

Dissertation zur Erlangung des Doktorgrades
der Fakultät für Chemie und Pharmazie
der Ludwig-Maximilians-Universität München

The Total Synthesis of (–)-Nitidasin,
Synthetic Studies Toward
Astellatol and Retigeranic Acid B,

And

Development of Novel Photochromic Ligands for
L-type Voltage-gated Calcium Channels

Vorgelegt von

FLORIAN MAURITIUS ERASMUS HUBER

aus München in Oberbayern
(Deutschland)

2014

Erklärung

Diese Dissertation wurde im Sinne von § 7 der Promotionsordnung vom 28. November 2011 von Herrn Prof. Dr. D. Trauner betreut.

Eidesstattliche Versicherung:

Diese Dissertation wurde eigenständig und ohne unerlaubte Hilfe erarbeitet.

München, den 17. Oktober 2014.

.....
(Florian M. E. Huber)

Dissertation eingereicht am: 17. Oktober 2014.

1. Gutachter: Prof. Dr. D. Trauner.

2. Gutachter: Prof. Dr. M. Heuschmann.

Mündliche Prüfung am: 12. November 2014.

– This work is dedicated to my family and my beloved Bianca.

Foreword

Parts of this doctoral thesis have been published in peer-reviewed journals:

D. T. Hog, F. M. E. Huber, D. Trauner, 'The Total Synthesis of (–)-Nitidasin', *Angew. Chem. Int. Ed.* **2014**, 53, 8513–8517; *Angew. Chem.* **2014**, 126, 8653–8657; *Synfacts* **2014**, 10, 902.

Parts of this doctoral thesis have presented at scientific conferences:

Oral presentations

'The Total Synthesis of (–)-Nitidasin and Synthetic Studies Toward Astellatol', *Seminar at the University of Toronto*, invited by Prof. Dr. M. Lautens, **2014**.

Poster presentations

'The Total Synthesis of (–)-Nitidasin and Synthetic Studies Toward Astellatol', *GRC The Central Role of Natural Products in Biology and Chemistry* (Andover, NH), **2014**.

'The Total Synthesis of (–)-Nitidasin', *SFB-749 annual meeting* (Venice), **2014**.

'Photocontrolling Ca_v Channels: Design and Synthesis of Potential Photochromic Blockers', *Frontiers in Medicinal Chemistry* (Munich), **2013**.

Abstract

The first part of present doctoral thesis is dedicated to sesterterpenoid natural products, which constitute a relatively small subclass of the family of terpenoid compounds. In particular, a small number of biosynthetically closely related *iso*-propyl-substituted *trans*-hydrindane-based congeners were chosen as targets for a synthetic program that envisioned their chemical construction *via* a unified approach. In this context, the first total synthesis of the complex tetracarbocyclic sesterterpenoid (–)-nitidasin was disclosed. To this end, a highly convergent installation of its western cyclopentane moiety was demonstrated by use of an unprecedented Li-alkenyl addition to a versatile *trans*-hydrindanone building block. An efficient closure of the central 8-membered carbocycle was achieved by means of ring-closing metathesis that benefitted from finely tuned conformational parameters of the employed substrate. In summary, the developed protocol provides a scalable and continuously high yielding route for the assembly of the rare carbon skeleton of (–)-nitidasin. Furthermore, advanced synthetic studies toward the pentacyclic natural products retigeranic acid B and astellatol are described. Notably, the latter involved a biomimetic retrosynthetic proposal for the elaboration of its unique fused ring system. Two different strategies were followed in order to access viable precursors for the suggested cationic cascade, of which the latter allowed for the investigation of the mentioned key step experimentally and *via* computational methods.

In the second section of this manuscript, the design and synthesis of the first known photochromic antagonist for L-type voltage-gated calcium channels is presented. The ultimate goal of this project lies in the establishment of a photopharmacological tool that supports the further elucidation of Ca^{2+} -dependent cellular events, especially in neurons. The central pharmacophore of the prepared compounds was derived from the benzothiazepine drug *cis*-(+)-diltiazem. This parent substance also served as the starting point for the developed short and convergent semisynthetic strategy. Thirteen analogues were synthesized in total and a preliminary lead structure was identified using electrophysiological methods. Based on these findings, two compounds of increased solubility and desirable photochemical properties were prepared. A possible explanation for their photodependent mode of action was proposed, which is currently subject of our ongoing investigations.

Acknowledgements

I want to thank Prof. Dr. D. Trauner for giving me the opportunity to conduct my doctoral research studies in his laboratories. Although the given projects posed considerable challenges, Dirk entrusted me to pursue my own strategies and always offered creative solutions to the occurring problems. I am very grateful for all the teaching tools he supplied for his group, like the weekly ‘Denksport’ or the retrosynthesis meetings. Furthermore, I really enjoyed the scientific conferences he enabled me to visit. These provided me with the chance to study state-of-the-art developments in chemistry and present my own experimental results. Another highly appreciated Trauner group activity was the annual skiing trip to Saalfelden. I would certainly like to study the behavior of the slope species ‘Black Mamba’ again in future years, if permitted. Due to Dirk’s extensive knowledge in chemistry and his inspiring enthusiasm for scientific questions, I learned what is needed to become a dedicated, efficient and better chemist.

I am grateful to Professor Dr. M. Heuschmann for examining my doctoral thesis as well as Prof. Dr. P. Knochel, Prof. Dr. K. Karaghiosoff, Prof. Dr. F. Bracher and Prof. Dr. W. Steglich for joining on my defense committee.

I am also thankful to my collaborators Dr. D. T Hog, Dr. T. Fehrentz, B.Sc. M. Maier and Dr. C. A Kuttruff for an ever-pleasant teamwork and stimulating scientific discussions. Together, we certainly got some projects going.

Furthermore, I want to acknowledge the former and present members of the Trauner group. Starting with a warm welcome, I soon felt at home amongst you. Especially my two earliest labmates Dr. B. Gaspar and J. Schwarz became dear friends to me. I will never forget our evenings at Kilians Irish pub. But also Dr. D. Stichnoth, who accompanied me for more than 4 years in the orange lab, and R. Meier (‘horny Robin’) have become almost indispensable daily companions, who I will miss greatly. Thanks to ‘Kuttiman’ and ‘Mesiman’ for the funny Paintball sessions. Thank you to all orange lab members of today and from the past: Dr. L. Salonnen, Dr. E. Herrero-Gómez, Dr. M. Kienzler, Dr. P. Stawski, G. Veits, A. Rizzo, L. Schreyer and S. Gerndt. Thank you, Dr. D. Barber, for improving my English skills by proofreading manuscripts. I also want to thank Dr. T. Magauer for helpful discussions.

I would like to thank the permanent staff of the Trauner laboratories, T. Kauer, C. Louis, L. de la Osa de la Rosa and Dr. M. Sumser for their helping hands and providing me with everything I needed. Special acknowledgements have to be addressed to H. Traub and A. Sarman Grilic for organizing the group and helping with all formalities.

Furthermore, I want to acknowledge my former undergraduate interns S. M. Janich ('Spatzl'), S. Linke ('Blaubarschbube') and E. Uhl, who helped me with lab work and gave me the opportunity to improve my teaching skills.

I am especially indebted to the analytical department (Dr. W. Spahl, S. Kosak, Dr. Stevenson, C. Dubler and Dr. P. Mayer) and the people, who keep the department running at different places and have always supplied me with precious dry ice.

Regarding the preparation of this manuscript, I am very thankful to Dr. N. Armanio, Dr. J. Shaw, Dr. H. Toombs-Ruane, P. Ellerbrock, Dr. M. Sumser, Dr. D. Stichnoth, R. Meier, B. Williams and A. Rizzo for their critical reading and helpful suggestions.

I am also very grateful to my friends at home, especially to the infamous 'Ammerseer Baumschubser' and my best friend M. Augustine, who helped me to recognize that there is life outside the lab.

Last but not least, I want to express my deep gratitude for my family. Thanks to my parents for supporting me and believing in me over the course of the last 30 years. And thanks to my sister for taking care of the royal member of the household, the cat. I also want to thank my grandparents for help and sponsorship. The future will hopefully hold more time for family boat trips on lake Ammersee.

TABLE OF CONTENTS

Erklärung.....	II
Foreword.....	IV
Abstract.....	V
Acknowledgements.....	VI
Table of Contents	VIII

THE TOTAL SYNTHESIS OF (–)-NITIDASIN AND SYNTHETIC STUDIES TOWARD RETIGERANIC ACID B AND ASTELLATOL

1. Introduction	3
1.1 Terpenoids: Definition, Subclasses and Biosynthesis.....	3
1.2 Terpenoids: Pharmaceutical Relevance and Synthetic Aspects.....	12
1.3 Sesterterpenoids: Chemical Synthesis, Subtypes and Background.....	18
1.4 <i>iso</i> -Propyl-substituted <i>trans</i> -Hydrindane Sesterterpenoids.....	29
1.4.1 <i>Comprehensive Overview of the Subclass</i>	29
1.4.2 <i>Literature-known Synthetic Approaches</i>	34
1.4.3 <i>Evolution of a Unified Synthetic Approach</i>	42
1.5 Project Outline.....	44
2. Synthetic Studies Toward Retigeranic Acid B	47
2.1 A Comprehensive Introduction to Retigeranic Acid A and B	47
2.2 Retrosynthetic Analysis.....	49
2.3 Synthesis of a Model System for the <i>trans</i> -Hydrindanone Moiety.....	50
2.4 Synthesis of the Cyclopentane Moiety.....	54
2.5 Model Studies on the Fragment Combination.....	57
2.6 Conclusion and Future Aspects.....	60

3.	The Total Synthesis of (–)-Nitidasin	62
3.1	A Comprehensive Introduction to (–)-Nitidasin.....	62
3.2	Retrosynthetic Analysis	64
3.3	Synthesis of the Vinyl Cyclopentane Moiety	66
3.4	Synthesis of the <i>trans</i> -Hydrindanone Moiety	70
3.5	Model Studies Toward the Construction of the Central Cyclooctane Motif	79
3.6	The Stage is Set – Completion of (–)-Nitidasin	87
3.7	A Brief Synthetic Digression Toward Alborosin	92
3.8	Conclusion and Future Aspects	94
4.	Synthetic Studies Toward Astellatol	97
4.1	A Comprehensive Introduction to Astellatol	97
4.2	Retrosynthetic Analysis	99
4.3	Enantioselective Synthesis of the Cyclopentenol Triflate Fragment.....	100
4.4	Model Studies on the Fragment Combination and Cyclooctadiene Formation	105
4.5	Second-generation Approach: Branching Off at the (–)-Nitidasin Synthesis ..	111
4.6	Theoretical Investigations on the Envisaged Cationic Cascade	114
4.7	Conclusion and Future Aspects	118
5.	Experimental Section.....	121
6.1	General Notes	121
6.2	Experimental Procedures for Chapter 2: ‘Synthetic Studies Toward Retigeranic Acid B’	124
6.3	Experimental Procedures for Chapter 3: ‘The Total Synthesis of (–)-Nitidasin’	143
6.4	Experimental Procedures for Chapter 4: ‘Synthetic Studies Toward Astellatol’	203

DEVELOPMENT OF NOVEL PHOTOCHROMIC LIGANDS FOR L-TYPE VOLTAGE-GATED CALCIUM CHANNELS

1.	Introduction	241
1.1	The Physiological Role of Calcium	241
1.2	Voltage-gated Calcium Channels: Structural Composition and Subtypes.....	243
1.3	L-Type Calcium Channels: Pharmacological and Functional Aspects	247
1.3.1	<i>Channel Gating and Inactivation</i>	247
1.3.2	<i>Overview on the Known Agonists and Antagonists</i>	249
1.3.3	<i>Dihydropyridine-based LTCC Blockers</i>	251
1.3.4	<i>Benzo(thi)azepine-based LTCC Blockers</i>	252
1.4	Project Outline.....	254
2.	Development of Photochromic Ligands for LTCCs	256
2.1	An Enantioselective Approach Toward Benzothiazepine-based Photochromic LTCC Blockers	256
2.2	Semisynthesis of Diltiazem-derived Photochromic LTCC Blockers.....	260
2.3	Electrophysiological Evaluation of Diltiazem-derived Photochromic LTCC Antagonists.....	268
2.4	Conclusion and Future Aspects.....	271
3.	Experimental Section	273
3.1	General Notes	273
3.2	Experimental Procedures for Chapter 2: ‘Development of Photochromic Ligands for LTCCs’	276

APPENDIX

I.	Summary	345
II.	Computational Methods.....	353
III.	X-Ray Crystallographic Data	354
IV.	^1H and ^{13}C NMR Spectra	376
V.	Additional Data	532
VI.	List of Abbreviations	547
VII.	References.....	554
VIII.	Curriculum Vitae.....	580

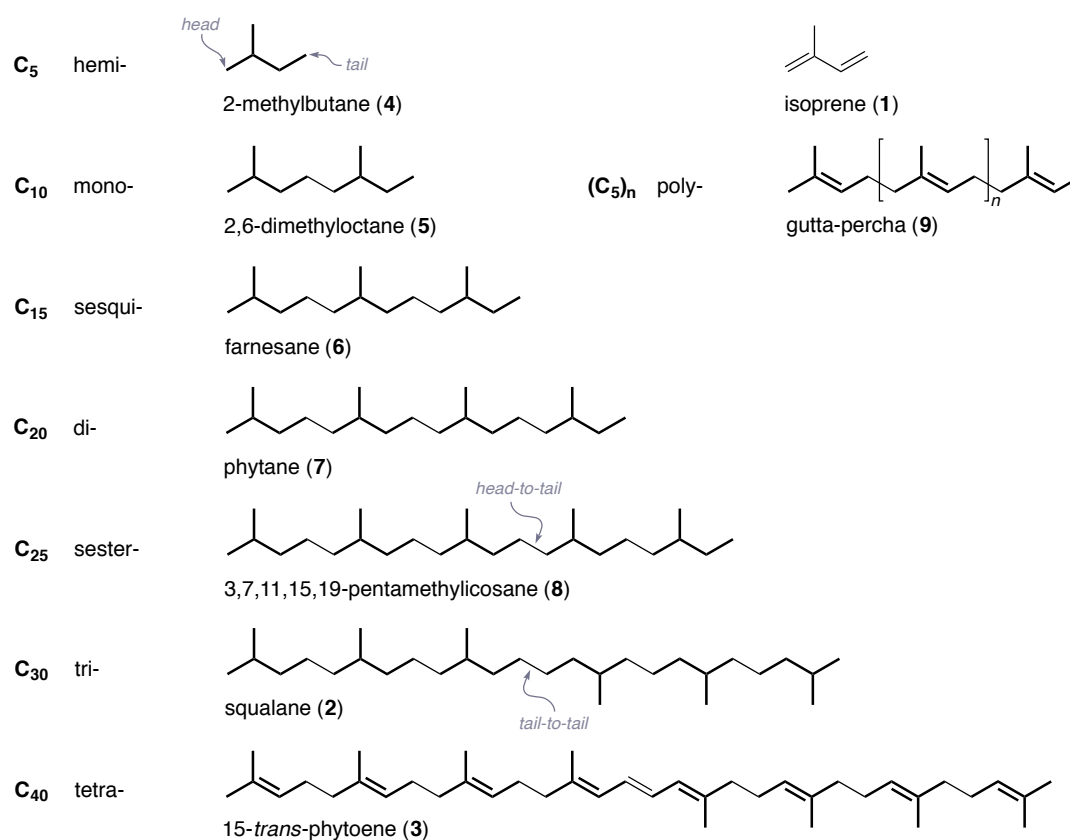
THE TOTAL SYNTHESIS OF (–)-NITIDASIN
AND
SYNTHETIC STUDIES TOWARD
RETIGERANIC ACID B AND ASTELLATOL

1. Introduction

1.1 Terpenoids: Definition, Subclasses and Biosynthesis

Terpenoids are an ubiquitous class of natural products and represent the largest and most diverse collection of secondary metabolites, with over 55.000 members isolated to date.^[1] For mankind, these functional molecules truly hold a special place in both world and chemical history, as their deliberate use can be traced back as far as ancient Egypt. Since then, scientists and non-scientists have found numerous applications for terpenoids, ranging from flavours, fragrances, hormones and therapeutical agents to even functional materials like rubber.^[2]

Originally, the term ‘terpenes’ had been coined by Kekulé to refer to the hydrocarbon content of the tree gum turpentine (lat. *Balsamum terebinthinae*).^[3] This definition has been extended since then and today all natural compounds built up by isoprene units are typically included. Although the terms ‘terpenes’ and ‘terpenoids’ are often used synonymously for this type of molecule, official nomenclature according to IUPAC^[4] states that the former comprises only

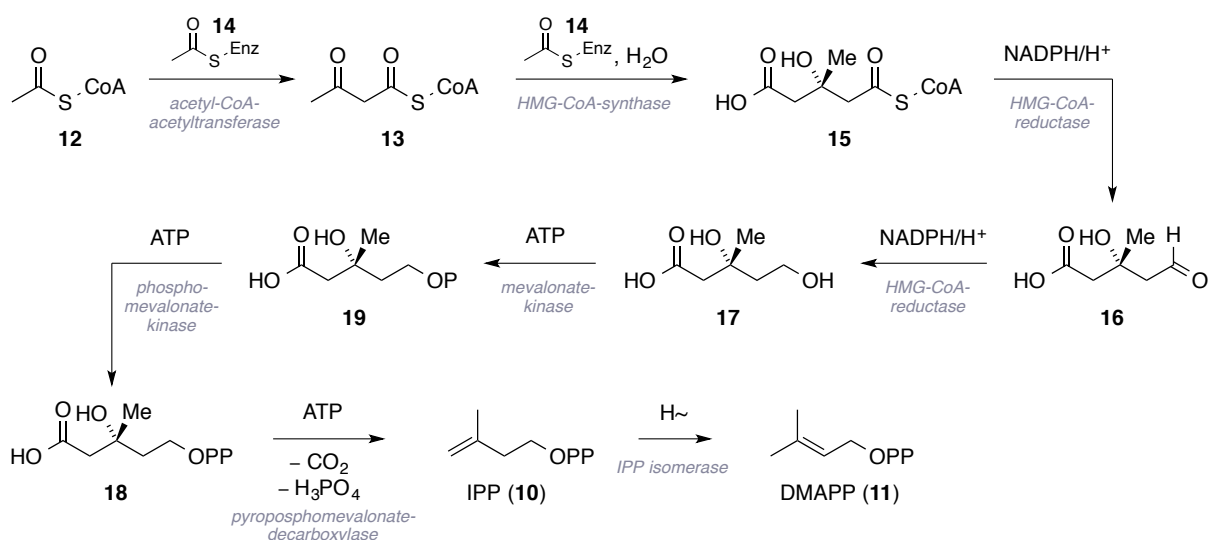


Scheme 1.1: Classification of terpenoids according to the number of included C₅ isoprene units. Phytoene (3) was drawn in the unnatural 15-*trans* configuration for simplicity.

pure hydrocarbons of biological origin, whereas the latter refers to oxygenated and further functionalized congeners.ⁱ

The search for the biosynthetic origin of terpenoid natural products in general and in particular has motivated innumerable scientific studies ever since the dawn of organic chemistry. In the beginning, the ground breaking studies by Wallach^[5] and later by Ruzicka^[6] led to the formulation of the already indicated ‘isoprene rule’, which states that all members of this family of compounds are built up from a varying number of a fundamental monomer, namely isoprene (**1**). Therefore, terpenoids are also sometimes denoted as ‘isoprenoids’, even though mentioned monomer itself is not involved in their biosynthesis. In nature, they occur predominately as functionalized or elaborately cyclized versions of their basic parent hydrocarbons, which are depicted in scheme 1.1. According to the number of C₅ building blocks, these natural products are subdivided in the classes of hemi-, mono-, sesqui-, di-, sester-, tri-, tetra- and polyterpenoids. As it can be seen in the exemplified tri-(**2**) and tetraterpenoid (**3**) chains, biosynthesis not only arranges *tail-to-head* connectivity but also *tail-to-tail* linkage is possible. This further structural diversification was first recognized by Ruzicka in 1953 in his extended ‘biogenetic isoprene rule’.^[7]

Identification of the actual biosynthetic precursors of natural occurring terpenoids was reported in the seminal investigations of Bloch^[8] and Lynen.^[9] In their studies, both authors disclosed that the two activated C₅ building blocks isopentenyl pyrophosphate (IPP, **10**) and dimethylallyl pyrophosphate (DMAPP, **11**) are nature’s equivalents for isoprene (**1**). After

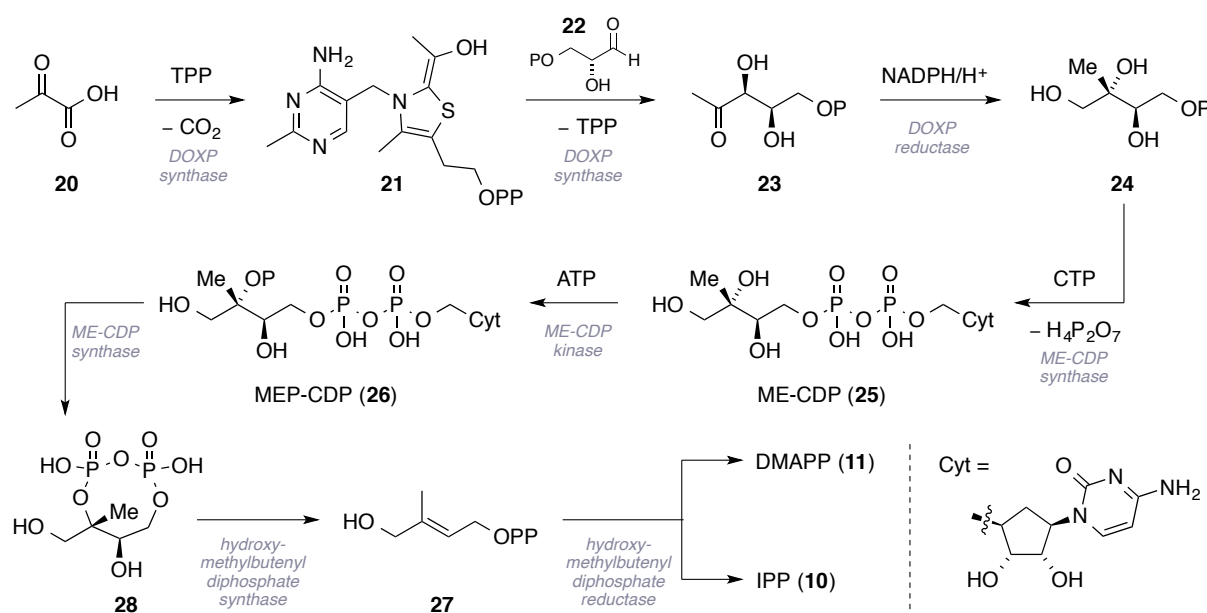


Scheme 1.2: The mevalonate pathway as the first elucidated biosynthetic origin of IPP (**10**) and DMAPP (**11**). Involved enzymes are indicated grey.

ⁱFor the sake of consistency, present doctoral thesis will only use the term ‘terpenoid(s)’.

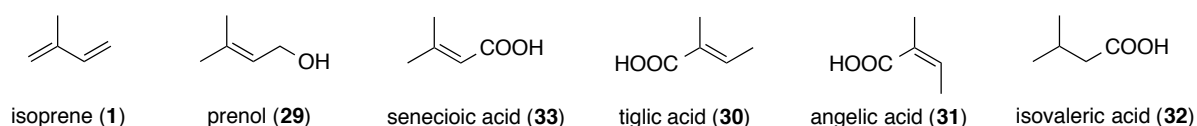
the fundamental discovery that both compounds can be traced back to acetyl-CoA (**12**), subsequent investigations led to the formulation and refinement of the so-called mevalonate pathway (scheme 1.2) and marked the first detailed mechanistic insights into terpenoid biogenesis.^[10] To this end, it was proven that initially an equivalent of acetyl-CoA (**12**) reacts with an enzyme-bound acetyl function to furnish diketone **13**, in a manner resembling a Claisen condensation. The resulting natural analogue of acetoacetate then undergoes diastereo-selective aldol addition of another thioester bound acetyl group (**14**). Ensuing hydrolysis accounts for the formation of β -hydroxy- β -methylglutaryl-CoA (**15**), which in turn is reduced by dihydronicotinamide adenine dinucleotide (NADPH/H⁺) to mevaldic acid (**16**). A second NADPH/H⁺-mediated reduction step then gives rise to (*R*)-mevalonic acid (MVA, **17**), the key intermediate that serves as eponym for this pathway. In the following, two sequential phosphorylation steps, which are mediated by one equivalent of adenosine triphosphate (ATP) each, form the pyrophosphate **18**. In a final ATP-assisted enzymatic transformation, substance **18** is decarboxylated and dehydrated to IPP (**10**). This first important building block can in turn be converted to the second – DMAPP (**11**) – by the thiol-based IPP isomerase.^[2] Interestingly, this formal [1,3]-hydride shift has been proposed to proceed *via* a two-base mechanism and starts with the stereospecific enzymatic removal of the *pro-R* proton in IPP (**10**).^[11]

For several decades, these milestone achievements completely eclipsed the existence of a second metabolic route for the biosynthesis of IPP (**10**) and DMAPP (**11**), mainly occurring



Scheme 1.3: The non-mevalonate pathway as the major source of IPP (**10**) and DMAPP (**11**) in plants.

in plants, protozoa, bacteria and algae.^[12] The methylerythriol phosphate (MEP) pathway, which has also come to be known as the non-mevalonate pathway, was pioneered by the groups of Rohmer^[13] and Arigoni.^[14] In detail, the sequence starts with pyruvic acid (**20**), which upon reaction with thiamine pyrophosphate (TPP) forms thiazole **21** under extrusion of carbon dioxide.^[15] After this umpolung step, the enamine in substance **21** can nucleophilically attack glyceraldehyde 3-phosphate (**22**), giving rise to 1-desoxy-D-xylulose-5-phosphate (DOXP, **23**). Notably, this intermediate is also the branching point for the biogenesis of pyridoxal (vitamin B₆, not shown) and thiamine (vitamin B₁, not shown). Along the terpenoid avenue, an enzyme-promoted skeletal rearrangement that is accompanied by a NADPH/H⁺-dependent reduction leads to the generation of MEP (**24**). Subsequently, an ester interchange between MEP (**24**) and the nucleotide cytidine triphosphate (CTP) forms the mixed diphosphate **25** (ME-CDP), driven by the expulsion of a molecule of pyrophosphate. An additional kinase promoted phosphorylation of the tertiary alcohol function (**26**, MEP-CDP) is then followed by intramolecular cyclization, proceeding again *via* transesterification and the release of cytidine monophosphate (CMP). Reductive ring opening toward phosphorylated alcohol **27** is achieved by a ferredoxin containing enzyme complex and delivers the last precursor for the formation of IPP (**10**) and DMAPP (**11**). This final step comes along with the oxidation of one equivalent of NADPH/H⁺ and the release of water, eventually yielding IPP (**10**) and DMAPP (**11**) in a ratio of 5:1 to 4:1. However, the mechanism for this transformation has not been fully clarified to date.

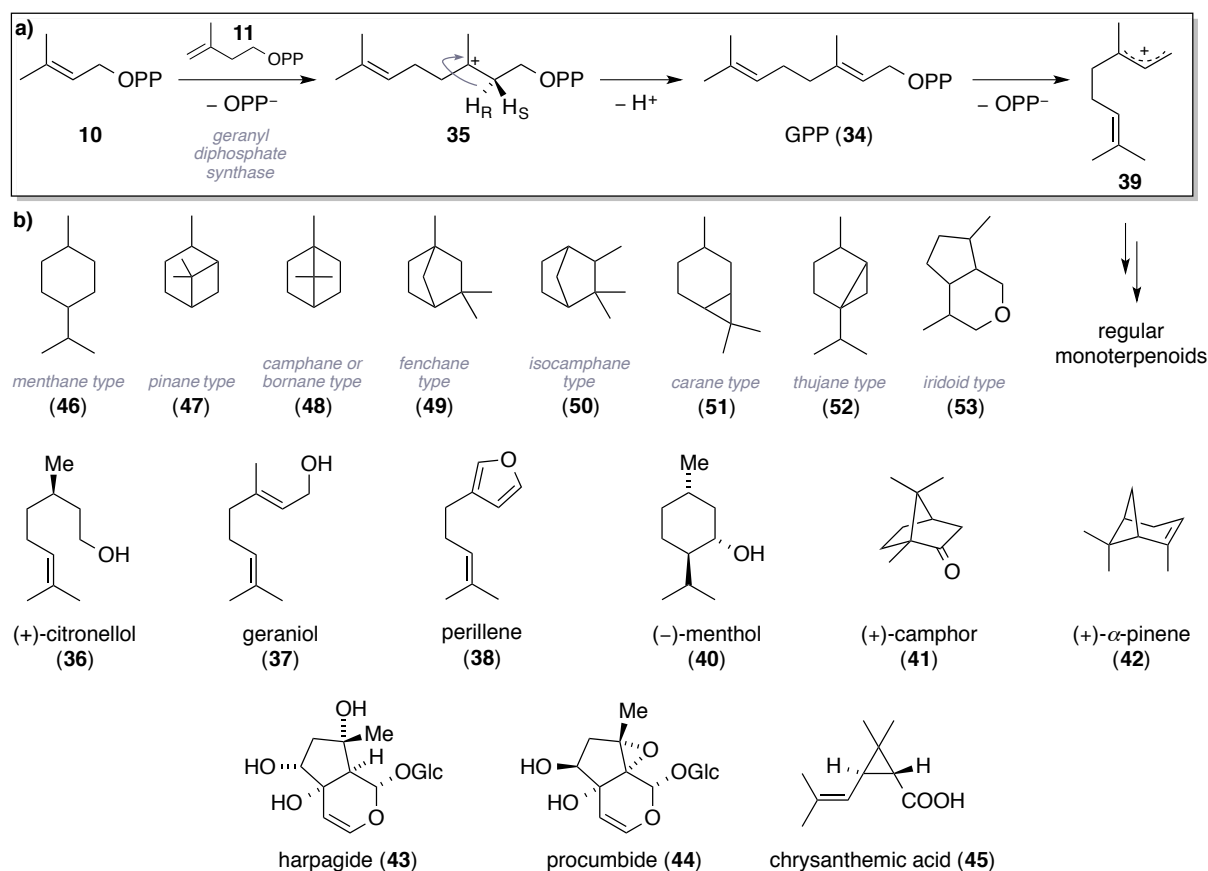


Scheme 1.4: Selected hemiterpenes as imminent biosynthetic descendants of IPP (**10**) or DMAPP (**11**).

The smallest subclass of terpenoids, the hemiterpenes, only consists of about 50 known congeners, which are directly synthesized from either one of the presented C₅ precursors.^[2] In nature they rarely occur in an unbound state, but rather are found as their respective glycoside or phosphate derivatives. Isoprene (**1**) itself is formed in plants from DMAPP (**11**) – assisted by the isoprene synthase – and represents the only true hemiterpene that is isolable from natural sources. Other important members of this subclass are prenol (**29**), tiglic acid (**30**), angelic acid (**31**), isovaleric acid (**32**) and senecioic acid (**33**), of which the latter four often appear as their respective esters in alkaloid natural products (scheme 1.4).

The biosynthetic diversion to more complex terpenoid structures starts with the formation of geranyl pyrophosphate (GPP, **34**) by a prenyl transferase-promoted nucleophilic attack of

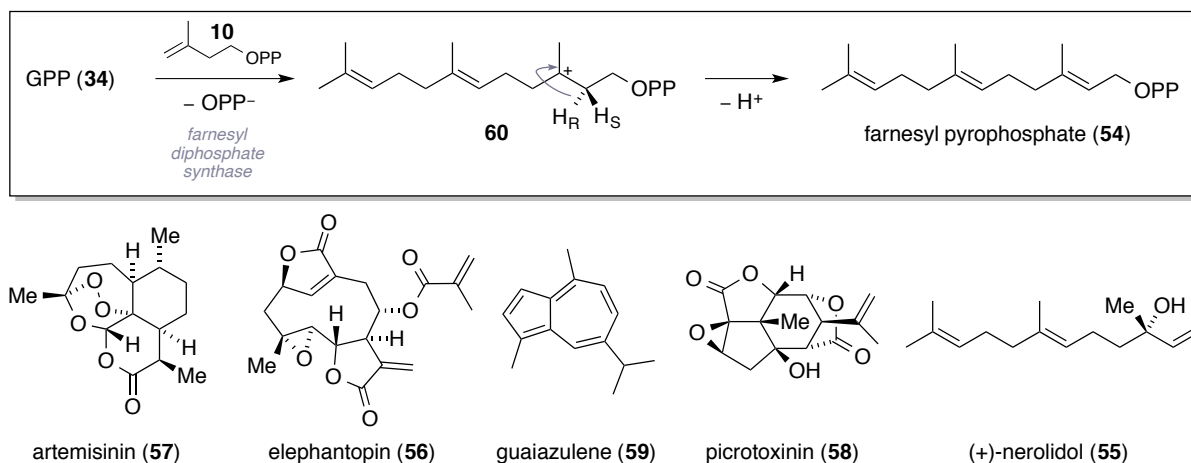
IPP (**10**) at an allylic cation generated from DMAPP (**11**). This initial *head-to-tail* connection is followed by the stereospecific elimination of the *pro-R* proton from cation **35** and leads to the fundamental all-carbon precursor of all monoterpenoids (scheme 1.5a).^[10d] Approximately 1500 naturally occurring monoterpenes have been documented to date.^[2] Besides the basic open-chain members of this subtype, which comprise the fragrances (+)-citronellol (**36**), geraniol (**37**) and perillene (**38**), also more interlaced carbocyclic architectures are found. Upon elimination of pyrophosphate from GPP (**34**), the generated allylic cation (**39**) can undergo a variety of cyclization reactions. These ring formations often represent only the first part of more substantial skeletal rearrangements that are concomitant to cationic cascades. Scheme 1.5b lists the basic mono- and bicyclic architectures observed in nature and showcases some prominent oxygenated derivatives, like for instance (–)-menthol (**40**), (+)-camphor (**41**) and (+)- α -pinene (**42**). Furthermore, the so-called iridoids constitute an important subclass of monoterpenoids, whose biogenesis has been traced back to geraniol (**37**).^[10d] Important congeners are the constituents of devil's claw, harpagide (**43**) and procumbide (**44**), which have been demonstrated to inhibit thromboxane biosynthesis similarly to aspirin (not shown).^[16] A somewhat special category of C₁₀ terpenoids are the



Scheme 1.5: Biosynthesis of GPP (**34**), basic carbon skeletons of monoterpenoids and selected examples.

irregular monoterpenoids like chrysanthemic acid (**45**), which have been found exclusively in the *Compositae/Asteraceae* plant family. Although IPP (**10**) and DMAPP (**11**) have been proven to be part of their biosynthesis, GPP (**34**) or related *head-to-tail* connected intermediates appear not to be involved.

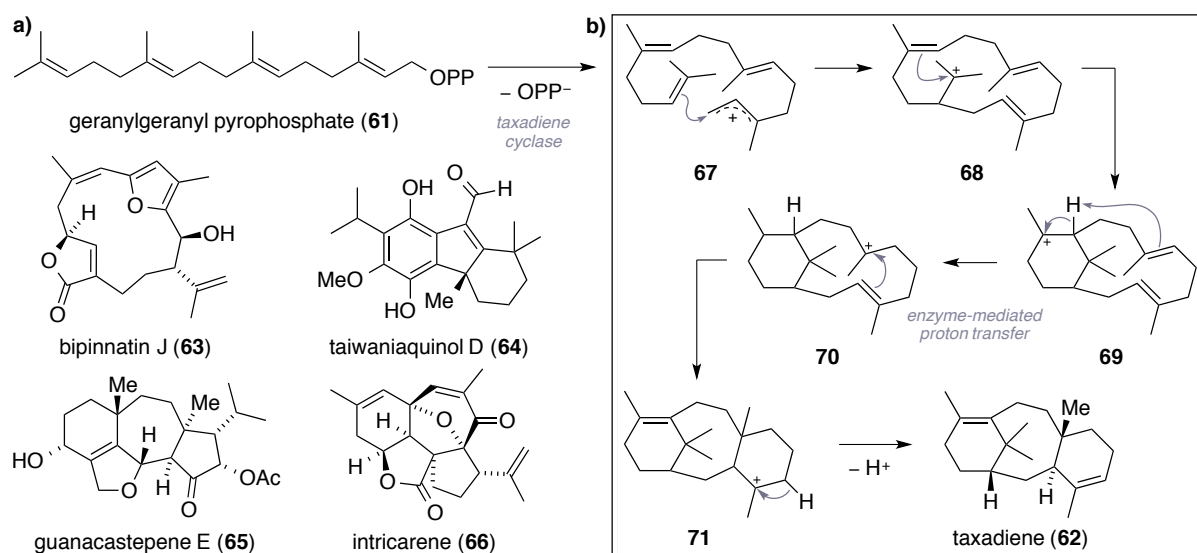
Analogously to the assembly of GPP (**34**), its carbon chain can be elongated even further by another C₅ unit, which consequently leads to the formation of farnesyl pyrophosphate (**54**). This activated allylic compound is then biosynthetically processed in a fashion, which is comparable to the one that has been detailed for the generation of monoterpenoids previously (scheme 1.6). Because of the increased chain length and the additional carbon–carbon double bond, the number of possible cyclization modes is vastly increased, which is why already over 10000 sesquiterpenoids have been isolated so far.^[2] While (+)-nerolidol (**55**) constitutes a simple acyclic sesquiterpenoid and is commonly used in perfumery, the mono- and bicarbocyclic elephantopin (**56**), artemisinin (**57**) and picrotoxinin (**58**) represent highly functionalized and potent bioactive derivatives. A fascinating aromatic sesquiterpenoid that can be isolated from the gorgonian *Euplexaura erecta* is guaiazulene (**59**). This compound features a deep blue colour, which is due to the charge separation that is inherent to the azulene core and establishes a stable chromophore.



Scheme 1.6: Chain elongation of GPP (**34**) to farnesyl pyrophosphate (**54**) and selected sesquiterpenoids.

It is not surprising that both the C₂₀ diterpenoids and C₂₅ sesterterpenoids are biosynthesized from their respective isoprene-elongated versions of farnesyl pyrophosphate (**54**). Whilst the subclass of sesterterpenoids will be discussed in more detail later (*cf.* chapter 1.3), scheme 1.7a provides a short selection of exemplary diterpenoids, which have been synthesized in the Trauner research group recently.^[17] Although the number of realizable polycyclic architectures increases even further for the diterpenoids, only approximately 5000 natural descendants of geranylgeranyl pyrophosphate (**61**) are known to date.^[18] To provide a

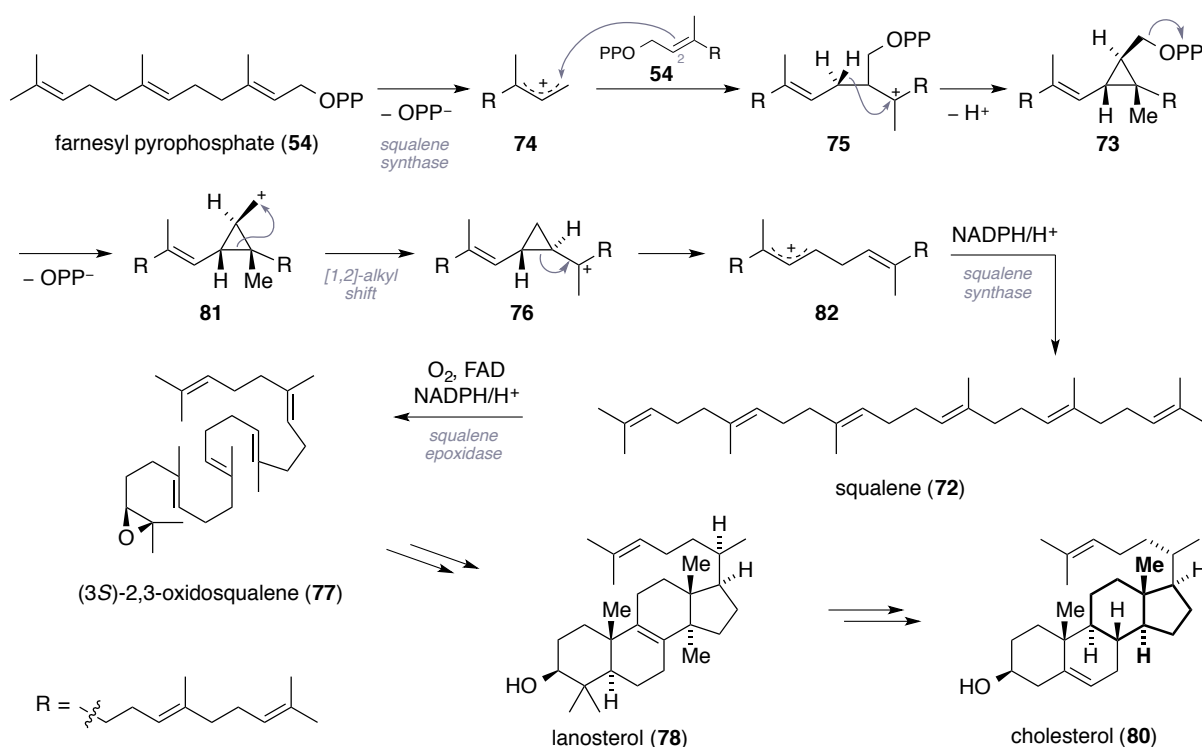
single but significant example for the complexity of the observed carbon frameworks, taxadiene (**62**) shall be named. This skeleton is the central motif of a prominent class of anticancer drugs and is enzymatically formed by the taxadiene cyclase. A special feature that was first discovered at this terpene cyclase is its ability to utilize an intermediary released proton for reprotonation of another, distant double bond to effectively relocate the cationic center during the biosynthetic cascade (1.7b).^[19]



Scheme 1.7: a) Geranylgeranyl pyrophosphate (**61**) and selected sesquiterpenoids recently accessed by total synthesis in the Trauner group. b) Biosynthetic formation of the taxadiene scaffold (**62**).

Interestingly, the natural precursors for tri- and tetraterpenoids are not assembled by the outlined IPP (**10**) homologation, but rather by a complex dimerization process of two molecules of farnesyl- (**54**) or geranylgeranyl pyrophosphate (**61**), respectively. In the case of triterpenoids, the mechanism of squalene (**72**) biosynthesis has been established in the 1970s after the isolation of presqualene diphosphate (**73**), an intermediate in the reaction sequence (scheme 1.8).^[20] This pathway commences with a nucleophilic attack of the C-2 situated double bond onto a previously formed farnesyl cation (**74**) upon which intermediate **75** is generated. A subsequent enzymatically catalyzed proton loss is accompanied with the formation of a cyclopropane moiety and leads directly to presqualene diphosphate (**73**). The ensuing expulsion of the pyrophosphate substituent comes along with a Wagner-Meerwein-type [1,2]-alkyl shift and gives rise to cyclopropane compound **76**. This species ultimately undergoes a ring-opening reaction and NADPH/H⁺-dependent reduction to yield squalene (**72**). Further transformations, like site-selective epoxidation to (3*S*)-2,3-oxido-squalene (**77**), set the stage for a series of thoroughly investigated epoxide-opening cascades.^[21] Triggered cationic cyclizations and rearrangements are the basic principles for the biogenesis of tetra-

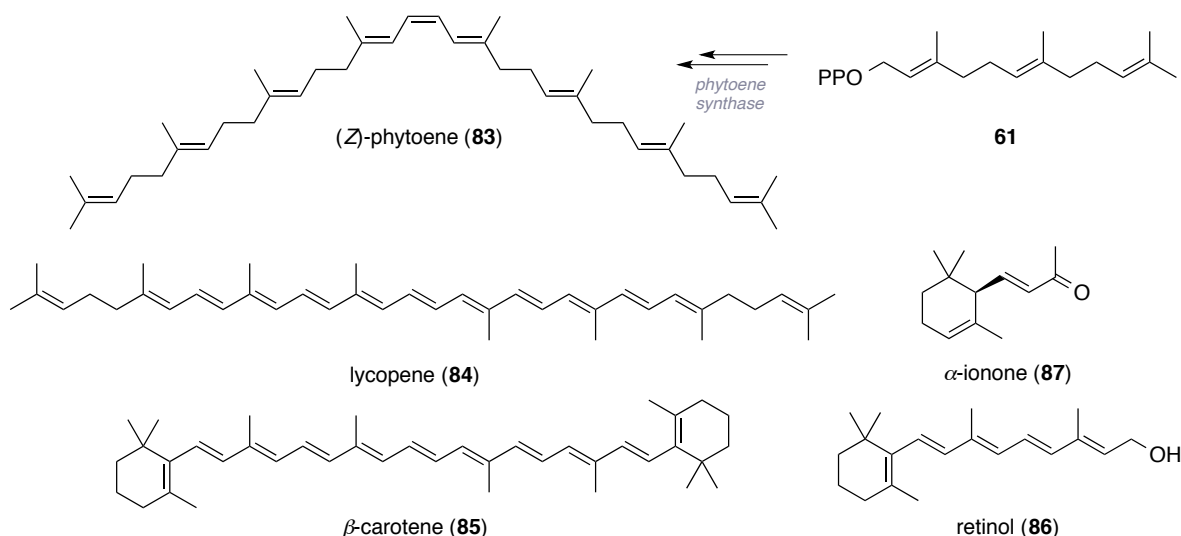
and pentacarboxylic triterpenoids like lanosterol (**78**) or similar steroid precursors. A thorough discussion of the natural product class of steroids that are, strictly speaking, classified as *nor*-terpenoidsⁱⁱ would be beyond the scope of this thesis. At this point, only two examples shall be given: namely the complex octacyclic *nor*-terpenoid micrandilactone A (**79**, scheme 1.17)^[22] and cholesterol (**80**), which is one of many steroid congeners possessing a *trans*-hydrindane substructure (*cf.* chapter 1.4).



Scheme 1.8: Biogenesis of the triterpenoid precursor squalene (**72**) and further epoxidation/cyclization to lanosterol (**78**) and steroids like cholesterol (**80**). The *trans*-hydrindane portion of the latter was highlighted bold.

The last category of naturally occurring classical oligoterpenoids are the C₄₀ tetraterpenoids, of which approximately 500 natural abundant congeners are known to date.^[2] Their common biosynthetic precursor is the C₂₀ symmetric substance (*Z*)-phytoene (**83**, scheme 1.9), which is processed from two molecules of geranylgeranyl pyrophosphate (**61**) in similar manner as already described earlier for squalene (**72**, *vide supra*). As this subclass is only represented by one group of compounds, they are also often referred to as ‘carotenoids’. Although (*Z*)-phytoene (**83**) itself is colourless, the extended π -electron system of most derived tetraterpenoids confers colour to them. Lycopene (**84**), for example, is the characteristic pigment in ripe tomato fruits and β -carotene (**85**) accounts for the orange colour of carrots. Apart from their function as natural dyes, carotenoids also exhibit favourable anti-oxidant

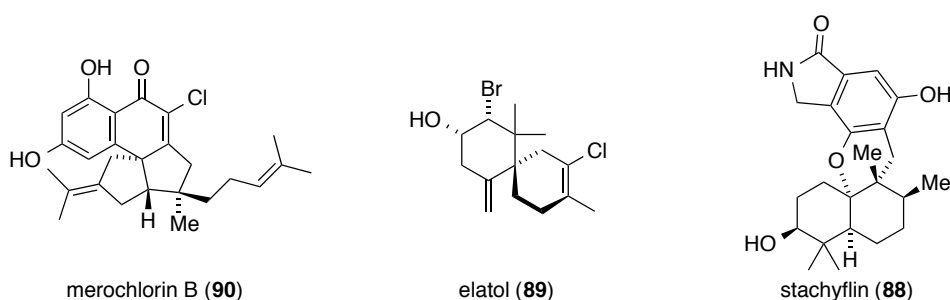
ⁱⁱThis classification refers to the frequently observed biosynthetic degradation of their carbon skeletons.



Scheme 1.9: Biosynthetic origin of (Z)-phytoene (83) and molecular structures of selected carotenoids, apocarotenoids and megastigmanes.

properties and play an important role in photosynthesis and the vision process.^[10d] Natural degradation products of the tetraterpenoids are the apocarotenoids, diapocarotenoids and megastigmanes. The first two substance groups are formed *via* oxygenative double bond cleavage of one or two terminal sections in, for example, β -carotene (85). They include retinol (86) that is also known as vitamin A₁. The megastigmanes involve even further biosynthetic degradation and are the most important fragrant components of flowers of various plant types, as it is the case for α -ionone (87).

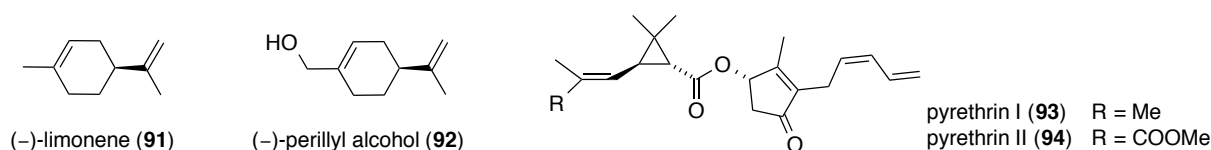
It shall be mentioned that besides the described more ‘classical’ terpenoid subtypes, also meroterpenoids and higher – most often polymeric – terpenoids exist in nature. Especially the meroterpenoids constitute a widespread class of natural products.^[23] In addition to the terpenoid portion, their carbon skeletons usually include structural elements that are derived from other metabolic sources, *e.g.* from the acetate and the shikimate pathway, or even from amino acid biosynthesis. For instance, an interesting structural mixture is present in stachyflin (88, scheme 1.10) and related compounds, which also exhibit interesting antiviral properties due to their interference with low-pH conformational change of hemagglutinin.^[24] Furthermore, several terpenoids with halogenated and polyhalogenated carbon frameworks,



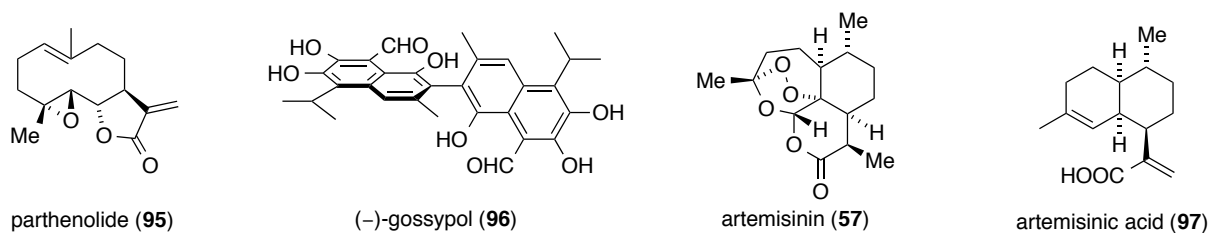
Scheme 1.10: Selected examples for meroterpenoids and halogenated terpenoids.

The biological role of terpenoid natural products is manifold and varies amongst the different organisms they are found in. Plants produce them, in part as defense agents against microorganisms and insects but also for the fulfillment of other important functions, as for instance carotenoids for photosynthesis or volatile molecules for their pollinator-attractive properties. In mammals, terpenoids contribute to stabilizing cell membranes, participate in metabolic pathways, and act as regulators in some enzymatic reactions.^[28] In general, the large structural diversity inherent to this class of secondary metabolites ensures a broad range of biological properties, which has ultimately led to their use in treatment of human diseases. This is exemplified by their current clinical application in treatment of malaria and certain types of cancer.^[29] This chapter will provide a selection of pharmaceutically relevant terpenoids and illustrate how their laboratory preparation has propelled the development of new synthetic strategies and methodologies in organic synthesis.

Already some of the small monoterpenoids, which are best known as constituents in essential oils, have been shown to possess anti-tumor activity. Primarily limonene (**91**) and perillyl alcohol (**92**) have long been established as chemopreventive and therapeutic agents against many tumor cell lines (scheme 1.11) and their clinical trials have progressed to phase 1 and phase 2,^[30,31] respectively.^[29] Their mechanism of action involves the induction of apoptosis and interference of the prenylation of key regulatory proteins.^[32] Furthermore, the pyrethrins (**93** and **94**), which are members of a small group of related monoterpenoid esters, exhibit valuable insecticidal properties and are used for the treatment of skin parasites such as head lice.^[33] Due to their ability to block sodium channel repolarization in arthropod neurons, their application leads to paralysis and death of target vermin.^[34] Today, several synthetic



Scheme 1.11: Molecular structures of selected pharmaceutically relevant monoterpenoids.



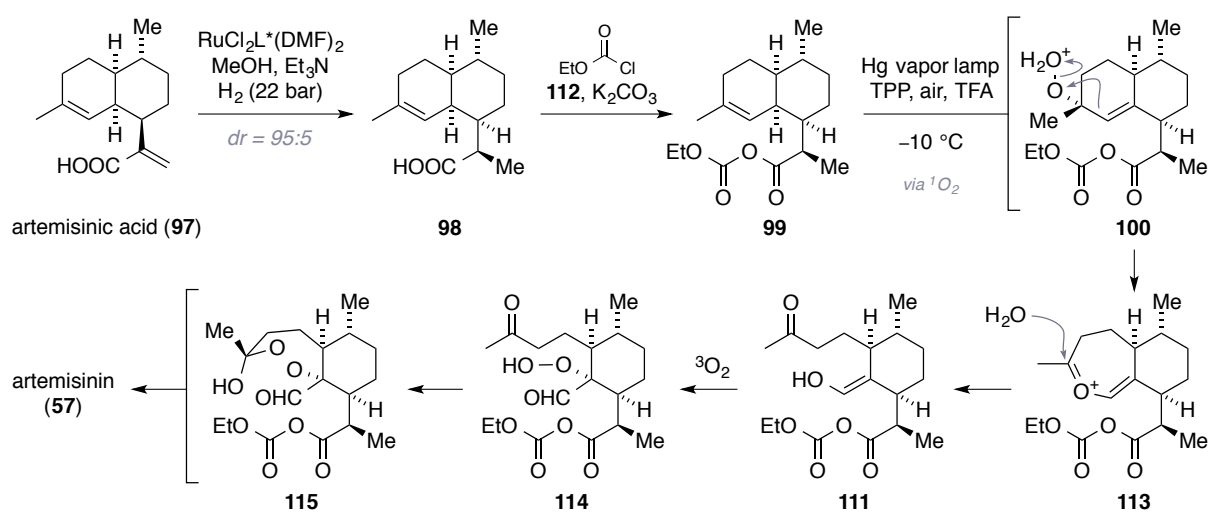
Scheme 1.12: Molecular structures of selected bioactive sesquiterpenoids and artemisinic acid (97).

analogues with increased toxicity and resistance against biodegradation have been developed and become widely used household and agricultural insecticides.^[10d]

The sesquiterpenoid lactone parthenolide (95, scheme 1.12) is the major active component of one of the oldest traditional remedies that comes from the plant *Tanacetum parthenium*. This plant is commonly called feverfew and is today widely used for the relief of arthritis, migraine, asthma and psoriasis.^[29] However, parthenolide (95) may occasionally cause some allergic side effects, due to its capability to alkylate proteogenic thiol groups.^[10d] (-)-Gossypol (96), an interesting dimerized sesquiterpenoid, is one of the major components in cottonseed and has been found to act as a male contraceptive. Extensive clinical trials in China established that the antifertility effect is usually reversible after stopping the treatment, provided that the consumption has not been too prolonged.^[35] Besides its desired function in altering sperm maturation, spermatozoid motility and inactivation of sperm enzymes necessary for fertilization, severe side effects were observed including high rates of hypokalemia among test subjects.^[36] Another drawback for its clinical use is the toxicity of the concomitant atropisomer (+)-gossypol (not shown), which cannot be separated fully upon isolation. Hence, research on this compound was widely abandoned in the late 1990's.^[37]

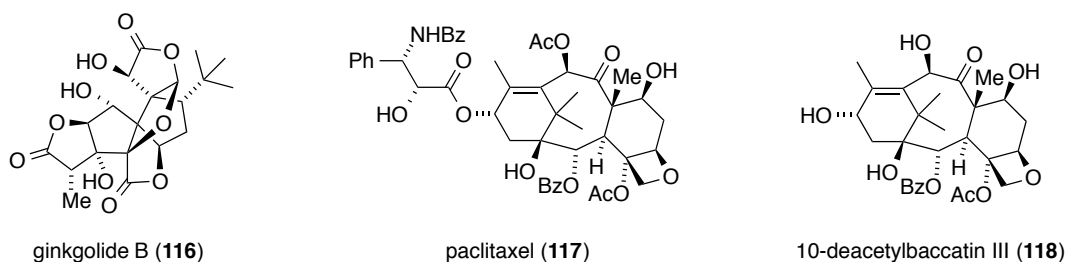
In contrast, the sesquiterpenoid artemisinin (57) is an approved drug for the treatment of malaria. It is isolated in 0.1–0.4 wt-% from the widespread herb species *Artemisia annua*. Early records reveal that this plant was already used by Chinese herbalists more than two thousand years ago.^[10d] Although the discovery of artemisinin (57) and the first investigations on its mode of action were part of a secret Chinese military project, it is today accepted that Y. Tu was the original principal investigator back in 1969.^[38] In 2012, it was reported that artemisinin-based therapies were the most effective clinical treatment of malaria at that time.^[39] The actual mode of artemisinin's (57) anti-malarial action is still a topic of considerable debate. One mechanism that is discussed refers to the effect of the endoperoxide group on free Fe^{3+} , which is released during digestion of hemoglobin. It is suggested that the iron directly reduces the peroxide bond in artemisinin (57), generating high-valent iron-oxo species. This supposedly results in a cascade of reactions that produce reactive

oxygen radicals, which ultimately damage the parasite and lead to its death.^[40] Today, artemisinin (**57**) is largely accessed *via* isolation and semisynthesis, starting from the naturally more abundant relative artemisinic acid (**97**). Industrial semisynthesis was first conducted by the company Amyris and was accomplished according to the ground breaking work of Acton, Roth^[41] and Brown.^[42] Very recently, the company Sanofi published their improved semisynthetic protocol, which is detailed in scheme 1.13.^[43] It features a highly diastereoselective hydrogenation of the exocyclic double bond of artemisinic acid (**97**) using a Ru(II)- and (*R*)-DTMB-SEGPPOS-based (not shown) catalyst system. After transformation of substance **98** to activated mixed anhydride **99**, an initial Schenck ene reaction^[44] with singlet oxygen leads to peroxide **100**, which undergoes sequential protonation and Hock cleavage^[45] to intermediate **111**. Final oxygenation and cyclization then yield the desired drug (**57**) in 55% over three steps. Notably, Sanofi uses a modification of Keasling's biosynthetic pathway for the *in vivo* preparation of artemisinic acid (**97**) in yeast.^[46] Although a plethora of total syntheses of artemisinin (**57**) has been disclosed in the past, none of those can compete with the semisynthetic approach in terms of cost.^[47]



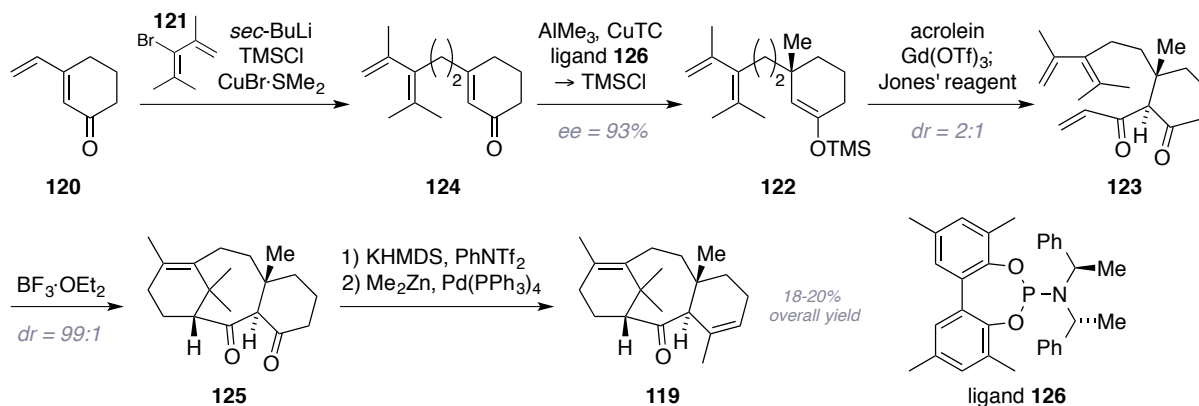
Scheme 1.13: Sanofi's semisynthesis of artemisinin (**57**) from biochemically prepared precursor **97**. The Ligand L equals to (*R*)-DTMB-SEGPPOS.

Regarding diterpenoid natural products, the ginkgolides represent a structurally intriguing bioactive subclass and can be isolated from *Ginkgo biloba*.^[48] The standardized extracts of the plant leaves are marketed for treatment of cerebral vascular disease and senile dementia, for which virtually all clinical studies have reported positive results. After the discovery that especially ginkgolide B (**116**, scheme 1.14) is an antagonist of the platelet-activating factor (PAF) receptor, extensive clinical studies on their potential use against respiratory infections were initiated.^[48] Although these studies could show that the compound is well tolerated with



Scheme 1.14: Structures of selected bioactive diterpenoids and of natural occurring Taxol[®] precursor **118**.

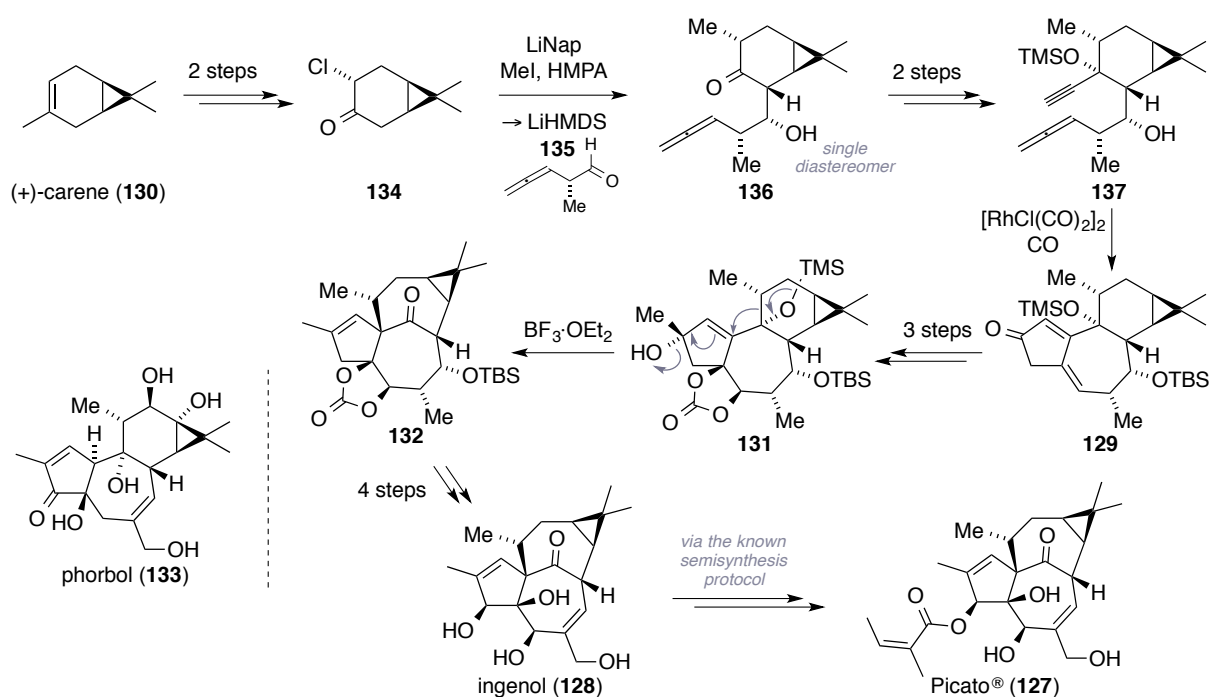
very few side effects, it was never registered as a drug due to a lack of efficacy. The probably best-investigated and pharmaceutically most valuable class of diterpenoids are the taxanes. Over 100 different species have been characterized to date, one of which is paclitaxel (**117**, Taxol[®]) that is clinically used for the treatment of ovarian and breast cancer.^[10d] First isolated from the bark of the pacific yew tree *Taxus brevifolia* in 1967, the natural product underwent thorough investigation until it was eventually approved as a drug by the FDA in 1992.^[49] Several increasingly soluble and potent synthetic analogues have been subjected to clinical trials, aiming at countering multiple drug resistance.^[50] Like several other anticancer drugs, paclitaxel (**117**) interacts with tubulin (more accurately the β -tubulin subunit) and effectively inhibits cell proliferation. Several in-depth studies have established that the drug retards microtubule depolymerization by formation of unusually stable microtubules.^[51] This leads to a disruption of the dynamic reorganization of the microtubule network, thus causing cellular arrest in the G₂/M phase of the mitotic cycle. By 1992, about 30 research teams were working on a total synthesis of paclitaxel (**117**),^[52] which culminated in a ‘photo finish’ between the groups of Nicolaou^[53] and Holton,^[54] who both have to be credited for the first independent successfully disclosed syntheses. Besides numerous studies, which have made substantial contributions to the development of synthetic methodology, to date seven total syntheses and two formal syntheses of paclitaxel (**117**) are known.^[55] However, today plant cell fermen-



Scheme 1.15: Baran's synthesis of taxadienone (**119**). Compounds **120** and **121** are prepared in one step each.

tation from specific *Taxus* cell lines has relieved the former less economic semisynthetic process.^[56] The latter starts from 10-deacetylbaccatin III (**118**), a more abundant taxane derivative, which is isolated predominately from European yew.^[57] Although still not being competitive in terms of cost, Baran and co-workers recently published a high yielding short sequence toward taxadienone (**119**, scheme 1.15)^[53] that exemplifies the ongoing advances in organic synthesis. After combining two very easily prepared building blocks (**120** and **121**) *via* Lewis acid assisted organocopper 1,6-addition, they demonstrated an elegant use of Alexakis' enantioselective conjugate addition methodology^[58] to access enantioenriched TMS ether **122**. Ensuing Mukaiyama^[59] aldol addition under Kobayashi's conditions^[60] and one-pot treatment with Jones' reagent^[61] forged precursor **123** for the substrate-controlled key Diels-Alder reaction. Although the aldol addition step suffers from low diastereoselectivity, the high overall yield (18–20%) of this scalable route poses an impressive synthetic achievement.

Omitting the large family of steroid-based pharmaceuticals, the diterpenoid ingenol mebutate (**127**) shall be mentioned as a last, synthetically relevant example of a successfully approved drug. The parent natural product ingenol (**128**) was first isolated in 1968^[62] from *Euphorbia ingens* and soon attracted chemists after the elucidation of its intriguing strained molecular structure.^[63] Several ester derivatives of this diterpenoid have been reported to exhibit important *in-vivo* anti-HIV or anticancer activity due to their interaction with protein kinase C.^[64] Ingenol mebutate (**127**) itself is currently sold by LEO Pharma under the name Picato[®] as a first-class treatment of actinic keratosis, a precancerous skin condition.^[65] The

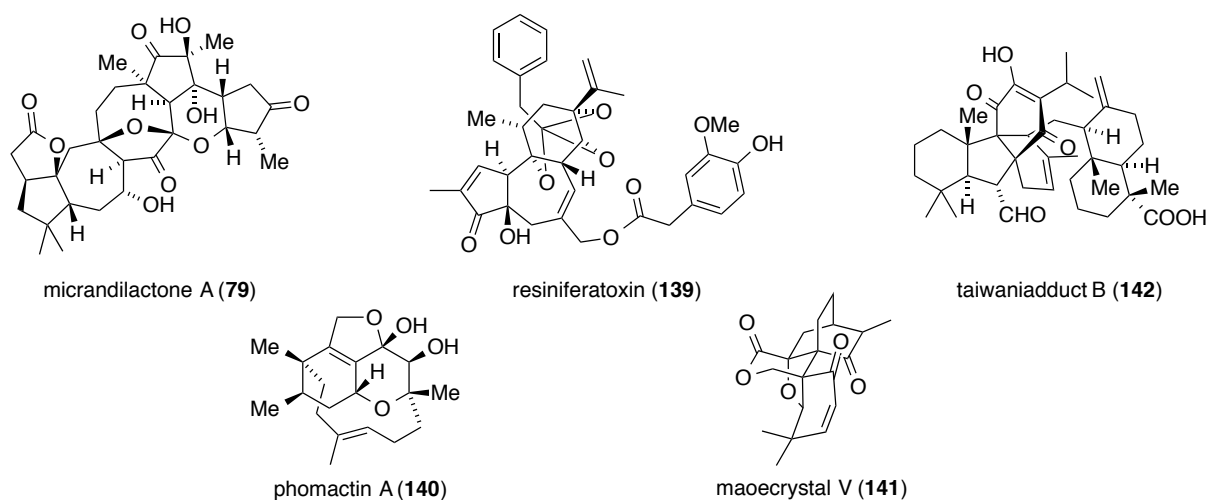


Scheme 1.16: Baran's synthesis of ingenol (**128**) and molecular structures of phorbol (**133**) and Picato[®] (**127**).

drug is produced by semisynthesis starting from ingenol (**128**), which can be obtained by a tedious isolation protocol in a low yield of approximately 250 mg/kg.^[66] Consequently, chemists have invested several decades of effort to provide the compound more economically, which culminated in four total syntheses and numerous approaches toward its carbon skeleton.^[65,67] Interestingly, the most recent approach, disclosed by Baran and co-workers and supported by LEO Pharma, has the potential to become one of the few total syntheses that are applied for the industrial production of a therapeutic compound. In their ingenious 14-step synthesis (scheme 1.16), they demonstrate the construction of all-carbon precursor **129** in only six transformations starting from the readily available monoterpene (+)-carene (**130**). Prominent features are a one-pot methylation/aldol addition protocol and a rhodium-catalyzed allenic Pauson-Khand reaction.^[68] Continuing in the sequence, a most intriguing and possibly biomimetic^[65,69] vinylogous pinacol rearrangement is applied to convert the phorbol-type carbon skeleton (**131**) into the strained ingenol system (**132**). The announced further development to an industrial process would prove the viability of economic large-scale total syntheses of complex organic molecules.

Terpenoids in general have attracted synthetic chemists ever since the dawn of modern organic chemistry. A major stimulus has come from the quest for the discovery of novel bioactivity and the potential development and large-scale production of therapeutic compounds. Additionally, the sheer challenge of constructing the complex molecular frameworks devised by nature has often been an inherent motivation. Since Komppa established the first process for the industrial preparation of camphor (**41**) in the early 1900's,^[70] a plethora of synthetic methodologies was devised and substantial mechanistic insights in organic transformations were gained in the course of terpenoid total syntheses. Prominent examples for elucidated novel modes of reactivity are, for instance, the Wagner-Meerwein rearrangement,^[71] or biomimetic epoxide opening^[72] and cationic cyclization cascades.^[73] Further important contributions to the evolution of synthesis stem from the long-lasting extensive explorations in steroid chemistry, which involved Woodward's pioneering use of Diels-Alder reactions.^[74] Organocatalysis and its important applications in modern asymmetric synthesis can also be traced back to the seminal work published on the construction of the Wieland-Miescher ketone^[75] (not shown) and the Eder-Sauer-Wiechert-Hajos-Parrish ketone (**138**, *cf.* chapter 2.3).^[76] Furthermore, essential principles in chemistry such as retrosynthetic^[77] and conformational analysis^[78] were originally developed and adopted for terpenoid synthesis. Last but not least, total synthesis of natural products still remains an indispensable technique for structural elucidation, although the advent of modern

analytical methods such as two-dimensional NMR spectroscopy and X-ray crystallography provides relief in many cases.^[1a] In particular, the absolute stereochemical configuration of complex polycyclic skeletons can often only be established by means of preparative synthetic methods, which is exemplified by the *nor*-terpenoid micrandilactone A (**79**, scheme 1.17).^[22] Selected examples of renowned, recently disclosed terpenoid syntheses comprise the intricate molecules resiniferatoxin (**139**, Wender, 1997),^[79] phomactin A (**140**, 2002, Pattenden),^[80] maoecrystal V (**141**, 2011, Reisman)^[81] and taiwaniadduct B (**142**, 2014, Li).^[82]

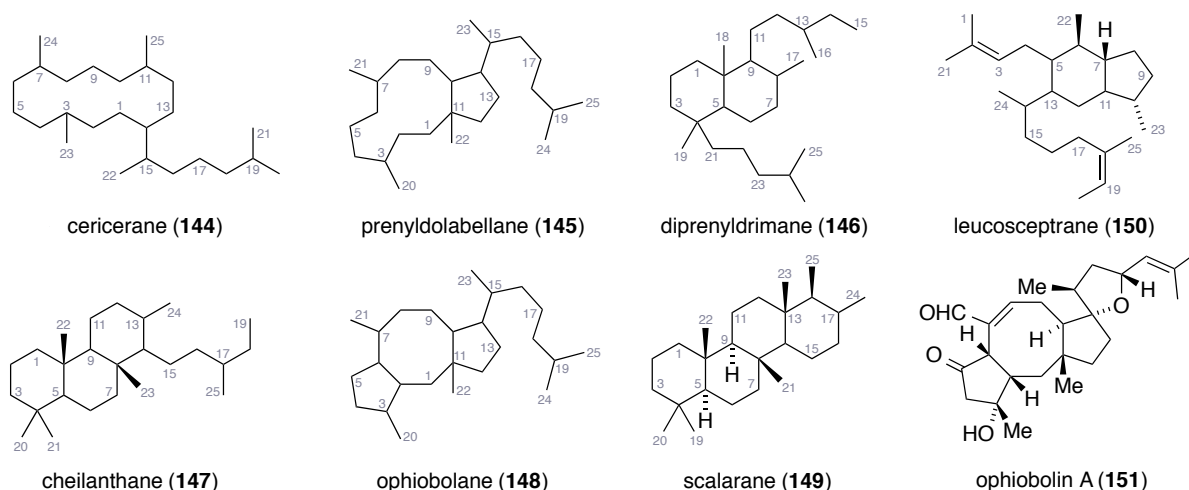


Scheme 1.17: Complex polycyclic terpenoids, of which compounds **139** to **142** were recently accessed by means of total synthesis.

1.3 Sesterterpenoids: Chemical Synthesis, Subtypes and Background

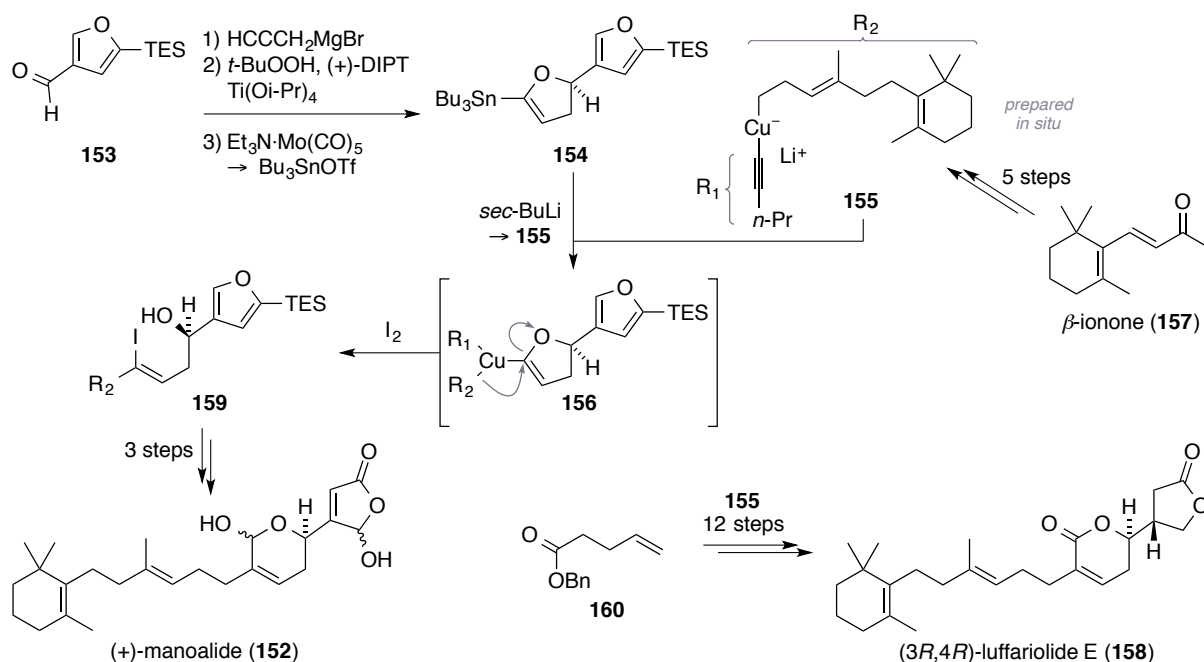
In this chapter, the subclass of sesterterpenoids will be introduced in detail, for one target of this doctoral thesis is the development of the first total syntheses of a certain type of biosynthetically closely related congeners (*cf.* chapter 1.5). At first, the most prominent parent architectures will be categorized and short biological profiles will be provided.

The sesterterpenoids represent, with about 1000 currently characterized compounds, a relatively small subgroup of terpenoid natural products. This is surprising with regard to their comparatively large size, structural complexity and molecular diversity.^[83] Scientists have recovered them from widespread biological sources comprising distinct organisms like terrestrial fungi, lichens, higher plants, insects and various marine species,^[84] particularly sponges.^[85] They contain two and a half (*lat. sester*) ‘terpene units’, which is related to a historic nomenclature and based on the outdated assumption that terpenoids are assembled



Scheme 1.18: Common carbon frameworks found in sesterterpenoid natural products and ophiobolin A (**151**).

from pieces made of ten carbons.^[2b] Accordingly, sesterterpenoids are constituted of C_{25} (or slightly fewer) architectures and essentially originate from their previously discussed biogenesis (*cf.* chapter 1.1) that branches off at the shared precursor geranylarnesyl pyrophosphate (**143**, *cf.* scheme 2.3). In this context, terpene cyclase-mediated cationic cascade reactions, enzymatic oxygenations and partial skeletal degradations provide a multitude of intricate polycyclic frameworks. These pose highly attractive targets for total synthesis and allow for the validation of new chemical methodology at complex molecular settings.^[83] Over the course of the last decades, an increasing number of review articles has been dedicated to this family of compounds, which is partially attributed to intensified studies on their biological properties.^[86] Commonly, sesterterpenoids are classified with respect to their basic carbon skeletons that include linear, mono-, di-, tri-, tetra- and even pentacarbocyclic congeners. Furthermore, six major subtypes of ring systems have been observed to occur more frequently in nature (scheme 1.18), namely the cericeranes (**144**), prenyldolabellanes (**145**), diprenyldrimanes (**146**), cheilanthanes (**147**), ophiobolanes (**148**) and scalaranes (**149**).^[2b] A very recent addition to this list is denoted by the leucosceptroids (**150**), of which already 23 family members have been isolated to date.^[87] The first characterization of a natural occurring sesterterpenoid was reported in 1958 by Nakamura.^[88] The compound was named ophiobolin A (**151**), according to its host organism *Ophiobolus miyabeanus*, and was early on described as an antibiotic. After the elucidation of its molecular structure *via* X-ray crystallographic analysis,^[89] more than 20 related compounds were found that share the central fused 5-8-5-membered ring system. They have been evidenced as potent agents against certain strains of bacteria and fungi, as well as anticancer cycotoxins.^[90] The largest



Scheme 1.19: Kocienski's asymmetric syntheses of (+)-manoalide (**152**) and (3R,4R)-luffariolide E (**158**).

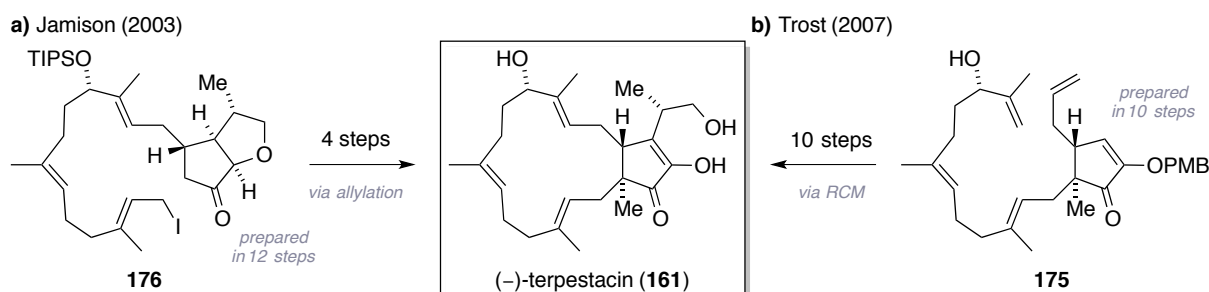
family of sesterterpenoids are the cheilanthanes, with over 50 currently known members. Several total synthesis have been published on this subtype in the past, of which the majority focused on semisynthetic approaches and have been reviewed elsewhere.^[86g] The total number of syntheses of – or synthetic studies toward – sesterterpenoid natural products still remains in the two-digit regime. A comprehensive summary dedicated to this topic has been published by Hog *et al.* in 2012 and served as model for the following second part of this chapter.^[83] Progressing from mono- to pentacarboxylic architectures, a selection of distinguished strategies toward some of the most prominent congeners of this substance class will be presented.ⁱⁱⁱ In addition, the advances published in this field over the last two years will be added. To this end, the focus will lie on transformations dealing with the construction of the central carbon ring systems and showcase the key intermediates utilized therein.

The discussion starts with the relatively simple monocarbocyclic sesterterpenoid (+)-manoalide (**152**) that was isolated in 1980 by Silva and Scheuer from *Luffariella variabilis*, a marine sponge.^[91] Although it bears only one stereocenter, seven racemic and two enantioselective total syntheses have already been reported by the groups of Katsamura,^[92] Garst,^[93] Sandano,^[94] Hoffmann,^[95] and Kocienski.^[96] This can be attributed to the significant pro-inflammatory properties of this natural product, which are due to a potent irreversible inhibition of phospholipase A2.^[97] The latest asymmetric approach that was disclosed by Kocienski and co-workers in 2003 starts from furyl aldehyde **153** and sets the

ⁱⁱⁱThe entirety of known total syntheses of *iso*-propyl *trans*-hydrindane sesterterpenoids will be discussed in chapter 1.4.2.

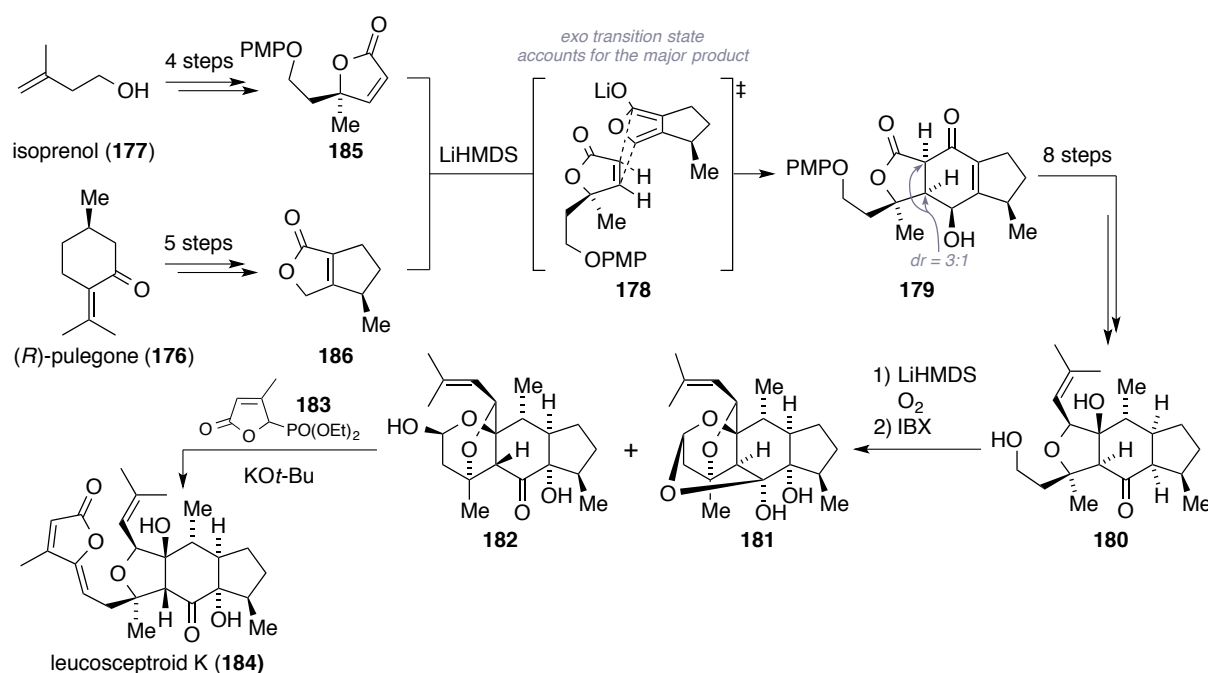
characterized early on as a promising candidate for the treatment of HIV, as it inhibits the formation of syncytia, *i.e.* multinuclear cell bodies that are an indirect but major cause of infection-induced death of T4 cells.^[100] The intriguing molecular structure, which comprises four stereogenic centers and a fused 15-membered ring system with three internal trisubstituted olefins, renders this natural product an archetype for the strategic application of modern synthetic carbon–carbon bond forming methodologies. Hence, it is not surprising that seven total syntheses have been devised to date, four of which are enantioselective. Four of those successful strategies involved macrocyclization *via* means of a Horner-Wadsworth-Emmons (HWE) reaction and were reported by the groups of Tatsuta (1998),^[101] Tius (2007)^[102] and Qui (2012).^[103] Tius' exemplary work allows access to the racemic natural product in only 15 consecutive reactions in a highly convergent manner and excellent 6.4% overall yield (scheme 1.20a). Starting from γ -butyrolactone (**162**), the authors set the initial stereocenter *via* allenyl ether Nazarov cyclization^[104] (**163**). Next, they used the stereochemical bias of the resulting cyclopentene system (**164**) to direct an alkylation with allylic bromide **165**. Ensuing deprotection, oxidation and HWE olefination under modified Masamune-Roush conditions^[105] gave rise to the bicyclic core structure (**166**). A final 6-step sequence was required to arrive at (\pm)-terpestacin (**161**).

Myers' enantioselective synthesis from 2002^[106] introduces chirality *via* ψ -ephedrine derived building block **167** that can be accessed using the method for asymmetric, auxiliary-assisted alkylation reactions developed in the same group (scheme 1.20b).^[107] To begin, a 4-step protocol sets the stage for the key fragment combination of lactone **168** with allylic bromide **169**, which proceeded *via* substrate-controlled enolate alkylation and forms substance **170**. Later in the synthesis, the authors describe another intramolecular enolate allylation to construct the desired fused 12-membered carbocycle (**171**) diastereoselectively. The natural product was then obtained after seven further transformations.



Scheme 1.21: Key intermediates **176** and **175** in a) Jamison's and b) Trost's syntheses of terpestacin (**161**).

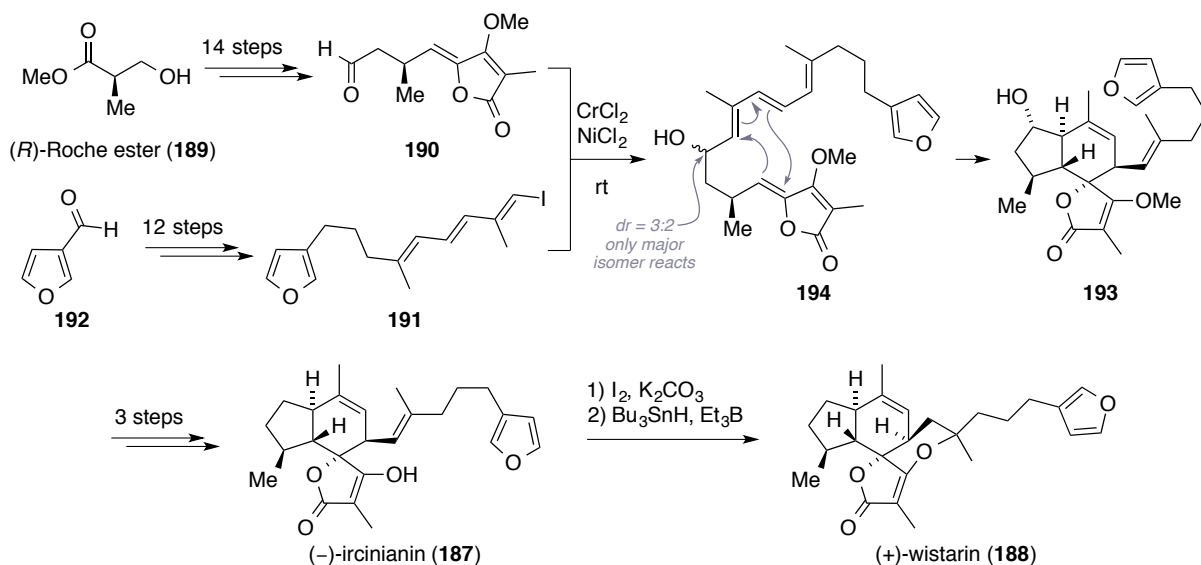
Two more enantioselective syntheses of (–)-terpestacin (**161**) have been disclosed by Jamison (2003)^[108] and by Trost (2007),^[109] respectively. The first of these resorted again to an intramolecular allylation protocol that bears similarities to Myers' approach (scheme 1.21a). In contrast, the second case describes the use of a RCM reaction to achieve the key ring closure (scheme 1.21b), which is facilitated by the allylic alcohol function (*cf.* chapter 3.5) in pentaene precursor **175**.



Scheme 1.22: Magauer's synthesis of (+)-norleucosceptroid A (**180**), (–)-norleucosceptroid B (**181**) and leucosceptroid K (**184**).

A novel synthetic challenge is presented by the relatively young class of leucosceptroid sesterterpenoids, of which the first member was isolated from *Leucosceptrum canum* only 10 years ago.^[110] Attracted by the plant's high resistance to herbivores and pathogens, it was soon established that this natural product class in general displays potent antifeedant activity. Consequently, these compounds have been considered as an alternative to conventional synthetic pesticides.^[87,111] Structurally, all members share a highly functionalized 5,6,5-membered polycyclic framework that differs in the oxidation state at C-11 and the substitution of the C-14 ethyl linkage (*cf.* scheme 1.18). Following the pioneering work of Horne and co-workers,^[112] who reported a first approach to the core of the leucosceptroids, the group of Liu published the first total synthesis of leucosceptroid B (not shown) in 2013.^[113] Very recently, Magauer and co-worker reported a general entry to this substance class, which allowed them to complete three of its congeners whilst constructing the basic bicarbocyclic core in only 5 steps (scheme 1.22).^[87] Starting from the two small terpenoids (*R*)-pulegone (**176**) and isoprenol (**177**), they prepared the precursors for the key

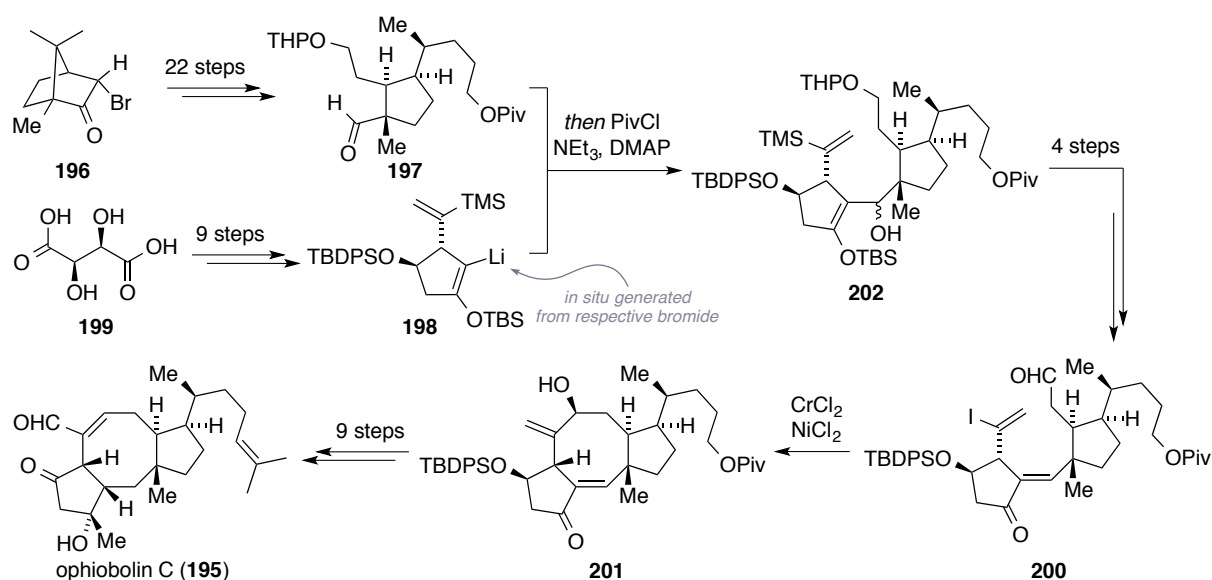
Hauser-Kraus-type annulation^[114] (**178**) that in turn furnished tricycle **179** in a 3:1 mixture of diastereomers on multi-gram scale. Although they encountered an unexpected retro-Claisen condensation *en route*, they were able to circumvent this reactivity and accessed building block **180** in eight further steps. When this material was submitted to regioselective hydroxylation and subsequent IBX-mediated intramolecular acetal formation, (+)-norleucosceptroid A (**181**) and (–)-norleucosceptroid B (**182**) were isolated as the major and minor products, respectively. A final HWE-type olefination with phosphonate **183** gave rise to leucosceptroid K (**184**) in 18 steps longest linear sequence.



Scheme 1.23: Uenishi's biomimetic synthesis of (–)-ircinianin (**187**) and (+)-wistarin (**188**).

Two complex bicyclic furanosesterterpenoids, namely (–)-ircinianin (**187**)^[115] and (+)-wistarin (**188**)^[116] were isolated from marine sponges of the genus *Ircinia* in 1977 and 1982, respectively. Inspired by the published biosynthetic proposal, Yoshii and Takeda achieved the first racemic synthesis of ircinianin (**187**) in 1986.^[117] Several years later, Uenishi and co-workers refined this strategy and devised a successful enantioselective route to both related natural products **187** and **188** (scheme 1.23).^[118] Their approach hinged on a key fragment coupling by means of a Nozaki-Hiyama-Kishi reaction^[119] between (R)-Roche ester (**189**) derived aldehyde **190** and alkenyl iodide **191**, which was accessed in 12 steps from 3-furyl aldehyde (**192**). Interestingly, only the main diastereomer that was produced in this reaction immediately underwent the biomimetic intramolecular Diels-Alder cyclization to yield *trans*-hydrindane system **193**. However, the authors showed that Lewis acid catalysis by the present CrCl_2 was crucial for this reaction to proceed at room temperature. Three further transformations led to (–)-ircinianin (**187**), which in turn was converted to (+)-wistarin (**188**)

via a two-step iodolactonization/radical dehalogenation protocol. Notably, the compound was the first example of a sesterterpenoid that occurs naturally in both enantiomeric forms.^[120] Regarding the family of tricycyclic sesterterpenoids, the previously mentioned ophiobolins have been the target of a considerable amount of synthetic studies since their initial discovery 56 years ago (*vide infra*).^[83] From a structural point of view, the artificial construction of their highly functionalized fused 5-8-5-carbocyclic framework poses an intricate challenge even to modern chemistry. Especially the closure of 8-membered ring systems still requires careful retrosynthetic planning and was of high significance for the reported studies on ophiobolin natural products,^[121] as well as for the experimental work of the present doctoral thesis. To this end, the only two completed total syntheses of (+)-ophiobolin C (**195**, 1989, Kishi)^[61] and (+)-ophiobolin A (**151**, 2011, Nakada)^[122,123] shall showcase late-stage cyclization strategies.

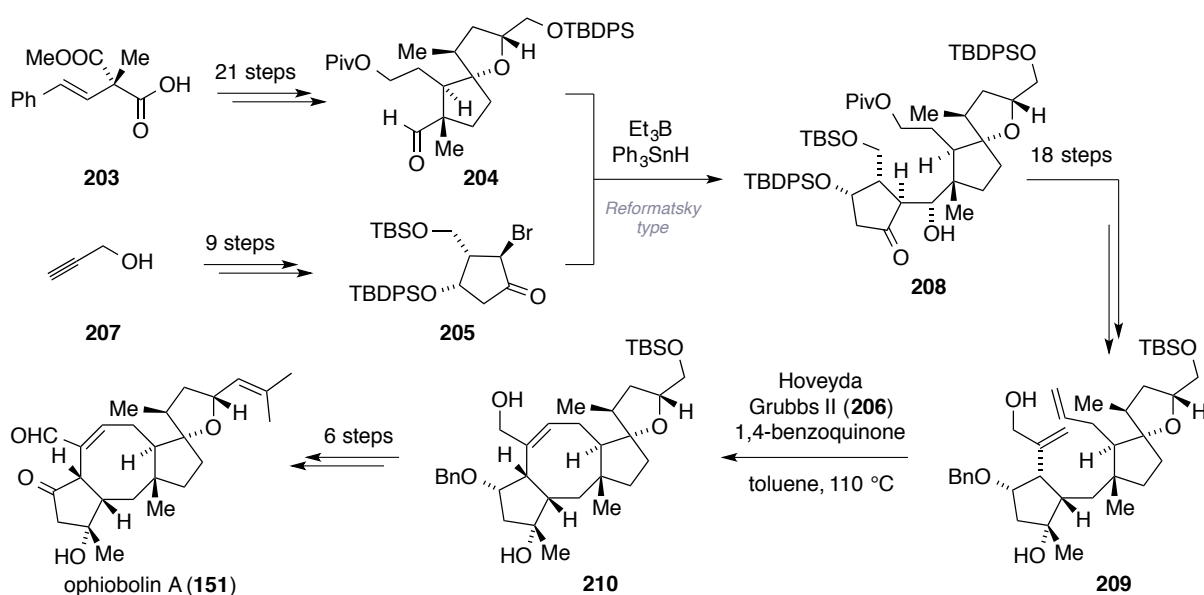


Scheme 1.24: Kishi's enantioselective synthesis of (+)-ophiobolin C (**195**), using an intramolecular Nozaki-Hiyama-Kishi reaction to construct the central cyclooctene ring system.

At the beginning of Kishi's successful enantioselective route, 3-*endo*-bromocamphor (**196**) was transformed over a series of 22 steps into aldehyde **197** (scheme 1.24). This compound was then coupled to *in situ* generated vinyl lithium reagent **198**, which was in turn prepared from (-)-tartaric acid (**199**) in 9 steps. Iododesilylation, selective deprotection of the THP ether function and Swern oxidation finally provided aldehyde **200**. This substance was the envisaged intermediate for the subsequent ring closure, which relied on an intra-molecular Nozaki-Hiyama-Kishi reaction.^[119] The product (**201**) of this key reaction was obtained as a single isomer with its relative stereochemistry assigned according to model studies.^[124] Final

adjustment of the substitution pattern required another 9 transformations to complete (+)-ophiobolin C (**195**).

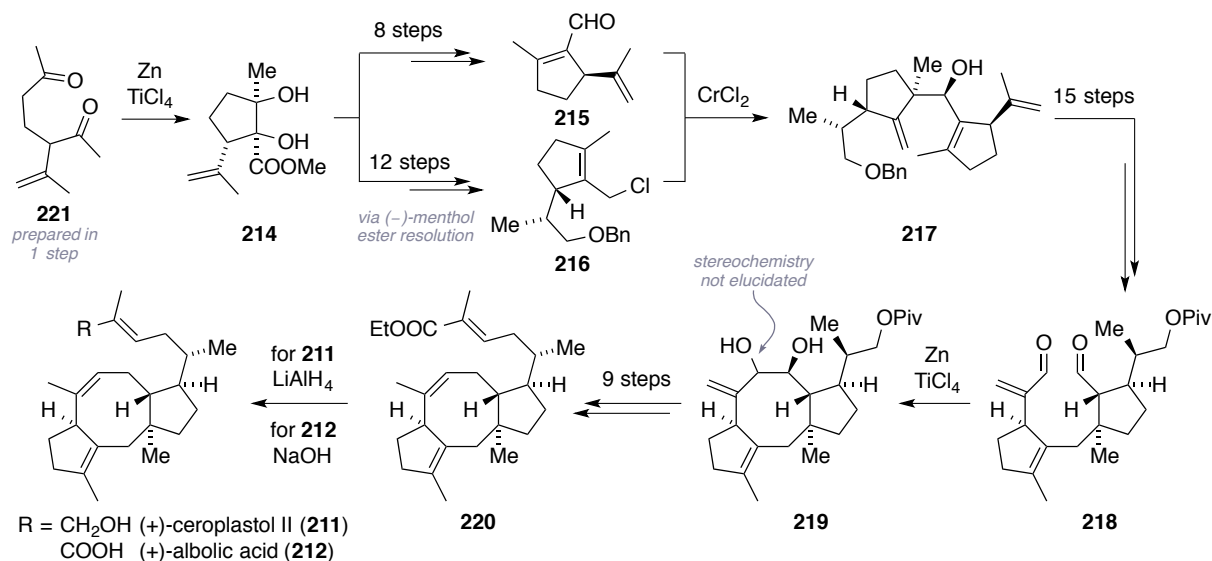
The more recent synthesis of (+)-ophiobolin A (**151**), which was published by Nakada and co-workers, made elegant use of the considerable advancement of modern Ru-catalyzed olefin metathesis chemistry (scheme 1.25).^[125] However, the preparation of a suitable diene precursor had to comply with the overall complexity of the molecule and required 40 steps from acid **203** that in turn was accessed by an enzymatic desymmetrization protocol. Notably, a highly diastereoselective Reformatsky-type reaction^[126] between aldehyde **204** and bromide **205** was applied in order to install the western cyclopentane moiety in a more convergent manner. The following sequence was mainly shaped by protecting group manipulations, as the RCM reaction turned out to be highly sensitive toward steric congestion at the reaction sites. The actual RCM reaction was conducted with Hoveyda-Grubbs II catalyst (**206**, cf. scheme 3.19) under the addition of 1,4-benzoquinone (not shown), which was required to prevent undesired double bond isomerization. As demonstrated in Trost's terpestacin (**161**) synthesis, an allylic alcohol was used to facilitate the key step (*vide infra*). An ensuing 6-step sequence furnished the natural product in an overall remarkable synthetic effort.



Scheme 1.25: Nakada's enantioselective strategy toward (+)-ophiobolin A (**151**), closing the 8-membered ring via a highly optimized RCM reaction.

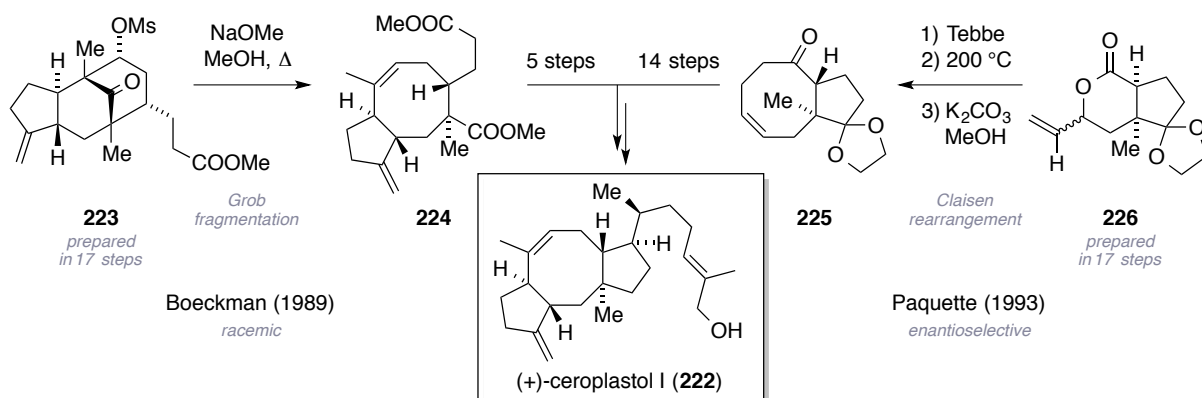
A related subclass of natural products are the ceroplastins, which were discovered only shortly after the ophiobolins in 1965 and are composed of the same, though somewhat less functionalized, ophiobolane-type carbon skeletons.^[127] The central challenge in their construction is again the octanoid ring system that is embedded in a 5-8-5-tricarbocyclic backbone. In 1988, Kato and co-workers described the first asymmetric total syntheses of

(+)-ceroplastol II (**211**) and albolic acid (**212**),^[128] both isolated previously from the wax secretion of the scale insect *Ceroplastes albolineatus*.^[129] Their approach resorted to a Ti(II)-mediated reductive carbonyl-carbonyl coupling strategy (scheme 1.26) and served as an important example of the feasibility of the later described first-generation retrosynthetic analysis of astellatol (**213**, *cf.* chapter 4.2). Despite its overall length, with 42 synthetic steps, Kato's synthesis features interesting transformations such as the initial diol formation toward substance **214** that once more employs *in situ* generated TiCl_2 reagent.^[130] In the following, an optical resolution of the corresponding (–)-menthyl esters (not shown) was conducted and both enantiomers were processed to building blocks **215** and **216** in 8 and 14 steps, respectively. A CrCl_2 -promoted reductive coupling of both compounds gave rise to intermediate **217**, which was converted to bisaldehyde **218** in 15 further steps. Interestingly the key ring closure to tricycle **219** was not accompanied by any vinylogous side reactions (*cf.* chapter 4.4) and provided a remarkable 96% yield. In nine final transformations, ester **220** was accessed and either reduced to (+)-ceroplastol II (**211**) or saponified to albolic acid (**212**).



Scheme 1.26: Kato's enantioselective route toward (+)-ceroplastol II (**211**) and (+)-albolic acid (**212**), featuring an intramolecular reductive diol formation to construct the 8-membered carbocycle.

In close progression, Boeckman (1989, racemic)^[131] and Paquette (1993, enantioselective)^[132] published their syntheses of (+)-ceroplastol I (**222**), which opted for ring opening and ring expansion strategies, respectively, to elaborate the cyclooctane framework. Scheme 1.27 illustrates the key intermediates that were involved in both strategies. Boeckman and co-workers used a base-induced Grob fragmentation^[133] to convert tricycle **223** to cyclooctene **224**. In contrast, Paquette and co-workers devised a sequential Tebbe olefination^[134] and Claisen rearrangement^[135] protocol to construct cyclooctenone **225**. In summary, both

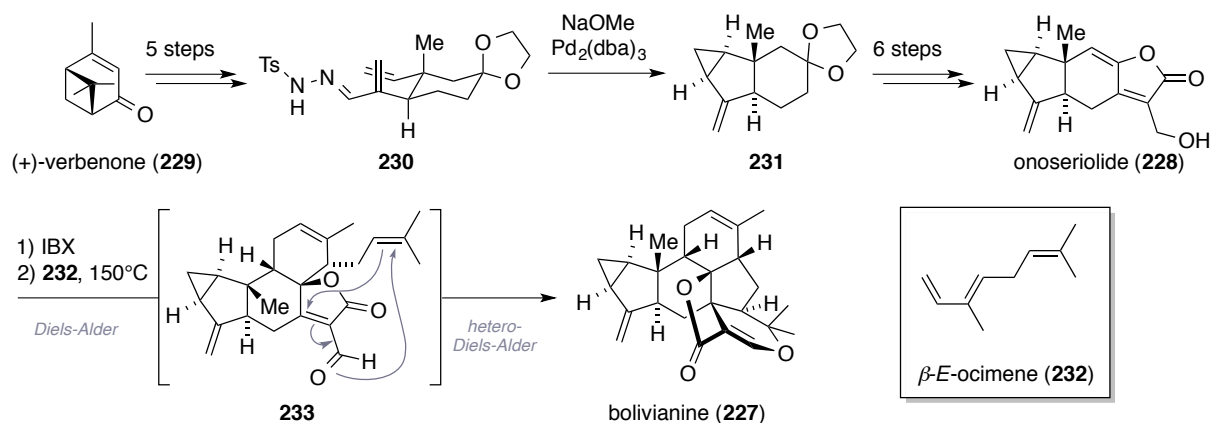


Scheme 1.27: Total syntheses of ceroplastol I (**222**) published by the groups of Boeckman and Paquette.

approaches are of similar length and reach completion of the natural product after 23 and 27 steps, respectively.

For tetracarboxyclic sesterterpenoids, largely semisyntheses of scalarane-type natural products^[136] and one successful approach toward cerorubenic acid III (not shown)^[137] are known. Instead, Liu's very recently published first total synthesis of the structurally complex pentacarboxylic molecule bolivianine (**227**),^[138] which was isolated in 2007 from *Hedyosmum angustifolium*,^[139] will be presented as a closing example for this chapter. Although no biological properties of the compound are known to date, an interesting biosynthetic proposal was put forward. It was hypothesized that the known sesquiterpenoid onoseriolide (**228**) might undergo condensation with an equivalent of geranyl pyrophosphate (**34**) and – after further processing – react in an intramolecular hetero-Diels-Alder cyclization to yield bolivianine (**227**).^[138] In their enantioselective synthesis, Liu and co-workers started from the naturally abundant monoterpene (+)-verbenone (**229**) and accessed hydrazone **230** in an initial 5-step sequence (scheme 1.28). From this substance, the western 3- and 5-membered rings in *trans*-hydrindane system **231** were constructed *via* palladium-catalyzed cyclopropanation. After another six transformations they obtained onoseriolide (**228**). This material was oxidized with IBX and the resulting aldehyde was submitted to a sealed tube thermal Diels-Alder/hetero-Diels-Alder cascade reaction using the monoterpene β -(*E*)-ocimene (**232**) as the initial diene. In total, only 14 steps were needed to construct the natural product's highly convoluted heptacyclic framework and to provide experimental proof of the proposed modified biogenetic pathway.

The synthetic strategies outlined in this chapter exemplify that – like ever so often in terpenoid chemistry – the artificial construction of sesterterpenoids is greatly shaped by the challenges that lie in the formation of fused- and macrocyclic ring systems, as well as in the



Scheme 1.28: Liu's biomimetic synthesis of bolivianine (227), featuring a Diels-Alder/hetero-Diels-Alder cascade.

construction of their concomitant non-heteroatom-substituted stereogenic centers. The presented natural product syntheses have spurred the development of a variety of chemical methodologies, like the different protocols that were devised to construct the 8-membered ring system of the ophiobolane framework (*vide infra*). Besides supplying material for biological studies, also these indirect proof of proposed biosynthetic pathways could be given. The next chapter will focus more on the last members of the sesterterpenoid family that have not yet been discussed, namely the *iso*-propyl-substituted *trans*-hydrindane sesterterpenoids.

1.4 *iso*-Propyl-Substituted *trans*-Hydrindane Sesterterpenoids

1.4.1 Comprehensive Overview of the Subclass

Amongst the sesterterpenoid natural products isolated so far,^[84–86] 20 compounds have been documented to share a common structural feature, namely a *trans*-fused hydrindane system, which is additionally substituted by an angular methyl group at the ring junction and an *iso*-propyl-type function at the C-3 position.^{iv} In almost all cases, the remaining carbon atoms of the biosynthetic precursor geranylarnesyl pyrophosphate (**143**, *cf.* chapter 1.1) are incorporated in intricate fused ring systems and no chain-like substructures are formed. A further plausible classification, according to the connectivity of mentioned *trans*-hydrindane moiety to the respective other carbocycles, was suggested by Hog^[140] and was adopted for the discussions presented in this doctoral thesis (scheme 1.29). Correspondingly, congeners of this sesterterpenoid subclass are distinguished as type A (**234**) and type B (**235**), where ring fusion occurs either at the C-5 to C-6 edge or the neighboring C-4 to C-5 edge of the

^{iv}The nomenclature for hydrindane-type carbocyclic systems was adopted from the IUPAC.^[4]

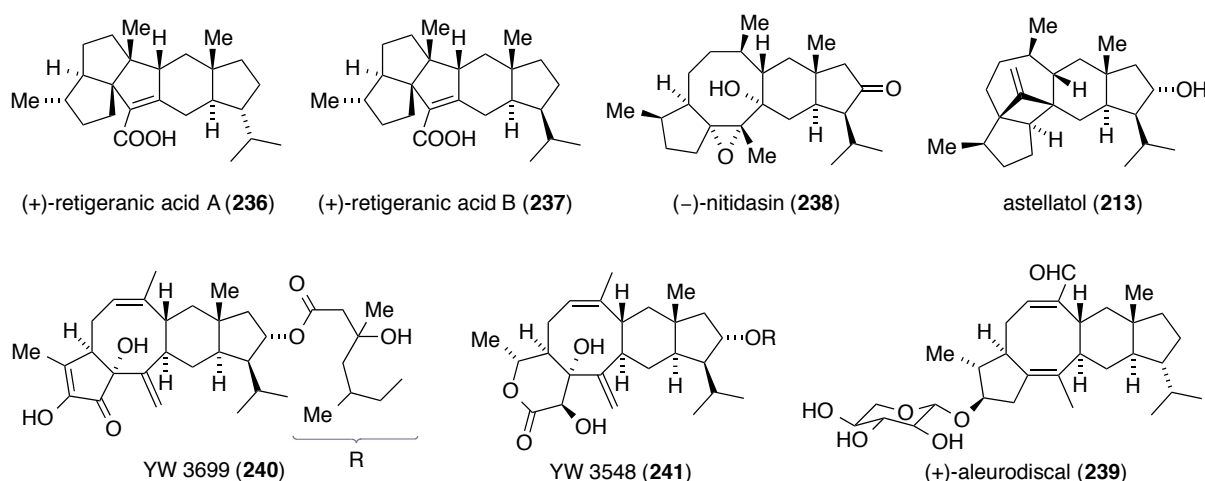
hydrindane hexacycle, respectively. Interestingly, both epimers of the C-3 stereocenter have been described for molecules of type A, whilst only the *trans*-orientation of the angular methyl group and the *iso*-propyl substituent is known for type B. Amongst the latter family, a concomitant unsaturation to an *iso*-propenyl functionality is encountered frequently. For the sake of a simplified structural comparison, some compounds were drawn as their unnatural enantiomers in the following section.^v



Scheme 1.29: Classification of known *iso*-propyl-substituted *trans*-hydrindane sesterterpenoids into type A (**234**) and type B (**235**), according to Hog.

In 1965, the first *iso*-propyl-substituted *trans*-hydrindane sesterterpenoid was isolated from a Himalayan lichen species and named retigeranic acid A (**236**, scheme 1.30).^[141–143] Besides the in detail discussed hydrindane motif, ongoing investigations revealed an at that time unprecedented angular triquinane portion.^[144–146] Further details on its structural elucidation, proposed biosynthesis, and the discovery of its C-3 epimer retigeranic acid B (**237**) are provided in chapter 2.1, where experimental results of our synthetic studies toward these natural products will be presented. Notably, retigeranic acid A (**236**) was the only member of this family that had been successfully addressed by total synthesis prior to 2014. Attracted by its daunting structure, the groups of Corey,^[147,148] Paquette,^[149,150] Hudlicky^[151,152] and Wender^[153] published their synthetic studies in the late 1980's, which have since then become classics in terpenoid synthesis and are detailed in the next chapter. Two related type A natural products are nitidasin (**238**)^[154] and astellatol (**213**),^[155] found in *Gentiana nitida* and *Aspergillus variegator*, respectively. For both compounds, a very similar cationic cascade is part of their biogenesis and was of central importance for the retrosynthetic approaches developed over the course of this doctoral thesis (*cf.* chapters 3 and 4). At this point, the completed synthesis of nitidasin (**238**)^[156] and previous synthetic investigations towards the construction of astellatol (**213**) that were conducted in our group shall be referenced.^[157] Historically, the tetracyclic sesterterpenoid aleurodiscal (**239**) was the first known congener of the discussed family that possesses the characteristic 5-8-6-5-membered ring

^vIf no sign of the optical rotation is provided (dexrotatory or levrotatory), the absolute configuration of the natural product has not been assigned yet, to the best of our knowledge.

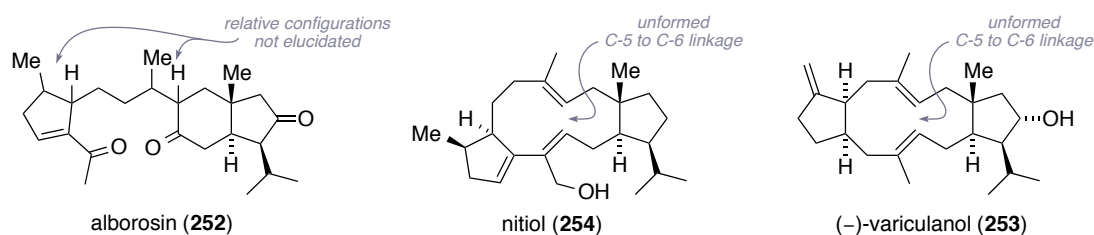


Scheme 1.30: Molecular structures of all seven known type A *iso*-propyl-substituted *trans*-hydrindane sesterterpenoids. Compounds **236**, **237** and **239** were drawn as their unnatural enantiomers.

system of nitidasin (**238**) and was isolated in 1989 from the fungus *Aleurodiscus mirabilis*.^[157] Concomitant with the isolation, its structure was verified *via* X-ray crystallography and the absolute configuration was elucidated by means of hydrolytic cleavage of the glycoside linkage to D-(+)-xylose (not shown). Although the natural product showed promising antifungal activity by inhibiting the incorporation of *N*-acetyl-D-glucosamine (not shown) into chitin and chitosan, no further studies on its bioactivity have been published so far. Aleurodiscal (**239**) and retigeranic acid A (**236**) are unique amongst the type A subclass, as they feature a *trans*-relationship between the *iso*-propyl residue and the angular methyl group at the hydrindane system. From a synthetic point of view, the double unsaturation of the central cyclooctadiene framework in aleurodiscal (**239**) poses a considerable challenge in terms of chemoselectivity and could not yet be found in any other natural occurring substances. One last type A sesterterpenoid that comprises the 5-8-6-5 carbocyclic backbone has been isolated by Wang *et. al* from the fungal strain *Codinaea simplex* in 1998 and was entitled YW 3699 (**240**).^[158] The molecular structure and relative configuration of its stereocenters was elucidated by means of 2D NMR spectroscopical investigations. Although the relative stereochemistry of the heptanoate side chain could not be assigned, several studies on the bioactivity of this compound have been described so far. Therein, it was disclosed that both YW 3699 and the related lactone YW 3548 (**241**)^[159] exhibit potent and selective inhibition of the GPI-anchoring biosynthesis in mammalian cells.^[160] In combination with their extended SAR studies, Wang and co-workers proposed that the YW compounds exert their toxicity by preventing the incorporation of [³H]*myo*-inositol (not shown) into proteins, which in turn frustrates the transport of GPI-anchored proteins to the Golgi apparatus.^[159,160]



surely represents a daunting target for synthetic chemists, which is emphasized by the natural product's potent inhibitory properties against *Mycobacterium tuberculosis* protein tyrosine phosphatase B.^[167] This enzyme is secreted by the parent microbe and manipulates the host's signal transduction in order to facilitate the infection process. Thus, inhibitors like asperterpenoid A (**251**) are currently considered to be promising targets for curing pulmonary tuberculosis.^[168]



Scheme 1.32: Molecular structures of the three non-canonical *iso*-propyl *trans*-hydrindane type sesterterpenoids alborosin (**252**), nitinol (**254**) and variculanol (**253**). The carbon atom numbering refers to the nomenclature given in scheme 1.29.

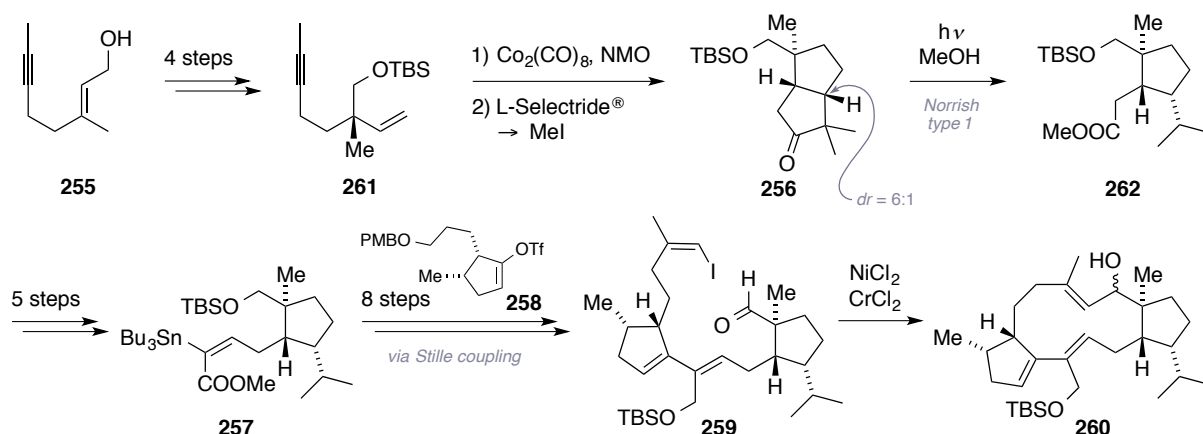
Besides the shown canonical type A and type B *iso*-propyl *trans*-hydrindane sesterterpenoids, three further natural occurring molecules shall be included in the parent classification. The first of those is the tricycyclic triketone alborosin (**252**), which was named according to its biological source *Gentaniella alborosea* by Kawahara and co-workers in 2000 (scheme 1.4.4).^[169] Comparison to nitidasin (**238**, *vide supra*) suggests that this substance is biosynthetically formed *via* oxidative carbon–carbon bond cleavage of a 1,2-diol function, that would be generated previously upon E1cB-type eliminative epoxide opening. Although the original investigators could not establish four of the stereocenters contained in this degradation product, it is reasonable to assume that they match the configurations encountered in nitidasin (**238**). In chapter 3.7, our experimental efforts to achieve this diol cleavage with chemical tools will be discussed briefly. In contrast, variculanol (**253**)^[170] and nitinol (**254**)^[171] possess a central 10-membered ring system, which is fused to two pentacyclic moieties. Their isolation sources were the already mentioned organisms *Aspergillus varicolor* and *Gentaniella nitida*, which indicates a possible biosynthetic relationship to the variecolins and nitidasin (**238**), respectively. Indeed, when drawing their structures in an appropriate fashion, it becomes apparent that the C-5 to C-6 linkage of the imaginary hydrindane system is missing. This finding might be explained either by a differing cyclization mode upon biogenesis from geranylfarnesyl pyrophosphate (**143**), or *via* a late-stage enzymatic ring opening, similar to the alborosin (**252**) case. However, the observed oxygenation pattern rather supports the first proposal. Whilst no data on the bioactivity of variculanol (**253**) has been published so far, the biological properties of nitinol (**254**) will be

detailed in chapter 3.1 in the course of the introduction of nitidasin (**238**). Although their hydrindane portions remain unfinished, both substance **253** and **254** were adopted into the discussed family of compounds with regard to the presumable common biosynthetic origin and the obvious similarities in substitution patterns.

1.4.2 Literature-known Synthetic Approaches

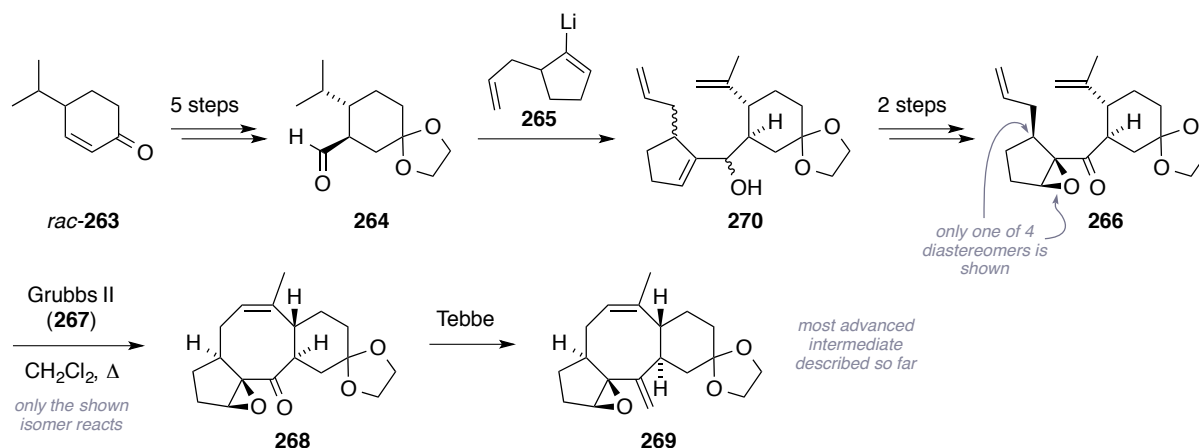
Although the *iso*-propyl-substituted *trans*-hydrindane sesterterpenoids display some of the most intriguing polycyclic frameworks found in terpenoid chemistry, only a very limited number of synthetic studies has been dedicated to those commonly potent bioactive compounds so far. The major reason for this might lie in the concomitant occurrence of highly substituted and strained *trans*-hydrindane motifs, together with the frequently observed fused cyclooctane ring systems, which were identified early on as a major challenge in the construction of ophiobolin-type natural products (*vide infra*). In the following section, an outline of the known synthetic strategies for the construction of retigeranic acid A (**236**), the variecolin family, nitiol (**254**), aleurodiscal (**239**) and YW 3699 (**240**) shall be provided. In this context, the transformations that led to the construction of the crucial ring junctions and thereby generated selectivities will take center stage, as they constitute the most direct showcases for the experimental work of this doctoral thesis.

To begin, the efforts of Dake and co-workers toward an enantioselective total synthesis of nitiol (**254**) shall be mentioned, even though this target omits the difficulty of the installment of a *trans*-hydrindane system.^[172] Their approach was published in 2001 and hinged on a convergent combination of two cyclopentane building blocks, of which the first was accessed in a 12-step sequence from geraniol derived alcohol **255** (scheme 1.33). The ring



Scheme 1.33: Dake's enantioselective synthetic approach toward the tricyclic sesterterpenoid nitiol (**254**).

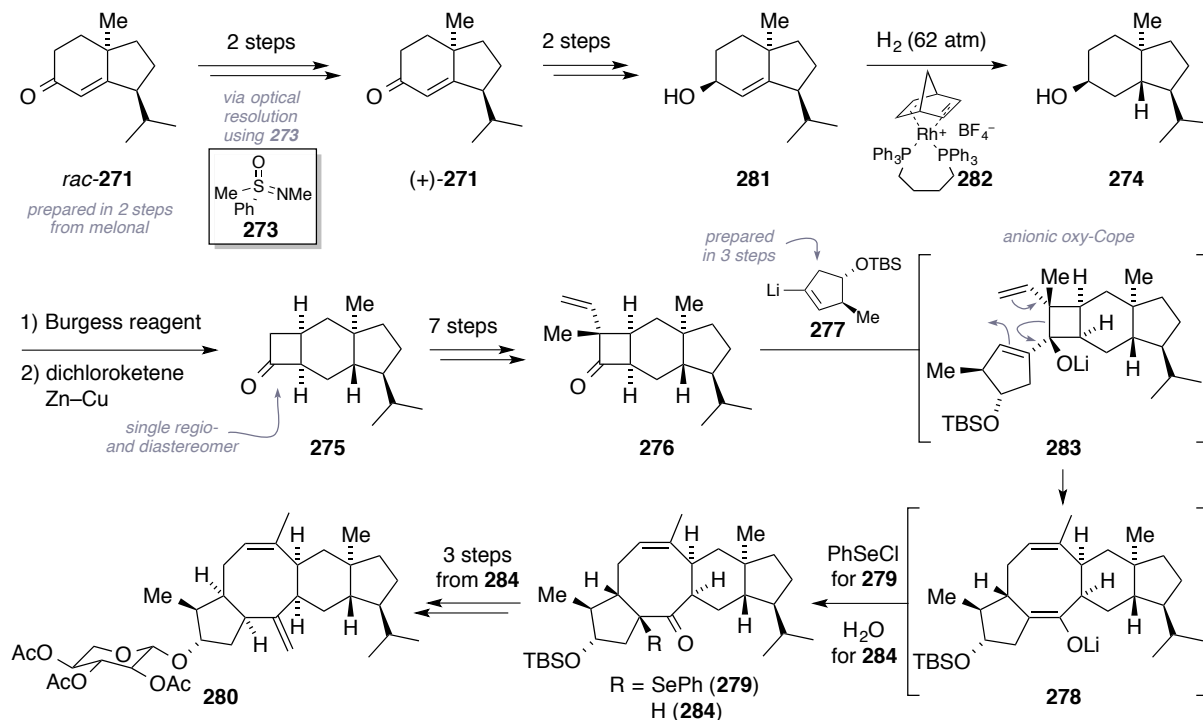
closure was achieved with a diastereoselectivity of 6:1 (**256**) by means of a Pauson-Khand reaction^[68] and subsequent vinylogous reduction with L-Selectride[®]. This was followed by the elegant use of a photoinduced Norrish-type 1 fragmentation^[173] to effect the desired substitution pattern at the western ring system of nitiol (**254**). Five further transformations then gave rise to alkenyl stannane **257**. An ensuing Pd(PPh₃)₄-catalyzed Stille cross-coupling^[174] to triflate **258** provided the first connectivity of the macrocycle, at which the second fragment was prepared in 5 steps from a readily accessible, literature-known compound. Over the course of the investigation of several macrocyclization strategies, the obtained intermediate was further processed to iodide **259** in seven steps and then successfully reacted to tricycle **260** under Nozaki-Hyama-Kishi-type conditions.^[119] However, the required final deoxygenation that would yield nitiol (**254**) remained unfeasible in their hands.



Scheme 1.34: A RCM-based strategy toward YW-3699 (**240**), published by Tori and co-workers in 2009.

Tori's synthetic studies on the natural product YW 3699 (**240**), which were published in 2009, describe the racemic construction of its 5-8-6-membered ring system and neglect the *trans*-hydrindane substructure (scheme 1.34).^[175] In the beginning of the developed sequence, *rac*-enone **263** was transformed to aldehyde **264** in five steps, using amongst others a substrate-controlled 1,4-cuprate addition. Intermediate **264** was then combined with racemic alkenyl lithium species **265** that in turn can be prepared by a Shapiro reaction^[176] from the corresponding trisylhydrazone and *t*-BuLi. After two further steps, diene **266** was obtained as a mixture of four diastereomers, with respect to the configurations of the epoxide moiety and the allyl substituent. Surprisingly, only the illustrated species (**266**) underwent RCM reaction when 30 mol-% of Grubbs II (**267**, *cf.* scheme 3.19) catalyst were employed in refluxing CH_2Cl_2 . The identity of substance **268** was verified unambiguously *via* X-ray crystallographic analysis. Although no further explanation on the observed reactivity was provided by the authors, this case points out the strong dependency on conformational preorganization that

RCM reactions toward cyclooctene systems have repeatedly demonstrated in the past.^[177] It is noteworthy to mention, that Tori and co-workers were also able to install the required *exo*-methylene function in diene **269** using Tebbe's reagent.^[134]

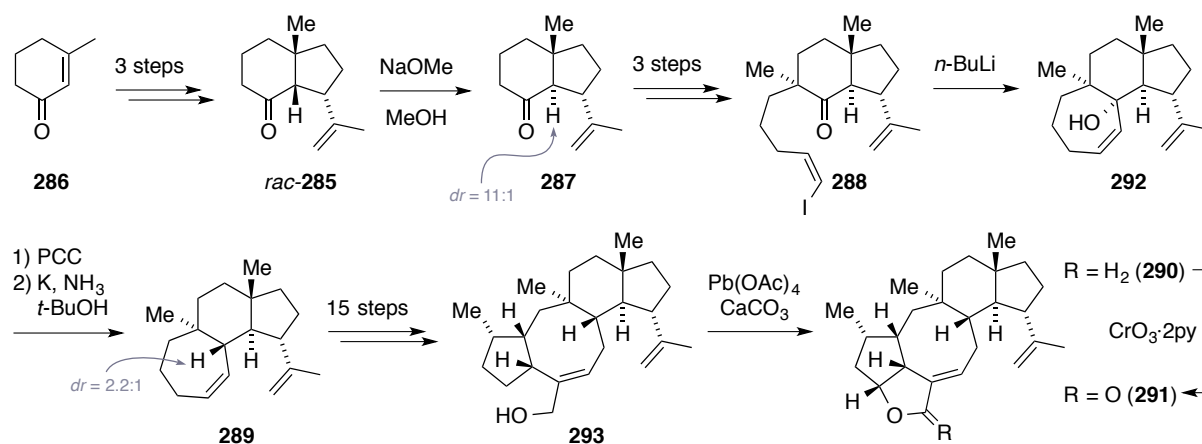


Scheme 1.35: Paquette's asymmetric approach toward aleurodiscal (**239**), using an anionic oxy-Cope rearrangement to construct the central cyclooctene ring system.

The first completion of a 5-8-6-5 carbocyclic backbone was described by Paquette and co-worker in 1998 in the course of their attempts to synthesize the β -D-xyloside sesterterpenoid aleurodiscal (**239**).^[178] Their enantioselective route started from hydrindenone **271**, which they prepared initially in a racemic fashion from commercially available melonal (**272**, *vide infra*), according to Corey^[147] and Snider.^[179,180] Using the lithium salt of Johnson's (+)-(*S*)-sulfoximine (**273**),^[181] a separation of the resulting diastereomers could be achieved and the ketone function was then regenerated *via* thermal induction of a retro-hetero-ene reaction. In order to introduce the *trans*-ring junction, they referred to a facially controlled hydrogenation protocol that was originally devised by Engler^[148] and delivered alcohol **274** as a single diastereomer. This material was then regioselectively dehydrated with Burgess reagent^[182] and subsequently reacted *via* [2+2] cycloaddition with dichloroketene in the presence of $Zn-Cu$ couple. Gratifyingly, the exclusive formation of the desired regio- and stereoisomer (**275**) was observed. Seven further transformations gave rise to tricyclic ketone **276**, which was then coupled with cyclopentenyl lithium reagent **277**, triggering an accompanying anionic oxy-Cope rearrangement.^[183] Interestingly, improved yields were obtained when the intermediary Li-enolate (**278**) was

scavenged with a selenium electrophile to furnish tetracycle **279**. However, at this stage the authors encountered severe problems when they tried to introduce the aldehyde function or at inverting the wrong set stereocenters at carbon C-5 (hydrindane numbering) and the western cyclopentane ring. The most advanced intermediate (**280**) was reached when enolate **278** was quenched by protonation and then submitted to a 3-step sequence that ultimately installed the glycosidic linkage of the natural product.

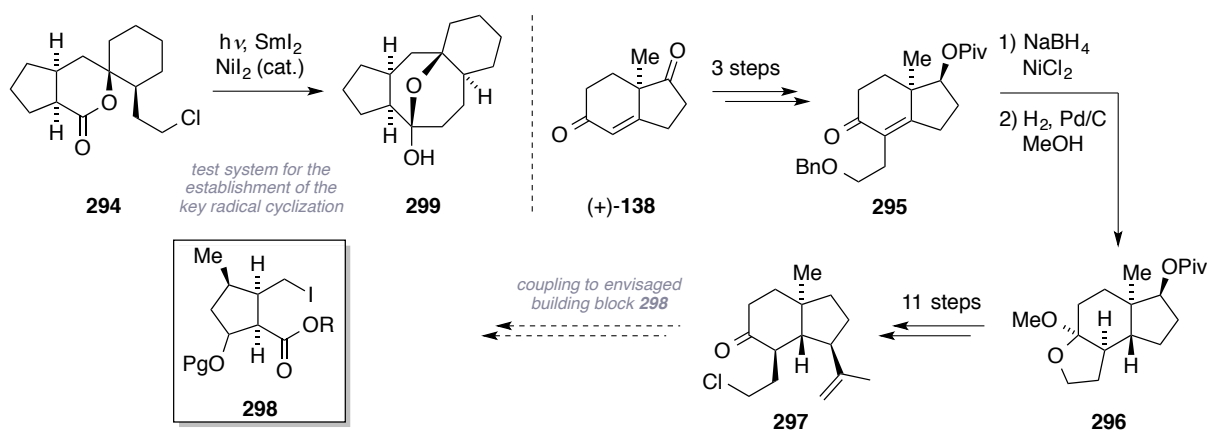
Progress toward the synthesis of the variecolin family has been reported by the research groups of Piers (1997)^[184] and Molander (2001).^[185] In 2002, Piers' work was complemented by the doctoral thesis of Walker, one of his co-workers (scheme 1.36).^[186] Their linear approach commences with the racemic 3-step preparation of bicyclic ketone **285** from 3-methyl cyclohexenone (**286**). This initial sequence comprised an optimized 1,4-cuprate addition/aldol condensation annulation protocol, followed by another highly diastereo-selective vinylogous nucleophilic attack of *iso*-propenyl cuprate. Biased by the newly set stereocenter, an ensuing base-promoted epimerization furnished the desired *trans*-ring junction in compound **287** in excellent selectivity (*cis/trans* = 11:1). Using kinetic deprotonation conditions, two consecutive alkylations and an iododestannylation reaction gave rise to intermediate **288**. This material was then submitted to iodine/lithium exchange with *n*-BuLi, which led to intramolecular 1,2-addition according to their previously established methodology.^[187] In order to correct the stereochemistry at carbon atom C-4, a combination of a Dauben oxidation^[188] and a Birch-type reduction was conducted and allowed access to ketone **289** in moderate selectivity (*dr* = 2.2:1). Afterwards, 15 transformations were required to relocate the carbonyl function, expand the 7-membered ring system and install the western cyclopentane moiety. Performing a hydroxyl group directed late-stage C–H activation



Scheme 1.36: Piers' racemic route toward variecolin-type sesterterpenoids, featuring a ring annulation *via* intramolecular Li-alkenyl addition.

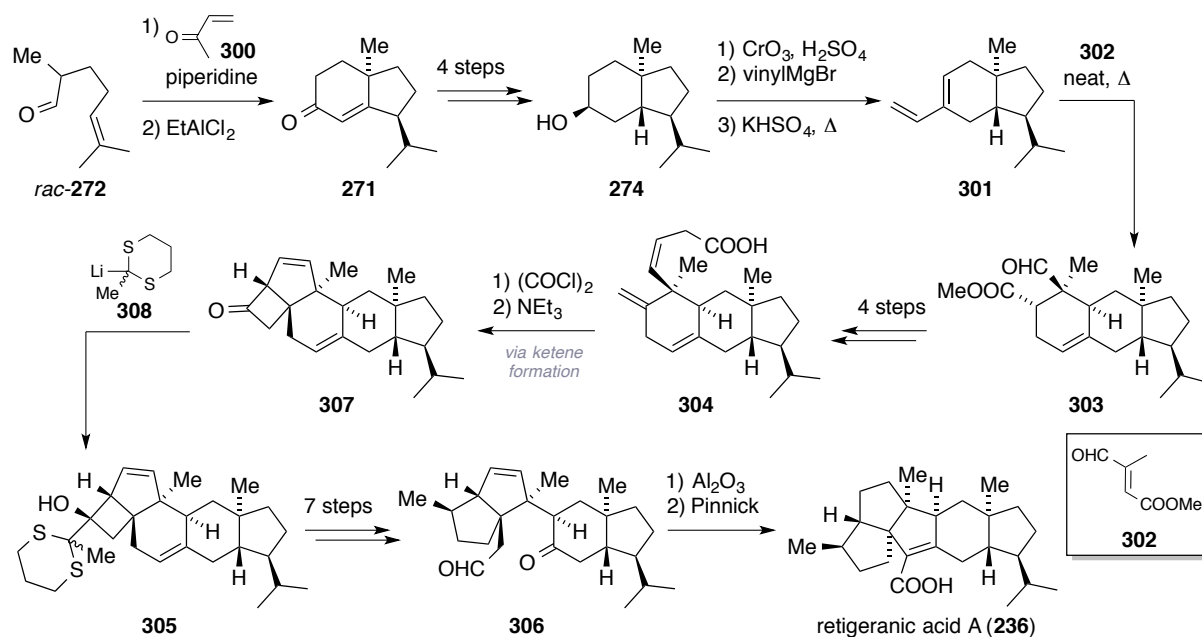
with $\text{Pb}(\text{OAc})_4$, 5-desoxyvariecolol (**290**) was obtained and further oxidized to 5-desoxy-variecolactone (**291**) with Collins' reagent^[189]. Unfortunately, a shortage of material prevented the authors from reaching the stage of a completed variecolin-type natural product.

In contrast, Molander's approach toward variecolin (**242**) was based on photochemical intramolecular radical addition of a primary chloride function, which was promoted by the addition of SmI_2 and catalytic amounts of NiI_2 (scheme 1.37).^[185] The viability of this transformation was proven on a model system (**294**) before they started to elaborate the building blocks for their envisaged key intermediate. The hydrindane-based portion was originally derived from enantiopure ketone (+)-**138** (*cf.* chapter 2.3) that was converted to enone **295** in a 3-step sequence. Their solution to install the critical *trans*-ring-fusion involved a nickel borate-mediated diastereoselective reduction. The obtained unstable intermediate was then immediately subjected to a one-pot hydrogenation/acetalization protocol to form tricyclic compound **296**. In eleven consequential reactions it was possible to access chloride **297**, which was meant to be coupled to cyclopentane system **298** according to the devised retrosynthetic plan. However, the synthesis of the latter fragment was not finished and the authors have published no further progress on this project so far.



Scheme 1.37: Synthetic studies toward variecolin (**242**) and evaluation of the envisaged key step on model compound **294**, published by Molander and co-workers.

The first successful total synthesis of an *iso*-propyl-substituted *trans*-hydrindane sesterterpenoid was described in 1985 by Corey and co-workers in their racemic strategy toward retigeranic acid A (**236**).^[147,148] Although the authors were mainly attracted by the angular triquinane ring system of the natural product, they also developed a new method to construct the required hydrindane portion that was later used by Paquette in his studies toward aleurodiscal (**239**, *vide supra*). To this end, they submitted melonal (**272**) to a Robinson-type annulation^[190] with methyl vinyl ketone (**300**) and subsequently obtained bicyclic enone **271** *via* a Lewis acid-catalyzed Prins reaction^[191] (scheme 1.38). The following 4-step protocol



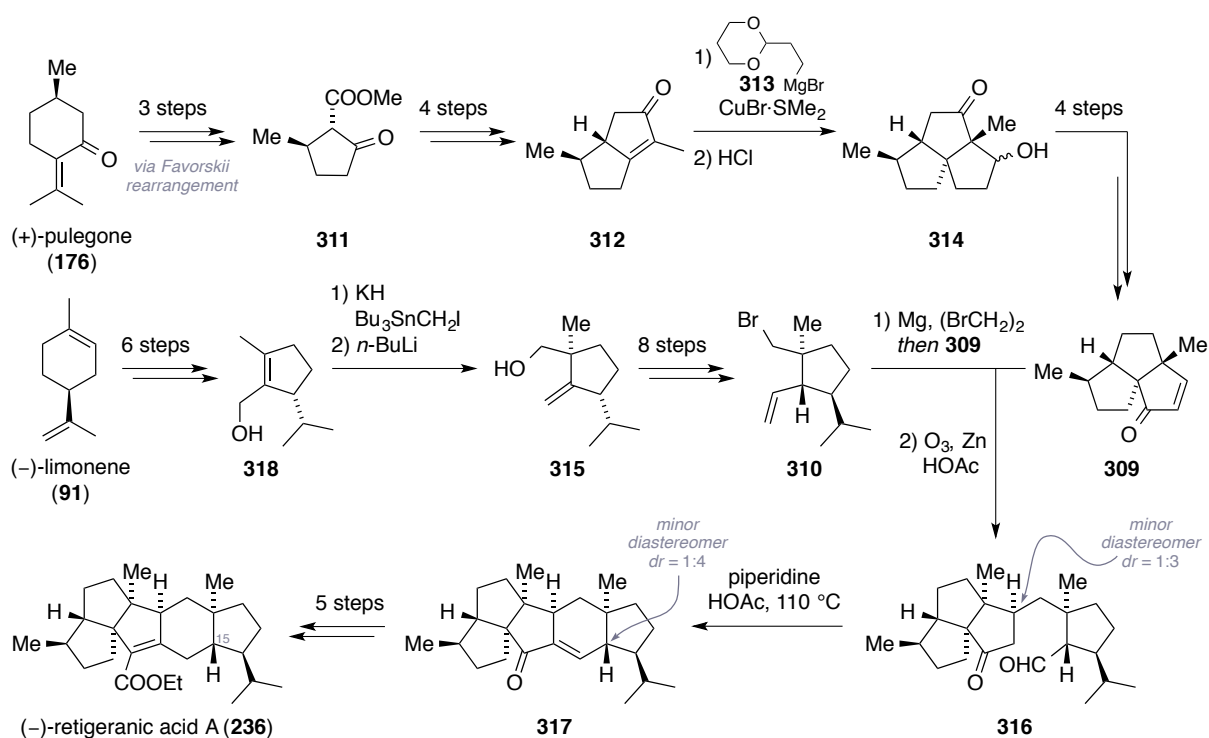
Scheme 1.38: Corey's racemic synthesis of retigeranic acid A (**236**), featuring a diastereoselective Diels-Alder reaction, a [2+2] ketene cycloaddition and an intramolecular aldol condensation.

that installed the *trans*-ring junction has been previously discussed (*cf.* scheme 1.35). Alcohol **274** was then sequentially oxidized with Jones' reagent^[192], reacted with vinyl Grignard and dehydrated with KHSO₄ to result in diene **301**. A thermally-induced Diels-Alder reaction with excess of dienophile **302** furnished the tricyclic system **303** as the major isomer in 61% yield. Six further transformations gave rise to acid **304**, which was reacted in a highly diastereoselective intramolecular [2+2] cycloaddition *via* the corresponding ketene generated *in situ*. The cyclobutane ring was then expanded in four steps by a CuOTf-mediated thio-pinacol rearrangement of intermediate **305** under concomitant installation of the western most methyl substituent. Fulfilling their synthetic plan, diketone compound **306** was reached in 7 additional reactions. This compound also represents an envisaged intermediate of the retrosynthetic plan that was pursued during the experimental work of present doctoral thesis (*cf.* chapter 2.2). Intramolecular aldol condensation and ensuing Pinnick oxidation^[193] eventually provided retigeranic acid A (**236**).

Two years later, Paquette and co-workers disclosed a more convergent route toward retigeranic acid A (**236**).^[149,150] Their synthetic plan envisaged the coupling of a triquinane building block (**309**) and a cyclopentane system (**310**) to implement the *trans*-fused 6-membered ring of the hydrindane system at a late stage (scheme 1.39). The construction of the first fragment started from the inexpensive monoterpene (+)-pulegone (**176**) and comprised an initial Favorskii rearrangement/ozonolysis protocol^[194] toward substance **311**, similar to the one utilized in present work (*cf.* chapter 2.4). Performing an alkylation and later an intramolecular aldol condensation, bicycle **312** was accessed in four further trans-

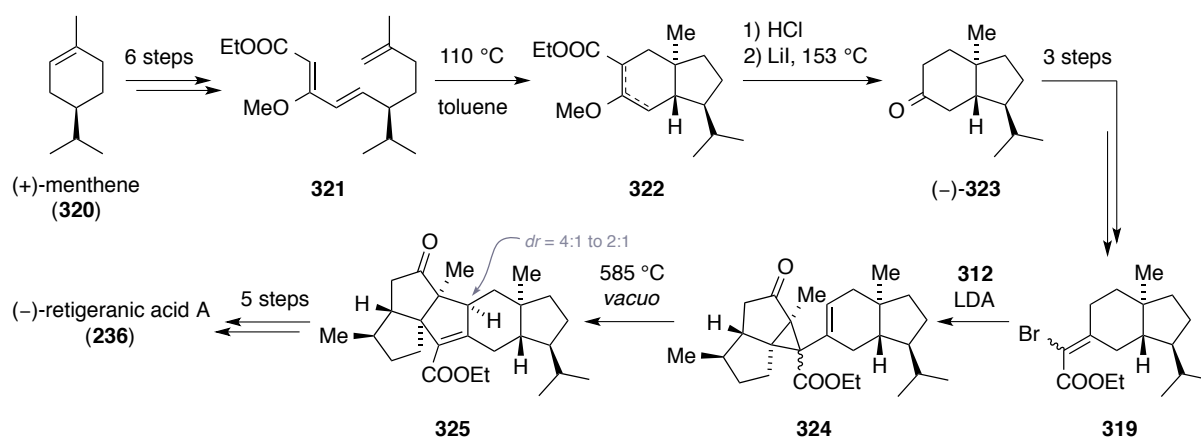
formations. This material was then submitted to a diastereoselective 1,4-addition of a cuprate side chain (**313**), followed by a one-pot deprotection and aldol addition to yield tricycle **314**. Chugaev elimination,^[195] Wolff-Kishner reduction and allylic oxidation eventually gave rise to triquinane **309**. The second key intermediate was elaborated in 16 steps from (–)-limonene (**91**), which involved amongst others a Wittig-Still rearrangement^[196] to install the *cis*-relationship between the angular methyl group and the *iso*-propyl moiety in compound **315**. Unfortunately, the nature of retigeranic acid B (**237**) had not been elucidated at that moment and the further synthetic sequence inverted the stereocenter of the larger substituent. Fragment combination was achieved *via* the respective Grignard reagent of bromide **310** and proceeded exclusively as the 1,4-addition. Unfortunately, the ensuing ozonolysis provided aldehyde **316** only as the minor diastereoisomer (*dr* = 1:3), thus indicating that the 1,4-addition had delivered the wrong selectivity. Furthermore, closure of the six-membered ring by aldol condensation required quite harsh conditions, namely piperidine and HOAc in toluene at 100 °C for 48 hours. As a consequence, epimerization was observed at C-15 (retigeranic acid numbering) and the *trans*-ring junction in pentacycle **317** was only obtained as the minor result (*dr* = 1:4) after HPLC purification. A final five-step sequence furnished the natural product for the first time in an enantiopure manner.

Building on the work of Corey and Paquette, an asymmetric total synthesis of retigeranic acid



Scheme 1.39: Paquette's convergent total synthesis of (–)-retigeranic acid A (**236**), constructing three of five ring systems *via* aldol addition chemistry.

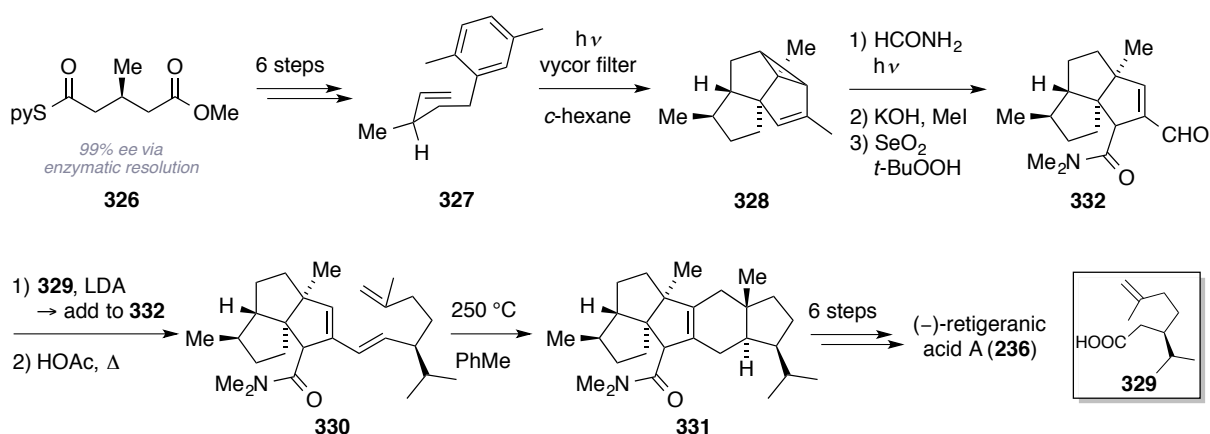
A (**236**) was published in 1988 by Hudlicky and co-workers.^[151,152] This work opted for the combination of *trans*-hydrindane compound **319** and bicycle **312** (*vide supra*), while postponing the construction of the central ring C (*cf.* scheme 2.1) to a later point of the sequence (scheme 1.40). Additionally, they devised a new strategy for the enantioselective preparation of the first intermediate that started from (+)-menthene (**320**). Referring to established chemistry, they produced triene **321** in six consecutive transformations. A thermally-induced intramolecular inverse electron-demand Diels-Alder cyclization gave rise to ester **322** as an inconsequential mixture of double bond isomers with complete selectivity for the *trans*-ring junction. Acid-catalyzed enol ether hydrolysis and subsequent Krapcho decarboxylation^[197] provided the known ketone **323** in 9 steps overall. Further elaboration of this material led to α -bromoester **319**, which was annulated to Paquette's diquinane **312** *via* dienolate-mediated 1,4-addition. A concomitant nucleophilic substitution of the bromide by the intermediary formed enolate yielded cyclopropane system **324** as a 1:1 mixture of stereoisomers. Flash vacuum pyrolysis (585 °C, 10⁻⁶ mm Hg) triggered the desired skeletal rearrangement and formed pentacarboxylic compound **325** in high yield, but with moderate diastereoselectivity (4:1 to 2:1, varying with the isomer of **324**). From this intermediate, five terminal reactions were needed to obtain the natural product in the shortest linear sequence of all successful approaches known to date (19 steps).



Scheme 1.40: Hudlicky's asymmetric approach toward (-)-retigeranic acid A (**236**), constructing the *trans*-hydrindane system *via* a diastereoselective Diels-Alder cyclization.

The last and most recent synthesis of retigeranic acid A (**236**) was disclosed by Wender *et al.* in 1990 and elaborates the molecule in a linear fashion *via* the angular triquinane ring system.^[153] Starting from ester **326**, which is readily available in 99% *ee* by enzymatic resolution of 3-methyl glutaric dimethyl ester (not shown), six transformations were applied to yield arene **327** (scheme 1.41). Making use of their previously established methodology for photochemical arene-alkene cycloadditions,^[198] they were able to isolate tetracycle **328** as the

minor constituent in a 1:2 mixture with the respective linear fused triquinane compound (not shown). However, the good overall yield of these reactions allowed access to the desired isomer in multi-gram quantities and thus rendered the reaction useful for preparative purposes. Subsequent ring opening of the cyclopropane moiety in compound **328** was accomplished by reaction with a photochemically generated acyl radical that led to fragmentation of the resulting intermediary cyclopropylcarbinyl radical. *N*-methylation, allylic oxidation, base-mediated condensation to acid **329** and decarboxylative dehydration gave rise to triene **330**, the envisaged precursor for a Diels-Alder cyclization to close the *trans*-hydrindane portion. Thus, the desired pentacycle (**331**) was obtained upon heating to 250 °C as the major isomer in a moderate overall yield of 64%. In the following, a 7-step sequence was required to relocate the carbon–carbon double bond into conjugation and finish the natural product, suffering from poor selectivity at the hydrogenative construction of the final stereocenter.

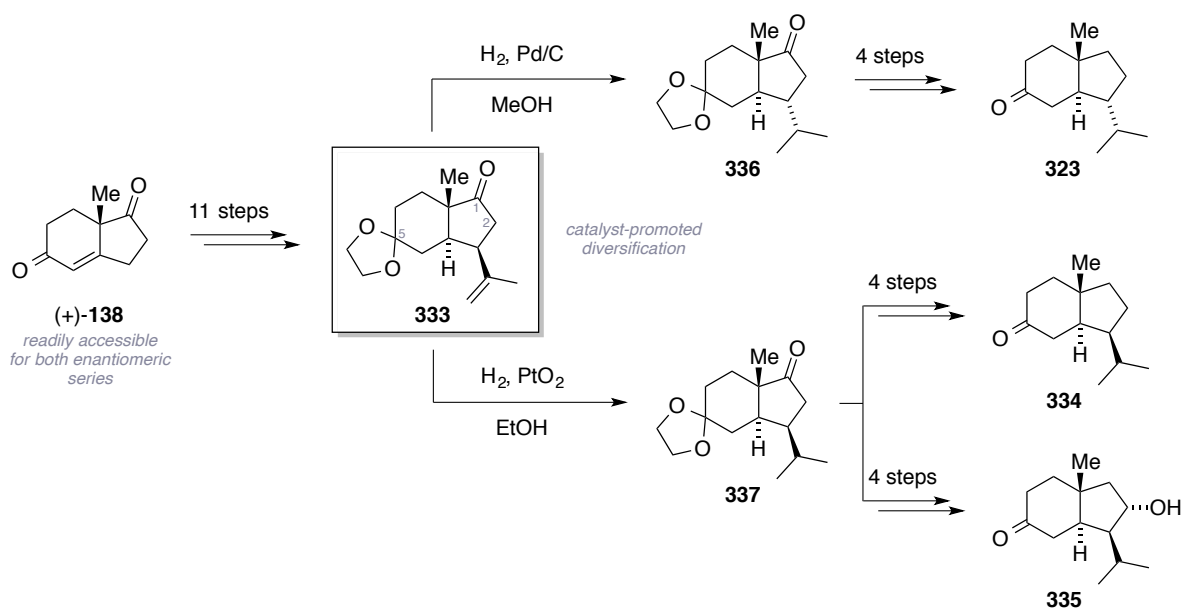


Scheme 1.41: Wender's synthetic strategy toward retigeranic acid A (**236**), making use of a photochemical arene-alkene cycloaddition and an intramolecular Diels-Alder reaction.

The last mentioned strategy illustrates again the complexity of the fused ring system inherent to the retigeranic acids and points out how troublesome the construction of the stereocenters at the respective junctions has been in the past. Additionally, no finished total synthesis of any cyclooctane containing *iso*-propyl-substituted *trans*-hydrindane sesterterpenoid had been published at the outset of this doctoral thesis.

1.4.3 Evolution of a Unified Synthetic Approach

Several years ago, the Trauner laboratories set out to develop a general synthetic approach toward *iso*-propyl *trans*-hydrindane sesterterpenoids. Pioneering work on this project was conducted by Dr. D. T. Hog and partially published in 2012 (scheme 1.42).^[140] The key sub-

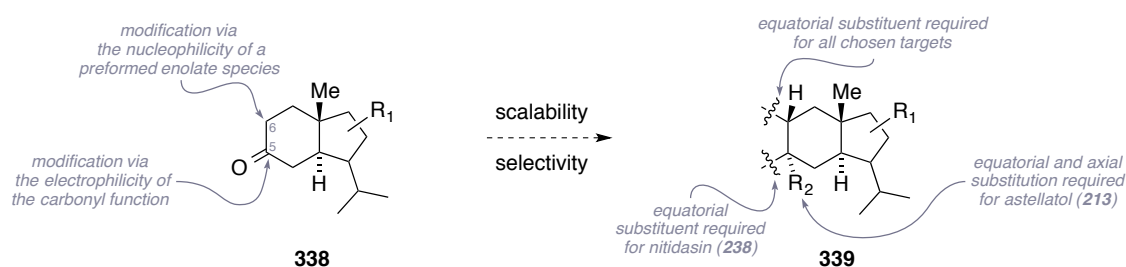


Scheme 1.42: The previously developed unified approach toward *iso*-propyl-substituted *trans*-hydrindane sesterterpenoids and branching points for their enantiopure preparation from ketone **(+)-138**.

structure that was identified as a suitable framework for outmost common intermediates was a *trans*-hydrindane system (**333**) with an oxygenation at its *C*-5 atom (*cf.* chapter 1.4.1) that would serve as a functional handle for the installation of further ring systems. To this end, three major building blocks (**323**, **334** and **335**) were accessed *via* a reliable and highly scalable route, which features several branching points for the variation of the substitution pattern of the cyclopentane moiety. The choice of Hajos-Parrish-Sauer-Eder-Wiechert ketone^[76] (**138**) as a starting point enables an easy transfer of all reactions to the complementary enantiomeric series. Furthermore, a catalyst-based diversification of the stereochemistry of the *iso*-propyl substituent was found when alkene **333** was subjected to either Pd/C - or Adams' catalyst^[199]-promoted hydrogenation. Thus, except for the variecolin-type natural products, all *iso*-propyl *trans*-hydrindane sesterterpenoids could in principle be traced back to alkene **333**. Further elaboration of both saturated epimers **336** and **337** gave rise to the oxygenation patterns of carbon atoms *C*-1 and *C*-2 so far observed in the target compound family. Experimental and theoretical details of the established synthetic protocols are discussed in chapters 2.3 and 3.3, as substances **334** and **335** played an essential role in the finished and attempted total syntheses described in present manuscript. Previously investigated synthetic approaches toward the natural products astellatol (**213**), nitiol (**254**) and YW 3548 (**241**), which were based on the above-described unified approach, are outlined in the doctoral thesis of Dr. D. T. Hog.^[156] Renewed synthetic investigations on the construction of YW 3548 (**241**) are currently in progress in the Trauner research group and are being carried out by B.Sc. M. Maier.

1.5 Project Outline

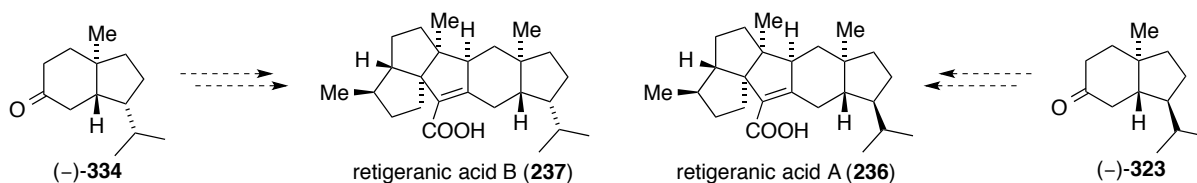
Building on the previously established chemistry of the above-described unified synthetic approach toward *iso*-propyl *trans*-hydrindane sesterterpenoids, the major goal of the present project was the elaboration of novel synthetic strategies to access, in particular, type A congeners of this class of natural products. As those structurally highly tangled compounds have proven to be formidable challenges even to modern synthetic chemistry (*cf.* chapter 1.4.2), a primary challenge lies in the successful incorporation of the developed *trans*-hydrindanone building blocks. To this end, further adjustments on their substitution pattern were not excluded in retrosynthetic planning.



Scheme 1.43: Initial challenges that are encountered for potential total syntheses of retigeranic acid B (**237**), nitidasin (**238**) and astellatol (**213**) commencing *via* the developed unified approach.

More precisely, we were inspired by the intriguing variation of ring size and cyclization pattern that is evident in the retigeranic acids (**236** and **237**), nitidasin (**238**) and astellatol (**213**), while frequently maintaining a similar configuration at their stereogenic centers. Consequently, a common target in our synthetic design was the stereoselective installation of a functional handle or beneficially an advanced side chain construct that would enable the required intramolecular closure of the unfinished carbocycles of these natural products. Two possible modifications were identified as an initial challenge, which would either exploit the nucleophilicity of the C-6 position in a preformed enolate species or refer to manipulation of the electrophilic carbonyl function at C-5 (scheme 1.43). Further requisitions to such a transformation were high scalability, selectivity and simple preparative purification, as the ensuing sequence toward the natural products would possibly involve several consecutive synthetic steps.

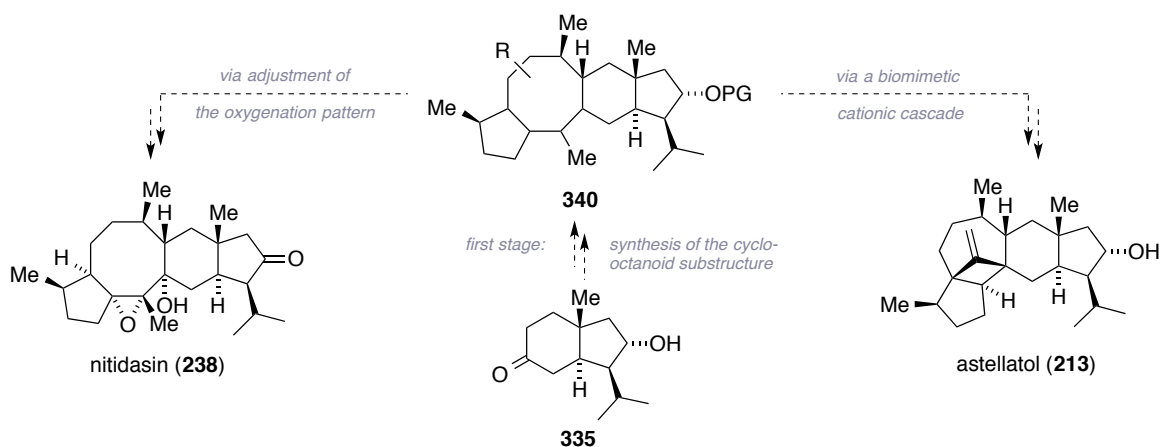
Motivated by the previously discovered convenient catalyst-promoted epimerization of the *iso*-propyl substituent (*cf.* chapter 1.4.3), it was our idea to utilize the rarely achieved *trans*-relationship to the angular methyl group for a potential first total synthesis of retigeranic acid B (**237**, scheme 1.44). Although the isomer retigeranic acid A (**236**) had been finalized



Scheme 1.44: Molecular structures of the sesterterpenoids retigeranic acid A (**237**) and B (**236**), and their proposed total syntheses from the known *trans*-hydrindane building blocks **323** and **334**.

several times before, all disclosed strategies either suffered from unfavourable selectivities or ample use of lengthy synthetic sequences. Thus, the project aimed at developing a convergent combination of *trans*-hydrindanones **323** or **334** with an appropriate building block that would enable a rapid substrate-controlled construction of the triquinane moiety, ideally *via* a one-pot reaction cascade. This more robust route was intended to be applied to both *iso*-propyl epimers and to give rise to substantial amounts of the natural products to elucidate their still unknown mode of bioactivity.

Furthermore, we recognized the close resemblance of the cationic intermediates proposed for the biogenesis^[200] of astellatol (**213**) to its close relative nitidasin (**238**) and were poised to investigate a simultaneous construction of both compounds from shared 5-8-6-5 carbocyclic precursors (scheme 1.45). We were especially fascinated by a supposedly biomimetic formation of the unique convoluted pentacarboxylic framework of astellatol (**213**) by a homoallyl-cyclopropylcarbiny-cyclobutyl rearrangement.^[201] This would not only allow to provide experimental proof of mentioned biosynthetic hypothesis, but also resemble the first application of this cascade reaction to preparative organic chemistry. Hence, the prominent task of this subproject was the preliminary assembly of the cyclooctanoid carbon skeleton (**340**), which had been preceded only by a single case prior to present doctoral thesis (*cf.* chapter 1.4.2). Once this ring system is completed, either adjustment of the oxygenation



Scheme 1.45: Molecular structures of the sesterterpenoids nitidasin (**238**) and astellatol (**213**), potentially accessible by total synthesis from a shared tetracarboxylic intermediate (**340**).

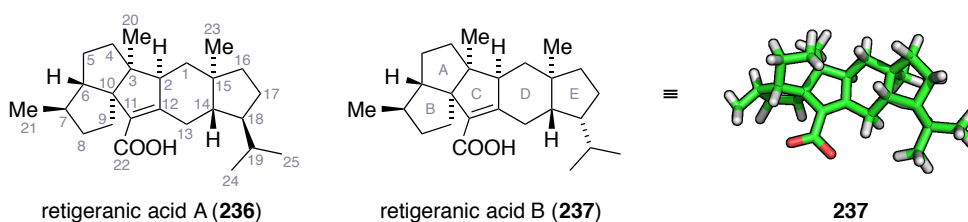
pattern or conversion to a stable entry point for the bioinspired rearrangement would have to be addressed in order to yield nitidasin (**238**) or astellatol (**213**), respectively. Again, manufacturing those molecules *via* total synthesis should allow further investigation of their biological activity, for which, in both cases, no relevant data has been published to date.

Last but not least, all chosen synthetic targets represent outstanding examples for the application and development of state-of-the-art organo chemical methodology on complex polycarbocyclic architectures. Specifically the establishment of cascade reactions has emerged as a figurehead of the synthetic programs launched in the Trauner research group^[27,202] and became a prevailing theme for the studies toward the total syntheses of type A *iso*-propyl-substituted *trans*-hydrindane sesterterpenoids that will be presented in the following chapters.

2. Synthetic Studies Toward Retigeranic Acid B

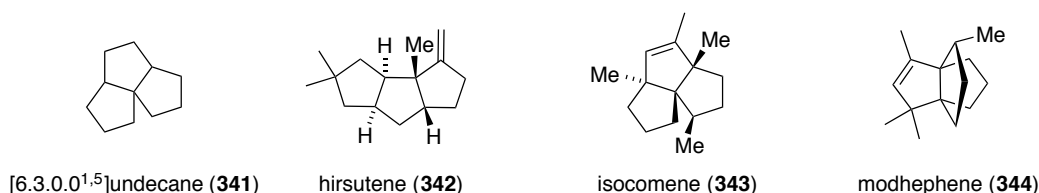
2.1 A Comprehensive Introduction to Retigeranic Acid A and B

The compounds which have come to be known as retigeranic acid A (**236**) and B (**237**) (scheme 2.1) were first isolated by Seshedari and co-workers^[141–143] in 1961 from a lichen species called *Lobaria retigera*, which was collected in different parts of the western Himalayas. It must be clarified, that at this point the retigeranic acids were obtained as a mixture but considered to be one single compound, simply named ‘retigeranic acid’. Later, in 1972, Shibata and co-workers isolated the same mixture from the related species *Lobaria isidiosa* and *Lobaria subretigera*, which they collected in eastern Bhutan.^[144,145] They found the retigeranic acids in the chloroform-soluble fractions of the ethereal extracts of those plants and were able to record first NMR spectra. By the additional use of mass spectroscopy, they identified the compounds as sesterterpenoids. Knowing of the presence of an α,β -unsaturated



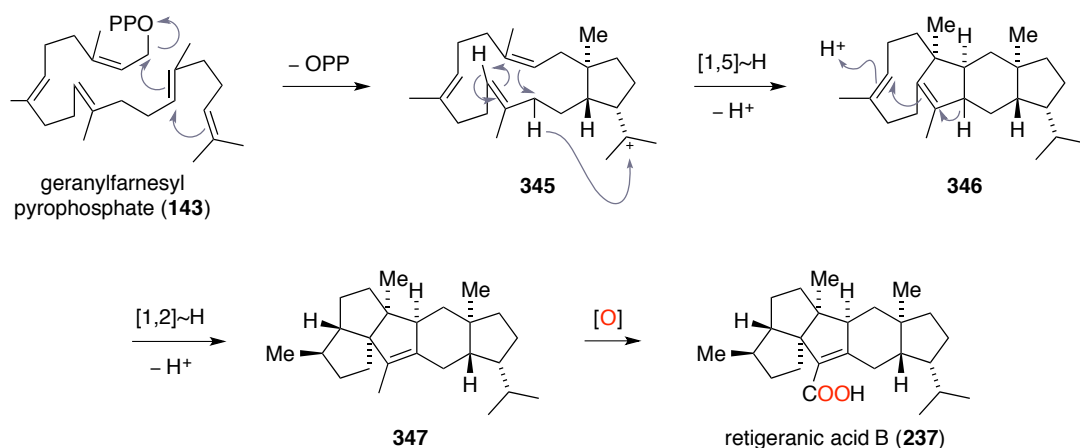
Scheme 2.1: Molecular structures of retigeranic acid A (**236**) and B (**237**) and crystal structure of the latter. Carbon and ring numbering was adopted from Shibata and co-workers.^[2,5]

acid from reaction with tetranitromethane and according to Liebermann-Burchard,^[203] they were able to obtain the corresponding *p*-bromoanilide of retigeranic acid A (**236**) and crystallized it from acetone to elucidate its structure. However, several years later Corey and co-workers managed to synthesize racemic ‘retigeranic acid’ for the first time.^[147] Modifying the natural product by means of esterification, they proved *via* HPLC separation that the isolated compound is a mixture of the minor, just synthesized retigeranic acid A (**236**) and the major, isomeric retigeranic acid B (**237**). Their suggestion that the two isomers vary at the stereocenter on C-7 (retigeranic acid numbering) was refuted by Shibata and co-workers in 1991.^[146] The authors were able to grow crystals of both isomers from different fractions obtained *via* HPLC methods. They could show that both compounds are diastereomeric in regard of the configuration of the *iso*-propyl substituent at C-18. Interestingly, they also managed to co-crystallize retigeranic acid A (**236**) and B (**237**) as a 1:1 mixture.



Scheme 2.2: Molecular structures of hirsutene (**342**), isocomene (**343**) and modhephene (**344**) as examples for linear, angular and propellane-type triquinane natural products.

The retigeranic acids possess some intriguing structural features, as foremost to mention their angular triquinane motif (rings A, B, C), which is based on the [6.3.0.0^{1,5}]undecane carbon skeleton (**341**, scheme 2.2). Notably, they were also the first structurally elucidated natural occurring compounds to have this substructure. In the years following their discovery, several other triquinane natural products like *e.g.* hirsutene (**342**),^[204] isocomene (**343**)^[205] and modhephene (**344**)^[206] were found. This led to a sheer race in total synthesis in the 1980's and 1990's, producing more than 130 different syntheses, of which the four previously mentioned retigeranic acid A (**236**) syntheses were amongst (*cf.* chapter 1.4.2). Furthermore, the retigeranic acids are constituted of 8 stereogenic centers, three of which are quaternary. They exhibit an extraordinarily low degree of functionalization, having only an α,β -unsaturated acid moiety. Last but not least, the retigeranic acids hold a sterically encumbered *iso*-propyl-substituted *trans*-hydrindane portion, characteristic for this subclass of natural products.



Scheme 2.3: Proposed biosynthesis for the formation of the retigeranic acids.^[2,4] Only one isomer is shown for clarity. The single oxidation event was highlighted in red.

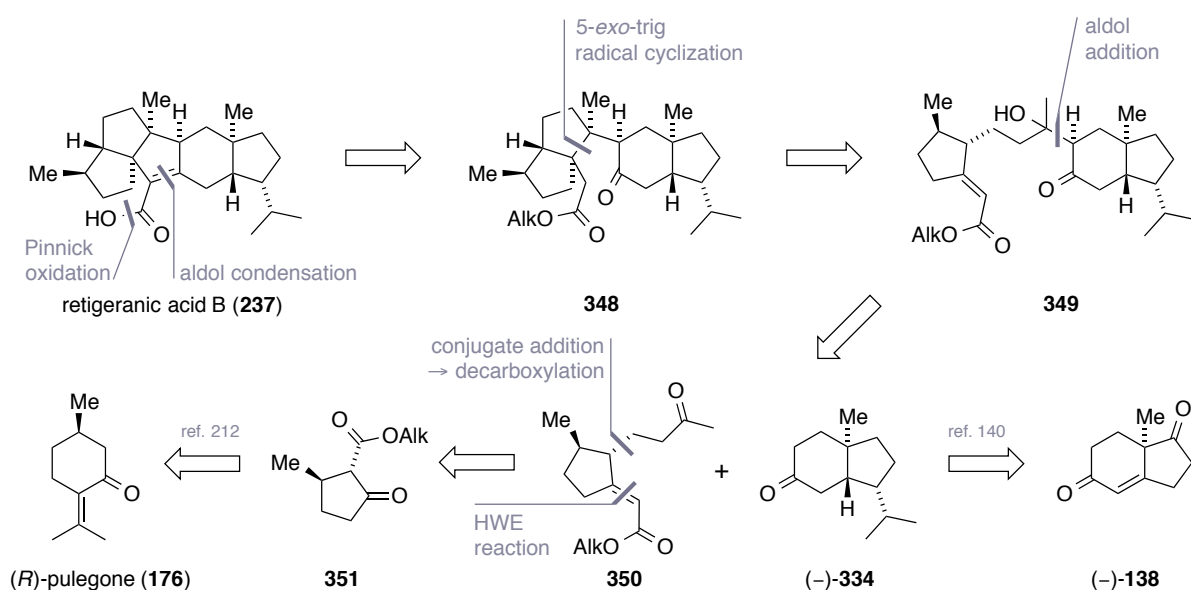
Despite their unique and synthetically challenging pentacarbocyclic structure that nature must have devised for a certain purpose, no data on the biological activity of both acids has been published, to the best of our knowledge. Solely the respective ozonide derivatives have been proven to act as anti-inflammatory agents.^[207] Concomitantly to their first structural investigations, Shibata and co-workers proposed a biosynthetic pathway^[144] (scheme 2.3), which involves the following sequential steps and starts from geranylfarnesyl pyrophosphate

(**143**): pyrophosphate elimination, 15-*endo*-trig and then 5-*exo*-trig cyclization (**345**), [1,5]-hydride shift, 6-*exo*-trig and subsequent 5-*exo*-trig cyclization, elimination (**346**), re-protonation and 5-*exo*-trig cyclization, [1,2]-hydride shift, elimination (**347**) and finally oxidation to yield the natural products. Nevertheless, no further chemical or theoretical proof of this hypothesis has been published yet.

As the major diastereomer retigeranic acid B (**237**) comprises the sterically more challenging substitution pattern at the *trans*-hydrindane moiety and due to the fact that it has not been accessed by total synthesis yet, we planned to synthesize this natural product. Our efforts to incorporate this project into the developed unified approach toward *iso*-propyl-substituted *trans*-hydrindane sesterterpenoids^[140] will be described in the following chapters.

2.2 Retrosynthetic Analysis

The pursued retrosynthetic strategy toward retigeranic acid B (**237**) commenced with the disconnection of pentacycle B (scheme 2.4). In the forward sense, this ring would be closed by a sequential aldol condensation and Pinnick oxidation^[193] that is based on Corey's racemic synthesis of retigeranic acid A (**236**)^[147] and requires a preceding ester reduction and re-oxidation to the corresponding aldehyde. All in all, this traces back to ketoester **348**. Closure of ring A should be addressed *via* a 5-*exo*-trig type vinylogous radical cyclization, at which the initial trisubstituted radical at C-3 should be generated possibly *via* the corresponding xantogenate of tertiary alcohol **349**. The formation of the desired stereochemistry at C-10 is

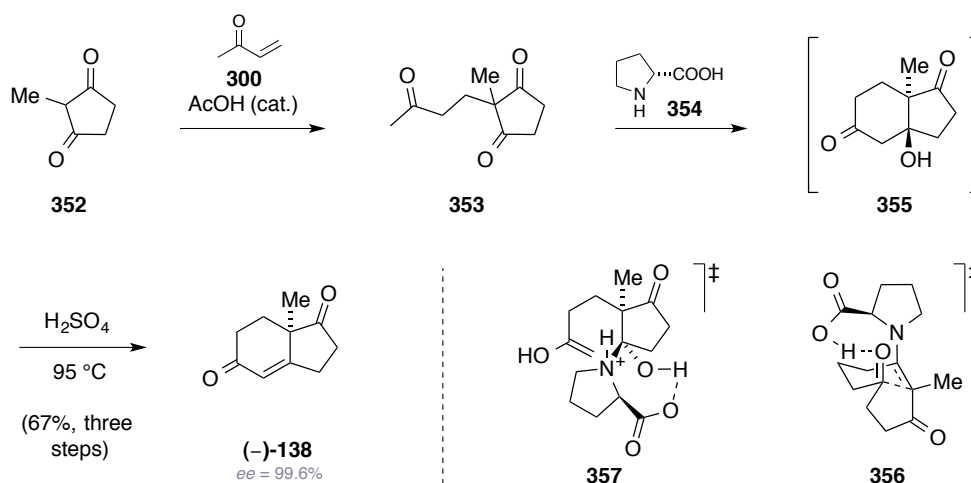


Scheme 2.4: Retrosynthetic analysis for the construction of retigeranic acid B (**237**) from *trans*-hydrindanone building block **334**, featuring an aldol addition and a radical cyclization key step.

well preceded for similar systems^[208] and would arise from the kinetic preference for the significantly less strained *cis*-diquinane system. Furthermore, it can be reasoned that the stereochemical outcome at C-3 would be favourably guided by the steric bulk of the neighboring *trans*-hydrindane substituent. It was speculated that by generating the initial C-3 centered radical *via* SmI₂-mediated conditions, the later on occurring α -keto radical intermediate could potentially combine with a C-12 located ketyl radical to additionally form ring C in the same step. This termination of the radical cascade bears similarities to samarium Barbier reactions, which have been investigated extensively in the past.^[209] Tertiary alcohol **349** itself should be synthesized *via* aldol-condensation between *trans*-hydrindanone **334** and ketone **350**. Such a fragment combination would probably involve the use of boron-based enolate conditions, which are known to stabilize the aldol product from retro-aldol reaction.^[210] *trans*-Hydrindanone **334** was intended to be prepared from Hajos-Parrish-Eder-Sauer-Wiechert ketone (**138**)^[211] by a 15-step sequence that had been published by the Trauner group previously.^[140] The cyclopentane building block **350** was planned to be accessed from ketoester **351** by performing a conjugate addition to methyl vinyl ketone (**300**). In the forward sense, subsequent decarboxylation and a final regioselective Horner-Wadsworth-Emmons olefination would install the desired α,β -unsaturated ester. Ketoester **351** itself can be readily obtained by a 3-step protocol, which proceeds *via* a Favorskii rearrangement^[194] and starts from the inexpensive chiral building block (*R*)-pulegone (**176**).^[212]

2.3 Synthesis of a Model System for the *trans*-Hydrindanone Moiety

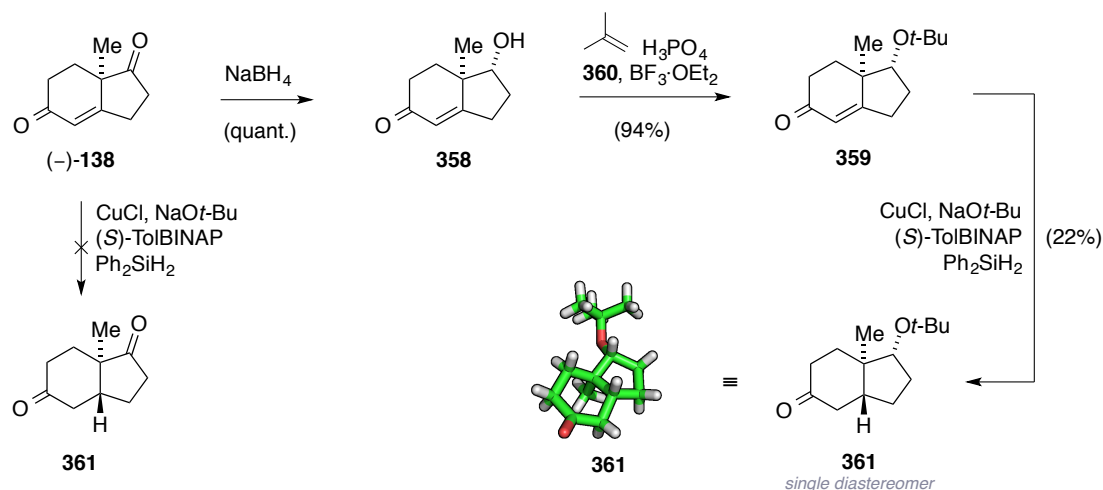
To reduce our retrosynthetic plan into practice, we started with the synthesis of a chiral building block for the envisaged *trans*-hydrindanone **334**. A common and well established precursor for the *trans*-hydrindane motif, which is also often found in steroid-type compounds, is the Hajos-Parrish-Eder-Sauer-Wiechert ketone (**138**).^[76] Following a detailed literature-known procedure,^[211] we reacted 100 g of diketone **352** with methyl vinyl ketone (**300**) using catalytic amounts of acetic acid to promote the occurring Michael-addition (scheme 2.5). Crude triketone **353** was then immediately subjected to (*R*)-proline (**354**) catalyzed aldol condensation, forming bicycle **355**. After acid-mediated elimination and thorough purification, 97 g of enone (–)-**138** were obtained from a single reaction batch in 67% yield (calculated from diketone **352**). The enantiomeric excess was determined to be an



Scheme 2.5: (*R*)-proline (**354**) catalyzed formation of chiral enone (–)-**138**, according to Hajos and Parrish.^[76] Transition states **357** and **356** have been proposed by the mentioned authors or by Houk and co-workers respectively.^[213]

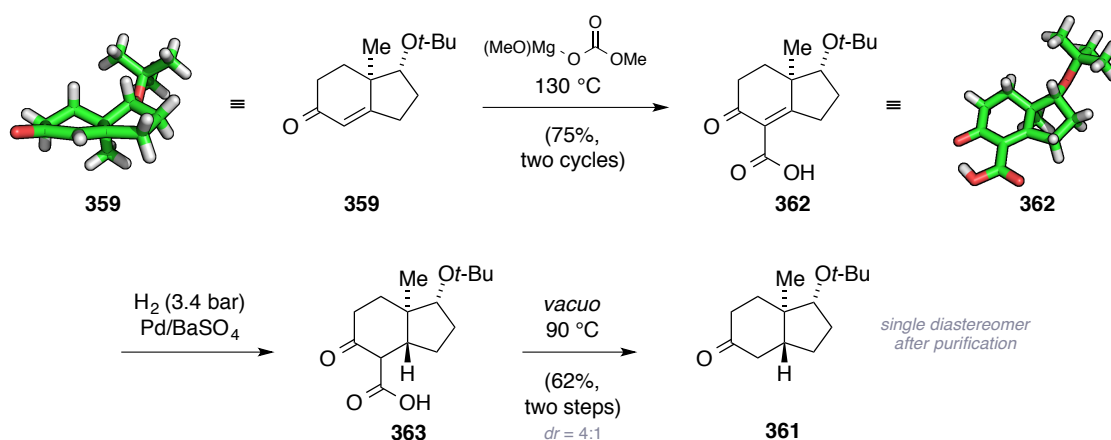
excellent 99.6% *via* optical rotation, which in this case has been accepted as the method of choice by the community.^[211] The transition state that accounts for the enantioselectivity of the reaction has been subject of considerable debate. Based on calculations, Houk proposed an enamine-type mechanistic model (**356**) in 2001.^[213] However, this has surprisingly been rejected by Hajos, who still held on to his originally proposed carbinolamine (**357**) mechanism.^[76,214]

In order to construct the desired *trans*-junction, several literature-known procedures were considered. As we knew from earlier experiments conducted in our group, the usage of bulky CuH species as described by Daniewski and co-workers,^[215,216] suffers from low reproducibility in terms of its yield, chemo-, and diastereoselectivity, as well as from insufficient scalability.^[156] Thus, we were curious to apply conditions that were established more recently by Buchwald and co-workers for an enantioselective 1,4-reduction of cyclic enone systems (scheme 2.6).^[217] At this, we speculated that, in a matched case, the utilized (*S*)-TolBINAP ligand (not shown) would enhance the diastereoselectivity of the CuH-mediated reduction. Unfortunately, we only observed 1,2-reduction of both ketone functionalities of compound (–)-**138**. Consequently, we had to refer to an industrial, scalable 5-step route,^[218] which has already been implemented in several total syntheses in the past.^[219] To this end, we first reduced the cyclopentanone moiety to alcohol **358** in quantitative yield and complete chemo- and stereoselectivity, using stoichiometric amounts of NaBH₄. Although TBS ethers have proven to be a viable protecting group for the generated alcohol in very similar synthetic sequences,^[220] we decided for the installment of a *tert*-butyl ether, which is a commonly used and less acid labile alternative. Furthermore, we had



Scheme 2.6: Attempts toward the scalable and selective installment of the *trans*-junction in compound **361**.

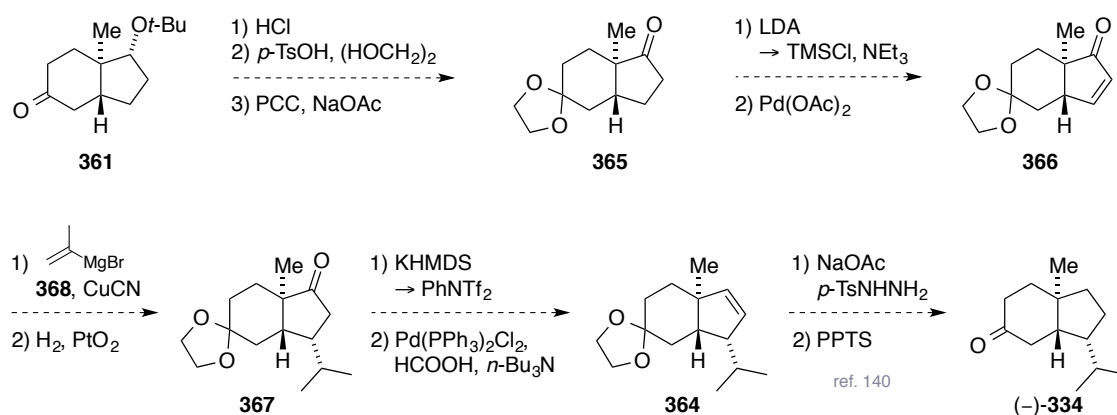
in mind that a more stable ether function would facilitate the use of substance **359** as a model system for screening purposes toward envisaged aldol addition step (*vide supra*). It must be mentioned that the original authors have described the presence of a sterically demanding residue as being crucial for the diastereoselectivity of the later on following hydrogenation step.^[218] Using *iso*-butylene (**360**) under H_3PO_4 - and $\text{BF}_3 \cdot \text{OEt}_2$ -mediated acid catalysis, we obtained ether **359** in excellent yield and could verify its structure *via* X-ray crystallography (scheme 2.7). Interestingly, reaction of ether **359** under Buchwald's conditions^[217] formed the desired hydrindane **361** with perfect *trans*-selectivity. However, 1,2-reduction was observed to be the major pathway again and was presumably caused by the inherent steric bulk of the chiral ligand. Hence, the 22% yield of substance **361** could not be improved by variation of the reaction parameters. Nevertheless, from this transformation we obtained material pure enough to grow crystals that were suitable for X-ray crystallographic analysis.



Scheme 2.7: Pursued industrial route for the preparation of *trans*-hydrindanone **361**.^[2,23] Indicated diastereomeric ratio refers to the crude reaction mixture.

According to the mentioned industrial route, ether **359** was α -carboxylated by employing Stiles reagent (scheme 2.7).^[221] Due to a momentarily lack in commercial availability of this reagent and its extremely laborious preparation, an aged batch was used, which led to somewhat lower conversion of ether **359** than previously reported.^[140] The concomitantly formed regioisomeric β -ketoacid (not shown) readily decarboxylated during acidic work up, which allowed for the convenient recovery of ether **359**. The solid-state structure obtained from the isolated material of compound **362** is shown in scheme 2.7. Although no obvious change in the overall shape of the molecule is noticeable when being compared to enone **359** or diketone (–)-**138**, hydrogenation of β -ketoacid **362** now preferentially led to the *trans*-fused system, whilst enone **359** would yield the corresponding *cis*-hydrindane as the major product.^[218] The reasons for these findings have not been clarified to date. It might be suspected that a possible interaction of the newly introduced carboxylic group with the surface of the employed heterogeneous Pd/BaSO₄ catalyst system alters the preferred face for the delivery of surface-bound hydrogen. Accordingly, when 3.4 atmospheres of hydrogen gas were applied, saturated β -ketoacid **363** could be obtained as a rather labile compound. Consequently, it was submitted to immediate decarboxylation at elevated temperature under reduced pressure. ¹H NMR analysis of the crude reaction mixture revealed a *cis/trans*-ratio of compound **361** of roughly 4:1. Thorough separation by column chromatography yielded pure *trans*-hydrindane **361** in good yield (62%, two steps) on multi-gram scale.

Due to the excellent disposability and inherent similarity of this compound in comparison to the envisioned final *trans*-hydrindanone building block **334**, it was used as a model system for the investigations toward a fragment combination with ketone **350** (*vide infra*). Therefore, attention was turned toward constructing this very ketone (**350**) at this point. Scheme 2.8

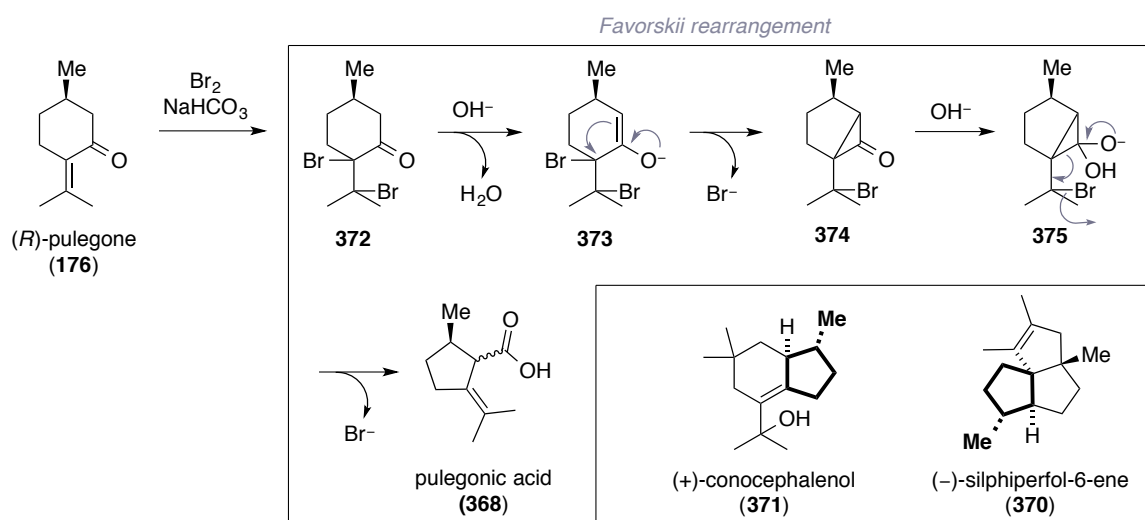


Scheme 2.8: Transformations required for the completion of *trans*-hydrindanone **334**. This synthetic sequence has been developed in the Trauner group previously and was published by Hog *et al.*^[140]

summarizes the transformations that are necessary for the completion of building block **334** and have been developed in the Trauner group previously.^[140] The majority of the steps will be outlined in detail in chapter 3.3 for the respective enantiomeric series. Final saturation of alkene **364** has been described by means of diimide reduction,^[222] as hydrogenation using Pd/C or PtO₂ would lead to epimerization of the neighboring *iso*-propyl-substituted stereocenter.^[140]

2.4 Synthesis of the Cyclopentane Moiety

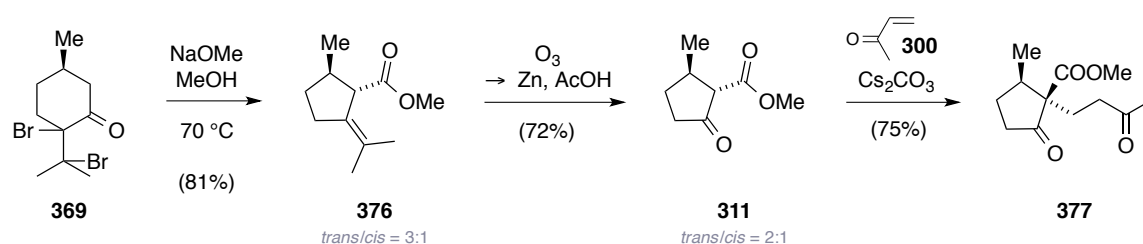
The synthesis of the B ring containing cyclopentane **350** started from (*R*)-pulegone (**176**), a common and inexpensive chiral building block. Already in 1918, Wallach described the formation of *cis*- and *trans*-pulegonic acid (**368**) when (*R*)-pulegone dibromide (**369**), which is readily available *via* bromination of (*R*)-pulegone (**176**), was treated with aqueous sodium hydroxide solution.^[223] Later, Wolinski and co-worker suggested that mechanistically a Favorskii rearrangement has to account for this transformation (scheme 2.9).^[224] Since then, several groups have used and refined this procedure to access chiral cyclopentane building blocks. Prominent examples were given by the groups of Hudlicky and Paquette during the construction of the triquinane portion of retigeranic acid A (**236**)^[2,32] or the synthesis of (–)-silphiperfol-6-ene (**370**),^[150] as well as by Cossy and co-workers during their synthesis of (+)-conocephalenol (**371**).^[225]



Scheme 2.9: Transformation of (*R*)-pulegone (**176**) to a mixture of pulegonic acids (**368**) *via* Favorskii rearrangement. Illustrated mechanism was adopted from Loftfield.^[226] The pulegone-derived parts of the natural products **370** and **371** have been highlighted in bold.

Accordingly, we started with the bromination of 25 g of (*R*)-pulegone (**176**) using stoichiometric amounts of bromine in NaHCO₃-buffered diethyl ether. Dibromide **369** was

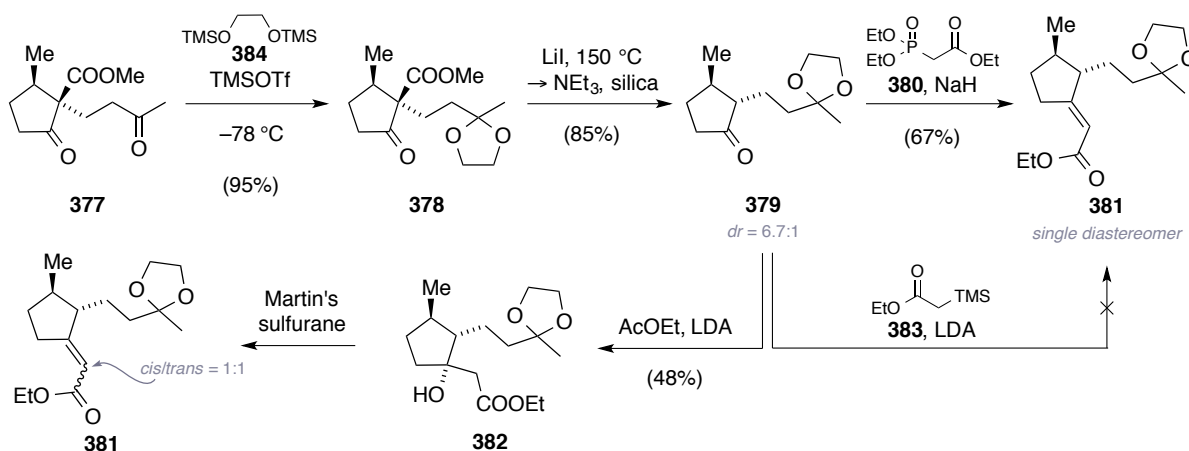
obtained quantitatively as deep purple oil and directly used for the following rearrangement step. Therefore, dibromide **369** was refluxed in a freshly prepared methanolic sodium methoxide solution and the resulting crude product was purified *via* distillation to yield methyl ester **376** in very good yield as a 3:1 mixture of *trans/cis*-isomers (scheme 2.10).^[227] Next, the alkene functionality was cleaved *via* ozonolysis with successive application of reductive work-up conditions. Hence, β -ketoester **311** was isolated in 72% yield in a *cis/trans* ratio of 1:2. This isomeric mixture was inconsequential for the following step and could be enhanced by base-catalyzed equilibration. Repeated column chromatography allowed for the separation and characterization of *trans*- β -ketoester **311**. Thereafter, the 1,4-addition of deprotonated β -ketoester **311** to methyl vinyl ketone (**300**) was investigated, at which the stereogenic methyl group would direct the attack to the desired face. Referring to conditions described by Santelli and co-workers,^[228] Cs₂CO₃ was employed as an enolizing base and diketone **377** could be isolated in 75% yield, along with trace amounts of the undesired diastereomer. It was found that the actual 1,4-addition step starts proceeding at approximately –35 °C and becomes sufficiently fast at –25 °C. Warmer reaction temperatures led to the formation of significant amounts of polymeric side products.



Scheme 2.10: Conducted transformations toward diketone **377**, comprising a Favorskii rearrangement, an ozonolysis with reductive work-up and a base-promoted addition to methyl vinyl ketone (**300**).

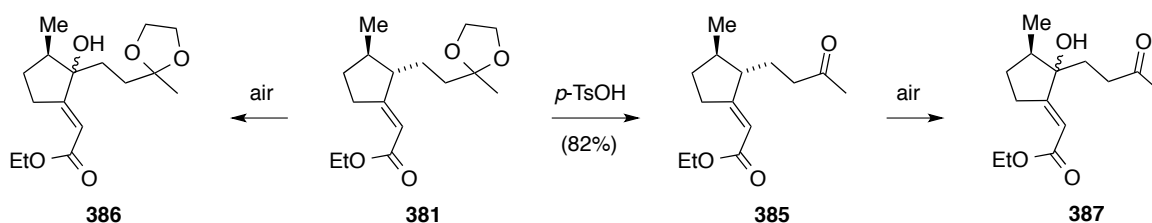
From the seminal work of Paquette *et. al.* on the construction of angular triquinane systems, it is known that compounds similar to diketone **377** tend to react *via* intramolecular aldol addition at elevated temperatures,^[150] which are usually required for the envisaged Krapcho decarboxylation.^[197] To circumvent this undesired reactivity, it was planned to selectively protect the acyclic, less sterically hindered ketone functionality to the respective 1,3-dioxolane (scheme 2.11). Transformations like this are possible by using a protocol developed by Noyori,^[229] at which TMS⁺ serves as a proton-like catalyst.^[230] Due to the low reaction temperatures involved, site-selectivity of the acetal formation could be demonstrated in several cases.^[231] When diketone **377** was subjected to these conditions, dioxolane **378** was obtained in almost quantitative yield on multi-gram scale. Subsequent Krapcho decarboxylation with lithium iodide in DMF at 150 °C^[152a] went smoothly and provided

substance **379** in an excellent yield (85%). The initially observed *cis/trans* ratio of 1:3.4 could be improved conveniently to 1:6.7 by conducting the chromatographic step with triethylamine-deactivated silica.



Scheme 2.11: Synthesis of α,β -unsaturated ester **381** via selective dioxolane formation, Krapcho decarboxylation and Horner-Wadsworth-Emmons olefination.

When the construction of the α,β -unsaturated ester functionality was investigated, conditions reported by Nangia *et al.* in their (–)-mitsugashiwalactone (not shown) synthesis for the olefination of a very similar cyclopentanone were first evaluated.^[232] These authors describe the application of classical Horner-Wadsworth-Emmons conditions as being superior to a wide variety of methods, but only when using super-stoichiometrical amounts of triethyl phosphonoacetate (**380**) and sodium hydride in THF. The same finding held true for cyclopentenone **379** and the oxygen-sensitive α,β -unsaturated ester **381** was obtained in 67% yield. Further screened reaction conditions (bases: KH, *n*-BuLi, KO*t*-Bu, NaO*t*-Bu; DBU, LiCl, MeCN; MeOC(O)CHPPh₃, toluene, 110 °C) unfortunately failed to improve the yield of this transformation. Repeated attempts to apply a Peterson olefination protocol that was known from different cyclopentanone syntheses^[233] remained futile. This is probably due to the steric hindrance exerted by the α -substituent at the electrophilic carbonyl functionality. Interestingly, deprotonated ethyl acetate could be added to compound **379** and gave rise to tertiary alcohol **382** in moderate yield as a single diastereomer. Although literature suggests that elimination of such an alcohol using Martin's sulfurane^[234] would preferentially yield the *E*-alkene,^[233b] we only observed a 1:1 ratio of isomers in ¹H NMR spectra recorded from the crude reaction mixture. Since this reflects an unselective E1 mechanism, and because of competing decomposition reactions, we dismissed this two-step sequence.



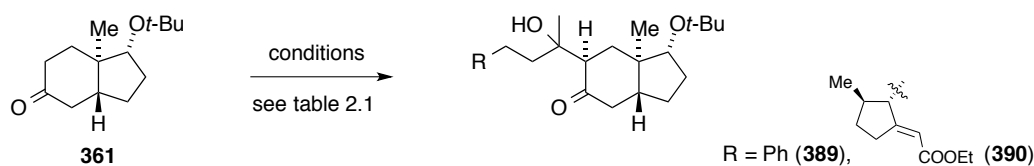
Scheme 2.12: Final deprotection step yielding desired diketone **385**. Both compounds **381** and **385** degrade to their respective γ -hydroxy esters **386** and **387** when exposed to air.

Final dioxolane cleavage was achieved with *para*-toluenesulfonic acid (*p*-TsOH) in a mixture of water and THF and provided **385** in 82% yield (scheme 2.12). Due to the long reaction duration of 7 days, the formation of two oxygenated byproducts **386** and **387** was observed, which were isolated in low quantities using HPLC methods. The structures of compounds **386** and **387** were assigned *via* NMR spectroscopy and the corresponding mass were found by EI-HRMS measurements. Both γ -hydroxy esters occurred as 1:1 diastereomeric mixtures, which suggests that they are formed *via* radical attack of oxygen at the stabilized γ -position and by subsequent reductive breakdown of an intermediary generated peroxy species.

2.5 Model Studies on the Fragment Combination

With completed fragment **385** and model system **361** in our hands, we started to investigate aldol addition-type coupling conditions. Although ketone-ketone aldol additions are supposed to be slightly endothermic processes as such,^[210] retro-aldol reactions can be circumvented. Modern aldol chemistry provides a variety of protocols, such as Mukaiyama aldol^[59] or boron and titanium Lewis acid-catalyzed reactions, which stabilize the aldol product either as the respective silyl ether or as its respective metal complex.

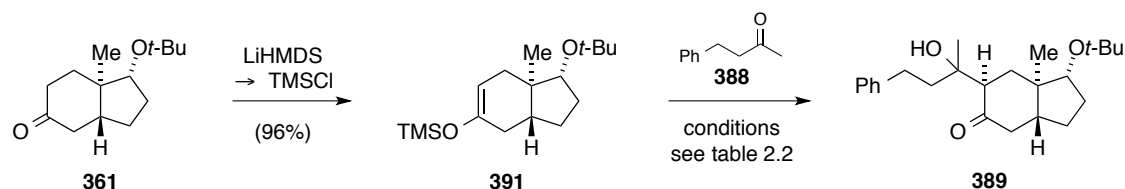
Table 2.1 summarizes the conditions evaluated for envisaged combination of model ketone **361** with either cyclopentane **385** or the in principle equivalent, but commercially available 4-phenylbutan-2-one (**388**, scheme 2.13). Simple enolization of ketone **361** or ZnCl₂-mediated reactions did not result in any of the desired products **389** and **390**, respectively (entries 1,2). Even when the sterically less demanding acetone was used as electrophilic coupling partner, no conversion could be induced. It has to be noted that acetone is well preceded in such ketone-ketone coupling reactions.^[235] Boron-based reagents proved to be ineffective as well (entries 3,4). In 2012, Nakajima and co-workers published a protocol specifically dedicated to enantioselective ketone-ketone aldol additions.^[236] Referring to the concept developed by Denmark,^[237] they describe the use of SiCl₃OTf as

Table 2.5.1: Model studies on the envisaged fragment combination *via* aldol addition.

entry	ketone ^a	solvent	reagents	T [°C]	t [h]	observation
1	388	THF	KHMDS	−78 to rt	2 h	n.r.
2	385, 388	THF	LDA, ZnCl ₂	−78 to rt	5 h	n.r.
3	388	Et ₂ O	(<i>n</i> -Bu) ₂ BOTf ^b , DIPEA	−50 to rt	4 h	n.r.
4	388	Et ₂ O	(Ipc) ₂ BCl, Et ₃ N	−20 to rt	4 h	n.r.
5	385, 388	<i>i</i> -PrCN	Cl ₃ SiOTf ^b , DIPEA, BINAPO	−60 to rt	6 h	n.r.

a) The ketone entry denotes the respective reaction partner of *trans*-hydrindanone **361**. b) The reagent was prepared according to ref. 238.

the Lewis acid and BINAPO (not shown) as the Lewis base activator. In summary, their methodology produces yields up to 88% and *ee*-values that reach 83%. Performing an initial control experiment with ketone **388** and cyclohexanone, the viability of this methodology could be confirmed, although aldol condensation was observed as a significant side reaction. However, when these conditions were applied to substances **361** and **388**, no reaction was triggered at all (entry 5).

**Scheme 2.13:** Synthesis of TMS ether **391** as substrate for Mukaiyama-type aldol additions.

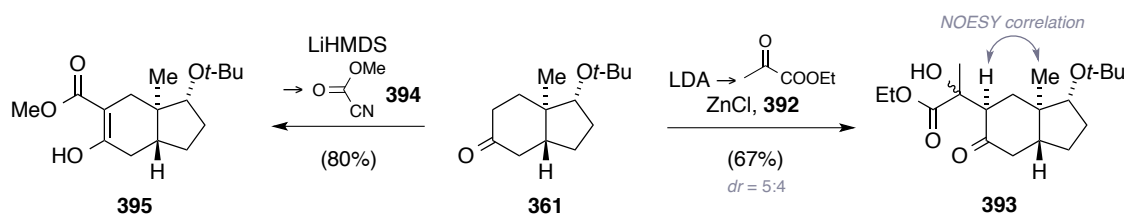
Meanwhile, we also investigated Mukaiyama-type aldol reactions.^[59] Therefore, we prepared TMS ether **391** by deprotonating ketone **361** with LiHMDS and trapping of resulting enolate species with TMSCl in excellent yield (scheme 13). It was observed that the usage of less bulky bases like LDA would result in the formation of considerable amounts of the respective regioisomeric TMS ether. Table 2.2 lists the screened literature-known Mukaiyama aldol protocols. We hoped, that the method developed by Yamamoto and co-workers^[239] would prevent retro-aldol reaction by the *in situ* formation of the respective TMS ethers of the desired aldol products **389** or **390**. Unfortunately, none of the applied conditions worked as intended.

Table 2.5.1: Evaluated literature-known Mukaiyama aldol conditions.

entry	solvent	reagents	T [°C]	t [h]	observation
1	CH ₂ Cl ₂	TiCl ₄ ^a	−78 to rt	2 h	decomp.
2	CH ₂ Cl ₂	TMSOTf	−78 to rt	5 h	loss of TMS
3	CH ₂ Cl ₂	SnCl ₄	−50 to rt	4 h	loss of TMS
4	CH ₂ Cl ₂	Sn(OTf) ₂ , N-ethyl piperidine	0 to rt	4 h	loss of TMS
5	Et ₂ O	HNTf ₂	−60 to rt	6 h	n.r.

a) Commercial and self-prepared solutions of TiCl₄ were tried.

At this point we reasoned that the nucleophilicity of the enolate of *trans*-hydrindane **361** might be too low, or its steric bulk too high, to react with non-activated ketones. To prove this hypothesis, we tried to react substrate **361** with increasingly electrophilic carbonyl compounds like ethyl pyruvate (**392**) under the already investigated ZnCl₂-mediated conditions (scheme 2.14). As suspected, this transformation proceeded smoothly and furnished α -hydroxyester **393** in good yield as a 5:4 mixture of diastereomers. Although the stereochemistry at carbon atom C-2 (retigeranic acid numbering) was elucidated by NOESY NMR measurements to be of the desired *R*-configuration, the obtained diastereomers could not be assigned to the respective configurations of the tertiary alcohol function. The addition of Mander's reagent^[240] (**394**) was reproduced in the course of present doctoral thesis and proceeded with somewhat higher yield of methyl ester **395** than reported previously.^[156]

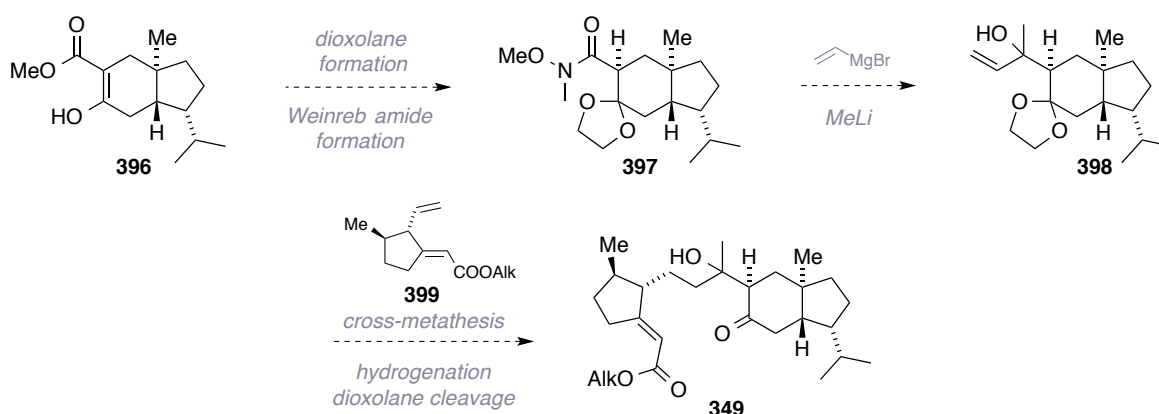
**Scheme 2.14:** Addition of enolized hydrindanone **361** to ethyl pyruvate (**392**) and Mander's reagent (**394**).

In light of the outcome of the conducted experiments, it was decided to abandon the ketone-ketone aldol addition approach. In order to functionalize the C-2 position of substrate **361**, future approaches will have to consider more electrophilic or less sterically demanding reagents.

2.5 Conclusion and Future Aspects

In summary, the synthesis of the B-ring containing cyclopentane building block **385** was accomplished in 8 steps with 20% overall yield and started from commercially available (*R*)-pulegone (**176**) (*cf.* chapter 2.3). To this end, a literature-known three-step sequence was used to access ketoester **311** on a multi-gram scale. Selective 1,3-dioxolane formation *via* Noyori's conditions and subsequent Krapcho decarboxylation formed cyclopentenone **379**, which was successfully olefinated by optimized Horner-Wadsworth-Emmons conditions. Concomitant to the final deprotection step the two decomposition products **386** and **387**, which were formed upon exposure to air, were isolated and characterized. Furthermore, enantiopure *trans*-hydrindanone **361** was synthesized on a multi-gram scale and used as a model system when screening aldol addition conditions (*cf.* chapter 2.2). However, studies toward a more direct installation of the required *trans*-junction in compound **361** were hampered by unprofitably low yields.

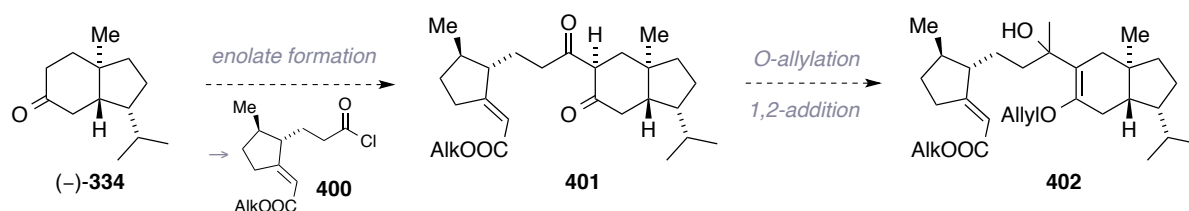
Unfortunately, all conducted attempts toward the desired fragment combination *via* ketone-ketone aldol addition were met with failure (*cf.* chapter 2.4). Although regioselective enolate formation could be demonstrated *via* the synthesis of TMS ether **391**, bisalkyl-substituted carbonyl electrophiles did not react with any of the preformed enolate species. Performing an addition to ethyl pyruvate (**392**) and Mander's reagent (**394**), it was shown that more electrophilic carbonyl species would undergo the desired coupling reaction. Furthermore, the formation of the desired stereochemistry at carbon atom C-2 was proven *via* NOESY correlation in diastereomeric α -hydroxyesters **393**.



Scheme 2.15: Possible second-generation approach toward radical cyclization precursor **349**.

Future approaches toward the desired radical cyclization precursor (**349**) might, for example, start from β -ketoester **396** (scheme 2.15). Transformation to the respective Weinreb amide^[241] and protection of C-12 centered carbonyl as 1,3-dioxolane (**397**) would allow for the addition

of vinyl magnesium bromide.^[242] Subsequent 1,2-addition of methyl lithium^[242], olefin cross-metathesis of alkene **398** with, for instance, building block **399**, hydrogenation and dioxolane cleavage could ultimately yield the desired precursor (**349**). Due to steric hindrance, the metathesis step would most likely require the use of special catalysts systems developed by Stewart and Grubbs.^[244]



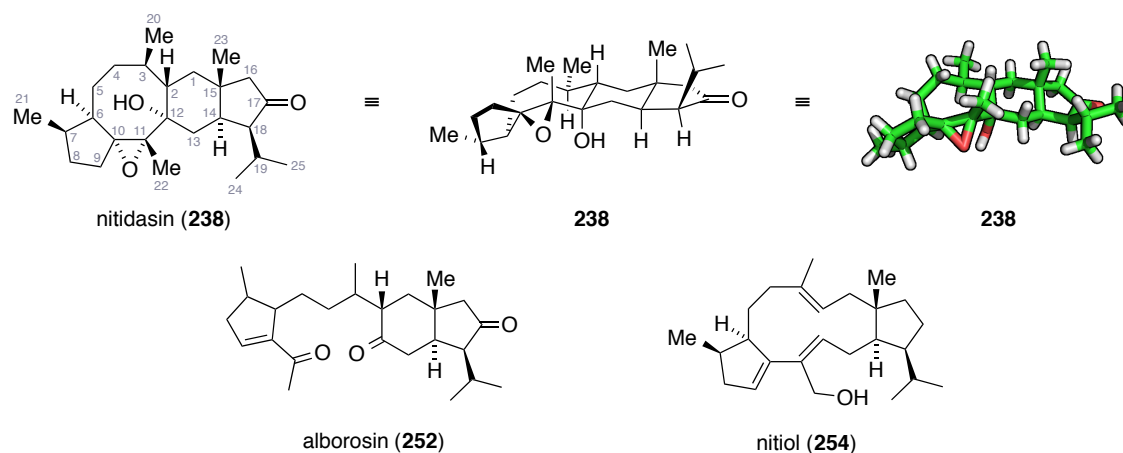
Scheme 2.16: A potential convergent synthesis of envisaged radical cyclization precursor **349**.

Another, more convergent strategy might aim for the construction of a more electrophilic handle for the cyclopentane coupling partner (scheme 2.16). One could envision an enolate addition to acid chloride **400**, which would require an ensuing discrimination of the ketone functionalities in structure **401** in order to selectively install the desired tertiary alcohol at C-3. A possible way to achieve this selectivity was demonstrated by Shibasaki and co-workers *via O-allylation* at a similar 1,3-diketone system for their racemic synthesis of Garsubellin A^[245] (not shown). At this point, selective 1,2-addition to the C-3 centered ketone could prove challenging, but should be achievable by Lewis acid-promoted activation of the ketone functionality. Removal of the allyl moiety in compound **402** would then forge the aspired precursor (**349**).

3. The Total Synthesis of (–)-Nitidasin

3.1 A Comprehensive Introduction to (–)-Nitidasin

The sesterterpenoid nitidasin (**238**) was first isolated in 1997 by the Kawahara group from the biennial plant *Gentaniella nitida*, which can be found in the Andes region.^[154] This gentian species and its close relative *Gentaniella alborosea* together compose the Peruvian traditional folk medicine ‘Hercampuri’, which is used as an aqueous whole plant extract for the treatment of hepatitis, diabetes, hypertension and obesity.^[246] Nitidasin (**238**) was found in the CH₂Cl₂-soluble fractions of the methanolic extract of *G. nitida*, along with various xanthones



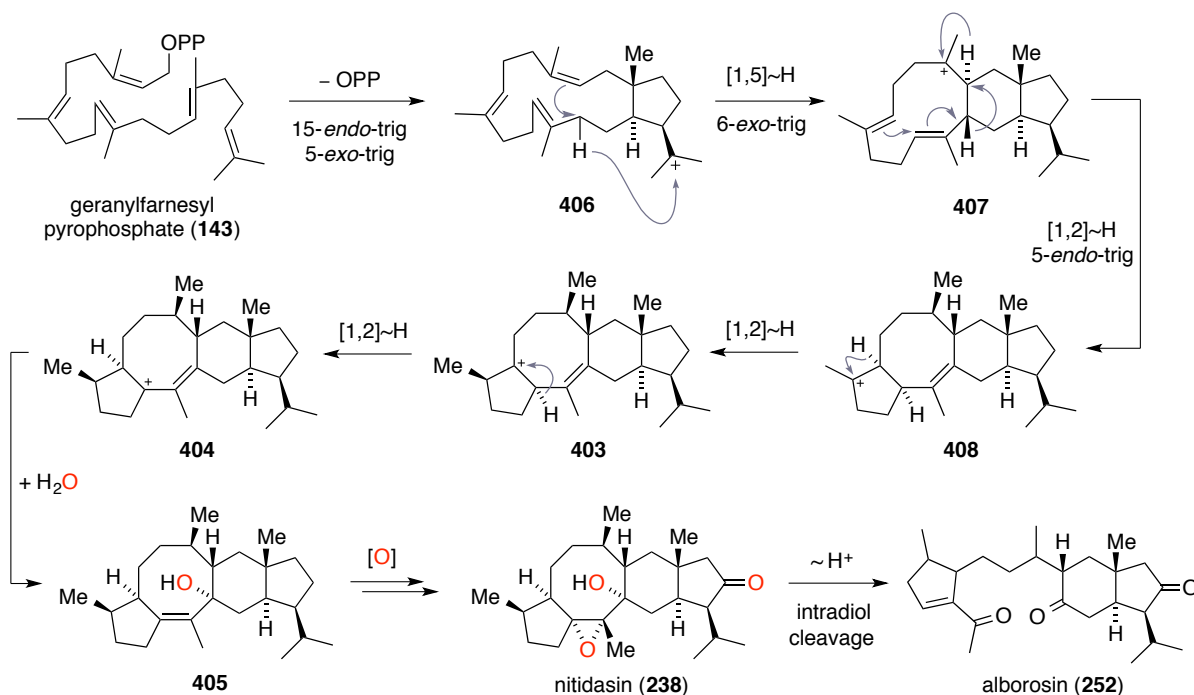
Scheme 3.1: The three sesterterpenoids nitidasin (**238**, flat structure, three-dimensional drawing and crystal structure), alborosin (**252**) and nitiol (**254**), all isolated from the same plant mixture.

and phenolic compounds, and then purified *via* silica gel column chromatography, followed by reversed-phase low-pressure liquid chromatography. Its molecular structure was first proposed by Kawahara and co-worker on the basis of extensive use of 2D NMR methods and later confirmed by X-ray crystallographic analysis (scheme 3.1).^[154]

After aleurodiscal (**239**), nitidasin (**238**) was only the second natural product to be isolated that possesses the extremely rare 5-8-6-5-membered pentacarboxyclic ring system. In total, nitidasin (**238**) contains 10 stereogenic centers, one of which is quaternary. Furthermore, it incorporates the sterically encumbered *iso*-propyl-substituted *trans*-hydrindane portion, which is a common feature of the parent subclass of sesterterpenoids (*cf.* chapter 1.4.1). From a synthetic point of view, nitidasin's (**238**) highly substituted, boat-chair-configured cyclooctane ring poses a considerable challenge. Heteroatom substituents exist only in form of a ketone and a tetrasubstituted epoxide with an adjacent tertiary alcohol. Thus, the

construction of this complex carbon skeleton requires a carefully elaborated retrosynthetic analysis.

To the best of our knowledge, a detailed biosynthetic pathway for the construction of nitidasin (**238**) has not been proposed so far. Due to its inherent structural similarity to astellatol (**213**) and retigeranic acids B (**237**), we reason that the mechanism shown in scheme 3.2 is most likely accountable for nitidasin's (**238**) formation in nature. In this context, the biosynthetic steps starting from geranylfarnesyl pyrophosphate (**143**) to homoallyl cation **403** are the same as published for the biosynthesis of astellatol (**213**) by Simpson *et al.* (*cf.* chapter 4.1).^[200] An ensuing [1,2]-hydride shift would generate the stabilized allyl cation **404**, which then could be trapped by a molecule of water to yield **405**. Epoxidation and final oxidation of carbon C-17 to the ketone functionality will furnish nitidasin (**238**). However, no investigations of the biosynthetic clusters of this and familiar sesterterpenoids have been published up to date.



Scheme 3.2: Proposed biosynthesis of nitidasin (**238**) and alborosin (**252**). Similarities to the biogenesis of retigeranic acid B (**237**) are indicated *via* mimetic drawing (*cf.* scheme 2.3). The oxygen introducing events were highlighted in red.

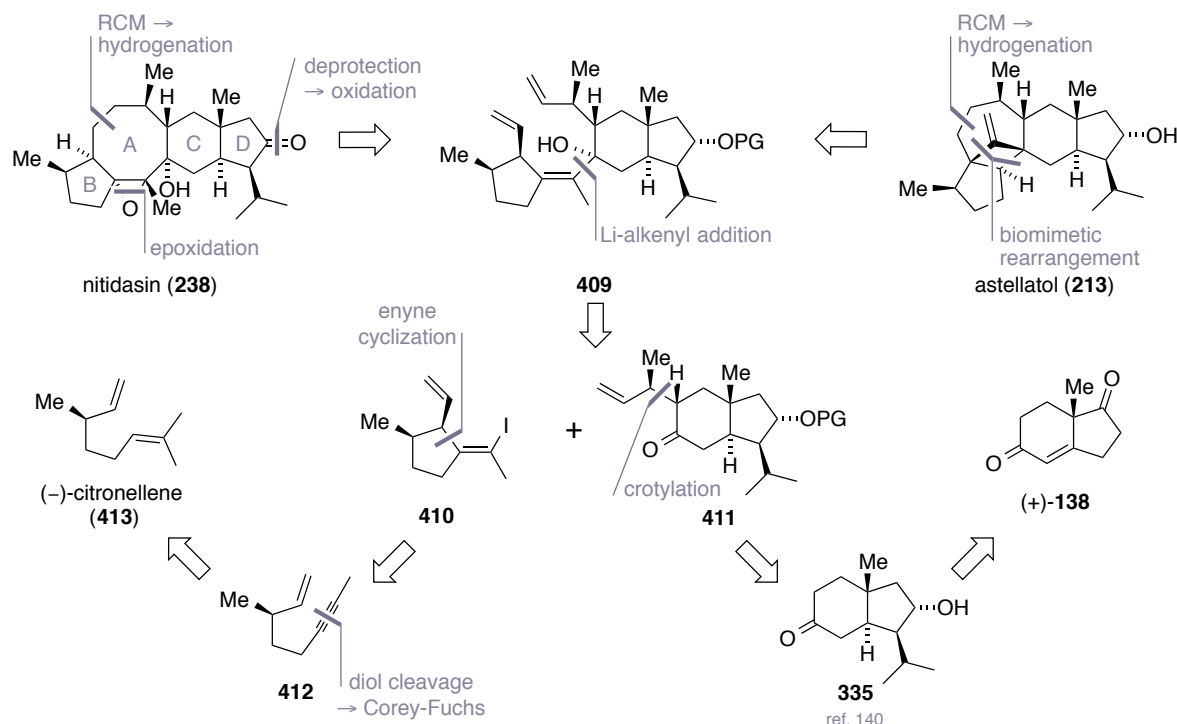
Regarding nitidasin's (**238**) biosynthesis, two directly related natural products have to be mentioned. Again, both compounds were found in 'Hercampuri', as reported by Kawahara and co-workers in 1999. The first was nitiol (**254**),^[171] which was isolated from *G. nitida* itself. The second was named alborosin (**252**)^[169] and was purified from the chloroform extract of *G. alborosea*. Although the relative stereochemistry of alborosin's (**252**) C-3, C-6 and C-7 (nitidasin numbering) located stereocenters was not elucidated, its biosynthetic origin

is hardly speculative. Epoxide opening *via* E1cB-type elimination at atom C-8 and subsequent diol-cleavage by an intradiol enzyme would directly yield alborosin (**252**) from nitidasin (**238**). It has to be noted that despite the solved X-ray structure of nitidasin (**238**), the absolute configurations of the three mentioned sesterterpenoids **238**, **252** and **254** had not been determined prior to present doctoral thesis.

For nitidasin (**238**) itself, no studies on its bioactivity have been published to date. However, it has been shown that the same extracts that contain the identified sesterterpenoids act antifungally against *Candida albicans*, *Trichophyton mentagrophytes* and *Microsporum gypseum*.^[247] Interestingly, nitiol (**254**) has been found to enhance gene expression of interleukin-2 (IL-2) raising its mRNA levels in Jurkat cells by a factor of three.^[171] IL-2 is a polypeptide, responsible for the growth and proliferation of T cells, thus being relevant for the immunotherapy of renal cell cancer and malignant melanoma.^[248] To the surprise of the authors, nitidasin (**238**) did not show any effect in these studies, which levels the question to what purpose this molecule might serve in nature. It was our intention that a total synthesis of nitidasin (**238**), which will be described in the following sections, would provide enough material to continue the investigations into nitidasin's (**238**) biological activity. Synthetic work presented in these chapters was conducted over large parts in cooperation with Dr. D. T. Hog, to whom the author would like to address a special acknowledgement.

3.2 Retrosynthetic Analysis

The retrosynthetic analysis of nitidasin (**238**), which had evolved from more obvious but unsuccessful approaches, envisioned a late-stage substrate-controlled epoxidation and a deprotection/oxidation sequence of a C-17 (nitidasin numbering) located alcohol moiety (scheme 3.3). A first disconnection of the ring system was planned at the C4–C5 bond. In the forward sense, the central ring A was meant to be closed by means of RCM reaction of the corresponding diene containing precursor **409**. Although it was known that approaches toward cyclooctane carbon frameworks generally suffer from predominant side reactions,^[177] it was reasoned that in the presented case the low degree of rotational freedom of structure **409** could possibly result in a favourable conformational preorganization of the system. Triene **409** in turn should be accessed by a highly convergent Li-alkenyl addition of metallated vinyl cyclo-pentane **410** to the ketone functionality of *trans*-hydrindanone **411**. Although this reaction type was unprecedented for tetrasubstituted alkenes, previous experiments conducted



Scheme 3.3: Retrosynthetic analysis for the construction of nitidasin (**238**) from *trans*-hydrindanone **411** and vinyl cyclopentane **410** and possible access to astellatol (**213**) from a common intermediate.

in the Trauner research group had shown that addition to similar *trans*-hydrindane based ketones proceeds smoothly with the desired stereochemical outcome.^[140] A key feature of this retrosynthetic approach is the possibility to access astellatol (**213**) from triene **409** as well, which will be discussed in detail later on (*cf.* chapter 4).

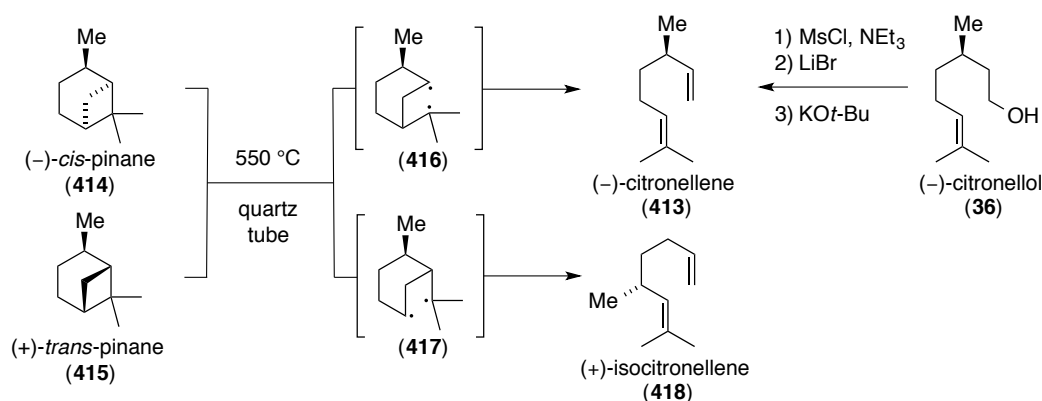
For the preparation of vinyl cyclopentane building block **410**, which comprises a *cis-cis-cis* relationship of its ring and double bond substituents that had not been accessed prior to this work, an iodide source-quenched metalla-enyne cyclization was envisaged. In the forward sense, this should be followed by an elimination/hydroboration sequence to correct the stereochemistry at C-6. Thereafter, oxidation to the aldehyde and subsequent Wittig olefination would construct the desired monosubstituted alkene. Enyne **412** was planned to be obtained from commercially available (-)-citronellene (**413**) *via* a literature-known diol cleavage protocol,^[249] followed by a methyl iodide-quenched Corey-Fuchs homologation.

Ketone building block **411** would in principle arise *via* diastereoselective crotylation of alcohol protected *trans*-hydrindanone **335**. Initially, we planned to address this challenging transformation by an *O*-alkylation/Claisen rearrangement procedure or by regioselective intramolecular allylation, which had been reported for similar systems by Nicolaou and co-workers in their colombiasin A synthesis (not shown).^[250] However, we eventually had to use a more lengthy, but scalable 9-step route. This protocol was originally investigated by Dr. D. T. Hog^[156] and was modified to the more robust SEM protecting group for C-17 centered

alcohol (*cf.* chapter 3.4). The synthesis of required alcohol **335** has been published previously by the Trauner laboratories and would be achieved in eight transformations on the respective enantiomeric series of already the described *trans*-hydrindane **361** (*cf.* chapter 2.3).^[140]

3.3 Synthesis of the Vinyl Cyclopentane Moiety

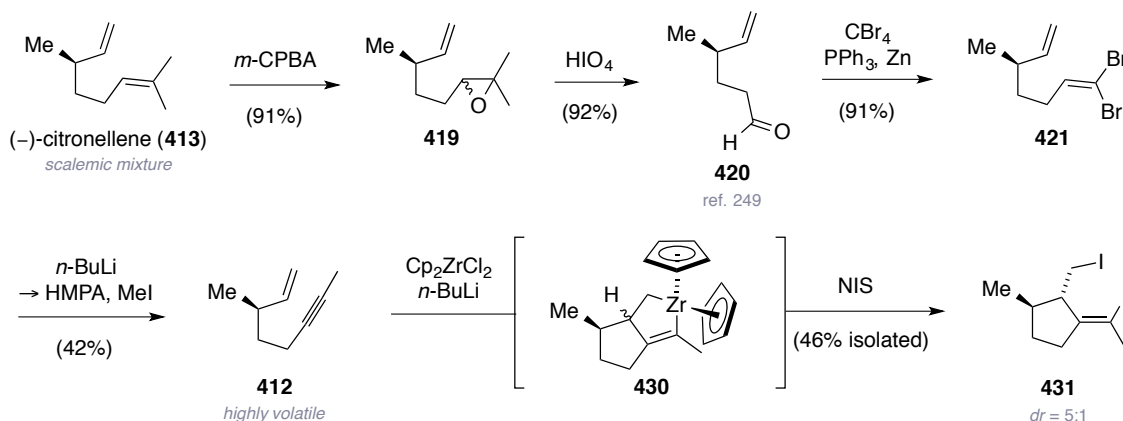
Presented studies toward the synthesis of vinyl cyclopentane **410** commenced from commercially available (–)-citronellene (**413**), which was at that time available as a technical grade, enantioenriched mixture. This mixture results from its industrial origin, where it is prepared *via* pyrolysis from (–)-*cis*- (**414**) and (+)-*trans*-pinane (**415**), which in turn often stem from synthesis *via* catalytic hydrogenation of pinene composites.^[251,252] Detailed mechanistic studies on this thermal transformation have been published, revealing that a biradical mechanism (**416** and **417**) has to be accounted for and that the formation of (–)-citronellene (**414**) itself would be highly enantioselective (scheme 3.4).^[253] Thus, the exact enantiomeric ratio of the employed starting material was unknown initially and would depend on the purity of its pinane precursor. Nevertheless, it was reasoned that it should be sufficient for initial synthetic studies. Enantiopure diene **413** can be accessed *via* a bromination/elimination sequence from commercial, but somewhat expensive, (–)-citronellol (**36**).^[254]



Scheme 3.4: Industrial synthesis of (–)-citronellene (**413**) and its side product **418**, together with a possible literature-known route toward enantiopure (–)-citronellene (**413**).^[253,254]

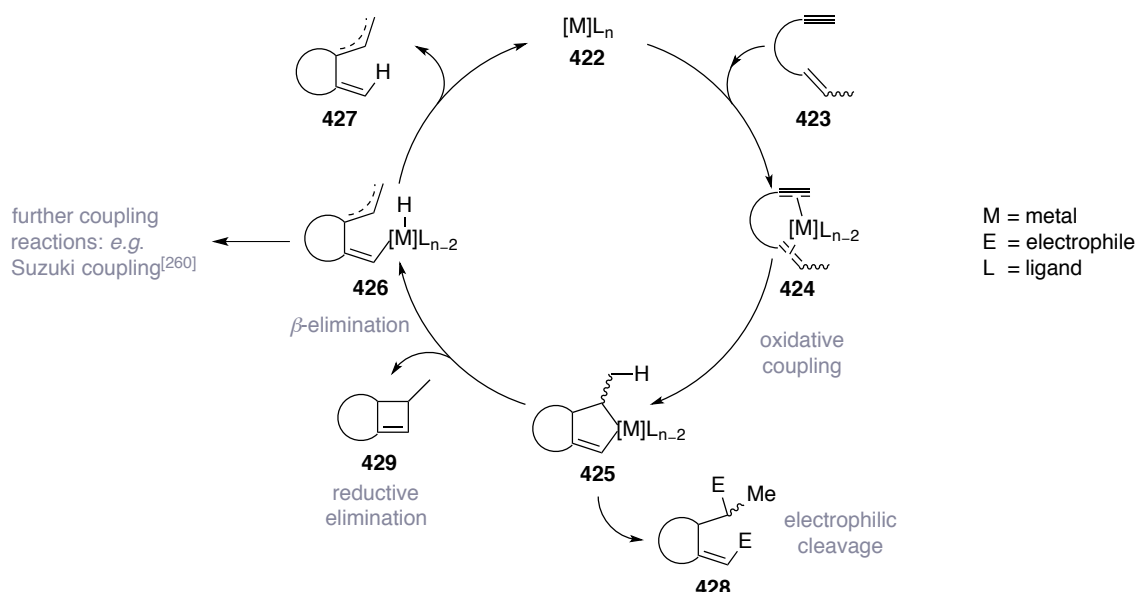
Using the scalemic mixture of diene **413**, the trisubstituted and more electron-rich double bond was first epoxidized chemoselectively with *m*-CPBA in CH₂Cl₂. The isolated inconsequential mixture of diastereomers (**419**) was then submitted to periodic acid-mediated diol cleavage conditions in diethyl ether, all according to a published protocol (scheme 3.5).^[249] Yields and analytical data toward aldehyde **420** were comparable to the literature and are not further specified in the experimental section of present manuscript. Subsequent transformation of aldehyde **420** to dibromoalkene **421** proceeded smoothly in

good yield *via* modified Ramirez reaction conditions,^[255] employing zinc to lower the required amount of PPh₃ and resulting OPPh₃ to one equivalent. When standard Corey-Fuchs homologation conditions were applied to dibromoalkene **421**,^[256] quenching the *via* Fritsch-Buttenberg-Wiechell rearrangement^[257] intermediary formed alkynyl lithium species with methyl iodide, complete and clean conversion was observed. However, enyne **412** proved to be highly volatile, which significantly decreased the obtained yield to 42%, even when being concentrated carefully from *n*-pentane by distillation using a Vigreux column.



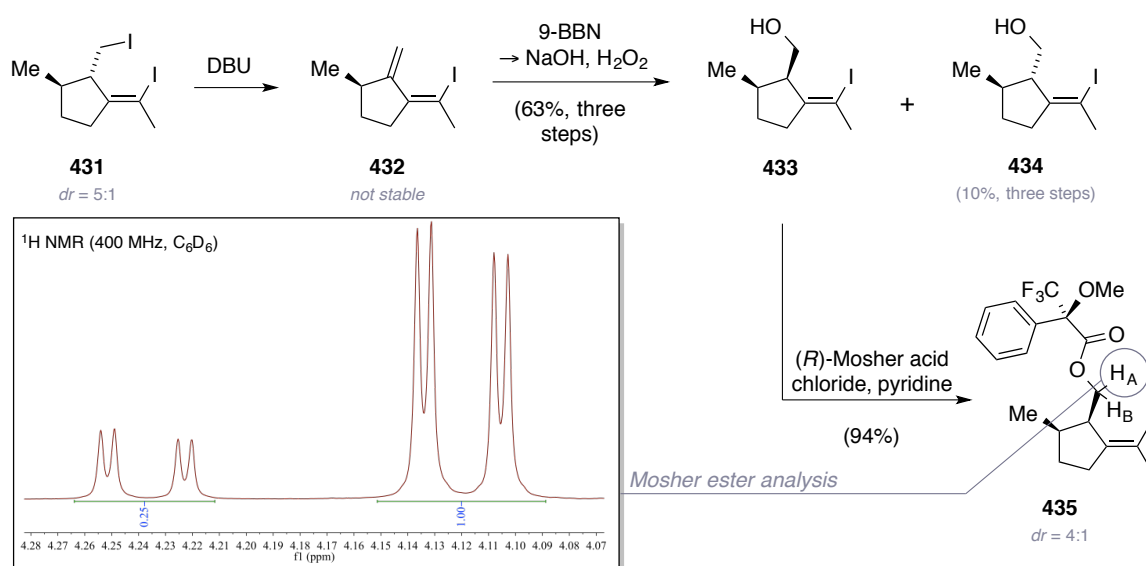
Scheme 3.5: Synthesis of diiodide **431**, starting from commercially available scalemic (-)-citronellene (**413**). Only the major diastereomer of diiodide **431** is shown for clarity.

Next, the focus was turned toward the planned enyne cyclization step, for which a variety of different methods has been developed over the years.^[258] Scheme 3.6 provides a general version of the catalytic cycle present in those transformations. As a metal source, different possible options exist, ranging from Pd, Pt, Ru, Ni, Au, Fe, Co, In to Ti and Zr. Even combinations of these with other organometallic reagents have been reported. In the begin-



Scheme 3.6: General catalytic cycle for metal-mediated enyne cyclization reactions.

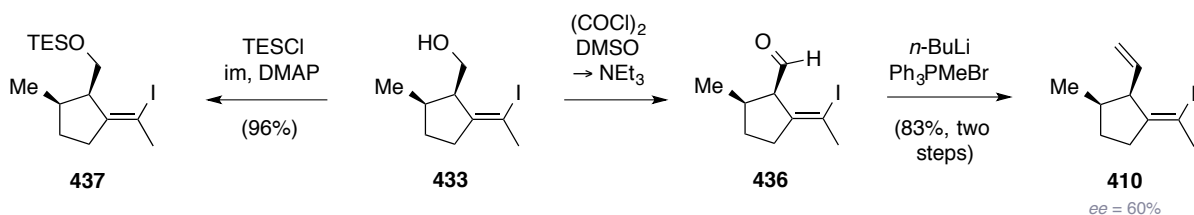
ning, the metal species (**422**) coordinates to an enyne substrate (**423**) and forms a chelated π -complex (**424**). An oxidative coupling then generates a metallacycle (**425**). However, most of the described choices for the metal would preferentially undergo β -elimination at this intermediate (**425**). This would yield an alkene substituent (*cf.* structures **426** and **427**) at carbon C-6 (nitidasin numbering) with an undesired *trans*-configuration in respect to the C-7 centered methyl group.^[258] Several synthetic steps would be required to correct mentioned stereocenter and thereafter to restore the alkene functionality. Although Pd-catalyzed protocols have been published, *e.g.* by Lu and co-workers, that target the construction of a *cis*-relationship at C-6 and C-7, those methods suffer from inversion of the stereochemistry of the halogen substituent.^[259] Metallacycles derived from group 4 metals (Ti, Zr) possess no vacant site of coordination and are inert toward β -elimination. Consequently, they are able to react selectively with one or two equivalents of an electrophile (*cf.* structure **428**).^[258] In this context, especially a method developed in 1992 by Negishi and co-workers seemed attractive, where the authors describe the stoichiometric use of a 14-electron Cp_2Zr species that can be generated from two equivalents *n*-BuLi and Cp_2ZrCl_2 .^[261] By reacting the intermediary formed zirconacycle with two equivalents of I_2 , it was possible to access the respective alkenyl-alkyl-diiodides, having the desired stereochemistry at the iodoalkene moiety. When this methodology was adopted for substrate **413**, the best results were obtained when quenching the initially formed complex **430** with NIS.^[262] Cp_2TiCl_2 showed the same reactivity, but did not result in improved yields.^[263]



Scheme 3.7: Elimination/hydroboration sequence to synthesize alcohol **433** and Mosher ester analysis thereof (**435**, only major isomer shown). The magnified ¹H NMR spectra exemplifies the obtained ratio of diastereomers, arising from scalemic (–)-citronellene (**413**).

Purification *via* column chromatography allowed for the isolation of diiodide **431** as an inconsequential diastereomeric mixture of 5:1 in an acceptable 46% yield.

As diiodide **431** was not indefinitely stable and still somewhat volatile, we were delighted when it was found that yields would significantly rise, when diiodide **431** was only shortly filtered over silica and used as such for further transformations (scheme 3.7). Elimination of the alkyl iodide substituent with DBU furnished diene **432**, which exhibited partial isomerization at the *cis*-iodo position to the *trans*-compound on an hour time scale upon purification. The driving force of this isomerization is most likely the inherent high 1,3-allylic strain of the molecule. Thus, the following hydroboration step was conducted with crude diene **432** immediately after its extraction. For this transformation, 9-BBN was found to be the best choice as the bulkiness of this hydroboration reagent enhances the facial bias of the stereogenic methyl group of the substrate. Counting from enyne **412**, the desired alcohol **433** could be obtained on gram scale in three steps in excellent 63% yield along with 10% of the undesired isomer (**434**).



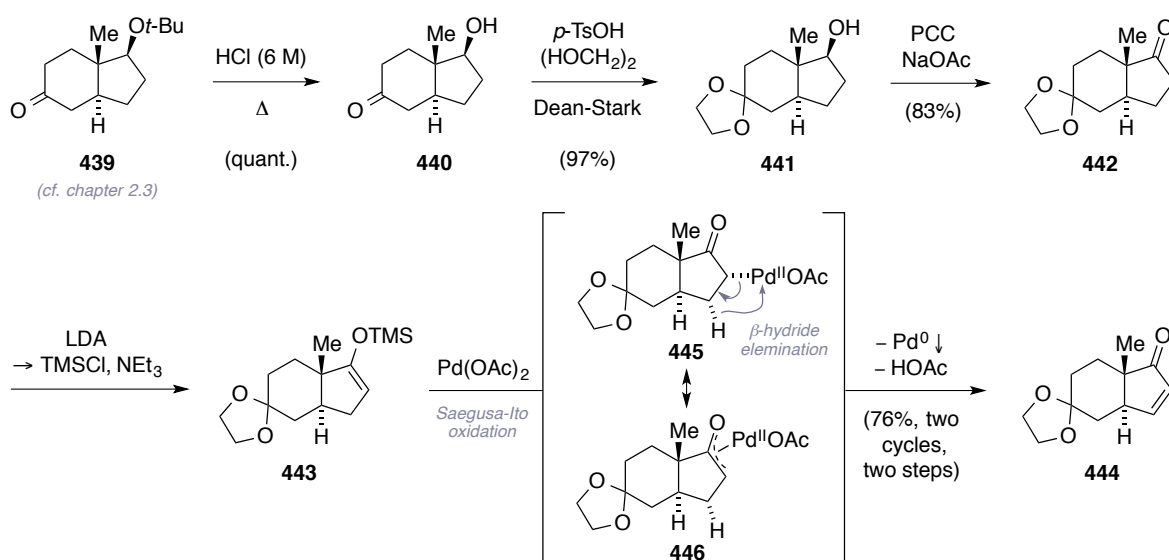
Scheme 3.8: Synthesis of diene **410** and TES protected alcohol **437** as substrates for envisaged Li-alkenyl addition step (*cf.* chapter 3.2).

Having set the desired stereochemistry, preferably neutral pH conditions were screened for the oxidation of alcohol **433** to aldehyde **436** as an olefination precursor (scheme 3.8). Initial experiments referred to classical Swern conditions, using oxalyl chloride, DMSO and then DIPEA, or Dess-Martin periodinane-mediated oxidation, failed and led to decomposition of alcohol **433**. Ley oxidation, which is supposed to be one of the mildest methods,^[264] did result in the formation of aldehyde **436**, but only in moderate yield. Interestingly, when we revisited Swern-type conditions, this time using triethylamine as a base- and phosphate-buffered work-up, aldehyde **436** was furnished cleanly as a single diastereomer. This indicated that no epimerization at C-6 had taken place. Otherwise, a thermodynamic mixture of isomers would be expected to be visible in ¹H NMR spectra of the crude reaction mixture. It is assumed that considerable 1,3-allylic strain renders enolization energetically unfavourable in this system, despite the potentially resulting conjugated system. Subsequent Wittig olefination with *in situ* generated Ph₃PCH₂ proceeded smoothly and yielded stable diene **410** in excellent 83% over two steps. Whilst investigating the oxidation/olefination protocol, the TES protected alcohol

437 was already synthesized as an alternative coupling partner for the envisaged fragment combination step (*cf.* chapter 3.2). On the one hand, this would require a less convergent construction of the *C*-7 alkene handle after coupling, but on the other hand provide a possibly more stable lithium alkenyl species ($pK_A \approx 42$), due to the lack of a comparably acidic bisallylic proton at carbon *C*-6 ($pK_A \approx 35$).^[265]

3.4 Synthesis of the *trans*-Hydrindanone Moiety

The following chapter will describe the syntheses of coupling fragment **411** and of the more conveniently accessible model system **438** (*cf.* scheme 3.16), which start from Hajos-Parrish-Eder-Sauer-Wiechert ketone (**138**).^[76] As the first steps toward ketone **439** have already been described in detail in chapter 2.3 at the respective enantiomeric series, they will not be shown again. The synthetic protocol for the preparation of alcohol **335** has been published by the Trauner research group previously.^[140,156] The detailed evolution of these methods is outlined in corresponding references.^{vi} Present manuscript will only provide information about the successfully adopted transformations.

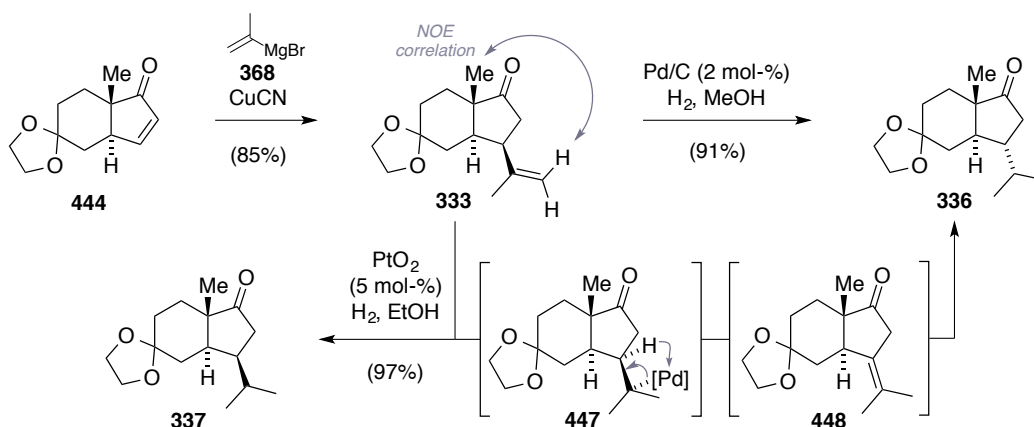


Scheme 3.9: Synthesis of enone **444** from **439** and the involved intermediary formed Pd-allyl species **445** and **446** of the Saegusa-Ito oxidation step.

The sequence commenced with the deprotection of ether **439** with aqueous HCl (6 M) in ethanol under refluxing conditions (scheme 3.9). Although these conditions are quite harsh, no elimination or rearrangement-caused side products were observed and alcohol **440** was furnished quantitatively. Protection of compound **440** with ethylene glycol was carried out

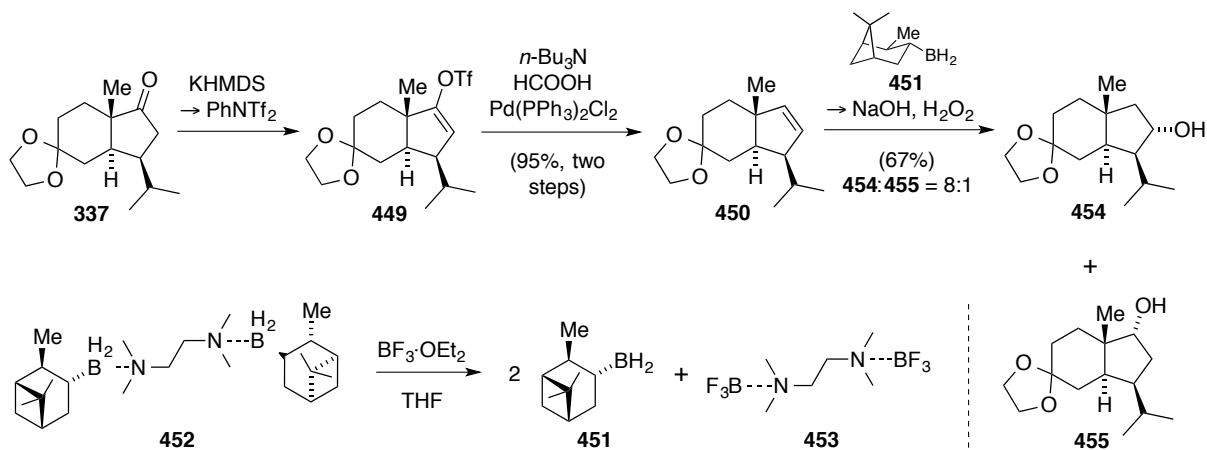
^{vi}Employed synthetic protocols have been developed by Dr. D. T. Hog.

under standard acid-catalyzed (*p*-TsOH) conditions, removing the formed water *via* azeotropic distillation from toluene using a Dean-Stark apparatus.^[266] Thus, 1,3-dioxolane **441** was isolated in excellent yield on multi-gram scale. The following transformation to ketone **442** was achieved *via* NaOAc-buffered PCC oxidation. When conducted on large scale, it proved to be crucial to thoroughly elutriate and wash the resulting slimy precipitate of reduced chromium species to achieve consistency of the yields. In such a way, ketone **442** was obtained as a highly crystalline solid and could be purified from remaining trace amounts of respective *cis*-hydrindane derivative (not shown), *via* recrystallization from *n*-hexane at 4 °C. Notably, the determined yield exceeded the previously described one by 12%.^[140] With this material in hand, the unsaturation of the cyclopentanone moiety was center stage. Previous experiments had shown that classical Saegusa-Ito conditions^[267] would perform best in this transformation.^[156] Conversion of ketone **442** to TMS ether **443** proceeded smoothly by deprotonating with LDA and intercepting the formed enolate with TMSCl in the presence of triethylamine. Silyl ether **443** was used crude after simple basic work up, extraction and thorough drying *in vacuo*. Oxidation with stoichiometric amounts of Pd(OAc)₂ in a mixture of CH₂Cl₂ and MeCN at 40 °C yielded enone **444**, along with small quantities of recovered ketone **442**. This is due to TMS ether cleavage by acetic acid that takes place over the course of the reaction. Resubmitting this material to the same two-step protocol led to an overall yield of enone **444** of 76%. At the Saegusa-Ito oxidation the mechanistically relevant η^1 -allyl (**445**) and η^3 -allyl (**446**) Pd^{II} species undergo β -hydride elimination and subsequent reductive formation of acetic acid under concomitant precipitation of Pd⁰.^[268] Due to the high costs of stoichiometric use of Pd reagents, either recovery of formed Pd⁰ *via* filtration (conducted during present thesis) and laborious re-conversion to Pd(OAc)₂,^[269] or the utilization of catalytic variants of the Saegusa-Ito oxidation are worth considering. Various methods for the *in situ* re-oxidation of Pd⁰ to Pd^{II} have been described, such as the use of benzoquinone,^[270] oxygen atmosphere using DMSO as a solvent or in combination with enamine co-catalysis,^[271] Pd(OH)₂ with *t*-BuOOH,^[272] and the oxidation of allyl enol carbonates by catalytic amounts of Pd(OAc)₂ and diphenylphosphinoethane.^[273] Unfortunately, those methods suffer from lower and sometimes not consistently reproducible yields. However, Lebel and co-workers recently published a method that employs inexpensive Oxone[®] as co-oxidant and could demonstrate that this allows obtaining yields largely comparable with the uncatalytic parent protocol.^[274] As the focus of present doctoral studies lay on the principal development of a synthetic route toward nitidasin (**238**), we have not revisited this synthetic step by evaluating Lebel's conditions, yet.



Scheme 3.10: Stereoselective cuprate addition and stereochemical diversification by hydrogenation with different heterogeneous metal catalysts.

For the installation of the *iso*-propyl substituent at C-18 the use of Normant-cuprate-based nucleophiles was intended. This was largely encouraged by procedures published by Molander and Bull, at which they surprisingly observed the addition of methyl or *iso*-propenyl cuprates from the more sterically hindered *pro-S* face of their *trans*-hydrindane system.^[275] In our hands, *iso*-propyl-based cuprate addition had only given unsatisfying results,^[156] presumably due to lower reactivity compared to alkenyl cuprates and the inherent tendency toward β -hydride elimination.^[276] Addition of superstoichiometric amounts of *iso*-propenyl-based Normant-cuprate, generated from two equivalents *iso*-propenyl magnesium bromide (**368**) and CuCN at $-78\text{ }^{\circ}\text{C}$, yielded desired saturated *trans*-hydrindanone **333** in 85% on 1.8 g scale (scheme 3.10). Reaction on higher scale was avoided due to a decrease in yield, which is probably attributed to a less efficient heat transfer that leads to undesired side reactions. The structure of addition product **333** was confirmed *via* NOE correlation of the angular methyl group to the *iso*-propenyl substituent and later on unambiguously *via* X-ray crystallographic analysis.^[156] In collaboration with the research group of Houk we set out to investigate the observed selectivity theoretically and the identified determinants will be published in due course. Reduction of the introduced alkene *via* heterogeneous catalytic hydrogenation had previously yielded an unexpected diversification that became the central motif of our unified approach toward *iso*-propyl-substituted *trans*-hydrindane sesterterpenoids (*cf.* chapter 1.4.3).^[140] When Pd/C (2 mol-%) was employed in methanol as solvent system, hydrogenation (1 atm H₂) resulted in a concomitant inversion of the stereogenic *iso*-propyl substituent and primarily ketone **336** was yielded.^[256] This is attributed to the inherent ability of transition metal-based catalysts to achieve the involved initial hydropalladation step (**447**) in equilibrium, thus rendering double bond migration into neighboring positions possible.^[277] In the presented case, this led



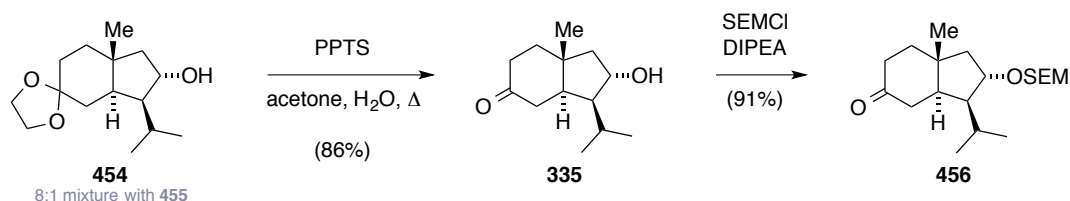
Scheme 3.11: Stereocontrolled installation of the C-17 centered alcohol functionality and preparation of (-)-Ipc borane (**451**) for the hydroboration step.

to isomerization of stereocenter C-18. At this, hydrogenation of alkene **448** would again occur *syn* to the angular methyl substituent (scheme 3.10). Gratifyingly, when Adams' catalyst (PtO₂, 5 mol-%) was used instead and the solvent system altered to ethanol, desired hydrindanone **337** was obtained exclusively. The latter finding was also reported by Reddy *et al.* on a similar *trans*-hydrindane-based substrate.^[278]

Next, the construction of the C-17 centered alcohol was conducted, which had to be achieved stereoselectively for a potential synthesis of astellatol (**213**) and the YW compounds (**240** and **241**) from common intermediates. In order to access alcohol **335**, an alkene functionality was introduced first *via* a two-step Pd-catalyzed reductive hydride coupling (scheme 3.11). To this end, ketone **337** was converted to its respective enol triflate (**449**), using KHMDS and then PhNTf₂. After extraction and removal of the solvents *in vacuo*, the crude triflate was heated with *n*-Bu₃N, formic acid and Pd(PPh₃)₂Cl₂ in DMF. Under these conditions, that were originally developed by Cacchi and co-workers,^[279] a Pd–H source is generated from formic acid by expelling CO₂. This Pd–H species then undergoes reductive coupling to the alkenyl-ligand generated from the oxidative insertion of Pd⁰ into the carbon-oxygen bond of triflate **449**. The whole two-step protocol proved to be highly scalable and yielded alkene **450** in excellent 95% on 4.7 gram scale.

Hydroboration of alkene **450** was best achieved using chiral (-)-Ipc borane (**451**) in a matched case. It has been shown that different borane-based reagents would result in lower diastereo- and regioselectivity of the transformation.^[156] Due to a lack of commercial availability, (-)-Ipc borane (**451**) had to be prepared freshly from (S)-Alpine-BoramineTM (**452**) by addition of two equivalents of BF₃·OEt₂.^[280] After separation from precipitated TMEDA adduct **453**, (-)-Ipc borane (**451**) was obtained as a solution in THF and immediately used for hydroboration of alkene **450** in THF at 0 °C. Ensuing treatment with

H₂O₂ and aqueous NaOH furnished alcohol **454** in perfect facial selectivity in an 8:3 mixture with its regioisomer **455**. Thorough separation by flash column chromatography allowed enriching of alcohol **454** to a ratio of 8:1 in 67% yield.

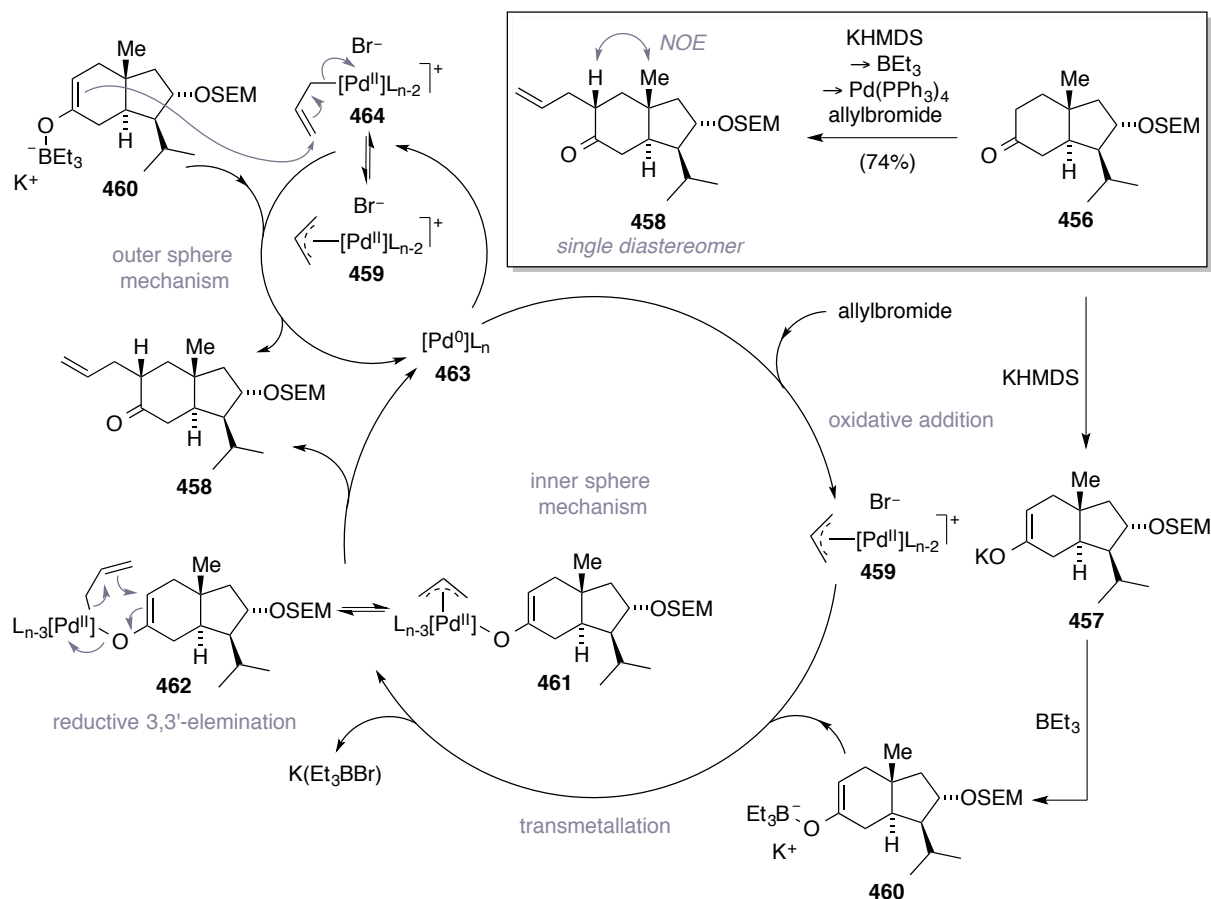


Scheme 3.12: Dioxolane cleavage and SEM ether formation toward *trans*-hydrindanone **456**.

Having synthesized gram quantities of dioxolane **454**, the ketone protecting group was removed using PPTS in an acetone/water mixture,^[281] in order to activate position C-2 for further functionalization (scheme 3.12). Here it was possible to remove remaining contents of the regioisomeric alcohol conveniently *via* flash column chromatography. In the following, it was intended to protect the alcohol functionality in substance **335**. Earlier experiments had shown that a TBS ether would not allow for an orthogonal cleavage of a secondary TES ether (*vide infra*) in the later stages of the synthesis.^[156] Besides, we were hesitant to employ hydrogenation labile hydroxyl protecting groups like benzyl ethers,^[266] as for a potential total synthesis of astellatol (**213**), its *exo*-methylene group would pose a venturous selectivity challenge. Hence, the 2-(trimethylsilyl)ethoxymethyl (SEM) protecting group was chosen, which would on the one hand provide considerable stability against a variety of chemical transformations and on the other hand should be cleavable *via* basic fluoride conditions.^[266] Using SEMCl in DIPEA, SEM ether **456** was isolated in excellent yield on gram scale.

A further challenge in our retrosynthetic plan was the installation of the stereocenters located at C-2 and C-3.^{vii} As it was already demonstrated that the stereo selectivity of enolate-based functionalizations at C-2 (*cf.* chapter 2.5) proceeds in favour of the desired configuration, it was tried to adopt these findings for a stereocontrolled crotylation of ketone **456**. Tsuji crotylations *via* a mixed carbonate were ruled out due to the difficulties associated with diastereoselectivity and mixtures of branched and linear products.^[250,282] Furthermore, early experiments in our group revealed that *O*-alkylation of enolates, generated from similar *trans*-hydrindanones, would not proceed or rather yield attack *via* the non-stabilized carbon centered anion.^[156] Accordingly, a Claisen rearrangement approach that would form both stereocenters *via* a chair-like 6-membered transition state, could not be evaluated to date.

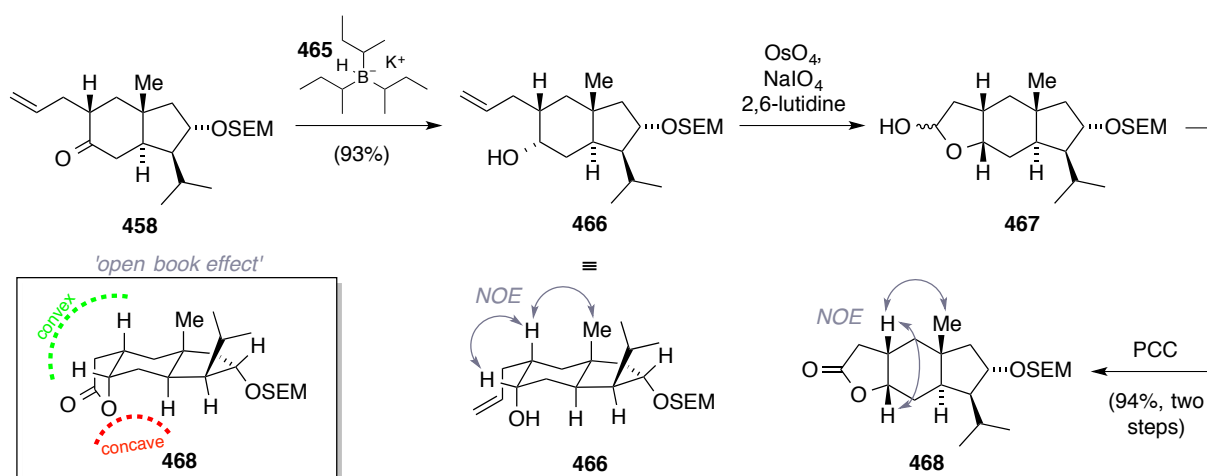
^{vii}The further synthetic sequence until alkene **475** was first evaluated on test system **439** by Dr. D. T. Hog^[156] and experimental work toward the preparation of alkene **477** was conducted in cooperation.



Scheme 3.13: Pd-catalyzed allylation of SEM ether **456**. Outer and inner sphere mechanisms are still subject of scientific debate.

Fortunately, studies published by Covey and co-workers on the construction of rearranged steroid systems had shown that *trans*-hydrindanone **439** can be regioselectively allylated with allylic electrophiles.^[283] Using potassium enoxyborates in the presence of catalytic amounts of Pd(PPh₃)₄, they were able to achieve allylation at carbon C-2 with the required diastereoselectivity. Employed methodology was originally developed by Negishi and co-workers in the early 1980's and can be applied to a broad variety of ketones.^[284] When this protocol was adopted, Covey's results on ketone **439** were reproduced first (*cf.* chapter 4.2) and it was recognized that this procedure is highly sensitive toward oxygen, presumably due to the use of alkylboron species. Gratifyingly, the established SEM ether **456** underwent the envisioned allylation as well (scheme 3.13). Regioselective generation of the potassium enolate (**457**) with KHMDS at room temperature was followed by transmetalation to boron using a self-prepared and thoroughly degassed solution of triethylborane at –78 °C. Subsequent addition of distilled allylbromide and Pd(PPh₃)₄ (7.5 mol-%) resulted in 74% yield of alkene **458** as a single diastereomer. The relative configuration at the newly formed stereocenter was again proven by 2D NOESY correlation between the angular methyl group and the C-2 located methine proton. The mechanisms of Tsuji-Trost allylations are currently

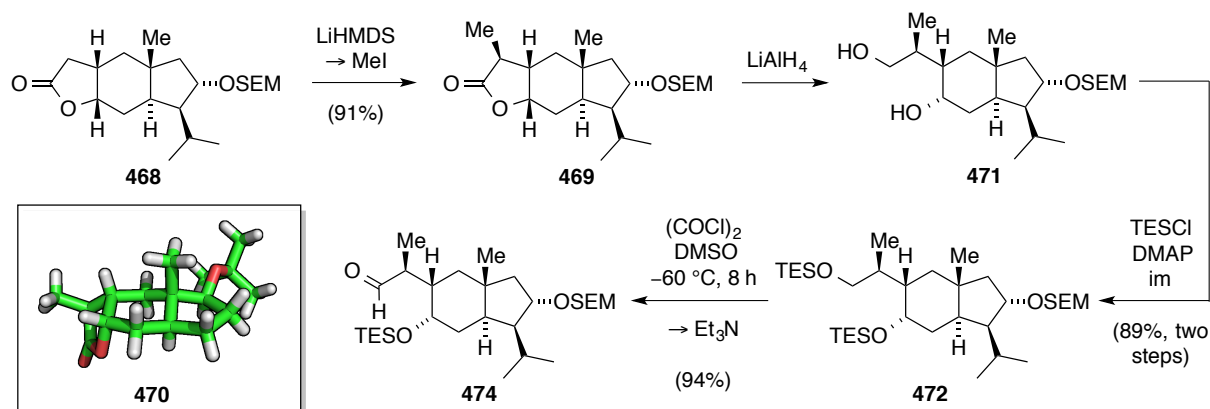
still under investigation by the chemical community.^[282d] It is undisputed that the catalytic cycle begins with the oxidative addition of Pd⁰ to allyl bromide to form Pd^{II} π -allyl species **459**. For a so-called inner sphere mechanism, transmetalation of enoxyboronate **460** would yield a Pd^{II} π -allyl species, which could be formulated either as a η^1, η^3 - (**461**) or as the respective η^1, η^1 -complex (**462**). A reductive 3,3'-elimination process then furnishes the desired allylated compound **458** and regenerates the initial Pd⁰ species (**463**). Evidence for the inner sphere mechanism has been given by Stoltz and Goodard by their calculations on enantioselective decarboxylative Tsuji allylations.^[285] However, calculated differences in transition state energies for inner- and outer sphere mechanisms sometimes resided only in the region of 1.6 kcal/mol.^[285b] Notably, the described 7-membered transition states, which are comparable to structure **462**, seem to be 41 kcal/mol lower in energy than the respective 'conventional' 3-center reductive elimination. The inner sphere mechanism provides a convenient explanation for the regioselectivity often observed for branched substrates.^[286] The outer sphere mechanism can be formulated as an S_N2'-type attack of enoxyboronate **460** at η^1 -Pd^{II} π -allyl species **464**. Proof for the occurrence of such a reaction pathway has been found by Helmchen and co-workers for Pd-catalyzed allylations of stabilized enolates.^[287]



Scheme 3.14: Synthesis of tricyclic lactone **468** and illustration of the so-called 'open book effect' on a three-dimensional drawing of this compound.

In order to construct the C-3 located stereocenter, it was planned to perform a substrate-controlled diastereoselective methylation. In particular, it was intended to tie back the allyl substituent to the cyclic carbon skeleton, preferably as a lactone to facilitate C–H activation. In literature this is often described using a reduction/ozonolysis sequence with subsequent oxidation of formed cyclic lactole.^[288] Accordingly, we reduced ketone **458** with the sterically demanding hydride source K-Selectride® (**465**) in THF, which selectively furnished alcohol **466** in excellent yield (scheme 3.14).^[288b,289] This proceeds *via* an equatorial nucleophilic

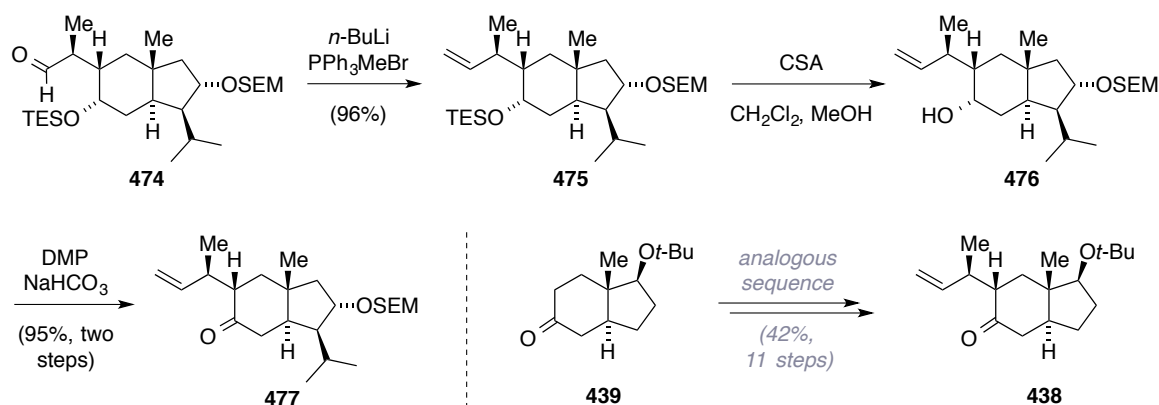
attack that is directed by the steric clash between the angular methyl group and the hydride source **465**. The configuration of formed stereogenic alcohol was elucidated *via* 2D NOESY experiments. In the following, a Lemieux-Johnson oxidation protocol^[290] proved to be best for the conversion of substrate **466** to cyclic lactol **467**. This procedure includes dihydroxylation, diol cleavage and intramolecular lactone formation in one-pot. Using catalytic amounts of OsO₄, accompanied by NaIO₄ and 2,6-lutidine in 1,4-dioxane/water at room temperature, lactol **467** was obtained as an inconsequential mixture of diastereomers, which was immediately subjected to PCC-mediated oxidation. Thus, γ -lactone **468** could be isolated in 94% yield over two steps. Scheme 3.14 illustrates the so-called ‘open book effect’ inherent to bicyclic systems with *cis*-junction. Any kind of reagent will approach from the convex rather than from the considerably more shielded concave face. The desired methylation then proceeded smoothly in excellent 91% yield and produced lactone **469** as a single diastereomer by deprotonating with LiHMDS in THF (scheme 3.15). A similar methylation of a *cis*-hexahydrobenzofuranone system has been described *e.g.* by Wipf *et al.* in their synthesis of (-)-tuberostemonine (not shown).^[291] Although the stereochemical outcome of these methylations is well preceded in literature,^[292] it was additionally verified *via* X-ray crystallography on model system **470** in a prior report.^[156,293]



Scheme 3.15: Diastereoselective methylation of lactone **468** and further transformation to aldehyde **474** *via* reduction with LiAlH₄, double TES protection and deprotective Swern oxidation. The crystal structure of lactone **470** was reproduced from ref. 156.

In order to restore the alkene handle required for the envisaged RCM step, lactone **469** was reduced with LiAlH₄ in THF, which furnished diol **471** cleanly. In principle, diol **471** was already pure enough for the following TES protection after simple extraction and concentration. Thus, bis-silyl ether **472** was accessed *via* reaction with TESCl and imidazole using catalytic amounts of DMAP in 89% yield over two steps. The use of more expensive TESOTf in combination with the base 2,6-lutidine was also possible and led to equally good

yields for test system **473** (*cf.* chapter 4.3). For the selective deprotection and oxidation of the primary alcohol function in compound **472**, a deprotective Swern oxidation protocol was applied, which is known to be able to discriminate between primary and secondary TES protected alcohols.^[294] Using the standard reagents DMSO and oxalyl chloride, substrate **472** had to be reacted at $-60\text{ }^{\circ}\text{C}$ for 8 hours or longer before addition of NEt_3 could follow. If in this first part of the procedure the temperature exceeded $-60\text{ }^{\circ}\text{C}$, isolable yields would significantly diminish due to double deprotection and oxidation. However, performing thorough temperature control, aldehyde **474** could be obtained in 94% yield as a single diastereomer without any observable epimerization (judged by NMR analysis). Following this, a Wittig olefination was conducted with excess of *in situ* generated Ph_3PCH_2 in THF at $0\text{ }^{\circ}\text{C}$ (scheme 3.16). After one hour, full conversion was achieved and alkene **475** was isolated in 96% yield, again as single diastereomer. Altogether, 1.1 g of this advanced intermediate was prepared and kept at this stage for the time being, in order to allow for the investigation of alternative synthetic strategies.



Scheme 3.16: Final steps toward envisioned building block **477**. Model system **438** was constructed employing the same synthetic procedures starting from hydrindanone **439**.

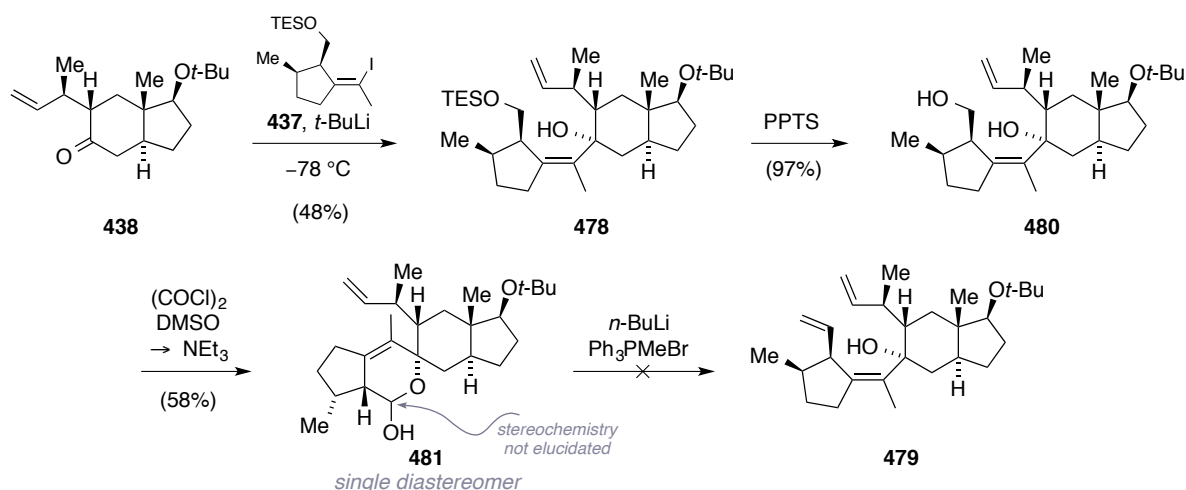
Moving forward to the required orthogonal deprotection of the secondary TES ether, substoichiometric amounts of (*R*)-campher sulfonic acid (CSA) were used in a solvent mixture of CH_2Cl_2 and methanol. Gratifyingly, we observed outright selectivity and alcohol **476** was cleanly formed without loss of its SEM ether. Thus obtained crude material was immediately subjected to Dess-Martin periodinane-mediated oxidation, being buffered with NaHCO_3 . Counting from TES ether **475**, the finished *trans*-hydrindanone building block **477** was isolated in almost quantitative yield (95%).

Summarizing, we synthesized coupling fragment **477** from known alcohol **335** in outstanding 41% by a scalable 12-step protocol that allowed the construction of chiral centers C-2 and C-3 in a highly diastereoselective manner. To conserve this valuable and highly advanced

intermediate, a model compound (**438**) was elaborated in 11 steps starting from ether **439** in again excellent yield (42%). This largely similar *trans*-hydrindanone compound (**438**) was employed for all initial studies toward fragment combination and construction of the 5-8-6-5-membered carbon skeleton that are described in the following section (*vide infra*).

3.5 Model Studies Toward the Construction of the Central Cyclooctane Motif

With substantial amounts of alkenyl iodides **410** and **437** and of model hydrindanone **438**^{viii} in hand, the planned fragment coupling *via* lithium alkenyl addition was investigated. Since we were worried that the alkenyl lithium species of diene **410** might be prone to undergo 1,3-metallotropic rearrangement similar to arylalkynes,^[295] or suffer from intramolecular proton shift, silyl ether **437** was employed initially (scheme 3.17). The required Li-alkenyl species was prepared in THF *in situ* *via* addition of two equivalents of *t*-BuLi at $-78\text{ }^{\circ}\text{C}$.^[296] When ketone **438** was added slowly to this solution, we were delighted to see a facile reaction course, furnishing tertiary alcohol **478** in 48% yield. It was possible to separate the undesired diastereomer (not shown) resulting from scalemic alkenyl iodide **437** by flash column chromatography. Furthermore, it was recognized that one has to employ slightly substoichiometric amounts of lithiation reagent, because any surplus amount of *t*-BuLi would add itself into the carbonyl functionality of substrate **438** and consequentially lower the obtained yield. The reactivity shown in this transformation is particularly worth noting since tetrasubstituted alkenyl lithium species are rarely used in organic synthesis. Especially

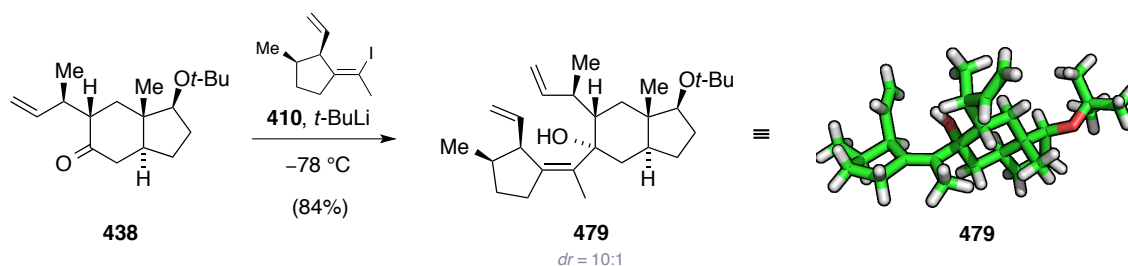


Scheme 3.17: First synthetic investigations toward the construction of triene **479** *via* Li-alkenyl addition.^{ix}

^{viii} Approximately one gram of model system **438** was provided by Dr. D. T. Hog.

^{ix} Depicted experiments were carried out together with Dr. D. T. Hog.

addition to ketones, particularly to sterically encumbered ones such as ketone **438**, are unprecedented to the best of our knowledge.^[297] In order to elaborate envisaged metathesis precursor **479**, the TES ether was cleaved next using PPTS under conditions similar to those described before (*cf.* chapter 3.4). Fortunately, the allylic alcohol moiety did not react *via* elimination and diol **480** was obtained almost quantitatively. Swern oxidation of the primary alcohol functionality was accompanied with spontaneous intramolecular cyclization to lactol **481**, which was isolated as a single isomer.^[298] Although the stereochemistry at the newly formed lactol center could not be elucidated by means of 2D NMR methods, compound **481** provided indirect proof that the double bond geometry of employed alkenyl iodide **437** had been retained upon lithiation. Next it was tried to react lactol **481** directly under Wittig olefination conditions using *in situ* generated Ph_3PCH_2 , which has been preceded for similar lactol systems frequently.^[299] Unfortunately, lactol **481** was not converted in the desired fashion, even when the temperature was risen to refluxing conditions.

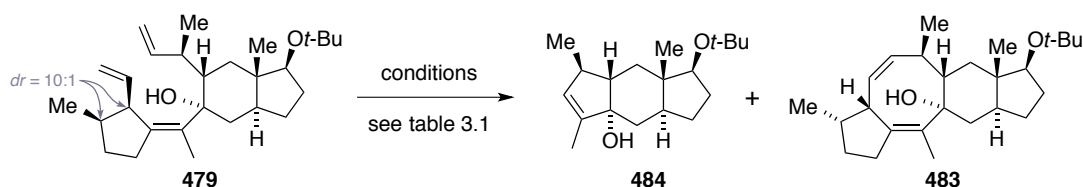


Scheme 3.18: Fragment coupling toward triene **479**, accompanied by kinetic resolution of scalemic **410**.

Encouraged by these results, it was tried to transfer the developed lithiation and addition conditions to diene **410** (scheme 3.18). To our delight the procedure furnished triene **479** smoothly, but as an inseparable mixture of diastereomers, due to the low *ee*-value (60%) of diene **410**. Interestingly, when 1.3 equivalents of the scalemic lithium alkenyl species were employed, triene **479** was obtained in a diastereomeric ratio of 10:1. This reflects a kinetic resolution of iodide **410** under the reaction conditions, which gratifyingly leads to preferential addition of the desired enantiomer. Furthermore, it was recognized that the addition speed of ketone **438** is a crucial parameter for this reaction. Supposedly, generated alcoholate of triene **479** started to enolize substrate **438** *in situ*, when extended exposure due to inhomogeneous distribution occurred. When addition times were prolonged to 30 min, yields would reach to excellent 84%. X-ray crystallographic analysis allowed for the verification of the relative configuration of all stereogenic centers and the alkene geometry. Careful inspection of the solid-state structure of triene **479** also revealed a close proximity between both terminal alkene functionalities. Solely, a 120° rotation around the C2–C3 axis would be required to result in an ideal conformational preorganization for envisaged RCM step.

With this knowledge in mind, we were poised to explore the key closure of nitidasin's (**238**) central octacycle by means of ring-closing metathesis. As literature precedence is comparably marginal anyway, there is no catalyst system reported to be superior for the construction of 8-membered ring systems.^[177] However, Nakada and co-workers had successfully employed ruthenium-based Grubbs catalysts in their recent synthesis of ophiobolin A on a similar system (**209**, cf. chapter 1.3).^[122,123] Table 3.1 summarizes the conditions screened for the transformation of triene **479**. Interestingly, when using Grubbs first-generation catalyst (**482**, *vide infra*) in CH₂Cl₂ at 40 °C (entry 1), traces of a cyclized product were observed by ¹H NMR and EI mass spectroscopy, which was tentatively assigned as tetracycle **483**. Similar results were obtained employing Grubbs second-generation catalyst (**267**) in both CH₂Cl₂ at 40 °C and DCE at 82 °C (entries 2,3). Exchange of the chlorinated solvents for benzene led to quick consumption of triene **484** and a new product was formed selectively. Surprisingly, NMR spectroscopic analysis revealed that the tetrasubstituted double bond had participated in the metathesis reaction and that ring B (nitidasin notation) had been expelled accordingly. Careful chromatographic purification using triethylamine (1 vol.-%) in the eluent mixture was required to obtain highly acid sensitive tricycle **484** in 60% yield. Otherwise allylic transposition of the tertiary alcohol functionality was effected and led to a 1:1 mixture of diastereomeric products.

Table 3.1: Model studies on the formation of nitidasin's (**238**) 8-membered carbocycle *via* RCM.

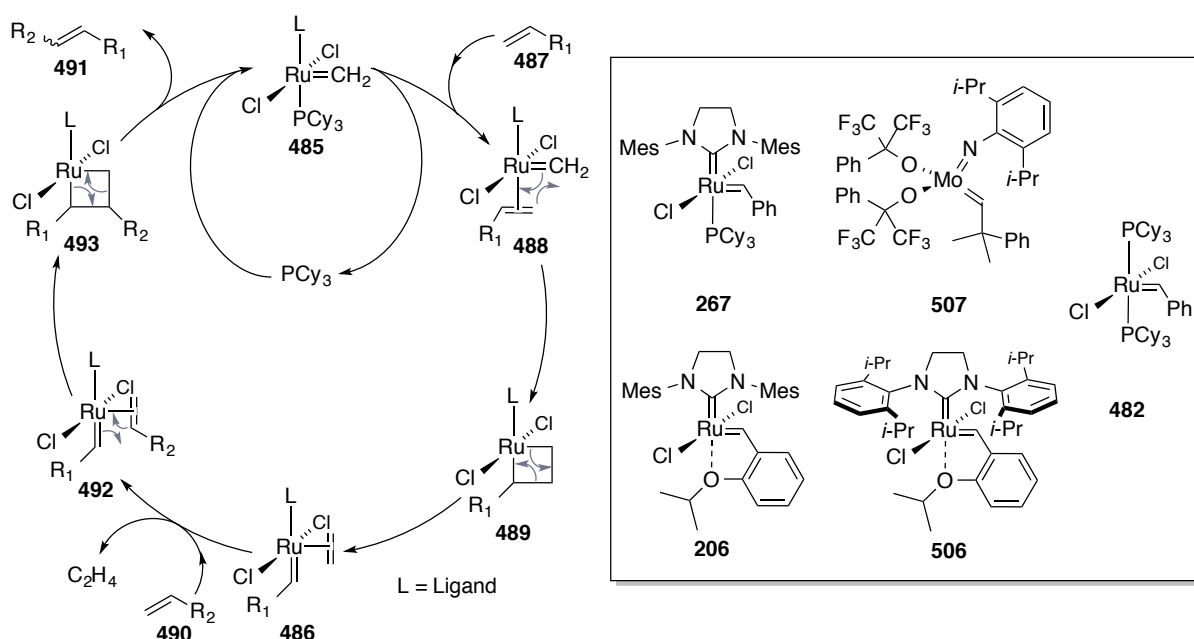


entry ^a	catalyst ^b	solvent ^c	T [°C]	t [h]	observation
1	Grubbs I (482)	CH ₂ Cl ₂	40	16 h	483 (traces)
2	Grubbs II (267)	CH ₂ Cl ₂	40	16 h	483 (traces)
3	Grubbs II (267)	DCE	82	16 h	483 (traces)
4	Grubbs II (267)	C ₆ H ₆	85	2 h	484 (60%) ^d , 483 (traces)

a) All reactions were carried out on 4 mg scale in 0.8 mM dilution. b) Catalyst loadings were 10 mol-%. For catalyst structures see scheme 3.19. c) Solvents were degassed prior to addition of the catalyst (Ar bubbling). d) Catalyst loading was 15 mol-%.

It was reasoned that this finding is most likely attributed to the presence of the tertiary allylic alcohol next to the tetrasubstituted double bond. Regarding the general catalytic cycle for olefin metathesis, which was first proposed by Chauvin^[300] in 1971 and later on elucidated in

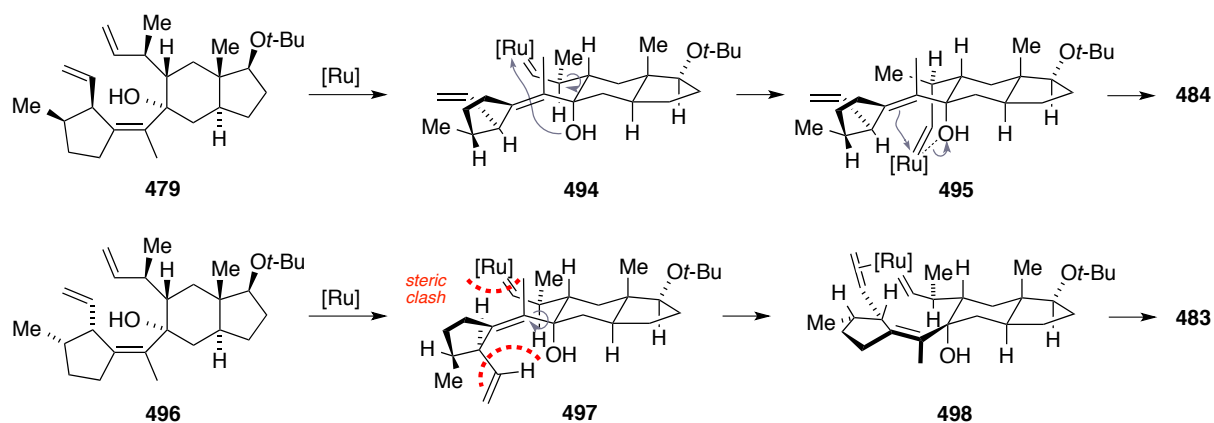
more detail by Grubbs,^[301] one recognizes that the site of catalyst initiation at substrate **479** is the key determinant of its cyclization mode. The catalytic cycle that is generally accepted for Ru-based catalyst systems^[362] starts with the formation of Ru-alkylidene **485** by the so-called catalyst initiation (scheme 3.19). This happens *via* a series of transformations analogue to the one that is described to lead from alkylidene **485** to complex **486**, involving: ligand dissociation to an active 16-electron species, alkene (**487**) coordination to π -complex **488**, cyclization to metallacyclobutane **489** and subsequent ring opening *via* the productive retro-reaction. Repetition of this sequence with another alkene molecule (**490**) ultimately yields desired metathesis product **491**, at which the carbon–carbon bond geometry may be tuned by the choice of catalyst. General driving force of this equilibrium process is the expulsion of ethane or similar low molecular-weight congeners. It is known from several studies that free tertiary allylic alcohols enhance the rate of metathesis of alkene substrates significantly.^[303] The reason for this is not undisputed. Hoyer *et al.* propose in their systematic studies that a rapid and reversible ligand exchange with the alkoxy functionality promotes reaction *via* pre-association.^[304] However, Grubbs and co-workers suggest that rather the electron donating properties of oxygen account for faster and more efficient alkylidene formation. The latter mentioned authors state that chelation in the allylic position of the metal alkylidene to the metal center should be disfavoured, forming a strained, four-membered ring.^[305]



Scheme 3.19: Dissociative mechanism of olefin metathesis after Chauvin and Grubbs, Grubbs-Hoveyda catalyst (**206**) and catalyst systems used in the course of present work.^[300,301]

In the presented case, catalyst initiation at the lower terminal double bond of triene **479** is unlikely, because this would involve the formation of a thermodynamically disfavoured,

strained cyclopropene (scheme 3.20). We reason that initiation takes places at the C-4 centered double bond (**494**), upon which the tertiary alcohol reversibly binds to the catalyst center. This renders the sterically highly encumbered tetrasubstituted double bond more accessible to the now close Ru-alkylidene (**495**). Due to the electronically activating effect of the allylic hydroxyl substituent, this double bond now reacts rapidly in metallacycle formation, not allowing the catalyst to reach for the remaining terminal double bond. For the minor diastereomer **496**, it may be suggested that the altered position of the C-6 substituent exerts increased steric hindrance on the allylic tertiary alcohol (**497**), effectively blocking it from the Ru-catalyst. Thus, structure **498** transforms smoothly to cyclooctadiene **483**, whereas desired substrate **479** preferably undergoes described side reaction. It was also tried to protect the tertiary alcohol of triene **479** as bulky as possible (**499**), in order to prevent speculated reversible catalyst coordination. Unfortunately, all attempts to functionalize this oxygen atom remained unfruitful, which is attributed to the overall steric encumbrance at C-12 (table 3.2).



Scheme 3.20: Possible mechanistic explanation for the formation of cyclooctadiene **483** and cyclopentene **484**.

Illustrated 3-dimensional drawings were derived in style of the solid-state structure of triene **479**.

Eventually this strategy was abandoned and a relay ring-closing metathesis-based (RRCM) approach was devised. This aimed at a shift of catalyst initiation from the C-4 centered double bond to the second terminal double bond of triene **479**. The concept of RRCM was originally developed by Hoyer *et al.* and allows directing metal movement throughout olefin metathesis *via* installation of least substituted, more accessible carbon-carbon double bonds.^[306] Exploiting the privileged formation of pentacyclic systems in RCM reactions, the additional relay handle would be expelled, thus forming the respective Ru-alkenylidene required for target ring formation.

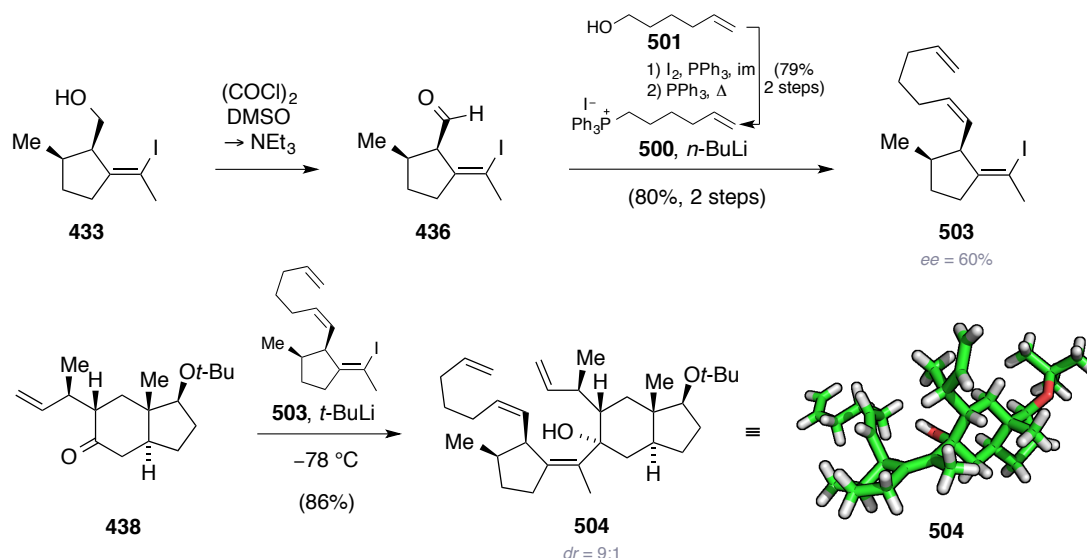
To reduce this plan into practice, the vinyl cyclopentane building block was modified as shown in scheme 3.21. The needed Wittig salt **500** was synthesized from commercially

Table 3.2: Conditions screened for protection of the tertiary alcohol functionality of triene **479**.

entry ^a	reagents ^b	solvent	T [°C] ^c	t [h]	observation
1	TESCl, im, DMAP	DMF	0 to 50	6 h	n.r.
2	TESOTf, 2,6-lutidine	CH ₂ Cl ₂	0 to 40	6 h	n.r.
3	NaH; TMSCl	THF	0 to 40	5 h	n.r.
4	<i>n</i> -BuLi; TMSOTf	THF	−78 to rt	2 h	n.r.
5	NaH; MeI	DMF	0 to 50	6 h	n.r.
6	NaH; Me ₂ SO ₄	DMF	0 to 50	12 h	traces ^d
7	NaH; MeSO ₃ F	DMF	0 to 50	12 h	n.r.

a) Reactions were carried out on 2 or 4 mg scale. b) Reagents were used in large excess to triene **479**. c) The temperature was raised gradually, monitoring the reaction course *via* TLC analysis. d) Observed *via* TLC and MS, but not isolated.

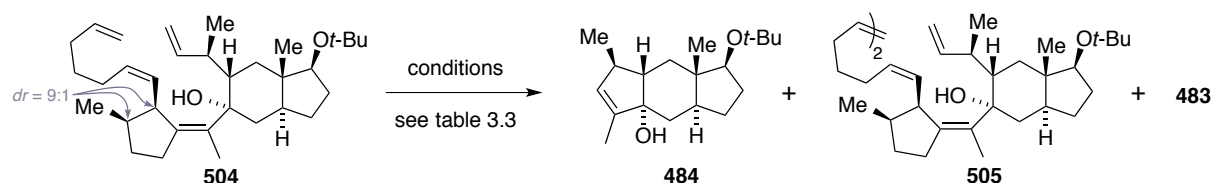
available alcohol **501** as described by Hiersemann and co-worker.^[307] Using their two-step protocol, which proceeds *via* Appel reaction^[308] and subsequent S_N2-type substitution of the furnished iodide (**502**) with triphenylphosphine, reagent **500** was isolated in 79% over two steps. Compound **500** was then reacted with known aldehyde **436** under the previously employed Wittig conditions (*cf.* chapter 3.3), at which triene **503** was obtained as a single double bond isomer in very good yield. Lithiation of **503** and subsequent addition to model system **438** furnished the desired RRCM precursor (**504**) in excellent 86% yield. Again, a kinetic resolution of scalemic alkenyl iodide **503** took place, although in somewhat lesser

**Scheme 3.21:** Synthesis of RRCM precursor **504**, using a modified vinyl cyclopentane building block (**503**).

extent than reported for the previous explorations. Despite the flexible alkene handle of tetraene **504**, single crystals suitable for X-ray crystallographic analysis could be grown, revealing a similar conformational arrangement as discussed for triene **479** (*vide supra*).

Next, RRCM reaction conditions were screened as outlined in table 3.3. Unfortunately, when using the Grubbs first- (**482**) or second-generation (**267**) catalyst in benzene, again tricycle **484** was formed accompanied with varying amounts of homodimer **505** and known diastereomer **483** (entries 1,2). Upon changing the solvent system to DCE, only dimer **505** could be observed (entry 3). In order to enhance the catalyst's preference to initiate at the least substituted double bond, catalyst **506** was employed, which was developed by Stewart and Grubbs.^[244] Unfortunately this only led to formation of significantly increased amounts of homodimer **505** (entries 4,5). Ultimately, we examined the activity of Schrock's catalyst (**507**),^[309] which interestingly did not result in any reaction (entry 6).

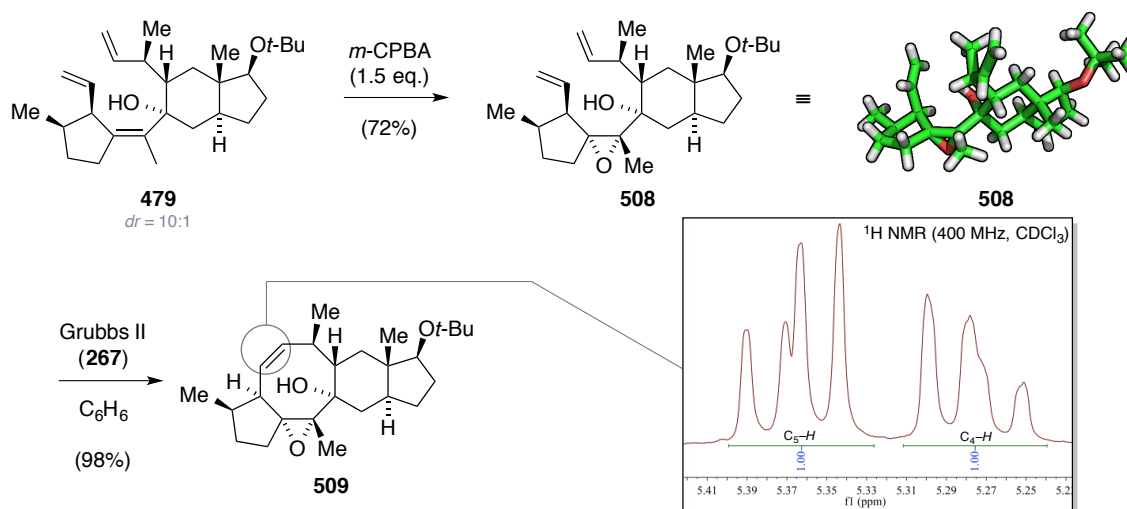
Table 3.3: Conditions screened for RRCM reaction of tetraene **504** and observed products (*cf.* table 3.1).



entry ^a	catalyst ^b	solvent ^c	T [°C]	t [h]	observation
1	Grubbs I (482)	C ₆ H ₆	85	3 h	483 (traces), 505 (traces)
2	Grubbs II (267)	C ₆ H ₆	85	3 h	484 (11%)
3	Grubbs II (267)	DCE	82	8 h	505 (traces)
4	catalyst 506	C ₆ H ₆	85	5 h	505 (31%)
5	catalyst 506	DCE	82	5 h	505 (traces)
6	Schrock's catalyst (507)	C ₆ H ₆	40; 85	3 h	n.r.

a) All reactions were carried out on 3 mg scale in 0.6 mM dilution. b) Catalyst loadings were in all cases 10 mol-%. For catalyst structures see scheme 3.19. c) Solvents were degassed prior to addition of the catalyst (Ar bubbling).

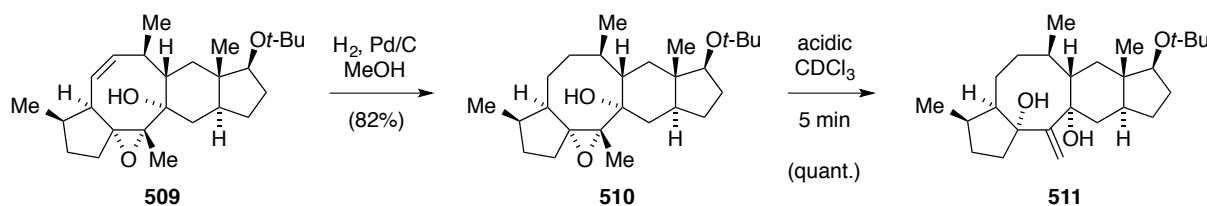
Since all attempts to circumvent participation of the tetrasubstituted double bond in RCM had failed so far, it was decided to mask this reaction site. Changing the order of events, it was considered bringing forward the envisaged late-stage epoxidation (*cf.* chapter 3.2). Gratifyingly, exposure of triene **479** to *m*-CPBA led to clean, chemoselective and diastereoselective reaction (scheme 3.22). Virtually no epoxidation of the terminal double bonds was observed under applied reaction conditions, even when a large excess of reagent was used. Purification *via* flash column chromatography allowed for the separation of



Scheme 3.22: Selective formation of epoxide **508** and key-step RCM, forming cyclooctene **509**. The magnified characteristic ^1H NMR signals belong to the alkene function of tetracycle **509**.

undesired isomers that resulted from employed 10:1 diastereomeric mixture of triene **479**. This provided pure epoxide **508** in 72% yield. Due to the lack of meaningful NOE signals, the identity of the newly formed stereogenic centers had to be elucidated by X-ray crystallographic analysis. The obtained structure again shows close proximity of the terminal double bonds and confirms that desired epoxide was formed. Since unique reactivity of triene **479** was observed when using Grubbs second-generation catalyst (**267**) in benzene, diene **508** was submitted to the very same reaction conditions. To our delight, this time ring-closing metathesis occurred uneventfully and delivered the desired tetracycle **509** in almost quantitative yield. Scheme 3.22 illustrates the characteristic alkene signals of recorded ^1H NMR spectra, which constitute the anticipated doublet of doublet splitting pattern. Although no single crystals could be grown from this material, 2D NMR analysis confirmed the closure of the central 8-membered ring unambiguously.

To complete the synthesis of nitidasin's (**238**) carbon framework at rings A, B and C, alkene **509** was hydrogenated in the presence of Pd/C (20 mol-%) in methanol (scheme 3.23). Although prolonged exposure to these conditions resulted in increased fractions of unaccounted side-reaction, desired saturated tetracycle **510** was obtained in 82% after three hours reaction duration. In order to compare model compound **510** with the data recorded from isolated nitidasin (**238**), we dissolved it in CDCl_3 as NMR solvent. Interestingly, rapid conversion of epoxide **510** was triggered to the corresponding *exo*-methylene compound **511**. This is attributed to trace amounts of DCl, causing proton-catalyzed epoxide opening that is followed by E1-type elimination. Notably, the newly formed allylic alcohol motif of

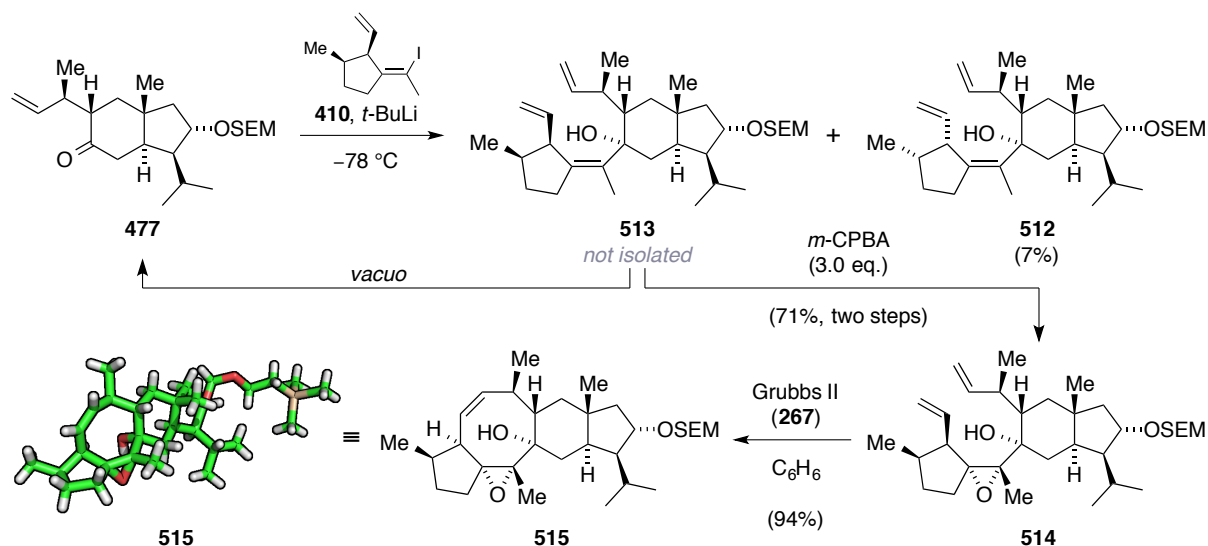


Scheme 3.23: Completion of the chosen model system for nitidasin's (**238**) tetracyclic carbon skeleton and acid catalyzed epoxide opening to *exo*-methylene compound **511**.

tetracycle **511** resembles YW 3699 (**240**) and YW 3548 (**241**) at respective carbon centers (*cf.* chapter 1.4.1). Consequently, this finding might be of synthetic usefulness for an aspired total synthesis of those natural products. Although NMR spectroscopic comparison of compound **511** to nitidasin (**238**) remained impractical, we were confident that we had completed the natural product, except for the substitution pattern on ring D. Thus, we moved on to apply developed transformations to *trans*-hydrindanone **477**.

3.6 The Stage is Set – Completion of (-)-Nitidasin

Encouraged by the presented model studies, we now exposed the further elaborated *trans*-hydrindanone **477** to lithiated vinyl cyclopentane **410** (scheme 3.24). For this substrate, increasing the equivalents of lithium organyl to 2.2 equivalents provided optimized results. In agreement with the previous results, the addition to the carbonyl functionality was found to be completely diastereoselective regarding the newly formed stereogenic center at carbon C-12 (nitidasin numbering). The diastereomers originating from scalemic iodide **410** were readily separable *via* flash column chromatography and 7% of the minor adduct (**512**) were isolated. Interestingly, the desired major isomer **513** turned out to be unstable upon concentration *in vacuo*. At this, the reconstitution of ketone **477** and the formation of a not ascertained low molecular weight fragment was observed. Consequently, triene **513** was directly employed for following epoxidation step, although being not thoroughly dried from *n*-pentane. Exposure to three equivalents of *m*-CPBA under the established reaction conditions yielded desired diene **514**, again with chemo- and diastereoselectivity. Accordingly, the desired RCM precursor (**514**) was obtained in very good 71%, counting over two steps. Although the yield of triene **513** could not be determined, the value calculated for the consecutive transformation allows to conclude that for the Li-alkenyl addition the previously described kinetic resolution had afforded a diastereomeric mixture equal to or higher than 10:1 (*cf.* chapter 3.5). The ensuing RCM proceeded smoothly, using Grubbs second-generation catalyst (**267**) in benzene



Scheme 3.24: Synthesis of tetracycle **515**, using the established 3-step sequence. The solid-state structure of **515** verified the correct relative configuration for all stereocenters found in the natural product.

as established on model system **508**. However, in present case, better yields were obtained when fresh catalyst **267** was added in three batches each hour, employing 5 mol-% loading at a time. Doing so, envisioned cyclooctene **515** was isolated in 94% yield and it became possible to grow crystals suitable for X-ray crystallographic analysis. This solid-state structure for the first time verified the relative configuration of all eleven stereogenic centers embedded in the carbon framework.

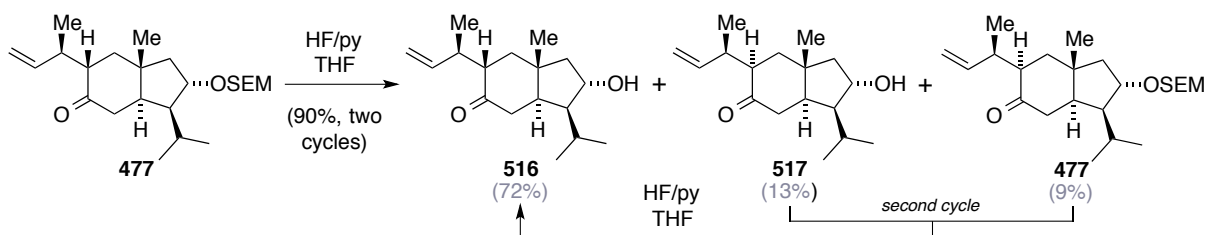
Furthermore, it was noticed that obtained tetracycle **515** was only poorly soluble in protic solvents, due to its inherent lipophilic nature caused by the flat, steroid-like shape. Hence, it was aspired to postpone hydrogenation of its alkene moiety after deprotection of the SEM ether, as this was established on model system **509** using methanol as a solvent system. The sensitivity of tetracycle **515**, combined with little amounts of material available for testing purposes prompted us to investigate the deprotection at a less advanced intermediate, namely ketone **456**. Table 3.4 outlines the screened conditions. Although being promising due the reported mildness, a protocol published by Hoffmann and co-worker^[310] that suggests the use of anhydrous MgBr_2 in a mixture of MeNO_2 and diethyl ether did not result in any reaction with model compound **456** (entry 1). Procedures based on basic fluoride sources did not yield conversion either at room temperature (entries 2–4). At this, elevated temperatures led to decomposition of the starting material. The use of strong Brønsted acids like TFA in CH_2Cl_2 or HCl in methanol (entries 5,6) gave rise to alcohol **335**, but was accompanied with unaccounted side reaction, observed by TLC analysis. To our delight, switching to less acidic HF/py in four volumes of THF led to clean formation of alcohol **335** in 92% yield (entry 7).

Table 3.4: Investigated conditions for the deprotection of SEM ether **456**.

entry ^a	reagent	solvent	T [°C]	t [h]	observation
1	MgBr ₂	Et ₂ O, MeNO ₂	rt to 30	12 h	n.r.
2	TASF	HMPA	50	12 h	decomp.
3	TBAF, 4 Å MS	DMPU	rt to 50	5 h	n.r. then decomp.
4	TBAF·3H ₂ O, 4 Å MS	THF	rt to 40	2 h	n.r. then decomp.
5	TFA	CH ₂ Cl ₂	0	5 h	335 (66%)
6	HCl (0.05 M) ^b	MeOH	rt	6 h	335 (75%)
7	HF/py	THF	rt	36 h	335 (92%)

a) All reactions were carried out on 10 mg scale under strict anhydrous conditions. b) The reagent was prepared freshly *via* addition of AcCl to MeOH.

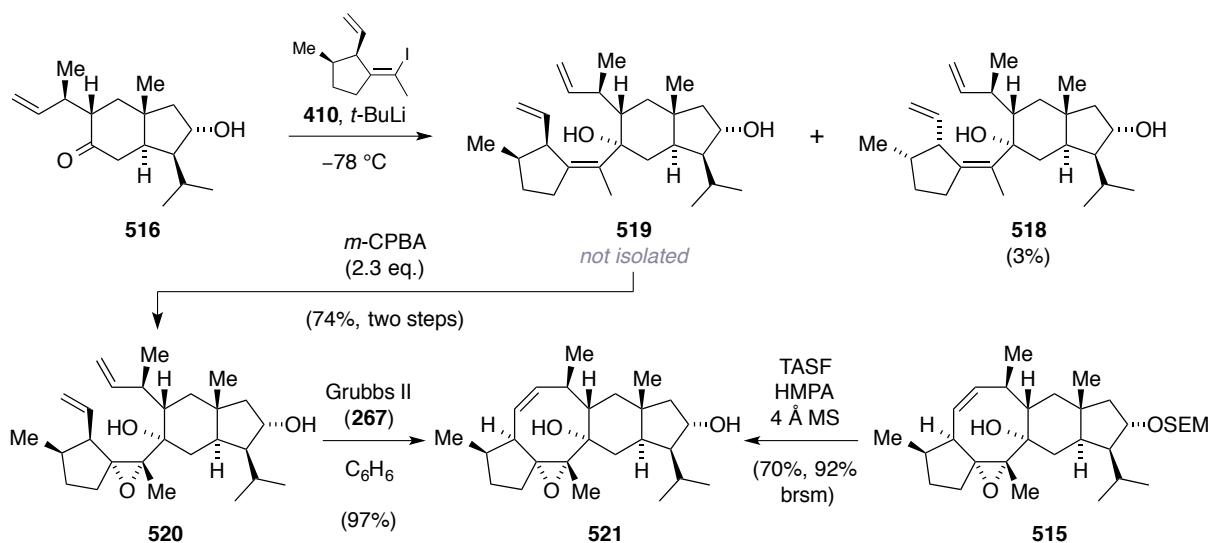
Keeping in mind that the epoxide functionality of tetracycle **515** suffers from pronounced lability toward acidic conditions, it was decided to remove the SEM group in advance of established fragment combination. Generated free alcohol would then require the use of an additional, sacrificial equivalent of the lithiated species of **410**. Therefore, it was intended to free the secondary alcohol in *trans*-hydrindanone **477** (scheme 3.25). When this building block was submitted to HF/py in THF as described above, initially only 72% of alcohol **516** were obtained, together with recovered starting material and epimerized alcohol **517**. The latter two fractions were resubmitted to the original reaction conditions, which led to an overall yield of 90% of desired deprotected ketone **516**.



Scheme 3.25: Deprotection of the SEM ether in *trans*-hydrindanone **477**. Grey hued yields refer to the first reaction cycle.

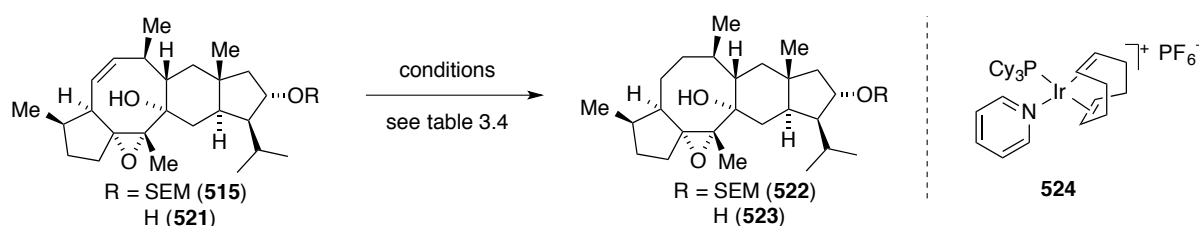
Gratifyingly, addition of 3.1 equivalents of the Li-alkenyl of **410** resulted in similar reactivity as observed before (scheme 3.26). The diastereomeric mixture originating from scalemic iodide **410** was again separated *via* flash column chromatography and 3% of the undesired adduct (**518**) were isolated. On the basis of the discussed results for compound **513** we

directly employed the major isomer **519** for following transformation as a not completely solvent free mixture. Substrate-controlled chemoselective epoxidation of triene **519** with 2.3 equivalents of *m*-CPBA then provided diene **520** in excellent 74% yield over two steps. Comparison of yields determined for isomer **518** and diene **520** suggests that for the Li-alkenyl addition the known kinetic resolution had afforded a diastereomeric mixture equal to or higher than 25:1. Following the obvious trend in this series, it becomes clear that increasing the amount of Li-alkenyl leads to a favoured formation of the respective desired tertiary alcohol adducts. However, this requires incremental wasteful use of synthetically precious vinyl cyclopentane building block **410**. Subsequent RCM reaction of diene **520** gave best results when fresh catalyst **267** was added in three batches each hour, as described previously (*vide supra*). Employing a total of 15 mol-% catalyst loading, desired unprotected tetracycle **521** was isolated in almost quantitative yield. Interestingly, the dilution of diene **520** had to be increased slightly to 0.6 mM to prevent formation of minor amounts of homodimeric side products.



Scheme 3.26: Three-step synthesis of unprotected tetracycle **521** and an alternative route, using modified SEM deprotection conditions.

Having established a reliable route toward alkene **521**, the SEM ether removal was revisited on leftover material of substrate **515**. Using TBAF in DMPU, solely slow decomposition was induced. The application of TBAF·3H₂O and 4 Å MS in THF simply triggered the loss of the TMS moiety without concomitant ether cleavage. Switching the fluoride source to TASf and the solvent to HMPA at elevated temperature did not provide any transformation at first. However, addition of thoroughly activated 4 Å MS led to the formation of freed alcohol **521** in 72% along with recovered starting material. Hence, an alternative route to substance **521**

Table 3.5: Evaluated hydrogenation conditions toward unsaturation of the cyclooctene moiety.

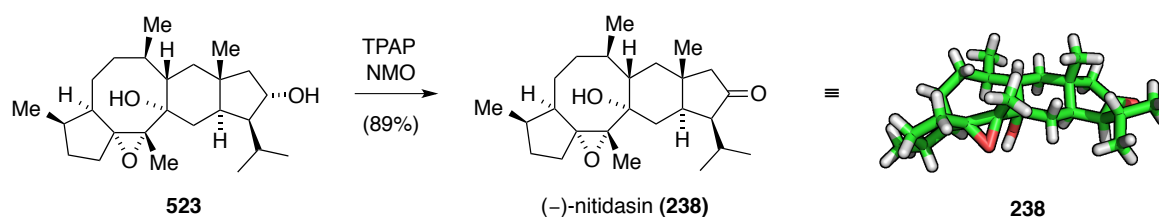
entry ^a	R	catalyst	loading	solvent	p(H ₂)	t [h]	observation ^d
1	SEM	Pd/C ^b	0.2 eq.	MeOH	1 bar	24	522 (20%)
2	H	Pd/C ^b	0.2 eq.	MeOH	1 bar	4	30% consumption
3	SEM	Pd/C ^b	0.2 eq.	EtOAc	8 bar	6	40% consumption
4	H, SEM	Pd/C ^b	0.2 eq.	EtOAc	20 bar	12	60% consumption
5	H	Pd/C ^b	0.2 eq.	MeOH	30 bar	10	full consumption
6	H	PtO ₂	0.1 eq.	EtOH	1 bar	10	slow decomp.
7	SEM	catalyst 524	0.1 eq.	CH ₂ Cl ₂	1 bar	1	rapid decomp.
8	SEM	Rh/Al ₂ O ₃ ^c	0.2 eq.	EtOH	1 bar	25	80% consumption
9	H	Pd/C ^b	3 eq.	MeOH	1 bar	1.25	523 (90%)
10	SEM	Pd/C ^b	3 eq.	MeOH	1 bar	1.25	522 (85%)

a) Reactions were carried out on 0.5 or 1.0 mg scale, except for entries 1,9 and 10. b) 10 wt-% Pd. c). 5 wt-% Rh. d) For entries 2–5 and 8, converted material was a mixture of **522** or **523** and decomposition products.

was established *via* a previously unknown modification of SEM ether deprotection conditions.^[266]

In order to complete nitidasin (**238**), we meanwhile had moved on to hydrogenate alkene **515** under the conditions employed for model system **509** (*cf.* chapter 3.5). This resulted in comparably slow conversion and only 20% of desired saturated substrate **522** were isolated, due to prevailing decomposition. It was suspected that mentioned low solubility of tetracycle **515** in methanol might be responsible. Thus, different solvent systems and catalysts were screened and the effect of increasing the applied hydrogen pressure (table 3.5) was evaluated. The variation of pressure and solvent system did not speed up the reaction sufficiently to compete with decomposition side reactions, when using catalytic amounts of Pd/C (entries 1–5). Furthermore, the use of Adams' catalyst^[199] in ethanol did not result in any product formation at all (entry 6). Crabtree's catalyst (**524**),^[311] which is known to coordinate to nearby alcohol functionalities, thus rendering even hindered alkenes accessible for hydrogenation, led to rapid decomposition. This is presumably due to its Lewis acidic nature (entry 7). Catalytic amounts of Rh/Al₂O₃, which is supposed to exhibit hydrogenation rates superior to Pd/C, also failed to effect improved results (entry 8).^[312] To our delight,

simply increasing the catalyst loading of Pd/C to three equivalents yielded desired cyclooctanes **522** and **523** at reduced reaction durations and in very good yield (entries 9,10). A reasonable explanation for this finding involves the predominant coordination of substrates **515** and **521** to the catalytic sites of employed heterogeneous systems, thereby effectively blocking hydrogen transfer to the alkene moieties. As application of superstoichiometrical amounts of catalyst obviously provides the needed active catalytic sites, the speculated coordinative deactivation must be caused either by the epoxide, the tertiary alcohol or by the protected and unprotected secondary alcohol functions in compounds **515** and **521**.



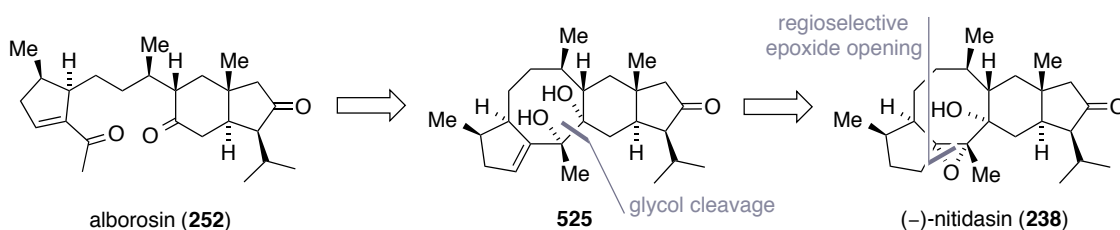
Scheme 3.27: Completion of (–)-nitidasin (**238**) *via* Ley oxidation of nitidasol (**523**). Depicted solid-state structure was produced from data recorded from synthetically obtained material.

Final transformation of ‘nitidasol’ (**523**), which might be the direct biosynthetic precursor of nitidasin (**238**), had to resort to non-acidic, mild methodologies. Already the use of NaHCO₃-buffered DMP oxidation conditions led to complete decomposition of alcohol **523**. To our delight, Ley oxidation with TPAP/NMO^[264] furnished the natural product in very good 89% yield (scheme 3.27). Unambiguous confirmation of the molecular structure of our synthetic material was achieved *via* X-ray crystallographic analysis. Obtained solid-state structure was identical to the one published by Kawahara and co-workers.^[154] In order to compare NMR spectroscopic data of the synthesized compound to the isolated material, thoroughly acid-freed CDCl₃ had to be prepared.^[313] A complete lineup of recorded ¹H and ¹³C NMR data and published values can be found in section V of the appendix. The optical rotation of the artificial sample was levorotatory as reported for the natural sample. The developed total synthesis enabled the preparation of all in all 16.3 mg of (–)-nitidasin (**238**) over the course of present doctoral thesis.

3.7 A Brief Synthetic Digression Toward Alborosin

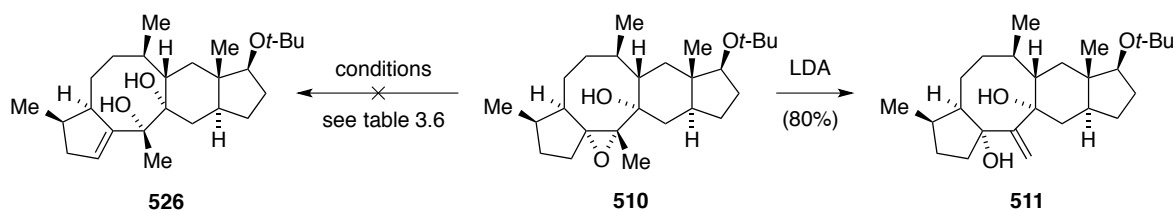
The assumed biosynthetic origin of alborosin (**252**) is nitidasin (**238**), as already outlined earlier (*cf.* chapter 3.1). Having access to the latter substance *via* the established total synthesis and to model system **510**, we were curious to examine whether their epoxide functionality could be opened regioselectively to form a 1,2-diol (**525**) with adjacent tertiary

alcohol (scheme 3.28). It was recognized that for this transformation a concomitant elimination would have to be triggered rather into the *C*-9 than into the *C*-6 position (nitidasin numbering), in order to form the required double bond. A glycol cleavage of intermediate **525** would then directly furnish alborosin (**525**), assuming drawn stereochemistry matches the isolated compound.



Scheme 3.28: Retrosynthetic analysis for a semisynthesis of alborosin (**525**) starting from nitidasin (**238**).

It was known from previous experiments that proton-catalyzed epoxide opening would furnish respective 1,3-diol motif (*vide supra*), rather than envisioned 1,2-diol **526** (scheme 3.29). Therefore, based-promoted epoxide opening *via* E1cB mechanism was investigated next. However, the use of LDA in diethyl ether on model system **510** led to clean formation of *exo*-methylene compound **511** with complete regioselectivity. This finding is explained by the increased steric encumbrance of methylene carbon *C*-9, compared to methyl carbon *C*-20. Furthermore, the solid-state structure of nitidasin (**238**) reveals that both hydrogen atoms at *C*-9 cannot not easily be aligned in a proper antiperiplanar fashion, which is ideally required for an E1cB-type epoxide opening. Consequently, we turned our attention to Lewis acid-promoted epoxide openings. It was reasoned that regioselective opening would be favoured, if precoordination of the Lewis acid with the tertiary alcohol function and the epoxide could be achieved. Table 3.6 summarizes the conducted efforts, which were limited by the quantity of available epoxide **510**. Most promising seemed the methodology published by Kita and co-workers, using hypervalent iodine(III) reagents to open 2,3-epoxy alcohols and achieve glycol cleavage in one step.^[314] Unfortunately, treatment of model system **510** with PIFA did not result in any reaction at all (entry 1). The effect of $\text{Ti}(\text{O}i\text{-Pr})_4$ was also examined at varying reaction temperatures, as this reagent was shown to affect desired



Scheme 3.29: Selective base-promoted epoxide opening to *exo*-methylene compound **511**.

transformation for less hindered 2,3-epoxy alcohol systems (entries 3,4).^[315] Again, this did not provide any reaction until slow decomposition of substrate **510** was initiated at 110 °C. Furthermore, the use of Pb(OAc)₄ did not promote desired reactivity either (entry 4). Interestingly, when compound **510** was treated with HIO₄ in diethyl ether, the slow formation of a new product was observed, of which it was not possible to elucidate the structure *via* NMR spectroscopic analysis. However, using mass spectroscopy we saw, that characteristic desired product signals were absent in this sample. We stopped our investigations on the semisynthesis of alborosin (**252**) at this point, due to a lack of material for screening purposes.

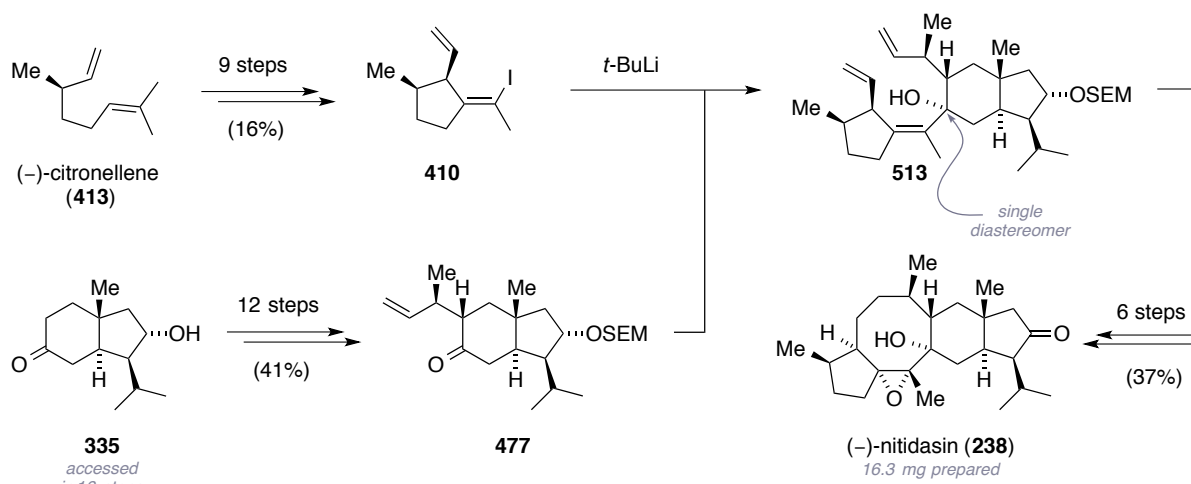
Table 3.6: Investigated conditions for the regioselective epoxide opening (*cf.* scheme 3.29)

entry ^a	reagent	solvent	T [°C]	t [h]	observation
1	PIFA	CH ₃ CN, H ₂ O	0 to rt	6 h	n.r.
2	Ti(Oi-Pr) ₄ ^b	CH ₂ Cl ₂	0 to rt	6 h	n.r.
3	Ti(Oi-Pr) ₄ ^b	toluene	rt to 110	6 h	n.r. then decomp.
4	Pb(OAc) ₄	CH ₂ Cl ₂	rt	24 h	n.r. then decomp.
5	HIO ₄	Et ₂ O	0 to rt	12 h	u.p. ^c

a) All reactions were carried out on 0.5 mg scale. b) Reagent was freshly distilled. c) The identity of the product of this reaction could not be elucidated.

3.8 Conclusion and Future Aspects

In conclusion, we have successfully established the first total synthesis of the complex sesterterpenoid (–)-nitidasin (**238**). The presented convergent synthetic route features several highly diastereoselective transformations, which enabled the construction of nine of nitidasin's (**238**) ten stereogenic centers from scratch. The natural product was prepared from inexpensive, commercially available starting materials in 34 steps (longest linear sequence) in 1.8% overall yield (scheme 3.30). In addition, obtained synthetic material allowed to assign the relative stereochemistry of the natural product by comparing measured optical rotations. Initiated by previous work conducted in the Trauner laboratories,^[140,156] we developed *trans*-hydrindane building block **475**. This versatile compound served not only as an advanced intermediate in the nitidasin (**238**) synthesis, but also takes a central role in currently ongoing synthetic investigations toward total syntheses of astellatol (**213**), alborosin (**252**), YW 3699 (**240**) and YW 3548 (**241**). The outlined synthetic sequence is especially

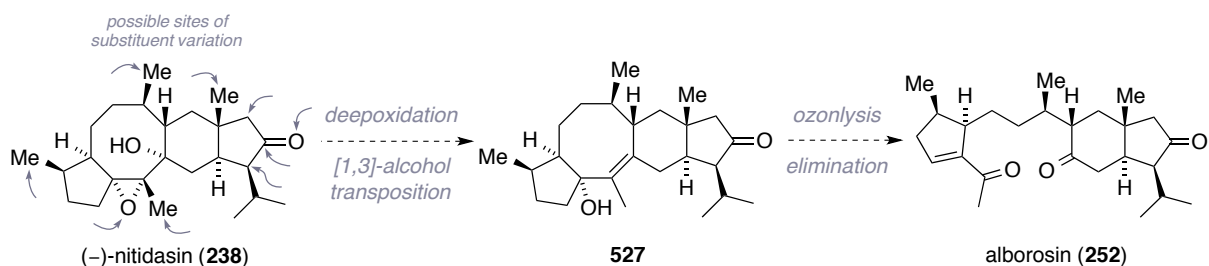


Scheme 3.30: The total synthesis of (–)-nitidasin (**238**), starting from commercial scalemic citronellene (**413**) and known *trans*-hydrindanone **477**.

marked by its reliable, scalable and high yielding transformations, *e.g.* affording *trans*-hydrindane **477** in 41% over 12 steps starting from known alcohol **335** (*cf.* chapter 3.4). Furthermore, it was possible to construct vinyl cyclopentane **410** in gram quantity *via* zirconium-mediated enyne cyclization. This was followed by correction of the configuration of C-6 located stereocenter (nitidasin numbering), using an elimination/hydroboration sequence (*cf.* chapter 3.3). This building block possesses a literature unprecedented *cis-cis-cis* relationship in respect to its vinyl iodide and adjacent ring substituents. Subsequently, a fragment combination was achieved under kinetic resolution *via* a completely diastereoselective addition of a tetrasubstituted alkenyl lithium species – generated from scalemic compound **410** – to *trans*-hydrindanone **477**. Later on, a remarkably efficient RCM-based formation of the central, highly substituted 8-membered ring of nitidasin (**238**) was demonstrated. At this, several solid-state structures were obtained and provided insights in the conformational preorganization of prepared substrates and the presumable course of their RCM reactions (*cf.* chapter 3.5 and 3.6).

Prepared synthetic (–)-nitidasin (**238**) is currently subject of investigation, regarding its bioactivity. However, first evaluation on the effect of the natural product on proliferation and induction of cell-death on MDA-MB-231 breast cancer cells did not show any effect so far.^x Once nitidasin's (**238**) biological purpose and mode of activity has been revealed, future work might aim at a modification of the established synthetic route in order to prepare analogues with possibly increased potency. Scheme 3.31 highlights the positions of the natural product at which differing substitution patterns would be accessible most easily. Although our efforts

^xThese experiments were conducted in co-work with the group of Prof. Dr. A. Vollmar.



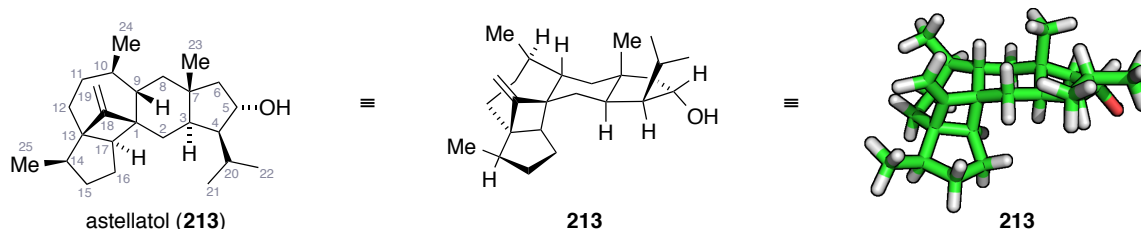
Scheme 3.31: An alternative route for the semisynthesis of alborosin (**252**), starting from nitidasin (**238**). Grey arrows indicate sites, at which variation of the substitution pattern can be easily achieved.

toward a semisynthesis of alborosin (**252**) have remained unfruitful so far (*cf.* chapter 3.7), a different synthetic approach would be conceivable. If one would de-epoxidize nitidasin (**238**) using Sharpless' protocol,^[316] an allylic transposition of the tertiary alcohol could yield structure **527**. Disconnection of the carbon-carbon double bond *via* ozonolysis and a final regioselective elimination step would provide alborosin (**252**) in a slightly longer sequence than previously aspired.

4. Synthetic Studies Toward Astellatol

4.1 A Comprehensive Introduction to Astellatol

In 1989 Simpson and Sadler isolated the sesterterpenoid astellatol (**213**) from the fungus *Aspergillus variegatus* (*syn. A. stellatus*) within their studies on a series of xanthone pigments.^[155] The authors were able to grow crystals of both, the natural product and its oxidatively derived ketone (not shown), which however were not suitable for X-ray crystallographic analysis. Hence, astellatol's (**213**) molecular structure was established by application of a variety of one- and two-dimensional NMR techniques (scheme 4.1).^[317] Its

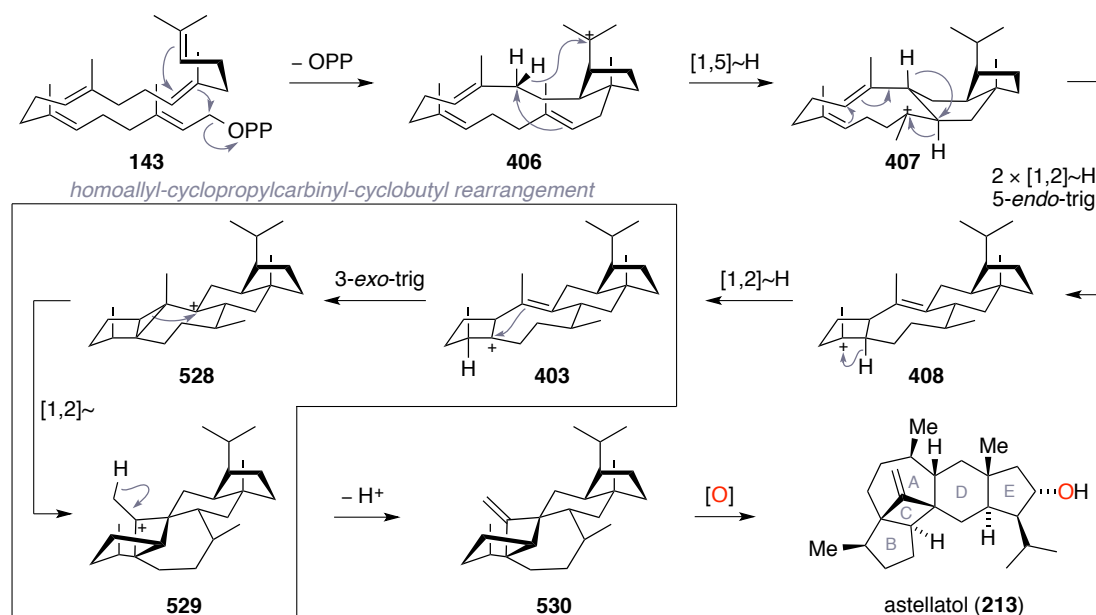


Scheme 4.1: The sesterterpenoid astellatol (**213**): flat generic structure, three-dimensional drawing and force field refined structure (MMFF94).

unique pentacyclic carbon backbone comprises a four-, two five-, a six- and a seven-membered ring, that are fused over edges and at the atoms C-1 and C-13 (astellatol numbering) *via* two spiro centers. Astellatol (**213**) features in total ten stereogenic centers, three of which are quaternary all-carbon-substituted. In similarity to nitidasin (**238**), present natural product also incorporates an *iso*-propyl-substituted *trans*-hydrindane motif. Its *exo*-methylene-substituted cyclobutane ring system and the single secondary alcohol pose the only two functional handles of the molecule, which renders the construction of its carbocyclic skeleton an intricate synthetic challenge.

Together with mentioned NMR studies, Simpson conducted labeling experiments at which [1,2-¹³C₂]acetate was fed to cultures of the parent fungus.^[200] The observed ¹³C-coupling pattern was consistent with the biosynthetic pathway shown in scheme 4.2. Accordingly, it was proposed that geranylfarnesyl pyrophosphate (**143**) undergoes initial folding and cyclization, corresponding to the proposed biosynthesis of retigeranic acid A (**236**) and B (**237**), to give the bicyclic intermediate **406** (*cf.* chapter 3.1). An ensuing [1,5]-hydride shift, which has been observed in the biosynthesis of a number of different sesterterpenoids,^[318] and a subsequent 6-*exo*-trig cyclization complete the *trans*-hydrindane system and lead to tricyclic tertiary carbocation **407**. This species now undergoes a series of stereospecific [1,2]-hydride

shifts, which are accompanied by a 5-*endo*-trig cyclization to yield in tetracyclic cation **408**. This intermediate also represents the branching point for the formation of nitidasin (**238**) as proposed earlier (*cf.* chapter 3.1). In the case of the formation of astellatol (**213**), homoallyl cation **403** is the entry to a so-called homoallyl-cyclopropylcarbinyl-cyclobutyl rearrangement, which has been found to be an equilibrium process.^[319] This intriguing cationic rearrangement proceeds *via* an initial 3-*exo*-trig cyclization (**528**), which is followed by a [1,2]-migration that forms the bond between C-1 and C-17 in a stereoselective manner (**529**). Final elimination to *exo*-methylene compound **530** delivers the thermodynamic driving force and terminates the cationic cascade. Stereoselective enzymatic oxidation of C-5 then completes the natural product. To date, there is no published data on astellatol's (**213**) biological activity. Notably, its D and E ring systems are identical to those found in the potent GPI-anchor inhibitors YW 3699 (**240**) and YW 3548 (**241**).^[160]

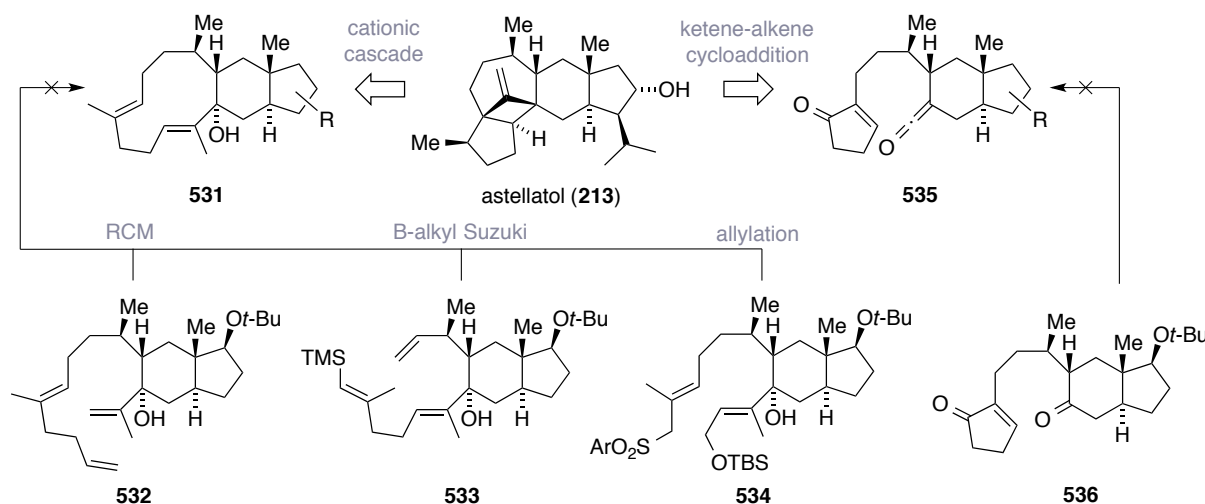


Scheme 4.2: Proposed biosynthesis of astellatol (**213**). The single oxidation step is highlighted red.

Shown biosynthetic pathway puts forth an compelling retrosynthetic disconnection for the artificial construction of astellatols (**213**) central 5-4-7-6-membered ring system. If one could address carbocation **403** or any later ionic intermediate by means of total synthesis, this would allow for the biomimetic formation of the desired carbon skeleton in an otherwise unfeasible efficient way. To the best of our knowledge, this would also be the first synthetic application of mentioned cationic rearrangement. Thus, a total synthesis of astellatol (**213**) would not only provide the chance to thoroughly investigate its bioactivity, but it would additionally establish its absolute configuration, confirm its structure unambiguously and prove the synthetic usefulness of the homoallyl-cyclopropylcarbinyl-cyclobutyl rearrangement.

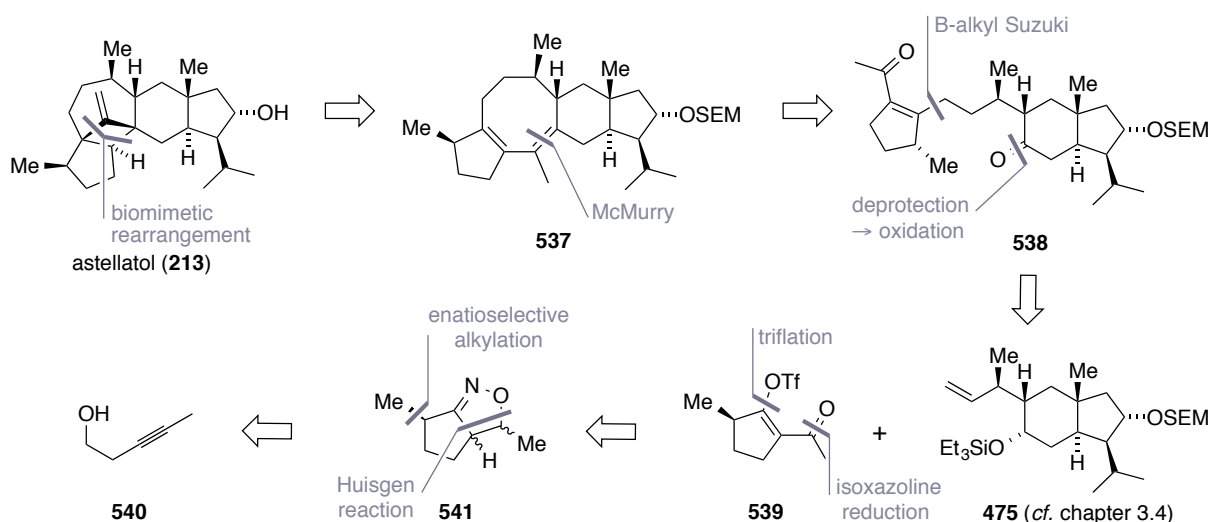
4.2 Retrosynthetic Analysis

In the forefront of discussing novel synthetic approaches toward astellatol (**213**), a short overview of unsuccessful retrosyntheses, which had been investigated in the Trauner laboratories previously will be presented (scheme 4.3). Research conducted in this field was carried out by Dr. D. T. Hog and is outlined in his doctoral thesis.^[156] In short, two distinct ideas to construct astellatol (**213**) were at hand. The first strategy envisaged the use of the natural product's biosynthetic cationic cascade (*cf.* scheme 4.2), which was meant to be entered at a stage similar to cation **407** *via* ionization of allylic alcohol **531**. Attempts to close the required 11-membered ring by means of RCM (**532**), B-alkyl Suzuki coupling (**533**) or intramolecular allylation (**534**) failed. This was either due to predominant side reactions during the ring closure or because the desired precursor could not be accessed. In a second attempt, it was tried to access the central polycyclic ring motif *via* ketene-alkene cycloaddition (**535**).^[320,321] At this, no reliable route toward a viable ketene precursor could be found, yet.



Scheme 4.3: Synthetic approaches toward astellatol (**213**) previously investigated in the Trauner research group. Depicted late-stage intermediates **532**, **533**, **534** and **536** are the most advanced compounds reliably accessed at respective routes.

In light of these previous endeavors, it was sought to establish a more convergent strategy for a potential biomimetic total synthesis of astellatol (**213**). In particular, we opted for a route involving a 5-8-6-5-membered ring system that would have the correct relative configuration at carbon *C*-14 (astellatol numbering) already in place and thus reduce the number of events in the key cascade. As outlined in scheme 4.4, diene **537** was envisioned as key precursor for a biomimetic synthesis of astellatol (**213**). Upon treatment with acid, protonation was supposed to trigger the homoallyl-cyclopropylcarbinyl-cyclobutyl rearrangement. Closure of

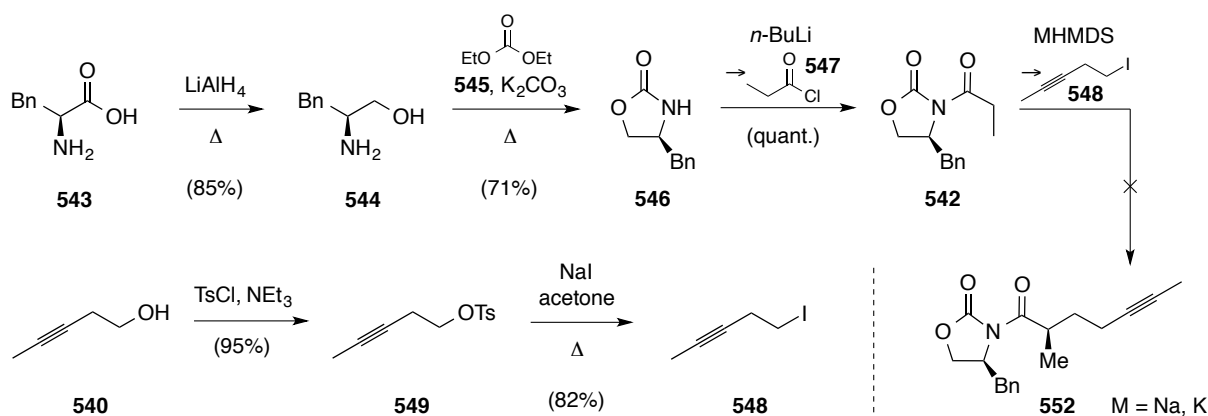


Scheme 4.4: Retrosynthetic analysis of astellatol (213), relying on the construction of cyclooctadiene **537** via means of reductive carbonyl-carbonyl coupling. Not specified stereocenters are inconsequential.

the central 8-membered carbocycle should be achieved by reductive carbonyl-carbonyl coupling, *e.g.* under McMurry conditions.^[322–324] The required diketone (**538**) was planned to arise from known SEM protected *trans*-hydrindane **475** (*cf.* chapter 3.4) and triflate **539**, using B-alkyl Suzuki coupling conditions. The latter fragment was meant to be prepared from 3-pentynol (**540**) in an enantioselective manner. At this, the required 1,3-diketone precursor (not shown) would be constructed *via* hydrogenative ring opening of isoxazoline **541** and subsequent oxidation of resulting β -keto alcohol function. Mentioned heterocycle could be obtained by means of 1,3-dipolar cycloaddition (Huisgen reaction)^[325] of an *in situ* generated nitrile oxide species. In addition, an auxiliary-controlled enantioselective alkylation could provide an entry for required open-chain building block and would refer to a suitable electrophilic derivative of commercially available alkyne **540**.^[326] A key feature of this retrosynthetic approach is the close structural similarity of envisioned intermediates **537** and **538** to the natural products nitidasin (**238**) and alborosin (**252**), respectively (*cf.* chapter 3). Thus, the outlined route would potentially allow to access three sesterterpenoids from common building blocks **539** and **475** in a highly convergent way.

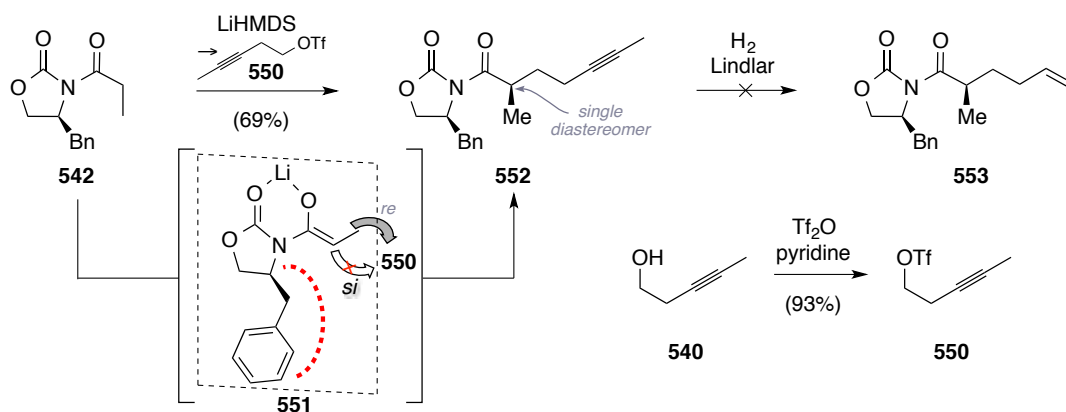
4.3 Enantioselective Synthesis of the Cyclopentenol Triflate Fragment

First attempts conducted in order to address an enantioselective entry by means of auxiliary-assisted nucleophilic substitution reaction, involved the use of propionylated oxazolidinone **542** in an Evans-type alkylation (scheme 4.5).^[327] This compound was prepared in three steps from (*S*)-phenylalanine (**543**) in 70% yield, according to well established literature



Scheme 4.5: Preparation of compound **542** and iodide **548** and unsuccessful coupling *via* Evans alkylation.

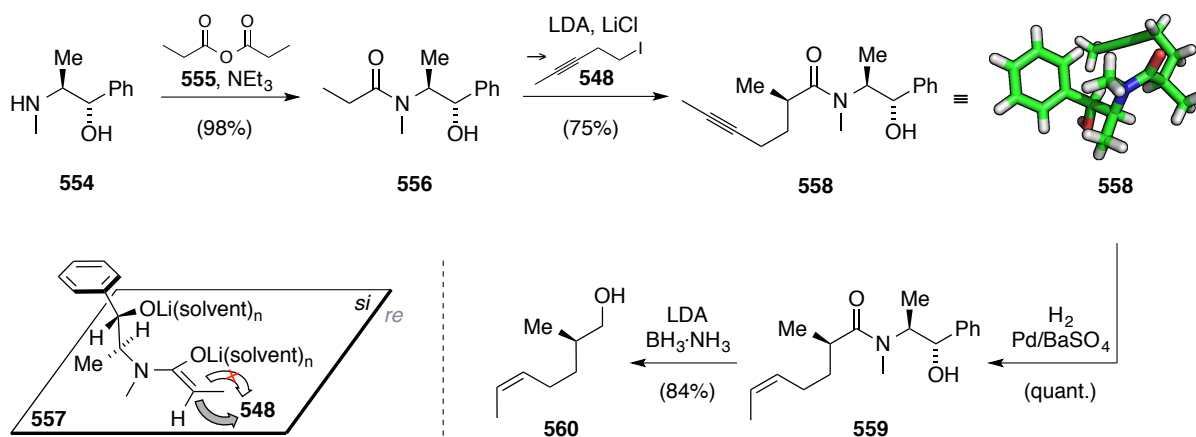
known procedures. In short, the performed transformations were: reduction with LiAlH_4 to aminoalcohol **544**,^[328] oxazolidinone formation with diethylcarbonate (**545**)^[329] and subsequent acylation of substance **546** using propionyl chloride (**547**).^[330] As electrophilic reaction partner, the known iodide **548** was prepared initially by a 2-step procedure. After almost quantitative tosylation of alkyne **540** with TsCl and triethylamine in CH_2Cl_2 , the sulfonate substituent in **549** was exchanged against iodine under classical Finkelstein conditions, employing NaI in acetone at 60°C . Purified by repeated distillation under inert gas atmosphere, electrophile **548** was obtained dry in 82% yield and was indefinitely stable as a solid upon storage at -20°C under exclusion of light. Unfortunately, when iodide **548** was added to the *in situ* generated Li- or Na-enolates of compound **542**, only trace amounts of the desired alkylation product were observed. It was reasoned that iodide **548** is not electrophilic enough to react with stabilized enolates, like those that are derived from oxazolidinones. Literature states that the respective triflates are more reactive and the reagents of choice in such cases.^[331] Accordingly, the very sensitive triflate **550** was prepared *via* addition of triflic anhydride to a mixture of alcohol **540** and pyridine in CH_2Cl_2 in excellent yield (scheme 4.6). As intended, this reagent underwent alkylation reaction with Li-enolate **551** to yield desired



Scheme 4.6: Evans alkylation of enolate **551** with triflate **550** and explanation of its stereochemical outcome.

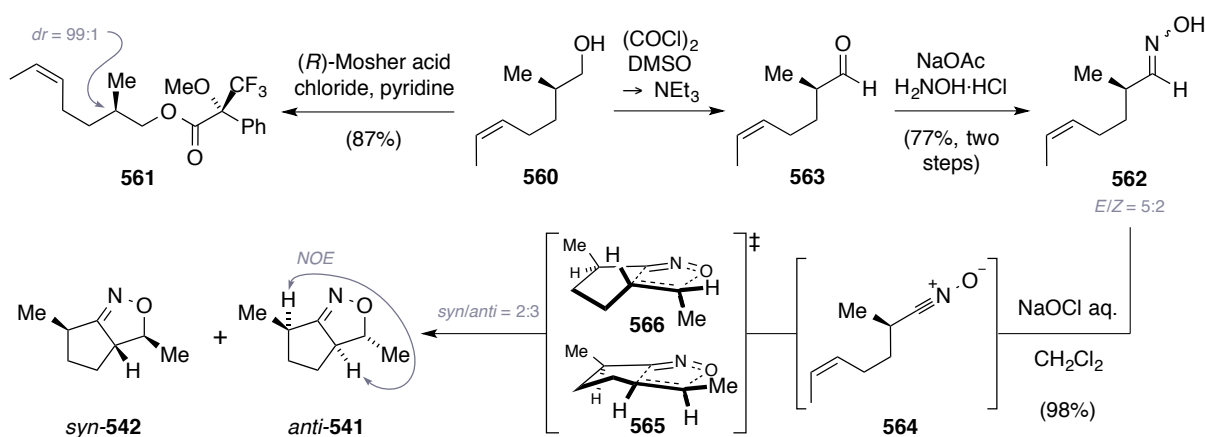
alkyne **552** as a single diastereomer in 69% yield. Observed selectivity can be explained by a conformational fixation of generated (*Z*)-enolate (**551**) *via* chelation of lithium to the 1,3-situated carbonyl functions.^[327] Consequently, the benzyl substituent shields the *si*-face of enolate **551** and directs electrophile **550** to the *re*-face. However, selective semi-hydrogenation of alkyne **552** to its respective alkene (**553**) remained unsuccessful. When Lindlar hydrogenation conditions (Pd/CaCO₃, poisoned with 5 wt-% Pb)^[332] were applied – with or without the addition of quinoline – overreduction of the alkyne function and decomposition of the oxazolidinone moiety was observed.

As Birch reduction conditions are obviously too harsh for substrate **552** and semi-reduction *via* diimide-mediated hydrogen transfer would be a capricious venture, it was tried to switch the chiral auxiliary and chosen to explore Myers' alkylation methodology with (1*S*,2*S*)-pseudoephedrine (**554**, scheme 4.7).^[107] Again, the auxiliary (**554**) was first acylated with propionic anhydride (**555**) as described in Myers' publication and amide **556** was obtained in excellent 98% yield. Beneficially, this detailed alkylation protocol allowed the use of less sensitive iodide **548**. When two equivalents of enolate species **557** were reacted, the desired product (**558**) was isolated in 75% yield with no observable formation of the respective diastereomer. Regarding the reaction mechanism, a complex three-dimensional model of formed (*Z*)-enolate **557** was proposed by the original authors, at which the *si*-face is sterically blocked due to oxygen centered solvated lithium ions.^[107] It shall be noted, that this rational has not been confirmed unambiguously up to date, as it does not account for the actual transition state.^[107,333] To our delight, we were able to obtain single crystals from amide **558**, which were suitable for X-ray crystallographic analysis and confirmed desired stereochemical outcome. Ensuing hydrogenation of alkyne **558** in the presence of Pd/BaSO₄ in pyridine selectively yielded corresponding *cis*-alkene **559**.^[334] Attempts, at



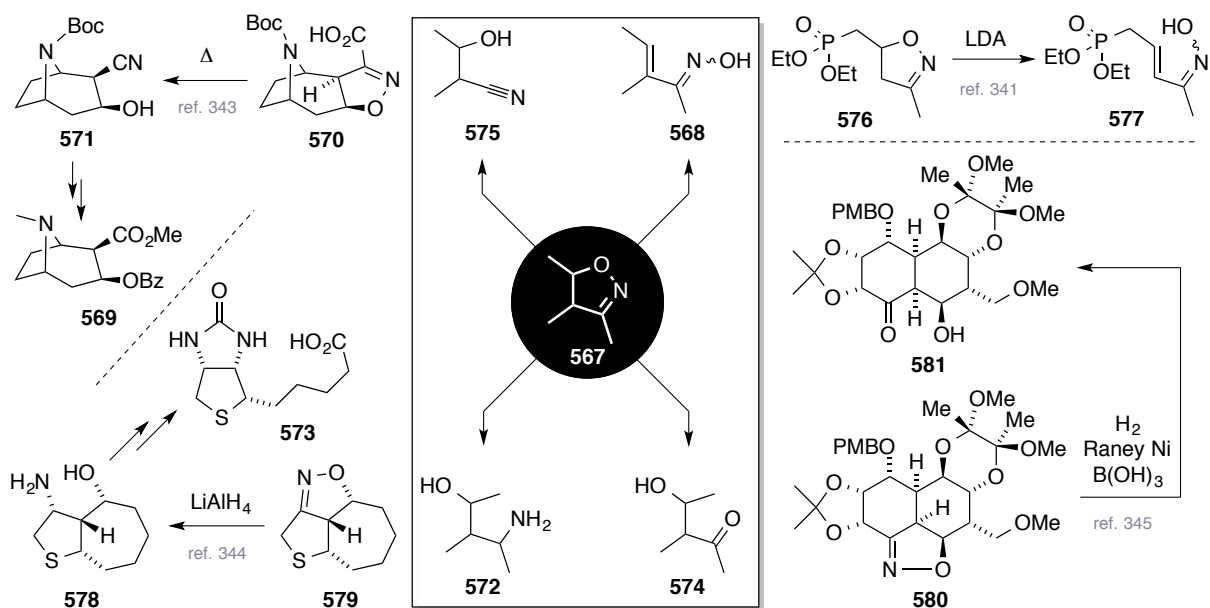
Scheme 4.7: Myers alkylation of enolate **557** with iodide **548**, explanation of its stereochemical outcome, semi-hydrogenation to alkene **559** and subsequent LAB reduction to alcohol **560**.

which classical Lindlar hydrogenation conditions^[332] were employed, resulted again in immediate overreduction to the respective alkane (not shown). Subsequent cleavage of the auxiliary with *in situ* generated lithium amidotrihydroborate (LAB) in THF led to clean formation of volatile alcohol **560**.^[335] At this stage, chiral intermediate **560** was converted to its respective Mosher ester (**561**, scheme 4.8) under the previously described conditions in 87% yield (*cf.* chapter 3.3). Evaluation of recorded ¹⁹F NMR spectra of ester **561** revealed an enantiomeric ratio of alcohol **560** of 99:1, which is consistent with the published data for comparable substrates.^[107] In order to synthesize envisaged isoxazoline **541**, it was first intended to transform alcohol **560** into its aldoxime congener (**562**). This functional group represents a well literature precedented precursor for the *in situ* generation of nitrile oxide species and has been used for intramolecular Huisgen reactions^{xi} before.^[336] Encouraged by previous positive results with Swern oxidations on α -chiral alcohols (*cf.* chapter 3), aldehyde **563** was synthesized under the same conditions. Due to its high volatility, intermediate **563** was not thoroughly freed from solvents, but directly employed for subsequent oxime formation. Upon reaction with NaOAc-buffered hydroxylamine hydrochloride in methanolic solution, the less volatile aldoxime **562** was obtained in 77% over two steps in an inconsequential 5:2 mixture of *E*- and *Z*-isomers. The focus was then directed toward the nitrile oxide (**564**) formation, which was first tried with aqueous sodium hypochloride in CH₂Cl₂. This transformation proved to be straightforward and yielded the product of the aspired intramolecular 1,3-dipolar cycloaddition in excellent 98% yield. In perfect agreement with studies on the diastereoselectivity of such Huisgen-type bicycle formations (*cf.* structures **565** and **566**) that were published by Houk^[337] and Kozikowski,^[338] a mixture of *syn*- and *anti*-**541** of 2:3 was observed. Using NOESY correlation, it was



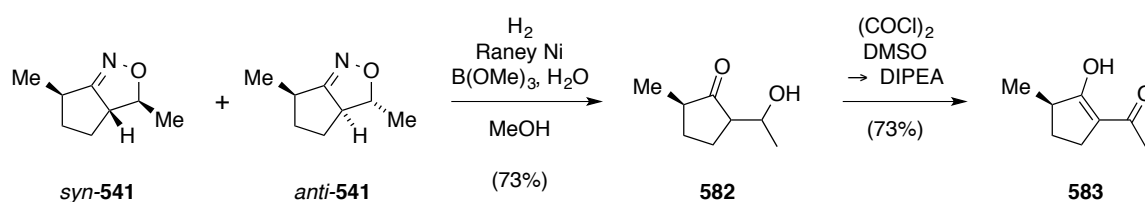
Scheme 4.8: Synthesis of isoxazoline **541** via Huisgen reaction and Mosher ester formation with alcohol **560**.

^{xi}This type of reaction has come to be known as intramolecular nitrile oxide cycloaddition (INOC).



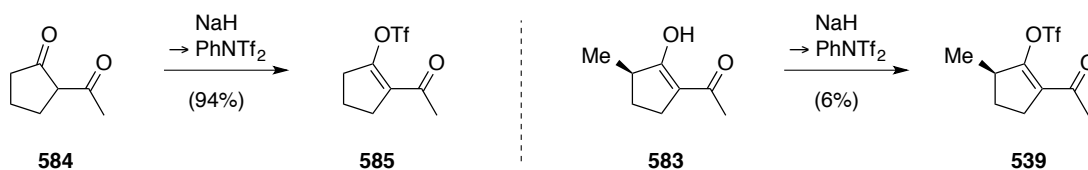
Scheme 4.9: Ring opening transformations of isoxazolines and examples for their application in synthesis.

possible to assign the major diastereomer to the *anti*-configuration. The isoxazoline heterocycle (**567**) has found numerous applications in total synthesis, as it can be transformed to a variety of functional group motifs (scheme 4.9), due its weak N–O bond (157 kJ/mol).^[339,340] Base-mediated ring opening with *e.g.* LDA may yield unsaturated α,β -oximes (**568**),^[341] whilst nucleophilic addition of Grignard reagents to the carbon–nitrogen double bond leads to respective isoxazolidinones (not shown).^[342] Lin *et al.* reported in their synthesis of (–)-cocaine (**569**) a decarboxylative fragmentation of an isoxazoline ring (**570**) under thermal conditions, yielding nitrile **571**.^[343] Furthermore, isoxazoline reduction by hydride sources or hydrogenation can provide the respective β -amino alcohols (**572**), which found its very first application in Confalone's racemic synthesis of biotin (**573**).^[344] For our synthetic route, the most relevant cleavage method is represented by the selective catalytic hydrogenation of the N–O bond. At this, the resulting iminium function first remains intact and is then hydrolyzed *in situ* to yield β -hydroxy carbonyls (**574**). The most commonly used protocol for this transformation was published by Curran in 1982 and employs borate or boronic acid buffered Raney[®] Nickel in wet methanolic



Scheme 4.10: Chemoselective hydrogenation of bicycle **541** and subsequent Swern oxidation toward enol **583**.

solution under an atmosphere of hydrogen.^[340,345] When the mixture of *syn*- and *anti*-**541** was submitted to these conditions, the expected hydroxy ketone **582** was isolated in 73% yield as a mixture of all four possible diastereomers (scheme 4.10). While oxidation with DMP and according to Ley^[264] led to complete decomposition of substrate **541**, Swern oxidation conditions furnished the desired product, which exists predominately in its enol form **583**, according to NMR spectroscopy. Although TLC analysis indicated a clean transformation, only a moderate 67% yield was realized and attributed to the volatility of product **583**.



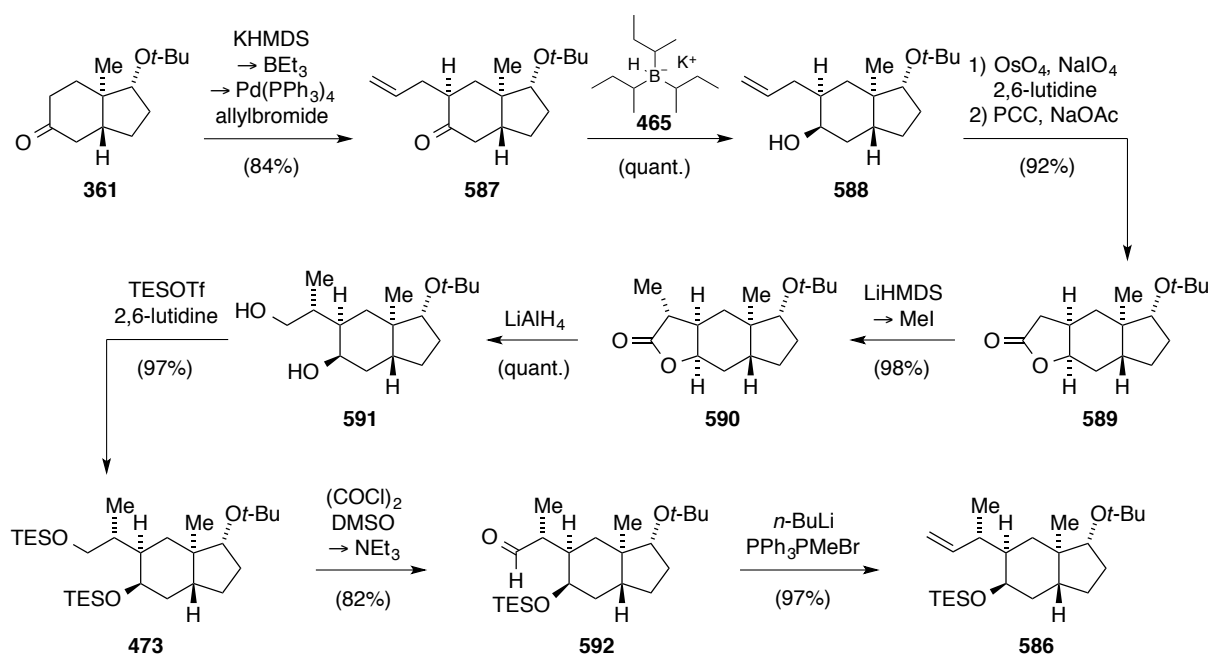
Scheme 4.11: Triflate formation on model system **584** and on advanced intermediate **583**.

The final triflate formation was first investigated on commercially available diketone **584** (scheme 4.11). The use of sodium hydride as base and subsequent addition of triflic anhydride resulted in surprisingly low yields, which is why the use of the milder triflation reagent PhNTf₂ was evaluated. Under these conditions triflate **585** was obtained in excellent yield. Due to its convenient fast preparation, we used this material as a model system for investigating the planned fragment coupling (*vide infra*). Unfortunately, when the established conditions were applied to advanced intermediate **583**, only 6% of the desired triflate (**539**) could be isolated. Further attempts toward an improvement of the reaction yield remained unsuccessful so far.

4.4 Model Studies on the Fragment Combination and Cyclooctadiene Formation

In order to conserve *trans*-hydrindanone **475**, a model system was synthesized for investigating the envisaged fragment combination and the following transformations toward aspired rearrangement precursor **537**. As several grams of surplus ether **361** were available from our synthetic studies toward retigeranic acid B (**237**, *cf.* chapter 2.3), we applied the transformations already outlined in chapter 3.5 to access alkene **586**. It has to be noted that the use of non-chiral triflate **585** renders the absolute configuration of substance **586** irrelevant for screening purposes.

Hence, ether **361** was submitted to Tsuji allylation conditions^[283] and desired alkene **587** was obtained in an optimized reaction yield of 84% (scheme 4.12). Subsequent diastereoselective reduction with K-Selectride[®] (**465**) proceeded smoothly and alcohol **588** was isolated quanti-



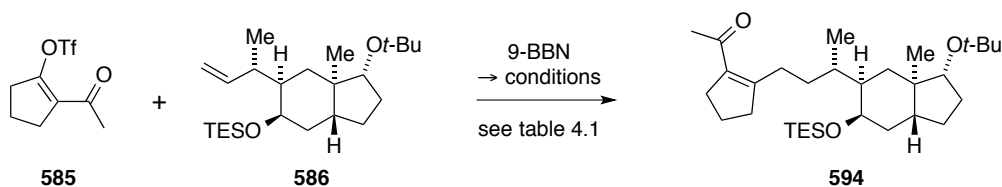
Scheme 4.12: Gram scale synthesis of model system **586** via the developed 9-step sequence (*cf.* chapter 3.4).

tatively. One-pot dihydroxylation and glycol cleavage under Lemieux-Johnson conditions^[290] was directly followed by PCC-mediated oxidation and gave rise to tricyclic lactone **589** in very good yield (92%). Next, the *C*-10 (astellatol numbering) centered stereogenic methyl group was installed *via* the established substrate-controlled alkylation procedure. Substance **590** was then reduced with LiAlH_4 , which allowed for the isolation of diol **591** in quantitative yield. The following double protection to silyl ether **473** was straightforward and was conducted with TESOTf and 2,6-lutidine in CH_2Cl_2 . When this material was reacted under deprotective Swern conditions, varying yields of aldehyde **592** were achieved (70–82%). Notably, the use of newly opened reagent batches did effect a less complete conversion of silyl ether **473**, which was presumably due to a reduced amount of available HCl traces.^[294] Final Wittig olefination of aldehyde **592** furnished alkene **586** without any observable side reaction. All in all, it was possible to synthesize 3.37 g of model compound **586** in an outstanding yield of 58% over 9 steps.

At this time it became possible to investigate the envisaged key intermolecular B-alkyl Suzuki coupling.^[346] Table 4.1 summarizes the conditions that were tested to achieve the fusion of alkene **586** and triflate **585**. For the initial hydroboration of substrate **586**, 9-BBN was employed in THF at 40 °C. At this, it was crucial to use two equivalents of the boron reagent to effect full conversion of the alkene functionality. Subsequently, an aqueous solution of either K_3PO_4 or Cs_2CO_3 was added to quench excess 9-BBN and to generate boronate **593** (scheme 4.13). This intermediate was then combined with triflate **585** in the presence of the respective Pd-based catalyst and solvent system. AsPh_3 was used optionally as

an additional ligand. The conditions originally published by Suzuki and co-workers for the coupling of aryl- and alkenyl triflates were evaluated first (entry 1).^[347] The low isolated yield prompted us to try the addition of frequently used AsPh_3 (entry 2), which has been proven to provide cleaner coupling reactions at higher turnover rates.^[348] Switching the catalyst to $\text{Pd}(\text{dppf})\text{Cl}_2$ (entry 3) and using Cs_2CO_3 as a base (entry 5), we literally optimized the reaction process to quantitative yield. Interestingly, conditions published by Carreira and Weiss for their (+)-daphmanidin E (not shown) synthesis,^[349] at which they describe $\text{Pd}_2(\text{dba})_3$ as being superior to phosphine ligand-based Pd^0 sources, produced enone **594** only in trace amounts (entry 4).

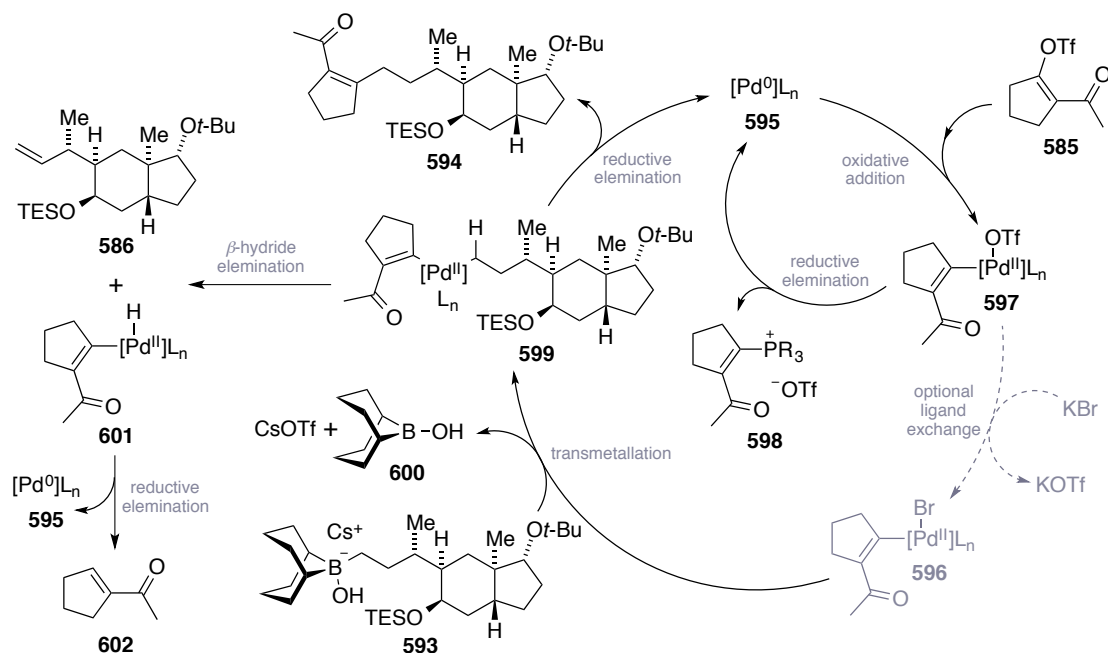
Table 4.1: Investigated conditions for B-alkyl Suzuki-type coupling of fragments **585** and **586**.



entry ^a	catalyst	additive ^d	solvent	T [°C]	t [h]	Yield
1	$\text{Pd}(\text{PPh}_3)_4$	K_3PO_4	1,4-dioxane	85	14 h	8% (72% brsm)
2	$\text{Pd}(\text{PPh}_3)_4$	Cs_2CO_3 , AsPh_3	1,4-dioxane	85	14 h	68%
3	$\text{Pd}(\text{dppf})\text{Cl}_2^b$	K_3PO_4 , AsPh_3	DMF	rt	18 h	82%
4	$\text{Pd}_2(\text{dba})_3^c$	K_3PO_4 , AsPh_3	DMF	45	14 h	traces
5	$\text{Pd}(\text{dppf})\text{Cl}_2^b$	Cs_2CO_3 , AsPh_3	DMF	rt	18 h	quant.

a) All reactions were carried out using 20 mg of alkene **586** and 2.0 eq. of triflate **585** at catalyst loadings of 5 mol-%. Solutions were thoroughly degassed *via* Ar bubbling. b) The more stable CH_2Cl_2 mono-adduct was used. c) The more stable CH_3Cl mono-adduct was used. d) Cs_2CO_3 and K_3PO_3 were used as 3 M aqueous solution.

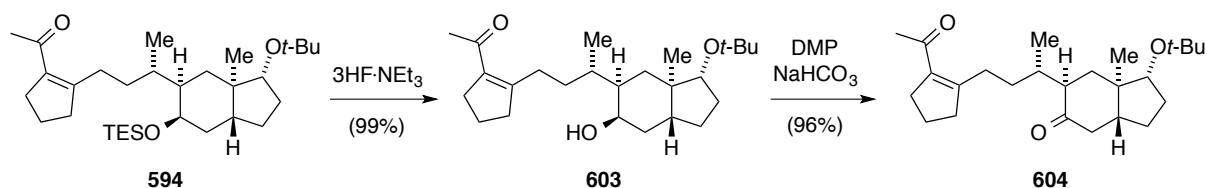
The mechanism of the B-alkyl Suzuki reaction is well understood and is illustrated in scheme 4.13 for Pd-based coupling.^[346] In most cases, the catalytically active Pd^0 species (**595**) are generated in the beginning *via* reduction that is induced *e.g.* by the phosphine ligand. Following oxidative addition of the alkenyl triflate (**585**) may be assisted by the use of KBr. The triggered ligand exchange (**596**) has been shown to suppress degradation of formed Pd^{II} species (**597**) by reductive elimination of phosphonium salts (**598**).^[347] Transmetalation of previously generated boronate **593** delivers intermediate **599** and byproduct **600**. Pd-complex **599** can either undergo reductive elimination to form desired coupling product **594**, thus closing the catalytic cycle, or react in β -hydride elimination of the alkyl ligand. This side reaction will lead to the backformation of



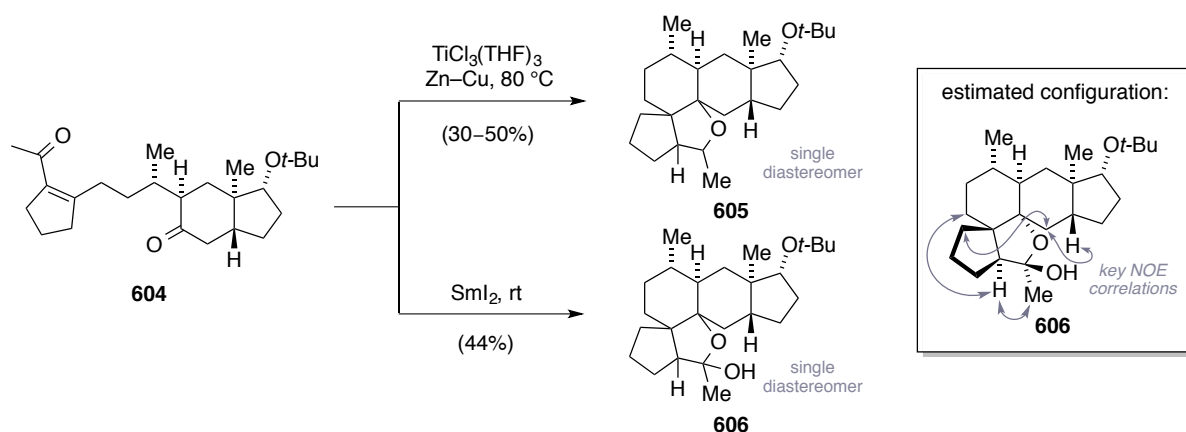
Scheme 4.13: Mechanism of the Pd-catalyzed B-alkyl Suzuki coupling reaction of preformed boronate **593** and triflate **585**. The optional ligand exchange step was not necessary in the presented case.

the initially employed alkene **586**. Concomitantly generated Pd–H species (**601**) would in turn instantly regenerate active Pd⁰ species **595** and yield the protodetriflated alkene **602**. It has been demonstrated that bidentate ligands with large bite angles, or monodentate ligands with bigger Tolman angles, effectively omit β -hydride elimination by acceleration of the reductive elimination in intermediate **599**.^[350] Hence, it is not surprising that dppf-ligand-based catalyst systems provided the best results in the presented investigations.

Ensuing TES deprotection was first evaluated using TBAF and 4 Å molecular sieves in THF. This led to significant amounts of decomposition, presumably due to the highly basic environment generated by this protocol. Gratifyingly, when the conditions were switched to acidic 3HF·NEt₃ in acetonitrile, clean cleavage of the ether function was observed and desired alcohol **603** was isolated in almost quantitative yield (scheme 4.14). Oxidation of this substrate, employing NaHCO₃-buffered Dess-Martin periodinane in CH₂Cl₂, was straightforward and gave rise to diketone **604**.



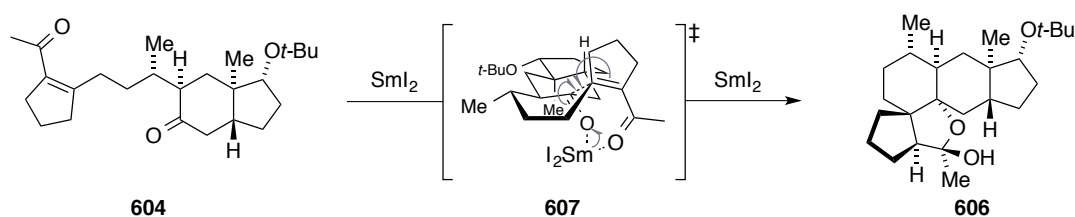
Scheme 4.14: Deprotection and oxidation sequence, yielding diketone **604**.



Scheme 4.15: Reaction of diketone **604** under McMurry or SmI_2 -mediated conditions. The relative configurations of the newly formed stereocenters of substances **605** and **606** could not be verified unambiguously.

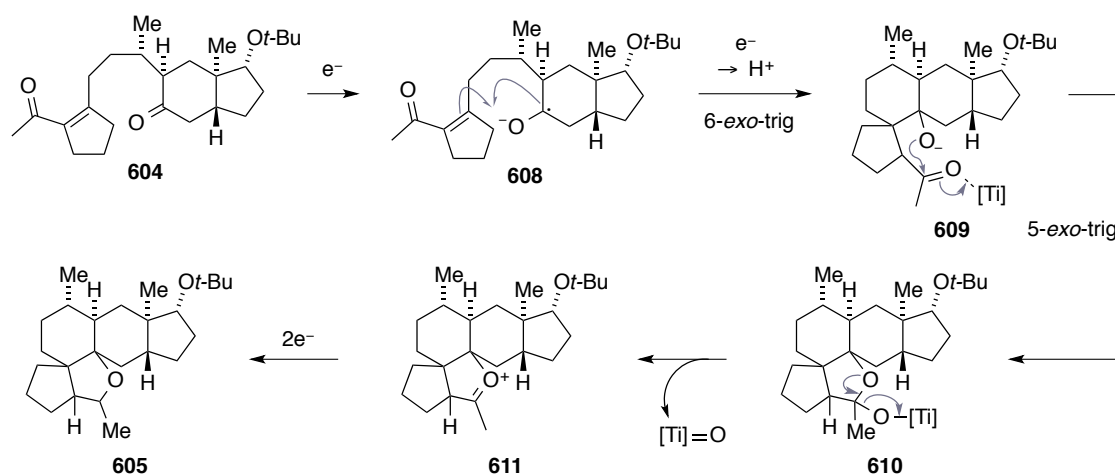
Having found a convenient route to model diketone **604**, we went on to investigate the envisaged reductive intramolecular carbonyl-carbonyl coupling. To this end, McMurry coupling protocols were tried first. Accordingly, substrate **604** was slowly added to a suspension of low-valent titanium, which was generated *in situ* from commercially available $\text{TiCl}_3(\text{THF})_3$ and freshly prepared Zn–Cu couple, in DME (scheme 4.15). Amongst various possible known reduction systems,^[323,324] these conditions are stated to be most reliable and reproducible.^[351] Interestingly, this reagent combination did not furnish the desired 8-membered ring, but resulted in the diastereoselective formation of pentacyclic product **605**. However, the configuration of the newly formed stereocenters could not be determined unambiguously, despite the use of extensive NMR spectroscopic studies. To the best of our knowledge, this type of cyclization cascade is unprecedented in literature and the resulting ring system has not been accessed by other means to date.

Since reductive carbonyl-carbonyl coupling can also be achieved *via* diol formation, we next turned our attention towards SmI_2 -mediated reactions.^[352,353] In agreement with the previous results from McMurry-type conditions, the envisioned 8-membered ring containing product was not observed. Instead, seemingly the same cyclization mode occurred and yielded pentacyclic hemiacetal **606** as a single diastereomer. Scheme 4.16 shows the isomer of the



Scheme 4.16: Possible 11-membered ring transition state, explaining the formation of the proposed *cis*-decalin junction at the SmI_2 -mediated cyclization of diketone **604**.

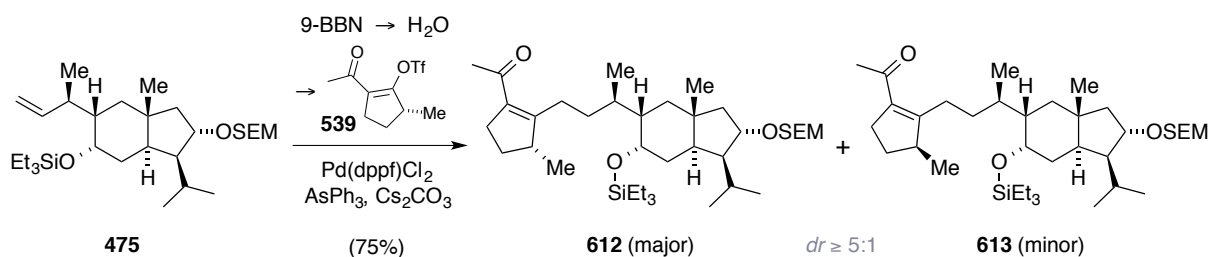
isolated substance **606** that represents the most probable relative configuration, according to observed NOESY signals. The proposed *cis*-decalin junction is in agreement with results published by Matsuda *et al.* In the course of their vinigrol (not shown) synthesis, these authors describe a comparable carbonyl-alkene coupling of a cyclohexanone moiety to a α,β -unsaturated ester function.^[354] In a study on asymmetric reductive cyclizations that was published by Little and co-worker, an 11-membered ring transition state is proposed. Transfer of this model to system **607** supports the stereochemistry that was deduced for the newly formed quaternary center (scheme 4.16).^[355] However, in the following drawings the configuration of those centers will be left undefined, in order to refrain from speculations.



Scheme 4.17: A plausible mechanism for observed reductive intramolecular cyclization cascade.

Mechanistically, we propose a general reaction pathway that is illustrated in scheme 4.17 for both the McMurry-type and the SmI_2 -mediated transformations. Upon formation of a ketyl radical at the more electrophilic carbonyl moiety of diketone **604**, intermediate **608** undergoes a Michael addition in a 6-*exo*-trig fashion.^[354,355] A subsequent one-electron reduction of the resulting oxygen centered radical is followed by protonation. Keto-enol tautomerization then generates the carbonyl functionality in alcoholate **609** that immediately cyclizes to form a hemiacetal **610**. The latter step and the following loss of oxygen is probably assisted by Lewis acidic titanium species. The resulting oxonium ion (**611**) would then be reduced in another two-electron step to corresponding ether **605**. The combination of milder reaction conditions with the less pronounced Lewis acidic properties of SmI_2 presumably account for the fact that in this case no final deoxygenation was observed.

A further screening of reaction conditions toward a reductive carbonyl-carbonyl coupling proved less fruitful. In light of these findings and the fact that the low yielding triflate formation remained a bottleneck in the synthetic roadmap for building block **539**, the

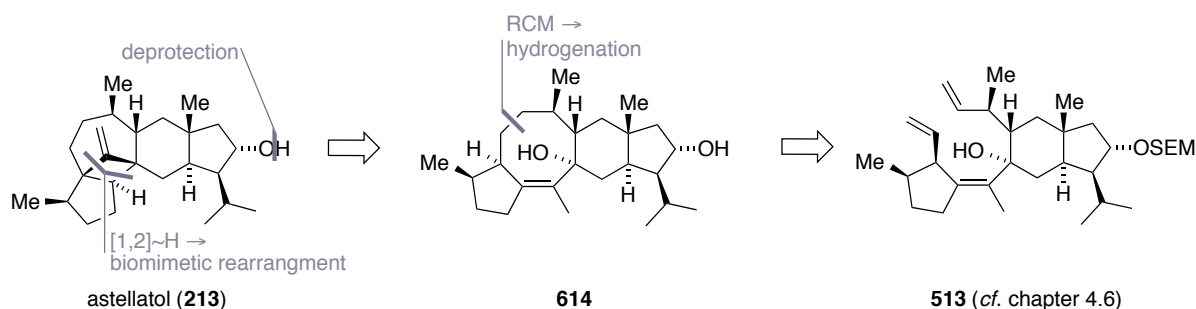


Scheme 4.18: B-alkyl Suzuki coupling of triflate **539** and *trans*-hydrindanone **475**.

presented strategy was abandoned at this point. It is worth to mention that the optimized B-alkyl Suzuki conditions also succeeded to couple both advanced fragments – triflate **539** and *trans*-hydrindane **475** – and delivered enone **612** in good yield (scheme 4.18). Concomitantly, a second diastereomer (**613**) was observed in this coupling, indicating that a partial epimerization of the selectively installed stereogenic center at carbon C-14 may have taken place in the course of pursued route (*cf.* chapter 4.3). A quantification of the ratio of those compounds was not feasible by means of HPLC, GCMS or LMCS methods. Calculating from the partially overlaying isomeric signals in recorded ^1H NMR spectra, the *dr*-value lies between 5:1 and 10:1 and is in favour of desired product **612**.

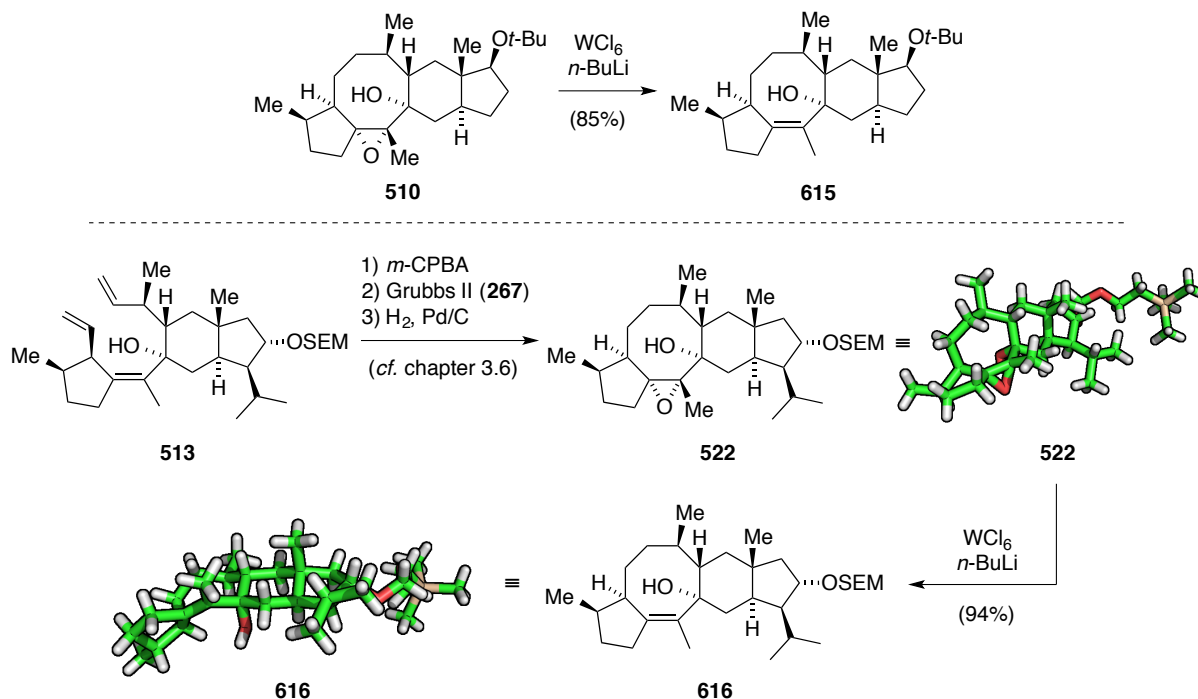
4.5 Second-generation Approach: Branching Off at the (–)-Nitidasin Synthesis

In chapter 3.2 it was already hinted that a different approach toward the construction of astellatol's (**213**) carbocyclic skeleton would be possible from common intermediate **513**. As outlined in the retrosynthetic analysis in scheme 4.19, it was envisioned to enter the proposed biomimetic rearrangement from allylic alcohol **614**. After an initial ionization, this would require an additional [1,2]-hydride shift to form the desired homoallyl cation. Although this hydride shift would clearly be endothermic for itself, the final formation of the stable natural product (**213**) was supposed to deliver the driving force for the equilibrium cationic cascade. A further disconnection of allylic alcohol **614** traces back to triene **513**. In



Scheme 4.19: Second-generation retrosynthetic analysis of astellatol **213**, starting from known triene **513**.

the forward sense, this triene (**513**) was originally planned to undergo RCM-mediated cyclization to yield the 5-8-6-5-membered ring system. However, it was not possible to access an cyclooctadiene system directly from triene **513** or from similar compounds by means of olefin metathesis-based approaches (*cf.* chapter 3.5). The unexpected participation of the tetrasubstituted double bond could only be avoided when this function was first epoxidized to diene **514**. Ensuing RCM reaction and hydrogenation, employing the previously established conditions, gave rise to saturated tetracycle **522** (scheme 4.20), of which crystals were obtained that were suitable for X-ray crystallographic analysis. With these results in mind, the synthetic strategy was changed and a protocol that was developed by Sharpless and co-workers was considered.^[316,356] This method allows for the transformation of epoxides to their respective alkenes, by using low valent tungsten species that are generated *in situ* from WCl_6 and two equivalents of *n*-BuLi. The mechanism of this reaction is still not clarified to date, but the original authors proposed that intermediary formed tungsten(IV) leads to a concerted deoxygenation and installment of the carbon–carbon double bond. Application of those conditions to model compound **510** resulted in clean conversion to desired allylic alcohol **615** in very good yield. Accordingly, transfer to advanced intermediate **522** finally provided the precursor (**616**) for the planned cationic cascade in excellent 94% yield. Since signal broadening thwarted the structure analysis by ^{13}C NMR spectroscopy for both allylic alcohols **615** and **616**, the identity of the latter compound had to be proven by means of X-ray

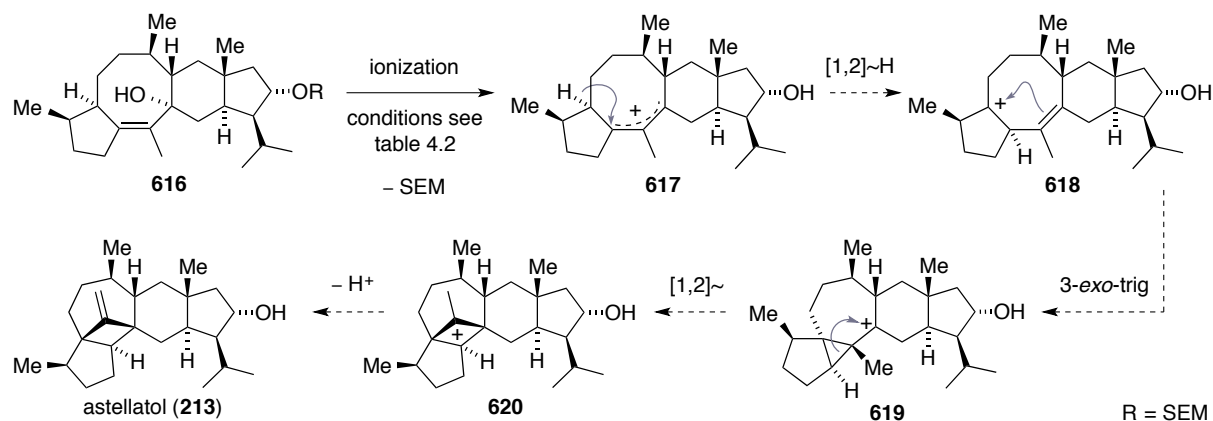


Scheme 4.20: Preparation of allylic alcohols **615** and **616**, using a tungsten(IV)-mediated deoxygenation.

crystallography. In summary, an epoxide function was effectively used as a protective group in order to achieve RCM-mediated closure of the 8-membered ring system.

At long last, we were now in the position to examine the proposed cationic cascade for the synthesis of astellatol (**213**) experimentally for the first time. In order to achieve the initial ionization step to species **617**, the use of Brønsted acids in a variety of solvent systems of

Table 4.2: Investigated conditions for the cationic cascade toward the construction of astellatol (**213**). Only the reaction pathway for allylic alcohol **616** is shown for clarity. SEM deprotection is optional.



entry ^a	substrate	reagent	solvent	T [°C]	observation
1	615	<i>p</i> -TsOH	toluene	60 to 120	elimination, deprotection
2	615 , 616	CSA	CH ₃ CN	rt	elimination, 621 ^c (1–2%)
3	615	Re ₂ O ₇	DCM	rt	elimination, deprotection
4	615	Re ₂ O ₇ , <i>p</i> -TsOH	DCE	60	elimination, deprotection
5	615	TFA-d ₁	CDCl ₃	rt	elimination, decomp.
6	616	CSA	THF/H ₂ O	rt to 65	elimination, deprotection
7	616	HF/py	THF	rt	elimination, 621 ^c (5–7%), deprotection
8	616	CSA	acetone	rt to 60	elimination
9	616	CSA	1,4-dioxane	rt to 65	elimination, 621 ^c (3–4%), deprotection
10	616	CSA	CH ₃ NO ₂	rt to 45	elimination, deprotection
11	616	HClO ₄	CH ₃ NO ₂	rt	decomp.
12	616	HCl ^b	MeOH	rt	elimination, deprotection
13	616	<i>p</i> -TsOH	TFE	rt	elimination, deprotection
14	616	CSA	DMF	rt to 60	elimination
15	616	CSA	DMSO/H ₂ O	rt to 60	elimination

^a) All reactions were carried out on 1.0 or 0.5 mg scale. ^b) Used in 1 M concentration and freshly prepared *via* addition of AcCl to dry MeOH. ^c) The identity of **621** could not be elucidated. ¹H NMR analysis suggests that **621** contains an *exo*-methylene function.

different polarities was investigated first (table 4.2). When no reaction could be observed, the temperature was raised gradually until conversion took place. Unfortunately, the prevailing reaction pathway led to the formation of several kinds of elimination products. This was accompanied by SEM or *t*-Bu group removal in certain cases. The addition of perrhenate species like Re_2O_7 , which are known to catalyze transposition of allylic alcohols,^[357] could not avoid the undesired elimination reactions either (entries 3,4). The characteristic signals of the *exo*-methylene group ($\delta = 4.80$ and 4.63 ppm) of astellatol (**213**) were observed at none of the presented cases when ^1H NMR spectra were recorded from the crude reaction mixtures.^[155] Under certain conditions a different *exo*-methylene containing compound (**621**, entries 2,7,9) was found, which showed clearly distinct chemical shifts for the relevant two protons ($\delta = 4.97$ and 4.84 ppm). However, the separation of this compound from the accompanying elimination products was impossible, due to the inherent low polarity of the mixture. Thus, the identity of this side product could not be elucidated further.

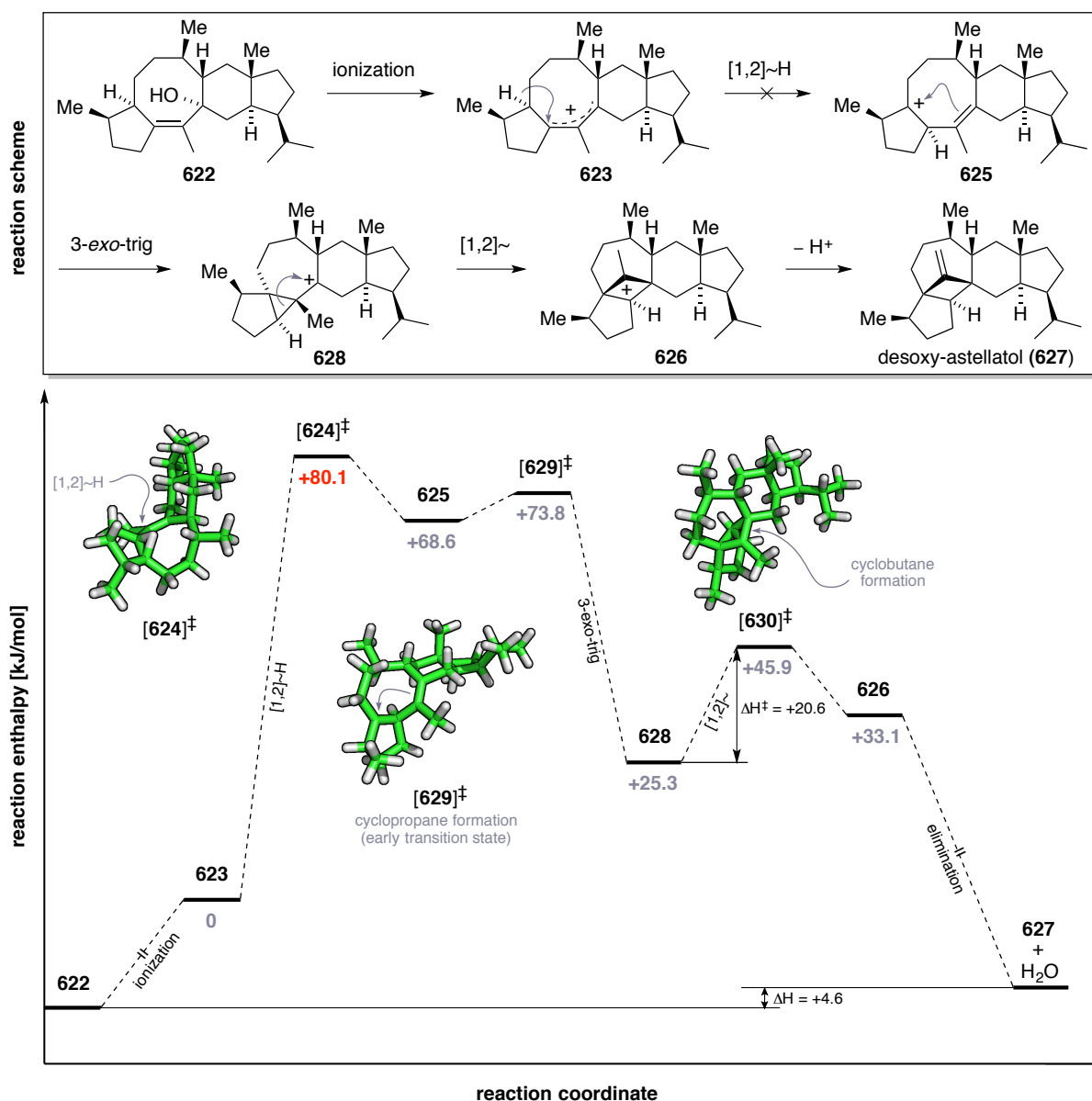
The same finding held true when Lewis acids (*e.g.* $\text{BF}_3 \cdot \text{OEt}_2$, $\text{Ti}(\text{OiPr})_4$, TiCl_4 , Cp_2ZrCl_2 , AlCl_3) were employed instead. In those cases, either elimination, no reaction or complete decomposition took place. According to those results, it is supposed that the required initial [1,2]-hydride shift toward homoallyl cation **618** exhibits an energetic barrier that is too high to compete with elimination side reactions into all possible four positions.

4.6 Theoretical Investigations on the Envisaged Cationic Cascade

In order to investigate the viability of the proposed cationic cascade and to provide further mechanistical insights into the presumably biomimetic homoallyl-cyclopropylcarbinyll-cyclobutyl rearrangement, we set out to conduct supporting theoretical studies. To this end, calculations on the relative energies of involved cationic intermediates and on the enthalpic outcome of the overall reaction were performed in cooperation with B.Sc. M. Maier. In order to reduce computational time and effort, we cut out the *C*-5 situated alkoxy substituent (astellatol numbering) of astellatol (**213**), as this function showed no obvious effect on the conformation of the direct reaction environment.

For the initial conformational search of allylic alcohol **622** (*vide infra*), we applied molecular mechanics on the MMFF94 force-field level.^[358] The number of found species of reasonable low energy was limited as it was expected according to the overall rigidity of the system. Only the B ring, the carbon atom chain from *C*-9 to *C*-13 and the *iso*-propyl group were able to adopt rotameric orientations. Hence, twelve relevant conformers were identified and

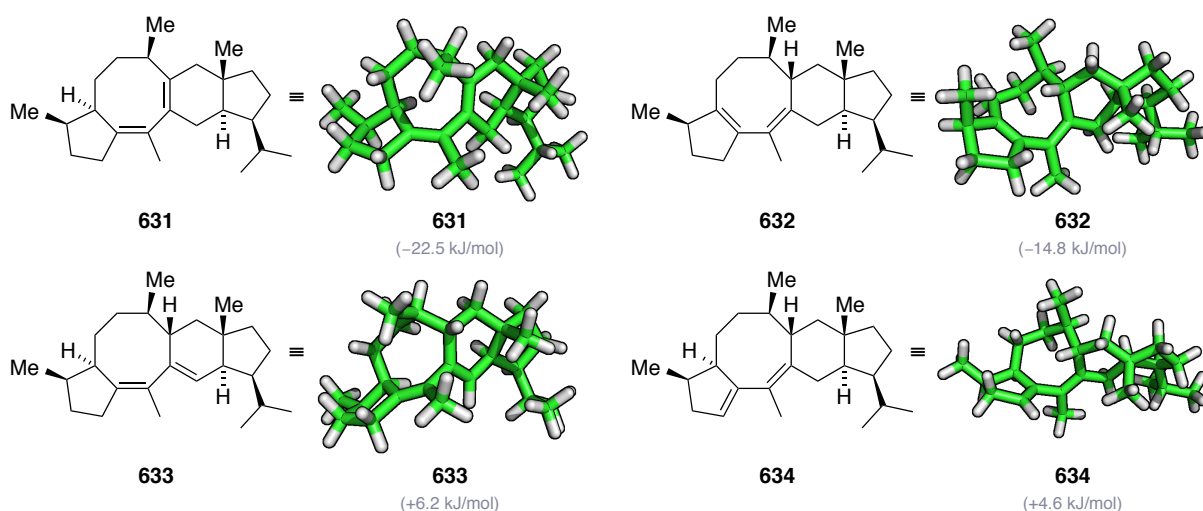
equivalent arrangements served as starting points for refinement of the geometries of determined reaction intermediates and transition states.^{xii} The computational investigations on the cationic cascade involved a two-level DFT approach. For structure optimization, the well-established B3LYP functional^[359] was used in combination with the def2-SVP basis set.^[360] For the approximation of solvation energies, the COSMO model^[361] was employed and THF was chosen as an appropriate polar environment^[201] with regard to the experimentally observed solubility properties of allylic alcohol **616**. Furthermore, the RIJCOSX and RI approximations,^[362] as well as the D3 and gCP corrections^[360] were applied to improve calculation speed and accuracy, respectively. Notably, the latter mentioned terms have



Scheme 4.21: Calculated energy profile for the proposed cationic rearrangement toward desoxy-astellatol (**627**).

^{xii}Reported results refer to the lowest energy conformers of respective species in THF. Gas-phase energies and further details on employed programs and methods are listed in sections I and V of the appendix.

been shown to provide results being superior to the commonly employed B3LYP/6-31G* approach.^[363] The found relative energies of all cationic intermediates and transition states are illustrated in scheme 4.21 in terms of a reaction profile. As a point of reference, allylic cation **623** was chosen. Most importantly, it was shown that the transition state **624** for the non-biomimetic [1,2]-hydride shift has an unexpected high energy of +80.1 kJ/mol. The calculated structure suggests that this is presumably a result of the high conformational change of the central 8-membered ring, which is required to effect the *syn*-periplanar orientation of the C-13 bound hydrogen and C-17 centered sp²-atom orbital. Starting from the favourable boat-chair configuration, the cyclooctene ring system gets distorted to the approximate shape of a hyperbolic paraboloid. In combination with the concomitant loss of the stabilizing conjugation effect, this accounts for the experimentally observed preference for reaction *via* elimination pathways. It was concluded that once the homoallyl cation corresponding to **625** can be addressed synthetically, the following steps of the cationic cascade would proceed without any difficulty, as the highest encountered barrier in energy is only of +20.6 kJ/mol. In summary, the actual biomimetic rearrangement is exothermic by –35.5 kJ/mol, when arriving at the final cyclobutyl cation **626**. Hence, ensuing elimination toward desoxy-astellatol (**627**) should effectively remove the cationic species from the equilibrium cascade. Nevertheless, future computational work will have to address the additionally conceivable elimination side reactions, which emanate from intermediary cationic species **625** and **628**.

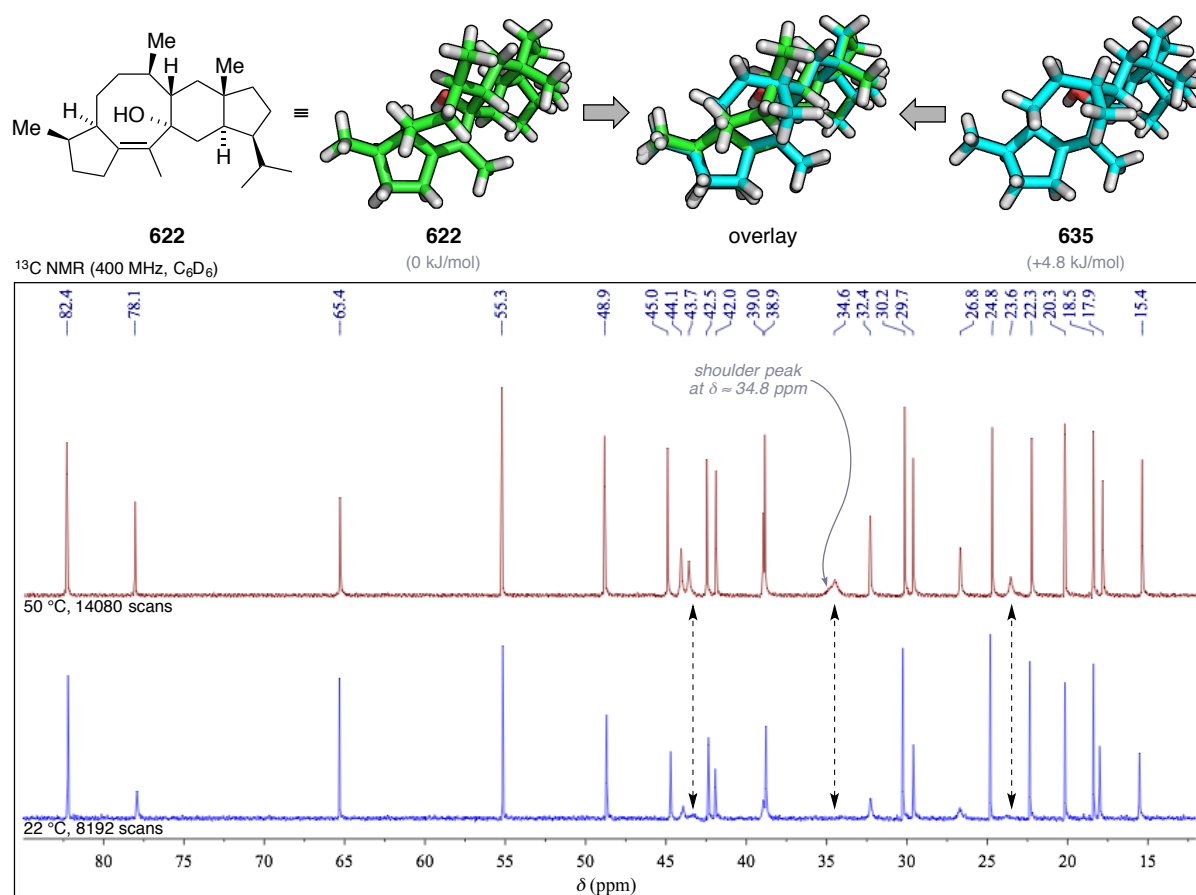


Scheme 4.22 Calculated energies and structures of possible elimination products of alcohol **622**. All values describe the respective generic dehydration reactions and refer to conformer **622** (*vide infra*).

It has to be mentioned, that both the starting allylic alcohol **622** and the ultimately resulting desoxy-astellatol **627** are not incorporated quantitatively, as initial ionization and final elimination steps are largely reagent-dependent processes. Interestingly, the overall reaction

enthalpy for a generic dehydration that yields water and pentacycle **627** shows a slightly positive value (+4.6 kJ/mol). However, this does not account for the favourable entropic contribution that arises from the formation the additional molecule of water, but states the high stability of allylic alcohol **622**. In line with this, the respective reaction enthalpies for the formation of all possible four elimination products of allylic cation **623** were calculated (scheme 4.22). Especially both the octadienes **631** and **632** seem to be energetically favoured. This suggests that the retrosynthetic approach presented in chapter 4.2, which envisages the very generation of the latter diene, would most likely suffer from the same problems as the second-generation approach. However, a more detailed theoretical investigation of involved transition states would be necessary to rigorously disprove this synthetic strategy.

Furthermore, the conducted conformational search of allylic alcohol **622** provided reasonable explanation for the experimentally observed signal broadening in recorded ^{13}C spectra. Although the solvent system differed for the calculations (THF), it can be seen that two energetically similar conformations prevail (scheme 4.23). These species exhibit significant spatial relocation of carbons C-10 to C-16, including the stereogenic methyl group C-24. The

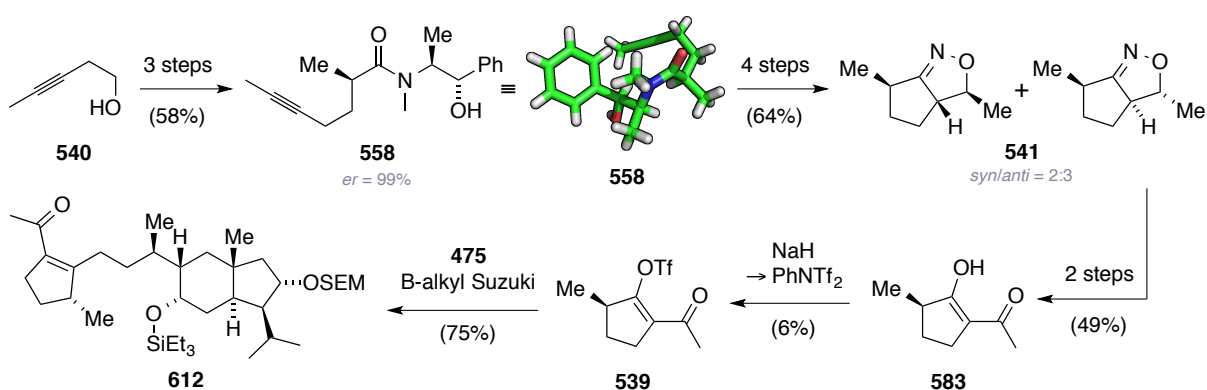


Scheme 4.23 Calculated structures **622** and **635** and relative energies for spectroscopically observed rotamers, as well as comparison of ^{13}C NMR spectra of substance **616** (*cf.* scheme 4.19) recorded at 22 (blue) and 50 °C (red), respectively.

transformation that is needed to interchange those rotamers requires the inward and outward flipping of methylene group C-11 and connected carbons C-10 and C-24, respectively. To prove the existence of a rotameric mixture of **622** and **635** in solution experimentally, high temperature ^{13}C NMR measurements were conducted at 50 °C. As expected, the so far missing carbon signals emerged and the already visible, but broadened peaks exhibited significantly narrowed line shapes. It has to be mentioned that two signals at $\delta = 34.6$ and 34.8 ppm could not be resolved completely and remained as a major and a shoulder peak, respectively. In order to preserve the valuable material that had to be employed in entirety, it was not tried to record spectra at even more elevated temperatures, as the required measurement times already exceeded 15 hours.

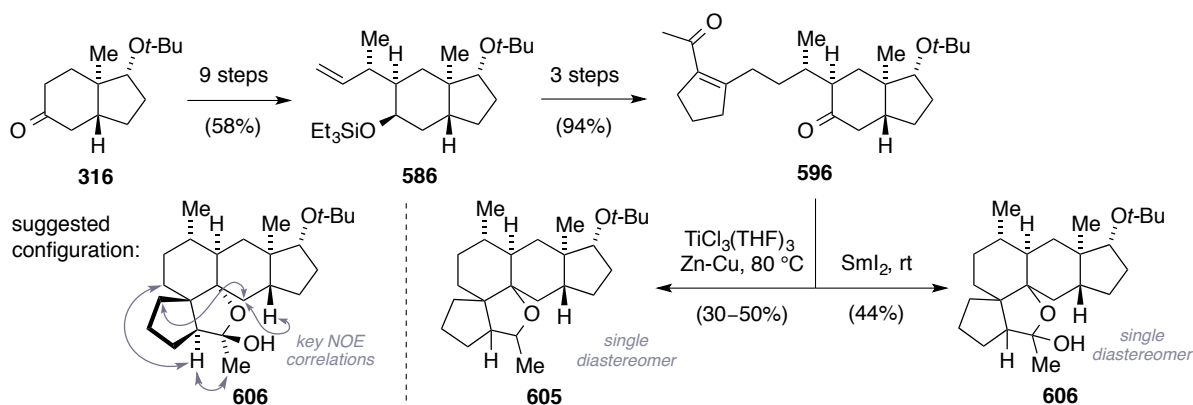
4.7 Conclusion and Future Aspects

In summary, two different synthetic approaches toward the sesterterpenoid astellatol (**213**) were presented, both of which planned to exploit the natural products biosynthetic cationic cascade for the assembly of its central ring motif in a final synthetic transformation.



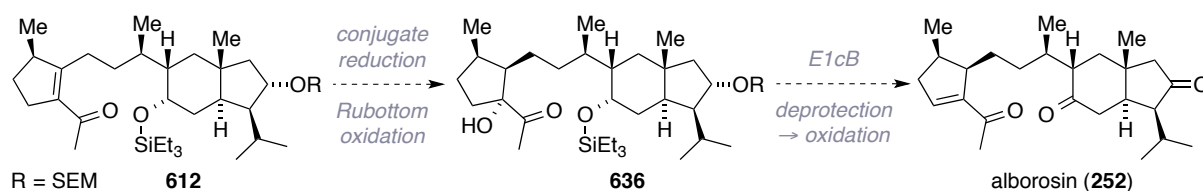
Scheme 4.24: Enantioselective 11-step synthesis of triflate **539** and B-alkyl-Suzuki coupling to substrate **475**.

The first approach relied on the construction of a fused cyclooctadien motif (**537**, scheme 4.4), which would allow entering the biomimetic rearrangement toward astellatol (**213**) upon initial protonation. Therefore, the envisaged cyclopentene triflate **539** was prepared by a enantioselective 11-step route, which was based on an early-stage introduction of the stereogenic center *via* Myers alkylation (scheme 4.24). Using the so-called INOC strategy, a highly efficient cyclization to a bicyclic isoxazoline ring system (**541**) could be demonstrated, which allowed for the reductive installation of required oxygenation pattern in an additional step. Unfortunately, the final triflate (**539**) formation remained a bottleneck in



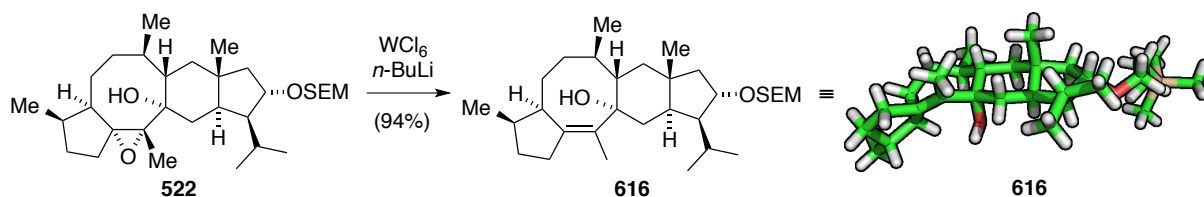
Scheme 4.25: Preparation of model system **586** and thereof synthesized pentacyclic compounds **605** and **606**.

this synthetic sequence, which leaves room for future optimization. At this, the effect of bases different from NaH or other transfer reagents like the increasingly reactive Comin's reagent^[364] might be explored. In addition, a highly efficient B-alkyl Suzuki coupling was presented on model system **586** and toward the authentic coupling product (**612**, cf. chapter 4.4). The application of reductive carbonyl-carbonyl coupling methods resulted in a literature unprecedented cyclization cascade (**605** and **606**, scheme 4.25). A plausible mechanism for this cyclization mode and a suggestion for the not unambiguously clarified stereochemical outcome were given. Although the formed pentacyclic skeleton is not included in any reported natural product or synthetic target, the discovered cyclization reactions provide an intriguingly fast construction of three fused ring systems and four adjacent stereogenic centers, two of which are quaternary.



Scheme 4.26: A possible synthetic route for the preparation of alborosin **252** from enone **612**. R = SEM.

Furthermore, this synthetic route might lead to a future total synthesis of the related sesterterpenoid alborosin (**252**, scheme 4.26), as the inherent structural similarity to the already accessed enone **612** suggests. Although the C-13 (astellatol numbering) located sp^2 -center is highly substituted, introduction of required stereochemistry could possibly be achieved using substrate- or reagent-controlled CuH-based 1,4-reduction methods.^[217,365,366] A thus generated enolate could be trapped as silyl ether and directly employed in a Rubottom oxidation.^[367] The selective formation of alcohol **636** could be biased by the adjacent ring substituents or by using an asymmetric modification.^[368] Subsequent conversion to an

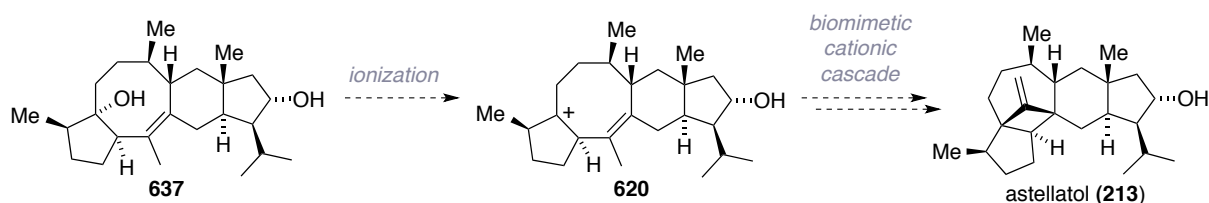


Scheme 4.27: Synthesis of alcohol **616** as precursor for proposed cationic cascade toward astellatol (**213**).

appropriate leaving group and elimination *via* an E1cB mechanism would then provide the desired unsaturation pattern. Final deprotection and oxidation to the natural product should be straightforward.

The second investigated approach toward astellatol (**213**) originally opted for the use of triene **513** as a precursor being common to the nitidasin (**238**) synthesis (*cf.* chapter 3.5). To this end, a tungsten(IV)-based deoxygenation protocol was applied to **522** in order to access the envisaged allylic alcohol **616** (scheme 4.27). However, experimental investigations on the proposed cationic cascade did not provide the carbon skeleton of the natural product under a variety of conditions. In parallel conducted theoretical investigations were in agreement with the experimental results and suggested that aspired initial [1,2]-hydride shift exhibits an energetic barrier (+80.1 kJ/mol), which is too high to compete with elimination reactions. According to those calculations, the actual homoallyl-cyclopropylcarbinyl-cyclobutyl rearrangement would proceed smoothly, once the homoallyl cation corresponding to species **625** can be addressed by synthesis (*cf.* chapter 4.6). From this point onward, the most endothermic transition state between involved cationic species was determined to have a relative energy of only +20.6 kJ/mol.

In the light of these results, it is reasoned that homoallyl alcohol **637** (scheme 4.27) represents the appropriate precursor for the biomimetic formation of astellatol (**213**). However, at this point reasonable retrosynthetic proposal for its construction is lacking, as this would probably require a complete redesign of the established 8-membered ring formation sequence.



Scheme 4.28: Homoallyl alcohol **637** as a potential target for future synthetic approaches toward a total synthesis of astellatol (**213**)

5. Experimental Section

5.1 General Notes

All reactions were magnetically stirred and carried out under a positive pressure of inert gas (N_2 or argon) utilizing standard Schlenk-techniques. Glassware was dried in an oven at $120\text{ }^\circ\text{C}$ and repeatedly at $650\text{ }^\circ\text{C}$ *in vacuo* prior to use. Liquid reagents and solvents were added by syringes or oven-dried stainless steel cannulas through rubber septa. Solids were added under inert gas counter flow or were dissolved in appropriate solvents. Low-temperature reactions were carried out in a Dewar vessel filled with a cooling agent: acetone/dry ice ($-78\text{ }^\circ\text{C}$), acetonitrile/liquid N_2 ($-40\text{ }^\circ\text{C}$), NaCl /ice ($-20\text{ }^\circ\text{C}$) or H_2O /ice ($0\text{ }^\circ\text{C}$). Reaction temperatures above room temperature were conducted in a heated oil bath. High-pressure reactions were carried out in a miniclave steel apparatus from *BÜCHI AG*. If literature-known procedures were followed, the respective references were given in the discussion part. Yields refer to isolated homogenous and spectroscopically pure materials, if not indicated otherwise.

Solvents and Reagents

Tetrahydrofuran (THF) and diethyl ether (Et_2O) were distilled under N_2 atmosphere from Na /benzophenone as drying reagent prior to use. Triethylamine (Et_3N), diisopropylamine (DIPA) and Hünig's base (DIPEA) were distilled under N_2 atmosphere from CaH_2 as drying agent prior to use. Further dry solvents such as dichloromethane (CH_2Cl_2), *N,N*-dimethylformamide (DMF), acetonitrile (MeCN), HMPA, acetone, methanol (MeOH), benzene and toluene were purchased from commercial suppliers and used as received. (*S*)-Alpine-BoramineTM (**452**) was purchased from *Sigma-Aldrich* and stored in a UNILab glove-box from *MBRAUN*. Methyl vinyl ketone (**300**) and allyl bromide were distilled prior to use and stored under an argon gas atmosphere. Solvents for extraction, crystallization and flash column chromatography were purchased in technical grade and distilled under reduced pressure prior to use. (+)-Eder-Sauer-Wiechert-Hajos-Parrish ketone (**138**),^[211] aldehyde **420**,^[249] DMP,^[369] Zn-Cu couple,^[351a] oxazolidinone **542**,^[328–330] and amide **556**,^[107] were prepared as described previously. Solutions of BEt_3 were freshly prepared from neat BEt_3 and thoroughly degassed THF ($3 \times$ freeze-pump-thaw). All other reagents and solvents

were purchased from chemical suppliers (*Sigma-Aldrich*, *Acros Organics*, *Alfa Aesar*, *Strem Chemicals*, *ABCR*, *TCI Europe*) and were used as received.

Chromatography

Reactions and chromatography fractions were monitored by qualitative thin-layer chromatography (TLC) on silica gel F₂₅₄ TLC plates from *Merck KGaA*. Analytes on the glass plates were visualized by irradiation with UV-light and/or by immersion of the TLC plate in an appropriate staining solution followed by heating with a hot-air gun (350 °C). The following staining solutions were applied:

- *p*-anisaldehyde staining solution (3.7 mL *p*-anisaldehyde (**671**), 5.0 mL concentrated aqueous H₂SO₄, 1.5 mL glacial AcOH, 135 mL EtOH).
- Hanessian's staining solution (CAM, 5.0 g, Ce(SO₄)₂, 25 g (NH₄)₆Mo₇O₂₄·4H₂O, 50 mL concentrated aqueous H₂SO₄, 450 mL H₂O).
- KMnO₄ staining solution, (3.0 g KMnO₄, 20 g K₂CO₃, 5.0 mL aqueous 5% NaOH, 300 mL H₂O).

Flash column chromatography was performed on Geduran[®] Si60 (40–63 µm) silica gel from *Merck KGaA*. All fractions containing a desired substrate were combined and solvents were removed under reduced pressure followed by drying *in high vacuo* (10⁻² mbar).

NMR spectroscopy

NMR spectra were measured on a *Bruker Avance III HD* 400 MHz spectrometer equipped with a CryoProbe[™] operating at 400 MHz for proton nuclei (100 MHz for carbon nuclei) or by the analytic section of the Department of Chemistry of the *Ludwig-Maximilians-Universität München* using *Bruker AXR300*, *Varian VXR400 S* and *Bruker AMX600* spectrometers operating at 300 MHz, 400 MHz and 600 MHz for proton nuclei (75 MHz, 100 MHz, 150 MHz for carbon nuclei, 382 MHz for fluoride nuclei), respectively. CDCl₃ and C₆D₆ were purchased from *Sigma-Aldrich* and *Euriso-top*. The ¹H NMR shifts are reported in ppm related to the residual shift of TMS. ¹H NMR shifts were calibrated to residual solvent resonances: CDCl₃ (7.26 ppm), C₆D₆ (7.16 ppm). ¹³C NMR shifts were calibrated to the center of the multiplet signal of the residual solvent resonance: CDCl₃ (77.16 ppm), C₆D₆ (128.06 ppm). ¹H NMR spectroscopic data are reported as follows: Chemical shift in ppm (multiplicity, coupling constants *J*, integration intensity). The multiplicities are

abbreviated with s (singlet), br (broad signal), d (doublet), t (triplet), q (quartet), m (multiplet) and m_C (centrosymmetric multiplet). In case of combined multiplicities, the multiplicity with the larger coupling constant is stated first. Except for multiplets, the chemical shift of all signals, as well for centrosymmetric multiplets, is reported as the center of the resonance range. Additionally to ¹H, ¹⁹F and ¹³C NMR measurements, 2D NMR techniques as homonuclear correlation spectroscopy (COSY), heteronuclear single quantum coherence (HSQC) and heteronuclear multiple bond coherence (HMBC) were used to assign signals. For further elucidation of 3D structures of the analytes, nuclear Overhauser enhancement spectroscopy (NOESY) was conducted. Coupling constants *J* are reported in Hz. All NMR spectra were analyzed using the program *MestRe NOVA 8.1* from *Mestrelab Research S. L.*

Mass spectrometry

All mass spectra were measured by the analytic section of the Department of Chemistry of the *Ludwig-Maximilians-Universität München*. Mass spectra were recorded on the following spectrometers (ionization mode in brackets): MAT 95 (EI) and MAT 90 (ESI) from *Thermo Finnigan GmbH* or JMS-700 (FAB) from *Jeol Ltd.* Mass spectra were recorded in high-resolution and the only characteristic molecule fragments or molecule ion peaks are indicated for each analyte. The used method is reported at the relevant section of the experimental part.

IR spectroscopy

IR spectra were recorded on a *PerkinElmer* Spectrum BX II FT-IR system. If required, substances were dissolved in CH₂Cl₂ prior to direct application on the ATR unit. The measured wave numbers are reported in cm⁻¹.

Optical rotation

Optical rotation values were recorded on a polarimeter P8000-T from *A. Krüss Optronic GmbH* or on a *PerkinElmer* 241 polarimeter. The specific rotation is calculated as follows:

$$[\alpha]_{\lambda}^{\vartheta} = \frac{\alpha \cdot 100}{c \cdot d}$$

Thereby, the wavelength λ is reported in nm and the measuring temperature ϑ in °C. α resembles the recorded optical rotation at the apparatus, c the concentration of the analyte in

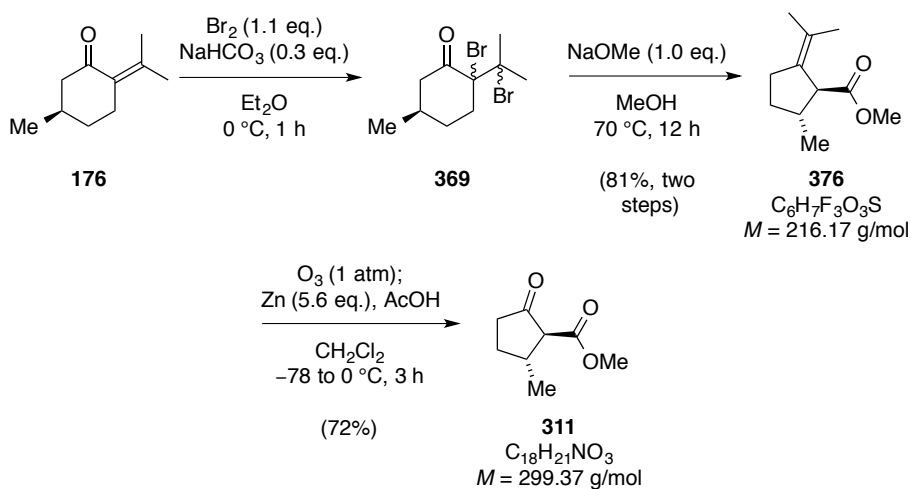
10 mg/mL and d the length of the cuvette in dm. Thus, the specific rotation is given in $10^{-1} \cdot \text{deg} \cdot \text{cm}^2 \cdot \text{g}^{-1}$. Usage of the sodium D line ($\lambda = 589 \text{ nm}$) is indicated by D instead of the wavelength in nm. The respective concentration as well as the solvent is denoted in the analytical part of the experimental description.

Melting points

Melting points were measured on the apparatus *BÜCHI* Melting Point B-540 from *BÜCHI Labortechnik AG* or on an EZ-Melt apparatus from *Stanford Research Systems* and are uncorrected.

5.2 Experimental Procedures for Chapter 2: ‘Synthetic Studies Toward Retigeranic Acid B’

Synthesis of Ester 311



To a solution of (*R*)-pulegone (**176**, 25.0 g, 164 mmol, 1.0 eq.) in dry diethyl ether (190 mL) was added NaHCO_3 (4.14 g, 49.0 mmol, 0.3 eq.) and the mixture was cooled to 0°C . Then, bromine (9.25 mL, 181 mmol, 1.1 eq.) was added dropwise over a period of 15 min. The reaction mixture was stirred for 50 min at this temperature before it was quenched *via* the slow addition of saturated aqueous $\text{Na}_2\text{S}_2\text{O}_3$ (80 mL). After diluting with saturated aqueous NaCl (200 mL) the layers were separated and the aqueous phase was extracted with diethyl ether ($3 \times 100 \text{ mL}$). The combined organic layers were dried over Na_2SO_4 and carefully concentrated *in vacuo* (min. 50 mbar, 30°C) yielding dibromide **369** as a purple, viscous oil, which was used for the next synthetic step without further purification.

Small chunks of sodium (11.3 g, 493 mmol, 3.0 eq.) were slowly added to dry methanol (160 mL) at 0 °C. After stirring for one hour at this temperature, the ice bath was removed and stirring was continued for another hour at room temperature. Subsequently, the mixture was heated to reflux for two hours until all sodium was consumed. Then, a solution of dibromide (assumed 164 mmol, 1.0 eq.) in dry methanol (25 mL) was added at room temperature and the resulting solution was heated to reflux for 12 hours. After treatment with aqueous HCl (200 mL, 5 wt-%), the mixture was extracted with diethyl ether (3 × 200 mL) and the combined organic layers were dried over Na₂SO₄. The crude mixture was carefully concentrated *in vacuo* (50 mbar, 30 °C) the product was purified *via* distillation (boiling point = 56 °C, 1 mbar) to yield ester **376** (24.1 g, 132 mmol, 81%) as a colorless liquid as a mixture of *cis/trans* isomers in a ratio of 1:3.

$R_f = 0.85$ (*i*-Hex:EtOAc = 20:1).

¹H NMR (CDCl₃, 200 MHz, characteristic signals): δ = 3.06 (s, br, 1H), 2.92 (s, br, 1H), 1.01 (d, J = 6.8 Hz, 3H), 0.95 (d, J = 6.8 Hz, 3 H) ppm.

EI-MS for C₁₁H₁₈O₂⁺ [M⁺]:
calcd. 182.1307
found 182.1299.

IR (ATR): $\tilde{\nu}/\text{cm}^{-1}$ = 2951, 2926, 2870, 1728, 1684, 1454, 1433, 1373, 1348, 1287, 1257, 1234, 1190, 1167, 1144, 1091, 1074, 1026, 1010, 954, 931, 909, 891, 840, 804, 779, 742 .

$[\alpha]_D^{20} = +43.0$ (c 1.00, CH₂Cl₂).

Ester **376** (10 g, 54.9 mmol, 1.0 eq.) was dissolved in dichloromethane (180 mL) and cooled to −78 °C. Ozone was bubble thorough this solution at a constant flow for 50 min until the reaction mixture had acquired a deep blue color. Then, argon was bubble through the blue solution for 20 min until the color had disappeared completely. After the slow addition of glacial acetic acid (100 mL), zink powder (20.1 g, 307 mmol, 5.6 eq.) was added in one portion and the resulting suspension was stirred for one hour at 0 °C. Having filtrated the reaction mixture over a plug of Celite[®] (CH₂Cl₂ washings), saturated aqueous NaHCO₃ was added until pH = 7 was reached. Then, the layers were separated, the aqueous phase was extracted with dichloromethane (3 × 100 mL) and the combined organic layers were dried

over Na₂SO₄. The solvents were evaporated under reduced pressure and the crude product was purified by flash column chromatography (silica, *i*-Hex:EtOAc = 97:3 to 9:1) to yield the title ester **311** (6.13 g, 39.3 mmol, 72%) as a colorless oil as an inseparable mixture of diastereomers (*cis/trans* = 1:2). For NMR analysis, a sample was enriched with the *trans*-isomer to a *dr* of 93:7 *via* repeated flash column chromatography.

$$R_f = 0.35 \text{ (} i\text{-Hex:EtOAc} = 20:1\text{)}.$$

¹H NMR (CDCl₃, 600 MHz, major isomer quoted): δ = 3.76–3.70 (s, 3H), 2.79–2.73 (d, *J* = 11.5 Hz 1H), 2.57 (m_C, 1H), 2.43–2.36 (m, 1H), 2.33–2.26 (m, 1H), 2.19–2.14 (m, 1H), 1.53–1.41 (m, 1H), 1.17–1.12 (m, 3H) ppm.

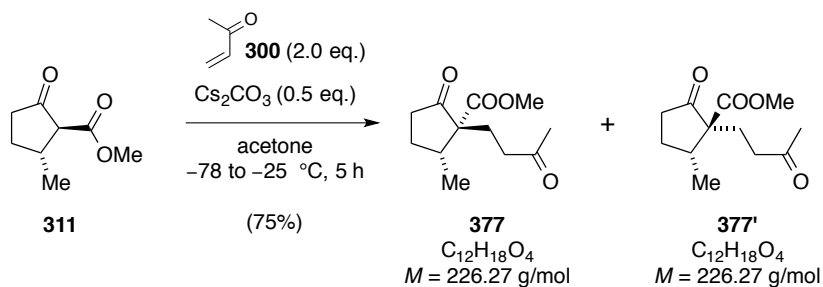
¹³C NMR (CDCl₃, 150 MHz, major isomer quoted): δ = 212.1, 169.7, 63.0, 52.5, 38.9, 36.4, 29.4, 19.3 ppm.

EI-MS for $\text{C}_8\text{H}_{12}\text{O}_3^+ [\text{M}^+]$:	calcd.	156.0786
	found	156.0777.

IR (ATR): $\tilde{\nu}/\text{cm}^{-1}$ = 3458, 2957, 2873, 1753, 1723, 1658, 1619, 1458, 1436, 1406, 1380, 1364, 1334, 1286, 1258, 1229, 1202, 1179, 1154, 1125, 1076, 1046, 1004, 956, 930, 909, 887, 844, 797, 775, 751, 663.

$$[\alpha]_D^{20} = +88.4 (c\ 1.00, \text{CH}_2\text{Cl}_2).$$

Synthesis of Diketone 377



CS₂CO₃ (16.7 g, 51.0 mmol, 0.5 eq.) was added in one portion to a stirred solution of ester **311** (16.0 g, 102 mmol, 1.0 eq.) in dry acetone (800 mL) at −78 °C. After having stirred the mixture for 10 min, freshly distilled methyl vinyl ketone (**300**, 16.7 g, 51.0 mmol, 0.5 eq.)

was added dropwise. The reaction was carefully and gradually warmed to $-25\text{ }^{\circ}\text{C}$ over a period of five hours. Subsequently, saturated aqueous NaHCO_3 (200 mL) was added and the layers were separated. The aqueous phase was extracted with dichloromethane ($3 \times 200\text{ mL}$), the combined organic layers were dried over Na_2SO_4 , and the solvent was removed *in vacuo* (caution: residual methyl vinyl ketone will co-evaporate!). The crude product was combined with another reaction batch, at which 15.0 g of ester **311** were transformed. Purification by flash column chromatography (silica, *i*-Hex:EtOAc = 9:1 to 3:1) to yielded the title compound (**377**, 33.6 g, 148 mmol, 75%) as a colorless oil.

On a smaller reaction scale 5.00 g of ester **311** were transformed, at which diketone **377** (5.02 g, 22.1 mmol, 69%) and its diastereomer **377'** (106 mg, 4.68 mmol, 2%) were isolated.

Analytical data for diketone **377**:

$R_f = 0.50$ (*i*-Hex:EtOAc = 3:2).

^1H NMR (CDCl_3 , 600 MHz): $\delta = 3.68$ (s, 3H), 2.83 (ddd, $J = 17.8, 10.3, 5.0\text{ Hz}$, 1H), 2.53–2.45 (m, 2H), 2.26 (ddd, $J = 19.0, 11.1, 8.9\text{ Hz}$, 1H), 2.19–2.03 (m, 3H), 2.12 (s, 3H), 1.85 (ddd, $J = 14.5, 10.3, 5.0\text{ Hz}$, 1H), 1.73 (dtd, $J = 12.6, 11.1, 8.5\text{ Hz}$, 1H), 1.02 (d, $J = 6.9\text{ Hz}$, 3H) ppm.

^{13}C NMR (CDCl_3 , 150 MHz): $\delta = 216.5, 208.2, 170.9, 61.8, 52.0, 42.2, 38.7$ (2C), 30.0, 28.3, 26.6, 16.0 ppm.

EI-MS for $\text{C}_{12}\text{H}_{18}\text{O}_4^+ [\text{M}^+]$:
calcd. 226.1205
found 226.1202.

IR (ATR): $\tilde{\nu}/\text{cm}^{-1} = 3454, 2957, 1746, 1726, 1711, 1455, 1434, 1405, 1356, 1291, 1272, 1235, 1190, 1160, 1125, 1058, 995, 953, 912, 888, 867, 812, 766, 711$.

$[\alpha]_D^{20} = +50.8$ ($c\ 1.00, \text{CH}_2\text{Cl}_2$).

Analytical data for diketone **377'**:

$R_f = 0.49$ (*i*-Hex:EtOAc = 3:2).

^1H NMR (CDCl_3 , 600 MHz): δ = 3.70 (s, 3H), 2.71–2.63 (m, 2H), 2.57 (ddd, J = 18.7, 8.0, 5.6 Hz, 1H), 2.42–2.27 (m, 2H), 2.12–2.03 (m, 1H), 2.09 (s, 3H), 1.99 (ddd, J = 13.9, 8.0, 5.6 Hz, 1H), 1.86 (ddd, J = 14.6, 8.0, 6.6 Hz, 1H), 1.72 (m_c , 1H), 1.04 (d, J = 7.0 Hz, 3H) ppm.

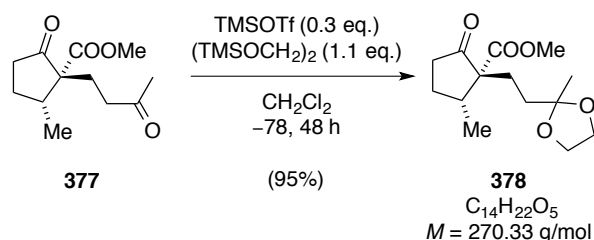
^{13}C NMR (CDCl_3 , 150 MHz): δ = 215.5, 208.2, 172.6, 62.3, 52.4, 41.3, 38.3, 37.7, 30.1, 27.6, 20.2, 14.1 ppm.

EI-MS for $\text{C}_{12}\text{H}_{18}\text{O}_4^+$ [M^+]:
calcd. 226.1205
found 226.1203.

IR (ATR): $\tilde{\nu}/\text{cm}^{-1}$ = 3448, 2958, 1742, 1712, 1460, 1434, 1406, 1367, 1353, 1289, 1250, 1206, 1164, 1129, 1105, 1053, 1022, 989, 889, 868, 795, 781, 738, 712.

$[\alpha]_D^{20}$ = +26.0 (c 0.50, CH_2Cl_2).

Synthesis of Dioxolane **378**



Diketone **377** (5.00 g, 22.1 mmol, 1.0 eq.), which was freed of water traces *via* azeotropic removal together with benzene, was dissolved in dry CH_2Cl_2 (100 mL) and cooled to -78°C . To this, 1,2-bis(trimethylsiloxy)ethane (**384**, 5.96 mL, 24.3 mmol, 1.1 eq.) and TMSOTf (1.00 mL, 5.52 mmol, 0.25 eq.) were added sequentially. The mixture was stirred for 48 hours at this temperature before being quenched *via* the addition of dry pyridine (1 mL). Then, saturated aqueous NaHCO_3 (50 mL) was added and the layers were separated after being warmed to room temperature. The aqueous phase was extracted with CH_2Cl_2 ($3 \times 100\text{ mL}$) and the combined organic layers were dried over Na_2SO_4 . After removal of the solvent *in vacuo*, the crude product was purified by flash column chromatography (silica, *i*-Hex:EtOAc = 9:1 to 4:1) to yield the title dioxolane **378** (5.65 g, 20.8 mmol, 95%) as a colorless oil.

Note: Dioxolane **378** and diketone **377** behaved co-polar on common silica TLC plates. The given R_f -value refers to basic alumina TLC plates.

$R_f = 0.54$ (*n*-pentane:Et₂O = 4:3).

¹H NMR (CDCl₃, 600 MHz): δ = 3.92–3.87 (m, 4H), 3.64 (s, 3H), 2.52–2.47 (m, 1H), 2.23–2.10 (m, 2H), 2.02 (m_C, 1H), 1.94–1.90 (m, 1H), 1.82–1.70 (m, 3H), 1.50–1.44 (m, 1H), 1.29 (s, 3H), 1.01 (d, J = 6.9 Hz, 3H) ppm.

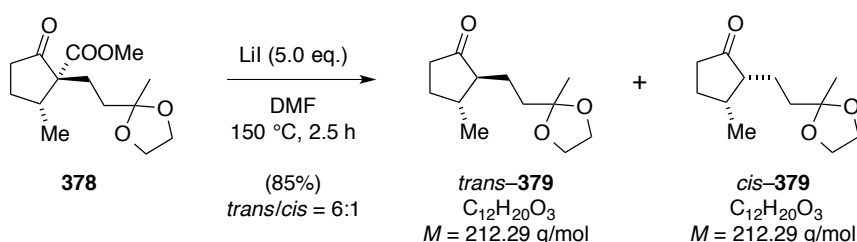
¹³C NMR (CDCl₃, 150 MHz): δ = 216.3, 171.1, 109.8, 64.7 (2C), 62.4, 51.8, 40.2, 38.8, 33.3, 28.3, 26.4, 23.8, 16.0 ppm.

EI-MS for C₁₄H₂₂O₅⁺ [M⁺]:
calcd. 270.1467
found 270.1466.

IR (ATR): $\tilde{\nu}/\text{cm}^{-1}$ = 3449, 2958, 2880, 1746, 1727, 1452, 1433, 1404, 1378, 1345, 1331, 1290, 1227, 1190, 1163, 1117, 1055, 996, 947, 917, 877, 849, 812, 793, 765, 697.

$[\alpha]_D^{20} = +64.0$ (c 1.00, CH₂Cl₂).

Synthesis of Cyclopentanone **379**



To a solution of dioxolane **378** (1.13 g, 4.18 mmol, 1.0 eq.) in dry DMF (12 mL) was added lithium iodide (2.80 g, 20.9 mmol, 5.0 eq.). The resulting suspension was vigorously stirred and heated to 150 °C for a period of 2.5 hours. After cooling to room temperature, CH₂Cl₂ (100 mL) was added and the mixture was washed with saturated aqueous NaCl (100 mL). The aqueous phase was extracted with CH₂Cl₂ (3 × 50 mL) and the combined organic layers were dried over Na₂SO₄. After removal of the solvent *in vacuo*, the crude product was purified by flash column chromatography (silica, deactivated with 1 wt-% NEt₃, *i*-Hex:EtOAc = 9:1 to

17:3) to yield the title cyclopentanone **379** (0.76 g, 3.56 mmol, 85%) as a colorless oil in a *trans/cis* isomeric ratio of 6.7:1. Analytical data were recorded from this mixture.

*Note: Without using thoroughly deactivated silica for flash column chromatography, cyclopentanone **379** was obtained in a trans/cis isomeric ratio of 3.4:1.*

$$R_f = 0.48 \text{ (} n\text{-pentane:Et}_2\text{O} = 3:2\text{)}.$$

¹H NMR (CDCl₃, 600 MHz, major isomer quoted): δ=3.95–3.89 (m, 4H), 2.34–2.29 (m, 1H), 2.10–2.03 (m, 2H), 1.99–1.77 (m, 2H), 1.68–1.59 (m, 4H), 1.41–1.36 (m, 1H), 1.31 (s, 3H), 1.14 (d, *J* = 6.5 Hz, 3H) ppm.

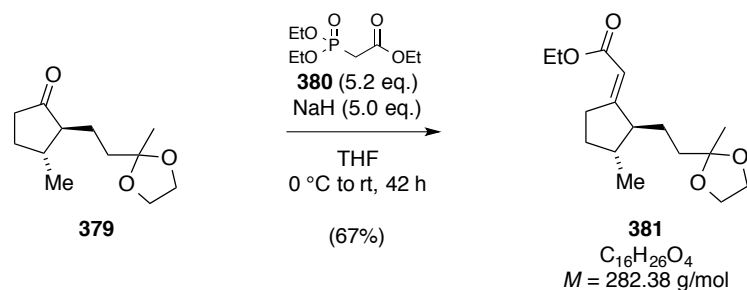
¹³C NMR (CDCl₃, 150 MHz, major isomer quoted): δ = 220.9, 110.0, 64.7 (2C), 56.2, 38.2, 37.1, 36.1, 29.7, 23.8, 22.3, 19.8 ppm.

EI-MS for C ₁₂ H ₂₀ O ₃ ⁺ [M ⁺]:	calcd.	212.1412
	found	212.1421

IR (ATR): $\tilde{\nu}/\text{cm}^{-1} = 3357, 2954, 2872, 1734, 1454, 1407, 1376, 1286, 1218, 1156, 1044, 947, 865, 829, 789$.

$$[\alpha]_D^{20} = +40.0 (c\ 1.00, \text{CH}_2\text{Cl}_2).$$

Synthesis of Ester 381



To a suspension of sodium hydride (188 mg, 60% wt-% in mineral oil, 4.70 mmol, 5.0 eq.) in dry THF (3 mL) was added phosphonate **380** (0.97 mL, 4.90 mmol, 5.2 eq.) dropwise at 0 °C. The resulting mixture was stirred for one hour at room temperature before a solution of cyclopentanone **379** (200 mg, 0.94 mmol, 1.0 eq.) in dry THF (1 mL) was added slowly. After stirring for 41 hours, water (2 mL) and then CH₂Cl₂ (30 mL) were added. The layers

were separated and the aqueous phase was extracted with CH_2Cl_2 (3×50 mL). Having dried the combined organic layers over Na_2SO_4 , the solvents were removed *in vacuo*. The crude product was purified by flash column chromatography (silica, *i*-Hex:EtOAc = 47:3) to yield ester **381** (207 mg, 0.73 mmol, 67%) as a colorless oil.

Note: Ester 381 was not air-stable in our hands. Therefore, analytical data were recorded from material that was freshly purified via reversed-phase HPLC ($R_t = 54$ min, $\text{CH}_3\text{CN}:\text{H}_2\text{O} = 1:1$).

$R_f = 0.40$ (*n*-pentane:Et₂O = 3:2).

^1H NMR (C_6D_6 , 600 MHz): $\delta = 6.10$ (q, $J = 2.5$ Hz, 1H), 4.23–4.14 (m, 2H), 3.65–3.60 (m, 4H), 3.35 (m_C, 1H), 2.85 (m_C, 1H), 1.97–1.94 (m, 1H), 1.81–1.70 (m, 5H), 1.57 (m_C, 1H), 1.37 (s, 3H), 1.12 (t, $J = 7.1$ Hz, 4H), 0.91 (d, $J = 6.6$ Hz, 3H) ppm.

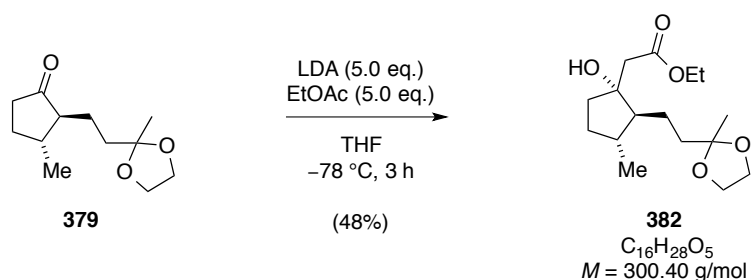
^{13}C NMR (C_6D_6 , 150 MHz): $\delta = 171.1$, 166.7, 112.4, 110.1, 64.7 (2C), 59.4, 53.6, 37.8, 35.9, 32.9, 32.2, 25.1, 24.1, 19.0, 14.5 ppm.

EI-MS for $\text{C}_{16}\text{H}_{26}\text{O}_4^+$ [M^+]:
calcd. 282.1831
found 282.1820.

IR (ATR): $\tilde{\nu}/\text{cm}^{-1} = 3371$, 2952, 2873, 1709, 1648, 1453, 1417, 1370, 1344, 1255, 1192, 1136, 1095, 1038, 947, 864, 790.

$[\alpha]_D^{20} = +10.4$ (c 1.00, CH_2Cl_2).

Synthesis of Alcohol 382



To a solution of diisopropylamine (0.17 mL, 1.18 mmol, 5.0 eq.) in dry THF (1.4 mL) at -78°C was added *n*-BuLi (0.49 mL, 2.4 M solution in hexanes, 1.18 mmol, 5.0 eq.) dropwise.

After stirring for 15 min, dry ethylacetate (0.12 mL, 1.18 mmol, 5.0 eq.) was added slowly and the reaction mixture was then stirred for another 30 min. Subsequently, a solution of ketone **379** (0.05 g, 0.24 mmol, 1.0 eq.) in dry THF (0.5 mL) was added dropwise and stirring was continued for 3 hours. After the addition of saturated aqueous NH_4Cl (10 mL), the mixture was warmed to room temperature and extracted with CH_2Cl_2 (3×25 mL). The combined organic layers were dried over Na_2SO_4 and the solvents were removed *in vacuo*. Thus alcohol **382** (34 mg, 0.11 mmol, 48%) was obtained as colorless oil.

Note: Alcohol 382 decomposes on silica and by time in CDCl_3 .

$R_f = 0.20$ (*n*-pentane: $\text{Et}_2\text{O} = 1:1$).

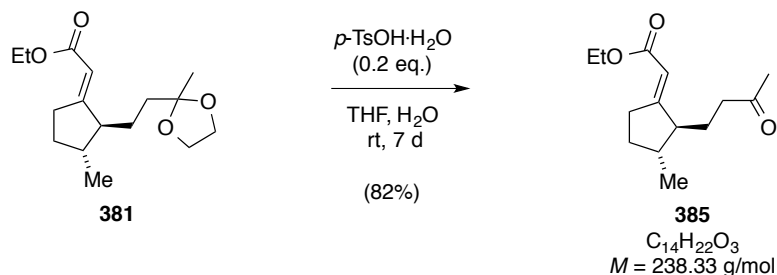
^1H NMR (CDCl_3 , 200 MHz): $\delta = 4.17$ (q, $J = 7.1$ Hz, 2H), 3.95–3.90 (m, 4H), 2.71 (d, $J = 15.5$ Hz, 1H), 2.35 (d, $J = 15.5$ Hz, 1H), 2.04–1.83 (m, 2H), 1.83–1.61 (m, 5H), 1.59–1.36 (m, 2H), 1.32 (s, 3H), 1.27 (t, $J = 7.1$ Hz, 3H), 1.20–1.06 (m, 1H), 1.01 (d, $J = 6.5$ Hz, 3H) ppm.

EI-MS for $\text{C}_{15}\text{H}_{25}\text{O}_5^+$ [(M- CH_3) $^+$]: calcd. 285.1697
found 285.1658.

IR (ATR): $\tilde{\nu}/\text{cm}^{-1} = 3451, 2970, 2901, 1730, 1460, 1452, 1401, 1352, 1308, 1258, 1208, 1180, 1117, 1109, 1046, 1011, 888, 832, 815, 732, 709$.

$[\alpha]_D^{20} = +26.3$ (*c* 0.33, CH_2Cl_2).

Synthesis of Ketoester **385**



Ester **381** (168 mg, 0.59 mmol, 1.0 eq.) was dissolved in a thoroughly degassed mixture of THF (5.3 mL) and water (0.9 mL). After the addition of *p*-toluenesulfonic acid (17.0 mg, 0.09 mmol, 0.15 eq.), the resulting mixture was stirred for one week at room temperature.

Subsequently water (20 mL) and CH₂Cl₂ (50 mL) were added and the layers were separated. The aqueous phase was extracted with CH₂Cl₂ (3 × 50 mL) and the combined organic layers were dried over Na₂SO₄. The crude product was purified *via* flash column chromatography (silica, *i*-Hex:EtOAc = 23:2) to yield ketoester **385** (116 mg, 0.49 mmol, 82%) as a colorless oil.

Note: Ketoester 381 was not air-stable in our hands. Therefore, analytical data were recorded from material that was freshly purified via reversed-phase HPLC (R_t = 41 min, CH₃CN:H₂O = 1:1).

R_f = 0.32 (*n*-pentane:Et₂O = 3:2).

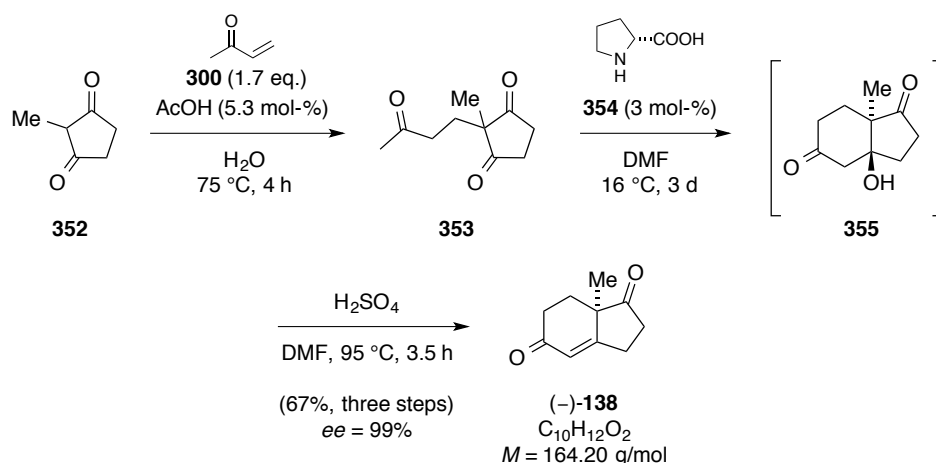
¹H NMR (C₆D₆, 600 MHz): δ = 5.82 (q, J = 2.4 Hz, 1H), 4.09 (qd, J = 7.1, 0.9 Hz, 2H), 3.22 (dddd, J = 19.7, 8.4, 3.6, 2.3 Hz, 1H), 2.73–2.64 (m, 1H), 2.69 (m_C, 2H), 1.95–1.85 (m, 2 H), 1.76–1.73 (m, 1H), 1.70–1.62 (m, 3H), 1.59 (s, 3H), 1.30 (m_C, J = 8.3, 6.3, 1H), 1.04 (t, J = 7.1 Hz, 3H), 0.97 (dq, J = 12.4, 8.7 Hz, 1H), 0.76 (d, J = 6.6 Hz, 3H) ppm.

¹³C NMR (C₆D₆, 150 MHz): δ = 205.8, 170.7, 166.6, 112.6, 59.5, 53.0, 39.6, 37.9, 32.7, 32.1, 29.4, 24.6, 19.0, 14.5 ppm.

EI-MS for C₁₄H₂₂O₃⁺ [M⁺]:
calcd. 238.1569
found 238.1527.

IR (ATR): $\tilde{\nu}/\text{cm}^{-1}$ = 3451, 2978, 2910, 2852, 1726, 1479, 1456, 1392, 1368, 1355, 1345, 1321, 1311, 1258, 1207, 1186, 1163, 1115, 1102, 1048, 1019, 967, 890, 850, 836, 814, 784, 774, 733, 709.

$[\alpha]_D^{20}$ = +8.0 (*c* 1.00, CH₂Cl₂).

Synthesis of Hajos-Parrish-Sauer-Eder-Wiechert-ketone (**138**)

To a suspension of 2-methyl-1,3-cyclopentadione (**352**, 100 g, 892 mmol, 1.0 eq.) in water (205 mL) was added freshly distilled methyl vinyl ketone (**300**, 129 mL, 1.53 mol, 1.7 eq.) and then glacial acetic acid (2.68 mL, 47.0 mmol, 5.3 mol-%). The reaction mixture was heated to 75 °C under exclusion of light for 4 hours. After cooling to room temperature CH₂Cl₂ (500 mL) was added and the layers were separated. The aqueous phase was extracted with CH₂Cl₂ (2 × 100 mL) and the combined organic layers were washed with saturated aqueous NaCl (2 × 250 mL). After re-extraction with CH₂Cl₂ (2 × 100 mL) the combined organic layers were dried over Na₂SO₄. Having removed the solvent *in vacuo*, triketone **353** (154 g, 845 mmol, 95%) was obtained as slightly yellow oil, which used for further syntheses. A degassed (3 × freeze-pump-thaw) suspension of (R)-proline (**354**, 2.92 g, 25.4 mmol, 3 mol-%) in dry DMF (666 mL) was stirred at 16 °C under the exclusion of light for one hour. Subsequently, a degassed solution of triketone **353** (154 g, 845 mmol, 1.0 eq.) in dry DMF (220 mL) was added and the resulting mixture was stirred for 3 days at 14 to 18 °C, upon which TLC analysis suggested complete consumption of the starting material.

Then, a solution of H₂SO₄ in DMF – being prepared *via* dropwise addition of concentrated H₂SO₄ (6.66 mL) to dry DMF (121 mL) – was added at –20 °C. This mixture was then heated to 95 °C for a period of 3.5 hours, before being cooled to room temperature again. After removal of the solvent *in vacuo*, the remaining dark brown oil was re-dissolved in CH₂Cl₂ (1.20 L), washed with NaCl-saturated aqueous H₂SO₄ (1 M, 500 mL), NaCl-saturated aqueous NaHCO₃ (2 × 200 mL), as well as saturated aqueous NaCl (500 mL) and then each aqueous layer was re-extracted with the same fraction of CH₂Cl₂ (2 × 200 mL). The combined organic layers were dried over Na₂SO₄, concentrated *in vacuo* and the crude product was taken up in EtOAc (200 mL). After filtration over a plug of dry silica (EtOAc washings) the obtained brown solid was subjected to bulb-to-bulb distillation (185 °C, 0.2 mbar). The resulting pale

yellow solid was recrystallized (Et₂O/*n*-hexane) to yield the title diketone (–)-**138** (96.6 g, 588 mmol, 67%) as colorless crystals.

$R_f = 0.30$ (*i*-Hex:EtOAc = 1:1).

Melting point = 63.5–64.3 °C (Et₂O/*n*-hexane)

¹H NMR (CDCl₃, 600 MHz): δ = 5.96 (d, J = 2.4 Hz, 1H), 2.94 (dddd, J = 17.1, 11.0, 9.9, 2.4 Hz, 1H), 2.81–2.71 (m, 2H), 2.58–2.36 (m, 3H), 2.09 (ddd, J = 13.6, 5.3, 2.2 Hz, 1H), 1.84 (dddd, J = 14.2, 13.5, 5.2, 0.7 Hz, 1H), 1.31 (s, 3H) ppm.

¹³C NMR (CDCl₃, 150 MHz): δ = 216.6, 198.2, 169.8, 124.0, 48.8, 36.0, 33.0, 29.3, 27.0, 20.7 ppm

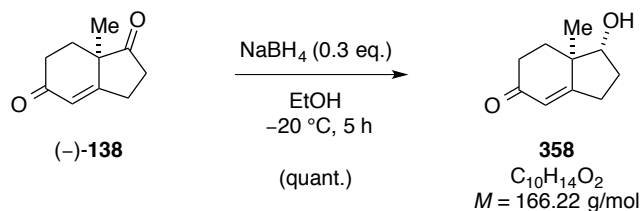
EI-MS for C₁₀H₁₂O₂⁺ [M⁺]: calcd. 164.0837

found 164.0833.

IR (ATR): $\tilde{\nu}/\text{cm}^{-1}$ = 2954, 1740, 1696, 1656, 1453, 1418, 1404, 1375, 1317, 1293, 1255, 1228, 1218, 1202, 1194, 1146, 1061, 996, 975, 962, 939, 891, 869, 846, 813, 767, 713, 670.

$[\alpha]_D^{20} = -384.6$ (c 1.00, toluene).

Synthesis of Alcohol 358



A stirred solution of diketone (–)-**138** (25.0 g, 152 mmol, 1.0 eq.) in absolute ethanol (370 mL) was cooled to –20 °C and subsequently NaBH₄ (1.59 g, 41.9 mmol, 0.3 eq.) that was dissolved in absolute ethanol (250 mL) was added dropwise over a period of 4 hours. After being stirred for another hour, the reaction was slowly quenched *via* the addition of aqueous HCl (10 wt-%) until pH = 5 was reached. The ethanol was then removed *in vacuo* and the residual aqueous phase was extracted with EtOAc (4 × 250 mL). The combined

organic layers were dried over Na₂SO₄ and the solvent was removed under reduced pressure. The crude product was purified *via* flash column chromatography (silica, CH₂Cl₂:MeOH = 93:7) to yield alcohol **358** (25.2 g, 152 mmol, quant.) as a slightly yellow solid.

R_f = 0.30 (CH₂Cl₂:MeOH = 20:1).

Melting point = 22.0–23.3 °C (CH₂Cl₂/MeOH)

¹H NMR (CDCl₃, 600 MHz): δ = 5.76 (s, 1H), 3.83 (dd, *J* = 10.4, 7.6 Hz, 1H), 2.69 (ddtd, *J* = 19.8, 11.6, 2.3, 0.7 Hz, 1H), 2.50 (ddd, *J* = 17.8, 14.4, 5.4 Hz, 1H), 2.46–2.34 (m, 3H), 2.15–2.08 (m, 2H), 1.85–1.73 (m, 2H), 1.13 (s, 3H) ppm.

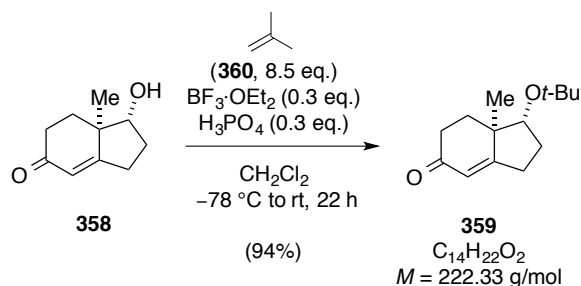
¹³C NMR (CDCl₃, 150 MHz): δ = 199.5, 175.5, 123.5, 80.7, 45.3, 34.2, 33.4, 29.2, 26.6, 15.2 ppm.

EI-MS for C₁₀H₁₄O₂⁺ [M⁺]:
calcd. 166.0994
found 166.0989.

IR (ATR): $\tilde{\nu}/\text{cm}^{-1}$ = 3357, 2962, 2931, 2910, 2867, 1693, 1632, 1469, 1446, 1416, 1371, 1349, 1333, 1324, 1307, 1288, 1269, 1258, 1220, 1205, 1136, 1074, 1037, 1016, 1006, 973, 954, 932, 901, 870, 847, 802, 768, 720.

$[\alpha]_D^{20} = -82.6$ (*c* 1.00, CH₂Cl₂).

Synthesis of Ether **359**



Alcohol **358** (28.7 g, 173 mmol, 1.0 eq.) was dissolved in dry CH₂Cl₂ (290 mL) and cooled to –20 °C. To the stirred solution was added H₃PO₄ (3.2 mL, prepared from 2.0 g P₂O₅ and 6.5 mL conc. H₃PO₄, 0.3 eq.), isobutene (**360**, approximately 140 mL, 1.47 mmol, 8.5 eq.)

and subsequently boron trifluoride etherate (7.37 mL, 58.7 mmol, 0.3 eq.). The reaction was stirred for 30 min at this temperature and then gradually warmed to room temperature over the course of 6 hours. Meanwhile, isobutene was re-condensed into the reaction *via* the use of a dry ice reflux condenser. Thereafter stirring was continued for another 16 hours, upon which aqueous ammonia (2 M, 280 mL) was added. The layers were separated and the aqueous phase was extracted with CH₂Cl₂ (4 × 250 mL). The combined organic layers were dried over Na₂SO₄, concentrated *in vacuo* and the crude product was purified *via* flash column chromatography (silica, *i*-Hex:EtOAc = 3:1 to 2:1) to yield ether **359** (36.2 g, 173 mmol, 94%) as a colorless solid.

Crystals suitable for X-ray analysis were obtained by slow evaporation of a solution of ether **359** from *n*-Hex at −20 °C.

R_f = 0.65 (*i*-Hex:EtOAc = 3:1).

Melting point = 61.9–62.9 °C (CH₂Cl₂/MeOH)

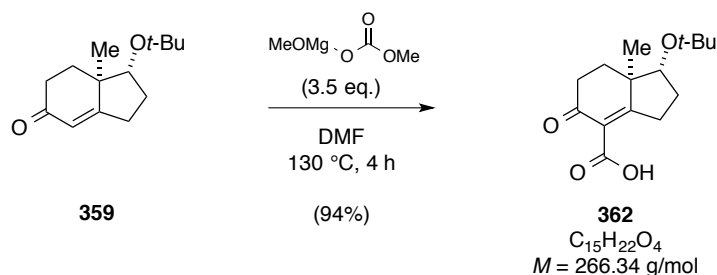
¹H NMR (CDCl₃, 600 MHz): δ = 5.75 (s, 1H), 3.56 (dd, *J* = 9.9, 7.6 Hz, 1H), 2.68 (ddt, *J* = 19.6, 11.7, 2.4 Hz, 1H), 2.50 (ddd, *J* = 17.8, 14.5, 5.4 Hz, 1H), 2.39–2.32 (m, 2H), 2.04–1.95 (m, 2H), 1.78 (dddd, *J* = 13.1, 11.7, 9.9, 8.8 Hz, 1H), 1.71 (td, *J* = 13.8, 5.0 Hz, 1H), 1.17 (s, 9H), 1.10 (s, 3H) ppm.

¹³C NMR (CDCl₃, 150 MHz): δ = 199.6, 175.6, 123.0, 79.8, 73.2, 45.0, 34.5, 33.6, 29.7, 15.9 ppm.

EI-MS for C₁₄H₂₃O₂⁺ [M⁺]:
calcd. 223.1693
found 223.1697.

IR (ATR): $\tilde{\nu}/\text{cm}^{-1}$ = 3029, 2969, 2937, 2905, 2864, 1699, 1668, 1639, 1454, 1415, 1392, 1369, 1361, 1343, 1333, 1321, 1303, 1261, 1249, 1224, 1214, 1198, 1190, 1130, 1088, 1045, 1028, 1002, 977, 957, 932, 909, 891, 865, 806, 766, 757, 732, 683.

$[\alpha]_D^{20} = -52.8$ (*c* 1.00, CH₂Cl₂).

Synthesis of Ketoacid **362**

Magnesium methyl carbonate (78.7 mL, 2 M in DMF, 15.7 mmol, 3.5 eq.) was added slowly to a solution of ether **359** (10.0 g, 45.0 mmol, 1.0 eq.) in dry DMF (98 mL). After degassing the mixture (Ar bubbling, 10 min), the reaction vessel was added to an oil bath (pre-heated to 130 °C) and the reaction was stirred for 4 hours. After cooling to 0 °C, aqueous HCl (2 M) was added until the mixture solidified. Subsequently, diethyl ether (80 mL) was added, followed by conc. aqueous HCl until a pH of 2–3 was reached and two homogenous layers had formed. The layers were separated and the aqueous phase was extracted with diethyl ether (5 × 100 mL). The combined organic layers were dried over Na₂SO₄, concentrated *in vacuo* and the crude product was recrystallized from *n*-hexane at –78 °C to yield ketoacid **362** (4.62 g, 17.3 mmol, 39%) as a colorless solid. The mother liquor was then concentrated and the resulting mixture was submitted to flash column chromatography (silica, *i*-Hex:EtOAc:HOAc = 9:1:0.05 to 4:1:0.08) to yield additional ketoacid **362** (520 mg, 1.95 mmol, 2%) and ether **359** (4.97 g, 22.3 mmol, 49%) as a colorless wax. The recovered starting material was subjected to another reaction cycle. Overall ketoacid **362** (9.01 g, 33.8 mmol) was obtained in 75% yield.

Crystals suitable for X-ray analysis were obtained by slow evaporation of a solution of ketoacid **362** from *n*-Hex at –20 °C.

$R_f = 0.30$ (*i*-Hex:EtOAc:HOAc = 4:1:0.05).

Melting point = 31.7–43.3 °C (*n*-Hex)

¹H NMR (CDCl₃, 600 MHz): δ = 13.10 (s, 1H), 3.66 (dd, J = 10.3, 7.2 Hz, 1H), 3.31–3.17 (m, 2H), 2.78 (ddd, J = 18.7, 14.4, 5.8 Hz, 1H), 2.64 (ddd, J = 18.7, 5.4, 1.8 Hz, 1H), 2.13–2.02 (m, 2H), 1.92–1.77 (m, 2H), 1.19 (s, 12H) ppm.

^{13}C NMR (CDCl_3 , 150 MHz): δ = 203.0, 196.3, 164.4, 120.5, 79.0, 73.6, 48.5, 33.7, 32.1, 31.6, 30.1, 28.8, 16.4 ppm.

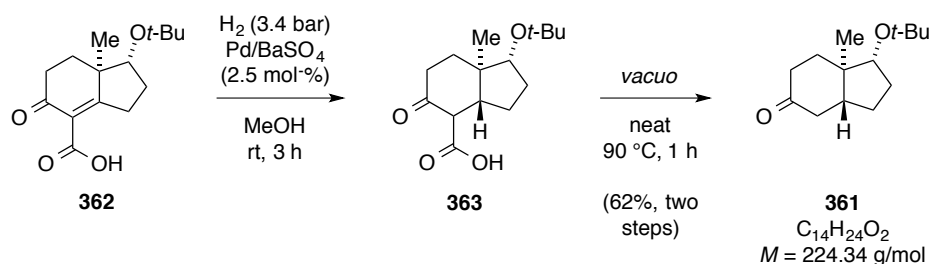
ESI-MS for $\text{C}_{15}\text{H}_{21}\text{O}_4^-$ $[(\text{M}-\text{H})^-]$: calcd. 265.1445

found 265.1440.

IR (ATR): $\tilde{\nu}/\text{cm}^{-1}$ = 2976, 2966, 2938, 2908, 2870, 2763, 1734, 1623, 1597, 1437, 1415, 1388, 1359, 1351, 1338, 1320, 1309, 1283, 1274, 1263, 1221, 1208, 1190, 1142, 1098, 1029, 1018, 992, 979, 940, 923, 890, 855, 818, 798, 771, 759, 709, 686.

$[\alpha]_D^{20} = -29.2$ (c 1.00, CH_2Cl_2).

Synthesis of Hydrindanone 361



A stirred suspension of ketoacid **362** (3.00 g, 11.3 mmol 1.0 eq.) and Pd/BaSO_4 (600 mg, 5 wt-% Pd, 0.28 mmol, 2.5 mol-%) in dry methanol (24 mL) was pressurized with H_2 (3.4 bar) for 4 hours. Thereafter, the pressure was released and the crude mixture was filtered over a pad of Celite[®] (MeOH washings). After removal of the solvent *in vacuo*, the crude saturated ketoacid **363** was obtained as pale yellow foam and directly employed for further reaction.

Saturated ketoacid **363** was transferred to a flask with high inner surface area, which was then evacuated (1 mbar) and subsequently heated to 90 °C for a period of one hour. After cooling to room temperature the crude product was purified by flash column chromatography (silica, *i*-Hex:EtOAc = 1:0 to 19:1) to yield hydrindanone **361** (1.56 g, 6.95 mmol, 62%) as a colorless solid as a single diastereomer.

Crystals suitable for X-ray analysis were obtained by slow evaporation of a solution of hydrindanone **361** from *n*-Hex at −20 °C.

$R_f = 0.70$ (*i*-Hex:EtOAc = 16:1).

Melting point = 40.2–40.9 °C (*n*-Hex)

^1H NMR (CDCl_3 , 400 MHz): $\delta = 3.46$ (dd, $J = 9.1, 7.6$ Hz, 1H), 2.42 (ddd, $J = 16.4, 13.0, 6.9$ Hz, 1H), 2.34–2.28 (m, 3H), 2.04–1.92 (m, 2H), 1.77–1.68 (m, 1H), 1.64–1.55 (m, 2H), 1.47–1.36 (m, 2H), 1.14 (s, 9H), 0.97 (d, $J = 0.7$ Hz, 3H) ppm.

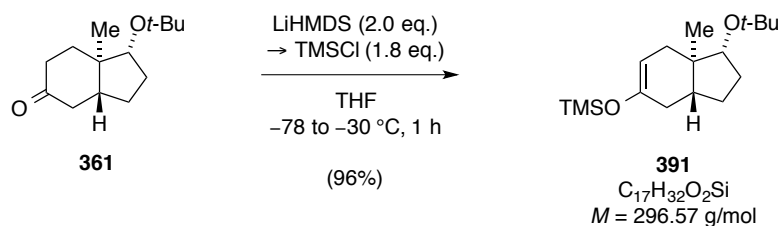
^{13}C NMR (CDCl_3 , 100 MHz): $\delta = 212.3, 79.5, 72.7, 44.8, 43.1, 42.2, 37.6, 35.4, 31.9, 28.8, 25.9, 10.4$ ppm.

EI-MS for $\text{C}_{14}\text{H}_{24}\text{O}_2^+ [\text{M}^+]$:
calcd. 224.1776
found 224.1778.

IR (ATR): $\tilde{\nu}/\text{cm}^{-1} = 2971, 2874, 1708, 1463, 1412, 1390, 1361, 1336, 1317, 1289, 1252, 1224, 1193, 1122, 1104, 1059, 1032, 998, 967, 934, 917, 901, 853, 754, 685$.

$[\alpha]_D^{20} = -84.8$ (c 1.00, CH_2Cl_2).

Synthesis of Enol Ether **391**



To a solution of hydrindanone **361** (20 mg, 0.9 mmol, 1.0 eq.) in dry THF (1 mL) at -78 °C was added LiHMDS (0.2 mL, 1 M solution in THF, 1.8 mmol, 2.0 eq.). After stirring for 15 min freshly distilled TMSCl (20 μL , 1.6 mmol, 1.8 eq.) was added and the reaction mixture was warmed to -30 °C for 30 min. Subsequently, saturated aqueous NaHCO_3 (5 mL) was added and the resulting solution was extracted with diethyl ether (3×10 mL). The combined organic layers were dried over Na_2SO_4 and concentrated *in vacuo* to yield enol ether **391** (25 mg, 0.9 mmol, 96%) as colorless oil, which required no further purification.

$R_f = 0.95$ (*i*-Hex:EtOAc = 20:1).

^1H NMR (C_6D_6 , 600 MHz): δ = 4.94 (dtd, J = 5.8, 2.0, 0.7 Hz, 1H), 3.30 (t, J = 8.4 Hz, 1H), 2.13 (ddd, J = 16.6, 5.3, 2.3 Hz, 1H), 2.02 (ddd, J = 15.9, 5.8, 2.0 Hz, 1H), 1.99–1.94 (m, 1H), 1.87–1.83 (m, 1H), 1.82–1.76 (m, 1H), 1.59 (dddd, J = 13.3, 11.7, 8.0, 3.7 Hz, 1H), 1.55–1.44 (m, 2H), 1.29–1.22 (m, 1H), 1.09 (s, 9H), 0.97 (s, 3H), 0.21 (s, 9H) ppm.

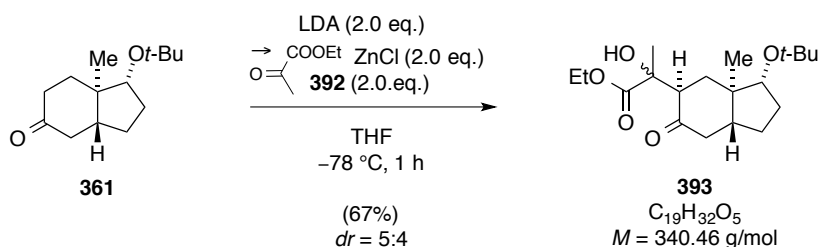
^{13}C NMR (C_6D_6 , 150 MHz): δ = 150.6, 128.3, 103.4, 80.5, 72.2, 41.6, 36.8, 33.8, 32.1, 28.9, 26.1, 11.0, 0.5 ppm.

EI-MS for $\text{C}_{17}\text{H}_{32}\text{O}_2\text{Si}^+ [\text{M}^+]$:
calcd. 296.22
found 296.22.

IR (ATR): $\tilde{\nu}/\text{cm}^{-1}$ = 2971, 1714, 1655, 1462, 1389, 1362, 1251, 1190, 1142, 1115, 1069, 1059, 1021, 901, 886, 844, 755.

$[\alpha]_D^{20}$ = -89.6 (c 0.25, CH_2Cl_2).

Synthesis of Hydroxy Ester **393**



To a solution of ketone **361** (0.03 g, 0.13 mmol, 1.0 eq.) in dry THF (1 mL) at $-78\text{ }^\circ\text{C}$ was added LDA (0.13 mL, 2 M solution in THF, 0.27 mmol, 2.0 eq.) dropwise. The resulting solution was stirred 10 min at this temperature and additional 30 min at room temperature. After being re-cooled to $-78\text{ }^\circ\text{C}$, a premixed solution of ethyl pyruvate (**392**, 0.03 mL, 0.27 mmol, 2.0 eq.) and ZnCl_2 (0.27 mL, 1 M solution in THF, 0.27 mmol, 2.0 eq.) in dry THF (1 mL) was added slowly. The reaction was stirred for one hour upon which half-saturated aqueous NH_4Cl (10 mL) was added. After warming to room temperature, the mixture was extracted with CH_2Cl_2 ($3 \times 25\text{ mL}$). The combined organic layers were dried over Na_2SO_4 and the solvents were removed *in vacuo*. The crude product was purified *via* flash column chromatography (silica, $i\text{-Hex}:\text{EtOAc} = 40:1$ to $20:1$) to yield hydroxy ester **393** (30.6 mg, 0.09 mmol, 67%) as colorless oil and as a 5:4 mixture of diastereomers.

Note: ^1H and ^{13}C NMR signals were attributed to the major and minor isomer according to 2D NMR spectroscopy.

$R_f = 0.30$ (*i*-Hex:EtOAc = 10:1).

^1H NMR (C_6D_6 , 600 MHz, major isomer): $\delta = 4.28\text{--}4.14$ (m, 2H), 3.52 (dd, $J = 9.0, 7.5$ Hz, 1H), 3.32 (s, br, 1H), 3.03 (dd, $J = 12.9, 6.5$ Hz, 1H), 2.33–2.29 (m, 2H), 2.09 (dd, $J = 12.5, 6.4$ Hz, 1H), 2.04–1.92 (m, 2H), 1.63–1.57 (m, 3H), 1.54 (t, $J = 12.6$ Hz, 1H), 1.29–1.25 (m, 3H), 1.27 (s, 3H), 1.16 (s, 9H), 1.02 (s, 3H) ppm.

^1H NMR (C_6D_6 , 600 MHz, minor isomer): $\delta = 4.28\text{--}4.14$ (m, 2H), 3.45 (dd, $J = 8.8, 7.7$ Hz, 1H), 3.34 (s, br, 1H), 2.99 (dd, $J = 12.6, 0.9$ Hz, 1H), 2.33–2.29 (m, 1H), 2.33–2.28 (m, 1H), 2.03–1.96 (m, 1H), 1.95–1.88 (m, 2H), 1.73–1.64 (m, 2H), 1.63–1.55 (m, 1H), 1.49–1.37 (m, 1H), 1.34 (s, 3H), 1.29–1.25 (m, 3H), 1.13 (s, 9H), 1.07–1.03 (m, 3H) ppm.

^{13}C NMR (CDCl_3 , 150 MHz, major isomer): $\delta = 211.9, 177.3, 79.6, 73.9, 72.8, 61.8, 53.1, 44.6, 42.9, 42.3, 35.6, 32.0, 28.9, 25.9, 25.8, 14.2, 11.5$ ppm.

^{13}C NMR (CDCl_3 , 150 MHz, minor isomer): $\delta = 213.1, 177.3, 78.9, 74.5, 72.8, 61.7, 58.5, 46.0, 43.7, 37.8, 35.4, 32.1, 28.8, 27.0, 23.9, 14.2, 11.8$ ppm.

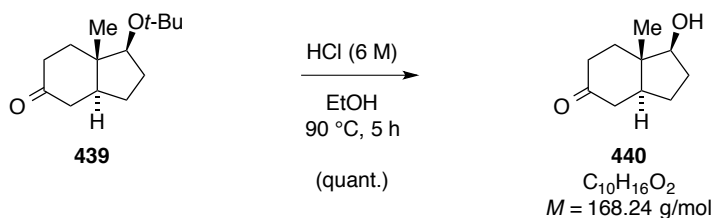
EI-MS for $\text{C}_{19}\text{H}_{32}\text{O}_5^+$ [M^+]:	calcd. 340.2250
	found 340.2246.

IR (ATR): $\tilde{\nu}/\text{cm}^{-1} = 3507, 2973, 2940, 2905, 2874, 1732, 1706, 1559, 1540, 1465, 1447, 1423, 1389, 1362, 1340, 1292, 1241, 1192, 1175, 1121, 1108, 1063, 1028, 974, 963, 941, 902, 865, 848, 804, 761, 712$.

Since the product was isolated as a mixture of diastereomers, the optical rotation of the product mixture was not determined.

5.3 Experimental Procedures for Chapter 3: ‘The Total Synthesis of (–)-Nitidasin’

Synthesis of Alcohol 440



Hydrindanone **439** (6.80 g, 30.3 mmol) was dissolved in ethanol (70 mL) and aqueous HCl (6 M, 10 mL) was added. The resulting solution was heated to reflux (90 °C oil bath) for 5 hours and then cooled to 0 °C. The pH of the mixture was adjusted to 7 *via* addition of neat Na_2CO_3 , upon which the solvent was removed *in vacuo*. The residue was re-dissolved in CH_2Cl_2 (100 mL) and water (50 mL) was added. The layers were separated and the aqueous phase was extracted with CH_2Cl_2 (3 × 100 mL). Subsequently, the combined organic layers were dried over Na_2SO_4 , concentrated *in vacuo* and the crude product was purified by flash column chromatography (silica, *i*-Hex:EtOAc = 3:2 to 1:1) to yield alcohol **440** (5.09 g, 30.3 mmol, quant.) as colorless wax.

$R_f = 0.20$ (*i*-Hex:EtOAc = 1:1).

^1H NMR (CDCl_3 , 400 MHz): δ = 3.74 (t, J = 8.6 Hz, 1H), 2.45–2.22 (m, 4H), 2.21–2.11 (m, 1H), 2.00 (ddd, J = 12.9, 6.8, 2.1 Hz, 1H), 1.91 (s, br, 1H), 1.75 (m_C , 1H), 1.66–1.54 (m, 2H), 1.50–1.39 (m, 2H), 0.98 (s, 3H) ppm.

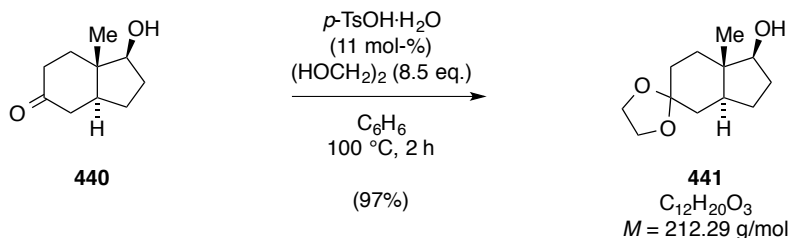
^{13}C NMR (CDCl_3 , 100 MHz): δ = 211.8, 80.4, 44.8, 43.0, 42.5, 37.3, 34.8, 31.2, 25.3, 9.8 ppm.

EI-MS for $\text{C}_{10}\text{H}_{16}\text{O}_2^+$ [M^+]:	calcd.	168.1150
	found	168.1145.

IR (ATR): $\tilde{\nu}/\text{cm}^{-1}$ = 3404, 2950, 2870, 1697, 1464, 1453, 1443, 1415, 1383, 1368, 1353, 1315, 1289, 1239, 1223, 1199, 1155, 1122, 1101, 1041, 1024, 996, 962, 914, 852, 826, 794, 729, 686.

$$[\alpha]_D^{20} = +76.1 (c\ 1.00, \text{CH}_2\text{Cl}_2).$$

Synthesis of Dioxolane **441**



Alcohol **440** (5.04 g, 30.2 mmol, 1.0 eq.) was dissolved in dry benzene (110 mL) and ethylene glycol (14.3 mL, 257 mmol, 8.5 eq.) and *p*-toluenesulfonic acid (0.63 g, 3.33 mmol, 11 mol-%) were added. The resulting mixture was stirred vigorously and heated to reflux (100 °C oil bath) for two hours, at which the newly formed water was removed *via* a Dean-Stark apparatus. After cooling to room temperature, saturated aqueous NaHCO_3 (100 mL) was slowly added and the layers were separated. The aqueous phase was extracted with EtOAc ($3 \times 100\text{ mL}$), and the combined organic layers were then dried over Na_2SO_4 and concentrated *in vacuo*. The crude product was purified by flash column chromatography (silica, *i*-Hex:EtOAc = 3:2) to yield dioxolane **441** (6.09 g, 28.7 mmol, 97%) as colorless solid.

$R_f = 0.48$ (*i*-Hex:EtOAc = 1:1).

^1H NMR (CDCl_3 , 400 MHz): $\delta = 3.94\text{--}3.89$ (m, 4H), 3.70 (t, $J = 7.8\text{ Hz}$, 1H), 2.10 (m_C , 1H), 1.76–1.43 (m, 9H), 1.36–1.27 (m, 2H), 0.80 (s, 3H) ppm.

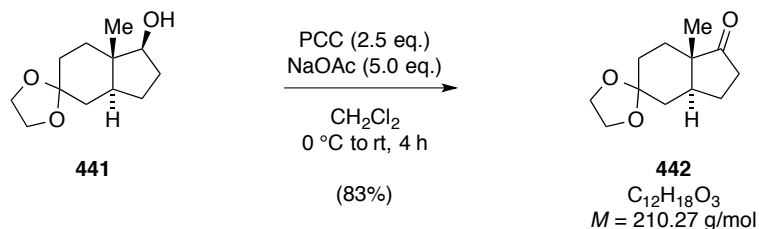
^{13}C NMR (CDCl_3 , 100 MHz): $\delta = 110.1, 81.1, 64.4, 64.3, 42.6, 42.5, 35.8, 33.7, 31.2, 31.1, 25.1, 9.7$ ppm.

EI-MS for $\text{C}_{12}\text{H}_{20}\text{O}_3^+ [M^+]$:	calcd.	212.1412
	found	212.1400.

IR (ATR): $\tilde{\nu}/\text{cm}^{-1} = 3476, 2953, 2938, 2873, 2855, 1469, 1449, 1444, 1430, 1407, 1375, 1347, 1334, 1325, 1305, 1290, 1261, 1253, 1226, 1233, 1189, 1136, 1112, 1071, 1043, 986, 972, 949, 943, 938, 897, 886, 856, 830, 800, 763, 734, 701, 677$.

$[\alpha]_D^{20} = +18.8$ (c 1.00, CH_2Cl_2).

Synthesis of Ketone **442**



Dioxolane **441** (6.10 g, 28.7 mmol, 1.0 eq.) was dissolved in dry CH_2Cl_2 (34 mL). This solution was then added dropwise to an ice-cold suspension of PCC (15.5 g, 71.8 mmol, 2.5 eq.) and NaOAc (11.8 g, 144 mmol, 5.0 eq.) in dry CH_2Cl_2 (160 mL). After warming to room temperature, the mixture was stirred for 4 hours, before being directly applied to flash column chromatography (silica, *i*-Hex:EtOAc = 2:1). Thus obtained crude ketone **442** (5.90 g, 28.1 mmol, 98%) was further purified *via* recrystallization from *n*-Hex at 4 °C to yield the title compound **442** (5.03 g, 23.9 mmol, 83%) as a colorless solid.

$R_f = 0.65$ (*i*-Hex:EtOAc = 1:1).

Melting point = 75.3–76.9 °C (*n*-Hex).

^1H NMR (CDCl_3 , 400 MHz): δ = 3.62–3.51 (m, 4H), 2.15–1.98 (m, 2H), 1.87–1.62 (m, 7H), 1.38 (dddd, J = 12.3, 8.9, 5.9, 1.3 Hz, 1H), 1.18 (m_c , 1H), 0.66 (s, 3H) ppm.

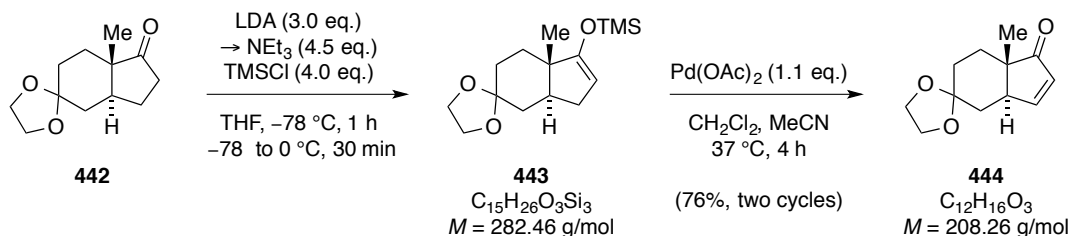
^{13}C NMR (CDCl_3 , 150 MHz): δ = 219.8, 109.6, 64.7, 64.4, 47.2, 42.8, 36.2, 35.6, 30.9, 28.7, 23.7, 12.3 ppm.

EI-MS for $\text{C}_{12}\text{H}_{18}\text{O}_3^+$ [M^+]:	calcd.	210.1256
	found	210.1270.

IR (ATR): $\tilde{\nu}/\text{cm}^{-1}$ = 2956, 2939, 2881, 2859, 1728, 1688, 1485, 1464, 1451, 1434, 1408, 1380, 1350, 1338, 1325, 1305, 1286, 1266, 1233, 1203, 1185, 1140, 1117, 1092, 1081, 1065, 1035, 1014, 1001, 986, 970, 947, 937, 925, 898, 856, 823, 806, 768, 678.

$$[\alpha]_D^{20} = +84.8 \text{ (} c \text{ 1.00, CH}_2\text{Cl}_2\text{)}.$$

Synthesis of Enone 444



A solution of diisopropylamine (12.0 mL, 85.6 mmol, 3.0 eq.) in dry THF (120 mL) at $-78\text{ }^\circ\text{C}$ was slowly treated with *n*-BuLi (34.2 mL, 2.51 M solution in hexanes, 85.6 mmol, 3.0 eq.) and the resulting mixture was stirred for 10 min at this temperature and for 15 min at $0\text{ }^\circ\text{C}$, before being cooled to $-78\text{ }^\circ\text{C}$ again. Then, ketone **442** (6.00 g, 28.5 mmol, 1.0 eq.) that was dissolved in dry THF (25 mL) was added over the course of 20 min. Stirring was continued for 45 min, at which point NEt_3 (17.9 mL, 128 mmol, 4.5 eq.) and freshly distilled TMSCl (14.4 mL, 114 mmol, 4.0 eq.) were added sequentially. The reaction was stirred for another 30 min and then allowed to warm to $0\text{ }^\circ\text{C}$. After the addition of half-saturated NaHCO_3 (100 mL), the mixture was diluted with *n*-pentane (200 mL) and the layers were separated. The aqueous phase was extracted with *n*-pentane ($3 \times 150\text{ mL}$) and the combined organic layers were dried over Na_2SO_4 . Careful evaporation of the solvents ($30\text{ }^\circ\text{C}$, min. 100 mbar) yielded silyl enol ether **443**, being pure enough for the use in further transformations.

Thus obtained silyl enol ether **443** was re-dissolved in dry CH_2Cl_2 (100 mL) and dry acetonitrile (34 mL). Pd(OAc)_2 (7.42 g, 31.3 mmol, 1.1 eq.) was added to this solution in one portion. This mixture was then added to an oil bath (pre-heated to $37\text{ }^\circ\text{C}$) and vigorously stirred for 4 hours. The resulting black suspension was directly applied to brief flash column chromatography (silica, *i*-Hex:EtOAc = 1:1). After removal of the solvents, further purification *via* flash column chromatography (silica, *i*-Hex:EtOAc = 8:1 to 6:1 to 4:1) yielded enone **444** (3.61g, 17.3 mmol, 61%) as colorless crystals, along with recovered ketone **442** (1.45 g, 6.90 mmol, 24%). Performing a second cycle of the above-described reaction conditions led to an overall yield of enone **444** (4.51g, 21.7 mmol) of 76%.

$R_f = 0.45$ (*i*-Hex:EtOAc = 1:1).

Melting point = $125.3\text{--}126.9\text{ }^\circ\text{C}$ (CH_2Cl_2).

^1H NMR (CDCl_3 , 600 MHz): δ = 7.38 (dd, J = 6.0, 0.8 Hz, 1H), 6.03 (dd, J = 5.9, 3.2 Hz, 1H), 3.99–3.94 (m, 4H), 3.05 (m_{C} , 1H), 1.95–1.89 (m, 3H), 1.78 (m_{C} , 2H), 1.70 (td, J = 13.2, 4.9 Hz, 1H), 1.14 (s, 3H) ppm.

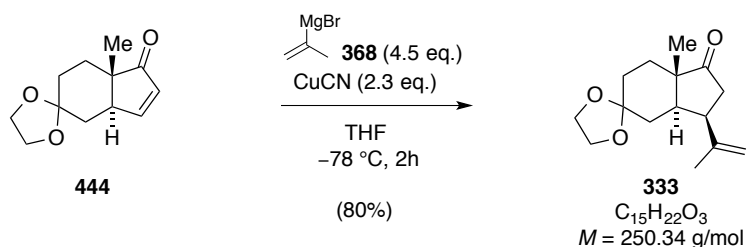
^{13}C NMR (CDCl_3 , 150 MHz): δ = 211.8, 160.6, 132.0, 109.7, 64.8, 64.3, 50.7, 48.1, 33.6, 31.7, 26.9, 19.4 ppm.

EI-MS for $\text{C}_{12}\text{H}_{16}\text{O}_3^+$ [M^+]:
calcd. 208.1100
found 208.1087.

IR (ATR): $\tilde{\nu}/\text{cm}^{-1}$ = 2963, 2931, 2862, 2878, 1695, 1660, 1560, 1484, 1466, 1454, 1444, 1436, 1377, 1370, 1351, 1344, 1314, 1274, 1251, 1229, 1206, 1179, 1133, 1086, 1066, 1035, 1002, 990, 971, 956, 938, 934, 894, 879, 827, 807, 767, 744, 711, 683, 669.

$[\alpha]_{\text{D}}^{20}$ = -66.4 (c 1.00, CH_2Cl_2).

Synthesis of Alkene 333



Powdered CuCN (1.77 g, 19.8 mmol, 2.3 eq.) was suspended in dry diethyl ether (58 mL) and cooled to 0 °C. Then, *iso*-propylmagnesium bromide (**368**, 79.0 mL, 0.5 M solution in THF, 19.8 mmol, 4.5 eq.) was added slowly and the resulting mixture was stirred for 30 min before being cooled to $-78\text{ }^\circ\text{C}$. After the dropwise addition of a solution of enone **444** (1.83 g, 8.79 mmol, 1.0 eq.) in dry THF (18 mL), the reaction was stirred for additional two hours. Saturated aqueous NH_4Cl (50 mL) was then added and the reaction was warmed to room temperature, filtered over a plug of Celite[®] (Et_2O washings) and the resulting layers were separated. The aqueous phase was extracted with diethyl ether ($3 \times 75\text{ mL}$) and the combined organic layers were dried over Na_2SO_4 and concentrated *in vacuo*. The crude products of several reaction batches of similar size were then combined and purification *via* flash column chromatography (silica, *i*-Hex: EtOAc = 8:1 to 5:1) to yield alkene **333** as colorless solid.

Overall enone **444** (7.83 g, 37.6 mmol) was converted to alkene **333** (7.52 g, 30.2 mmol) in 80% yield.

$R_f = 0.50$ (*i*-Hex:EtOAc = 3:1).

Melting point = 69.0–70.1 °C (CH₂Cl₂).

¹H NMR (CDCl₃, 400 MHz): δ = 4.96 (s, 1H), 4.83 (s, 1H), 3.99–3.92 (m, 4H), 2.86 (t, J = 8.3 Hz, 1H), 2.77 (dd, J = 19.7, 1.8 Hz, 1H), 2.48 (dd, J = 19.7, 9.1 Hz, 1H), 2.38 (dt, J = 9.9, 7.5 Hz, 1H), 1.96–1.93 (m, 2H), 1.80 (s, 3H), 1.79–1.60 (m, 3H), 1.42 (td, J = 13.2, 4.8 Hz, 1H), 1.03 (s, 3H) ppm.

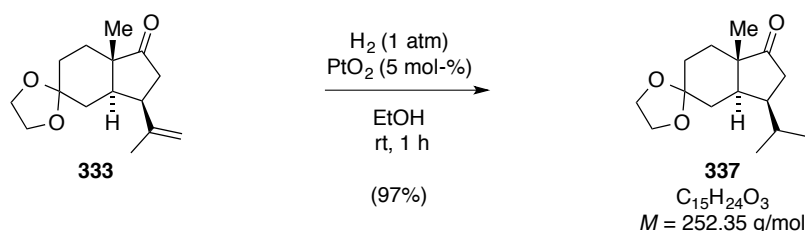
¹³C NMR (CDCl₃, 150 MHz): δ = 220.6, 146.1, 112.3, 109.8, 64.7, 64.4, 47.1, 45.7, 42.2, 41.9, 35.7, 30.9, 30.9, 24.9, 15.3 ppm.

EI-MS for C ₁₅ H ₂₂ O ₃ ⁺ [M ⁺]:	calcd.	250.1569
	found	250.1561.

IR (ATR): $\tilde{\nu}/\text{cm}^{-1}$ = 2952, 2886, 1734, 1644, 1432, 1378, 1345, 1295, 1234, 1188, 1153, 1136, 1093, 1052, 1032, 1012, 997, 967, 948, 940, 930, 923, 904, 862, 815, 770, 747, 678.

$[\alpha]_D^{20} = +31.0$ (*c* 1.00, CH₂Cl₂).

Synthesis of Ketone **337**



Alkene **333** (10.0 g, 40.0 mmol, 1.0 eq.) was dissolved in absolute ethanol (750 mL) and PtO₂ (554 mg, 2.00 mmol, 5 mol-%) was added in one batch. The resulting suspension was vigorously stirred, saturated with hydrogen (3 × evacuate and backfill) and then stirred under a hydrogen gas atmosphere (1 atm) for one hour. Thereafter, the mixture was filtered over

a plug of Celite[®] (Et₂O washings) and the solvents were removed *in vacuo*. The crude product was purified *via* flash column chromatography (silica, *i*-Hex:EtOAc = 5:1) to yield ketone **337** as colorless solid.

$R_f = 0.55$ (*i*-Hex:EtOAc = 3:1).

Melting point = 62.6–64.0 °C (CH₂Cl₂).

¹H NMR (CDCl₃, 400 MHz): δ = 3.98–3.90 (m, 4H), 2.49 (dd, J = 19.7, 2.4 Hz, 1H), 2.37 (dd, J = 19.8, 8.6 Hz, 1H), 2.28 (ddd, J = 13.6, 7.0, 3.3 Hz, 1H), 2.00 (t, J = 13.1 Hz, 1H), 1.93–1.61 (m, 6H), 1.44 (td, J = 13.0, 5.2 Hz, 1H), 1.04 (s, 3H), 0.96 (d, J = 6.0 Hz, 3H), 0.88 (d, J = 6.2 Hz, 3H) ppm.

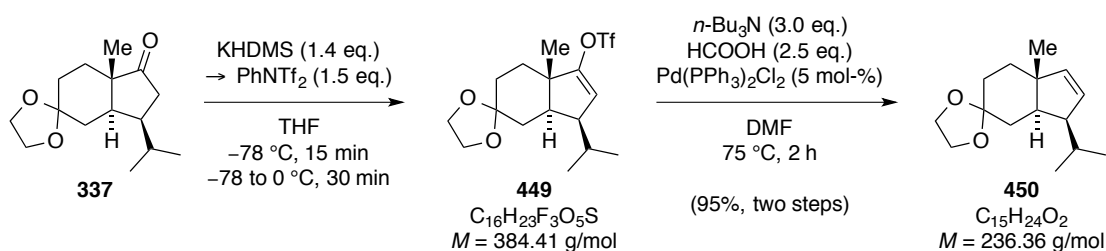
¹³C NMR (CDCl₃, 100 MHz): δ = 220.7, 109.9, 64.6, 64.4, 46.5, 45.5, 43.5, 41.9, 35.8, 30.7, 30.6, 29.9, 23.7, 23.2, 15.9 ppm.

EI-MS for C₁₅H₂₄O₃⁺ [M⁺]:
calcd. 252.1725
found 252.1728.

IR (ATR): $\tilde{\nu}/\text{cm}^{-1}$ = 2953, 2927, 2879, 1734, 1470, 1430, 1405, 1382, 1347, 1327, 1305, 1290, 1262, 1230, 1209, 1171, 1138, 1112, 1102, 1084, 1067, 1043, 1010, 989, 969, 948, 941, 919, 884, 860, 814, 768, 721, 680, 667.

$[\alpha]_D^{20} = +55.0$ (c 1.00, CH₂Cl₂).

Synthesis of Alkene **450**



To a solution of ketone **337** (5.23 g, 20.7 mmol, 1.0 eq.) in dry THF (205 mL) was added KHMDS (58.0 mL, 0.5 M solution in toluene, 29.0 mmol, 1.4 eq.) dropwise at -78 °C and the

resulting yellow mixture was stirred for 15 min. Then, PhNTf₂ (11.1 g, 31.1 mmol, 1.5 eq.) was added in five portions and stirring was continued for 5 min. The reaction was allowed to warm to 0 °C and stirred for 30 min. Half-saturated aqueous NH₄Cl (80 mL) and diethyl ether (200 mL) were added. The layers were separated and the aqueous phase was extracted with diethyl ether (3 × 50 mL). The combined organic layers were dried over Na₂SO₄ and then carefully concentrated *in vacuo* (30 °C, min. 100 mbar). Thus obtained crude enol triflate **449** was immediately used for the next transformation without further purification.

Enol triflate **449** was re-dissolved in dry DMF (52 mL) and *n*-Bu₃N (14.7 mL, 62.2 mmol, 3.0 eq.), formic acid (1.95 mL, 51.8 mmol, 2.5 eq.) and Pd(PPh₃)₂Cl₂ (726 mg, 1.04 mmol, 5 mol-%) were added sequentially. The yellow suspension was added to an oil bath (pre-heated to 75 °C) and vigorously stirred for one hour. The formed black suspension was cooled to room temperature and quenched *via* the addition of water (50 mL). After filtration over a plug of Celite[®] (Et₂O washings), the aqueous layer was separated and extracted with diethyl ether (3 × 50 mL). The combined organic layers were dried over Na₂SO₄ and then carefully concentrated *in vacuo* (30 °C, min. 500 mbar). The crude product was purified by flash column chromatography (silica, *n*-pentane:Et₂O = 50:1 to 30:1) to yield alkene **450** (4.65 g, 19.7 mmol, 95%) as colorless oil.

R_f = 0.40 (*i*-Hex:EtOAc = 10:1).

¹H NMR (CDCl₃, 400 MHz): δ = 5.85 (d, *J* = 6.0 Hz, 1H), 5.80 (dd, *J* = 5.9, 2.8 Hz, 1H), 3.97–3.94 (m, 4H), 2.17 (ddd, *J* = 11.3, 7.5, 5.4 Hz, 1H), 2.08 (m_C, 1H), 1.92–1.86 (m, 2H), 1.81 (dd, *J* = 13.8, 5.3 Hz, 1H), 1.76–1.64 (m, 2H), 1.60–1.45 (m, 2H), 1.01 (s, 3H), 0.90 (d, *J* = 6.4 Hz, 3H), 0.84 (d, *J* = 6.7 Hz, 3H) ppm.

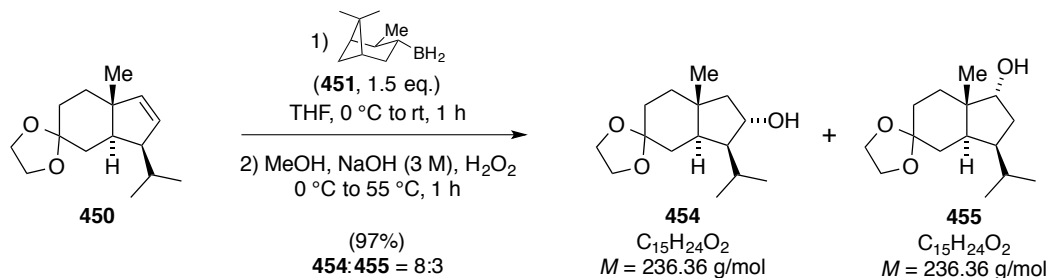
¹³C NMR (CDCl₃, 100 MHz): δ = 141.6, 134.1, 110.6, 64.5, 64.3, 54.2, 48.3, 45.8, 35.1, 35.0, 32.1, 29.8, 23.7, 22.5, 21.3 ppm.

EI-MS for C ₁₅ H ₂₄ O ₂ ⁺ [M ⁺]:	calcd.	236.1776
	found	236.1762.

IR (ATR): $\tilde{\nu}/\text{cm}^{-1}$ = 3047, 2953, 2931, 2870, 1465, 1432, 1383, 1364, 1349, 1291, 1249, 1185, 1120, 1108, 1084, 1052, 1014, 986, 972, 942, 879, 782, 740, 718, 671.

$$[\alpha]_D^{20} = -73.6 (c\ 1.00, \text{CH}_2\text{Cl}_2).$$

Synthesis of Alcohol 454



A solution of (+)-IpcBH₂ (**451**, ca. 1 M in THF) was freshly prepared as followed: A solution of (*S*)-Alpine-BoramineTM (**452**, 3.15 g, 7.57 mmol, 1.0 eq.) in dry THF (12 mL) was treated with BF₃·Et₂O (1.87 mL, 1.51 mmol, 2.0 eq.) at room temperature and the resulting mixture was stirred for two hours. The formed colorless precipitate was filtered off *via* syringe filter and the remaining solution was used for the generation of alcohol **454**.

To a solution of alkene **451** (1.38 g, 5.82 mmol, 1.0 eq.) in dry THF (150 mL) at 0 °C was dropwise added the prepared solution of (+)-IpcBH₂ (**451**, 8.73 mL, ca. 1 M in THF, 8.73 mmol, 1.5 eq.) and the resulting mixture was allowed to warm to room temperature. After stirring for one hour the reaction was cooled to 0 °C and methanol (2 mL), aqueous NaOH (3 M, 25 mL) and aqueous H₂O₂ (30 wt-%, 25 mL) were added sequentially. The biphasic mixture was heated to 55 °C for one hour and was then diluted with half-saturated aqueous NH₄Cl (100 mL) and diethyl ether (50 mL) at room temperature. The layers were separated and the aqueous phase was extracted with diethyl ether (3 × 75 mL). The combined organic layers were dried over Na₂SO₄ and concentrated *in vacuo*. The crude product was submitted to brief flash column chromatography (silica, *i*-Hex:EtOAc = 2:1), yielding alcohol **454** (1.43 g, 5.63 mmol, 97%) as a 8:3 mixture with isomeric alcohol **455**. Subsequent two cycles of flash column chromatography (silica, *i*-Hex:EtOAc = 4:1 to 3:1) yielded alcohol **454** (1.12 g, 4.40 mmol, 75%) as colorless oil as an 8:1 mixture with its regioisomer **455**.

Note: An analytical sample of alcohol 454 (purity as judged from ¹H NMR: 95 mol-%) was obtained by repeated flash column chromatography.

R_f = 0.35 (*i*-Hex:EtOAc = 2:1).

¹H NMR (CDCl₃, 400 MHz): δ = 4.33 (ddd, *J* = 8.9, 7.1, 4.3 Hz, 1H), 3.97–3.92 (m, 4H), 2.25 (ddd, *J* = 13.8, 10.3, 3.3 Hz, 1H), 2.01 (dd, *J* = 11.6, 7.1 Hz, 1H), 1.86 (ddd, *J* = 12.6,

3.2, 2.2 Hz, 1H), 1.76–1.38 (m, 8H), 1.29–1.15 (m, 1H), 1.00 (d, $J = 6.6$ Hz, 3H), 0.94 (d, $J = 6.3$ Hz, 3H), 0.87 (s, 3H) ppm.

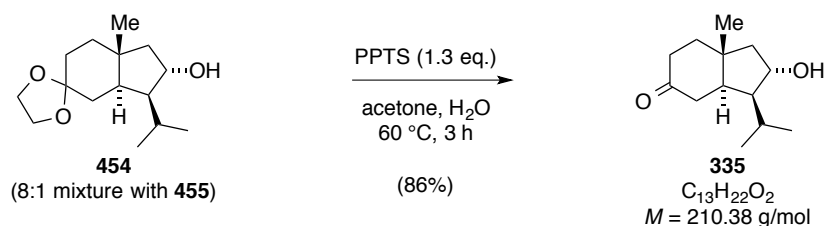
^{13}C NMR (CDCl_3 , 100 MHz): $\delta = 110.4, 77.9, 64.5, 64.3, 57.2, 50.1, 46.9, 41.2, 36.9, 34.8, 30.8, 29.9, 24.1, 22.0, 19.1$ ppm.

EI-MS for $\text{C}_{15}\text{H}_{26}\text{O}_3^+ [\text{M}^+]$:
 calcd. 254.1882
 found 254.1868.

IR (ATR): $\tilde{\nu}/\text{cm}^{-1} = 3293, 2941, 2890, 1469, 1455, 1383, 1366, 1351, 1289, 1254, 1191, 1168, 1158, 1139, 1107, 1093, 1082, 1064, 1038, 1002, 992, 945, 938, 928, 891, 874, 821, 767, 716, 706, 651, 638, 609$.

$[\alpha]_D^{20} = -3.0$ (c 1.00, CH_2Cl_2).

Synthesis of Hydrindanone 335



A solution of an 8:1 mixture of alcohols **454** and **455** (200 mg, 0.79 mmol, 1.0 eq.) in acetone (16 mL) and water (1.6 mL) was treated with PPTS (257 mg, 1.02 mmol, 1.3 eq.). The resulting mixture was heated to 60 °C for 3 hours. After cooling to room temperature, half-saturated aqueous NaHCO_3 (30 mL) and diethyl ether (50 mL) were added. The layers were separated and the aqueous phase was extracted with diethyl ether (3×25 mL). The combined organic layers were dried over Na_2SO_4 and then concentrated *in vacuo*. Purification *via* flash column chromatography (silica, *i*-Hex:EtOAc = 3:1 to 5:2) yielded pure alcohol **335** (142 mg, 0.67 mmol, 86%) as colorless solid.

$R_f = 0.20$ (*i*-Hex:EtOAc = 2:1).

Melting point = 54.0–55.3 °C (CH_2Cl_2).

^1H NMR (CDCl_3 , 400 MHz): δ = 4.41 (ddd, J = 8.9, 7.0, 4.8 Hz, 1H), 2.57 (dt, J = 13.5, 2.1 Hz, 1H), 2.44–2.29 (m, 4H), 2.09 (dd, J = 11.8, 7.0 Hz, 1H), 1.83 (ddd, J = 13.1, 6.9, 2.2 Hz, 1H), 1.73–1.53 (m, 2H), 1.62–1.53 (m, 2H), 1.30 (dd, J = 11.8, 9.3 Hz, 1H), 1.03 (s, 3H), 1.03 (d, J = 6.1 Hz, 1H), 0.93 (d, J = 6.3 Hz, 3H) ppm.

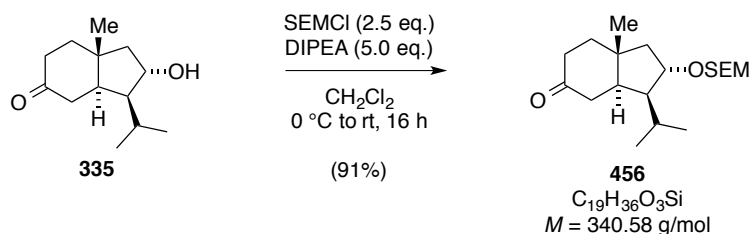
^{13}C NMR (CDCl_3 , 100 MHz): δ = 212.2, 77.6, 56.5, 49.3, 48.5, 41.6, 40.9, 37.7, 37.2, 29.2, 24.2, 21.7, 19.0 ppm.

EI-MS for $\text{C}_{13}\text{H}_{22}\text{O}_2^+$ [M^+]:
calcd. 210.1620
found 210.1621.

IR (ATR): $\tilde{\nu}/\text{cm}^{-1}$ = 3270, 2938, 2860, 1702, 1461, 1423, 1385, 1368, 1320, 1287, 1273, 1260, 1230, 1218, 1170, 1149, 1129, 1099, 1035, 1002, 954, 939, 926, 877, 811, 760, 693, 667, 639, 621.

$[\alpha]_D^{20}$ = +75.2 (c 0.50, CH_2Cl_2).

Synthesis of Ketone **456**



To a solution of alcohol **335** (630 mg, 3.00 mmol, 1.0 eq.) in CH_2Cl_2 (30 mL) at 0 °C were consecutively added DIPEA (2.60 mL, 15.0 mmol, 5.0 eq.) and SEMCl (1.30 mL, 7.50 mmol, 2.5 eq.). The mixture was allowed to warm to room temperature and stirred for 16 h. Then, EtOH (2.5 mL) was added and the mixture was stirred for an additional 15 min, before being diluted with saturated aqueous NaHCO_3 (30 mL). The layers were separated and the aqueous phase was extracted with CH_2Cl_2 (3 \times 50 mL). The combined organic layers were washed with saturated aqueous NaCl (40 mL) and dried over MgSO_4 . The solvents were evaporated under reduced pressure and the crude product was purified by flash column chromatography (silica, *i*-Hex:EtOAc = 20:1 to 7:1) to yield ketone **456** (934 mg, 2.74 mmol, 91%) as a colorless oil.

On a slightly larger scale, alcohol **335** (1.09 g, 5.19 mmol) was converted to ketone **456** (1.56 g, 4.58 mmol) in 88% yield.

$R_f = 0.23$ (*i*-Hex:EtOAc = 10:1).

^1H NMR (CDCl_3 , 400 MHz): $\delta = 4.68$ (d, $J = 7.0$ Hz, 1H), 4.63 (d, $J = 7.0$ Hz, 1H), 4.29 (ddd, $J = 8.7, 6.9, 4.0$ Hz, 1H), 3.68–3.52 (m, 2H), 2.58 (ddd, $J = 14.6, 3.9, 1.5$ Hz, 1H), 2.46–2.35 (m, 2H), 2.35–2.22 (m, 2H), 2.18 (dd, $J = 11.8, 7.0$ Hz, 1H), 1.84 (ddd, $J = 13.0, 6.8, 2.2$ Hz, 1H), 1.75–1.66 (m, 2H), 1.57 (ddd, $J = 12.9, 12.9, 6.1$ Hz, 1H), 1.27 (dd, $J = 11.6, 8.9$ Hz, 1H), 1.03 (s, 3H), 0.99 (d, $J = 6.1$ Hz, 3H), 0.96–0.89 (m, 5H), 0.01 (s, 9H) ppm.

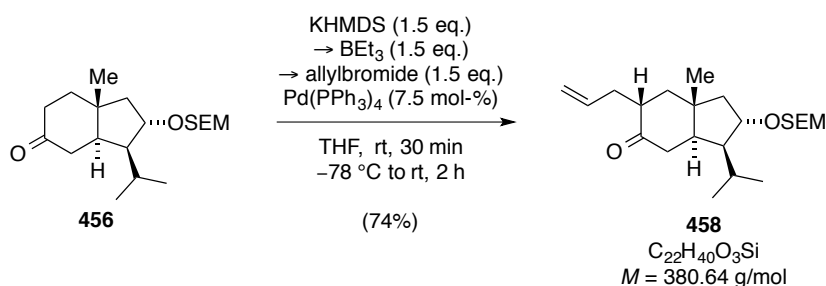
^{13}C NMR (CDCl_3 , 100 MHz): $\delta = 212.1, 93.6, 82.2, 65.4, 53.9, 48.2, 47.0, 41.5, 40.8, 37.9, 37.3, 28.9, 24.4, 21.5, 19.0, 18.2, -1.3$ ppm.

EI-MS for $\text{C}_{17}\text{H}_{32}\text{O}_3\text{Si}^+ [(\text{M}-\text{C}_2\text{H}_4)^+]$: calcd. 312.2115
found 312.2119.

IR (ATR): $\tilde{\nu}/\text{cm}^{-1} = 2954, 2927, 1710, 1463, 1420, 1388, 1248, 1107, 1058, 1029, 936, 860, 835$.

$[\alpha]_D^{20} = +43.2$ (c 1.00, CH_2Cl_2).

Synthesis of Ketone **458**



To a solution of ketone **456** (876 mg, 2.58 mmol, 1.0 eq.) in degassed THF (40 mL) was added KHMDS (7.70 mL, 0.5 M solution in toluene, 3.75 mmol, 1.5 eq.) at room temperature and the resulting yellow solution was stirred for 30 min, before being cooled to -78 $^\circ\text{C}$. Then,

Et₃B (7.70 mL, 0.5 M freshly prepared solution in THF, 3.75 mmol, 1.5 eq.) was added dropwise and the mixture was stirred for 5 min. After slowly adding a solution of Pd(PPh₃)₄ (223 mg, 194 μmol, 7.5 mol-%) and allyl bromide (334 μL, 3.85 mmol, 1.5 eq.) in degassed THF (5 mL), the cold bath was removed and the mixture was stirred for 2 hours at room temperature. The reaction was quenched by addition of saturated aqueous NH₄Cl (30 mL) and diluted with Et₂O (30 mL). The layers were separated and the aqueous phase was extracted with Et₂O (3 × 50 mL). The combined organic layers were washed with saturated aqueous NaCl (50 mL) and dried over MgSO₄. The solvents were evaporated under reduced pressure and the crude product was purified by flash column chromatography (silica, *i*-Hex:EtOAc = 34:1 to 24:1) to yield ketone **458** (725 mg, 1.90 mmol, 74%) as a colorless oil. On a slightly larger scale, ketone **456** (1.43 g, 4.21 mmol) was converted to its allylated congener **458** (1.09 g, 2.87 mmol) in 68% yield.

R_f = 0.47 (*i*-Hex:EtOAc = 10:1)

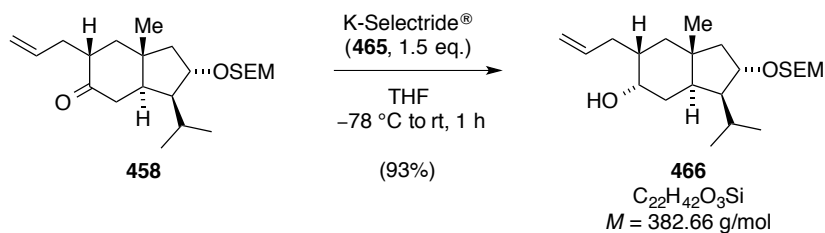
¹H NMR (CDCl₃, 600 MHz): δ = 5.74 (m_C, 1H), 5.04–4.97 (m, 2H), 4.67 (d, *J* = 7.0 Hz, 1H), 4.63 (d, *J* = 7.0 Hz, 1H), 4.30 (m_C, 1H), 3.66–3.54 (m, 2H), 2.63–2.54 (m, 2H), 2.48–2.37 (m, 2H), 2.23–2.15 (m, 2H), 2.02–1.94 (m, 2H), 1.74–1.66 (m, 2H), 1.27–1.22 (m, 2H), 1.08 (s, 3H), 0.99 (d, *J* = 6.1 Hz, 3H), 0.95–0.89 (m, 5H), 0.01 (s, 9H) ppm.

¹³C NMR (CDCl₃, 150 MHz): δ = 212.0, 136.6, 116.5, 93.6, 82.2, 65.4, 54.3, 49.4, 47.0, 45.2, 44.9, 41.9, 41.6, 33.9, 29.1, 24.3, 21.6, 19.9, 18.2, –1.3 ppm.

EI-MS for C₂₂H₄₀O₃Si⁺ [M⁺]: calcd. 380.2741
 found 380.2732.

IR (ATR): $\tilde{\nu}/\text{cm}^{-1}$ = 3076, 2955, 2928, 1708, 1464, 1388, 1249, 1162, 1099, 1058, 1033, 917, 860, 836.

$[\alpha]_D^{20}$ = +27.4 (*c* 0.50, CH₂Cl₂).

Synthesis of Alcohol **466**

To a solution of ketone **458** (1.08 g, 2.84 mmol, 1.0 eq.) in THF (30 mL) was added K-Selectride[®] (**465**, 4.26 mL, 1.0 M solution in THF, 4.26 mmol, 1.5 eq.) dropwise at -78 °C. The mixture was stirred for 10 min at this temperature, an additional 50 min at room temperature and then cooled to 0 °C. Then, MeOH (4.9 mL) was added followed by aqueous NaOH (3 M, 8.0 mL) and H₂O₂ (30 wt-%, 6.5 mL). The mixture was stirred at room temperature for 1.5 h and subsequently diluted with saturated aqueous NH₄Cl (40 mL). The layers were separated and the aqueous phase was extracted with Et₂O (3 × 50 mL). The combined organic layers were washed with saturated aqueous NaCl (40 mL) and dried over MgSO₄. The solvents were evaporated under reduced pressure and the crude product was purified by flash column chromatography (silica, *n*-pentane:Et₂O = 2:1) to yield alcohol **466** (1.01 g, 2.64 mmol, 93%) as a colorless oil.

$R_f = 0.22$ (*i*-Hex:EtOAc = 7:1)

¹H NMR (CDCl₃, 400 MHz): δ = 5.81 (ddt, J = 17.2, 10.0, 7.0 Hz, 1H), 5.06 (m_C, 1H), 5.01 (m_C, 1H), 4.68 (d, J = 7.1 Hz, 1H), 4.63 (d, J = 7.1 Hz, 1H), 4.21 (m_C, 1H), 3.97 (m_C, 1H), 3.69–3.53 (m, 2H), 2.28 (m_C, 1H), 2.20–2.12 (m, 1H), 2.06 (dd, J = 11.5, 7.1 Hz, 1H), 2.03–1.91 (m, 2H), 1.72–1.58 (m, 4H), 1.43–1.36 (m, 2H), 1.32–1.20 (m, 2H), 0.98–0.91 (m, 8H), 0.82 (s, 3H), 0.01 (s, 9H) ppm.

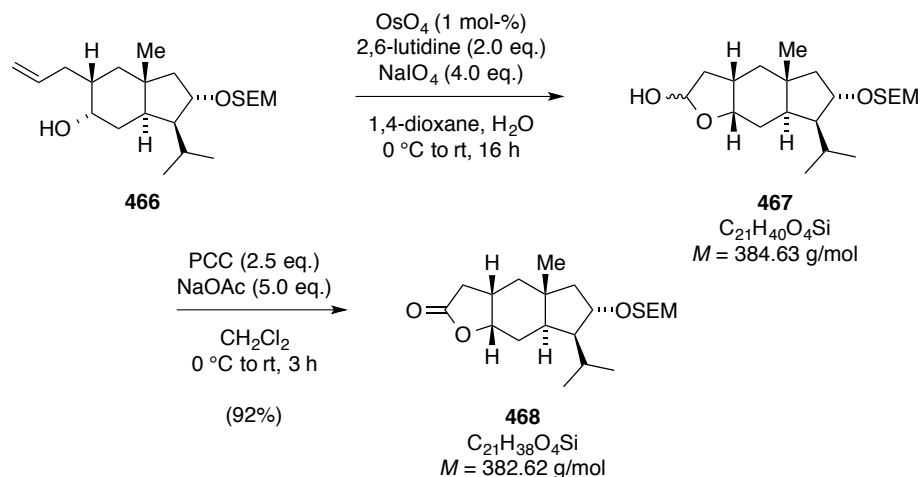
¹³C NMR (CDCl₃, 100 MHz): δ = 137.5, 116.0, 93.5, 81.7, 69.2, 65.3, 54.2, 48.0, 42.0, 41.9, 41.4, 37.3, 36.7, 32.4, 29.6, 24.4, 21.9, 19.8, 18.3, -1.3 ppm.

ESI-MS for C₂₂H₄₆O₃SiN⁺ [(M+NH₄)⁺]: calcd. 400.3241
found 400.3240.

IR (ATR): $\tilde{\nu}/\text{cm}^{-1}$ = 3474, 3076, 2953, 2929, 1462, 1378, 1250, 1100, 1056, 1026, 911, 860, 836.

$$[\alpha]_D^{20} = +21.6 (c\ 0.50, \text{CH}_2\text{Cl}_2).$$

Synthesis of Lactone 468



To a solution of alkene **466** (640 mg, 1.68 mmol, 1.0 eq.) and 2,6-lutidine (390 μL , 3.35 mmol, 2.0 eq.) in a mixture of 1,4-dioxane (24 mL) and H_2O (8 mL) were sequentially added OsO_4 (170 μL , 4 wt-% solution in H_2O , 16.8 μmol , 1 mol-%) and NaIO_4 (1.44 g, 6.70 mmol, 4.0 eq.) at $0\text{ }^\circ\text{C}$. The mixture was allowed to warm to room temperature and was stirred for 16 h, forming a white suspension. The mixture was partitioned between H_2O (30 mL) and CH_2Cl_2 (50 mL) and the layers were separated. The aqueous phase was extracted with CH_2Cl_2 ($3 \times 50\text{ mL}$) and the combined organic layers were washed with saturated aqueous NaCl (40 mL). After drying over MgSO_4 , the solvents were evaporated under reduced pressure to yield crude lactol **467** ($R_f = 0.19$, $i\text{-Hex}:\text{EtOAc} = 4:1$) which was used in the next step without further purification.

To a suspension of PCC (905 mg, 4.20 mmol, 2.5 eq.) and NaOAc (689 mg, 8.40 mmol, 5.0 eq.) in CH_2Cl_2 (30 mL) was added a solution of crude lactol **467** (assumed 1.68 mmol, 1.0 eq.) in CH_2Cl_2 (4 mL) at $0\text{ }^\circ\text{C}$. The mixture was allowed to warm to room temperature and stirred for 3 hours before being directly applied to flash column chromatography (silica, $i\text{-Hex}:\text{EtOAc} = 4:1$). The title compound (**468**, 611 mg, 1.59 mmol, 94% over two steps) was obtained as pale yellow oil.

On a slightly larger scale, alkene **466** (995 mg, 2.60 mmol) was converted to lactone **468** (910 mg, 2.38 mmol) in an overall yield of 91%.

$R_f = 0.27$ ($i\text{-Hex}:\text{EtOAc} = 4:1$).

^1H NMR (CDCl_3 , 400 MHz): δ = 4.68–4.59 (m, 3H), 4.17 (m_C , 1H), 3.67–3.53 (m, 2H), 2.71 (dd, J = 16.8, 7.0 Hz, 1H), 2.49 (m_C , 1H), 2.35 (m_C , 1H), 2.17 (d, J = 16.8 Hz, 1H), 2.13–2.04 (m, 2H), 1.81–1.62 (m, 4H), 1.23–1.17 (m, 1H), 1.11 (m_C , 1H), 0.99–0.89 (m, 8H), 0.82 (s, 3H), 0.01 (s, 9H) ppm.

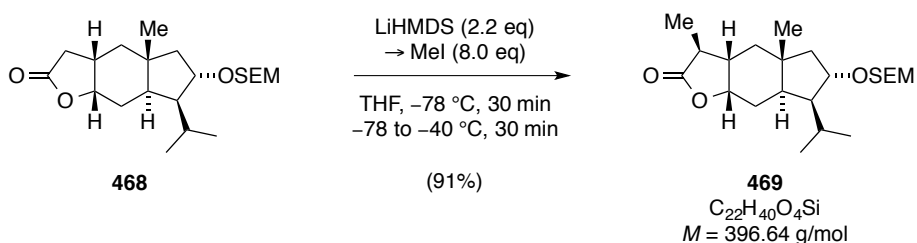
^{13}C NMR (CDCl_3 , 100 MHz): δ = 177.1, 93.6, 81.2, 80.0, 65.4, 53.2, 47.3, 42.3, 41.1, 40.4, 38.3, 32.3, 29.2, 26.4, 24.5, 21.7, 19.1, 18.3, –1.3 ppm.

ESI-MS for $\text{C}_{21}\text{H}_{42}\text{O}_4\text{Si}^+[(\text{M}+\text{NH}_4)^+]$: calcd. 400.2878
found 400.2876.

IR (ATR): $\tilde{\nu}/\text{cm}^{-1}$ = 2952, 1779, 1462, 1422, 1387, 1287, 1248, 1192, 1156, 1103, 1056, 1031, 942, 906, 861, 835.

$[\alpha]_D^{20} = -0.8$ (c 0.50, CH_2Cl_2).

Synthesis of Lactone 469



To a solution of lactone **468** (910 mg, 2.38 mmol, 1.0 eq.) in THF (40 mL) was added LiHMDS (5.24 mL, 1.0 M solution in THF, 5.24 mmol, 2.2 eq.) dropwise at $-78\text{ }^\circ\text{C}$ and the resulting mixture was stirred for 30 min. Then, MeI (1.19 mL, 19.0 mmol, 8.0 eq.) was added and the mixture was allowed to warm to $-40\text{ }^\circ\text{C}$. After stirring for an additional 30 min at this temperature, the reaction was quenched by addition of half-saturated aqueous NH_4Cl (40 mL). The biphasic mixture was allowed to warm to room temperature and diluted with Et_2O (50 mL). The layers were separated and the aqueous phase was extracted with Et_2O ($3 \times 50\text{ mL}$). The combined organic layers were consecutively washed with saturated aqueous $\text{Na}_2\text{S}_2\text{O}_3$ (40 mL), saturated aqueous NaCl (30 mL) and dried over MgSO_4 . The solvents were evaporated under reduced pressure and the crude product was purified by flash column

chromatography (silica, *i*-Hex:EtOAc = 5:1) to yield lactone **469** (857 mg, 2.16 mmol, 91%) as a colorless oil.

R_f = 0.47 (*i*-Hex:EtOAc = 4:1).

^1H NMR (CDCl_3 , 400 MHz): δ = 4.75 (m_C , 1H), 4.67 (d, J = 7.1 Hz, 1H), 4.62 (d, J = 7.2 Hz, 1H), 4.16 (m_C , 1H), 3.66–3.53 (m, 2H), 2.39–2.27 (m, 2H), 2.15–2.02 (m, 3H), 1.80–1.61 (m, 4H), 1.29 (d, J = 7.6 Hz, 3H), 1.19 (m_C , 1H), 1.09 (m_C , 1H), 0.99–0.89 (m, 8H), 0.80 (s, 3H), 0.01 (s, 9H) ppm.

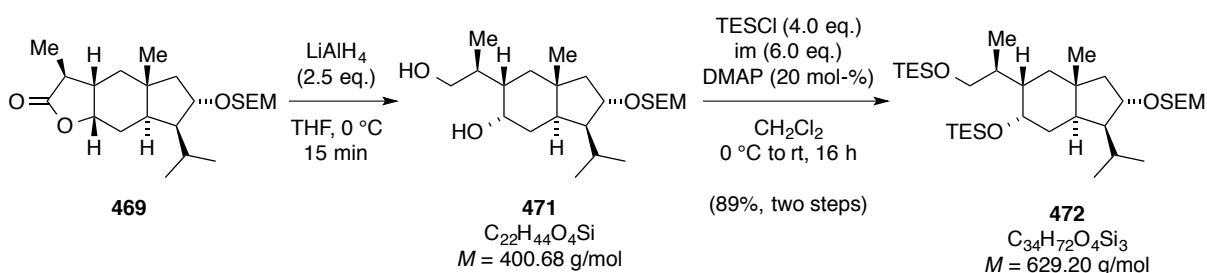
^{13}C NMR (CDCl_3 , 100 MHz): δ = 180.2, 93.6, 81.2, 77.8, 65.4, 53.2, 47.3, 44.8, 42.7, 41.2, 40.4, 39.1, 29.2, 26.4, 24.5, 21.7, 19.0, 18.3, 14.9, –1.3 ppm.

ESI-MS for $\text{C}_{22}\text{H}_{40}\text{O}_4\text{NaSi}^+$ [MNa^+]: calcd. 419.2588
found 419.2589.

IR (ATR): $\tilde{\nu}/\text{cm}^{-1}$ = 2952, 2900, 1772, 1460, 1385, 1248, 1190, 1098, 1057, 1031, 942, 860, 836.

$[\alpha]_D^{20}$ = –6.8 (c 0.50, CH_2Cl_2).

Synthesis of Silyl Ether **472**



To a suspension of LiAlH_4 (201 mg, 5.29 mmol, 2.5 eq.) in THF (26 mL) at 0 °C was added a solution of lactone **469** (840 mg, 2.12 mmol, 1.0 eq.) in THF (10 mL) dropwise and the mixture was stirred for 15 min. The reaction was quenched by careful addition of half-saturated aqueous Rochelle salt (50 mL), diluted with Et_2O (30 mL) and the biphasic mixture was stirred vigorously at room temperature for one hour. The layers were separated and the aqueous phase was extracted with Et_2O ($3 \times 50\text{ mL}$). The combined organic layers were

washed with saturated aqueous NaCl (30 mL) and dried over MgSO₄. Having evaporated the solvents under reduced pressure, the crude product was purified by brief flash column chromatography (silica, CH₂Cl₂:MeOH = 40:1) to yield diol **471**, which was immediately used in the next reaction.

To a solution of diol **471** (assumed 2.12 mmol, 1.0 eq.) in CH₂Cl₂ (20 mL) were sequentially added imidazole (865 mg, 12.7 mmol, 6.0 eq.), DMAP (52.0 mg, 0.42 mmol, 20 mol-%) and Et₃SiCl (1.44 mL, 8.50 mmol, 4.0 eq.) at 0 °C. The mixture was allowed to warm to room temperature and stirred for 16 hours. The reaction was filtered over a pad of Celite[®] (CH₂Cl₂ washings) and the clear solution was washed with saturated aqueous NaHCO₃ (30 mL). The aqueous phase was extracted with CH₂Cl₂ (3 × 50 mL) and the combined organic layers were washed with saturated aqueous NaCl (40 mL). After drying over MgSO₄, the solvent was evaporated under reduced pressure and the crude product was purified by flash column chromatography (silica, *i*-Hex:EtOAc = 100:1 to 60:1) to yield the title compound **472** (1.19 g, 1.89 mmol, 89% over two steps) as a colorless oil.

R_f = 0.24 (*i*-Hex:EtOAc = 30:1).

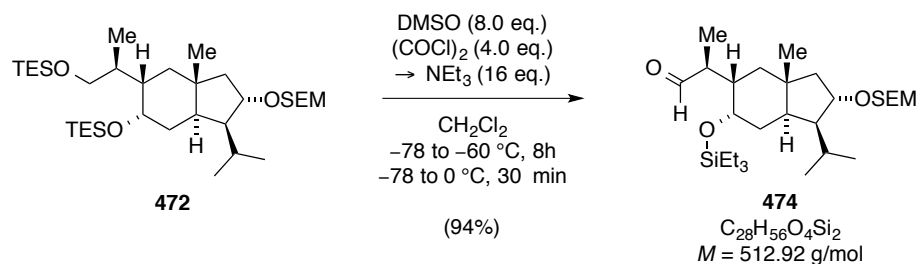
¹H NMR (CDCl₃, 400 MHz): δ = 4.70 (d, *J* = 7.1 Hz, 1H), 4.65 (d, *J* = 7.1 Hz, 1H), 4.22 (m_C, 1H), 4.07 (m_C, 1H), 3.72–3.54 (m, 2H), 3.51–3.42 (m, 2H), 2.37 (m_C, 1H), 2.05 (dd, *J* = 11.4, 7.0 Hz, 1H), 1.84 (m_C, 1H), 1.70–1.50 (m, 5H), 1.39–1.29 (m, 2H), 1.23 (m_C, 1H), 0.99–0.91 (m, 26H), 0.86 (d, *J* = 6.9 Hz, 3H), 0.80 (s, 3H), 0.63–0.54 (m, 12H), 0.01 (s, 9H) ppm.

¹³C NMR (CDCl₃, 100 MHz): δ = 93.5, 81.9, 70.6, 66.3, 65.3, 54.3, 48.3, 41.8, 41.6, 38.0 (2C), 37.2, 33.3, 29.8, 24.4, 21.9, 20.0, 18.3, 15.0, 7.2, 7.0, 5.5, 4.6, –1.3 ppm.

ESI-MS for C₃₄H₇₆O₄NSi₃⁺ [(M+NH₄)⁺]: calcd. 646.5077
 found 646.5085.

IR (ATR): $\tilde{\nu}/\text{cm}^{-1}$ = 2952, 2910, 2875, 1459, 1414, 1388, 1249, 1097, 1056, 949, 859, 835, 726.

$[\alpha]_D^{20}$ = +24.4 (*c* 0.50, CH₂Cl₂).

Synthesis of Aldehyde **474**

To a solution of dry DMSO (670 μ L, 9.52 mmol, 8.0 eq.) in dry CH₂Cl₂ (20 mL) at -78 °C was added dropwise oxalyl chloride (2.38 mL, 2.0 M solution in CH₂Cl₂, 4.78 mmol, 4.0 eq.) and the mixture was stirred for 15 min at this temperature. Then, a solution of silyl ether **472** (750 mg, 1.19 mmol, 1.0 eq.) in CH₂Cl₂ (4 mL) was added over 30 min. The mixture was allowed to warm to -60 °C and was stirred for 8 hours at -65 to -60 °C. The reaction was then cooled to -78 °C and Et₃N (2.65 mL, 19.0 mmol, 16 eq.) was added dropwise. The cold bath was replaced by an ice/water bath and the mixture was stirred for 30 min at 0 °C, at which point the reaction was quenched by addition of H₂O (40 mL) and diluted with CH₂Cl₂ (40 mL). The layers were separated and the aqueous layer was extracted with CH₂Cl₂ (3 \times 40 mL). The combined organic layers were washed with saturated aqueous NaCl (50 mL) and dried over MgSO₄. Having evaporated the solvents under reduced pressure, the crude product was purified by flash column chromatography (silica, *i*-Hex:EtOAc = 40:1 to 20:1) to yield aldehyde **474** (577 mg, 1.12 mmol, 94%) as a pale yellow oil.

On a larger scale, silyl ether **472** (1.18 g, 1.88 mmol) was converted to aldehyde **474** (657 mg, 1.28 mmol) in 69% yield. In addition, unreacted starting material **472** (225 mg, 385 μ mol, 30%) was recovered.

R_f = 0.22 (*i*-Hex:EtOAc = 15:1).

¹H NMR (CDCl₃, 400 MHz): δ = 9.73 (d, *J* = 1.7 Hz, 1H), 4.70 (d, *J* = 7.1 Hz, 1H), 4.65 (d, *J* = 7.1 Hz, 1H), 4.22 (m_C, 1H), 4.11 (m_C, 1H), 3.70–3.55 (m, 2H), 2.42–2.32 (m, 2H), 2.08 (dd, *J* = 11.4, 7.1 Hz, 1H), 1.93–1.83 (m, 2H), 1.69–1.53 (m, 4H), 1.38 (dd, *J* = 12.3, 3.7 Hz, 1H), 1.25 (dd, *J* = 11.3, 8.5 Hz, 1H), 1.05 (d, *J* = 7.2 Hz, 3H), 0.98–0.91 (m, 17H), 0.84 (s, 3H), 0.62–0.54 (m, 6H), 0.01 (s, 9H) ppm.

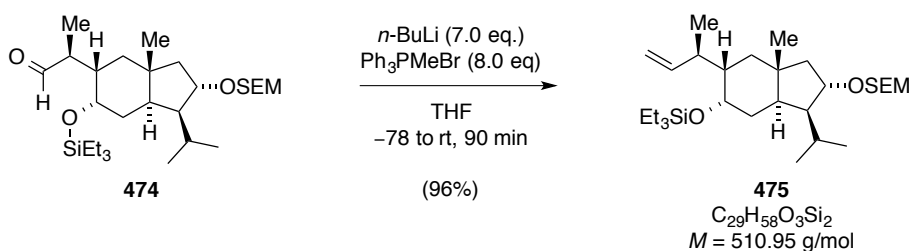
¹³C NMR (CDCl₃, 100 MHz): δ = 205.1, 93.5, 81.7, 68.8, 65.3, 54.2, 48.3, 48.1, 41.9, 41.5, 39.7, 39.1, 32.5, 29.7, 24.4, 21.9, 19.8, 18.3, 12.1, 7.1, 5.3, -1.3 ppm.

ESI-MS for $C_{28}H_{57}O_4Si_2^+$ $[MH^+]$: calcd. 513.3790
 found 513.3797.

IR (ATR): $\tilde{\nu}/cm^{-1}$ = 2951, 2875, 1725, 1457, 1379, 1248, 1100, 1055, 946, 859, 835, 730.

$[\alpha]_D^{20}$ = +48.0 (*c* 0.25, CH_2Cl_2).

Synthesis of Alkene **475**



To a suspension of Ph_3PMeBr (3.31 g, 9.28 mmol, 8.0 eq.) in THF (50 mL) was added *n*-BuLi (3.25 mL, 2.5 M solution in hexanes, 8.12 mmol, 7.0 eq.) dropwise at 0 °C and the mixture was allowed to warm to room temperature. The suspension was stirred for one hour and subsequently cooled to -78 °C. Then, a solution of aldehyde **474** (594 mg, 1.16 mmol, 1.0 eq.) in THF (10 mL) was added slowly. The cold bath was removed and the mixture was stirred for 1.5 hours at room temperature. Then, the reaction was quenched by addition of half-saturated aqueous NH_4Cl (30 mL) and the biphasic mixture was extracted with Et_2O ($3 \times 50 \text{ mL}$). The combined organic layers were washed with saturated aqueous NaCl (30 mL) and were dried over $MgSO_4$. Having evaporated the solvents under reduced pressure, the crude product was purified by flash column chromatography (silica, *i*-Hex:EtOAc = 100:1 to 40:1) to yield alkene **475** as a colorless oil.

Flash column chromatography was performed combined with the crude product of a smaller reaction batch. Overall, aldehyde **474** (645 mg, 1.26 mmol) was converted to alkene **475** (617 mg, 1.21 mmol) in 96% yield.

R_f = 0.38 (*i*-Hex:EtOAc = 15:1).

1H NMR ($CDCl_3$, 400 MHz): δ = 5.74 (ddd, J = 17.3, 10.2, 8.3 Hz, 1H), 4.97 (m_C , 1H), 4.92 (m_C , 1H), 4.70 (d, J = 7.0 Hz, 1H), 4.65 (d, J = 7.1 Hz, 1H), 4.22 (m_C , 1H), 4.07 (m_C , 1H), 3.70–3.54 (m, 2H), 2.37 (m_C , 1H), 2.20 (m_C , 1H), 2.05 (dd, J = 11.2, 7.1 Hz, 1H), 1.85 (m_C ,

1H), 1.68–1.47 (m, 3H), 1.40 (dd, $J = 11.3, 2.6$ Hz, 1H), 1.34–1.19 (m, 3H), 1.00–0.87 (m, 20H), 0.79 (s, 3H), 0.63–0.55 (m, 6H), 0.01 (s, 9H) ppm.

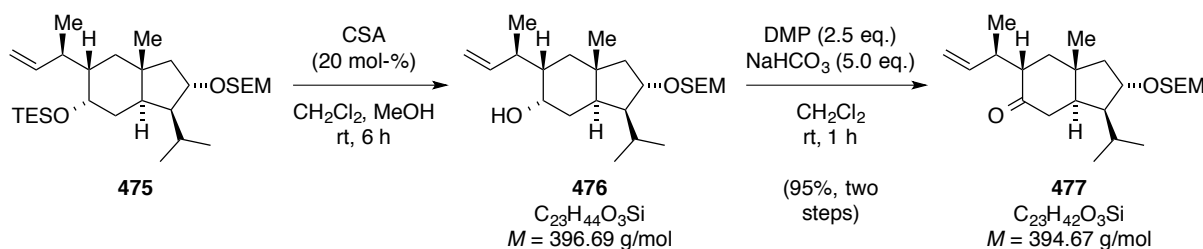
^{13}C NMR (CDCl_3 , 100 MHz): $\delta = 144.8, 113.1, 93.5, 81.9, 69.5, 65.3, 54.2, 48.2, 42.9, 41.9, 41.6, 38.9, 38.6, 33.1, 29.8, 24.4, 21.9, 20.1, 18.6, 18.3, 7.3, 5.6, -1.3$ ppm.

EI-MS for $\text{C}_{27}\text{H}_{53}\text{O}_3\text{Si}_2^+$ $[(\text{M}-\text{C}_2\text{H}_5)^+]$: calcd. 481.3528
found 481.3530.

IR (ATR): $\tilde{\nu}/\text{cm}^{-1} = 3076, 2954, 2877, 1460, 1415, 1370, 1260, 1099, 1048, 946, 910, 859, 835, 794, 727$.

$[\alpha]_D^{20} = +28.5$ (c 0.33, CH_2Cl_2).

Synthesis of Ketone 477



To a solution of TES ether **475** (200 mg, 391 μmol , 1.0 eq.) in a mixture of CH_2Cl_2 (28 mL) and MeOH (4 mL) was added CSA (18.0 mg, 78.0 μmol , 20 mol-%) and the mixture was stirred for 6 hours. The reaction was quenched by the addition of saturated aqueous NaHCO_3 (40 mL) and was then diluted with CH_2Cl_2 (30 mL). The layers were separated and the aqueous phase was extracted with CH_2Cl_2 (3×50 mL). The combined organic layers were washed with saturated aqueous NaCl (20 mL) and dried over Na_2SO_4 . The solvents were removed under reduced pressure to give crude alcohol **476** ($R_f = 0.20$, $i\text{-Hex}:\text{EtOAc} = 7:1$), which was directly used without further purification.

To a solution of crude alcohol **476** (assumed 391 μmol , 1.0 eq.) in CH_2Cl_2 (20 mL) was consecutively added NaHCO_3 (164 mg, 1.96 mmol, 5.0 eq.) and Dess-Martin periodinane (415 mg, 978 μmol , 2.5 eq.) and the suspension was stirred for one hour. The reaction was carefully quenched by the addition of saturated aqueous NaHCO_3 , saturated aqueous $\text{Na}_2\text{S}_2\text{O}_3$ and H_2O (1:1:1, 20 mL). The resulting mixture was vigorously stirred until two distinct layers

were obtained. The phases were separated and the aqueous layer was extracted with CH₂Cl₂ (3 × 50 mL). The combined organic layers were dried over Na₂SO₄ and the solvent was evaporated under reduced pressure. The crude product was purified by flash column chromatography (silica, *i*-Hex:EtOAc = 20:1) to yield ketone **477** (147 mg, 373 μmol, 95% over two steps) as a highly viscous, colorless oil.

$R_f = 0.50$ (*i*-Hex:EtOAc = 7:1).

¹H NMR (CDCl₃, 400 MHz): δ = 5.79 (m_C, 1H), 5.03–4.95 (m, 2H), 4.68 (d, J = 7.1 Hz, 1H), 4.63 (d, J = 7.1 Hz, 1H), 4.29 (m_C, 1H), 3.68–3.54 (m, 2H), 2.89 (m_C, 1H), 2.59 (dd, J = 14.7, 4.0 Hz, 1H), 2.45–2.36 (m, 2H), 2.23–2.14 (m, 2H), 1.78 (dd, J = 12.8, 6.3 Hz, 1H), 1.74–1.64 (m, 2H), 1.37 (dd, J = 13.0, 13.0 Hz, 1H), 1.27 (dd, J = 11.7, 8.7 Hz, 1H), 1.04 (s, 3H), 0.99 (d, J = 6.1 Hz, 3H), 0.97–0.89 (m, 8H), 0.01 (s, 9H) ppm.

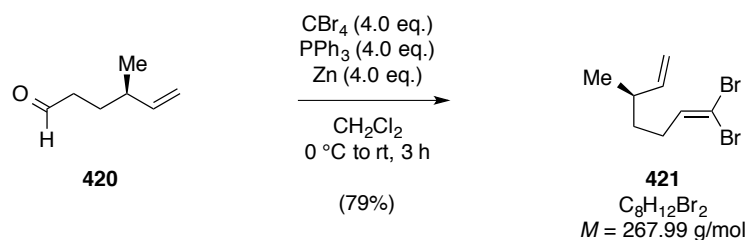
¹³C NMR (CDCl₃, 100 MHz): δ = 211.5, 142.6, 113.9, 93.6, 82.1, 65.4, 54.2, 49.7, 48.5, 47.3, 42.0, 41.2, 39.4, 35.5, 29.0, 24.3, 21.6, 19.7, 18.2, 14.8, –1.3 ppm.

EI-MS for C₂₃H₄₂O₃Si⁺ [M⁺]:
calcd. 394.2898
found 394.2914.

IR (ATR): $\tilde{\nu}/\text{cm}^{-1}$ = 3075, 2955, 2932, 2876, 1705, 1462, 1382, 1372, 1249, 1160, 1103, 1058, 1030, 936, 915, 860, 835.

$[\alpha]_D^{20} = +29.8$ (*c* 0.50, CH₂Cl₂).

Synthesis of Dibromide **421**



To a suspension of Zn (10.5 g, 160 mmol, 4.0 eq.) in CH₂Cl₂ (300 mL) was added PPh₃ (41.9 g, 160 mmol, 4.0 eq.) at 0 °C and the mixture was stirred for 5 min. Then, CBr₄

(53.0 g, 160 mmol, 4.0 eq.) was added and the resulting green suspension was stirred for an additional 90 min. at 0 °C. At this point, a solution of aldehyde **420** (4.48 g, 40.0 mmol, 1.0 eq.) in CH₂Cl₂ (20 mL) was added. The cold bath was removed and the mixture was stirred for 3 hours at room temperature, changing its color to dark brown. The suspension was diluted with *n*-pentane (300 mL) and the solvents were decanted. The resulting brown solid was suspended in CH₂Cl₂ (50 mL). *n*-Pentane (50 mL) was added before the solvents were decanted again. This wash was repeated two more times and the suspension was filtered over a plug of silica (*n*-pentane washings). The solvent of the product containing fractions was carefully removed under reduced pressure and the crude product was purified by flash column chromatography (silica, *n*-pentane) to yield dibromoalkene **421** (8.42 g, 31.4 mmol, 79%) as a light yellow liquid.

$R_f = 0.88$ (*n*-pentane).

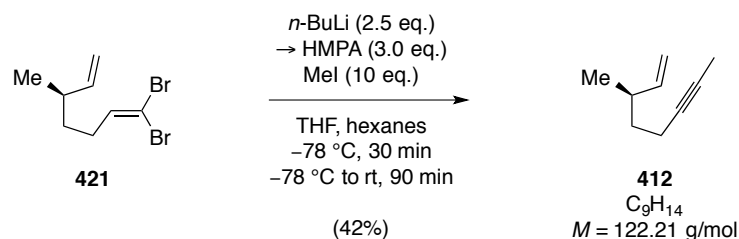
¹H NMR (CDCl₃, 400 MHz): δ = 6.40 (t, J = 7.3 Hz, 1H), 5.69 (ddd, J = 17.3, 10.2, 7.7 Hz, 1H), 5.05–4.95 (m, 2H), 2.22–2.02 (m, 3H), 1.48–1.40 (m, 2H), 1.03 (d, J = 6.9 Hz, 3H) ppm.

¹³C NMR (CDCl₃, 100 MHz): δ = 143.8, 138.8, 113.5, 88.7, 37.5, 34.6, 31.0, 20.3 ppm.

EI-MS for C ₈ H ₁₁ Br ₂ ⁺ [(M–H) ⁺]:	calcd.	264.9222
	found	264.9207.

IR (ATR): $\tilde{\nu}/\text{cm}^{-1}$ = 3076, 2955, 2923, 2862, 1807, 1704, 1638, 1452, 1417, 1373, 1270, 1233, 1144, 994, 912, 796, 749, 665.

$[\alpha]_D^{20} = -1.2$ (c 1.00, CH₂Cl₂).

Synthesis of Enyne **412**

To a solution of dibromoalkene **421** (7.70 g, 28.7 mmol, 1.0 eq.) in THF (56 mL) at $-78\text{ }^{\circ}\text{C}$ was added dropwise $n\text{-BuLi}$ (28.7 mL, 2.5 M solution in hexanes, 72.8 mmol, 2.5 eq.) and the resulting mixture was stirred for 30 min. Then, HMPA (12.5 mL, 72.8 mmol, 2.5 eq.) was added and the mixture was stirred for an additional 5 min, at which point MeI (17.9 mL, 287 mmol, 10 eq.) was added dropwise. The mixture was stirred for 30 min at $-78\text{ }^{\circ}\text{C}$ and for 90 min at room temperature. Then, the reaction was quenched by the addition of half-saturated NH_4Cl (100 mL) and the mixture was diluted with $n\text{-pentane}$ (100 mL). The phases were separated and the aqueous layer was extracted with $n\text{-pentane}$ ($3 \times 80\text{ mL}$). The combined organic layers were subsequently washed with H_2O ($3 \times 100\text{ mL}$), saturated aqueous $\text{Na}_2\text{S}_2\text{O}_3$ (100 mL) and saturated aqueous NaCl ($2 \times 100\text{ mL}$). After drying over MgSO_4 , the solvents were distilled off at atmospheric pressure (20 cm Vigreux) and the resulting residue was purified by flash column chromatography (silica, $n\text{-pentane}$) to yield the desired enyne **412** (1.83 g, 5:2 mixture with $n\text{-pentane}$, 12.1 mmol, 42%) as a light yellow, volatile liquid.

Note: The solvent of the product containing fractions was distilled off at atmospheric pressure.

$R_f = 0.29$ ($n\text{-pentane}$).

^1H NMR (CDCl_3 , 400 MHz): $\delta = 5.65$ (m_C , 1H), 4.98 (m_C , 1H), 4.93 (m_C , 1H), 2.25 (m_C , 1H), 2.18–2.03 (m, 2H), 1.77 (t, $J = 2.6\text{ Hz}$, 3H), 1.47 (m, 2H), 0.99 (d, $J = 6.6\text{ Hz}$, 3H) ppm.

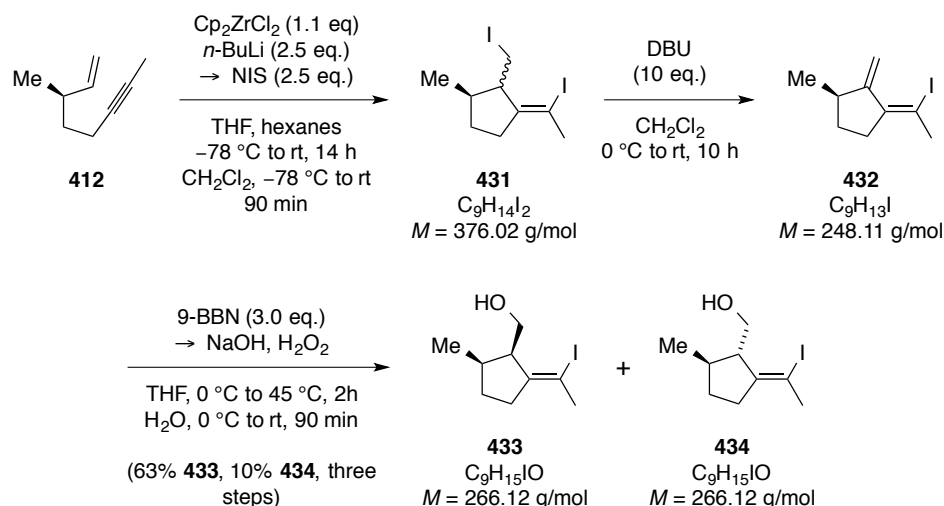
^{13}C NMR (CDCl_3 , 100 MHz): $\delta = 143.9$, 113.3, 79.3, 75.6, 37.0, 35.9, 20.0, 16.7, 3.6 ppm.

EI-MS for $\text{C}_9\text{H}_{13}^+$ [(M-H) $^+$]:	calcd.	121.1012
	found	121.1020.

IR (ATR): $\tilde{\nu}/\text{cm}^{-1}$ = 3078, 2958, 2919, 2861, 1829, 1639, 1454, 1433, 1419, 1373, 1346, 1309, 1148, 1111, 1075, 995, 911, 771, 680.

$[\alpha]_D^{20} = -22.4$ (c 0.50, CH_2Cl_2).

Synthesis of Alcohols 433 and 434



To a solution of Cp₂ZrCl₂ (1.84 g, 6.29 mmol, 1.05 eq.) in THF (39 mL) was added *n*-BuLi (4.73 mL, 2.65 M solution in hexanes, 12.8 mmol, 2.1 eq.) dropwise at -78 °C and the resulting yellow solution was stirred at this temperature for one hour. Then, a solution of enyne **412** (730 mg, 5.99 mmol, 1.00 eq.) in THF (5 mL) was added within 20 min. The mixture was allowed to warm to room temperature over the course of two hours and stirred for an additional 14 hours, changing its color to light red. The resulting intermediate was added to a solution of NIS (3.37 g, 15.0 mmol, 2.5 eq.) in CH₂Cl₂ (40 mL) at -78 °C within 90 min. The mixture was stirred for 15 min at -78 °C, for 30 min at -50 °C and an additional hour at room temperature. The reaction was quenched by the addition of saturated aqueous NH₄Cl (30 mL) and diluted with *n*-pentane (40 mL). The resulting suspension was filtered over a pad of Celite® (*n*-pentane washings). The layers were separated and the aqueous layer was extracted with *n*-pentane (3 × 40 mL). The combined organic layers were consecutively washed with saturated aqueous Na₂S₂O₃ (50 mL), saturated aqueous NaHCO₃ (50 mL) and saturated aqueous NaCl (50 mL). After drying over Na₂SO₄, the solvents were evaporated under reduced pressure and the crude product was purified by flash column chromatography (silica, *n*-pentane) to yield crude diiodide **431** (2.05 g, 5.45 mmol, 85%) as a brownish liquid. Such material was obtained as an inconsequential 3:1 to 5:1 mixture of diastereomers and was

employed in the next step without further purification. An analytical sample was obtained by repeated flash column chromatography.

$R_f = 0.57$ (*n*-pentane).

^1H NMR (C_6D_6 , 400 MHz, only major isomer quoted): $\delta = 3.37$ (dd, $J = 9.7, 3.1$ Hz, 1H), 2.90 (m_C , 1H), 2.48 (m_C , 1H), 2.16–2.06 (m, 4H), 2.04–1.93 (m, 1H), 1.93–1.82 (m, 1H), 1.56 (m_C , 1H), 1.10 (m_C , 1H), 0.75 (d, $J = 7.1$ Hz, 3H) ppm. Characteristic signal for minor isomer: $\delta = 1.00$ (d, $J = 6.9$ Hz, 3H) ppm.

^{13}C NMR (C_6D_6 , 100 MHz, only major isomer quoted): $\delta = 149.4, 91.6, 60.5, 39.0, 32.2, 30.8, 29.5, 20.1, 10.2$ ppm.

EI-MS for $\text{C}_9\text{H}_{14}\text{I}_2^+$ [M^+]:	calcd.	375.9180
	found	375.9185.

IR (ATR): $\tilde{\nu}/\text{cm}^{-1} = 2951, 2922, 2866, 2840, 1641, 1453, 1431, 1418, 1374, 1348, 1312, 1286, 1263, 1243, 1211, 1199, 1173, 1159, 1145, 1102, 1058, 1016, 968, 948, 912, 879, 833, 790, 763, 679, 655$.

Since this compound was obtained as a mixture of diastereomers, no optical rotation was measured.

To a solution of diiodide **431** (2.05 g, 5.45 mmol, 1.0 eq.) in CH_2Cl_2 (110 mL) was slowly added DBU (7.93 mL, 54.5 mmol, 10 eq.) at 0 °C. The mixture was allowed to warm to room temperature and stirred for 10 hours. The reaction was quenched by the addition of H_2O (50 mL) and the resulting mixture was diluted with *n*-pentane (100 mL). The layers were separated and the aqueous phase was extracted with *n*-pentane (3×100 mL). The combined organic layers were consecutively washed with saturated aqueous NH_4Cl (100 mL), saturated aqueous NaCl (100 mL) and were dried over Na_2SO_4 . The solvents were carefully removed under reduced pressure and the obtained crude diene **432** was immediately used in the next step.

Note: Intermediate 432 is very prone to decomposition. A sample suitable for NMR analysis could be obtained by quick flash column chromatography (silica, n-pentane).

$R_f = 0.64$ (*n*-pentane).

^1H NMR (C_6D_6 , 400 MHz): $\delta = 6.42$ (d, $J = 2.2$ Hz, 1H), 4.90 (d, $J = 1.6$ Hz, 1H), 2.33 (s, 3H), 2.37–2.26 (m, 1H), 2.17 (m_C , 1H), 2.05–1.94 (m, 1H), 1.51 (m_C , 1H), 0.95 (d, $J = 6.8$ Hz, 1H), 0.99–0.88 (m, 3H) ppm.

^{13}C NMR (C_6D_6 , 100 MHz): $\delta = 154.1, 142.3, 109.1, 86.7, 41.4, 33.7, 32.2, 32.1, 18.6$ ppm.

To a solution of crude diene **432** (assumed 4.79 mmol, 1.0 eq.) in THF (90 mL) was slowly added 9-BBN (29 mL, 0.5 M solution in THF, 14.5 mmol, 3.0 eq.) at 0 °C. The reaction was allowed to warm to room temperature and stirred for one hour at 45 °C. The mixture was cooled to 0 °C and EtOH (9.0 mL) was added slowly. The mixture was stirred for 10 min and subsequently NaOH (32.0 mL, 3.0 M solution in H_2O , 96.0 mmol, 20 eq.) and H_2O_2 (9.60 mL, 30 wt-%, 96.0 mmol, 20 eq.) were added. After stirring for 90 min at room temperature, H_2O (50 mL) was added and the biphasic mixture was extracted with Et_2O (3×100 mL). The combined organic layers were washed with saturated aqueous NaCl (30 mL) and dried over Na_2SO_4 . Having evaporated the solvents under reduced pressure, the crude product was purified by flash column chromatography (silica, *n*-pentane/ Et_2O = 6:1 to 5:1) to yield the desired alcohol **433** (1.01 g, 3.76 mmol, 63% over three steps) as a colorless low melting solid along with its diastereomer **434** (170 mg, 639 μmol , 10% over three steps) as a colorless oil.

Analytical data for major isomer **433**:

$R_f = 0.29$ (*n*-pentane/ Et_2O = 20:1).

Melting point = 28–31 °C (*n*-pentane).

^1H NMR (C_6D_6 , 600 MHz): $\delta = 3.79$ –3.69 (m, 1H), 3.57–3.49 (m, 1H), 2.56 (m_C , 1H), 2.17 (q, $J = 1.4$ Hz, 3H), 2.14–2.04 (m, 1H), 1.99–1.84 (m, 2H), 1.73–1.63 (m, 1H), 1.57–1.49 (m, 1H), 1.02 (d, $J = 7.1$ Hz, 3H), 0.73–0.61 (m, 1H) ppm.

^{13}C NMR (C_6D_6 , 150 MHz): $\delta = 150.0, 88.6, 61.2, 56.9, 37.4, 34.2, 30.7, 30.5, 15.5$ ppm.

EI-MS for $\text{C}_9\text{H}_{15}\text{IO}^+ [\text{M}]^+$: calcd. 266.0162
 found 266.0147.

IR (ATR): $\tilde{\nu}/\text{cm}^{-1} = 3366, 2951, 2869, 1646, 1472, 1454, 1429, 1373, 1321, 1294, 1260, 1213, 1181, 1132, 1100, 1074, 1055, 1036, 1000, 982, 950, 933, 839, 802, 703, 673.$

$[\alpha]_D^{20} = -56.0$ (c 0.10, C_6D_6).

Analytical data for minor isomer **434**:

$R_f = 0.26$ (n -pentane/ $\text{Et}_2\text{O} = 20:1$).

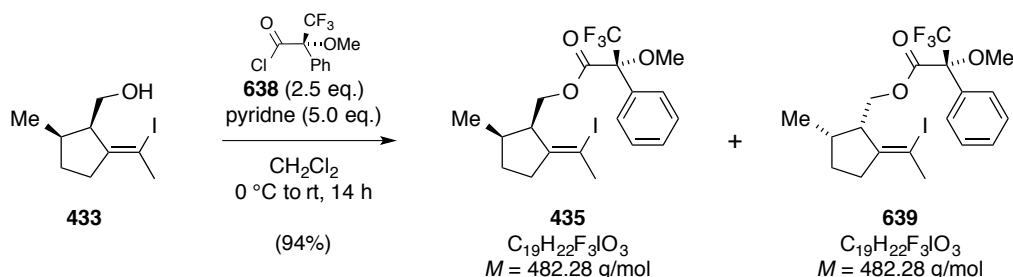
^1H NMR (C_6D_6 , 400 MHz): $\delta = 3.71\text{--}3.65$ (m, 1H), 3.39 (m_C , 1H), 2.42–2.34 (m, 1H), 2.24–2.16 (m, 1H), 2.19 (m_C , 3H), 2.16–2.07 (m, 1H), 1.98–1.88 (m, 1H), 1.76 (m_C , 1H), 1.19 (m_C , 1H), 0.88 (br s, 1H), 0.85 (d, $J = 7.0$ Hz, 3H) ppm.

^{13}C NMR (C_6D_6 , 100 MHz): $\delta = 148.4, 89.6, 63.1, 61.2, 35.7, 32.9, 31.0, 30.1, 20.5$ ppm.

EI-MS for $\text{C}_9\text{H}_{15}\text{IO}^+ [\text{M}]^+$: calcd. 266.0162
 found 266.0157.

IR (ATR): $\tilde{\nu}/\text{cm}^{-1} = 3259, 2952, 2867, 1640, 1455, 1428, 1379, 1312, 1260, 1238, 1209, 1175, 1059, 1027, 1016, 983, 970, 899, 855, 798, 731, 685.$

$[\alpha]_D^{20} = +25.6$ (c 0.25, C_6D_6).

Preparation of Mosher Ester **435**

To a solution of alcohol **433** (10 mg, 38 μmol , 1.0 eq.) in CH_2Cl_2 (1.0 mL) was added pyridine (15 μL , 0.2 mmol, 5.0 eq.) at 0 $^\circ\text{C}$. Subsequently, (*R*)-Mosher's acid chloride (**638**, 18 μL , 94 μmol , 2.5 eq.) was added and the resulting mixture was stirred for 14 hours at room temperature. After the addition of half-saturated aqueous NaHCO_3 solution (10 mL), the mixture was extracted with CH_2Cl_2 ($3 \times 10 \text{ mL}$). The combined organic layers were dried over Na_2SO_4 and concentrated under reduced pressure. ^1H NMR analysis of the crude reaction mixture indicated a diastereomeric mixture of **435**:**639** = 4:1. The crude product was purified *via* flash column chromatography (silica, *n*-pentane/ Et_2O = 19:1) to yield the ester **435** (17 mg, 35 μmol , 94%) as a colorless oil, which retained its content mixture of **435**:**639** = 4:1.

$R_f = 0.74$ (*i*-Hex / EtOAc = 25:1).

^1H NMR (C_6D_6 , 400 MHz, both isomers quoted): δ = 7.72–7.60 (m, 2H, **435**, **639**), 7.12–6.94 (m, 3H, **435**, **639**), 4.60–4.55 (m, 1H, **435**, **639**), 4.24 (dd, J = 11.4, 2.0 Hz, 1H, **639**), 4.12 (dd, J = 11.4, 2.1 Hz, 1H, **435**), 3.43–3.43 (m, 3H, **435**), 3.39–3.37 (m, 3H, **639**), 2.65 (t, J = 7.0 Hz, 1H, **435**), 2.59 (t, J = 7.0 Hz, 1H, **639**), 2.12 (m_C , 3H, **639**), 2.04–2.02 (m, 3H, **435**), 1.80–1.59 (m, 3H, **435**, **639**), 1.58–1.45 (m, 1H, **435**, **639**), 1.22 (m, 1H, **435**, **639**), 0.72 (d, J = 7.0 Hz, 3H, **435**), 0.71 (d, J = 7.0 Hz, 3H, **639**) ppm.

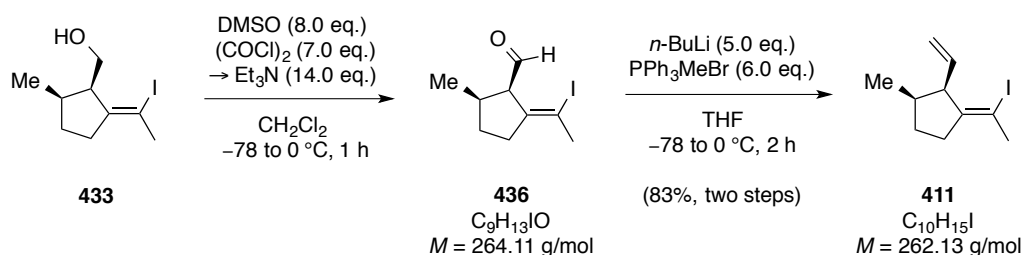
^{13}C NMR (C_6D_6 , 100 MHz, only major isomer quoted): δ = 166.4, 148.2, 133.4, 129.5, 128.5, 127.6, 125.7, 89.8, 85.4–84.6 (m), 64.4, 55.6, 53.2, 36.9, 33.8, 30.4, 30.3, 15.1 ppm.

EI-MS for $\text{C}_{19}\text{H}_{22}\text{F}_3\text{IO}_3^+$ [M] $^+$:	calcd.	482.0560
	found	482.0567.

IR (ATR): $\tilde{\nu}/\text{cm}^{-1}$ = 2952, 2875, 2846, 1747, 1648, 1497, 1451, 1376, 1323, 1271, 1253, 1165, 1120, 1104, 1079, 1058, 1040, 1028, 1012, 1000, 950, 916, 802, 764, 731, 717, 695, 676.

$[\alpha]_D^{20} = -12.4$ (c 0.50, CH_2Cl_2).

Synthesis of Diene 411



To a solution of dry DMSO (850 μL , 12.0 mmol, 8.0 eq.) in CH_2Cl_2 (20 mL) was slowly added oxalyl chloride (5.36 mL, 2.0 M solution in CH_2Cl_2 , 10.5 mmol, 7.0 eq.) at -78°C and the mixture was stirred for 15 min. Then, a solution of alcohol **433** (400 mg, 1.50 mmol, 1.0 eq.) in CH_2Cl_2 (6 mL) was added dropwise and the mixture was stirred for an additional two hours before adding Et_3N (2.93 mL, 21.0 mmol, 14 eq.). The reaction mixture was allowed to warm to 0°C over a period of 60 min and was then quenched by the addition of aqueous phosphate buffer (10 mL, 2 M, $\text{pH} = 6.3$). After separating the phases, the aqueous layer was extracted with *n*-pentane (3×50 mL). The combined organic layers were washed with aqueous phosphate buffer (10 mL, 2 M, $\text{pH} = 6.3$) and dried over Na_2SO_4 . The solvents were carefully removed under reduced pressure and the crude product was purified by quick flash column chromatography (silica, *n*-pentane/ Et_2O = 9:1) to yield aldehyde **436** (392 mg, 1.48 mmol, 99%), which was immediately used in the next step.

$R_f = 0.68$ (*i*-Hex: EtOAc = 20:1).

^1H NMR (C_6D_6 , 400 MHz): δ = 9.55 (dd, J = 3.3, 0.6 Hz, 1H), 3.31 (m, 1H), 2.17–2.07 (m, 1H), 2.10 (s, 3H), 1.79 (m, 2H), 1.63–1.49 (m, 1H), 1.41–1.25 (m, 1H), 0.82 (d, J = 7.0 Hz, 3H) ppm.

^{13}C NMR (C_6D_6 , 100 MHz): δ = 199.6, 146.3, 91.5, 67.0, 38.7, 34.5, 31.1, 30.3, 15.4 ppm.

EI-MS for $\text{C}_9\text{H}_{13}\text{IO}^+$ [M^+]:
calcd. 264.0006.
found 263.9996.

IR (ATR): $\tilde{\nu}/\text{cm}^{-1}$ = 2955, 2872, 2717, 1715, 1647, 1459, 1431, 1378, 1347, 1274, 1213, 1175, 1133, 1119, 1097, 1058, 1009, 971, 945, 899, 789, 722, 676.

$[\alpha]_D^{20} = -20.8$ (c 0.50, *n*-pentane).

To a suspension of Ph_3PMeBr (3.21 g, 9.0 mmol, 6.0 eq.) in THF (50 mL) was slowly added *n*-BuLi (2.80 mL, 2.7 M solution in hexanes, 7.50 mmol, 5.0 eq.) at 0 °C. The resulting orange suspension was allowed to warm to room temperature and stirred for 60 min, before being cooled to –78 °C. A solution of aldehyde **436** (392 mg, 1.48 mmol, 1.0 eq.) in THF (8.5 mL) was then added slowly. The cold bath was replaced by an ice/water bath and the mixture was stirred for additional 60 min at 0 °C, prior to quenching the reaction by the addition of half-saturated aqueous NH_4Cl (30 mL). The layers were separated and the aqueous layer was extracted with *n*-pentane (3 × 50 mL). The combined organic layers were washed with saturated aqueous NaCl (50 mL) and dried over Na_2SO_4 . Having carefully removed the solvents under reduced pressure, the crude product was purified by flash column chromatography (silica, *n*-pentane) to yield diene **411** (326 mg, 1.2 mmol, 83% over the two steps) as a colorless oil.

$R_f = 0.90$ (*i*-Hex:EtOAc = 20:1).

^1H NMR (C_6D_6 , 600 MHz): δ = 5.53–5.39 (m, 1H), 5.22–5.15 (m, 2H), 3.17 (t, J = 7.5 Hz, 1H), 2.20 (q, J = 1.3 Hz, 3H), 2.13–2.08 (m, 1H), 2.00–1.93 (m, 1H), 1.86–1.78 (m, 1H), 1.67–1.62 (m, 1H), 1.33–1.25 (m, 1H), 0.84 (d, J = 6.8 Hz, 3H) ppm.

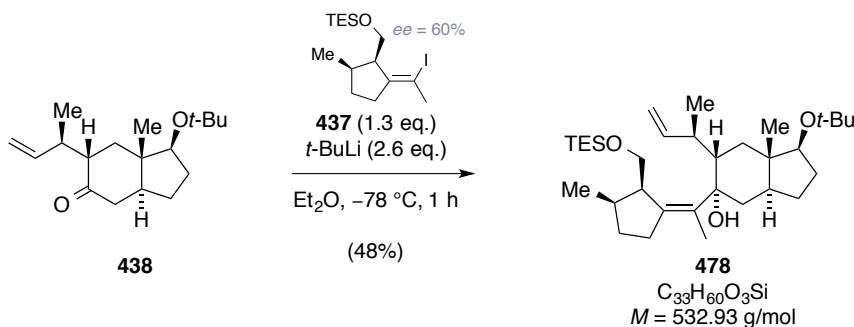
^{13}C NMR (C_6D_6 , 100 MHz): δ = 149.2, 133.6, 117.2, 89.2, 60.2, 38.2, 33.2, 30.3 (2C), 15.7 ppm.

EI-MS for $\text{C}_{10}\text{H}_{15}\text{I}^+$ [M^+]:
calcd. 262.0213.
found 262.0213.

IR (ATR): $\tilde{\nu}/\text{cm}^{-1}$ = 2951, 2909, 2872, 1648, 1457, 1412, 1374, 1282, 1237, 1183, 1137, 1085, 1064, 1009, 987, 962, 941, 895, 875, 817, 790, 741, 724, 667.

$[\alpha]_D^{20} = -48.4$ (c 0.50, C_6D_6).

Synthesis of Allylic Alcohol **478**



To a solution of vinyl iodide **437** (57.1 mg, 0.15 mmol, 1.3 eq.) in Et_2O (6.0 mL) at $-78\text{ }^\circ\text{C}$ was slowly added $t\text{-BuLi}$ (0.17 mL, 1.7 M solution in n -pentane, 0.29 mmol, 2.6 eq.) and the mixture was stirred for one hour at this temperature. Then, a solution of ketone **438** (31.7 mg, 0.11 mmol, 1.0 eq.) in Et_2O (2.5 mL) was added dropwise. The resulting mixture was stirred for one hour at $-78\text{ }^\circ\text{C}$, at which point the reaction was quenched by the addition of half-saturated aqueous NH_4Cl (6 mL). The mixture was allowed to warm to room temperature and the phases were separated. The aqueous layer was extracted with Et_2O ($3 \times 10\text{ mL}$) and the combined organic layers were washed with saturated aqueous NaCl (10 mL). After drying over MgSO_4 , the solvents were evaporated under reduced pressure and the crude product was purified by flash column chromatography (silica, n -pentane: Et_2O = 80:1 to 30:1) to yield the title compound **478** (28.2 mg, 0.53 mmol, 48%) as a colorless oil.

$R_f = 0.27$ (i -Hex: EtOAc = 30:1).

^1H NMR (C_6D_6 , 400 MHz): δ = 6.01 (ddd, J = 17.3, 10.2, 7.2 Hz, 1H), 5.09 (m_C , 1H), 4.98 (m_C , 1H), 4.06 (s, 1H), 3.87–3.73 (m, 2H), 3.52–3.38 (m, 2H), 2.63 (m_C , 1H), 2.45–2.23 (m, 2H), 2.20–2.06 (m, 2H), 1.96–1.84 (m, 2H), 1.77 (dd, J = 12.3, 3.8 Hz, 1H), 1.73–1.67 (m, 4H), 1.66–1.52 (m, 5H), 1.43–1.32 (m, 1H), 1.40 (d, J = 7.1 Hz, 3H), 1.27–1.16 (m, 1H), 1.11 (s, 9H), 1.04–0.97 (m, 12H), 0.91 (d, J = 7.1 Hz, 3H), 0.70–0.60 (m, 6H) ppm.

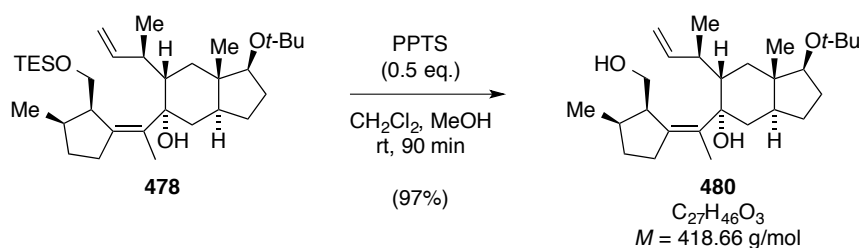
^{13}C NMR (C_6D_6 , 100 MHz): δ = 145.8, 139.0, 136.4, 111.6, 81.2, 80.4, 72.2, 61.8, 47.5, 42.5, 41.0, 39.7, 39.1, 37.8, 36.9, 34.3, 31.6, 31.0, 29.6, 28.5, 25.9, 17.6, 17.3, 15.2, 11.0, 6.6, 4.1 ppm.

EI-MS for $\text{C}_{33}\text{H}_{60}\text{O}_3\text{Si}^+ [\text{M}^+]$:
 calcd. 532.4306
 found 532.4308

IR (ATR): $\tilde{\nu}/\text{cm}^{-1}$ = 3446, 3072, 2955, 2875, 1460, 1361, 1238, 1195, 1130, 1061, 1004, 906, 802, 743.

$[\alpha]_D^{20} = -8.0$ (c 0.20, CH_2Cl_2).

Synthesis of Diol **480**



To a solution of silyl ether **478** (21 mg, 39 μmol , 1.0 eq.) in a mixture of CH_2Cl_2 (11 mL) and MeOH (1.5 mL), PPTS (5.0 mg, 20 μmol , 0.5 eq.) was added in one portion and the resulting mixture was stirred for 90 min at this temperature. The reaction was quenched by the addition of saturated aqueous NaHCO_3 (10 mL). The layers were separated and the aqueous phase was extracted with CH_2Cl_2 (3×10 mL). The combined organic layers were washed with saturated aqueous NaCl (10 mL), and dried over MgSO_4 . After evaporation of the solvents under reduced pressure and subsequent co-evaporation with benzene (3×3 mL), diol **480** (16 mg, 38 μmol , 97%) was obtained as colorless oil, which required no further purification.

$R_f = 0.23$ (i -Hex:EtOAc = 7:1).

^1H NMR (C_6D_6 , 400 MHz): δ = 5.97 (ddd, J = 17.3, 10.3, 6.7 Hz, 1H), 5.08 (m_C , 1H), 4.98 (m_C , 1H), 3.87 (m_C , 1H), 3.51 (m_C , 1H), 3.46 (dd, J = 9.9, 5.2 Hz, 1H), 2.97 (dd, J = 11.8, 9.9 Hz, 1H), 2.59 (m_C , 1H), 2.35–2.07 (m, 4H), 1.99–1.80 (m, 2H), 1.79–1.51 (m, 7H), 1.66

(s, 3H), 1.44–1.30 (m, 2H), 1.27 (d, $J = 7.0$ Hz, 3H), 1.14 (s, 9H), 1.03 (s, 3H), 0.80 (d, $J = 7.0$ Hz, 3H) ppm.

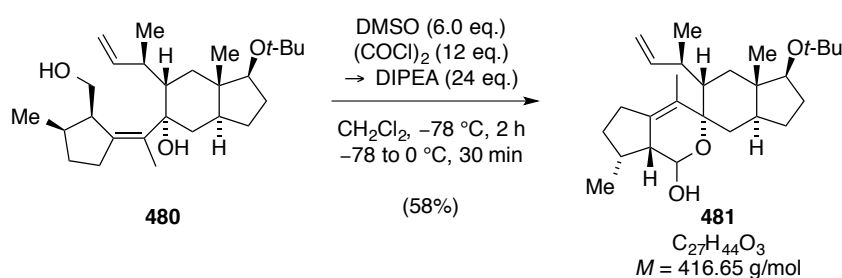
^{13}C NMR (C_6D_6 , 100 MHz): $\delta = 146.1, 138.1, 136.4, 111.6, 81.2, 81.1, 72.2, 59.8, 46.8, 43.0, 41.4, 39.6, 39.4, 38.0, 36.7, 33.9, 32.1, 32.0, 29.9, 29.0, 26.3, 17.9, 16.2, 15.2, 11.5$ ppm.

EI-MS for $\text{C}_{27}\text{H}_{46}\text{O}_3^+ [\text{M}^+]$:
calcd. 418.3441
found 418.3442.

IR (ATR): $\tilde{\nu}/\text{cm}^{-1} = 3279, 2955, 2874, 1461, 1361, 1195, 1129, 1061, 906$.

$[\alpha]_D^{20} = +18.0$ (c 0.50, CH_2Cl_2).

Synthesis of Lactol **481**



To a solution of dry DMSO (24.1 μL , 0.34 mmol, 12 eq.) in CH_2Cl_2 (4.0 mL) was slowly added oxalyl chloride (90.0 μL , 2.0 M solution in CH_2Cl_2 , 0.18 mmol, 6.0 eq.) at $-78\text{ }^\circ\text{C}$ and the resulting mixture was stirred for 15 min. Then, a solution of diol **480** (12.0 mg, 28.7 μmol , 1.0 eq.) in CH_2Cl_2 (1.0 mL) was added and the mixture was stirred for two hours. Subsequently, DIPEA (125 μL , 696 μmol , 24 eq.) was added and the mixture was allowed to warm to $0\text{ }^\circ\text{C}$ and. After being stirred for 30 min, the reaction was quenched by the addition of H_2O (5 mL) and was then diluted with CH_2Cl_2 (5 mL). The layers were separated and the aqueous phase was extracted with CH_2Cl_2 (3×7 mL). The combined organic layers were washed with saturated aqueous NaCl (10 mL) and dried over MgSO_4 . Having evaporated the solvent under reduced pressure, the crude product was purified by flash column chromatography (silica, $i\text{-Hex}:\text{EtOAc} = 7:1$) to yield lactol **481** (7.0 mg, 17 μmol , 58%) as a colorless oil and as single diastereomer. The relative stereochemistry at the lactol moiety was not elucidated.

$R_f = 0.23$ (*i*-Hex:EtOAc = 7:1).

^1H NMR (C_6D_6 , 400 MHz): $\delta = 5.83$ (m_C , 1H), 4.97 (m_C , 1H), 4.89 (m_C , 1H), 4.81 (dd, $J = 7.7$ Hz, 1H), 3.51 (m_C , 1H), 2.43 (m_C , 1H), 2.32 (m_C , 1H), 2.20–2.05 (m, 2H), 2.01–1.89 (m, 3H), 1.76–1.43 (m, 11H), 1.38–1.25 (m, 2H), 1.19 (d, $J = 6.9$ Hz, 3H), 1.13 (s, 9H), 0.98 (s, 3H), 0.77 (d, $J = 7.1$ Hz, 3H) ppm.

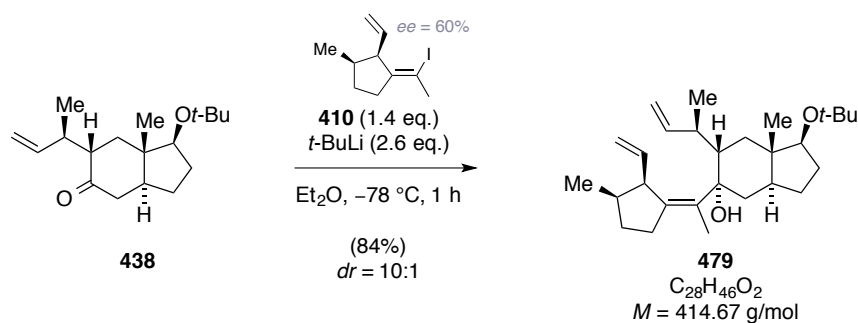
^{13}C NMR (C_6D_6 , 100 MHz): $\delta = 145.4$, 134.9, 130.4, 111.9, 94.5, 84.2, 81.2, 72.2, 50.4, 42.9, 40.8, 39.4, 39.1, 36.7, 34.9, 34.1, 32.5, 32.0, 29.0, 27.6, 26.2, 15.7, 15.3, 14.3, 11.3 ppm.

EI-MS for $\text{C}_{27}\text{H}_{44}\text{O}_3^+ [\text{M}^+]$:
 calcd. 416.3285
 found 416.3291.

IR (ATR): $\tilde{\nu}/\text{cm}^{-1} = 3432$, 3074, 2969, 2955, 2869, 1460, 1388, 1375, 1361, 1254, 1192, 1132, 1061, 907.

$[\alpha]_D^{20} = +12.8$ (c 0.25, CH_2Cl_2).

Synthesis of Triene 479



To a solution of vinyl iodide **410** (48.0 mg, 18.4 μmol , 1.4 eq.) in Et_2O (3.4 mL) was added $t\text{-BuLi}$ (195 μL , 1.8 M solution in *n*-pentane, 34.2 μmol , 2.6 eq.) at -78°C and the resulting mixture was stirred for 45 min. Then, a solution of ketone **438** (36.6 mg, 13.2 μmol , 1.0 eq.) in Et_2O (1.6 mL) was added dropwise over a period of 20 min. The reaction was stirred for an additional 90 min and was then quenched by the addition of half-saturated aqueous NH_4Cl (8 mL). The mixture was allowed to warm to room temperature and was extracted with diethyl ether (3×25 mL). The combined organic layers were washed with saturated aqueous NaCl (20 mL) and dried over Na_2SO_4 . The solvents were evaporated under reduced

pressure and the crude product was purified by flash column chromatography (silica, *n*-pentane:Et₂O = 98:1) to yield the title compound (**479**, 46.0 mg, 11.1 μmol, 84%) as a colorless solid and as an inseparable mixture 10:1 mixture of diastereomers, originating from the moderate enantiomeric excess of vinyl iodide **410**.

Crystals suitable for X-ray analysis were grown from slow evaporation of a solution of triene **479** in MeOH/Et₂O/*n*-pentane.

$R_f = 0.69$ (*i*-Hex:EtOAc = 10:1).

Melting point = 113.5–114.5 °C (MeOH/*n*-pentane/Et₂O).

¹H NMR (C₆D₆, 400 MHz, only major isomer quoted): δ = 5.87 (m_C, 1H), 5.77 (m_C, 1H), 5.09–4.98 (m, 3H), 4.93 (m_C, 1H), 4.04 (m_C, 1H), 3.46 (m_C, 1H), 2.43–2.36 (m, 2H), 2.25–2.19 (m, 2H), 2.15–2.07 (m, 2H), 1.98–1.80 (m, 2H), 1.71–1.48 (m, 10H), 1.37–1.29 (m, 1H), 1.21–1.10 (m, 13H), 0.98 (s, 3H), 0.90 (d, *J* = 6.9 Hz, 3H) ppm.

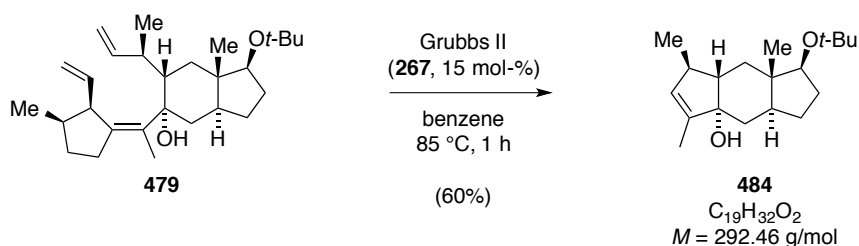
¹³C NMR (C₆D₆, 100 MHz, only major isomer quoted): δ = 145.5, 141.4, 139.6, 134.5, 115.7, 112.0, 82.5, 81.2, 72.2, 51.5, 43.0, 41.2, 40.0, 39.0, 38.0, 36.9, 33.9, 33.2, 32.0, 30.1, 29.0, 26.2, 17.7, 16.5, 16.2, 11.4 ppm.

EI-MS for C ₂₈ H ₄₆ O ₂ ⁺ [M ⁺]:	calcd.	414.3492
	found	414.3477.

IR (ATR): $\tilde{\nu}/\text{cm}^{-1}$ = 3583, 3073, 2970, 2955, 2870, 1636, 1459, 1388, 1375, 1361, 1254, 1197, 1127, 1063, 1001, 907.

Since the product was isolated as a mixture of diastereomers, the optical rotation of the product mixture was not determined.

Synthesis of Tricycle 484



To a solution of triene **479** (4.0 mg, 9.7 μmol , 1.0 eq.) in degassed benzene (12 mL) was added Grubbs second-generation catalyst (**267**, 1.2 mg, 1.5 μmol , 15 mol-%). The mixture was placed in an oil bath (pre-heated to 85 $^\circ\text{C}$) and stirred at this temperature for one hour, before being allowed to cool to room temperature. The solvent was evaporated under reduced pressure and the obtained crude product was purified by flash column chromatography (silica, deactivated with NEt_3 , n -pentane: Et_2O = 24:1 to 23:2) to yield the cyclized product **484** (1.7 mg, 5.8 μmol , 60%) as a colorless oil.

Note: This material decomposes in CDCl_3 by time. Measurement in C_6D_6 is recommended.

$R_f = 0.39$ (i -Hex: EtOAc = 50:3).

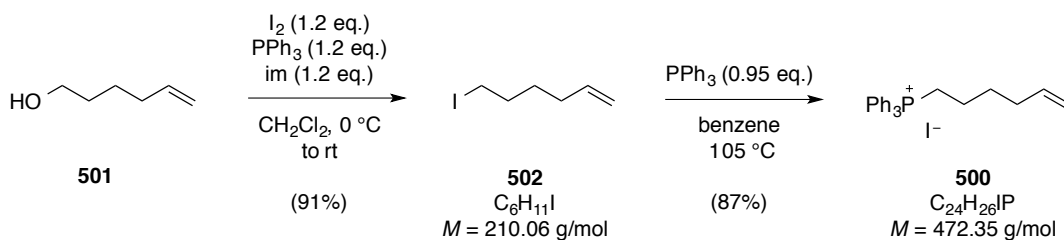
^1H NMR (C_6D_6 , 400 MHz): δ = 5.24–5.23 (m_C , 1H), 3.48 (dd, J = 8.9, 7.1 Hz, 1H), 2.31–2.15 (m, 2H), 1.97–1.88 (m, 1H), 1.79 (dd, J = 11.0, 2.4 Hz, 1H), 1.70 (dd, J = 12.2, 3.5 Hz, 1H), 1.67–1.60 (m, 1H), 1.63 (dd, J = 2.4, 1.7 Hz, 3H), 1.43–1.20 (m, 4H), 1.12 (s, 9H), 0.97–0.93 (m, 6H), 0.47 (s, br, 1H) ppm.

^{13}C NMR (C_6D_6 , 100 MHz): δ = 146.2, 135.4, 83.4, 80.3, 72.2, 54.2, 44.2, 39.8, 38.7, 34.0, 33.7, 32.5, 29.0, 26.1, 17.2, 12.3, 12.0 ppm.

EI-MS for $\text{C}_{19}\text{H}_{32}\text{O}_2^+ [\text{M}^+]$:	calcd.	292.2397
	found	292.2393.

IR (ATR): $\tilde{\nu}/\text{cm}^{-1}$ = 3472, 2953, 2923, 2868, 2851, 1740, 1444, 1387, 1373, 1361, 1260, 1196, 1117, 1094, 1063, 1033, 998, 980, 946, 924, 915, 863, 849, 802, 729.

$[\alpha]_D^{20} = +40.0$ (c 0.10, CH_2Cl_2).

Synthesis of Wittig Salt **500**

To a solution of PPh_3 (15.7 g, 59.9 mmol, 1.2 eq.) and imidazole (4.08 g, 59.9 mmol, 1.2 eq.) in CH_2Cl_2 (100 mL) was added I_2 (15.2 g, 59.9 mmol, 1.2 eq.) in portions at 0 °C over 10 min and the resulting solution was stirred for an additional 15 min. Subsequently, 5-hexen-1-ol (**501**, 5.00 g, 49.9 mmol, 1.0 eq.) was added dropwise over a period of 5 min. The resulting mixture was warmed to room temperature and stirred for 2.5 hours. After filtration over a pad of Celite[®] (*n*-pentane washings) the solvents were removed under reduced pressure (min. 500 mbar). The crude product was purified by flash column chromatography (silica, *n*-pentane) and the product containing fractions were carefully concentrated under reduced pressure (min. 100 mbar) to yield iodide **502** (9.54 g, 4.54 mmol, 91%) as colorless oil.

$R_f = 0.92$ (*n*-pentane:Et₂O = 25:1).

^1H NMR (C_6D_6 , 400 MHz): $\delta = 5.58$ (ddt, $J = 17.6, 9.7, 6.7$ Hz, 1H), 4.97–4.84 (m, 2H), 2.68 (t, $J = 7.0$ Hz, 2H), 1.75 (m_C, 2H), 1.47–1.34 (m, 2H), 1.19–1.08 (m, 2H) ppm.

^{13}C NMR (C_6D_6 , 100 MHz): $\delta = 138.3, 115.1, 33.1, 32.9, 29.8, 6.5$ ppm.

EI-MS for $\text{C}_6\text{H}_{11}\text{I}^+ [\text{M}^+]$: calcd. 209.9900

found 209.9904.

IR (ATR): $\tilde{\nu}/\text{cm}^{-1} = 3075, 2997, 2975, 2930, 2854, 1930, 1640, 1453, 1426, 1349, 1281, 1246, 1214, 1173, 1080, 988, 910, 854, 788, 735, 724$.

To a solution of PPh_3 (3.56 g, 13.6 mmol, 0.95 eq.) in benzene (20 mL) was added iodide **502** (3.00 g, 14.3 mmol, 1.0 eq.) and the mixture was heated in a pressure tube at 105 °C for 11 hours. After cooling to room temperature, the precipitate was filtered off and washed with benzene. Recrystallization (CH_2Cl_2 /benzene) afforded Wittig salt **500** (5.58 g, 11.8 mmol, 87%) as colorless solid.

Melting point = 167.3–169.2 °C (CH₂Cl₂/benzene).

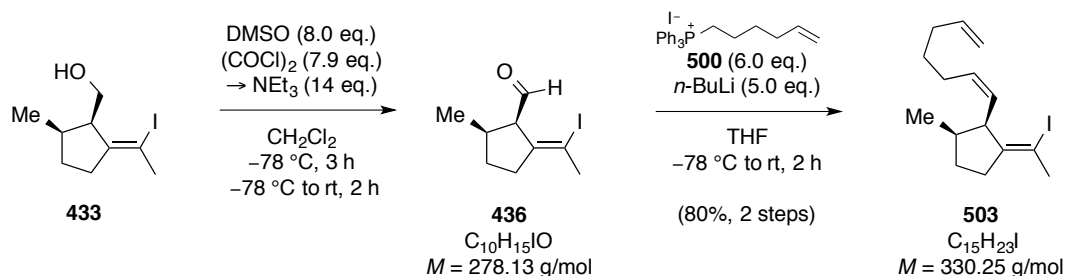
¹H NMR (CDCl₃, 400 MHz): δ = 7.85–7.73 (m, 9H), 7.74–7.63 (m, 6H), 5.65 (ddt, J = 16.9, 10.2, 6.7 Hz, 1H), 4.97–4.81 (m, 2H), 3.63 (m_C, 2H), 2.04 (q, J = 7.0 Hz, 2H), 1.80–1.69 (m, 2H), 1.69–1.53 (m, 2H) ppm.

¹³C NMR (CDCl₃, 100 MHz): δ = 137.5, 135.2, 135.2, 133.7, 133.6, 130.7, 130.5, 118.4, 117.6, 115.4, 32.9, 29.3, 29.1, 23.2, 22.7, 21.8, 21.7 ppm.

ESI-MS for C₂₄H₂₆P⁺ [M⁺]: calcd. 345.17666
 found 345.17619.

IR (ATR): $\tilde{\nu}/\text{cm}^{-1}$ = 3040, 3010, 2989, 2889, 2863, 2798, 1640, 1585, 1485, 1438, 1413, 1344, 1332, 1316, 1261, 1242, 1191, 1171, 1162, 1113, 1027, 995, 918, 888, 856, 810, 788, 761, 744, 737, 722, 699, 688.

Synthesis of Triene 503



To a solution of dry DMSO (63.9 μL , 900 μmol , 8.0 eq.) in CH₂Cl₂ (1.5 mL) was slowly added oxalyl chloride (394 μL , 2.0 M solution in CH₂Cl₂, 788 μmol , 7.9 eq.) at -78°C and the mixture was stirred for 15 min. Then, a solution of alcohol **433** (30.0 mg, 107 μmol , 1.0 eq.) in CH₂Cl₂ (0.3 mL) was added dropwise and the reaction was stirred for an additional 2 hours before adding Et₃N (220 μL , 1.60 mmol, 14 eq.). The solution was allowed to warm to 0°C over a period of 60 min and was then quenched by the addition of aqueous phosphate buffer (5.0 mL, 2 M, pH = 6.3). The layers were separated, the aqueous layer was extracted with *n*-pentane (3 \times 50 mL) and the combined organic layers were washed with saturated aqueous phosphate buffer (10 mL, 2 M, pH = 6.3). After drying over Na₂SO₄, the solvents were carefully removed under reduced pressure and the crude product was purified by quick

flash column chromatography (silica, *n*-pentane:Et₂O = 9:1) to yield aldehyde **436** as a yellow oil, which was immediately used in the next step.

To a suspension of Wittig salt **500** (320 mg, 678 μ mol, 6.0 eq.) in THF (4 mL) was slowly added *n*-BuLi (196 μ L, 2.86 M solution in hexanes, 560 μ mol, 5.0 eq.) at 0 °C. The resulting red solution was allowed to warm to room temperature and stirred for 60 min, before being cooled to -78 °C. Then, a solution of aldehyde **436** (assumed 110 μ mol, 1.0 eq.) in THF (1 mL) was added slowly. The cold bath was replaced by an ice/water bath and the mixture was stirred for additional 60 min at 0 °C, prior to quenching the reaction by the addition of half-saturated aqueous NH₄Cl (15 mL). The layers were separated and the aqueous phase was extracted with *n*-pentane (3 \times 50 mL). The combined organic layers were washed with saturated aqueous NaCl (25 mL) and dried over Na₂SO₄. Having carefully removed the solvents under reduced pressure, the crude product was purified by flash column chromatography (silica, *n*-pentane) to yield triene **503** (29.9 mg, 90.4 μ mol, 80% over two steps) as colorless oil and as inseparable mixture of double bond isomers (*E*:*Z* = 19:1).

R_f = 0.95 (*i*-Hex:EtOAc = 20:1).

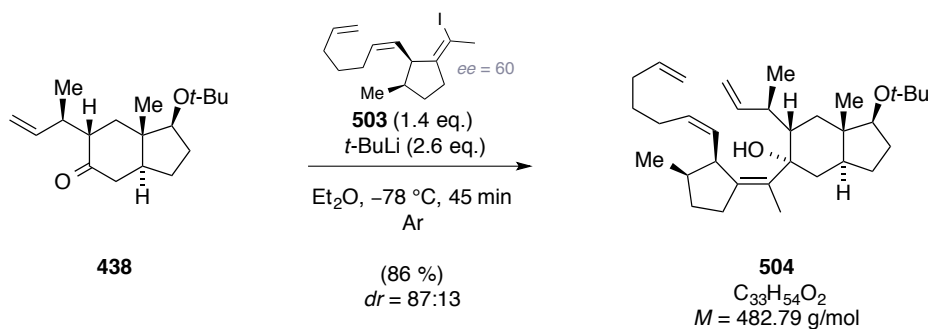
¹H NMR (C₆D₆, 400 MHz, only major isomer quoted): δ = 5.83 (ddt, *J* = 16.9, 10.1, 6.6 Hz, 1H), 5.59–5.48 (m, 1H), 5.16–4.89 (m, 3H), 3.45 (dd, *J* = 10.9, 6.8 Hz, 1H), 2.42–2.27 (m, 1H), 2.26–1.93 (m, 5H), 2.20 (m_C, 3 H), 1.88 (m_C, 1H), 1.75–1.39 (m, 3H), 1.41–1.21 (m, 1H), 0.88 (d, *J* = 6.8 Hz, 3H) ppm.

¹³C NMR (C₆D₆, 100 MHz, only major isomer quoted): δ = 150.8, 139.1, 131.5, 125.0, 114.8, 87.9, 54.7, 38.8, 34.2, 33.5, 30.5, 30.4, 29.7, 28.3, 15.9 ppm.

EI-MS for C ₁₅ H ₂₃ I ⁺ [M ⁺]:	calcd.	330.0839.
	found	330.0846.

IR (ATR): $\tilde{\nu}$ /cm⁻¹ = 3073, 3003, 2923, 2868, 1640, 1451, 1431, 1374, 1347, 1311, 1285, 1247, 1176, 1130, 1096, 1055, 986, 964, 908, 869, 799, 728, 675.

$[\alpha]_D^{20}$ = -35.6 (*c* 0.50, CH₂Cl₂).

Synthesis of Tetraene **504**

To a solution of alkenyl iodide **503** (20.0 mg, 60.5 μmol , 1.4 eq.) in Et_2O (1.4 mL) at $-78\text{ }^\circ\text{C}$ was added $t\text{-BuLi}$ (68.0 μL , 1.65 M solution in $n\text{-pentane}$, 112 μmol , 2.6 eq.) and the resulting mixture was stirred for 45 min. Then, a solution of ketone **438** (12 mg, 43.2 μmol , 1.0 eq.) in Et_2O (1.0 mL) was added dropwise. The mixture was stirred for an additional 45 min and the reaction was quenched by the addition of half-saturated aqueous NH_4Cl (10 mL). The mixture was allowed to warm to room temperature and was extracted with Et_2O ($3 \times 25\text{ mL}$). The combined organic layers were washed with saturated aqueous NaCl (10 mL) and dried over Na_2SO_4 . The solvents were evaporated under reduced pressure and the crude product was purified by flash column chromatography (silica, $n\text{-pentane}:\text{Et}_2\text{O} = 200:1$ to $100:1$) to yield the title compound (**504**, 17.9 mg, 37.1 μmol , 86%) as a colorless solid and as an inseparable 87:13 mixture of diastereomers, originating from the moderate enantiomeric excess of vinyl iodide **503**.

Crystals suitable for X-ray analysis were grown by slow evaporation of a solution of tetraene **504** in $n\text{-pentane}/\text{MeOH}$.

$R_f = 0.72$ ($i\text{-Hex}:\text{EtOAc} = 25:1$).

Melting point = $86.2\text{--}88.7\text{ }^\circ\text{C}$ ($n\text{-pentane}/\text{MeOH}$).

^1H NMR (C_6D_6 , 400 MHz, only major isomer quoted): $\delta = 5.89$ (ddt, $J = 17.2, 10.3, 6.9\text{ Hz}$, 1H), 5.74 (ddt, $J = 16.9, 10.1, 6.7\text{ Hz}$, 1H), 5.47–5.37 (m, 1H), 5.28–5.14 (m, 1H), 5.11–4.88 (m, 4H), 4.35 (dd, $J = 10.8, 6.6\text{ Hz}$, 1H), 3.41 (dd, $J = 8.9, 7.3\text{ Hz}$, 1H), 2.51–2.38 (m, 2H), 2.36–2.04 (m, 6H), 2.04–1.81 (m, 4H), 1.78–1.63 (m, 3H), 1.66–1.39 (m, 6H), 1.59 (s, 3H), 1.40–1.13 (m, 2H), 1.18 (d, $J = 6.9\text{ Hz}$, 3H), 1.10 (s, 9H), 1.03–0.89 (m, 6H) ppm.

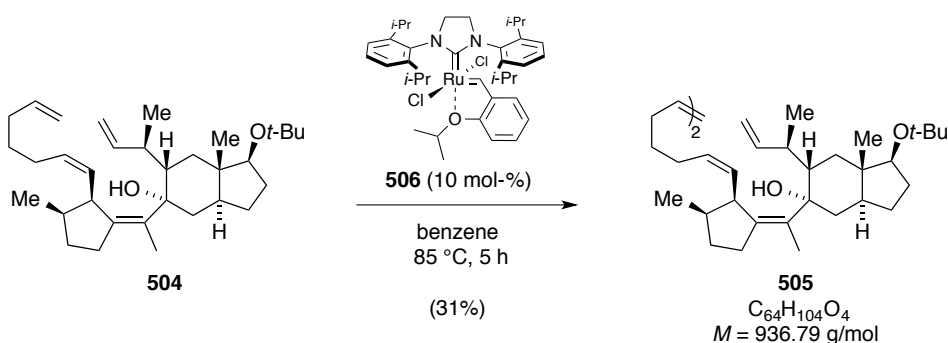
^{13}C NMR (C_6D_6 , 100 MHz, only major isomer quoted): δ = 145.6, 141.1, 138.8, 133.4, 131.1, 130.6, 114.8, 112.0, 82.4, 81.1, 72.2, 45.7, 43.0, 41.1, 40.9, 38.9, 38.1, 36.9, 34.0 (2C), 33.3, 32.0, 30.7, 29.5, 28.9, 27.8, 26.2, 17.9, 16.6, 16.2, 11.4 ppm.

EI-MS for $\text{C}_{33}\text{H}_{54}\text{O}_2^+$ [M^+]:
calcd. 482.4118
found 482.4130.

IR (ATR): $\tilde{\nu}/\text{cm}^{-1}$ = 3564, 3080, 2969, 2927, 2869, 1633, 1454, 1409, 1386, 1360, 1265, 1252, 1195, 1144, 1124, 1095, 1063, 1039, 1011, 1000, 945, 921, 907, 874, 865, 806, 722, 695.

Since the product was isolated as a mixture of diastereomers, the optical rotation of the product mixture was not determined.

Synthesis of Homodimer **505**



Tetraene **504** (2.0 mg, 4.14 μmol , 1.0 eq.) was dissolved in benzene (6.7 mL) and the resulting solution was degassed ($3 \times$ freeze-pump-thaw). Then, catalyst **506** (0.3 mg, 0.41 μmol , 5 mol-%) was added and the mixture was heated to 85 $^\circ\text{C}$ for 3 hours. After addition of a second batch of catalyst **506** (0.3 mg, 0.41 μmol , 5 mol-%), heating was continued for another 2 hours, before the reaction mixture was cooled to room temperature and concentrated *in vacuo*. The crude product was purified by flash column chromatography (silica, *n*-pentane:Et₂O = 500:1) to yield the title compound (**505**, 1.2 mg, 1.28 μmol , 31%) as a colorless wax and as a single diastereomer.

R_f = 0.66 (*i*-Hex:EtOAc = 25:1).

^1H NMR (C_6D_6 , 400 MHz): δ = 5.89 (ddd, J = 17.1, 10.3, 6.8 Hz, 2H), 5.51–5.37 (m, 4H), 5.29–5.17 (m, 2H), 5.11–4.93 (m, 4H), 4.39–4.33 (m, 2H), 3.50–3.38 (m, 2H), 2.47–2.43 (m, 2H), 2.37–2.22 (m, 8H), 2.16–2.07 (m, 4H), 2.04–1.87 (m, 8H), 1.76–1.65 (m, 6H), 1.64–1.50 (m, 8H), 1.59 (s, 6H), 1.50–1.42 (m, 4H), 1.41–1.25 (m, 4H), 1.20 (d, J = 7.0 Hz, 6H), 1.14–1.11 (m, 18H), 1.00 (s, 12H) ppm.

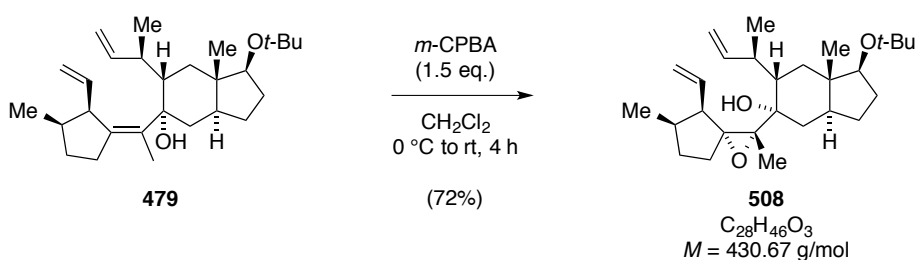
^{13}C NMR (C_6D_6 , 100 MHz): δ = 145.6, 141.2, 133.3, 131.3, 130.6, 130.5, 112.0, 82.4, 81.1, 72.2, 45.7, 43.0, 41.1, 41.0, 38.9, 38.7, 38.1, 36.8, 33.9, 33.3, 32.9, 32.0, 30.7, 30.2, 29.0, 27.9, 26.2, 18.0, 16.6, 16.3, 11.4 ppm.

ESI-MS for $\text{C}_{64}\text{H}_{104}\text{ClO}_4^-$ [(M+Cl) $^-$]:
 calcd. 971.7623
 found 971.7619.

IR (ATR): $\tilde{\nu}/\text{cm}^{-1}$ = 3567, 3075, 2955, 2870, 1457, 1388, 1373, 1361, 1318, 1261, 1231, 1196, 1127, 1098, 1062, 1008, 970, 945, 905, 875, 856, 802, 734, 663.

$[\alpha]_D^{20}$ = -101 (c 0.08, C_6D_6).

Synthesis of Epoxide **508**



To a solution of triene **479** (29 mg, 70 μmol , 1.0 eq.) in CH_2Cl_2 (8.1 mL) at 0 $^\circ\text{C}$ was slowly added *m*-CPBA (524 μL , 0.2 M solution in CH_2Cl_2 , 105 μmol , 1.5 eq.). The mixture was stirred for 45 min at this temperature and an additional 3 hours at room temperature. The reaction was quenched by the addition of saturated aqueous NaHCO_3 (10 mL) and the layers were separated. The aqueous phase was extracted with CH_2Cl_2 ($3 \times 10 \text{ mL}$) and the combined organic layers were consecutively washed with saturated aqueous K_2CO_3 (10 mL), saturated aqueous NaCl (10 mL) and dried over Na_2SO_4 . Having evaporated the solvents under reduced pressure, the crude product was purified by flash column chromatography (silica,

n-pentane:Et₂O = 20:1 to 10:1) to yield epoxide **508** (22 mg, 50 μmol, 72%) as colorless solid and as single diastereomer.

Crystals suitable for X-ray analysis were grown from slow evaporation of a solution of epoxide **508** in *n*-pentane/Et₂O/MeOH.

R_f = 0.31 (*i*-Hex:EtOAc = 10:1).

Melting point = 132.2–135.3 °C (*n*-pentane/Et₂O/MeOH).

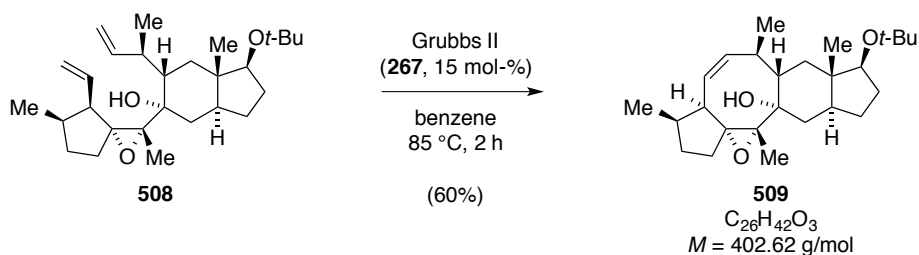
¹H NMR (C₆D₆, 400 MHz): δ = 5.85 (m_C, 1H), 5.41 (m_C, 1H), 5.07–4.91 (m, 4H), 3.41 (m_C, 1H), 2.74 (dd, *J* = 10.2, 5.6 Hz, 1H), 2.49–2.36 (m, 2H), 2.10–2.01 (m, 1H), 1.98–1.73 (m, 5H), 1.73–1.55 (m, 4H), 1.53–1.38 (m, 2H), 1.32 (m_C, 1H), 1.24 (s, 3H), 1.12 (s, 9H), 1.08 (d, *J* = 6.9 Hz, 3H), 1.10–1.02 (m, 1H), 0.92 (s, 3H), 0.91 (d, *J* = 7.0 Hz, 3H) ppm.

¹³C NMR (C₆D₆, 100 MHz): δ = 145.4, 134.8, 118.0, 111.8, 81.1, 79.7, 77.8, 72.2, 69.5, 55.3, 42.9, 39.4, 38.7, 38.5, 35.6, 35.3, 34.0, 33.0, 31.9, 28.9, 28.3, 26.1, 19.9, 17.2, 16.3, 11.3 ppm.

EI-MS for C ₂₈ H ₄₆ O ₃ ⁺ [M ⁺]:	calcd.	430.3441
	found	430.3434.

IR (ATR): $\tilde{\nu}/\text{cm}^{-1}$ = 3562, 3478, 2073, 2969, 2870, 1636, 1462, 1374, 1361, 1197, 1130, 1064, 992, 907.

$[\alpha]_D^{20}$ = +36.4 (*c* 0.50, C₆D₆).

Synthesis of Tetracycle **509**

To a solution of diene **508** (17 mg, 40 μmol , 1.0 eq.) in degassed benzene (48 mL) was added Grubbs second-generation catalyst (**267**, 5.0 mg, 5.9 μmol , 15 mol-%). The mixture was placed in an oil bath (pre-heated to 85 $^\circ\text{C}$) and stirred for 2 hours, before being allowed to cool to room temperature. The solvent was evaporated under reduced pressure and the obtained crude product was purified by flash column chromatography (silica, *n*-pentane:Et₂O = 20:1) to yield the cyclized product (**509**, 15.6 mg, 39 μmol , 98%) as a colorless, fluffy solid.

Note: This material decomposes in CDCl₃ by time. Measurement in C₆D₆ is recommended.

$R_f = 0.48$ (*i*-Hex:EtOAc = 10:1).

Melting point = 54.0–55.5 $^\circ\text{C}$ (Et₂O/*n*-pentane).

¹H NMR (CDCl₃, 400 MHz): δ = 5.44 (dd, J = 10.9, 7.8 Hz, 1H), 5.34 (m_C, 1H), 3.45 (m_C, 1H), 3.19 (m_C, 1H), 2.89 (m_C, 1H), 2.73 (s, 1H), 2.40–2.31 (m, 1H), 2.27 (m_C, 1H), 1.99–1.83 (m, 2H), 1.89 (dd, J = 13.0, 13.0 Hz, 1H), 1.80 (dd, J = 12.7, 5.1 Hz, 1H), 1.75–1.58 (m, 2H), 1.56–1.40 (m, 4H), 1.40–1.22 (m, 2H), 1.26 (s, 3H), 1.14 (s, 9H), 1.03 (m_C, 1H), 1.01 (d, J = 6.8 Hz, 3H), 0.94 (d, J = 6.9 Hz, 3H), 0.69 (s, 3H) ppm.

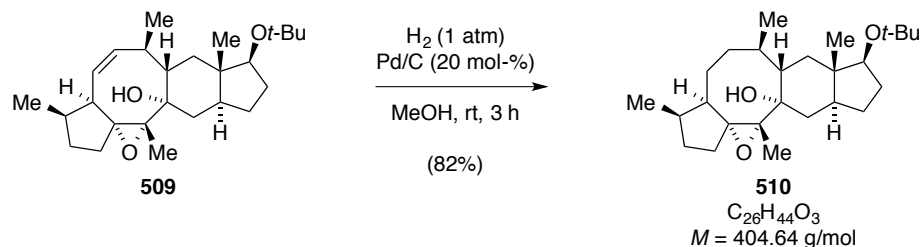
¹³C NMR (CDCl₃, 100 MHz): δ = 141.1, 128.0, 84.6, 81.1, 76.1, 72.5, 66.8, 46.4, 42.0, 40.5, 39.8, 38.4, 37.7, 35.0, 33.0, 32.4, 31.2, 28.9, 27.5, 25.5, 20.9, 17.0, 16.4, 10.7 ppm.

EI-MS for C ₂₆ H ₄₂ O ₃ ⁺ [M ⁺]:	calcd.	402.3128
	found	402.3127.

IR (ATR): $\tilde{\nu}/\text{cm}^{-1}$ = 3480, 3007, 2968, 2871, 1460, 1376, 1361, 1235, 1196, 1150, 1134, 1092, 1072, 1007, 987.

$$[\alpha]_D^{20} = +1.2 \text{ (} c \text{ 0.33, CH}_2\text{Cl}_2\text{)}.$$

Synthesis of Tetracycle **510**



To a solution of alkene **509** (3.3 mg, 8.2 μmol , 1.0 eq.) in MeOH (2.5 mL) was added Pd/C (10 wt-% Pd, 2.1 mg, 1.6 μmol , 20 mol-%) and the resulting suspension was stirred under an atmosphere of H_2 for 3 hours. The mixture was filtered over a pad of Celite[®] (Et_2O washings) and the solvent was evaporated under reduced pressure. The crude product was purified by flash column chromatography (silica, n -pentane: Et_2O = 15:1) to yield tetracycle **510** (2.7 mg, 6.7 μmol , 82%) as colorless oil.

*Note: Substrate **509** and product **510** behaved co-polar at TLC analysis.*

$R_f = 0.48$ (i -Hex: EtOAc = 10:1).

^1H NMR (C_6D_6 , 400 MHz): δ = 3.36 (m_C, 1H), 2.68–2.58 (m, 1H), 2.47–2.37 (m, 1H), 2.31 (s, 1H), 2.03–1.69 (m, 7H), 1.67–1.57 (m, 1H), 1.55–1.37 (m, 4H), 1.37–1.17 (m, 5H), 1.19 (s, 3H), 1.16–1.05 (m, 1H), 1.11 (s, 9H), 1.00 (d, J = 7.1 Hz, 3H), 0.99–0.89 (m, 1H), 0.92 (s, 3H), 0.87 (d, J = 6.8 Hz, 3H) ppm.

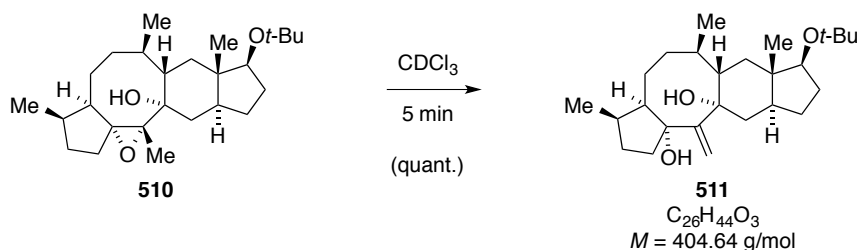
^{13}C NMR (C_6D_6 , 100 MHz): δ = 81.1, 78.6, 75.2, 72.2, 67.2, 43.0, 42.8, 42.6, 40.0, 38.0, 37.8, 36.4, 35.5, 32.6, 32.5, 31.9, 28.9, 27.0, 25.9, 25.2, 23.5, 16.4, 15.2, 11.4 ppm.

EI-MS for $\text{C}_{26}\text{H}_{44}\text{O}_3^+$ [M^+]:	calcd.	404.3285
	found	404.3292.

IR (ATR): $\tilde{\nu}/\text{cm}^{-1}$ = 3489, 2969, 2872, 1461, 1374, 1361, 1197, 1067.

$$[\alpha]_D^{20} = +28.0 \text{ (} c \text{ 0.10, CH}_2\text{Cl}_2\text{)}.$$

Synthesis of Diol **511**

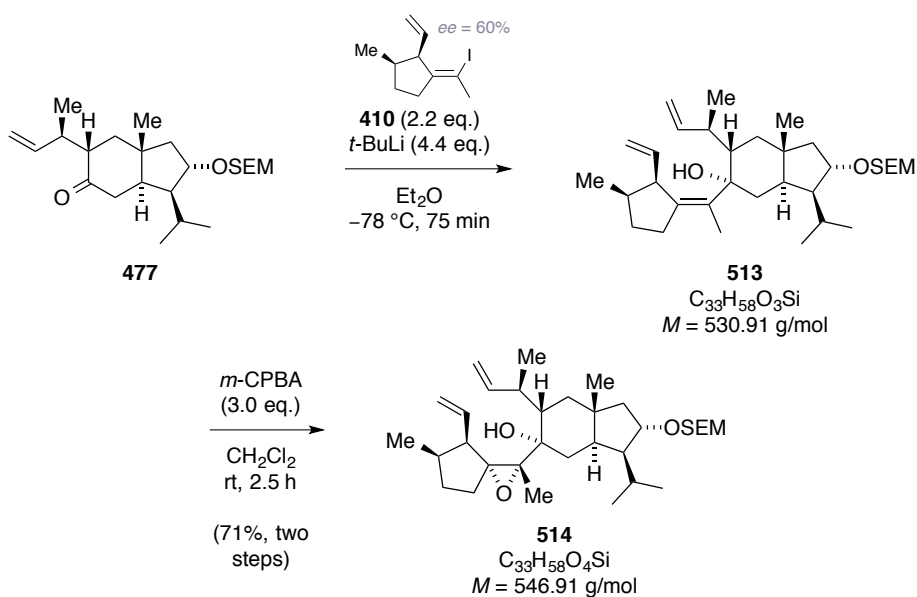


A sample of epoxide **510** was dissolved in CDCl_3 and NMR spectra were recorded immediately. The NMR analysis showed complete conversion to tetracycle **511**. This compound slowly reacted further in the NMR solvent to a mixture of unknown compounds. Thus, no further analytical data could be determined.

^1H NMR (CDCl_3 , 400 MHz): $\delta = 5.18$ (s, 1H), 4.98 (s, 1H), 3.46 (m_C , 1H), 2.82–2.64 (m, 2H), 2.31 (m_C , 1H), 2.09 (m_C , 1H), 1.97–1.85 (m, 3H), 1.85–1.70 (m, 3H), 1.68–1.61 (m, 1H), 1.59–1.39 (m, 7H), 1.38–1.18 (m, 2H), 1.17–1.08 (m, 1H), 1.14 (s, 9H), 1.05–0.98 (m, 1H), 0.96–0.85 (m, 1H), 0.93 (d, $J = 6.7 \text{ Hz}$, 3H), 0.88 (d, $J = 6.9 \text{ Hz}$, 3H), 0.78 (s, 3H) ppm.

^{13}C NMR (CDCl_3 , 100 MHz): $\delta = 160.6$, 110.5, 87.9, 80.9, 79.4, 72.4, 51.7, 46.5, 45.2, 42.6, 38.7, 38.5, 35.2, 34.5(2), 31.5, 30.7, 28.9, 27.4, 25.5, 24.8, 23.5, 15.7, 11.1 ppm.

Synthesis of Epoxide **514**



To a solution of vinyl iodide **410** (56 mg, 0.21 mmol, 2.2 eq.) in Et_2O (3.6 mL) was slowly added $t\text{-BuLi}$ (0.25 mL, 1.7 M solution in $n\text{-pentane}$, 0.42 mmol, 4.4 eq.) at -78°C and the

resulting mixture was stirred for 45 min at this temperature. Then, a solution of ketone **477** (38 mg, 0.10 mmol, 1.0 eq.) in Et₂O (1.4 mL) was added within 30 min and stirring was continued for an additional 45 min. The reaction was quenched by the addition of half-saturated aqueous NH₄Cl (10 mL) and was then allowed to warm to room temperature. The phases were separated and the aqueous layer was extracted with Et₂O (3 × 75 mL). The combined organic layers were washed with saturated aqueous NaCl (10 mL) and dried over Na₂SO₄. The solvents were carefully removed under reduced pressure (min. 500 mbar) and the crude product was purified by flash column chromatography (silica, *n*-pentane:Et₂O = 97:3). The solvents of the product containing fractions were carefully removed under reduced pressure (min. 300 mbar) and the obtained addition product **513** was immediately used in the next step.

To a solution of triene **513** (41 mg, assumed 77 μmol, 1.0 eq.) in CH₂Cl₂ (8.9 mL) was added *m*-CPBA (0.80 mL, 0.2 M solution in CH₂Cl₂, 0.16 mmol, 2.0 eq.) and the mixture was stirred for 90 min at room temperature, at which point additional *m*-CPBA (0.40 mL, 0.2 M solution in CH₂Cl₂, 80 μmol, 1.0 eq.) was added. Stirring was continued for one hour and the reaction was then quenched by the addition of saturated aqueous NaHCO₃ (10 mL). The phases were separated and the aqueous layer was extracted with CH₂Cl₂ (3 × 50 mL). The combined organic layers were consecutively washed with saturated aqueous K₂CO₃ (10 mL), saturated aqueous NaCl (10 mL) and dried over Na₂SO₄. The solvents were evaporated under reduced pressure and the crude product was purified by flash column chromatography (silica, *n*-pentane:Et₂O = 23:2 to 9:1) to yield epoxide **514** (38 mg, 69 μmol, 71% over two steps) as colorless oil and as a single diastereomer.

$R_f = 0.33$ (*i*-Hex:EtOAc = 10:1).

¹H NMR (C₆D₆, 400 MHz): δ = 5.82 (m_C, 1H), 5.38 (m_C, 1H), 5.04–4.93 (m, 4H), 4.78 (d, *J* = 7.0 Hz, 1H), 4.73 (d, *J* = 6.9 Hz, 1H), 4.37 (m_C, 1H), 3.79 (m_C, 1H), 3.71 (m_C, 1H), 2.68 (dd, *J* = 10.3, 5.8 Hz, 1H), 2.48 (m_C, 1H), 2.45–2.33 (m, 2H), 2.15 (dd, *J* = 11.5, 7.0 Hz, 1H), 2.09–1.97 (m, 2H), 1.97–1.80 (m, 3H), 1.74–1.57 (m, 3H), 1.53 (m_C, 2H), 1.45 (m_C, 1H), 1.32 (dd, *J* = 12.3, 3.8 Hz, 1H), 1.24 (s, 3H), 1.10 (d, *J* = 6.8 Hz, 3H), 1.07–0.96 (m, 3H), 1.02 (d, *J* = 6.3 Hz, 3H), 0.99 (d, *J* = 6.9 Hz, 3H), 0.92 (d, *J* = 6.9 Hz, 3H), 0.77 (s, 3H), 0.02 (s, 9H) ppm.

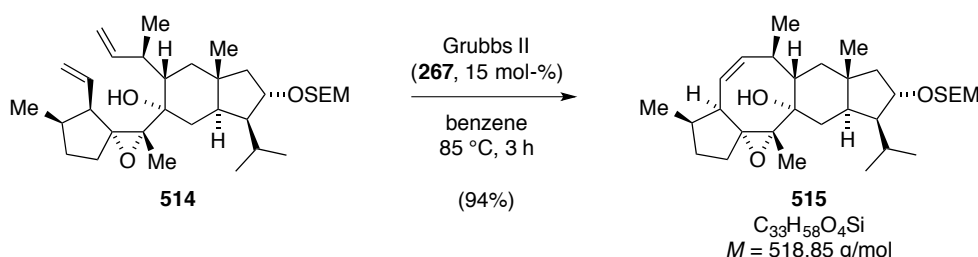
^{13}C NMR (C_6D_6 , 100 MHz) δ = 145.4, 134.6, 118.0, 111.8, 93.7, 81.9, 79.7, 77.9, 69.5, 65.3, 55.2, 55.0, 43.0, 41.7, 38.8, 38.4, 36.9, 35.6, 33.8, 33.1, 29.9, 28.3, 24.8, 22.7, 22.1, 19.9, 19.8, 18.4, 17.0, 16.3, -1.3 ppm.

ESI-MS for $\text{C}_{33}\text{H}_{62}\text{O}_4\text{NSi}^+ [(\text{M}+\text{NH}_4)^+]$: calcd. 546.4443
found 546.4445.

IR (ATR): $\tilde{\nu}/\text{cm}^{-1}$ = 3575, 3248, 3079, 2967, 2871, 1697, 1634, 1460, 1412, 1387, 1370, 1362, 1263, 1197, 1160, 1126, 1099, 1066, 1033, 1014, 1000, 992, 948, 924, 905, 874, 857, 815, 755, 703, 678.

$[\alpha]_D^{20} = -3.0$ (c 1.00, C_6D_6).

Synthesis of Tetracycle **515**



To a solution of diene **514** (40.4 mg, 73.9 μmol , 1.0 eq.) in degassed benzene (116 mL) was added a solution of Grubbs second-generation catalyst (**267**, 8.3 mg, 9.7 μmol , 15 mol-%) in degassed benzene (1.0 mL). The mixture was placed in an oil bath (pre-heated to 85 $^\circ\text{C}$) and stirred at this temperature for 3 hours, before being allowed to cool to room temperature. The solvent was evaporated under reduced pressure and the obtained crude product was purified by flash column chromatography (silica, n -pentane: Et_2O = 93:7) to yield the cyclized product **515** (36.2 mg, 69.8 μmol , 94%) as colorless needles.

Note: Substrate 514 and product 515 behaved almost co-polar at TLC analysis. However, the product appears less intense blue when staining the TLC plate with PAA.

Crystals suitable for X-ray analysis were obtained by slow evaporation of a solution of alkene **515** in n -pentane/MeOH.

R_f = 0.33 (i -Hex: EtOAc = 10:1).

Melting point = 122.1–122.9 °C (*n*-pentane/MeOH).

^1H NMR (C_6D_6 , 400 MHz): δ = 5.45–5.30 (m, 2H), 4.77 (d, J = 6.9 Hz, 1H), 4.73 (d, J = 7.0 Hz, 1H), 4.33 (m_C , 1H), 3.82–3.67 (m, 2H), 3.43 (m_C , 1H), 3.20 (m_C , 1H), 2.88 (d, J = 1.4 Hz, 1H), 2.63 (m_C , 1H), 2.33–2.21 (m, 1H), 2.19–2.01 (m, 3H), 1.95 (ddd, J = 10.3, 10.3, 4.4 Hz, 1H), 1.87–1.72 (m, 3H), 1.70–1.52 (m, 3H), 1.51–1.36 (m, 3H), 1.20 (s, 3H), 1.10 (d, J = 6.6 Hz, 3H), 1.06–1.00 (m, 2H), 0.96 (d, J = 6.3 Hz, 3H), 0.95–0.90 (m, 6H), 0.71 (s, 3H), 0.02 (s, 9H) ppm.

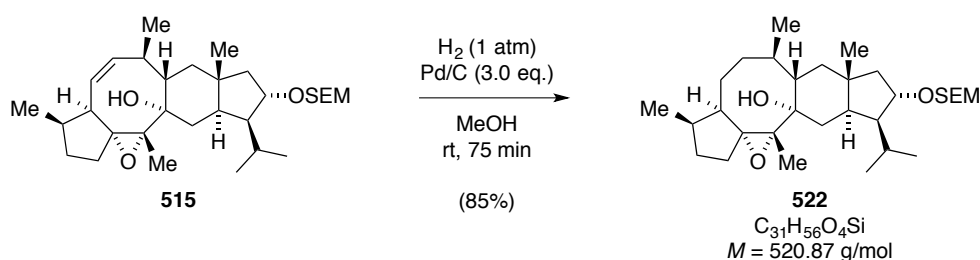
^{13}C NMR (C_6D_6 , 100 MHz) δ = 141.4, 128.1 (obscured by residual solvent), 93.8, 84.6, 81.9, 76.4, 66.4, 65.3, 54.8, 48.7, 46.6, 43.5, 42.1, 41.3, 39.7, 37.1, 35.1, 33.3, 32.4, 30.0, 27.6, 24.6, 22.3, 21.0, 19.9, 18.4, 17.1, 16.4, –1.3 ppm.

EI-MS for $\text{C}_{31}\text{H}_{54}\text{O}_4\text{Si}^+ [\text{M}^+]$:
 calcd. 518.3786
 found 518.3770.

IR (ATR): $\tilde{\nu}/\text{cm}^{-1}$ = 3480, 2951, 1459, 1377, 1248, 1101, 1057, 937, 860.

$[\alpha]_D^{20}$ = +6.4 (c 0.25, C_6D_6).

Synthesis of Tetracycle **522**



To a solution of alkene **515** (36.2 mg, 69.8 μmol , 1.0 eq.) in MeOH (80 mL) was added Pd/C (10 wt-% Pd, 268 mg, 209 μmol , 3.0 eq.) and the suspension was stirred under an atmosphere of H_2 for 75 min. The mixture was filtered over a pad of Celite[®] (Et_2O washings) and the solvent was evaporated under reduced pressure. The crude product was purified by flash column chromatography (silica, *n*-pentane: Et_2O = 93:7) to yield substance **522** (30.9 mg, 59.3 μmol , 85%) as colorless solid.

Note: Substrate 515 and product 522 behave co-polar at TLC analysis.

Crystals suitable for X-ray analysis were obtained by slow evaporation of a solution of **522** in *n*-pentane/MeOH.

$R_f = 0.81$ (*n*-pentane:Et₂O = 1:3).

Melting point = 120.1–121.3 °C (*n*-pentane/MeOH).

¹H NMR (C₆D₆, 400 MHz): δ = 4.78 (d, J = 7.0 Hz, 1H), 4.73 (d, J = 7.0 Hz, 1H), 4.38–4.33 (m_C, 1H), 3.84–3.64 (m, 2H), 2.70–2.57 (m, 2H), 2.43–2.35 (m_C, 1H), 2.22 (s, 1H), 2.13 (dd, J = 11.5, 6.9 Hz, 1H), 2.04–1.88 (m, 2H), 1.87–1.58 (m, 6H), 1.49–1.20 (m, 7H), 1.23 (s, 3H), 1.12 (d, J = 6.6 Hz, 3H), 1.15–1.01 (m, 3H), 0.97 (d, J = 6.3 Hz, 3H), 0.94–0.83 (m, 7H), 0.75 (s, 3H), 0.02 (s, 9H) ppm.

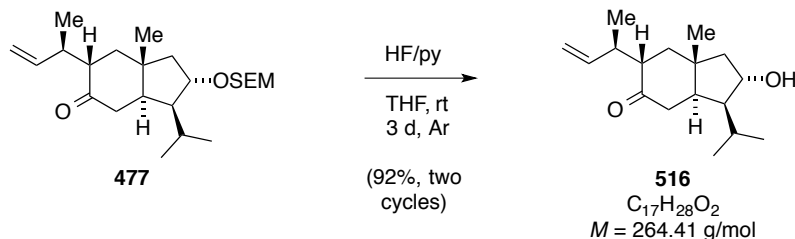
¹³C NMR (C₆D₆, 100 MHz): δ = 93.7, 82.1, 78.6, 75.4, 67.2, 65.3, 54.8, 48.6, 42.9, 42.5, 42.3, 42.1, 41.9, 36.4 (2C), 35.5, 32.6, 32.4, 30.2, 27.0, 25.1, 24.7, 23.4, 22.3, 20.1, 18.4, 16.5, 15.2, –1.2 ppm.

ESI-MS for C₃₁H₆₀NO₄Si⁺ [(M+NH₄)⁺]: calcd. 538.4286
found 538.4287.

IR (ATR): $\tilde{\nu}/\text{cm}^{-1}$ = 3490, 2953, 2924, 1558, 1458, 1377, 1261, 1250, 1097, 1057, 1029, 940, 860, 834, 880, 688, 669.

$[\alpha]_D^{20} = +26.0$ (c 0.20, C₆D₆).

Synthesis of Alcohol **516**



To a solution of ketone **477** (100 mg, 253 μmol , 1.0 eq.) in THF (14 mL) was added HF/pyridine (4.0 mL) at 0 °C. The resulting mixture was stirred at room temperature for

12 hours, at which point additional HF/pyridine (0.4 mL) was added. After stirring for further 44 hours, the reaction mixture was poured into saturated aqueous NaHCO₃ solution (200 mL) and subsequently extracted with CH₂Cl₂ (3 × 150 mL). The combined organic layers were dried over Na₂SO₄, concentrated under reduced pressure and the crude product was purified *via* flash column chromatography (silica, *n*-pentane:Et₂O = 3:1 to 7:3) to yield alcohol **516** (49.7 mg, 0.19 mmol, 74%) as a colorless solid, as well as recovered ketone **477** (8.5 mg, 0.02 mmol, 8.5%) and epimerized alcohol **517** (9.0 mg, 0.04 mmol, 13%).

When epimerized alcohol **517** and the re-isolated ketone **477** were submitted to the same reaction conditions as described above, further alcohol **516** (12 mg, 46 μmol, 18%) could be obtained.

$R_f = 0.30$ (*i*-Hex:EtOAc = 5:2).

Melting point = 75.3–75.7 °C (Et₂O).

¹H NMR (C₆D₆, 400 MHz): δ = 5.89–5.74 (m, 1H), 5.07–4.94 (m, 2H), 4.05 (m_C, 1H), 3.02 (m_C, 1H), 2.45 (dd, J = 14.1, 3.7 Hz, 1H), 2.12 (m_C, 1H), 1.99 (m, 1H), 1.91–1.71 (m, 2H), 1.51 (dd, J = 12.6, 6.2 Hz, 1H), 1.43–1.22 (m, 2H), 1.21–1.09 (m, 2H), 1.05 (d, J = 6.9 Hz, 3H), 1.03–0.98 (m, 1H), 0.91 (d, J = 6.3 Hz, 3H), 0.76 (d, J = 6.0 Hz, 3H), 0.61 (s, 3H) ppm.

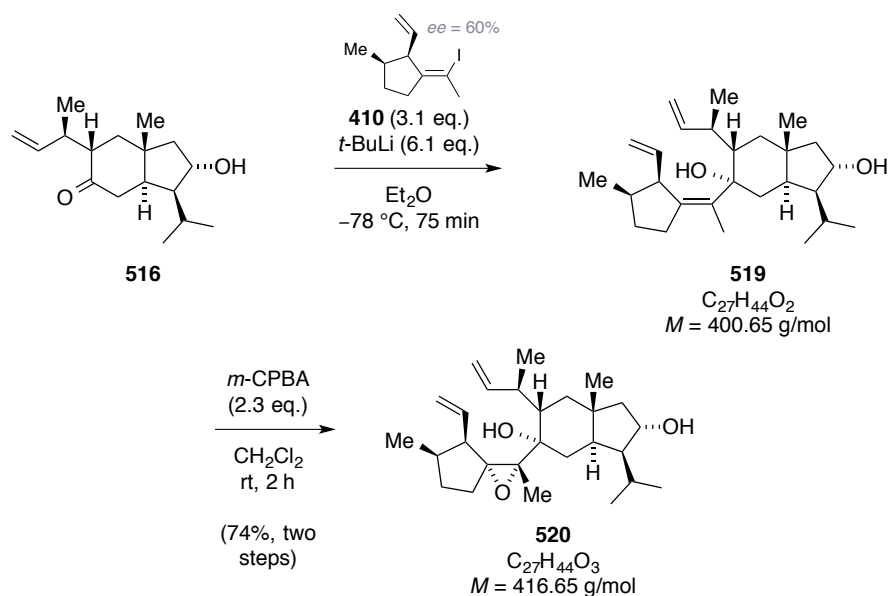
¹³C NMR (C₆D₆, 100 MHz) δ = 208.7, 143.0, 113.8, 77.3, 56.8, 50.0, 49.6, 48.8, 41.9, 41.1, 39.5, 36.0, 29.4, 24.1, 21.7, 19.4, 15.1 ppm.

EI-MS for C ₁₇ H ₂₈ O ₂ ⁺ [M ⁺]:	calcd.	264.2084
	found	264.2098.

IR (ATR): $\tilde{\nu}/\text{cm}^{-1}$ = 3249, 2958, 2932, 2868, 1695, 1638, 1462, 1387, 1369, 1354, 1262, 1226, 1101, 1035, 992, 909, 871, 816, 754, 682.

$[\alpha]_D^{20} = +11.4$ (*c* 1.00, C₆D₆).

Synthesis of Epoxide 520



To a solution of vinyl iodide **410** (76.9 mg, 0.29 mmol, 3.10 eq.) in Et₂O (5.3 mL) was slowly added *t*-BuLi (0.34 mL, 1.7 M solution in *n*-pentane, 0.57 mmol, 6.05 eq.) at -78 °C and the resulting mixture was stirred for 45 min at this temperature. Then, a solution of ketone **516** (25.0 mg, 9.46 μmol, 1.00 eq.) in Et₂O (1.4 mL) was added within 30 min and the mixture was stirred for an additional 45 min. The reaction was quenched by the addition of half-saturated aqueous NH₄Cl (10 mL) and was then warmed to room temperature. The phases were separated and the aqueous layer was extracted with Et₂O (3 × 100 mL). The combined organic layers were washed with saturated aqueous NaCl (20 mL) and dried over Na₂SO₄. The solvents were carefully removed under reduced pressure (min. 500 mbar) and the crude product was purified by flash column chromatography (silica, *n*-pentane:Et₂O = 17:3). The solvent of the product containing fractions was carefully removed under reduced pressure (min. 300 mbar) and the obtained addition product **519** was immediately used for the next transformation.

To a solution of triene **519** (assumed 9.46 μmol, 1.00 eq.) in CH₂Cl₂ (8.7 mL) was added *m*-CPBA (0.85 mL, 0.2 M solution in CH₂Cl₂, 0.17 mmol, 1.90 eq.) and the mixture was stirred for 90 min at room temperature. After the addition of further *m*-CPBA (0.20 mL, 0.2 M solution in CH₂Cl₂, 40.0 μmol, 0.40 eq.), stirring was continued for 30 min. The reaction was quenched by the addition of saturated aqueous NaHCO₃ (10 mL) and the phases were separated. The aqueous layer was extracted with CH₂Cl₂ (3 × 100 mL). The combined organic layers were consecutively washed with saturated aqueous K₂CO₃ (10 mL), saturated aqueous NaCl (10 mL) and dried over Na₂SO₄. The solvents were evaporated under

reduced pressure and the crude product was purified by flash column chromatography (silica, *n*-pentane:Et₂O = 19:6 to 16:9) to yield epoxide **520** (29.3 mg, 70.3 μmol, 74%) as colorless solid and as a single diastereomer.

$R_f = 0.42$ (*i*-Hex:EtOAc = 3:1).

Melting point = 166.7–167.3 °C (C₆D₆).

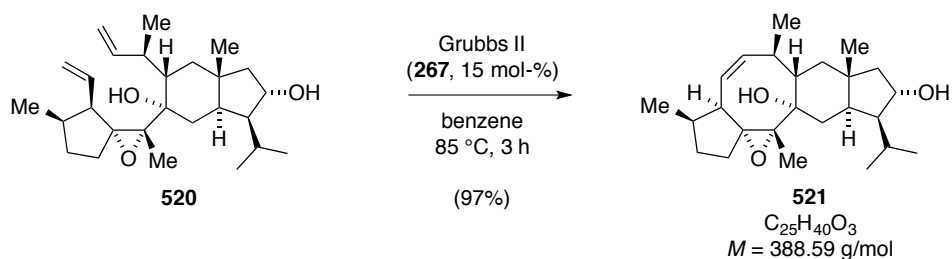
¹H NMR (C₆D₆, 600 MHz): δ = 5.85–5.79 (m_C, 1H), 5.43–5.36 (m_C, 1H), 5.09–4.93 (m, 4H), 4.19–4.16 (m_C, 1H), 2.76 (dd, J = 10.4, 5.7 Hz, 1H), 2.51–2.32 (m, 3H), 2.08–2.03 (m_C, 1H), 1.99 (dd, J = 13.6, 3.4 Hz, 1H), 1.93 (dd, J = 11.5, 7.1 Hz, 1H), 1.89–1.80 (m, 2H), 1.73–1.65 (m, 1H), 1.65–1.48 (m, 4H), 1.34–1.26 (m, 3H), 1.23 (s, 3H), 1.10–1.02 (m, 1H), 1.02–0.98 (m, 9H), 0.94 (d, J = 6.8 Hz, 3H), 0.73 (s, 3H) ppm.

¹³C NMR (C₆D₆, 100 MHz) δ = 145.4, 134.6, 118.1, 111.8, 79.7, 78.0, 77.3, 69.6, 57.7, 55.1, 51.2, 43.3, 41.8, 38.8, 38.5, 36.8, 35.6, 33.8, 33.1, 30.2, 28.3, 24.5, 22.1, 19.9, 19.8, 17.0, 16.4 ppm.

ESI-MS for C ₂₇ H ₄₅ O ₃ ⁺ [M ⁺]:	calcd.	417.3363
	found	417.3378.

IR (ATR): $\tilde{\nu}/\text{cm}^{-1}$ = 3422, 2966, 2954, 2927, 2888, 1635, 1464, 1410, 1389, 1369, 1302, 1273, 1222, 1192, 1135, 1086, 1060, 1044, 1029, 1010, 991, 959, 944, 934, 901, 871, 860, 804, 776, 754, 723, 693, 681, 667.

$[\alpha]_D^{20} = -28.4$ (c 0.50, C₆D₆).

Synthesis of Tetracycle **521**

To a solution of diene **520** (15 mg, 36 μmol , 1.0 eq.) in degassed benzene (30 mL) was added Grubbs second-generation catalyst (**267**, 1.5 mg, 1.8 μmol , 5 mol-%). The mixture was placed in an oil bath (pre-heated to 85 $^\circ\text{C}$) and stirred at this temperature. After one and two hours, respectively, another two batches of Grubbs second-generation catalyst (**267**, 1.5 mg, 1.8 μmol , 5 mol-%) were added and stirring was continued to a total reaction time of 3 hours. The reaction mixture was allowed to cool to room temperature. The solvent was evaporated under reduced pressure and the obtained crude product was purified by flash column chromatography (silica, *n*-pentane:Et₂O = 3:1 to 7:3) to yield the cyclized product **521** (11 mg, 21 μmol , 86%) as a colorless wax.

$R_f = 0.38$ (*i*-Hex:EtOAc = 3:1).

¹H NMR (C₆D₆, 600 MHz): δ = 5.40 (dd, J = 10.7, 8.0 Hz, 1H), 5.34 (dd, J = 10.7, 8.1 Hz, 1H), 4.12 (m_C, 1H), 3.45 (t, J = 6.6 Hz, 1H), 3.25–3.15 (m, 1H), 2.94 (s, 1H), 2.54 (m_C, 1H), 2.35–2.22 (m, 1H), 2.12 (m_C, 1H), 2.00 (t, J = 13.2 Hz, 1H), 1.88 (dd, J = 11.4, 7.0 Hz, 1H), 1.84–1.72 (m, 2H), 1.62 (dd, J = 12.4, 4.9 Hz, 1H), 1.60–1.41 (m, 4H), 1.38–1.25 (m, 1H), 1.36 (t, J = 12.4 Hz, 1H), 1.25–1.12 (m, 5H), 1.00 (d, J = 6.4 Hz, 3H), 0.98–0.89 (m, 9H), 0.66 (s, 3H) ppm.

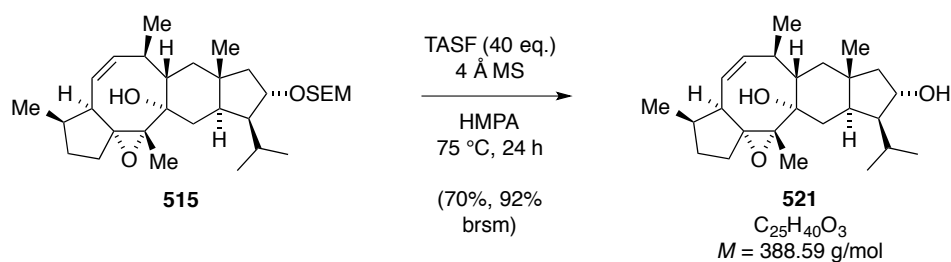
¹³C NMR (C₆D₆, 100 MHz) δ = 141.4, 128.1 (obscured by residual solvent), 84.7, 77.3, 76.4, 66.4, 57.5, 51.6, 46.7, 43.3, 42.4, 41.3, 39.6, 37.1, 35.2, 33.2, 32.4, 30.3, 27.6, 24.4, 22.2, 21.0, 19.8, 17.1, 16.4 ppm.

EI-MS for C ₂₅ H ₄₀ O ₃ ⁺ [M ⁺]:	calcd.	388.2972
	found	388.2968.

IR (ATR): $\tilde{\nu}/\text{cm}^{-1}$ = 3495, 3266, 2950, 2930, 2873, 1457, 1378, 1329, 1260, 1233, 1170, 1148, 1096, 1075, 1040, 1011, 986, 970, 942, 914, 883, 862, 841, 794, 778, 734, 711, 684, 668, 663.

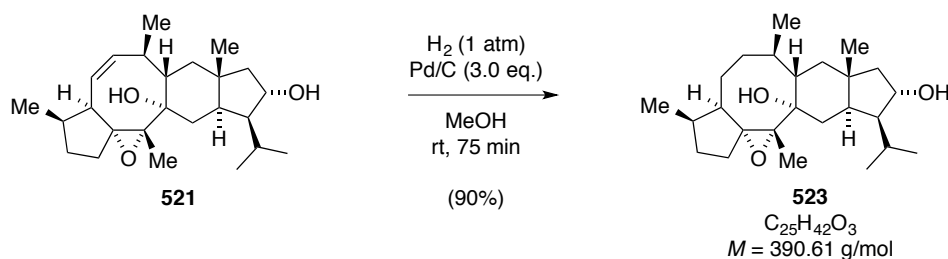
$[\alpha]_D^{20} = -32.5$ (c 0.85, C_6D_6).

Synthesis of Tetracycle **521**



To a solution of compound **515** (5.0 mg, 9.5 μmol , 1.0 eq.) and TASf (50 mg, 1.9 mmol, 20 eq.) in HMPA (4.5 mL) were added molecular sieves (4 Å, 50 mg). The vessel was transferred to an oil bath (pre-heated to 75 °C) and the reaction was stirred for 16 hours. After the addition of further TASf (50 mg, 1.9 mmol, 20 eq.) and molecular sieves (4 Å, 50 mg) in HMPA (1 mL), stirring was continued for another 8 hours at 75 °C. The reaction was allowed to cool to room temperature and the mixture was diluted with water (20 mL), and extracted with Et_2O (4×50 mL). The combined organic layers were washed with half-saturated aqueous NaCl (2×10 mL), dried over Na_2SO_4 and the solvents were evaporated under reduced pressure. The crude product was purified by flash column chromatography (silica, n -pentane: Et_2O = 3:1 to 7:3) to yield the alcohol **521** (2.6 mg, 7.0 μmol , 70%) as a colorless wax, along with recovered starting material **515** (1.1 mg, 2.1 μmol , 22%).

*Note: The measured analytical data was identical to the data of the material obtained from ring-closing metathesis of triene **520** (vide supra).*

Synthesis of Tetracycle **523**

To a solution of alkene **521** (4.0 mg, 10 μmol , 1.0 eq.) in MeOH (8 mL) was added Pd/C (10 wt-% Pd, 40 mg, 31 μmol , 3.0 eq.). The argon atmosphere was exchanged with hydrogen (1 atm) and the suspension was stirred for 75 min. The mixture was filtered over a pad of Celite[®] (Et₂O washings) and the solvents were evaporated under reduced pressure. Purification of the crude product by flash column chromatography (silica, *n*-pentane:Et₂O = 1:1) yielded alcohol **523** (3.5 mg, 9.0 μmol , 90%) as colorless oil.

On a slightly higher reaction scale, alkene **521** (13 mg, 33 μmol) was hydrogenated to alcohol **523** (12 mg, 30 μmol) in 90% yield.

Note: Product 523 and alkene 521 behaved co-polar at TLC analysis.

$R_f = 0.24$ (*i*-Hex:EtOAc = 4:1).

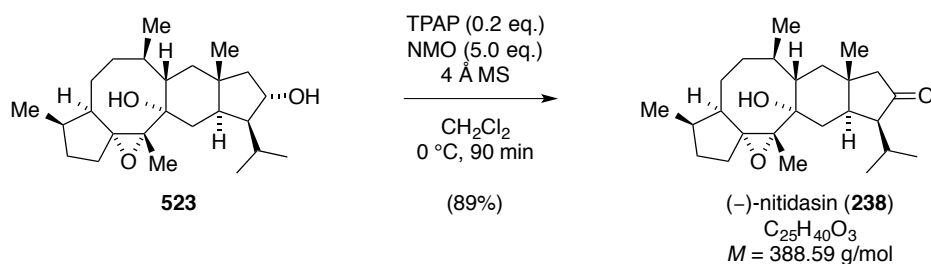
¹H NMR (C₆D₆, 400 MHz): $\delta = 4.13$, (m_C, 1H), 2.69–2.50 (m, 2H), 2.47–2.34 (m, 1H), 2.27 (s, 1H), 1.97–1.85 (m, 2H), 1.84–1.67 (m, 4H), 1.63 (dd, $J = 11.9, 3.9 \text{ Hz}$, 1H), 1.59–1.49 (m, 1H), 1.47–1.26 (m, 5H), 1.26–1.17 (m, 6H), 1.14–1.06 (m, 1H), 1.00 (d, $J = 6.6 \text{ Hz}$, 3H), 0.95–0.85 (m, 10H), 0.70 (s, 3H) ppm.

¹³C NMR (C₆D₆, 100 MHz) $\delta = 78.6, 77.5, 75.4, 67.2, 57.5, 51.5, 42.6, 42.5, 42.4, 42.2, 41.9, 36.5, 36.4, 35.5, 32.6, 32.4, 30.5, 27.0, 25.1, 24.4, 23.5, 22.2, 20.0, 16.5, 15.2 \text{ ppm}$.

EI-MS for C ₂₅ H ₄₂ O ₃ ⁺ [M ⁺]:	calcd.	390.3129
	found	390.3145.

IR (ATR): $\tilde{\nu}/\text{cm}^{-1} = 3464, 2930, 2870, 1459, 1044$.

$[\alpha]_D^{20} = +6.2$ (*c* 0.50, CH₂Cl₂).

Synthesis of (–)-Nitidasin (**238**)

To a solution of alcohol **523** (11.0 mg, 28.2 μ mol, 1.0 eq.) in CH₂Cl₂ (7.3 mL) were added molecular sieves (4 Å, 55.0 mg) and the suspension was cooled to 0 °C. Then, NMO (26.0 mg, 225 μ mol, 5.0 eq.) and TPAP (1.98 mg, 5.64 μ mol, 20 mol-%) were consecutively added and the mixture was stirred for one hour. The reaction was filtered over a pad of silica (Et₂O washings) and the solvents were evaporated under reduced pressure. The crude product was purified by flash column chromatography (silica, *n*-pentane:Et₂O = 9:1 to 17:3) to yield (–)-nitidasin (**238**, 9.8 mg, 25.2 μ mol, 89%) as a colorless solid.

Crystals suitable for X-ray crystallography were obtained from slow evaporation of a solution of (–)-nitidasin (**238**) in MeOH at –20 °C.

R_f = 0.67 (*i*-Hex:EtOAc = 4:1).

Melting point = 145.7–146.3 °C (C₆D₆), Lit.:^[154] 145–147 °C (MeOH).

¹H NMR (C₆D₆, 400 MHz): δ = 2.63–2.48 (m, 2H), 2.41 (m_C, 1H), 2.29 (s, 1H), 2.01 (t, *J* = 13.1 Hz, 1H), 1.98 (d, *J* = 17.0 Hz, 1H), 1.83–1.59 (m, 7H), 1.53 (dd, *J* = 12.3, 4.0 Hz, 1H), 1.47–1.27 (m, 3H), 1.27–1.14 (m, 3H), 1.20 (s, 3H), 1.18 (d, *J* = 6.3 Hz, 3H), 1.12–1.06 (m, 1H), 0.95–0.81 (m, 10H), 0.71 (s, 3H) ppm.

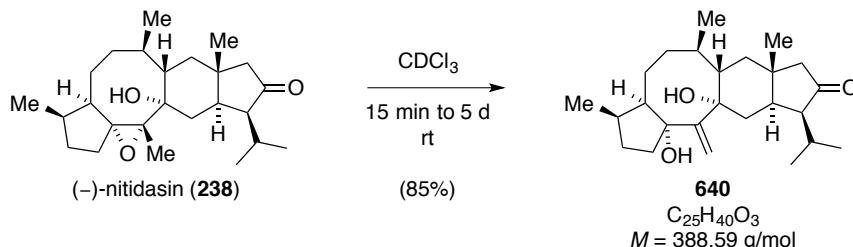
¹³C NMR (C₆D₆, 100 MHz) δ = 217.5, 78.7, 75.1, 67.0, 55.7, 55.6, 42.7, 42.5, 42.0, 41.8, 39.1, 36.4, 35.3, 34.7, 32.6, 32.3, 28.7, 27.0, 25.5, 25.1, 23.4, 21.6, 20.2, 16.4, 15.2 ppm.

EI-MS for C₂₅H₄₀O₃⁺ [M⁺]:
calcd. 388.2972
found 388.2976.

IR (ATR): $\tilde{\nu}$ /cm^{–1} = 3480, 2954, 2872, 1732, 1461, 1378; Lit.:^[154] $\tilde{\nu}$ /cm^{–1} = 3423, 1738.

$$[\alpha]_D^{20} = -102 (c\ 0.10, \text{CHCl}_3), \text{Lit.:}^{[154]} [\alpha]_D^{20} = -41.4 (c\ 0.28, \text{CHCl}_3).$$

Synthesis of Diol **640** – Transformation of (-)-Nitidasin (**238**) in Acidic CDCl_3



A sample of (-)-nitidasin (**238**, 1.3 mg, 2.8 μmol) was dissolved in CDCl_3 (0.7 mL) that was taken from a fresh ampule and the NMR spectra were immediately recorded. NMR analysis showed complete conversion to diol **640** after five days. After removal of the solvent *in vacuo* diol **640** (1.1 mg, 2.4 μmol , 85%) was obtained as colorless oil. This compound reacted further in the NMR solvent at prolonged exposure to a mixture of unknown compounds.

Note: The reaction time was dependent on the HCl content of the employed CDCl_3 and cannot be estimated easily. Even different ampullas of the same 10-ampullas box led to unequal reaction times, ranging from 15 min to 5 days.

^1H NMR (CDCl_3 , 400 MHz): $\delta = 5.26$ (s, 1H), 5.07 (s, 1H), 4.18 (br s, 1H), 2.84–2.69 (m, 2H), 2.63 (ddd, $J = 13.1, 8.9, 3.2$ Hz, 1H), 2.38 (ddd, $J = 13.5, 11.9, 6.9$ Hz, 1H), 2.23 (t, $J = 13.3$ Hz, 1H), 2.18–2.00 (m, 3H), 1.99–1.80 (m, 4H), 1.74 (ddd, $J = 12.6, 3.5, 2.2$ Hz, 2H), 1.70–1.61 (m, 1H), 1.54 (s, 2H), 1.37–1.22 (m, 3H), 1.20–1.11 (m, 1H), 1.04–0.98 (m, 7H), 0.98–0.91 (m, 6H), 0.87 (d, $J = 7.2$ Hz, 3H) ppm.

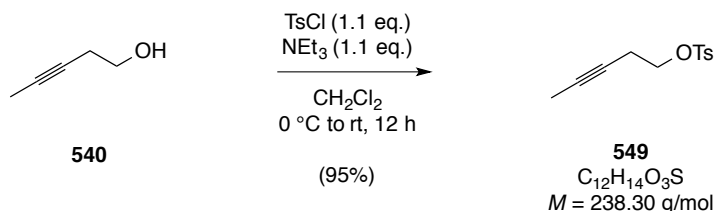
^{13}C NMR (CDCl_3 , 100 MHz): $\delta = 160.3, 111.1, 88.2, 79.0, 56.1, 56.0, 51.6, 46.3, 42.6, 42.3, 40.9, 39.5, 35.5, 34.5, 34.4, 30.6, 29.9, 28.6, 27.3, 25.7, 24.7, 23.5, 21.3, 20.4, 15.7$.ppm.

EI-MS for $\text{C}_{25}\text{H}_{40}\text{O}_3^+ [\text{M}^+]$:
 calcd. 388.2972
 found 388.2965.

IR (ATR): $\tilde{\nu}/\text{cm}^{-1} = 3417, 2956, 2925, 2865, 1732, 1560, 1540, 1452, 1383, 2361, 1175, 1096, 1025, 947, 898, 799$.

$$[\alpha]_D^{20} = -51.8 (c\ 0.73, \text{CHCl}_3).$$

5.4 Experimental Procedures for Chapter 2: ‘Synthetic Studies Toward Astellatol’

Synthesis of Tosylate **549**

To a solution of 3-pentynol (**540**, 5.0 g, 59.4 mmol, 1.0 eq.) and Et₃N (9.1 mL, 65.4 mmol, 1.1 eq.) in CH₂Cl₂ (60 mL) was added TsCl (12.5 g, 65.4 mmol, 1.1 eq.) at 0 °C in one portion and the resulting solution was stirred at room temperature for 12 hours. After diluting with H₂O (100 mL), the layers were separated and the aqueous phase was extracted with CH₂Cl₂ (3 × 75 mL). The combined organic layers were dried over Na₂SO₄ and concentrated under reduced pressure. The crude product was purified by flash column chromatography (silica, *i*-Hex:EtOAc = 19:1 to 17:3) to yield tosylate **549** (13.4 g, 56.3 mmol, 95%) as a colorless solid.

R_f = 0.93 (*i*-Hex:EtOAc = 3:2).

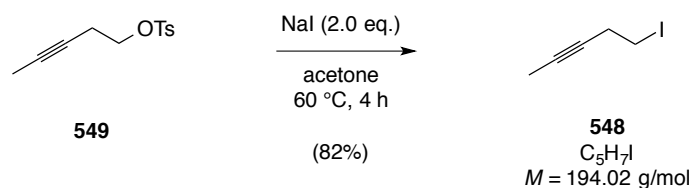
Melting point = 40–41 °C (*i*-Hex/EtOAc).

¹H NMR (CDCl₃, 300 MHz): δ = 7.69–7.63 (m, 2H), 7.25–7.18 (m, 2H), 3.91 (td, *J* = 7.1, 0.6 Hz, 2H), 2.40–2.26 (m, 2H), 2.31 (m_C, 3H), 1.57 (td, *J* = 2.6, 0.6 Hz, 3H) ppm.

¹³C NMR (CDCl₃, 75 MHz): δ = 144.9, 133.0, 129.9, 127.9, 78.2, 73.2, 68.3, 21.6, 19.7 (2C), 3.4 ppm.

EI-MS for C ₁₂ H ₁₄ O ₃ S ⁺ [M ⁺]:	calcd.	238.0664.
	found	238.0667.

IR (ATR): $\tilde{\nu}/\text{cm}^{-1}$ = 2960, 2893, 1590, 1357, 1195, 1186, 1172, 1091, 1067, 940 760, 691, 660.

Synthesis of Iodide **548**

To a solution of tosylate **549** (10.8 g, 45.3 mmol, 1.0 eq.) in acetone (85 mL) was added NaI (13.6 g, 90.6 mmol, 2.0 eq.) in one portion. The resulting mixture was heated to 60 °C and stirred under exclusion of light for 4 hours. Subsequently, the mixture was diluted with Et₂O (300 mL) and washed with H₂O (100 mL). The aqueous phase was re-extracted with Et₂O (3 × 40 mL). The combined organic layers were dried over Na₂SO₄ and concentrated under reduced pressure (200 mbar, 30 °C). The crude product was purified by distillation (boiling point = 65 °C, 14 mbar) under an argon atmosphere to yield iodide **548** (7.18 g, 37.0 mmol, 82%) as a colorless oil, which was indefinitely stable as a solid upon storage at −20 °C under exclusion of light.

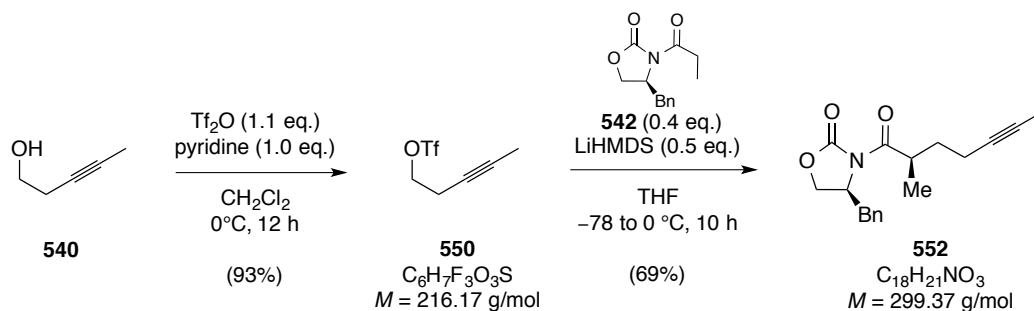
$R_f = 0.96$ (*i*-Hex:EtOAc = 3:1).

¹H NMR (CDCl₃, 400 MHz): δ = 3.20 (t, J = 7.4 Hz, 2H), 2.71 (tq, J = 7.4, 2.5 Hz, 2H), 1.77 (t, J = 2.5 Hz, 3H) ppm.

¹³C NMR (CDCl₃, 100 MHz): δ = 78.1, 77.9, 24.3, 3.7, 2.7 ppm.

EI-MS for C ₅ H ₇ I ⁺ [M ⁺]:	calcd.	193.9587.
	found	193.9587.

IR (ATR): $\tilde{\nu}/\text{cm}^{-1}$ = 2963, 2916, 2851, 1434, 1421, 1377, 1333, 1248, 1170, 1151, 1029, 904, 840, 774, 727.

Synthesis of Alkyne **542**

To a solution of 3-pentynol (**540**, 1.08 g, 12.9 mmol, 1.0 eq.) and pyridine (1.04 mL, 12.9 mmol, 1.0 eq.) in CH_2Cl_2 (12 mL) was added freshly distilled Ti_2O (2.39 mL, 14.2 mmol, 1.1 eq.) dropwise at 0°C and the resulting mixture was stirred for 30 min. The reaction was quenched by the addition of H_2O (20 mL). The layers were separated and the aqueous phase was extracted with CH_2Cl_2 ($3 \times 10 \text{ mL}$). The combined organic layers were dried over Na_2SO_4 and then carefully concentrated under reduced pressure (400 mbar, 30°C). The resulting crude product was filtered through a short Na_2SO_4 plug (CH_2Cl_2 washings) and was again concentrated to yield triflate **550** (2.58 g, 11.9 mmol, 93%), which was used immediately in the next reaction.

*Note: Triflate **550** could not be stored longer than two days at -20°C before decomposition took place.*

$R_f = 0.95$ (*i*-Hex:EtOAc = 3:2).

^1H NMR (C_6D_6 , 400 MHz): $\delta = 3.85$ (m_c , 2H), 1.98 (m_c , 2H), 1.49 (td, $J = 2.5, 0.5 \text{ Hz}$, 3H) ppm.

^{13}C NMR (C_6D_6 , 100 MHz): $\delta = 119.3$ (q, $J = 319 \text{ Hz}$), 79.2, 74.6, 72.4, 20.0, 3.0 ppm.

^{19}F NMR (C_6D_6 , 376 MHz): $\delta = -75.4 \text{ ppm}$

EI-MS for $\text{C}_6\text{H}_6\text{F}_3\text{O}_3\text{S}^+ [(M-H)^+]$:	calcd.	214.9984.
	found	214.9983.

IR (ATR): $\tilde{\nu}/\text{cm}^{-1} = 2955, 2935, 2876, 1460, 1414, 1380, 1361, 1237, 1200, 1128, 1060, 1000, 960, 947, 860, 792, 710$.

To a solution of oxazolidinone **542** (100 mg, 0.43 mmol, 1.0 eq.) in THF (1.5 mL) was added LiHMDS (0.47 mL, 1 M solution in THF, 0.47 mmol, 1.1 eq.) dropwise at $-78\text{ }^{\circ}\text{C}$. The resulting mixture was stirred for 30 min, upon which a solution of freshly prepared triflate **550** (0.28 g, 1.29 mmol, 3.0 eq.) in THF (0.5 mL) was added dropwise. After stirring for an additional 30 min, the reaction was allowed to warm to room temperature over 10 hours. The resulting viscous mixture was diluted with CH_2Cl_2 (20 mL) and washed with saturated aqueous NaCl (20 mL). The aqueous phase was extracted with CH_2Cl_2 ($3 \times 20\text{ mL}$) and the combined organic layers were dried over Na_2SO_4 . The solvent was removed under reduced pressure and the crude product was purified by flash column chromatography (silica, *i*-Hex:EtOAc = 9:1 to 17:3) to yield alkyne **542** (89 mg, 0.30 mmol, 69%) as a colorless oil and a single diastereomer.

$R_f = 0.60$ (*i*-Hex:EtOAc = 3:1).

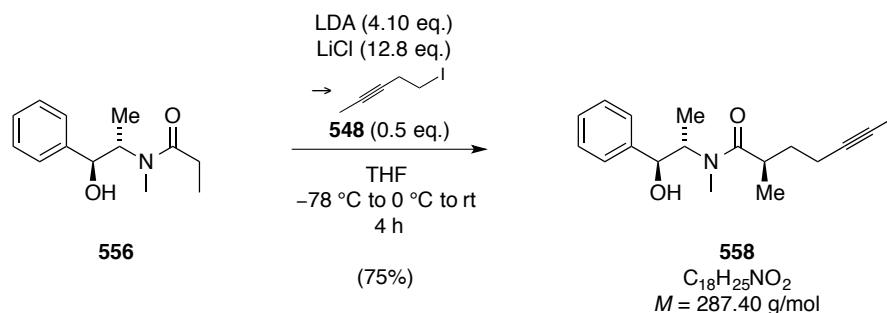
^1H NMR (CDCl_3 , 600 MHz): $\delta = 7.35\text{--}7.30$ (m, 2H), 7.29–7.25 (m, 1H), 7.24–7.18 (m, 2H), 4.67 (ddt, $J = 9.6, 7.7, 3.2\text{ Hz}$, 1H), 4.20–4.10 (m, 2H), 3.88 (sept, $J = 6.8\text{ Hz}$, 1H), 3.29 (dd, $J = 13.4, 3.4\text{ Hz}$, 1H), 2.74 (dd, $J = 13.4, 9.7\text{ Hz}$, 1H), 2.22–2.19 (m, 2H), 2.01 (dq, $J = 13.4, 7.2\text{ Hz}$, 1H), 1.77 (t, $J = 2.6\text{ Hz}$, 3H), 1.63 (m_C , 1H), 1.19 (d, $J = 6.9\text{ Hz}$, 3H) ppm.

^{13}C NMR (CDCl_3 , 150 MHz): $\delta = 176.8, 153.1, 135.4, 129.5, 129.1, 127.4, 78.2, 76.5, 66.1, 55.5, 38.1, 37.0, 32.9, 17.0, 16.7, 3.6\text{ ppm}$.

EI-MS for $\text{C}_{18}\text{H}_{21}\text{NO}_3^+ [\text{M}^+]$:	calcd.	299.1521.
	found	299.1518.

IR (ATR): $\tilde{\nu}/\text{cm}^{-1} = 2955, 2935, 2876, 1460, 1414, 1380, 1361, 1237, 1200, 1128, 1060, 1000, 960, 947, 860, 792, 710$.

$[\alpha]_D^{20} = +26.8$ ($c\ 1.00, \text{CH}_2\text{Cl}_2$).

Synthesis of Alkyne **558**

To a suspension of flame-dried LiCl (8.27 g, 0.19 mol, 12.8 eq.) in THF (90 mL) was added freshly distilled diisopropylamine (8.77 mL, 62.5 mmol, 4.15 eq.) and the resulting mixture was cooled to $-78\text{ }^{\circ}\text{C}$. Then, *n*-BuLi (20.8 mL, 2.95 M solution in hexanes, 61.5 mmol, 4.1 eq.) was added dropwise and the suspension was stirred for 15 min at -78 and 5 min at $0\text{ }^{\circ}\text{C}$. After being cooled to $-78\text{ }^{\circ}\text{C}$, a solution of amide **556** (7.00 g, 31.6 mmol, 2.1 eq.) in THF (41 mL) was added dropwise over a period of 15 min. The reaction was stirred at this temperature for one hour, at $0\text{ }^{\circ}\text{C}$ for 15 min and at room temperature for another 5 min. Subsequently, iodide **548** (2.92 g, 15.0 mmol, 1.0 eq.) was added dropwise at $0\text{ }^{\circ}\text{C}$ and the mixture was stirred for 5 hours before being warmed slowly to room temperature over night. The reaction was quenched by the addition of saturated aqueous NH_4Cl (50 mL) and diluted with CH_2Cl_2 (50 mL). The layers were separated and the aqueous phase was extracted with CH_2Cl_2 ($3 \times 75\text{ mL}$). The combined organic layers were dried over Na_2SO_4 and concentrated *in vacuo*. Purification by flash column chromatography (silica, *i*-Hex:EtOAc = 7:3 to 6:4 to 0:1) yielded alkyne **558** (6.81 g, 23.7 mmol, 75%) as a colorless oil, which slowly solidified upon prolonged drying *in vacuo*. Furthermore, amide **556** (3.01 g, 13.6 mmol) could be re-isolated.

Note: The employed LiCl had to be flame-dried thoroughly and needed to be ground under argon gas atmosphere. Yields were significantly lower when the LiCl was not dried or ground properly.

$R_f = 0.68$ (*i*-Hex:EtOAc = 1:3).

Melting point = $94.3\text{--}95.9\text{ }^{\circ}\text{C}$ (CH_2Cl_2).

^1H NMR (C_6D_6 , 400 MHz, major rotamer): $\delta = 7.34\text{--}7.28$ (m, 2H), $7.19\text{--}7.12$ (m, 2H), $7.11\text{--}7.06$ (m, 1H), 4.92 (s, br 1H), 4.55 (d, $J = 7.0\text{ Hz}$, 1H), 4.26 (s, br, 1H), $2.66\text{--}2.56$ (m,

1H), 2.39 (s, 3H), 2.12–2.00 (m, 2H), 1.99–1.88 (m, 1H), 1.52 (t, $J = 2.5$ Hz, 3H), 1.41 (m, 1H), 0.99 (d, $J = 6.9$ Hz, 3H), 0.96 (d, $J = 6.8$ Hz, 3H) ppm.

^1H NMR (C_6D_6 , 400 MHz, minor rotamer): $\delta = 7.34\text{--}7.28$ (m, 2H), 7.19–7.12 (m, 2H), 7.11–7.06 (m, 1H), 4.92 (s, br 1H), 4.25 (d, $J = 10.0$ Hz, 1H), 4.04 (m_{C} , 1H), 3.10 (m_{C} , 1H), 2.80 (s, 3H), 2.32–2.27 (m, 2H), 1.60 (t, $J = 2.4$ Hz, 3H), 1.04 (d, $J = 6.8$ Hz, 3H), 0.66 (d, $J = 6.7$ Hz, 3H) ppm.

^{13}C NMR (C_6D_6 , 100 MHz, major rotamer): $\delta = 177.7, 143.8, 128.4, 127.4, 126.8, 79.1, 76.4, 75.9, 59.5, 35.5, 33.5, 33.3$ (br), 17.3, 17.0, 14.4, 3.3 ppm.

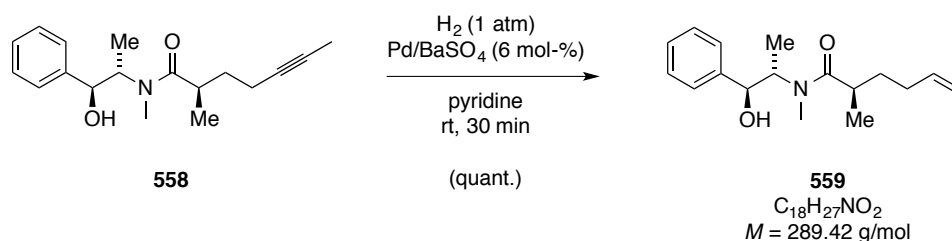
^{13}C NMR (C_6D_6 , 100 MHz, minor rotamer): $\delta = 176.6, 142.8, 128.7, 127.5, 126.8, 79.9, 76.2, 75.5, 58.1, 35.0, 33.7, 27.0, 18.1, 17.3, 15.4, 3.7$ ppm.

ESI-MS for $\text{C}_{18}\text{H}_{26}\text{NO}_2^+$ [MH^+]:
calcd. 288.1958.
found 288.1958.

IR (ATR): $\tilde{\nu}/\text{cm}^{-1} = 3374, 3030, 2968, 2933, 2874, 1613, 1451, 1409, 1374, 1302, 1257, 1199, 1108, 1080, 1049, 1028, 918, 838, 761, 700$.

$[\alpha]_{\text{D}}^{20} = +26.4$ (c 1.00, CH_2Cl_2).

Synthesis of Alkene 559



A suspension of Pd/BaSO_4 (740 mg, 5 wt-% Pd, 350 μmol , 5 mol-%) in dry pyridine (60 mL) was saturated with hydrogen *via* bubbling for 10 min. A solution of alkyne **558** (2.00 g, 6.96 mmol, 1.0 eq.) was then added and the reaction was stirred at room temperature under hydrogen atmosphere (1 atm) for 30 min. After filtration over Celite[®] (EtOAc washings), the reaction mixture was concentrated under reduced pressure. The crude product was purified by

flash column chromatography (silica, *i*-Hex:EtOAc = 1:1) to yield alkene **559** (2.00 g, 6.96 mmol, quant.) as a colorless oil.

R_f = 0.62 (*i*-Hex:EtOAc = 2:3).

^1H NMR (C_6D_6 , 400 MHz, major rotamer): δ = 7.36–7.34 (m, 2H), 7.25–7.14 (m, 2H), 7.12–7.05 (m, 1H), 5.49–5.41 (m, 1H), 5.38–5.28 (m, 1H), 4.98 (s, br, 1H), 4.55 (t, J = 6.9 Hz, 1H), 4.38 (s, br, 1H), 2.31 (s, 3H), 2.33–2.27 (m, 1H), 2.03–1.82 (m, 3H), 1.50 (d, J = 6.5 Hz, 3H), 1.34–1.24 (m, 1H), 0.98 (d, J = 6.7 Hz, 3H) 0.97 (d, J = 5.9 Hz, 3H) ppm.

^1H NMR (C_6D_6 , 400 MHz, minor rotamer): δ = 7.36–7.34 (m, 2H), 7.25–7.14 (m, 2H), 7.12–7.05 (m, 1H), 5.66–5.50 (m, 2H), 4.24 (d, J = 8.2 Hz, 1H), 3.93 (quin, J = 6.9 Hz, 1H), 3.12 (m, 1H), 2.86–2.80 (m, 1H), 2.83 (s, 3H), 2.26–2.12 (m, 3H), 1.64 (d, J = 6.5 Hz, 3H), 1.60–1.53 (m, 1H), 1.07 (d, J = 6.9 Hz, 3H), 0.68 (d, J = 6.7 Hz, 3H) ppm.

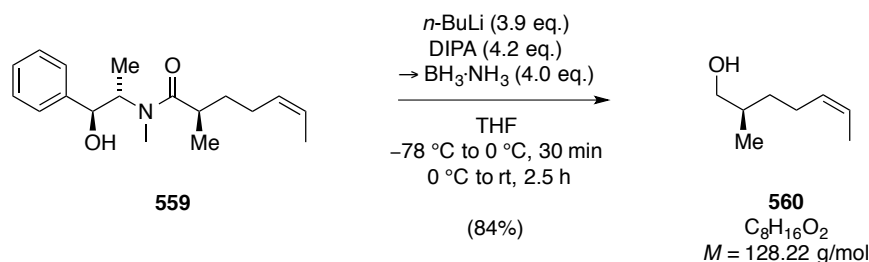
^{13}C NMR (C_6D_6 , 100 MHz, major rotamer): δ = 178.0, 143.8, 130.6, 128.4, 127.4, 126.9, 124.5, 76.4, 58.9 (br), 36.0, 34.0, 32.7 (br), 25.0, 17.7, 14.4, 12.9 ppm.

^{13}C NMR (C_6D_6 , 100 MHz, minor rotamer): δ = 176.9, 142.9, 131.3, 128.6, 127.4, 126.9, 124.2, 75.5, 58.1, 35.7, 34.3, 27.2, 25.4, 18.3, 15.4, 13.1 ppm.

ESI-MS for $\text{C}_{18}\text{H}_{28}\text{NO}_2^+$ [MH^+]: calcd. 290.21146.
 found 290.21149.

IR (ATR): $\tilde{\nu}/\text{cm}^{-1}$ = 3376, 3061, 3008, 2967, 2932, 2871, 1613, 1478, 1450, 1405, 1371, 1316, 1299, 1257, 1197, 1107, 1082, 1048, 1027, 986, 915, 837, 753, 698, 608.

$[\alpha]_D^{20}$ = +67.0 (c 1.00, CDCl_3).

Synthesis of Alcohol **560**

To a solution of diisopropylamine (4.07 mL, 29.0 mmol, 4.2 eq.) in THF (29 mL) at $-78\text{ }^\circ\text{C}$ was added $n\text{-BuLi}$ (8.70 mL, 3.10 M solution in hexanes, 27.0 mmol, 3.9 eq.) dropwise. The resulting mixture was stirred for 15 min at -78 and another 15 min at $0\text{ }^\circ\text{C}$. Then, borane-ammonia complex (0.85 g, 27.7 mmol, 4.0 eq.) was added in one portion. The resulting mixture was stirred for 15 min at $0\text{ }^\circ\text{C}$ and for 15 min at room temperature, before being cooled to $0\text{ }^\circ\text{C}$ again. Subsequently, a solution of alkene **559** (2.0 g, 6.96 mmol, 1.0 eq.) in THF (17 mL) was added dropwise over a period of 10 min and the resulting solution was stirred at room temperature for two hours. After cooling to $0\text{ }^\circ\text{C}$, aqueous HCl (3 M, 60 mL) was added slowly and the mixture was stirred for 10 min at room temperature. The layers were separated and the aqueous phase was extracted with Et_2O ($4 \times 10\text{ mL}$). The combined organic layers were dried over Na_2SO_4 and carefully concentrated under reduced pressure (400 mbar, $30\text{ }^\circ\text{C}$). The crude product was purified by flash column chromatography (silica, $n\text{-pentane}:\text{Et}_2\text{O} = 17:3$ to $7:3$) to yield alcohol **560** (747 mg, 5.82 mmol, 84%) as a colorless liquid.

$R_f = 0.84$ ($i\text{-Hex}:\text{EtOAc} = 3:2$).

^1H NMR (CDCl_3 , 400 MHz): $\delta = 5.41$ (m_C , 2H), 3.54–3.49 (m, 1H), 3.46–3.41 (m, 1H), 2.18–1.96 (m, 2H), 1.69–1.57 (m, 4H), 1.47 (dddd, $J = 13.3, 9.3, 6.7, 5.3\text{ Hz}$, 1H), 1.35 (s, br, 1H), 1.18 (dddd, $J = 13.3, 9.3, 8.2, 6.0\text{ Hz}$, 1H), 0.94 (d, $J = 6.7\text{ Hz}$, 3H) ppm.

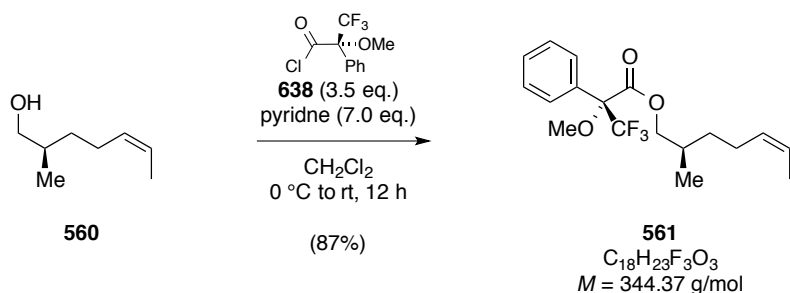
^{13}C NMR (CDCl_3 , 100 MHz): $\delta = 130.7, 124.1, 68.4, 35.5, 33.0, 24.4, 16.6, 12.9\text{ ppm}$.

EI-MS for $\text{C}_8\text{H}_{16}\text{O}^+$ [M^+]:	calcd.	128.1196.
	found	128.1185.

IR (ATR): $\tilde{\nu}/\text{cm}^{-1}$ = 3332, 3012, 2953, 2915, 2872, 1656, 1454, 1403, 1376, 1251, 1225, 1190, 1099, 1034, 995, 905, 763, 698, 628, 619, 605.

$[\alpha]_D^{20}$ = +8.0 (c 0.50, CDCl_3).

Preparation of Mosher Ester **561**



To a solution of alcohol **560** (3.0 mg, 23.4 μmol , 1.0 eq.) in CH_2Cl_2 (1.0 mL) were consecutively added pyridine (13 μL , 0.16 mmol, 7.0 eq.) and (*R*)-Mosher's acid chloride (**638**, 15 μL , 81.9 μmol , 3.5 eq.) at 0 $^\circ\text{C}$. The resulting mixture was stirred for 12 hours at room temperature. The reaction was quenched by the addition of half-saturated aqueous NaHCO_3 (10 mL) and was then extracted with CH_2Cl_2 ($3 \times 10 \text{ mL}$). The combined organic layers were dried over Na_2SO_4 and concentrated under reduced pressure. ^1H NMR analysis of the crude reaction mixture did not indicated the existence of any second diastereomer. The crude product was purified *via* flash column chromatography (silica, *n*-pentane/ Et_2O = 199:1) to yield ester **561** (7 mg, 20.3 μmol , 87%) as a colourless wax.

Note: ^{19}F NMR spectra recorded of the purified product revealed a diastereomeric mixture of Mosher ester **561** of 99:1.

R_f = 0.50 (*i*-Hex: EtOAc = 25:1).

^1H NMR (CDCl_3 , 400 MHz): δ = 7.54–7.49 (m, 2H), 7.42–7.38 (m, 3H), 5.48–5.39 (m, 1H), 5.34–5.27 (m, 1H), 4.21–4.13 (m, 2H), 3.55 (m_C , 3H), 2.10–1.97 (m, 2H), 1.92–1.84 (m, 1H), 1.59 (d, J = 6.7 Hz, 3H), 1.45–1.38 (m, 1H), 1.31–1.17 (m, 1H), 0.94 (d, J = 6.8 Hz, 3H) ppm.

^{13}C NMR (CDCl_3 , 100 MHz): δ = 166.8, 132.5, 130.0, 129.7, 128.5, 127.5, 124.4, 84.8 (q, J = 27.5 Hz), 71.2, 55.6, 32.9, 32.2, 29.9, 24.1, 16.8, 12.9 ppm.

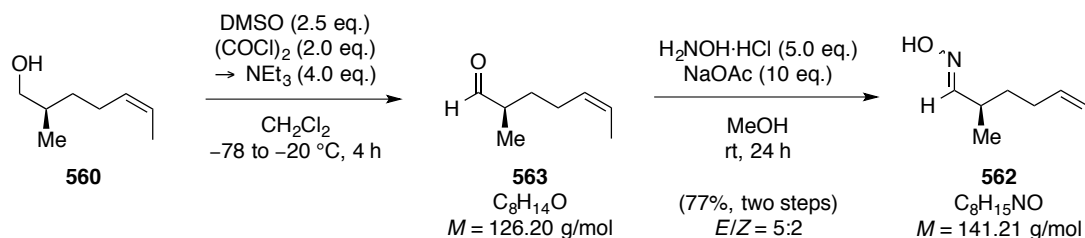
^{19}F NMR (CDCl_3 , 382 MHz): $\delta = -71.4$ (minor), -71.6 (major) ppm

ESI-MS for $\text{C}_{18}\text{H}_{23}\text{ClF}_3\text{O}_3^-$ $[(\text{M}+\text{Cl})^-]$: calcd. 379.12878.
found 379.12886.

IR (ATR): $\tilde{\nu}/\text{cm}^{-1} = 3067, 3012, 2958, 2856, 1746, 1658, 1606, 1497, 1463, 1451, 1404, 1388, 1378, 1259, 1167, 1121, 1106, 1081, 1019, 1001, 966, 917, 802, 764, 718, 695$.

$[\alpha]_D^{20} = +28.0$ (c 0.1, CDCl_3).

Synthesis of Oxime **562**



To a solution of dry DMSO (1.04 mL, 14.6 mmol, 2.5 eq.) in CH_2Cl_2 (50 mL) was added oxalyl chloride (5.85 mL, 2 M solution in CH_2Cl_2 , 11.7 mmol, 2.0 eq.) dropwise at -78 °C. The resulting mixture was stirred for 15 min, before a solution of alcohol **560** (750 mg, 5.85 mmol, 1.0 eq.) in CH_2Cl_2 (4 mL) was added over a period of 10 min. Stirring was continued for two hours, at which Et_3N (3.24 mL, 23.4 mmol, 4.0 eq.) was added slowly. This mixture was stirred for an additional two hours at -78 °C, before being gradually warmed to -20 °C over one hour. The reaction was quenched by addition of aqueous phosphate buffer (10 mL, 2 M, pH = 6.5) and the layers were separated. The aqueous phase was extracted with Et_2O (4×10 mL). The combined organic layers were subsequently dried over Na_2SO_4 and carefully concentrated under reduced pressure (400 mbar, 30 °C). The crude product was purified by flash column chromatography (silica, n -pentane: Et_2O = 19:1) to yield aldehyde **563** (628 mg, 4.97 mmol, 85%) as a 2:15 mixture with n -pentane as a colorless liquid, which was immediately used in the next step.

$R_f = 0.95$ (i -Hex: EtOAc = 10:1).

To a mixture of hydroxylamine hydrochloride (1.45 g, 20.9 mmol, 5.0 eq.) and NaOAc (3.43 g, 41.8 mmol, 10 eq.) in MeOH (26 mL), a solution of aldehyde **563** (528 mg, 12 mol-% solution in *n*-pentane, 4.19 mmol, 1.0 eq.) in MeOH (2 mL) was added. The reaction was stirred for 24 hours at room temperature before being quenched by the addition of half-saturated aqueous NaHCO₃ (20 mL). After extraction with Et₂O (4 × 25 mL) the combined organic layers were dried over Na₂SO₄ and concentrated under reduced pressure (300 mbar, 30 °C). The crude product was purified by flash column chromatography (silica, *n*-pentane:Et₂O = 9:1 to 4:1) to yield oxime **562** (639 mg, 4.52 mmol, 72%) as a colorless liquid as a 5:2 mixture of *E/Z* isomers and in a 21:1 mixture with *n*-pentane.

Note: The stated yields were deduced from ¹H NMR of respective mixtures with n-pentane. A spectroscopically pure sample of oxime 562 was obtained by repeated concentration from CDCl₃.

$R_f(E\text{-}\mathbf{562}) = 0.32$ (*i*-Hex:EtOAc = 20:1).

$R_f(Z\text{-}\mathbf{562}) = 0.30$ (*i*-Hex:EtOAc = 20:1).

¹H NMR (CDCl₃, 400 MHz, *E*-**562**): δ = 8.06 (s, br, 1H), 7.30 (d, J = 7.0 Hz, 1H), 5.52–5.28 (m, 2H), 2.39 (sept, J = 6.9 Hz, 1H), 2.06 (m, 2H), 1.59 (m, 3H), 1.56–1.34 (m, 2H), 1.09 (d, J = 6.9 Hz, 3H) ppm.

¹H NMR (CDCl₃, 400 MHz, *Z*-**562**): δ = 8.33 (s, br, 1H), 6.53 (d, J = 7.7 Hz, 1H), 5.54–5.26 (m, 2H), 3.16 (sept, J = 6.9 Hz, 1H), 2.06 (m, 2H), 1.64–1.55 (m, 3H), 1.55–1.32 (m, 2H), 1.05 (d, J = 6.9 Hz, 3H) ppm.

¹³C NMR (CDCl₃, 100 MHz, *E*-**562**): δ = 156.5, 129.8, 124.6, 34.5, 34.2, 24.5, 18.1, 12.9 ppm.

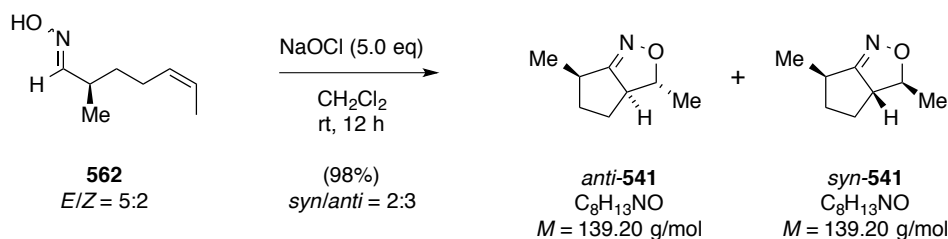
¹³C NMR (CDCl₃, 100 MHz, *Z*-**562**): δ = 157.4, 129.9, 124.5, 34.6, 29.4, 24.8, 17.5, 12.9 ppm.

EI-MS for C ₈ H ₁₅ NO ⁺ [M ⁺]:	calcd.	141.1154.
	found	141.1154.

IR (ATR): $\tilde{\nu}/\text{cm}^{-1}$ = 3274, 3012, 2962, 2918, 2854, 1657, 1453, 1404, 1375, 1332, 1308, 1278, 1122, 1081, 1029, 948, 933, 873, 702.

$[\alpha]_D^{20} = -18.4$ (c 0.50, CDCl_3).

Synthesis of Isoxazole **541**



To a solution of oxime **562** (580 mg, 4.11 mmol, 1.0 eq.) in CH_2Cl_2 (22 mL) was slowly added aqueous NaOCl (22 mL, 7 wt-% NaOCl, 20.5 mmol, 5.0 eq.). The resulting mixture was stirred at room temperature for 12 hours, before being diluted with H_2O (20 mL) and Et_2O (25 mL). The layers were separated and the aqueous phase was extracted with Et_2O ($4 \times 10 \text{ mL}$). The combined organic layers were dried over Na_2SO_4 and carefully concentrated under reduced pressure (400 mbar, 30°C). The crude product was purified by flash column chromatography (silica, n -pentane: Et_2O = 4:1) to yield isoxazole **541** (543 mg, 4.03 mmol, 98%) as a colorless liquid as a *syn/anti* isomeric mixture of 2:3.

Note: The syn/anti isomeric ratio of compound 541 was determined via GCMS measurements. The identity of the isomers was deduced from NOESY and HMBC NMR spectra.

$R_f = 0.44$ (i -Hex: EtOAc = 10:1).

^1H NMR (CDCl_3 , 400 MHz, signals not separable): δ = 4.75 (m_C , 1H), 3.89–3.74 (m, 1H), 2.83–2.71 (m, 1H), 2.52 – 2.32 (m, 1H), 1.84–1.54 (m, 3H), 1.25–1.22 (2d, J = 7.1, 6.8 Hz, 3H), 1.12–1.09 (2d, J = 6.6, 6.6 Hz, 3H) ppm.

^{13}C NMR (CDCl_3 , 100 MHz, *anti*-**541**): δ = 174.3, 78.7, 57.0, 38.9, 29.7, 22.8, 18.8, 16.5 ppm.

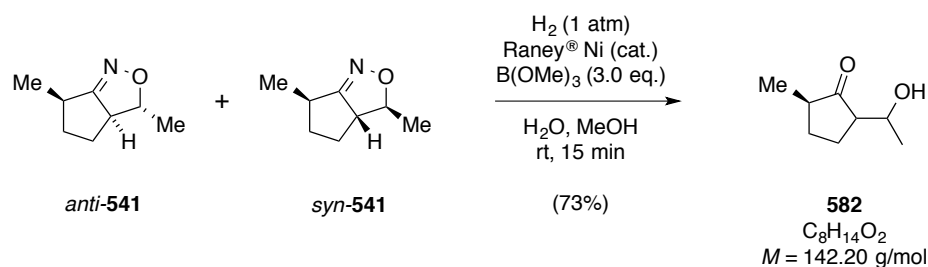
^{13}C NMR (CDCl_3 , 100 MHz, *syn*-**541**): δ = 174.4, 79.2, 57.3, 38.2, 30.1, 20.8, 17.4, 16.2 ppm.

EI-MS for $C_8H_{13}NO^+$ [M^+]:
calcd. 139.0992.
found 139.0984.

IR (ATR): $\tilde{\nu}/cm^{-1}$ = 2964, 2928, 2870, 1452, 1374, 1334, 1295, 1250, 1177, 1167, 1140, 1109, 1084, 1046, 1017, 994, 948, 910, 862, 830, 812, 770, 730, 660.

$[\alpha]_D^{20} = +8.4$ (c 0.50, $CDCl_3$).

Synthesis of Alcohol **582**



To a solution of isoxazole **541** (200 mg, 1.44 mmol, 1.0 eq.) in MeOH (20 mL) and H_2O (4 mL) was consecutively added $B(OMe)_3$ (490 μ L, 4.30 mmol, 3.0 eq.) and Raney[®] Ni 2400 (0.1 mL, 50 wt-% suspension in MeOH). The reaction mixture was purged with hydrogen (3 times) and stirred under an hydrogen atmosphere (1 atm) for 30 min. After diluting the reaction with H_2O (20 mL) and Et_2O (50 mL), the layers were separated and the aqueous phase was extracted with Et_2O (4×10 mL). The combined organic layers were dried over Na_2SO_4 and then carefully concentrated under reduced pressure (400 mbar, 30 $^\circ C$). The crude product was purified by flash column chromatography (silica, n -pentane: Et_2O = 7:3 to 3:2) to yield alcohol **582** (150 mg, 1.06 mmol, 73%) as a mixture of all four possible diastereomers.

Note: Due to the obtained mixture of diastereomers, interpretation of the 1H NMR spectrum proved to be extremely complicated. As a consequence, only the ^{13}C shifts for all isomers are reported.

$R_f = 0.25$ – 0.30 (i -Hex: $EtOAc$ = 10:1).

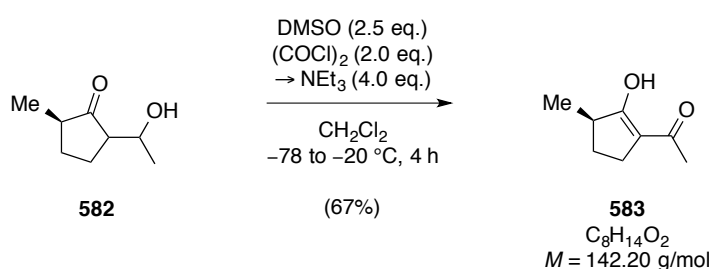
^{13}C NMR ($CDCl_3$, 150 MHz): δ = 225.4, 225.2, 223.5, 222.6, 69.1, 67.0, 66.9, 66.5, 55.5, 55.1, 54.5 (2C), 45.6, 44.8, 43.4, 43.0, 29.8 (2C), 29.3, 28.8, 24.9, 23.9, 22.5, 21.6, 21.5, 21.3, 21.0, 20.9, 15.3, 14.6, 14.4, 14.2 ppm.

EI-MS for $\text{C}_8\text{H}_{14}\text{O}_2^+$ [M^+]: calcd. 142.0994.
 found 142.0993.

IR (ATR): $\tilde{\nu}/\text{cm}^{-1}$ = 3453, 2964, 2932, 2871, 1727, 1453, 1395, 1373, 1329, 1282, 1250, 1155, 1128, 1096, 1049, 1017, 986, 949, 917, 887, 852, 835, 742, 600.

$[\alpha]_D^{20} = -69.6$ (c 0.33, CDCl_3).

Synthesis of Diketone **583**



To a solution of dry DMSO (161 μL , 2.29 mmol, 2.5 eq.) in CH_2Cl_2 (8.8 mL) was added oxalyl chloride (914 μL , 2 M solution in CH_2Cl_2 , 1.83 mmol, 2.0 eq.) dropwise at -78°C . The resulting mixture was stirred for 15 min before a solution of alcohol **582** (130 mg, 0.91 mmol, 1.0 eq.) in CH_2Cl_2 (1.5 mL) was added over a period of 10 min. Stirring was continued for two hours. Thereafter, Et_3N (622 μL , 3.66 mmol, 4.0 eq.) was added slowly. This reaction was stirred for an additional two hours at -78°C , before being warmed gradually to -20°C over one hour. The reaction was quenched by the addition of aqueous phosphate buffer (5 mL, 2 M, pH = 6.5) and the layers were separated. The aqueous phase was extracted with Et_2O ($4 \times 10 \text{ mL}$) and the combined organic layers were subsequently dried over Na_2SO_4 and carefully concentrated *in vacuo* (400 mbar, 30°C). Purification by flash column chromatography (silica, *n*-pentane: Et_2O = 19:1 to 9:1) yielded diketone **583** (86 mg, 6.13 mmol, 67%) as a colorless liquid.

*Note: ^1H NMR revealed that diketone **583** exists predominately as the depicted enol tautomer and is in equilibrium with both possible diastereomers of the diketo form.*

$R_f = 0.85$ (*i*-Hex: EtOAc = 3:1).

^1H NMR (CDCl_3 , 400 MHz, only major tautomer quoted): δ = 13.47 (s, br, 1H), 2.48 (m, 3H), 2.53–2.42 (m, 2H), 1.98 (s, 3H), 1.46 (dq, J = 12.5, 8.9 Hz, 1H), 1.14 (d, J = 7.0 Hz, 3H)

ppm. Characteristic signals for the diketo tautomers: $\delta = 3.51$ (dd, $J = 8.6, 4.0$ Hz, 1H), 3.38 (dd, $J = 9.9, 8.3$ Hz, 1H), 2.34 (s, 3H), 2.32 (s, 3H) ppm.

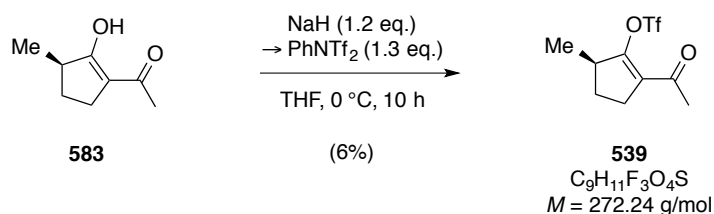
^{13}C NMR (CDCl_3 , 100 MHz, only major tautomer quoted): $\delta = 207.9, 174.9, 109.6, 42.7, 29.9, 24.1, 20.6, 15.4$ ppm. Characteristic signals for the diketo tautomers: $\delta = 214.5, 214.0, 202.8, 202.2$ ppm.

ESI-MS for $\text{C}_8\text{H}_{11}\text{O}_2^-$ [(M-H) $^-$]:
calcd. 139.07645.
found 139.07644.

IR (ATR): $\tilde{\nu}/\text{cm}^{-1} = 2963, 2931, 2871, 1742, 1709, 1654, 1608, 1453, 1430, 1385, 1357, 1321, 1283, 1218, 1177, 1144, 1083, 1033, 994, 967, 948, 889, 729, 706$.

$[\alpha]_D^{20} = -16.8$ (c 0.33, CDCl_3).

Synthesis of Triflate **539**



To a stirred suspension of NaH (17 mg, 60 wt-% in mineral oil, 428 μmol , 1.2 eq.) in THF (1.4 mL) was added a solution of diketone **583** (50 mg, 357 μmol , 1.0 eq.) in THF (350 μL) dropwise at 0 $^\circ\text{C}$ and the mixture was stirred for 30 min. Then, a solution of PhNTf₂ (159 mg, 446 μmol , 1.3 eq.) in THF (350 μL) was added and the reaction was stirred for 10 hours at 0 $^\circ\text{C}$. Subsequently, the reaction was diluted with H₂O (10 mL) and extracted with Et₂O (3 \times 15 mL). The combined organic layers were dried over Na₂SO₄ and concentrated under reduced pressure (500 mbar, 30 $^\circ\text{C}$). The crude product was purified by flash column chromatography (silica, *n*-pentane:Et₂O = 19:1 to 9:1) to yield the title compound **539** (5.4 mg, 19.8 μmol , 6%) as a colorless oil.

$R_f = 0.45$ (*i*-Hex:EtOAc = 20:1).

^1H NMR (CDCl_3 , 400 MHz): δ = 3.16 (m_C , 1H), 2.67–2.62 (m, 2H), 2.36 (s, 3H), 2.24 (m_C , 1H), 1.62–1.53 (m, 2H), 1.22 (d, J = 6.9 Hz, 3H) ppm.

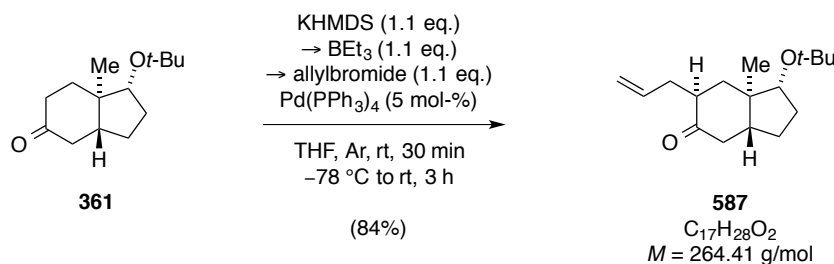
^{13}C NMR (CDCl_3 , 100 MHz): δ = 194.7, 156.0, 129.7, 118.4 (q, J = 320 Hz), 39.7, 29.9, 27.8, 18.0 ppm.

EI-MS for $\text{C}_9\text{H}_{11}\text{F}_3\text{O}_4\text{S}^+ [\text{M}^+]$:
 calcd. 272.0330.
 found 272.0347.

IR (ATR): $\tilde{\nu}/\text{cm}^{-1}$ = 2970, 2938, 2878, 1698, 1677, 1639, 1457, 1424, 1379, 1362, 1337, 1289, 1248, 1203, 1168, 1135, 1099, 1082, 1034, 976, 921, 905, 876, 834, 768, 707, 661.

$[\alpha]_D^{20}$ = +70.8 (c 0.33, CDCl_3).

Synthesis of Alkene **587**



KHMDS (35.3 mL, 0.5 M solution in toluene, 17.7 mmol, 1.1 eq.) was added to a solution of hydrindanone **361** (3.60 g, 16.1 mmol, 1.0 eq.) in dry THF (144 mL) at room temperature. The yellow mixture was stirred for 30 min before being cooled to $-78\text{ }^\circ\text{C}$. After the slow addition of triethylborane (17.7 mL, 1.0 M freshly prepared solution in THF, 17.7 mmol, 1.1 eq.) the reaction was stirred for 5 min before $\text{Pd}(\text{PPh}_3)_4$ (927 mg, 0.80 mmol, 5 mol-%) and subsequently a solution of allyl bromide (1.53 mL, 17.7 mmol, 1.1 eq.) in dry THF (14 mL) were added. The mixture was allowed to warm to room temperature and then stirred for another 2.5 hours. The reaction was quenched *via* addition of saturated aqueous NH_4Cl (100 mL) and then diluted with diethyl ether (200 mL). The layers were separated and the aqueous phase was extracted with diethyl ether ($3 \times 100\text{ mL}$). The combined organic layers were dried over Na_2SO_4 , concentrated *in vacuo* and the resulting crude product was purified by flash column chromatography (silica, *i*-Hex:EtOAc = 40:1 to 20:1) to yield alkene **587** (3.58 g, 13.5 mmol, 84%) as colorless oil and as single diastereomer.

$R_f = 0.75$ (*i*-Hex:EtOAc = 13:1).

^1H NMR (CDCl_3 , 600 MHz): $\delta = 5.75$ (dddd, $J = 16.8, 10.1, 7.6, 6.5$ Hz, 1H), 5.01–4.96 (m, 2H), 3.43 (dd, $J = 8.9, 7.5$ Hz, 1H), 2.54 (m_C , 1H), 2.40 (m_C , 1H), 2.36–2.27 (m, 2H), 2.05 (dd, $J = 12.8, 6.2$ Hz, 1H), 2.00–1.94 (m, 2H), 1.65 (dddd, $J = 13.2, 11.9, 7.0, 4.9$ Hz, 1H), 1.60–1.53 (m, 2H), 1.44–1.37 (m, 1H), 1.12 (s, 9H), 1.07 (t, $J = 12.6$ Hz, 1H), 1.00 (s, 3H) ppm.

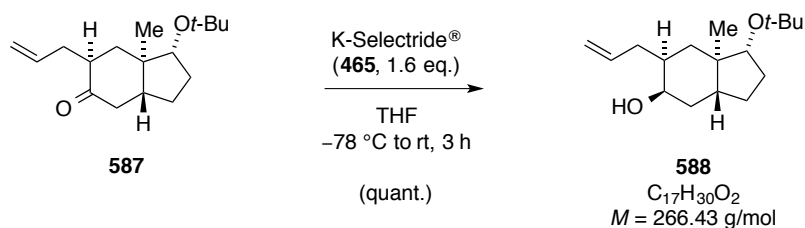
^{13}C NMR (CDCl_3 , 150 MHz): $\delta = 212.0, 136.8, 116.3, 79.5, 72.7, 45.8, 45.3, 43.0, 42.7, 42.3, 34.1, 31.9, 28.8, 25.9, 11.3$ ppm.

EI-MS for $\text{C}_{17}\text{H}_{28}\text{O}_2^+ [\text{M}^+]$:
calcd. 264.2089
found 264.2071.

IR (ATR): $\tilde{\nu}/\text{cm}^{-1} = 2974, 2934, 2875, 2851, 1701, 1642, 1462, 1431, 1386, 1361, 1296, 1259, 1228, 1190, 1142, 1110, 1026, 998, 967, 916, 899, 849, 774, 754, 723, 693$.

$[\alpha]_D^{20} = -32.8$ (c 1.00, CH_2Cl_2).

Synthesis of Alcohol **588**



To a stirred solution of alkene **587** (3.50 g, 13.2 mmol, 1.0 eq.) in dry THF (130 mL) at $-78\text{ }^\circ\text{C}$ was added K-Selectride[®] (**465**, 20.5 mL, 1 M solution in THF, 20.5 mmol, 1.6 eq.) dropwise over a period of 20 min. After being stirred for further 10 min at this temperature, the reaction mixture was allowed to warm to room temperature over the course of two hours. Then, the reaction was cooled to $0\text{ }^\circ\text{C}$ and excess reagent was quenched with methanol (25 mL). Subsequently, aqueous NaOH (3 M, 47 mL) and H_2O_2 (30 wt-%, 35 mL) were added and the biphasic mixture was thoroughly stirred for two hours at room temperature. Thereafter, saturated aqueous NH_4Cl (50 mL) was added and the mixture was extracted with diethyl ether (3×150 mL). The combined organic layers were dried over Na_2SO_4 ,

concentrated *in vacuo* and the resulting crude product was purified by flash column chromatography (silica, *i*-Hex:EtOAc = 20:1 to 10:1) to yield alcohol **588** (3.51 g, 13.2 mmol, quant.) as colorless oil and as single diastereomer.

R_f = 0.60 (*i*-Hex:EtOAc = 10:1).

^1H NMR (CDCl_3 , 600 MHz): δ = 5.82 (dddd, J = 16.9, 10.1, 7.6, 6.7 Hz, 1H), 5.05 (m_C , 1H), 5.00 (m_C , 1H), 3.91 (q, J = 2.8 Hz, 1H), 3.43 (dd, J = 8.9, 7.4 Hz, 1H), 2.18–2.13 (m, 1H), 2.04–1.99 (m, 1H), 1.93–1.86 (m, 1H), 1.71–1.63 (m, 3H), 1.53–1.40 (m, 5H), 1.31–1.24 (m, 1H), 1.11 (s, 9H), 1.08 (t, J = 12.7 Hz, 1H), 0.72 (s, 3H) ppm.

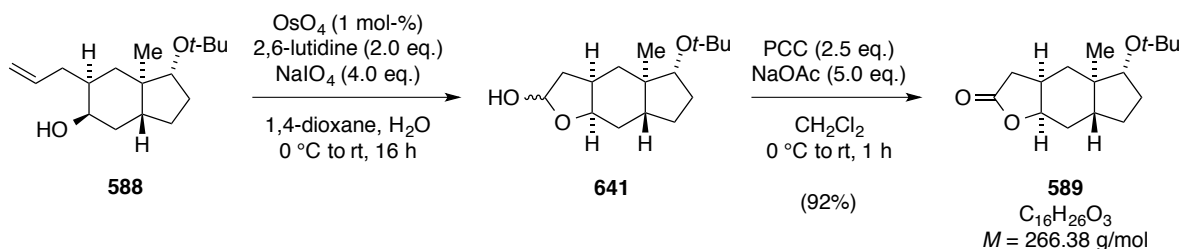
^{13}C NMR (CDCl_3 , 150 MHz): δ = 137.7, 115.8, 80.6, 72.3, 68.9, 43.0, 38.6, 37.6, 37.5, 37.4, 33.6, 31.3, 28.9, 25.6, 10.9 ppm.

EI-MS for $\text{C}_{17}\text{H}_{28}\text{O}^+$ [(M-H₂O)⁺]:
calcd. 248.2140
found 248.2136.

IR (ATR): $\tilde{\nu}/\text{cm}^{-1}$ = 3390, 3076, 2973, 2927, 11462, 1441, 1388, 1361, 1311, 1253, 1195, 1127, 1110, 1065, 1028, 1004, 976, 948, 906, 863, 753.

$[\alpha]_D^{20}$ = -45.2 (c 1.00, CH_2Cl_2).

Synthesis of Lactone **589**



To a stirred solution of alcohol **588** (2.70 g, 10.1 mmol, 1.0 eq.) in 1,4-dioxane (114 mL) and water (37 mL) at 0 °C was added 2,6-lutidine (2.35 mL, 20.3 mmol, 2.0 eq.) and then OsO_4 (0.64 mL, 4 wt-% solution in H_2O , 0.10 mmol, 1 mol-%). Subsequently, NaIO_4 (8.67 g, 40.5 mmol, 4.0 eq.) was added in one portion and the resulting mixture was allowed to warm to room temperature. After being stirred for 16 hours, the reaction was diluted with water (200 mL) and extracted with CH_2Cl_2 (4×100 mL). The combined organic layers were dried

over Na₂SO₄, concentrated *in vacuo* to yield lactol **641** ($R_f = 0.20$, *i*-Hex:EtOAc = 4:1) as colorless solid as inconsequential mixture of epimers, requiring no further purification.

Thus obtained lactol **641** was re-dissolved in dry CH₂Cl₂ (35 mL) and then slowly added to an ice-cold stirred suspension of PCC (5.46 g, 25.3 mmol, 2.5 eq.) in dry CH₂Cl₂ (148 mL) over the course of 15 min. The resulting mixture was allowed to warm to room temperature and stirred for further 45 min. After being directly applied to flash column chromatography (silica, *i*-Hex:EtOAc = 3:1), the still crude product was purified *via* a second flash column chromatography (silica, *i*-Hex:EtOAc = 10:1 to 9:1) step to yield title lactone **589** (2.50 g, 9.31 mmol, 92%) as a colorless solid.

$R_f = 0.55$ (*i*-Hex:EtOAc = 4:1).

Melting point = 120.0–121.3 °C (CH₂Cl₂).

¹H NMR (CDCl₃, 600 MHz): δ = 4.56 (td, J = 4.0, 2.0 Hz, 1H), 3.39 (dd, J = 8.9, 7.8 Hz, 1H), 2.73 (dd, J = 16.8, 7.0 Hz, 1H), 2.51 (m_C, 1H), 2.20 (d, J = 16.8 Hz, 1H), 2.11 (dt, J = 14.0, 2.4 Hz, 1H), 1.95–1.88 (m, 1H), 1.81 (dd, J = 13.1, 6.4 Hz, 1H), 1.62–1.42 (m, 4H), 1.30 (qd, J = 11.8, 6.2 Hz, 1H), 1.12 (s, 9H), 0.90 (t, J = 12.6 Hz, 1H), 0.72 (s, 3H) ppm.

¹³C NMR (CDCl₃, 150 MHz): δ = 177.4, 80.2, 80.1, 72.6, 42.1, 39.5, 38.4, 37.0, 33.1, 30.8, 28.9, 28.5, 25.3, 10.4 ppm.

EI-MS for C ₁₆ H ₂₆ O ₃ ⁺ [M ⁺]:	calcd. 266.1882
	found 266.1882.

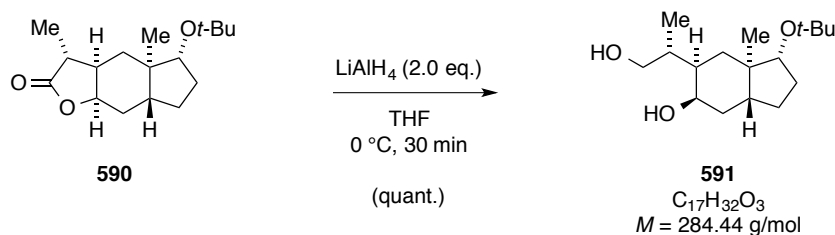
IR (ATR): $\tilde{\nu}/\text{cm}^{-1}$ = 2972, 2934, 2869, 1763, 1464, 1426, 1390, 1363, 1334, 1293, 1278, 1254, 1241, 1214, 1194, 1179, 1156, 1121, 1098, 1062, 1043, 1028, 999, 966, 946, 912, 880, 858, 818, 738, 693.

$[\alpha]_D^{20} = -13.6$ (c 1.00, CH₂Cl₂).

IR (ATR): $\tilde{\nu}/\text{cm}^{-1}$ = 2964, 2937, 2877, 1764, 1458, 1385, 1360, 1311, 1200, 1184, 1128, 1107, 1084, 1061, 1042, 1024, 976, 945, 905, 882, 808, 716, 674.

$[\alpha]_D^{20}$ = +4.2 (c 1.00, CH_2Cl_2).

Synthesis of Diol **591**



A solution of lactone **590** (2.72 g, 9.70 mmol, 1.0 eq.) in dry THF (36 mL) was slowly added to a stirred suspension of LiAlH_4 (0.74 g, 19.4 mmol, 2.0 eq.) in dry THF (54 mL) at 0 °C over the course of 20 min. The resulting mixture was stirred for another 30 min at this temperature before being carefully quenched *via* the addition of half-saturated Rochelle salt (80 mL). After being vigorously stirred for another hour, CH_2Cl_2 (200 mL) was added and the layers were separated. The aqueous phase was extracted with CH_2Cl_2 ($3 \times 200 \text{ mL}$) and the combined organic layers were dried over Na_2SO_4 . Concentration under reduced pressure yielded diol **591** (2.75 g, 9.70 mmol, quant.) as colorless solid, which required no further purification.

R_f = 0.35 (CH_2Cl_2 : MeOH = 20:1).

Melting point = 130.3–131.8 °C (CH_2Cl_2 / MeOH).

^1H NMR (CDCl_3 , 600 MHz): δ = 4.08 (q, J = 2.8 Hz, 1H), 3.65–3.52 (m, 2H), 3.60 (s, br, 2H), 3.46 (dd, J = 8.9, 7.3 Hz, 1H), 1.89 (m_c , 1H), 1.75–1.62 (m, 3H), 1.52–1.39 (m, 5H), 1.30–1.23 (m, 2H), 1.12 (s, 9H), 0.98 (d, J = 7.1 Hz, 3H), 0.71 (s, 3H) ppm.

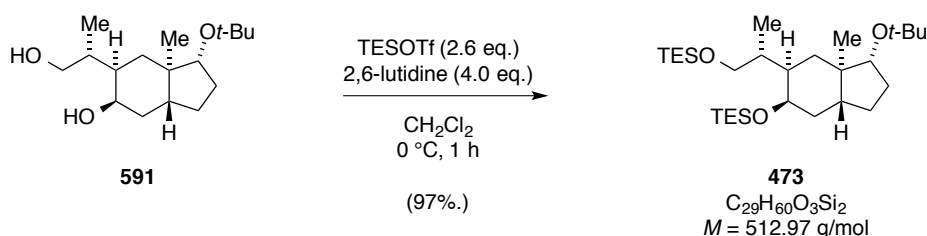
^{13}C NMR (CDCl_3 , 150 MHz): δ = 80.8, 72.4, 66.6, 65.4, 43.0, 42.2, 38.2, 37.6, 37.5, 33.5, 31.4, 28.9, 25.6, 16.3, 10.9 ppm.

EI-MS for $C_{17}H_{32}O_3^+ [M^+]$: calcd. 284.2351
 found 284.2330.

IR (ATR): $\tilde{\nu}/\text{cm}^{-1}$ = 3149, 2969, 2928, 2909, 2869, 1461, 1437, 1377, 1359, 1342, 1292, 1278, 1253, 1233, 1191, 1161, 1117, 1090, 1066, 1050, 1033, 1005, 969, 936, 903, 877, 860, 822, 731.

$[\alpha]_D^{20} = -40.0$ (c 1.00, CH_2Cl_2).

Synthesis of Bis-silyl Ether **473**



To a solution of diol **591** (3.29 g, 11.6 mmol, 1.0 eq.) in dry CH_2Cl_2 (110 mL) was added 2,6-lutidine (5.36 mL, 46.3 mmol, 4.0 eq.) and then TESOTf (6.80 mL, 30.7 mmol, 2.6 eq.) dropwise at 0 °C. After being stirred for one hour at this temperature, the reaction was quenched with saturated aqueous NaHCO_3 (66 mL) and the resulting layers were separated. The aqueous phase was extracted with CH_2Cl_2 ($3 \times 150\text{ mL}$), the combined organic layers were dried over Na_2SO_4 and concentrated under reduced pressure. Purification *via* flash column chromatography (silica, *i*-Hex:EtOAc = 100:1 to 75:1) yielded bis-silyl ether **473** (5.73 g, 11.2 mmol, 97%) as colorless oil.

$R_f = 0.95$ (*i*-Hex:EtOAc = 40:1).

^1H NMR (CDCl_3 , 600 MHz): δ = 4.01 (q, J = 2.7 Hz, 1H), 3.52 (dd, J = 9.6, 4.9 Hz, 1H), 3.53–3.41 (m, 2H), 1.90 (m_C , 1H), 1.76–1.67 (m, 2H), 1.56–1.52 (m, 2H), 1.46–1.38 (m, 4H), 1.25 (qd, J = 12.3, 6.5 Hz, 1H), 1.14 (s, 9H), 0.96 (t, J = 8.0 Hz, 18H), 0.89 (d, J = 6.9 Hz, 3H), 0.70 (s, 3H), 0.64–0.54 (m, 12H) ppm.

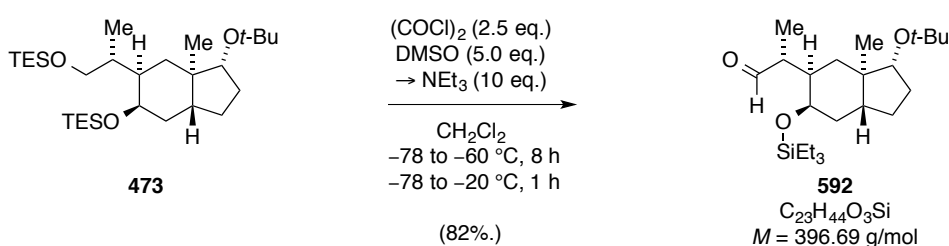
^{13}C NMR (CDCl_3 , 150 MHz): δ = 81.0, 72.3, 70.5, 66.5, 42.7, 38.7, 37.4, 35.0, 34.7, 31.5, 29.0, 25.6, 15.1, 11.1, 7.2, 5.5, 4.6 ppm.

EI-MS for $C_{29}H_{60}O_3Si_2^+$ [M^+]: calcd. 512.4081
 found 512.4071.

IR (ATR): $\tilde{\nu}/cm^{-1}$ = 2954, 2911, 2876, 1459, 1414, 1388, 1361, 1238, 1195, 1060, 1005, 975, 944, 902, 861, 796, 723.

$[\alpha]_D^{20} = -23.8$ (c 1.00, CH_2Cl_2).

Synthesis of Aldehyde **592**



To a solution of DMSO (760 μ L, 10.7 mmol, 5.0 eq.) in dry CH_2Cl_2 (21 mL) was added oxalyl chloride (2.67 mL, 2 M solution in CH_2Cl_2 , 5.34 mmol, 2.5 eq.) dropwise at -78 °C. The resulting mixture was stirred for 15 min before a solution of bis-silyl ether **473** (1.06 g, 2.14 mmol, 1.0 eq.) in CH_2Cl_2 (4.2 mL), was added over a period of 30 min. The reaction was subsequently warmed to -60 °C and kept at this temperature for 7.5 hours (note: temperature control is very significant for this reaction!). Thereafter, Et_3N (2.98 mL, 21.4 mmol, 10 eq.) was added slowly and the resulting mixture was stirred for one hour at -78 °C, before being warmed gradually to -20 °C over the course of another hour. The reaction was quenched by the addition of water (20 mL) and the layers were separated. The aqueous phase was extracted with CH_2Cl_2 , (4×100 mL) and the combined organic layers were subsequently dried over Na_2SO_4 and concentrated *in vacuo*. Purification by flash column chromatography (silica, *i*-Hex:EtOAc = 60:1 to 40:1) yielded aldehyde **592** (703 mg, 1.77 mmol, 82%) as a colorless liquid.

$R_f = 0.55$ (*i*-Hex:EtOAc = 40:1).

1H NMR ($CDCl_3$, 600 MHz): δ = 9.74 (d, J = 1.7 Hz, 1H), 4.04 (q, J = 2.7 Hz, 1H), 3.44 (dd, J = 9.0, 7.3 Hz, 1H), 2.40 (m_C , 1H), 1.95–1.86 (m, 2H), 1.73 (m_C , 1H), 1.60 (dt, J = 13.7,

3.2 Hz, 1H), 1.58–1.40 (m, 4H), 1.35 (t, $J = 12.4$ Hz, 1H), 1.31–1.24 (m, 1H), 1.15 (s, 9H), 1.07 (d, $J = 7.2$ Hz, 3H), 0.94 (t, $J = 8.0$ Hz, 9H), 0.74 (s, 3H), 0.58 (q, $J = 7.8$ Hz, 6H) ppm.

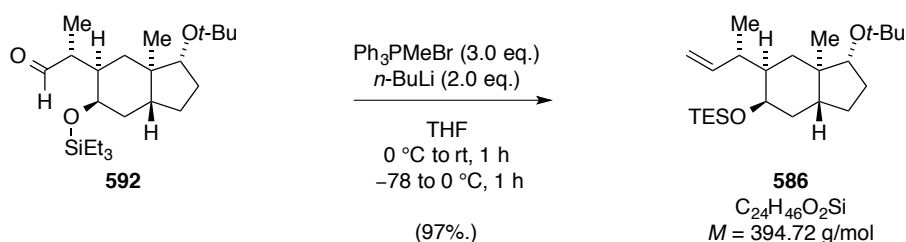
^{13}C NMR (CDCl_3 , 150 MHz): $\delta = 205.2, 80.8, 72.4, 68.7, 48.5, 42.9, 40.3, 37.2, 36.2, 33.9, 31.4, 29.0, 25.5, 12.2, 10.9, 7.2, 5.3$ ppm.

ESI-MS for $\text{C}_{23}\text{H}_{45}\text{O}_3\text{Si}^+$ [MH^+]:
calcd. 397.3133
found 397.3142.

IR (ATR): $\tilde{\nu}/\text{cm}^{-1} = 2955, 2876, 2697, 1721, 1460, 1414, 1389, 1378, 1361, 1237, 1195, 1126, 1058, 1043, 1004, 972, 944, 918, 902, 860, 822, 795, 724$.

$[\alpha]_D^{20} = -65.2$ (c 1.00, CH_2Cl_2).

Synthesis of Alkene **586**



To a suspension of Ph_3PMeBr (2.97 g, 8.32 mmol, 3.0 eq.) in THF (40 mL) at -78 °C was slowly added $n\text{-BuLi}$ (2.05 μL , 2.70 M solution in hexanes, 5.55 mmol, 2.0 eq.). The resulting orange solution was allowed to warm to room temperature and stirred for 60 min, before being cooled to -78 °C again. Then, a solution of aldehyde **592** (1.10 g, 2.77 mmol, 1.0 eq.) in THF (6 mL) was added dropwise. The cold bath was replaced by an ice/water bath and the mixture was stirred for additional 60 min at 0 °C prior to quenching the reaction by the addition of saturated aqueous NH_4Cl (50 mL). The layers were separated and the aqueous phase was extracted with diethyl ether (3×100 mL). The combined organic layers were dried over Na_2SO_4 , concentrated under reduced pressure and the crude product was then purified by flash column chromatography (silica, $i\text{-Hex}:\text{EtOAc} = 100:1$) to yield alkene **586** (1.06 g, 2.69 mmol, 97%) as colorless oil.

$R_f = 0.85$ ($i\text{-Hex}:\text{EtOAc} = 60:1$).

^1H NMR (CDCl_3 , 600 MHz): δ = 5.77 (ddd, J = 17.1, 10.3, 8.2 Hz, 1H), 4.98 (ddd, J = 17.3, 2.1, 1.0 Hz, 1H), 4.92 (ddd, J = 10.3, 2.1, 0.7 Hz, 1H), 4.00 (q, J = 2.4 Hz, 1H), 3.43 (dd, J = 8.9, 7.4 Hz, 1H), 2.22 (m_c , 1H), 1.94–1.87 (m, 1H), 1.74 (m_c , 1H), 1.58–1.52 (m, 2H), 1.46–1.36 (m, 3H), 1.29–1.21 (m, 2H), 1.15 (s, 9H), 1.07 (t, J = 12.4 Hz, 1H), 0.97–0.94 (m, 12H), 0.70 (s, 3H), 0.61–0.56 (m, 6H) ppm.

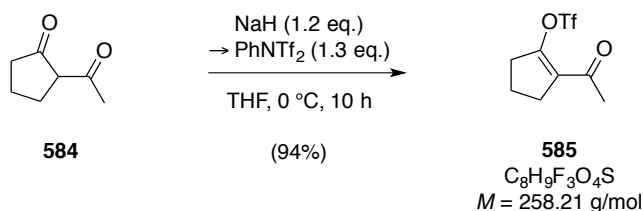
^{13}C NMR (CDCl_3 , 150 MHz): δ = 144.9, 112.8, 80.7, 72.1, 69.2, 43.4, 42.6, 38.8, 37.1, 35.4, 34.2, 31.4, 28.8, 25.3, 18.5, 11.0, 7.1, 5.4 ppm.

EI-MS for $\text{C}_{24}\text{H}_{46}\text{O}_2\text{Si}^+$ [MH^+]:
calcd. 394.3267
found 394.3254.

IR (ATR): $\tilde{\nu}/\text{cm}^{-1}$ = 2955, 2909, 2876, 1460, 1415, 1388, 1361, 1237, 1195, 1128, 1101, 1058, 1044, 1004, 974, 941, 908, 861, 796, 723.

$[\alpha]_D^{20}$ = -41.4 (c 1.00, CH_2Cl_2).

Synthesis of Triflate **585**



To a stirred suspension of NaH (228 mg, 60% wt-% in mineral oil, 9.51 mmol, 1.2 eq.) in THF (30 mL) was added dropwise a solution of diketone **584** (1.00 g, 7.92 mmol, 1.0 eq.) in THF (5 mL) at 0 °C. After 30 min, a solution of PhNTf₂ (3.54 g, 9.91 mmol, 1.3 eq.) in THF (5 mL) was added and the resulting mixture was stirred for 10 hours at 0 °C. Subsequently, the reaction was diluted with H₂O (40 mL) and extracted with Et₂O (3 × 40 mL). The combined organic layers were dried over Na₂SO₄ and concentrated under reduced pressure (500 mbar, 30 °C). The crude product was purified by flash column chromatography (silica, *n*-pentane:Et₂O = 9:1) to yield the title compound **585** (1.92 g, 7.41 mmol, 94%) as a colorless oil.

R_f = 0.71 (*i*-Hex:EtOAc = 3:1).

^1H NMR (C_6D_6 , 400 MHz): δ = 2.25–2.17 (m, 2H), 2.15–2.07 (m, 2H), 1.99 (s, 3H), 1.20–1.06 (q, J = 7.81 Hz, 2H) ppm.

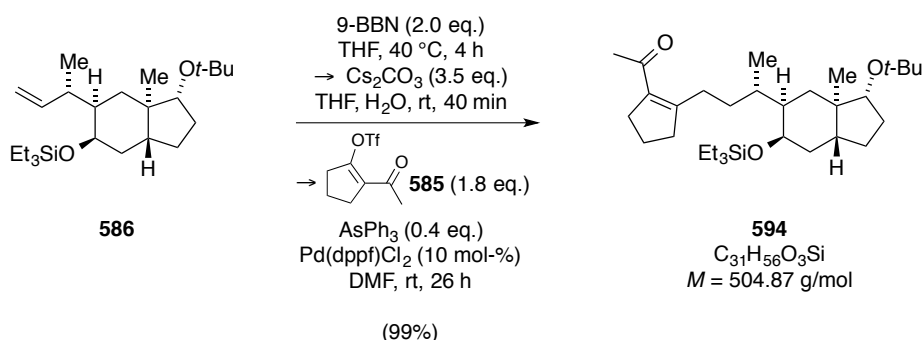
^{13}C NMR (C_6D_6 , 100 MHz): δ = 192.1, 151.9, 129.7, 118.8 (d, J = 320 Hz), 32.5, 29.5, 28.9, 18.5 ppm.

^{19}F NMR (C_6D_6 , 375 MHz): δ = –74.6 ppm

EI-MS for $\text{C}_8\text{H}_9\text{F}_3\text{O}_4\text{S}^+ [\text{M}^+]$:
 calcd. 258.0168.
 found 258.0164.

IR (ATR): $\tilde{\nu}/\text{cm}^{-1}$ = 2974, 2920, 2890, 1683, 1650, 1420, 1390, 1370, 1320, 1280, 1250, 1203, 1138, 1100, 1082, 1011, 920, 901, 875, 830, 767, 710.

Synthesis of Enone **594**



To a solution of alkene **586** (600 mg, 1.52 mmol, 1.0 eq.) in THF (12 mL) was added 9-BBN (6.10 mL, 0.5 M solution in THF, 3.04 mmol, 2.0 eq.) and the resulting solution was heated to 40 °C for 3.5 hours. The mixture was then cooled to 0 °C and degassed aqueous Cs_2CO_3 (3 M, 1.78 mL, 5.30 mmol, 3.5 eq.) was added. The reaction was vigorously stirred at room temperature for 40 min. Subsequently, a solution of triflate **585** (707 mg, 2.74 mmol, 1.8 eq.) and AsPh_3 (186 mg, 6.08 mmol, 0.4 eq.) was added. The resulting mixture was degassed and $\text{Pd(dppf)Cl}_2 \cdot \text{CH}_2\text{Cl}_2$ (124 mg, 1.52 mmol, 10 mol-%) was added in one portion. The mixture was stirred for 26 hours and then partitioned between H_2O (20 mL) and Et_2O (50 mL). The aqueous layer was extracted with Et_2O ($3 \times 50 \text{ mL}$) and the combined organic layers were dried over Na_2SO_4 . Then, the solvents were removed under reduced pressure and the crude product was purified by flash column chromatography (silica, *i*-Hex:EtOAc = 60:1 to 50:1) to yield enone **594** (760 mg, 1.50 mmol, 99%) as a colorless oil.

$R_f = 0.68$ (*i*-Hex:EtOAc = 20:1).

^1H NMR (CDCl_3 , 400 MHz): $\delta = 4.04$ (m_C, 1H), 3.42 (dd, $J = 8.9, 7.3$ Hz, 1H), 2.71–2.58 (m, 3H), 2.56–2.43 (m, 2H), 2.43–2.32 (m, 1H), 2.22 (s, 3H), 1.96–1.67 (m, 4H), 1.65–1.50 (m, 3H), 1.50–1.34 (m, 4H), 1.34–1.17 (m, 3H), 1.14 (s, 9H), 1.14–1.07 (m, 1H), 0.99–0.92 (t, $J = 7.9$ Hz, 9H), 0.90 (d, $J = 6.7$ Hz, 3H), 0.69 (s, 3H), 0.62–0.52 (m, 6H) ppm.

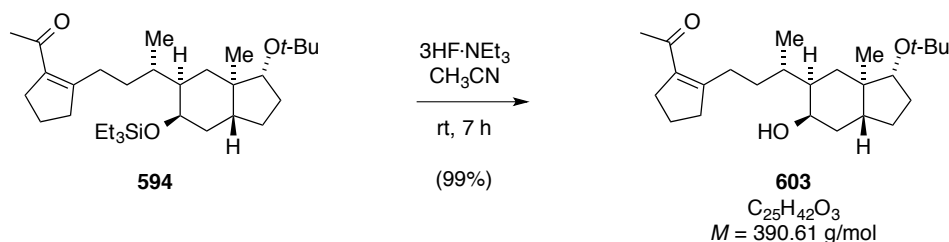
^{13}C NMR (CDCl_3 , 100 MHz): $\delta = 198.5, 159.2, 135.3, 81.0, 72.3, 70.1, 42.7, 42.2, 38.6, 37.4, 35.3, 34.7$ (2C), 34.5, 33.5, 31.6, 30.5, 29.0, 27.9, 25.5, 21.8, 17.2, 11.1, 7.2, 5.5 ppm.

EI-MS for $\text{C}_{31}\text{H}_{56}\text{O}_3\text{Si}^+ [\text{M}^+]$:
calcd. 504.3993.
found 504.3985.

IR (ATR): $\tilde{\nu}/\text{cm}^{-1} = 2953, 2912, 2875, 1712, 1678, 1656, 1608, 1460, 1433, 1417, 1378, 1359, 1297, 1253, 1236, 1195, 1128, 1106, 1060, 1043, 1005, 976, 943, 925, 902, 860, 796, 723, 701$.

$[\alpha]_D^{20} = -43.2$ (c 0.50, CH_2Cl_2).

Synthesis of Alcohol 603



To a solution of enone **594** (750 mg, 1.49 mmol, 1.0 eq.) in MeCN (11.5 mL), $3\text{HF}\cdot\text{NEt}_3$ (1.21 mL, 5.94 mmol, 5.0 eq.) was added dropwise. The resulting mixture was stirred for 7 hours. Subsequently, the reaction was quenched by the addition of saturated aqueous NaHCO_3 (25 mL) and extracted with CH_2Cl_2 (4×50 mL). The combined organic layers were dried over Na_2SO_4 and concentrated *in vacuo*. Purification by flash column chromatography (silica, *i*-Hex:EtOAc = 23:2 to 22:3) yielded alcohol **603** (575 mg, 1.48 mmol, 99%) as a colorless oil.

$R_f = 0.35$ (*i*-Hex:EtOAc = 4:1).

^1H NMR (CDCl_3 , 600 MHz): $\delta = 4.09$ (q, $J = 2.8$ Hz, 1H), 3.42 (dd, $J = 8.9, 7.3$ Hz, 1H), 2.64 (m_C , 2H), 2.54–2.43 (m, 4H), 2.19 (s, 3H), 1.92–1.85 (m, 1H), 1.83–1.77 (m, 2H), 1.65 (m_C , 4H), 1.52–1.38 (m, 4H), 1.33–1.22 (m, 3H), 1.11 (s, 9H), 1.01 (t, $J = 12.9$ Hz, 1H), 0.92 (d, $J = 6.7$ Hz, 3H), 0.68 (s, 3H) ppm.

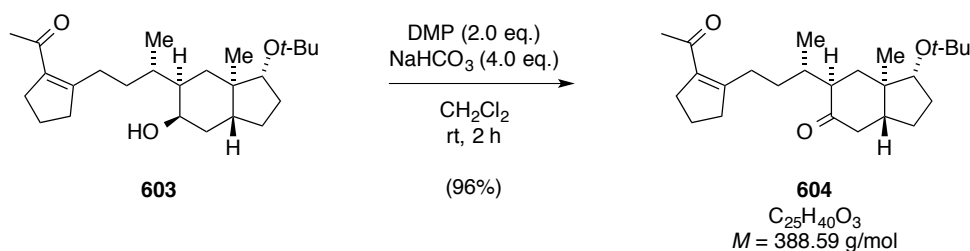
^{13}C NMR (CDCl_3 , 150 MHz): $\delta = 198.8, 159.7, 135.2, 80.8, 72.4, 68.0, 42.8, 42.1, 38.7, 37.5, 36.2, 34.7, 34.6, 34.0, 32.8, 31.4, 30.5, 28.9, 28.3, 25.6, 21.9, 17.7, 11.0$ ppm.

ESI-MS for $\text{C}_{25}\text{H}_{42}\text{NaO}_3^+ [\text{MNa}^+]$:
 calcd. 413.3032.
 found 413.3023.

IR (ATR): $\tilde{\nu}/\text{cm}^{-1} = 3466, 2971, 2930, 2871, 1707, 1669, 1604, 1462, 1431, 1388, 1360, 1302, 1256, 1195, 1125, 1061, 1006, 973, 944, 903, 876, 860, 804, 753, 733, 701$.

$[\alpha]_D^{20} = -22.8$ (c 0.50, CH_2Cl_2).

Synthesis of Diketone **604**



To a suspension of alcohol **603** (570 mg, 1.46 mmol, 1.0 eq.) and NaHCO_3 (245 mg, 5.80 mmol, 4.0 eq.) in CH_2Cl_2 (30 mL) was added Dess-Martin periodinane (1.24 g, 2.92 mmol, 2.0 eq.) in one portion. The mixture was stirred for two hours at room temperature, subsequently diluted with a mixture of aqueous saturated $\text{Na}_2\text{S}_2\text{O}_3$, aqueous saturated NaHCO_3 , as well as H_2O (1:1:1, 20 mL) and extracted with CH_2Cl_2 (4×50 mL). The combined organic layers were dried over Na_2SO_4 and concentrated under reduced pressure. The crude product was purified by flash column chromatography (silica, *i*-Hex:EtOAc = 23:2 to 22:3) to yield diketone **604** (544 mg, 1.40 mmol, 96%) as a colorless oil.

$R_f = 0.58$ (*i*-Hex:EtOAc = 4:1).

^1H NMR (CDCl_3 , 600 MHz): $\delta = 3.49\text{--}3.44$ (dd, $J = 8.9, 7.7$ Hz, 1H), 2.66 (m_C , 2H), 2.63–2.56 (m, 1H), 2.52–2.42 (m, 3H), 2.40 (m_C , 1H), 2.32–2.26 (m, 2H), 2.23–2.28 (m, 1H), 2.21 (s, 3H), 2.01–1.95 (m, 1H), 1.89 (dd, $J = 12.5, 6.3$ Hz, 1H), 1.82 (quin, $J = 7.6$ Hz, 2H), 1.68–1.52 (m, 3H), 1.45–1.30 (m, 3H), 1.18 (t, $J = 12.8$ Hz, 1H) 1.15 (m, 9H), 0.99 (s, 3H), 0.81 (d, $J = 6.8$ Hz, 3H) ppm.

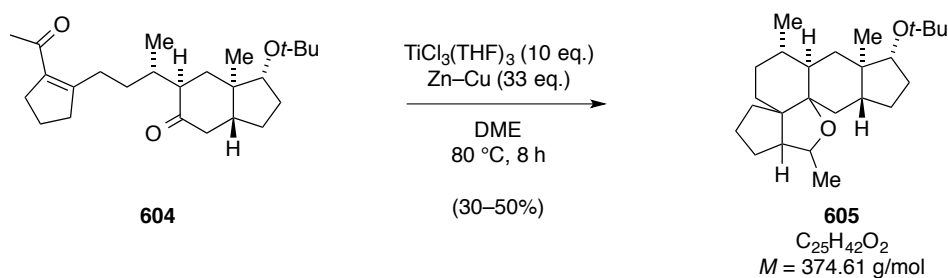
^{13}C NMR (CDCl_3 , 150 MHz): $\delta = 212.5, 198.6, 158.3, 135.6, 78.0, 72.7, 49.3, 44.8, 43.3, 42.3, 38.4, 35.8, 34.7, 33.0, 31.9, 31.0, 30.5, 28.9, 28.5, 25.9, 21.8, 16.1, 11.2$ ppm.

EI-MS for $\text{C}_{25}\text{H}_{40}\text{O}_3^+ [\text{M}^+]$:
calcd. 388.2972.
found 388.2968.

IR (ATR): $\tilde{\nu}/\text{cm}^{-1} = 3347, 2967, 2873, 1703, 1677, 1608, 1461, 1430, 1389, 1350, 1290, 1255, 1191, 1110, 1060, 1025, 970, 901, 854, 803, 755$.

$[\alpha]_D^{20} = -28.0$ (c 0.25, CH_2Cl_2).

Synthesis of Ether **605**



To a vigorously stirred suspension of $\text{TiCl}_3(\text{THF})_3$ (229 mg, 2.01 mmol, 10 eq.) and Zn–Cu couple (106 mg, 1.68 mmol, 33 eq.) in dimethoxyethane (14 mL), a solution of diketone **604** (20 mg, 51.5 μmol , 1.0 eq.) in dimethoxyethane (5 mL) was added at 80 °C *via* syringe pump over a period of 6 hours. The reaction mixture was stirred for an additional two hours, subsequently cooled to room temperature and filtered over Celite[®] (Et_2O washings). The crude mixture was washed with saturated aqueous NaHCO_3 (20 mL) and the aqueous phase was extracted with Et_2O (3×20 mL). The combined organic layers were dried over Na_2SO_4 and concentrated under reduced pressure. Purification by flash column chromatography

(silica, *n*-pentane:Et₂O = 200:1) yielded ether **605** (14 mg, 30–50%) as a colorless wax and as a single diastereomer.

*Note: The yield of this reaction was approximated from ¹H NMR, but could not be determined properly due to residual silicon grease that eluted co-polar with ether **605**.*

R_f = 0.85 (*i*-Hex:EtOAc = 40:1).

¹H NMR (CDCl₃, 600 MHz): δ = 3.49–3.35 (m, 2H), 1.91–1.78 (m, 4H), 1.75–1.56 (m, 6H), 1.53–1.44 (m, 2H), 1.45–1.32 (m, 3H), 1.33–1.15 (m, 2H), 1.12 (d, *J* = 6.0 Hz, 3H), 1.16–0.95 (m, 5H), 1.10 (s, 9H), 0.86 (d, *J* = 6.9 Hz 3H), 0.70 (s, 3H) ppm.

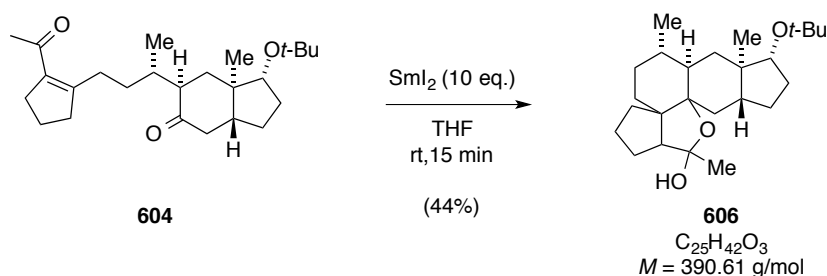
¹³C NMR (CDCl₃, 150 MHz): δ = 85.8, 80.8, 76.1, 72.4, 60.1, 58.9, 42.2, 41.7, 39.8, 39.6, 36.3, 35.1, 31.7, 30.5, 29.4, 29.3, 29.0, 28.8 (2C), 26.0, 21.6, 20.5, 11.3 ppm.

EI-MS for C₂₅H₄₂O₂⁺ [M⁺]:
calcd. 374.3179.
found 374.3174.

IR (ATR): $\tilde{\nu}/\text{cm}^{-1}$ = 2960, 2927, 2865, 1455, 1386, 1373, 1360, 1259, 1196, 1094, 1062, 1020, 951, 940, 918, 902, 859, 799, 753, 723, 705, 660.

$[\alpha]_D^{20} = -25.8$ (*c* 1.00, CH₂Cl₂).

Synthesis of Hemiacetal **606**



To a commercial deep blue solution of SmI₂ (14.3 mL, 0.072 M solution in THF, 1.03 mmol, 10 eq.) was added a solution of diketone **604** (40 mg, 0.10 mmol, 1.0 eq.) in THF (2 mL) dropwise at room temperature *via* syringe pump over a period of one hour. The reaction was stirred for further 15 min, upon which it was diluted with Et₂O (40 mL). The now colorless mixture was washed with saturated aqueous NaHCO₃ (20 mL) and the aqueous layer was re-

extracted with Et₂O (3 × 20 mL). The combined organic layers were dried over Na₂SO₄ and concentrated under reduced pressure. Purification by flash column chromatography (silica, *n*-pentane:Et₂O = 19:1 to 9:1) yielded hemiacetal **606** (18 mg, 46.1 μmol, 44%) as a colorless wax and as a single diastereomer.

R_f = 0.90 (*i*-Hex:EtOAc = 4:1).

¹H NMR (C₆D₆, 600 MHz): δ = 3.50 (dd, *J* = 8.9, 7.3 Hz, 1H), 2.25 (dd, *J* = 12.8, 3.0 Hz, 1H), 2.20 (dd, *J* = 9.1, 3.8 Hz, 1H), 2.09–1.92 (m, 6H), 1.80–1.52 (m, 5H), 1.51–1.40 (m, 3H), 1.38–1.30 (m, 2H), 1.33 (s, 3H), 1.21 (m, 1H), 1.15–1.11 (m, 1H), 1.13 (s, 9H), 1.10–1.01 (m, 2H), 0.97 (s, 3H), 0.94 (d, *J* = 6.9 Hz, 3H) ppm.

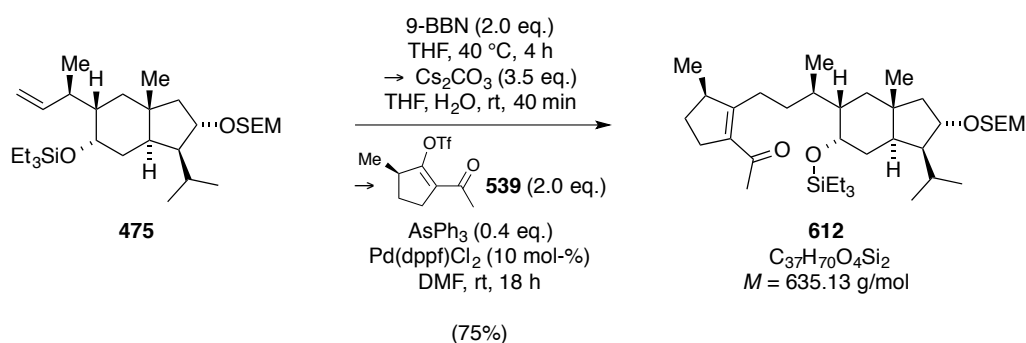
¹³C NMR (C₆D₆, 150 MHz): δ = 103.8, 87.3, 81.5, 72.5, 61.2, 59.5, 42.9, 42.5, 40.7, 39.9, 36.6, 35.1, 34.2, 32.6, 30.0, 29.7, 29.4, 29.3, 29.1, 27.0, 26.6, 22.0, 12.3 ppm.

EI-MS for C₂₅H₄₂O₃⁺ [*M*⁺]:
calcd. 390.3129.
found 390.3119.

IR (ATR): $\tilde{\nu}$ /cm⁻¹ = 3465, 2969, 2929, 2667, 1460, 1375, 1360, 1253, 1233, 1193, 1122, 1063, 1026, 1012, 981, 953, 936, 904, 862, 835, 753, 733.

$[\alpha]_D^{20} = -17.3$ (*c* 0.50, CH₂Cl₂).

Synthesis of Enone **612**



To a solution of alkene **475** (1.1 mg, 2.10 μmol, 1.0 eq.) in THF (300 μL) was added 9-BBN (9 μL, 0.5 M solution in THF, 4.20 μmol, 2.0 eq.) and the resulting solution was heated to 40 °C for 3.5 hours. The mixture was then cooled to 0 °C, degassed aqueous Cs₂CO₃ (3 M,

3 μL , 7.34 μmol , 3.5 eq.) was added and the reaction was stirred vigorously at room temperature for 40 min. Subsequently, a solution of triflate **539** (1.1 mg, 4.20 μmol , 2.0 eq.) and AsPh_3 (0.3 mg, 0.84 μmol , 0.4 eq.) in DMF (500 μL) was added. The resulting mixture was degassed and $\text{Pd}(\text{dppf})\text{Cl}_2 \cdot \text{CH}_2\text{Cl}_2$ (0.2 mg, 0.21 μmol , 10 mol-%) was added in one portion. The mixture was stirred for 26 hours and then partitioned between H_2O (10 mL) and Et_2O (20 mL). The aqueous layer was extracted with Et_2O (3×10 mL) and the combined organic layers were dried over Na_2SO_4 . The solvents were removed under reduced pressure and the crude product was purified by flash column chromatography (silica, $i\text{-Hex}:\text{EtOAc} = 49:1$ to $19:1$ to $9:1$) to yield enone **612** (1.0 mg, 1.57 μmol , 75%) as a colorless oil as a diastereomeric mixture of 5:1 together with **613**.

Note: The diastereomeric ratio, which refers to the stereogenic methyl group of the cyclopentene subunit, was determined from ^1H NMR as HPLC methods did not achieve proper separation of the isomers.

$R_f = 0.50$ ($i\text{-Hex}:\text{EtOAc} = 25:2$).

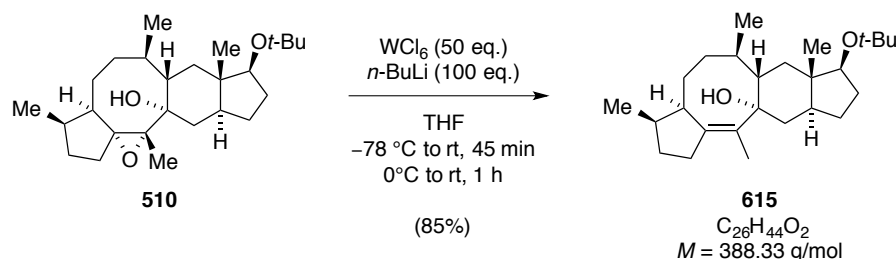
^1H NMR (C_6D_6 , 400 MHz): $\delta = 4.76$ (d, $J = 7.0$ Hz, 1H), 4.72 (d, $J = 7.0$ Hz, 1H), 4.39 (td, $J = 7.6, 4.0$ Hz, 1H), 4.32–4.25 (m, 1H), 3.77 (td, $J = 9.3, 7.2$ Hz, 1H), 3.68 (td, $J = 9.3, 7.2$ Hz, 1H), 3.34–3.17 (m, 1H), 2.73–2.63 (m, 2H), 2.42–2.33 (m, 1H), 2.30–2.22 (m, 1H), 2.20–2.07 (m, 2H), 2.04–1.91 (m, 2H), 1.93 (s, 3H), 1.91–1.76 (m, 2H), 1.74–1.43 (m, 8H), 1.28–1.20 (m, 1H), 1.15 (d, $J = 6.6$ Hz, 3H), 1.12–1.00 (m, 8H), 1.06 (s, 9H), 0.98 (d, $J = 6.9$ Hz, 3H), 0.84 (s, 3H), 0.75–0.61 (m, 6H), 0.01 (s, 9H) ppm.

^{13}C NMR (C_6D_6 , 100 MHz): $\delta = 197.0, 161.7, 134.5, 93.7, 82.0, 70.7, 65.3, 54.9, 48.8, 43.6, 42.2, 42.1, 41.2, 38.8, 34.5, 33.7, 33.5, 32.8, 31.2, 30.2, 30.1, 24.9, 24.7, 22.2, 20.3, 18.5, 18.4, 17.6, 7.4, 5.8, -1.3$ ppm.

EI-MS for $\text{C}_{37}\text{H}_{70}\text{O}_4\text{Si}_2^+$ [M^+]:	calcd.	634.4813.
	found	634.4825.

IR (ATR): $\tilde{\nu}/\text{cm}^{-1} = 2951, 2930, 2873, 1740, 1677, 1655, 1605, 1457, 1416, 1376, 1354, 1248, 1195, 1159, 1100, 1048, 1029, 947, 921, 859, 834, 793, 740, 834, 691$.

$[\alpha]_D^{20} = +36.0$ (c 0.05, CDCl_3).

Synthesis of Allyl Alcohol **615**

To a stirred suspension of WCl_6 (240 mg, 610 μmol , 50 eq.) in THF (6.5 mL) was added $n\text{-BuLi}$ (423 μL , 2.86 M solution in hexanes, 1.21 mmol, 100 eq.) dropwise at $-78\text{ }^\circ\text{C}$. The resulting yellow solution was warmed to room temperature and was stirred for 45 min. After cooling to $0\text{ }^\circ\text{C}$, a solution of epoxide **510** (4.9 mg, 12.1 μmol , 1.0 eq.) in THF (2.0 mL) was added dropwise over a period of 15 min. The brown reaction mixture was then warmed to room temperature and stirred for one hour. Subsequently, half-saturated NaHCO_3 solution (5 mL) was added at $0\text{ }^\circ\text{C}$ and the layers were separated. The aqueous phase was extracted with n -pentane ($3 \times 20\text{ mL}$). The combined organic layers were washed with saturated aqueous NaHCO_3 solution (5 mL), dried over Na_2SO_4 and concentrated under reduced pressure. The crude product was purified by flash column chromatography (silica, n -pentane: $\text{Et}_2\text{O} = 197:1$ to $193:7$) to yield the title compound **615** (4.0 mg, 10.3 μmol , 85%) as a colorless foam.

Note: ^{13}C NMR analysis was thwarted by signal broadening. Undetected and broad signals are attributed to C3 to C9, including C20 (nitidasin numbering).

$R_f = 0.83$ ($i\text{-Hex}:\text{EtOAc} = 25:1$).

^1H NMR (C_6D_6 , 400 MHz): $\delta = 3.85$ (s, br, 1H), 3.36 (t, $J = 8.2\text{ Hz}$, 1H), 2.31–2.24 (m, 1H), 2.21–2.10 (m, 2H), 1.97–1.76 (m, 5H), 1.71–1.59 (m, 2H), 1.60 (s, 3H), 1.54–1.42 (m, 4H), 1.42–1.22 (m, 4H), 1.12 (s, 9H), 1.04–1.00 (m, 2H), 1.03 (d, $J = 7.0\text{ Hz}$, 3H), 1.01 (d, $J = 6.8\text{ Hz}$, 3H), 0.93 (s, 3H), 0.37 (s, br, 1H) ppm.

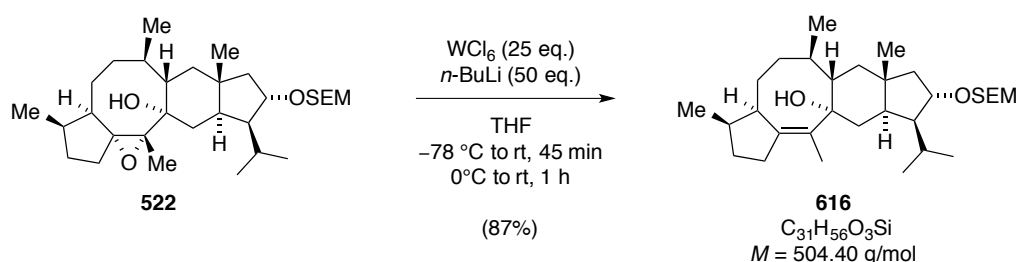
^{13}C NMR (C_6D_6 , 100 MHz, observable signals quoted): $\delta = 142.8, 133.1, 81.2, 77.9, 72.2, 45.4, 44.0$ (br), 43.0, 40.3, 39.0 (br), 38.1, 32.3 (br), 31.9, 29.6, 29.0, 26.7 (br), 26.1, 23.9 (br), 17.9, 15.5, 11.4 ppm.

EI-MS for $\text{C}_{26}\text{H}_{44}\text{O}_2^+$ [M^+]:	calcd.	388.3341.
	found	388.3321.

IR (ATR): $\tilde{\nu}/\text{cm}^{-1}$ = 3491, 2972, 2931, 2868, 1454, 1388, 1373, 1360, 1330, 1298, 1253, 1229, 1198, 1133, 1085, 1064, 1038, 1022, 1000, 987, 967, 944, 903, 862, 836, 810, 755, 720.

$[\alpha]_D^{20} = +152.8$ (c 1.00, C_6D_6).

Synthesis of Allyl Alcohol **616**



To a stirred suspension of WCl_6 (148 mg, 370 μmol , 25 eq.) in THF (4.1 mL) was added $n\text{-BuLi}$ (262 μL , 2.86 M solution in hexanes, 740 μmol , 50 eq.) dropwise at $-78\text{ }^\circ\text{C}$. The resulting yellow solution was warmed to room temperature and was stirred for 45 min. After cooling to $0\text{ }^\circ\text{C}$, a solution of epoxide **522** (7.8 mg, 14.9 μmol , 1.0 eq.) in THF (1.5 mL) was added dropwise over a period of 15 min. The brown reaction mixture was then warmed to room temperature and stirred for one hour. Subsequently, half-saturated NaHCO_3 solution (10 mL) was added at $0\text{ }^\circ\text{C}$ and the layers were separated. The aqueous phase was extracted with n -pentane ($3 \times 40\text{ mL}$). The combined organic layers were washed with saturated aqueous NaHCO_3 solution (10 mL), dried over Na_2SO_4 and concentrated under reduced pressure. The crude product was purified by flash column chromatography (silica, n -pentane: Et_2O = 187:13 to 37:3) to yield the title compound **616** (6.6 mg, 13.1 μmol , 85%) as colorless needles.

Note: ^{13}C NMR analysis was thwarted by signal broadening. Measurement at $50\text{ }^\circ\text{C}$ is recommended.

Crystals suitable for X-ray analysis were grown from slow evaporation of a solution of allyl alcohol **616** in n -pentane/MeOH.

$R_f = 0.46$ (i -Hex: EtOAc = 40:3).

Melting point = $141.6\text{--}143.0\text{ }^\circ\text{C}$ (n -pentane/MeOH).

^1H NMR (C_6D_6 , 400 MHz): δ = 4.78 (d, J = 6.9 Hz, 1H), 4.74 (d, J = 6.9 Hz, 1H), 4.36 (ddd, J = 8.3, 6.9, 4.1 Hz, 1H), 3.87–3.77 (m, 2H), 3.70 (td, J = 9.3, 7.3 Hz, 1H), 2.51–2.44 (m, 1H), 2.32–1.99 (m, 5H), 1.89 (td, J = 10.4, 4.1 Hz, 1H), 1.80 (s, br, 1H), 1.73–1.55 (m, 3H), 1.62 (s, 3H), 1.50–1.23 (m, 8H), 1.16 (d, J = 6.6 Hz, 3H), 1.08–1.00 (m, 3H), 1.03 (d, J = 6.3 Hz, 3H), 1.03 (d, J = 6.8 Hz, 3H), 0.94 (d, J = 7.2 Hz, 3H), 0.74 (s, 3H), 0.30 (s, 1H), 0.02 (s, 9H) ppm.

^{13}C NMR (C_6D_6 , 100 MHz, 50 °C): δ = 143.1, 133.1, 93.8, 82.4, 78.1, 65.4, 55.3, 48.9, 45.0, 44.2, 43.7, 42.6, 42.0, 39.0, 38.9, 34.6, 32.4, 30.2, 29.7, 26.8, 24.8, 23.7, 22.3, 20.3, 18.5, 17.9, 15.5, –1.2 ppm.

EI-MS for $\text{C}_{31}\text{H}_{54}\text{O}_2\text{Si}^+[(\text{M}-\text{H}_2\text{O})^+]$: calcd. 486.3893.
 found 486.3896.

IR (ATR): $\tilde{\nu}/\text{cm}^{-1}$ = 3482, 2952, 2921, 2871, 1462, 1451, 1372, 1302, 1250, 1229, 1204, 1163, 1146, 1106, 1058, 1031, 990, 858, 834, 758, 741, 710, 692.

$[\alpha]_D^{20}$ = +82.0 (c 1.00, C_6D_6).

**DEVELOPMENT OF NOVEL PHOTOCHROMIC
LIGANDS FOR
L-TYPE VOLTAGE-GATED CALCIUM CHANNELS**

1. Introduction

1.1 The Physiological Role of Calcium

Calcium ions play a manifold role in the physiology and biochemistry of essentially all higher organisms and their intra- and extracellular concentrations are tightly regulated.^[370] In vertebrates, the bones act as the major mineral storage site for Ca^{2+} and contain up to 99% of its total body content. At this site, it is bound mainly as hydroxylapatite ($\text{Ca}_{10}(\text{PO}_4)_6(\text{OH})_2$), but also as calcium phosphate, carbonate, citrate, fluoride and sulfate. Calcium is released from the bone tissue into the blood stream as free ions or bound to proteins like serum albumin in a controlled manner. The major regulation factors are the peptidal hormone parathyroid^[371] and the activated form of vitamin D_3 , calcitriol (not shown),^[372] which promote the resorption of Ca^{2+} from bone, kidney and the intestines. In contrast, the polypeptide calcitonin opposes the effect of parathyroid hormone and reduces the blood levels of Ca^{2+} .^[373,374] Within the cytoplasm of cells, membrane channels in the plasma membrane and in the organelles mediate the inward flow of Ca^{2+} , whereas ATPases, ion exchangers and the mitochondrial Ca^{2+} uptake system^[375] are responsible for its removal.^[370]

Calcium plays a pivotal part in a diverse array of cellular processes such as signal transduction as second messenger,^[376] neurotransmitter release from neurons,^[377] secretion of bioactive molecules,^[376,377] muscle contraction,^[378] gene expression^[379] and as a co-factor for several enzymes.^[380] Furthermore, the difference between intra- (~100 nM unbound) and extracellular Ca^{2+} concentrations allows for a precise temporal control of cellular processes and is *e.g.* about 20000-fold in different types of neurons.^[376d] In this cell type, voltage-gated calcium (Ca_v) and cation selective ligand-gated ion channels are primarily responsible for the spatially confined influx of Ca^{2+} ions, which is triggered upon membrane depolarization. Thus generated micro- and nanodomains of elevated Ca^{2+} levels are typically of a diameter of 10 to 1000 nm and are sufficient for the binding to the calcium sensor protein synaptogamin that is found in the membranes of the pre-synaptic vesicles.^[377b] The following exocytosis of those neurotransmitter-loaded vesicles is initiated by the so-called SNARE protein complex and is in turn dependent on Ca^{2+} -mediated displacement of complexin by synaptogamin.^[381] Release of the neurotransmitter may directly open ligand-gated ion channels in the post-synaptic cell membrane. Depending on the nature of the receptor and the neurotransmitter, this will cause ions to enter or exit the cell, thus changing the local transmembrane potential and propagating or inhibiting the action potential.^[372] In this context, the small molecules acetylcholine,

γ -amino-butyric acid (GABA), serotonin, histamine, dopamine and noradrenaline define the most significant inter-synaptic signaling systems in human physiology that are known to date.^[382] However, inhibition of neuronal activity can also occur from the pre-synaptic site and is frequently mediated by metabotropic GABA receptors or *e.g.* the muscarinic acetylcholine receptors and adenosine receptors.^[383] For this mode of action, overall a membrane hyperpolarization is induced by an increased chloride ion conductance that leads to a subsequent reduction of Ca^{2+} entry *via* Ca_v channels.^[384]

Another type of process that is associated with the synaptic uptake of calcium ions is the regulation of gene expression and dendritic differentiation in those cells. Especially the so-called L-type calcium channels (LTCCs), which are also voltage-gated and will be discussed in more detail in the following chapters, have been subject of numerous investigations on their effects on gene transcription.^[376e] Historically, in 1986 Greenberg *et al.* were the first to demonstrate that agonists of the nicotinic acetylcholine receptor and similar membrane depolarizing agents cause a fast and transient activation of the *c-fos* proto-oncogene in neuronal cell lines *via* induction of calcium influx through LTCCs.^[385] Following studies in this field have disclosed that *c-fos* is only one amongst several hundred genes that are controlled by neuronal activity throughout the formation and maturing of synapses.^[386] Interestingly, many of those genes seem to influence various aspects of synaptic function and development, as for instance the synthesis of the neurotrophin BDNF (dendritic growth), the cytoplasmic protein Arc (glutamate receptor endocytosis) and the formation of synaptic protein complexes, which is closely linked to *Homer1a*.^[376e] Considerable efforts were undertaken to elucidate the second messenger pathways which propagate the calcium signal to the nucleus and it was shown that three distinct mechanisms eventually focus on the phosphorylation of the Ser133 residue of the cAMP response element-binding protein (CREB). In its active form, this leucine-zipper-type DNA-binding protein constitutes an often encountered transcription factor and has amongst others been linked to the circadian clock.^[387]

The first of those signaling avenues that lead to CREB phosphorylation was originally reported by Deisseroth *et al.*^[388] and proceeds *via* the binding of up to four calcium ions to calmodulin (CaM), which is accommodated closely to the internal face of LTCCs.^[376d,389] The authors established that CaM translocation is fast enough (1–2 min) to account for the kinetics of nuclear CREB activation. In their studies it was proven that even large increases in bulk cellular Ca^{2+} concentration fail to promote the mentioned phosphorylation if not coupled to CaM. In addition, it was proposed that CaMKIV would be an intermediary nuclear target of

this mechanism, as it is the substrate of CaM-dependent kinases^[390] and had been implicated in neuronal activity-dependent CREB phosphorylation previously.^[391] Several years later, another pathway that acts on the same time scale and requires an initial binding of calcium ions to apo-CaM was discovered.^[392] A further event in this cascade is the activation of Ca^{2+} /CaM-dependent protein kinase II (CaMKII), which has been shown to associate for instance with $\text{Ca}_v1.2$ (*vide supra*).^[393] However, the ensuing signaling steps that finally result in CREB phosphorylation are still a matter of debate. Independent from this a third and comparably slow mechanism (30–60 min) has been shown to transmit the CREB activating signal *via* the Ras-MAP kinase pathway.^[394] Therefore, it was suggested that scaffolding proteins bound to an LTCC intracellular domain may recruit Ras-MAP kinase activators. This would allow CaM, which in this context seems to be basally tethered to the LTCC,^[395] to switch them on directly or indirectly by a conformational change of the channel.

As modern biochemistry has made decisive advances toward the understanding of the physiological role of calcium, especially its relevance in neuronal activity calls for the development of chemical tools that allow a spatial and temporal control of its concentration in living tissue. To understand the potential starting points for the design of related small molecule-based strategies, the following chapter will provide an introduction on the subtypes and structures of Ca_v channels.

1.2 Voltage-gated Calcium Channels: Structural Composition and Subtypes

Voltage-gated calcium channels are the principal source of depolarization-induced calcium influx in neurons and exhibit a great diversity of subtypes that is caused by the existence of multiple genes for calcium channel $\alpha 1$ subunits. Furthermore, coassembly with a variety of auxiliary calcium channel subunits and alternative gene splicing is observed throughout the whole class. This accounts for the high number of specialized roles that they fulfill in several distinct neuronal subtypes and particular subcellular loci. Since the discovery of manipulable calcium currents in neurons by the seminal investigations of Katz and Miledi,^[396] Hagiwara and Nakajima,^[397] as well as Reuter,^[398] several milestone achievements have led to the identification of ten sorts of humane Ca_v channels that show major differences in the composition of their $\alpha 1$ subunits.^[399] Commonly they are classified either according to those $\alpha 1$ domains or to a one letter code that refers to the respective electrophysiological properties and first site of characterization. Table 1.1 lists all congeners of this family known to date, as well as their primary physiological function and the established specific blocking

Table 1.1: Classification and function of known humane Ca_v channels according to Catterall.^[400]

Ca^{2+} current type	$\alpha 1$ subunit type	specific blocker ^a	primary physiological functions
L	$\text{Ca}_v1.1$		excitation-contraction coupling in skeletal muscle, transcription regulation
	$\text{Ca}_v1.2$	DHPs, BTZs, PAAs	excitation-contraction coupling in cardiac and smooth muscle, endocrine secretion, neuronal Ca^{2+} transients in cell bodies and dendrites, enzyme activity regulation, transcription regulation
	$\text{Ca}_v1.3$	(for all L-type)	endocrine secretion, cardiac pacemaking, neuronal Ca^{2+} transients in cell bodies and dendrites, auditory signal transduction
	$\text{Ca}_v1.4$		visual signal transduction
N	$\text{Ca}_v2.1$	ω -conotoxin GVIA ^[401]	neurotransmitter release, dendritic Ca^{2+} transients
P/Q	$\text{Ca}_v2.2$	ω -agatoxin ^[402]	neurotransmitter release, dendritic Ca^{2+} transients
R	$\text{Ca}_v2.3$	SNX-482 ^[403]	neurotransmitter release, dendritic Ca^{2+} transients
T	$\text{Ca}_v3.1$	—	pacemaking and repetitive firing
	$\text{Ca}_v3.2$	—	pacemaking and repetitive firing
	$\text{Ca}_v3.3$	—	pacemaking and repetitive firing

a) Small molecule based blockers like the dihydropyridines (DHPs) will be discussed in chapter 1.3.1. The remaining agents listed are peptide-based toxins.

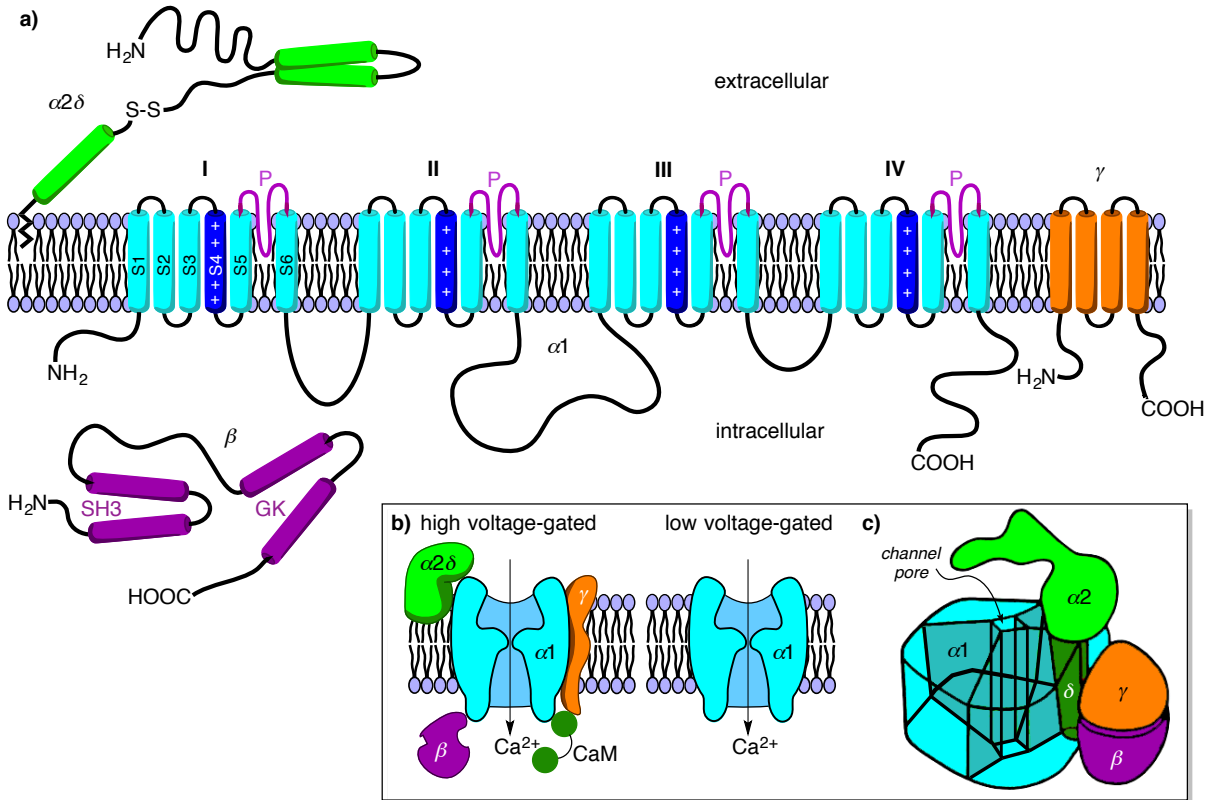
agents.^[400] Additionally, Ca_v channels can be distinct whether they are high voltage (about -20 mV) or low voltage (about -70 mV) activated. It has been shown that channels of the first type are constituted of heteromultimeric protein complexes that are formed by the assembly of a pore-forming $\alpha 1$ unit plus auxiliary β and $\alpha 2\delta$ subunits,^[404] whereas the second category appears to lack these auxiliary elements.^[405] Before discussing the structural features of Ca_v channels more in-depth, a short introduction on the single LTCCs shall be given, as they denote the relevant targets of the chemical tools developed within present doctoral thesis. The specific properties of N- ('neuronal'), P- ('purkinje'), Q- (first recorded in cerebellar granule neurons),^[406] R- ('residual') and T-type ('transient') Ca_v channels have been reviewed elsewhere.^[399,400,407]

The four LTCCs encoded by the human genome display slow voltage-dependent gating characteristics and therefore are long (L-type) lasting when Ba^{2+} is the current carrier and there is no Ca^{2+} -dependent inactivation.^[408] The first member $\text{Ca}_v1.1$ is mostly expressed in skeletal muscle and primarily acts as a voltage sensor, connecting depolarization to release of

intracellular calcium by activating the ryanodine receptor in the sarcoplasmic reticulum.^[409] The coupling of the opening of this channel to membrane depolarization has been shown to be rather inefficient and slow.^[410] $\text{Ca}_v1.2$ and $\text{Ca}_v1.3$ channels exhibit largely similar expression behavior in different tissues and are often localized in the same neuronal compartments – particularly dendrites – but their subcellular distributions appear distinct.^[411] Thus, both congeners can be found for example in pancreatic cells, smooth muscle or neurons, whereas solely ventricular cardiac muscles harbor $\text{Ca}_v1.2$ and atrial tissue only $\text{Ca}_v1.3$ channels, respectively.^[412] $\text{Ca}_v1.2$ helps defining the shape of the action potential in cardiac and smooth muscle and triggers the signaling cascade that leads to the contraction of those muscles by its primary function, the actual Ca^{2+} influx.^[413] In neurons, $\text{Ca}_v1.2$ has been evidenced to couple membrane depolarization to regulation of gene expression (*vide supra*).^[394,414] At this, $\text{Ca}_v1.3$ has been demonstrated to induce higher levels of CREB phosphorylation.^[415] A common feature of both channels is their role in hormone secretion, which is particularly well studied in adrenal chromaffin cells, where calcium that enters *via* this source drives much of the release of catecholamine.^[416] Their channel kinetics are faster than those of $\text{Ca}_v1.1$ and they will open at membrane potentials of approximately -20 mV and -40 mV, at which $\text{Ca}_v1.3$ requires less depolarization.^[412] The $\text{Ca}_v1.4$ -encoding gene is expressed almost exclusively in the retina and is connected to the rare disorder stationary night blindness.^[417] However, RNA that is translated to this channel has also been found in dorsal root ganglia.^[418] $\text{Ca}_v1.4$ is located at synaptic terminals of retinal bipolar cells and is specifically responsible for Ca^{2+} entry that triggers exocytosis of neurotransmitters.^[419] In comparison to other LTCCs, this channel undergoes no calcium-dependent inactivation due to an autoinhibitory domain at its intracellular C-terminus.^[420]

Although the molecular structure of Ca_v channels has been investigated intensely, still no solid-state structure of their central pore-forming $\alpha 1$ domain has been published in literature to date. Knowledge about their structural features and functions thereof is based on sequence homology to other channel types (especially K_v channels), site-directed mutagenesis and analysis of the biochemical properties, glycosylation, and hydrophobicity,^[399,400] which all became possible after the first cloning and expression of a Ca^{2+} channel gene by Tanabe and co-workers in 1987.^[410c,421] Scheme 1.1 illustrates the basic constituents of Ca_v channels in a flat and three-dimensional drawing, of which the latter is based on cryo-electronmicroscopic measurements on $\text{Ca}_v1.1$.^[422]

All ten known $\alpha 1$ subunits share a common topology of four homologue transmembrane domains (I-IV), each of which contain six membrane-spanning α -helices (S1-S6). Generally,



Scheme 1.1: a) Subunit composition and transmembrane topology of Ca_v subunits. The zigzag line on the $\alpha 2\delta$ portion illustrates the GPI-anchor. The positive charges denote the voltage sensor regions located at the S4 helices. b) Side view of native high and low voltage-gated Ca^{2+} channels and their respective subunits. c) Illustration of the $\text{Ca}_v 1.1$ channel based on cryo-electronmicroscopic images (reproduced from ref. 400).

the $\alpha 1$ domain contains about 2000 amino acids and has a mass of roughly 190 kDa.^[399,400] Like in similar ion channels, a positively charged S4 segment imparts voltage-dependent activation and a re-entrant loop motif (P) between S5 and S6 composes the ion-permeating pathway. Those P-loop sequences contain highly conserved negatively charged amino acids and their amide carbonyl and side chain carboxylic acid functions form a pore that is highly selective for permeating cations such as calcium.^[423] The greatest sequence variation amongst Ca_v subtypes is given between the major membrane domains I-IV in the cytoplasmic linker regions, which mediates important protein-protein interactions with regulatory and second messenger elements such as G proteins and protein kinases.^[424]

For the $\text{Ca}_v\beta$ subunits, there are currently four encoding genes ($\beta 1$ – $\beta 4$) and several alternative splice transcripts known.^[425] This type of protein is located on the cytoplasmic site of Ca_v channels and contains conserved SH3 and GK domains, of which the latter enables the association to the loop region between the domain I and II of an $\alpha 1$ unit.^[399] As a consequence of this interaction, a modification of the gating properties of the pore-forming core^[425,426] and increased cell surface trafficking is observed. In this regard, it has been proven that the

β -subunit leads to an inhibition of ubiquitination and degradation of the channels, as well as to a masking of intrinsic endoplasmatic reticulum (ER) retention signals located on the $\alpha 1$ part. Currently, four isoforms of the $\alpha 2\delta$ subunit have been identified ($\alpha 2\delta 1$ – $\alpha 2\delta 4$), which are all transcribed and translated as a single protein, post-translationally cleaved to the $\alpha 2$ and δ portion, and then recombined *via* disulfide linkage.^[427] Recent findings oppose the original thought that the $\alpha 2\delta$ complex spans the membrane and indicate that it is attached to the extracellular site by a glycoposphatidylinositol (GPI) anchor.^[428] Although the overall effect of the $\alpha 2\delta$ part on channel function seems to be relatively small,^[429] increased levels of expression in neurons have been linked to improved pre-synaptic abundance of Ca_v channels and enhanced synaptic release probability.^[430]

In skeletal muscle the ancillary $\text{Ca}_v\gamma$ subunit can be found, which is a glycoprotein that comprises four transmembrane helices.^[431] So far, the genes of seven potential isoforms have been identified, including $\text{Ca}_v\gamma 2$ ('stargazin').^[432] Besides their evidenced effects of whole-cell current density,^[433] also association with other cellular functions such as AMPA receptor trafficking has been described.^[434] Furthermore, considerable evidence has been provided that all high voltage-gated Ca_v channels associate with CaM, suggesting that CaM should be considered as the fifth calcium channel subunit.^[399,435]

1.3 L-Type Calcium Channels: Pharmacological and Functional Aspects

Whilst presented knowledge has contributed much to the understanding of regulation mechanisms in Ca_v channels, drug interactions still have to be calculated using homology models with other channel types. The next chapters will provide a short overview of blocking agents for LTCCs and will specifically focus on the class of dihydropyridines (DHPs) and benzo(thi)azepines (BTZs). To this end, the known structure-activity relationship (SAR) studies for the latter compounds will be summarized, as they were of central importance for the development of the photoswitchable Ca_v ligands that were prepared in the course of present doctoral thesis.

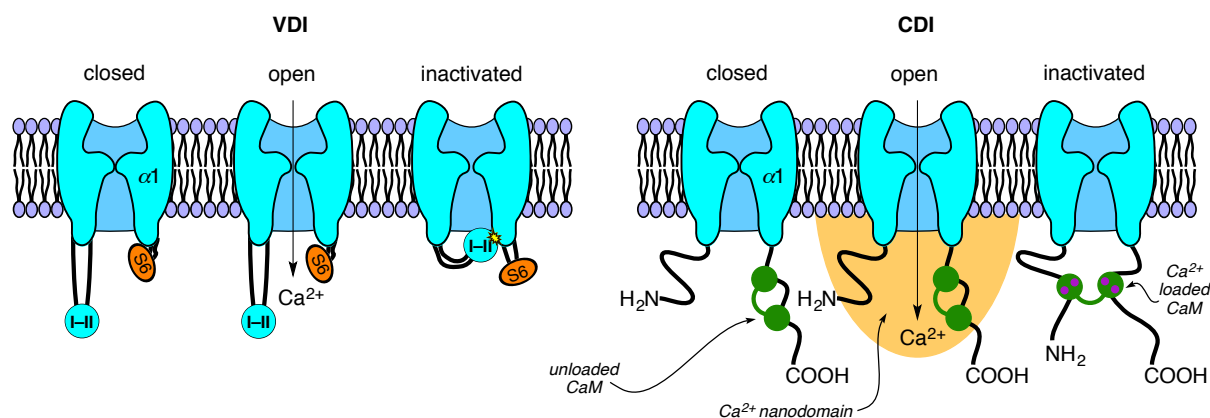
1.3.1 Channel Gating and Inactivation

In order to understand the mode of action of possible Ca_v agonists or antagonists, the different states which LTCCs undergo while ion gating is initialized or deactivated have to be considered.

The actual ion filter of the channel pore is composed by the previously mentioned four P-loop regions and has recently been investigated by electrophysiological and X-ray crystallographic analyses of a mutated Na_vAb channel.^[423] Introduction of the three aspartate residues of the Ca_v P-loop sequence conferred Ca^{2+} selectivity to the channel chimera and the authors could deduce the structural basis for this finding. Interestingly, it was found that most or all interactions of Ca^{2+} ions with the pore are made through its inner hydration shell. A set of three Ca^{2+} binding sites was identified, cooperating in a knock-off mechanism, at which the selectivity filter oscillates between two states with either one hydrated Ca^{2+} ion bound at a central site or two hydrated Ca^{2+} ions bound at the respective distal sites.

The primary opened or closed states of the channel are determined by the S4 voltage sensor segments of the homologous domains, respectively.^[400] Upon membrane depolarization those helices move outward and rotate under the influence of the electric field. Thus, a conformational change is initiated that opens the pore gate, which is formed by the S6 sections and represents an important part of the receptor sites for pore-blocking drugs specific for LTCCs (*vide supra*).^[436]

Besides, two major pathways for Ca_v inactivation have to be accounted for, which prevent Ca^{2+} overload in response to prolonged membrane depolarization. Understanding of how these modes work at a molecular level is particularly important, given that for instance clinically used DHP- or benzo(thi)azepine-based drugs show different channel affinities in the order inactivated > open > closed state.^[437,438] Common to all Ca_v subtypes is the voltage-dependent inactivation (VDI), which varies in its extent throughout the channel isoforms and is potentially modulated by the β subunit.^[439] In their studies, Zamponi and co-workers proposed a mechanistic model that involves a structural rearrangement of the S6 segments in response to sustained depolarization (scheme 1.2a).^[440] This change would presumably lead to the exposure of a docking site for the domain I-II linker region, thus giving rise to a hinged-lid-like gating particle.^[439] Notably, in $\text{Ca}_v1.3$ channels, this docking process has been found to be modified by an additional inhibitory element, which was termed the ‘inactivation shield’.^[441] In contrast, calcium-dependent inactivation (CDI) becomes apparent when Ca_v channel currents are compared in the presence of Ba^{2+} or Ca^{2+} .^[442] For this case it is believed that calcium-free CaM preassociates with the C-terminus of the channel in such a way that both ends of CaM are bound to specific domains thereon (scheme 1.2b).^[443] The rise of intracellular Ca^{2+} levels ultimately promotes molecular repositioning of fully loaded CaM that in turn triggers additional interactions with the N-terminus and consequently results in CDI.



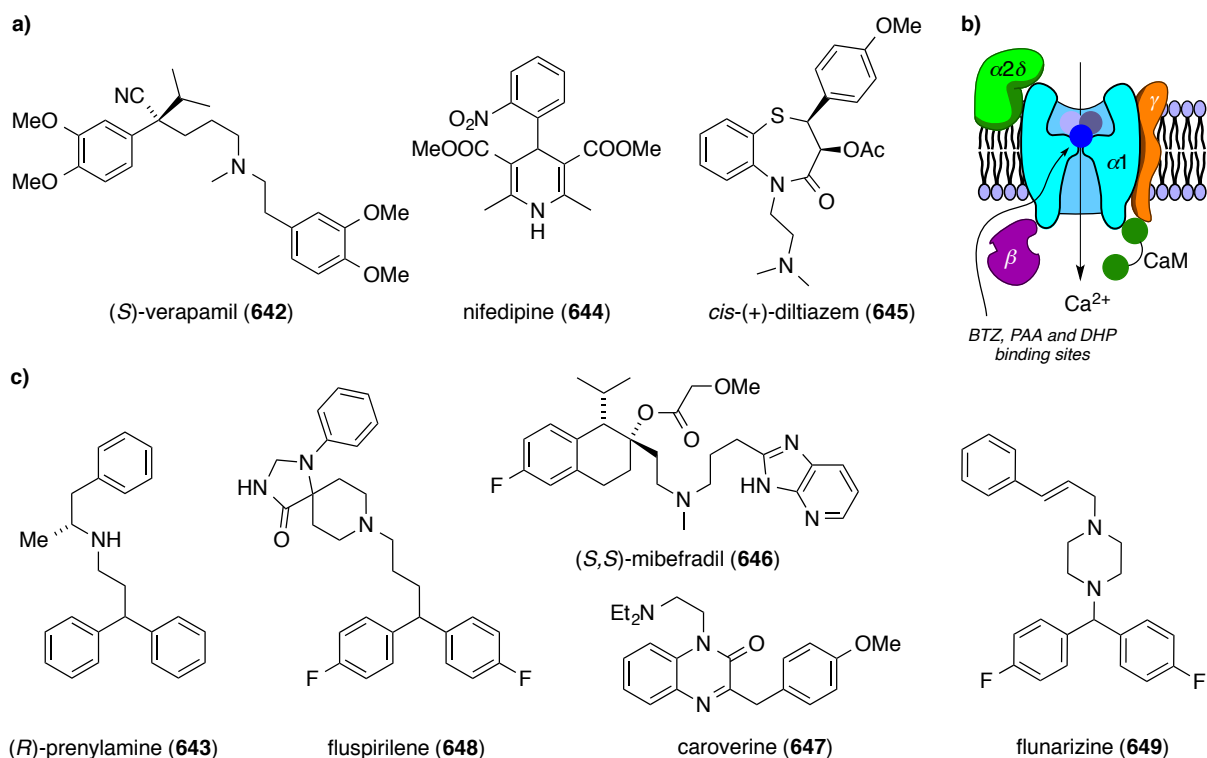
Scheme 1.2: Mechanisms of a) voltage-dependent inactivation (VDI) and b) calcium-dependent inactivation (CDI) of Ca_V channels. CaM can accommodate four calcium ions (purple dots).

At this, it has been proven that already the formation of calcium nanodomains is sufficient for $\text{Ca}_V1.2$ and $\text{Ca}_V1.3$ channels to initiate this mechanism.^[444]

From an electrophysiological point of view, a simplified consideration of gating in LTCCs has led to two main kinetic models,^[445] which suggest multiple closed states and one open species. Investigations thereof are mainly linked to the elucidation of the voltage-dependent block of DHP antagonists.^[446]

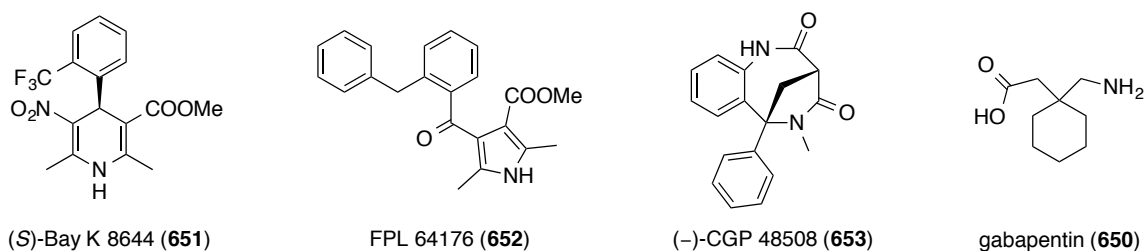
1.3.2 Overview on the Known Agonists and Antagonists

In regard of the crucial importance of Ca_V and especially LTCCs channels for the human physiology, the artificial control of their function has become the focus of numerous scientific and clinical studies. In 1882, Ringer described for the first time that calcium influences the contraction of heart muscle tissue, which was quickly lost when Ca^{2+} was deprived from employed media.^[447] The discovery of Ca^{2+} antagonism for the use in coronary drugs was first reported in 1964 by Fleckstein and co-workers, who found that verapamil (**642**) and prenylamine (**643**), mimic the cardiac effects of simple calcium withdrawal (scheme 1.3).^[448] In the following years, their laboratories identified a considerable number of similarly acting compounds, which were either based on the phenylalkylamine (PAA) structure similar to verapamil (**642**) or congeners of the new class of dihydropyridines (DHPs), like nifedipine (**644**).^[449] Diltiazem (**645**), the archetype of the benzo(thi)azepine (BTZ) family, was initially published by a Japanese group of scientists in 1975 for its antagonistic effects on Ca^{2+} currents.^[450] Later on, it was proven that most members of the



Scheme 1.3: Molecular structures of a) representative selective LTCC antagonists and b) an illustration of the location of their binding sites in LTCCs, as well as c) unselective LTCC antagonists.

above named substance classes would act with high selectivity (90–100%) on Ca²⁺-type, rather than on Na⁺- or K⁺-type currents.^[449] It was soon established that LTCCs are the primary physiological target of those compounds.^[446c,451] In the beginning of 1975, nifedipine (Adalat[®], **644**) was approved for treatment of coronary diseases in Germany.^[452] Since then, several derivatives thereof have been introduced to the market for the reduction of systemic vascular resistance and arterial pressure at symptoms like hypertension or for the treatment of angina pectoris.^[446c,453] Further investigations by means of photoaffinity labeling and antibody mapping suggested that all mentioned types of selective LTCC antagonists reside in three distinct, but overlapping binding sites near the S6 domain of the channel pore.^[454] A plethora of studies has been designated to the identification and characterization of those binding sites, which mainly referred to mutagenesis experiments.^[453,455] The concomitantly generated SAR data will be presented in chapter 1.3.4 for the case of BTZ-type Ca_v channel blockers. Notably, only peptide toxins are currently available as selective probes for the different members of the non-L-type Ca_v channel family. Besides this, several rather unselective antagonists like mibefradil (**646**),^[456] caroverine (**647**),^[449] fluspirilene (**648**)^[457] and flunarizine (**649**),^[458] are known. Furthermore, gabapentin (**650**) and related compounds have been evidenced to disrupt Ca_v channel trafficking by

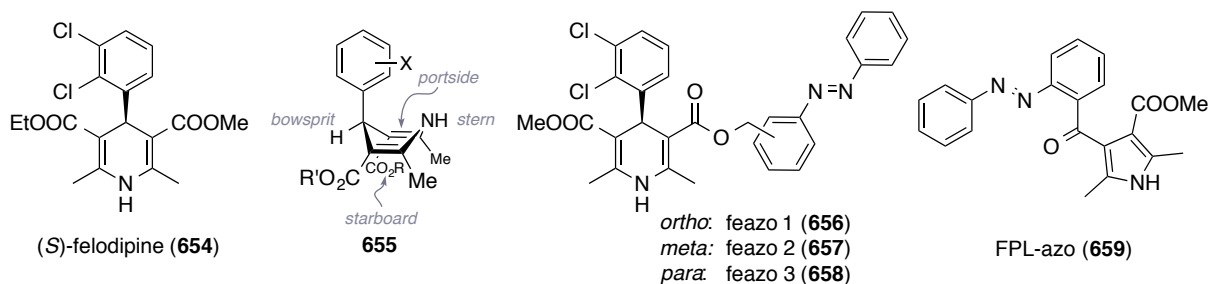


Scheme 1.4: Molecular structures of prominent LTCC activators and of the $\alpha 2\delta$ subunit modulator gabapentin (**650**).

targeting the $\alpha 2\delta$ subunit (scheme 1.4).^[459] Drugs that promote current through LTCCs (Ca_v channel activators) have also been described and prominent examples are the dihydropyridine (–)-BAY K 8644 (**651**),^[460] the benzoylpyrrole FPL 64176 (**652**)^[461] and the benzodiazocine CGP 48508 (**653**).^[462]

1.3.3 Dihydropyridine-based LTCC Blockers

The class of DHP-based Ca_v channel ligands is probably the most well investigated and since their discovery a considerable number of studies have tried to elucidate their binding site at the ion gating enzymes. Thus it was recognized that LTCCs are not all inhibited equally by DHP antagonists. Specifically $\text{Ca}_v 1.3$ and $\text{Ca}_v 1.4$ channels are significantly less sensitive when compared to $\text{Ca}_v 1.2$.^[412,463] One of the most potent congeners developed so far is the racemic compound felodipine (**654**), which exhibits an IC_{50} value of 14.9 nM (scheme 1.5).^[464] An interesting approach toward probing for the binding pocket of DHPs involved a molecular tape measurement, at which a positively charged quaternary ammonium function was attached to a DHP core structure *via* an alkyl linker of varying length.^[465] Thus it was estimated, that the antagonist resides approximately 11–14 Å away from the channels' extracellular face. Furthermore, a “sidewalk” pathway was found that allows the blockers to access the channel interior from the external, but not from the internal side.^[466] Today it is known that this DHP receptor site lies between the transmembrane helices III-S5, III-S6, IV-S6 and the pore loop region III-P.^[467] However, due to the lack of crystallographic data on $\text{Ca}_v \alpha 1$ domains, the exact interactions between the drugs and the channels remain unknown. Modern approaches addressing this problem rely on computational methods and employ homology models, as for instance demonstrated by Zhorov *et al.*^[467e] These authors used a mixed construct, where the open state was calculated in analogy to K_vAP , the closed state according to a KcsA template and the selectivity filter was based on a $\text{Na}_v 1.4$ P-loop domain



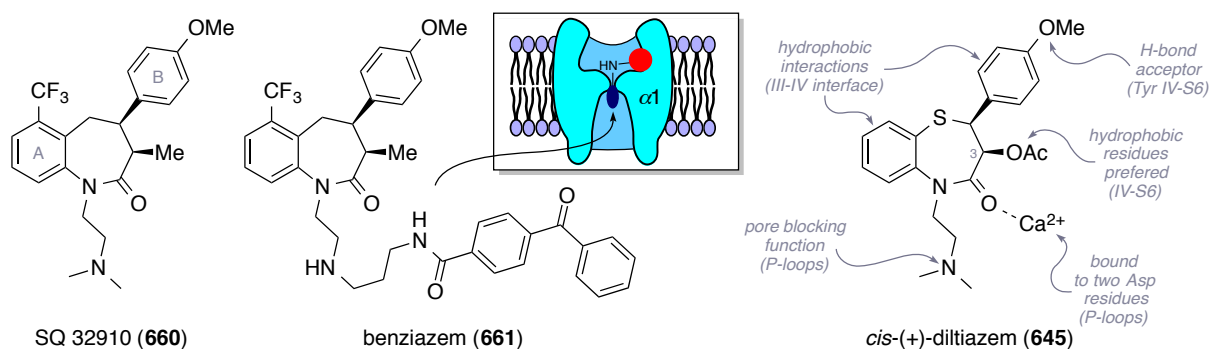
Scheme 1.5: The LTCC blocker felodipine (**654**), an illustration of a commonly used DHP nomenclature and the ineffective azobenzene derivatives (**656–659**) previously evaluated in the Trauner laboratories.

model. As a consequence, four models of DHP-bound LTCCs have been published to date.^[468] The major consensus found in these hypotheses is, that the portside group of DHP structures (*cf.* structure **655**) is oriented toward the ring of hydrophobic residues in the C-terminal halves of S6 helices. Thus, hydrophobic groups at the portside of the DHP-type antagonists are proposed to stabilize the closed state of the activation gate, whereas hydrophilic groups would act in converse manner.

With these findings in mind, the Trauner laboratories had set out to design and synthesize potential photochromic versions of the mentioned DHP felodipine (**654**).^[469] To this end, the compounds Feazo 1–3 (**656–658**), as well as the FPL 64176 analogue FPL-azo (**659**) were prepared and electrophysiologically evaluated. Although the photochromic DHP derivatives remained potent $\text{Ca}_v1.3$ blockers, no control of Ca^{2+} currents could be achieved with light. The same held true for FPL-azo (**659**), which additionally induced significantly less activation of Ca^{2+} influx than its respective parent compound.

1.3.4 Benzo(thi)azepine-based LTCC blockers

Benzo(thi)azepines (BTZs) are complex molecules with many different functional groups and so is their mode of action as LTCC antagonists, which exhibits several observable dependencies. Frequency-dependent block has been demonstrated by increasing the number of depolarization stimuli in a given time window. In general this leads to more effective inhibition of Ca^{2+} currents.^[470] This ‘use-dependent block’ termed behavior is consistent with the hypothesis that the distinct functional states of the channel have different affinities for those drugs (*vide infra*). Furthermore, raising Ca^{2+} or Ba^{2+} concentrations counteracts the effect of *e.g.* diltiazem (**645**), at which the channel block is stronger when calcium is used as charge carrier.^[471] Thus, the function of BTZs is considered to be potentiated by Ca^{2+} ,



Scheme 1.6: Molecular structures of SQ 32910 (**660**) and benziazem (**661**). The calculated binding mode of the latter BTZ was illustrated next to it, with the basic pharmacophore (red) and the photolabeling side chain (dark blue). The most significant interactions of BTZs and LTCCs known from SAR studies were indicated at the structure of diltiazem (**645**).

suggesting that the presence of those ions in the channel is required for high affinity binding.^[437] A third characteristic of BTZs was revealed when tertiary amine and quaternary ammonium containing analogues were either applied from the extra- or intracellular side. Interestingly, BTZs did not result in significant block from the cytoplasmic face, leading to the conclusion that they enter LTCCs *via* an extracellular pathway.^[472] In contrast to this, more recent studies, which employed a quaternary ammonium version of diltiazem (**645**), have disclosed that use-dependent current inhibition is induced by the protonated form of diltiazem from the inside.^[473] Concomitantly, it was proposed that this derivative accesses the same binding pocket as externally applied BTZs *via* a similar pathway previously found for charged PAA antagonists. An early approach to identify this receptor site was conducted by Kraus *et al.* *via* labeling of LTCCs purified from skeletal muscle by photoincorporation of [³H]benziazem (not shown).^[474] Accordingly, the ligand could be detected in four tryptic fragments of the III-S6 and IV-S6 regions at the $\alpha 1$ domain (*cf.* chapter 1.2). Further elucidation of the BTZ-sensing residues of LTCCs was achieved by different mutational studies, which were complicated by the unequal effects on distinct BTZ drugs or the characteristics of blocked Ca²⁺ currents.^[475] A common finding was that selectivity filter mutations do not alter diltiazem block of closed channels in Ba²⁺ containing media, but disrupt frequency-dependent block and potentiation by calcium ions.^[471] Besides, some other residues of the P-loops on the SIII and SIV segments seemed to be involved in BTZ-binding.^[475] The determinants for the atomic-level mechanism of block by BTZ-type Cav channel antagonists remained largely unclear until Zhorov and Tikhonov published their computational analysis, which referred to a homology model of Cav1.2 to KvAP and KscA.^[437] In their docking experiments, the two ligands SQ 32910 (**660**)^[476] and benziazem (**661**)^[477] were used to account for BTZs with small and large substituents at the essential

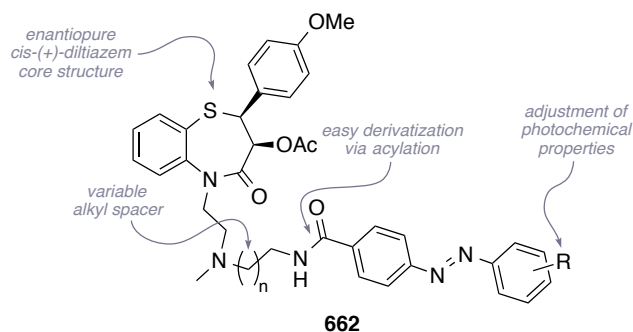
amino function. Scheme 1.6 illustrates the determined interactions of those ligands with the channel model on the exemplary structure of diltiazem (**645**). In the proposed binding mode, the carbonyl oxygen of BTZs directly connects with a calcium ion, that in turn is associated to two glutamic acid residues in the selectivity filter region of the P-loops of segments III and IV. An interpretation of the state-dependent binding of BTZs was given by the calculated possibility of the amino group to bind either at the focus of P-helices (channel pore) in the presence of Ca^{2+} , or to a selectivity filter glutamate in the absence thereof. In the closed-state of the channel, specific hydrophobic interactions to a phenylalanine and isoleucine residue on the III-S6 and IV-S6 helices were lost, explaining the experimentally observed lower affinity to the ligand (*vide supra*). A viable entry for BTZs to the receptor site was confirmed and would proceed *via* the III/IV domain interface. Notably, benizazem (**661**) was found to bind in the same mode as smaller BTZs, at which the large substituent on the amino function protrudes into the channel pore, being directed toward the cell interior.

In this context, the previously established SAR data^[476,478] on BTZ-type Ca_V channel ligands was reinvestigated. A decisive feature for BTZ potency is administered by the methoxy function at the aromatic ring A. Whilst larger substituents, like *e.g.* an ethyl moiety, were proven to result in a pronounced drop in blocking efficiency,^[478c] the calculations showed an H-bond to a tyrosine residue on the IV-S6 helix that is specific for LTCCs.^[437] Both aromatic portions exhibit important interactions with hydrophobic residues of the channel interface, whereas the substituent at position C-3 of the 7-membered ring system seems to have only a moderate effect on the BTZ potency.^[478c] However, the absolute and relative configuration of the two adjacent stereocenters was demonstrated to be crucial for the efficacy of diltiazem (**645**).^[479] The already mentioned amino functionality that constitutes the actual pore-blocking moiety can only be substituted by other hydrophilic groups under substantial loss of potency.^[437,471] However, a multitude of derivatives having large substituents tethered to this function were published in the past,^[476,478] which is why this position drew our attention for the potential installment of an azobenzene side chain.

1.4 Project Outline

As outlined in the preceding chapters, Ca^{2+} is a major determinant in neurotransmitter release and gene regulation *via* second messenger pathways in neurons. Controlling the influx of Ca^{2+} through Ca_V channels in a light-dependent manner would allow studying these events in more detail. A chemical tool that mediates such a behavior would potentially lead to a deeper

understanding of the temporal and spatial correlations of LTCC activity and its downstream signaling events.



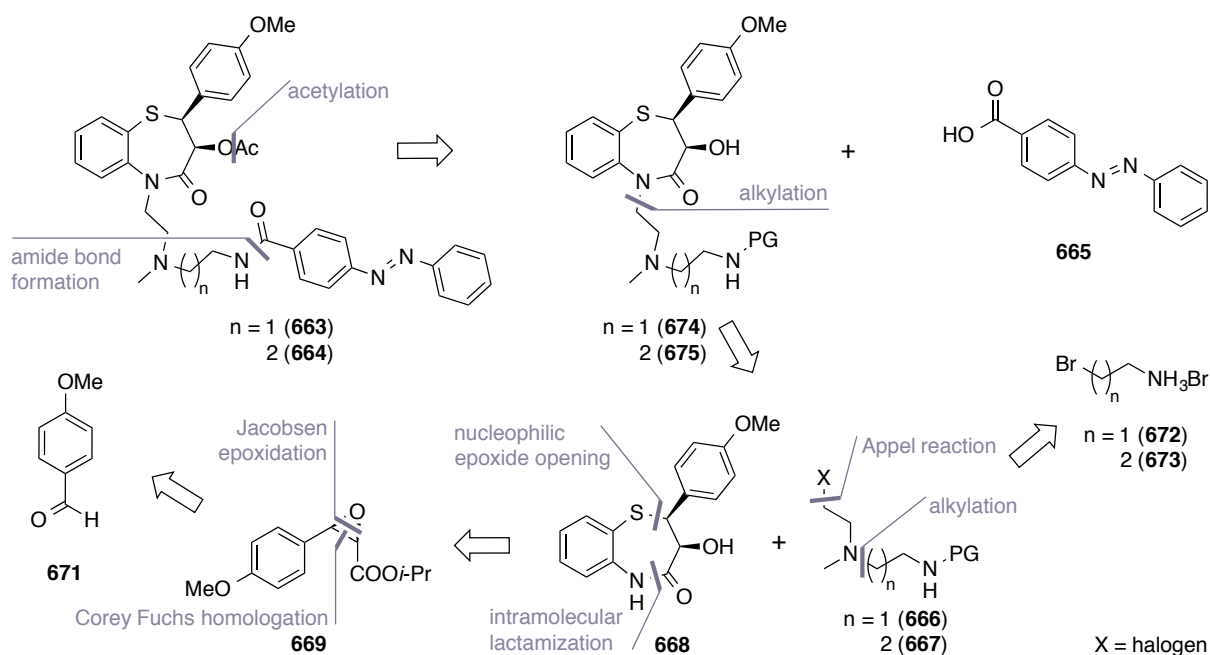
Scheme 1.7: Design of a potential photochromic LTCC antagonist, based on the diltiazem (**645**) core structure and featuring various potential sites for convenient chemical modification.

The present project aimed at the development of novel, benzo(thi)azepine-based photochromic ligands for LTCCs. To this end, it was envisioned to attach an azobenzene moiety as molecular switch to an appropriate site of the BTZ pharmacophore. This concept has become a leitmotif of the Trauner laboratories and has previously enabled the photocontrol of *e.g.* K_V or Na_V channels, as well as ionotropic glutamate receptors.^[480] Based on the known SAR data and homology models (*cf.* chapter 1.3.4) structure **662** was designed as an initial target for a synthetic program (scheme 1.7). Similar to benziazem (**661**), the large aromatic azobenzene core was linked to the pore-blocking amino function. The length of the alkyl spacer was considered to be variable and the optimal size would be determined by means of electrophysiological evaluation of a compound library. However, it was reasoned that shorter distances between the blocking amino function and the azobenzene switch could potentially yield higher efficacies of block and unblock, due to a more pronounced effect of the change in spatial demand and dipole moment on the position of the amino function. For the terminus of this linking chain, an amide function was chosen, which would provide a convenient way to attach several azobenzene substructures with desirable substitution patterns and photochemical properties. The introduction of more red-shifted and faster relaxing diazene switches might be necessary to adjust the ligand to the gating kinetics of the target channel. Diltiazem (**645**) was meant to be the basic pharmacophore, as several laboratory and industrial syntheses thereof have been described in literature.^[481] In principle those synthetic protocols should enable a broader insight in feasible chemical modifications of the bicyclic core, once the need to introduce additional structural modifications arises.^[482] The second stage of the project would involve the electrophysiological evaluation of the synthesized compounds and the chemical optimization of a potential lead structure to ultimately combine potent LTCC antagonism and efficient light-induced block and unblock.

2. Development of Photochromic Ligands for LTCCs

2.1 An Enantioselective Approach Toward Benzothiazepine-based Photochromic LTCC Blockers

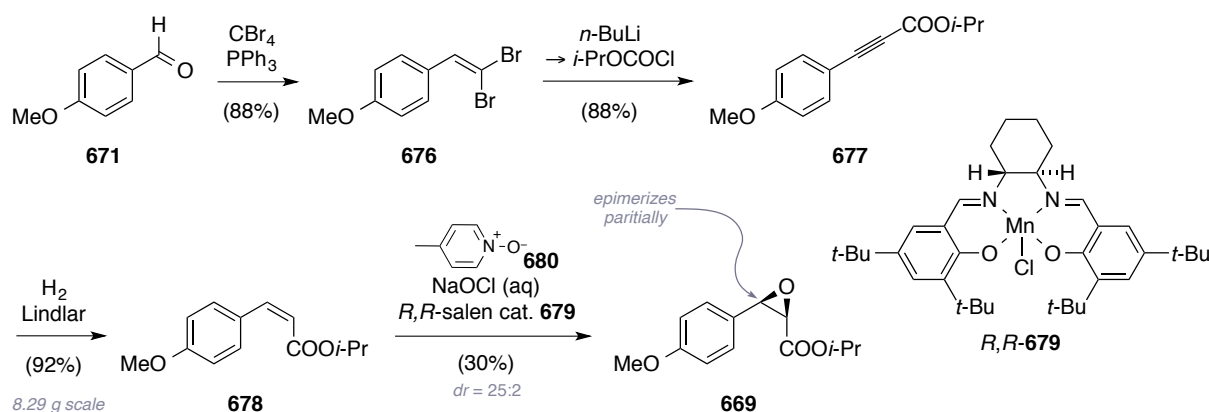
Based on the considerations discussed in the project outline, the presented synthetic program initially aimed for the synthesis of two prototypic azobenzene analogues of diltiazem (**663** and **664**). The retrosynthetic plan for these targets envisioned placing the first disconnection at the amide bond to 4-(phenylazo)benzoic acid (**665**). In order to allow a most convergent preparation of several analogues, further cleavage was planned at the alkyl linkage to the amide nitrogen of the 7-membered ring system and the C-3 located acetyl group (scheme 2.1). Previous syntheses of diltiazem (**645**) have shown that the first mentioned bond can be formed *via* convenient alkylation procedures,^[481b,c] which traces the molecule back to the halogenated linker fragments **666** and **667** and the tricyclic core of diltiazem (**668**). The latter was meant to be accessible in an enantiopure fashion *via* modification of the synthetic protocol disclosed by Jacobsen *et al.*^[481g] To this end, the central thiazepine ring system would arise from intramolecular lactam formation between the ester moiety of epoxide precursor **669** and the aniline nitrogen. The latter function would be present after stereospecific addition of *o*-nitro-thiophenol (**670**) to this very epoxide (**669**) and subsequent Béchamp reduction thereof.^[483] Substance **669** should be synthesized asymmetrically from the



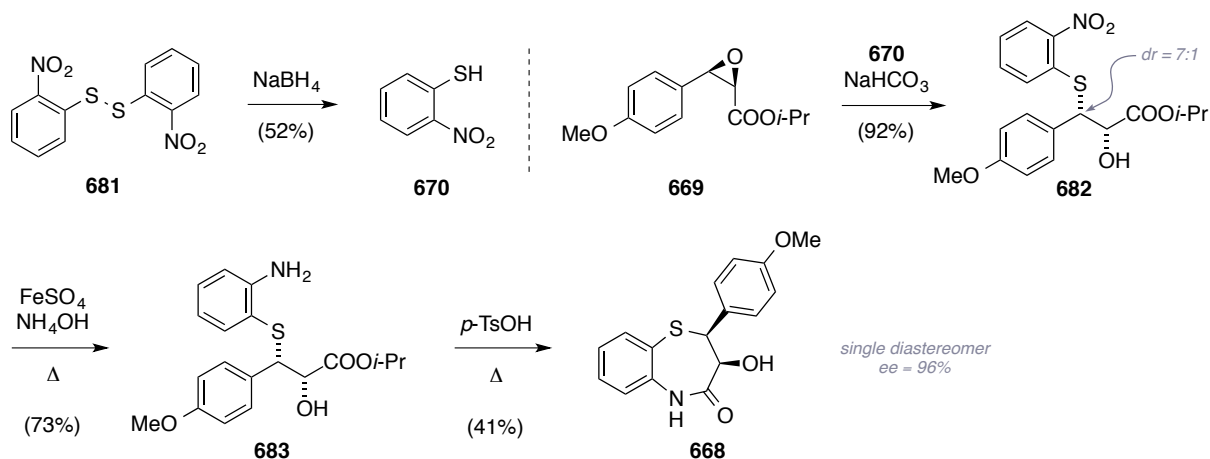
Scheme 2.1: First-generation retrosynthetic analysis for the enantioselective and convergent synthesis of the potential photochromic LTCC antagonists **663** and **664**.

respective *Z*-cinnamon ester (not shown) by Jacobsen-Katsuki epoxidation,^[484] which is well established for those substrates.^[481g] To address the required ester, it was intended to employ a literature-known sequence^[481g] that proceeds *via* Corey-Fuchs homologation^[256] and Lindlar reduction^[332] of inexpensive *para*-anisaldehyde (**671**). The respective halogenated side chains **666** and **667** should be obtained by *e.g.* Appel reaction^[308] of the corresponding alcohols, which would stem from an alkylation of the appropriately protected versions of the commercially available bromoalkylamines **672** and **673**.

To reduce this plan into practice, the synthesis of thiazepine core **668** was commenced by submitting *p*-anisaldehyde (**671**) to classical Ramirez conditions^[255] and dibromide **676** was obtained in good yield (scheme 2.2). This material was then reacted with *n*-BuLi in a Corey-Fuchs-type homologation, at which the intermediary generated Li-alkynyl species was quenched with excess *iso*-propyl chloroformate according to the published protocol.^[481g] Thus, alkyne **677** was accessed on multi-gram scale in a yield being 29% higher than reported previously. Subsequent hydrogenation under Lindlar conditions^[332] was performed in a solvent mixture of *n*-hexane and 1-hexene and turned out to be highly dependent on the scale of the reaction. Due to an increased availability of hydrogen in larger amounts of solvent, the reaction sped up from 22 hours (100 mg scale) to one hour (8.39 g scale) and gave rise to alkene **678** in complete *Z*-selectivity without any overreduction. Next, the described Jacobsen epoxidation was evaluated, using *R,R*-salen catalyst **679**, picoline *N*-oxide (**680**) and common bleach solution as terminal oxidant in benzene. Initial experiments provided epoxide **669** only in half amounts of the expected yield. Variation of the additive to 4-phenylpyridine *N*-oxide (not shown),^[481g] the reaction temperature, the reaction duration, the solvent system to 1,2-dichloroethane and of the catalyst loading to lower (5 mol-%) and higher (30 mol-%) values did not effect any significant change. Notably, an improved diastereomeric ratio of



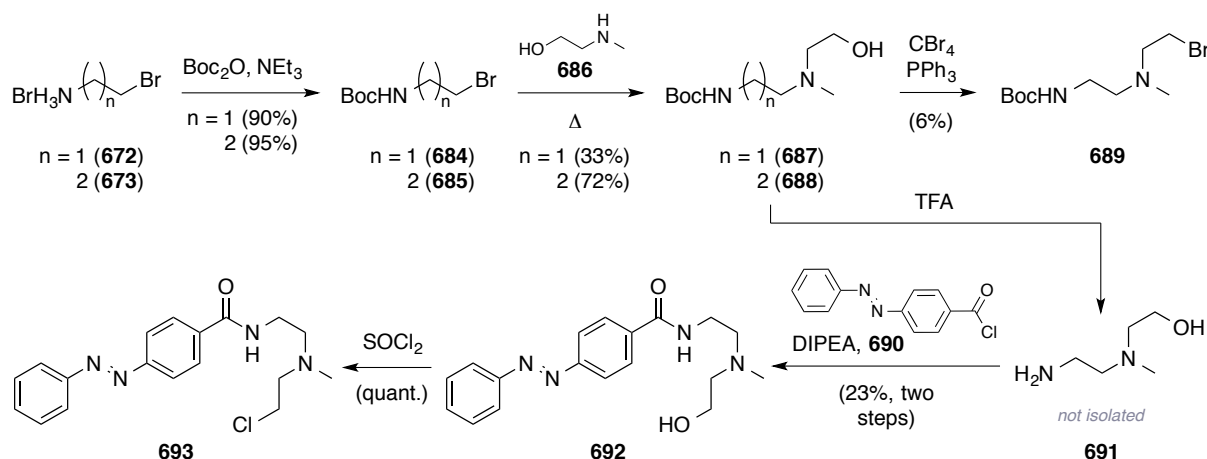
Scheme 2.2: Initial 4-step sequence for the asymmetric preparation of glycidate **669**, using a protocol that was established previously by Jacobsen *et al.*^[481g]



Scheme 2.3: Synthesis of thiazepine core **668** via nucleophilic epoxide opening with freshly prepared thiophenol **670**, Béchamp reduction and acid catalyzed lactam formation.

25:2 was observed, which stems from the partial inversion of involved radical intermediate.^[481g] Due to this isomeric mixture, the enantiomeric excess was not determined at this stage. However, measurement of the optical activity indicated that the reaction had proceeded in an asymmetric fashion.

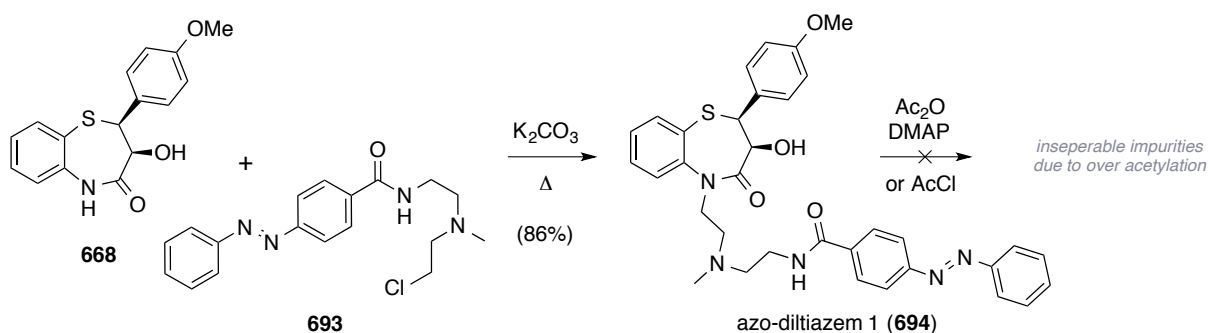
For the envisaged nucleophilic epoxide opening, air sensitive thiophenol **670** was freshly prepared from the respective inexpensive disulfide **681** via reduction with NaBH₄ (scheme 2.3). The moderate yield of compound **670** was attributed to partial reoxidation during the work-up and purification steps. Reaction of this material with epoxide **669** was conducted in ethanol under base catalysis with NaHCO₃. Lewis acid catalysis (*e.g.* with MgCl₂) or elevated temperatures^[485] led to increased amounts of the respective *erythro* isomer (not shown) via a S_N1-type mechanism. Although the desired thioether **682** could be obtained in 92% and with a *threo/erythro* ratio of 7:1, the procedure failed at times, presumably when the presence of oxygen was not excluded rigorously. Subsequent Béchamp reduction^[483] was straightforward and furnished the desired aniline (**683**) in good yield. The undesired isomers that originated from the epoxidation and thiol ether formation could be separated at this stage. To achieve thiazepine formation, conditions described by Adger *et al.* were chosen, at which substance **683** was directly cyclized employing catalytic amounts of *p*-TsOH under refluxing conditions in *m*-xylene.^[486] Unfortunately, the achieved moderate yield could not be optimized by the two-step procedure described by Jacobsen *et al.* that proceeds by ester hydrolysis and separate lactam formation.^[481g] Comparison of the optical rotation of thiazepine **668** to literature-known values indicated an *ee*-value of 96%.^[487] It has to be mentioned that on some occasions the transformation provided only very poor yield and no reasonable cause could be identified.



Scheme 2.4: A unoptimized sequence toward the β -amino chloride containing azobenzene fragment **693**.

In order to construct the linker fragment between the thiazepine core **668** and an azobenzene chromophore, inexpensive ammonium salts **672** and **673** were first protected as their respective Boc versions (**684** and **685**, scheme 2.4). Subsequent nucleophilic substitution with 2-(methylamino)ethanol (**686**) under refluxing conditions yielded the amino alcohols **687** and **688** in moderate and good yield, respectively. Unfortunately, all attempts toward converting those substances to their respective chlorides, bromides or iodides *via* Appel reaction^[308] or treatment with SOCl_2 in CH_2Cl_2 led to complete decomposition or provided very poor yield of bromide **689** (6%). Hence, it was tried to install the planned azobenzene moiety directly by first deprotecting the amine function in carbamate **687** with TFA in CH_2Cl_2 and ensuing treatment with freshly prepared acid chloride **690**. Gratifyingly, only *N*-acylation of amine **691** was observed, although the 2-step procedure suffered from low yields. At this point, the search for a more feasible synthesis of intermediate **692** was postponed and a potential halogenation of its alcohol function was investigated. This time, reaction with SOCl_2 promoted a clean formation of the desired chloride **693**, presumably *via* a $\text{S}_{\text{N}}1$ mechanism.^[488] Apparently, the Boc protecting group present in previous experiments had been to labile and undesired side reactions were caused by the *in situ* freed amino functionality.

With little amounts of both coupling partners in hand, the desired alkylation of the thiazepine core was evaluated. Applying conditions described by Schwartz *et al.* for their enantioselective synthesis of diltiazem (**645**),^[481e] chloride **693** was reacted with lactam **668**, deprotonating the amide function with K_2CO_3 in refluxing, wet EtOAc (scheme 2.5). Thus, azo-diltiazem **1** (**694**) was obtained in 84% yield, albeit in low quantities (17.4 mg). When this compound was submitted to acetylation protocols using AcCl or Ac_2O and DMAP, a concomitant participation of the amide function of the azobenzene moiety was triggered. The resulting impurity could not be separated by means of chromatography. In the following, a



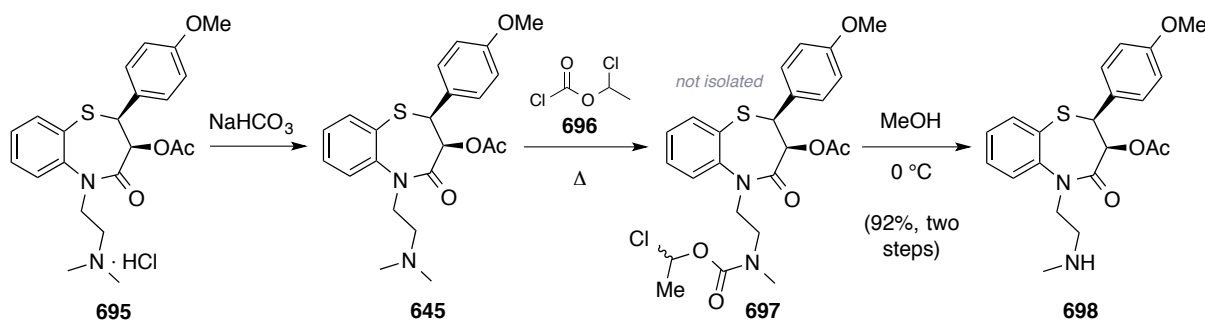
Scheme 2.5: Successful coupling of fragments **668** and **693**, yielding the first completed azobenzene derivative of diltiazem (**694**) and acetylation conditions applied thereto.

shortage of material hampered further investigation of reaction conditions and we chose to conserve the remaining azo-diltiazem 1 (**694**) for biological testing as the substituent on C-3 has been shown to be of rather small significance for drug potency (*cf.* chapter 1.3.4). Although the presented route had ultimately given rise to a potential photochromic LTCC antagonist (**694**), encountered low yields and unreliable transformations marked this strategy as unsuitable to be performed on larger scale, being necessary in order to establish a compound library.

2.2 Semisynthesis of Diltiazem-derived Photochromic LTCC Blockers

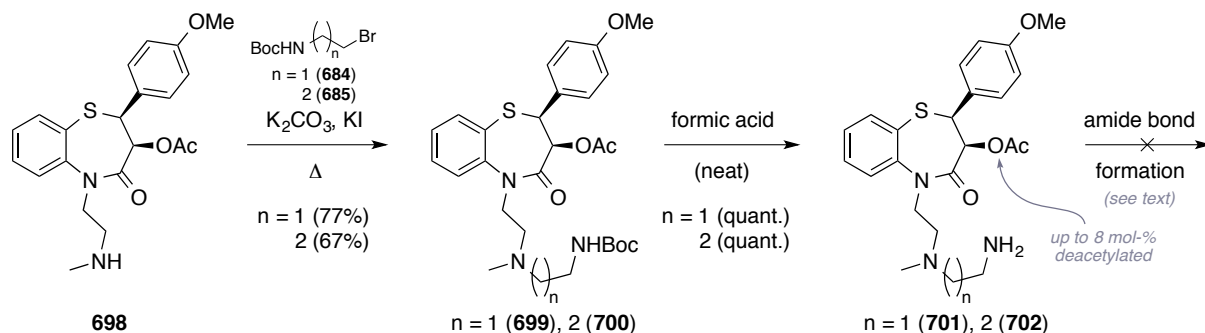
As (+)-*cis*-diltiazem hydrochloride (**695**) itself was commercially available at reasonable pricing, we became attracted by a method described by Alexander, which allows for the selective mono demethylation of the drug.^[489] The generated secondary amine was intended to be alkylated or submitted to reductive amination, thus representing a readily available precursor for the attachment of several azobenzene-substituted alkyl linker fragments.

Referring to Olofson's chemistry,^[490] the described demethylation process requires the use of stoichiometric amounts of the reagent 1-chloroethyl chloroformate (**696**) in refluxing DCE (scheme 2.6). From a mechanistic point of view, this transformation proceeds *via* an initial acylation of the tertiary amide in diltiazem (**645**) to yield in an intermediary acyl ammonium species (not shown). Under the employed elevated temperatures, the freed chloride ion then removes one methyl group by S_N2 -type nucleophilic substitution.^[490] The formed carbamate (**697**) is then no longer reactive enough to undergo a second acylation/demethylation event. Accordingly, the respective moisture sensitive carbamate (**697**) could be obtained after simple removal of the volatiles from the reaction vessel. However, when this material was subjected to hydrolysis in refluxing methanol, the respective deacetylated and mono dimethyl-



Scheme 2.6: Optimized two-pot protocol for the gram scale preparation of mono desmethyl diltiazem (**698**).

ated compound constituted the major product. Analysis *via* LCMS methods suggested that this ester cleavage had not occurred during the acylation/demethylation step. Furthermore, purifying the labile carbamate **697** by means of extraction and chromatography led to a significant loss of material. Gratifyingly, conducting the hydrolysis step at 0°C with prolonged reaction times suppressed the undesired deacetylation to 1–5 mol-% and mono desmethyl diltiazem (**698**) could be isolated in 92% over three steps on multi-gram scale. Similar reactivity was demonstrated on benzazepine-type LTCC blockers by using 2,2,2-trichloroethyl chloroformate and subsequent treatment with Zn in acetic acid.^[476] Due to the thioether function in substrate **645**, this reagent combination proved to be not applicable.

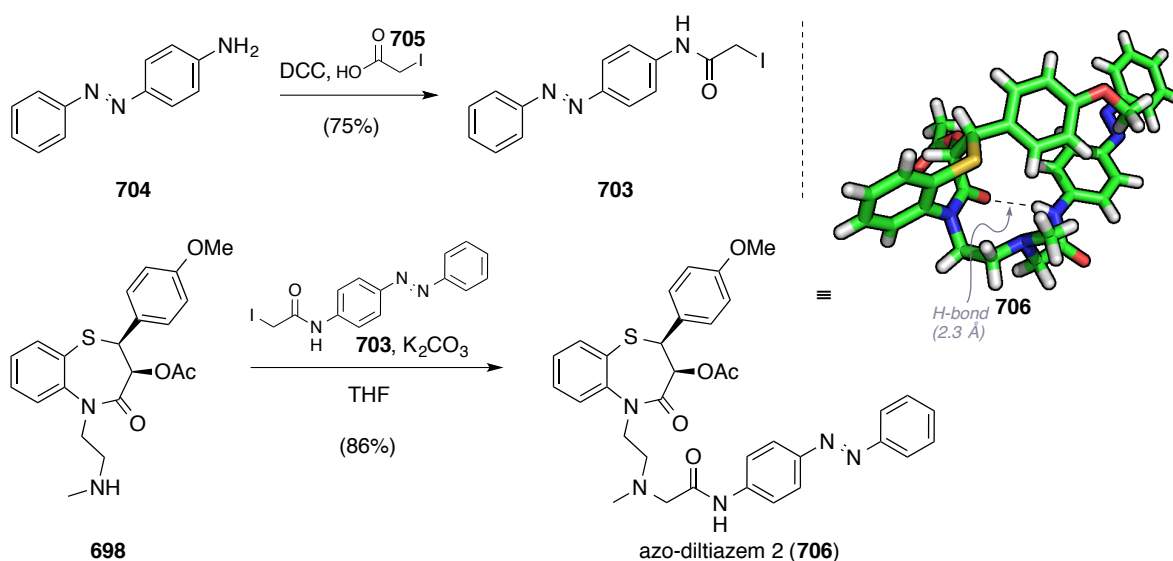


Scheme 2.7: First-generation approach for the elongation of mono desmethyl diltiazem (**698**) by alkylation and investigated further transformations of obtained carbamates **699** and **700**.

Next, it was planned to install an alkyl handle for the linkage to various photoswitchable diazene chromophores and nucleophilic addition to the previously synthesized Ω -bromo carbamates **684** and **685** (scheme 2.7) was investigated. In both cases, alkylation in the presence of potassium iodide furnished the desired tertiary amines **699** and **700** in good yields. The ensuing removal of the respective Boc protecting groups turned out to be surprisingly intricate, as standard acidic conditions^[266] like TFA in CH_2Cl_2 , HCl in MeOH, HCl in dioxane, TMSOTf and 2,6-lutidine in CH_2Cl_2 and *p*-TsOH in THF/ CH_2Cl_2 concomitantly promoted the hydrolysis of the acetyl function. Additionally, silica gel under heat and reduced pressure did not effect any reaction until decomposition set in at 200°C .

Interestingly, stirring the compounds in neat formic acid at room temperature, allowed for the isolation of desired free amines (**701** and **702**) in quantitative yields with less than 8% of the deacetylated side product. Ensuing attachment of the diazene unit was first tried with the preformed acid chloride **690** (*cf.* scheme 2.4), but resulted in the formation of an inseparable bisacylated side product. On the contrary, usage of the coupling reagents DCC and EDCI did not trigger any reaction at all.

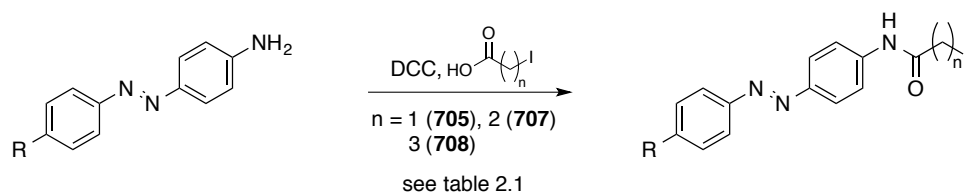
Hence, the strategy was changed once again and it was aimed at a possible alkylation of mono desmethyl diltiazem (**698**) by electrophilic reagents that already bear the azobenzene moiety. To this end, initially iodide **703** was prepared from commercially available aniline **704** and iodoacetic acid (**705**) by reaction with DCC (scheme 2.8). Although residual amounts of the hardly separable urea that is generated in the process contaminated the product at times, this method provided a convenient and fast entry to viable coupling partners for the diltiazem core **698**. Reaction of the latter mentioned amine with the activated α -carbonyl iodo compound **703** in THF furnished azo-diltiazem 2 (**706**) in excellent yield and the structure of this compound could be verified by X-ray crystallographic analysis. The obtained solid-state structure of **706** showed a densely packed conformation of the polycyclic molecule. At this, an H-bond of 2.3 Å length^[491] between the thiazepine carbonyl and the hydrogen atom of the newly formed amide functionality mediates additional folding. Notably, mentioned connectivity might explain both, the experimentally observed tendency of similar amides to undergo two consecutive acylation events (*vide supra*) and the inherent low solubility of *e.g.* azo-diltiazem 2 (**706**) in aqueous media.



Scheme 2.8: Alkylation of mono desmethyl diltiazem (**698**) with acetamide **703** and the solid-state structure of synthesized azo-diltiazem 2 (**706**). The intramolecular H-bond is indicated by a dashed line.

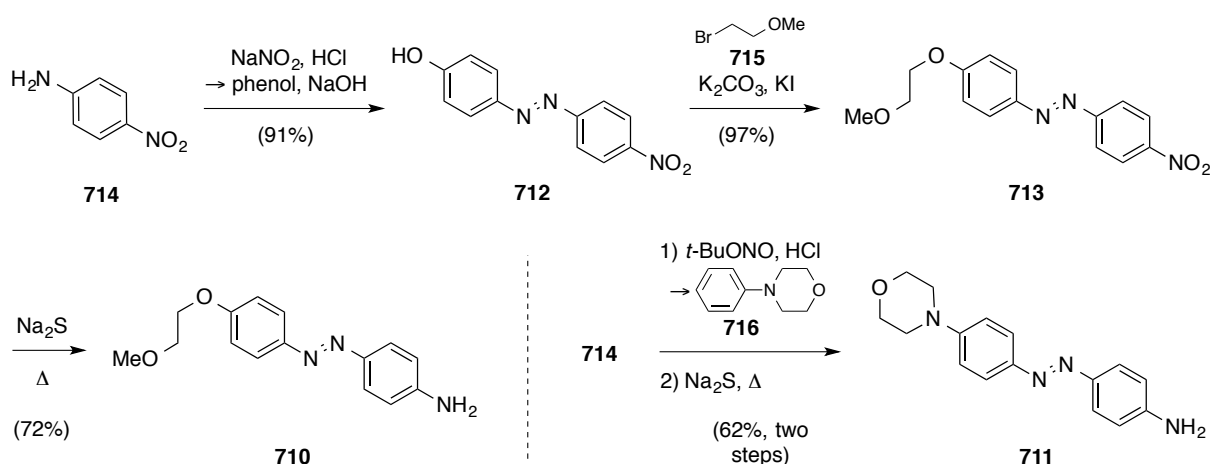
Encouraged by these results, we set out to synthesize a small compound library by modifying the azobenzene building block, either bearing an elongated alkyl chain, or *via* substitution with an electron donating dimethyl amino portion (table 2.1). At this, the yields for the DCC-promoted coupling reaction were generally lower, when 3-iodopropanoic acid (**707**) or 4-iodobutanoic acid (**708**) were employed. In the case of butanamide **709** (entry 7) the residual starting aniline **704** could not be separated fully by means of flash column chromatography. Furthermore, we prepared glycol ether- (**710**) and morpholino-substituted (**711**) anilines, in order to increase the solubility of the final diltiazem derivatives. Attachment of those polar tail functions is an often found concept in medicinal chemistry.^[492] The synthesis of those anilines is summarized in scheme 2.9 and comprises well established azo coupling chemistry (**712**), an alkylation step (**713**) and in both cases the reduction of respective nitro functions with aqueous sodium sulfide (**710** and **711**).^[480a,493] To the best of our knowledge, the latter conditions represent the only known method to achieve chemoselective reduction of aryl nitro groups reliably in the presence of a diazene bond.

Table 2.1: Synthesized Ω -iodoalkyl amides for the alkylation of mono desmethyl diltiazem (**698**).



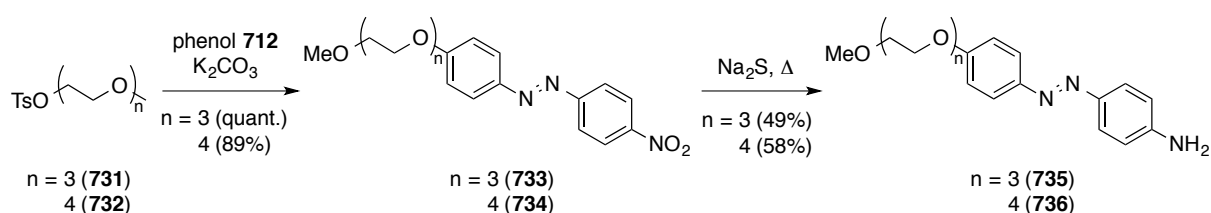
entry ^a	aniline	n	R	product	yield
1	704	1	H	703	75%
2	717	1	NMe ₂	718	38%
3	710	1	OCH ₂ CH ₂ OMe	719	52%
4	711	1	N-morpholino	720	77%
5	704	2	H	721	51%
6	717	2	NMe ₂	722	49%
7	704	3	H	709	25–38% ^b
8	717	3	NMe ₂	723	37%
9	735	3	O(CH ₂ CH ₂ O) ₃ Me	737	28–35% ^b
10	736	3	O(CH ₂ CH ₂ O) ₄ Me	738	68–73% ^b

a) Reactions were carried out in THF and stirred over night according to the general procedure given at the experimental section in chapter 3.2. b) Those compounds were contaminated with inseparable amounts of the respective starting aniline.



Scheme 2.9: Preparation of anilines **710** and **711** from nitroaniline **714** via common azo coupling chemistry.

Coupling of those reagents to mono desmethyl diltiazem (**698**) showed the expected trend that the electronically activated iodoacetamides would react faster and result in better yields (table 2.2). The synthesized derivatives that had no – or a dimethyl amino substituent – at the 4' position of the azobenzene unit (**706**, **724–728**), unfortunately suffered from very low solubility in aqueous media, even when their respective hydrochloride salts were formed by precipitation from HCl (1 M) in diethyl ether. The preparation of the glycol ether derivate **729** and the morpholino-substituted compound **730** could not improve this finding either. Notably, azo-diltiazem **8** (**729**) delivered crystals suitable for X-ray crystallographic analysis (table 2.2) that revealed a similar molecular arrangement as already described for azo-diltiazem **2** (**706**). Meanwhile conducted electrophysiological evaluation (*cf.* chapter 2.3) indicated that photoswitchable currents can be realized with compounds **729** and **727** indeed, at which the latter case showed the most promising results. However, only very low concentrations could be realized in physiological buffer solutions (HEPES, $\text{pH} = 7.4$), which is why small-chain PEGylated versions, having the same alkyl spacer length to the pore-blocking amino function as azo-diltiazem **4** (**727**), were synthesized. The required aniline building blocks were accessed from phenol **712** via alkylation with tosylates **731** and **732** (scheme 2.10). In both cases, the high polarity of the generated polyethers (**733** and **734**) complicated their separation from residual alkylating reagents by means of flash

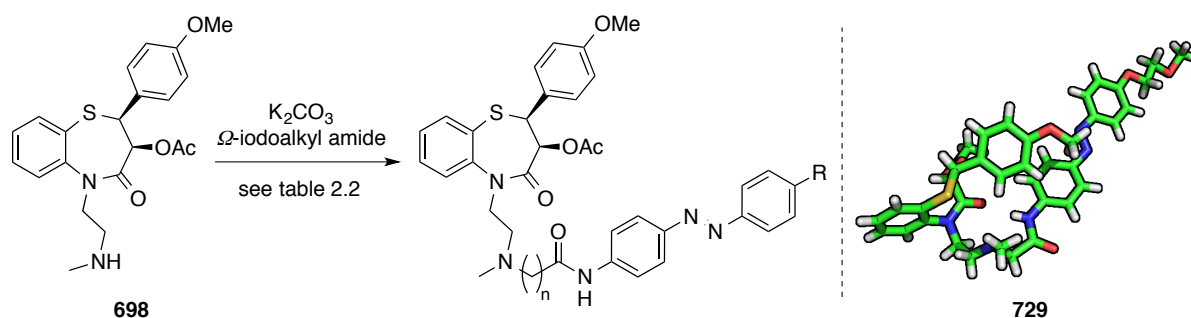


Scheme 2.10: Syntheses of PEGylated azobenzenes **735** and **736**. The preparation of employed tosylates **731** and **732** is described in the experimental section at chapter 3.2.

column chromatography. The remaining minor impurities were lost upon ensuing reduction with sodium sulfide. Thus, anilines **735** and **736** were obtained in moderate yields and employed for further coupling to 4-iodobutanoic acid (**708**) as detailed in table 2.1 (entries 9,10). When the resulting alkylating reagents (**737** and **738**) were used for the synthesis of azo-diltiazem derivatives **739** and **740**, moderate to good yields were achieved (table 2.2, entries 9,10). Despite their highly polar behavior that was observed at the chromatographic purification, the PEGylated compounds only exhibited slightly improved solubility in water in form of their respective hydrochloride salts. Transfer to physiological buffer solutions (DPBS, HEPES) resulted again in predominant precipitation, due to the increased polarity mediated by therein dissolved ions. Hence, those compounds have not been evaluated as photochromic LTCC blockers by means of *in vivo* experiments so far.

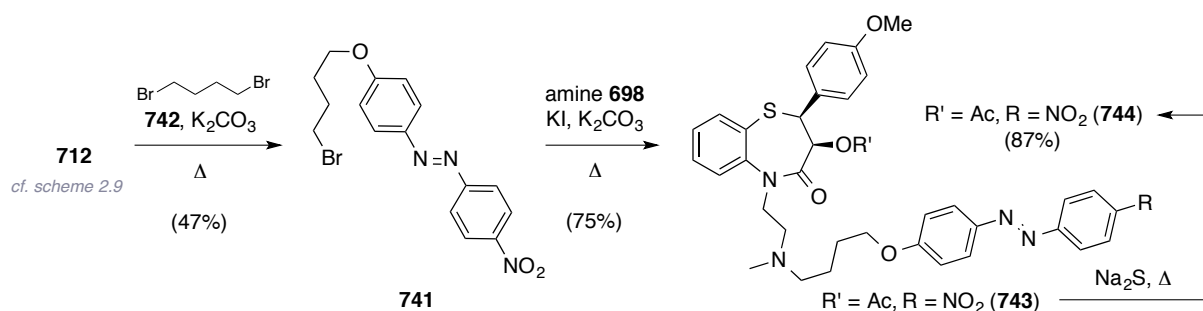
Instead, it was envisaged to raise the solubility in aqueous media by installing a permanent charge at the 4' position of the azobenzene moiety. In this context, it was tried to substitute the amide function by an ether linkage, in order to avoid observed conformational folding *via*

Table 2.2: Synthesis of azo-diltiazem derivatives **706**, **724–730**, **739** and **740** *via* an alkylation strategy.



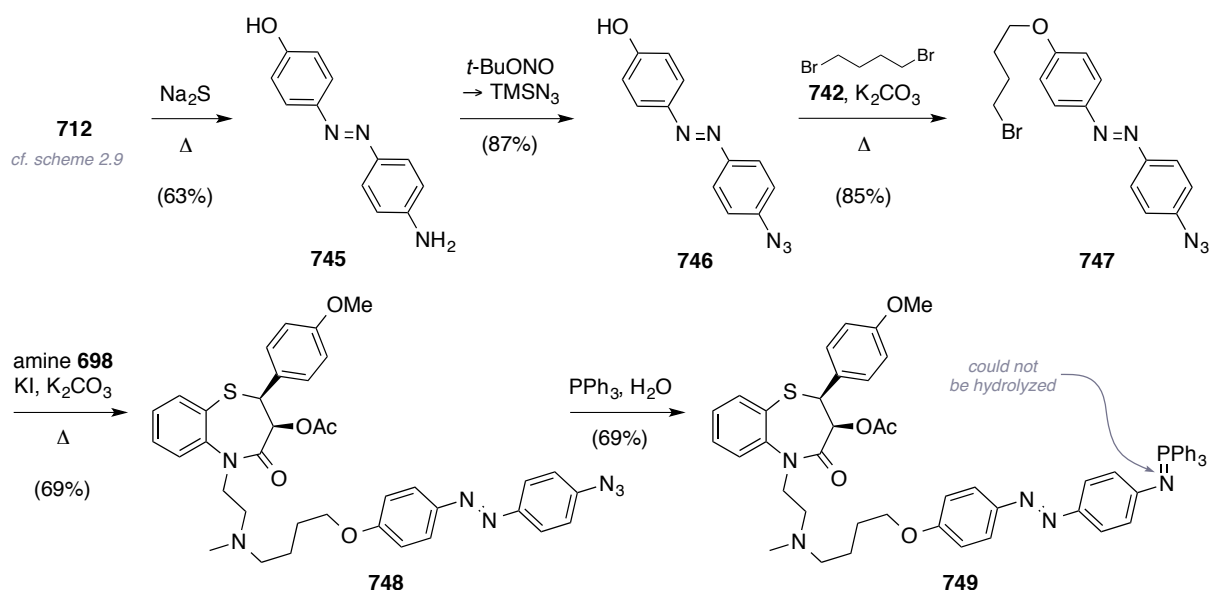
entry ^a	amide	n	R	product	yield
1	703	1	H	azo-diltiazem 2 (706)	86%
2	718	1	NMe ₂	azo-diltiazem 5 (724)	91%
3	719	1	OCH ₂ CH ₂ OMe	azo-diltiazem 8 (729)	95%
4	720	1	N-morpholino	azo-diltiazem 9 (730)	94%
5	721	2	H	azo-diltiazem 3 (725)	51%
6	722	2	NMe ₂	azo-diltiazem 6 (726)	32%
7	709	3	H	azo-diltiazem 4 (727)	32%
8	723	3	NMe ₂	azo-diltiazem 7 (728)	58%
9	737	3	O(CH ₂ CH ₂ O) ₃ Me	azo-diltiazem 10 (739)	69%
10	738	3	O(CH ₂ CH ₂ O) ₄ Me	azo-diltiazem 11 (740)	61%

^a) Reactions were carried out in THF at room temperature with super-stoichiometrical amounts of the respective Ω-iodoalkyl amide. Detailed experimental procedures are given in the experimental section in chapter 3.2.



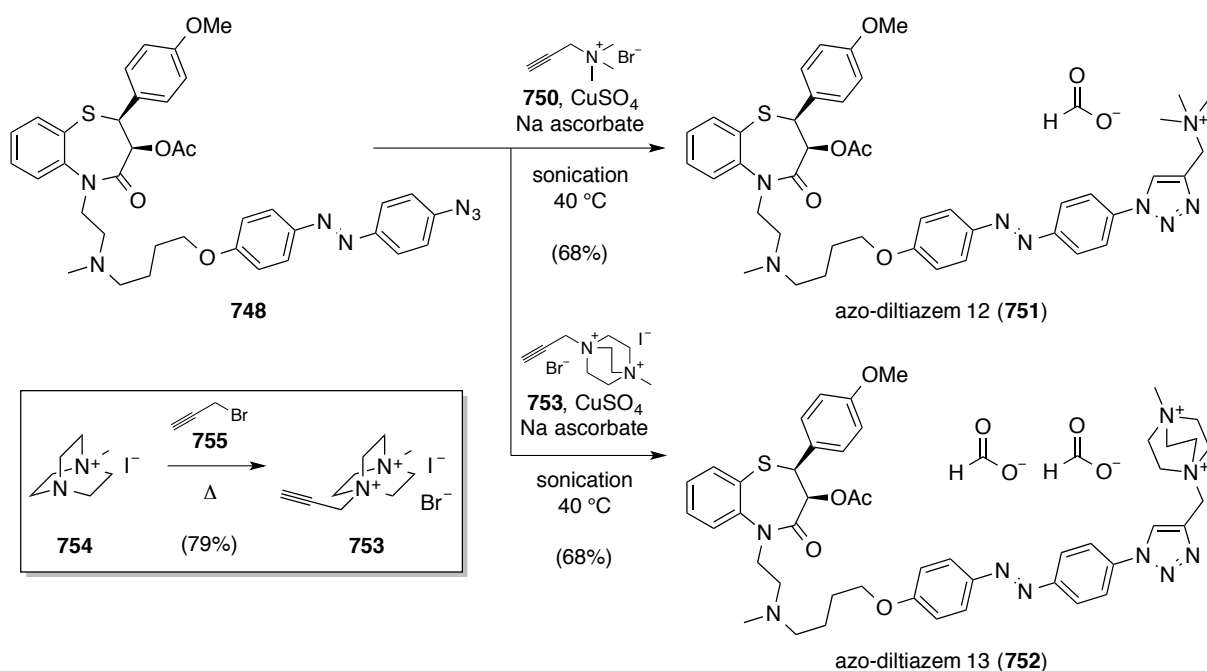
Scheme 2.11: Unsuccessful approach toward a permanently charged azo-diltiazem derivative.

intramolecular H-bond formation. To this end, alkyl bromide **741** was prepared from phenol **712** by reaction with stoichiometric amounts of dibromide **742** (scheme 2.11). Subsequent alkylation of mono desmethyl diltiazem (**698**) provided a higher yield (75%) when KI was added for an *in situ* Finkelstein-type halogen exchange. In the following, reaction conditions for a chemoselective reduction of the nitro function of substance **743** to the respective aniline were investigated. Whilst treatment with Zn in HOAc induced an undesired cleavage of the diazene bond, sodium sulfide-promoted reduction caused a simultaneous saponification of the acetyl ester (**744**). As a consequence, the planned ensuing acylation with a betaine-derived acid chloride^[480a] did not proceed in a site-selective manner. To circumvent the basic reduction conditions, the nitro group was exchanged against an azide substituent according to Moses and co-workers,^[494] by reacting aniline **745** with *t*-BuONO and quenching with TMSN₃ (scheme 2.12). For the mechanism of this reaction, several intermediates have been postulated and evidenced. Depending on the reaction temperature, either nucleophilic attack of an azide anion at the intermediary generated diazonium salt and a subsequent expel of gaseous N₂, or a sequential 1,3-dipolar cycloaddition and retro-cyclo-



Scheme 2.12: Synthesis of azide containing derivative **749** and unsuccessful Staudinger reduction thereof.

addition takes place.^[495] Accordingly, azide **746** could be accessed in 87% on gram scale. The following alkylation with dibromide **742** showed a significantly improved yield, when four equivalents of the reagent were used instead of one (*vide supra*). The coupling of the obtained bromide **747** to mono desmethyl diltiazem (**698**) required a threefold prolonged reaction time compared to nitro compound **741**. In the process, about 30 mol-% of the respective saponified congener were isolated as an inseparable mixture with the desired product **748**. Gratifyingly, complete re-acetylation could be achieved using unbuffered acetyl chloride and catalytic amounts of DMAP in CH₂Cl₂. With this material in hand, PPh₃ in wet acetonitrile was applied in order to effect a Staudinger-type reduction.^[496] Interestingly, the transformation stopped at the phosphazene intermediate (**749**), which could be isolated in almost quantitative yield. However, this compound could not be hydrolyzed to the desired aniline and remained inert even under forcing conditions (H₂O:AcOH = 1:1, 100 °C, 12 h).^[497] Therefore, the strategy was altered and the attachment of alkyne **750** by means of ‘Click’-chemistry^[498] (azide-alkyne Huisgen reaction^[499]) was investigated. Optimal reaction conditions involved the use of CuSO₄·5H₂O and sodium ascorbate in a thoroughly degassed mixture of DMSO, CH₃CN and water at 40 °C under constant sonication (scheme 2.13). Typically, full conversion was reached after 2 to 4 hours and the product (**751**) could then be obtained as the respective formate salt *via* reversed-phase column chromatography using formic acid (0.1 vol.-%) as an additive in the eluent mixture. Additionally bisammonium salt **752** was prepared in a similar fashion from alkyne **753**. Both compounds showed the desired increased solubility in water, as well as in physiological buffer solutions, and concentrations up to 250 µL could be reached



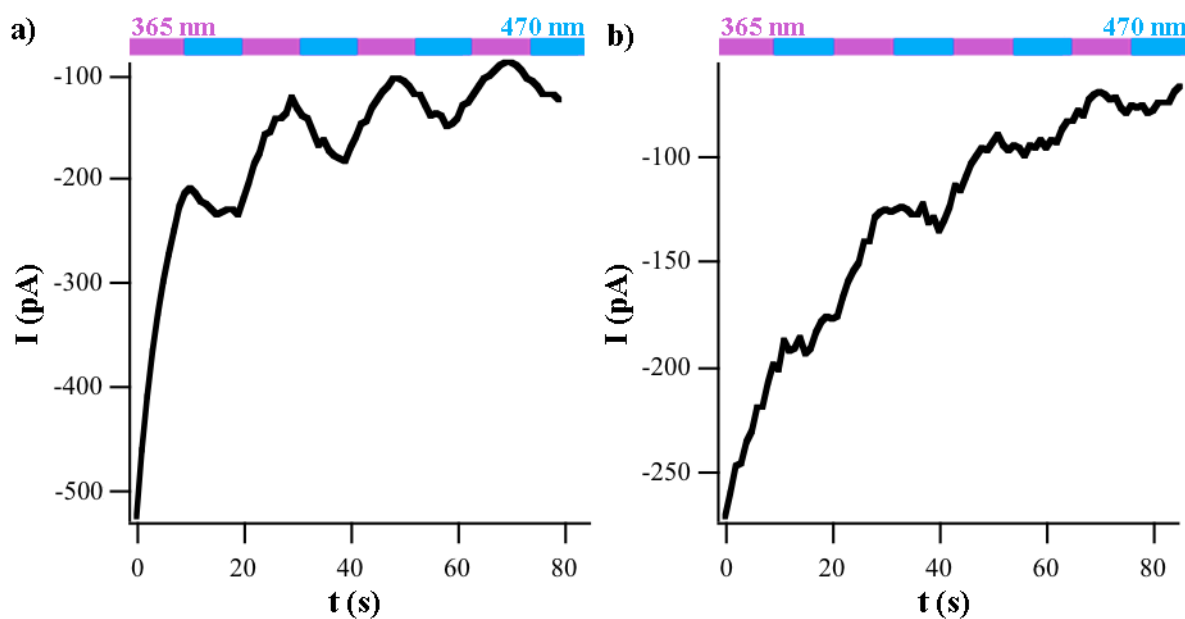
Scheme 2.13: Synthesis of permanently charged azo-diltiazems **751** and **752** using ‘click’-chemistry.

without any difficulty. So far, azo-diltiazem 13 (**752**) represents the furthestmost optimized structure for photochromic LTCC antagonists.

2.3 Electrophysiological Evaluation of Diltiazem-derived Photochromic LTCC Antagonists

The experimental work required for the electrophysiological evaluation of the synthesized azo-diltiazems derivatives was conducted by Dr. T. Fehrentz and was still ongoing as present chapter was written. Only preliminary results will be outlined in the following, as it is planned to publish the majority of the established data in due course.

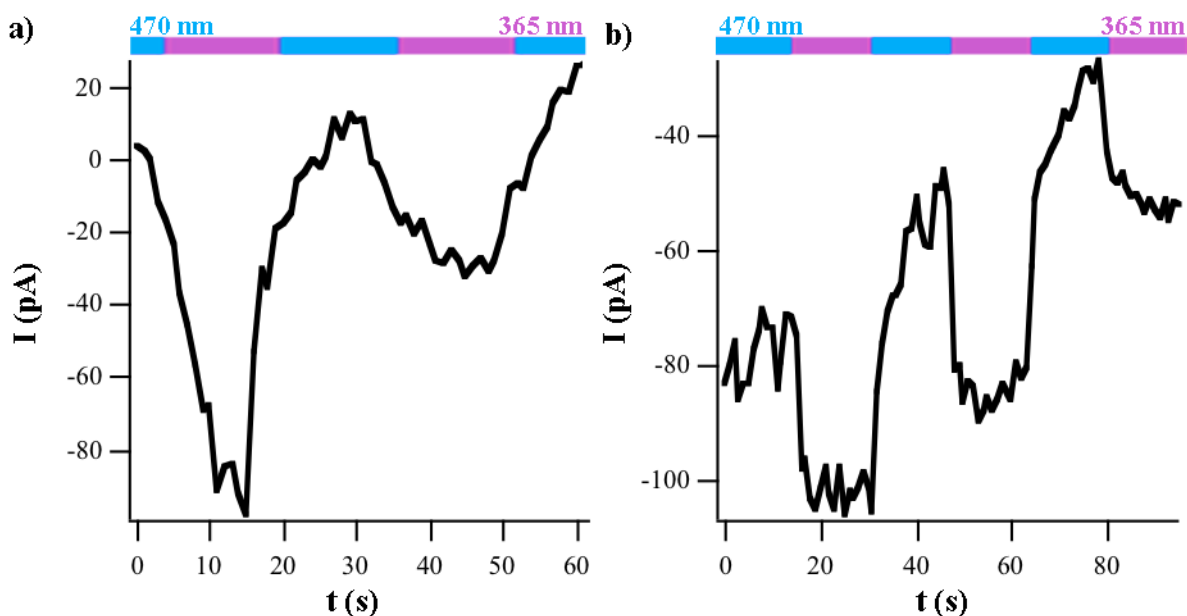
For presented measurements, HEK293T cells were transfected with 1 μg $\text{Ca}_v1.3\alpha1$, $\text{Ca}_v\beta3$ and $\text{Ca}_v\alpha2\delta$ in a molar ratio of 1:1:1 using the calcium phosphate method. To simplify the detection of transfected cells, eGFP (enhanced green fluorescent protein) was co-transfected. The employed electrophysiological protocol is described in detail in references 463 and 469. As calcium ion conductance in $\text{Ca}_v1.3\alpha1$ goes along with CDI of the channel current (*cf.* chapter 1.3.1), this effect was dampened by replacing Ca^{2+} with Ba^{2+} in the external recording solution.^[463] Current traces were recorded whilst irradiating the cells with two different wavelengths in an alternating mode, in order to switch the diazene bond from *trans* to *cis* or *cis* to *trans* configuration, respectively. Those wavelengths were determined for each compound by preceding UV-Vis spectroscopic measurements in water, which addressed the



Scheme 2.14: Current traces of representative a) azo-diltiazem 4 (**727**) and b) azo-diltiazem 8 (**729**) photoswitching events on $\text{Ca}_v1.3\alpha1$ channels expressed in HEK293T cells. The data indicates that longer alkyl spacer length to the pore-blocking amino function is desirable.

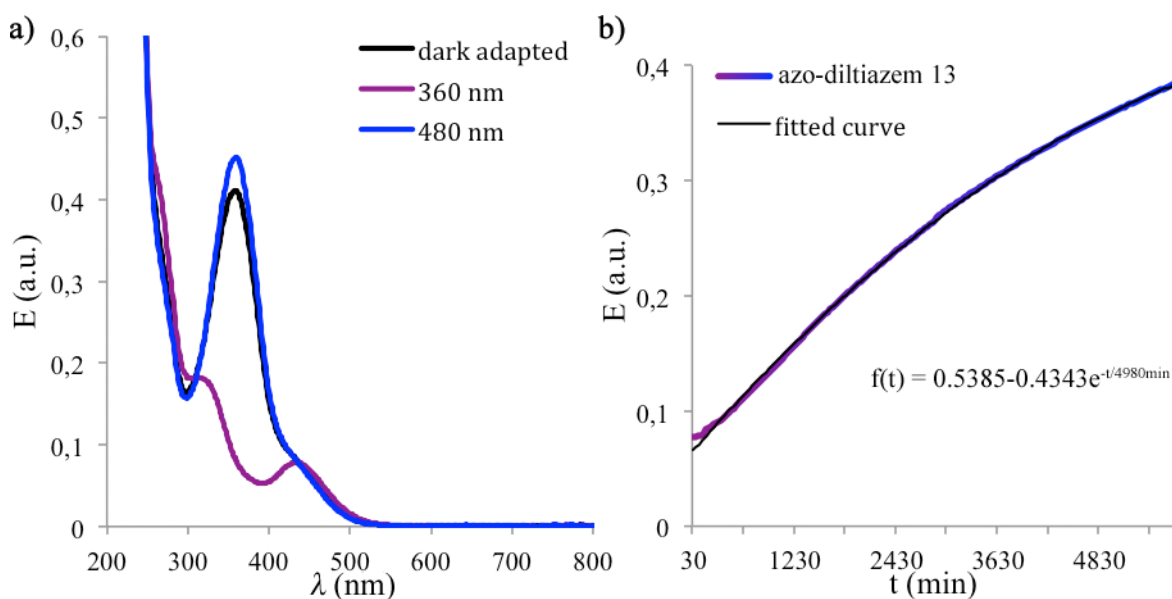
photostationary states with the respective maximum achievable *trans*- or *cis*-azobenzene content.

Thus recorded current traces are depicted in scheme 2.14 for azo-diltiazem 4 (**727**) and 8 (**729**) and the respective irradiation events are indicated at the time scale. The molecular concentrations of the antagonists in the external bath solution that were perfused on the cells were 40 μM (azo-diltiazem 4) and 40 μM (azo-diltiazem 8). It has to be mentioned that the general drop in current strength is attributed to the so-called rundown effect.^[500] Despite this, a significantly stronger pronounced increase in current was observed for substance **727**, when 470 nm were applied to switch the compound to its *trans*-state. Accordingly, both compounds become more potent LTCC blockers whilst having a *cis*-configured diazene bond. Notably, this was unexpected in regard to the previously calculated orientation of benziazem (**661**, *cf.* chapter 1.3.4) in LTCCs, which would suggest that a *cis*-configured azobenzene should exert increased steric demand in the channel pore, thus leading to unblock of the channel. Scheme 2.15 illustrates similar measurements for the charged and doubly charged derivatives azo-diltiazem 12 (**751**, 25 μM) and 13 (**752**, 25 μM). Unfortunately, the quality of grown cells did not allow recording comparable data sets, yet. Current efforts are directed toward the establishment of a more stable gene expression in order to obtain $\text{Ca}^{2+}/\text{Ba}^{2+}$ currents of improved consistency. Despite this, it can be seen that those water-soluble compounds act at least with similar efficacy as photochromic LTCC antagonists as azo-diltiazem 4 (**727**), but



Scheme 2.15: Current traces of representative a) azo-diltiazem 12 (**751**) and b) azo-diltiazem 13 (**752**) photoswitching events on $\text{Ca}_v1.3\alpha1$ channels expressed in HEK293T cells. For both compounds pronounced differences in cell currents were recorded, in respect to the triggered photostationary states.

can in principal be introduced in higher concentrations. In contrast to *cis*-blocker **727**, the permanently charged substances reduced Ca^{2+} currents preferentially when their diazene bonds were *trans*-configured. As especially azo-diltiazem **13** (**752**) has a large molecular weight (860 Da) and possesses a highly polar tail group, it is speculated that this compound might be unable to enter the plasma membrane fully and acts similarly to the ‘molecular tapes’ previously developed as DHP-based LTCC antagonists (*cf.* chapter 1.3.3).^[465] Support for this hypothesis was found when we measured the distribution of azo-diltiazem **13** (**752**) between water (100 μM) and octan-1-ol, at which the latter is considered as a satisfactory surrogate for membrane vesicles.^[501] Taking samples of both the aqueous and the organic layer and submitting them to LCMS measurements, virtually no ions of the benzothiazepine compound (**752**) could be detected in the octan-1-ol phase and recorded UV-Vis traces showed no absorption at the λ_{max} -value (360 nm). To quantify this finding, LTCC antagonists having the same chromophore, but shorter or longer alkyl spacer units, are envisaged targets for future synthesis.



Scheme 2.16: a) Recorded UV-Vis spectra of azo-diltiazem **13** (**752**) in water at its dark adapted state (black) and at the *cis* (purple) and *trans* photostationary (blue) states. b) Thermal relaxation after preirradiation with 360 nm for 10 minutes.

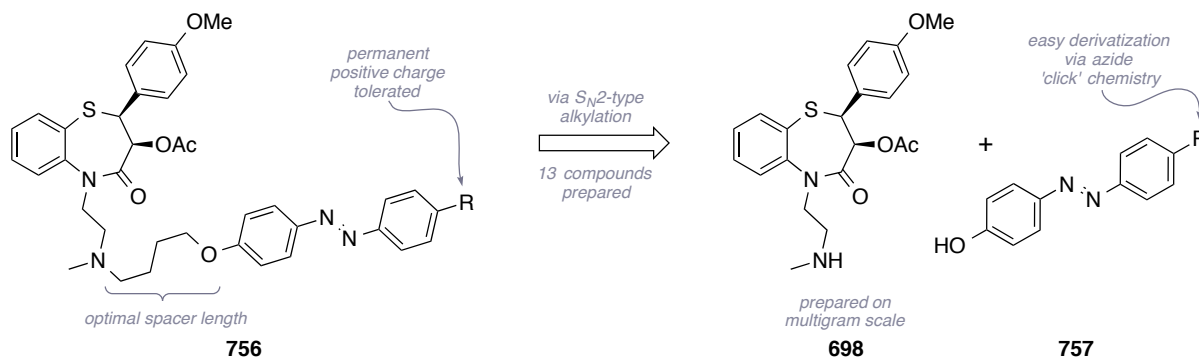
Additionally, all synthesized LTCC antagonists were characterized *via* UV-Vis spectroscopy in respect to their photostationary states and thermal relaxations from *cis*- to *trans*-configuration of the diazene units. These results are intended to be subject to publication as mentioned before, which is why only representative data is illustrated for azo-diltiazem **13** (**752**) in scheme 2.16. Interestingly, the compound exhibits extremely slow thermal relaxation in water with a half-life of 2.40 ± 0.01 days. This property is highly

desirable for testing, as the antagonist can be preirradiated conveniently and then perfused on the cells. Furthermore, largely stable states of channel block and unblock might be achieved that allow for a temporal control of Ca^{2+} currents without constant irradiation.

2.4 Conclusion and Future Aspects

In summary, we have successfully established the first photochromic antagonists for L-type voltage-gated calcium channels on basis of the pharmacophore of *cis*-(+)-diltiazem (**645**). A compound library of 13 azobenzene modified benzothiazepine channel blockers was synthesized and a preliminary lead structure (**756**) was identified by means of electrophysiological evaluation on the LTCC subtype $\text{Ca}_v1.3$ (scheme 2.17).

Whilst azo-diltiazem **4** (**727**) and **8** (**729**) showed more potent channel block in their *cis*-diazene photostationary states, the permanently charged versions **751** and **752** exerted more pronounced inhibition of Ca^{2+} currents, when having their azobenzene moieties *trans*-configured. Furthermore, the latter two derivatives exhibited improved solubility in water and physiological buffer solutions. Consequently, azo-diltiazem **13** (**752**) represents the most promising candidate for an efficient photocontrol of Ca^{2+} currents. This antagonist is marked by an unusual long thermal relaxation of its diazene bond and it was proposed that it acts as a molecular tape. This means that the charged tail group would reside at the extracellular side of the cell membrane and only the pharmacophore could reach to the BTZ receptor site (*cf.* chapter 1.3). To verify this hypothesis, we envisage synthesizing analogues of this compound, which vary only in the distance between the pore-blocking amino function and the chromophore. Ideally, these experiments should show a maximum in efficacy of photocontrol of Ca^{2+} currents for a specific alkyl spacer length.



Scheme 2.17: Developed convergent semisynthesis of photochromic LTCC antagonists. Structure **756** constitutes the assessed lead motif for further optimization of pharmacological properties.

In regard of the conducted synthetic experiments, a scalable and short semisynthetic route was successfully developed (*cf.* chapter 2.2) that allows attaching substituted diazene compounds to the parent drug diltiazem (**645**). To this end, the convergent coupling of mono desmethyl diltiazem (**698**) to a variety of alkylating agents was demonstrated. Crystal structures of the compounds azo-diltiazem **2** (**706**) and **8** (**729**) were obtained and a plausible explanation for their low solubility in aqueous media was deduced. Syntheses of permanently charged antagonists were achieved *via* convenient late-stage coupling of modified alkyne reagents using 1,3-dipolar cycloadditions ('click' reaction). In contrast, the attempted total synthetic route (*cf.* chapter 2.1) toward this type of antagonists suffered from low yields and not consistently reproducible procedures. Future work in this field might rather focus on the construction of benzoazepine-derived structures like SQ 32910 (**660**), which do not bear the sensitive thioether and acetyl ester portions (*cf.* chapter 1.3.4).

Currently, further physiological experiments are being performed by Dr. T. Fehrentz and quantifiable data regarding the efficacy of LTCC photocontrol and general drug potency are gathered. We expect that those investigations disclose potential chemical modifications of the determined lead structure and allow for the establishment of a useful photopharmacological tool for the elucidation of *e.g.* Ca^{2+} signaling pathways in neurons.

3. Experimental Section

3.1 General Notes

All reactions were magnetically stirred and carried out under a positive pressure of inert gas (N_2 or argon) utilizing standard Schlenk-techniques. Glassware was dried in an oven at $120\text{ }^\circ\text{C}$ and repeatedly at $650\text{ }^\circ\text{C}$ *in vacuo* prior to use. Liquid reagents and solvents were added by syringes or oven-dried stainless steel cannulas through rubber septa. Solids were added under inert gas counter flow or were dissolved in appropriate solvents. Low-temperature reactions were carried out in a Dewar vessel filled with a cooling agent: acetone/dry ice ($-78\text{ }^\circ\text{C}$) or $\text{H}_2\text{O}/\text{ice}$ ($0\text{ }^\circ\text{C}$). Reaction temperatures above room temperature were conducted in a heated oil bath. If literature-known procedures were followed, the respective reference was added to the experimental details. Yields refer to isolated homogenous and spectroscopically pure materials, if not indicated otherwise.

Solvents and Reagents

Tetrahydrofuran (THF) and diethyl ether (Et_2O) were distilled under N_2 atmosphere from Na/benzophenone as drying reagent prior to use. Triethylamine (Et_3N) and Hünig's base (DIPEA) were distilled under N_2 atmosphere from CaH_2 as drying agent prior to use. Further dry solvents such as dichloromethane (CH_2Cl_2), *N,N*-dimethylformamide (DMF), acetonitrile (MeCN), acetone, dimethyl sulfoxide (DMSO), methanol (MeOH), benzene, *m*-xylene, and toluene were purchased from commercial suppliers and used as received. Solvents for extraction, crystallization and flash column chromatography were purchased in technical grade and distilled under reduced pressure prior to use. Alkyne **750**^[502] and quaternary ammonium salt **754**^[503] were prepared according to literature-known procedures. All other reagents and solvents were purchased from chemical suppliers (*Sigma-Aldrich*, *Acros Organics*, *Alfa Aesar*, *TCI Europe*, *ABCR*) and were used as received.

Chromatography

Reactions and chromatography fractions were monitored by qualitative thin-layer chromatography (TLC) on silica gel F254 TLC plates from *Merck KGaA*. Analytes on the glass plates were visualized by irradiation with UV-light and/or by immersion of the TLC

plate in an appropriate staining solution followed by heating with a hot-air gun (350 °C). The following staining solutions were applied:

- *p*-anisaldehyde staining solution (3.7 mL *p*-anisaldehyde (**671**), 5.0 mL concentrated aqueous H₂SO₄, 1.5 mL glacial AcOH, 135 mL EtOH).
- Hanessian's staining solution (CAM, 5.0 g, Ce(SO₄)₂, 25 g (NH₄)₆Mo₇O₂₄·4H₂O, 50 mL concentrated aqueous H₂SO₄, 450 mL H₂O).
- KMnO₄ staining solution, (3.0 g KMnO₄, 20 g K₂CO₃, 5.0 mL aqueous 5% NaOH, 300 mL H₂O).

Flash column chromatography was performed on Geduran[®] Si60 (40–63 µm) silica gel from *Merck KGaA* or on C18-reversed-phase silica gel from *Waters Corporation*. All fractions containing a desired substrate were combined and solvents were removed under reduced pressure followed by drying *in high vacuo* (10⁻² mbar).

NMR spectroscopy

NMR spectra were measured on a *Bruker* Avance III HD 400 MHz spectrometer equipped with a CryoProbeTM operating at 400 MHz for proton nuclei (100 MHz for carbon nuclei) or by the analytic section of the Department of Chemistry of the *Ludwig-Maximilians-Universität München* using *Bruker* AXR300, *Varian* VXR400 S and *Bruker* AMX600 spectrometers operating at 300 MHz, 400 MHz and 600 MHz for proton nuclei (75 MHz, 100 MHz, 150 MHz for carbon nuclei), respectively. DMF-d₇, CD₃OD, DMSO-d₆, CDCl₃ and C₆D₆ were purchased from *Sigma-Aldrich* and *Euriso-top*. The ¹H NMR shifts are reported in ppm related to the residual shift of TMS. ¹H NMR shifts were calibrated to residual solvent resonances: DMF-d₇ (8.02 ppm), CD₃OD (3.31 ppm), DMSO-d₆ (2.50 ppm), CDCl₃ (7.26 ppm), C₆D₆ (7.16 ppm). ¹³C NMR shifts were calibrated to the center of the multiplet signal of the residual solvent resonance: DMF-d₇ (162.50 ppm), CD₃OD (49.00 ppm), DMSO-d₆ (29.84 ppm), CDCl₃ (77.16 ppm), C₆D₆ (128.06 ppm). ¹H NMR spectroscopic data are reported as follows: Chemical shift in ppm (multiplicity, coupling constants *J*, integration intensity). The multiplicities are abbreviated with s (singlet), br (broad signal), d (doublet), t (triplet), q (quartet), m (multiplet) and m_C (centrosymmetric multiplet). In case of combined multiplicities, the multiplicity with the larger coupling constant is stated first. Except for multiplets, the chemical shift of all signals, as well for centrosymmetric multiplets, is reported as the center of the resonance range. Additionally to ¹H and ¹³C NMR measurements, 2D NMR techniques as homonuclear correlation spectroscopy (COSY),

heteronuclear single quantum coherence (HSQC) and heteronuclear multiple bond coherence (HMBC) were used to assign signals. For further elucidation of 3D structures of the analytes, nuclear Overhauser enhancement spectroscopy (NOESY) was conducted. Coupling constants J are reported in Hz. All NMR spectra were analyzed using the program MestRe NOVA 8.1 from *Mestrelab Research S. L.*

Mass spectrometry

All mass spectra were measured by the analytic section of the Department of Chemistry of the *Ludwig-Maximilians-Universität München*. Mass spectra were recorded on the following spectrometers (ionization mode in brackets): MAT 95 (EI) and MAT 90 (ESI) from *Thermo Finnigan GmbH* or JMS-700 (FAB) from *Jeol Ltd.* Mass spectra were recorded in high-resolution and the only characteristic molecule fragments or molecule ion peaks are indicated for each analyte. The used method is reported at the relevant section of the experimental part. Liquid chromatography–mass spectrometry (LCMS) was conducted on a 1260 Infinity LC unit that was attached to a 1100 Series LC/MSD mass spectrometer, both being from *Agilent Technologies Inc.*

IR spectroscopy

IR spectra were recorded on a *PerkinElmer* Spectrum BX II FT-IR system. If required, substances were dissolved in CH_2Cl_2 prior to direct application on the ATR unit. The measured wave numbers are reported in cm^{-1} .

Optical rotation

Optical rotation values were recorded on a polarimeter P8000-T from *A. Krüss Optronic GmbH* or on a *PerkinElmer* 241 polarimeter. The specific rotation is calculated as follows:

$$[\alpha]_{\lambda}^{\vartheta} = \frac{\alpha \cdot 100}{c \cdot d}$$

Thereby, the wavelength λ is reported in nm and the measuring temperature ϑ in $^{\circ}\text{C}$. α resembles the recorded optical rotation at the apparatus, c the concentration of the analyte in 10 mg/mL and d the length of the cuvette in dm. Thus, the specific rotation is given in $10^{-1} \cdot \text{deg} \cdot \text{cm}^2 \cdot \text{g}^{-1}$. Usage of the sodium D line ($\lambda = 589 \text{ nm}$) is indicated by D instead of the

wavelength in nm. The respective concentration as well as the solvent is denoted in the analytical part of the experimental description. Optical rotations of azobenzene containing compounds were not recorded, due to the light dependent photostationary states of their diazene bonds.

Melting points

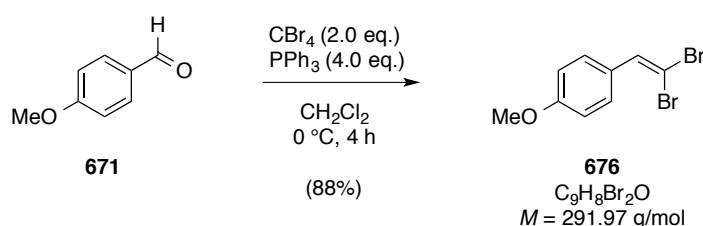
Melting points were measured on the apparatus *BÜCHI* Melting Point B-540 from *BÜCHI Labortechnik AG* or on an EZ-Melt apparatus from *Stanford Research Systems* and are uncorrected.

UV-Vis Spectroscopy

UV-Visible spectra were recorded on a *Varian Cary 50 Bio* UV-Visible Spectrophotometer using *Starna 29/B/12* quartz cuvettes with 10 mm section thickness. The evaluation of relaxation kinetics was conducted using the software *IGOR Pro 6.3* from *WaveMetrics Inc.*

3.2 Experimental Procedures for Chapter 2: ‘Development of Photochromic Ligands for LTCCs’

Synthesis of Dibromide 676



Tetrabromomethane (48.7 g, 146 mmol, 2.0 eq.) was dissolved in dry CH_2Cl_2 (150 mL) and cooled to 0 °C. Triphenylphosphine (77.2 g, 293 mmol, 4.0 eq.) was added to the stirred solution in portions. The resulting mixture was stirred for 15 min at 0 °C and a solution of *p*-anisaldehyde (**671**, 8.4 mL, 73 mmol, 1.0 eq.) in dry CH_2Cl_2 (28 mL) was then added dropwise over 20 min. After the mixture was stirred for additional 3 hours at 0 °C, saturated aqueous NaHCO_3 solution was added until the aqueous phase reached neutrality. The layers were separated and the organic layer was washed with portions of saturated aqueous NaCl ($3 \times 250\text{ mL}$) and dried over Na_2SO_4 . The solvent was removed *in vacuo* to give a pale yellow

solid. Purification by flash column chromatography (silica, *i*-Hex:EtOAc = 10:0 to 9:1) yielded compound **676** (18.9 g, 65 mmol, 88%) as slightly yellow solid.

R_f = 0.81 (*i*-Hex:EtOAc = 4:1).

Melting point = 34.9–35.3 °C (*i*-Hex:EtOAc).

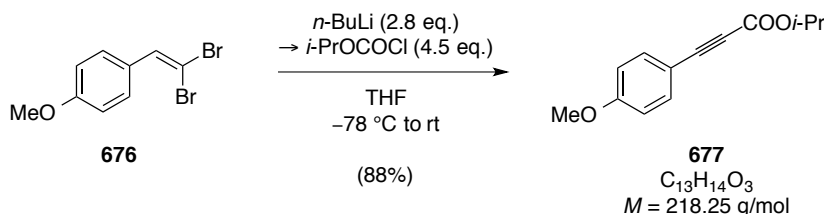
^1H NMR (CDCl_3 , 300 MHz): δ = 7.54–7.49 (m, 2H), 7.41 (s, 1H), 6.92 (m, 2H), 3.82 (s, 3H) ppm.

^{13}C NMR (CDCl_3 , 75 MHz): δ = 159.8, 136.4, 130.0, 128.0, 113.9, 87.4, 55.4 ppm.

EI-MS for $\text{C}_9\text{H}_8\text{Br}_2\text{O}^+$ [M^+]: calcd. 289.8936
 found 289.8934.

IR (ATR): $\tilde{\nu}/\text{cm}^{-1}$ = 3005, 2956, 2928, 2833, 1888, 1711, 1602, 1572, 1507, 1453, 1439, 1418, 1332, 1306, 1276, 1245, 1176, 1112, 1024, 858, 819, 800.

Synthesis of *iso*-Propyl Ester **677**



Dibromide **676** (20.0 g, 68.5 mmol, 1.0 eq.) was dissolved in dry THF (800 mL). A solution of *n*-BuLi (77 mL, 2.5 M solution in hexanes, 192 mmol, 2.8 eq.) was added dropwise at -78°C . After the mixture had been stirred for one hour, a solution of *iso*-propyl chloroformate (308 mL, 1.0 M solution in toluene, 308 mmol, 4.5 eq.) was added dropwise. The resulting mixture was stirred for 10 min at -78°C , allowed to warm up to room temperature, and then poured into saturated aqueous NaHCO_3 solution (300 mL). The mixture was diluted with EtOAc (300 mL) and the phases were separated. The aqueous layer was extracted with EtOAc ($2 \times 250 \text{ mL}$). The combined organic layers were sequentially washed with saturated aqueous NaHCO_3 (100 mL), saturated aqueous NaCl solutions (100 mL) and

then dried over Na_2SO_4 . Purification by flash column chromatography (silica, *i*-Hex:EtOAc = 10:0 to 9:1) yielded compound **677** (13.2 g, 60.3 mmol, 88%) as a slightly yellow solid.

R_f = 0.50 (*i*-Hex:EtOAc = 8:1).

Melting point = 59.4–60.3 °C (*i*-Hex:EtOAc).

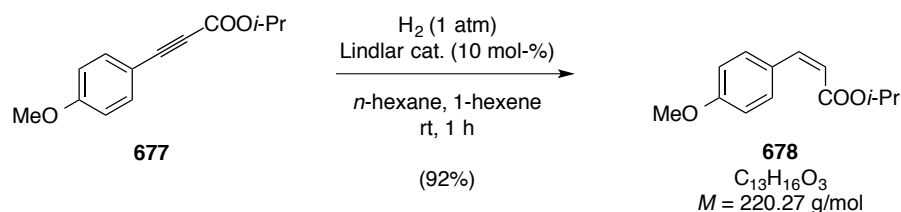
^1H NMR (CDCl_3 , 300 MHz): δ = 7.45–7.40 (m, 2H), 6.79–6.74 (m, 2H), 5.04 (sept, J = 6.3 Hz, 1H), 3.72 (s, 3H), 1.22 (d, J = 6.3 Hz, 6H) ppm.

^{13}C NMR (CDCl_3 , 75 MHz): δ = 161.8, 154.3, 135.3, 114.6, 111.9, 86.9, 80.9, 70.2, 55.8, 22.1 ppm.

EI-MS for $\text{C}_{13}\text{H}_{14}\text{O}_3^+$ [M^+]:
calcd. 218.0943
found 218.0936.

IR (ATR): $\tilde{\nu}/\text{cm}^{-1}$ = 2981, 2838, 2211, 1700, 1603, 1571, 1510, 1459, 1422, 1374, 1286, 1252, 1196, 1166, 1101, 1028, 961, 897, 828, 745.

Synthesis of *E*-Alkene **678**



Under an atmosphere of argon, *iso*-propyl ester **677** (8.99 g, 41.0 mmol, 1.0 eq.) was dissolved in a mixture of *n*-hexane and freshly distilled 1-hexene (411 mL, v/v = 2:1). Then freshly distilled quinoline (16 mL, 136 mmol, 3.3 eq.) was added and the mixture was degassed (3 × freeze-pump-thaw). Lindlar catalyst,^[332] that is Pd/CaCO₃ (5 % Pd) poisoned with lead (1.40 g, 4.12 mmol, 10 mol-%) was added. The resulting suspension was purged with hydrogen for 5 min and the reaction vessel was then connected to a hydrogen filled balloon (1 atm) and stirred at room temperature. TLC analysis indicated complete consumption of alkyne **677** after one hour. The hydrogen atmosphere was displaced by argon and the reaction mixture was then filtered through a Celite[®] pad. The filtrate was taken up in

EtOAc (300 mL) and washed with saturated aqueous NaCl solution (3×200 mL). The combined aqueous layers were re-extracted with ethyl acetate (3×200 mL). The combined organic layers was dried over Na_2SO_4 and purified *via* flash column chromatography (silica, *i*-Hex:EtOAc = 1:0 to 97:3), yielding compound **678** (8.39 g, 38.0 mmol, 92%) as a colourless liquid.

$R_f = 0.53$ (*i*-Hex:EtOAc = 8:1).

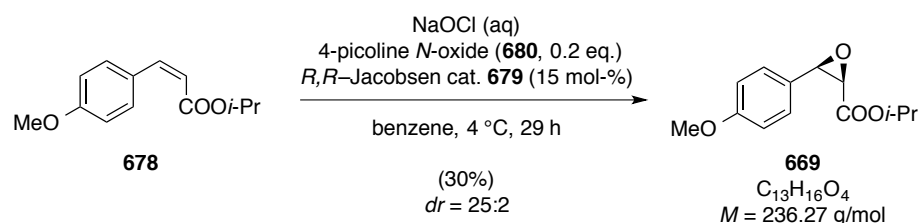
^1H NMR (CDCl_3 , 600 MHz): $\delta = 7.68\text{--}7.63$ (m, 2H), 6.87–6.83 (m, 2H), 6.80 (d, $J = 12.7$ Hz, 1H), 5.78 (d, $J = 12.7$ Hz, 1H), 5.05 (sept, $J = 6.3$ Hz, 1H), 3.81 (s, 3H), 1.24 (d, $J = 6.3$ Hz, 6H) ppm.

^{13}C NMR (CDCl_3 , 150 MHz): $\delta = 166.2, 160.4, 142.8, 132.2, 127.6, 118.0, 113.5, 67.7, 55.4, 22.0$ ppm.

EI-MS for $\text{C}_{13}\text{H}_{16}\text{O}_3^+$ [M^+]:
calcd. 220.1099
found 220.1082.

IR (ATR): $\tilde{\nu}/\text{cm}^{-1} = 2979, 2838, 1709, 1600, 1571, 1510, 1464, 1441, 1385, 1373, 1306, 1256, 1162, 1103, 958, 847, 785, 741, 698$.

Synthesis of Epoxide **669**



To a solution of *E*-alkene **678** (500 mg, 2.3 mmol, 1.0 eq.) in benzene (5 mL), 4-picoline *N*-oxide (**680**, 50.0 mg, 0.5 mmol, 0.2 eq.) and *R,R*-Jacobsen catalyst **679** (216 mg, 0.3 mmol, 15 mol-%) were added. The resulting mixture was combined with a pre-cooled bleach solution (5 mL), and the biphasic mixture was stirred for 23 hours at 4 °C. Then, another portion of catalyst (**679**, 72 mg, 0.1 mmol, 5 mol-%) and precooled bleach solution (1 mL) was added, and the mixture was stirred for further 6 hours at 4 °C. Diethyl ether (10 mL) was then added to the reaction mixture. The organic layer was separated, filtered through a pad of

Celite[®], washed with water (6×10 mL) and then dried over Na₂SO₄. The solvents were removed *in vacuo* and the residue was purified by flash chromatography (silica, deactivated with NEt₃, *i*-Hex:EtOAc = 1:0 to 19:1) to afford epoxide **669** (163 mg, 0.7 mmol, 30%) as a colourless liquid as a ratio of *syn/anti* diastereomers of 25:2.

Note: The enantiomeric excess of the product mixture was not determined due to its nature as mixture of diastereomers.

$R_f = 0.40$ (*i*-Hex:EtOAc = 9:1).

¹H NMR (CDCl₃, 600 MHz): δ = 7.26–7.21 (m, 2H), 6.77–6.72 (m, 2H), 4.77 (sept, $J = 6.3$ Hz, 1H), 4.10 (d, $J = 4.6$ Hz, 1H), 3.69 (s, 3H), 3.65 (d, $J = 4.6$ Hz, 1H), 0.91 (d, $J = 6.2$ Hz, 3H) ppm.

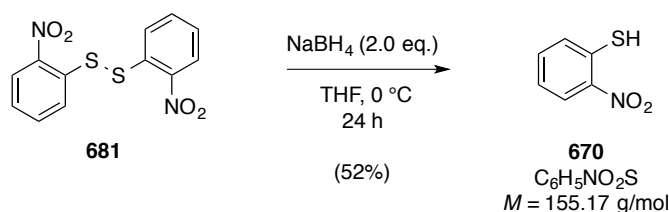
¹³C NMR (CDCl₃, 150 MHz): δ = 166.5, 159.8, 128.1, 125.1, 113.6, 69.2, 57.3, 56.1, 55.4, 21.7, 21.6 ppm.

EI-MS for C₁₃H₁₆O₄⁺ [M⁺]:
calcd. 236.1049
found 236.1046.

IR (ATR): $\tilde{\nu}/\text{cm}^{-1}$ = 2981, 2838, 1745, 1722, 1613, 1515, 1466, 1406, 1374, 1294, 1245, 1205, 1172, 1146, 1030, 971, 923, 866, 836, 806, 784, 722.

$[\alpha]_D^{20} = +15.1$ (c 1.00, CH₂Cl₂).

Synthesis of Thiophenol **670**



Disulfide **681** (5.00 g, 16.2 mmol, 1.0 eq.) was suspended in dry THF (20 mL) and the resulting yellow suspension was cooled to 0 °C. NaBH₄ (1.22 g, 32.4 mmol, 2.0 eq.) was added slowly in three portions. The red reaction mixture was then stirred for 24 hours. The reaction mixture was quenched with water (5 mL) and thereafter acidified with aqueous

sulfuric acid (15 vol.-%). The mixture was then extracted with diethyl ether (3 × 50 mL). The combined organic layers were washed with saturated aqueous NaCl solution (50 mL) and dried over Na₂SO₄. The solvents were evaporated *in vacuo* and the crude thiol compound was purified by flash column chromatography (silica, *i*-Hex:EtOAc = 10:1 to 5:1). 2-Nitrothiophenol (**670**, 1.3 g, 8.5 mmol, 52%) was obtained as yellow solid.

$R_f = 0.63$ (*i*-Hex:EtOAc = 4:1).

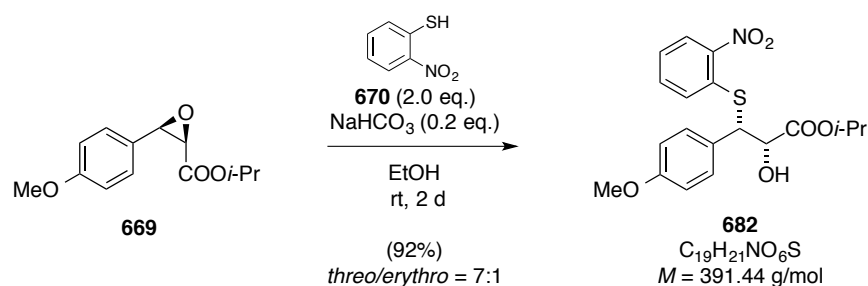
¹H NMR (CDCl₃, 300 MHz): δ = 8.19–8.11 (m, 1H), 7.38–7.31 (m, 2H), 7.25–7.12 (m, 1H) 3.93 (s, 1H) ppm.

¹³C NMR (CDCl₃, 75 MHz): δ = 133.8, 133.8, 132.2, 126.4, 125.9 ppm.

EI-MS for C₆H₅NO₂S⁺ [M⁺]:
calcd. 155.0041
found 155.0030

IR (ATR): $\tilde{\nu}/\text{cm}^{-1}$ = 2530, 1589, 1567, 1500, 1453, 1360, 1329, 1306, 1261, 1165, 1112, 1062, 1039, 979, 852, 783, 731, 678.

Synthesis of Thioether **682**



To a degassed (3 × freeze-pump-thaw) solution of 2-nitrothiophenol (**670**, 137 mg, 0.44 mmol, 2.0 eq.) and NaHCO₃ (7 mg, 0.09 mmol, 0.2 eq.) in ethanol (0.7 mL), epoxide **669** (104 mg, 0.88 mmol, 1.0 eq.) was added. The reaction mixture was stirred at room temperature for two days. Concentration under reduced pressure and purification by flash chromatography (silica, *i*-Hex:EtOAc = 9:1 to 4:1) afforded thioether **682** (159 mg, 0.41 mmol, 92%) as a yellow oil in a mixture of *threo* and *erythro* isomers of 7:1.

Note: The yield of this reaction dropped significantly when the employed solutions were not degassed thoroughly. The enantiomeric excess of the product mixture was not determined due to its nature as mixture of diastereomers.

$R_f = 0.27$ (*i*-Hex:EtOAc = 2:1).

^1H NMR (600 MHz, CDCl_3): $\delta = 7.93\text{--}7.89$ (m, 1H), 7.38–7.35 (m, 2H), 7.28–7.24 (m, 2H), 7.14–7.09 (m, 1H), 6.77–6.74 (m, 2H), 4.95 (sep, $J = 6.3$ Hz, 1H), 4.61 (d, $J = 3.7$ Hz, 1H), 4.42 (d, $J = 3.7$ Hz, 1H), 3.68 (s, 3H), 2.84 (br, s, 1H), 1.15 (d, $J = 6.2$ Hz, 4H), 1.02 (d, $J = 6.3$ Hz, 3H) ppm.

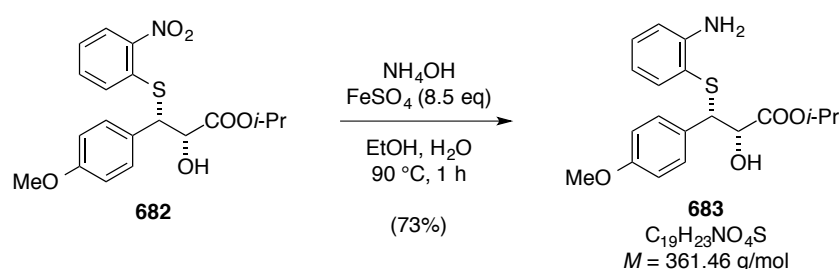
^{13}C NMR (CDCl_3 , 150 MHz): $\delta = 171.4$, 159.5, 147.9, 134.9, 133.2, 129.8, 129.5, 126.5, 125.8, 125.6, 114.3, 75.1, 70.8, 55.4, 55.3, 21.8, 21.6 ppm.

EI-MS for $\text{C}_{19}\text{H}_{21}\text{NO}_6\text{S}^+ [\text{M}^+]$:
calcd. 391.1090
found 391.1093.

IR (ATR): $\tilde{\nu}/\text{cm}^{-1} = 3466$, 2981, 2935, 2837, 1726, 1609, 1589, 1566, 1508, 1454, 1374, 1335, 1302, 1248, 1176, 1146, 1099, 1029, 906, 852, 834, 778, 730, 653.

$[\alpha]_D^{20} = +101.3$ (c 1.00, CH_2Cl_2).

Synthesis of Aniline **683**



The diastereomeric mixture of thioether **682** obtained as described above (0.17 g, 0.43 mmol, 1.0 eq.) was dissolved in a mixture of ethanol and water (3.4 mL, v/v = 1:1) and $\text{FeSO}_4 \cdot 7\text{H}_2\text{O}$ (1.01 g, 3.65 mmol, 8.5 eq.) was added. The resulting solution was heated to 90 °C for 30 min. Reflux was sustained as concentrated NH_4OH (1.2 mL) was added dropwise over 15 min. After additional 10 min of refluxing, the mixture was allowed to cool to room

temperature and was then extracted with EtOAc (3×10 mL). The organic layer was washed with saturated aqueous NaCl solution (10 mL) and dried over Na_2SO_4 . The solvents were removed *in vacuo* and the crude product was purified by flash chromatography (silica, *i*-Hex:EtOAc = 9:1 to 4:1) to afford substance **683** (113 mg, 0.32 mmol, 73%) as a colorless solid as a single diastereomer.

$R_f = 0.23$ (*i*-Hex:EtOAc = 2:1).

^1H NMR (CDCl_3 , 600 MHz): $\delta = 7.22\text{--}7.17$ (m, 2H), 7.01–6.96 (m, 2H), 6.72–6.67 (m, 2H), 6.58 (ddd, $J = 7.8, 1.3, 0.6$ Hz, 1H), 6.48 (td, $J = 7.5, 1.3$ Hz, 1H), 4.81 (sept, $J = 6.2$ Hz, 1H), 4.35 (d, $J = 3.5$ Hz, 1H), 4.27 (d, $J = 3.5$ Hz, 1H), 3.69 (s, 3H), 1.13 (d, $J = 6.2$ Hz, 3H), 1.00 (d, $J = 6.2$ Hz, 3H) ppm.

^{13}C NMR (CDCl_3 , 150 MHz): $\delta = 172.2, 159.2, 149.1, 137.7, 132.1, 130.6, 129.8, 118.8, 115.2, 113.8, 74.4, 70.2, 56.3, 55.4, 29.9, 21.9, 21.7$ ppm.

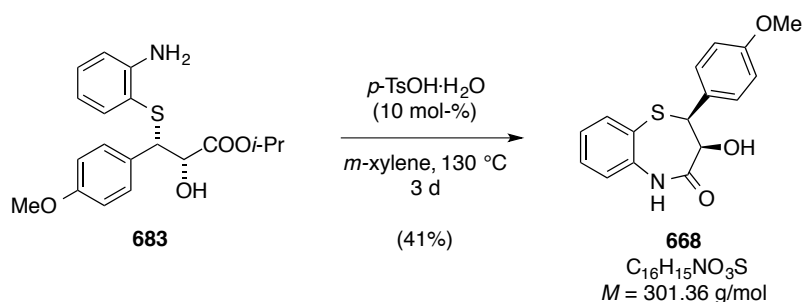
ESI-MS for $\text{C}_{19}\text{H}_{23}\text{NNaO}_4\text{S}^+ [\text{MNa}^+]$ calcd. 384.1245

found 384.1240.

IR (ATR): $\tilde{\nu}/\text{cm}^{-1} = 3452, 3359, 3064, 2979, 2957, 2923, 2852, 1725, 1609, 1587, 1510, 1479, 1465, 1449, 1423, 1386, 1375, 1303, 1248, 1177, 1146, 1101, 1031, 978, 939, 906, 855, 834, 817, 749, 680$.

$[\alpha]_D^{20} = +89.3$ (c 1.00, CH_2Cl_2).

Synthesis of Thiazepine **668**



Aniline **683** (60 mg, 0.16 mmol, 1.0 eq.) was dissolved in *m*-xylene (1.4 mL) in a Schlenk flask equipped with a Dean-Stark apparatus and a reflux condenser. *p*-Toluenesulfonic acid

(4.0 mg, 0.02 mmol, 10 mol-%) was added and the resulting solution was refluxed at 130 °C for 3 days. The reaction mixture was then cooled to room temperature, diluted with EtOAc (10 mL) and washed with saturated NaCl solution (10 mL). The aqueous phase was re-extracted with EtOAc (3× 20 mL). Subsequently, the combined organic layers were dried over Na₂SO₄ and the solvent was removed *in vacuo*. The crude product was purified by flash column chromatography (silica, *i*-Hex:EtOAc = 9:1 gradient to 13:7) to afford thiazepine **668** (17 mg, 0.06 mmol, 41%) as a colorless solid. The enantiomeric excess of thiazepine **668** was determined to 96% *via* comparison of the optical rotation value.

$R_f = 0.31$ (*i*-Hex:EtOAc = 1:1).

Melting point = 201.3–203.5 °C (*i*-Hex:EtOAc).

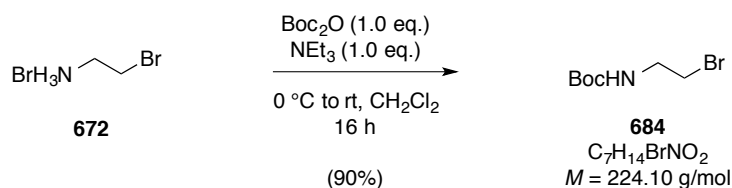
¹H NMR (600 MHz, CDCl₃): δ = 8.75 (s, 1H), 7.58 (dd, J = 7.7, 1.4 Hz, 1H), 7.39–7.33 (m, 2H), 7.29 (td, J = 7.7, 1.4 Hz, 1H), 7.13 (td, J = 7.7, 1.1 Hz, 1H), 7.03 (dd, J = 7.7, 1.1 Hz, 1H), 6.70–6.64 (m, 2H), 4.99 (d, J = 6.8 Hz, 1H), 4.38 (dd, J = 9.1, 6.8 Hz, 1H), 3.65 (s, 3H), 2.94 (d, J = 9.1 Hz, 1H) ppm.

¹³C NMR (150 MHz, CDCl₃): δ = 173.7, 160.1, 140.4, 134.9, 131.3, 131.2, 131.2, 131.2, 130.2, 130.2, 127.5, 127.1, 126.4, 123.2, 113.9, 113.8, 69.4, 57.6, 55.4, 55.4, 55.4 ppm.

ESI-MS for C₁₆H₁₆NNaO₃S⁺ [MNa⁺] calcd. 324.0664
found 324.0663.

IR (ATR): $\tilde{\nu}/\text{cm}^{-1}$ = 3334, 3187, 3118, 3074, 3006, 2961, 2906, 2835, 1680, 1640, 1608, 1584, 1571, 1512, 1474, 1438, 1420, 1359, 1338, 1306, 1253, 1178, 1107, 1034, 952, 922, 878, 870, 842, 816, 795, 772, 746, 728, 714, 698, 679, 664.

$[\alpha]_D^{20} = +119.3$ (*c* 1.00, EtOH).

Synthesis of Carbamate **684**

According to the literature,^[504] Boc₂O (10.7 g, 48.8 mmol, 1.0 eq.) was added to a suspension of (2-bromoethyl)amine hydrobromide (**672**, 10.0 g, 48.8 mmol, 1.0 eq.) in dry CH₂Cl₂ (250 mL). The reaction mixture was cooled to 0 °C and NEt₃ (6.8 mL, 48.8 mmol, 1.0 eq.) was added dropwise over one hour. Stirring was continued and the reaction mixture was allowed to warm to room temperature over night. Subsequently the organic phase was washed with saturated aqueous NaCl solution (3 × 50 mL). The combined aqueous layers were re-extracted with CH₂Cl₂ (3 × 100 mL). The organic layers were combined and dried over Na₂SO₄. After evaporation of the solvents, the crude product was purified *via* flash column chromatography (silica, CH₂Cl₂). Thus, carbamate **684** (9.9 g, 44.0 mmol, 90%) was obtained as a low melting colourless solid.

$R_f = 0.85$ (CH₂Cl₂:MeOH = 10:1).

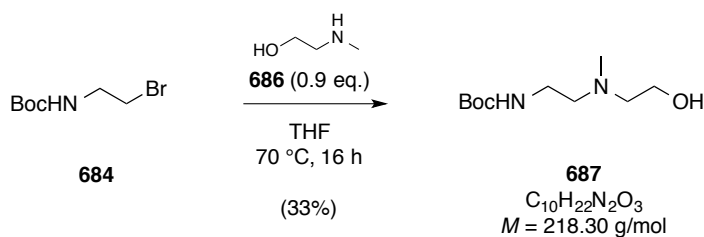
Melting point = 30–33 °C (CH₂Cl₂).

¹H NMR (CDCl₃, 300 MHz): δ = 4.93 (s, br, 1H), 3.48–3.19 (m, 4H), 1.31 (s, 9H) ppm.

¹³C NMR (CDCl₃, 75 MHz): δ = 155.7, 79.8, 42.4, 32.7, 28.4 ppm.

EI-MS for C₇H₁₄BrNO₂⁺ [M⁺]: calcd. 223.0208
 found 223.0209.

IR (ATR): $\tilde{\nu}/\text{cm}^{-1}$ = 3239, 2920, 1715, 1610, 1482, 1425, 1322, 1246, 1074, 1018, 961, 921m, 881, 817, 767, 715.

Synthesis of Aminoalcohol **687**

2-(Methylamino)ethanol (**686**, 1.4 g, 0.19 mmol, 1.0 eq.) and carbamate **684** (4.7 g, 0.21 mmol, 1.1 eq.) were dissolved in dry THF (80 mL). The reaction mixture was refluxed for 16 hours at 70 °C. The solvent was then removed under reduced pressure and the residue was purified by flash column chromatography (silica, CH_2Cl_2 :MeOH = 1:0 to 9:1) to yield compound **687** (1.36 g, 6.22 mmol, 33%) as a colorless oil.

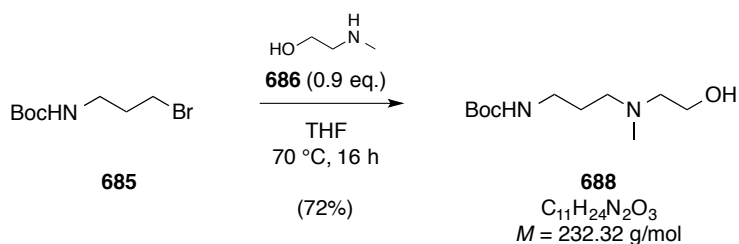
$R_f = 0.10$ (CH_2Cl_2 :MeOH = 9:1).

^1H NMR (CD_3OD , 400 MHz): δ = 3.69 (t, J = 5.7 Hz, 2H), 3.54 (s, 1H), 3.24 (t, J = 6.4 Hz, 2H), 2.79–2.63 (m, 4H), 2.46 (s, 3H), 1.44 (s, 9H) ppm.

^{13}C NMR (CD_3OD , 100 MHz): δ = 158.6, 80.3, 60.1, 59.2, 58.1, 42.3, 38.4, 28.7 ppm.

ESI-MS for $\text{C}_{10}\text{H}_{22}\text{N}_2\text{O}_3^+$ [MH^+]:
 calcd. 219.1709
 found 219.1705.

IR (ATR): $\tilde{\nu}/\text{cm}^{-1}$ = 3318, 2975, 1687, 1513, 1455, 1391, 1365, 1273, 1249, 1165, 1032, 968, 870, 780.

Synthesis of Aminoalcohol **688**

2-(Methylamino)ethanol (**686**, 143 mg, 1.91 mmol, 1.0 eq.) and carbamate **685** (500 mg, 2.09 mmol, 1.1 eq.) were dissolved in THF (15 mL). The reaction mixture was refluxed for

16 hours at 70 °C. The solvent was then removed under reduced pressure, and the residue was purified by flash column chromatography (silica, CH₂Cl₂:MeOH = 1:0 to 9:1) to yield compound **688** (353 mg, 1.52 mmol, 72%) as a colourless oil.

$R_f = 0.28$ (CH₂Cl₂:MeOH = 10:1).

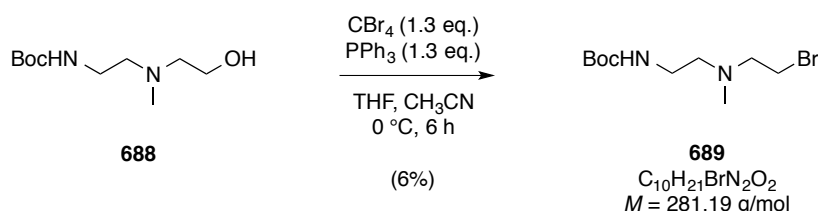
¹H NMR (CDCl₃, 300 MHz): δ = 5.43 (s, 1H), 3.97–3.83 (m, 2H), 3.36–3.01 (m, 7H), 2.82 (s, 3H), 1.99–1.87 (m, 2H), 1.28 (s, 9H) ppm.

¹³C NMR (CDCl₃, 75 MHz): δ = 156.6, 79.7, 57.9, 55.9, 54.6, 41.3, 37.5, 28.5, 24.7 ppm.

EI-MS for C₁₁H₂₄N₂O₃⁺ [M⁺]:
calcd. 232.1787
found 232.1791.

IR (ATR): $\tilde{\nu}/\text{cm}^{-1}$ = 3316, 2974, 2705, 1684, 1515, 1455, 1391, 1365, 1274, 1249, 1165, 1070, 1023, 866, 780.

Synthesis of Bromide **689**



Carbamate **688** (100 mg, 0.46 mmol, 1.0 eq.), and triphenylphosphine (213 mg, 0.81 mmol, 1.3 eq.) were dissolved in dry THF (2.4 mL). A solution of tetrabromomethane (269 mg, 0.81 mmol, 1.3 eq.) in acetonitrile (0.9 mL) was added at 0 °C and the mixture was stirred at that temperature for 6 hours. The solvent was then removed under reduced pressure and the residue was purified *via* flash column chromatography (silica, CH₂Cl₂:MeOH = 1:0 to 19:1) yielding bromide **689** (8 mg, 0.03 mmol, 6%) as a colourless oil.

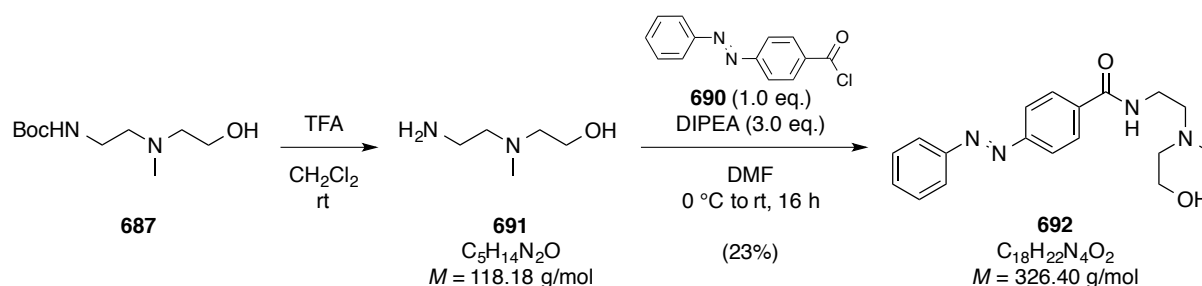
$R_f = 0.62$ (CH₂Cl₂:MeOH = 9:1).

¹H NMR (CD₃OD, 400 MHz): δ = 3.50 (t, J = 5.5 Hz, 2H), 3.17 (t, J = 6.7 Hz, 2H), 2.63 (t, J = 5.5 Hz, 2H), 2.53 (t, J = 6.8 Hz, 2H), 2.30 (s, 3H), 1.44 (s, 9H) ppm.

^{13}C NMR (CD_3OD , 100 MHz): δ = 154.8, 71.2, 59.0, 58.0, 57.7, 54.8, 42.8, 28.7 ppm.

EI-MS for $\text{C}_{10}\text{H}_{21}\text{BrN}_2\text{O}_2^+$ [M^+]: calcd. 280.0786
 found 280.0789.

Synthesis of Amide **692**



Carbamate **687** (200 mg, 0.92 mmol, 1.0 eq.) was dissolved in CH_2Cl_2 (4 mL) and trifluoroacetic acid (1 mL) was added. The resulting solution was stirred at room temperature for two hours and then concentrated *in vacuo*. The crude reaction product was dried thoroughly *in vacuo* and used for the next reaction step without further purification. 4-(Phenyldiazenyl)benzoic acid (207 mg, 0.92 mmol, 1.0 eq.) was dissolved in dry acetonitrile (5 mL) and dry DMF (2 drops) was added. Subsequently, oxalyl chloride (504 μL , 2 M solution in CH_2Cl_2 , 1.01 mmol, 1.1 eq.) was added dropwise. After one hour, when gas evolution had stopped, the reaction mixture was concentrated and dried *in vacuo* for 30 min. The resulting solid acid chloride was then re-dissolved in dry DMF (10 mL), cooled to 0 °C and DIPEA (0.16 mL, 2.75 mmol, 3.0 eq.) was added thereto. Subsequently, a solution of the crude deprotected amino alcohol (**691**) in dry DMF (10 mL) was added dropwise *via* cannula. The reaction mixture was allowed to warm to room temperature and was then stirred for 16 hours. Thereafter, EtOAc (30 mL) and saturated aqueous NaHCO_3 (30 mL) solution were added. The phases were separated and the aqueous layer was extracted with EtOAc (3×20 mL). The combined organic layers were dried over Na_2SO_4 and concentrated *in vacuo*. Purification *via* flash column chromatography (silica, CH_2Cl_2 :MeOH = 1:0 to 9:1) yielded amide **692** (70.1 mg, 0.21 mmol, 23%) as an orange solid.

R_f = 0.23 (CH_2Cl_2 :MeOH = 10:1).

^1H NMR (CDCl_3 , 600 MHz): δ = 7.87–7.83 (m, 2H), 7.82–7.77 (m, 4H), 7.42–7.35 (m, 3H), 7.24 (t, J = 4.9 Hz, 1H), 3.56 (t, J = 5.3 Hz, 2H), 3.46 (q, J = 5.5 Hz, 2H), 3.39 (s, 1H), 2.60 (t, J = 5.9 Hz, 2H), 2.52 (t, J = 5.3 Hz, 2H), 2.24 (s, 3H) ppm.

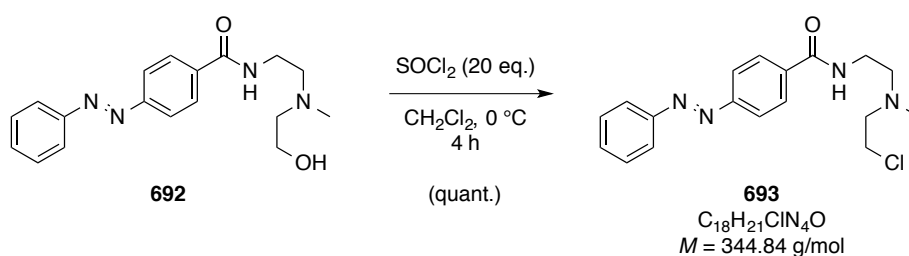
^{13}C NMR (CDCl_3 , 150 MHz): δ = 167.1, 154.2, 152.6, 136.3, 131.6, 129.2, 128.2, 123.1, 122.9, 59.1, 58.9, 56.4, 42.2, 37.6 ppm.

ESI-MS for $\text{C}_{18}\text{H}_{23}\text{N}_4\text{O}_2^+$ [MH^+]: calcd. 327.1816
found 327.1812.

IR (ATR): $\tilde{\nu}/\text{cm}^{-1}$ = 3540, 3267, 2930, 1680, 1645, 1595, 1580, 1523, 1442, 1440, 1423, 1380, 1331, 1290, 1154, 1140, 1120, 1063, 986, 965, 923, 821, 811, 790, 780, 755, 725.

UV-Vis (DMSO): λ_{max} = 381 nm.

Synthesis of Chloride **693**



Thionyl chloride (0.20 mL, 2.76 mmol, 20.4 eq.) was dissolved in dry CH_2Cl_2 (0.5 mL) and the mixture was then cooled to 0 °C. To this, a solution of amide **692** (40.0 mg, 0.12 mmol, 1.0 eq.) in dry CH_2Cl_2 (0.5 mL) was added dropwise *via* syringe pump over one hour. The mixture was stirred for further 3 hours at this temperature and subsequently quenched with aqueous sodium hydroxide solution (5 M, 2.2 mL). The phases were separated and the aqueous layer was extracted with dichloromethane ($3 \times 10 \text{ mL}$). The combined organic layers were dried over Na_2SO_4 and concentrated *in vacuo*. Purification *via* flash column chromatography (silica, CH_2Cl_2 :MeOH = 1:0 to 97:3) yielded chloride **693** (41.9 mg, 0.12 mmol, quant.) as an orange solid.

R_f = 0.85 (CH_2Cl_2 :MeOH = 10:1).

^1H NMR (CDCl_3 , 600 MHz): δ = 7.93–7.79 (m, 6H), 7.47–7.36 (m, 3H), 7.1 (s, br, 1H), 3.55 (t, J = 5.9 Hz, 2H), 3.49 (q, J = 5.3 Hz, 2H), 2.74 (t, J = 5.8 Hz, 2H), 2.63 (t, J = 5.4 Hz, 2H), 2.29 (s, 3H) ppm.

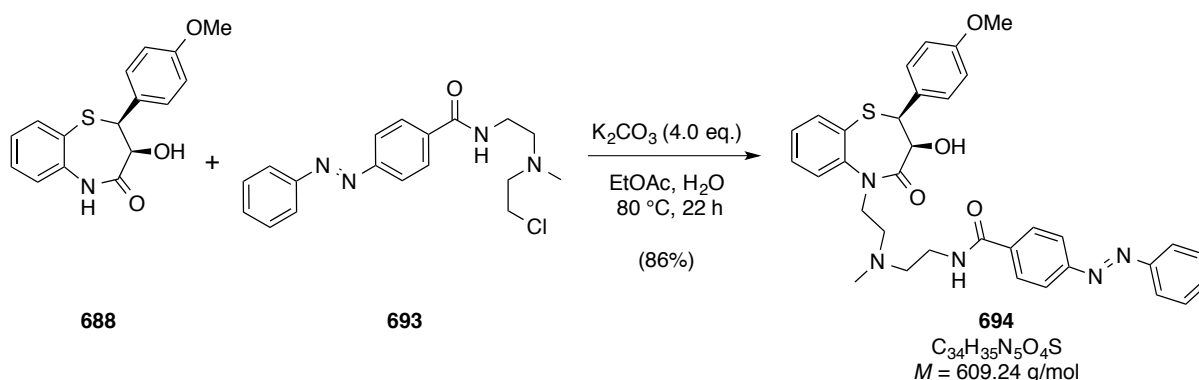
^{13}C NMR (CDCl_3 , 150 MHz): δ = 166.7, 154.3, 152.7, 136.3, 131.6, 129.3, 128.2, 123.2, 123.0, 58.6, 55.8, 41.7, 37.2 ppm.

ESI-MS for $\text{C}_{18}\text{H}_{22}\text{ClN}_4\text{O}^+$ [MH^+]: calcd. 345.1477
found 345.1480.

IR (ATR): $\tilde{\nu}/\text{cm}^{-1}$ = 2933, 1665, 1640, 1592, 1582, 1553, 1523, 1467, 1442, 1400, 1381, 1331, 1293, 1120, 1063, 982, 940, 923, 820, 813, 790, 781, 753, 726, 682.

UV-Vis (DMSO): λ_{max} = 380 nm.

Azo-diltiazem **1** (**694**)



To a solution of thiazepine **688** (10.1 mg, 33.2 μmol , 1.0 eq.) in EtOAc (0.40 mL) were added chloride **693** (18 mg, 66.4 μmol , 2.0 eq.), water (1 drop) and K_2CO_3 (18.0 mg, 133 μmol , 4.0 eq.). The resulting suspension was heated to reflux at 82 $^\circ\text{C}$ for 22 hours. Subsequently, the solvent was removed *in vacuo* and the crude mixture was purified *via* flash column chromatography (*i*-Hex:EtOAc = 1:1 to 0:1). Azo-diltiazem **1** (17.4 mg, 28.6 μmol , 86%) was obtained as an orange oil of 96% purity, as judged by ^1H NMR analysis. Further purification was achieved by reversed-phase HPLC ($\text{H}_2\text{O}:\text{CH}_3\text{CN}:\text{TFA}$ = 1:0:10 $^{-3}$ to 3:7:10 $^{-3}$). Thus obtained pure azo-diltiazem **694** (4.2 mg, 6.8 μmol , 21%) did show broadened signals for specific protons in the ^1H NMR, due to the basicity of the tertiary amine function.

$R_f = 0.30$ (EtOAc).

^1H NMR (CDCl_3 , 600 MHz): $\delta = 7.86\text{--}7.79$ (m, 2H), $7.77\text{--}7.67$ (m, 4H), $7.59\text{--}7.57$ (m, 1H), $7.44\text{--}7.33$ (m, 8H), $7.25\text{--}7.23$ (m, 3H), $6.68\text{--}6.67$ (m, 2H), 4.79 (d, $J = 7.2$ Hz, 1H), $4.63\text{--}4.59$ (m, 1H), 4.19 (d, $J = 7.2$ Hz, 1H), 3.64 (s, 3H), $3.62\text{--}3.54$ (m, 2H), $3.53\text{--}3.46$ (m, 1H), 2.83 (s, br, 1H), 2.72 (s, br, 1H), 2.53 (s, br, 2H), 2.36 (s, 3H) ppm.

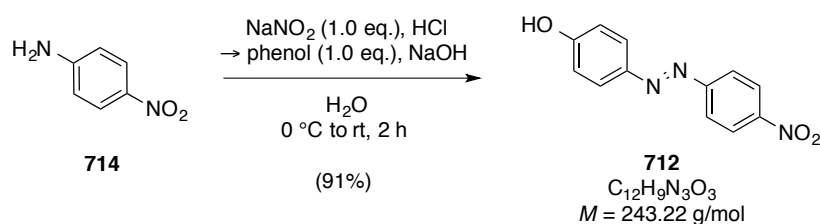
^{13}C NMR (CDCl_3 , 150 MHz): $\delta = 172.0, 167.5, 160.1, 154.1, 152.7, 144.5, 135.6, 131.5, 130.8, 129.2, 128.9, 128.4, 128.0, 126.0, 124.6, 123.2, 122.6, 120.8, 119.9, 113.7, 69.2, 56.8, 56.6, 56.3, 55.3, 47.2, 42.7, 37.7$ ppm.

ESI-MS for $\text{C}_{34}\text{H}_{36}\text{N}_5\text{O}_4\text{S}^+ [\text{MH}^+]$: calcd. 610.2483
found 610.2483.

IR (ATR): $\tilde{\nu}/\text{cm}^{-1} = 3337, 3.175, 3101, 3093, 2932, 2902, 1676, 1641, 1609, 1592, 1580, 1550, 1525, 1512, 1462, 1439, 1400, 1381, 1359, 1338, 1331, 1290, 1145, 1077, 982, 940, 923, 819, 810, 788, 778, 734, 718, 726, 682, 665$.

UV-Vis (DMSO): $\lambda_{\text{max}} = 380$ nm.

Synthesis of Phenol **712**



According to a literature-known procedure,^[493] 4-nitroaniline (**714**, 5.0 g, 36.0 mmol, 1.0 eq.) was suspended in water (36 mL) and concentrated aqueous HCl (9 mL) was added. The resulting mixture was heated until the aniline was completely dissolved. This solution was then cooled to 0°C and a mixture of sodium nitrite (2.5 g, 36.2 mmol, 1.0 eq.) in water (36 mL) was added slowly. The reaction mixture was stirred for one hour at this temperature and subsequently added to a solution of phenol (3.4 g, 36.2 mmol, 1.0 eq.) and NaOH (2.9 g, 72.5 mmol, 2.0 eq.) in water (36 mL) dropwise *via* cannula at 0°C . The resulting suspension was stirred for another hour. The formed yellow precipitate was filtered and thoroughly

washed with water. After drying *in vacuo*, phenol **712** (7.9 g, 32.8 mmol, 91%) was obtained as an orange solid, which required no further purification.

$R_f = 0.53$ (*i*-Hex:EtOAc = 9:1).

^1H NMR (CDCl_3 , 600 MHz): $\delta = 8.29\text{--}8.24$ (m, 2H), $7.90\text{--}7.87$ (m, 2H), $7.86\text{--}7.82$ (m, 2H), $6.91\text{--}6.85$ (m, 2H), 5.18 (s, br, 1H) ppm.

^{13}C NMR (CDCl_3 , 150 MHz): $\delta = 159.6, 156.1, 148.5, 147.3, 126.0, 124.9, 123.3, 116.2$ ppm.

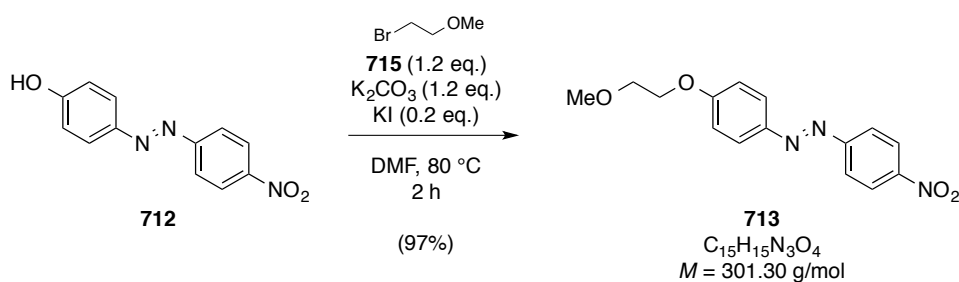
ESI-MS for $\text{C}_{12}\text{H}_8\text{N}_3\text{O}_3^-$ [(M-H) $^-$]: calcd. 242.0571

found 242.0567.

IR (ATR): $\tilde{\nu}/\text{cm}^{-1} = 3382, 1603, 1584, 1502, 1457, 1428, 1402, 1379, 1331, 1281, 1179, 1133, 1108, 1000, 1006, 860, 844, 836, 791, 755, 722, 686, 879$.

UV-Vis (DMSO): $\lambda_{\text{max}} = 386$ nm.

Synthesis of Methyl Ether **713**



Phenol **712** (3.00 g, 12.3 mmol, 1.0 eq.) was dissolved in dry DMF (17 mL). To this solution, K_2CO_3 (1.96 g, 14.2 mmol, 1.2 eq.), KI (0.41 g, 2.5 mmol, 0.2 eq.) and 1-bromo-2-methoxyethane (**715**, 1.97 g, 14.2 mmol, 1.2 eq.) were added. The resulting blue suspension was stirred at $83\text{ }^\circ\text{C}$ for two hours, upon which a colour change to red was observed. Subsequent cooling to room temperature led to solidification of the reaction mixture, which was then redissolved in EtOAc (200 mL), washed with saturated NaCl solution (2×100 mL), dried over Na_2SO_4 and concentrated *in vacuo*. The product was purified *via* flash column chromatography (silica, *i*-Hex:EtOAc = 1:0 to 0:1). Thus, methyl ether **713** (3.58 mg, 11.8 mmol, 97%) was obtained as an orange solid.

$R_f = 0.73$ (*i*-Hex:EtOAc = 3:2).

^1H NMR (CDCl_3 , 600 MHz): $\delta = 8.29\text{--}8.19$ (m, 2H), 7.91–7.81 (m, 4H), 7.02–6.92 (m, 2H), 4.12 (t, $J = 4.7$ Hz, 2H), 3.69 (t, $J = 4.7$ Hz, 2H), 3.37 (s, 3H) ppm.

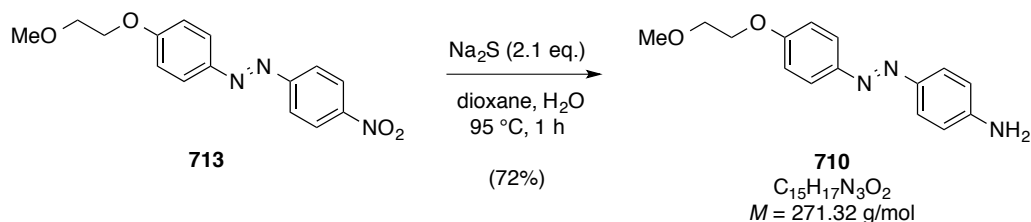
^{13}C NMR (CDCl_3 , 150 MHz): $\delta = 162.6, 156.1, 148.4, 147.1, 125.7, 124.8, 123.2, 115.2, 70.9, 67.9, 59.4$ ppm.

EI-MS for $\text{C}_{15}\text{H}_{15}\text{N}_3\text{O}_4^+$ [M^+]:
calcd. 301.1063
found 301.1048.

IR (ATR): $\tilde{\nu}/\text{cm}^{-1} = 3101, 2999, 2925, 2879, 2847, 2810, 1600, 1588, 1580, 1515, 1500, 1456, 1420, 1400, 1377, 1339, 1318, 1300, 1247, 1198, 1155, 1141, 1113, 1098, 1063, 1032, 951, 925, 856, 841, 832, 778, 756, 726, 689, 684$.

UV-Vis (DMSO): $\lambda_{\text{max}} = 376$ nm.

Synthesis of Aniline **710**



Nitro compound **713** (3.0 g, 10.0 mmol, 1.0 eq.) was dissolved in 1,4-dioxane (100 mL). To this, water (10 mL) and then Na_2S (1.6 g, 20.9 mmol, 2.1 eq.) were added. The resulting suspension was heated to 95 °C for one hour and the conversion was then judged to be complete *via* TLC analysis. Subsequently, the reaction mixture was poured into saturated aqueous NaHCO_3 solution (150 mL) and extracted with CH_2Cl_2 (3×200 mL). The combined organic layers were dried over Na_2SO_4 and concentrated *in vacuo*. Purification *via* flash column chromatography (silica, *i*-Hex:EtOAc = 1:0 to 0:1) provided aniline **710** (2.0 g, 7.22 mmol, 72%) as an orange solid.

$R_f = 0.36$ (*i*-Hex:EtOAc = 3:2).

^1H NMR (DMSO- d_6 , 400 MHz): δ = 7.77–7.67 (m, 2H), 7.66–7.57 (m, 2H), 7.11–7.01 (m, 2H), 6.72–6.61 (m, 2H), 5.95 (s, 2H), 4.16 (t, J = 4.5 Hz, 2H), 3.66 (t, J = 4.5 Hz, 1H), 3.32 (s, 3H) ppm.

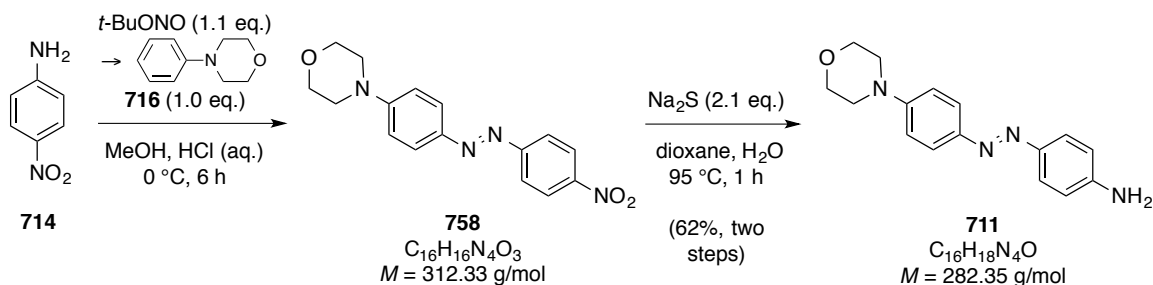
^{13}C NMR (DMSO- d_6 , 100 MHz): δ = 159.6, 152.1, 146.6, 142.8, 124.6, 123.3, 114.8, 113.4, 70.3, 67.2, 58.2 ppm.

ESI-MS for $\text{C}_{15}\text{H}_{18}\text{N}_3\text{O}_2^+$ [MH^+]: calcd. 272.1394
 found 272.1392.

IR (ATR): $\tilde{\nu}/\text{cm}^{-1}$ = 3460, 3368, 3234, 2978, 2926, 2891, 2820, 1640, 1594, 1578, 1506, 1499, 1454, 1428, 1405, 1371, 1311, 1296, 1251, 1197, 1190, 1145, 1120, 1107, 1057, 1031, 1002, 947, 857, 838, 766, 731.

UV-Vis (DMSO): λ_{max} = 403 nm.

Synthesis of Morpholine 711



4-Nitroaniline (**714**, 3.00 g, 21.7 mmol, 1.0 eq.) was dissolved in methanol (100 mL) and concentrated HCl (10 mL) was added. This solution was cooled to $0\text{ }^\circ\text{C}$ and $t\text{-BuONO}$ (2.35 g, 22.8 mmol, 1.05 eq.) was added slowly. The reaction mixture was stirred for one hour at this temperature and subsequently added to a solution of (4-morpholinyl)benzene (**716**, 3.56 g, 21.7 mmol, 1.0 eq.) in methanol (100 mL) and concentrated HCl (10 mL) dropwise *via* cannula at $0\text{ }^\circ\text{C}$. The resulting red solution was stirred for 5 hours and allowed to warm to room temperature. Subsequently, the reaction mixture was poured into saturated aqueous NaHCO_3 solution (200 mL) and extracted with EtOAc ($3 \times 200\text{ mL}$). The combined organic layers were dried over Na_2SO_4 and concentrated *in vacuo*. Purification *via* flash column chromatography (silica, CH_2Cl_2 : $i\text{-Hex}$ = 1:1 to 1:0) provided nitro compound **758** as an

orange solid, along with residual (4-morpholinyl)benzene (**716**, 5 mol-%) as judged by ^1H NMR analysis.

Thus obtained nitro compound **758** (5.0 g, 16.0 mmol, 1.0 eq.) was dissolved in 1,4-dioxane (160 mL). To this, water (16 mL) and then Na_2S (2.6 g, 33.6 mmol, 2.1 eq.) were added. The resulting suspension was heated to 95 °C for one hour and the reaction was then judged to be complete *via* TLC analysis. Subsequently, the reaction mixture was poured into saturated aqueous NaHCO_3 solution (200 mL) and extracted with CH_2Cl_2 (3×250 mL). The combined organic layers were dried over Na_2SO_4 and concentrated *in vacuo*. Purification *via* flash column chromatography (silica, *i*-Hex:EtOAc = 4:1 to 0:1) provided morpholine **711** (3.7 g, 13.0 mmol, 62%) as an orange solid.

$R_f = 0.76$ (*i*-Hex:EtOAc = 1:1).

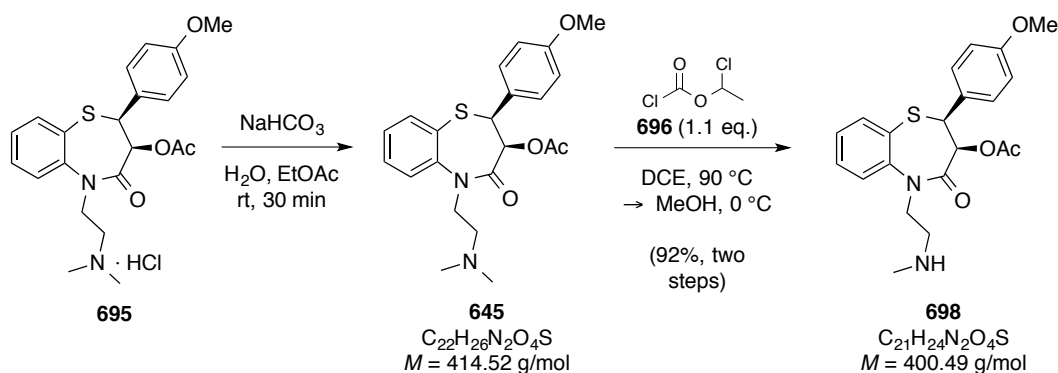
^1H NMR (CDCl_3 , 600 MHz): $\delta = 7.74\text{--}7.70$ (m, 2H), 7.68–7.63 (m, 2H), 6.88–6.84 (m, 2H), 6.66–6.62 (m, 2H), 3.86 (s, br, 2H), 3.78 (t, $J = 4.8$ Hz, 4H), 3.18 (t, $J = 4.8$ Hz, 4H) ppm.

^{13}C NMR (CDCl_3 , 150 MHz): $\delta = 152.5, 148.8, 146.3, 146.0, 124.6, 124.0, 114.9, 114.9, 66.9, 48.6$ ppm.

ESI-MS for $\text{C}_{16}\text{H}_{19}\text{N}_4\text{O}^+$ [MH^+]:
calcd. 283.1553
found 283.1558.

IR (ATR): $\tilde{\nu}/\text{cm}^{-1} = 3452, 3348, 3214, 3036, 2963, 2898, 2865, 2839, 1628, 1592, 1572, 1502, 1462, 1445, 1428, 1397, 1381, 1344, 1303, 1296, 1268, 1232, 1180, 1154, 1138, 1115, 1070, 1050, 1029, 961, 937, 924, 860, 832, 823, 796, 753, 734, 719$.

UV-Vis (DMSO): $\lambda_{\text{max}} = 453$ nm.

Synthesis of Mono Desmethyl Diltiazem (**698**)

Diltiazem hydrochloride **695** (7.23 g, 16.0 mmol, 1.0 eq.) was dissolved in EtOAc (20 mL) and saturated aqueous NaHCO_3 solution (100 mL) was added. The resulting solution was stirred for 30 min and then diluted with EtOAc (200 mL). Thereafter, the phases were separated and the aqueous layer was extracted with EtOAc ($3 \times 150 \text{ mL}$). The combined organic layers were dried over Na_2SO_4 and concentrated *in vacuo* to yield diltiazem (**645**) (6.64 g, 16.0 mmol, quant.) as colourless foam.

Diltiazem (**645**, 6.64 g, 16.0 mmol, 1.0 eq.) was dissolved in dry DCE (99 mL) and 1-chloroethyl chloroformate (**696**, 2.50 g, 17.5 mmol, 1.1 eq.) was added. The resulting solution was heated to 90°C for one hour and then cooled to room temperature. After concentrating *in vacuo* at 10^{-2} mbar for one hour, the obtained foamy 1-chloroethyl formamide (**697**, cf. scheme 2.6) was redissolved in dry MeOH (218 mL) at 0°C and stirred for 6 hours until TLC analysis indicated complete conversion. Thereafter, the reaction mixture was poured into saturated aqueous NaHCO_3 solution (200 mL) and extracted with EtOAc ($4 \times 200 \text{ mL}$). The combined organic layers were dried over Na_2SO_4 and concentrated *in vacuo*. Purification *via* flash column chromatography (silica, $\text{CH}_2\text{Cl}_2:\text{MeOH} = 1:0$ to $23:2$) provided mono desmethyl diltiazem **698** (5.84 g, 14.6 mmol, 92%) as foamy colourless solid.

$R_f = 0.28$ ($\text{CH}_2\text{Cl}_2:\text{MeOH}:\text{H}_2\text{O}:\text{NH}_4\text{OH} = 9.0:1.0:0.1:0.1$).

^1H NMR (CDCl_3 , 600 MHz): $\delta = 7.60$ (dd, $J = 7.7, 1.5 \text{ Hz}$, 1H), 7.41–7.28 (m, 4H), 7.17 (dt, $J = 7.7, 1.4 \text{ Hz}$, 2H), 6.80–6.78 (m, 2H), 5.06 (d, $J = 7.5 \text{ Hz}$, 1H), 4.92 (d, $J = 7.5 \text{ Hz}$, 1H), 4.49 (dt, $J = 13.7, 6.9 \text{ Hz}$, 1H), 3.72 (s, 3H), 3.59 (dt, $J = 13.7, 5.8 \text{ Hz}$, 1H), 2.77–2.72 (m, 2H), 2.31 (s, 3H), 1.80 (s, 3H) ppm.

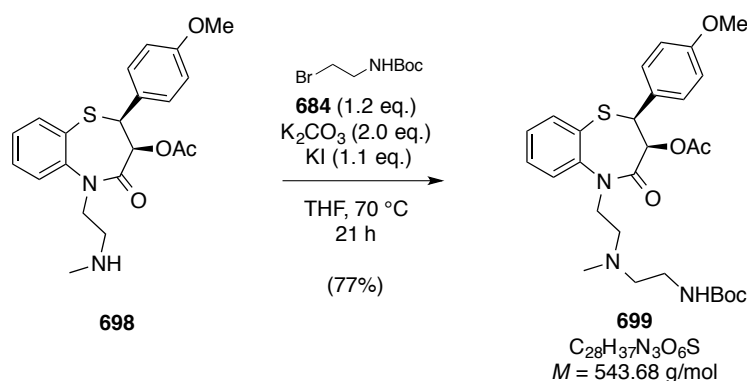
^{13}C NMR (CDCl_3 , 150 MHz): δ = 170.0, 167.1, 159.9, 145.4, 135.5, 131.3, 130.8, 128.5, 127.7, 126.6, 124.9, 114.0, 71.2, 55.4, 54.5, 49.4, 49.1, 36.1, 20.6 ppm.

ESI-MS for $\text{C}_{21}\text{H}_{25}\text{N}_2\text{O}_4\text{S}^+ [\text{MH}^+]$: calcd. 401.1530
found 401.1529.

IR (ATR): $\tilde{\nu}/\text{cm}^{-1}$ = 3319, 3063, 2936, 2838, 2797, 2248, 1743, 1675, 1609, 1584, 1512, 1471, 1444, 1407, 1370, 1304, 1293, 1223, 1179, 1140, 1113, 1852, 1061, 1031, 909s, 836, 818, 763, 725, 661, 645, 600, 565.

$[\alpha]_D^{20} = +43.6$ (c 1.00, CH_2Cl_2).

Synthesis of Carbamate **699**



Mono desmethyl diltiazem (**698**, 698 mg, 1.74 mmol, 1.0 eq.) was dissolved in dry THF (8 mL). To this, KI (318 mg, 1.92 mmol, 1.1 eq.), K_2CO_3 (482 mg, 3.49 mmol, 2.0 eq.), and substance **684** (469 mg, 2.09 mmol, 1.2 eq.) were added. The reaction mixture was then heated to 70 °C for 21 hours, cooled to room temperature and diluted with CH_2Cl_2 (40 mL). The organic phase was washed with saturated aqueous NaCl (20 mL) and the resulting aqueous layer was re-extracted with CH_2Cl_2 ($2 \times 20 \text{ mL}$). The combined organic layers were dried over Na_2SO_4 and concentrated *in vacuo*. Purification *via* flash column chromatography (silica, EtOAc) provided carbamate **699** (716 mg, 1.32 mmol, 77%) as a slightly yellow foam.

$R_f = 0.26$ (EtOAc).

^1H NMR (CDCl_3 , 600 MHz): δ = 7.58 (dd, J = 7.6, 1.4 Hz, 1H), 7.39–7.32 (m, 2H), 7.32–7.27 (m, 2H), 7.13 (dt, J = 7.6, 1.4 Hz, 1H), 6.78–6.73 (m, 2H), 5.02 (d, J = 7.5 Hz, 1H), 4.90 (s,

br, 1H), 4.88 (d, $J = 7.5$ Hz, 1H), 4.37–4.26 (m, 1H), 3.67 (s, 3H), 3.58 (dt, $J = 19.6, 6.5$ Hz, 1H), 3.05–2.97 (m, 2H), 2.63 (dt, $J = 12.8, 6.5$ Hz, 1H), 2.44 (dt, $J = 12.8, 6.5$ Hz, 1H), 2.38 (dt, $J = 11.7, 5.7$ Hz, 1H), 2.34–2.30 (m, 1H), 2.12 (s, 3H), 1.76 (s, 3H), 1.26 (s, 9H) ppm.

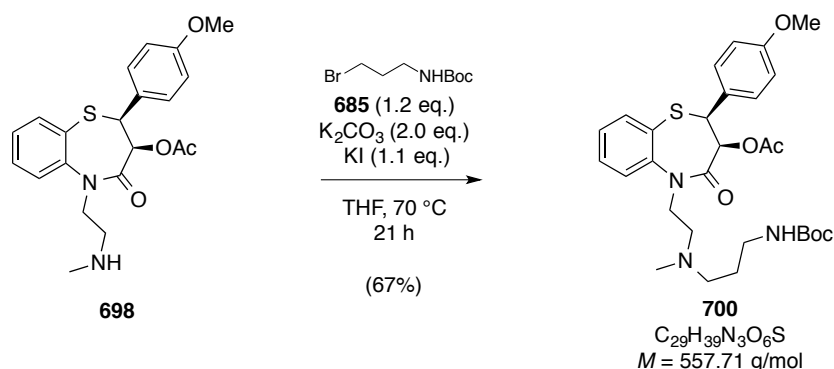
^{13}C NMR (CDCl_3 , 150 MHz): $\delta = 169.8, 166.9, 159.7, 156.0, 145.5, 135.4, 131.0, 130.8, 128.5, 127.4, 126.6, 124.5, 113.7, 78.8, 71.1, 56.8, 55.6, 55.2, 54.4, 47.5, 41.6, 37.9, 28.4, 20.5$ ppm.

ESI-MS for $\text{C}_{28}\text{H}_{38}\text{N}_3\text{O}_6\text{S}^+$ $[\text{MH}^+]$: calcd. 544.2476
found 544.2471.

IR (ATR): $\tilde{\nu}/\text{cm}^{-1} = 3374, 2974, 2838, 2802, 1746, 1707, 1678, 1610, 1584, 1512, 1472, 1445, 1391, 1391, 1365, 1304, 1248, 1169, 1114, 1062, 1033, 960, 922, 836, 764, 734, 661, 636, 603, 563$.

$[\alpha]_D^{20} = +80.4$ (c 1.00, CH_2Cl_2).

Synthesis of Carbamate 700



Mono desmethyl diltiazem (**698**, 670 mg, 1.67 mmol, 1.0 eq.) was dissolved in dry THF (8.0 mL). To this, KI (305 mg, 1.84 mmol, 1.1 eq.), K_2CO_3 (462 mg, 3.49 mmol, 2.0 eq.) and substance **685** (478 mg, 2.01 mmol, 1.2 eq.) were added. The reaction mixture was then heated to 70 °C for 23 hours, cooled to room temperature and diluted with CH_2Cl_2 (40 mL). The organic phase was washed with saturated aqueous NaCl (20 mL) and the resulting aqueous layer was re-extracted with CH_2Cl_2 (2×20 mL). The combined organic layers were dried over Na_2SO_4 and concentrated *in vacuo*. Purification *via* flash, column chromatography (silica, EtOAc) provided carbamate **685** (620 mg, 1.32 mmol, 77%) as a colourless foam.

$R_f = 0.58$ ($\text{CH}_2\text{Cl}_2:\text{MeOH}:\text{H}_2\text{O}:\text{NH}_4\text{OH} = 9.0:1.0:0.1:0.1$).

^1H NMR (CDCl_3 , 600 MHz): $\delta = 7.59$ (dd, $J = 7.7, 1.5$ Hz, 1H), 7.44–7.38 (m, 2H), 7.33–7.31 (m, 2H), 7.18–7.13 (m, 2H), 6.81–6.78 (m, 2H), 5.04 (d, $J = 7.5$ Hz, 1H), 4.95 (s, br, 1H), 4.90 (d, $J = 7.6$ Hz, 1H), 4.20–4.14 (m, 1H), 3.74–3.67 (m, 1H), 3.72 (s, 3H), 3.02–2.99 (m, 2H), 2.75–2.69 (m, 1H), 2.44–2.40 (m, 1H), 2.36–2.31 (m, 2H), 2.15 (s, 3H), 1.80 (s, 3H), 1.51–1.46 (m, 2H), 1.31 (s, 9H) ppm.

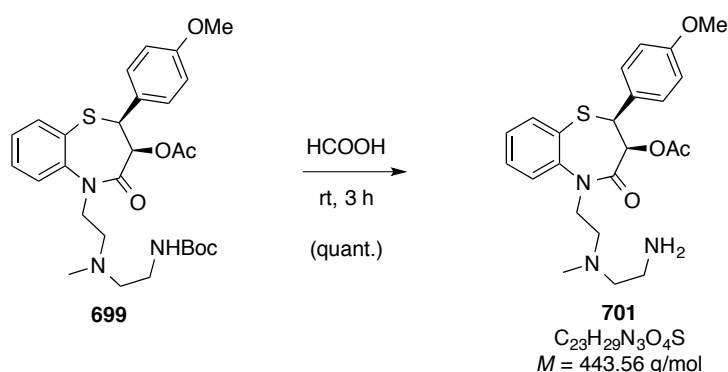
^{13}C NMR (CDCl_3 , 150 MHz): $\delta = 170.1, 167.1, 159.9, 156.2, 145.9, 135.5, 131.2, 130.9, 128.6, 127.5, 126.8, 124.9, 113.9, 79.0, 71.4, 56.0, 55.4, 55.4, 54.6, 48.4, 42.4, 39.3, 28.6, 27.5, 20.7$ ppm.

ESI-MS for $\text{C}_{29}\text{H}_{40}\text{N}_3\text{O}_6\text{S}^+$ [MH^+]: calcd. 558.2632
 found 558.2624.

IR (ATR): $\tilde{\nu}/\text{cm}^{-1} = 3367, 2934, 2837, 2799, 1745, 1676, 1609, 1583, 1511, 1471, 1444, 1407, 1390, 1364, 1304, 1224, 1166, 1062, 1030, 945, 919, 834, 818, 762, 735, 686, 660$.

$[\alpha]_D^{20} = +89.0$ (c 1.00, CH_2Cl_2).

Synthesis of Amine 701



Carbamate **699** (70 mg, 0.13 mmol) was dissolved in neat formic acid (1.8 mL) at room temperature. This solution was stirred for 3 hours until TLC analysis indicated complete conversion. Subsequently, saturated aqueous NaHCO_3 solution (20 mL) was added slowly and the resulting mixture was extracted with CH_2Cl_2 (3×20 mL). The combined organic layers were dried over Na_2SO_4 and concentrated *in vacuo*, yielding amine **701** (63 mg,

0.13 mmol, quant.) as a colourless foam. ^1H NMR analysis showed contamination of less than 5 mol-% of the respective deacetylated amine as an inseparable side product.

$R_f = 0.13$ ($\text{CH}_2\text{Cl}_2:\text{MeOH}:\text{H}_2\text{O}:\text{NH}_4\text{OH} = 9.0:1.0:0.1:0.1$).

^1H NMR (CDCl_3 , 600 MHz): $\delta = 7.6\text{--}7.57$ (m, 1H), 7.40–7.36 (m, 2H), 7.32–7.30 (m, 2H), 7.16–7.13 (m, 1H), 6.80–6.78 (m, 2H), 5.04 (d, $J = 7.5$ Hz, 1H), 4.90 (d, $J = 7.5$ Hz, 1H), 4.26 (ddd, $J = 14.0, 7.5, 6.6$ Hz, 1H), 3.71 (s, 3H), 3.66–3.61 (m, 1H), 2.69 (ddd, $J = 7.5, 6.6$ Hz, 1H), 2.61–2.58 (m, 2H), 2.49–2.46 (m, 1H), 2.36–2.32 (m, 2H), 2.15 (s, 3H), 1.98 (s, br, 2H), 1.79 (s, 3H) ppm.

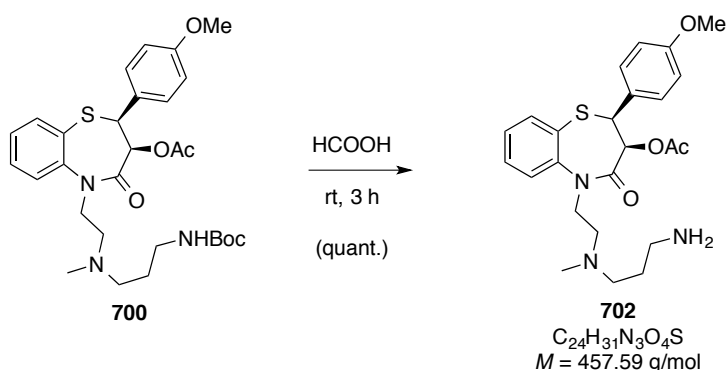
^{13}C NMR (CDCl_3 , 150 MHz): $\delta = 170.0, 167.1, 159.9, 145.8, 135.5, 131.2, 130.9, 128.6, 127.5, 126.8, 124.8, 113.9, 71.2, 60.4, 55.7, 55.4, 54.6, 48.1, 42.4, 39.5, 20.6$ ppm.

ESI-MS for $\text{C}_{23}\text{H}_{30}\text{N}_3\text{O}_4\text{S}^+$ [MH^+]: calcd. 444.1952
found 444.1950.

IR (ATR): $\tilde{\nu}/\text{cm}^{-1} = 2950, 2838, 2798, 2246, 1743, 1672, 1609, 1584, 1512, 1471, 1444, 1408, 1370, 1304, 1224, 1179, 1113, 1062, 1031, 909, 834, 763, 725, 662$.

$[\alpha]_D^{20} = +39.6$ (c 1.00, CH_2Cl_2).

Synthesis of Amine 702



Carbamate **700** (300 mg, 0.54 mmol) was dissolved in neat formic acid (3 mL) at room temperature. This solution was stirred for 3 hours until TLC analysis indicated complete conversion. Subsequently, saturated aqueous NaHCO_3 solution (40 mL) was added slowly

and the resulting mixture was extracted with CH_2Cl_2 (3×50 mL). The combined organic layers were dried over Na_2SO_4 and concentrated *in vacuo*, yielding amine **702** (246 mg, 0.54 mmol, quant.) as a colourless foam. ^1H NMR analysis showed contamination with less than 8 mol-% of the respective deacetylated amine as an inseparable side product.

$R_f = 0.16$ ($\text{CH}_2\text{Cl}_2:\text{MeOH}:\text{H}_2\text{O}:\text{NH}_4\text{OH} = 9.0:1.0:0.1:0.1$).

^1H NMR (CDCl_3 , 600 MHz): $\delta = 7.56\text{--}7.53$ (m, 1H), 7.37–7.30 (m, 4H), 7.29–7.25 (m, 2H), 7.12–7.09 (m, 1H), 6.75–6.73 (m, 2H), 4.99 (d, $J = 7.5$ Hz, 1H), 4.86 (d, $J = 7.5$ Hz, 1H), 4.19 (ddd, $J = 14.0, 7.5, 6.6$ Hz, 1H), 3.66 (s, 3H), 3.63–3.59 (m, 1H), 2.66 (ddd, $J = 7.5, 6.6$ Hz, 1H), 2.53–2.51 (m, 2H), 2.41–2.34 (m, 1H), 2.30–2.26 (m, 2H), 2.11 (s, 3H), 1.85 (s, br, 2H), 1.74 (s, 3H) ppm.

^{13}C NMR (CDCl_3 , 150 MHz): $\delta = 169.8, 166.8, 159.7, 145.7, 135.3, 131.3, 130.8, 128.5, 127.3, 126.7, 124.7, 113.7, 71.1, 56.7, 55.7, 55.2, 54.4, 48.0, 42.2, 40.4, 28.4, 20.5$ ppm.

ESI-MS for $\text{C}_{24}\text{H}_{32}\text{N}_3\text{O}_4\text{S}^+$ [MH^+]: calcd. 458.2108
 found 458.2108.

IR (ATR): $\tilde{\nu}/\text{cm}^{-1} = 3318, 3063, 2936, 2836, 2798, 1744, 1656, 1608, 1582, 1549, 1510, 1471, 1442, 1409, 1368, 1303, 1250, 1178, 1132, 1110, 1091, 1062, 1031, 911, 834, 818, 753, 729, 686, 663$.

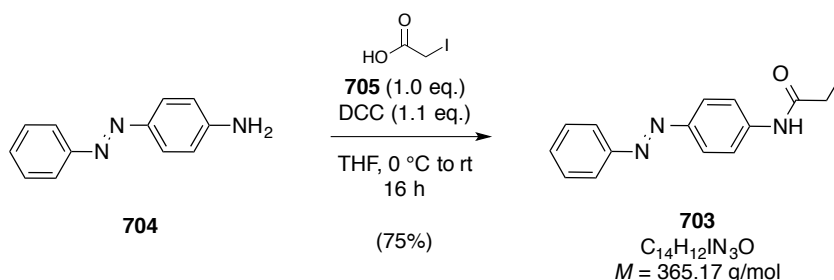
$[\alpha]_D^{20} = +104.8$ (c 1.00, CH_2Cl_2).

General Procedure for the Synthesis of Substituted Ω -Iodoalkyl Amides

The respective Ω -iodoalkanoic acid (1.00 mmol, 1.0 eq.) was dissolved in dry THF (4.9 mL) and cooled to 0°C under an argon gas atmosphere. To this solution the aniline of choice (1.00 mmol, 1.0 eq.) was added in portions and the resulting mixture was stirred for 10 min. Subsequently, a solution of N,N' -dicyclohexylcarbodiimide (1.10 mmol, 1.1 eq.) in dry THF (3.3 mL) was added dropwise *via* cannula over 15 min. The reaction mixture was stirred for one hour and then allowed to warm to room temperature over night. Thereafter, the formed precipitate was filtered off and washed thoroughly with Et_2O . The filtrate was concentrated

and purified *via* column chromatography to yield the respective Ω -iodoalkyl amide. In some cases contamination with 1,3-dicyclohexylurea (not shown) was observed, which did not influence reactivity or purification of the following synthetic steps.

Synthesis of Acetamide **703**



Following the general procedure for the synthesis of Ω -iodoalkyl amides, 2-iodoacetic acid (**705**, 1.89 g, 10.1 mmol, 1.0 eq.), aniline **704** (2.00 g, 10.1 mmol, 1.0 eq.) and *N,N*-dicyclohexylcarbodiimide (2.29 g, 11.1 mmol, 1.1 eq.) were reacted. Purification *via* flash column chromatography (silica, CH_2Cl_2 :*i*-Hex = 1:1 to 1:0) yielded acetamide **703** (2.76 g, 7.56 mmol, 75%) as an orange solid.

$R_f = 0.21$ (CH_2Cl_2).

^1H NMR (CDCl_3 , 600 MHz): $\delta = 7.88\text{--}7.83$ (m, 2H), 7.82–7.78 (m, 2H), 7.75 (s, br, 1H), 7.59 (d, $J = 8.8$ Hz, 2H), 7.44–7.39 (m, 2H), 7.39–7.34 (m, 1H), 3.80 (s, 2H) ppm.

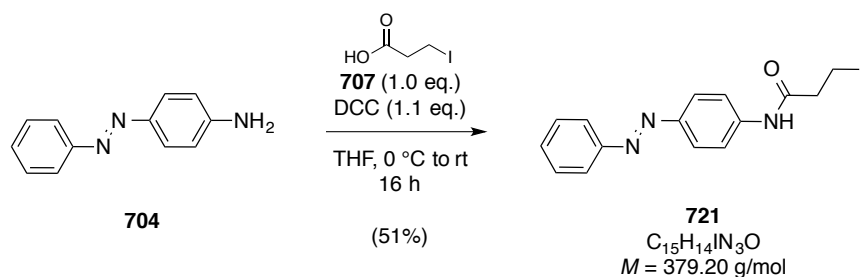
^{13}C NMR (CDCl_3 , 150 MHz): $\delta = 165.1, 152.8, 149.6, 139.9, 131.1, 129.2, 124.2, 123.0, 120.0, -0.1$ ppm.

ESI-MS for $\text{C}_{14}\text{H}_{13}\text{IN}_3\text{O}^+ [\text{MH}^+]$:
calcd. 366.0098
found 366.0099.

IR (ATR): $\tilde{\nu}/\text{cm}^{-1} = 3283, 2924, 1670, 1634, 1596, 1536, 1498, 1441, 1421, 1325, 1300, 1274, 1234, 1152, 1084, 1017, 968, 925, 872, 848, 832, 802, 765, 722, 686$.

UV-Vis (DMSO): $\lambda_{\text{max}} = 361 \text{ nm}$.

Synthesis of Propanamide **721**



Following the general procedure for the synthesis of Ω -iodoalkyl amides, 3-iodopropanoic acid (**707**, 2.03 g, 10.1 mmol, 1.0 eq.), aniline **704** (2.00 g, 10.1 mmol, 1.0 eq.) and *N,N'*-dicyclohexylcarbodiimide (2.29 g, 11.1 mmol, 1.1 eq.) were reacted. Purification *via* flash column chromatography (silica, EtOAc:*i*-Hex = 0:1 to 1:1) yielded propanamide **721** (1.98 g, 5.22 mmol, 51%) as an orange solid.

$R_f = 0.81$ (EtOAc:*i*-Hex = 2:3).

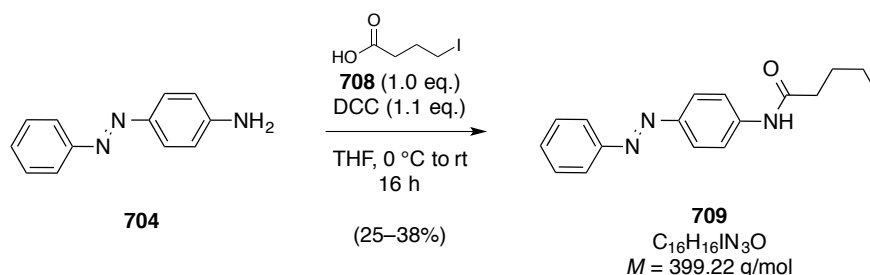
^1H NMR (DMSO- d_6 , 400 MHz): $\delta = 7.91\text{--}7.86$ (m, 3H), $7.60\text{--}7.54$ (m, 3H), 3.45 (t, $J = 6.7$ Hz, 1H), 3.07 (t, $J = 6.7$ Hz, 1H) ppm.

^{13}C NMR (DMSO- d_6 , 100 MHz): $\delta = 169.4, 152.0, 147.6, 142.0, 131.1, 129.4, 123.7, 122.3, 119.3, 36.6, 0.5$ ppm.

ESI-MS for $\text{C}_{15}\text{H}_{15}\text{IN}_3\text{O}^+$ [MH^+]:
 calcd. 380.0254
 found 380.0255.

IR (ATR): $\tilde{\nu}/\text{cm}^{-1} = 3280, 3040, 2925, 2850, 1661, 1623, 1593, 1582, 1524, 1483, 1464, 1448, 1438, 1403, 1373, 1299, 1258, 1247, 1205, 1185, 1166, 1154, 1142, 1126, 1104, 1087, 1069, 1045, 1018, 1001, 956, 912, 892, 833, 765, 720, 683$.

UV-Vis (DMSO): $\lambda_{\text{max}} = 361 \text{ nm}$.

Synthesis of Butanamide **709**

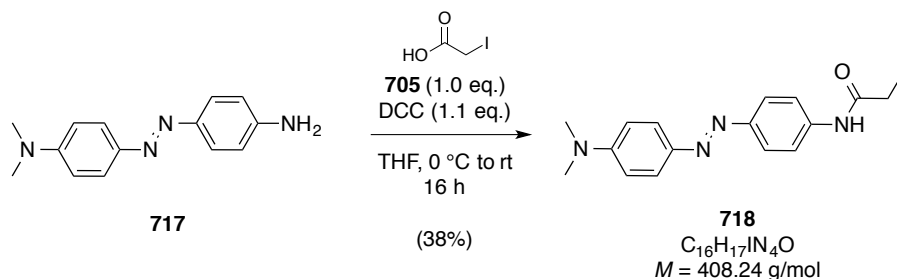
Following the general procedure for the synthesis of Ω -iodoalkyl amides, 4-iodobutanoic acid (**708**, 500 mg, 2.34 mmol, 1.0 eq.), aniline **704** (461 mg, 2.34 mmol, 1.0 eq.) and *N,N'*-dicyclohexylcarbodiimide (531 mg, 2.57 mmol, 1.1 eq.) were reacted. Purification *via* flash column chromatography (silica, EtOAc:*i*-Hex = 0:1 to 1:1) yielded butanamide **709** (350 mg, 0.89 mmol, 25–38%) as an orange solid, along with 20 mol-% of inseparable aniline **704**, as judged by ^1H NMR analysis.

Note: As a consequence of its impurity, more equivalents of butanamide 709 were employed for the alkylation reactions. Analytical data was recorded from the obtained mixture.

$R_f = 0.78$ (EtOAc:*i*-Hex = 2:3).

^1H NMR (DMSO- d_6 , 200 MHz, characteristic signals): $\delta = 7.92\text{--}7.54$ (m, 9H), 3.34 (t, $J = 6.8$ Hz, 2H), 2.52 (m, 2H), 2.22–1.93 (m, 2H) ppm.

ESI-MS for $\text{C}_{16}\text{H}_{17}\text{IN}_3\text{O}^+ [\text{MH}^+]$:
 calcd. 394.0411
 found 394.0413.

Synthesis of Acetamide **718**

Following the general procedure for the synthesis of Ω -iodoalkyl amides, 2-iodoacetic acid (**705**, 387 mg, 2.08 mmol, 1.0 eq.), bisaniline **717** (500 mg, 2.08 mmol, 1.0 eq.) and *N,N'*-dicyclohexylcarbodiimide (472 mg, 2.28 mmol, 1.1 eq.) were reacted. Purification *via*

flash column chromatography (silica, CH₂Cl₂:*i*-Hex = 1:1 to 1:0) yielded acetamide **718** (319 mg, 0.78 mmol, 38%) as a brownish solid.

R_f = 0.76 (EtOAc:*i*-Hex = 1:3).

¹H NMR (DMSO-*d*₆, 400 MHz): δ = 10.57 (s, 1H), 7.81–7.71 (m, 6H), 6.83–6.79 (m, 2H), 3.86 (s, 2H) 3.05 (s, 6H) ppm.

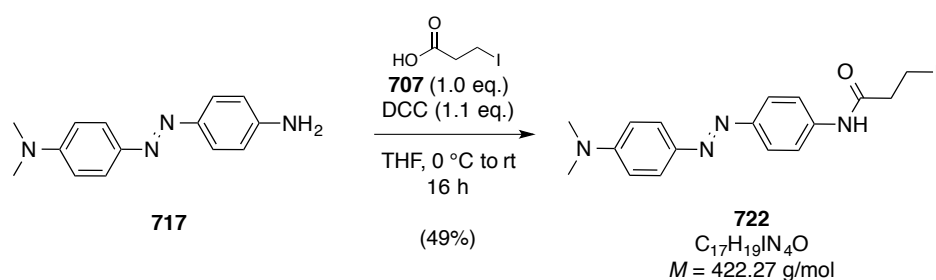
¹³C NMR (DMSO-*d*₆, 100 MHz): δ = 166.8, 152.3, 148.3, 142.6, 140.2, 124.5, 122.7, 119.3, 111.6, 39.9, 1.5 ppm.

ESI-MS for C₁₆H₁₈IN₄O⁺ [MH⁺]: calcd. 409.0520
 found 409.0519.

IR (ATR): $\tilde{\nu}/\text{cm}^{-1}$ = 3280, 3184, 3124, 2925, 2852, 1802, 1666, 1644, 1599, 1542, 1491, 1440, 1417, 1390, 1370, 1330, 1270, 1254, 1233, 1152, 1140, 1103, 1084, 1068, 985, 970, 944, 892, 870, 840, 824, 806, 766, 730, 738, 664.

UV-Vis (DMSO): λ_{max} = 439 nm.

Synthesis of Propanamide **722**



Following the general procedure for the synthesis of Ω -iodoalkyl amides, 3-iodopropanoic acid (**707**, 1.67 g, 8.33 mmol, 1.0 eq.), aniline **717** (2.00 mg, 8.33 mmol, 1.0 eq.) and *N,N'*-dicyclohexylcarbodiimide (1.89 g, 9.16 mmol, 1.1 eq.) were reacted. Purification *via* flash column chromatography (silica, CH₂Cl₂:EtOAc = 1:0 then 0:1) yielded propanamide **722** (1.72 g, 4.13 mmol, 49%) as a brownish solid.

R_f = 0.50 (EtOAc:*i*-Hex = 1:1).

^1H NMR (DMSO- d_6 , 600 MHz): δ = 7.77–7.76 (m, 6H), 6.84–6.82 (m, 2H), 3.45 (t, J = 6.7 Hz, 2H), 3.05 (m, 8H) ppm.

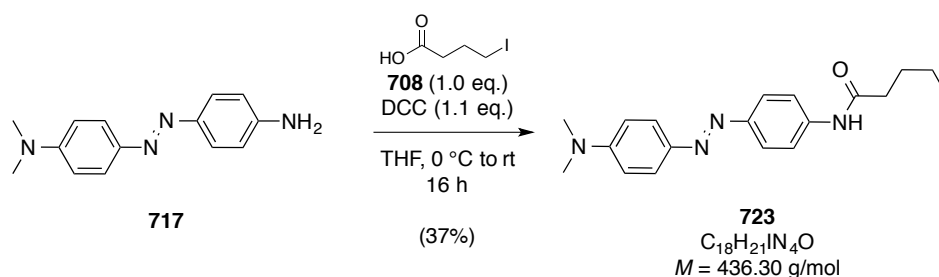
^{13}C NMR (DMSO- d_6 , 150 MHz): δ = 169.1, 152.2, 148.1, 142.6, 140.3, 124.4, 122.6, 119.3, 111.6, 39.8, 36.5, 0.6 ppm.

ESI-MS for $\text{C}_{17}\text{H}_{20}\text{IN}_4\text{O}^+$ [MH^+]: calcd. 423.0676
found 423.0677.

IR (ATR): $\tilde{\nu}/\text{cm}^{-1}$ = 3286, 3253, 3191, 3128, 3068, 2924, 2855, 2813, 1660, 1602, 1548, 1494, 1442, 1419, 1396, 1370, 1312, 1300, 1262, 1234, 1154, 1146, 1117, 1105, 1066, 1009, 962, 946, 918, 843, 834, 818, 731, 718, 686.

UV-Vis (DMSO): λ_{max} = 431 nm.

Synthesis of Butanamide **723**



Following the general procedure for the synthesis of Ω -iodoalkyl amides, 4-iodobutanoic acid (**708**, 0.89 g, 4.16 mmol, 1.0 eq.), aniline **717** (1.00 mg, 4.16 mmol, 1.0 eq.) and N,N' -dicyclohexylcarbodiimide (0.95 g, 4.58 mmol, 1.1 eq.) were reacted. Purification *via* flash column chromatography (silica, *i*-Hex:EtOAc = 1:0 to 1:1) yielded butanamide **723** (1.36 g, 3.11 mmol, 37%) as a brownish solid.

R_f = 0.63 (EtOAc:*i*-Hex = 3:2).

^1H NMR (DMSO- d_6 , 600 MHz): δ = 7.78–7.75 (m, 4H), 7.19 (d, J = 8.8 Hz, 2H), 6.89–6.85 (m, 2H), 4.25 (t, J = 7.0 Hz, 2H), 3.06 (s, 3H), 2.44–2.40 (m, 2H), 2.18–2.06 (m, 2H) ppm.

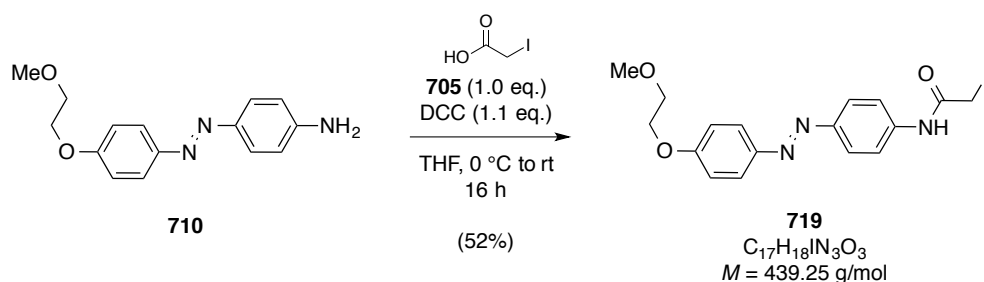
^{13}C NMR (DMSO- d_6 , 150 MHz): δ = 177.8, 156.6, 151.9, 142.7, 140.8, 124.5, 123.5, 120.3, 112.1, 68.3, 40.0, 27.4, 21.7 ppm.

ESI-MS for $\text{C}_{18}\text{H}_{22}\text{IN}_4\text{O}^+$ $[\text{MH}^+]$:
calcd. 437.0833
found 437.0830.

IR (ATR): $\tilde{\nu}/\text{cm}^{-1}$ = 3275, 2914, 1650, 1608, 1592, 1558, 1518, 1443, 1420, 1412, 1398, 1368, 1328, 1312, 1292, 1255, 1217, 1155, 1141, 1120, 1064, 977, 963, 839, 820, 796, 766, 730.

UV-Vis (DMSO): λ_{max} = 429 nm.

Synthesis of Acetamide **719**



Following the general procedure for the synthesis of Ω -iodoalkyl amides, 2-iodoacetic acid (**705**, 0.69 g, 3.69 mmol, 1.0 eq.), aniline **710** (1.00 mg, 3.69 mmol, 1.0 eq.) and *N,N*-dicyclohexylcarbodiimide (0.84 g, 4.05 mmol, 1.1 eq.) were reacted. Purification *via* flash column chromatography (silica, *i*-Hex:EtOAc = 1:0 to 2:3) yielded acetamide **719** (0.85 g, 1.92 mmol, 52%) as an orange solid.

R_f = 0.85 (EtOAc:*i*-Hex = 3:1).

^1H NMR (DMSO- d_6 , 400 MHz): δ = 7.86–7.74 (m, 4H), 7.17–7.05 (m, 2H), 4.24–4.14 (m, 2H), 3.87 (s, 2H), 3.74–3.63 (m, 2H), 3.32 (s, 3H) ppm.

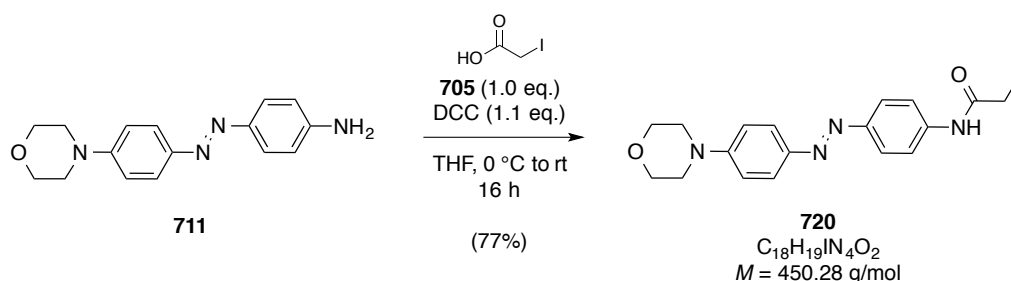
^{13}C NMR (DMSO- d_6 , 100 MHz): δ = 167.0, 161.0, 147.8, 146.2, 141.2, 124.3, 123.3, 119.3, 115.0, 70.2, 67.4, 58.2, 1.4 ppm.

ESI-MS for $C_{17}H_{19}IN_3O_3^+$ $[MH^+]$: calcd. 440.0466
found 440.0463.

IR (ATR): $\tilde{\nu}/\text{cm}^{-1}$ = 3236, 3191, 3122, 3450, 2925, 2848, 1652, 1595, 1581, 1532, 1495, 1450, 1420, 1406, 1371, 1320, 1305, 1297, 1249, 1196, 1153, 1131, 1107, 1096, 1059, 1035, 1010, 985, 973, 923, 846, 822, 814, 773, 735, 657.

UV-Vis (DMSO): λ_{max} = 371 nm.

Synthesis of Acetamide **720**



Following the general procedure for the synthesis of Ω -iodoalkyl amides, 2-iodoacetic acid (**705**, 0.59 g, 3.19 mmol, 1.0 eq.), aniline **711** (0.90 mg, 3.19 mmol, 1.0 eq.) and *N,N'*-dicyclohexylcarbodiimide (0.72 g, 3.51 mmol, 1.0 eq.) were reacted. Purification *via* flash column chromatography (silica, $\text{Et}_2\text{O}:\text{EtOAc}$ = 1:0 then 0:1) yielded acetamide **720** (1.11 g, 2.47 mmol, 77%) as a brown solid.

R_f = 0.55 (Et_2O).

^1H NMR (DMF-d_7 , 400 MHz): δ = 8.07–7.99 (m, 6H, obscured by residual solvent), 7.33–7.26 (m, 2H), 5.80 (s, br, 1H), 4.17 (s, 2H), 3.97 (d, J = 5.0 Hz, 4H), 3.52 (d, J = 5.0 Hz, 4H) ppm.

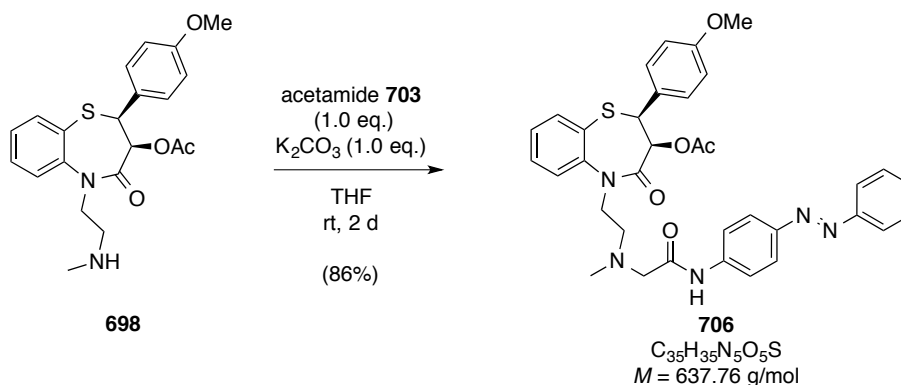
^{13}C NMR (DMF-d_7 , 100 MHz): δ = 167.5, 153.9, 149.2, 145.2, 141.7, 124.7, 123.5, 119.9, 114.7, 66.8, 48.2, 0.8 ppm.

ESI-MS for $C_{18}H_{20}IN_4O_2^+$ $[MH^+]$: calcd. 451.0625
found 451.0631.

IR (ATR): $\tilde{\nu}/\text{cm}^{-1}$ = 3283, 3251, 3289, 3123, 3055, 2956, 2924, 2849, 1657, 1596, 1547, 1507, 1446, 1421, 1400, 1346, 1324, 1307, 1266, 1253, 1234, 1180, 1156, 1120, 1086, 1069, 1050, 1025, 1008, 969, 927, 891, 843, 817, 759, 731, 715.

UV-Vis (DMSO): λ_{max} = 443 nm.

Synthesis of Azo-diltiazem **2** (**706**)



To a solution of mono desmethyl diltiazem (**698**, 400 mg, 1.00 mmol, 1.0 eq.) in dry THF (8 mL), acetamide **703** (365 mg, 1.00 mmol, 1.0 eq.) and K_2CO_3 (138 mg, 1.00 mmol, 1.0 eq.) were added. The resulting suspension was stirred at room temperature for two days, subsequently filtered and concentrated *in vacuo*. Purification *via* flash column chromatography (silica, *i*-Hex:EtOAc = 1:1 to 0:1) yielded diltiazem derivative **706** (546 mg, 0.86 mmol, 86%) as a red, foamy solid. The analytical sample was further purified by recrystallization from CHCl_3/n -hexane.

Crystals suitable for X-ray analysis were obtained by slow evaporation of a solution of **706** in CH_2Cl_2 .

R_f = 0.70 (EtOAc).

^1H NMR (CDCl_3 , 600 MHz): δ = 9.34 (s, br, 1H), 7.80–7.77 (m, 2H), 7.71–7.65 (m, 2H), 7.63 (dd, J = 7.7, 1.5 Hz, 1H), 7.53 (d, J = 8.6 Hz, 2H), 7.44–7.34 (m, 7H), 7.19 (td, J = 7.6, 1.4 Hz, 1H), 6.60 (d, J = 8.5 Hz, 2H), 5.07 (d, J = 7.6 Hz, 1H), 4.96 (d, J = 7.6 Hz, 1H), 4.63 (ddd, J = 13.5, 8.5, 4.6 Hz, 1H), 3.55 (d, J = 16.0 Hz, 1H), 3.44 (s, 3H), 3.35 (d, J = 15.2 Hz, 1H), 2.94 (d, J = 15.2 Hz, 1H), 2.73–2.55 (m, 2H), 2.37 (s, 3H), 1.84 (s, 3H) ppm.

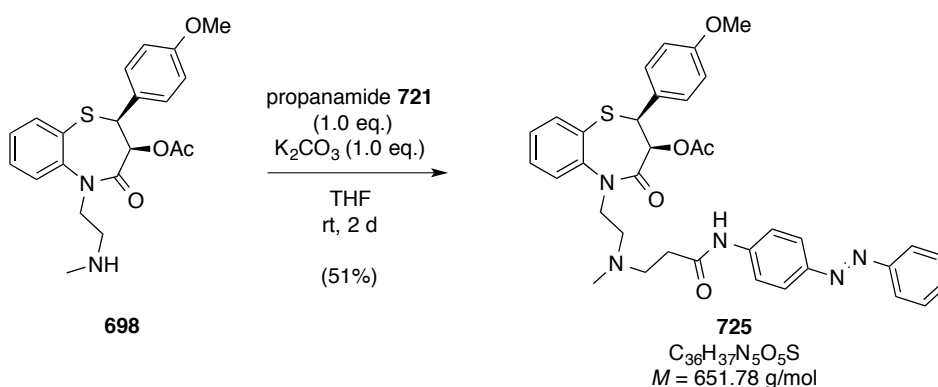
^{13}C NMR (CDCl_3 , 150 MHz): δ = 170.0, 169.5, 167.8, 155.9, 152.9, 145.1, 141.1, 135.8, 131.4, 130.7, 129.5, 129.2, 128.9, 128.0, 126.4, 124.8, 123.8, 122.8, 120.0, 114.1, 71.2, 62.7, 56.7, 55.2, 54.7, 48.0, 48.0, 44.3, 20.6 ppm.

ESI-MS for $\text{C}_{35}\text{H}_{36}\text{N}_5\text{O}_5\text{S}^+$ $[\text{MH}^+]$: calcd. 638.2432
found 638.2431.

IR (ATR): $\tilde{\nu}/\text{cm}^{-1}$ = 3265, 2944, 2835, 1744, 1669, 1591, 1583, 1511, 1471, 1461, 1439, 1406, 1369, 1303, 1251, 1237, 1223, 1180, 1152, 1142, 1111, 1087, 1057, 1034, 1000, 909, 847, 766, 734, 688, 661.

UV-Vis (DMSO): λ_{max} = 361 nm.

Synthesis of Azo-diltiazem **3** (**725**)



To a solution of mono desmethyl diltiazem (**698**, 500 mg, 1.25 mmol, 1.0 eq.) in dry THF (10 mL), propanamide **721** (761 mg, 1.87 mmol, 1.5 eq.) and K_2CO_3 (259 mg, 1.87 mmol, 1.5 eq.) were added. The resulting suspension was stirred at room temperature for two days, subsequently filtered and concentrated *in vacuo*. Purification *via* flash column chromatography (silica, *i*-Hex:EtOAc = 1:1 to 0:1) yielded diltiazem derivative **725** (414 mg, 0.64 mmol, 51%) as a red, foamy solid. The analytical sample was further purified by recrystallization from CHCl_3/n -hexane.

R_f = 0.20 (EtOAc).

^1H NMR (CDCl_3 , 600 MHz): δ = 9.95 (s, 1H), 7.81–7.79 (m, 2H), 7.77–7.75 (m, 2H), 7.57–7.47 (m, 4H), 7.42–7.39 (m, 2H), 7.35–7.28 (m, 4H), 7.08 (td, J = 7.6, 1.3 Hz, 1H),

6.81–6.79 (m, 2H), 5.03 (d, $J = 7.6$ Hz, 1H), 4.93 (d, $J = 7.6$ Hz, 1H), 4.01–3.93 (m, 2H), 3.70 (s, 3H), 2.99 (dt, $J = 13.1, 7.3$ Hz, 1H), 2.86–2.82 (m, 1H), 2.71–2.67 (m, 1H), 2.55 (ddd, $J = 12.7, 7.6, 4.8$ Hz, 1H), 2.42 (ddd, $J = 11.9, 7.4, 4.8$ Hz, 2H), 2.33 (s, 3 H), 1.84 (s, 3H) ppm.

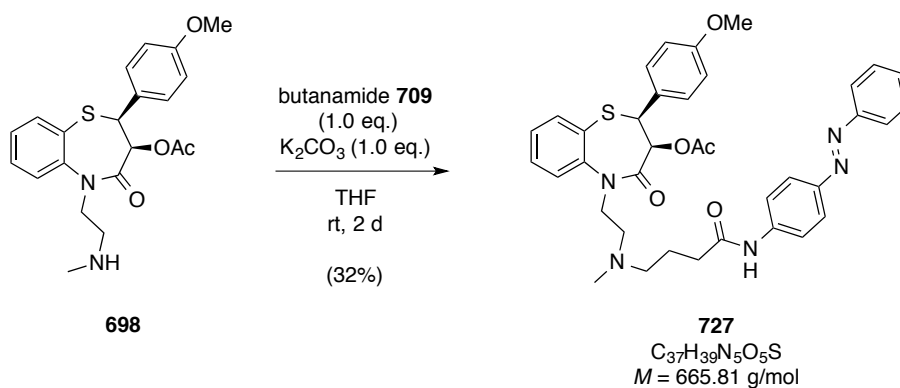
^{13}C NMR (CDCl_3 , 150 MHz): $\delta = 171.1, 170.5, 167.4, 159.9, 152.8, 148.6, 145.6, 141.5, 135.4, 131.4, 130.8, 130.7, 129.1, 127.9, 127.6, 126.5, 124.8, 124.0, 122.7, 119.6, 113.9, 71.5, 55.3, 54.6, 54.3, 53.6, 48.9, 42.5, 34.6, 20.7$ ppm.

ESI-MS for $\text{C}_{36}\text{H}_{38}\text{N}_5\text{O}_5\text{S}^+ [\text{MH}^+]$: calcd. 652.2588
found 652.2575.

IR (ATR): $\tilde{\nu}/\text{cm}^{-1} = 3316, 1953, 2835, 1745, 1673, 1592, 1532, 1511, 1471, 1440, 1406, 1369, 1300, 1222, 1178, 1151, 1141, 1060, 1030, 909, 843, 764, 723, 687$.

UV-Vis (DMSO): $\lambda_{\text{max}} = 360$ nm.

Synthesis of Azo-diltiazem **4** (**727**)



To a solution of mono desmethyl diltiazem (**698**, 100 mg, 0.25 mmol, 1.0 eq.) in dry THF (2 mL), butanamide **709** (197 mg, 0.50 mmol, 2.0 eq.) and K_2CO_3 (69 mg, 0.50 mmol, 2.0 eq.) were added. The resulting suspension was stirred at room temperature for two days, subsequently filtered, and concentrated *in vacuo*. Purification *via* flash column chromatography (silica, *i*-Hex:EtOAc = 1:1 to 0:1) yielded diltiazem derivative **727** (136 mg, 0.20 mmol, 32%) as an orange, foamy solid. The analytical sample was further purified by recrystallization from CHCl_3/n -hexane.

$R_f = 0.18$ (EtOAc).

^1H NMR (CDCl_3 , 600 MHz, 27 °C): δ = 9.18 (s, 1H), 7.79–7.77 (m, 2H), 7.70–7.66 (m, 2H), 7.61 (dd, J = 7.6, 1.4 Hz, 1H), 7.54–7.50 (m, 2H), 7.41–7.33 (m, 7H), 7.18 (dd, J = 7.4 Hz, 1H), 6.75–6.73 (m, 2H), 5.06 (d, J = 7.4 Hz, 1H), 4.94 (d, J = 7.4 Hz, 1H), 4.15 (dt, J = 14.4, 6.8 Hz, 1H), 3.80 (ddd, J = 13.3, 8.0, 4.8 Hz, 1H), 3.59 (s, 3H), 2.76 (dt, J = 14.4, 7.1 Hz, 1H), 2.48–2.38 (m, 5H), 2.22 (s, 3H), 1.85 (dt, J = 13.7, 6.8 Hz, 2H), 1.76 (s, 3H) ppm.

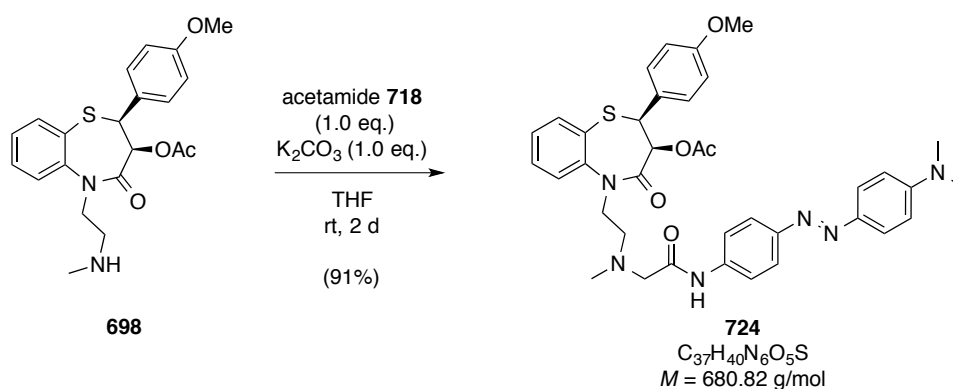
^{13}C NMR (CDCl_3 , 150 MHz, 27 °C): δ = 172.7, 170.0, 167.5, 160.0, 152.8, 148.5, 145.5, 141.7, 135.5, 131.3, 130.9, 130.6, 129.1, 128.4, 127.8, 126.4, 124.7, 123.8, 122.7, 119.5, 113.8, 71.4, 56.7, 55.2, 54.6, 53.5, 49.2, 43.3, 36.0, 23.9, 20.6 ppm.

ESI-MS for $\text{C}_{37}\text{H}_{40}\text{N}_5\text{O}_5\text{S}^+$ [MH^+]: calcd. 666.2745
found 666.2729.

IR (ATR): $\tilde{\nu}/\text{cm}^{-1}$ = 3318, 2935, 2797, 1745, 1659, 1593, 1530, 1511, 1471, 1440, 1405, 1368, 1298, 1250, 1222, 1178, 1152, 1141, 1061, 1031, 920, 845, 763, 735, 723, 688, 662.

UV-Vis (DMSO): λ_{max} = 361 nm.

Synthesis of Azo-diltiazem **5** (**724**)



To a solution of mono desmethyl diltiazem (**698**, 150 mg, 0.38 mmol, 1.0 eq.) in dry THF (3 mL), acetamide **718** (229 mg, 0.56 mmol, 1.5 eq.) and K_2CO_3 (104 mg, 0.56 mmol, 1.5 eq.) were added. The resulting suspension was stirred at room temperature for two days, subsequently filtered, and concentrated *in vacuo*. Purification *via* flash column chromatography (silica, *i*-Hex:EtOAc = 1:1 to 0:1) yielded diltiazem derivative **724** (232 mg,

0.34 mmol, 91%) as a red, foamy solid. The analytical sample was further purified by recrystallization from CHCl_3/n -hexane.

$R_f = 0.75$ (EtOAc).

^1H NMR (CDCl_3 , 600 MHz): $\delta = 9.21$ (s, br, 1H), 7.76–7.74 (m, 2H), 7.63–7.59 (m, 3H), 7.51–7.47 (m, 2H), 7.40 (ddd, $J = 8.0, 7.5, 1.5$ Hz, 1H), 7.36–7.32 (m, 3H), 7.19–7.14 (m, 1H), 6.66–6.61 (m, 4H), 5.06 (d, $J = 7.5$ Hz, 1H), 4.95 (d, $J = 7.5$ Hz, 1H), 4.59 (ddd, $J = 14.2, 8.1, 5.0$ Hz, 1H), 3.56 (dt, $J = 14.3, 5.1$ Hz, 1H), 3.47 (s, 3H), 3.30 (d, $J = 15.4$ Hz, 1H), 2.97 (s, 6H), 2.97–2.94 (m, 1H), 2.73–2.68 (m, 1H), 2.63–2.59 (m, 1H), 2.36 (s, 3H), 1.91 (s, 3H) ppm.

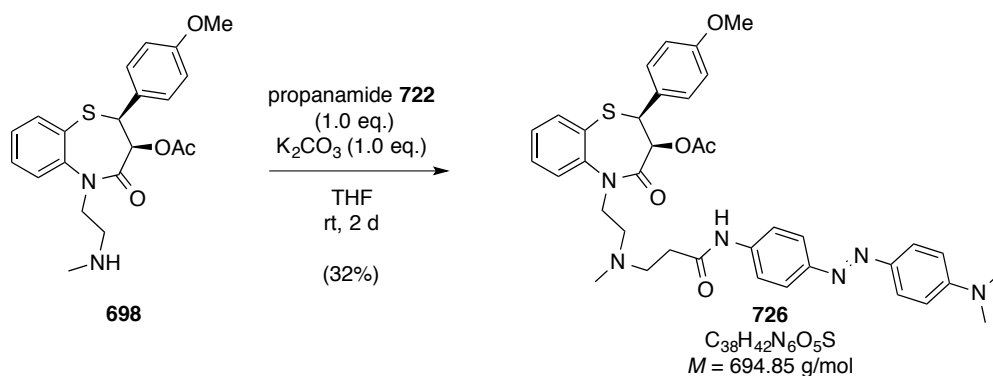
^{13}C NMR (CDCl_3 , 150 MHz): $\delta = 170.0, 169.1, 167.7, 159.9, 152.3, 149.4, 145.2, 143.8, 139.4, 135.7, 131.4, 130.7, 128.7, 127.9, 126.4, 124.8, 124.7, 122.9, 120.0, 114.0, 111.7, 71.2, 62.6, 56.6, 55.2, 54.7, 47.9, 44.1, 40.4, 20.6$ ppm.

ESI-MS for $\text{C}_{37}\text{H}_{41}\text{N}_6\text{O}_5\text{S}^+ [\text{MH}^+]$: calcd. 661.2854
found 661.2841.

IR (ATR): $\tilde{\nu}/\text{cm}^{-1} = 3261, 2881, 1744, 1668, 1597, 1511, 1471, 1442, 1400, 1361, 1304, 1223, 1179, 1152, 1139, 1060, 1029, 944, 844, 821, 763, 728$.

UV-Vis (DMSO): $\lambda_{\text{max}} = 428$ nm.

Synthesis of Azo-diltiazem **6** (**726**)



To a solution of mono desmethyl diltiazem (**698**, 400 mg, 1.00 mmol, 1.0 eq.) in dry THF (8 mL), propanamide **722** (632 mg, 1.50 mmol, 1.5 eq.), and K_2CO_3 (207 mg, 1.50 mmol,

1.5 eq.) were added. The resulting suspension was stirred at room temperature for two days, subsequently filtered, and concentrated *in vacuo*. Purification *via* flash column chromatography (silica, *i*-Hex:EtOAc = 1:1 to 0:1) yielded diltiazem derivative **726** (224 mg, 0.32 mmol, 32%) as a red, foamy solid. The analytical sample was further purified by recrystallization from CHCl₃/*n*-hexane.

R_f = 0.65 (EtOAc).

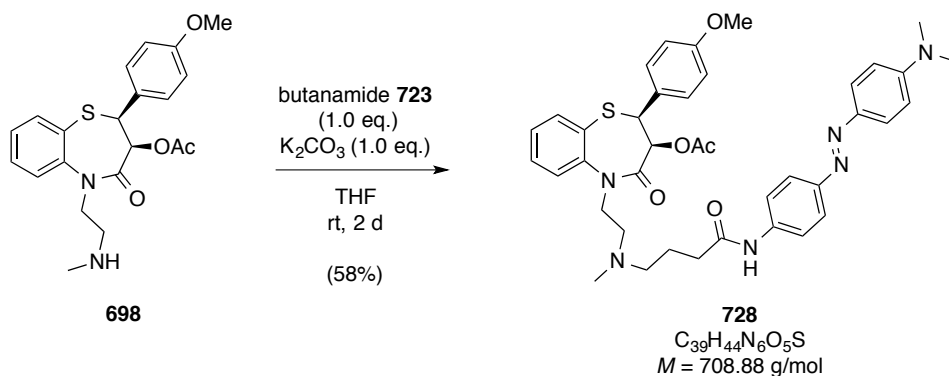
¹H NMR (CDCl₃, 600 MHz): δ = 9.83 (s, 1H), 7.77–7.74 (m, 2H), 7.69–7.65 (m, 2H), 7.55 (dd, *J* = 7.7, 1.6 Hz, 1H), 7.49–7.46 (m, 3H), 7.34–7.31 (m, 2H), 7.30–7.27 (m, 1H), 7.08 (td, *J* = 7.5, 1.2 Hz, 1H), 6.81–6.79 (m, 2H), 6.67–6.64 (m, 2H), 5.02 (d, *J* = 7.7 Hz, 1H), 4.93 (d, *J* = 7.6 Hz, 1H), 4.04–3.90 (m, 2H), 3.70 (s, 3H), 3.01–2.96 (m, 1H), 2.97 (s, 6H), 2.84 (m, *J* = 12.9, 8.1, 4.9 Hz, 1H), 2.73–2.66 (m, 1H), 2.55 (ddd, *J* = 12.7, 7.8, 4.7 Hz, 1H), 2.41 (ddd, *J* = 11.9, 7.1, 4.9 Hz, 2H), 2.34 (s, 3H), 1.84 (s, 3H) ppm.

¹³C NMR (CDCl₃, 150 MHz): δ = 170.9, 170.5, 167.5, 156.0, 152.4, 149.3, 145.7, 143.9, 140.1, 135.5, 131.5, 130.9, 128.0, 127.7, 126.6, 125.0, 124.9, 123.2, 119.8, 114.0, 111.7, 71.6, 55.4, 54.7, 54.4, 53.8, 48.9, 42.5, 40.5, 34.7, 20.8 ppm.

ESI-MS for C₃₈H₄₃N₆O₅S⁺ [MH⁺]: calcd. 695.3010
 found 695.3003.

IR (ATR): $\tilde{\nu}/\text{cm}^{-1}$ = 3316, 2938, 2801, 1742, 1671, 1596, 1511, 1471, 1443, 1422, 1398, 1361, 1223, 1178, 1151, 1138, 1087, 1060, 1029, 943, 907, 841, 821, 761, 726, 662.

UV-Vis (DMSO): λ_{max} = 429 nm.

Synthesis of Azo-diltiazem 7 (728)

To a solution of mono desmethyl diltiazem (**698**, 490 mg, 1.22 mmol, 1.0 eq.) in dry THF (10 mL), butanamide **723** (800 mg, 1.83 mmol, 1.5 eq.), and K_2CO_3 (253 mg, 1.83 mmol, 1.5 eq.) were added. The resulting suspension was stirred at room temperature for two days, subsequently filtered, and concentrated *in vacuo*. Purification *via* flash column chromatography (silica, *i*-Hex:EtOAc = 1:1 to 0:1) yielded diltiazem derivative **728** (504 mg, 0.71 mmol, 58%) as a red, foamy solid. The analytical sample was further purified by recrystallization from CHCl_3/n -hexane.

$R_f = 0.15$ (EtOAc).

^1H NMR (CDCl_3 , 600 MHz): δ = 9.00 (s, 1H), 7.76–7.73 (m, 2H), 7.63–7.59 (m, 3H), 7.47 (d, J = 8.8 Hz, 2H), 7.41–7.34 (m, 4H), 7.20–7.16 (m, 1H), 6.76–6.73 (m, 2H), 6.66–6.64 (m, 2H), 5.05 (d, J = 7.4 Hz, 1H), 4.93 (d, J = 7.4 Hz, 1H), 4.17 (dt, J = 14.2, 7.2 Hz, 1H), 3.85–3.80 (m, 1H), 3.61 (s, 3H), 2.97 (s, 6H), 2.82–2.76 (m, 1H), 2.53–2.38 (m, 5H), 2.25 (s, 3H), 1.89–1.80 (m, 2H), 1.77 (s, 3H) ppm.

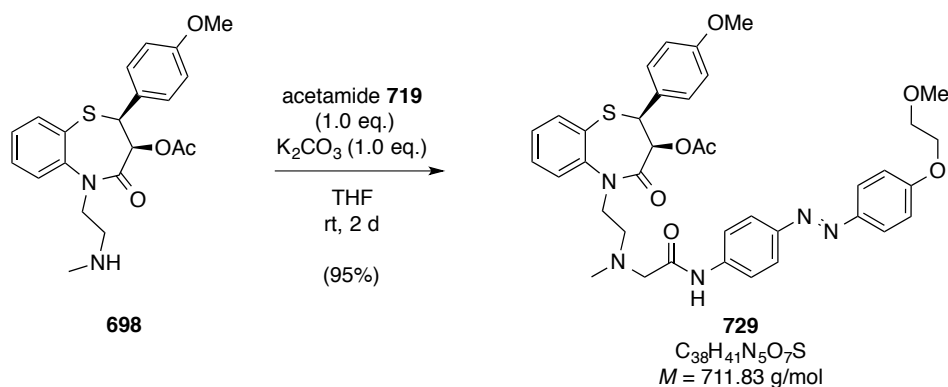
^{13}C NMR (CDCl_3 , 150 MHz): δ = 172.3, 170.2, 167.5, 160.1, 152.3, 149.2, 145.5, 143.8, 140.2, 135.6, 131.4, 130.9, 128.4, 127.8, 126.4, 124.8, 124.8, 123.1, 119.6, 113.9, 111.7, 71.4, 56.8, 55.3, 54.7, 53.7, 49.0, 43.2, 40.5, 36.0, 23.7, 20.6 ppm.

ESI-MS for $\text{C}_{39}\text{H}_{45}\text{N}_6\text{O}_5\text{S}^+ [\text{MH}^+]$: calcd. 709.3167
found 709.3165.

IR (ATR): $\tilde{\nu}/\text{cm}^{-1}$ = 3317, 2936, 2797, 1744, 1662, 1597, 1511, 1471, 1443, 1421, 1398, 1361, 1298, 1224, 1178, 1152, 1139, 1061, 1031, 944, 844, 821, 762, 735, 660.

UV-Vis (DMSO): $\lambda_{\text{max}} = 427 \text{ nm}$.

Synthesis of Azo-diltiazem **8** (**729**)



To a solution of mono desmethyl diltiazem (**698**, 365 mg, 0.91 mmol, 1.0 eq.) in dry THF (7 mL), acetamide **719** (600 mg, 1.37 mmol, 1.5 eq.) and K_2CO_3 (189 mg, 1.37 mmol, 1.5 eq.) were added. The resulting suspension was stirred at room temperature for two days, subsequently filtered, and concentrated *in vacuo*. Purification *via* flash column chromatography (silica, *i*-Hex:EtOAc = 1:1 to 0:1) yielded diltiazem derivative **729** (619 mg, 0.87 mmol, 95%) as an orange, foamy solid. The analytical sample was further purified by recrystallization from CHCl_3/n -hexane.

Crystals suitable for X-ray analysis were obtained by slow evaporation of a solution of **729** in CH_2Cl_2 .

$R_f = 0.57$ (EtOAc).

^1H NMR (CDCl_3 , 600 MHz): $\delta = 9.29$ (s, 1H), 7.78 (dd, $J = 9.4, 2.7 \text{ Hz}$, 2H), 7.64–7.61 (m, 3H), 7.52–7.49 (m, 2H), 7.40 (tt, $J = 7.7, 1.3 \text{ Hz}$, 1H), 7.36–7.32 (m, 3H), 7.19–7.16 (m, 1H), 6.94–6.92 (m, 2H), 6.60 (d, $J = 8.5 \text{ Hz}$, 2H), 5.06 (d, $J = 7.7 \text{ Hz}$, 1H), 4.95 (d, $J = 7.7 \text{ Hz}$, 1H), 4.71–4.66 (m, 1H), 4.11–4.09 (m, 2H), 3.69–3.68 (m, 2H), 3.55 (dt, $J = 14.3, 4.8 \text{ Hz}$, 1H), 3.44 (s, 3H), 3.37 (s, 3H), 3.32 (d, $J = 15.3 \text{ Hz}$, 1H), 2.94 (d, $J = 15.3 \text{ Hz}$, 1H), 2.69 (ddd, $J = 13.2, 8.2, 4.7 \text{ Hz}$, 1H), 2.59 (ddd, $J = 12.9, 4.7, 4.7 \text{ Hz}$, 1H), 2.36 (s, 3H), 1.83 (s, 3H) ppm.

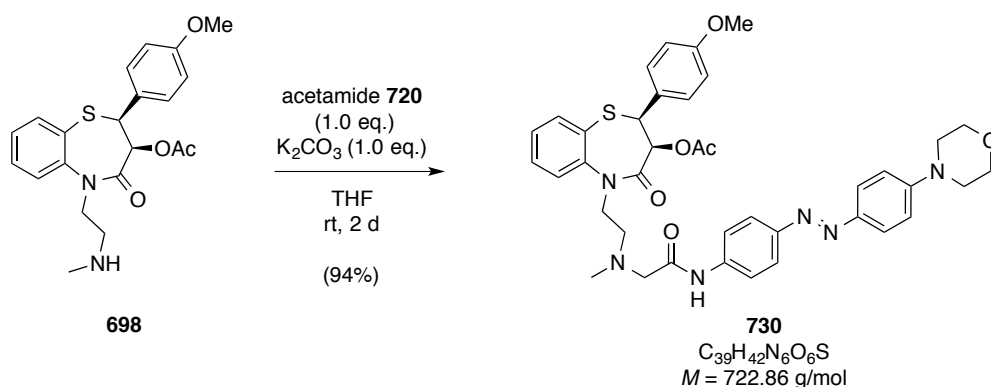
^{13}C NMR (CDCl_3 , 150 MHz): δ = 167.0, 169.4, 167.8, 161.0, 159.9, 148.8, 147.3, 145.1, 140.4, 135.8, 131.4, 130.7, 128.8, 128.0, 126.4, 124.8, 124.5, 123.4, 120.0, 114.9, 114.0, 71.2, 71.0, 67.7, 62.6, 59.4, 56.7, 55.2, 54.7, 47.9, 44.2, 20.6 ppm.

ESI-MS for $\text{C}_{38}\text{H}_{42}\text{N}_5\text{O}_7\text{S}^+ [\text{MH}^+]$: calcd. 712.2799
found 712.2797.

IR (ATR): $\tilde{\nu}/\text{cm}^{-1}$ = 3253, 3058, 2927, 2887, 2839, 1750, 1693, 1662, 1594, 1532, 1511, 1499, 1472, 1446, 1438, 1413, 1372, 1352, 1301, 1250, 1239, 1225, 1189, 1178, 1151, 1127, 1120, 1088, 1080, 1063, 1029, 1004, 965, 949, 927, 910, 855, 834, 819, 810, 767, 756, 739, 733, 689, 663.

UV-Vis (DMSO): λ_{max} = 369 nm.

Synthesis of Azo-diltiazem **9** (**730**)



To a solution of mono desmethyl diltiazem (**698**, 593 mg, 1.48 mmol, 1.0 eq.) in dry THF (12 mL), acetamide **720** (1.00 g, 2.22 mmol, 1.5 eq.) and K_2CO_3 (307 mg, 2.22 mmol, 1.5 eq.) were added. The resulting suspension was stirred at room temperature for two days, subsequently filtered, and concentrated *in vacuo*. Purification *via* flash column chromatography (silica, *i*-Hex:EtOAc = 1:1 to 0:1) yielded diltiazem derivative **730** (1.01 g, 1.39 mmol, 94%) as a deep red, foamy solid. The analytical sample was further purified by recrystallization from CHCl_3/n -hexane.

R_f = 0.65 (EtOAc).

^1H NMR (CDCl_3 , 600 MHz): δ = 9.25 (s, 1H), 7.77–7.75 (m, 2H), 7.64–7.61 (m, 3H), 7.52–7.48 (m, 2H), 7.42–7.39 (m, 1H), 7.37–7.32 (m, 3H), 7.18 (td, J = 7.6, 1.4 Hz, 1H), 6.88–6.86 (m, 2H), 6.63–6.59 (m, 2H), 5.07 (d, J = 7.6 Hz, 1H), 4.95 (d, J = 7.6 Hz, 1H), 4.60 (ddd, J = 14.2, 8.2, 4.8 Hz, 1H), 3.79–3.77 (m, 4H), 3.55 (dt, J = 14.2, 4.9 Hz, 1H), 3.45 (s, 3H), 3.31 (d, J = 15.4 Hz, 1H), 3.22–3.19 (m, 4H), 2.94 (d, J = 15.4 Hz, 1H), 2.69 (ddd, J = 13.2, 8.2, 4.9 Hz, 1H), 2.59 (dt, J = 13.2, 4.9 Hz, 1H), 2.36 (s, 3H), 1.83 (s, 3H) ppm.

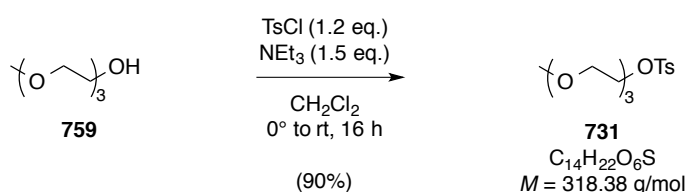
^{13}C NMR (CDCl_3 , 150 MHz): δ = 170.0, 169.3, 167.7, 159.9, 153.0, 149.1, 146.0, 145.2, 140.0, 135.8, 131.4, 130.7, 128.8, 128.0, 126.4, 124.8, 124.5, 123.2, 120.0, 114.7, 114.0, 71.2, 66.8, 62.6, 56.6, 55.2, 54.7, 48.4, 48.0, 44.2, 20.6 ppm.

ESI-MS for $\text{C}_{39}\text{H}_{43}\text{N}_6\text{O}_6\text{S}^+$ [MH^+]: calcd. 723.2959
found 723.2962.

IR (ATR): $\tilde{\nu}/\text{cm}^{-1}$ = 3262, 3056, 2955, 2834, 1743, 1668, 1596, 1508, 1470, 1445, 1417, 1402, 1376, 1302, 1226, 1179, 1154, 1120, 1110, 1087, 1049, 1028, 925, 844, 827, 762, 734, 715, 685, 660.

UV-Vis (DMSO): λ_{max} = 412 nm.

Synthesis of Tosylate **731**



According to the literature,^[505] methyl ether **759** (3.00 g, 18.3 mmol, 1.0 eq.) and NEt_3 (3.82 mL, 27.4 mmol, 1.5 eq.) were dissolved in dry CH_2Cl_2 (50 mL) and cooled to 0 °C. To this, a solution of tosylchloride (2.80 mL, 21.9 mmol, 1.2 eq.) in dry CH_2Cl_2 (10 mL) was added slowly over a period of 10 min. The resulting mixture was allowed to warm to room temperature and stirred for 16 hours. Thereafter, saturated aqueous NaHCO_3 (50 mL) was added and the layers were separated. The aqueous phase was extracted with CH_2Cl_2 ($3 \times 30 \text{ mL}$) and the combined organic layers were dried over Na_2SO_4 . After having removed the solvent *in vacuo*, purification of the crude product by flash column chromatography

(silica, *i*-Hex:EtOAc = 1:0 to 1:3) yielded tosylate **731** (5.24 g, 16.5 mmol, 90%) as colourless liquid.

$R_f = 0.58$ (*i*-Hex:EtOAc = 1:3).

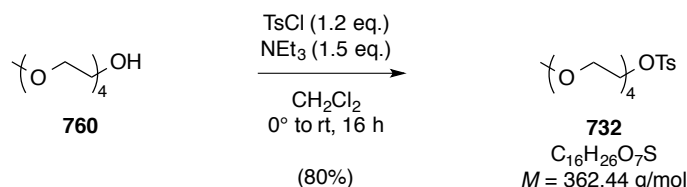
^1H NMR (CDCl_3 , 400 MHz): $\delta = 7.72\text{--}7.67$ (m, 2H), 7.24 (d, $J = 8.1$ Hz, 2H), 4.08–4.03 (m, 2H), 3.62–3.56 (m, 2H), 3.53–3.47 (m, 6H), 3.43 (dd, $J = 5.8, 3.4$ Hz, 2H), 3.27 (s, 3H), 2.35 (s, 3H) ppm.

^{13}C NMR (CDCl_3 , 100 MHz): $\delta = 144.9, 133.2, 123.0, 128.1, 72.1, 70.9, 70.7, 70.7, 69.4, 68.8, 59.2, 21.8$ ppm.

EI-MS for $\text{C}_{14}\text{H}_{22}\text{O}_6\text{S}^+ [\text{M}^+]$:
calcd. 318.1137
found 318.1135.

IR (ATR): $\tilde{\nu}/\text{cm}^{-1} = 2877, 1929, 1724, 1598, 1495, 1452, 1399, 1352, 1306, 1291, 1246, 1189, 1174, 1095, 1011, 916, 847, 815, 773, 705, 689, 661$.

Synthesis of Tosylate **732**



According to the literature,^[505] methyl ether **760** (3.00 g, 14.4 mmol, 1.0 eq.) and NEt_3 (3.01 mL, 21.6 mmol, 1.5 eq.) were dissolved in dry CH_2Cl_2 (57 mL) and cooled to 0°C . To this, a solution of tosylchloride (2.21 mL, 17.3 mmol, 1.2 eq.) in dry CH_2Cl_2 (10 mL) was added slowly over a period of 10 min. The resulting mixture was allowed to warm to room temperature and stirred for 16 hours. Thereafter, saturated aqueous NaHCO_3 (50 mL) was added and the layers were separated. The aqueous phase was extracted with CH_2Cl_2 (3×30 mL) and the combined organic layers were dried over Na_2SO_4 . After having removed the solvent *in vacuo*, purification of the crude product by flash column chromatography (silica, *i*-Hex:EtOAc = 1:0 to 1:2) yielded tosylate **732** (4.20 g, 16.5 mmol, 80%) as colourless liquid.

$R_f = 0.26$ (*i*-Hex:EtOAc = 1:2).

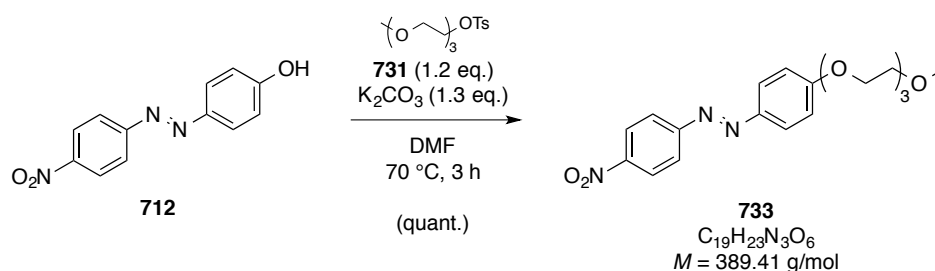
^1H NMR (CDCl_3 , 400 MHz): $\delta = 7.73\text{--}7.66$ (m, 2H), 7.23 (d, $J = 8.0$ Hz, 2H), 4.07–4.02 (m, 2H), 3.61–3.55 (m, 2H), 3.55–3.50 (m, 6H), 3.47 (s, 4H), 3.46–3.41 (m, 2H), 3.26 (s, 3H), 2.34 (s, 3H) ppm.

^{13}C NMR (CDCl_3 , 100 MHz): $\delta = 144.9$, 133.1, 129.9, 128.1, 72.1, 70.9, 70.7, 70.7, 70.7, 70.6, 69.4, 68.8, 59.2, 21.8 ppm.

EI-MS for $\text{C}_{16}\text{H}_{26}\text{O}_7\text{S}^+ [\text{M}^+]$:
 calcd. 362.1399
 found 362.1382.

IR (ATR): $\tilde{\nu}/\text{cm}^{-1} = 2879$, 1711, 1598, 1495, 1400, 1330, 1311, 1306, 1291, 1246, 1221, 1193, 1170, 1105, 1090, 1017, 917, 848, 830, 818, 770, 710, 696, 683, 662.

Synthesis of Polyether **733**



Phenol **712** (2.55 g, 10.4 mmol, 1.0 eq.) was dissolved in dry DMF (38 mL). To this, K_2CO_3 (1.88 g, 13.6 mmol, 1.3 eq.) and tosylate **731** (4.00 g, 12.6 mmol, 1.2 eq.) were added and the resulting mixture was heated to 70 °C for 3 hours. Subsequently, the suspension was cooled to room temperature and diluted with EtOAc (200 mL). The organic layer was washed with half-saturated aqueous NaCl solution (3×50 mL). The respective aqueous phases were re-extracted with EtOAc (50 mL) and the combined organic layers were dried over Na_2SO_4 . After having removed the solvent *in vacuo*, purification of the crude product by repeated flash column chromatography (silica, *i*-Hex:EtOAc = 1:1 to 1:2) yielded polyether **733** (4.03 g, 10.4 mmol, quant.) as an orange solid, which was contaminated with 5 mol-% of tosylate **731**, as judged by ^1H NMR.

$R_f = 0.80$ (EtOAc).

^1H NMR (CDCl_3 , 400 MHz): δ = 8.29–8.22 (m, 2H), 7.86 (m_C , 4H), 6.96 (m_C , 2H), 4.16–4.11 (m, 2H), 3.84–3.78 (m, 2H), 3.68–3.63 (m, 2H), 3.62–3.54 (m, 4H), 3.52–3.41 (m, 2H), 3.28 (s, 3H) ppm.

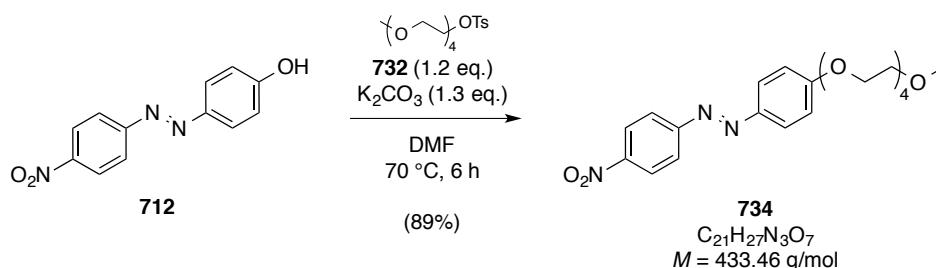
^{13}C NMR (CDCl_3 , 100 MHz): δ = 162.7, 156.2, 148.4, 147.1, 125.7, 124.8, 123.3, 115.2, 72.1, 71.1, 70.8, 70.8, 69.7, 68.0, 59.2 ppm.

ESI-MS for $\text{C}_{19}\text{H}_{24}\text{N}_3\text{O}_6^+$ [MH^+]: calcd. 390.1660
 found 390.1656.

IR (ATR): $\tilde{\nu}/\text{cm}^{-1}$ = 2928, 2888, 2829, 1601, 1579, 1550, 1516, 1492, 1476, 1450, 1421, 1399, 1379, 1365, 1294, 1335, 1294, 1246, 1197, 1175, 1135, 1113, 1092, 1068, 1054, 1020, 998, 957, 917, 850, 822, 778, 755, 723, 683, 663.

UV-Vis (DMSO): λ_{max} = 379 nm

Synthesis of Polyether **734**



Phenol **712** (2.00 g, 8.22 mmol, 1.0 eq.) was dissolved in dry DMF (32 mL). To this, K_2CO_3 (1.48 g, 10.7 mmol, 1.3 eq.) and tosylate **732** (3.58 g, 9.87 mmol, 1.2 eq.) were added and the resulting mixture was heated to 70 °C for 6 hours. Subsequently, the suspension was cooled to room temperature and diluted with EtOAc (150 mL). The organic layer was washed with half-saturated aqueous NaCl solution ($3 \times 50 \text{ mL}$). The respective aqueous phases were re-extracted with EtOAc (50 mL) and the combined organic layers were dried over Na_2SO_4 . After having removed the solvent *in vacuo*, purification of the crude product by repeated flash column chromatography (silica, *i*-Hex:EtOAc = 1:1 to 1:4) yielded polyether **734** (3.83 g, 8.84 mmol, 89%) as an orange solid, which was contaminated with 3 mol-% of tosylate **732**, as judged by ^1H NMR.

$R_f = 0.15$ (*i*-Hex:EtOAc = 3:2).

^1H NMR (CDCl_3 , 400 MHz): $\delta = 8.29\text{--}8.23$ (m, 2H), 7.87 (m_C, 4H), 6.96 (m_C, 2H), 4.14 (m_C, 2H), 3.84–3.78 (m, 2H), 3.67–3.63 (m, 2H), 3.62–3.50 (m, 8H), 3.47–3.42 (m, 2H), 3.27 (s, 3H) ppm.

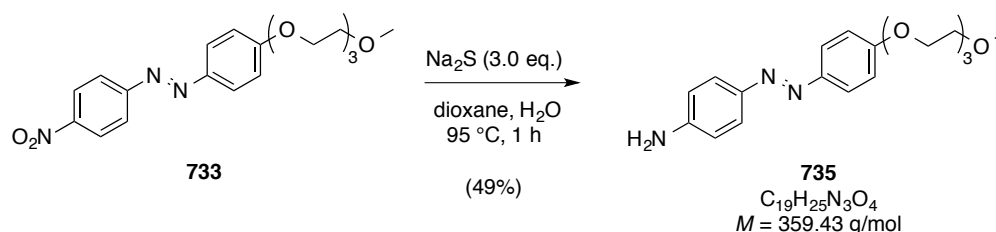
^{13}C NMR (CDCl_3 , 100 MHz): $\delta = 162.7, 156.2, 148.4, 147.3, 125.7, 124.9, 123.3, 115.2, 72.1, 71.1, 70.8, 70.8, 70.8, 70.7, 69.7, 68.0, 59.2$ ppm.

ESI-MS for $\text{C}_{21}\text{H}_{28}\text{N}_3\text{O}_7^+$ [MH^+]:
calcd. 434.1922
found 434.1919.

IR (ATR): $\tilde{\nu}/\text{cm}^{-1} = 2898, 1601, 1581, 1517, 1496, 1478, 1455, 1418, 1399, 1379, 1362, 1337, 1294, 1254, 1193, 1177, 1132, 1095, 1054, 1040, 1023, 1000, 948, 927, 887, 864, 856, 850, 824, 808, 779, 756, 724, 685, 663$.

UV-Vis (DMSO): $\lambda_{\text{max}} = 381$ nm.

Synthesis of Aniline **735**



Polyether **733** (4.00 g, 10.3 mmol, 1.0 eq.) was dissolved in 1,4-dioxane (100 mL). To this, water (10 mL) and Na_2S (2.41 g, 30.8 mmol, 3.0 eq.) were added. The resulting suspension was heated to 95 °C for one hour and the conversion was then judged to be complete *via* TLC analysis. Subsequently, the reaction mixture was poured into saturated aqueous NaHCO_3 solution (100 mL) and extracted with CH_2Cl_2 (3 \times 150 mL). The combined organic layers were dried over Na_2SO_4 and concentrated *in vacuo*. Purification *via* flash column chromatography (silica, *i*-Hex:EtOAc = 1:1 to 1:9) provided aniline **735** (1.81 g, 5.04 mmol, 49%) as a bright orange solid.

$R_f = 0.32$ (*i*-Hex:EtOAc = 1:4).

^1H NMR (CDCl_3 , 400 MHz): δ = 7.72 (m_C , 2H), 7.66 (m_C , 2H), 6.90 (m_C , 2H), 6.62 (m_C , 2H), 4.12–4.07 (m , 2H), 3.91 (s , br , 2H), 3.81–3.76 (m , 2H), 3.68–3.63 (m , 2H), 3.62–3.54 (m , 4H), 3.48–3.42 (m , 2H), 3.28 (s , 3H) ppm.

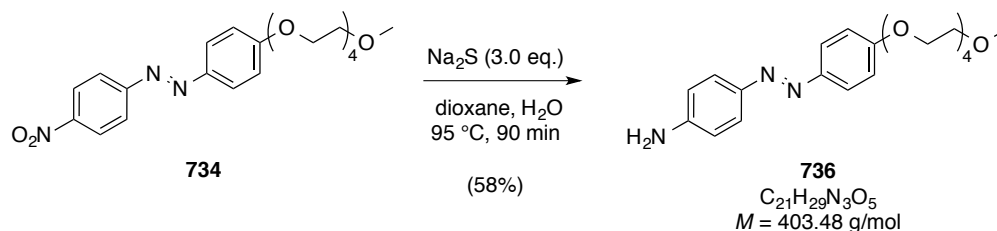
^{13}C NMR (CDCl_3 , 100 MHz): δ = 160.5, 149.2, 147.4, 145.7, 124.8, 124.1, 114.9, 114.8, 72.1, 71.0, 70.8, 70.7, 69.8, 67.8, 59.2 ppm.

ESI-MS for $\text{C}_{19}\text{H}_{26}\text{N}_3\text{O}_4^+$ [MH^+]:
calcd. 360.1918
found 360.1915.

IR (ATR): $\tilde{\nu}/\text{cm}^{-1}$ = 3424, 3345, 3235, 3053, 2993, 2941, 2915, 2875, 2846, 1640, 1597, 1573, 1536, 1507, 1495, 1469, 1451, 1430, 1408, 1391, 1363, 1348, 1319, 1298, 1283, 1253, 1192, 1148, 1134, 1125, 1104, 1091, 1060, 1022, 950, 934, 922, 854, 840, 833, 819, 767, 731.

UV-Vis (DMSO): λ_{max} = 405 nm.

Synthesis of Aniline **736**



Polyether **734** (3.50 g, 8.11 mmol, 1.0 eq.) was dissolved in 1,4-dioxane (100 mL). To this, water (10 mL) and Na_2S (1.89 g, 24.2 mmol, 3.0 eq.) were added. The resulting suspension was heated to 95 °C for 90 min and the conversion was then judged to be complete *via* TLC analysis. Subsequently, the reaction mixture was poured into saturated aqueous NaHCO_3 solution (100 mL) and extracted with CH_2Cl_2 ($3 \times 150 \text{ mL}$). The combined organic layers were dried over Na_2SO_4 and concentrated *in vacuo*. Purification *via* flash column chromatography (silica, *i*-Hex:EtOAc = 1:1 to 0:1) provided aniline **736** (1.89 g, 4.68 mmol, 58%) as a bright orange solid.

R_f = 0.41 (EtOAc).

^1H NMR (CDCl_3 , 400 MHz): δ = 7.72 (m_C , 2H), 7.66 (m_C , 2H), 6.90 (m_C , 2H), 6.62 (m_C , 2H), 4.11–4.07 (m, 2H), 3.92 (s, br, 2H), 3.80–3.76 (m, 2H), 3.66–3.62 (m, 2H), 3.62–3.52 (m, 8H), 3.46–3.41 (m, 2H), 3.27 (s, 3H) ppm.

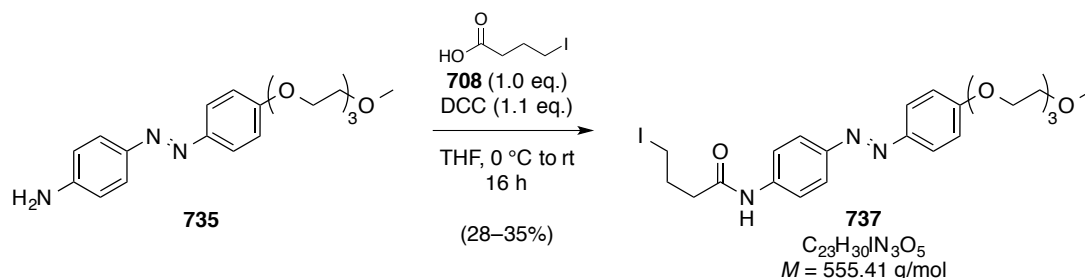
^{13}C NMR (CDCl_3 , 100 MHz): δ = 160.5, 149.2, 147.4, 145.7, 124.8, 124.1, 114.9, 114.8, 72.1, 71.0, 70.8, 70.8, 70.7, 70.7, 69.8, 67.8, 59.2 ppm.

ESI-MS for $\text{C}_{21}\text{H}_{30}\text{N}_3\text{O}_5^+$ [MH^+]: calcd. 404.2180
found 404.2177.

IR (ATR): $\tilde{\nu}/\text{cm}^{-1}$ = 3424, 3344, 3236, 3064, 2876, 2813, 1639, 1596, 1574, 1553, 1530, 1503, 1470, 1453, 1430, 1407, 1358, 1347, 1314, 1299, 1252, 1126, 1099, 1060, 1025, 953, 923, 843, 811, 766, 732, 672.

UV-Vis (DMSO): λ_{max} = 403 nm.

Synthesis of Butanamide **737**



Following the general procedure for the synthesis of Ω -iodoalkyl amides, 4-iodobutyric acid (**708**, 0.74 g, 3.48 mmol, 1.0 eq.), aniline **735** (1.25 g, 3.48 mmol, 1.0 eq.) and N,N' -dicyclohexylcarbodiimide (0.79 g, 3.83 mmol, 1.1 eq.) were reacted. Purification *via* flash column chromatography (silica, $\text{EtOAc}:\textit{i}$ -Hex = 1:0 to 1:0) yielded butanamide **737** (0.79 g, 7.56 mmol, 28–35%) as brown solid in a 4:1 mixture with inseparable aniline **735**, as judged by ^1H NMR.

Note: As a consequence of its impurity, more equivalents of butanamide **737** were employed for the alkylation reactions. Analytical data was recorded from the obtained mixture.

R_f = 0.36 (\textit{i} -Hex:EtOAc = 1:4).

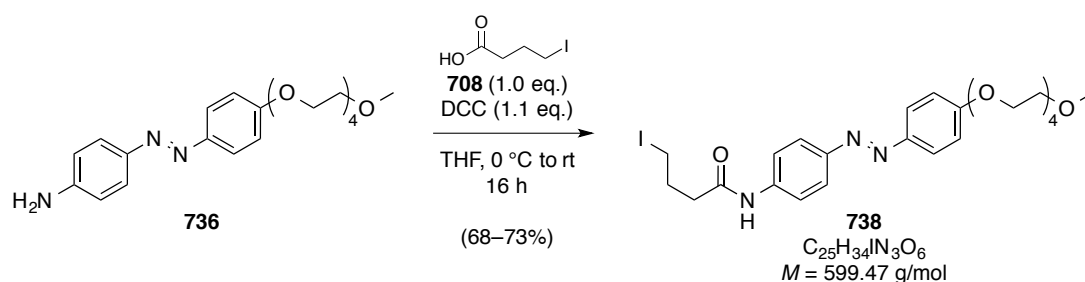
^1H NMR (CDCl_3 , 400 MHz, characteristic signals): δ = 7.83–7.73 (m, 4H), 7.57 (d, J = 8.7 Hz, 2H), 7.28 (s, br, 1H), 6.96–6.87 (m, 2H), 4.17–4.06 (m, 2H), 3.85–3.74 (m, 2H), 3.70–3.63 (m, 2H), 3.63–3.53 (m, 4H), 3.48–3.44 (m, 2H), 3.28 (s, 3H), 3.23 (t, J = 6.5 Hz, 2H), 2.46 (t, J = 7.0 Hz, 2H), 2.14 (quin, J = 6.7 Hz, 2H) ppm.

^{13}C NMR (CDCl_3 , 100 MHz, characteristic signals): δ = 169.6, 161.1, 149.2, 147.1, 139.6, 124.6, 123.7, 119.7, 114.8, 71.9, 70.9, 70.7, 70.6, 69.7, 67.7, 59.1, 34.0, 28.5, 6.5 ppm.

ESI-MS for $\text{C}_{23}\text{H}_{31}\text{IN}_3\text{O}_5^+$ [MH^+]: calcd. 556.1303
found 556.1301.

UV-Vis (DMSO): λ_{max} = 373 nm.

Synthesis of Butanamide **738**



Following the general procedure for the synthesis of Ω -iodoalkyl amides, 4-iodobutyric acid (**708**, 0.66 g, 3.10 mmol, 1.0 eq.), aniline **736** (1.25 g, 3.10 mmol, 1.0 eq.), and N,N' -dicyclohexylcarbodiimide (0.70 g, 3.41 mmol, 1.1 eq.) were reacted. Purification *via* flash column chromatography (silica, $\text{EtOAc}:\textit{i}$ -Hex = 4:1 to 1:0) yielded butanamide **738** (1.37 g, 2.30 mmol, 68–73%) as brown solid in a 6.7:1 mixture with inseparable aniline **736**, as judged by ^1H NMR.

Note: As a consequence of its impurity, more equivalents of butanamide 738 were employed for the alkylation reactions. Analytical data was recorded from the obtained mixture.

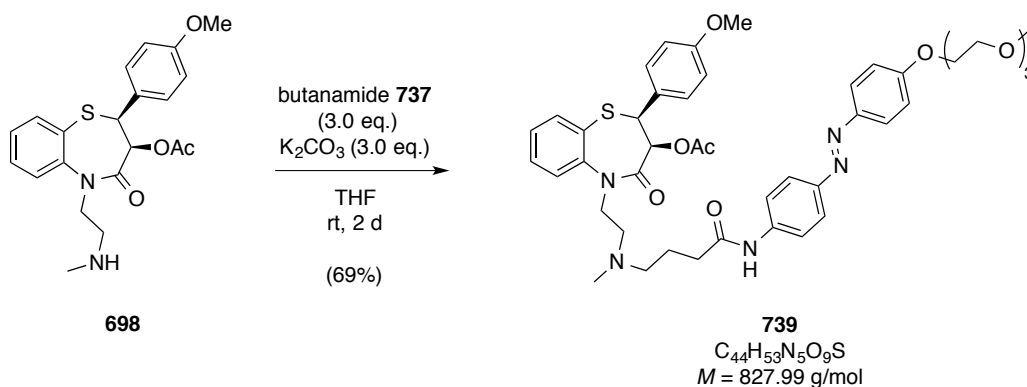
R_f = 0.43 (EtOAc).

^1H NMR (CDCl_3 , 400 MHz, characteristic signals): δ = 7.86–7.73 (m, 4H), 7.57 (d, J = 8.7 Hz, 2H), 7.25 (s, br, 1H), 7.03–6.86 (m, 2H), 4.14–4.06 (m, 2H), 3.84–3.76 (m, 2H), 3.69–3.50 (m, 10H), 3.48–3.41 (m, 2H), 3.28–3.22 (m, 2H), 3.27 (s, 53H), 2.46 (t, J = 7.0 Hz, 2H), 2.14 (quin, J = 6.8 Hz, 2H) ppm.

ESI-MS for $\text{C}_{25}\text{H}_{35}\text{IN}_3\text{O}_6^+$ $[\text{MH}^+]$: calcd. 600.1565
found 600.1563.

UV-Vis (DMSO): $\lambda_{\text{max}} = 391 \text{ nm}$.

Synthesis of Azo-diltiazem 10 (**739**)



To a solution of mono desmethyl diltiazem (**698**, 144 mg, 0.36 mmol, 1.0 eq.) in dry THF (3 mL), butanamide **737** (600 mg, 1.08 mmol, 3.0 eq.) and K_2CO_3 (100 mg, 0.72 mmol, 3.0 eq.) were added. The resulting suspension was stirred at room temperature for two days, subsequently filtered, and concentrated *in vacuo*. Purification *via* repeated flash column chromatography (silica, $\text{MeOH}:\text{EtOAc} = 0:1$ to $1:9$) yielded diltiazem derivative **739** (208 mg, 0.25 mmol, 69%) as an orange, foamy solid.

Note: Early fractions collected at the column chromatographic steps contained little amounts of the respective deacetylated compound and were discarded.

$R_f = 0.28$ ($\text{MeOH}:\text{EtOAc} = 1:19$).

^1H NMR (CDCl_3 , 600 MHz): $\delta = 9.06$ (s, br, 1H), 8.11–8.03 (m, 4H), 8.03–7.96 (m, 2H), 7.62–7.48 (m, 3H), 7.10–6.93 (m, 2H), 6.90–6.76 (m, 5H), 4.99 (d, $J = 7.4 \text{ Hz}$, 1H), 4.69 (d, $J = 7.4 \text{ Hz}$, 1H), 4.00 (dt, $J = 14.0, 7.1 \text{ Hz}$, 1H), 3.71 (dd, $J = 5.8, 4.1 \text{ Hz}$, 3H), 3.57–3.40 (m, 8H), 3.34 (dd, $J = 5.9, 4.0 \text{ Hz}$, 2H), 3.24 (s, 3H), 3.12 (s, 3H), 2.72–2.49 (m, 2H), 2.37 (mc, 2H), 2.24 (ddd, $J = 12.3, 7.8, 4.7 \text{ Hz}$, 1H), 2.10 (ddd, $J = 12.3, 6.6, 4.7 \text{ Hz}$, 1H), 1.95 (s, 3H), 1.95–1.88 (m, 1H), 1.87–1.73 (m, 1H), 1.47 (s, 3H) ppm

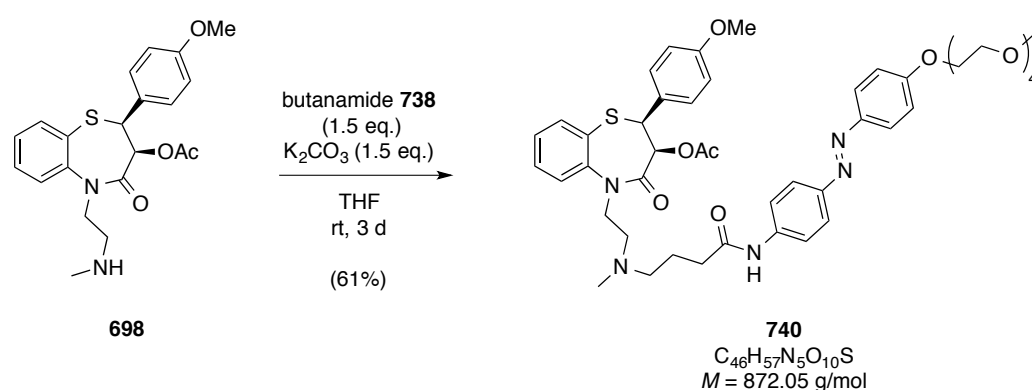
¹³C NMR (C₆D₆, 150 MHz): δ = 171.9, 169.8, 167.9, 161.5, 160.7, 149.1, 147.9, 146.4, 142.5, 135.5, 131.5, 131.1, 128.9, 127.4, 127.0, 125.0, 124.9, 124.2, 119.7, 115.1, 114.2, 72.4, 71.7, 71.2, 71.1, 71.0, 69.8, 67.9, 58.7, 56.8, 55.0, 54.8, 54.0, 49.7, 43.1, 36.1, 24.4, 20.1 ppm.

ESI-MS for C ₄₄ H ₅₄ N ₅ O ₉ S ⁺ [MH ⁺]:	calcd.	828.3637
	found	828.3630.

IR (ATR): $\tilde{\nu}/\text{cm}^{-1}$ = 3320, 3281, 3194, 3120, 3058, 2931, 2874, 2837, 2805, 1745, 1661, 1594, 1582, 1531, 1511, 1499, 1470, 1446, 1405, 1368, 1299, 1243, 1178, 1148, 1106, 1089, 1059, 1029, 942, 922, 845, 763, 735, 715, 687, 663.

UV-Vis (DMSO): $\lambda_{\text{max}} = 371$ nm.

Synthesis of Azo-diltiazem 11 (740)



To a solution of mono desmethyl diltiazem (**698**, 356 mg, 0.89 mmol, 1.0 eq.) in dry THF (6 mL), butanamide **738** (800 mg, 1.33 mmol, 1.5 eq.) and K₂CO₃ (184 mg, 1.33 mmol, 1.5 eq.) were added. The resulting suspension was stirred at room temperature for two days, subsequently filtered, and concentrated *in vacuo*. Purification *via* repeated flash column chromatography (silica, MeOH:EtOAc = 0:1 to 1:9) yielded diltiazem derivative **740** (478 mg, 0.58 mmol, 61%) as an orange, foamy solid.

Note: Early fractions collected at the column chromatographic steps contained little amounts of the respective deacetylated compound and were discarded.

$R_f = 0.25$ (MeOH:EtOAc = 1:19).

^1H NMR (C_6D_6 , 600 MHz): δ = 9.00 (s, br, 1H), 8.04 (d, J = 8.6 Hz, 2H), 8.00 (d, J = 8.7 Hz, 2H), 7.93 (d, J = 8.5 Hz, 2H), 7.50 (d, J = 8.4 Hz, 2H), 7.47 (d, J = 7.7 Hz, 2H), 7.02–6.92 (m, 2H), 6.80–6.71 (m, 4H), 4.93 (d, J = 7.4 Hz, 1H), 4.63 (d, J = 7.4 Hz, 1H), 3.94 (dt, J = 14.2, 7.2 Hz, 1H), 3.66 (t, J = 5.0 Hz, 3H), 3.46 (t, J = 5.0 Hz, 2H), 3.43–3.36 (m, 10H), 3.29 (dd, J = 5.8, 4.3 Hz, 2H), 3.18 (s, 3H), 3.06 (s, 3H), 2.58 (dt, J = 13.6, 7.1 Hz, 1H), 2.54–2.46 (m, 1H), 2.35 (ddd, J = 14.1, 8.6, 6.1 Hz, 1H), 2.28 (ddd, J = 12.8, 7.5, 5.0 Hz, 1H), 2.18 (ddd, J = 12.4, 7.8, 4.7 Hz, 1H), 2.05 (dt, J = 12.0, 5.6 Hz, 1H), 1.90 (s, 3H), 1.88–1.82 (m, 1H), 1.79–1.70 (m, 1H), 1.42 (s, 3H) ppm.

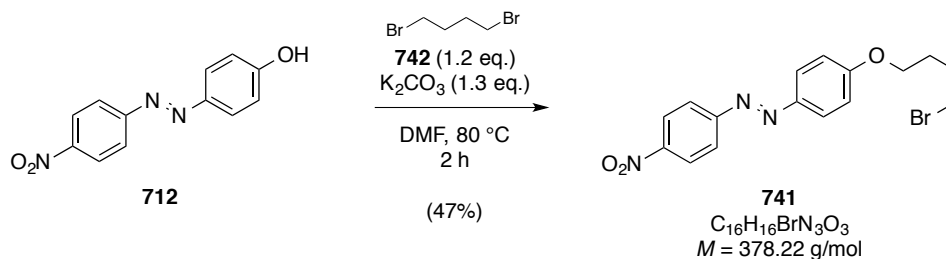
^{13}C NMR (C_6D_6 , 150 MHz): δ = 171.5, 169.3, 167.4, 161.1, 160.3, 148.7, 147.4, 145.9, 142.0, 135.1, 131.0, 130.6, 128.5, 128.1, 127.0, 126.5, 124.6, 124.5, 123.7, 122.8, 119.3, 114.7, 113.8, 72.0, 71.3, 70.8, 70.7, 70.5, 69.4, 67.4, 58.3, 56.3, 54.6, 54.4, 53.6, 49.3, 42.7, 35.7, 23.9, 19.7 ppm.

ESI-MS for $\text{C}_{46}\text{H}_{58}\text{N}_5\text{O}_{10}\text{S}^+ [\text{MH}^+]$: calcd. 872.3900
found 872.3888.

IR (ATR): $\tilde{\nu}/\text{cm}^{-1}$ = 3318, 3194, 3120, 3058, 2936, 2873, 2813, 1744, 1674, 1661, 1594, 1582, 1532, 1511, 1499, 1470, 1446, 1405, 1368, 1299, 1244, 1178, 1147, 1105, 1089, 1059, 1029, 943, 922, 845, 763, 735, 715, 686, 662.

UV-Vis (DMSO): λ_{max} = 371 nm.

Synthesis of Bromide **741**



To a solution of phenol **712** (500 mg, 2.06 mmol, 1.0 eq.) in dry DMF (8 mL), K_2CO_3 (369 mg, 2.67 mmol, 1.3 eq.) and dibromide **742** (0.30 mL, 2.47 mmol, 1.2 eq.) were added. The resulting suspension was heated to 80 °C for 2 hours until the conversion was complete, as judged *via* TLC analysis. Then, the reaction mixture was cooled to room temperature and

diluted with EtOAc (100 mL), as well as half-saturated aqueous NaCl solution (40 mL). The layers were separated and the aqueous phase was extracted with EtOAc (3×30 mL). Subsequently, the combined organic layers were dried over Na_2SO_4 and concentrated *in vacuo*. The crude product was purified *via* flash column chromatography (silica, *i*-Hex:EtOAc = 9:1). Thus, bromide **741** (369 mg, 0.98 mmol, 47%) was obtained as an orange solid.

$R_f = 0.95$ (*i*-Hex:EtOAc = 3:2).

^1H NMR (CDCl_3 , 400 MHz): $\delta = 8.27$ (m_C , 2H), 7.93–7.82 (m, 4H), 6.93 (m_C , 2H), 4.02 (t, $J = 6.0$ Hz, 2H), 3.41 (t, $J = 6.5$ Hz, 2H), 2.06–1.96 (m, 2H), 1.96–1.87 (m, 2H) ppm.

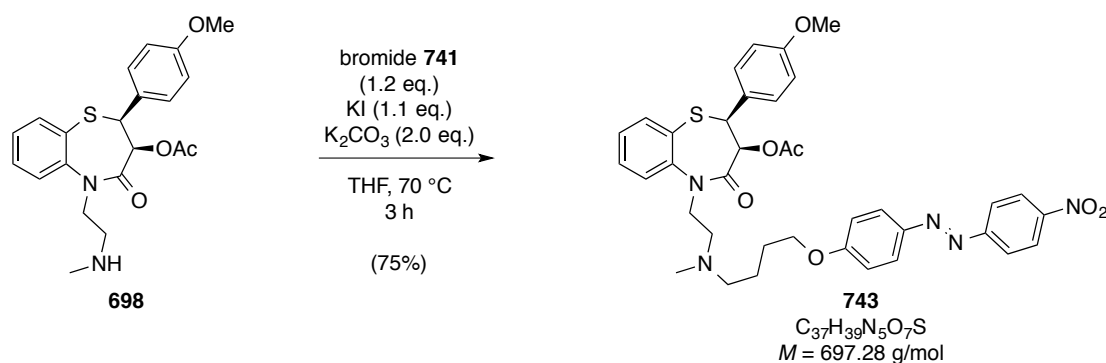
^{13}C NMR (CDCl_3 , 100 MHz): $\delta = 162.7$, 156.2, 148.4, 147.1, 125.8, 124.9, 123.3, 115.0, 67.5, 33.4, 29.5, 27.9 ppm.

EI-MS for $\text{C}_{16}\text{H}_{16}\text{BrN}_3\text{O}_3^+ [\text{M}^+]$:
calcd. 377.0375
found 377.0369.

IR (ATR): $\tilde{\nu}/\text{cm}^{-1} = 3109$, 2949, 1601, 1578, 1521, 1499, 1469, 1452, 1417, 1402, 1368, 1343, 1322, 1292, 1270, 1248, 1203, 1133, 1106, 1060, 1030, 1003, 953, 920, 861, 840, 806, 771, 754, 734, 723, 684.

UV-Vis (DMSO): $\lambda_{\text{max}} = 380$ nm.

Synthesis of Diltiazem Derivative **743**



To a stirred solution of mono desmethyl diltiazem (**698**, 200 mg, 0.50 mmol, 1.0 eq.) in dry THF (4 mL), K_2CO_3 (138 mg, 1.00 mmol, 2.0 eq.), KI (91 mg, 0.55 mmol, 1.1 eq.) and

bromide **741** (227 mg, 0.60 mmol, 1.2 eq.) were added. The resulting suspension was heated to 70 °C for 3 hours and then cooled to room temperature. Subsequently, water (10 mL) and CH₂Cl₂ (25 mL) were added and the layers were separated. The aqueous phase was extracted with CH₂Cl₂ (2 × 25 mL) and the combined organic layers were dried over Na₂SO₄. After having concentrated the solvents *in vacuo*, the crude product was purified by flash column chromatography (silica, *i*-Hex:EtOAc = 1:1 to 0:1) to yield diltiazem derivative **743** (260 mg, 0.37 mmol, 75%) as an orange foam.

R_f = 0.43 (EtOAc).

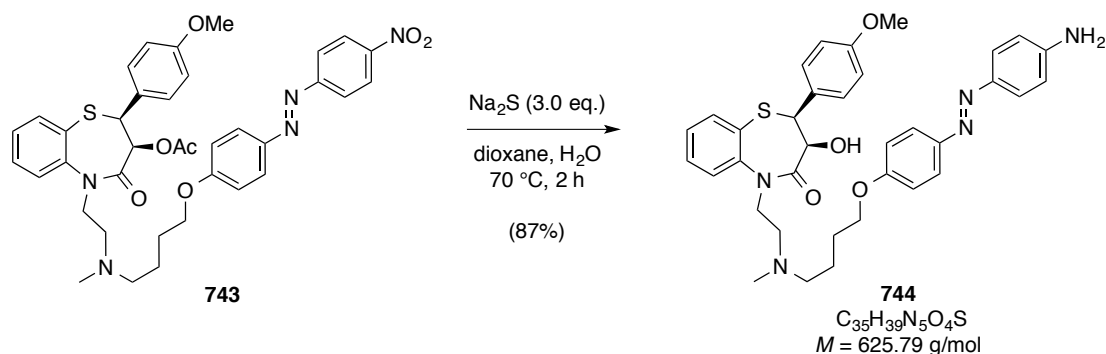
¹H NMR (CDCl₃, 600 MHz): δ = 8.26 (m_C, 2H), 7.90–7.83 (m, 4H), 7.60–7.59 (m, 1H), 7.42–7.35 (m, 2H), 7.35–7.30 (m, 2H), 7.18–7.13 (m, 1H), 6.90 (m_C, 2H), 6.79 (m_C, 2H), 5.06 (d, *J* = 7.5 Hz, 1H), 4.91 (d, *J* = 7.6 Hz, 1H), 4.34–4.27 (m, 1H), 3.94 (t, *J* = 6.5 Hz, 2H), 3.70 (s, 3H), 3.69–3.64 (m, 1H), 2.77–2.70 (m, 1H), 2.49 (s, br, 1H), 2.37 (t, *J* = 7.1 Hz, 2H), 2.18 (s, 3H), 1.80 (s, 3H), 1.73–1.64 (m, 2H), 1.56–1.49 (t, *J* = 9.6 Hz, 2H) ppm.

¹³C NMR (CDCl₃, 150 MHz): δ = 170.0, 167.0, 163.0, 159.9, 156.2, 148.3, 146.9, 145.8, 135.5, 131.5, 131.1, 130.9, 128.7, 127.5, 126.8, 125.7, 124.8, 123.2, 115.1, 113.9, 113.8, 71.3, 68.4, 57.6, 55.4, 54.6, 48.2, 42.3, 27.1, 24.0, 20.7 ppm.

ESI-MS for C₃₇H₄₀N₅O₇S⁺ [MH⁺]: calcd. 698.2643
 found 698.2637.

IR (ATR): $\tilde{\nu}/\text{cm}^{-1}$ = 3278, 3265, 2950, 2934, 2840, 2812, 1732, 1690, 1685, 1623, 1552, 1500, 1470, 1458, 1443, 1401, 1325, 1270, 1257, 1211, 1186, 1174, 1122, 1100, 1087, 1032, 1026, 987, 944, 872, 843, 818, 774, 723, 654.

UV-Vis (DMSO): λ_{max} = 378 nm.

Synthesis of Diltiazem Derivative **744**

Nitro compound **743** (163 mg, 0.23 mmol, 1.0 eq.) was dissolved in 1,4-dioxane (4.0 mL). To this, water (0.4 mL) and Na_2S (55.0 mg, 0.70 mmol, 3.0 eq.) were added. The resulting suspension was heated to $80\text{ }^\circ\text{C}$ for one hour and the conversion was then judged to be complete *via* TLC analysis. Subsequently, the reaction mixture was poured into saturated aqueous NaHCO_3 solution (20 mL) and extracted with CH_2Cl_2 ($3 \times 25\text{ mL}$). The combined organic layers were dried over Na_2SO_4 and concentrated *in vacuo*. Purification *via* flash column chromatography (silica, *i*-Hex:EtOAc = 1:9 to 0:1) provided diltiazem derivative **744** (127 mg, 0.20 mmol, 87%) as an orange foam.

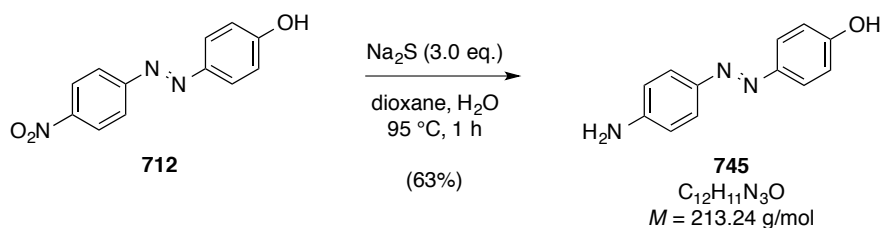
$R_f = 0.40$ (EtOAc).

^1H NMR (CDCl_3 , 400 MHz): $\delta = 7.74$ (m_C, 2H), 7.68 (m_C, 2H), 7.59 (dd, $J = 7.7, 1.5\text{ Hz}$, 1H), 7.38–7.27 (m, 4H), 7.18–7.11 (m, 1H), 6.88–6.76 (m, 4H), 6.62 (m_C, 2H), 4.81 (d, $J = 7.2\text{ Hz}$, 1H), 4.37 (ddd, $J = 14.1, 8.1, 6.4\text{ Hz}$, 1H), 4.21 (d, $J = 7.2\text{ Hz}$, 1H), 3.02 (s, br, 1H), 3.88 (t, $J = 6.4\text{ Hz}$, 4H), 3.69 (s, 3H), 3.67–3.61 (m, 1H), 2.80 (s, br, 1H), 2.72 (dt, $J = 14.1, 7.0\text{ Hz}$, 2H), 2.51 (ddd, $J = 13.0, 8.0, 5.3\text{ Hz}$, 1H), 2.34 (t, $J = 7.3\text{ Hz}$, 2H), 2.18 (s, 3H), 1.64 (quin, $J = 6.8\text{ Hz}$, 2H), 1.55–1.44 (m, 2H) ppm.

^{13}C NMR (CDCl_3 , 100 MHz): $\delta = 171.4, 160.7, 159.9, 149.2, 147.1, 145.6, 145.1, 135.4, 131.4, 130.6, 128.9, 127.5, 126.3, 124.7, 124.5, 124.1, 114.7, 114.7, 113.7, 69.3, 68.1, 57.6, 56.7, 55.3, 53.5, 47.7, 42.2, 27.0, 23.9\text{ ppm}$.

ESI-MS for $\text{C}_{35}\text{H}_{40}\text{N}_5\text{O}_4\text{S}^+ [\text{MH}^+]$:
 calcd. 626.2796
 found 626.2794.

Synthesis of Aniline **745**



Phenol **712** (2.70 g, 1.11 mmol, 1.0 eq.) was dissolved in 1,4-dioxane (100 mL). To this, water (10 mL) and Na_2S (2.60 g, 33.3 mmol, 3.0 eq.) were added. The resulting suspension was heated to reflux at 95 °C for one hour and the conversion was then judged to be complete *via* TLC analysis. Subsequently, the reaction mixture was poured into saturated aqueous NaHCO_3 solution (100 mL) and extracted with CH_2Cl_2 ($3 \times 150 \text{ mL}$). The combined organic layers were dried over Na_2SO_4 and concentrated *in vacuo*. Purification *via* flash column chromatography (silica, *i*-Hex:EtOAc = 6:4) provided aniline **745** (1.50 g, 7.03 mmol, 63%) as an orange solid.

$R_f = 0.66$ (*i*-Hex:EtOAc = 1:1).

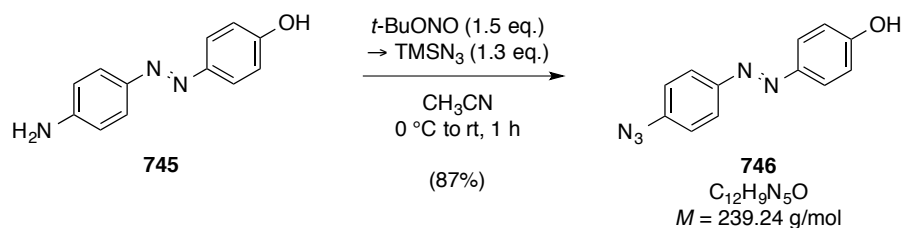
^1H NMR (DMSO- d_6 , 400 MHz): δ = 9.94 (s, 1H), 7.66–7.61 (m, 2H), 7.61–7.55 (m, 2H), 6.93–6.81 (m, 2H), 6.72–6.58 (m, 2H), 5.88 (s, br, 2H) ppm.

^{13}C NMR (DMSO- d_6 , 100 MHz): δ = 159.1, 151.8, 145.2, 142.8, 124.4, 123.6, 115.7, 113.4 ppm.

ESI-MS for $\text{C}_{12}\text{H}_{12}\text{N}_3\text{O}^+$ [MH^+]:
 calcd. 214.0975
 found 214.0974.

IR (ATR): $\tilde{\nu}/\text{cm}^{-1}$ = 3359, 3286, 3004, 2672, 1589, 1493, 1470, 1448, 1385, 1238, 1150, 1143, 1099, 1095, 1088, 1007, 948, 883, 836, 804, 762, 728, 710.

UV-Vis (DMSO): $\lambda_{\text{max}} = 403 \text{ nm}$.

Synthesis of Azide **746**

A stirred suspension of aniline **745** (1.40 g, 6.57 mmol, 1.0 eq.) in dry CH₃CN (28 mL) was cooled to 0 °C. Then, *t*-BuONO (1.02 g, 9.85 mmol, 1.50 eq.) was added slowly and the mixture was stirred for 10 min. To the resulting red solution, TMSN₃ (1.13 mL, 8.54 mmol, 1.3 eq.) was added dropwise over a period of 15 min. Subsequently, the reaction was allowed to warm to room temperature, stirred for one hour and concentrated under reduced pressure. The crude product was purified *via* flash column chromatography (silica, *i*-Hex:EtOAc = 17:3 to 4:1). Thus, azide **746** (1.37 g, 5.72 mmol, 87%) was obtained as a red solid.

$R_f = 0.78$ (*i*-Hex:EtOAc = 2:3).

¹H NMR (CDCl₃, 400 MHz): δ = 7.85–7.73 (m, 4H), 7.09–7.00 (m, 2H), 6.93–6.79 (m, 2H), 5.04 (s, br, 1H) ppm.

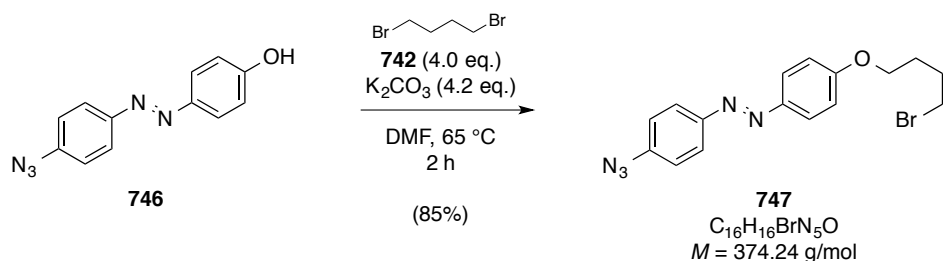
¹³C NMR (CDCl₃, 100 MHz): δ = 158.3, 150.0, 147.3, 142.2, 125.1, 124.4, 119.7, 116.0 ppm.

ESI-MS for C₁₂H₈N₅O⁺ [MH⁺]:
calcd. 238.0734
found 238.0734.

IR (ATR): $\tilde{\nu}/\text{cm}^{-1}$ = 3174, 2403, 2252, 2115, 1587, 1579, 1471, 1442, 1413, 1386, 1299, 1286, 1223, 1152, 1143, 1129, 1107, 1005, 944, 839, 813, 808, 773, 726, 709, 670.

UV-Vis (DMSO): $\lambda_{\text{max}} = 371$ nm.

Synthesis of Bromide 747



To a solution of azide **746** (800 mg, 3.34 mmol, 1.0 eq.) in dry DMF (15 mL), K₂CO₃ (1.94 g, 14.0 mmol, 4.2 eq.) and dibromide **742** (1.60 mL, 13.4 mmol, 4.0 eq.) were added. The resulting suspension was heated to 65 °C for 2 hours until the conversion was complete, as judged *via* TLC analysis. Then, the reaction mixture was cooled to room temperature and diluted with EtOAc (200 mL) and half-saturated aqueous NaCl solution (50 mL). The layers were separated and the aqueous phase was extracted with EtOAc (3 × 50 mL). Subsequently, the combined organic layers were dried over Na₂SO₄ and concentrated *in vacuo*. The crude product was purified *via* flash column chromatography (silica, *i*-Hex:EtOAc = 23:2 to 9:1). Thus, bromide **747** (1.10 g, 2.82 mmol, 85%) was obtained as an orange solid.

$$R_f = 0.90 \text{ (} i\text{-Hex:EtOAc} = 3:1\text{)}.$$

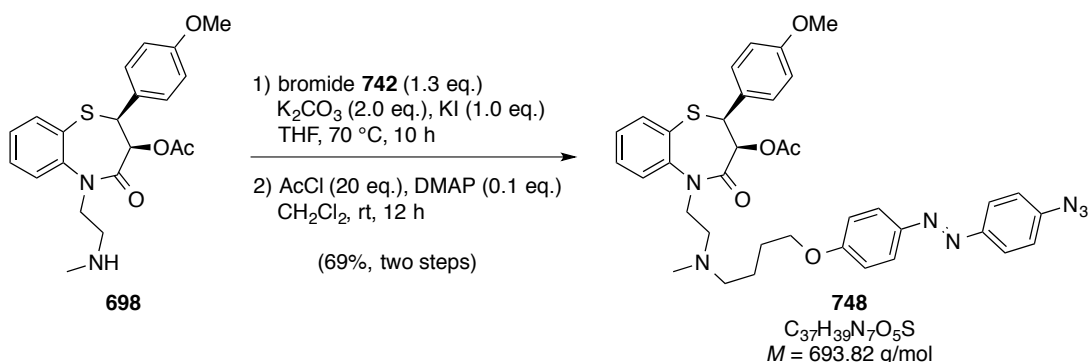
¹H NMR (CDCl₃, 400 MHz): δ = 7.83–7.76 (m, 4H), 7.07–7.01 (m, 2H), 6.94–6.86 (m, 2H), 3.99 (t, *J* = 6.0 Hz, 2H), 3.41 (t, *J* = 6.5 Hz, 2H), 2.06–1.95 (m, 2H), 1.93–1.86 (m, 2H) ppm.

¹³C NMR (CDCl₃, 100 MHz): δ = 161.5, 150.0, 147.0, 142.0, 124.9, 124.4, 119.7, 114.8, 67.3, 33.5, 29.5, 27.9 ppm.

EI-MS for C ₁₆ H ₁₇ BrN ₅ O ⁺ [M ⁺]:	calcd.	374.0611
	found	374.0609.

IR (ATR): $\tilde{\nu}/\text{cm}^{-1}$ = 2944, 2873, 2402, 2116, 1599, 1592, 1582, 1575, 1500, 1491, 1473, 1462, 1444, 1434, 1422, 1418, 1393, 1348, 1312, 1300, 1287, 1278, 1241, 1209, 1170, 1152, 1143, 1125, 1106, 1043, 1027, 1009, 966, 944, 844, 824, 830, 810, 779, 744, 737, 731, 679.

UV-Vis (DMSO): $\lambda_{\text{max}} = 369 \text{ nm}$.

Synthesis of Diltiazem Derivative **748**

To a stirred solution of mono desmethyl diltiazem (**698**, 412 mg, 1.03 mmol, 1.0 eq.) in dry THF (8 mL), K_2CO_3 (284 mg, 2.06 mmol, 2.0 eq.), KI (171 mg, 1.03 mmol, 1.0 eq.) and bromide **742** (500 mg, 1.34 mmol, 1.3 eq.) were added. The resulting suspension was heated to 70 °C for 10 hours and then cooled to room temperature. Subsequently, water (15 mL) and CH_2Cl_2 (30 mL) were added and the layers were separated. The aqueous phase was extracted with CH_2Cl_2 ($2 \times 30 \text{ mL}$) and the combined organic layers were dried over Na_2SO_4 . After having concentrated the solvents *in vacuo*, the crude product was purified by flash column chromatography (silica, *i*-Hex:EtOAc = 1:1 to 1:9) to yield diltiazem derivative **748** (507 mg, 0.73 mmol, 72%) as an orange foam, being contaminated by 30% of the respective deacetylated compound, as judged by 1H NMR.

Thus obtained partially deacetylated substance **748** was redissolved in dry CH_2Cl_2 (7 mL) and cooled to 0 °C. Under stirring, acetyl chloride (1.04 mL, 8.05 mmol, 20 eq.) and DMAP (9.0 mg, 0.07 mmol, 0.1 eq.) were added. The resulting solution was allowed to warm to room temperature and stirred for 12 hours, before being quenched by the addition of saturated aqueous $NaHCO_3$ (30 mL). Subsequently, the mixture was extracted with EtOAc ($3 \times 30 \text{ mL}$), the combined organic layers were dried over Na_2SO_4 and the solvents were removed under reduced pressure. Purification *via* flash column chromatography (silica, *i*-Hex:EtOAc = 1:9 to 0:1) yielded diltiazem derivative **748** (493 mg, 0.71 mmol, 69%) as an orange foam.

$R_f = 0.52$ (MeOH:EtOAc = 1:49).

1H NMR ($CDCl_3$, 400 MHz): $\delta = 8.00$ (m_C, 2H), 7.92 (m_C, 2H), 7.64 (m_C, 2H), 7.58 (dd, $J = 7.7, 1.6 \text{ Hz}$, 1H), 7.27 (dd, $J = 8.0, 1.3 \text{ Hz}$, 1H), 7.04 (td, $J = 7.7, 1.6 \text{ Hz}$, 1H), 6.89–6.79 (m, 5H), 6.76–6.70 (m, 2H), 5.15 (d, $J = 7.6 \text{ Hz}$, 1H), 4.77 (d, $J = 7.6 \text{ Hz}$, 1H), 4.34 (dt, $J = 13.7, 6.9 \text{ Hz}$, 1H), 3.75 (ddd, $J = 13.8, 7.0, 5.4 \text{ Hz}$, 1H), 3.58 (t, $J = 6.6 \text{ Hz}$, 2H), 3.24 (s,

3H), 2.88 (dt, $J = 13.3, 6.8$ Hz, 1H), 2.61 (ddd, $J = 12.7, 7.2, 5.4$ Hz, 1H), 2.23 (t, $J = 7.0$ Hz, 2H), 2.08 (s, 3H), 1.60–1.52 (m, 2H), 1.50 (s, 3H), 1.48–1.37 (m, 2H) ppm.

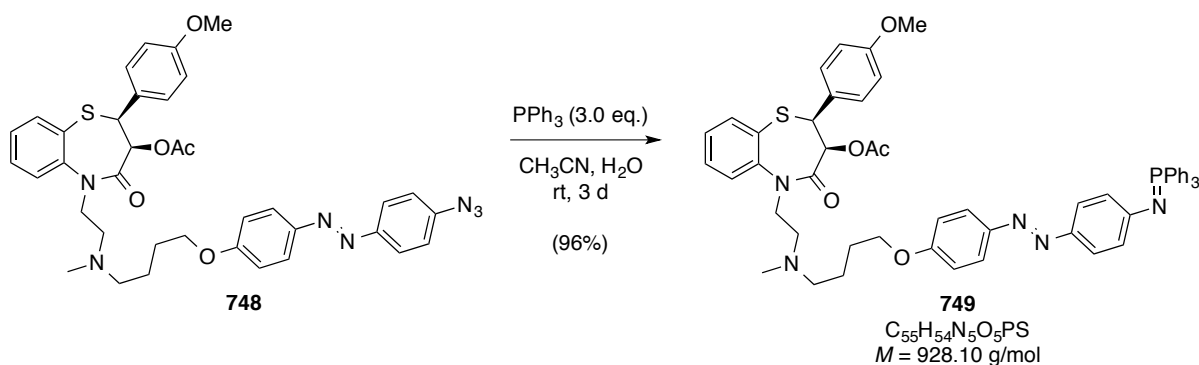
^{13}C NMR (CDCl_3 , 100 MHz): $\delta = 169.5, 167.3, 162.3, 160.4, 150.5, 147.5, 147.0, 142.2, 135.5, 131.6, 130.9, 129.1, 127.6, 126.9, 125.3, 125.0, 124.7, 119.8, 115.2, 114.2, 71.6, 68.3, 57.8, 56.2, 55.2, 54.7, 48.6, 42.1, 27.2, 24.2, 20.2$ ppm.

ESI-MS for $\text{C}_{37}\text{H}_{40}\text{N}_7\text{O}_5\text{S}^+ [\text{MH}^+]$: calcd. 694.2806
found 694.2804.

IR (ATR): $\tilde{\nu}/\text{cm}^{-1} = 2942, 2834, 2789, 2112, 1743, 1676, 1595, 1579, 1511, 1497, 1470, 1443, 1420, 1406, 1369, 1284, 1247, 1179, 1149, 1139, 1105, 1086, 1060, 1031, 943, 840, 817, 762, 762, 736, 711, 674$.

UV-Vis (DMSO): $\lambda_{\text{max}} = 369$ nm.

Synthesis of Phosphazene **749**



Diltiazem derivative **748** (0.08 g, 0.11 mmol, 1.0 eq.) was dissolved in a mixture of CH_3CN (3.2 mL) and water (0.3 mL). To this, triphenylphosphine (0.09 g, 3.46 mmol, 3.0 eq.) was added and the resulting solution was stirred at room temperature for 3 days. After removing the solvents *in vacuo*, the crude product was purified by flash column chromatography (silica, *i*-Hex:EtOAc = 1:0 to 0:1) to yield phosphazene **749** (103 mg, 0.11 mmol, 96%) as an orange foam.

Note: Phosphazene 749 and azide 748 behaved co-polar at TLC analysis. Due to overlapping signals in 2D NMR spectra, it was not possible to resolve the coupling constants of ^{31}P to ^{13}C nuclei. Hence, all observed signals are listed instead.

$R_f = 0.52$ (MeOH:EtOAc = 1:49).

^1H NMR (C_6D_6 , 400 MHz): $\delta = 8.21$ (m_C, 1H), 8.20–8.05 (m, 3H), 7.74 (m_C, 5H), 7.69–7.61 (m, 2H), 7.57 (ddd, $J = 7.7, 2.7, 1.6$ Hz, 1H), 7.30–7.23 (m, 2H), 7.12–6.93 (m, 9H), 6.89–6.76 (m, 5H), 6.30–6.23 (m, 1H), 5.14 (d, $J = 7.6$ Hz, 1H), 4.77 (d, $J = 7.6$ Hz, 1H), 4.34 (m_C, 1H), 3.82–3.68 (m, 1H), 3.59–3.55 (m, 2H), 3.23 (s, 3H), 2.97 (s, 1H), 2.87 (m_C, 1H), 2.61 (m_C, 1H), 2.20 (q, $J = 7.0$ Hz, 2H), 2.07 (s, 3H), 1.62–1.46 (m, 2H), 1.50 (s, 3H), 1.42 (ddd, $J = 15.1, 12.2, 6.7$ Hz, 2H) ppm.

^{13}C NMR (C_6D_6 , 100 MHz): $\delta = 169.5, 167.3, 161.3, 160.8, 160.4, 149.7, 148.3, 147.9, 147.0, 146.2, 146.0, 135.5, 134.9, 133.9, 132.9, 132.8, 132.5, 132.4, 131.9, 131.8, 131.8, 131.6, 131.6, 131.6, 130.9, 129.1, 129.0, 128.9, 128.7, 128.6, 128.5, 126.9, 125.2, 125.1, 124.7, 124.0, 123.9, 115.1, 115.0, 114.7, 114.1, 71.6, 68.1, 57.8, 56.2, 55.1, 54.7, 48.6, 42.1, 27.2, 24.3, 20.2$ ppm.

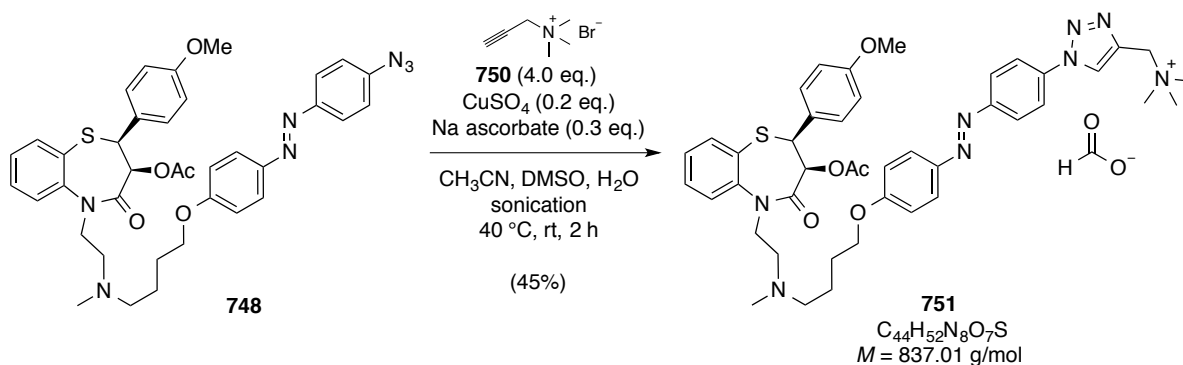
ESI-MS for $\text{C}_{55}\text{H}_{55}\text{N}_5\text{O}_5\text{PS}^+$ [MH^+]: calcd. 928.3656

found 928.3651.

IR (ATR): $\tilde{\nu}/\text{cm}^{-1} = 3452, 3346, 3218, 3051, 2941, 2837, 2785, 1743, 1673, 1595, 1583, 1551, 1510, 1492, 1436, 1404, 1341, 1304, 1237, 1179, 1143, 1105, 1061, 1019, 997, 943, 919, 837, 755, 718, 693$.

UV-Vis (DMSO): $\lambda_{\text{max}} = 408$ nm.

Synthesis of Azo-diltiazem 12 (751)



Alkyne **750** (92.0 mg, 0.52 mmol, 4.0 eq.) and diltiazem derivative **748** (90 mg, 0.13 mmol, 1.0 eq.) were dissolved in DMSO (14 mL) under an argon gas atmosphere and the resulting

solution was thoroughly degassed. To this, a degassed solution of $\text{CuSO}_4 \cdot 5\text{H}_2\text{O}$ (6.5 mg, 0.02 mmol, 0.2 eq.) and sodium ascorbate (5.7 mg, 0.3 mmol, 0.3 eq.) in water (5.6 mL) and acetonitrile (8.5 mL) was added. This mixture was sonicated at 40 °C for 2 hours until analysis *via* LCMS measurement indicated complete consumption. Subsequently, the solvents were removed *in vacuo* and the crude product was purified by repeated flash column chromatography (C-18 reversed-phase silica, $\text{H}_2\text{O}:\text{MeOH}:\text{HCOOH} = 0:1:10^{-3}$ to $1:1:10^{-3}$) to yield the title compound (**751**, 48.9 mg, 0.06 mmol, 45%) as an orange wax.

Note: The obtained ^1H NMR values varied slightly and exhibited sometimes significant line broadening, due to the basicity of the amino function.

$R_f = 0.00$ (MeOH:EtOAc = 1:49).

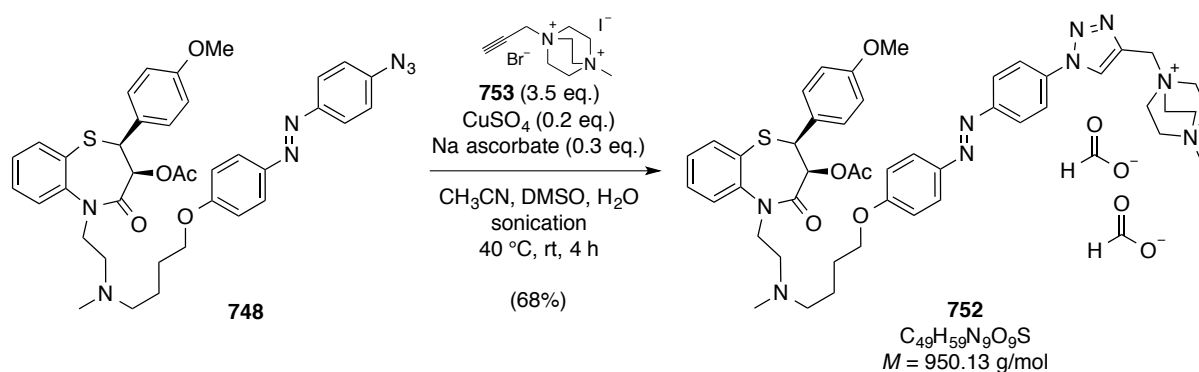
^1H NMR (CD_3OD , 400 MHz): $\delta = 9.04$ (s, 1H), 8.54 (s, br, 1H), 8.11–8.04 (m, 4H), 7.90 (d, $J = 8.4$ Hz, 2H), 7.74 (d, $J = 7.6$ Hz, 1H), 7.65–7.59 (m, 2H), 7.45–7.29 (m, 3H), 7.05 (d, $J = 8.5$ Hz, 2H), 6.87 (d, $J = 8.2$ Hz, 2H), 5.07 (s, 2H), 4.82 (s, br, 2H), 4.47 (m_c , 1H), 4.09 (s, 3H), 3.75 (s, 3H), 3.24 (s, 9H), 3.13–2.94 (m, 4H), 2.69 (s, 3H), 1.86 (s, 3H), 1.84 (s, br, 4H) ppm.

^{13}C NMR (CD_3OD , 100 MHz): $\delta = 171.3, 169.9, 169.6, 163.5, 161.3, 153.9, 148.1, 146.1, 138.9, 138.0, 136.6, 132.7, 132.0, 129.6, 129.4, 127.9, 127.6, 126.2, 125.8, 125.0, 122.3, 116.0, 114.6, 72.5, 68.9, 61.1, 57.5, 55.8, 55.5, 54.5, 53.5, 46.7, 41.6, 27.5, 23.2, 20.3$ ppm

ESI-MS for $\text{C}_{43}\text{H}_{51}\text{N}_8\text{O}_5\text{S}^+$ [M^+]: calcd. 791.3698
 found 791.3699.

IR (ATR): $\tilde{\nu}/\text{cm}^{-1} = 3402, 3047, 2951, 2781, 1740, 1670, 1653, 1597, 1581, 1559, 1540, 1508, 1472, 1460, 1444, 1406, 1372, 1303, 1224, 1180, 1140, 1109, 1049, 1021, 985, 897, 920, 844, 761, 732, 667$.

UV-Vis (H_2O): $\lambda_{\text{max}} = 357$ nm.

Synthesis of Azo-diltiazem **13** (**752**)

Alkyne **753** (47.0 mg, 0.13 mmol, 3.5 eq.) and diltiazem derivative **748** (25 mg, 0.04 mmol, 1.0 eq.) were dissolved in DMSO (3.5 mL) under an argon gas atmosphere and the resulting solution was thoroughly degassed. To this, a degassed solution of $\text{CuSO}_4 \cdot 5\text{H}_2\text{O}$ (1.8 mg, 0.01 mmol, 0.2 eq.) and sodium ascorbate (1.6 mg, 0.1 mmol, 0.3 eq.) in water (1.6 mL) and acetonitrile (2.4 mL) was added. This mixture was sonicated at $40\text{ }^\circ\text{C}$ for 4 hours until analysis *via* LCMS measurement indicated complete consumption. Subsequently, the solvents were removed *in vacuo* and the crude product was purified by repeated flash column chromatography (C-18 reversed-phase silica, $\text{H}_2\text{O}:\text{MeOH}:\text{HCOOH} = 0:1:10^{-3}$ to $9:11:10^{-3}$) to yield the title compound (**752**, 23.4 mg, 0.02 mmol, 68%) as an orange solid.

Note: The obtained ^1H NMR values varied slightly and exhibited sometimes significant line broadening, due to the basicity of the amino function.

$R_f = 0.00$ ($\text{MeOH}:\text{EtOAc} = 1:49$).

^1H NMR (CD_3OD , 400 MHz): $\delta = 9.12$ (s, br, 2H), 8.07 (t, $J = 6.4$ Hz, 4H), 7.97–7.85 (m, 2H), 7.79–7.71 (m, 1H), 7.70–7.54 (m, 2H), 7.47–7.40 (m, 2H), 7.39–7.29 (m, 1H), 7.12–7.00 (m, 2H), 6.97–6.78 (m, 3H), 5.19–5.04 (m, 4H), 4.43 (ddd, $J = 14.2, 8.6, 6.1$ Hz, 1H), 4.31–3.99 (m, 13H), 3.98–3.80 (m, 2H), 3.77 (s, 3H), 3.40 (s, 3H), 2.92 (ddd, $J = 13.6, 8.8, 6.1$ Hz, 1H), 2.66 (ddd, $J = 13.1, 8.5, 5.3$ Hz, 1H), 2.56 (t, $J = 7.5$ Hz, 2H), 2.34 (s, 3H), 1.87 (s, 3H), 1.82–1.75 (m, 2H), 1.71–1.63 (m, 2H) ppm.

^{13}C NMR (CD_3OD , 100 MHz): $\delta = 171.4, 170.1, 163.6, 161.4, 154.1, 148.2, 146.1, 138.9, 136.7, 136.2, 132.7, 132.0, 129.7, 129.5, 128.3, 127.9, 126.2, 125.8, 125.1, 122.4, 116.1, 114.7, 72.5, 68.8, 59.9, 57.5, 55.7, 55.5, 54.7, 54.4, 53.1, 52.5, 46.6, 41.4, 27.4, 23.0, 20.2$ ppm.

ESI-MS for $C_{47}H_{57}N_9O_5S^{2+}$ [M^{2+}]: calcd. 429.7
 found 429.7.

FAB-MS for $C_{47}H_{56}N_9O_5S^+$ [($M-H$) $^+$]: calcd. 858.4
 found 858.3.

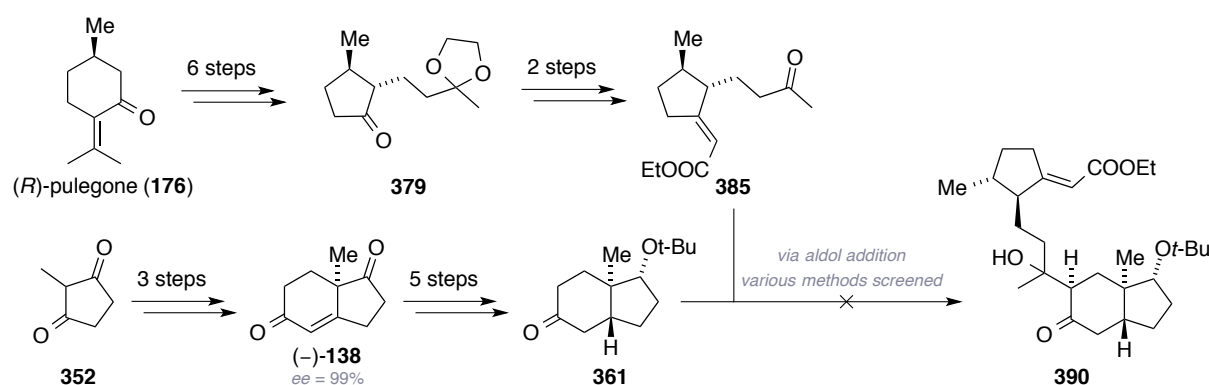
IR (ATR): $\tilde{\nu}/\text{cm}^{-1}$ = 3373, 3029, 2930, 2972, 2698, 1741, 1675, 1580, 1510, 1471, 1445, 1408, 1373, 1344, 1304, 1248, 1180, 1139, 1128, 1108, 1088, 1058, 1027, 990, 942, 848, 759, 730, 704, 663.

UV-Vis (H_2O): λ_{max} = 360 nm.

APPENDIX

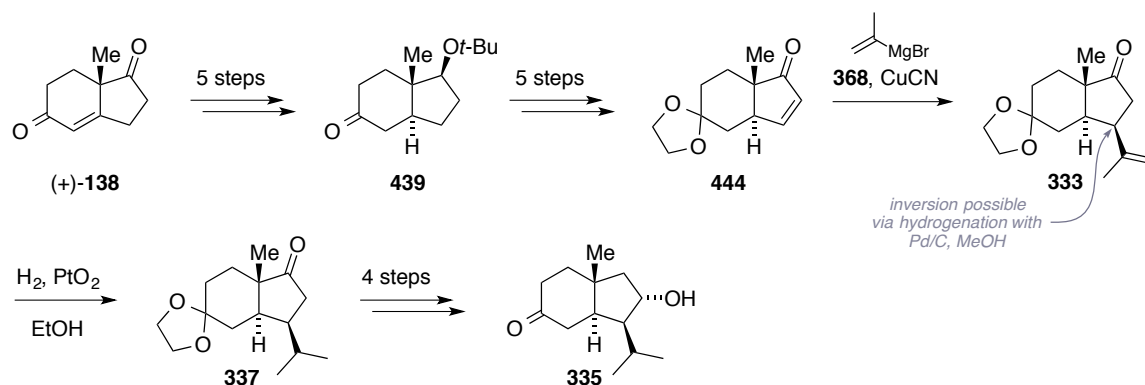
I. Summary

The first part of present doctoral thesis has detailed the synthetic efforts conducted toward the enantioselective construction of the biosynthetically closely related *iso*-propyl-substituted *trans*-hydrindane sesterterpenoids nitidasin (**238**), astellatol (**213**), retigeranic acid B (**237**) and alborosin (**252**). Developed retrosynthetic approaches relied on the previously established unified approach toward this class of natural products, which focused on *trans*-hydrindane-based building blocks.^[140,156] Owing to an inspiring and fruitful collaboration with Dr. D. T. Hog, our combined efforts eventually culminated in the first total synthesis of nitidasin (**238**).



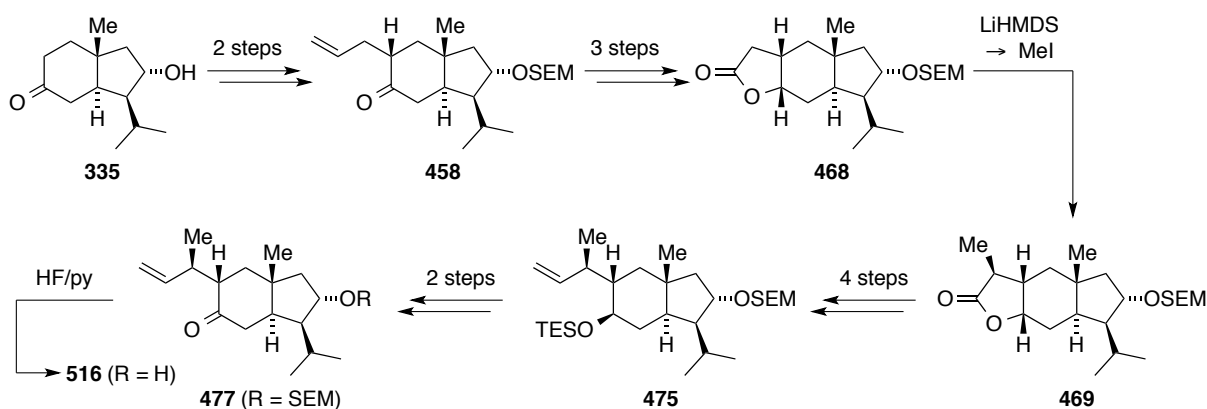
Scheme A.1: Conducted studies toward the construction of retigeranic acid B (**237**), using model system **361** and the newly accessed cyclopentane building block **385**.

The experimental research carried out toward a potential total synthesis of retigeranic acid B (**237**) was reported first. To this end, a retrosynthetic proposal was presented, which involved a convergent key fragment coupling by means of ketone-ketone aldol addition. The envisaged cyclopentane building block **385** was synthesized in a novel 8-step sequence in 20% overall yield (*cf.* chapter 2.4), starting from commercially available chiral (*R*)-pulegone (**176**). The developed route featured a vinylogous addition to methyl vinyl ketone (**300**), a regioselective dioxolane formation and a substrate-controlled diastereoselective Krapcho decarboxylation (scheme A.1) forming intermediate **379**. An ensuing Horner-Wadsworth-Emmons olefination and a final dioxolane cleavage completed the desired electrophile for the intended aldol addition. Unfortunately, all our attempts to affect the envisaged fragment coupling were met with failure (*cf.* chapter 2.5). Besides, it was possible to shed light on the reactivity of utilized *trans*-hydrindanone model system **361** at enolate-based addition reactions. Accordingly, it was demonstrated that more electrophilic reagents, like Mander's reagent (**394**) and ethylpyruvate (**392**), readily undergo nucleophilic attack by employed preformed enolate species.



Scheme A.2: Conducted synthetic route toward enantiopure alcohol **335**, according to Hog *et al.*^[140]

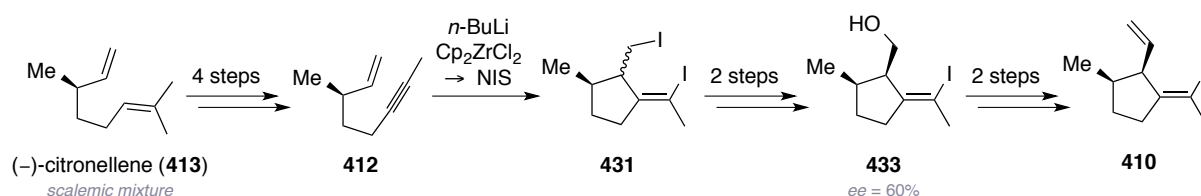
For the total synthesis of nitidasin (**238**), initially enantiopure alcohol **335** was prepared on multi-gram scale. To this end, a previously developed, reliable and high-yielding 10-step sequence was followed (scheme A.2). Required *trans*-hydrindanone **439** was accessed *via* the frequently used and conveniently scalable carboxylation/hydrogenation route, which ultimately starts by the preparation of (+)-Hajos-Parrish-Sauer-Eder-Wiechert ketone (**138**). In collaboration with the research group of K. Houk, we are currently working on a mechanistic explanation for the experimentally found stereochemical outcome of the cuprate-mediated formation of alkene **333** and its catalyst-promoted hydrogenative diversification, using computational methods.



Scheme A.3: Developed 12-step procedure toward *trans*-hydrindanone **477**, achieving the construction of stereocenters C-2, C-3 and required functional handles for the envisaged fragment combination.

Based on earlier experiments,^[156] the functional handles for a convergent construction of the central 8-membered ring motif of nitidasin (**238**) were installed (scheme A.3). The major portion of those investigations was conducted simultaneously to the reported synthetic studies toward astellatol (**213**), which is why intermediates being *en route* to both natural products took center stage. As a protective group for the C-17 (nitidasin numbering) centered alcohol function, a robust SEM ether was installed that proved compatible with all envisaged

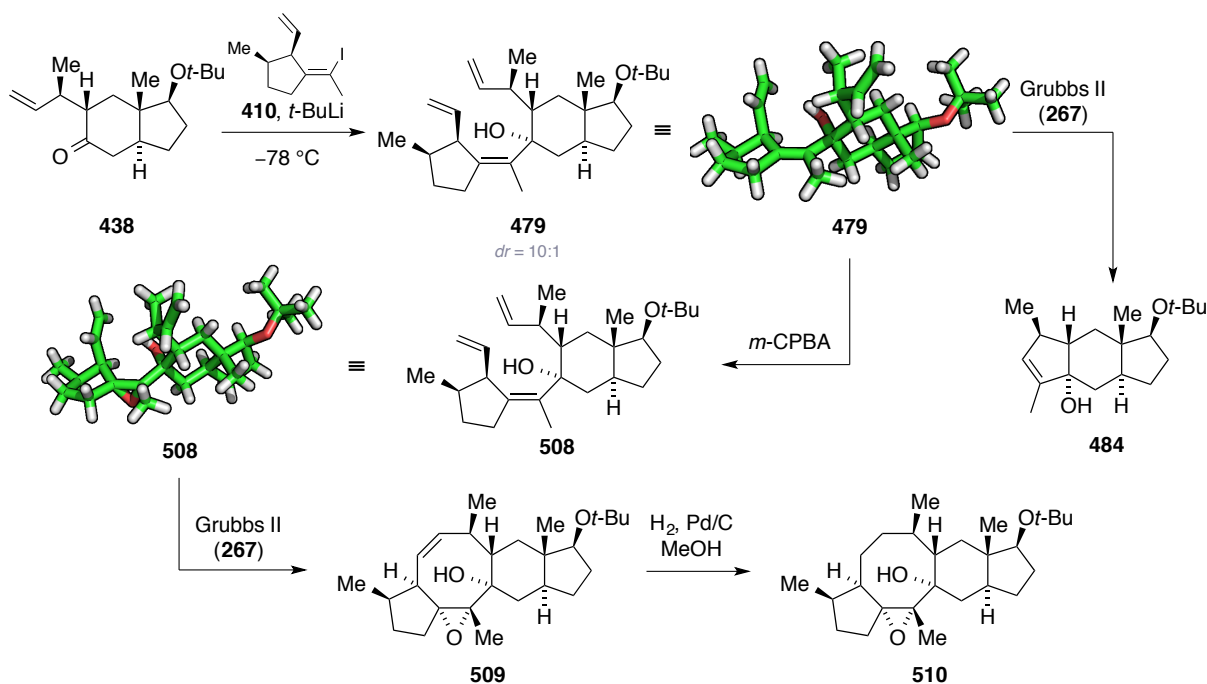
transformations. Starting from the SEM ether of alcohol **335**, the C-2 located stereocenter was set *via* a Pd-catalyzed Tsuji allylation (*cf.* chapter 3.4). The formation of the stereogenic methyl group at C-3 took advantage of the conformational bias of tricyclic system **468**. The restoration of the terminal alkene function at C-3 involved a reduction of substance **469**, a TES protection of the resulting alcohol functions, a chemoselective deprotective Swern oxidation and a final Wittig olefination. Orthogonal desilylation of **475** and DMP-mediated oxidation then gave rise to envisioned *trans*-hydrindanone **477**. Notably, conducted 12-step sequence allowed for the scalable preparation of this highly advanced intermediate in outstanding 41% yield, starting from alcohol **335**. As the majority of those transformations had been established on model system **438** previously, this more readily accessible compound was utilized for our initial screening phase of ensuing key fragment combination and RCM reaction (*vide infra*).



Scheme A.4: 9-step sequence toward building block **410**, featuring a zirconocene-mediated enyne cyclization.

Furthermore, the synthesis of vinyl cyclopentane **410** (scheme A.4) was established (*cf.* chapter 3.3). This compound possesses a literature unprecedented *cis-cis-cis* relationship in respect to its vinyl iodide function and adjacent ring substituents. Starting from inexpensive, but scalemic (–)-citronellene (**413**), building block **410** was prepared in gram quantities by a 9-step sequence that featured a zirconocene-mediated enyne cyclization. Treatment of intermediary generated zirconacycle furnished diiodide **431**, which could then be converted to alcohol **433** *via* elimination and subsequent substrate-controlled hydroboration. Mosher ester analysis of this compound allowed quantifying its enantiomeric excess to 60%. A final Swern oxidation/Wittig olefination protocol gave rise to stable diene **410** as a single diastereomer.

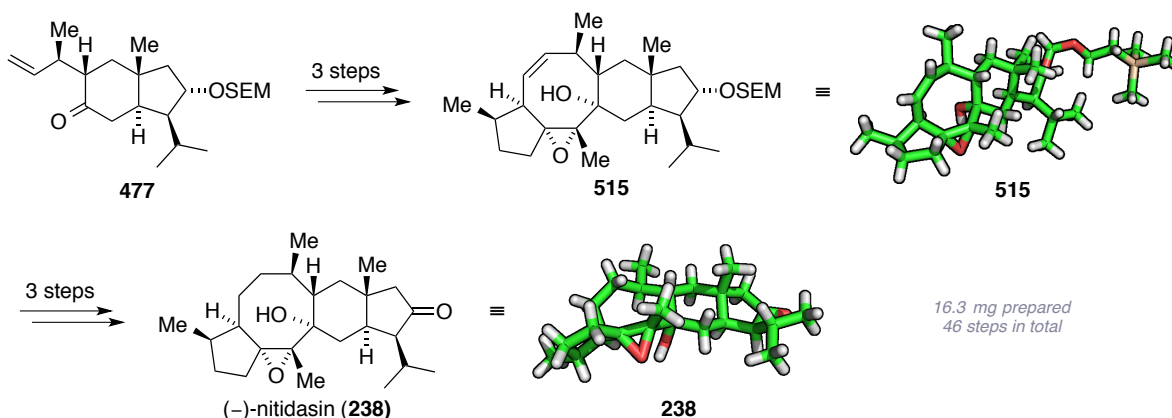
Model studies toward the completion of nitidasin's (**238**) carbocyclic backbone were reported in chapter 3.5. In this context, a literature unprecedented and highly diastereoselective addition of a tetrasubstituted Li-alkenyl species to a sterically congested *trans*-hydrindanone system (**438**, scheme A.5) could be demonstrated. A key feature of this remarkable transformation was the unexpected kinetic resolution of scalemic vinyl cyclopentane **410**, which fortunately proceeded in favour of the desired enantiomer. The following elaborate studies on RCM-based approaches toward closing of nitidasin's (**238**) central 8-membered



Scheme A.5: Successful construction of the 5-8-6-5 ring system of nitidasin (**238**) on a model system. Key features are the diastereoselective Li-alkenyl addition and the highly efficient RCM reaction.

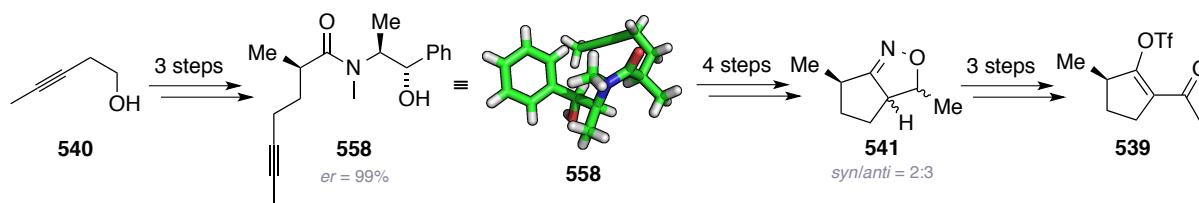
ring were hampered due to a predominant side reaction of triene **479**. The undesired formation of cyclopentene **484**, at which participation of the tetrasubstituted double bond is presumably induced by adjacent tertiary alcohol, could only be circumvented when planned epoxidation step was brought forward. Taking advantage of the system's stereochemical and electronic properties, nitidasin's (**238**) epoxide function could be installed in a chemo- and diastereoselective manner. Ensuing key RCM reaction furnished nitidasin's (**238**) completed carbon skeleton (**509**) in remarkably high yield, being assisted by the beneficial conformational preorganization of epoxide **508**.

Thus, the stage was set for the completion of nitidasin (**238**) (*cf.* chapter 3.6). The successful transfer of developed 3-step protocol allowed for the preparation of tetracycle **515** and the



Scheme A.6: Completion of the first total synthesis of the natural occurring sesterterpenoid nitidasin (**238**).

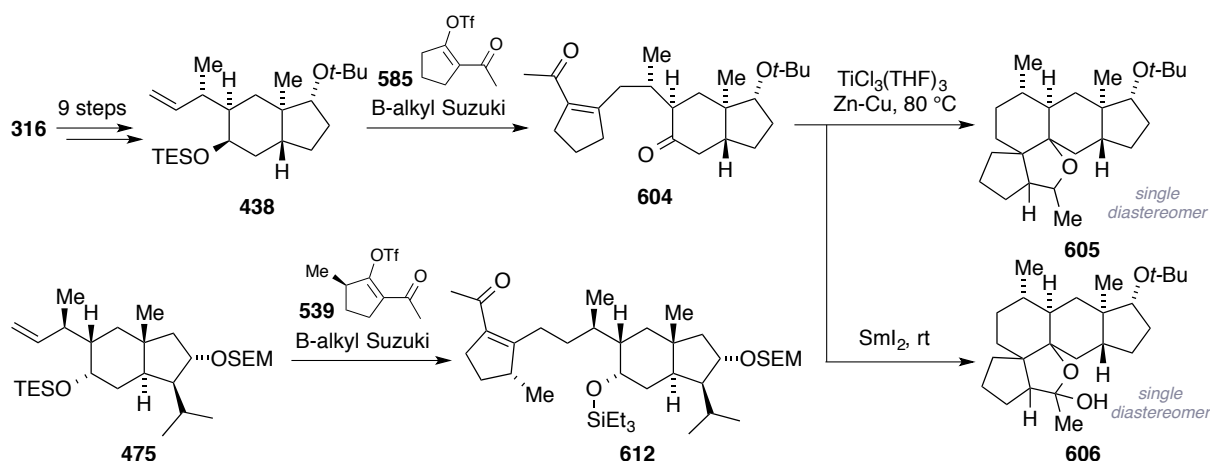
proper construction of all stereocenters could be verified by means of X-ray crystallographic analysis (scheme A.6). Extended screening provided conditions for the intricate SEM ether deprotection and the difficult hydrogenation of the remaining alkene function. Final Ley oxidation furnished (–)-nitidasin (**238**), whose identity was proven by the elucidation of its solid-state structure and by comparison of recorded NMR data to the published values of the isolated natural product. Furthermore, the absolute configuration of the natural product was established *via* its optical rotation. A total of 16.3 mg of nitidasin (**238**) were prepared in 34 steps (longest linear sequence, starting from ketone (+)-**138**) in 1.8% overall yield. It is our intention to subject this material to further biological testing, in order to shed light on nitidasin's (**238**) yet unknown bioactivity. It was also tried to synthesize alborosin (**252**) from nitidasin (**238**) biomimetically. These attempts were frustrated by the failure to open the epoxide function with the required regioselectivity (*cf.* chapter 3.7).



Scheme A.7: Established 11-step sequence toward the enantioselective construction of triflate **539**.

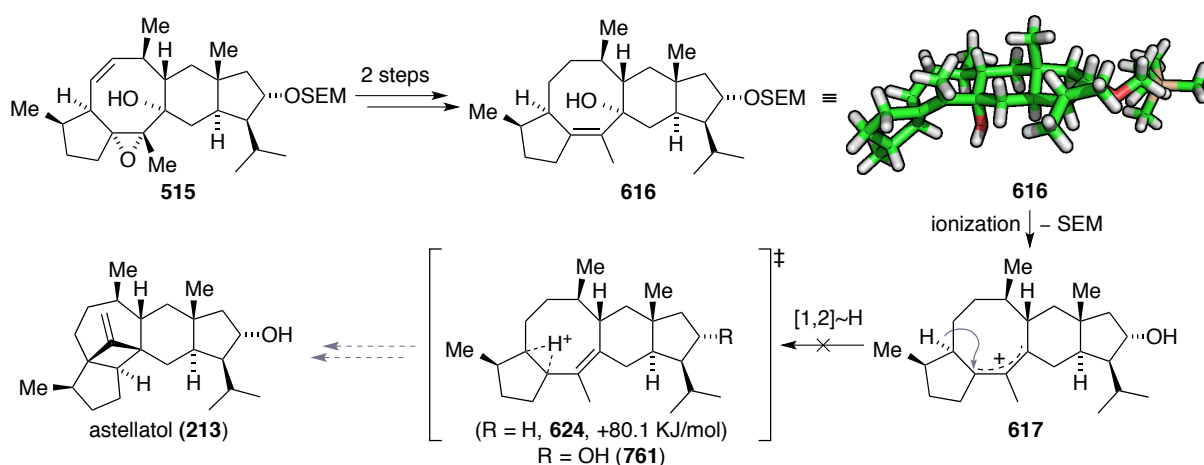
Regarding a potential total synthesis of the sesterterpenoid astellatol (**213**), two approaches were presented, both of which targeted the biomimetic cationic cascade that would potentially construct the natural product's elaborate carbocyclic backbone. The first strategy involved the asymmetric synthesis of vinyl triflate **539**, starting from achiral 3-pentynol (**540**, *cf.* chapter 4.3). In the process, a highly enantioselective Myers alkylation was devised for the preparation of intermediate **558** (scheme A.7). The further sequence featured an efficient intramolecular nitrile oxide cyclization toward bicycle **541** and a chemoselective hydrogenative ring opening that installed the required oxygenation pattern. However, the final low yielding triflation step remained as a bottleneck of this 11-step synthetic route.

In the following (*cf.* chapter 4.4), a highly optimized fragment combination by means of B-alkyl Suzuki coupling was reported, both on a model system (**438**) and on the actually envisaged intermediate (**475**, scheme A.8). The accessed diketone **604** served as a starting point for our investigations on reductive carbonyl-carbonyl coupling. Thereby, an unexpected novel cyclization cascade was discovered, which furnished pentacyclic compounds **605** and **606**, using low valent titanium- or SmI₂-mediated conditions, respectively. While the nature of all four newly formed stereocenters could not be elucidated unambiguously, we nevertheless provided a reasonable mechanistic explanation for mentioned cyclization mode.

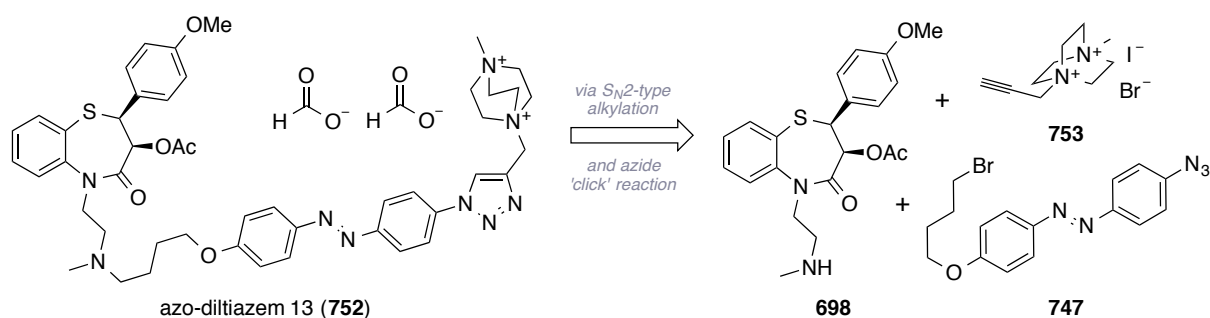


Scheme A.8: B-alkyl Suzuki coupling toward enones **605** and **612**, as well as reductive formation of pentacyclic products **605** and **606** by a literature unprecedented cyclization cascade.

Branching off at the nitidasin (**238**) synthesis at an even later stage, the presented second-generation approach toward astellatol (**213**) involved the preparation of allylic alcohol **616** (*cf.* chapter 4.5) using a tungsten(IV)-based protocol (scheme A.9). However, our experimental efforts to initiate the proposed cationic cascade did not provide the carbon skeleton of the natural product under a wide variety of reaction conditions. In parallel conducted theoretical investigations revealed that aspired initial [1,2]-hydride shift exhibits an energetic barrier (+80.1 kJ/mol), being too high to compete with the experimentally observed elimination reactions (*cf.* chapter 4.6). Moreover, according to these calculations, the biomimetic homoallyl-cyclopropylcarbinyl-cyclobutyl rearrangement would proceed smoothly, once a homoallylic cation (*cf.* structure **625**, scheme 4.21) can be addressed synthetically.



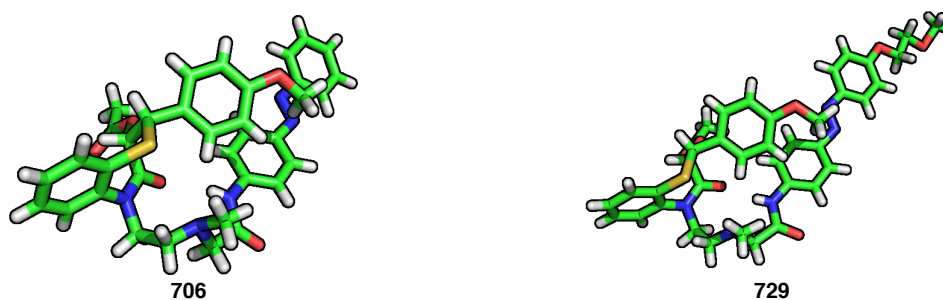
Scheme A.9: Second-generation approach toward astellatol (**213**) and computational rationalization (**624**) of the experimental results of conducted investigations on proposed cationic cascade.



Scheme A.10: Illustration of the developed semisynthetic approach toward photochromic benzothiazepine-based LTCC antagonists, exemplified for the most promising congener azo-diltiazem 13 (**752**).

The second part of this doctoral thesis presents the evolution and synthesis of novel, benzothiazepine-based photochromic ligands for L-type voltage-gated calcium channels. To this end, a short and scalable semisynthetic route was established (*cf.* chapter 2.2), starting from commercially available *cis*-(+)-diltiazem (**645**). By means of chemoselective mono demethylation, it was possible to access a versatile building block (**698**) that could be coupled to a variety of azobenzene-type chromophores *via* alkylation reaction methods (scheme A.10). Accordingly, a small compound library of 13 azobenzene-modified benzothiazepines (azo-diltiazems 1–13) was synthesized and a preliminary lead structure was determined by performing electrophysiological experiments^{xiii} on the channel subtype Ca_v1.3 (*cf.* chapter 2.3). In the process, crystal structures of azo-diltiazem 2 (**706**) and 8 (**729**) were elucidated and a plausible explanation for their low solubility in aqueous media was deduced (scheme A.11). In order to achieve higher drug concentrations in aqueous solutions, two permanently charged antagonists were prepared using a late-stage coupling of modified alkyne reagents *via* azide ‘click’ chemistry. Development of a total synthetic route toward this class of LTCC antagonists was hampered by low yields and not consistently reproducible procedures (*cf.* chapter 2.1).

Electrophysiological evaluation proved that azo-diltiazem derivatives **727** and **729** induce a



Scheme A.11: Solid-state structures of azo-diltiazem 2 (**706**) and 8 (**729**), both revealing folded molecular conformations.

^{xiii}Electrophysiological evaluation of synthesized compounds was conducted by Dr. T. Fehrentz.

more pronounced channel block in *cis* configuration of their respective diazene subunits. In contrast, charged substances **751** and **752** exert channel block preferentially in their *trans* configurations. Generally, azo-diltiazem 13 (**752**) is considered to be the most promising candidate for an efficient photochromic LTCC antagonist according to currently available data. This antagonist features an unusual slow thermal relaxation rate of its diazene bond and first evidence was presented that it may act as a molecular tape, at which the charged tail group would reside at the extracellular side of the cell membrane and only the pharmacophore reaches to the BTZ receptor site. Further chemical modification of the established lead structure is aspired and is directed toward the development of a useful small molecule-based photopharmacological tool for the temporal and spatial control of Ca^{2+} currents in living tissue.

II. Computational Methods

Conformational searches were conducted with a combination of two programs. An initial conformer library was created with the program VEGA ZZ 3.0.3 using the SP4 force-field. This was followed by manual search for further conformers *via* the program Avogadro 1.1.1 and the MMFF94 force-field method.^[358] From the obtained library, species of reasonable low energy were selected for further investigations.

For all quantum mechanical calculations, the program ORCA 3.0.2 was used.^[506] Tight convergence criteria were selected for structure optimization and SCF convergence. A DFT integration grid above the standard accuracy was selected according to the keyword “grid4”. Otherwise, the default settings were adopted. The RIJCOSX and RI approximations were employed to accelerate the SCF procedure for calculation of vibrational frequencies and for the MP2 contribution to the PWPB95 functional.^[362] The D3 correction with BJ damping was applied in all procedures and the gCP correction was used for calculations with the small def2-SVP basis set.^[360] The correct nature of all stationary points was verified by conducting a frequency analysis.

Structure optimizations were performed with the B3LYP functional^[359] and the def2-SVP basis set.^[360] Approximate structures for uncharged molecules were obtained from a conformational search and for ionic species derived from structures of similar uncharged molecules. Starting points for the transition state structures were obtained by relaxed potential energy scans along appropriate internal coordinates or constrained optimizations, if related structures were known from similar transition states. To identify or confirm the energy minima of the transition states, the respective structure was deformed along its reactive mode, which was followed by structure optimization in both directions.

For the located energy minima and transition states, single point energies were calculated with the PWPB95 functional and the def2-TZVPP basis set.^[360] Furthermore, single point energies were calculated with the B3LYP functional and the def2-SVP basis set in the gas phase and in THF ($\epsilon = 7.25$) by modeling the solvent *via* the COSMO method.^[361] Solvation energies can be calculated from the difference of the B3LYP/def2-SVP derived energy in the gas phase and in solution.

III. X-Ray Crystallographic Data

The data collections were performed on an Oxford Diffraction Xcalibur diffractometer or on a Bruker D8Quest diffractometer at 173 K using MoK α -radiation ($\lambda = 0.71073$ Å, graphite monochromator). The CrysAlisPro software (version 1.171.33.41)^[507] was applied for the integration, scaling and multi-scan absorption correction of the data. The structures were solved by direct methods with SIR97^[508] and refined by least-squares methods against F^2 with SHELXL-97.^[509] All non-hydrogen atoms were refined anisotropically. The hydrogen atoms were placed in ideal geometry, riding on their parent atoms. Further details are summarized in the tables at the respective sections.^[510]

Tetraene 504

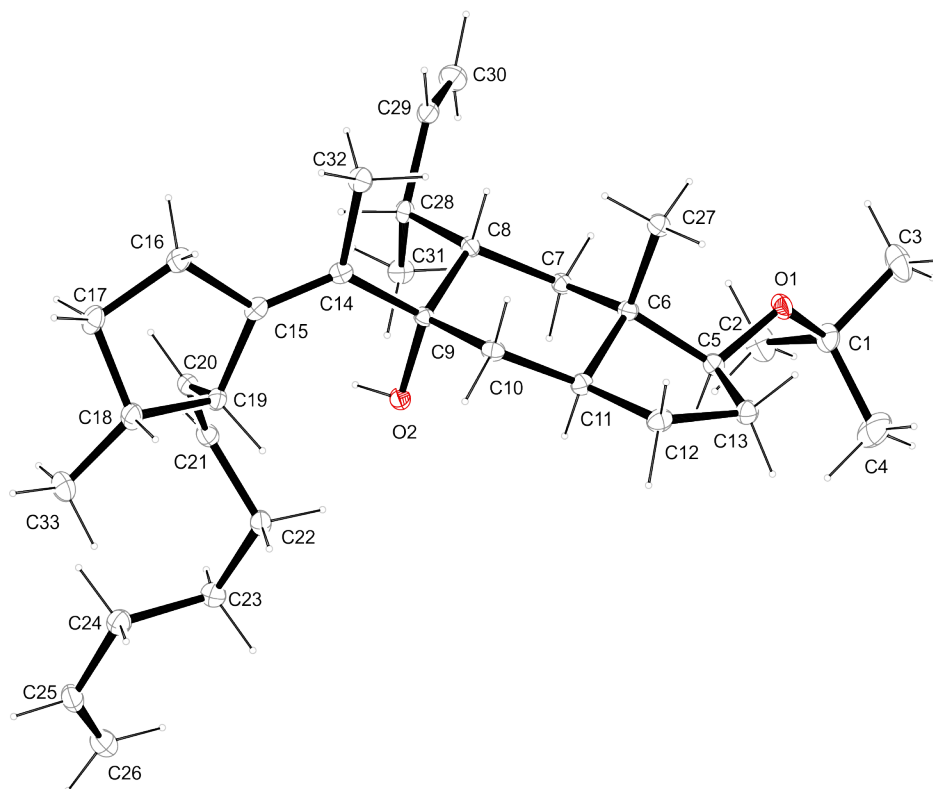
CCDC 1015223 contains the supplementary crystallographic data for tetraene **504**. These data can be obtained free of charge from the Cambridge Crystallographic Data Centre *via* www.ccdc.cam.ac.uk/data_request/cif.

Table A.1: Crystallographic data for tetraene **504**.

net formula	C ₃₃ H ₅₄ O ₂
$M_r/\text{g mol}^{-1}$	482.781
crystal size/mm	0.110 × 0.090 × 0.070
T/K	100(2)
radiation	MoK α
diffractometer	Bruker D8Venture
crystal system	triclinic
space group	$P1$
$a/\text{\AA}$	6.5679(8)
$b/\text{\AA}$	8.8671(10)
$c/\text{\AA}$	13.7516(15)
$\alpha/^\circ$	87.171(3)
$\beta/^\circ$	89.358(3)
$\gamma/^\circ$	69.215(3)
$V/\text{\AA}^3$	747.82(15)
Z	1
calc. density/ g cm^{-3}	1.0720(2)
μ/mm^{-1}	0.064

absorption correction	'multi-scan'
transmission factor range	0.6687–0.7454
refls. measured	11635
R_{int}	0.0302
mean $\sigma(I)/I$	0.0502
θ range	2.97–26.40
observed refts.	4944
x, y (weighting scheme)	0.0435, 0.0330
hydrogen refinement	mixed
Flack parameter	0.1(9)
refls in refinement	5757
Parameters	327
Restraints	3
$R(F_{\text{obs}})$	0.0405
$R_w(F^2)$	0.0885
S	1.051
shift/error _{max}	0.001
max electron density/ $\text{e} \text{ \AA}^{-3}$	0.178
min electron density/ $\text{e} \text{ \AA}^{-3}$	−0.193

C-bound H: constr, O-bound H: refall.



Allyl Alcohol 616

CCDC 1015224 contains the supplementary crystallographic data for allyl alcohol **616**. These data can be obtained free of charge from the Cambridge Crystallographic Data Centre *via* www.ccdc.cam.ac.uk/data_request/cif.

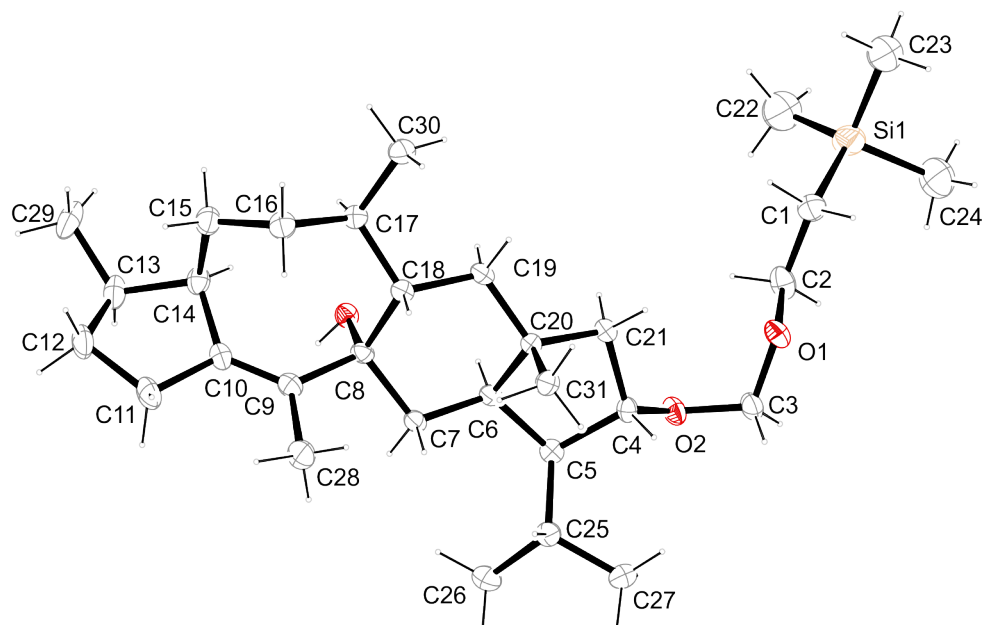
Table A.2: Crystallographic data for allyl alcohol **616**.

net formula	C ₃₁ H ₅₆ O ₃ Si
$M_r/\text{g mol}^{-1}$	504.860
crystal size/mm	0.20 × 0.15 × 0.12
T/K	173(2)
radiation	MoK α
diffractometer	Oxford XCalibur
crystal system	orthorhombic
space group	$P2_12_12_1$
$a/\text{\AA}$	10.7156(6)
$b/\text{\AA}$	17.0663(12)
$c/\text{\AA}$	17.2385(11)
$a/^\circ$	90
$b/^\circ$	90
$g/^\circ$	90
$V/\text{\AA}^3$	3152.5(3)
Z	4
calc. density/g cm ⁻³	1.06373(10)
m/mm ⁻¹	0.101
absorption correction	'multi-scan'
transmission factor range	0.97608–1.00000
refls. measured	16946
R_{int}	0.0730
mean $\sigma(I)/I$	0.1060
θ range	4.20–25.35
observed refls.	3713
x, y (weighting scheme)	0.0452, 0
hydrogen refinement	constr
Flack parameter	0.0(2)
refls in refinement	5734
Parameters	327

Restraints	0
$R(F_{\text{obs}})$	0.0600
$R_w(F^2)$	0.1296
S	1.019
shift/error _{max}	0.001
max electron density/e Å ⁻³	0.236
min electron density/e Å ⁻³	-0.290

Two Si-bound methyl groups disordered, split model applied, sof ratio

0.65/0.35, split atoms refined isotropically.



3.3 Alkyne 558

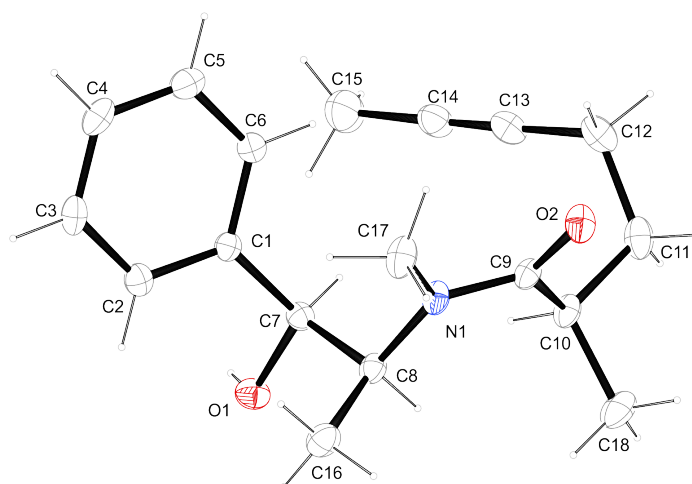
CCDC 1015225 contains the supplementary crystallographic data for alkyne **558**. These data can be obtained free of charge from the Cambridge Crystallographic Data Centre *via* www.ccdc.cam.ac.uk/data_request/cif.

Table A.3: Crystallographic data for alkyne **558**.

net formula	C ₁₈ H ₂₅ NO ₂
$M_r/\text{g mol}^{-1}$	287.397
crystal size/mm	0.110 × 0.08 × 0.04
T/K	173(2)
radiation	MoK α
diffractometer	Bruker D8 Venture
crystal system	orthorhombic

space group	$P2_12_12_1$
$a/\text{\AA}$	8.1742(6)
$b/\text{\AA}$	13.5997(8)
$c/\text{\AA}$	14.6764(9)
$a/^\circ$	90
$b/^\circ$	90
$g/^\circ$	90
$V/\text{\AA}^3$	1631.53(18)
Z	4
calc. density/ g cm^{-3}	1.17004(13)
m/mm^{-1}	0.075
absorption correction	'multi-scan'
transmission factor range	0.8360–0.9585
refls. measured	12988
R_{int}	0.0324
mean $\sigma(I)/I$	0.0324
θ range	3.15–26.42
observed refls.	2773
x, y (weighting scheme)	0.0380, 0.2338
hydrogen refinement	mixed
Flack parameter	0.3(12)
refls in refinement	3323
Parameters	198
Restraints	0
$R(F_{\text{obs}})$	0.0361
$R_w(F^2)$	0.0846
S	1.051
shift/error _{max}	0.001
max electron density/ e \AA^{-3}	0.155
min electron density/ e \AA^{-3}	−0.164

C-bound H: constr, O-bound H: refall.



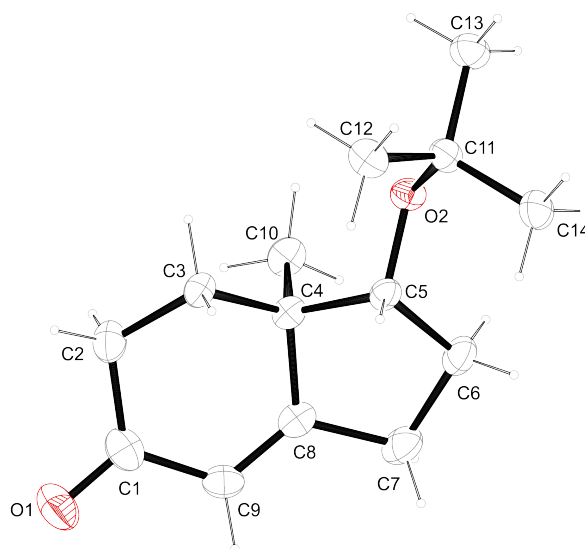
Ether 359

CCDC 1028518 contains the supplementary crystallographic data for ether **359**. These data can be obtained free of charge from the Cambridge Crystallographic Data Centre *via* www.ccdc.cam.ac.uk/data_request/cif.

Table A.4: Crystallographic data for ether **359**.

net formula	C ₁₄ H ₂₂ O ₂
$M_r/\text{g mol}^{-1}$	222.323
crystal size/mm	0.154 × 0.111 × 0.093
T/K	100(2)
radiation	MoK α
diffractometer	Bruker D8Venture
crystal system	orthorhombic
space group	$P2_12_12_1$
$a/\text{\AA}$	7.6811(6)
$b/\text{\AA}$	11.6826(10)
$c/\text{\AA}$	14.4895(12)
$a/^\circ$	90
$b/^\circ$	90
$c/^\circ$	90
$V/\text{\AA}^3$	1300.22(19)
Z	4
calc. density/ g cm^{-3}	1.13575(17)
m/mm^{-1}	0.074
absorption correction	'multi-scan'

transmission factor range	0.9385–0.9580
refls. measured	19361
R_{int}	0.0461
mean $\sigma(I)/I$	0.0237
θ range	3.17–25.41
observed refls.	2138
x, y (weighting scheme)	0.0299, 0.2453
hydrogen refinement	constr
Flack parameter	−0.2(11)
refls in refinement	2362
Parameters	149
Restraints	0
$R(F_{\text{obs}})$	0.0306
$R_w(F^2)$	0.0708
S	1.057
shift/error _{max}	0.001
max electron density/e \AA^{-3}	0.177
min electron density/e \AA^{-3}	−0.126



Ketoacid 362

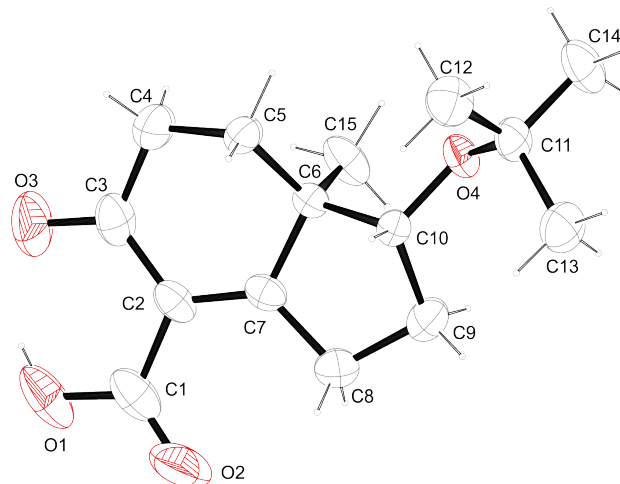
CCDC 1028519 contains the supplementary crystallographic data for ketoacid **362**. These data can be obtained free of charge from the Cambridge Crystallographic Data Centre *via* www.ccdc.cam.ac.uk/data_request/cif.

Table A.5: Crystallographic data for ketoacid **362**.

net formula	C ₁₅ H ₂₂ O ₄
$M_r/\text{g mol}^{-1}$	266.333
crystal size/mm	0.150 × 0.097 × 0.034
T/K	173(2)
radiation	MoK α
diffractometer	Bruker D8Venture
crystal system	orthorhombic
space group	$P2_12_12_1$
$a/\text{\AA}$	6.4353(13)
$b/\text{\AA}$	9.217(2)
$c/\text{\AA}$	24.531(5)
$a/^\circ$	90
$b/^\circ$	90
$g/^\circ$	90
$V/\text{\AA}^3$	1454.9(5)
Z	4
calc. density/ g cm^{-3}	1.2159(4)
m/mm^{-1}	0.087
absorption correction	'multi-scan'
transmission factor range	0.9475–0.9585
refls. measured	22678
R_{int}	0.0702
mean $\sigma(I)/I$	0.0498
θ range	3.27–25.06
observed refls.	1902
x, y (weighting scheme)	0.0270, 0.3196
hydrogen refinement	constr
Flack parameter	–1.3(14)
refls in refinement	2549
Parameters	177

Restraints	0
$R(F_{\text{obs}})$	0.0414
$R_w(F^2)$	0.0876
S	1.064
shift/error _{max}	0.001
max electron density/e Å ⁻³	0.152
min electron density/e Å ⁻³	-0.131

Flack test meaningless, correct structure derived from synthesis.



Hydrindanone 361

CCDC 1028520 contains the supplementary crystallographic data for hydrindanone **361**. These data can be obtained free of charge from the Cambridge Crystallographic Data Centre via www.ccdc.cam.ac.uk/data_request/cif.

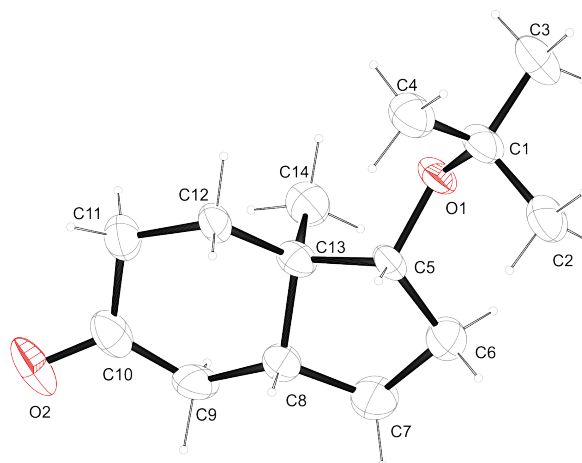
Table A.6: Crystallographic data for hydrindanone **361**.

net formula	C ₁₄ H ₂₄ O ₂
$M_r/\text{g mol}^{-1}$	224.339
crystal size/mm	0.3268 × 0.2540 × 0.1079
T/K	123(2)
radiation	MoK α
diffractometer	Oxford XCalibur
crystal system	monoclinic
space group	$P2_1$
$a/\text{\AA}$	12.2555(13)
$b/\text{\AA}$	12.0957(11)
$c/\text{\AA}$	19.4776(18)

$a/^\circ$	90
$b/^\circ$	108.240(10)
$g/^\circ$	90
$V/\text{\AA}^3$	2742.3(5)
Z	8
calc. density/ g cm^{-3}	1.08676(20)
m/mm^{-1}	0.070
absorption correction	'multi-scan'
transmission factor range	0.97161–1.00000
refls. measured	9337
R_{int}	0.0325
mean $\sigma(I)/I$	0.0809
θ range	4.33–25.34
observed refts.	5703
x, y (weighting scheme)	0.0299, 0
hydrogen refinement	constr
Flack parameter	–2.5(12)
refls in refinement	7464
Parameters	594
Restraints	1
$R(F_{\text{obs}})$	0.0526
$R_w(F^2)$	0.1036
S	1.033
shift/error _{max}	0.001
max electron density/ e \AA^{-3}	0.171
min electron density/ e \AA^{-3}	–0.178

Correct structure derived from synthesis.

Refined as pseudo-merohedral twin (TWIN –1 0 0 0 –1 0 1 0 1, BASF 0.46).



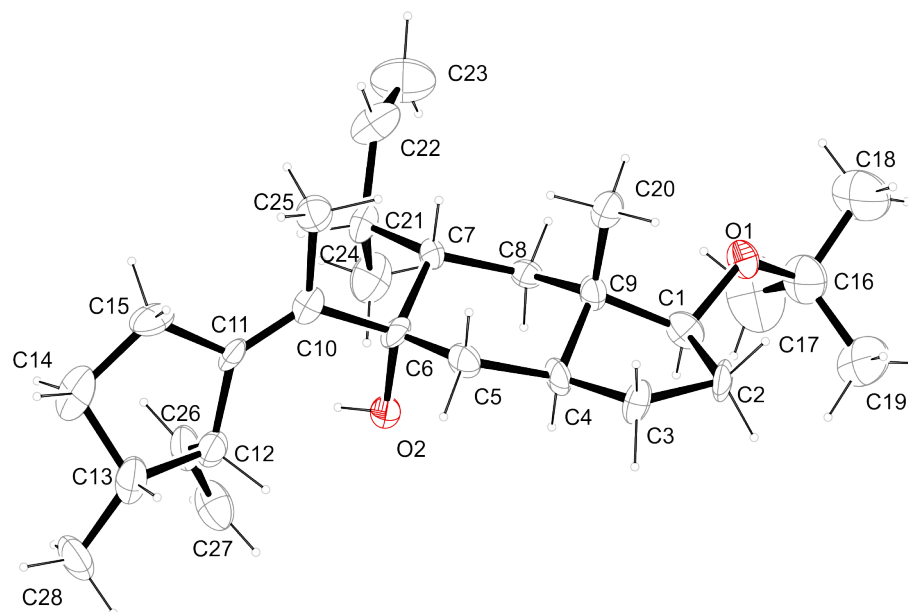
Triene 479

CCDC 987776 contains the supplementary crystallographic data for triene **479**. These data can be obtained free of charge from the Cambridge Crystallographic Data Centre *via* www.ccdc.cam.ac.uk/data_request/cif.

Table A.7: Crystallographic data for triene **479**.

net formula	C ₂₈ H ₄₆ O ₂
$M_r/\text{g mol}^{-1}$	414.664
crystal size/mm	0.339 × 0.075 × 0.045
T/K	173(2)
radiation	MoK α
diffractometer	'Bruker D8Quest'
crystal system	triclinic
space group	$P1$
$a/\text{\AA}$	6.4186(17)
$b/\text{\AA}$	11.485(3)
$c/\text{\AA}$	18.983(6)
a°	75.300(9)
b°	83.856(9)
g°	73.935(8)
$V/\text{\AA}^3$	1299.8(6)
Z	2
calc. density/ g cm^{-3}	1.0595(5)
m/mm^{-1}	0.064
absorption correction	multi-scan
transmission factor range	0.8645–0.9575
refls. Measured	16191
R_{int}	0.1056
mean $\sigma(I)/I$	0.1262
θ range	2.56–24.12
observed refls.	4261
x, y (weighting scheme)	0.1742, 0.0534
hydrogen refinement	mixed
Flack parameter	–2(3)
refls in refinement	5541
Parameters	556

Restraints	3
$R(F_{\text{obs}})$	0.1111
$R_w(F^2)$	0.2567
S	1.089
shift/error _{max}	0.001
max electron density/e Å ⁻³	0.679
min electron density/e Å ⁻³	-0.430



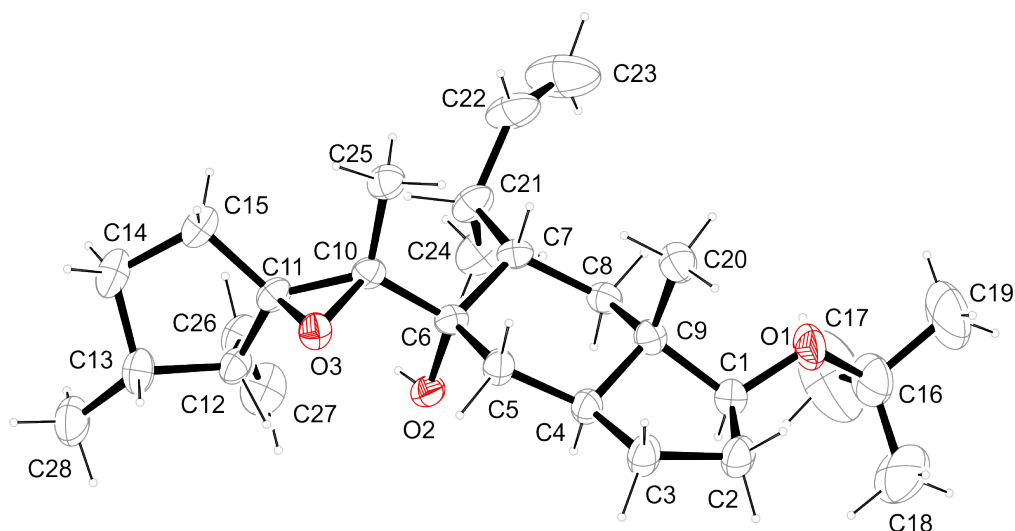
Epoxide 508

CCDC 987777 contains the supplementary crystallographic data for epoxide **508**. These data can be obtained free of charge from the Cambridge Crystallographic Data Centre *via* www.ccdc.cam.ac.uk/data_request/cif.

Table A.8: Crystallographic data for epoxide **508**.

net formula	C ₂₈ H ₄₆ O ₃
$M_r/\text{g mol}^{-1}$	430.663
crystal size/mm	0.414 × 0.173 × 0.062
T/K	173(2)
radiation	MoK α
diffractometer	'Bruker D8Quest'
crystal system	monoclinic
space group	$C2$
$a/\text{\AA}$	22.6781(16)

$b/\text{\AA}$	6.4165(4)
$c/\text{\AA}$	19.4911(13)
$a/^\circ$	90
$b/^\circ$	109.4868(19)
$g/^\circ$	90
$V/\text{\AA}^3$	2673.8(3)
Z	4
calc. density/ g cm^{-3}	1.06985(12)
m/mm^{-1}	0.067
absorption correction	multi-scan
transmission factor range	0.9096–0.9590
refls. Measured	20602
R_{int}	0.0454
mean $\sigma(I)/I$	0.0602
θ range	2.39–27.53
observed refls.	4457
x, y (weighting scheme)	0.0487, 0.9170
hydrogen refinement	constr
Flack parameter	−0.6(10)
refls in refinement	6072
Parameters	288
Restraints	1
$R(F_{\text{obs}})$	0.0536
$R_w(F^2)$	0.1125
S	1.023
shift/error _{max}	0.001
max electron density/ e \AA^{-3}	0.180
min electron density/ e \AA^{-3}	−0.212



Tetracycline 515

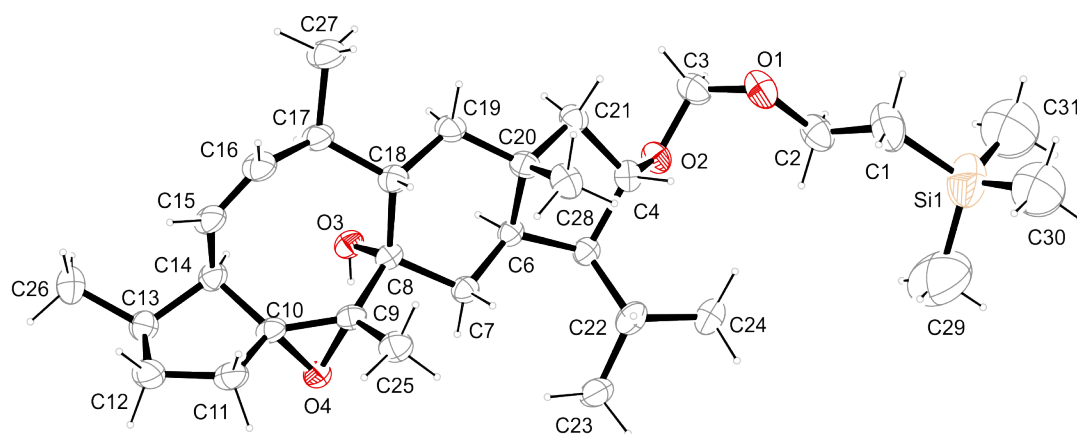
CCDC 987778 contains the supplementary crystallographic data for tetracycline **515**. These data can be obtained free of charge from the Cambridge Crystallographic Data Centre *via* www.ccdc.cam.ac.uk/data_request/cif.

Table A.9: Crystallographic data for tetracycline **515**.

net formula	C ₃₁ H ₅₄ O ₄ Si
<i>M_r</i> /g mol ⁻¹	518.844
crystal size/mm	0.357 × 0.116 × 0.078
<i>T</i> /K	173(2)
radiation	MoKα
diffractometer	'Bruker D8Quest'
crystal system	orthorhombic
space group	<i>P</i> 2 ₁ 2 ₁ 2 ₁
<i>a</i> /Å	9.7229(5)
<i>b</i> /Å	17.7799(10)
<i>c</i> /Å	18.6273(11)
<i>a</i> /°	90
<i>b</i> /°	90
<i>c</i> /°	90
<i>V</i> /Å ³	3220.1(3)
<i>Z</i>	4
calc. density/g cm ⁻³	1.07024(10)
<i>m</i> /mm ⁻¹	0.103

absorption correction	multi-scan
transmission factor range	0.9306–0.9705
refls. Measured	56340
R_{int}	0.0823
mean $\sigma(I)/I$	0.0401
θ range	2.36–25.14
observed refls.	4594
x, y (weighting scheme)	0.0471, 0.7328
hydrogen refinement	mixed
Flack parameter	−0.09(19)
refls in refinement	5731
Parameters	339
Restraints	0
$R(F_{\text{obs}})$	0.0461
$R_w(F^2)$	0.1043
S	1.074
shift/error _{max}	0.001
max electron density/ $\text{e} \text{ \AA}^{-3}$	0.250
min electron density/ $\text{e} \text{ \AA}^{-3}$	−0.331

C-bound H: constr, O-bound H: refall. Si-bound methyl groups partly disordered, split model applied, split atoms refined isotropically.



Tetracycle 522

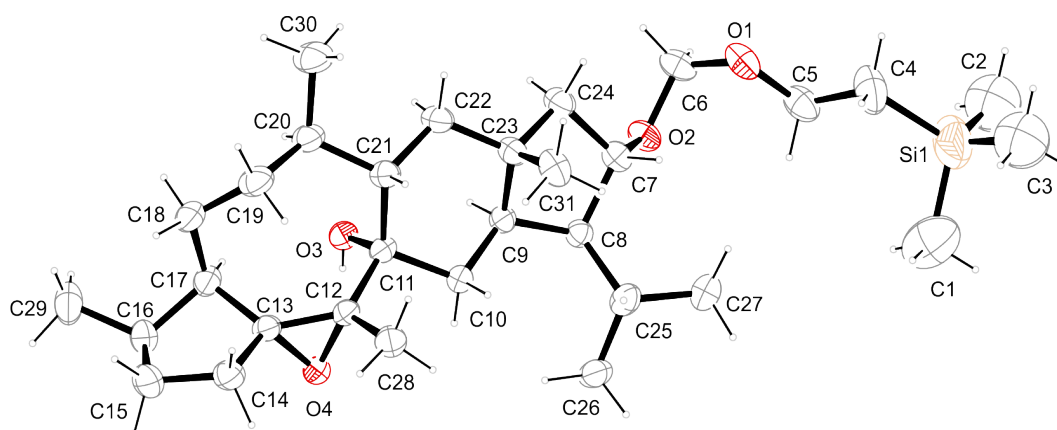
CCDC 988636 contains the supplementary crystallographic data for tetracycle **522**. These data can be obtained free of charge from the Cambridge Crystallographic Data Centre *via* www.ccdc.cam.ac.uk/data_request/cif.

Table A.10: Crystallographic data for tetracycle **522**.

net formula	C ₃₁ H ₅₆ O ₄ Si
$M_r/\text{g mol}^{-1}$	520.859
crystal size/mm	0.289 × 0.182 × 0.149
T/K	173(2)
radiation	MoK α
diffractometer	'Bruker D8Quest'
crystal system	orthorhombic
space group	$P2_12_12_1$
$a/\text{\AA}$	9.5112(5)
$b/\text{\AA}$	18.2926(10)
$c/\text{\AA}$	18.4951(11)
$a/^\circ$	90
$b/^\circ$	90
$g/^\circ$	90
$V/\text{\AA}^3$	3217.9(3)
Z	4
calc. density/ g cm^{-3}	1.07514(10)
m/mm^{-1}	0.103
absorption correction	multi-scan
transmission factor range	0.9250–0.9580
refls. Measured	53825
R_{int}	0.0532
mean $\sigma(I)/I$	0.0293
θ range	2.41–25.41
observed refls.	4905
x, y (weighting scheme)	0.0625, 1.5206
hydrogen refinement	mixed
Flack parameter	0.0(2)
refls in refinement	5910
Parameters	338

Restraints	4
$R(F_{\text{obs}})$	0.0519
$R_w(F^2)$	0.1315
S	1.052
shift/error _{max}	0.001
max electron density/e Å ⁻³	0.462
min electron density/e Å ⁻³	-0.563

C-bound H: constr, O-bound H: refall. Si-bound methyl partly disordered, split model, split atoms refined isotropically. Main part shown in figure.



(-)-Nitidasin (238)

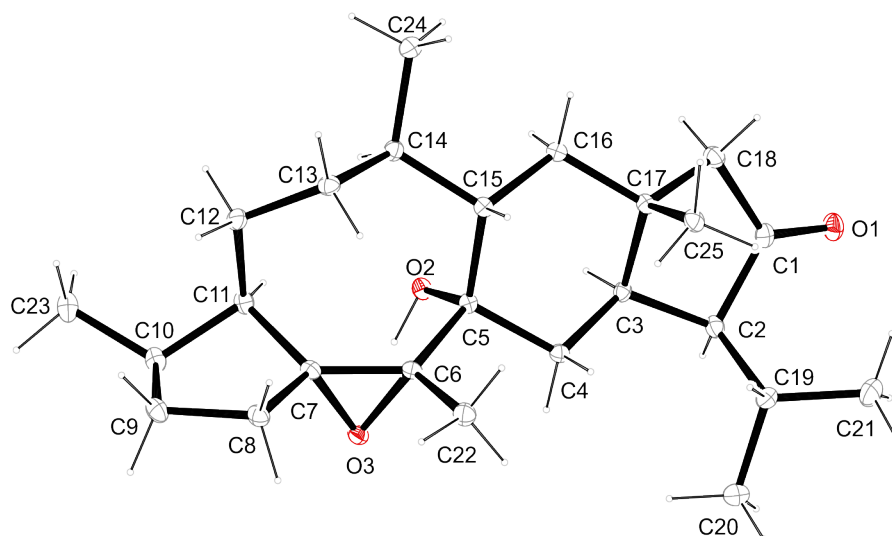
CCDC 990612 contains the supplementary crystallographic data for (-)-nitidasin (**238**). These data can be obtained free of charge from The Cambridge Crystallographic Data Centre *via* www.ccdc.cam.ac.uk/data_request/cif. The obtained crystallographic parameters were in agreement with those reported in the isolation publication.^[154] The isolation data can be obtained from The Cambridge Crystallographic Data Centre using the CSD code NUWMIB.

Table A.11: Crystallographic data for (-)-nitidasin (**238**).

net formula	C ₂₅ H ₄₀ O ₃
M_r /g mol ⁻¹	388.592
crystal size/mm	0.06 × 0.09 × 0.15
T /K	100(2)
radiation	MoK α
diffractometer	'Bruker D8Venture'
crystal system	orthorhombic
space group	$P2_12_12_1$

$a/\text{\AA}$	6.4061(4)
$b/\text{\AA}$	13.4536(10)
$c/\text{\AA}$	25.5219(17)
$a/^\circ$	90
$b/^\circ$	90
$g/^\circ$	90
$V/\text{\AA}^3$	2199.6(3)
Z	4
calc. density/ g cm^{-3}	1.17343(16)
m/mm^{-1}	0.075
absorption correction	multi-scan
transmission factor range	0.9072–0.9585
refls. Measured	23884
R_{int}	0.0433
mean $\sigma(I)/I$	0.0350
θ range	3.03–26.41
observed refls.	3921
x, y (weighting scheme)	0.0403, 0.4296
hydrogen refinement	mixed
Flack parameter	0.9(9)
refls in refinement	4482
Parameters	263
Restraints	0
$R(F_{\text{obs}})$	0.0360
$R_w(F^2)$	0.0830
S	1.039
shift/error _{max}	0.001
max electron density/ e \AA^{-3}	0.245
min electron density/ e \AA^{-3}	−0.186

C-bound H: constr, O-bound H: refall.



Azo-diltiazem 2 (706)

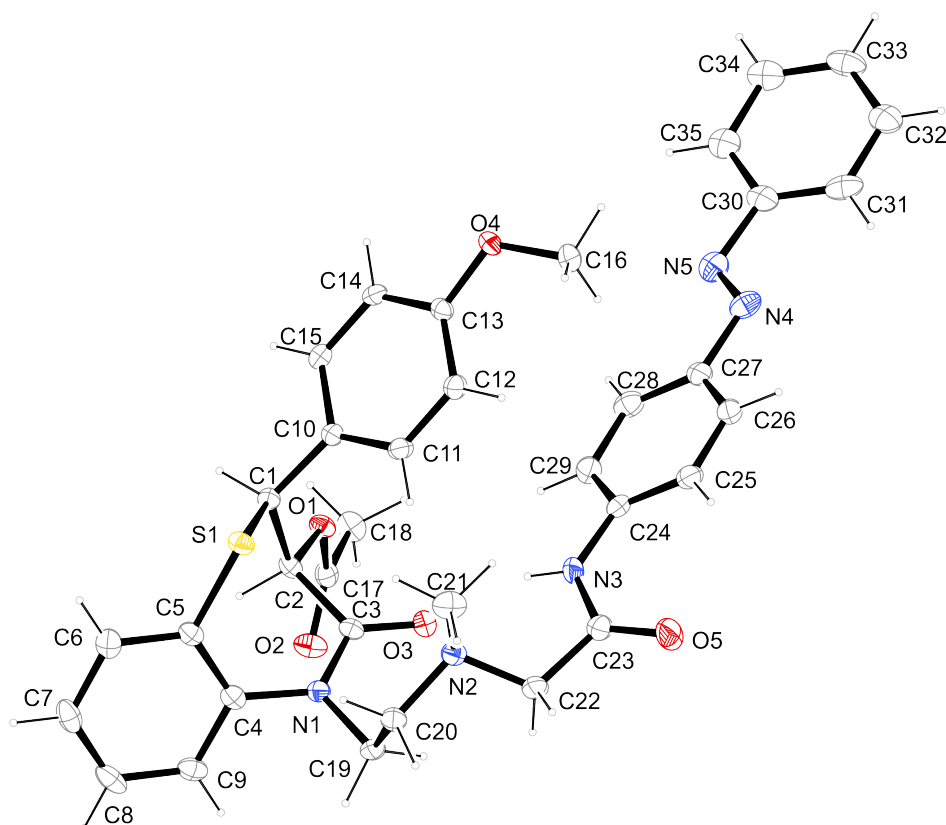
CCDC 1027093 contains the supplementary crystallographic data for azo-diltiazem 2 (**706**). These data can be obtained free of charge from The Cambridge Crystallographic Data Centre via www.ccdc.cam.ac.uk/data_request/cif.

Table A.12: Crystallographic data for azo-diltiazem 2 (**706**).

net formula	C ₃₅ H ₃₅ N ₅ O ₅ S
M_r /g mol ⁻¹	637.749
crystal size/mm	0.162 × 0.111 × 0.092
T /K	100(2)
radiation	MoK α
diffractometer	'Bruker D8Venture'
crystal system	orthorhombic
space group	$P2_12_12_1$
a /Å	8.8467(4)
b /Å	10.3973(4)
c /Å	33.9921(12)
a /°	90
b /°	90
c /°	90
V /Å ³	3126.7(2)
Z	4
calc. density/g cm ⁻³	1.35481(9)
m /mm ⁻¹	0.156

absorption correction	multi-scan
transmission factor range	0.9504–0.9679
refls. Measured	64458
R_{int}	0.0491
mean $\sigma(I)/I$	0.0225
θ range	3.02–25.51
observed refts.	5400
x, y (weighting scheme)	0.0284, 0.8739
hydrogen refinement	mixed
Flack parameter	–0.04(5)
refls in refinement	5746
Parameters	422
Restraints	0
$R(F_{\text{obs}})$	0.0286
$R_w(F^2)$	0.0643
S	1.075
shift/error _{max}	0.002
max electron density/ $\text{e} \text{ \AA}^{-3}$	0.238
min electron density/ $\text{e} \text{ \AA}^{-3}$	–0.167

C-bound H: constr, N-bound H: reffall.



Azo-diltiazem 8 (729)

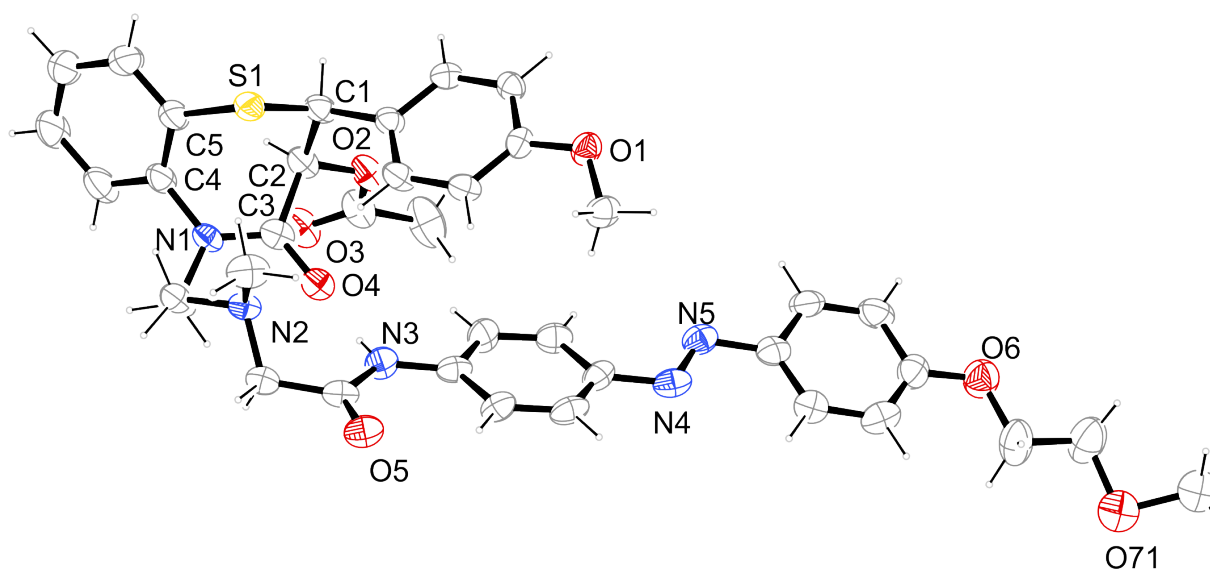
CCDC 1027094 contains the supplementary crystallographic data for azo-diltiazem 8 (**729**). These data can be obtained free of charge from The Cambridge Crystallographic Data Centre via www.ccdc.cam.ac.uk/data_request/cif.

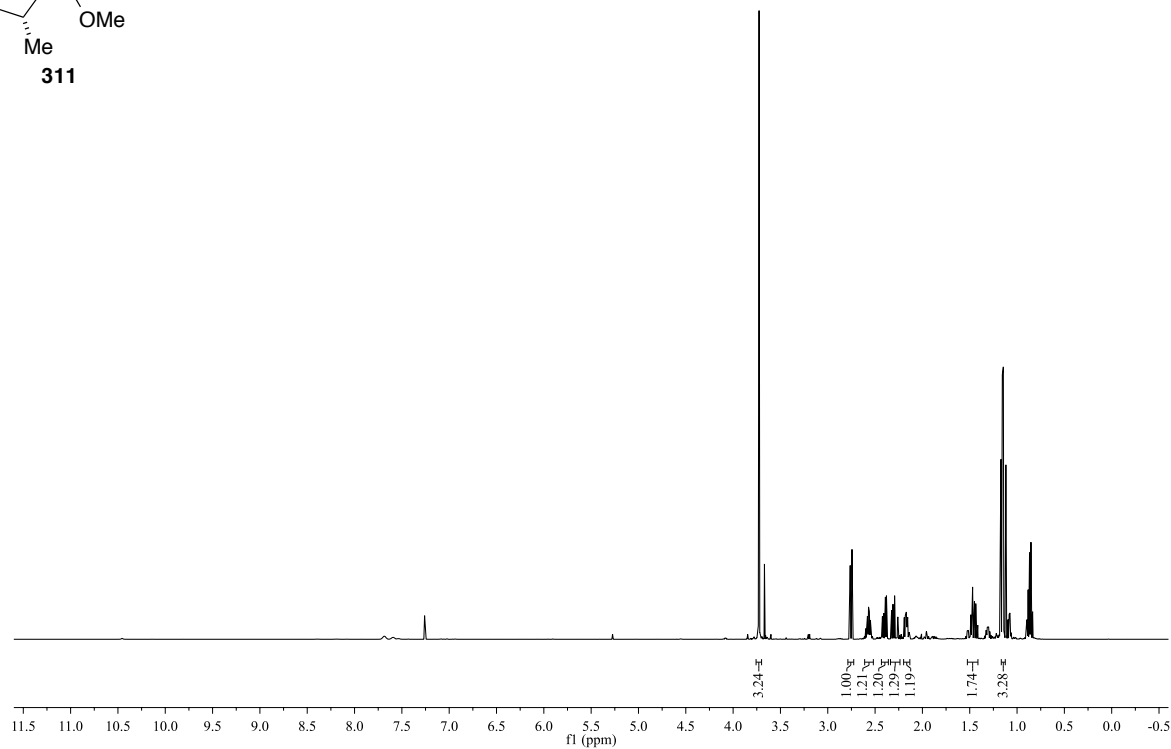
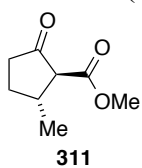
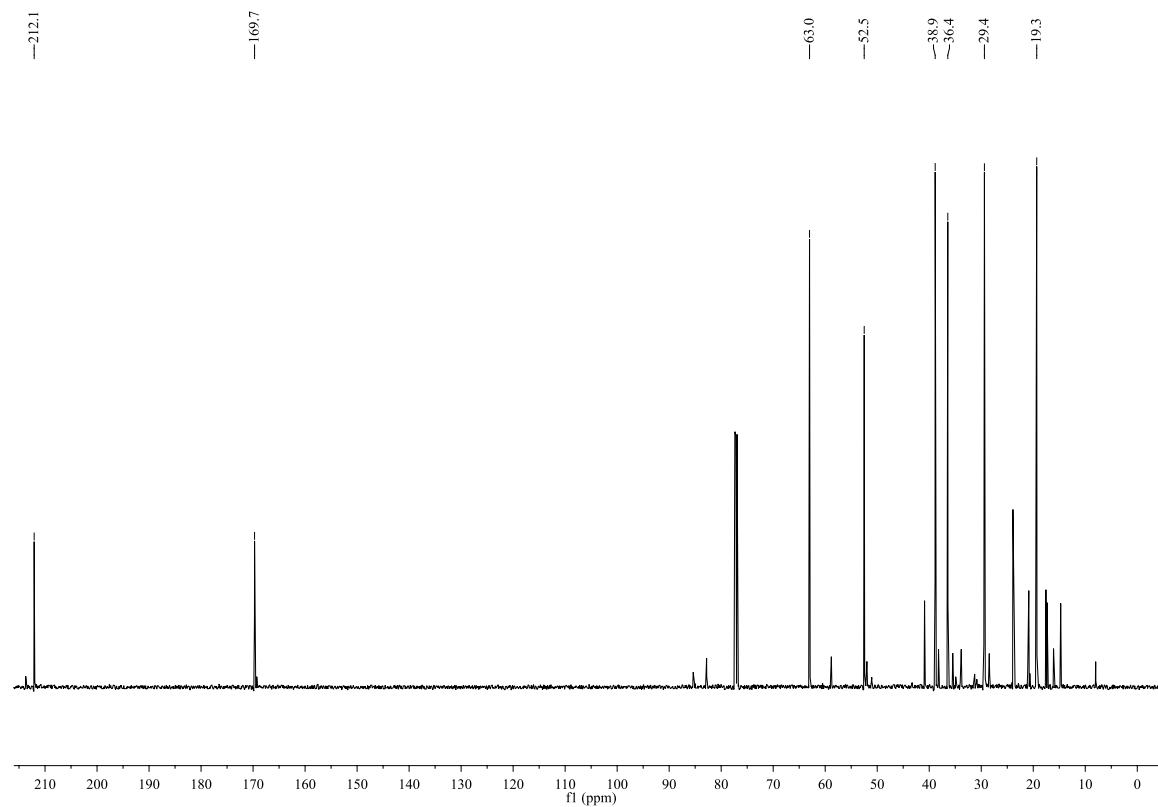
Table A.13: Crystallographic data for azo-diltiazem 8 (**729**).

net formula	C ₃₈ H ₄₁ N ₅ O ₇ S
<i>M_r</i> /g mol ⁻¹	711.828
crystal size/mm	0.177 × 0.128 × 0.110
<i>T</i> /K	123(2)
radiation	MoKα
diffractometer	'Bruker D8Venture'
crystal system	orthorhombic
space group	<i>P</i> 2 ₁ 2 ₁ 2 ₁
<i>a</i> /Å	9.6378(5)
<i>b</i> /Å	16.9354(8)
<i>c</i> /Å	23.5059(12)
<i>a</i> /°	90
<i>b</i> /°	90
<i>c</i> /°	90
<i>V</i> /Å ³	3836.6(3)
<i>Z</i>	4
calc. density/g cm ⁻³	1.23238(10)
<i>m</i> /mm ⁻¹	0.138
absorption correction	multi-scan
transmission factor range	0.9055–0.9705
refls. Measured	41701
<i>R</i> _{int}	0.0401
mean $\sigma(I)/I$	0.0246
θ range	2.99–25.02
observed refls.	6001
<i>x</i> , <i>y</i> (weighting scheme)	0.0869, 3.4367
hydrogen refinement	mixed
Flack parameter	0.00(12)
refls in refinement	6808
Parameters	468

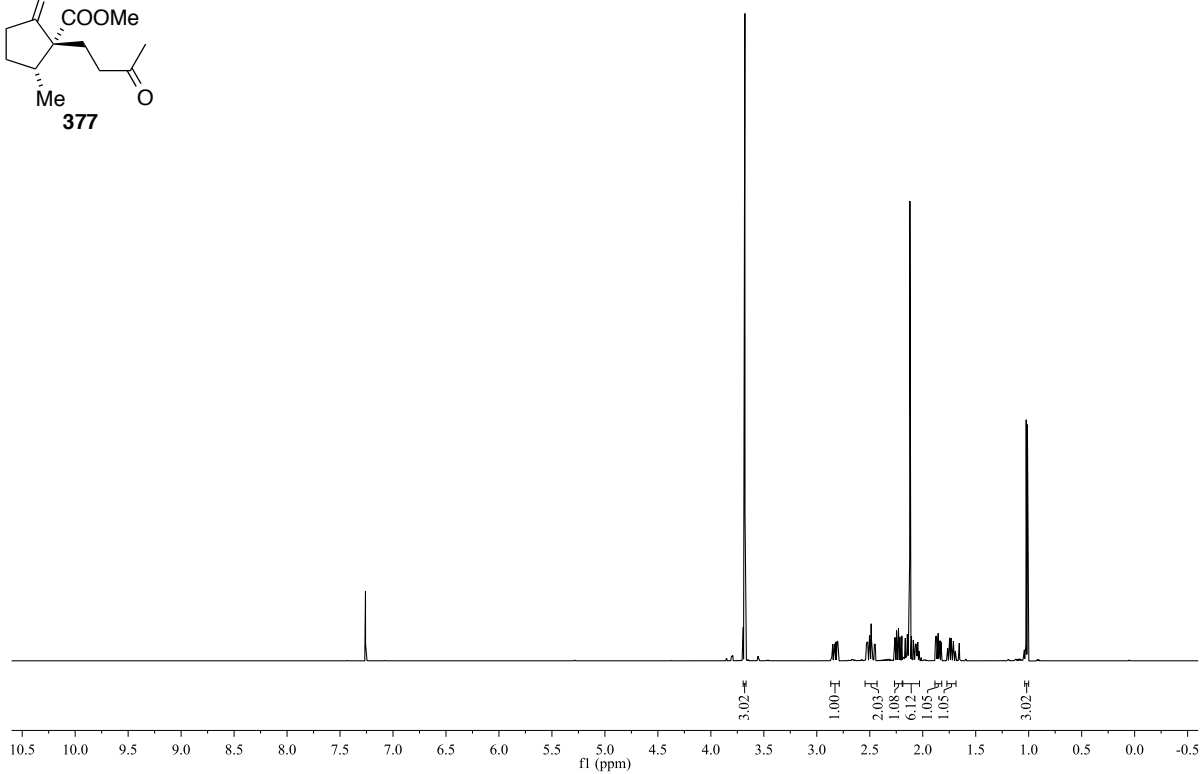
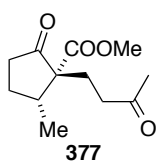
Restraints	0
$R(F_{\text{obs}})$	0.0566
$R_w(F^2)$	0.1681
S	1.104
shift/error _{max}	0.001
max electron density/e Å ⁻³	0.795
min electron density/e Å ⁻³	-0.467

C-bound H: constr, N-bound H: refall. Split model applied for the disorder of the OCH₃ group, sof ratio 1:1, split atoms refined isotropically.

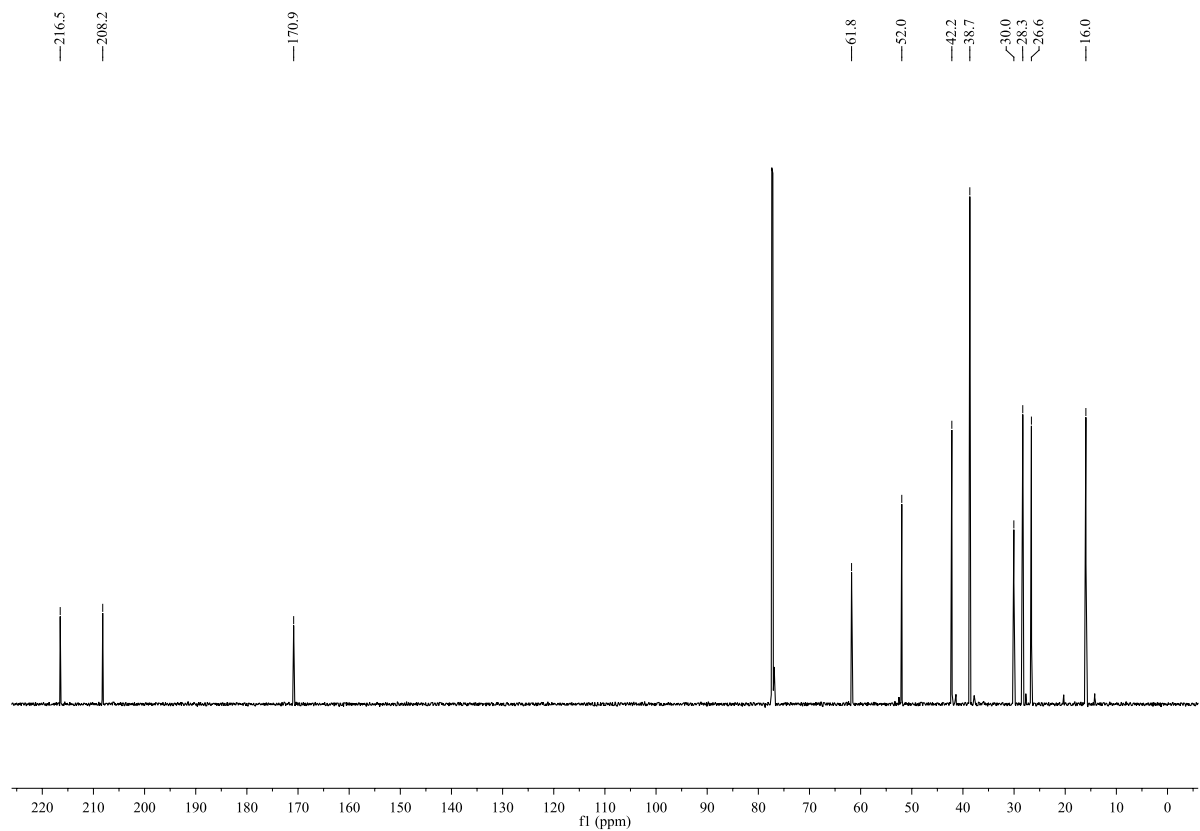


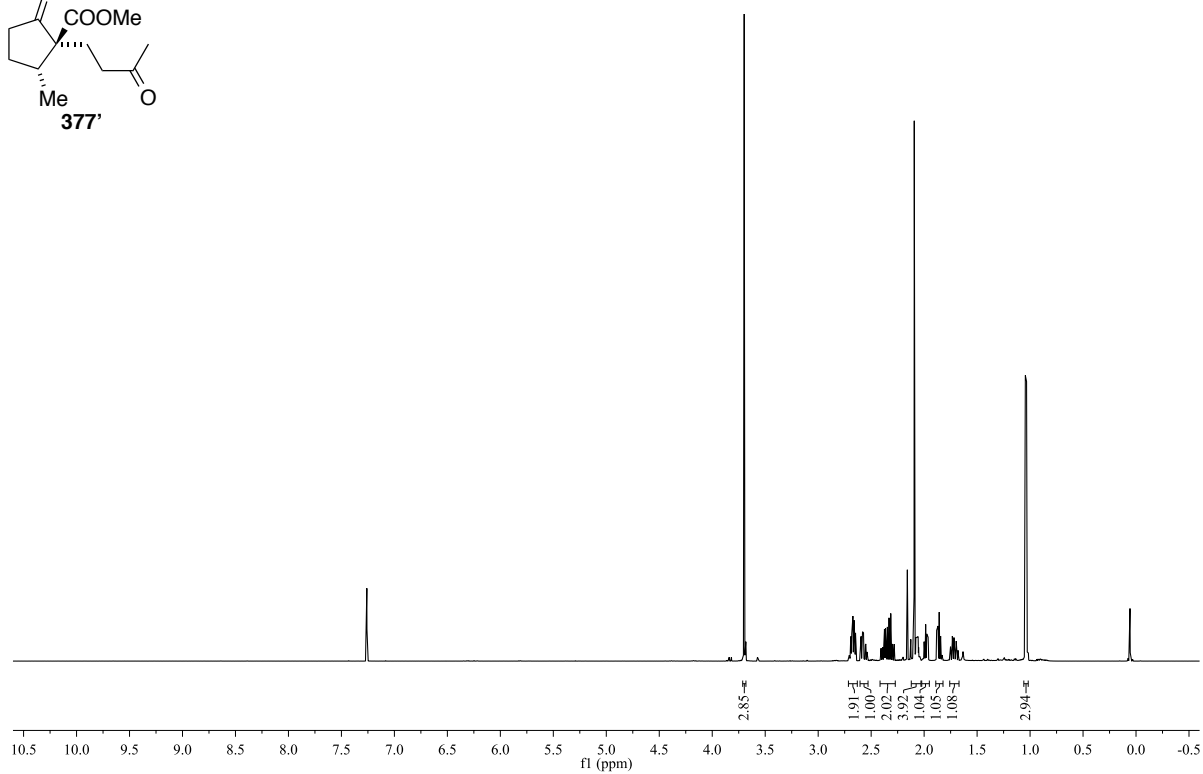
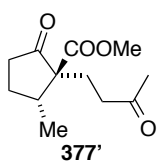
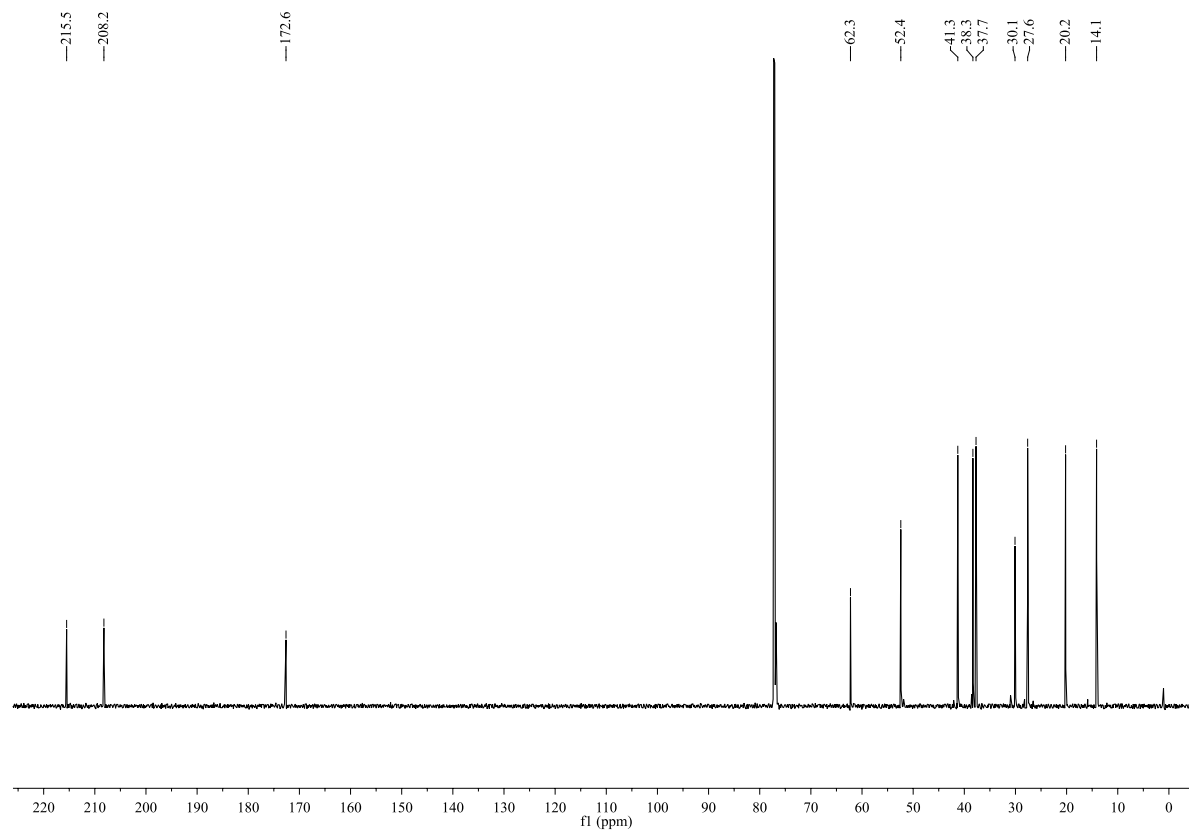
IV. ^1H and ^{13}C NMR Spectra ^1H NMR (CDCl_3 , 600 MHz): ^{13}C NMR (CDCl_3 , 150 MHz):

^1H NMR (CDCl_3 , 600 MHz):

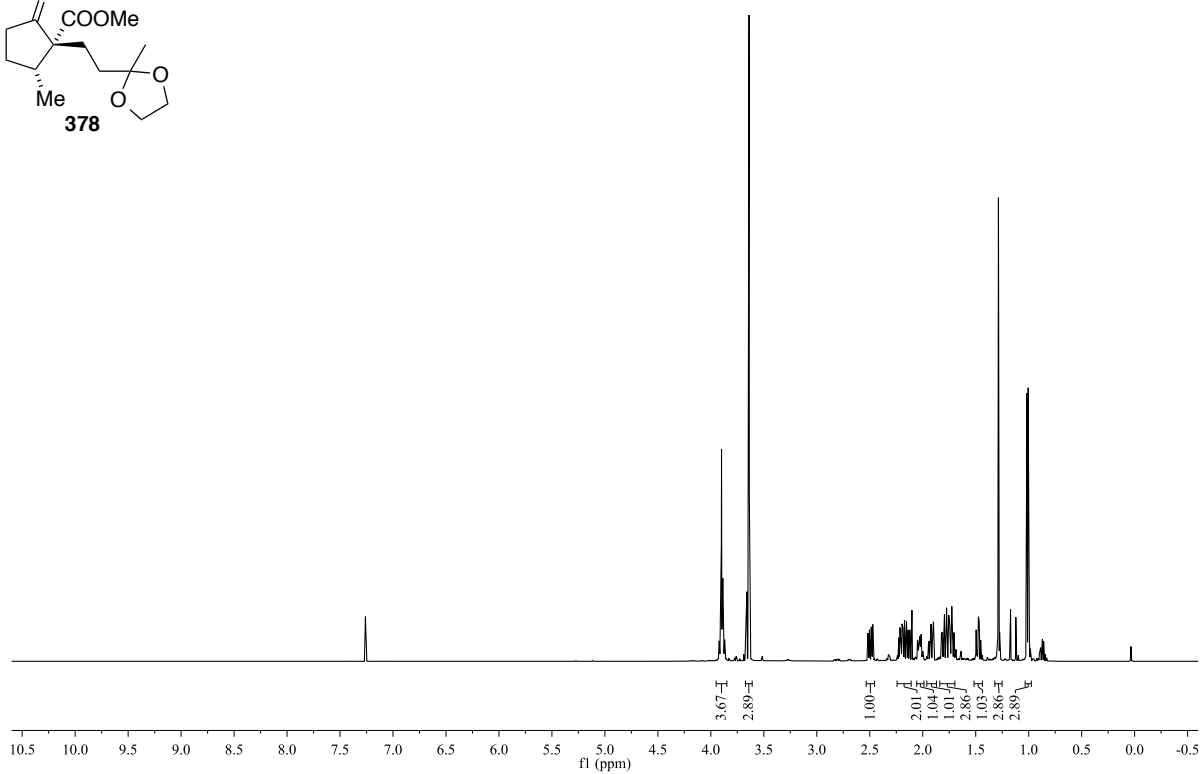
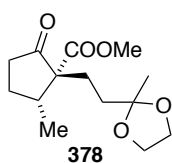


^{13}C NMR (CDCl_3 , 150 MHz):

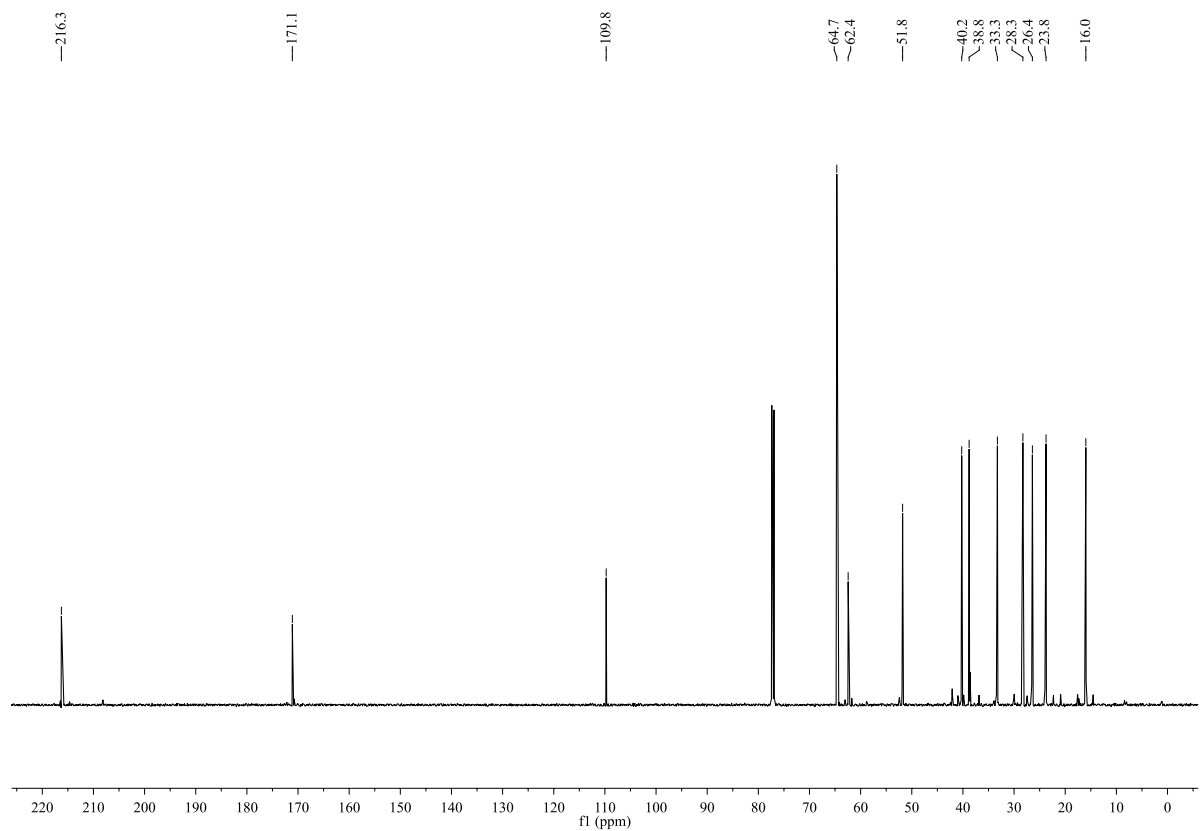


^1H NMR (CDCl_3 , 600 MHz): ^{13}C NMR (CDCl_3 , 150 MHz):

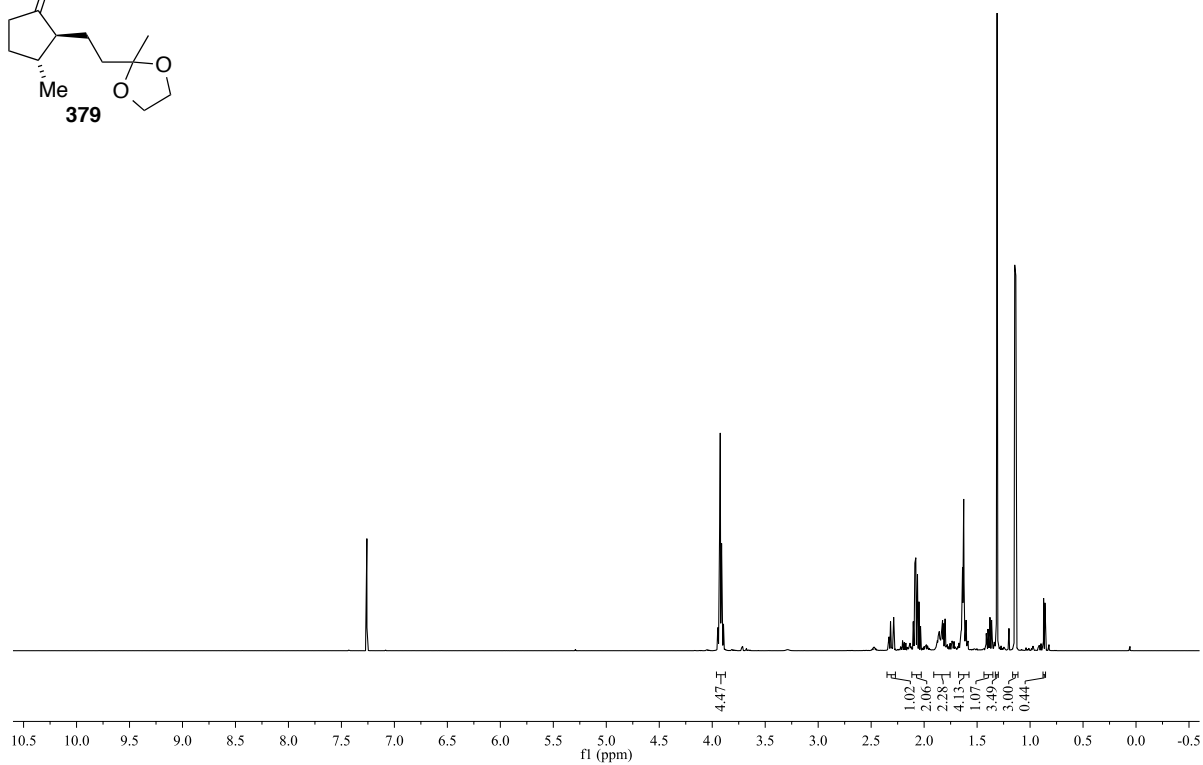
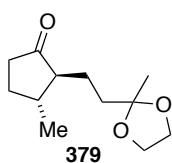
^1H NMR (CDCl_3 , 600 MHz):



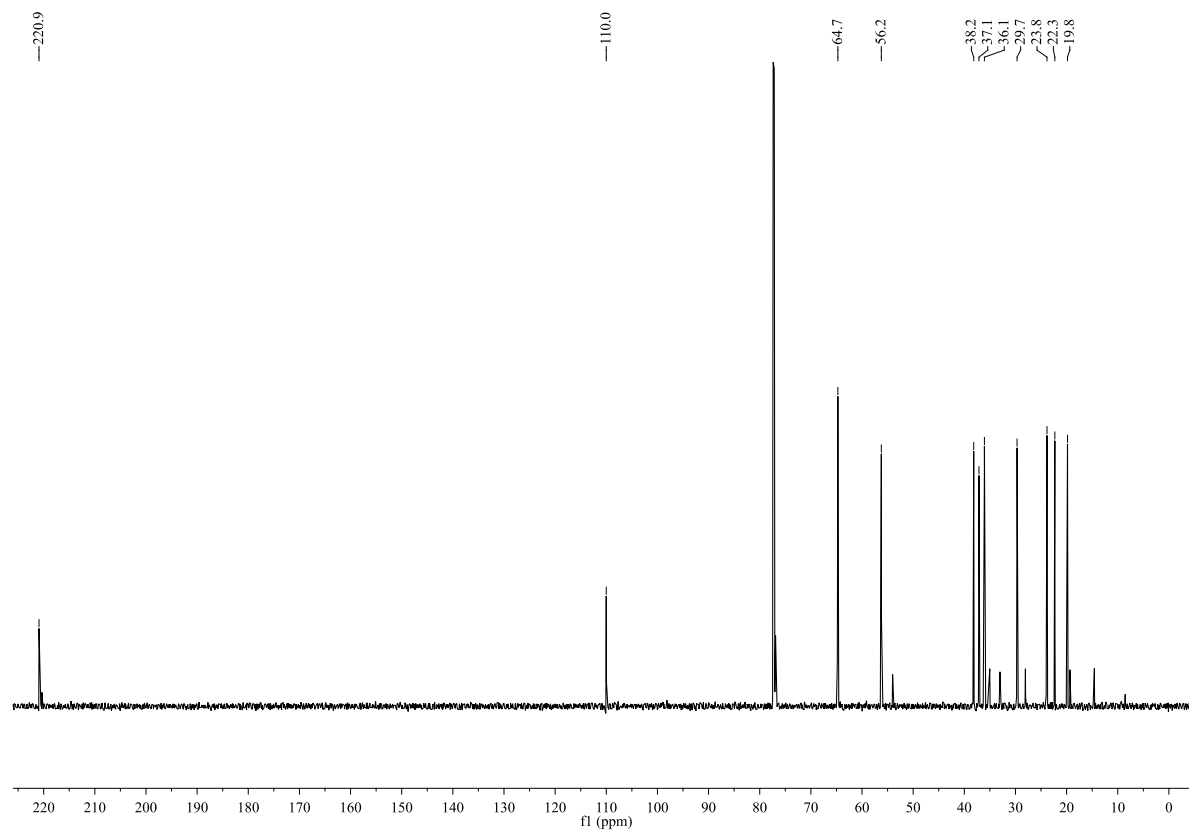
^{13}C NMR (CDCl_3 , 150 MHz):



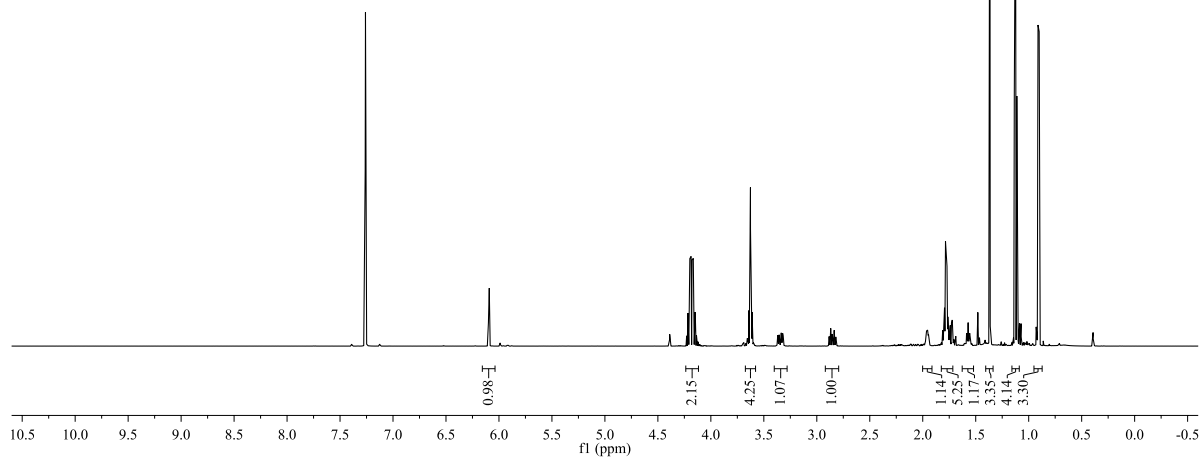
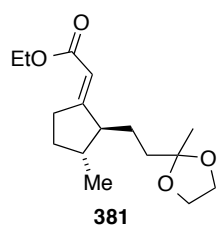
^1H NMR (CDCl_3 , 600 MHz):



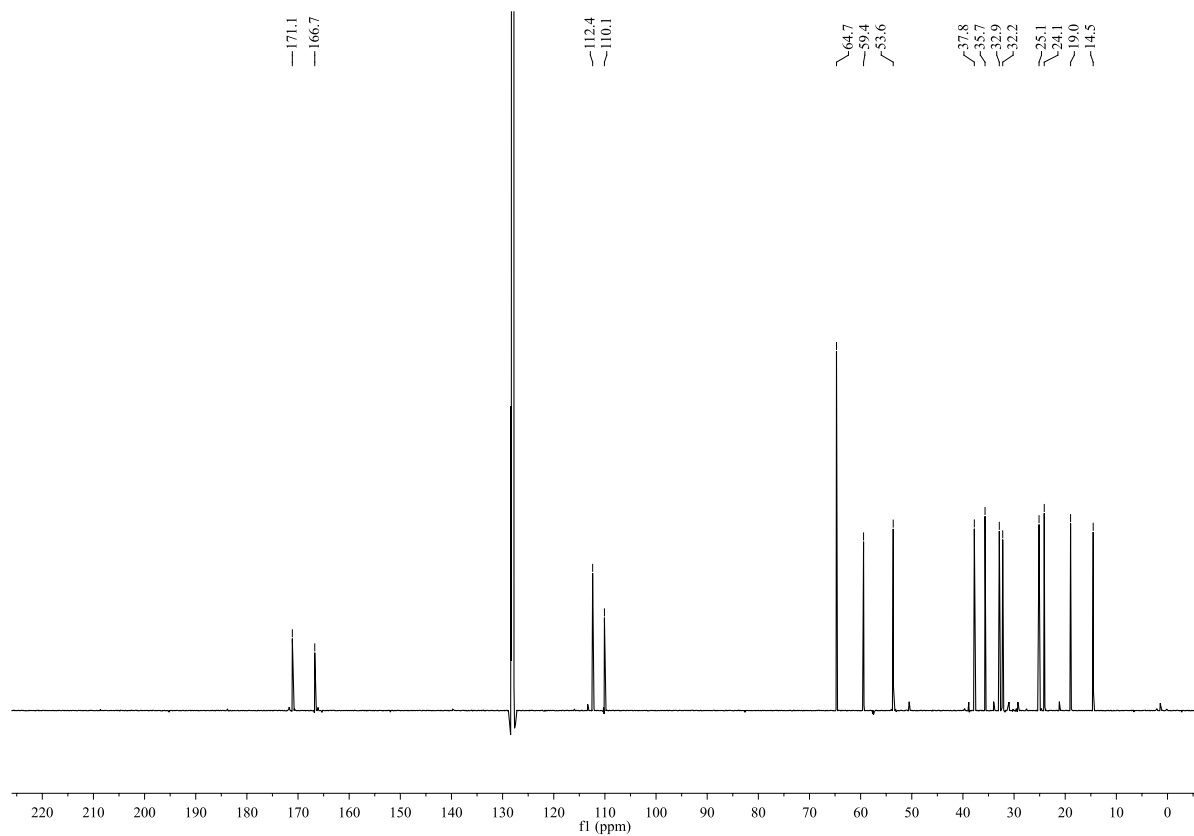
^{13}C NMR (CDCl_3 , 150 MHz):



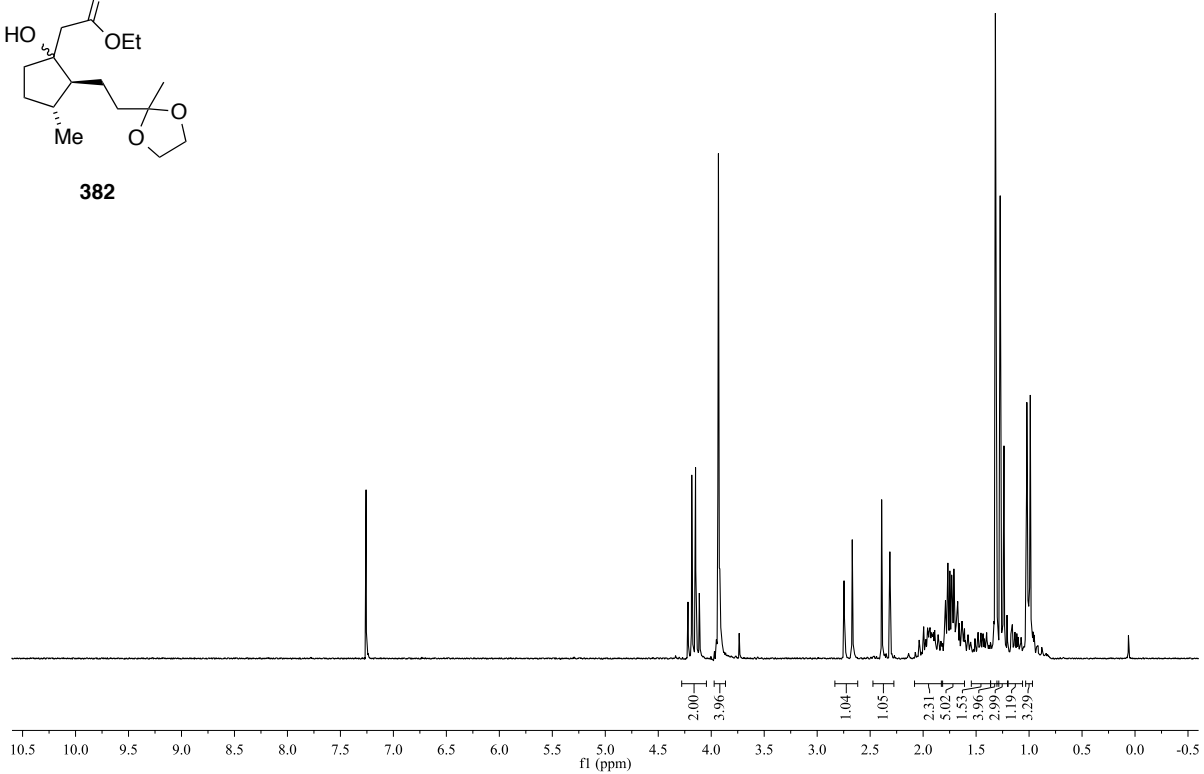
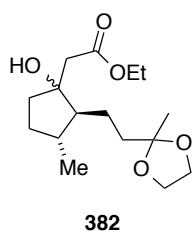
^1H NMR (C_6D_6 , 600 MHz):



^{13}C NMR (C_6D_6 , 150 MHz):

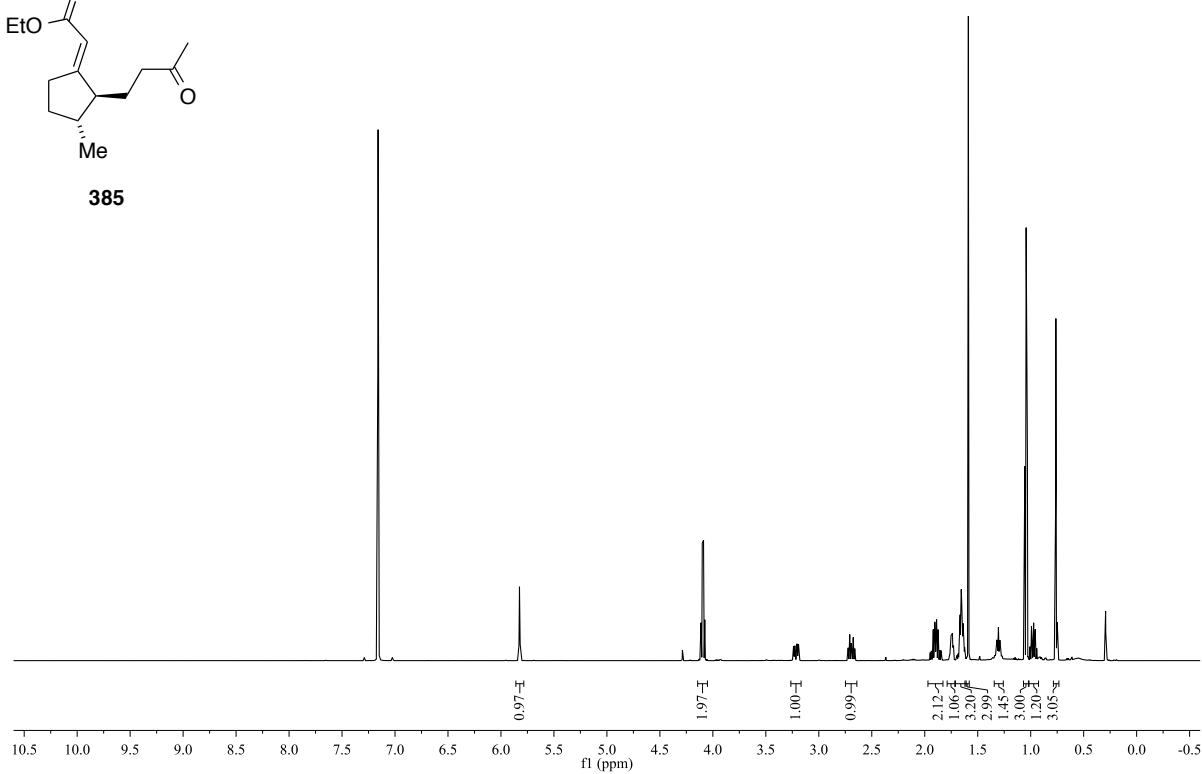
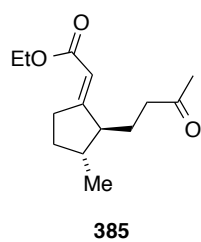


^1H NMR (CDCl_3 , 200 MHz):

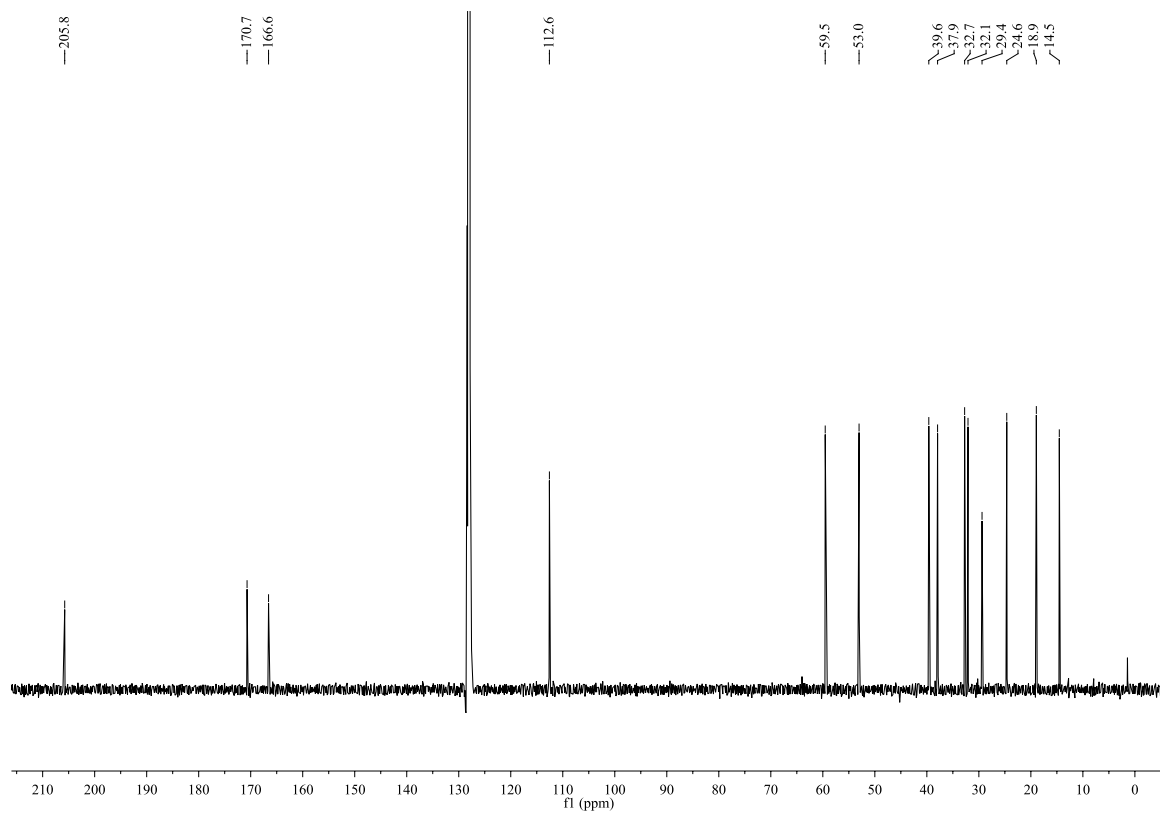


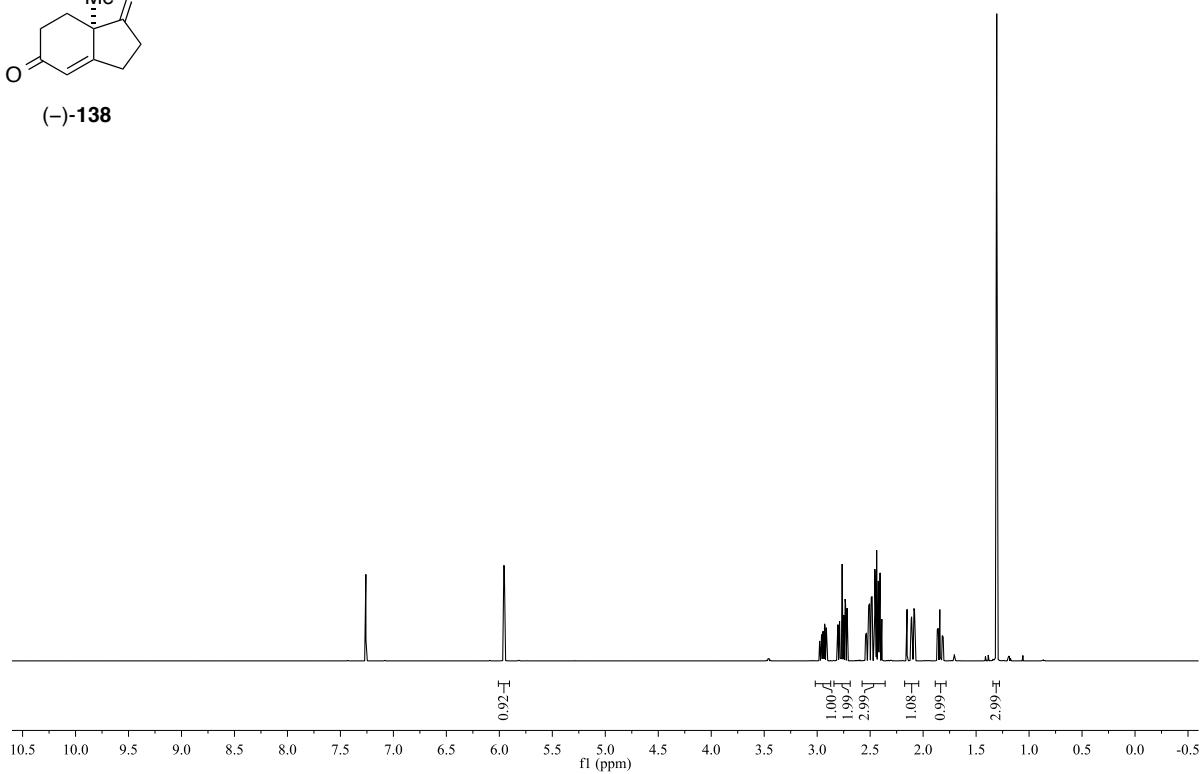
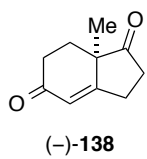
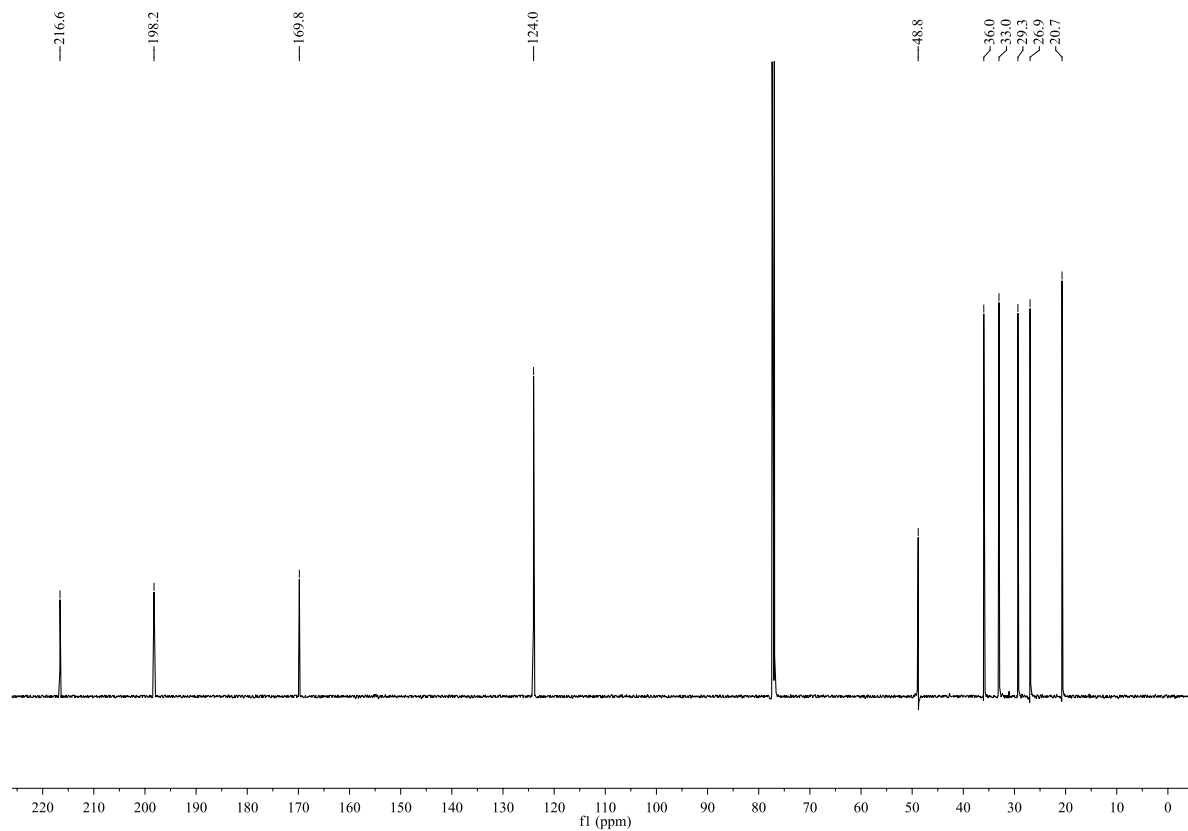
^{13}C NMR: *not recorded due to decomposition of substance **382** in the NMR solvent.*

^1H NMR (C_6D_6 , 600 MHz):

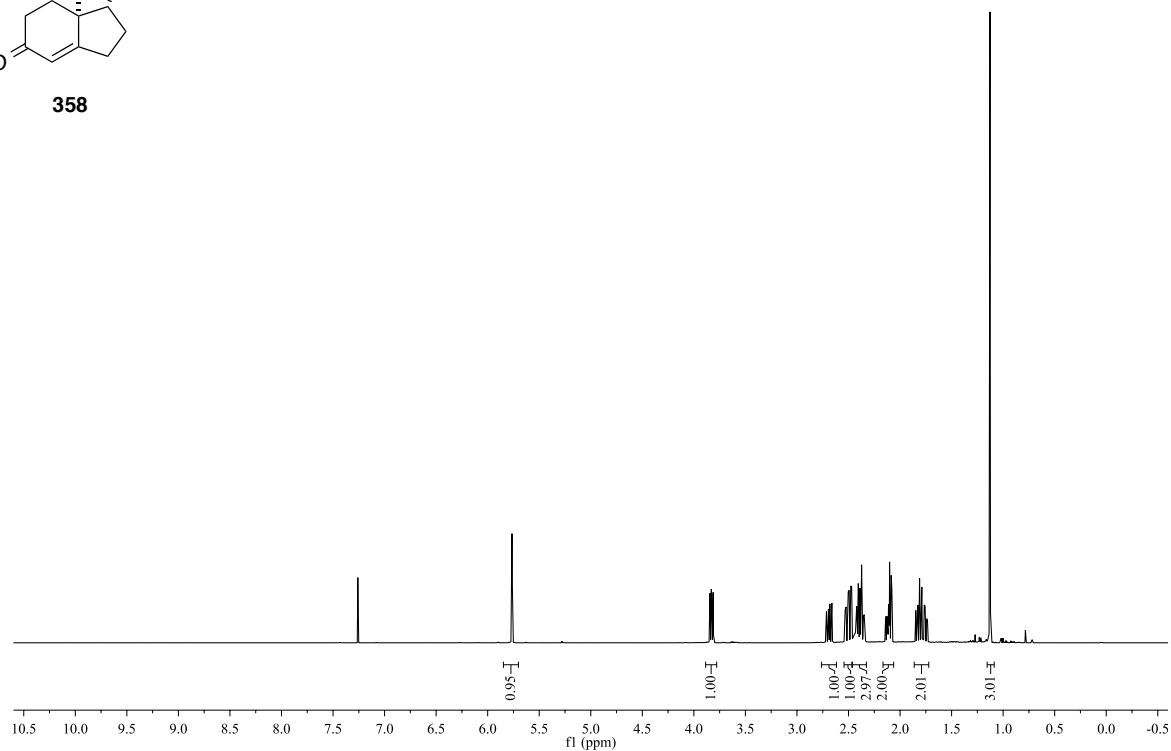
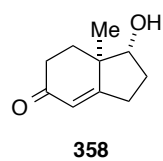


^{13}C NMR (C_6D_6 , 150 MHz):

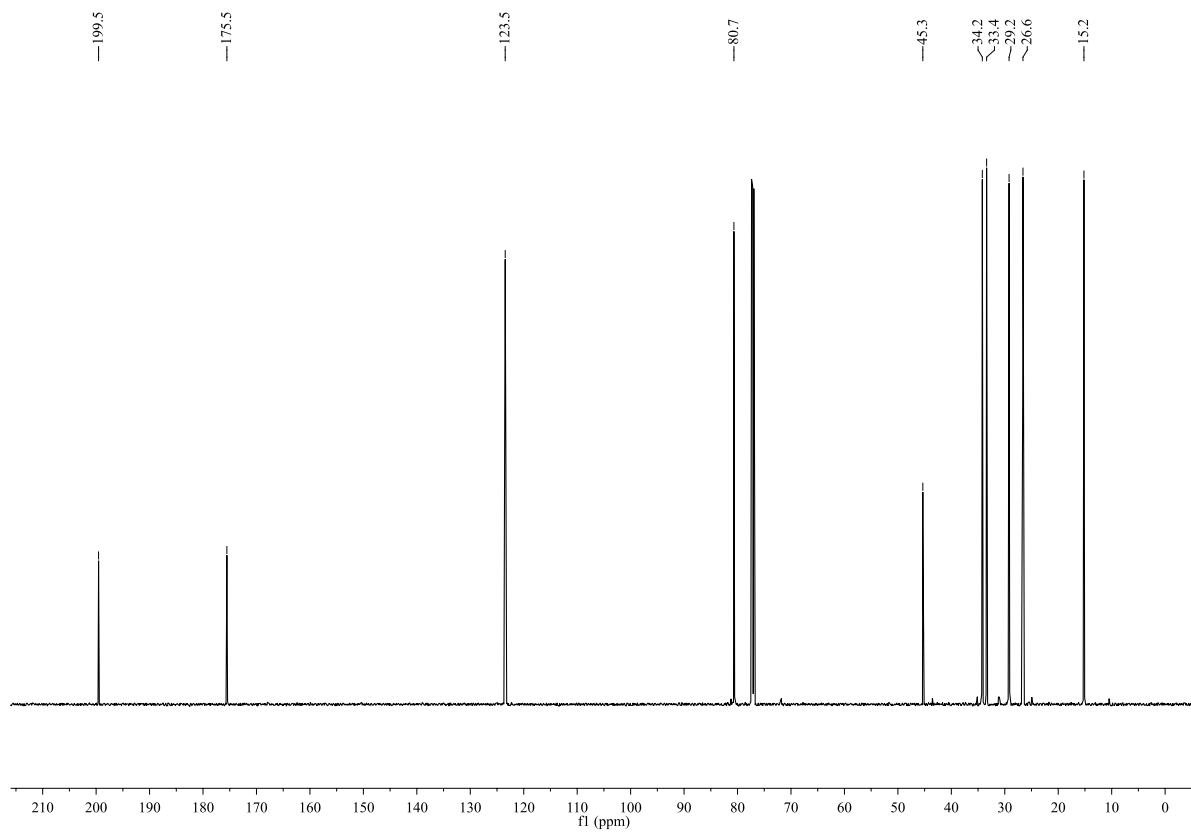


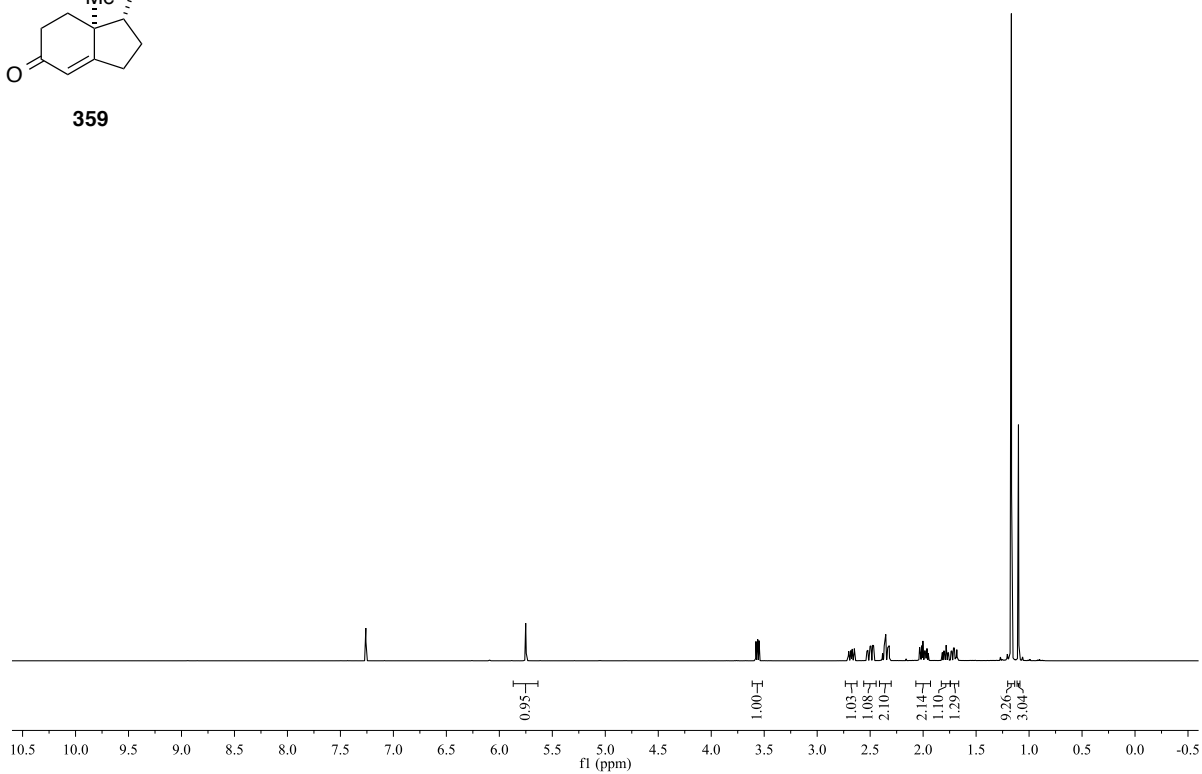
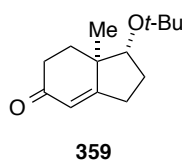
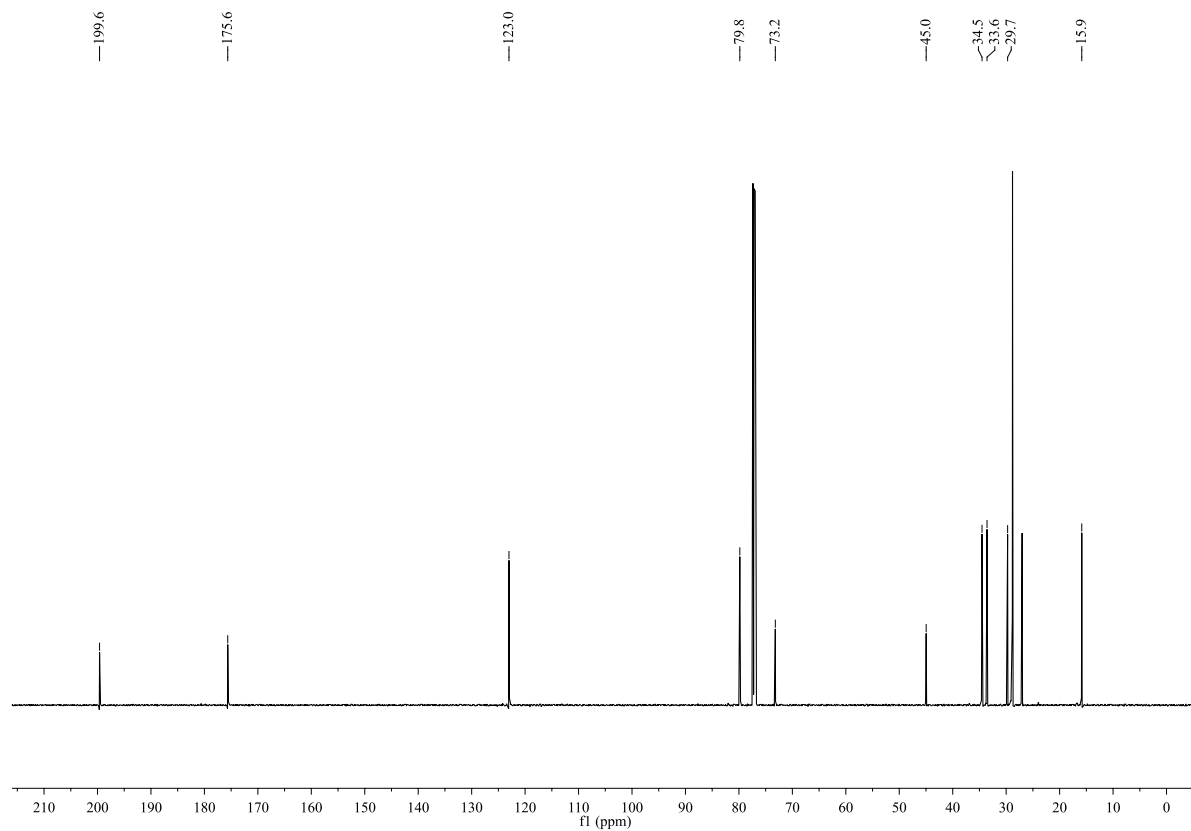
^1H NMR (CDCl_3 , 600 MHz): ^{13}C NMR (CDCl_3 , 150 MHz):

^1H NMR (CDCl_3 , 600 MHz):

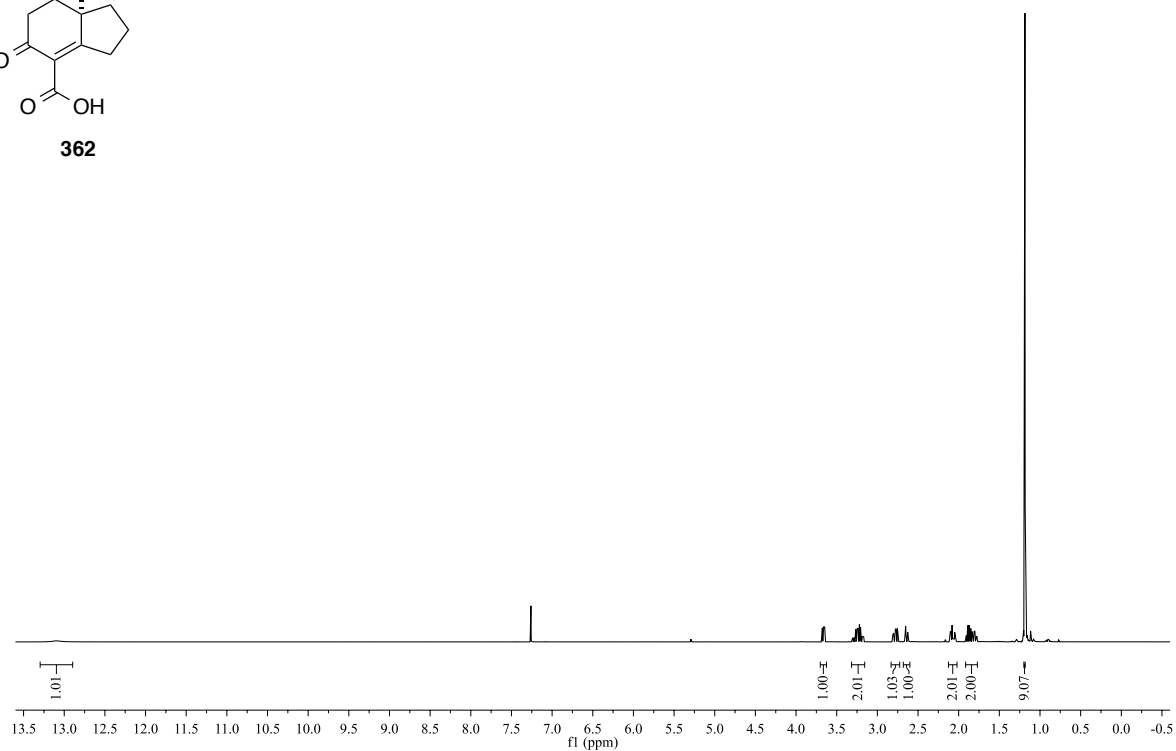
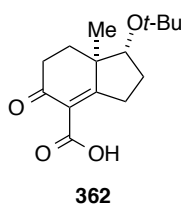


^{13}C NMR (CDCl_3 , 150 MHz):

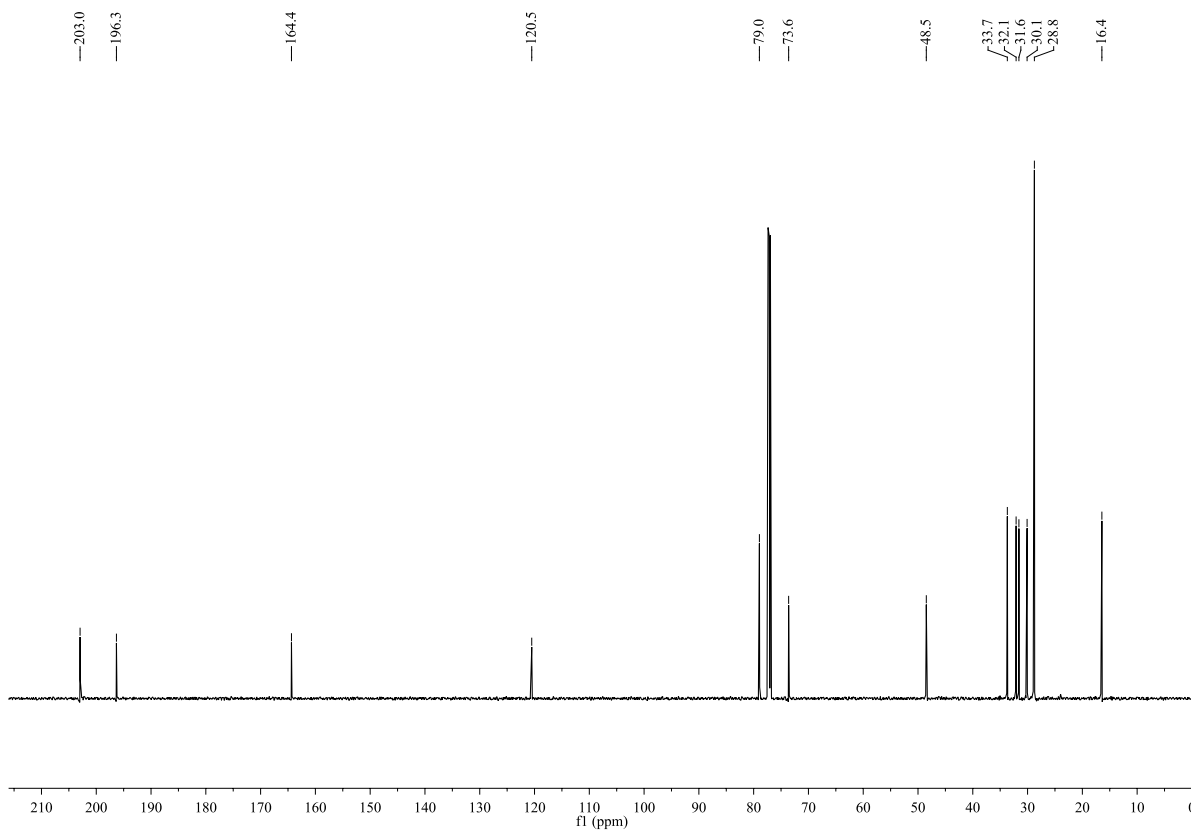


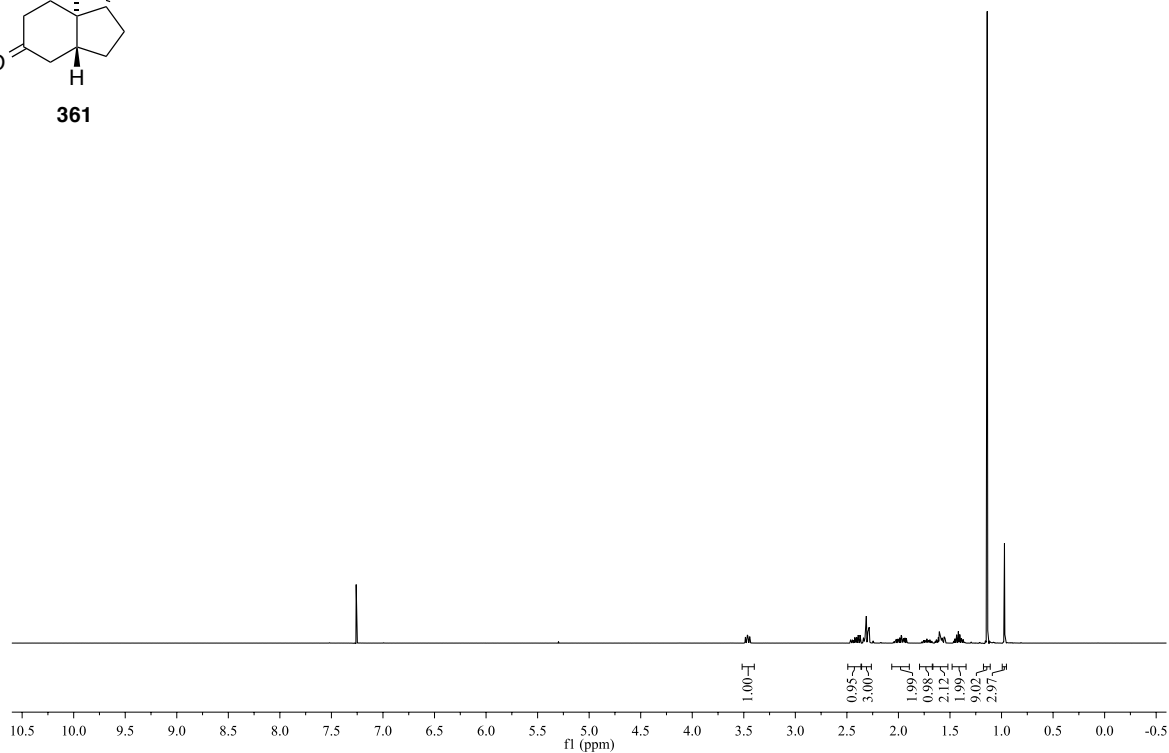
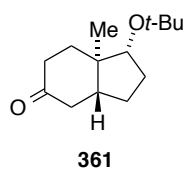
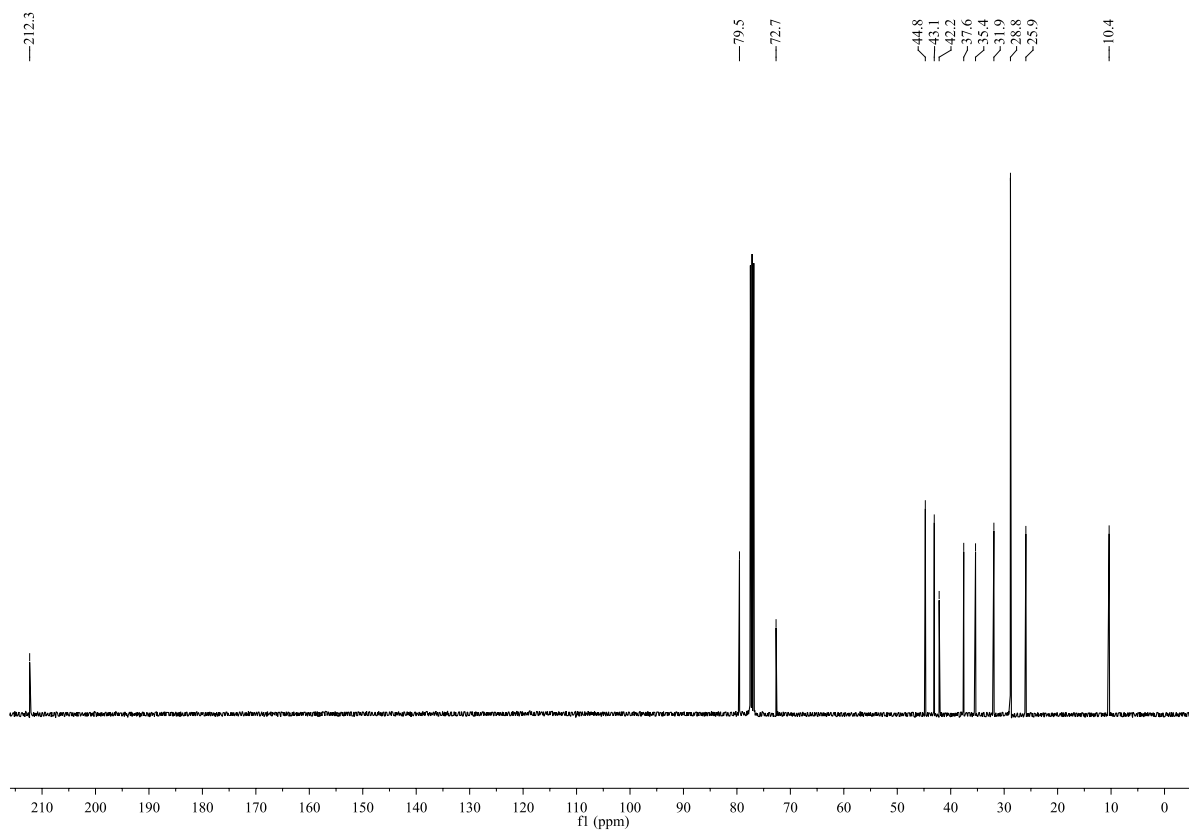
^1H NMR (CDCl_3 , 600 MHz): ^{13}C NMR (CDCl_3 , 150 MHz):

^1H NMR (CDCl_3 , 600 MHz):

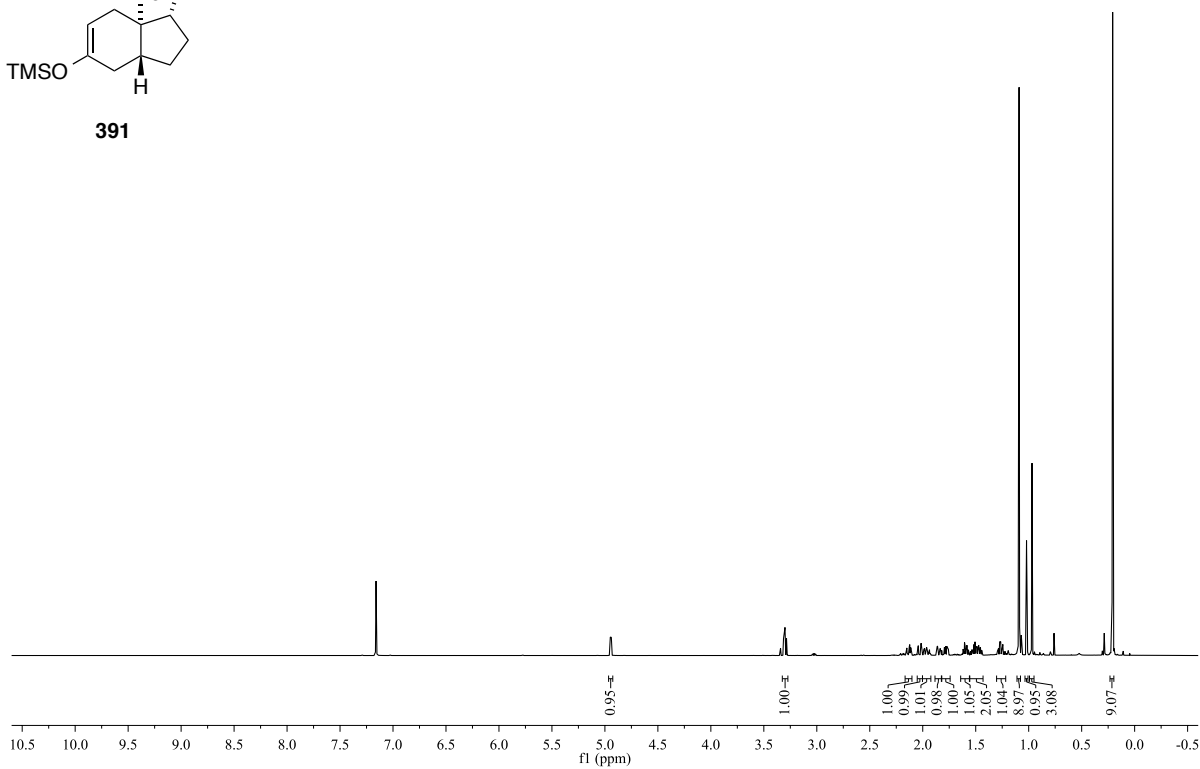
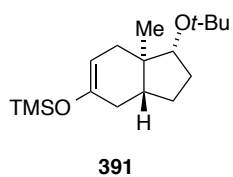


^{13}C NMR (CDCl_3 , 150 MHz):

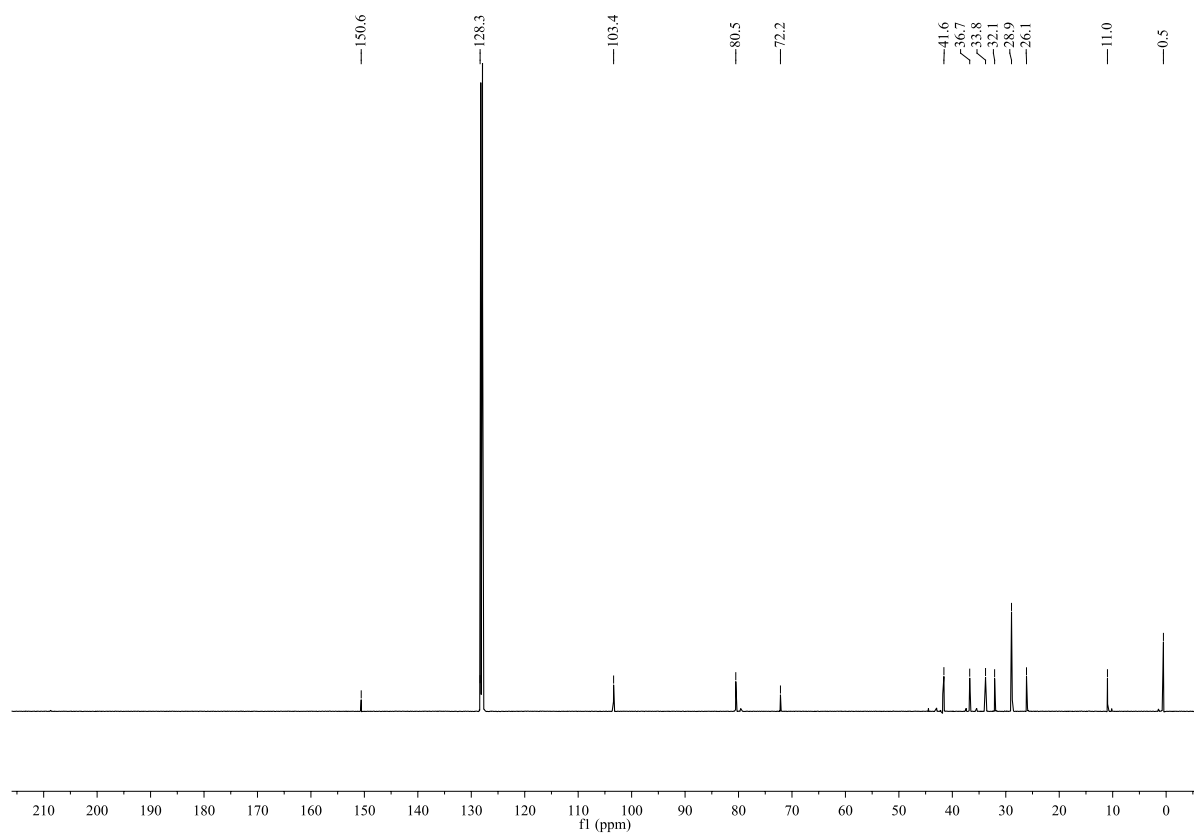


^1H NMR (CDCl_3 , 400 MHz): ^{13}C NMR (CDCl_3 , 100 MHz):

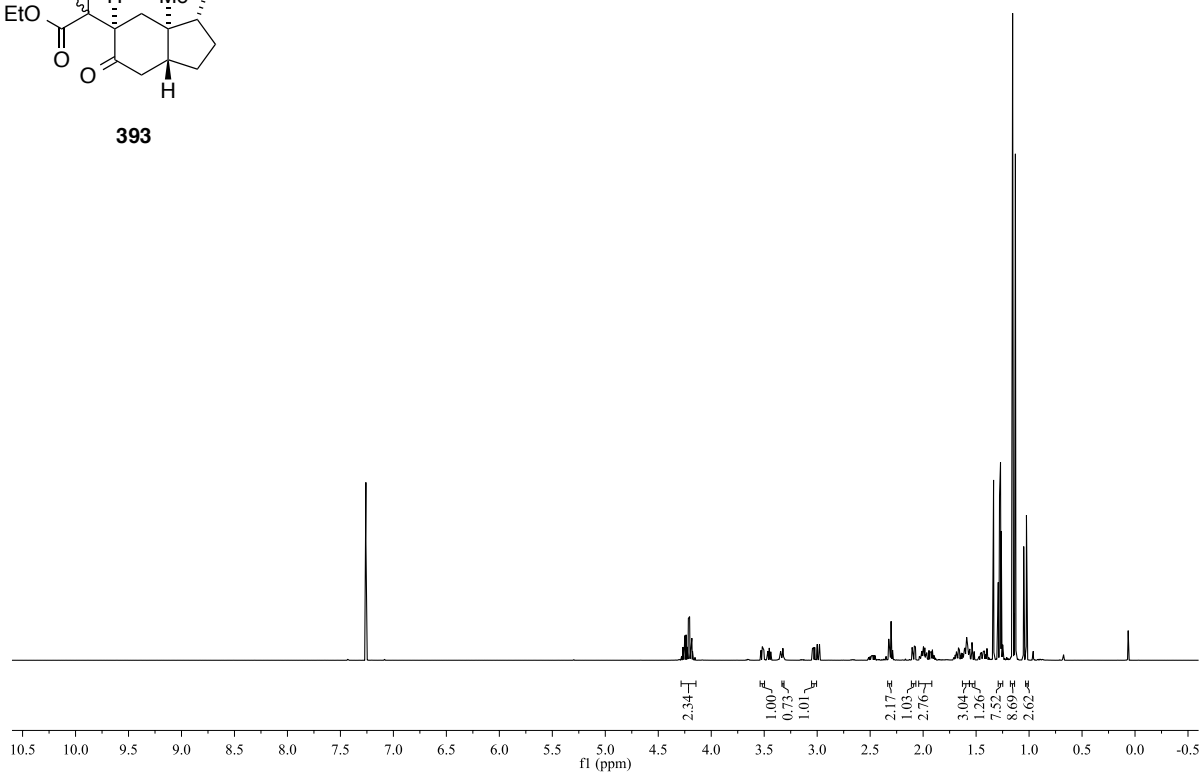
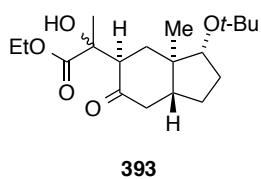
^1H NMR (C_6D_6 , 600 MHz):



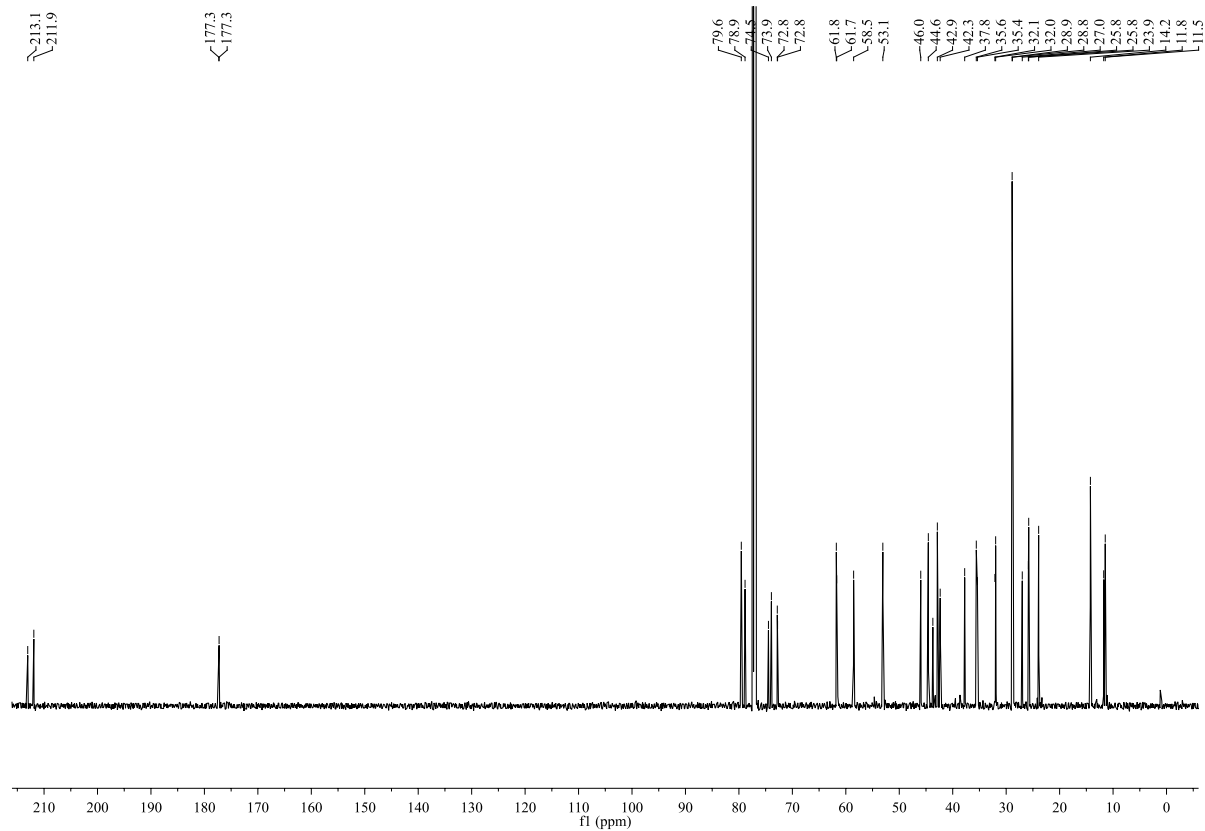
^{13}C NMR (C_6D_6 , 150 MHz):



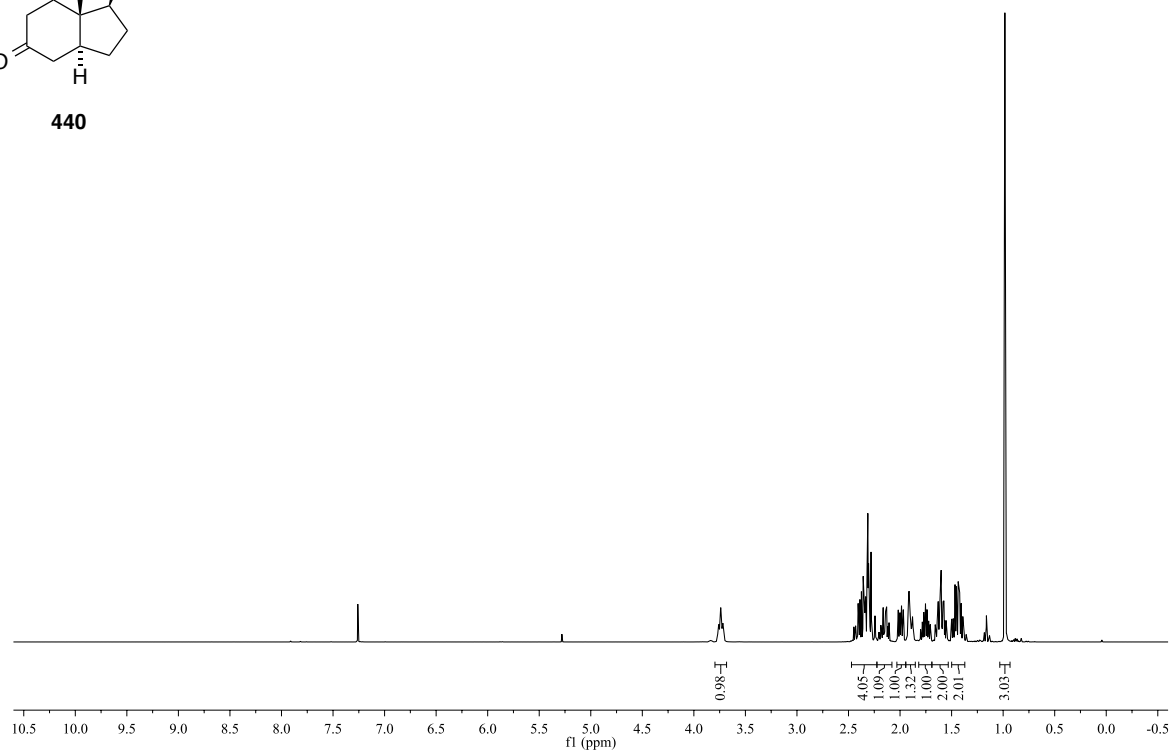
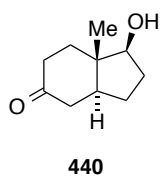
^1H NMR (C_6D_6 , 600 MHz):



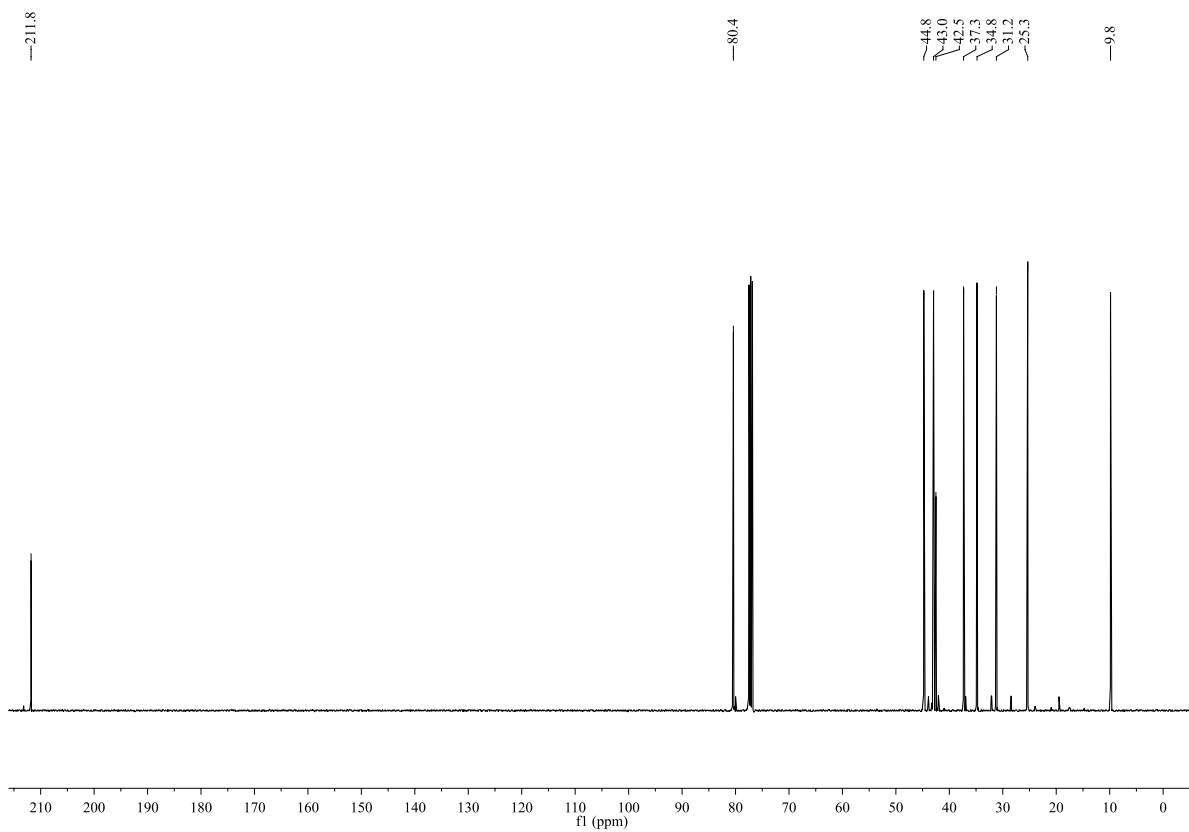
^{13}C NMR (C_6D_6 , 150 MHz):

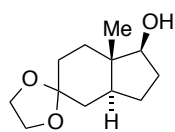
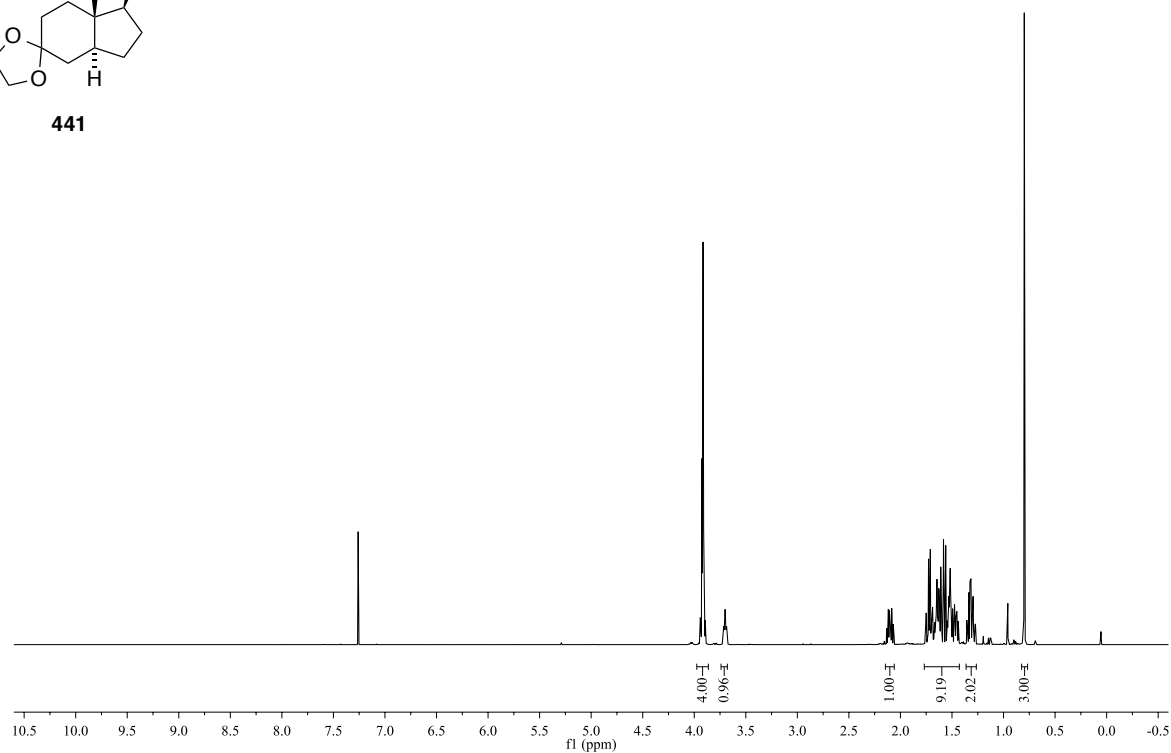
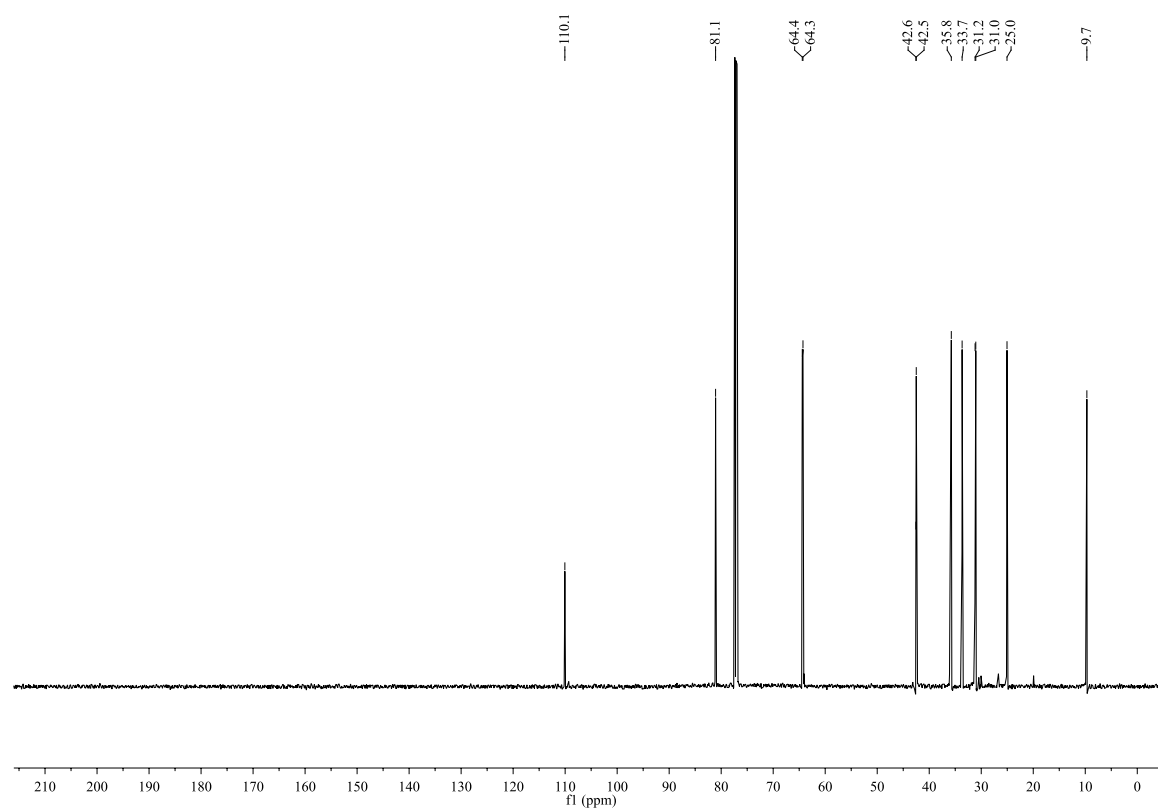


^1H NMR (CDCl_3 , 400 MHz):

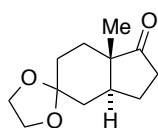


^{13}C NMR (CDCl_3 , 100 MHz):

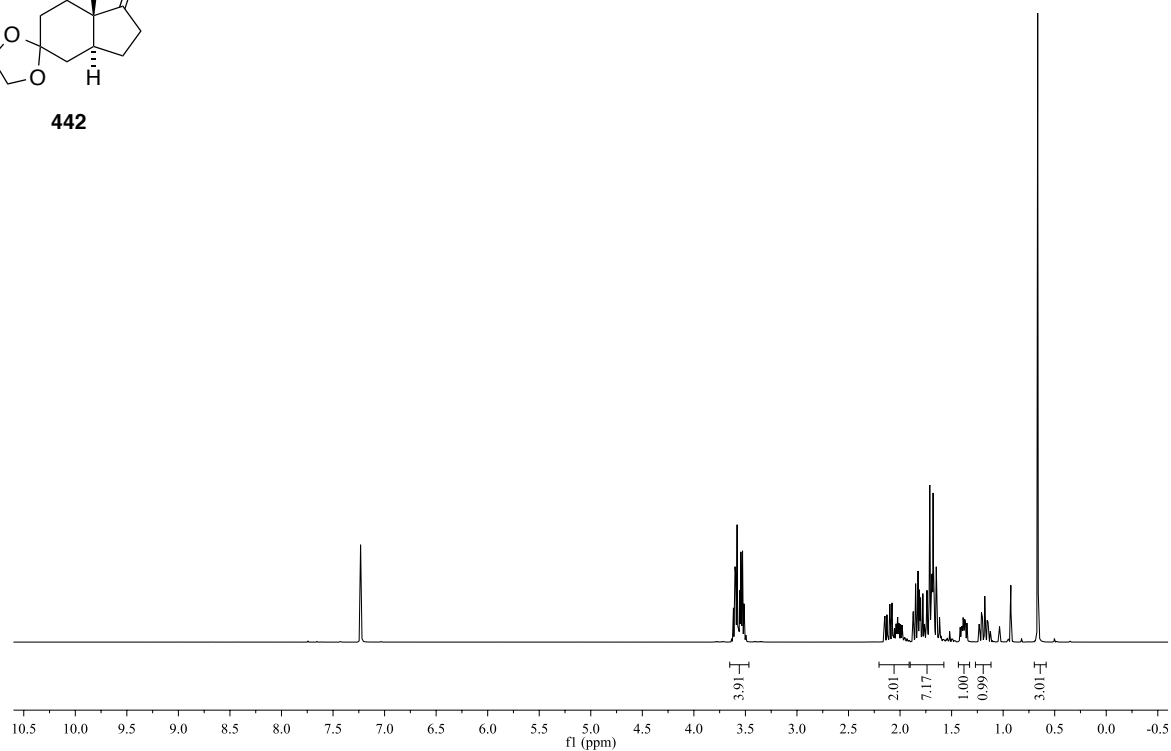


^1H NMR (CDCl_3 , 400 MHz):**441** ^{13}C NMR (CDCl_3 , 100 MHz):

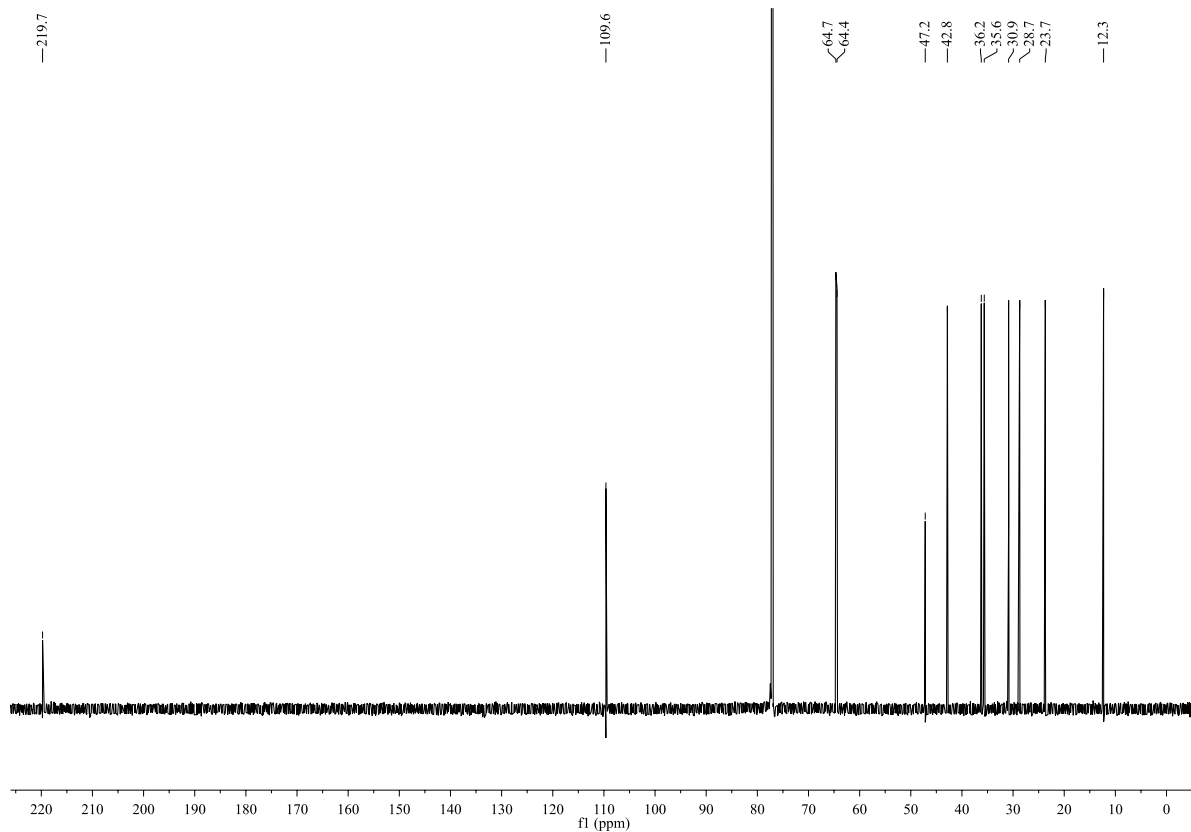
^1H NMR (CDCl_3 , 400 MHz):

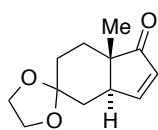
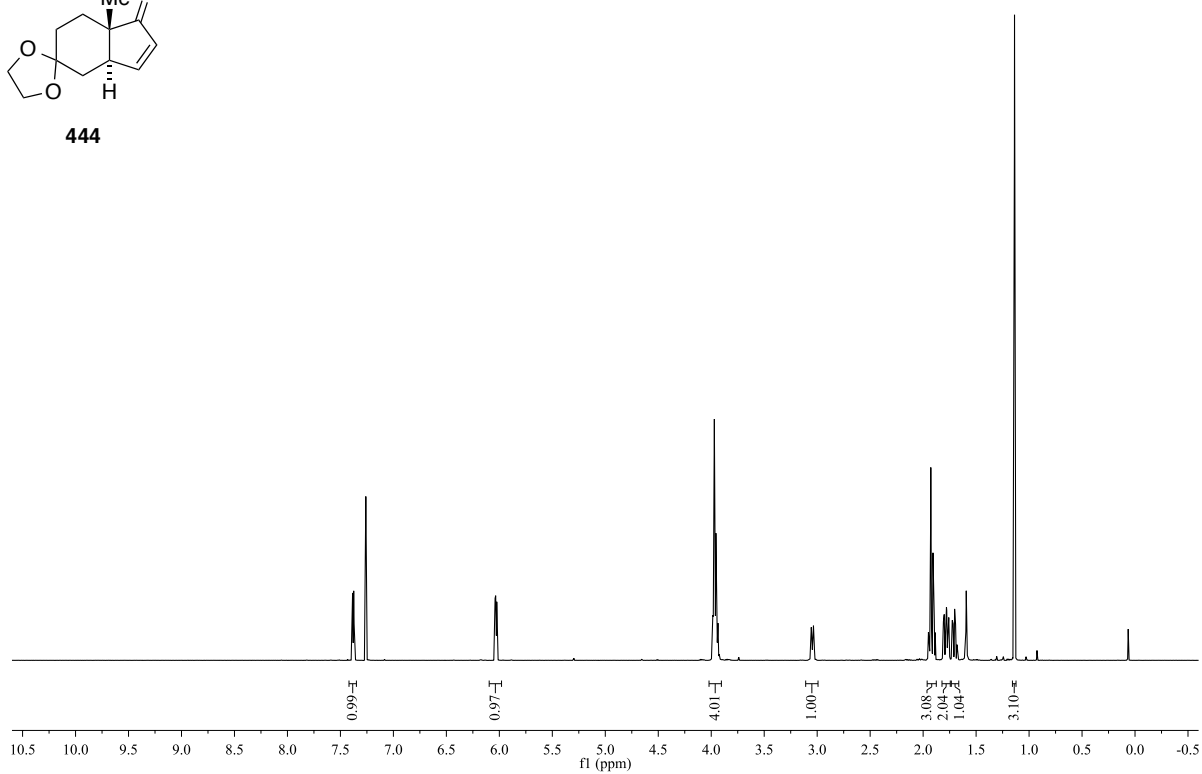
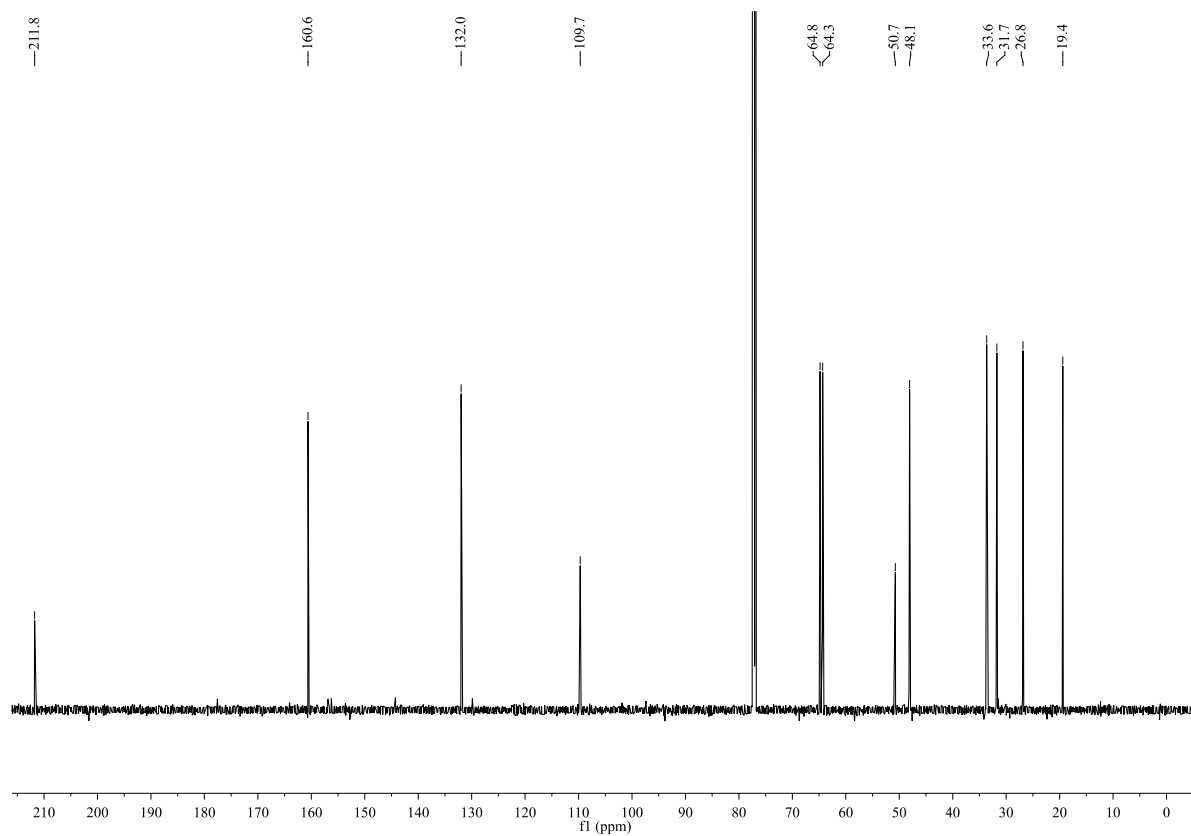


442

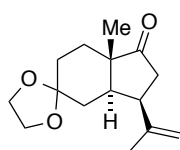


^{13}C NMR (CDCl_3 , 150 MHz):

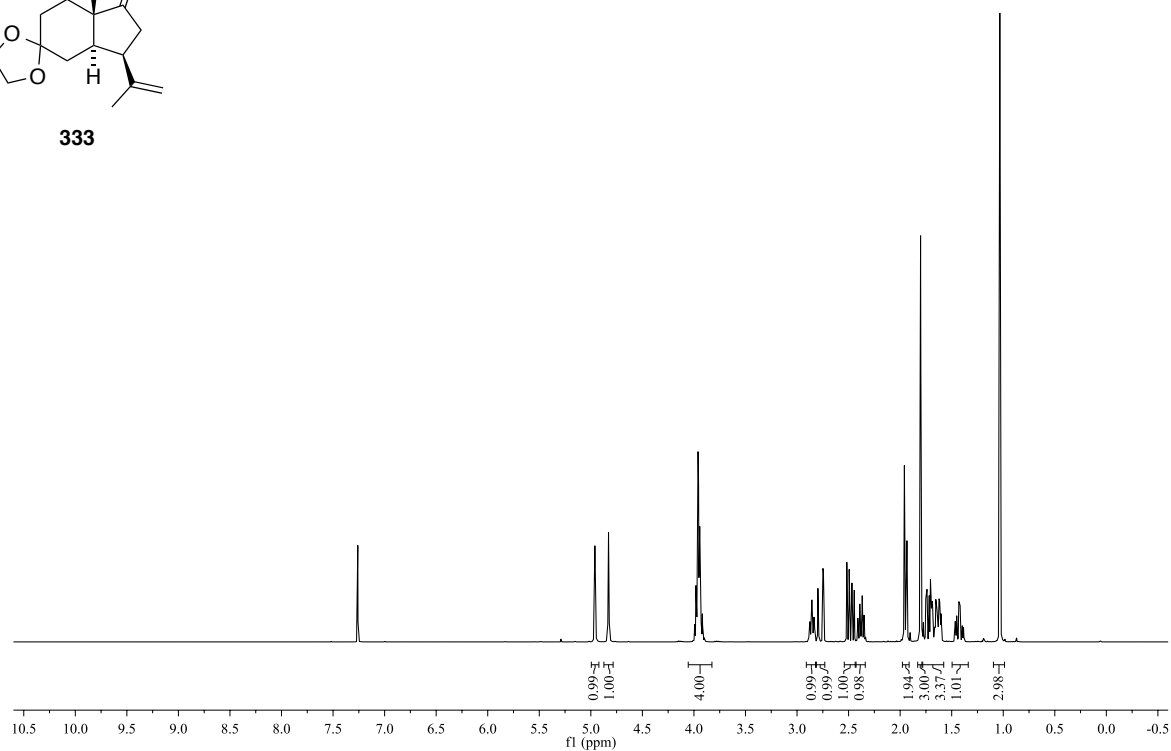


^1H NMR (CDCl_3 , 600 MHz):**444** ^{13}C NMR (CDCl_3 , 150 MHz):

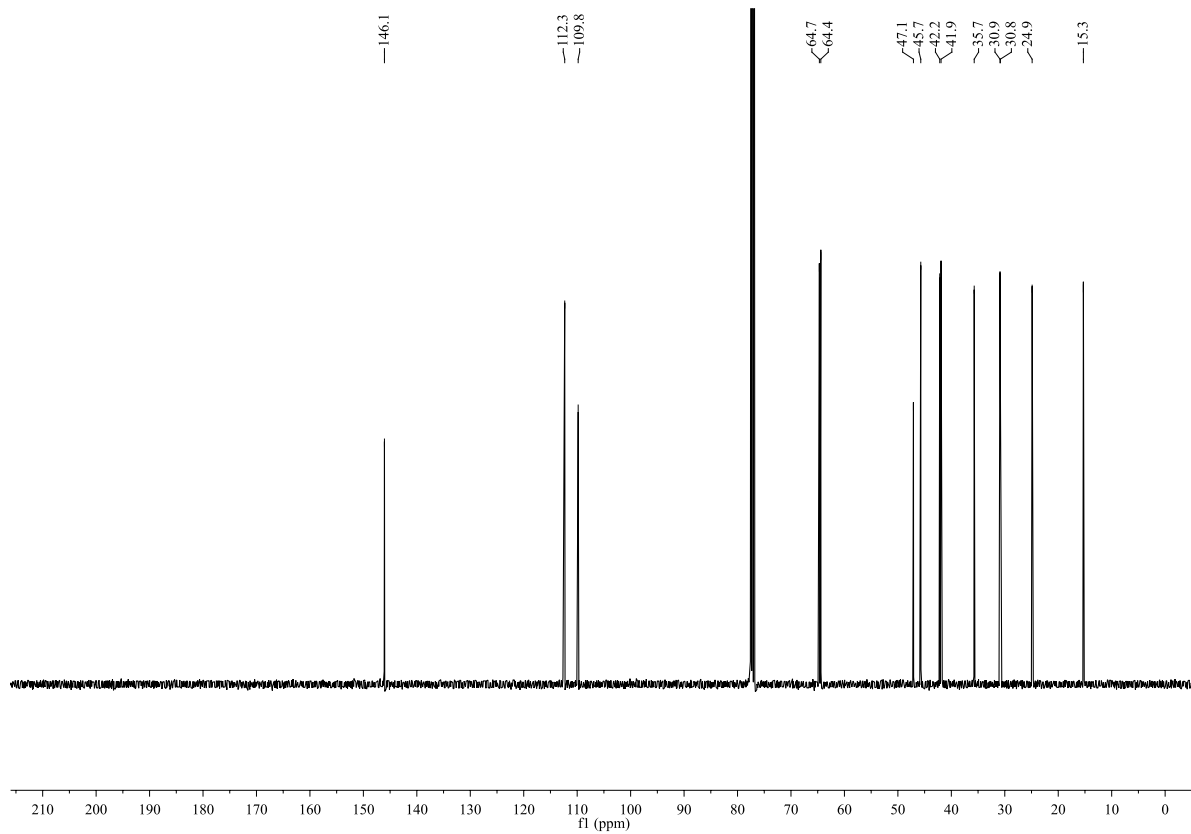
^1H NMR (CDCl_3 , 400 MHz):



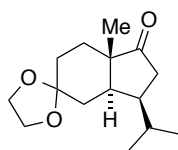
333



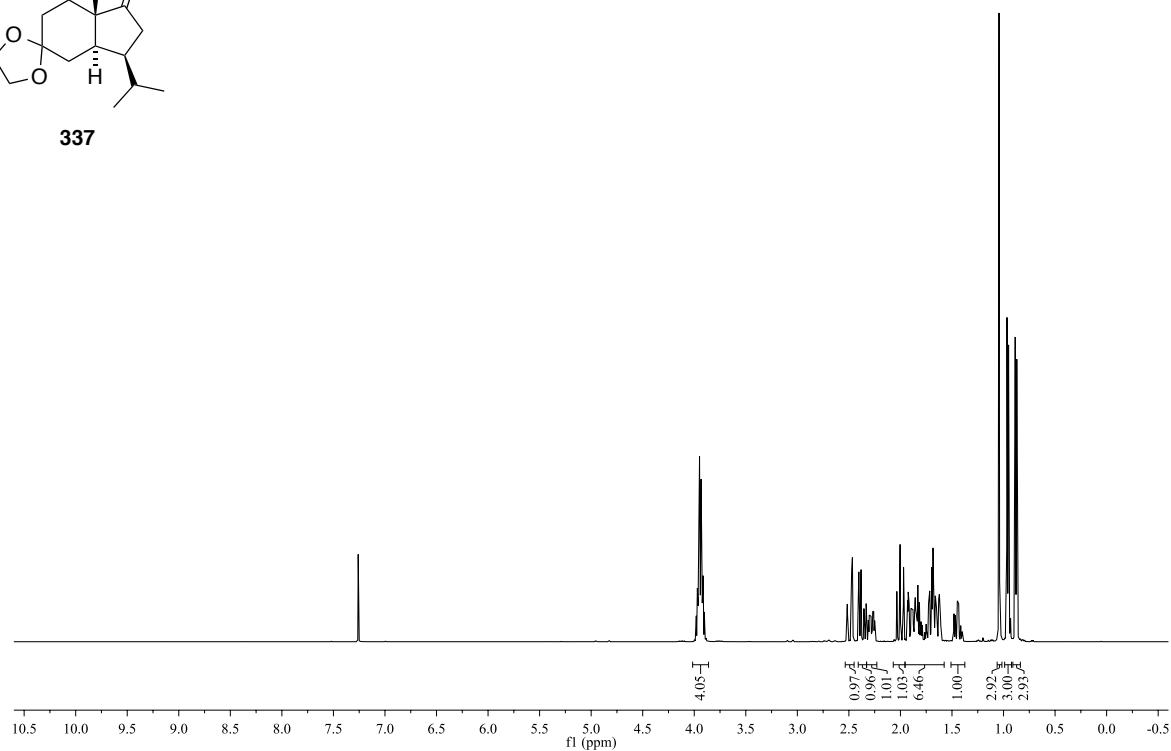
^{13}C NMR (CDCl_3 , 150 MHz):



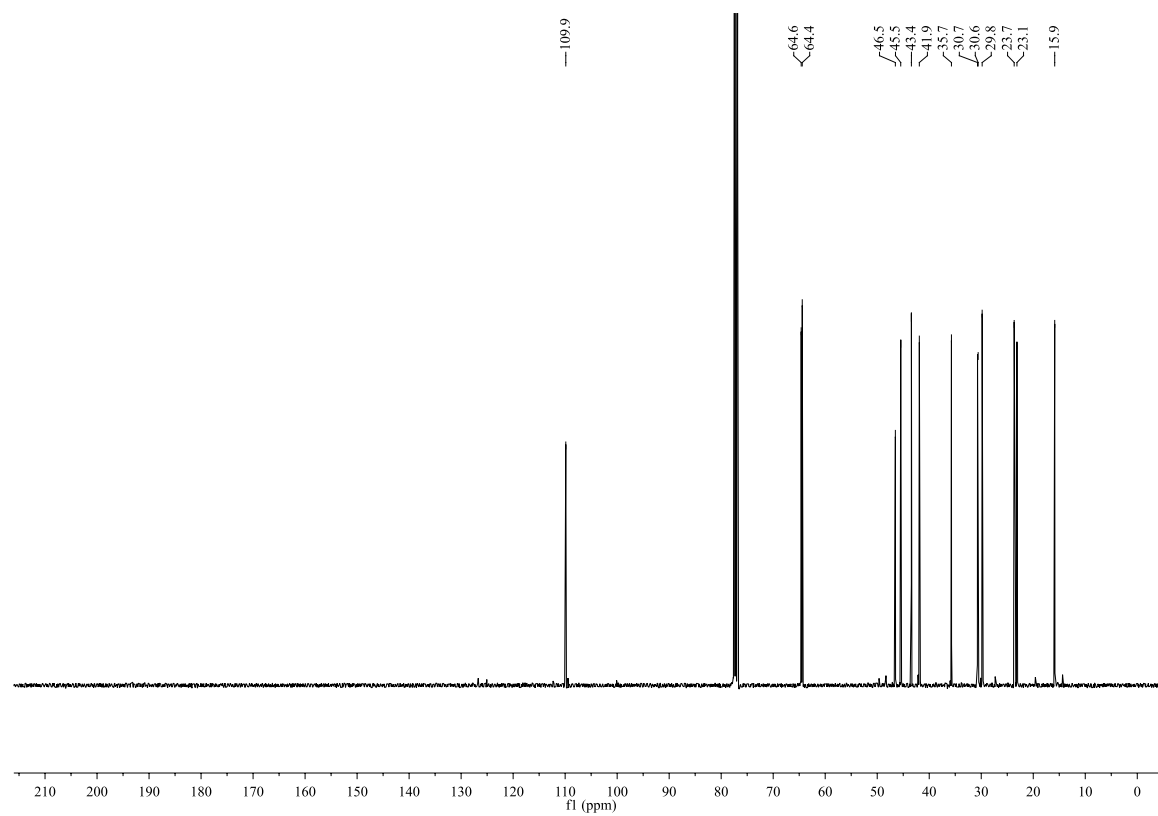
^1H NMR (CDCl_3 , 400 MHz):



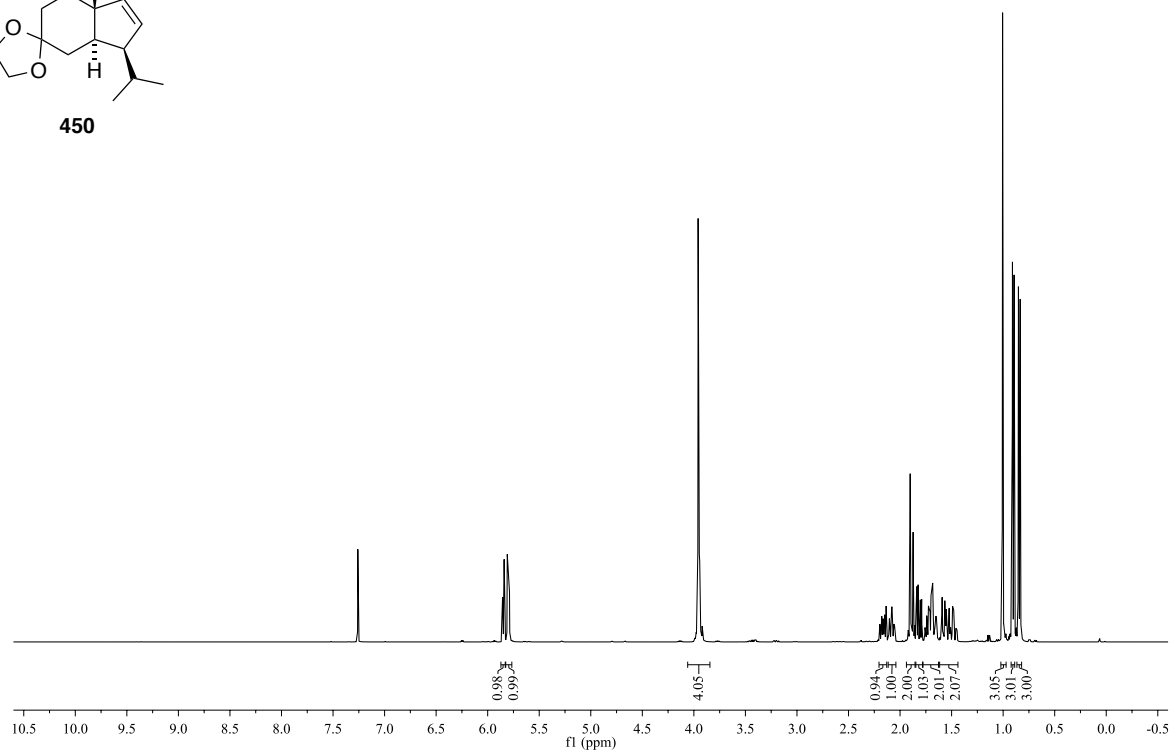
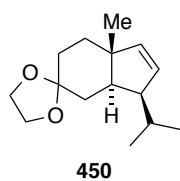
337



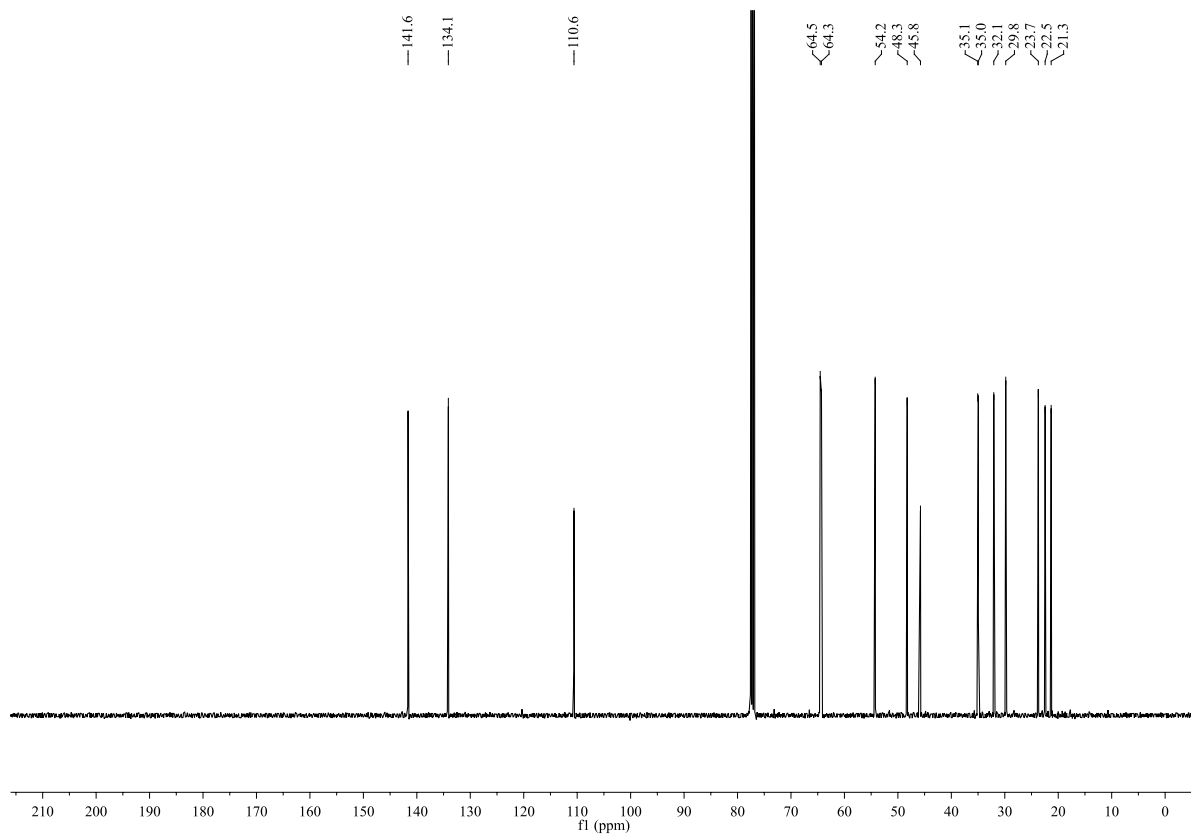
^{13}C NMR (CDCl_3 , 100 MHz):

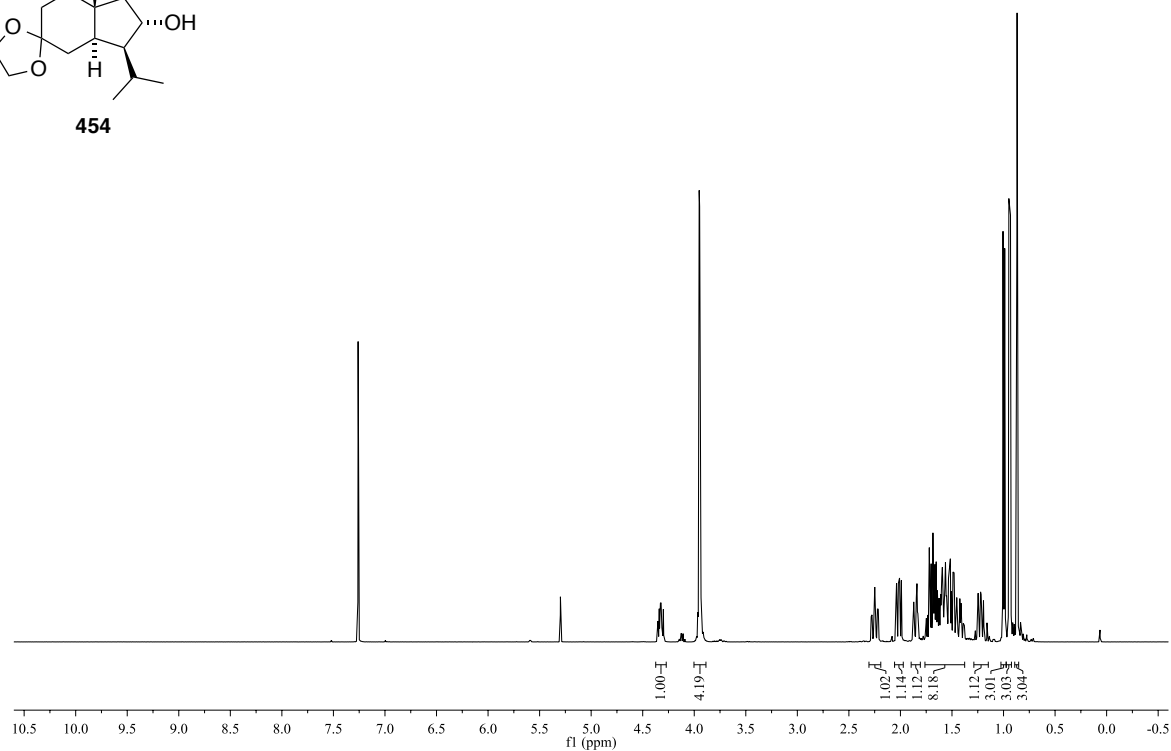
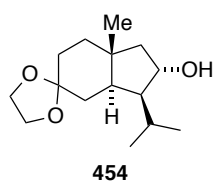
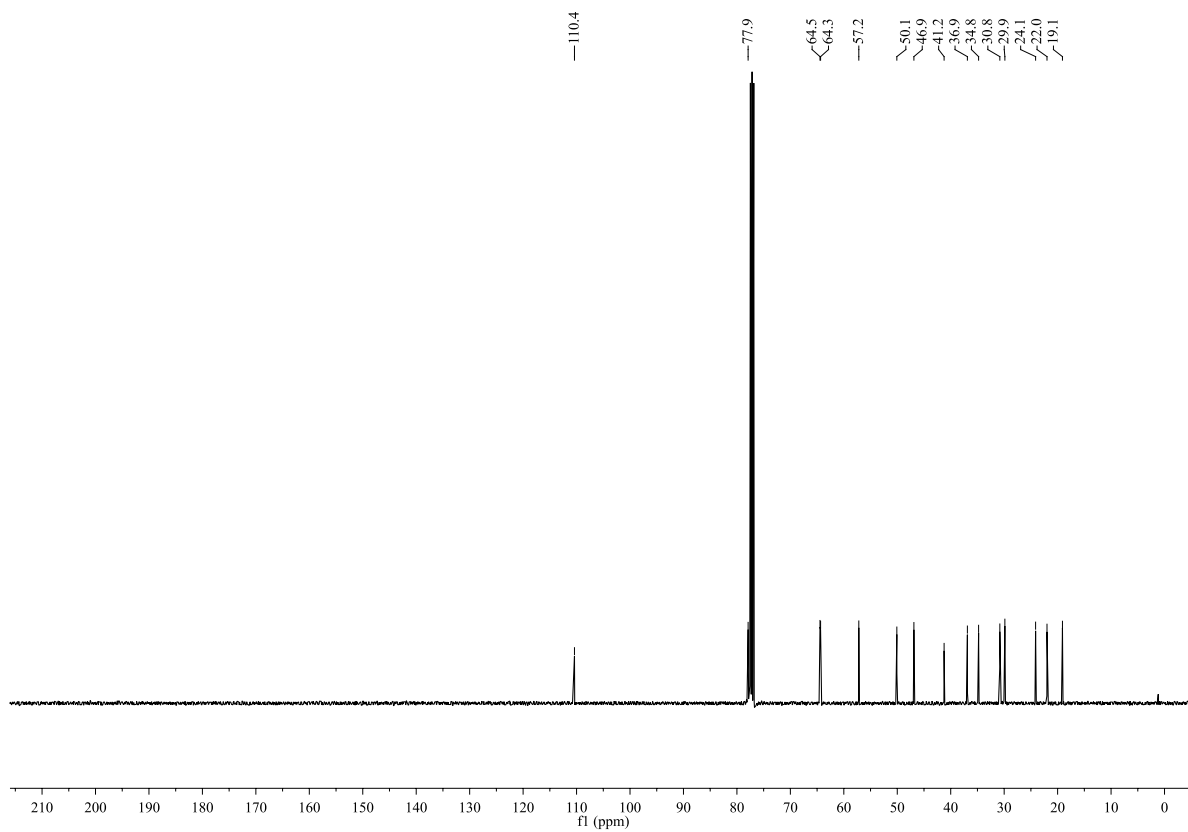


^1H NMR (CDCl_3 , 400 MHz):

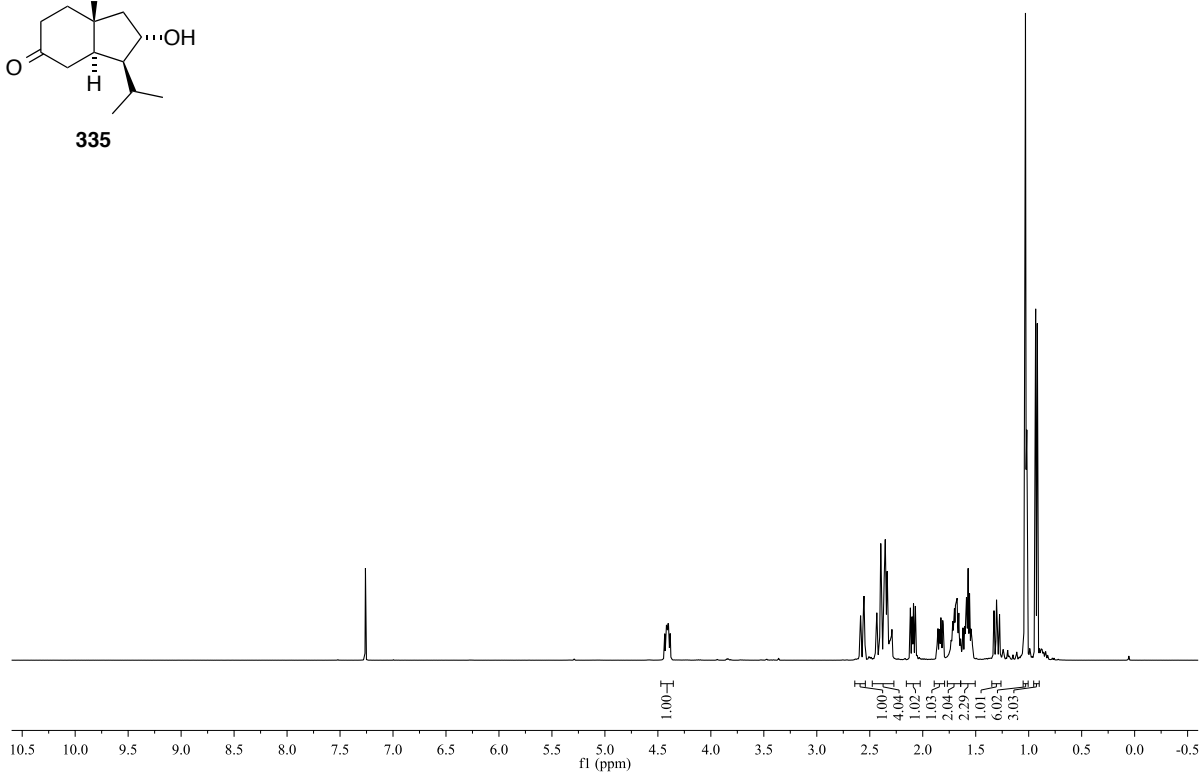
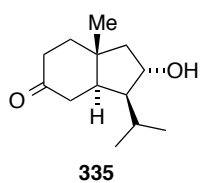


^{13}C NMR (CDCl_3 , 100 MHz):

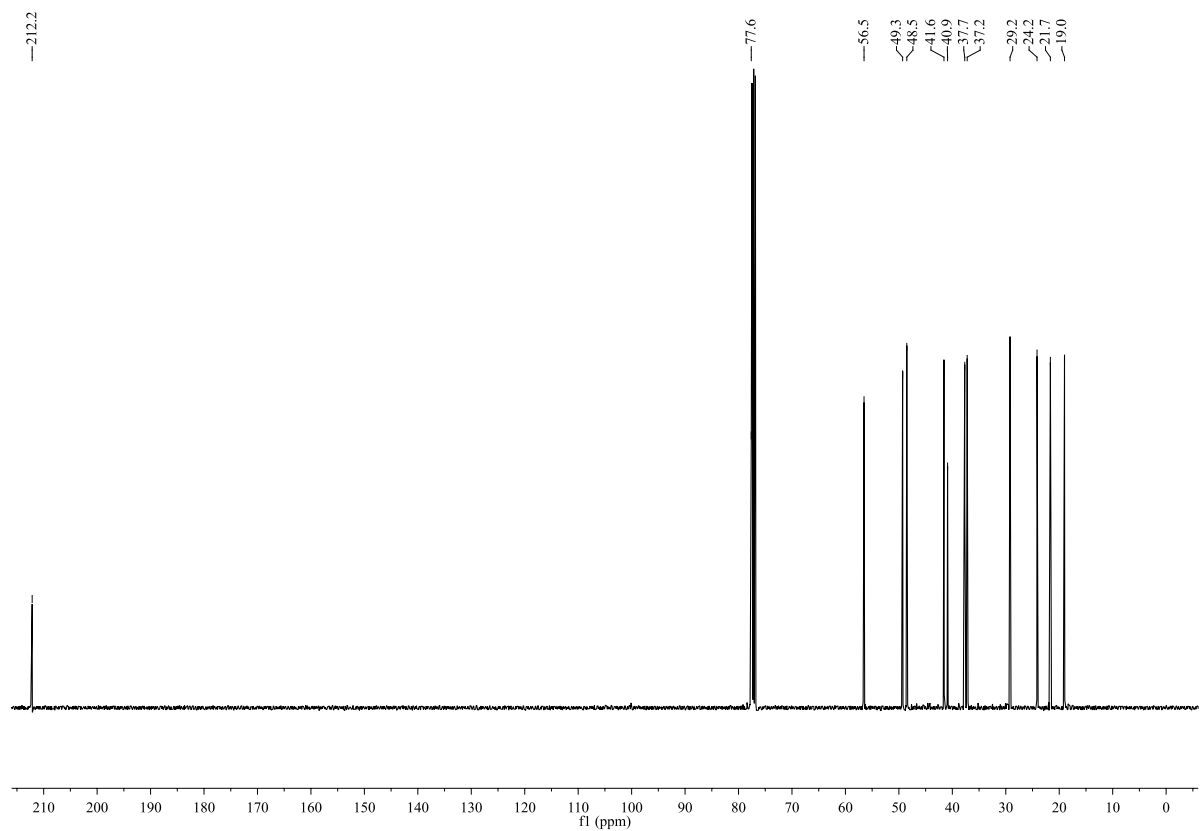


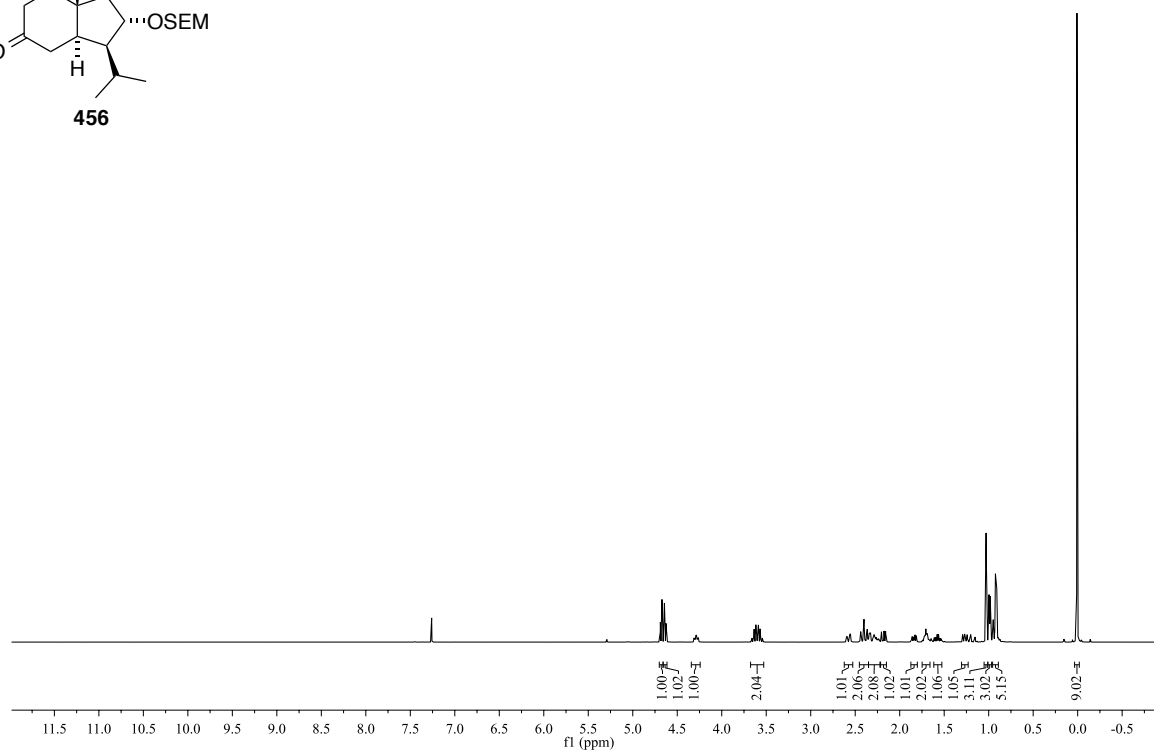
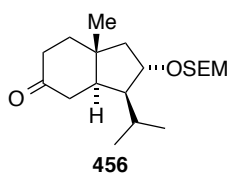
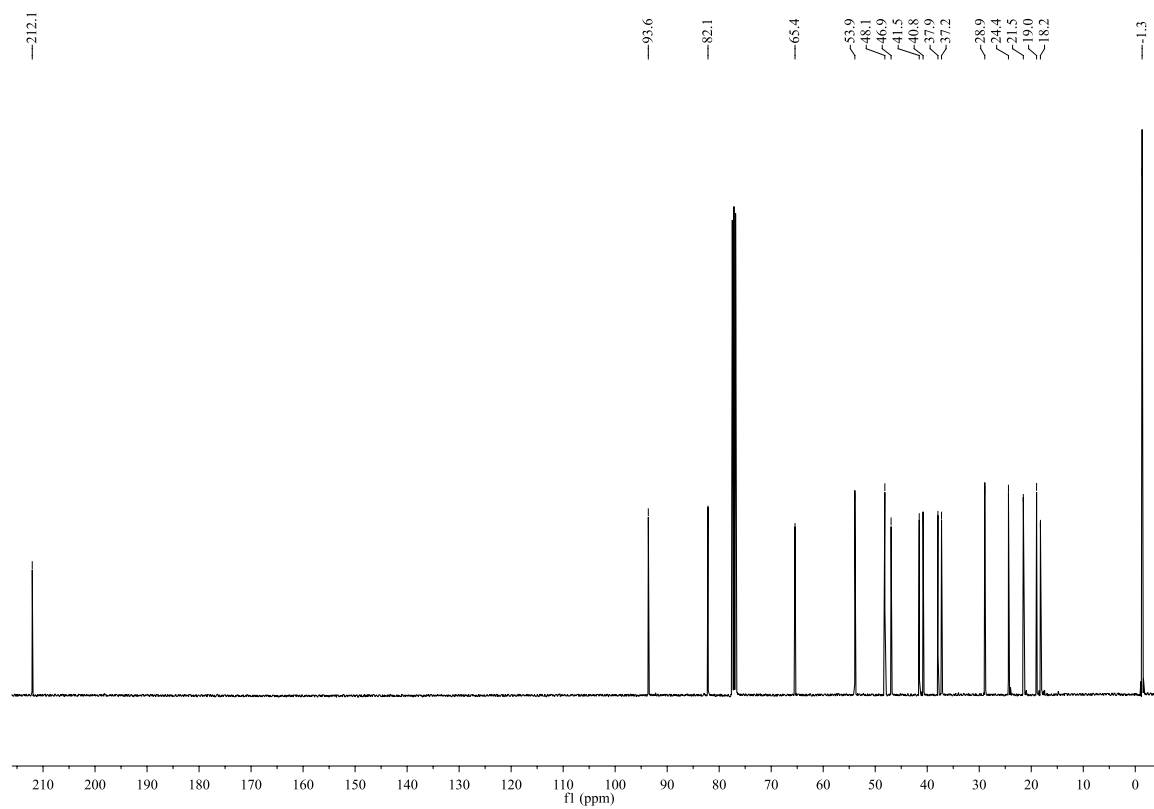
^1H NMR (CDCl_3 , 400 MHz): ^{13}C NMR (CDCl_3 , 100 MHz):

^1H NMR (CDCl_3 , 400 MHz):

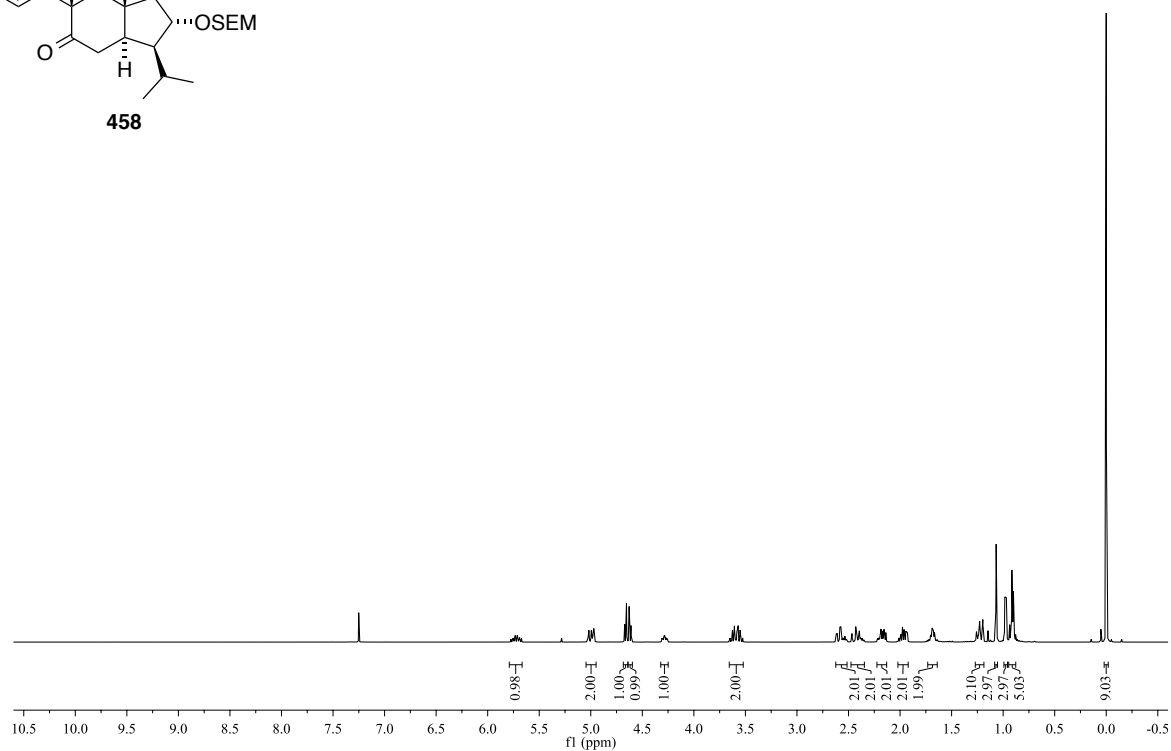
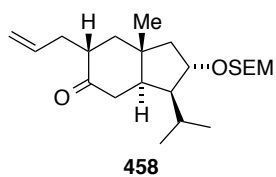


^{13}C NMR (CDCl_3 , 100 MHz):

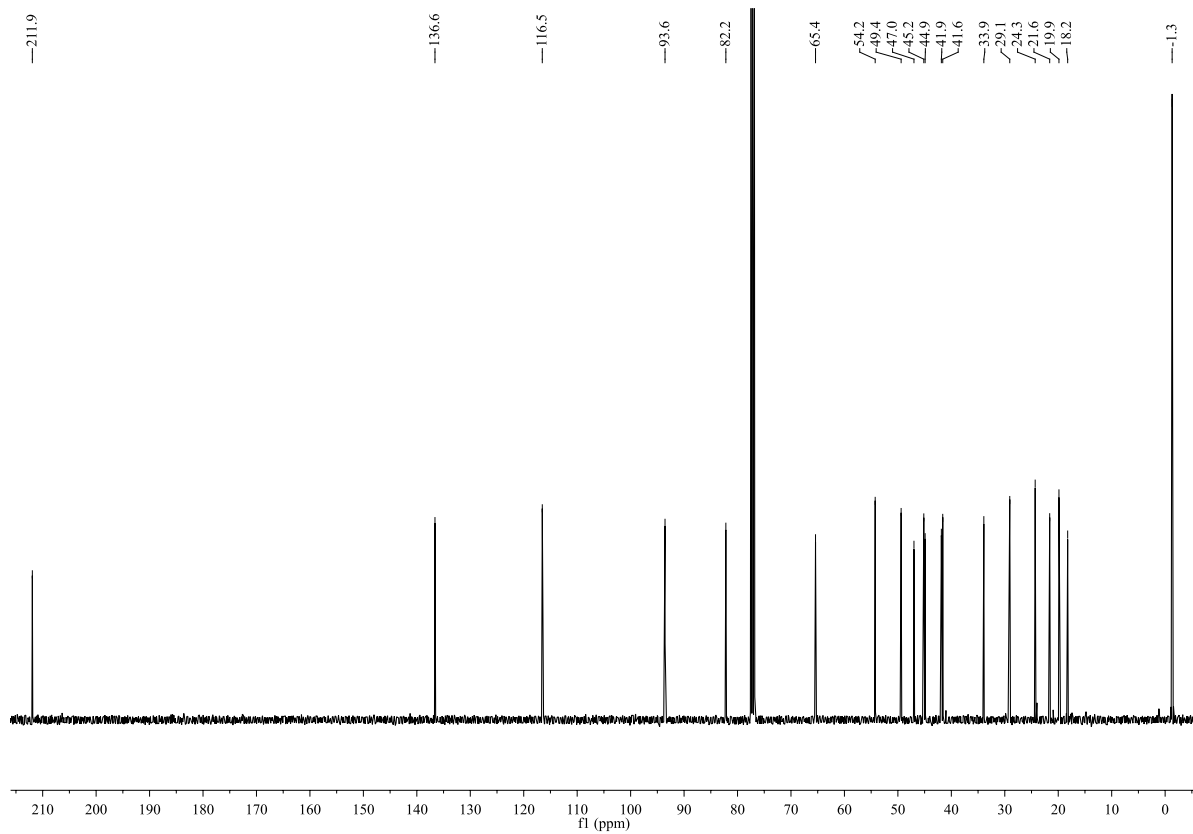


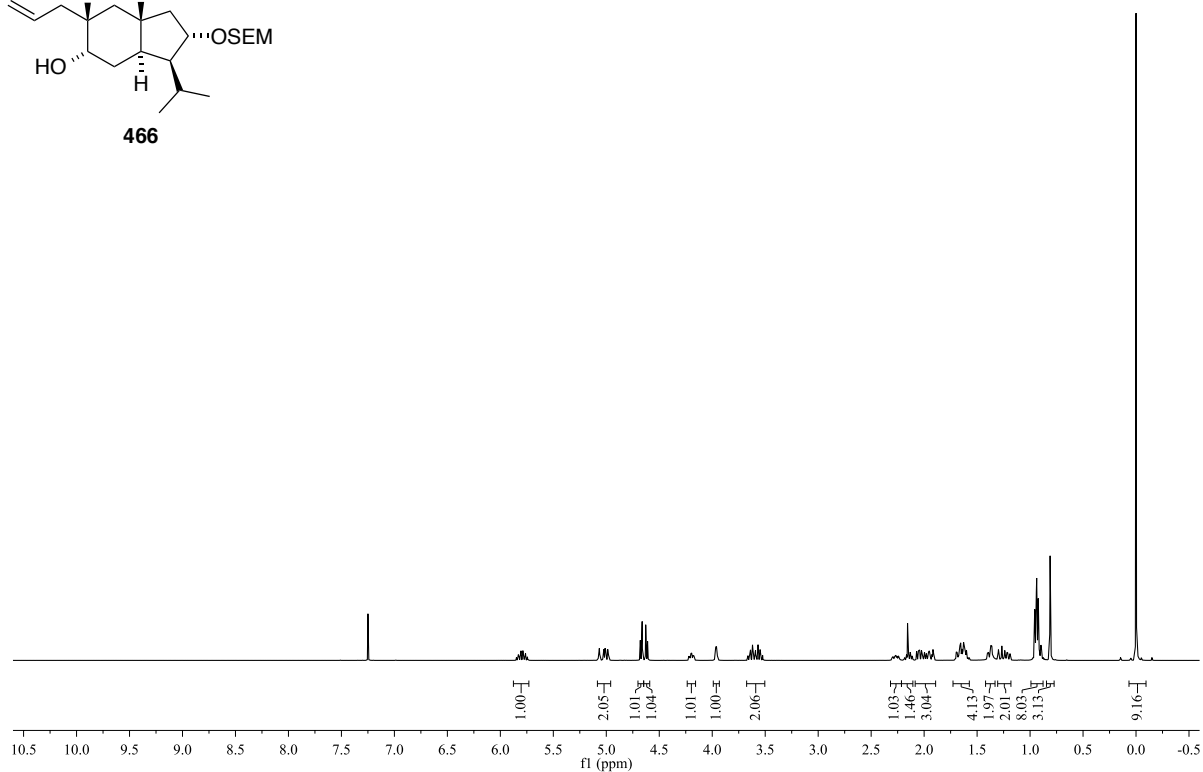
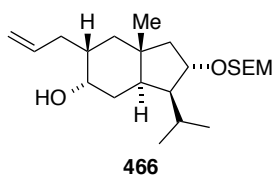
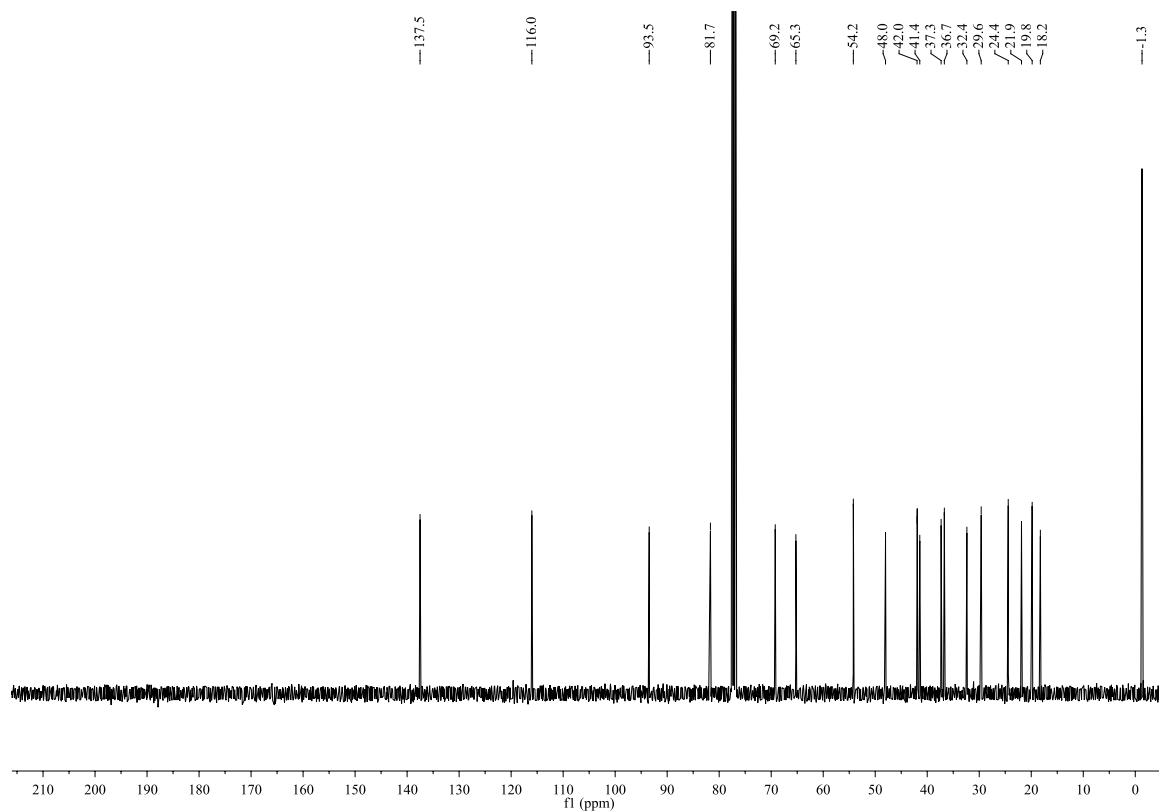
^1H NMR (CDCl_3 , 400 MHz): ^{13}C NMR (CDCl_3 , 100 MHz):

^1H NMR (CDCl_3 , 600 MHz):

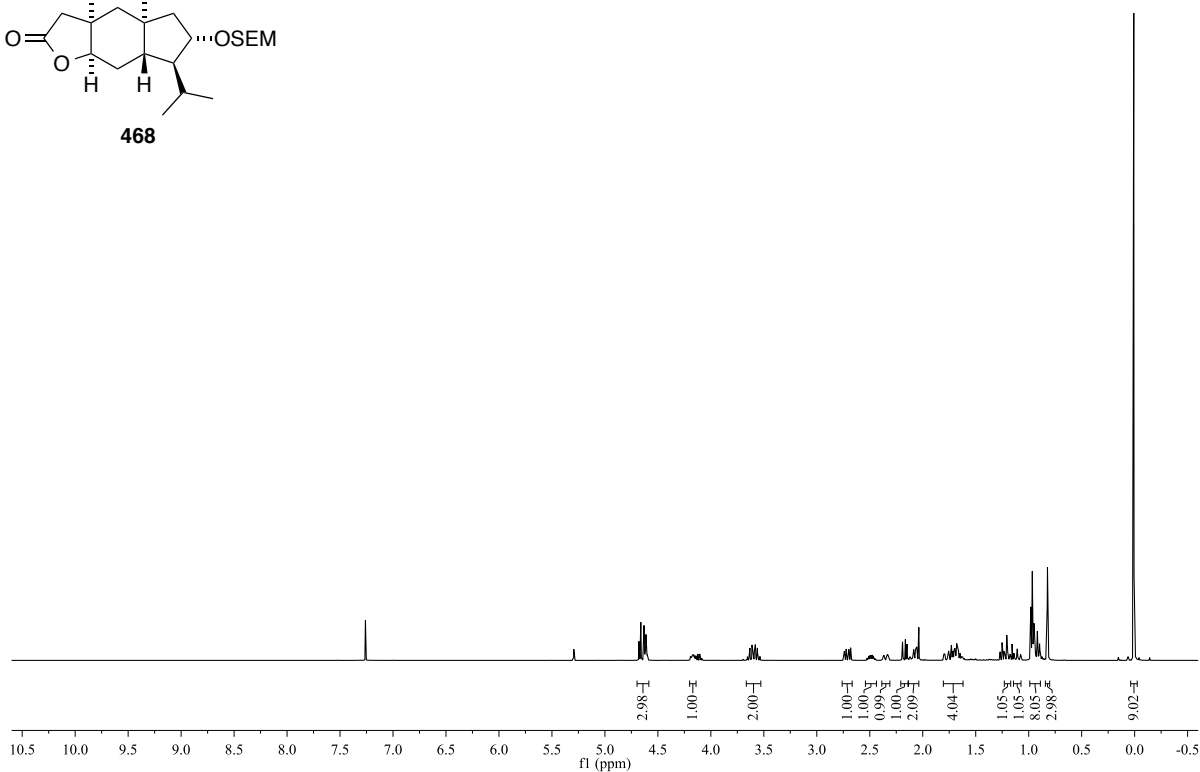
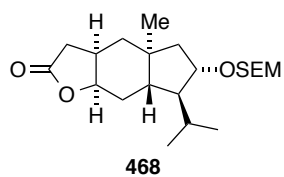


^{13}C NMR (CDCl_3 , 150 MHz):

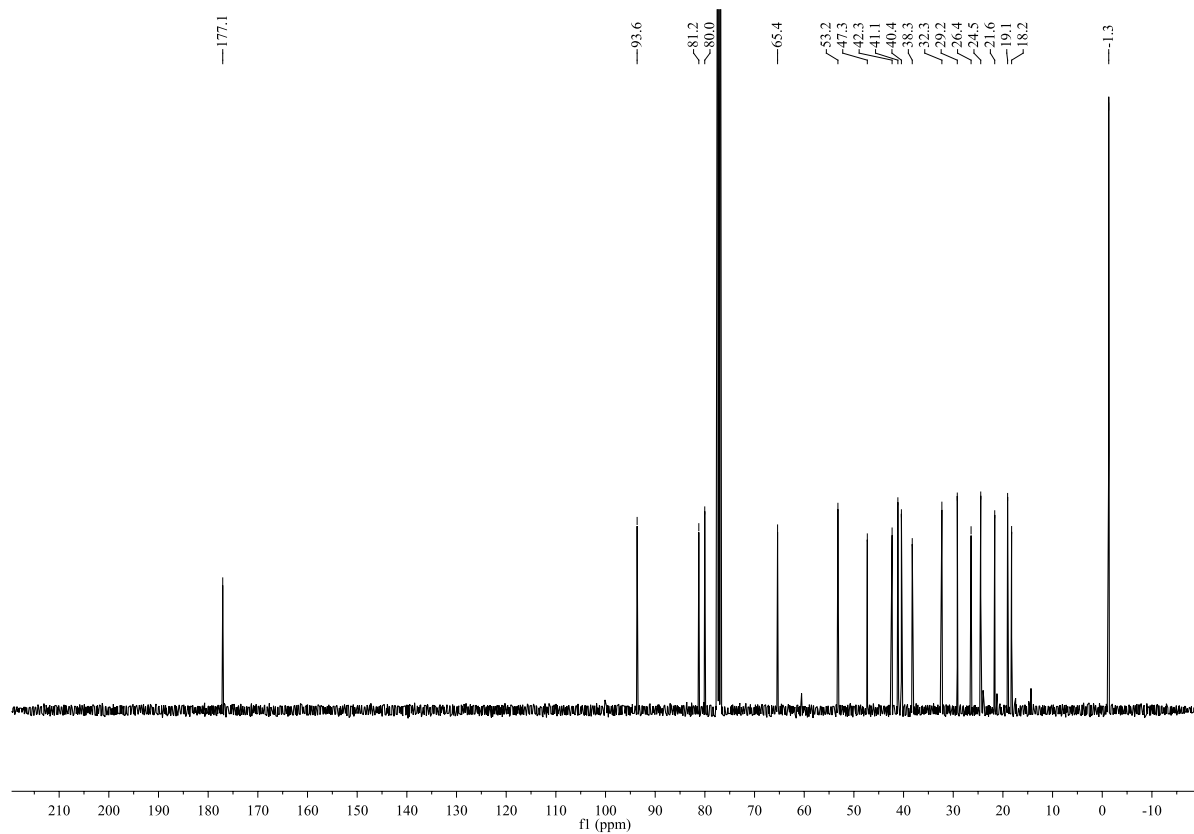


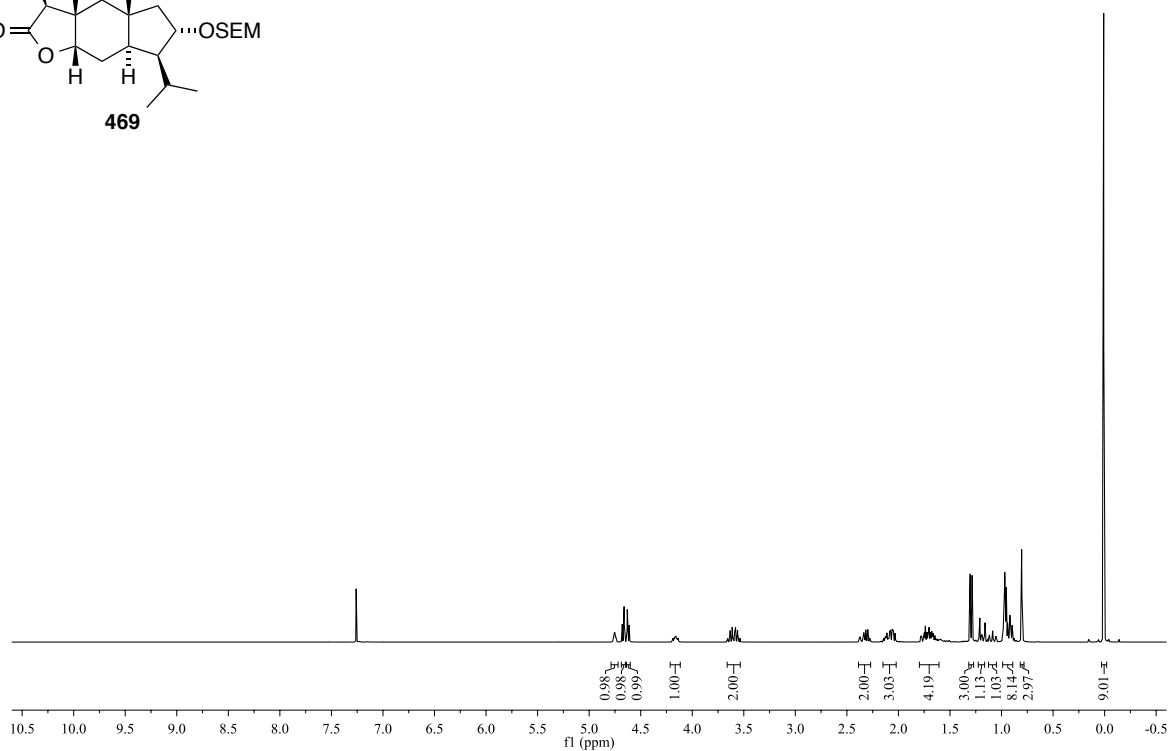
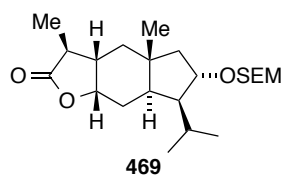
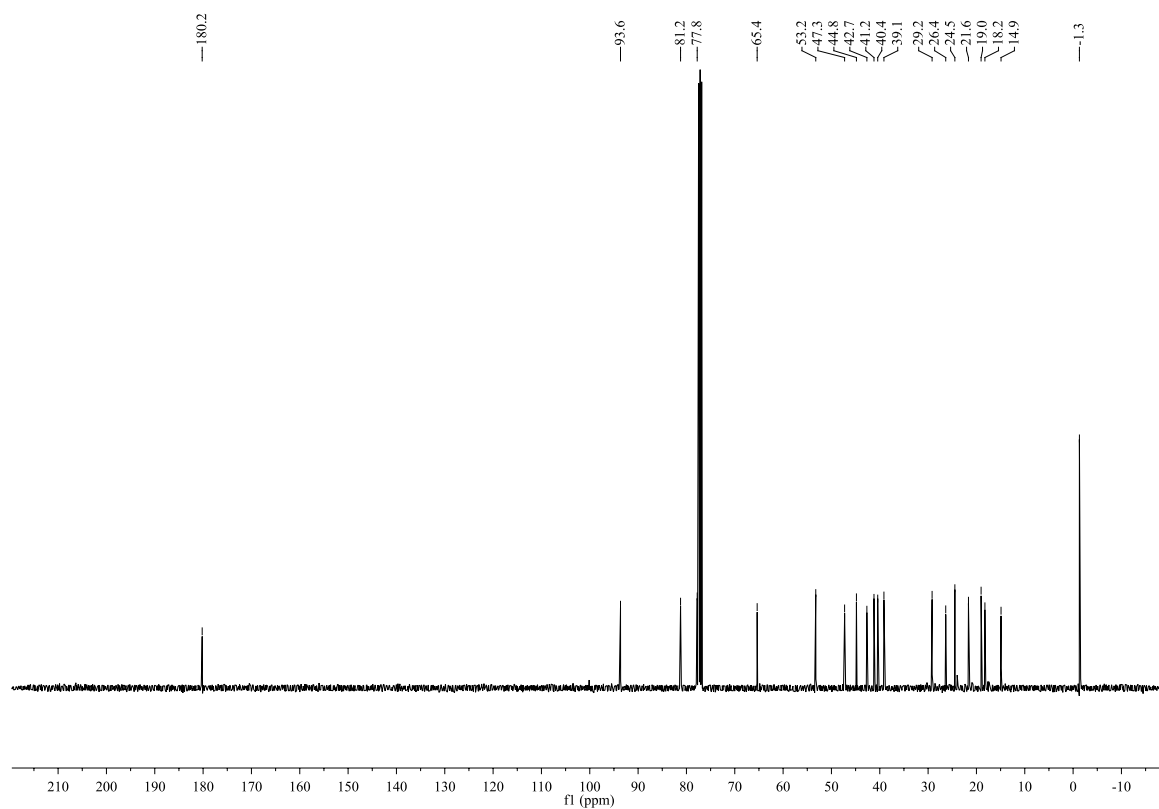
^1H NMR (CDCl_3 , 400 MHz): ^{13}C NMR (CDCl_3 , 100 MHz):

^1H NMR (CDCl_3 , 400 MHz):

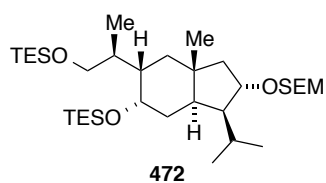


^{13}C NMR (CDCl_3 , 100 MHz):

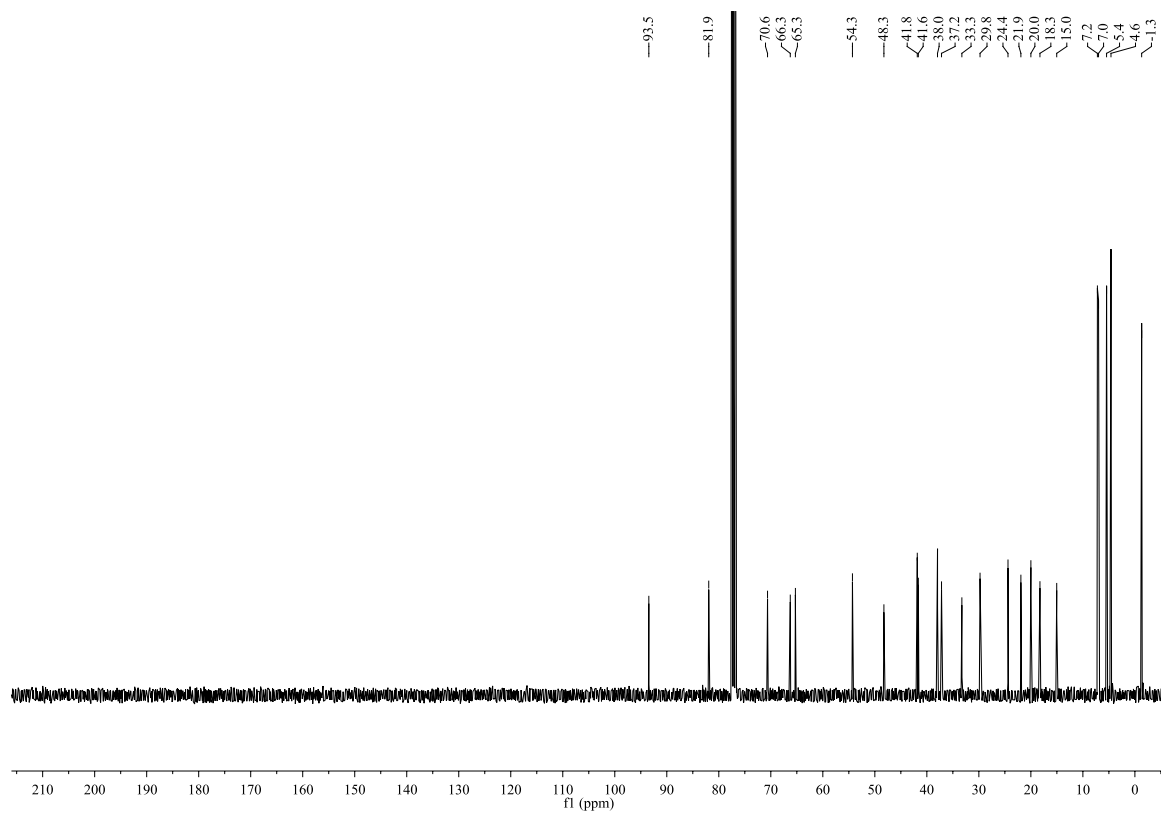


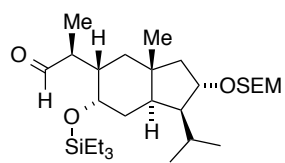
^1H NMR (CDCl_3 , 400 MHz): ^{13}C NMR (CDCl_3 , 100 MHz):

^1H NMR (CDCl_3 , 400 MHz):

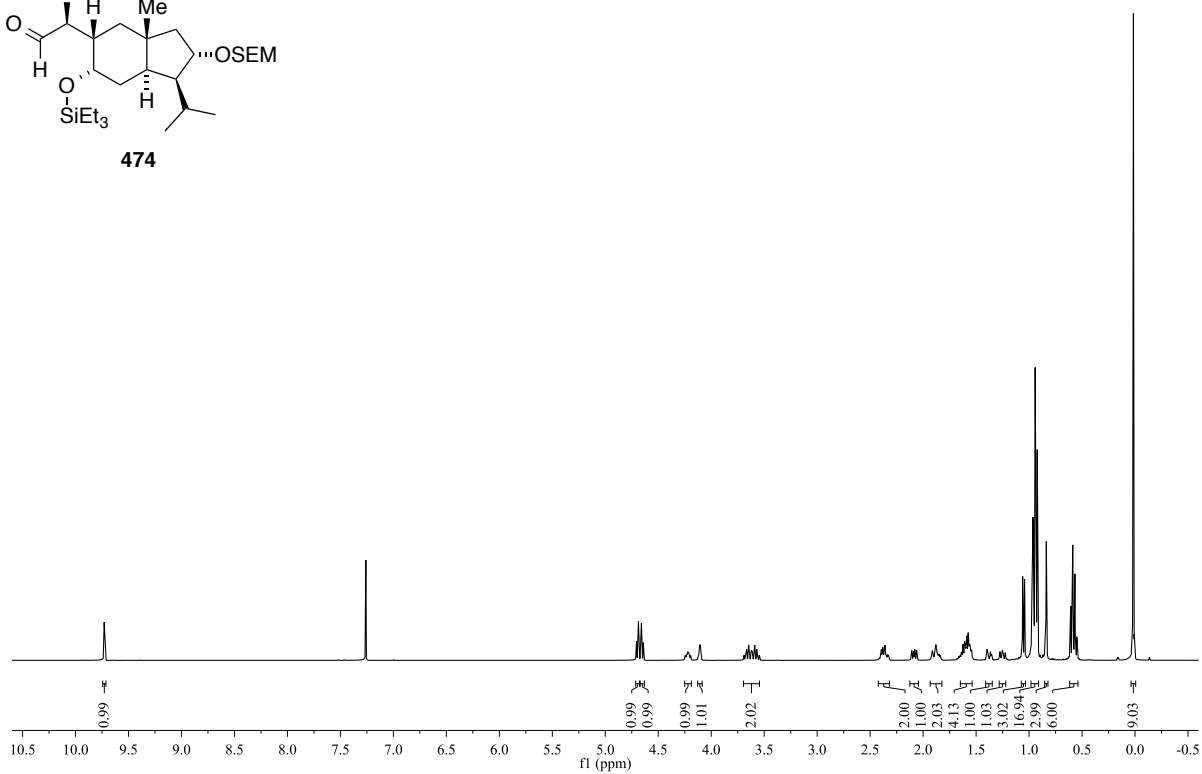
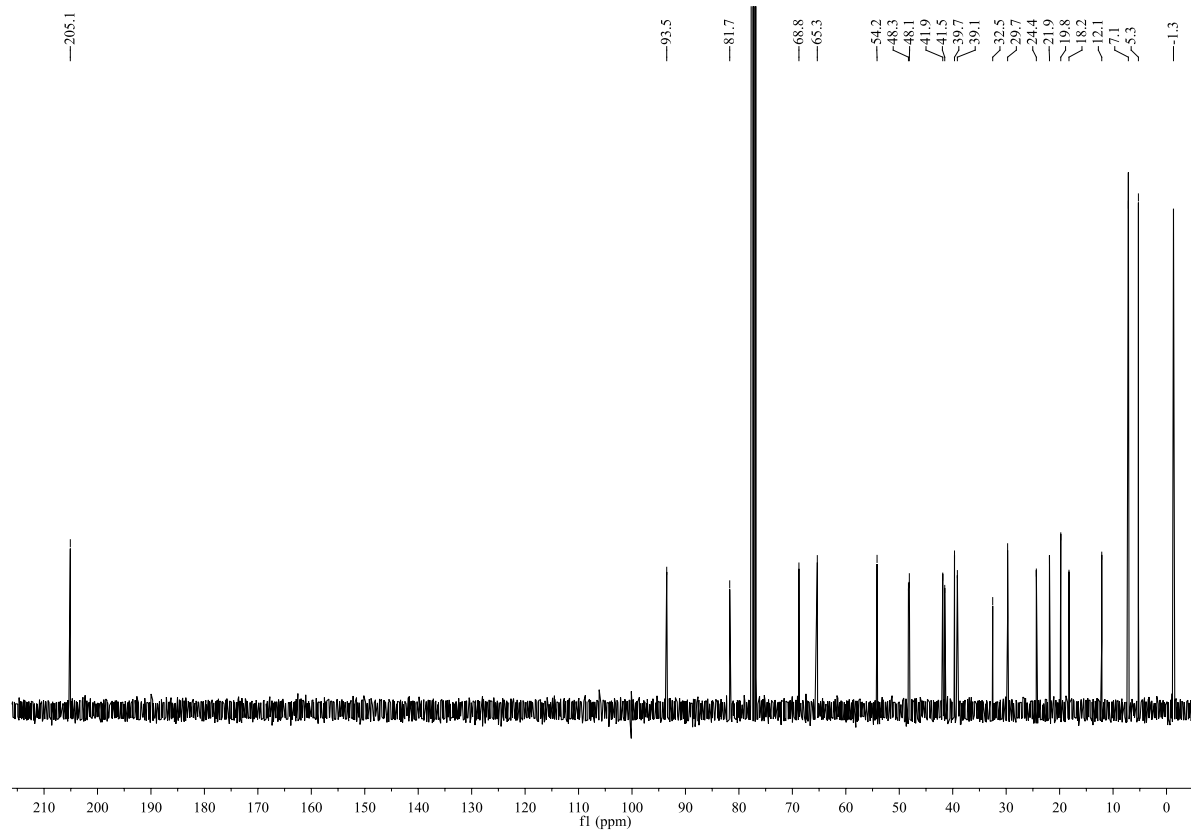


^{13}C NMR (CDCl_3 , 100 MHz):

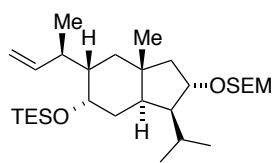


^1H NMR (CDCl_3 , 400 MHz):

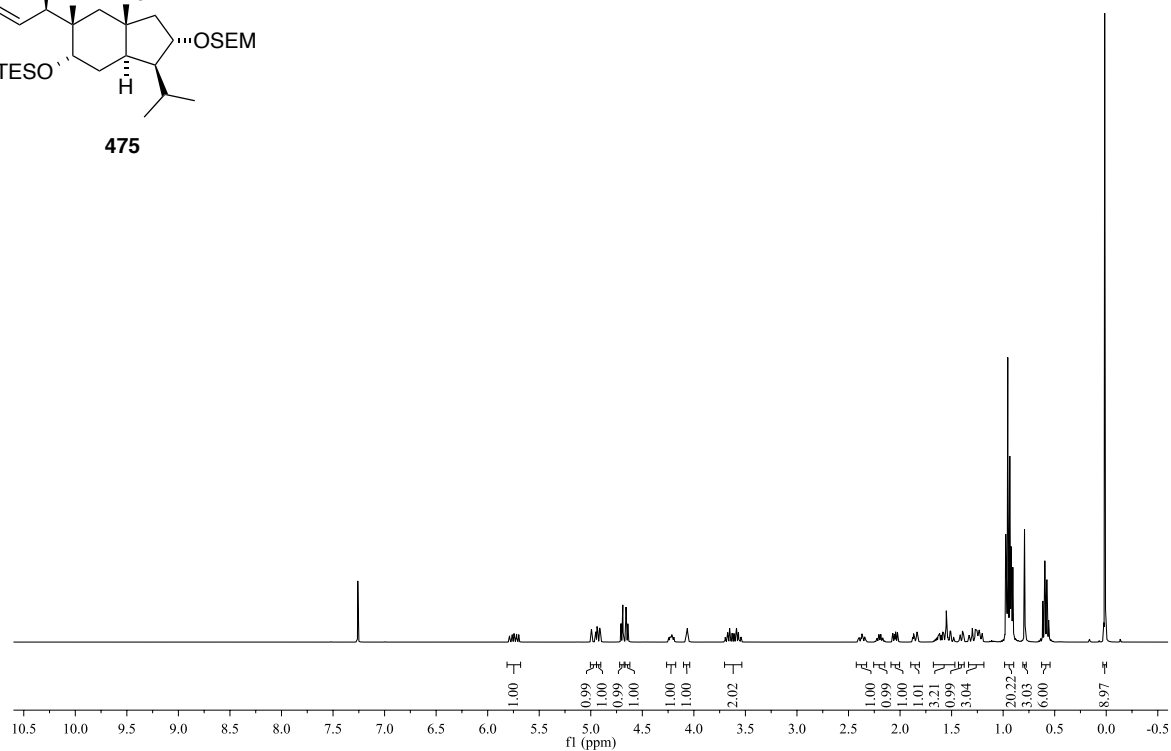
474

 ^{13}C NMR (CDCl_3 , 100 MHz):

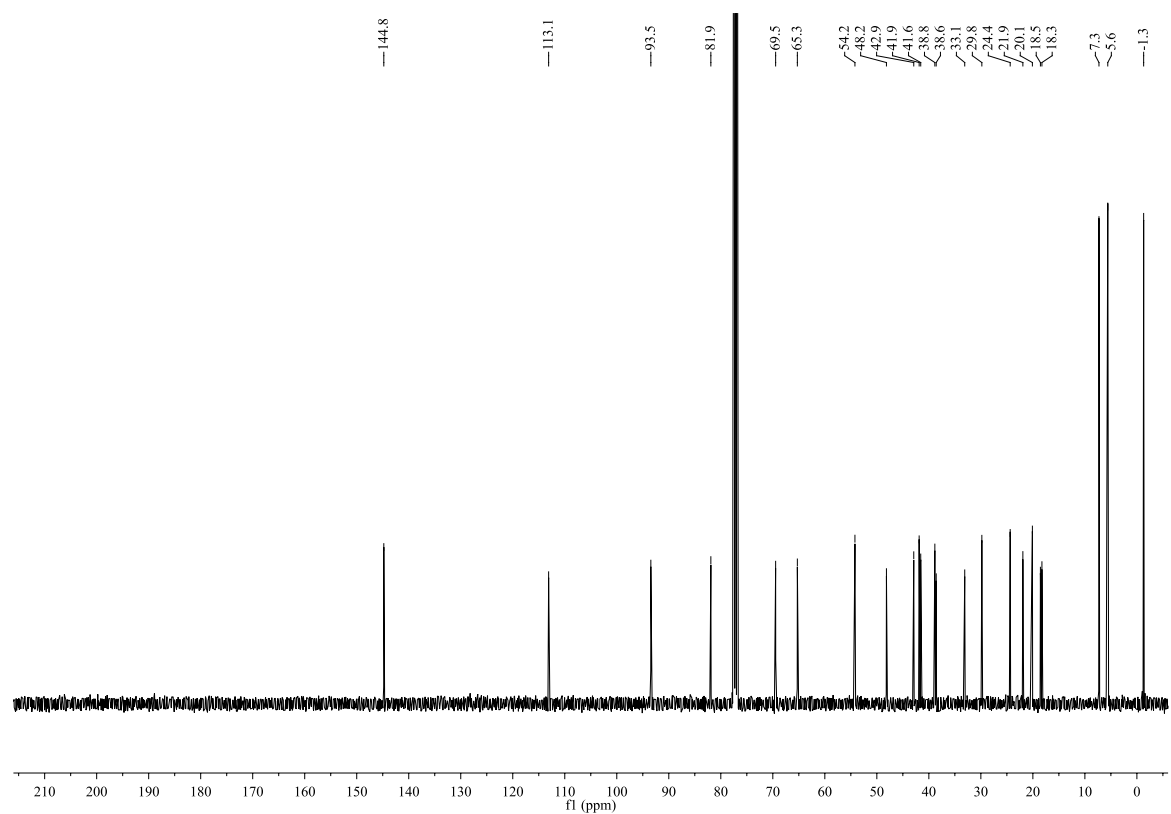
^1H NMR (CDCl_3 , 400 MHz):

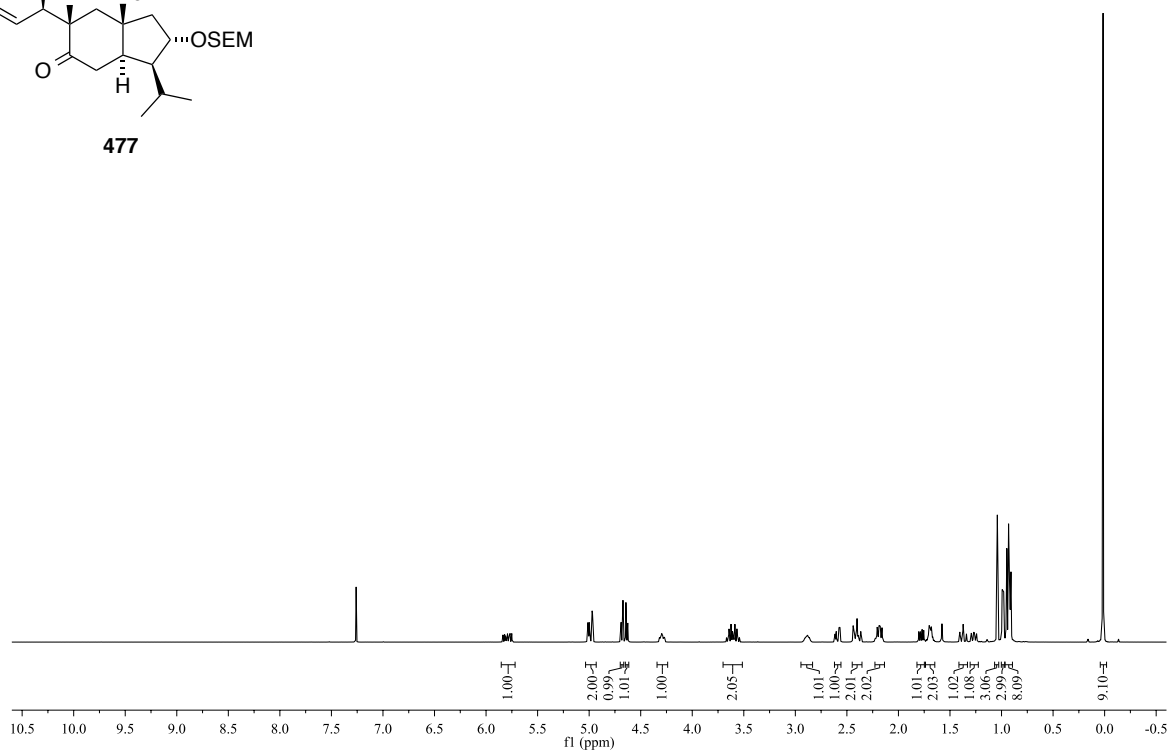
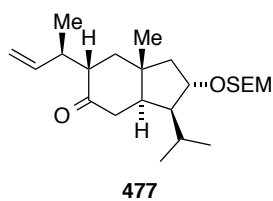
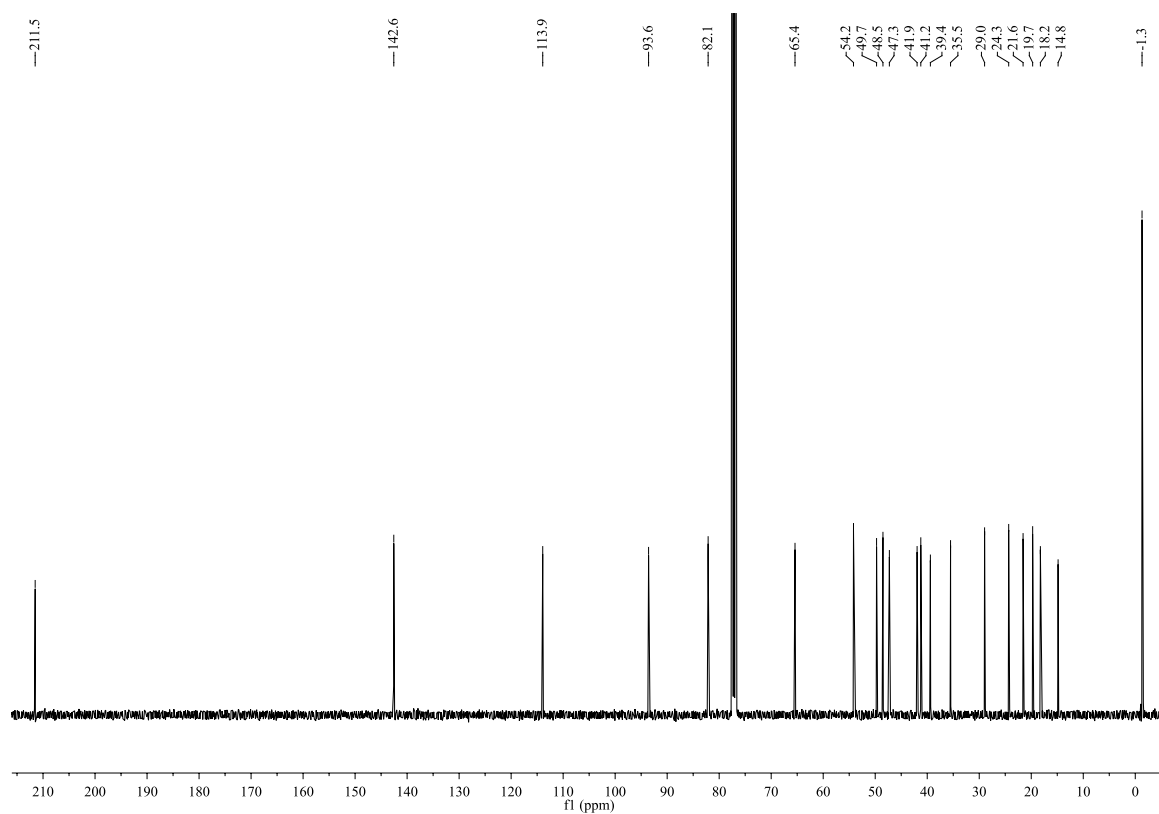


475

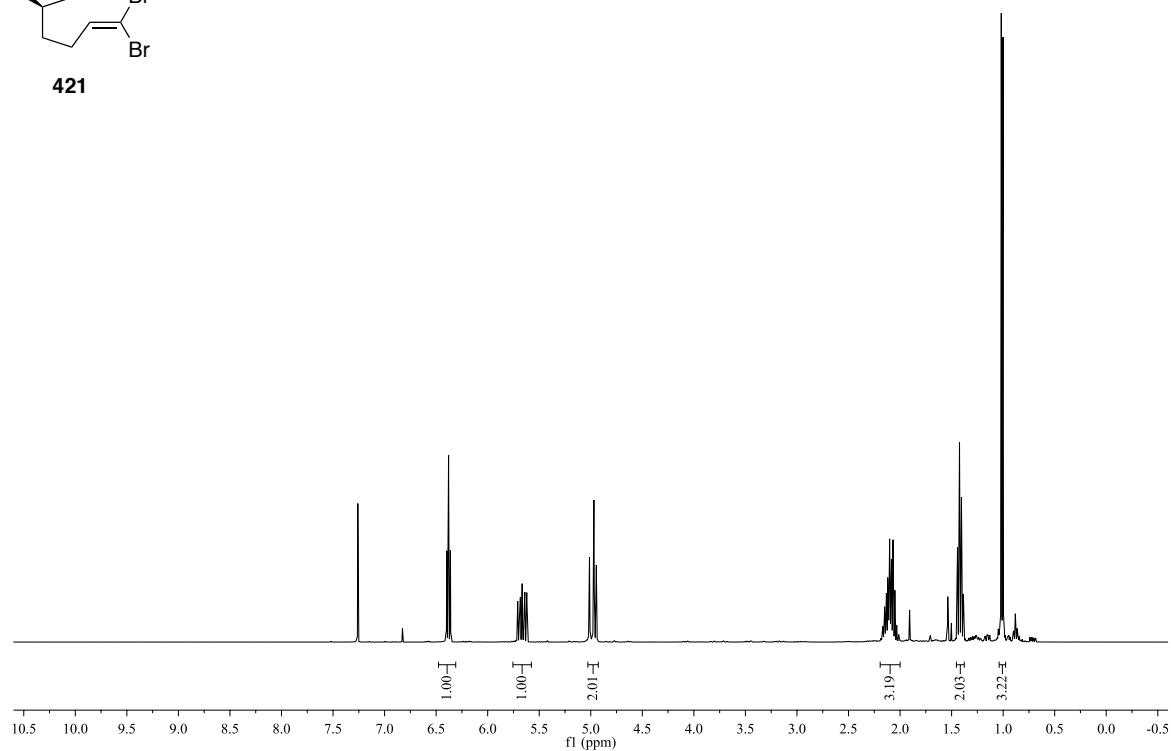
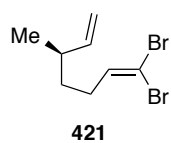


^{13}C NMR (CDCl_3 , 100 MHz):

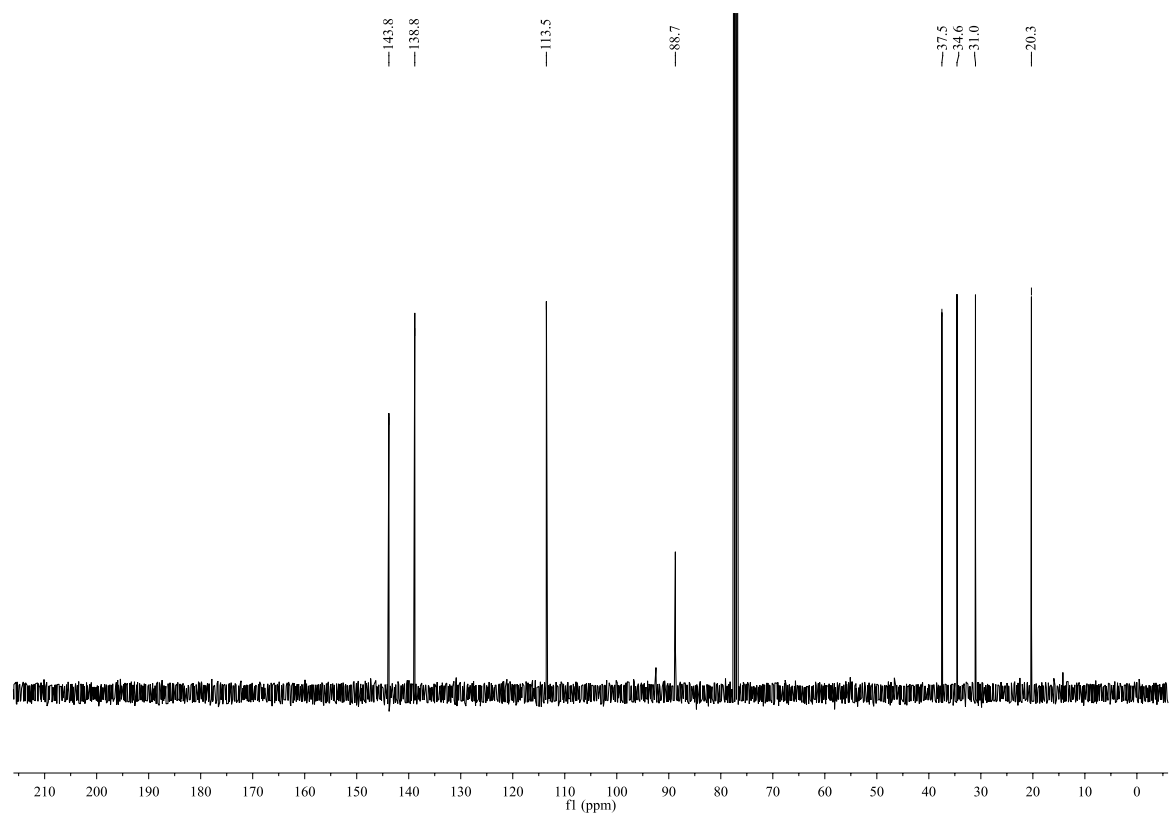


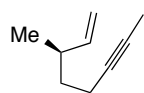
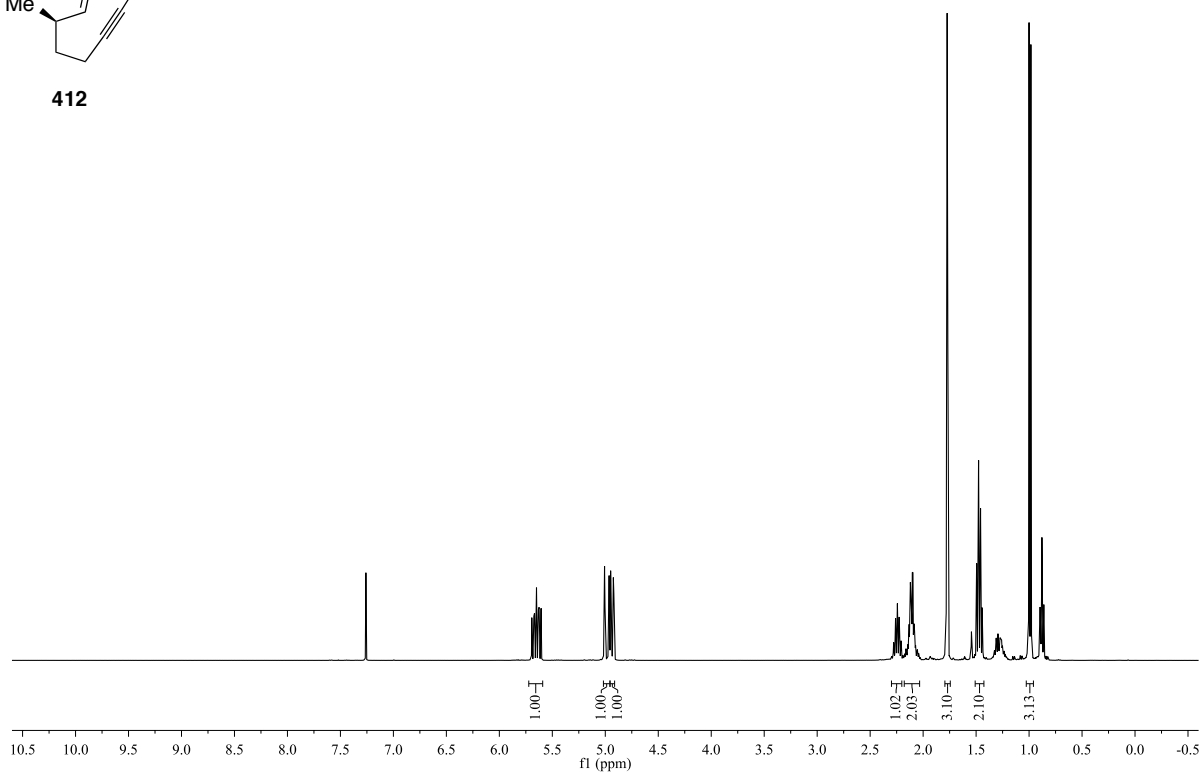
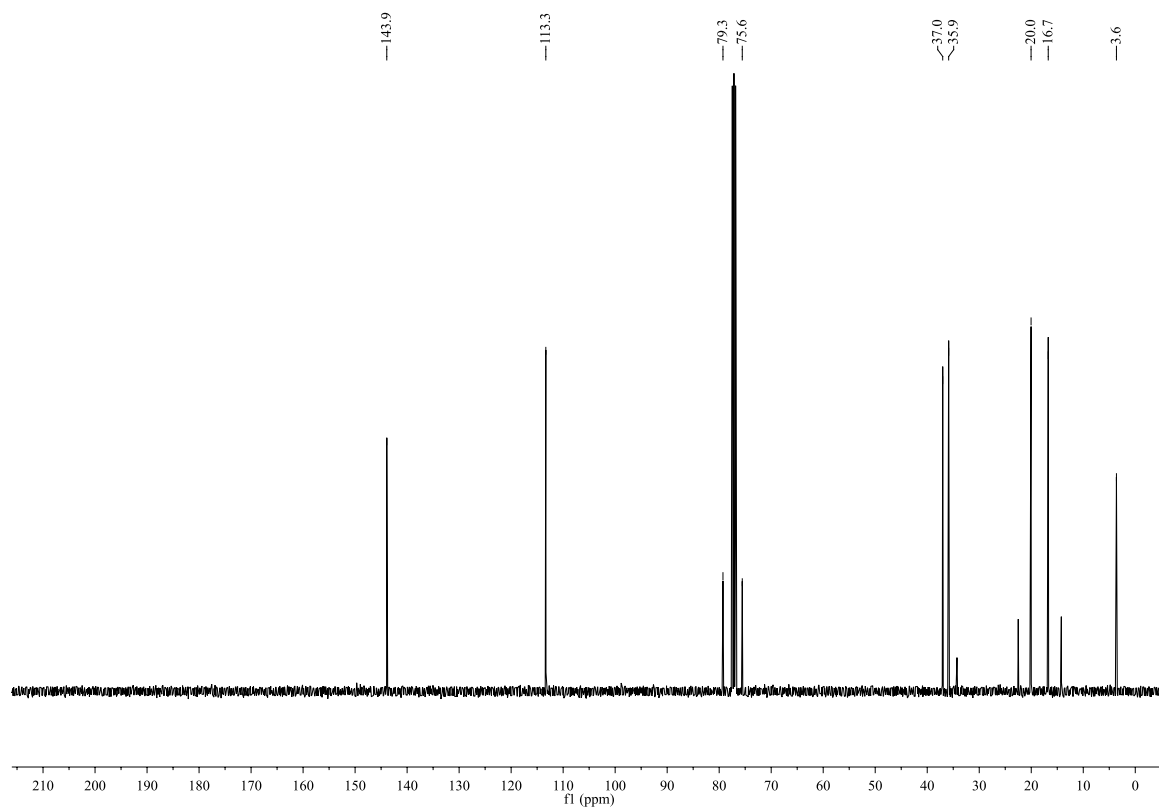
^1H NMR (CDCl_3 , 400 MHz): ^{13}C NMR (CDCl_3 , 100 MHz):

^1H NMR (CDCl_3 , 400 MHz):

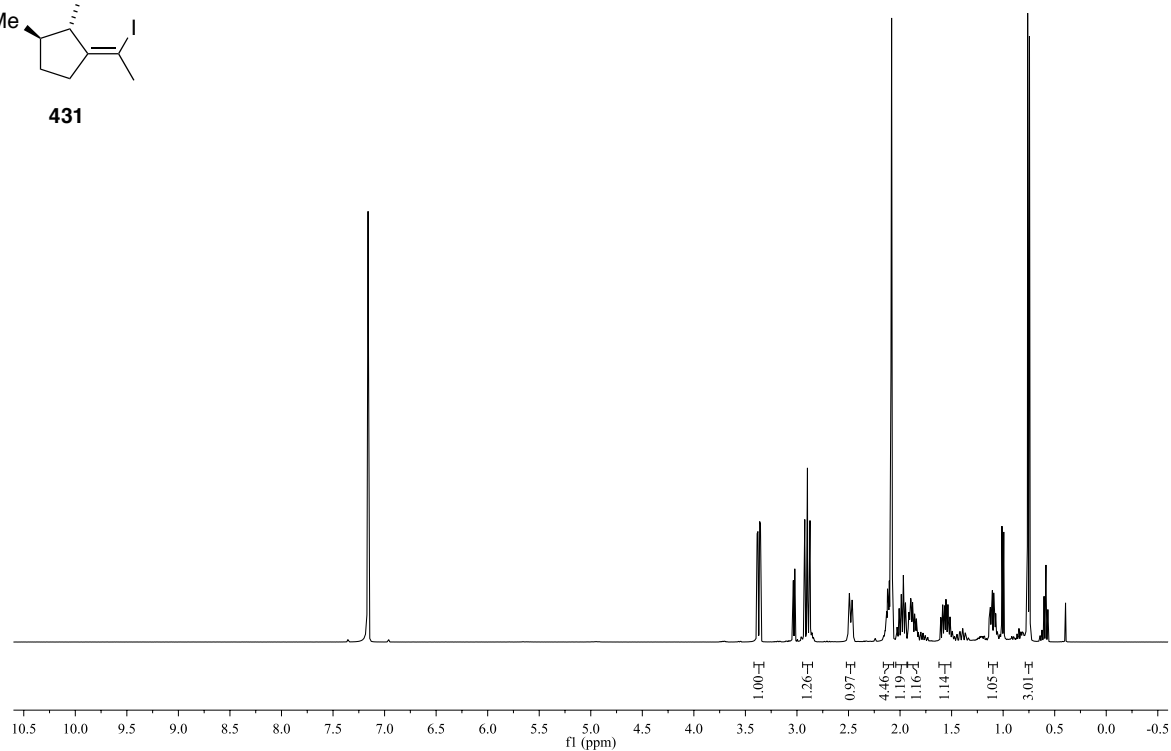
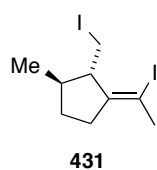


^{13}C NMR (CDCl_3 , 100 MHz):

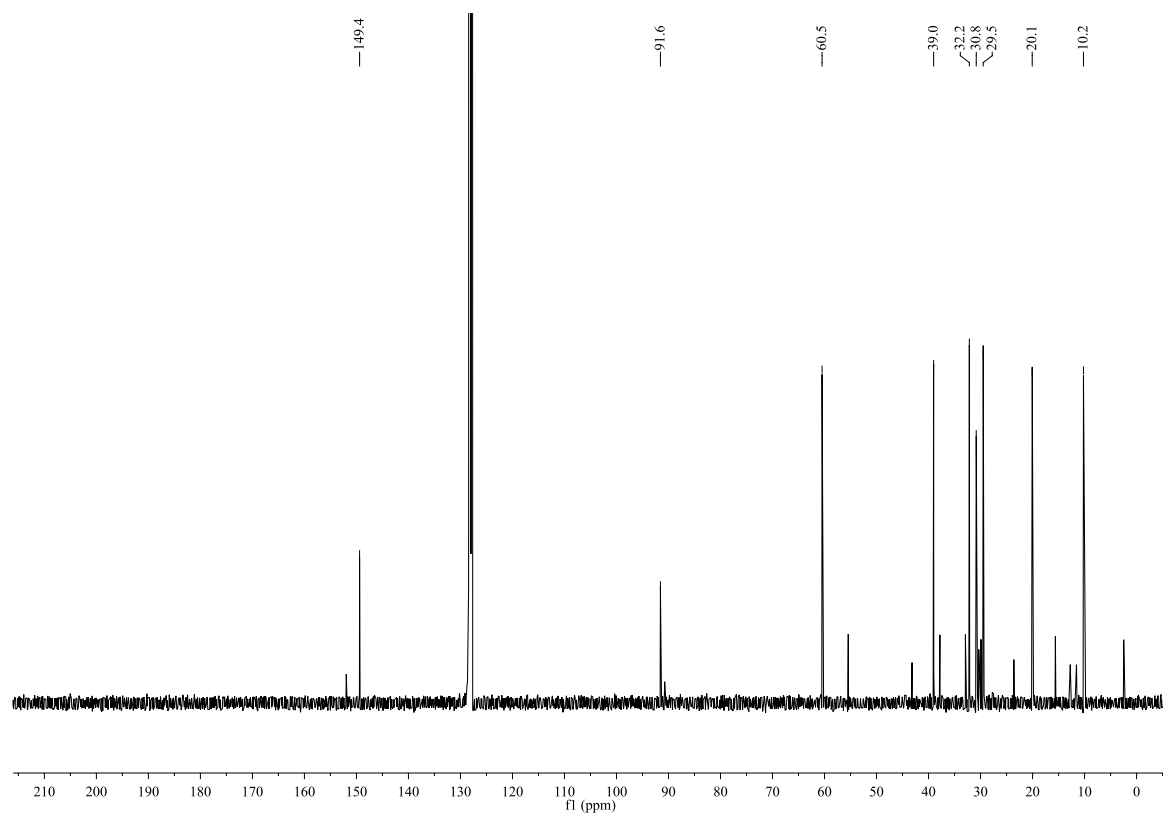


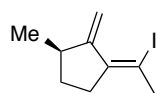
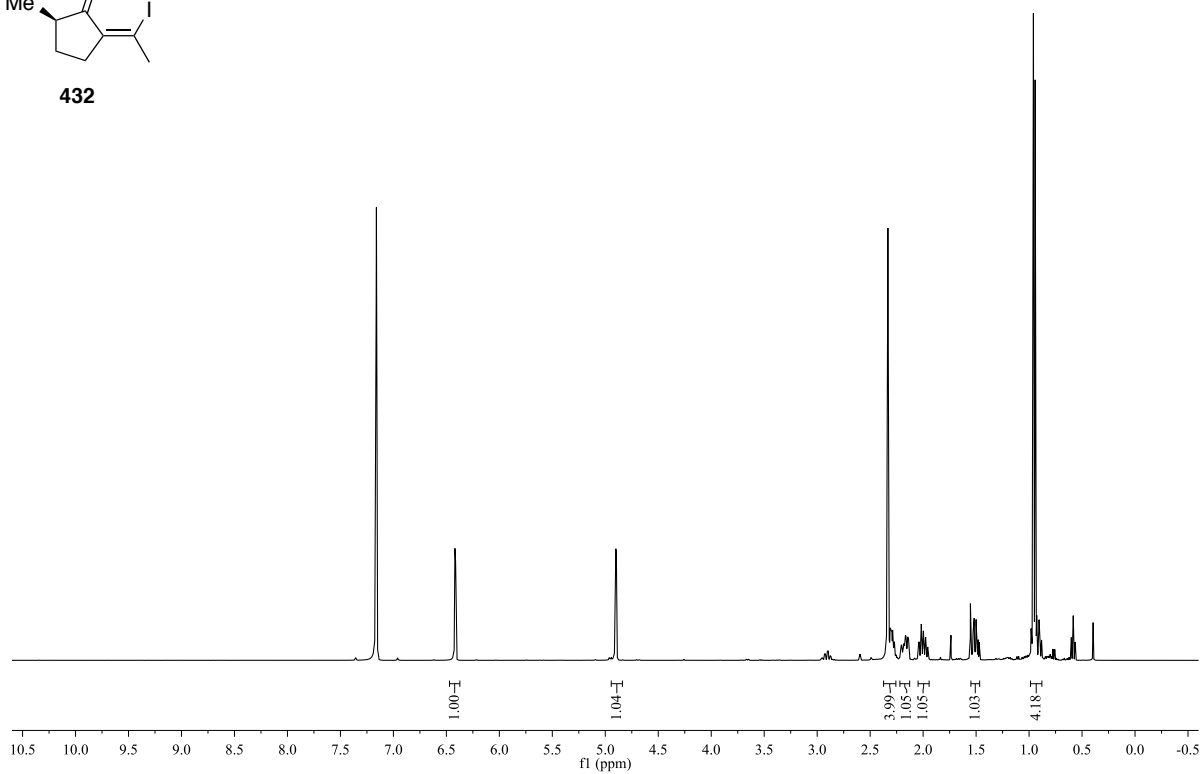
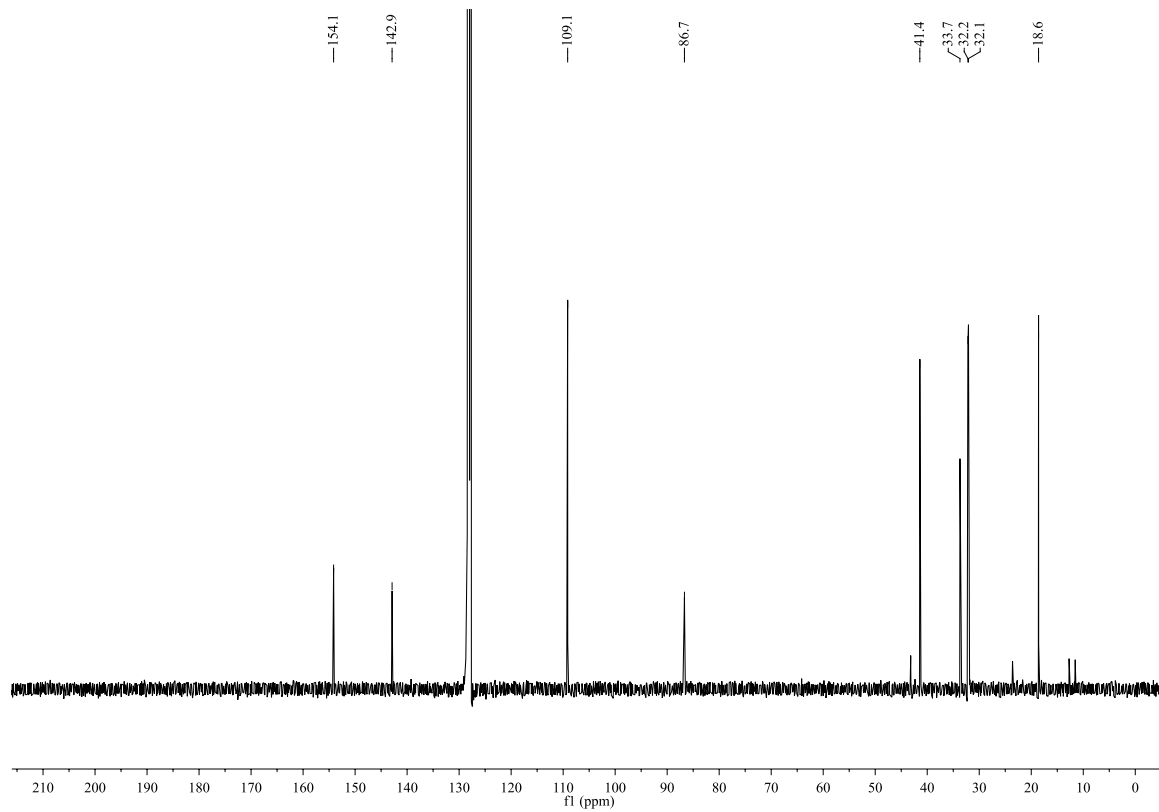
^1H NMR (CDCl_3 , 400 MHz):**412** ^{13}C NMR (CDCl_3 , 100 MHz):

^1H NMR (C_6D_6 , 400 MHz):

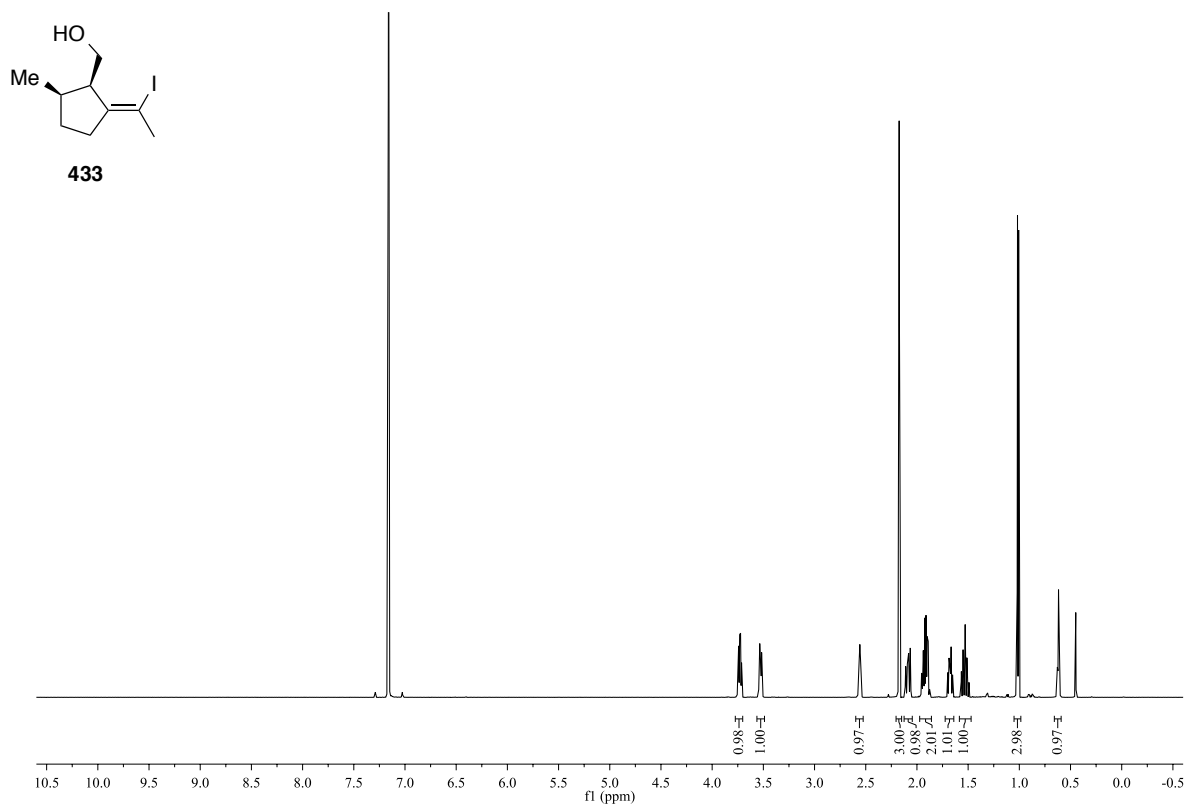


^{13}C NMR (C_6D_6 , 100 MHz):

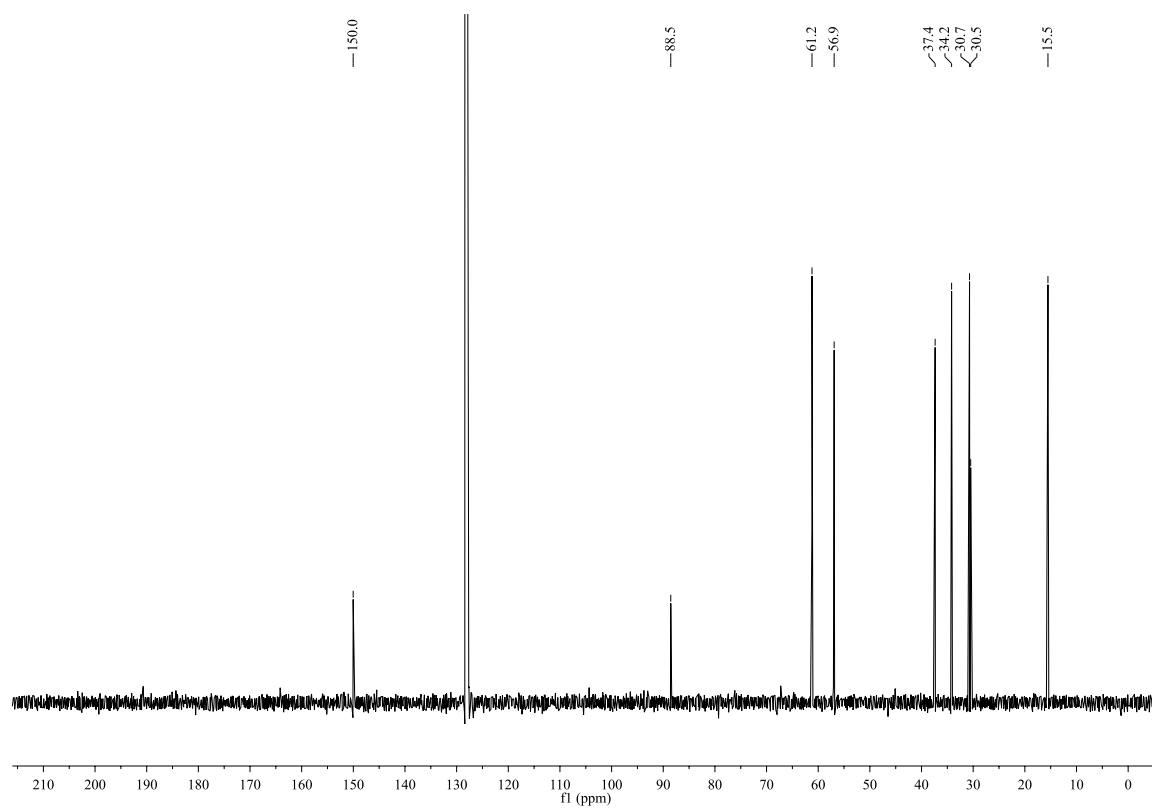


^1H NMR (C_6D_6 , 400 MHz):**432** ^{13}C NMR (C_6D_6 , 100 MHz):

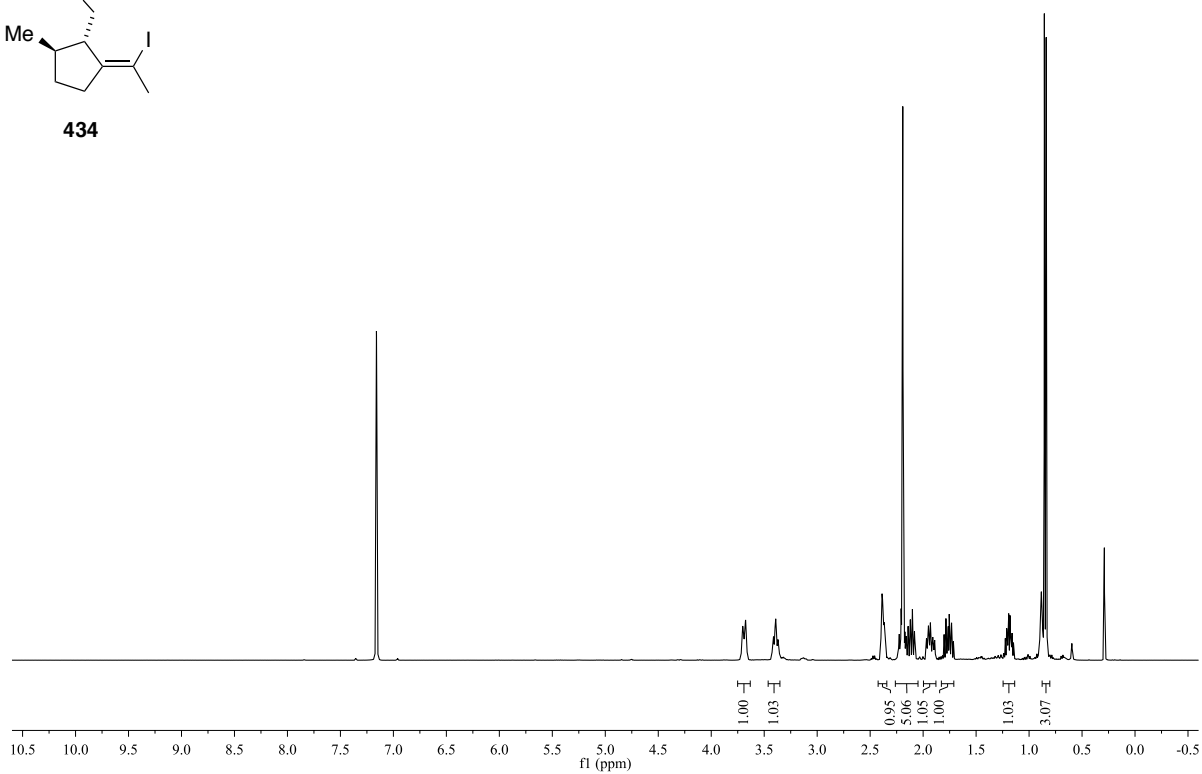
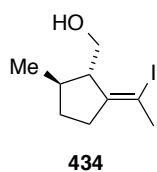
^1H NMR (C_6D_6 , 600 MHz):



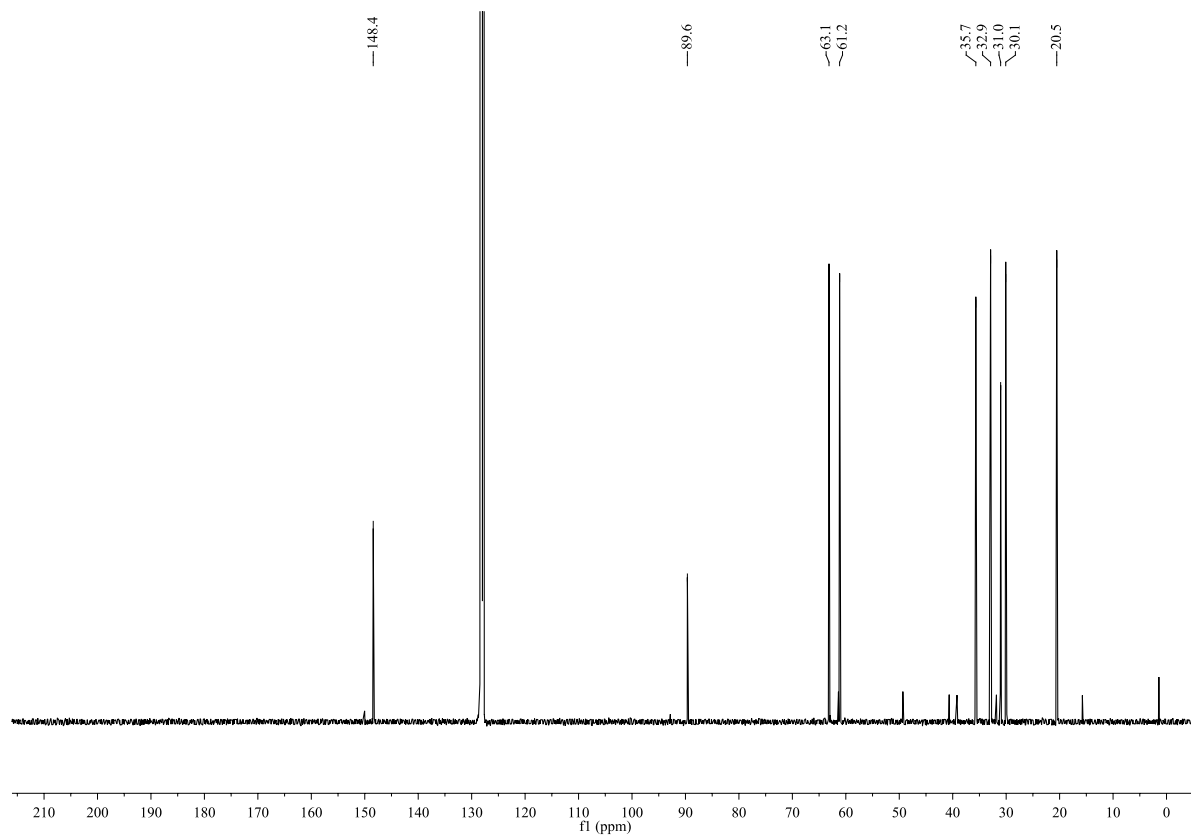
^{13}C NMR (C_6D_6 , 150 MHz):



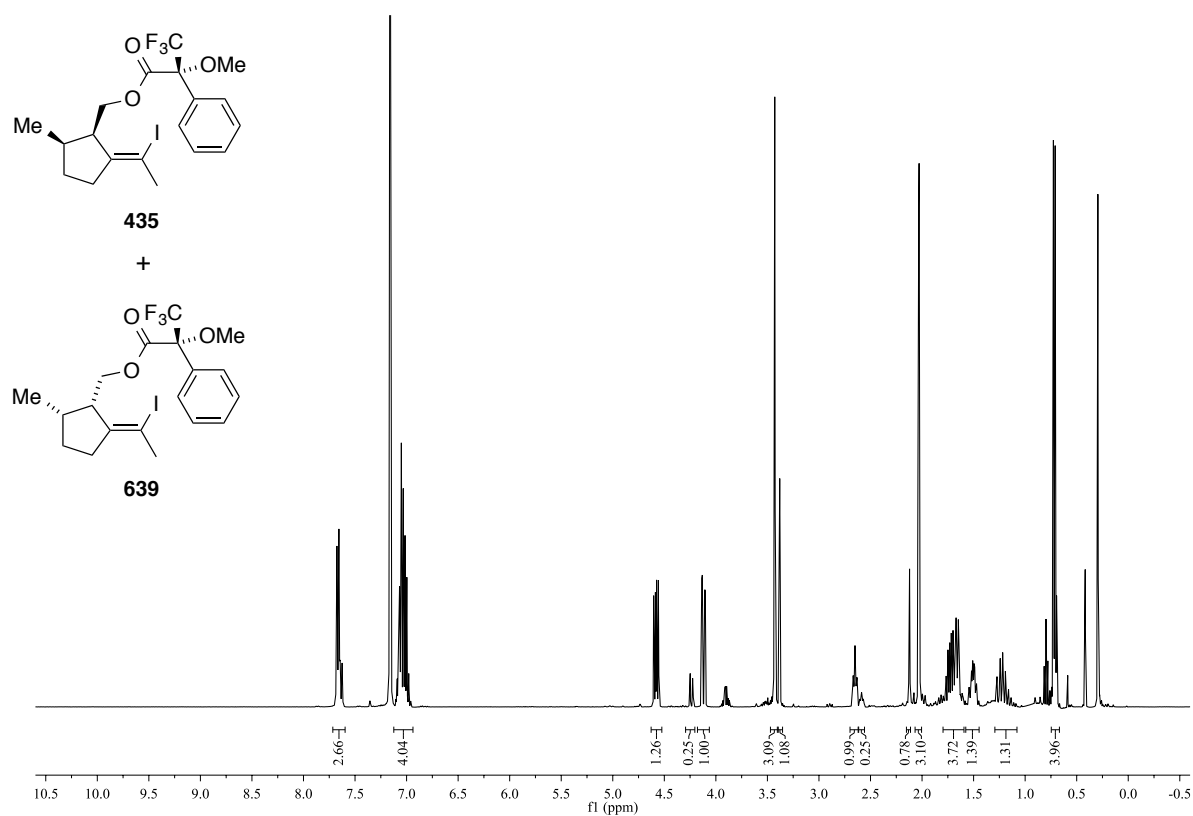
^1H NMR (C_6D_6 , 400 MHz):



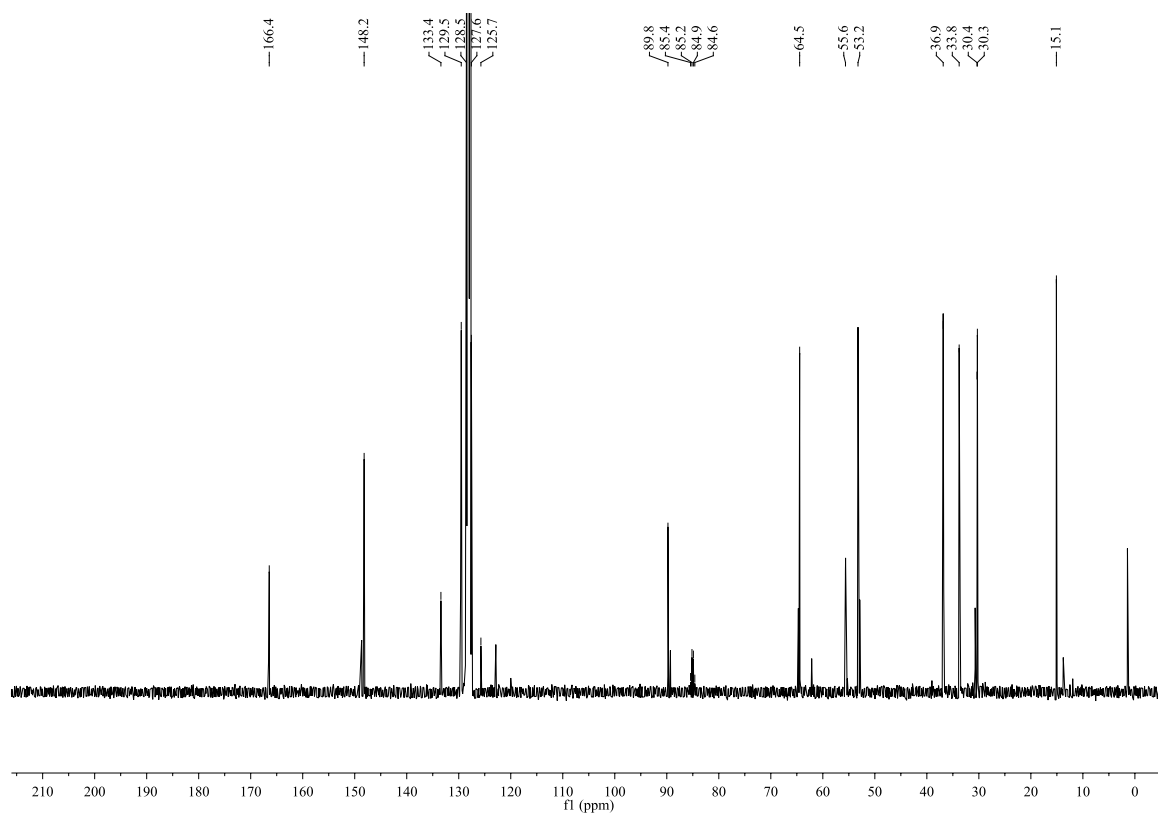
^{13}C NMR (C_6D_6 , 100 MHz):

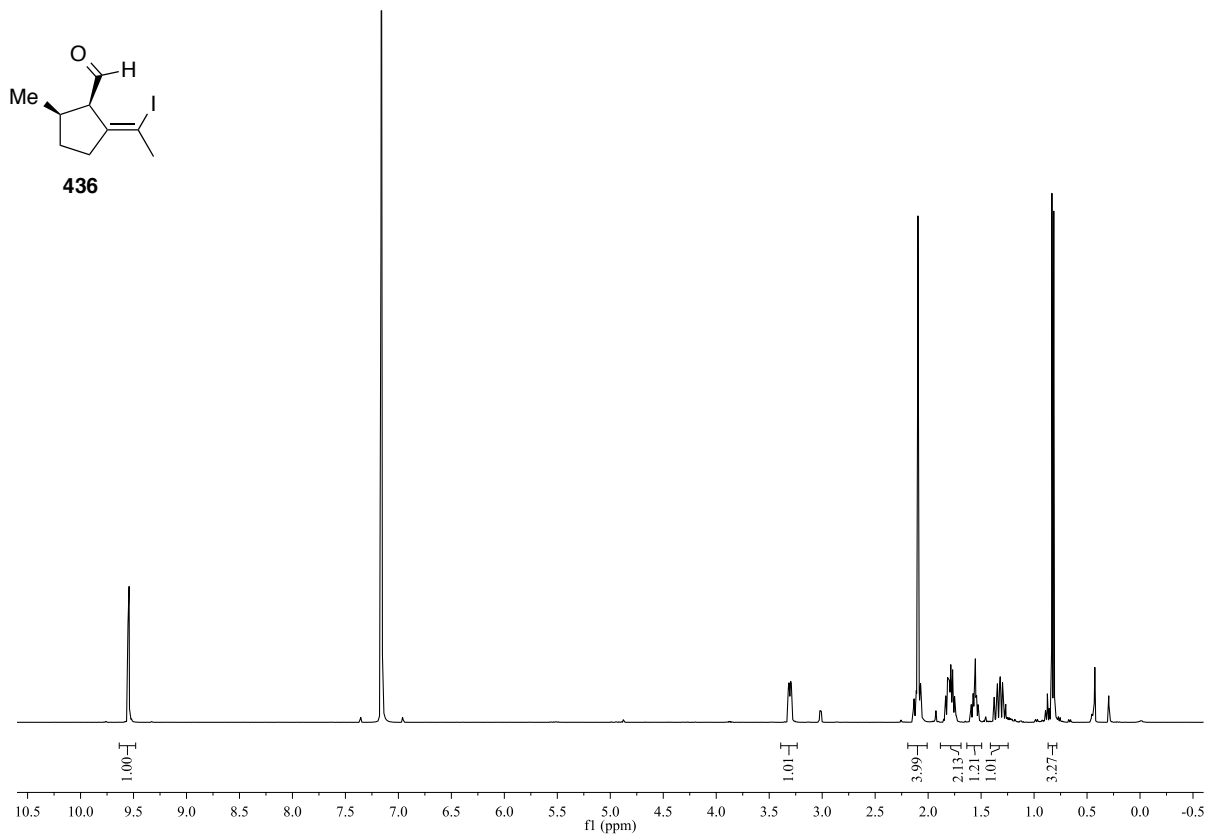
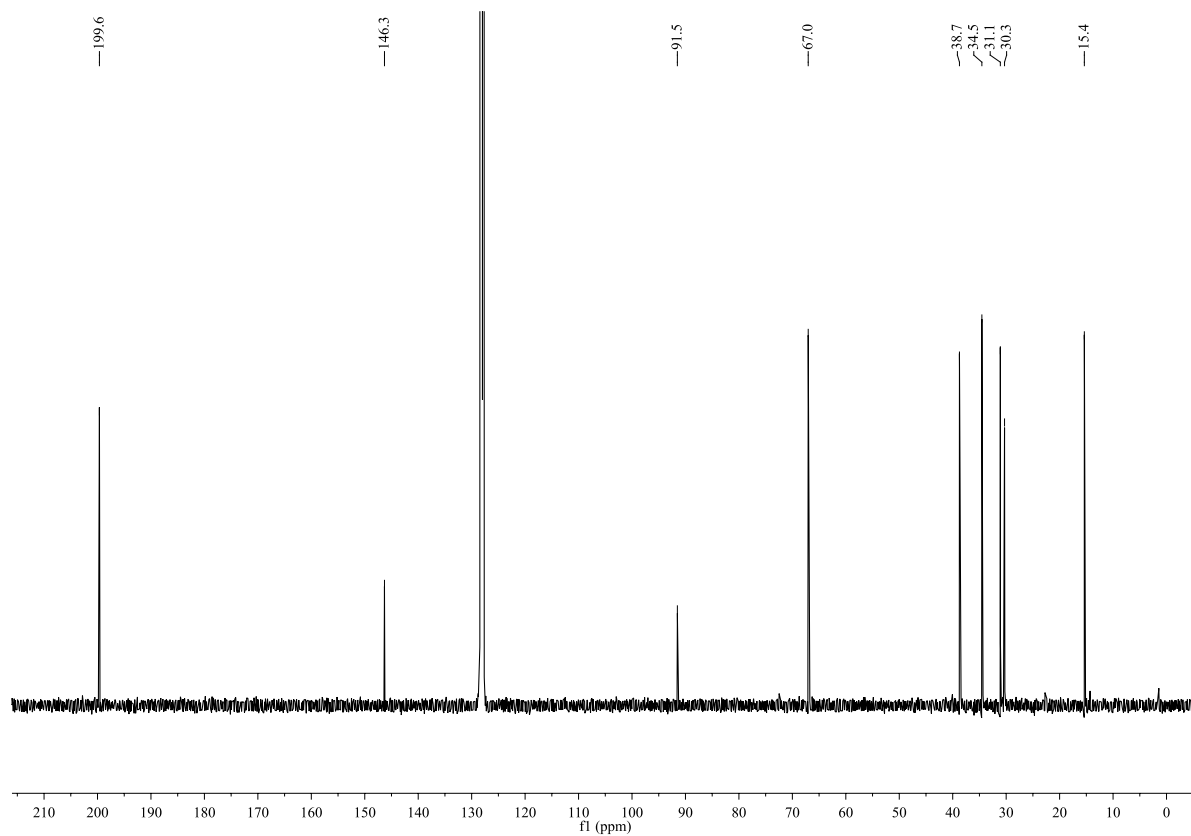


^1H NMR (C_6D_6 , 400 MHz):

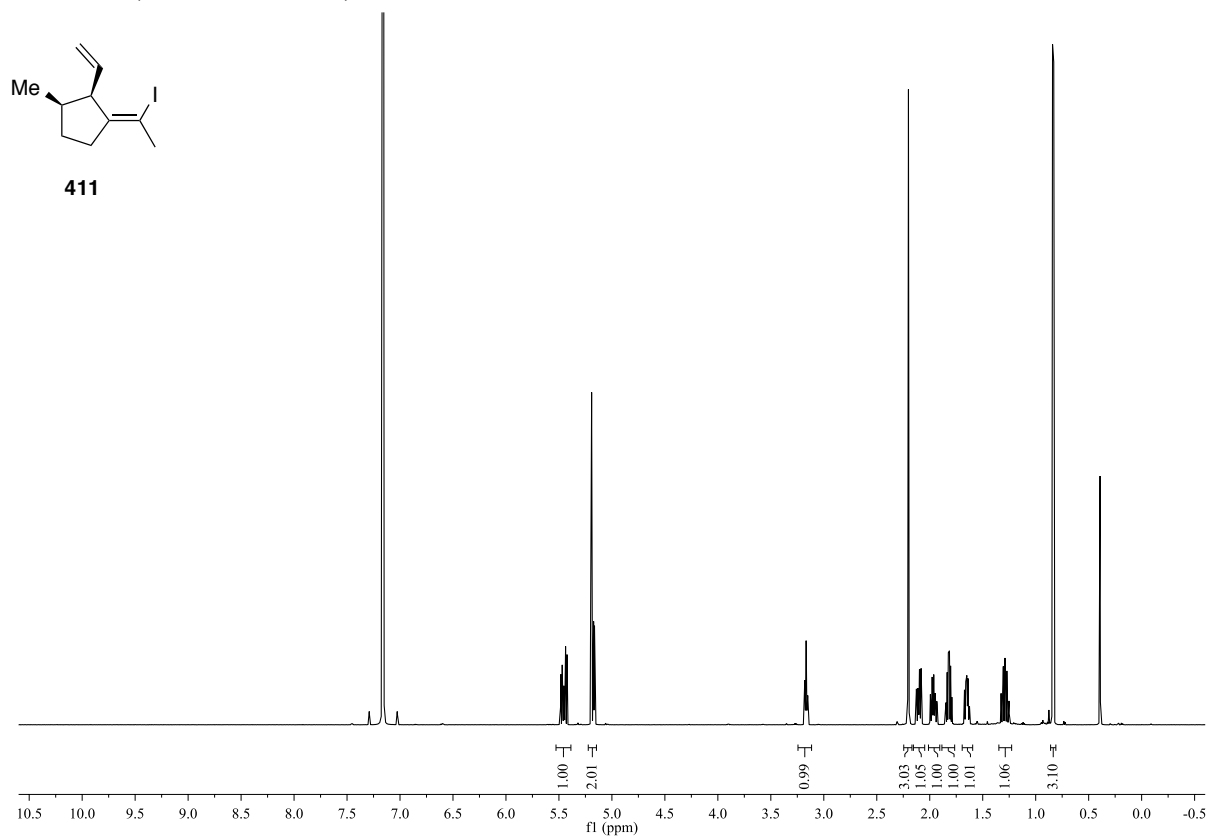


^{13}C NMR (C_6D_6 , 100 MHz):

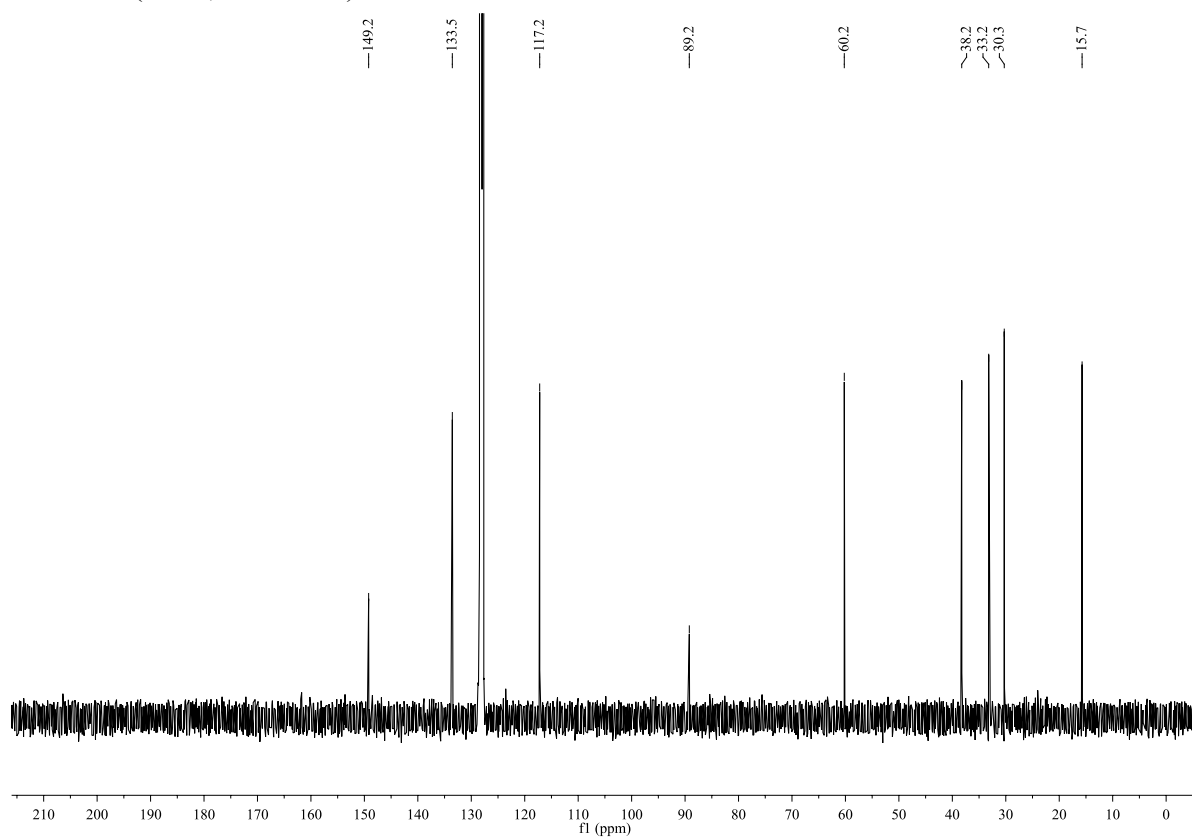


^1H NMR (C_6D_6 , 400 MHz): ^{13}C NMR (C_6D_6 , 100 MHz):

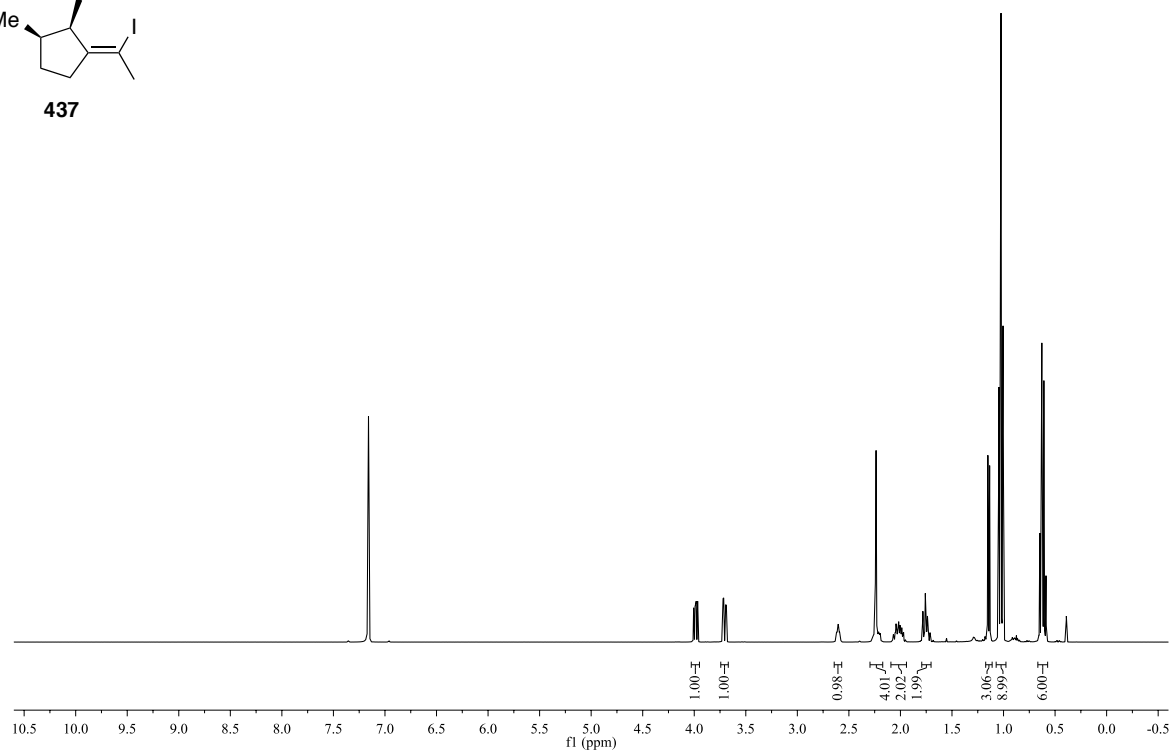
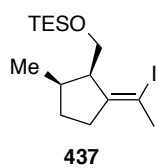
^1H NMR (C_6D_6 , 600 MHz):



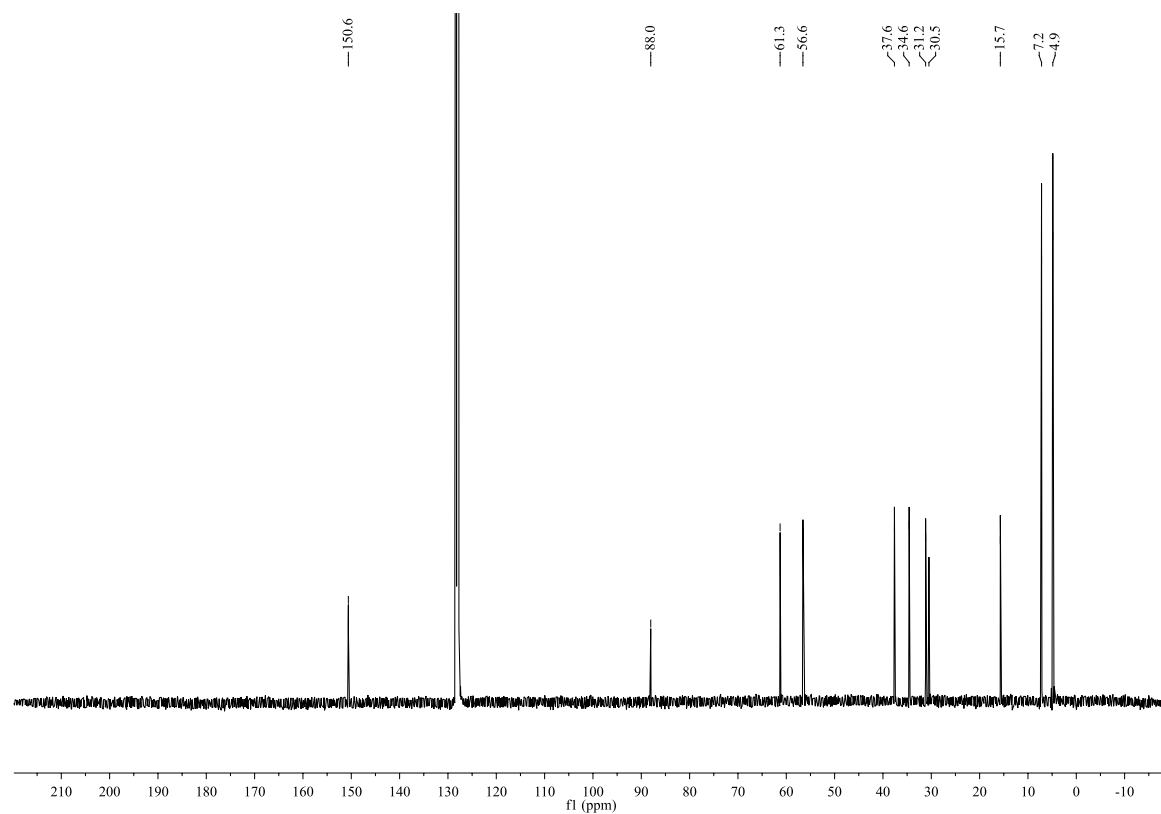
^{13}C NMR (C_6D_6 , 150 MHz):



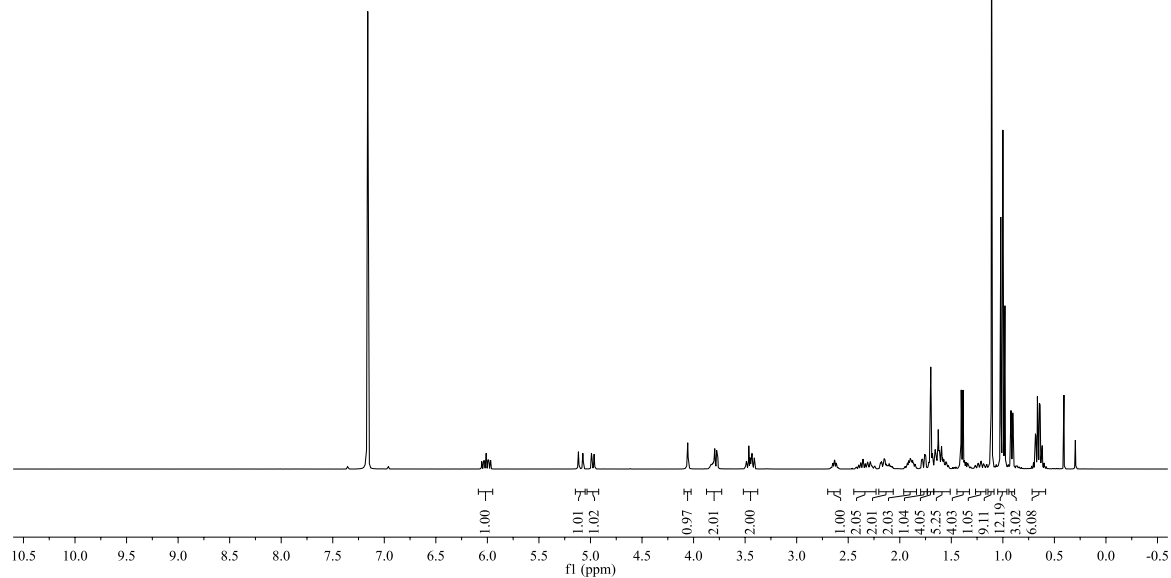
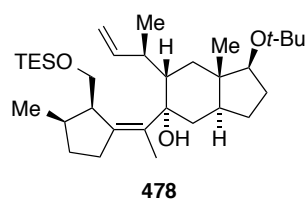
^1H NMR (C_6D_6 , 400 MHz):



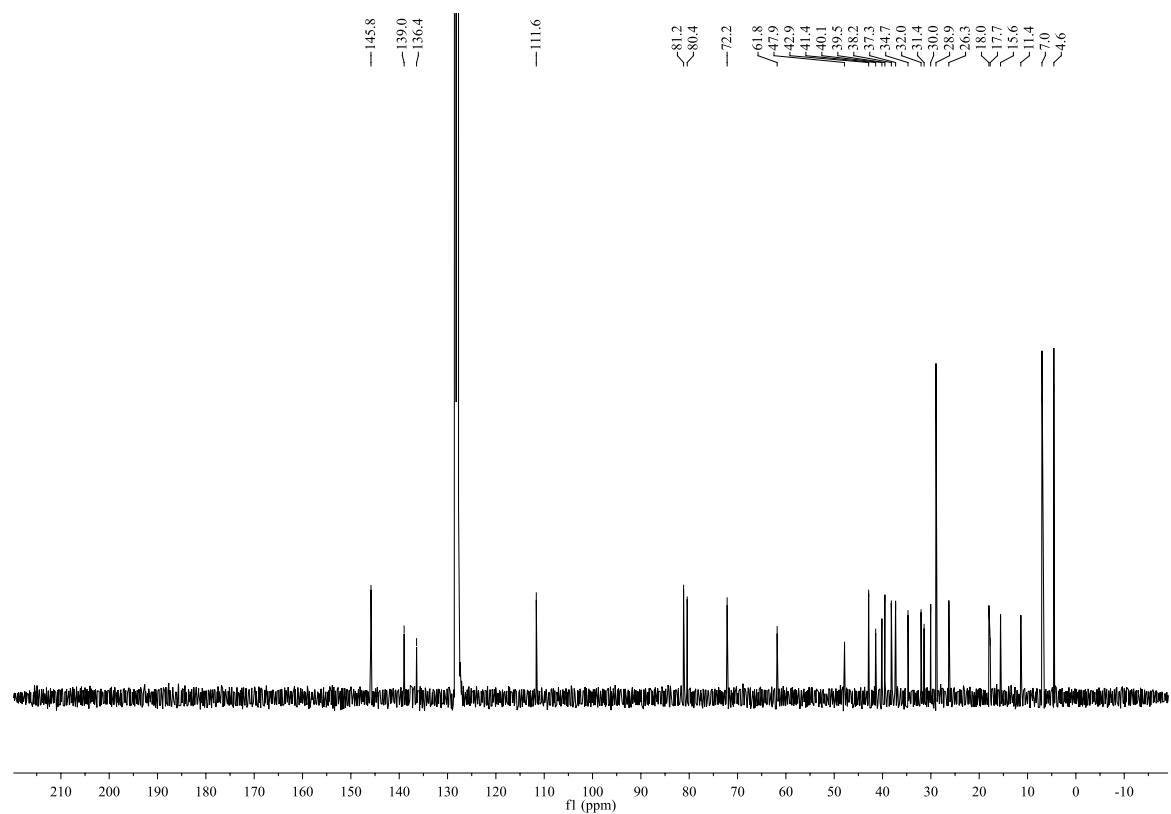
^{13}C NMR (C_6D_6 , 100 MHz):



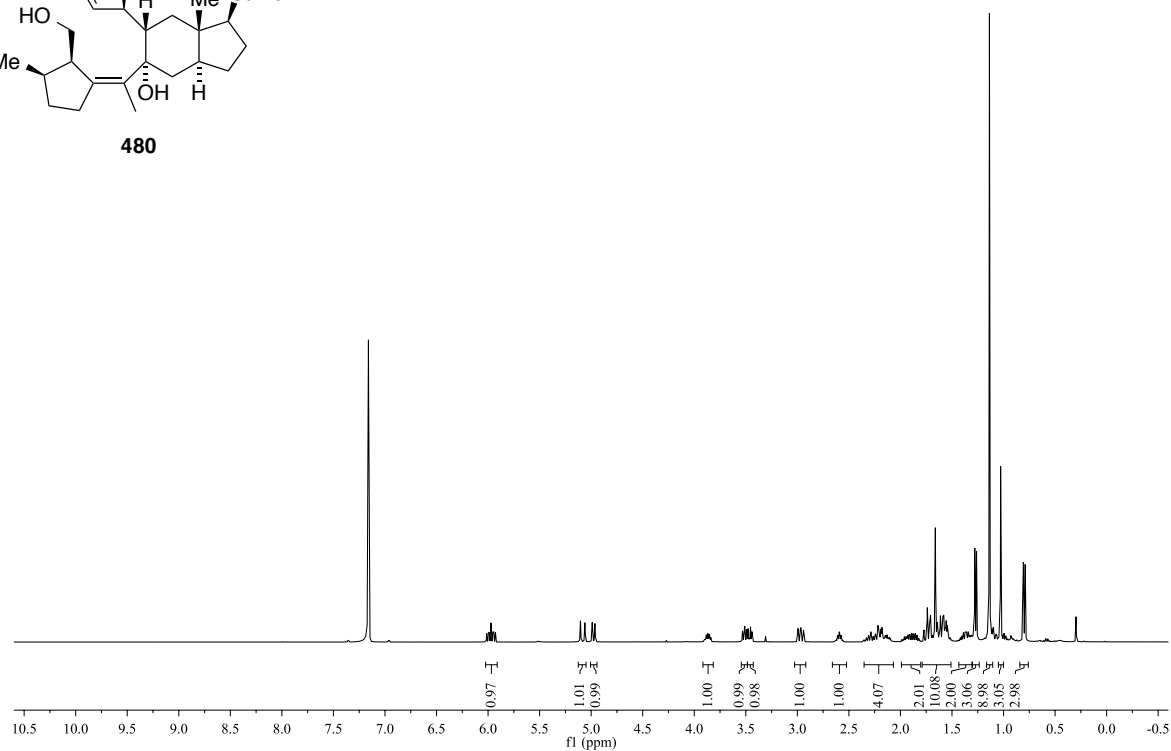
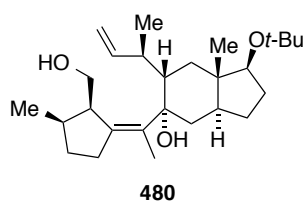
^1H NMR (C_6D_6 , 400 MHz):



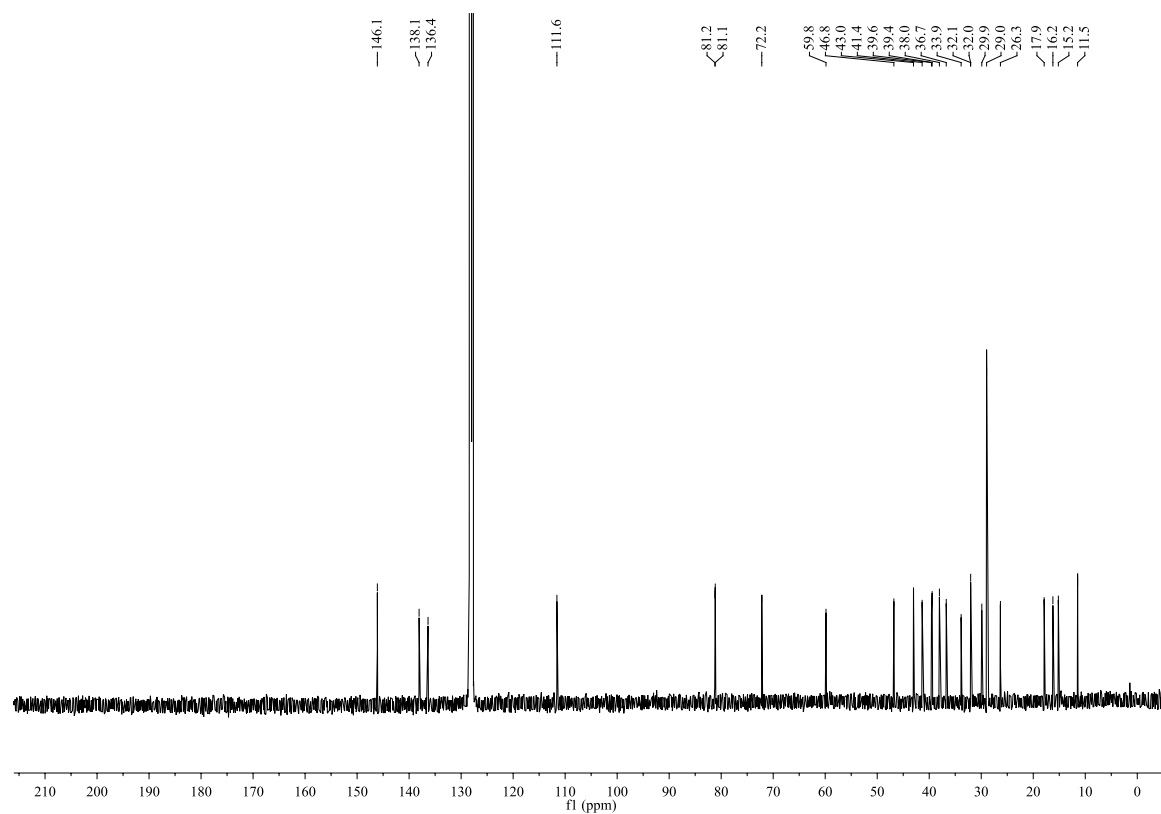
^{13}C NMR (C_6D_6 , 100 MHz):



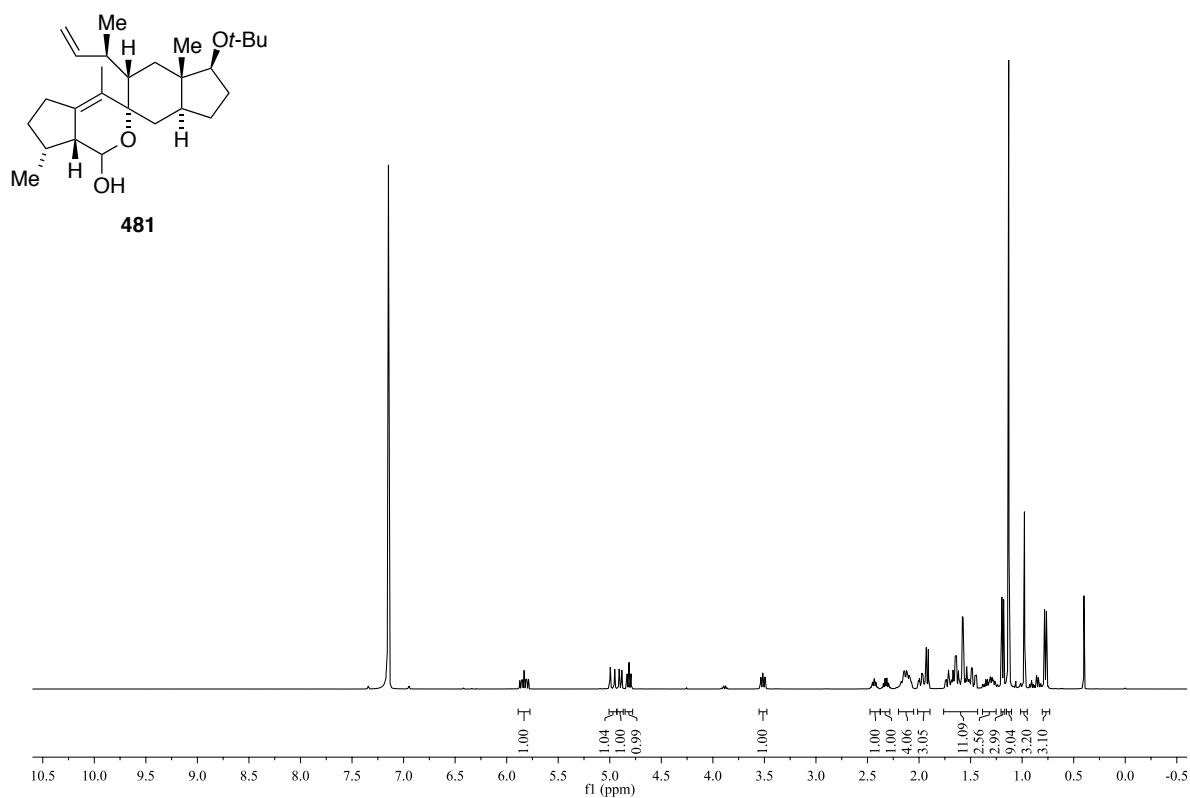
^1H NMR (C_6D_6 , 400 MHz):



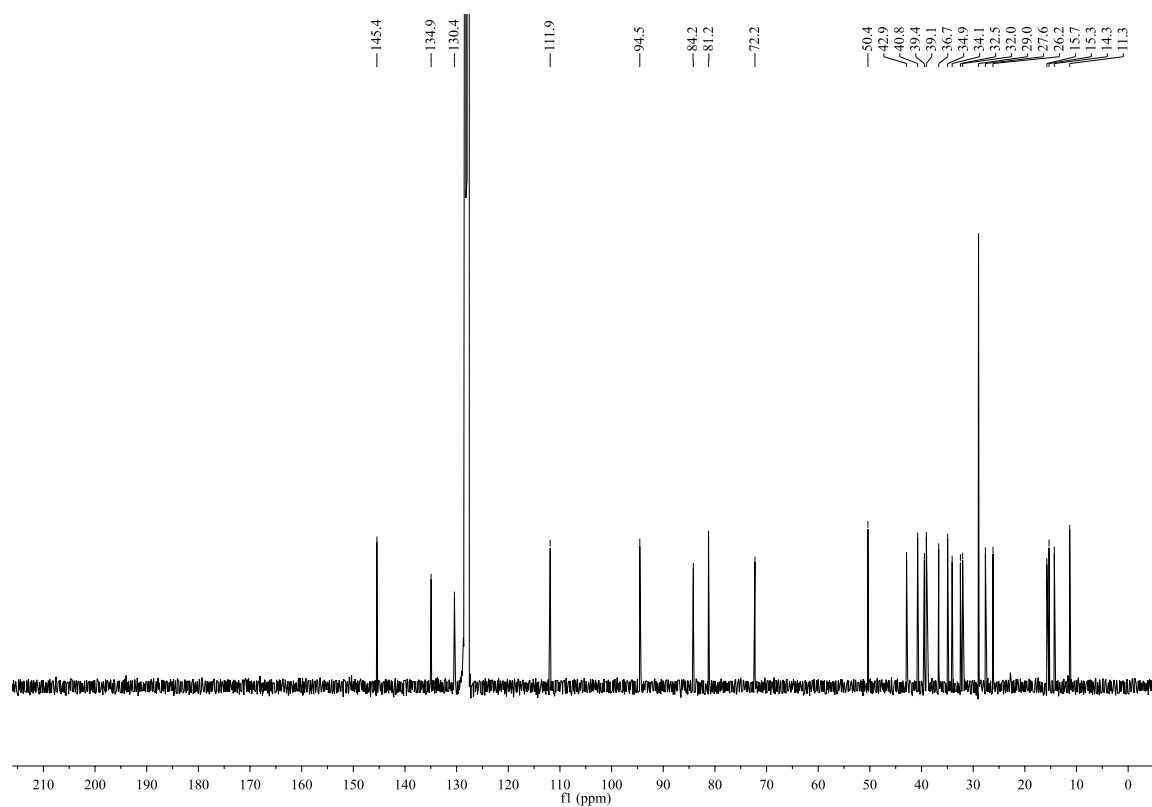
^{13}C NMR (C_6D_6 , 100 MHz):



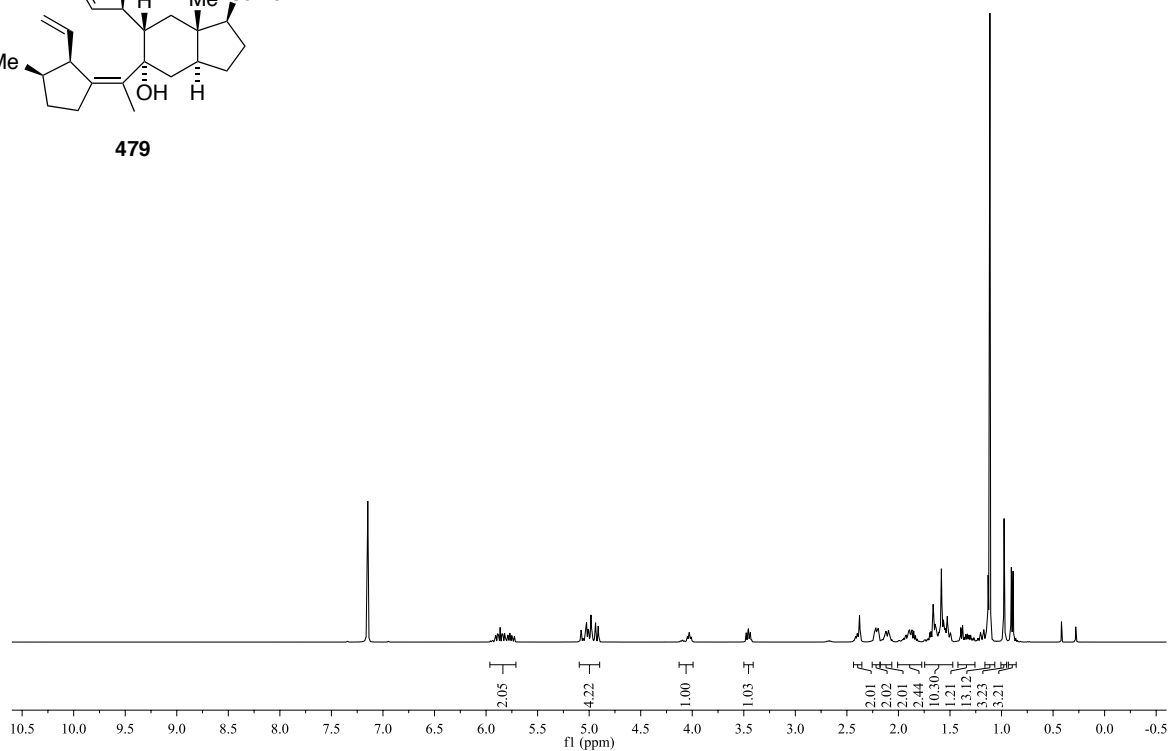
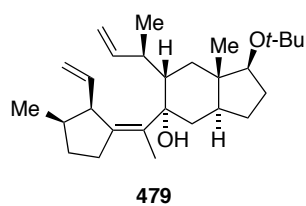
^1H NMR (C_6D_6 , 400 MHz):



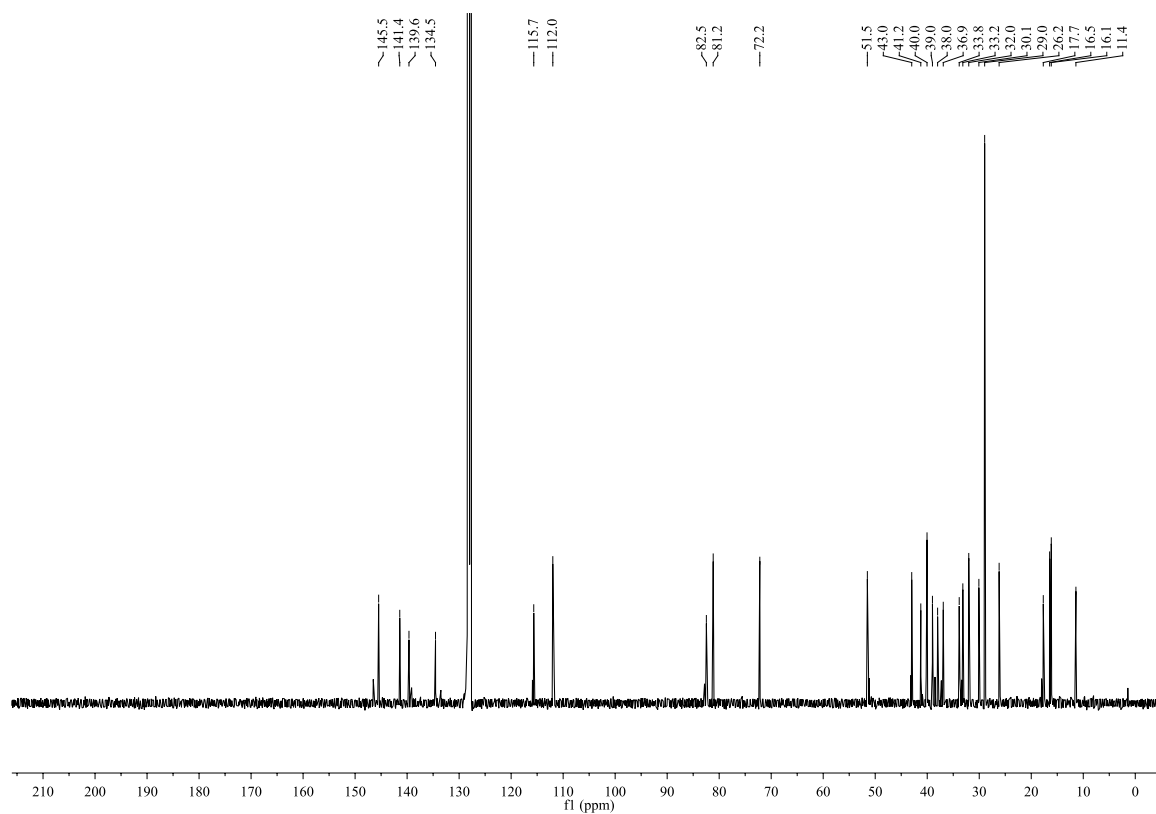
^{13}C NMR (C_6D_6 , 100 MHz):



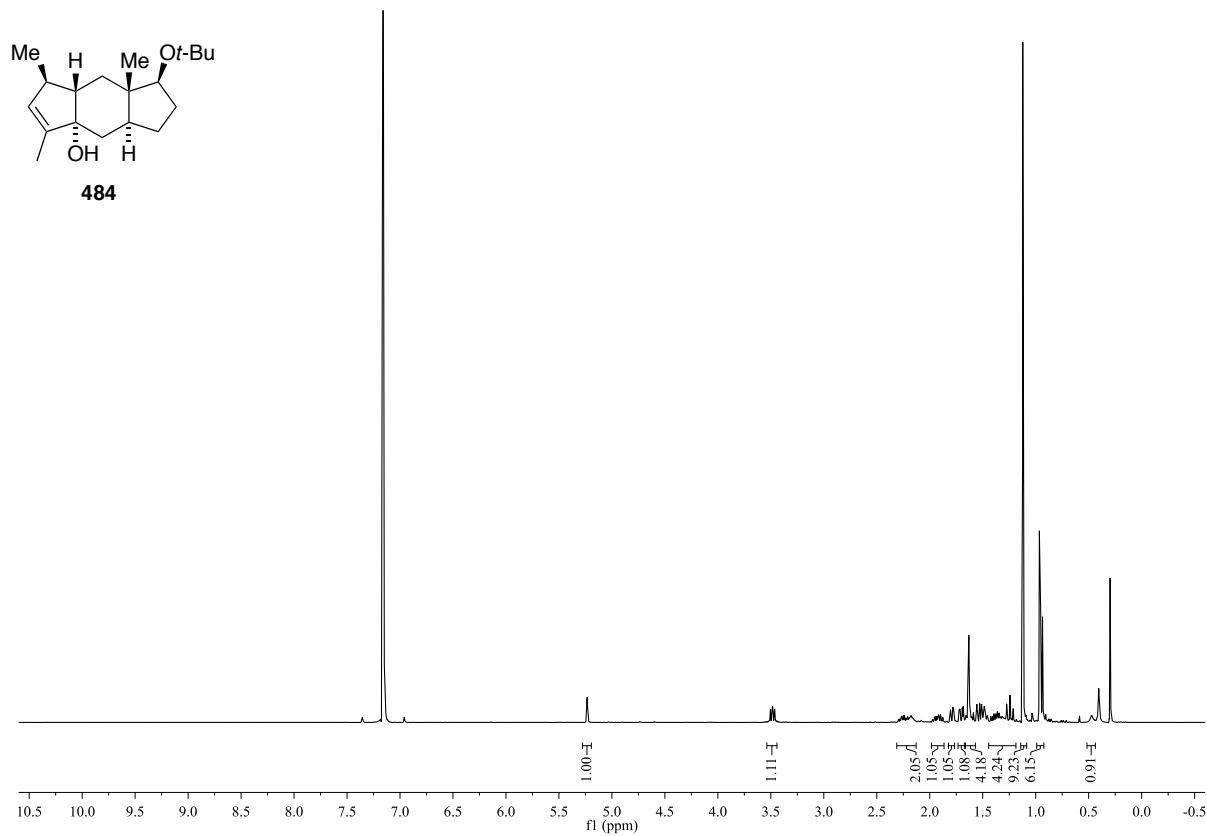
^1H NMR (C_6D_6 , 400 MHz):



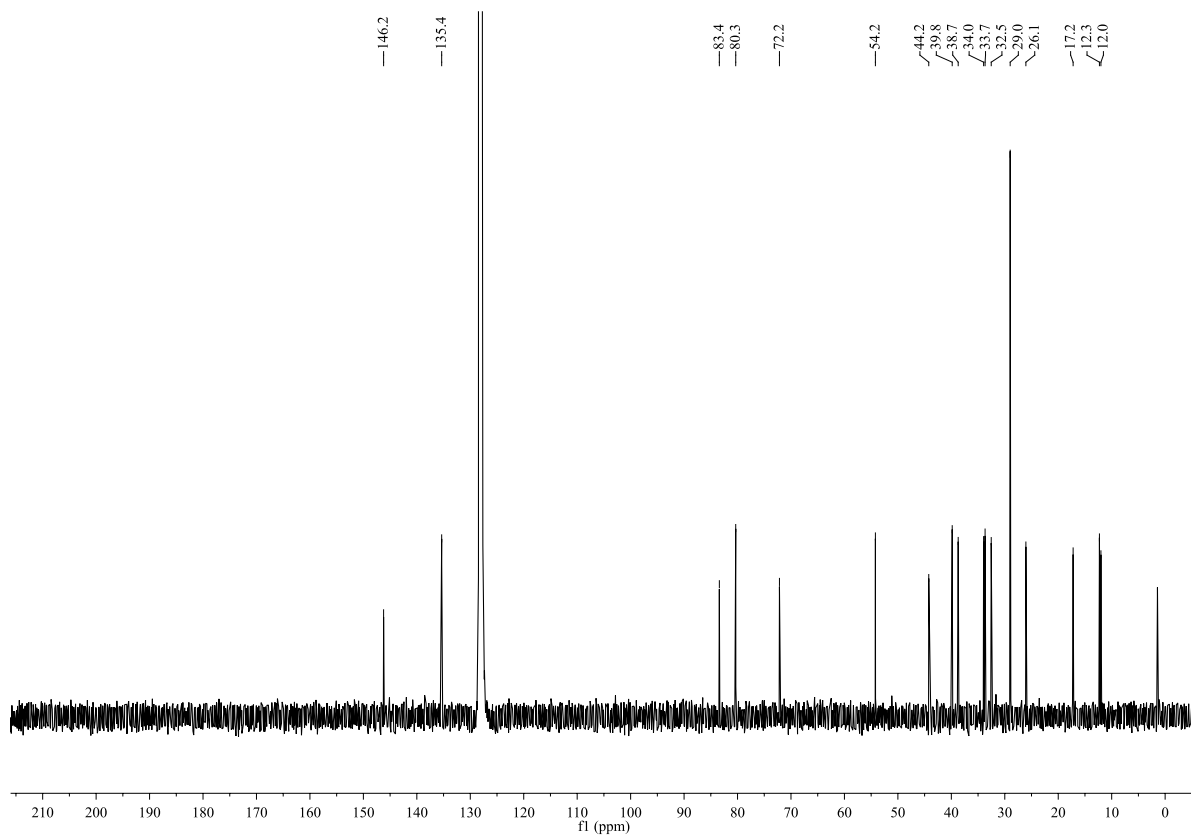
^{13}C NMR (C_6D_6 , 100 MHz):



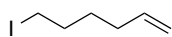
^1H NMR (C_6D_6 , 400 MHz):



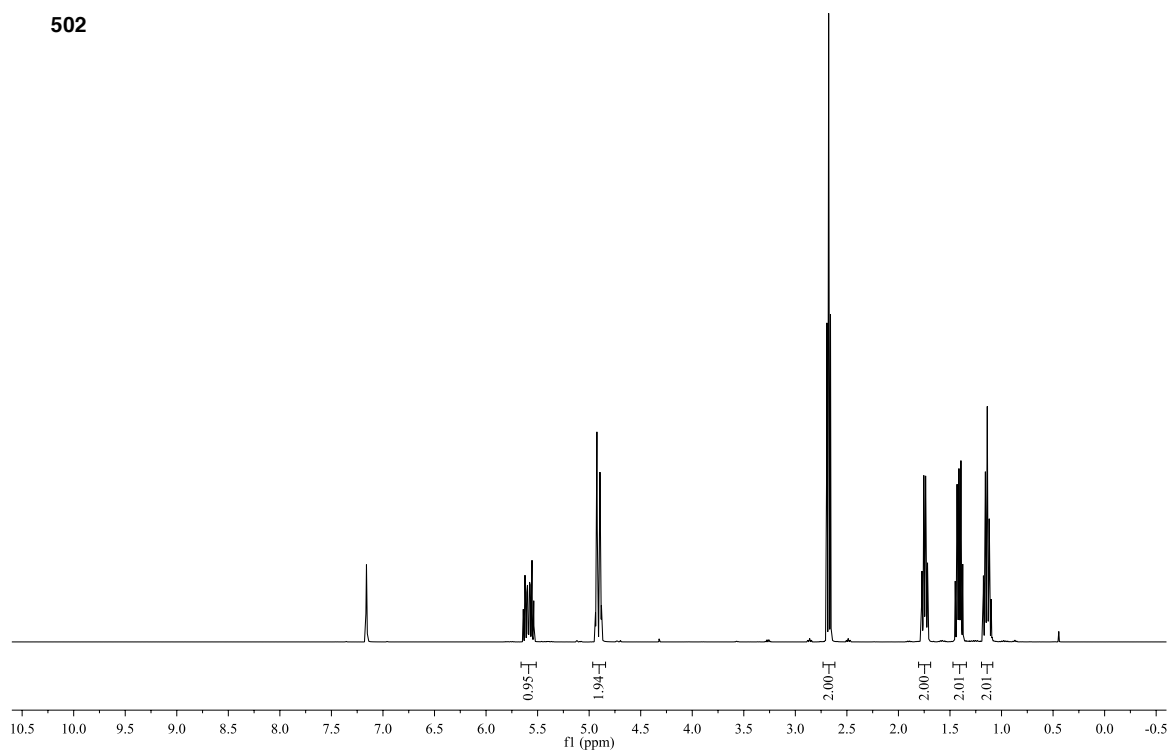
^{13}C NMR (C_6D_6 , 100 MHz):



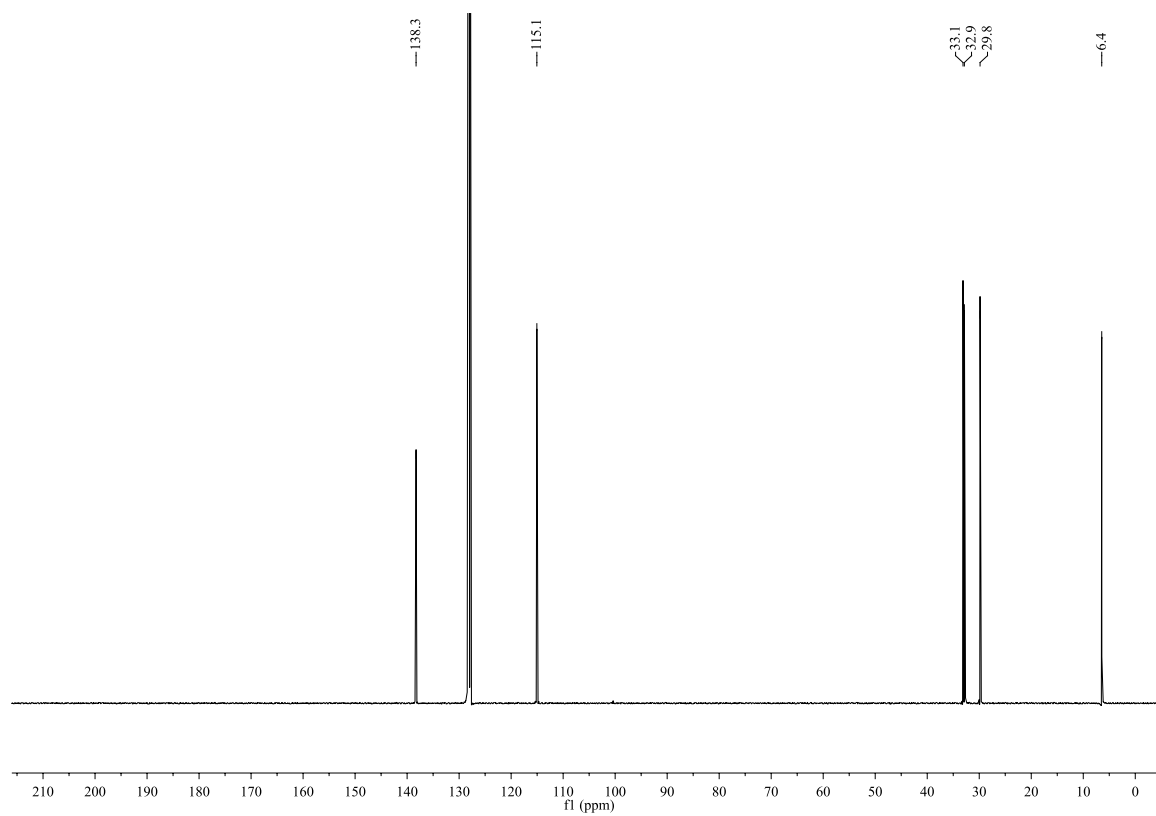
^1H NMR (C_6D_6 , 400 MHz):



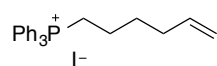
502



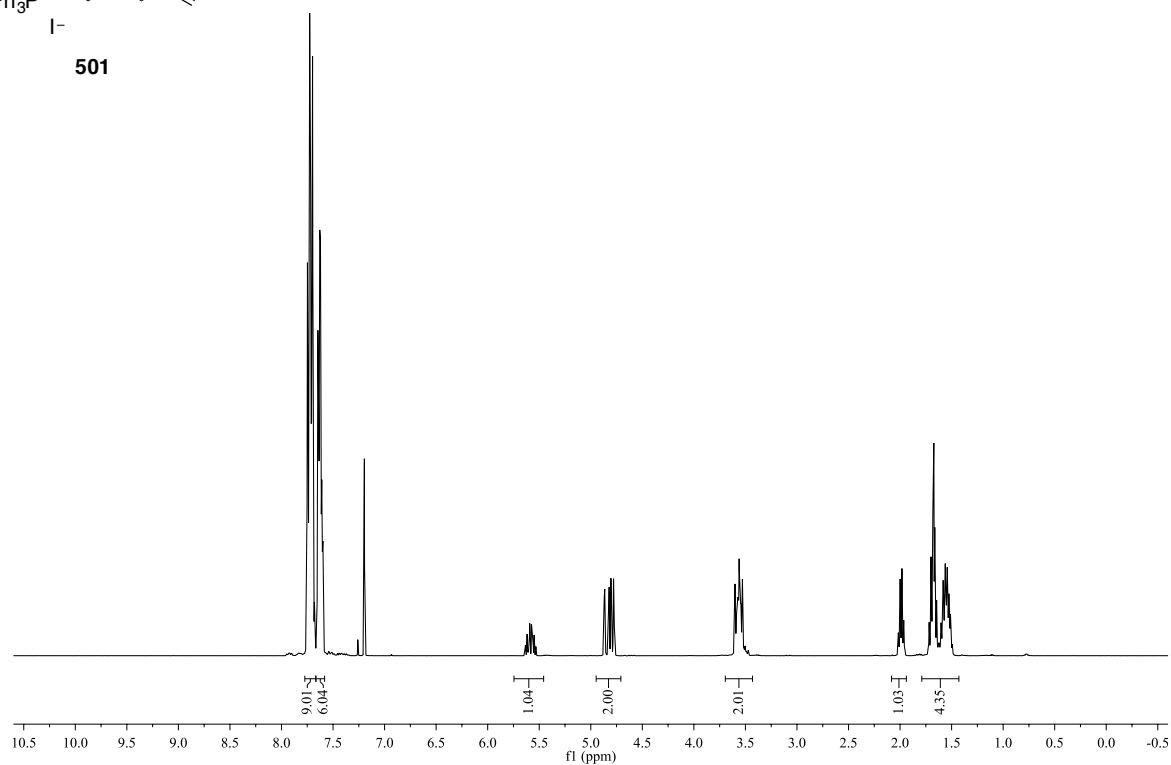
^{13}C NMR (C_6D_6 , 100 MHz):



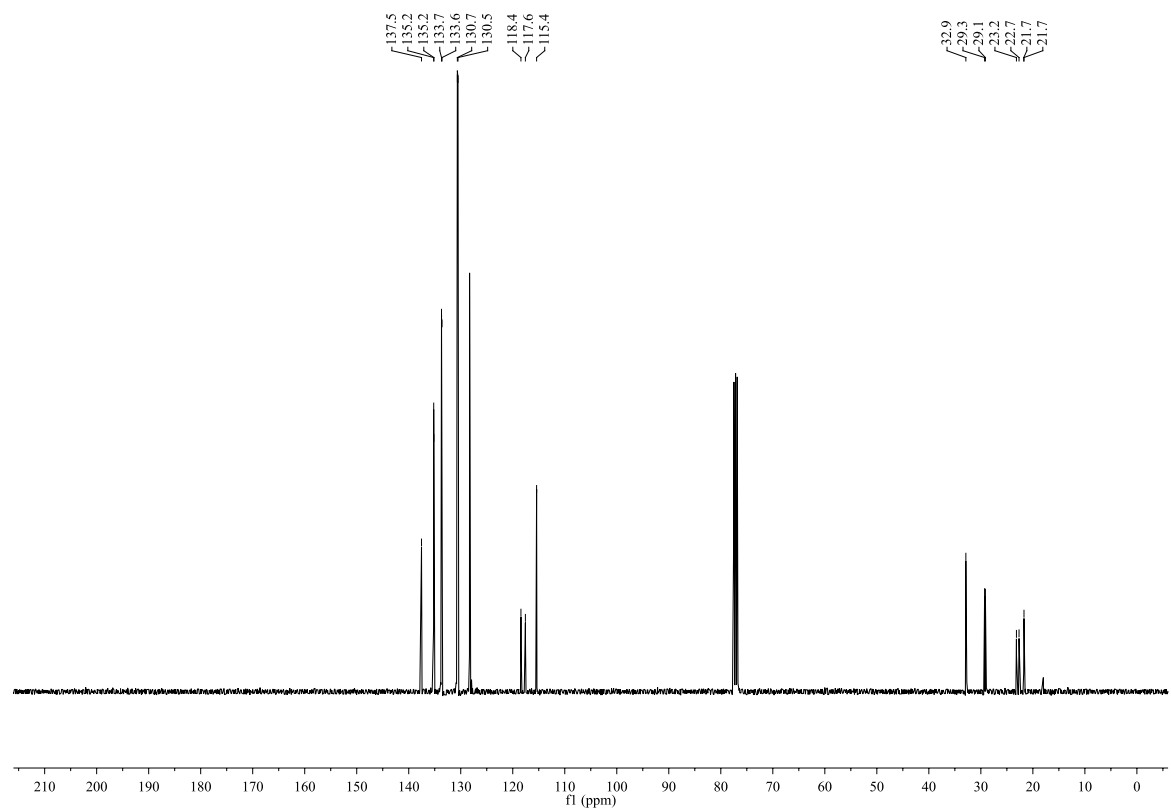
^1H NMR (CDCl_3 , 400 MHz):

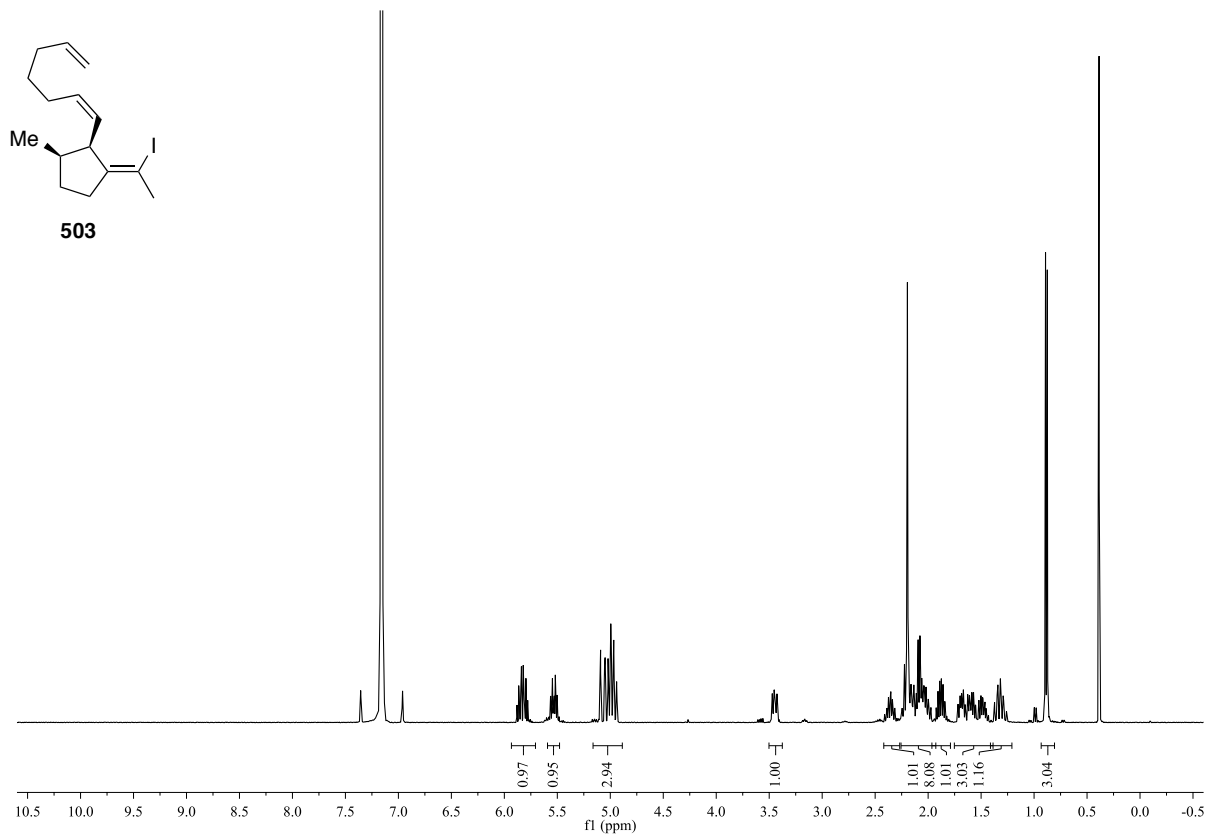
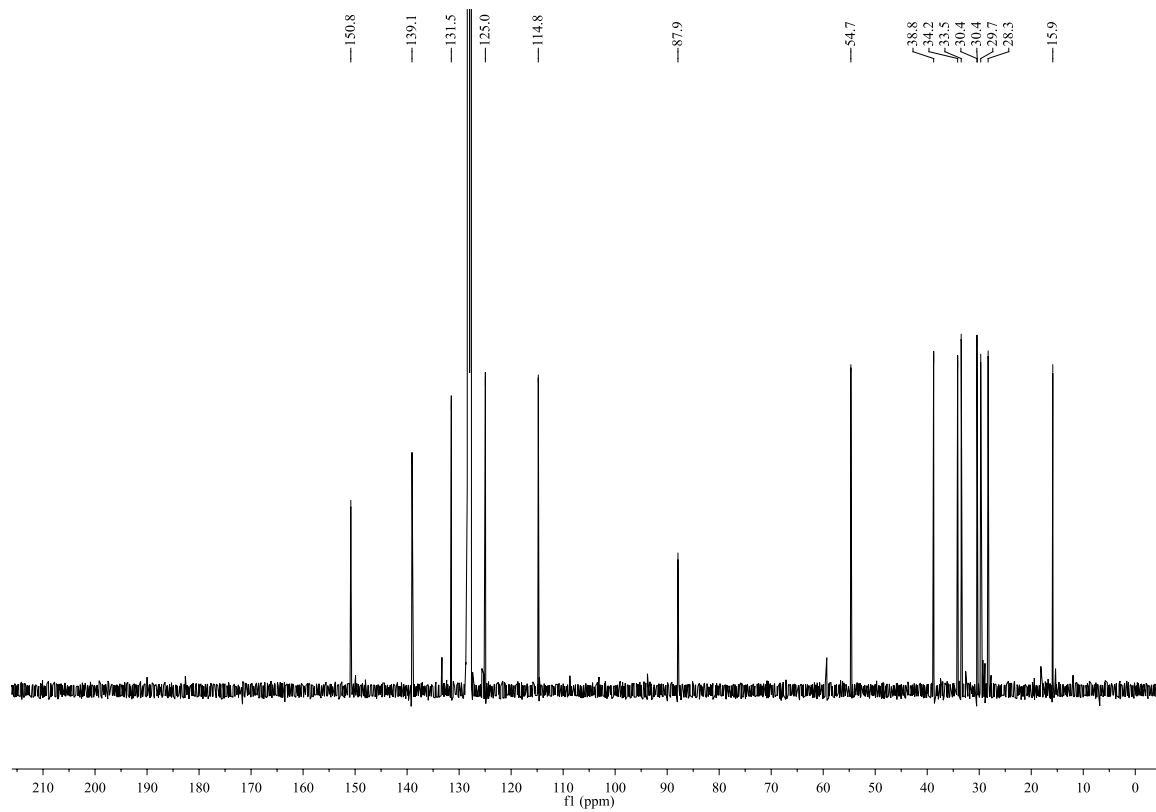


501

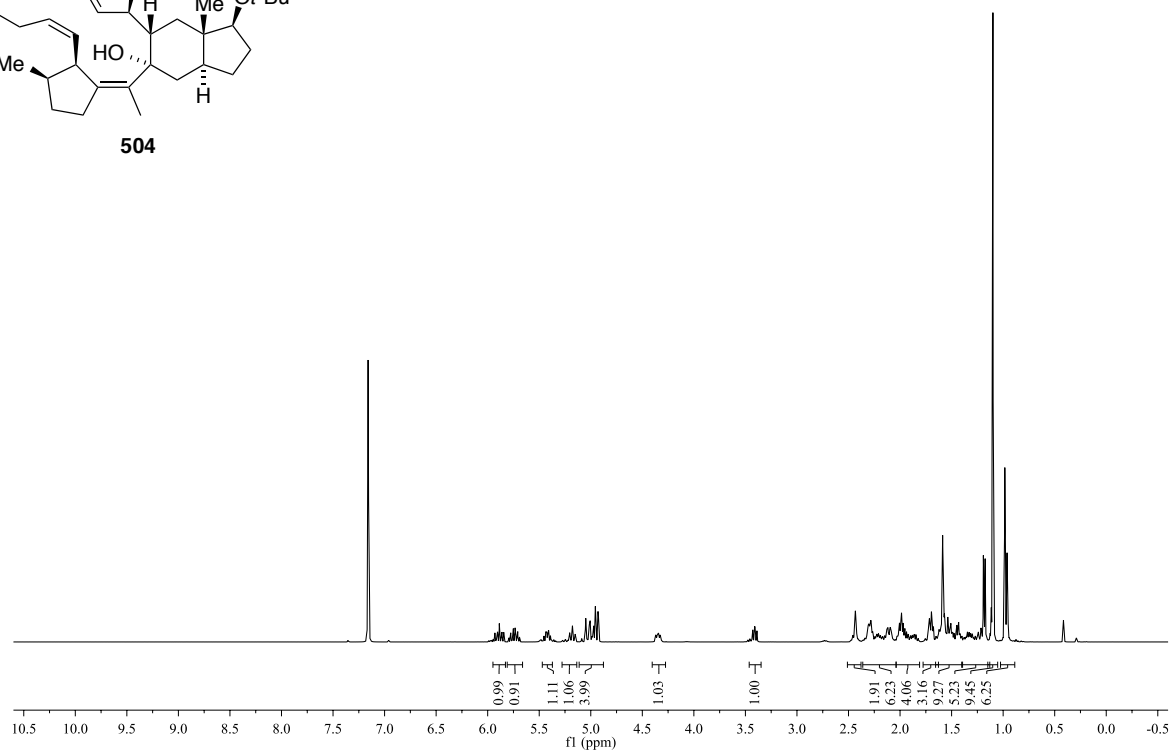
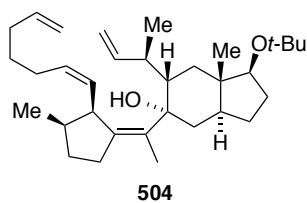


^{13}C NMR (CDCl_3 , 100 MHz):

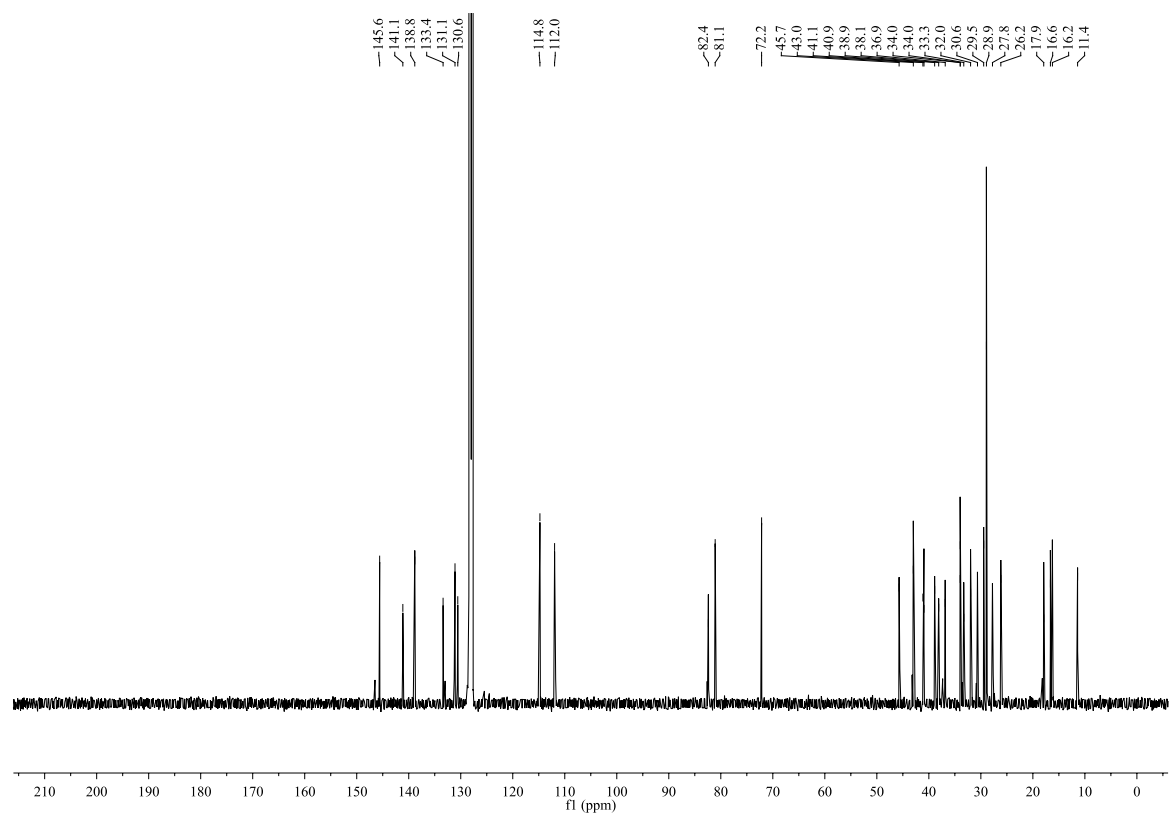


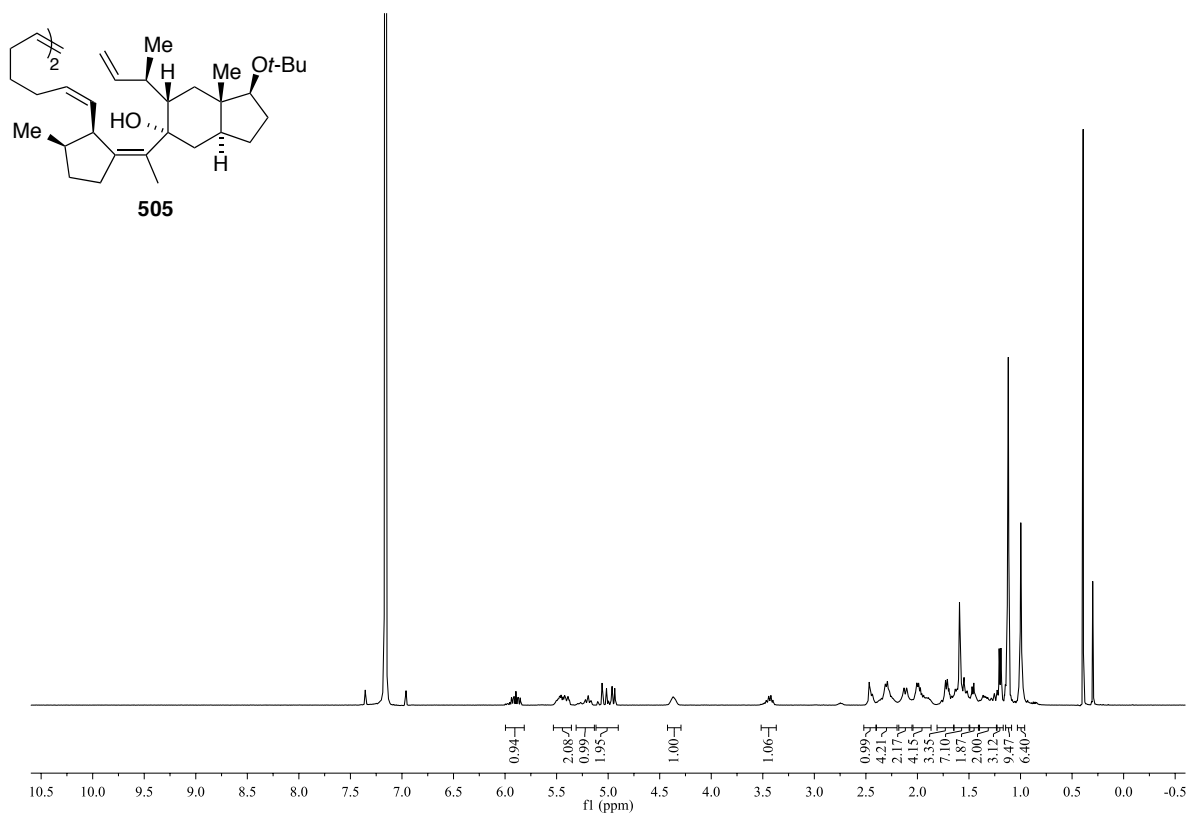
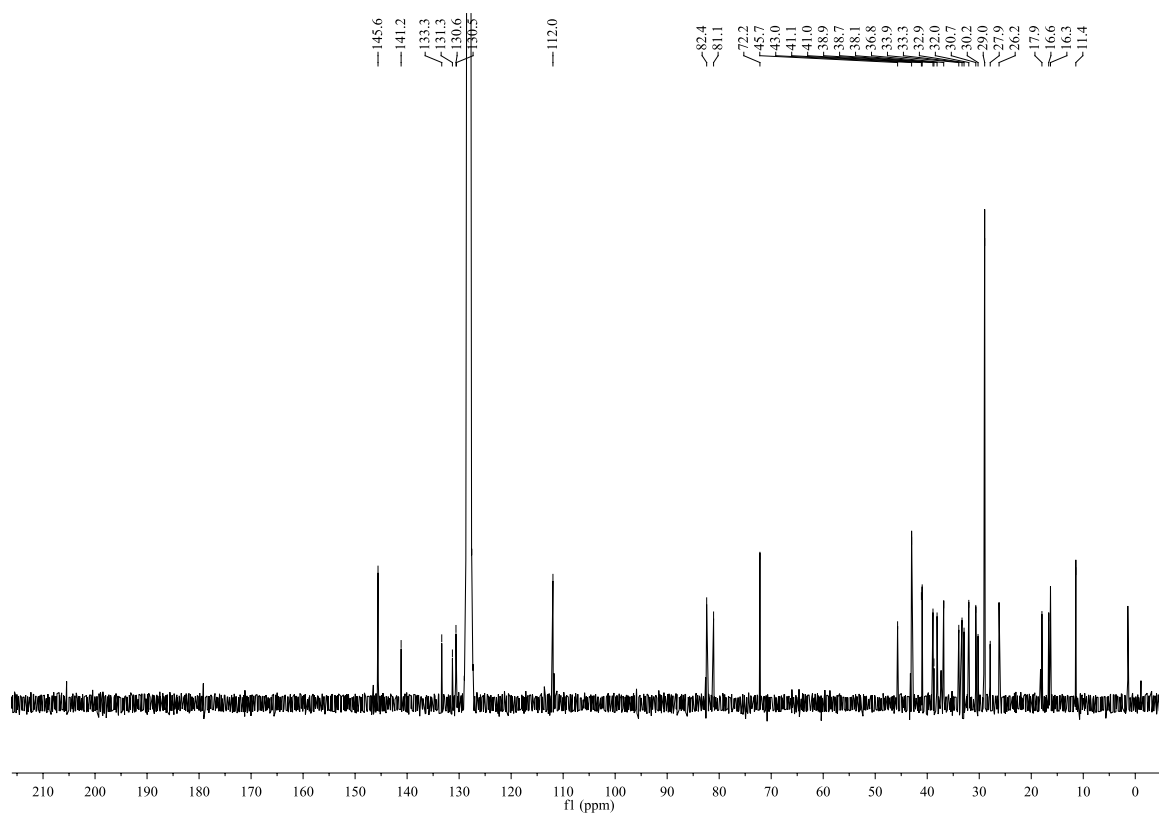
^1H NMR (C_6D_6 , 400 MHz): ^{13}C NMR (C_6D_6 , 100 MHz):

^1H NMR (C_6D_6 , 400 MHz):

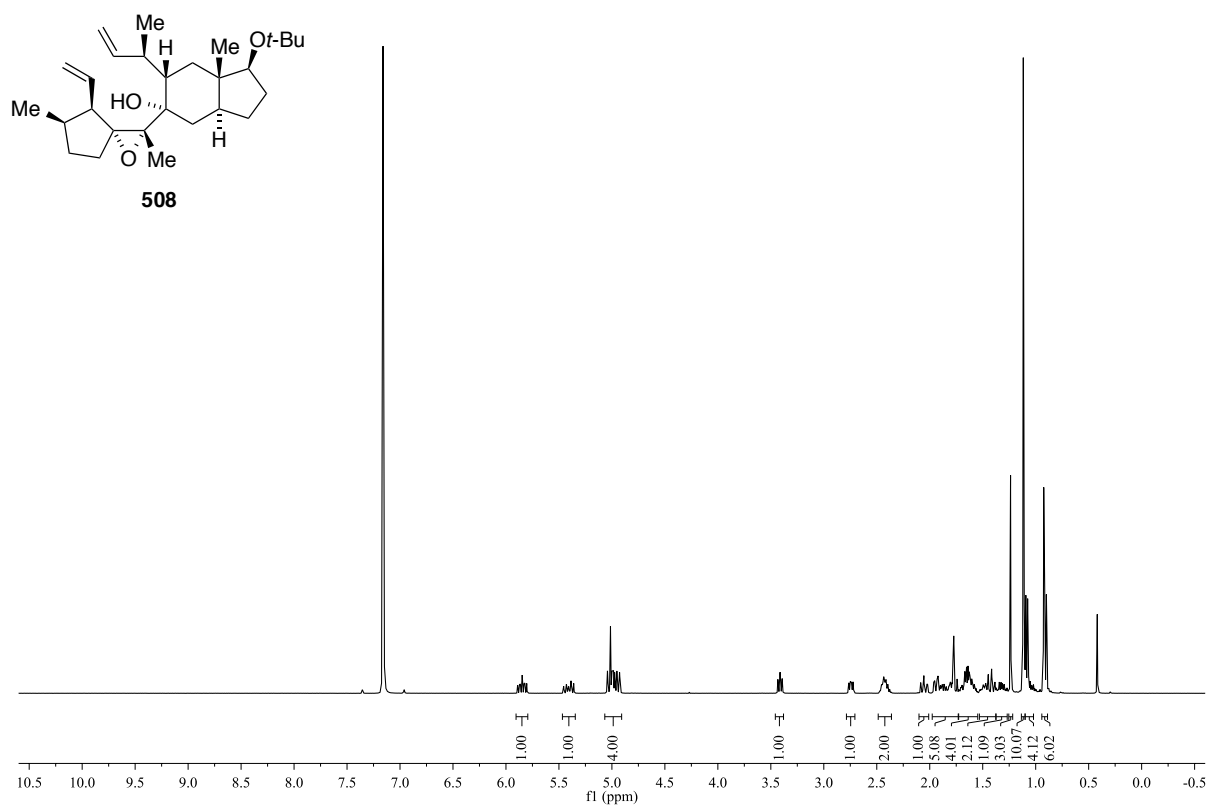


^{13}C NMR (C_6D_6 , 100 MHz):

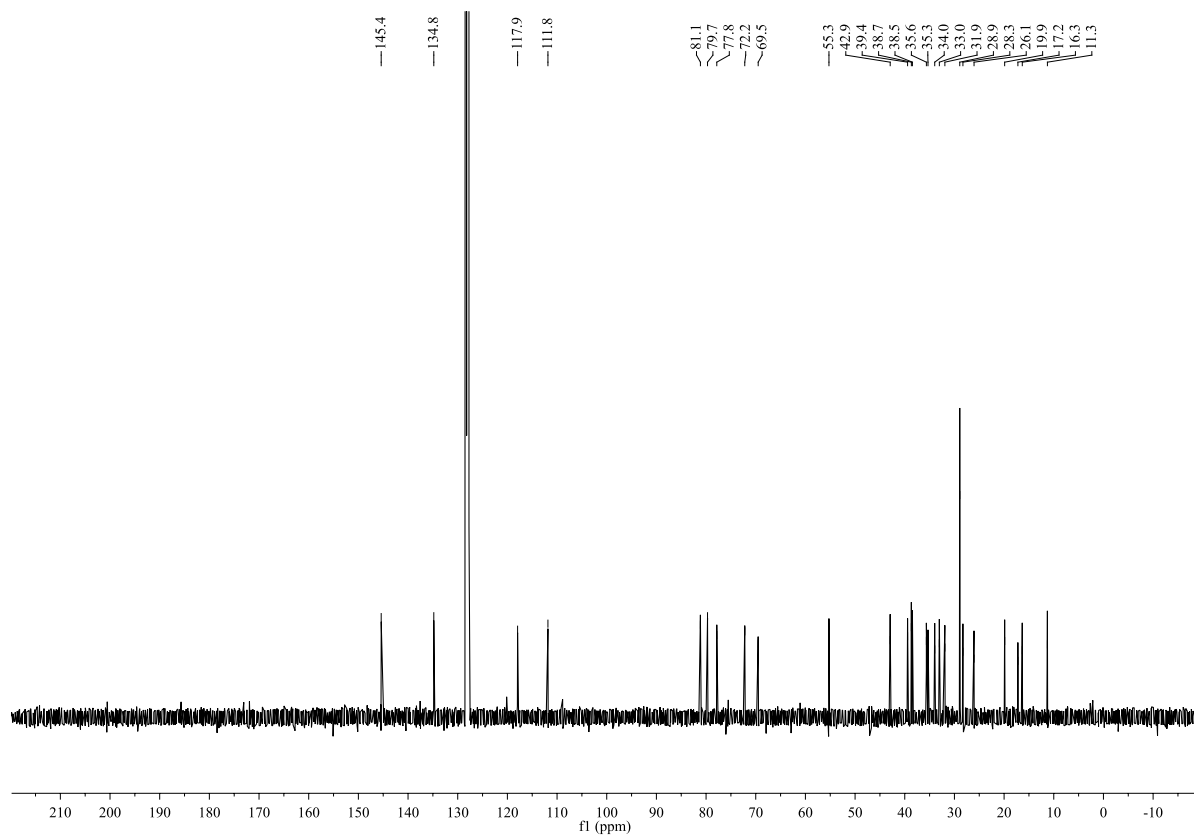


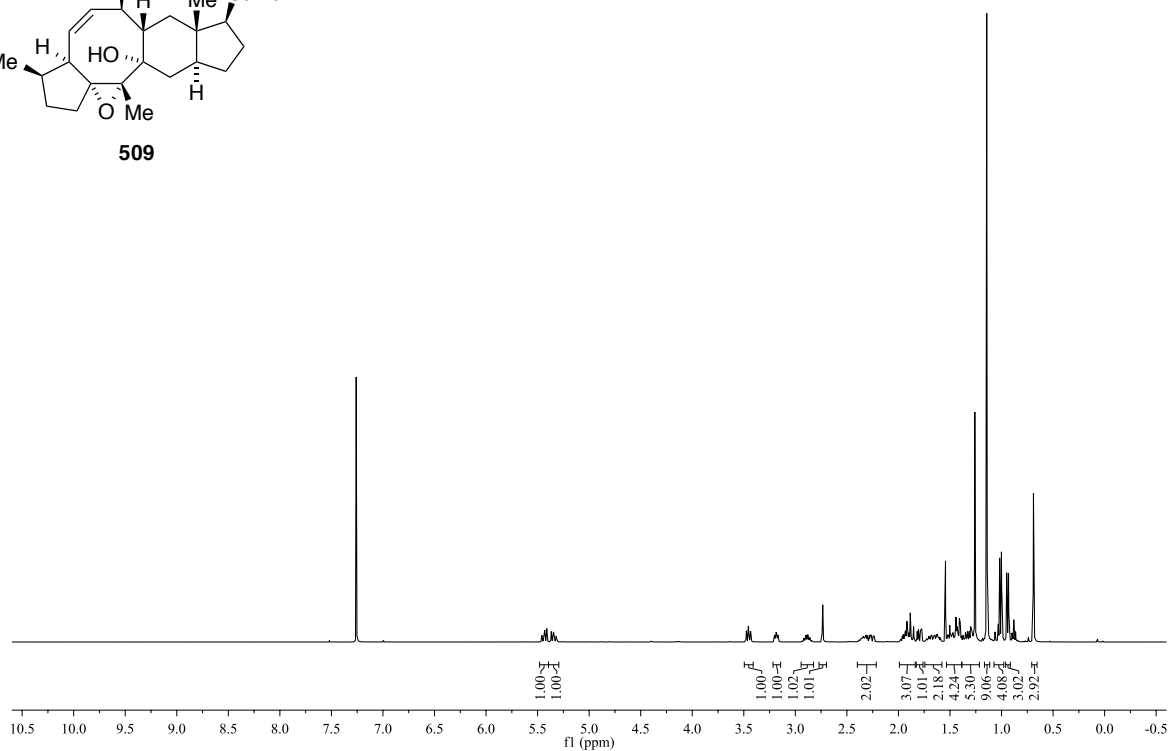
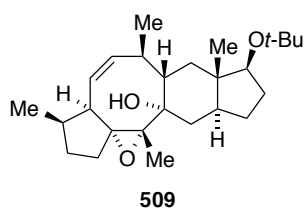
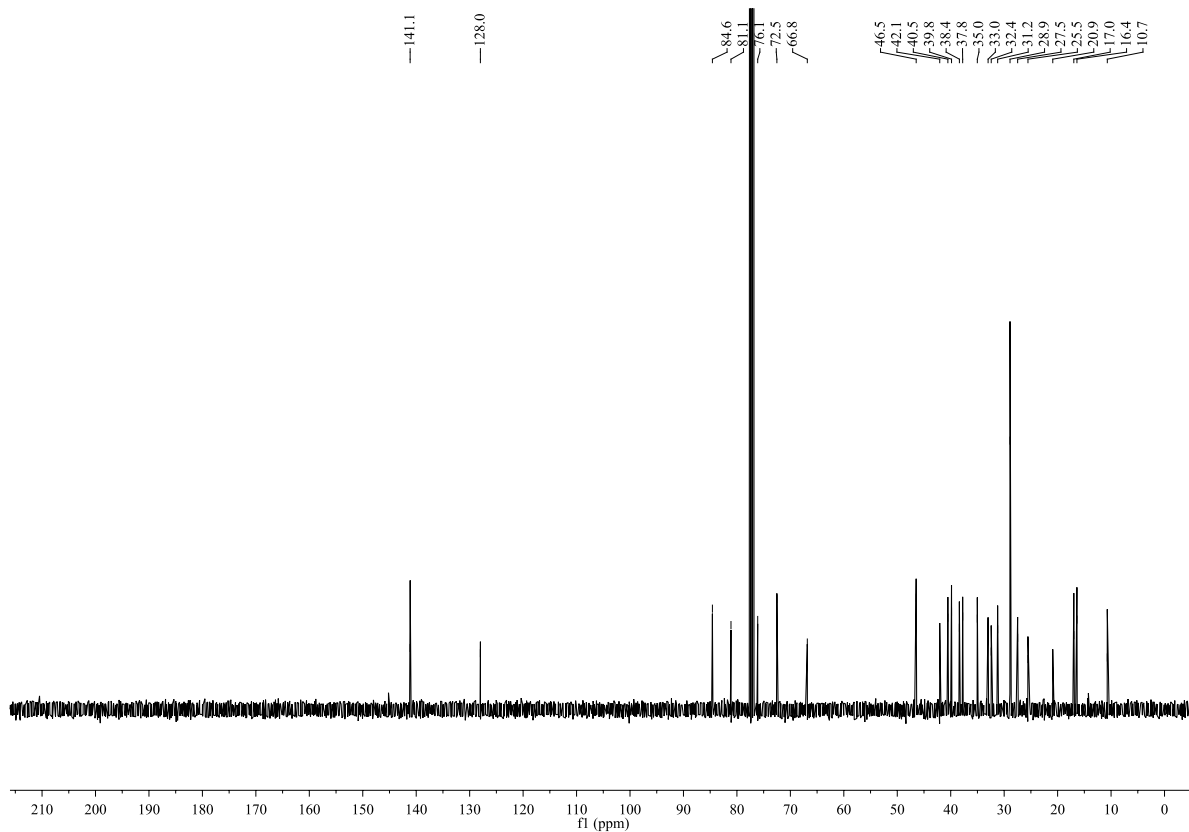
^1H NMR (C_6D_6 , 400 MHz): ^{13}C NMR (C_6D_6 , 100 MHz):

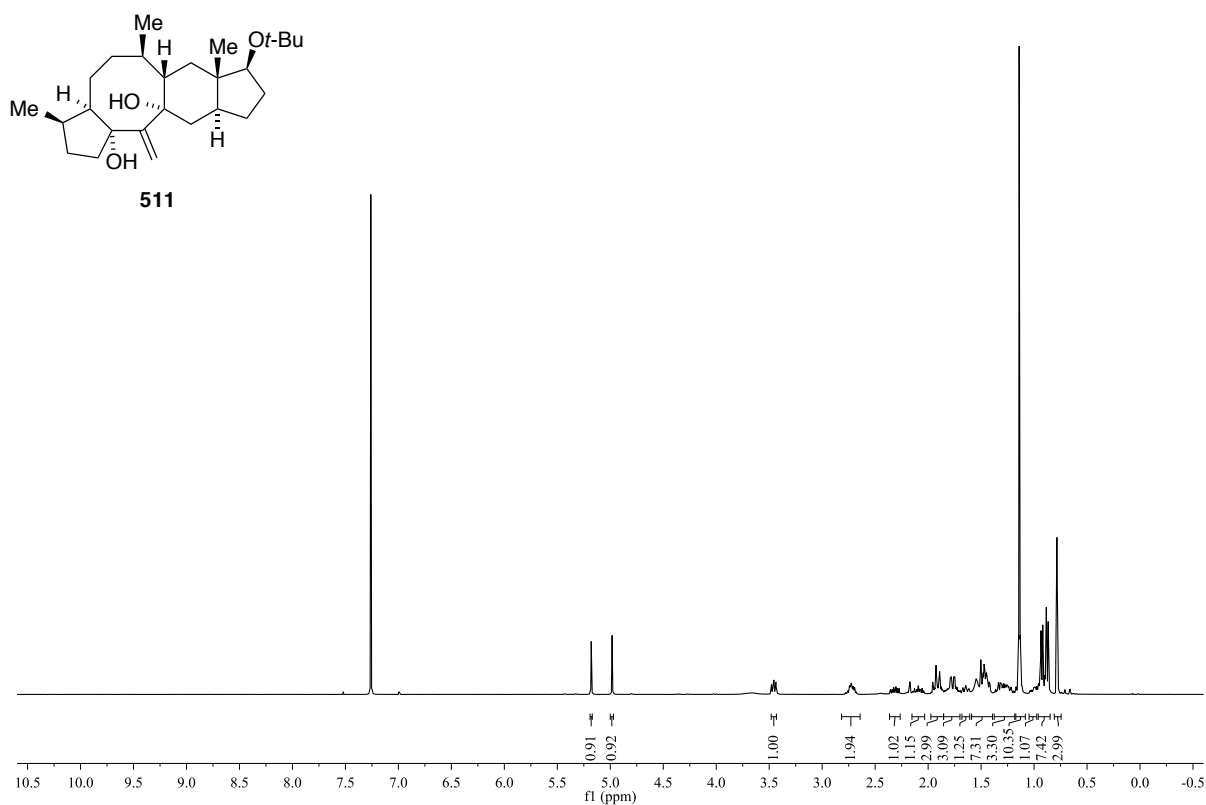
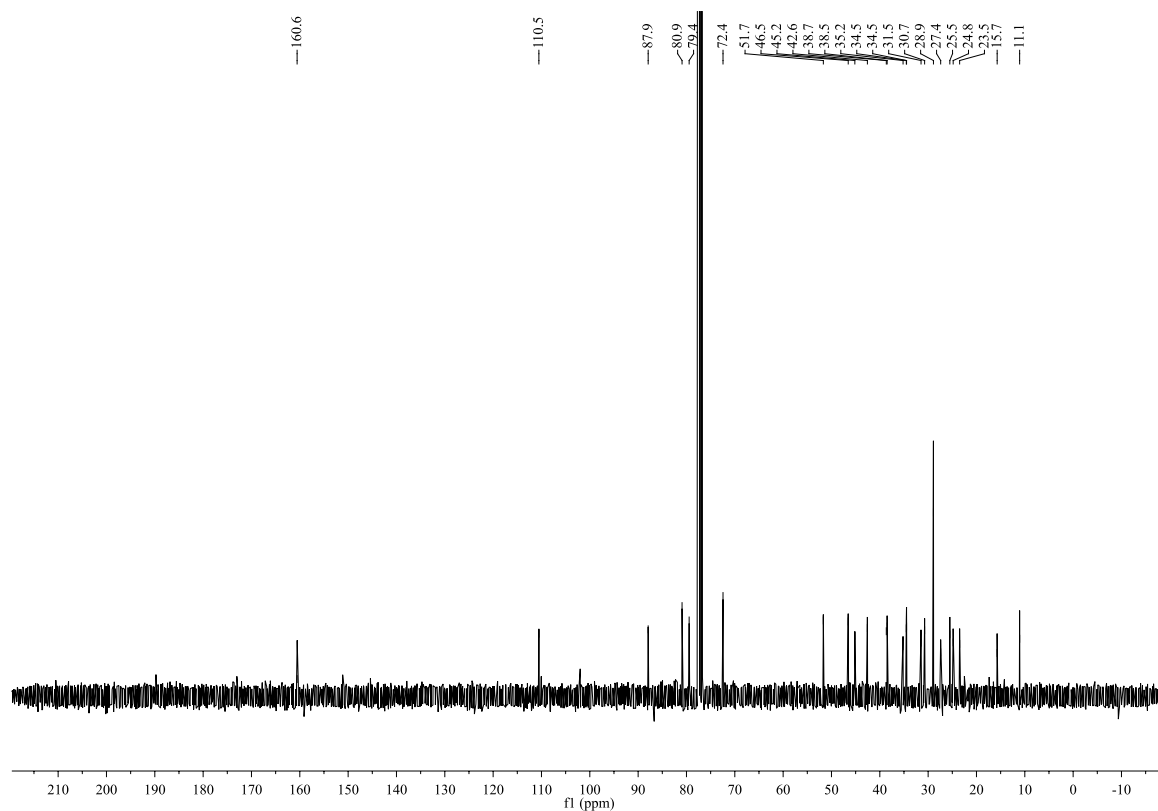
^1H NMR (C_6D_6 , 400 MHz):



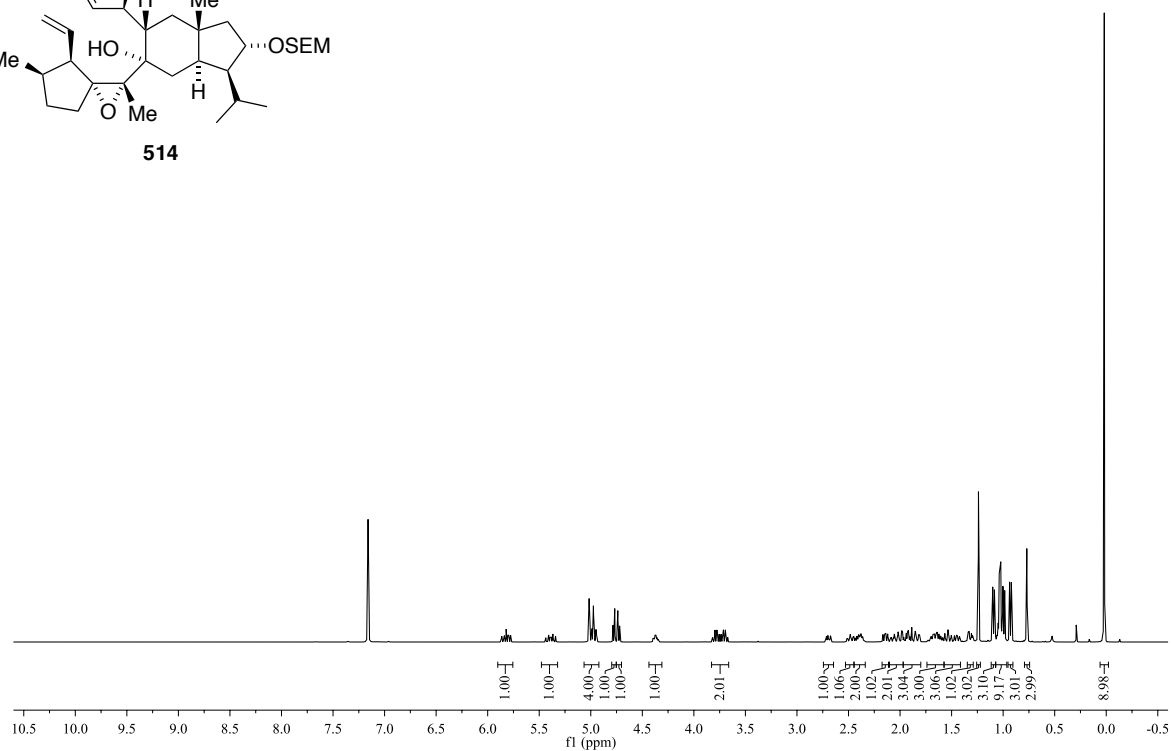
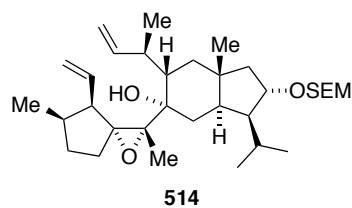
^{13}C NMR (C_6D_6 , 100 MHz):



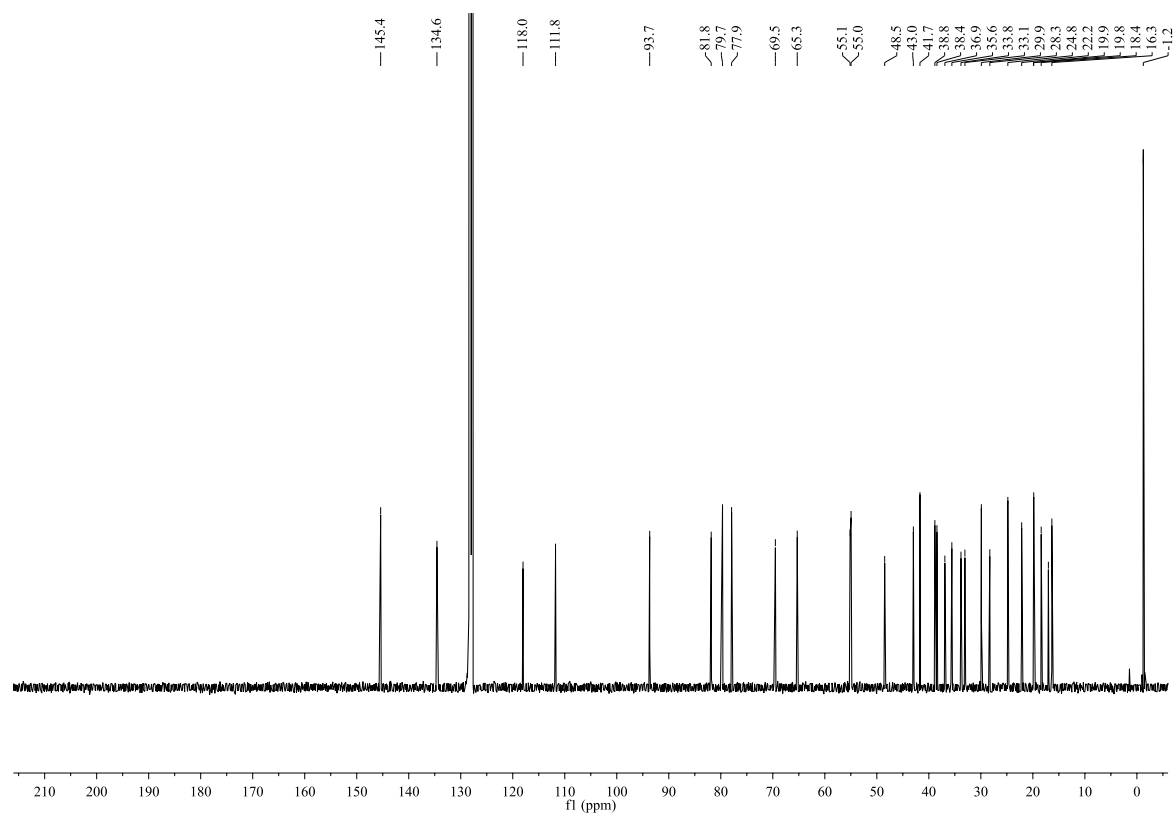
^1H NMR (CDCl_3 , 400 MHz): ^{13}C NMR (CDCl_3 , 100 MHz):

^1H NMR (CDCl_3 , 400 MHz): ^{13}C NMR (CDCl_3 , 100 MHz):

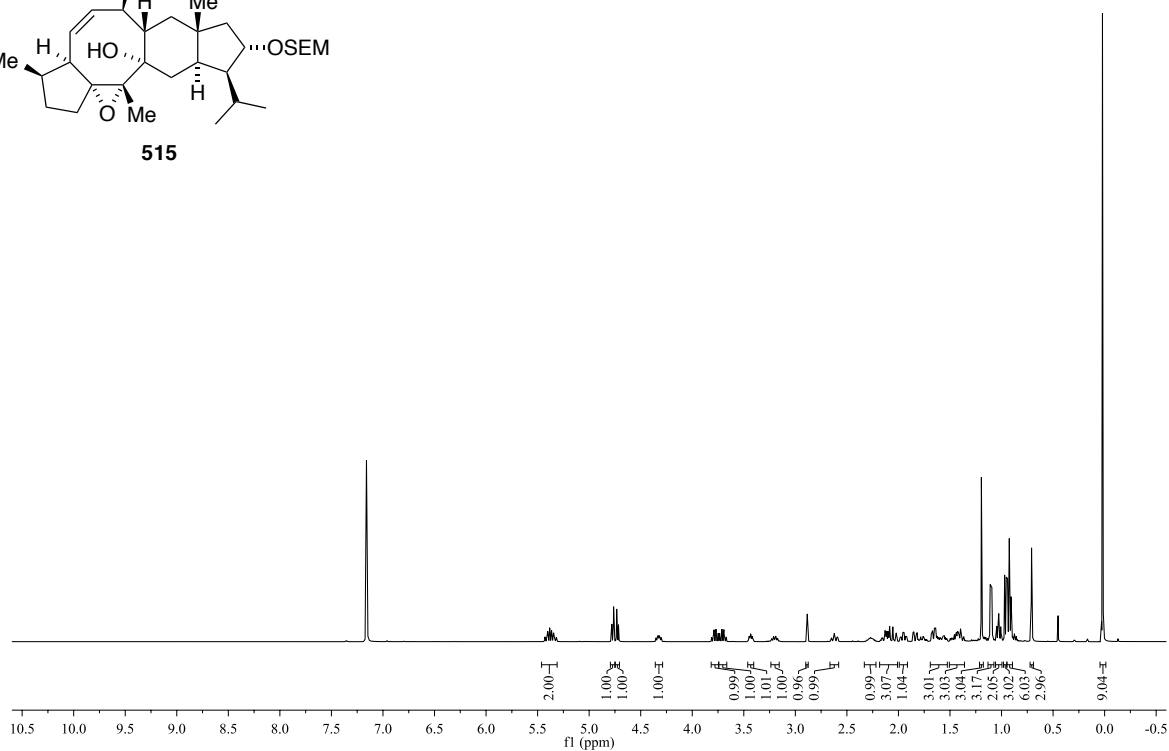
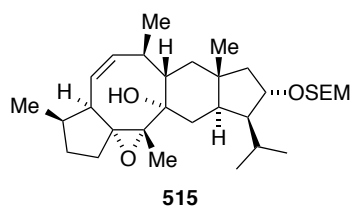
^1H NMR (C_6D_6 , 400 MHz):



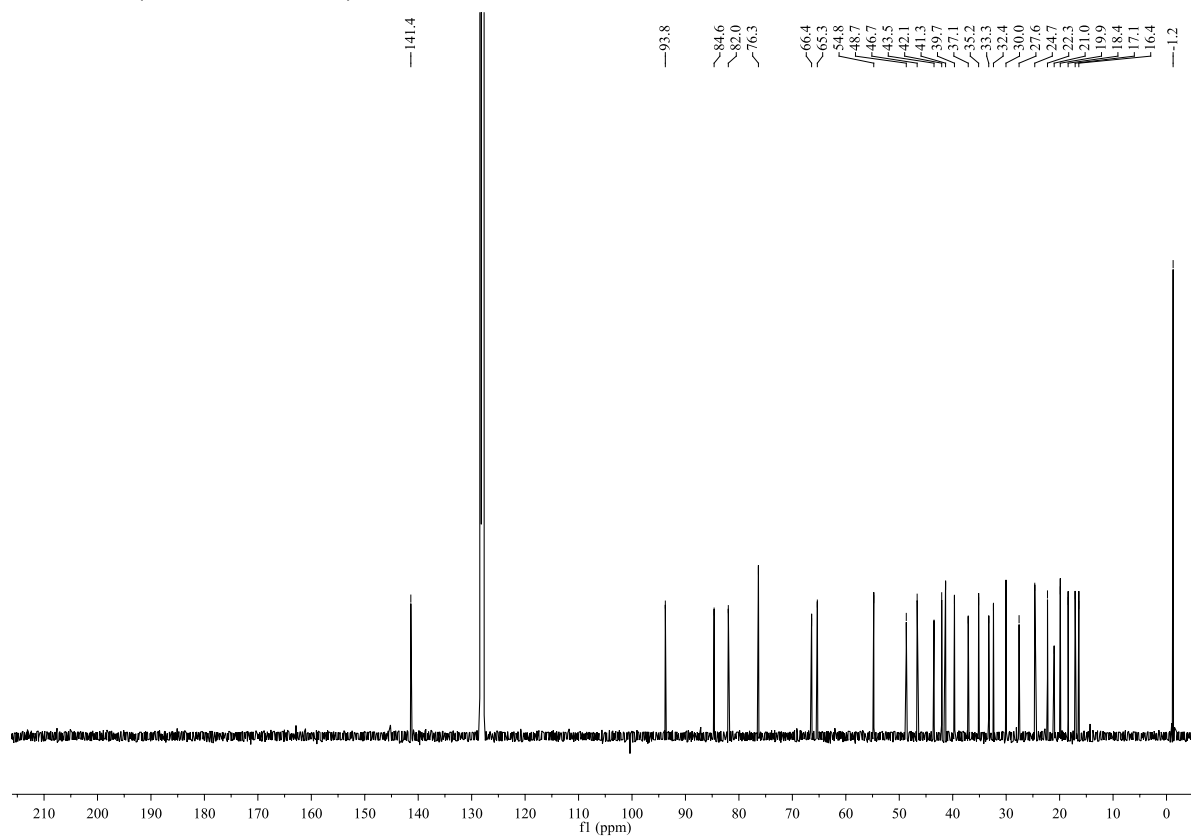
^{13}C NMR (C_6D_6 , 100 MHz):



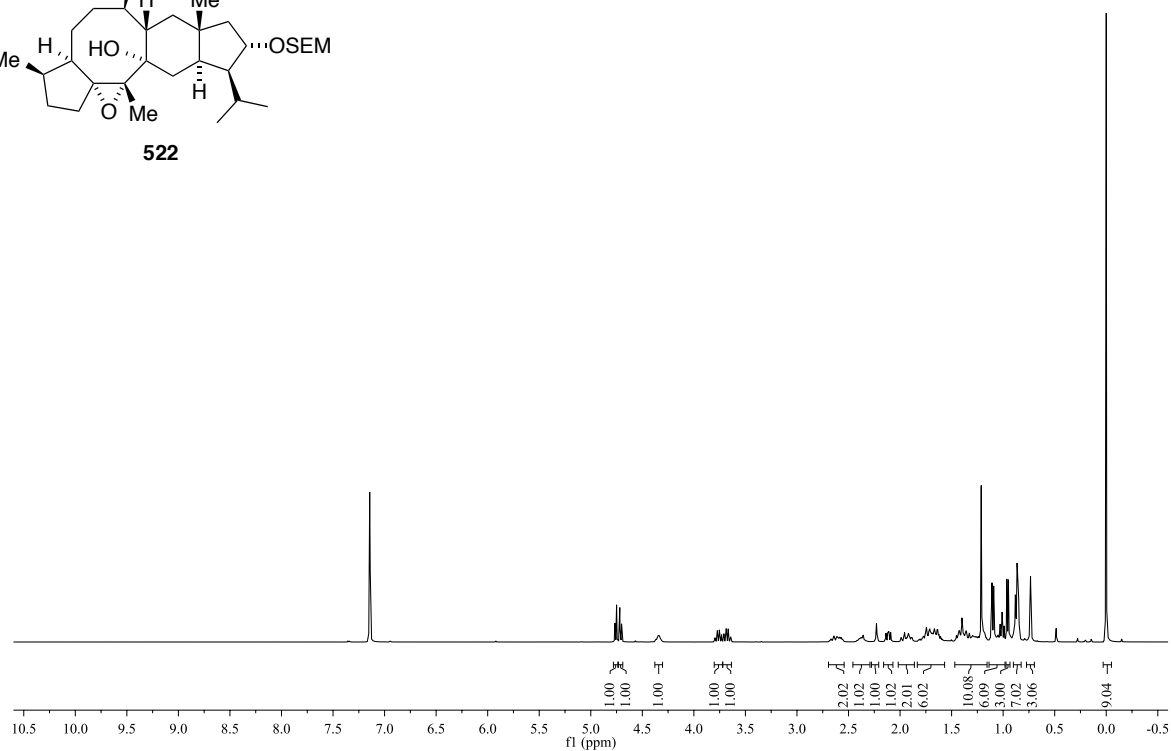
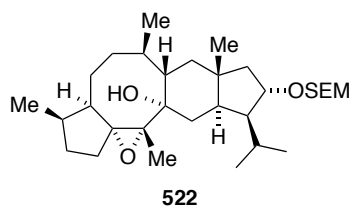
^1H NMR (C_6D_6 , 400 MHz):



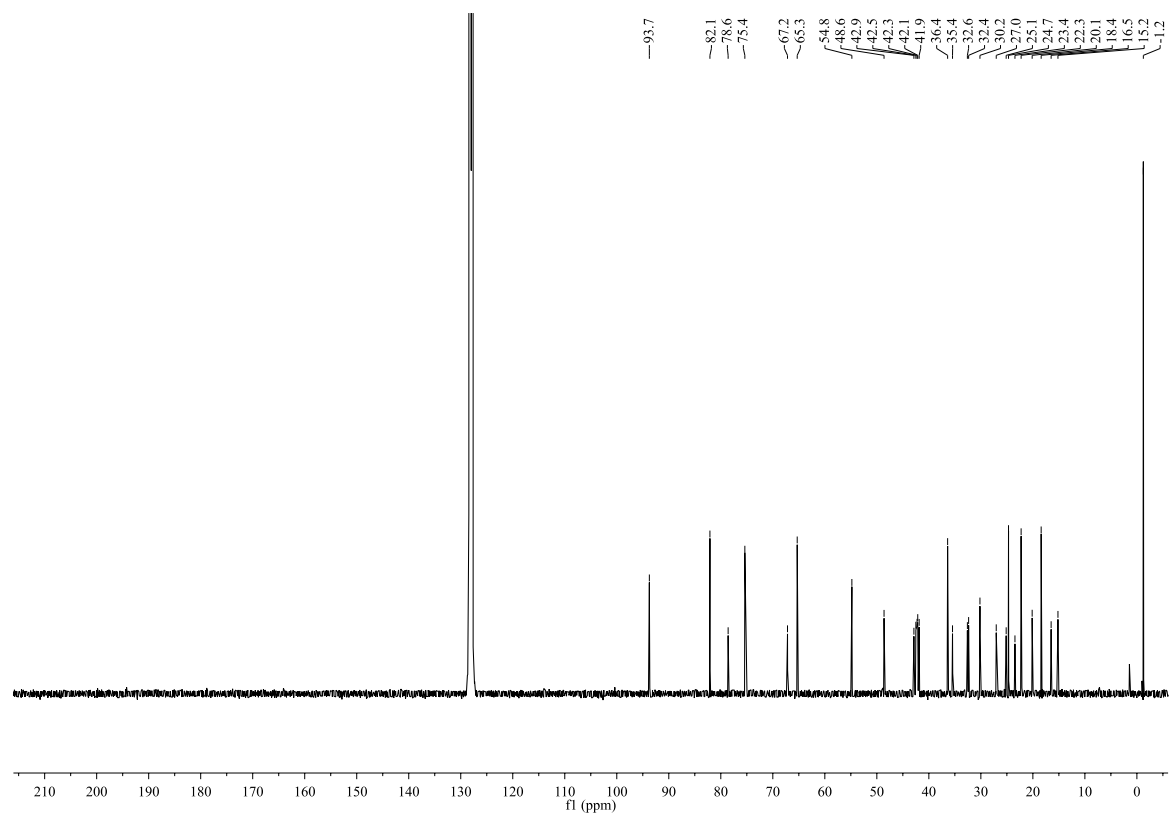
^{13}C NMR (C_6D_6 , 100 MHz):



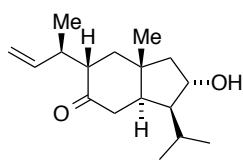
^1H NMR (C_6D_6 , 400 MHz):



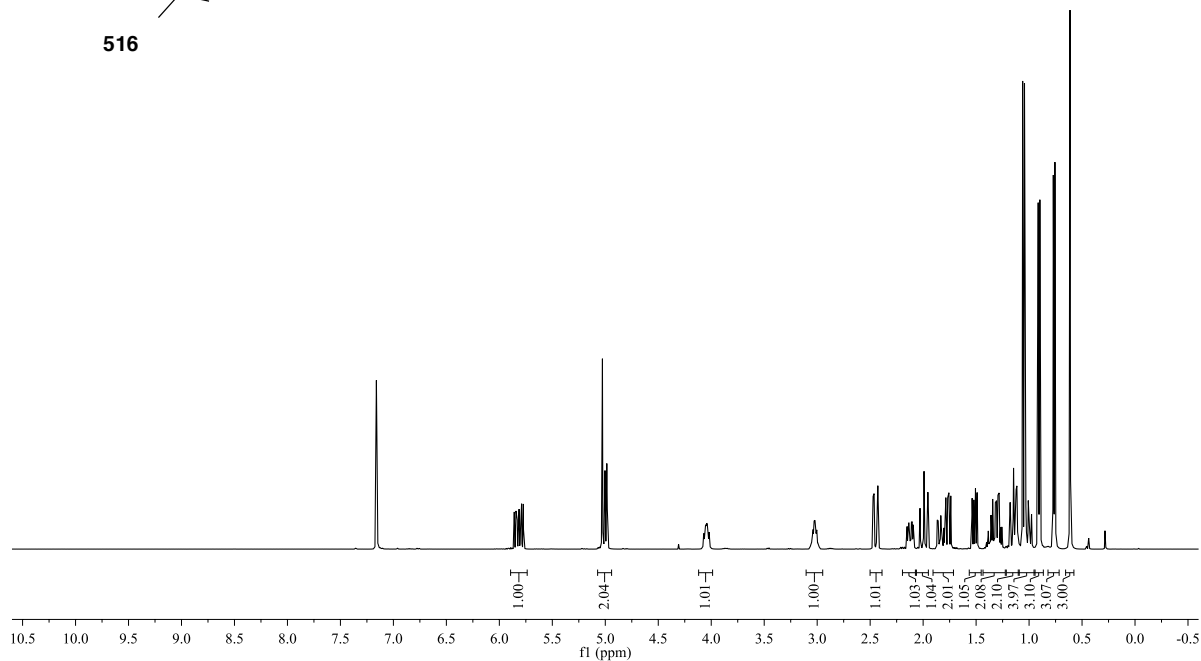
^{13}C NMR (C_6D_6 , 100 MHz):



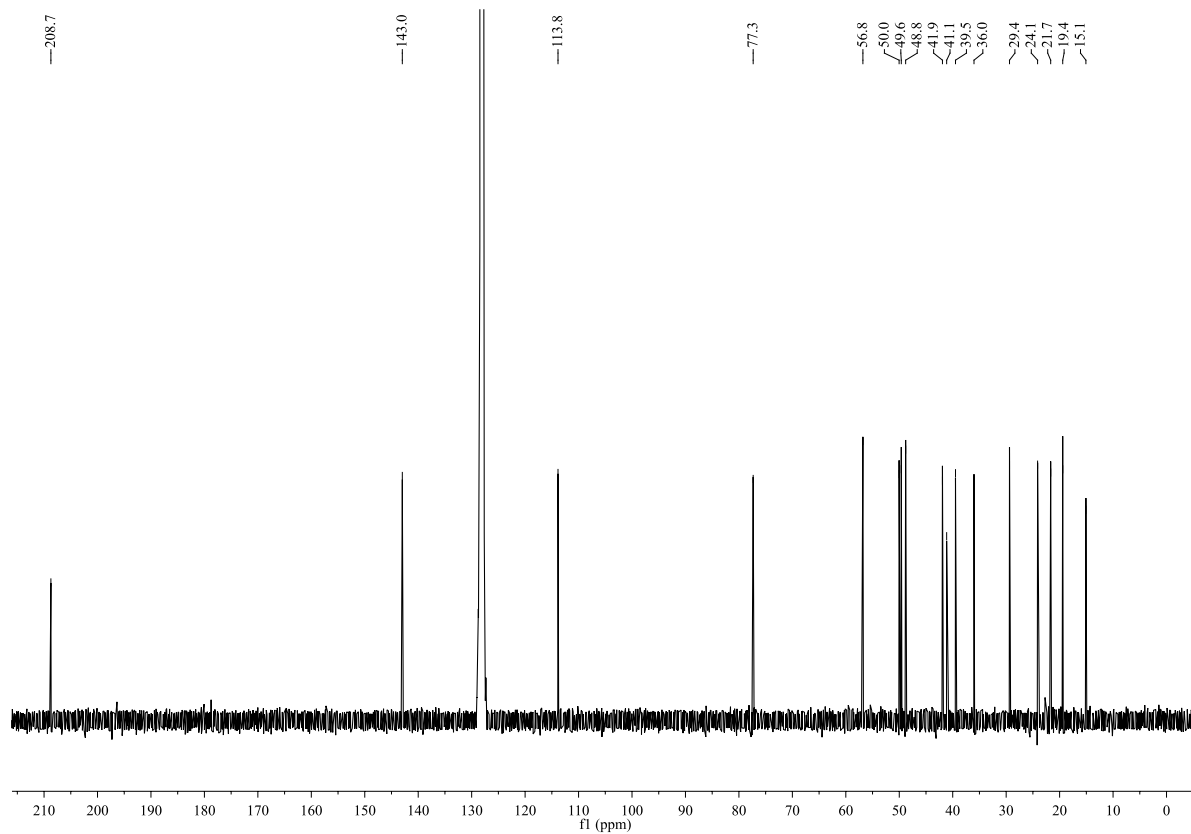
^1H NMR (C_6D_6 , 400 MHz):



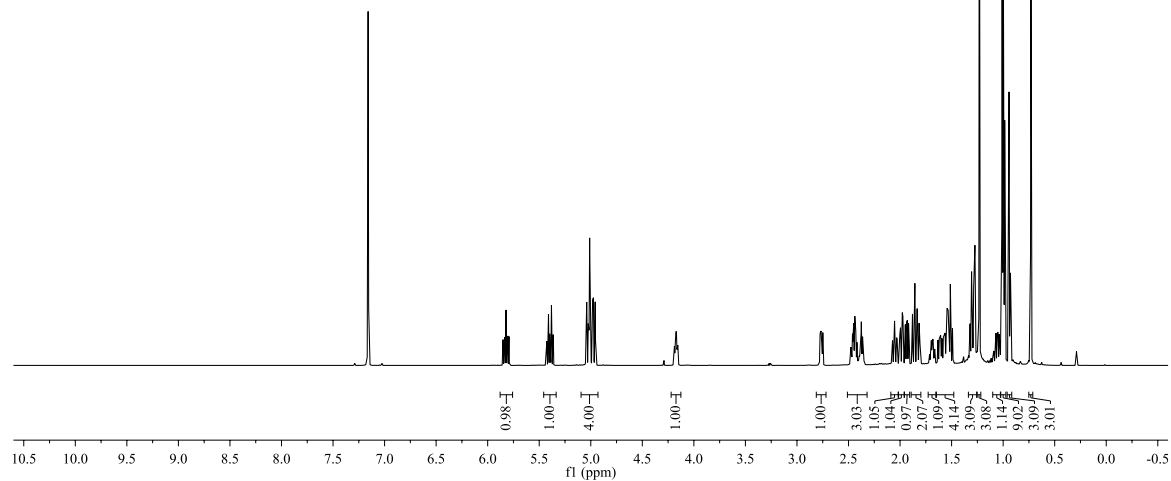
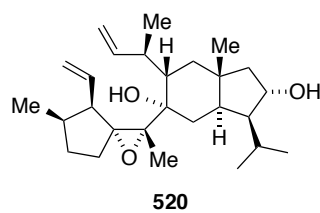
516



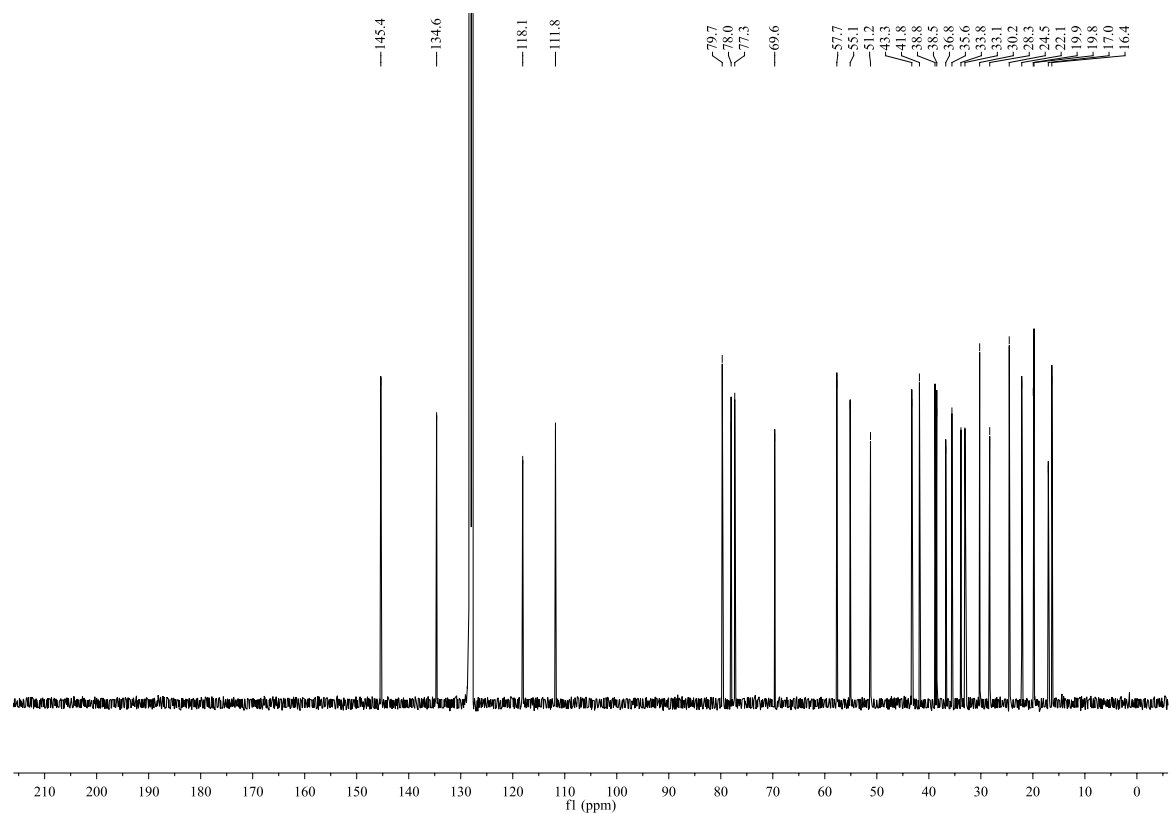
^{13}C NMR (C_6D_6 , 100 MHz):



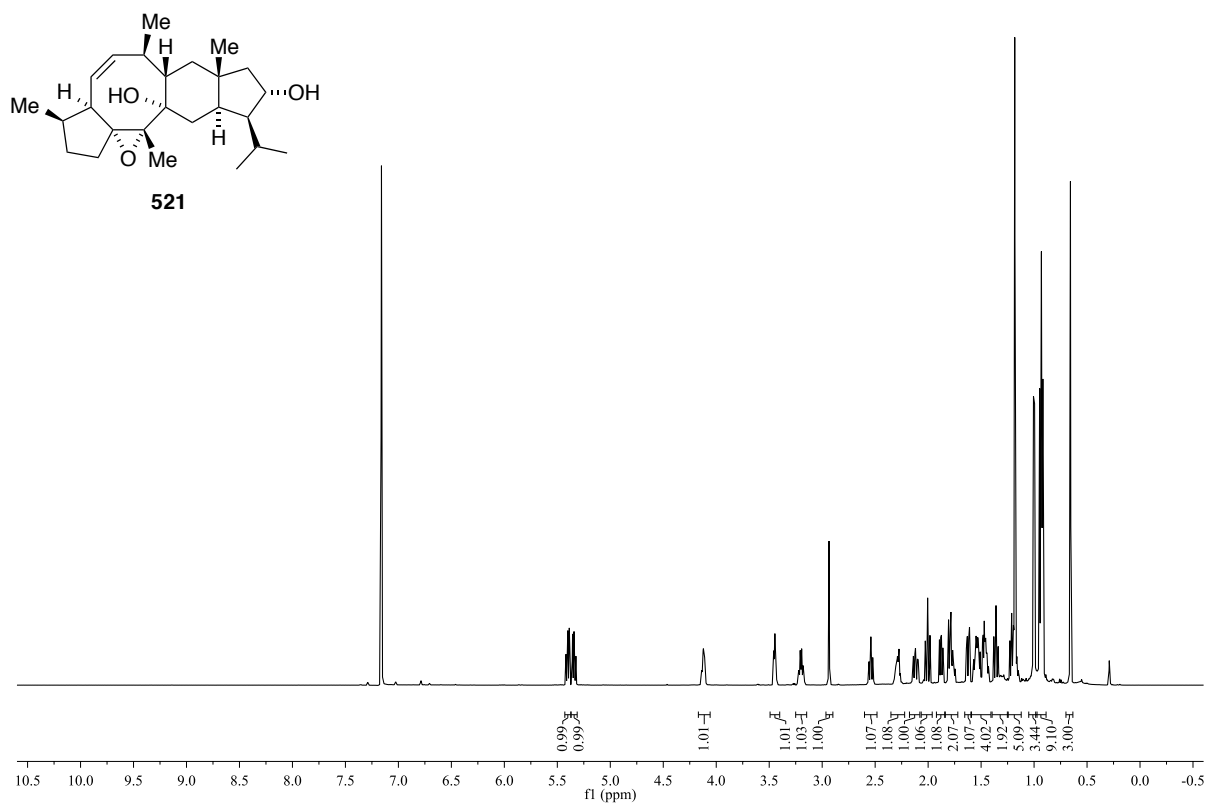
^1H NMR (C_6D_6 , 600 MHz):



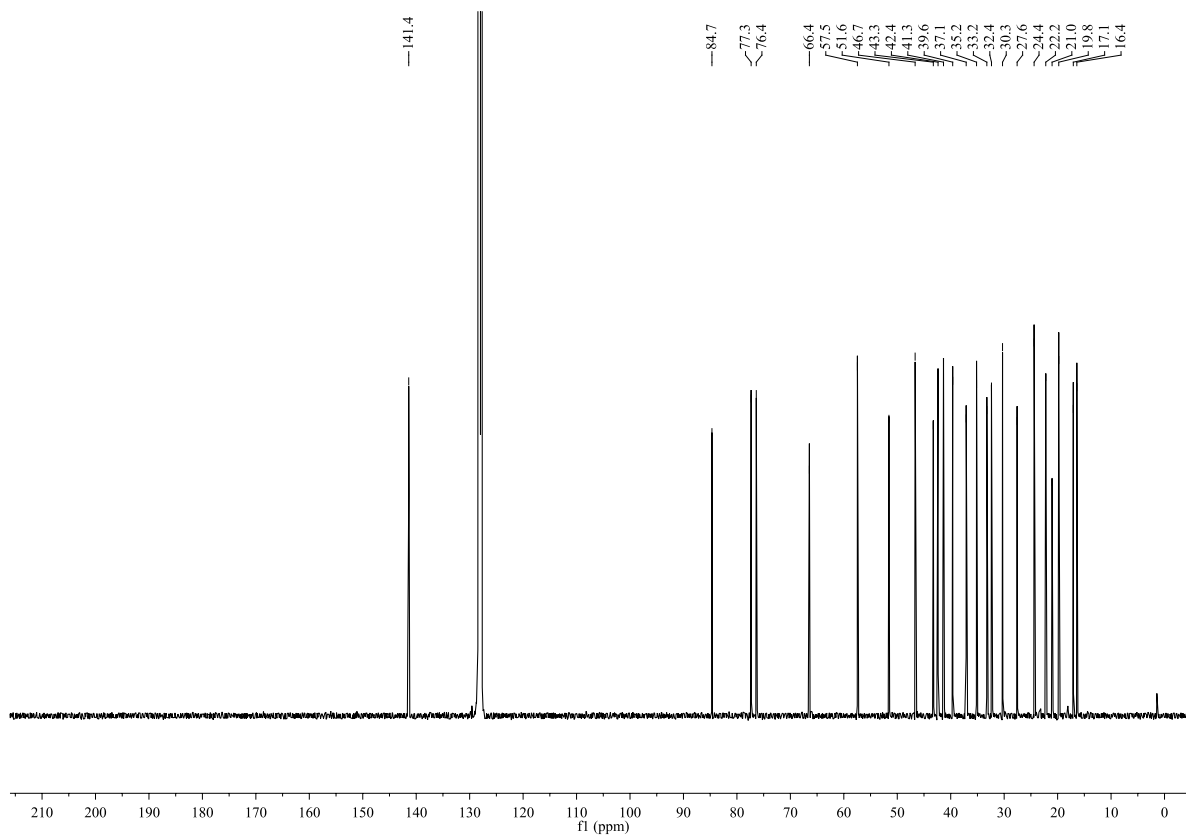
^{13}C NMR (C_6D_6 , 100 MHz):



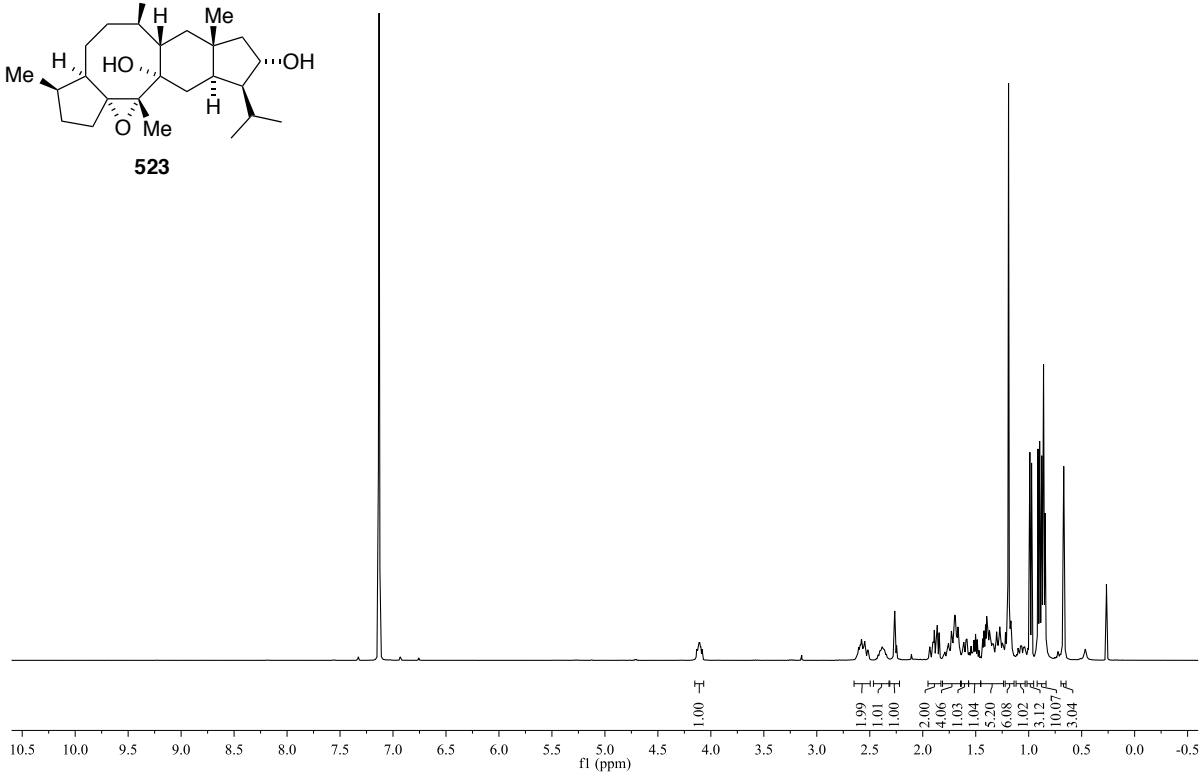
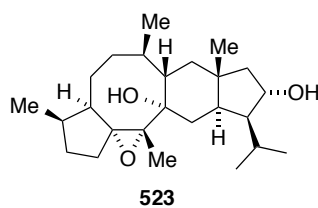
^1H NMR (C_6D_6 , 600 MHz):



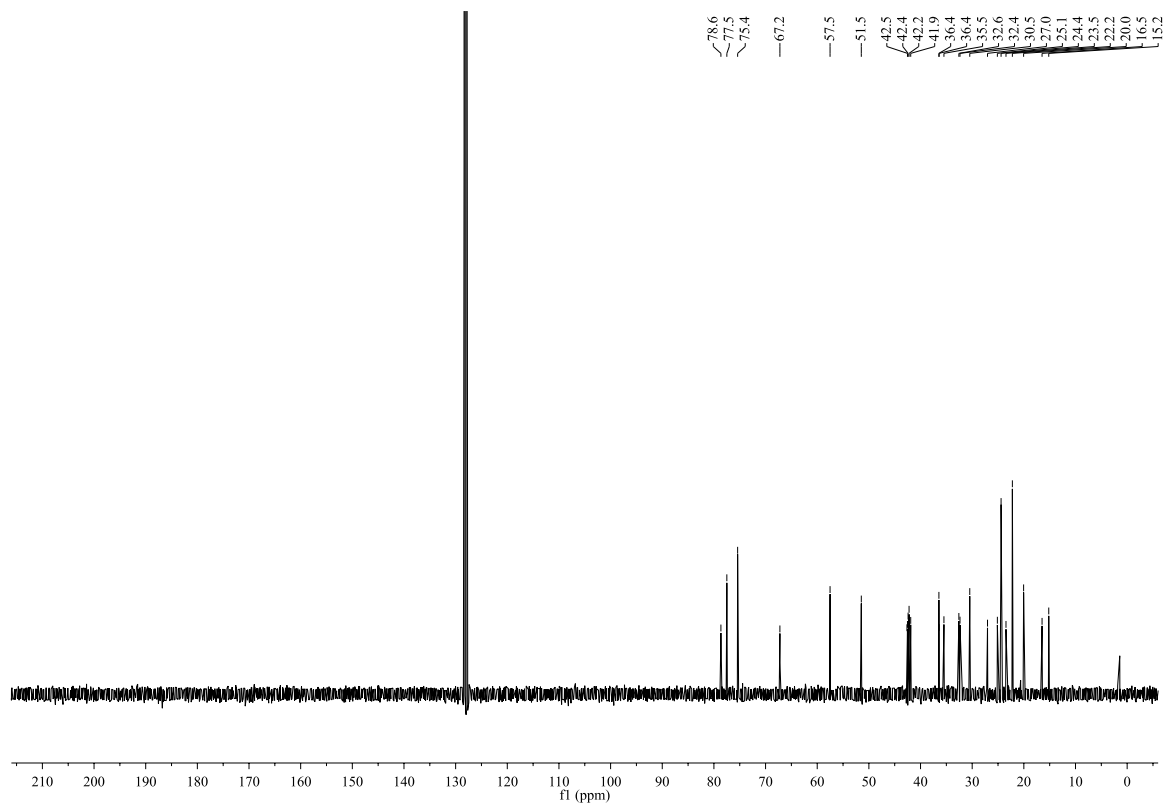
^{13}C NMR (C_6D_6 , 100 MHz):

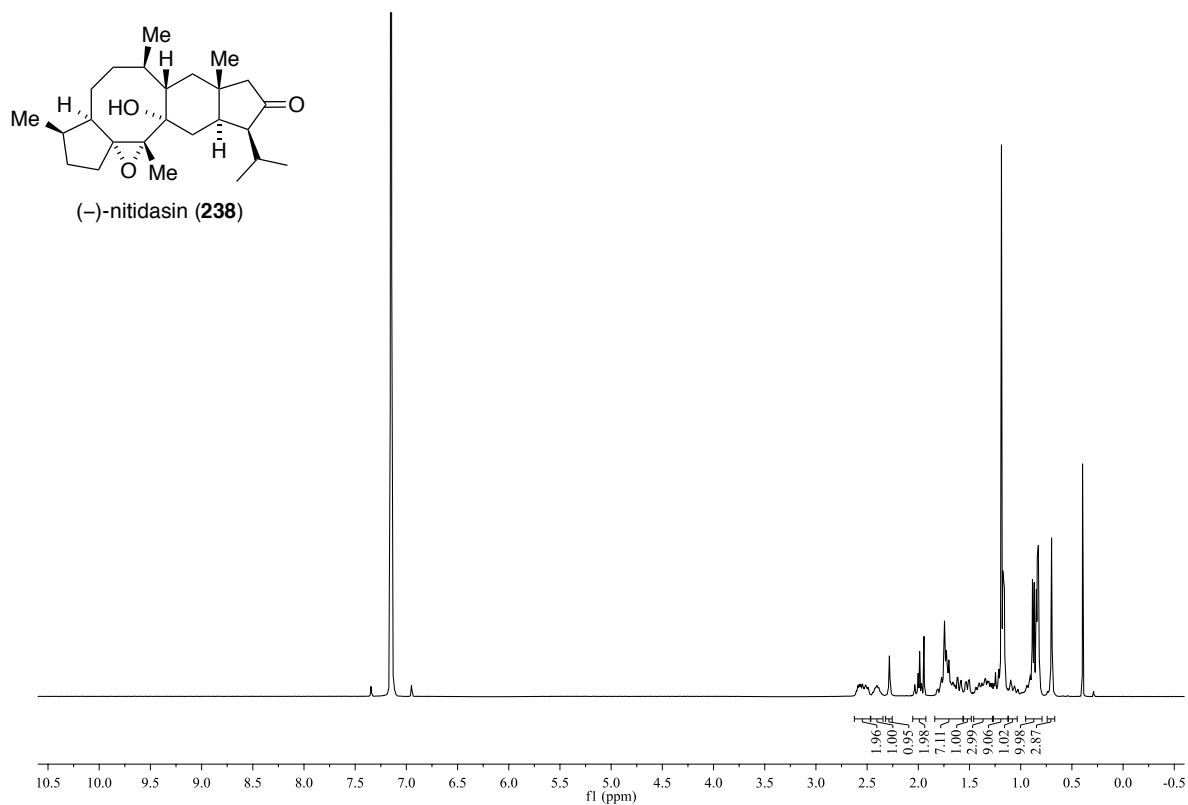
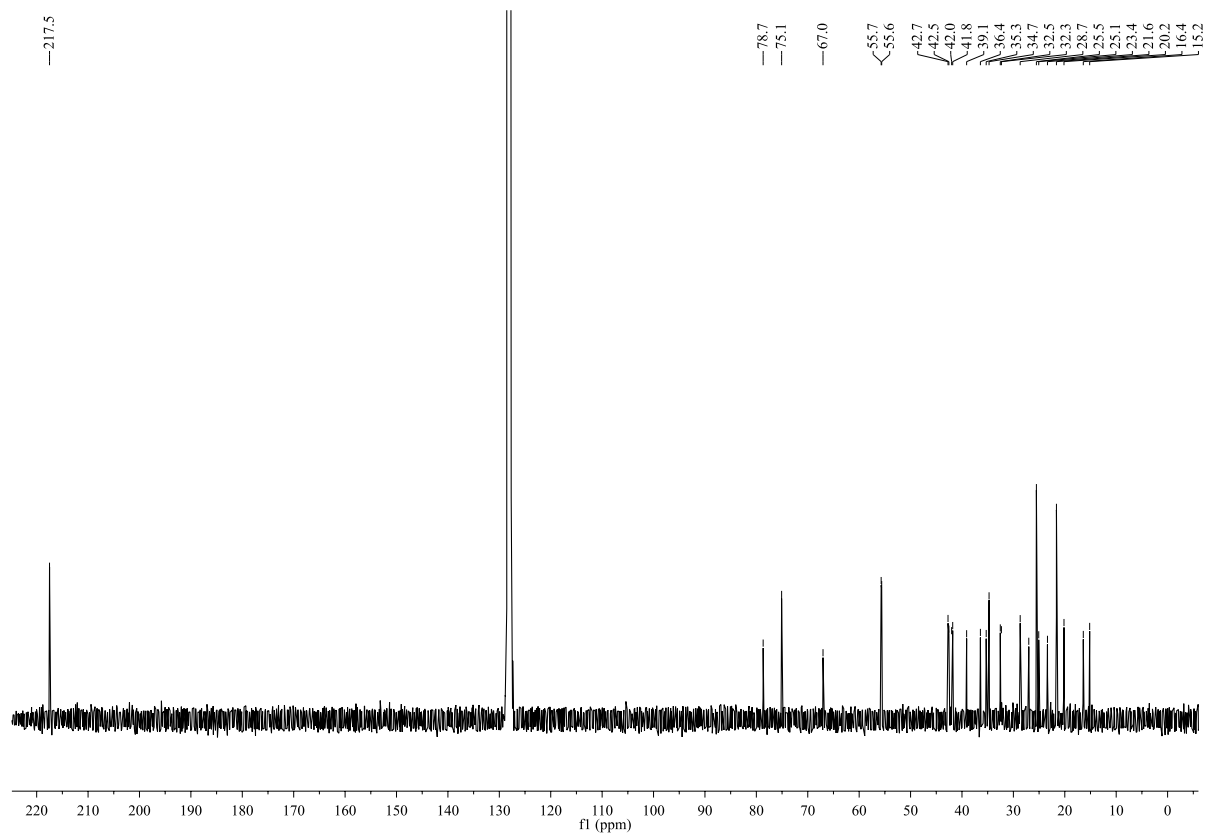


^1H NMR (C_6D_6 , 400 MHz):

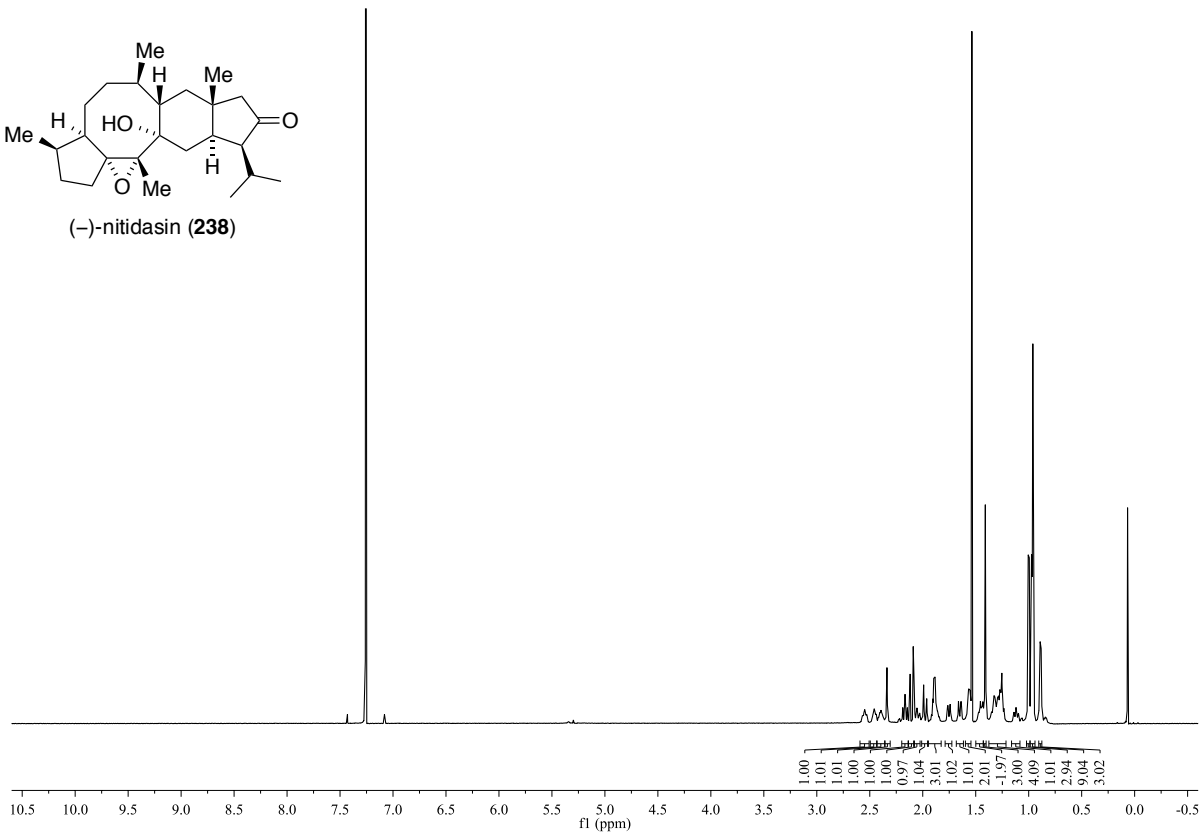
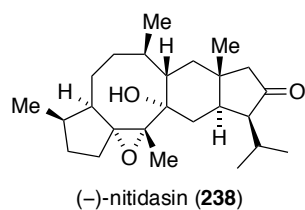


^{13}C NMR (C_6D_6 , 100 MHz):

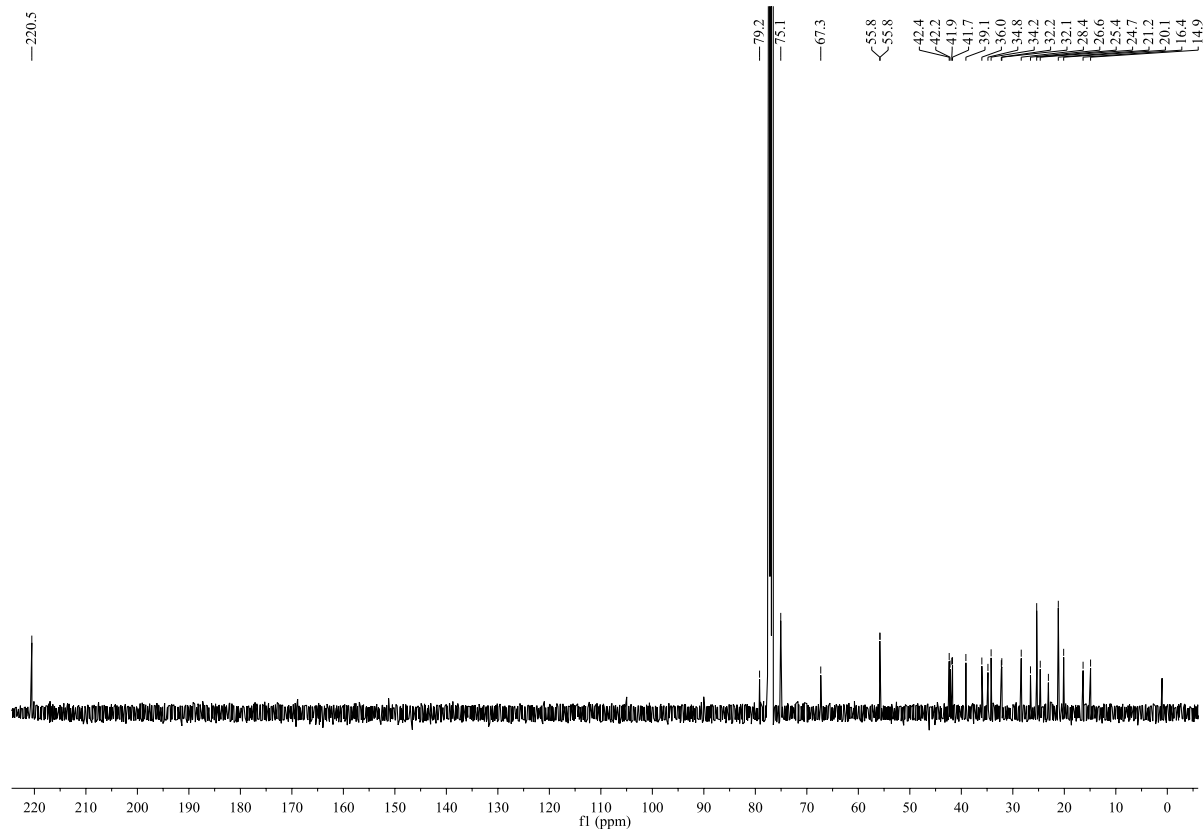


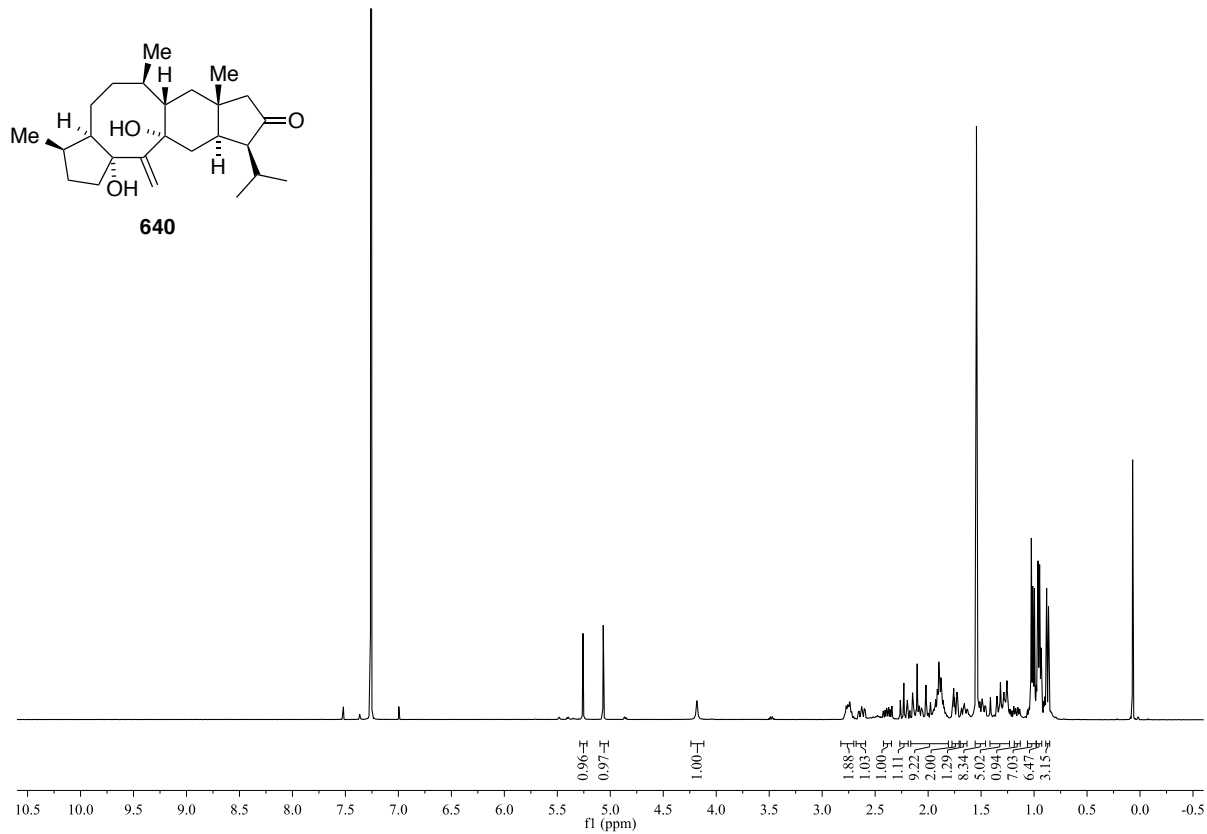
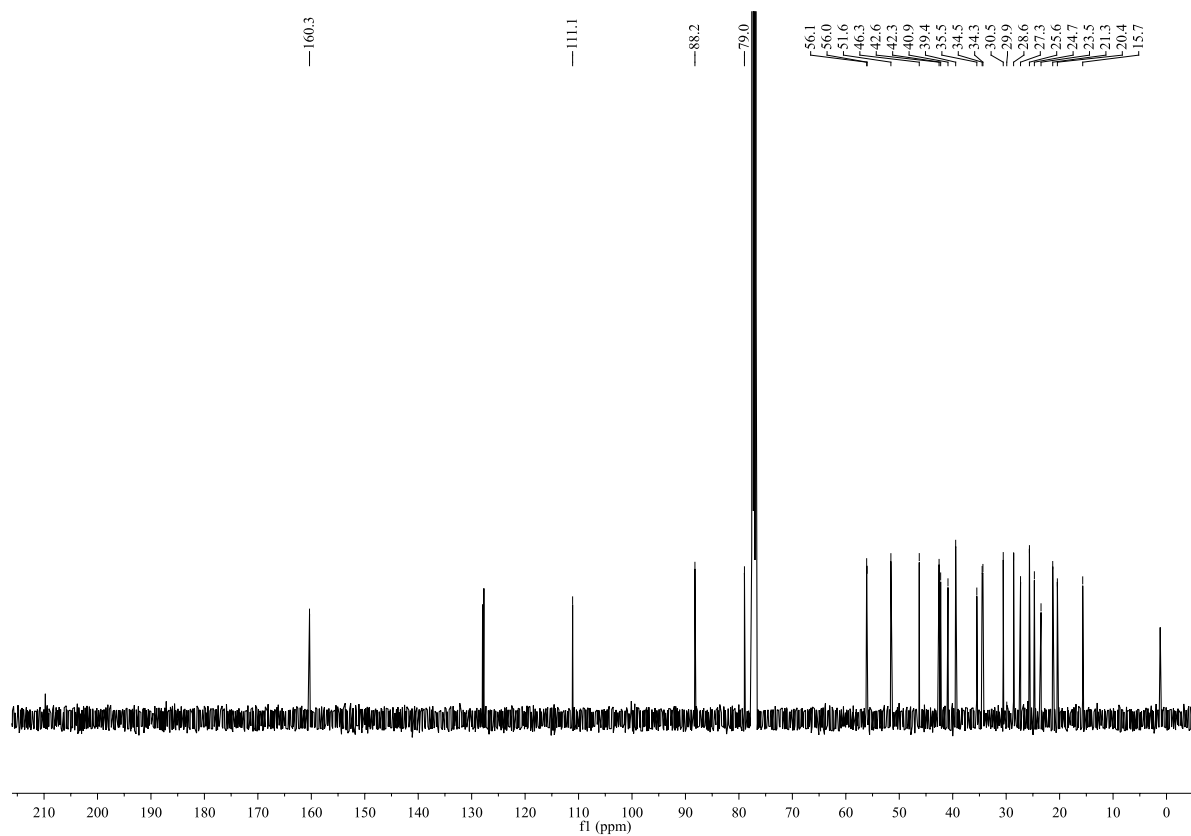
^1H NMR (C_6D_6 , 400 MHz): ^{13}C NMR (C_6D_6 , 100 MHz):

^1H NMR (CDCl_3 , 600 MHz):

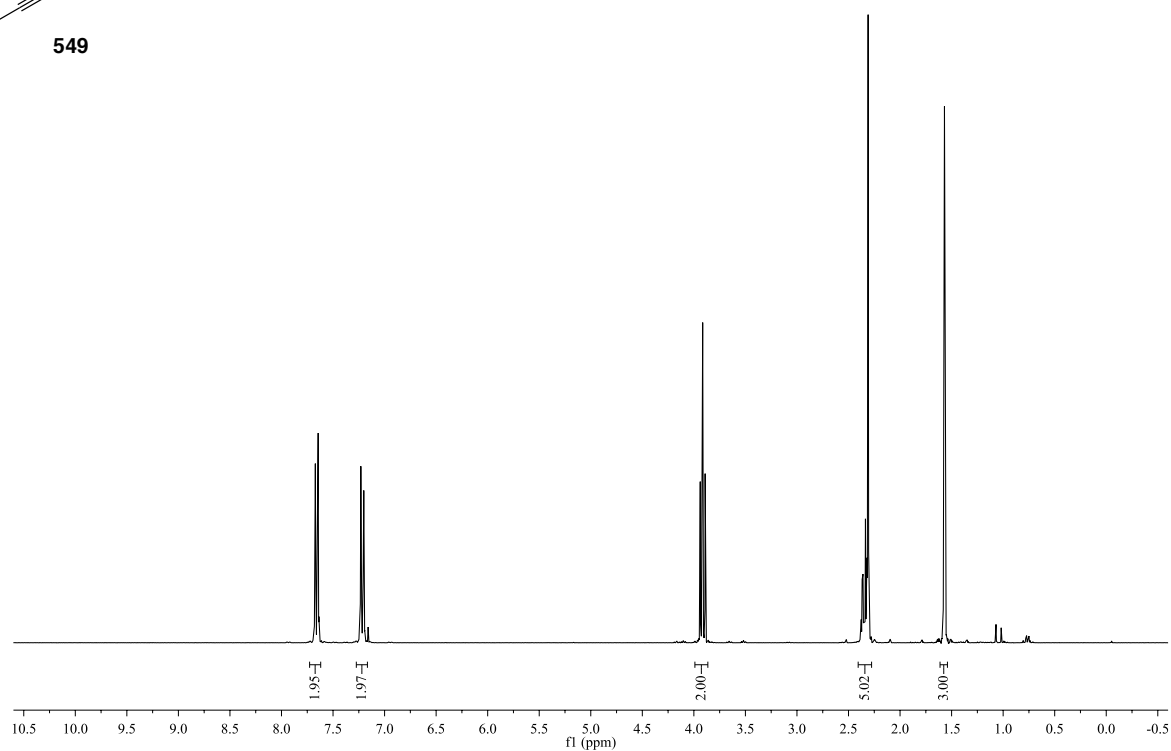
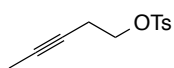


^{13}C NMR (CDCl_3 , 100 MHz):

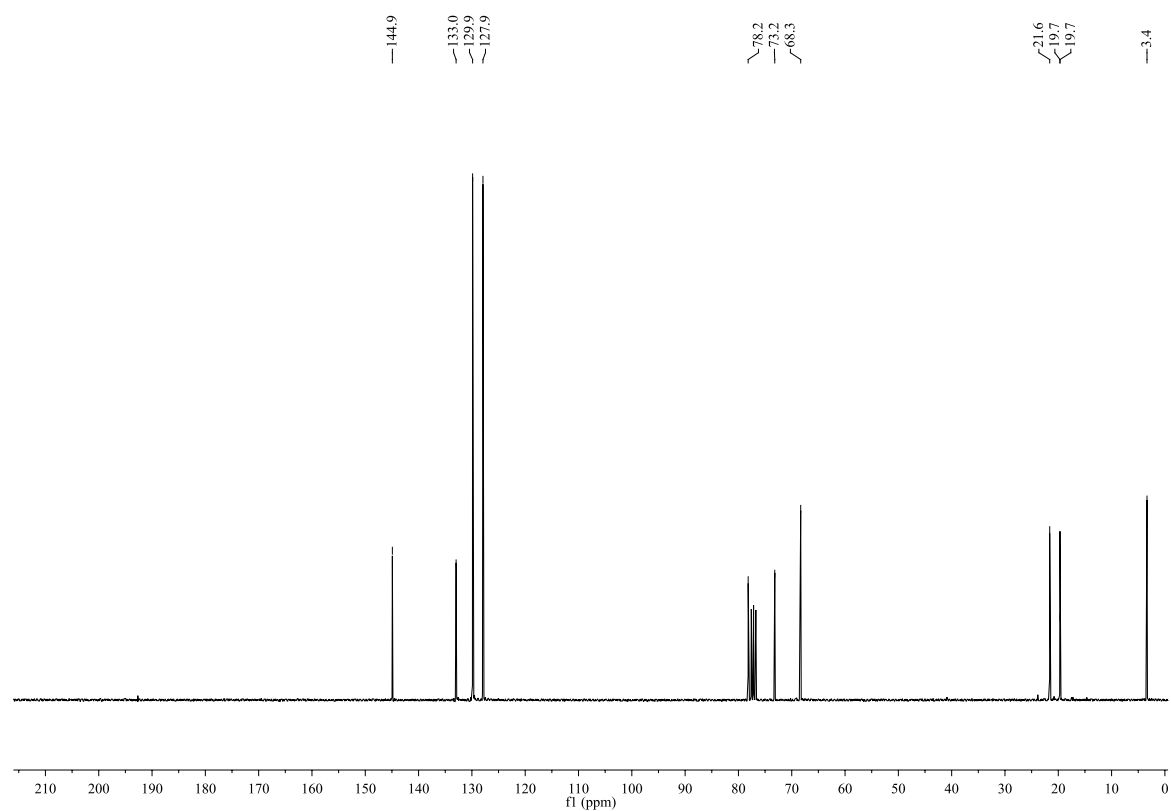


^1H NMR (CDCl_3 , 400 MHz): ^{13}C NMR (CDCl_3 , 100 MHz):

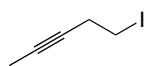
^1H NMR (CDCl_3 , 300 MHz):



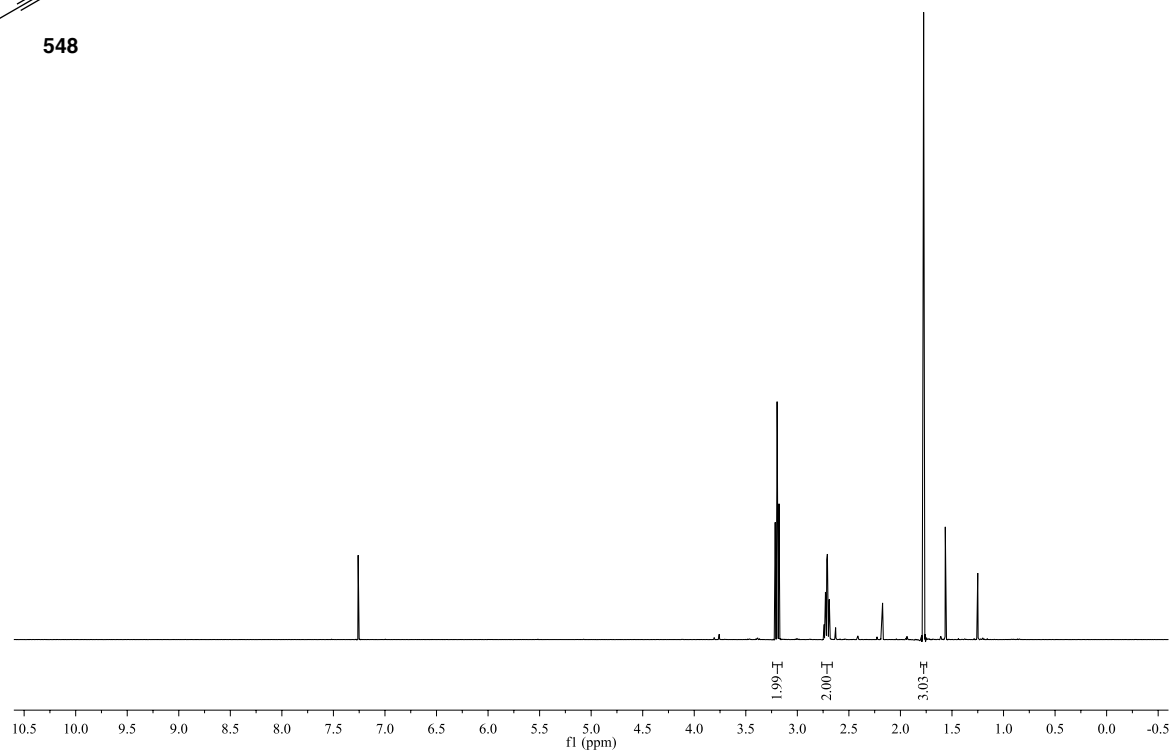
^{13}C NMR (CDCl_3 , 75 MHz):



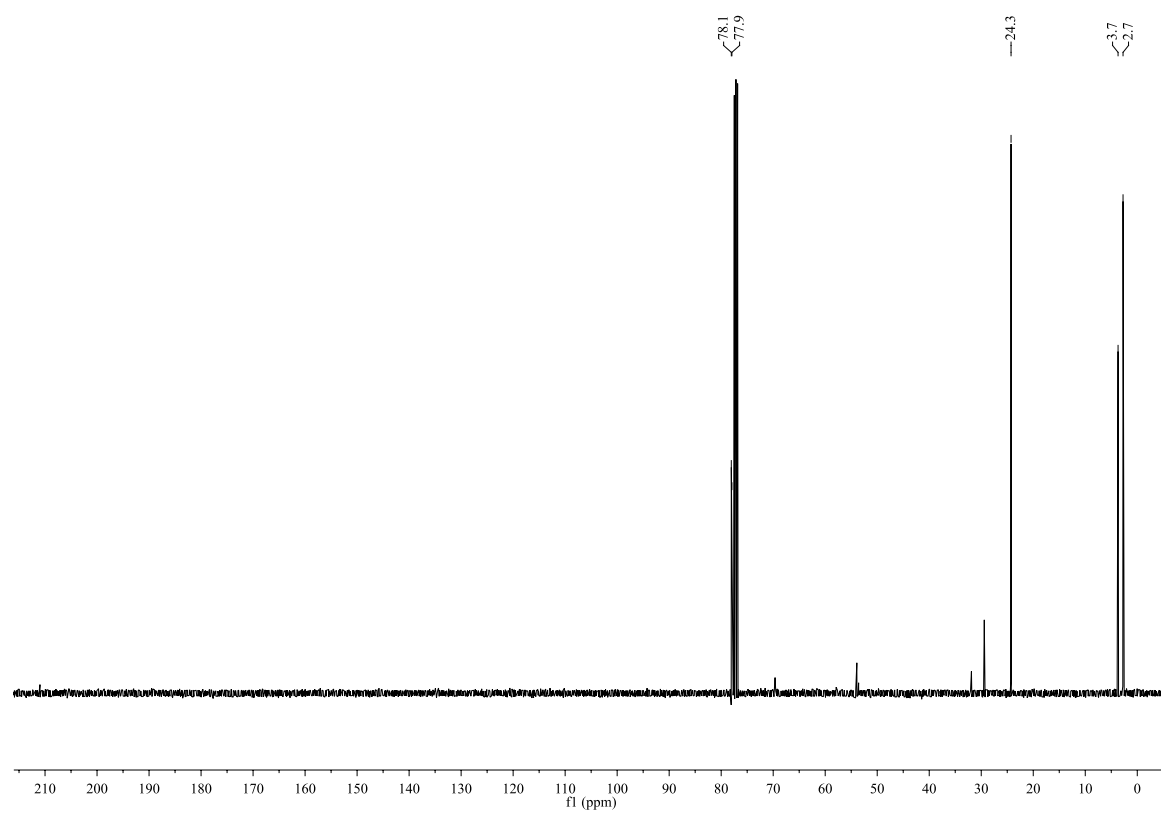
^1H NMR (CDCl_3 , 400 MHz):



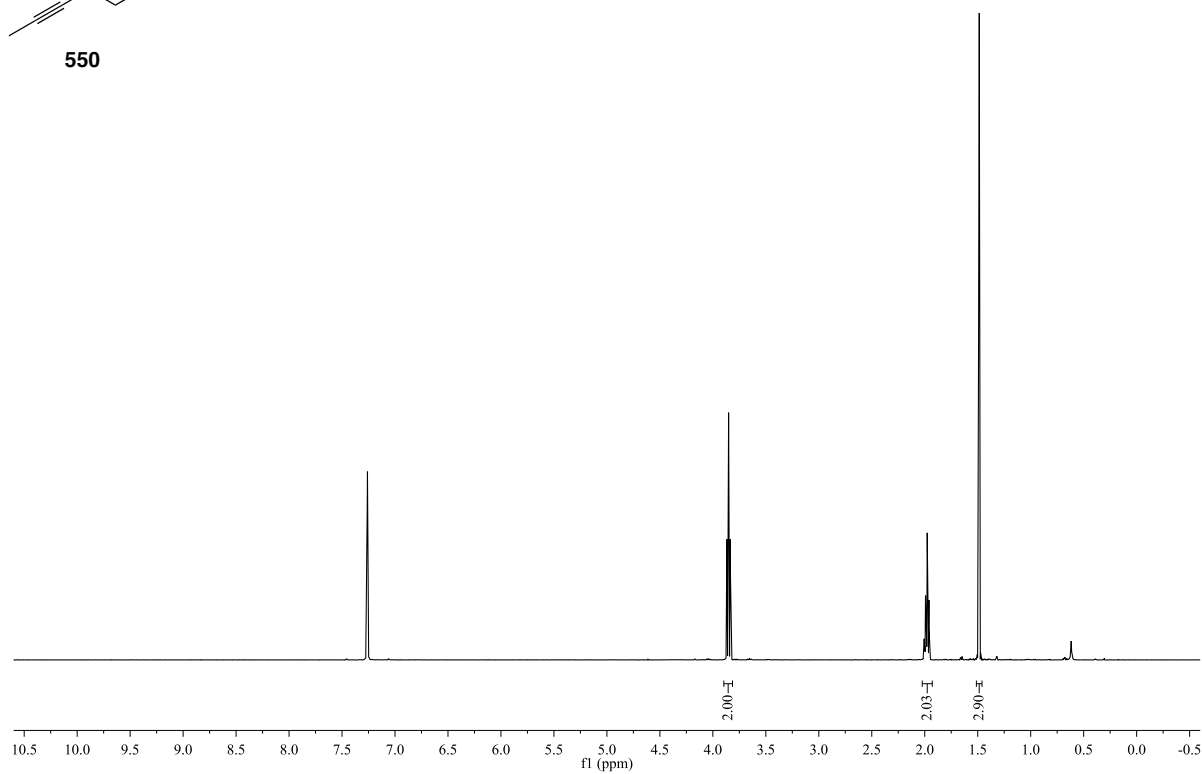
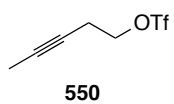
548



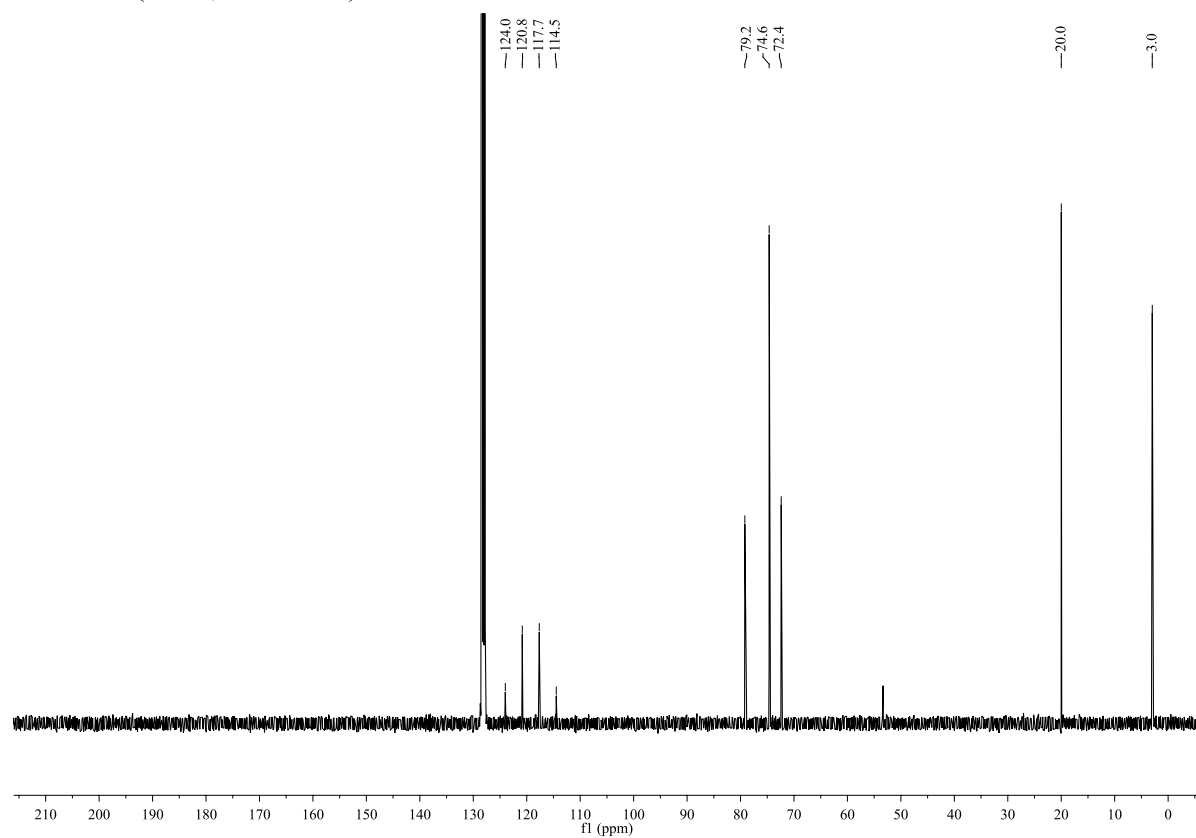
^{13}C NMR (CDCl_3 , 100 MHz):

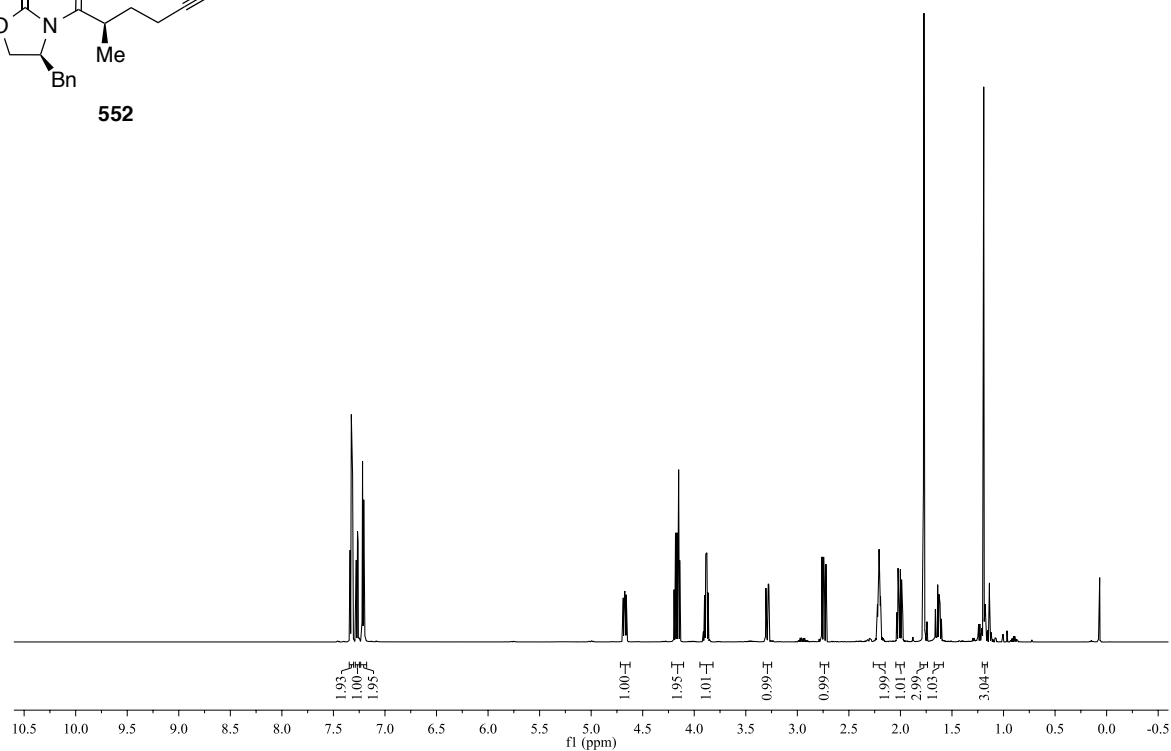
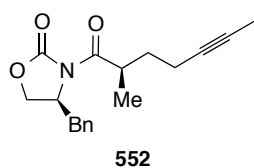
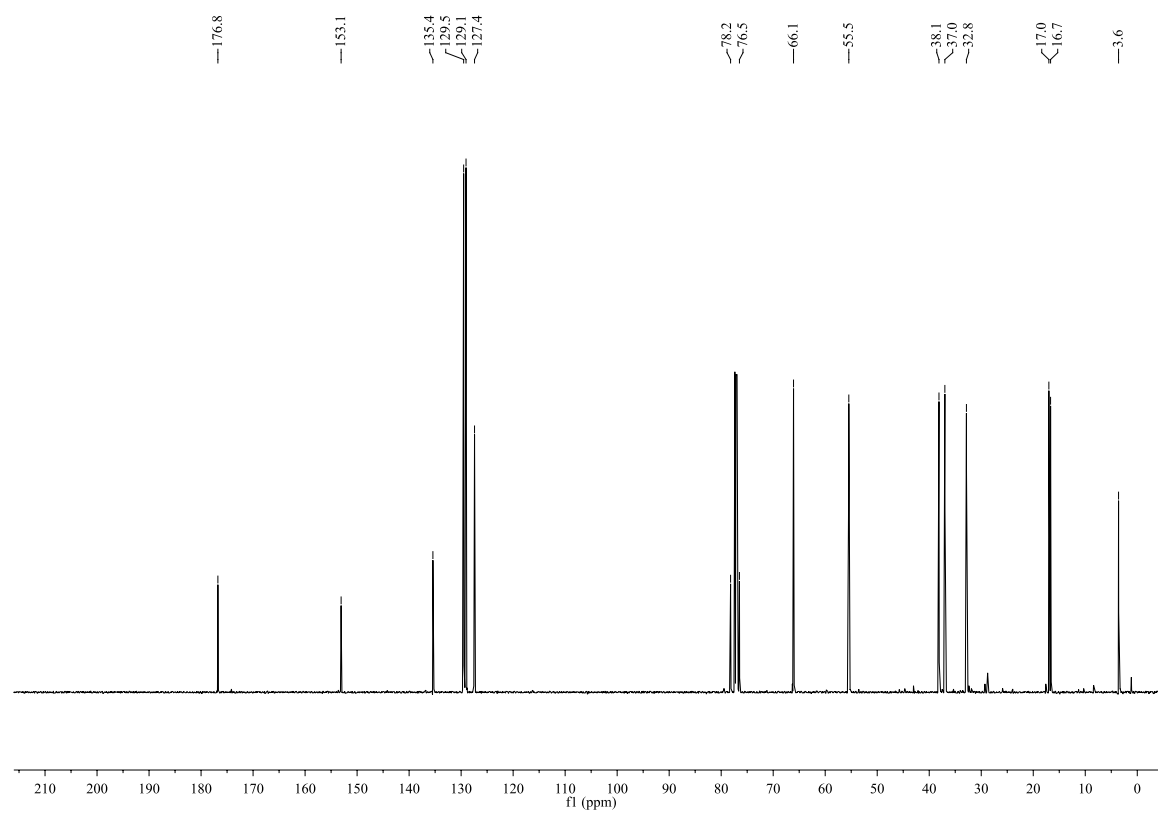


^1H NMR (C_6D_6 , 400 MHz):

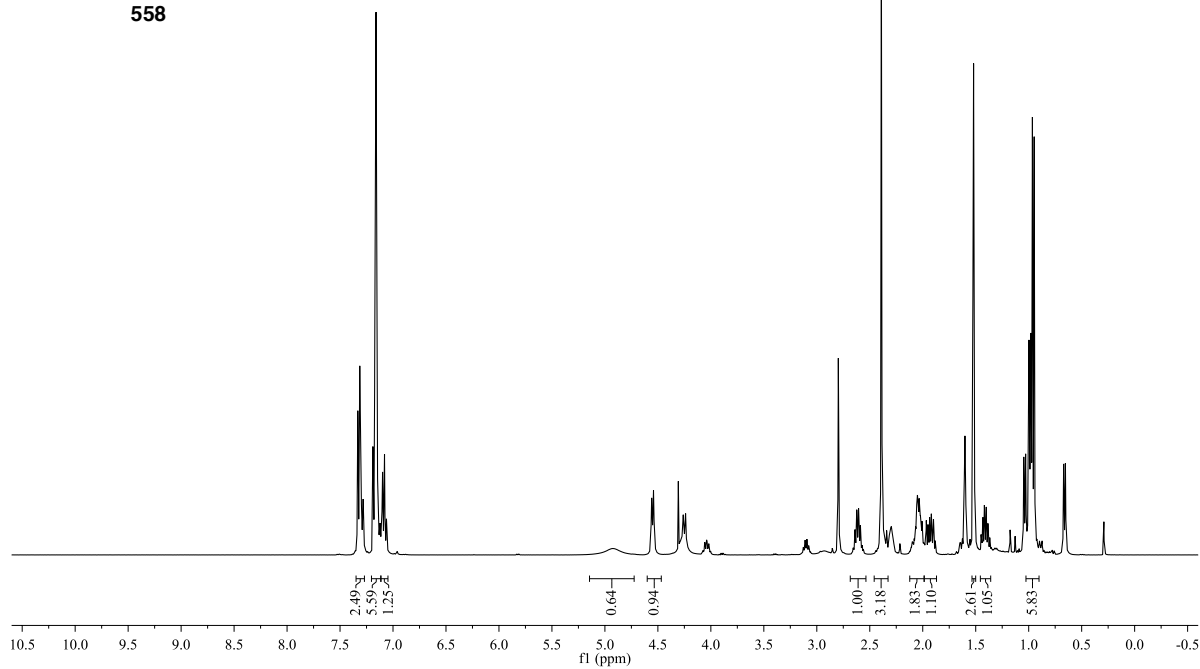
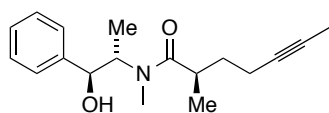


^{13}C NMR (C_6D_6 , 100 MHz):

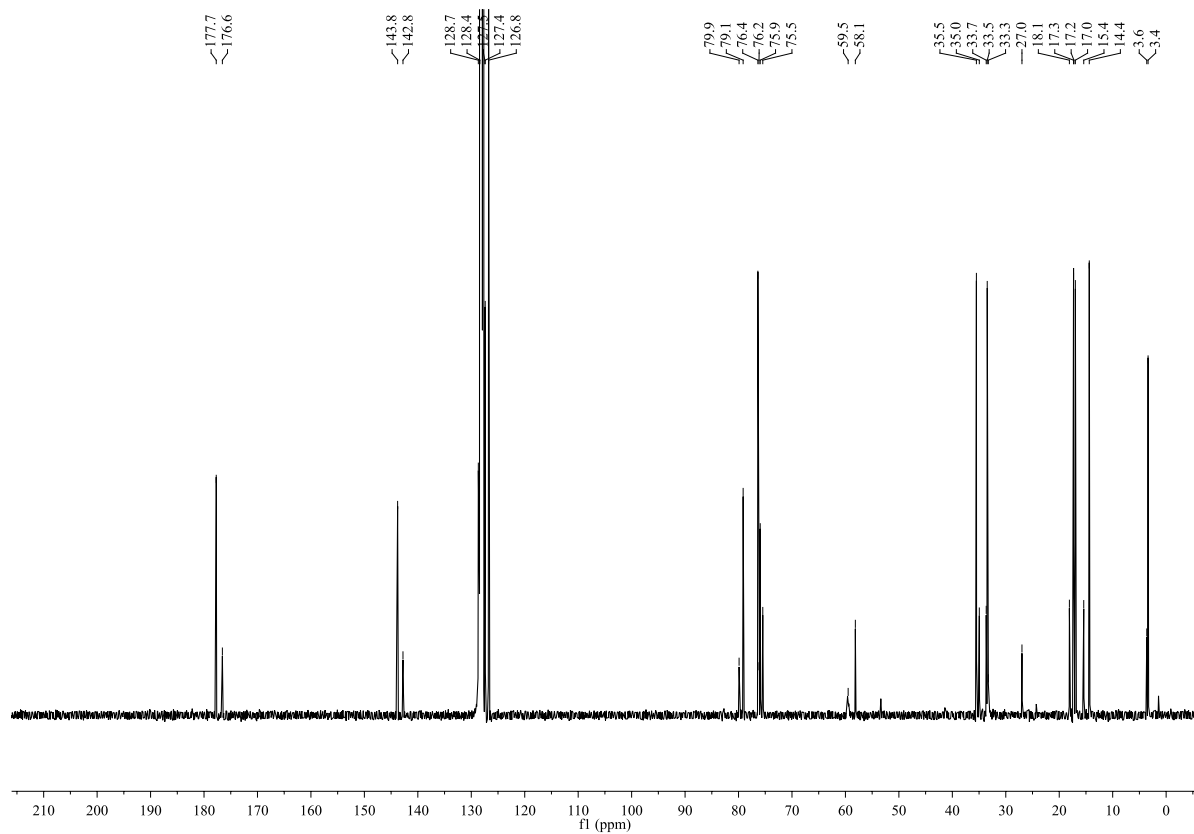


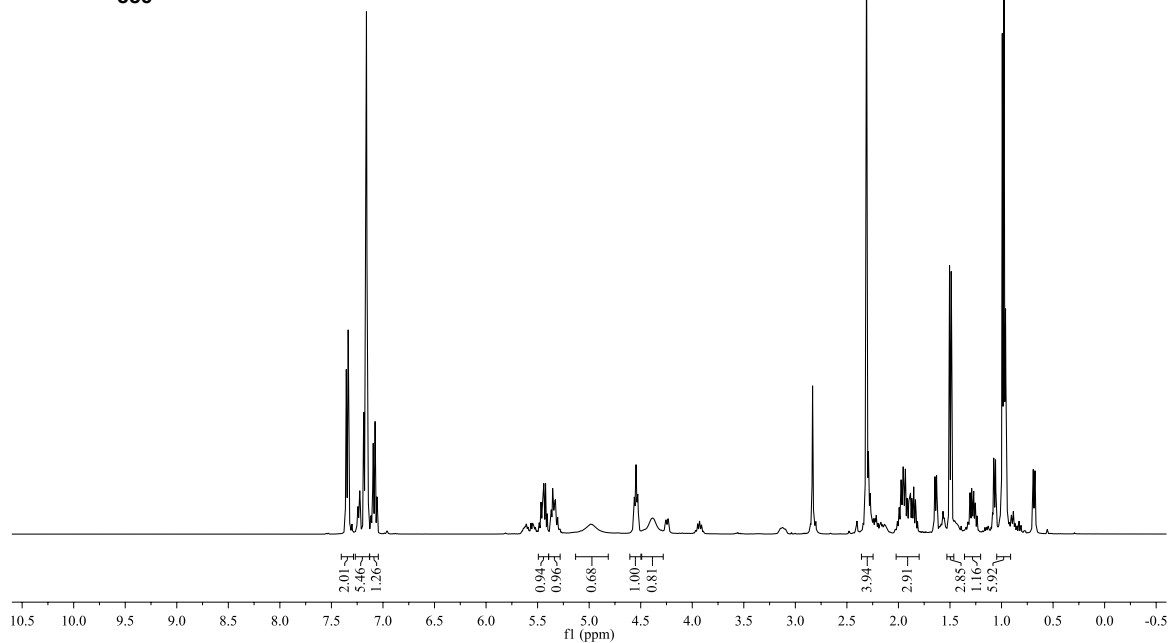
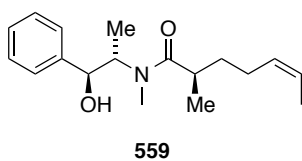
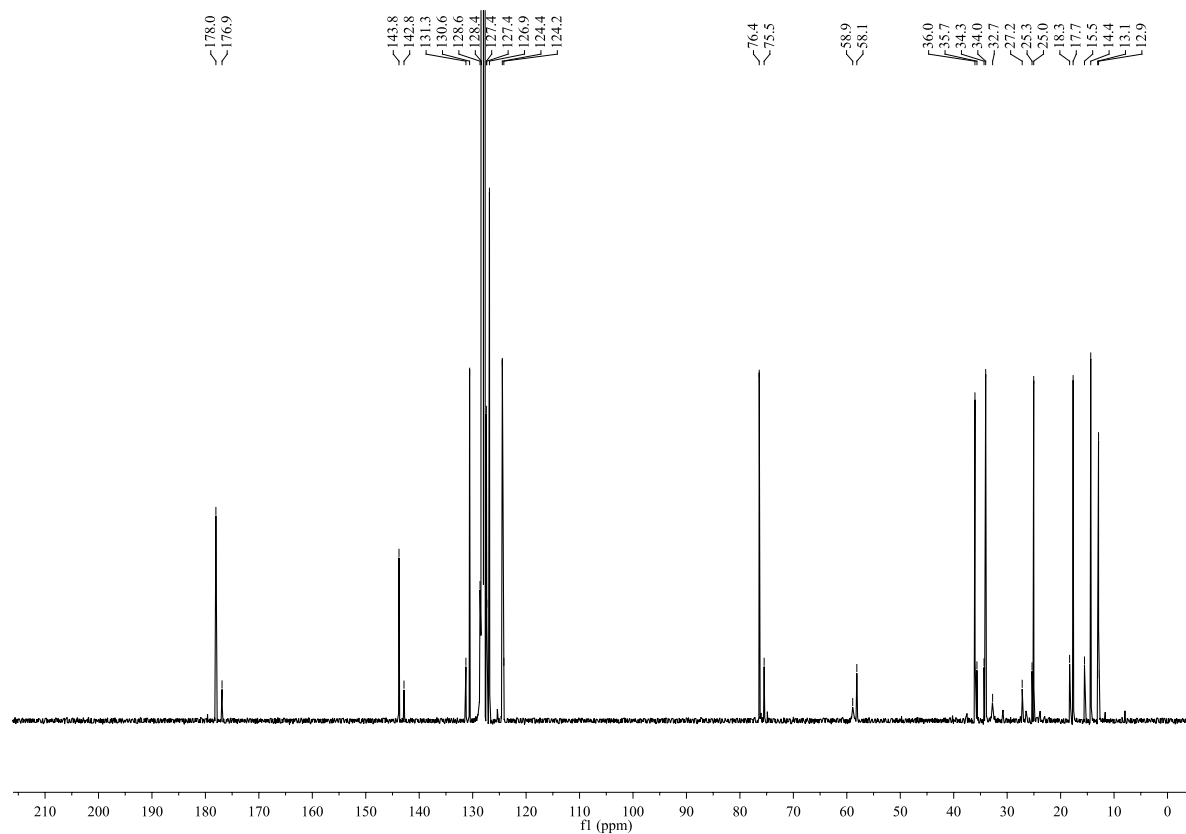
^1H NMR (CDCl_3 , 600 MHz): ^{13}C NMR (CDCl_3 , 150 MHz):

^1H NMR (C_6D_6 , 600 MHz):

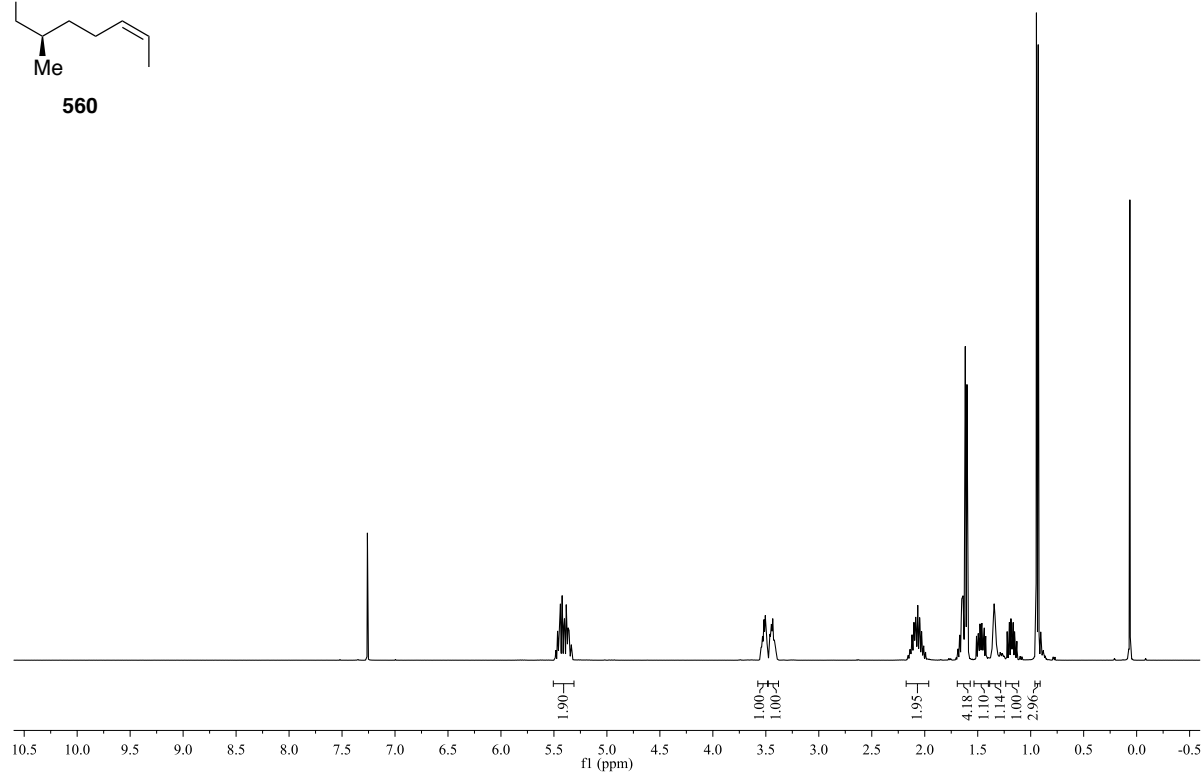
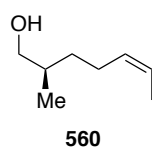


^{13}C NMR (C_6D_6 , 150 MHz):

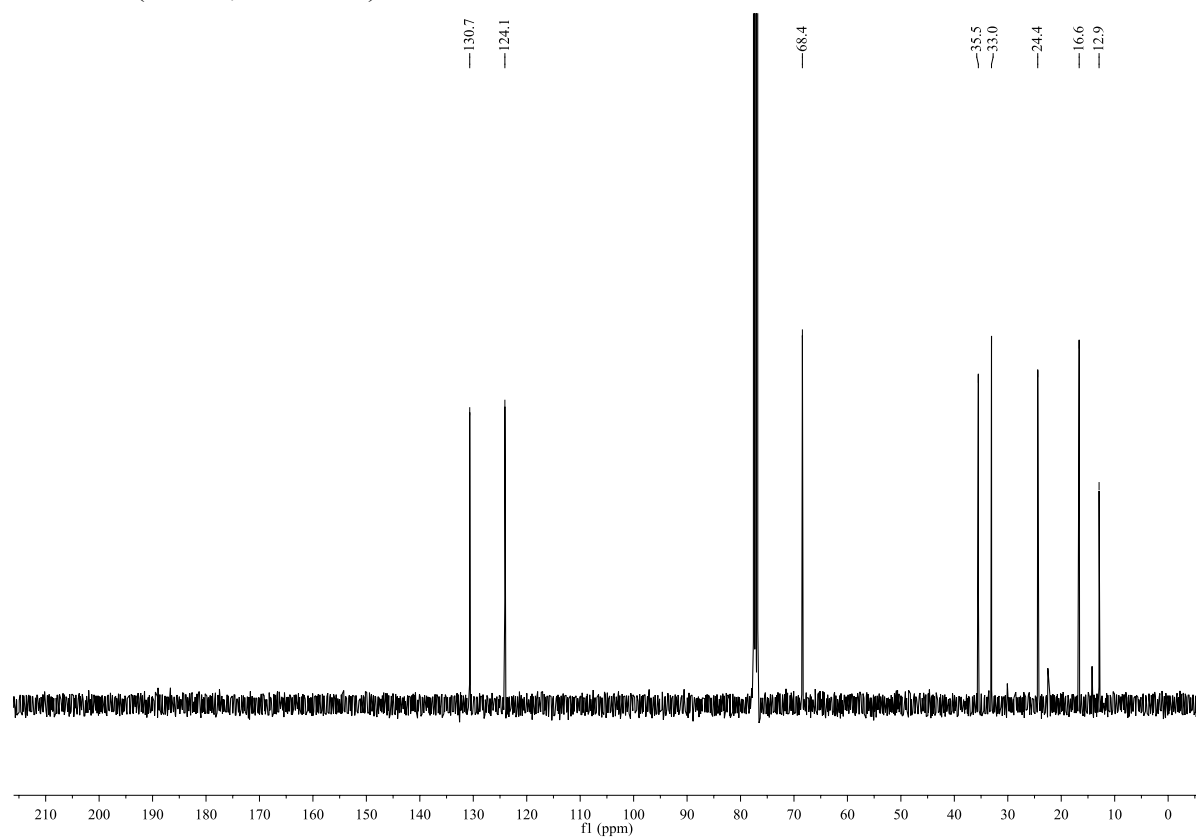


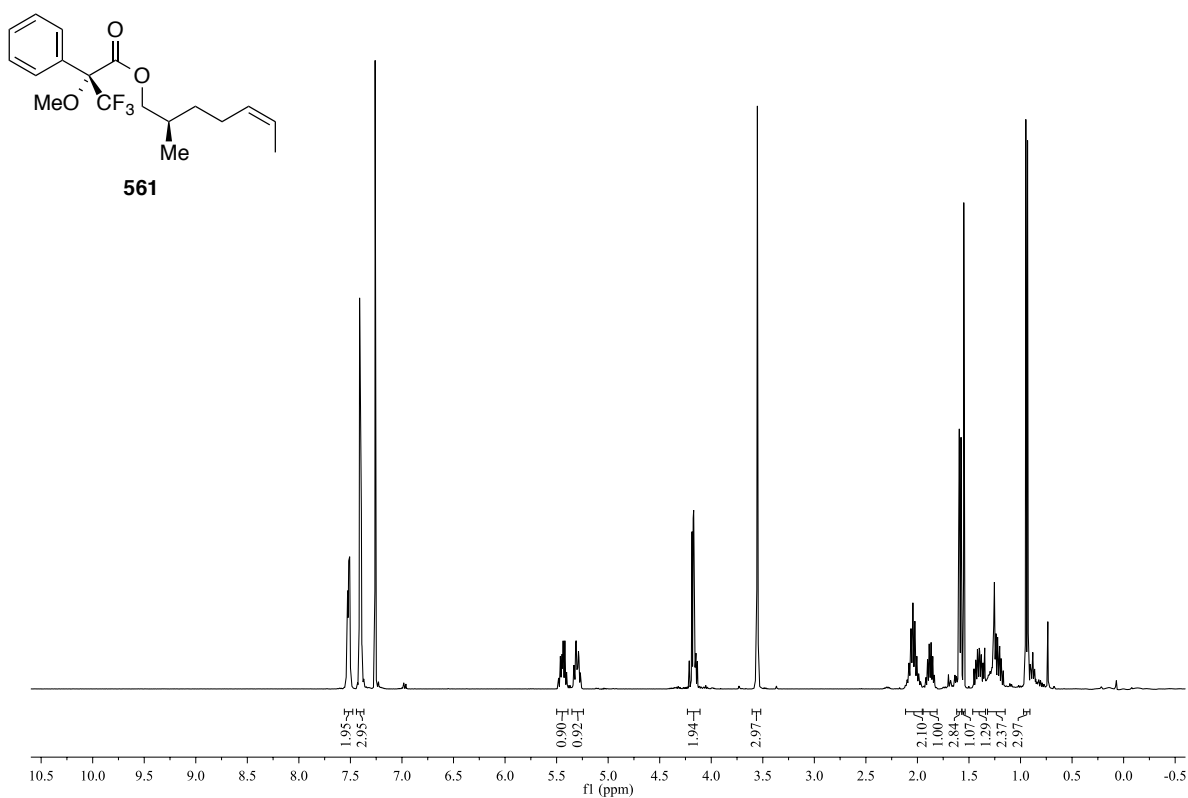
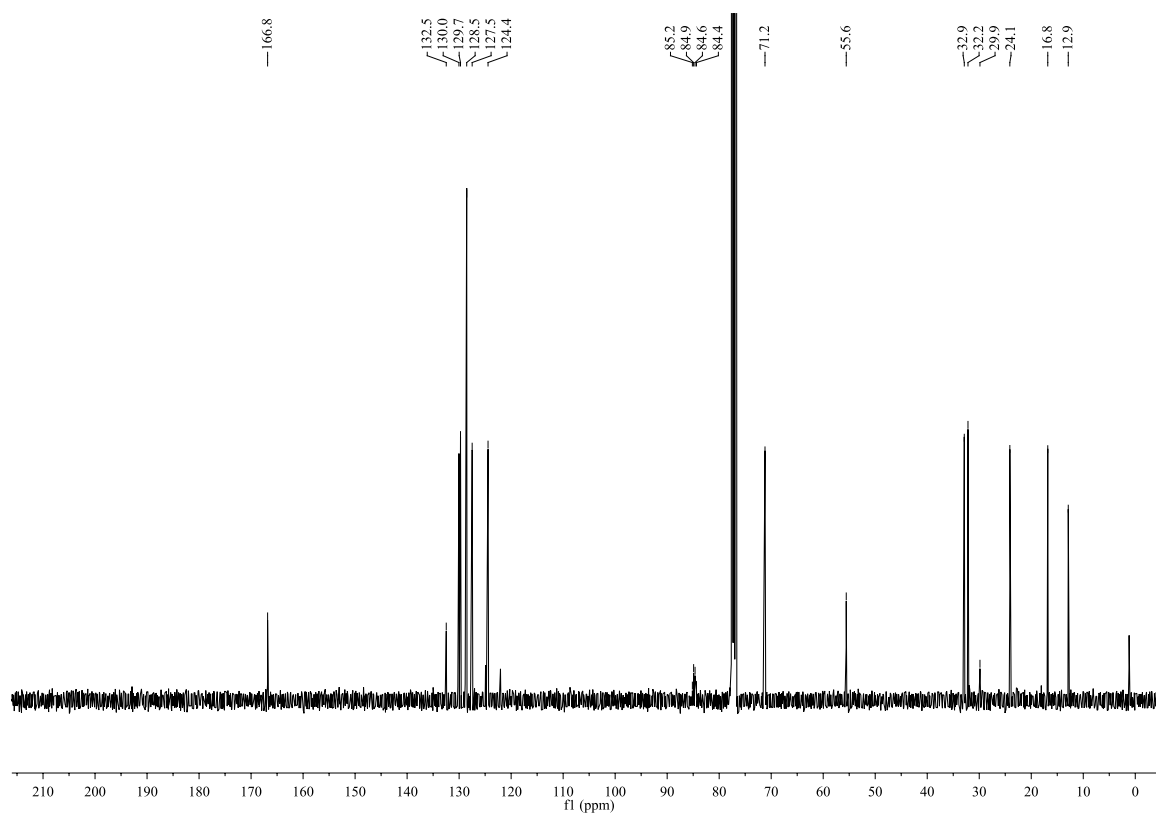
^1H NMR (C_6D_6 , 400 MHz): ^{13}C NMR (C_6D_6 , 100 MHz):

^1H NMR (CDCl_3 , 400 MHz):

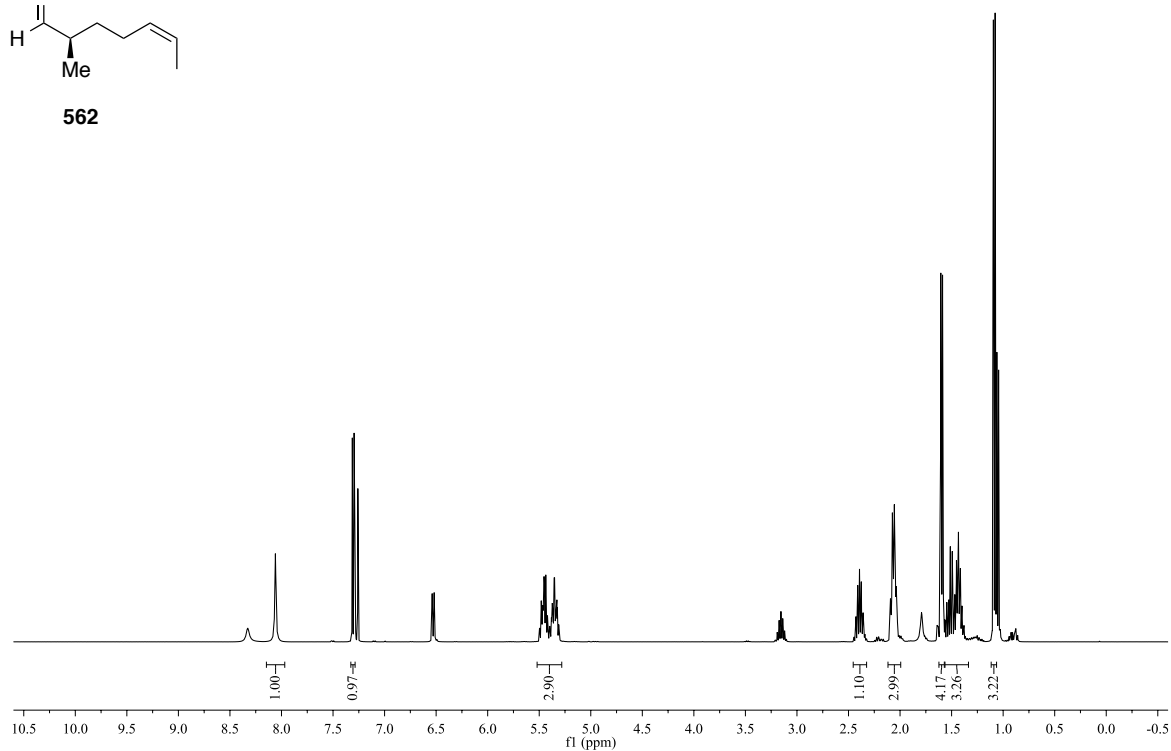
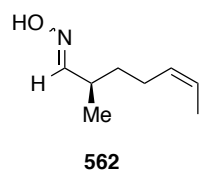


^{13}C NMR (CDCl_3 , 100 MHz):

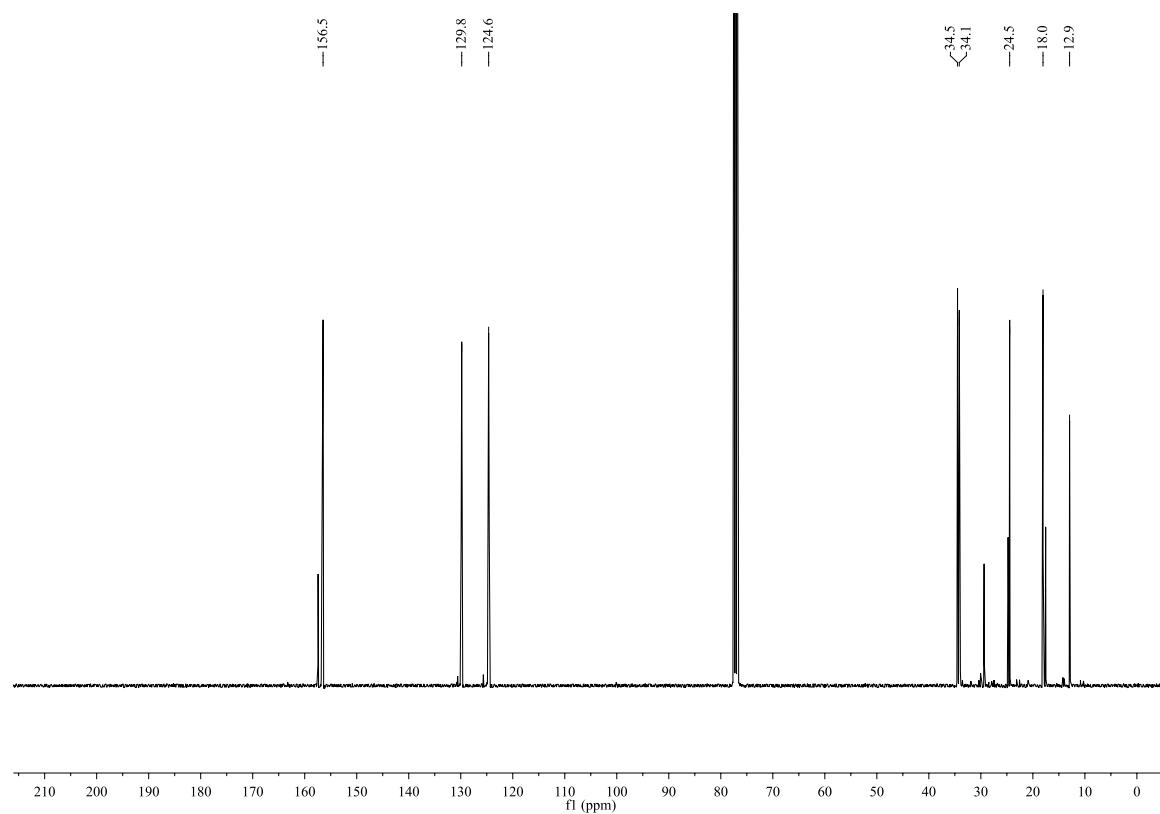


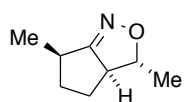
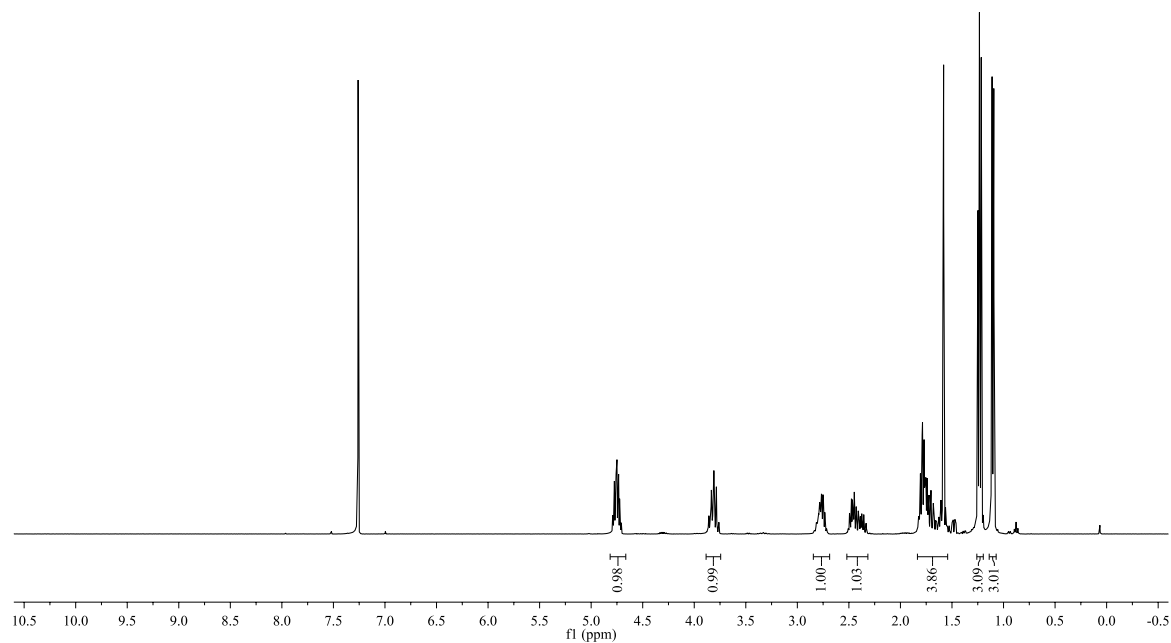
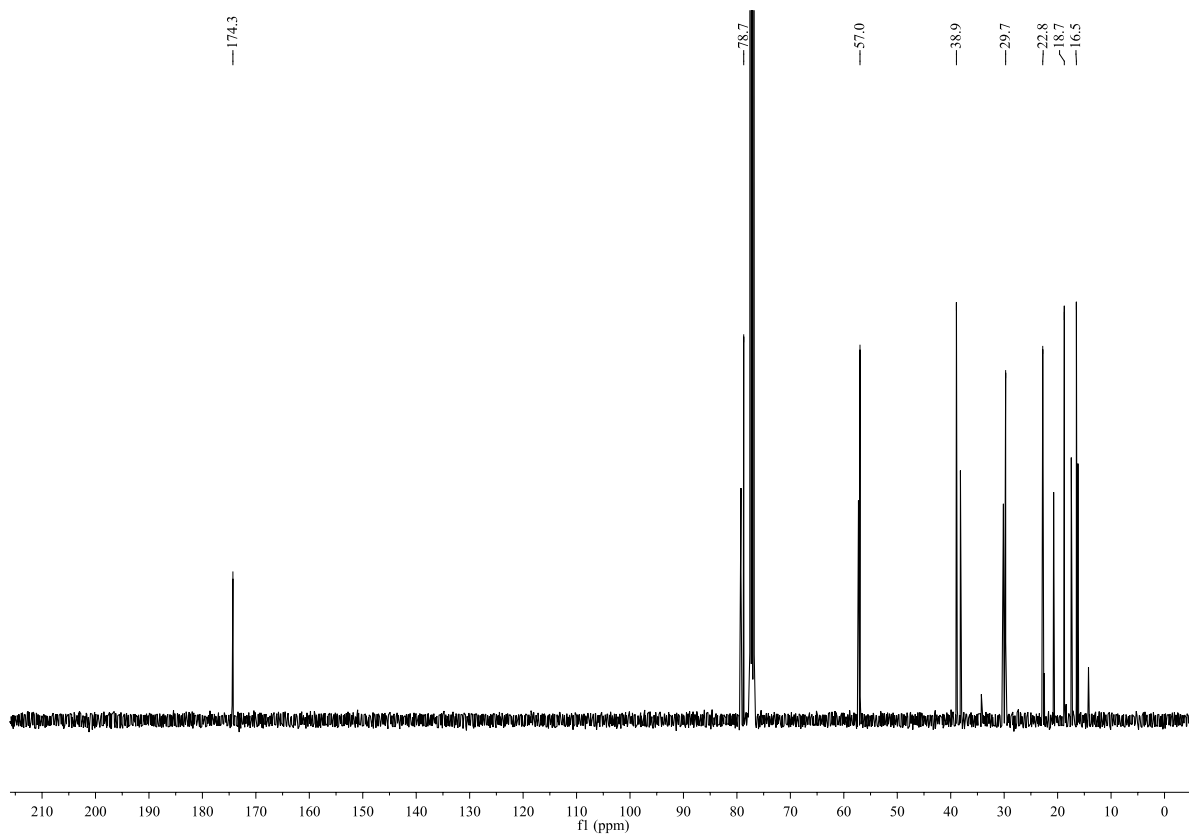
^1H NMR (CDCl_3 , 400 MHz): ^{13}C NMR (CDCl_3 , 100 MHz):

^1H NMR (CDCl_3 , 400 MHz):

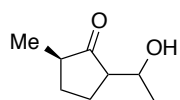


^{13}C NMR (CDCl_3 , 100 MHz):

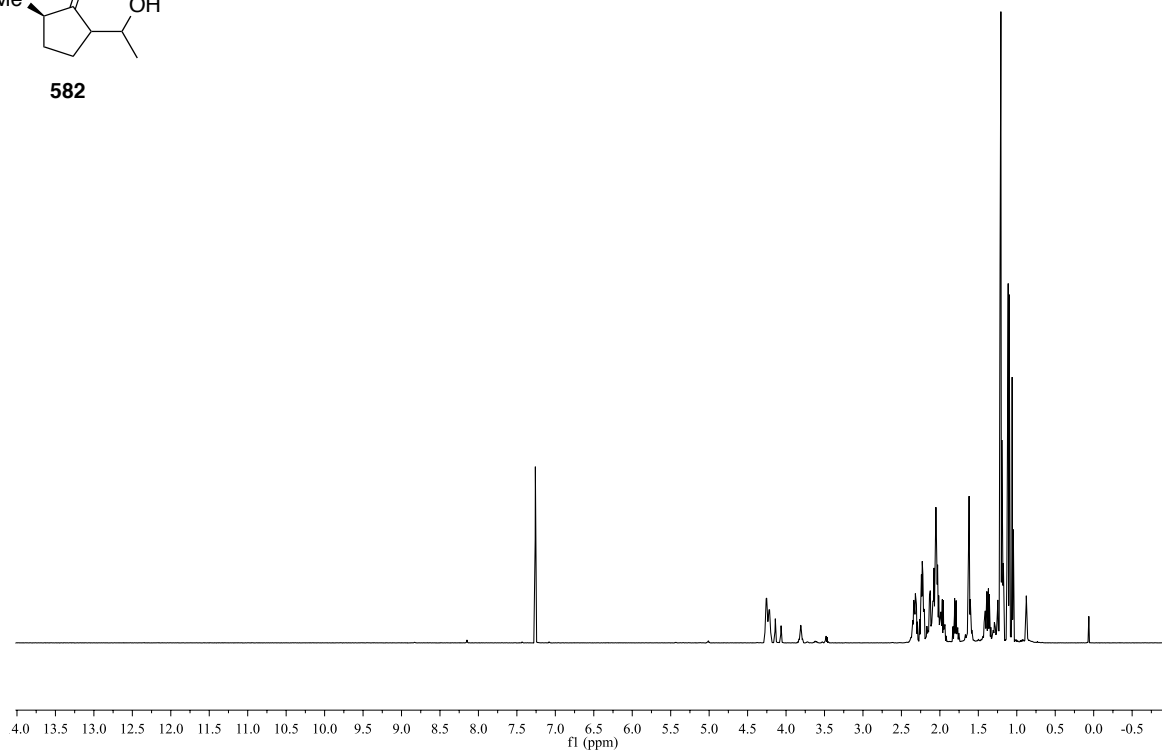


^1H NMR (CDCl_3 , 400 MHz):**541** ^{13}C NMR (CDCl_3 , 100 MHz):

^1H NMR (CDCl_3 , 600 MHz):

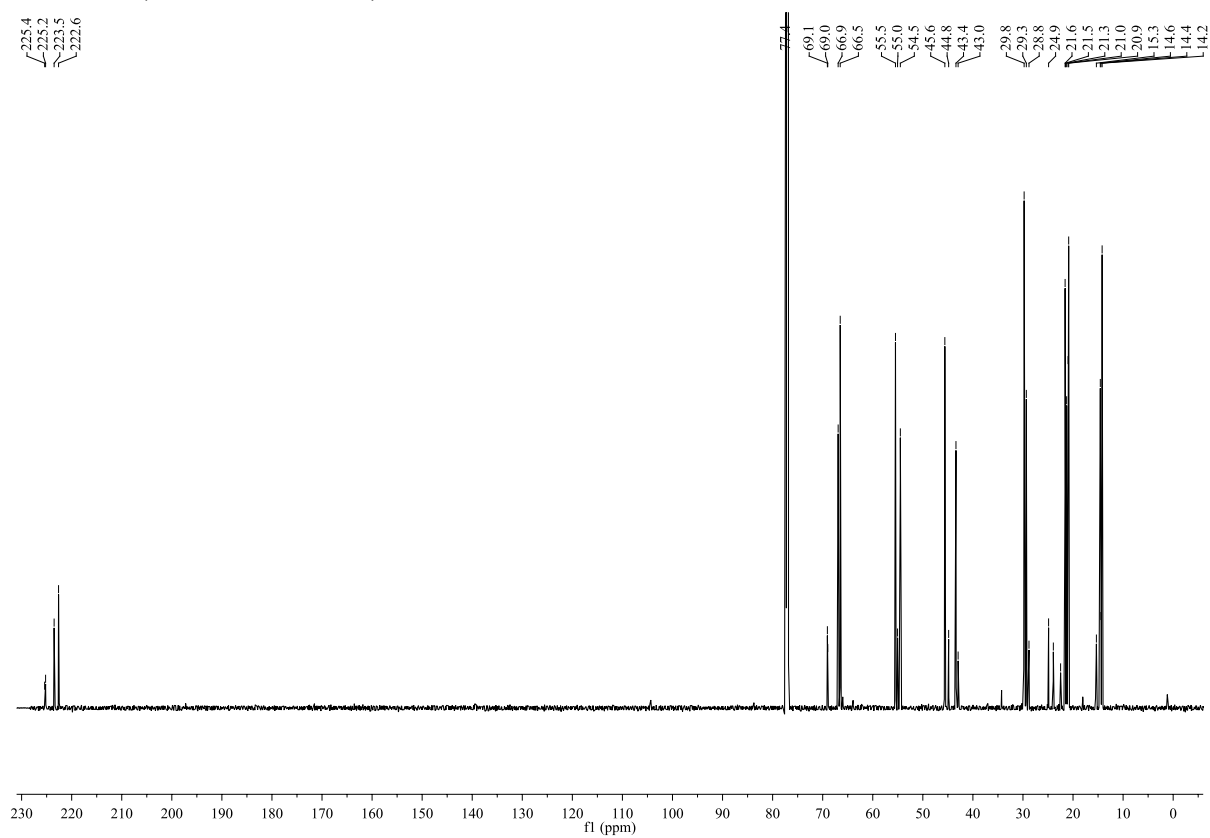


582

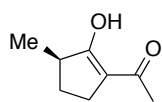


^{13}C NMR (CDCl_3 , 150 MHz):

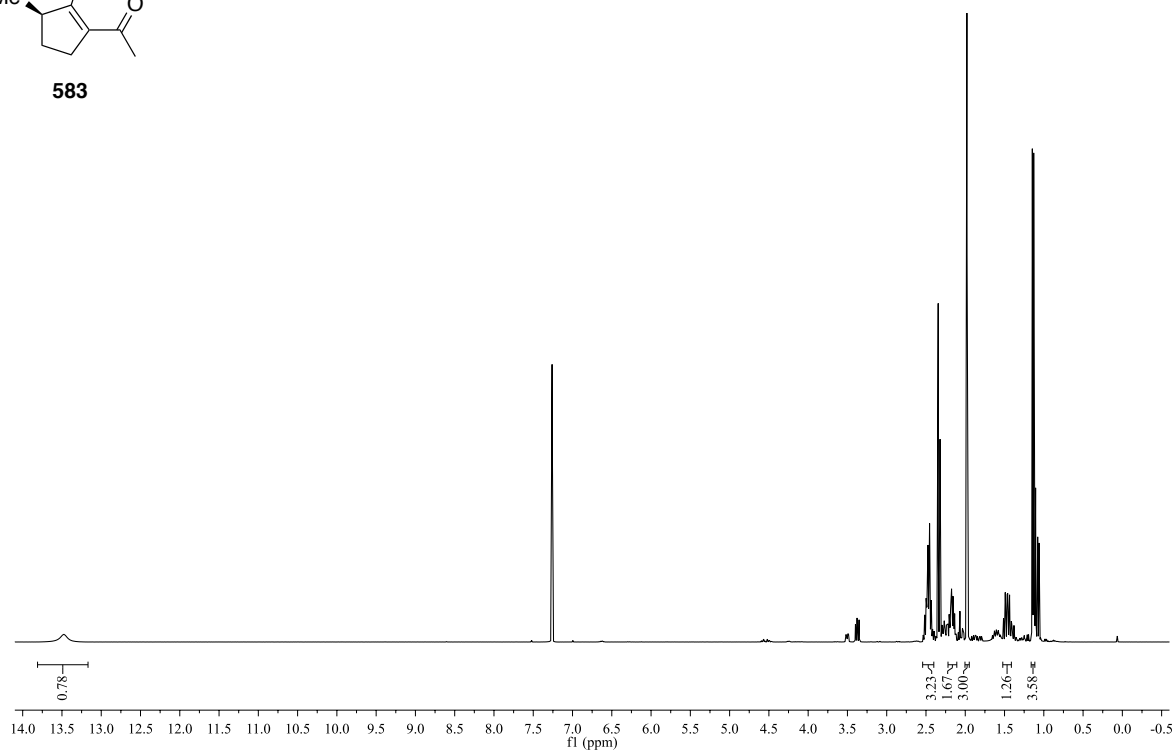
225.4
225.2
223.5
222.6



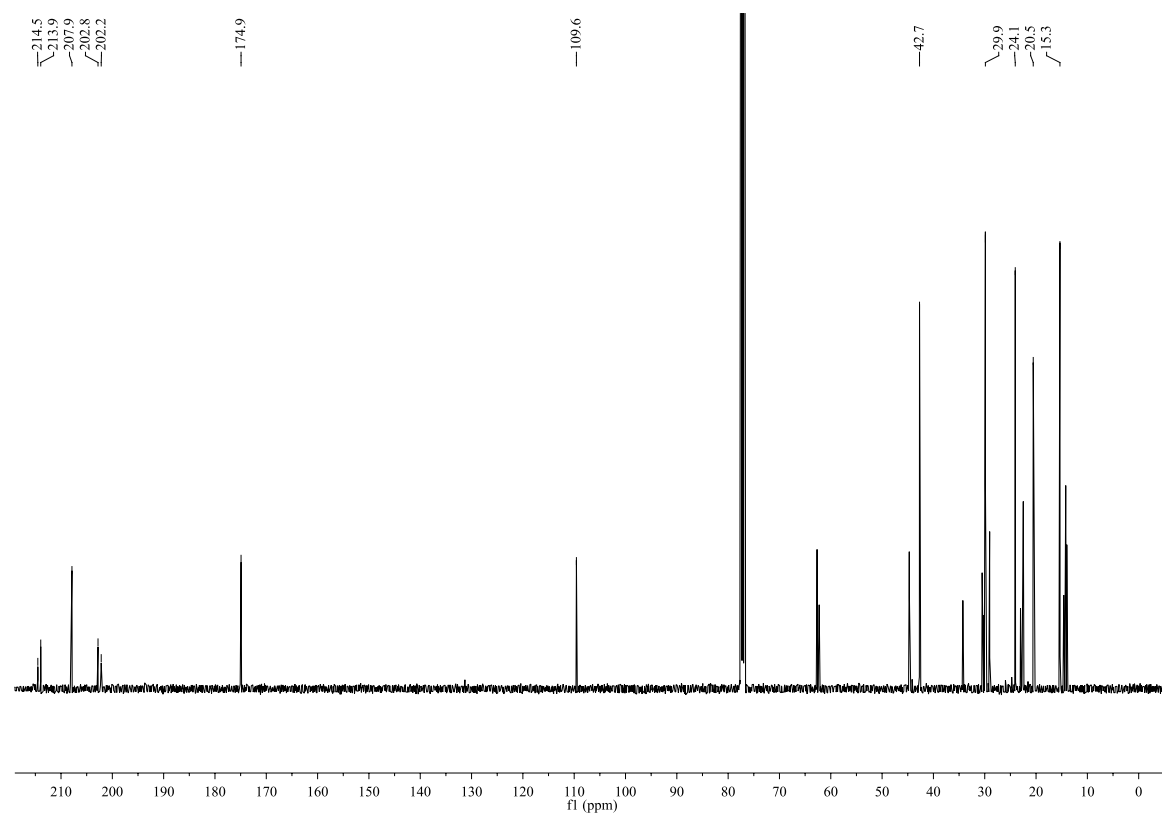
^1H NMR (CDCl_3 , 400 MHz):



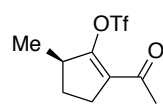
583



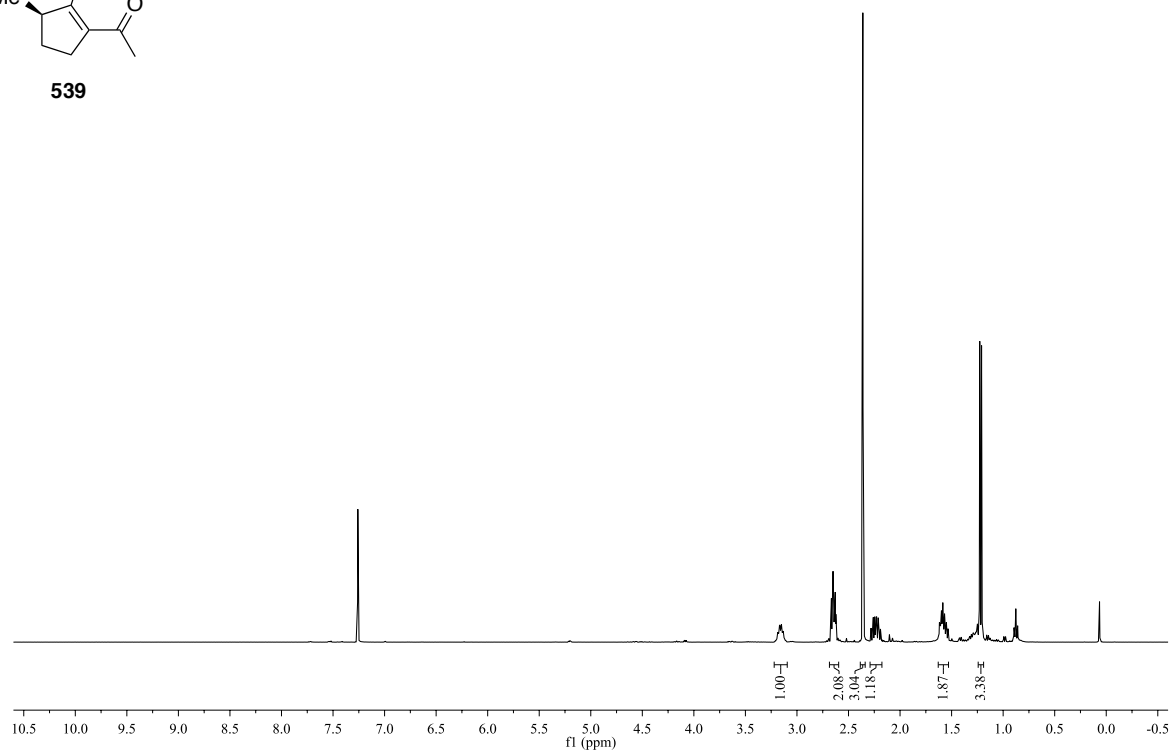
^{13}C NMR (CDCl_3 , 100 MHz):



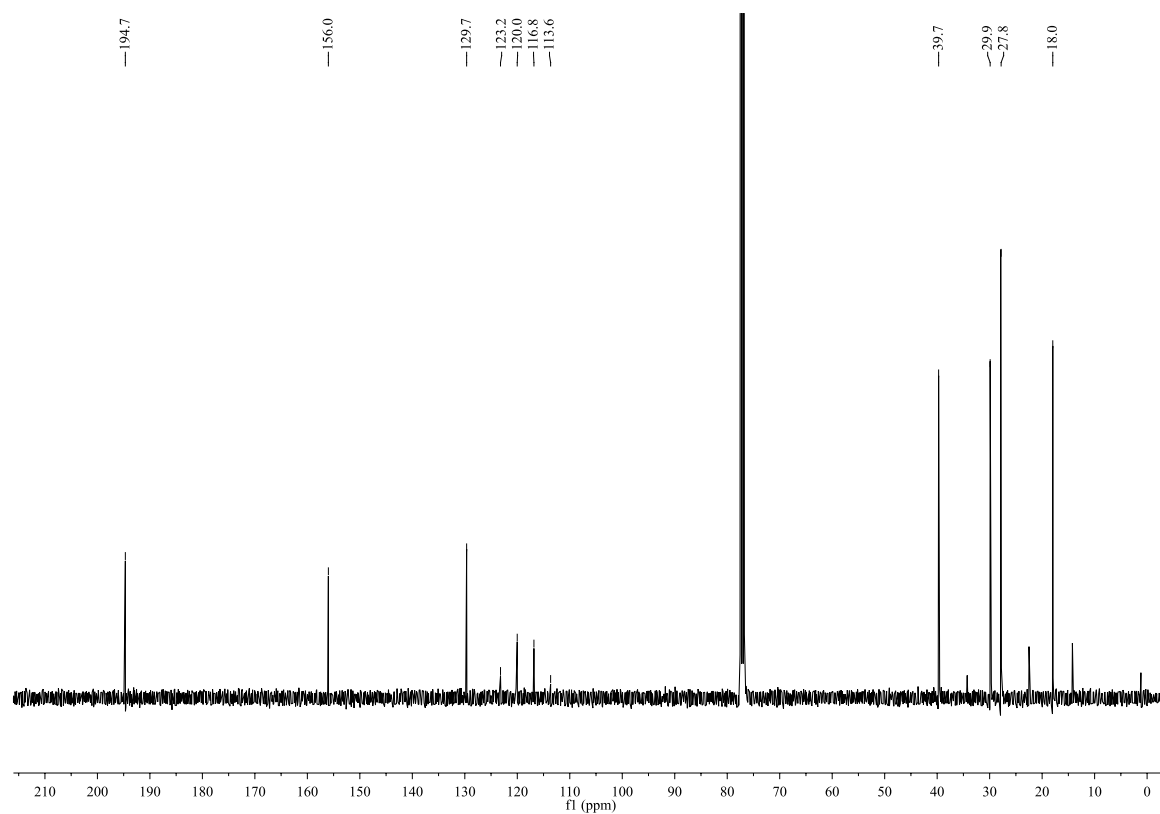
^1H NMR (CDCl_3 , 400 MHz):

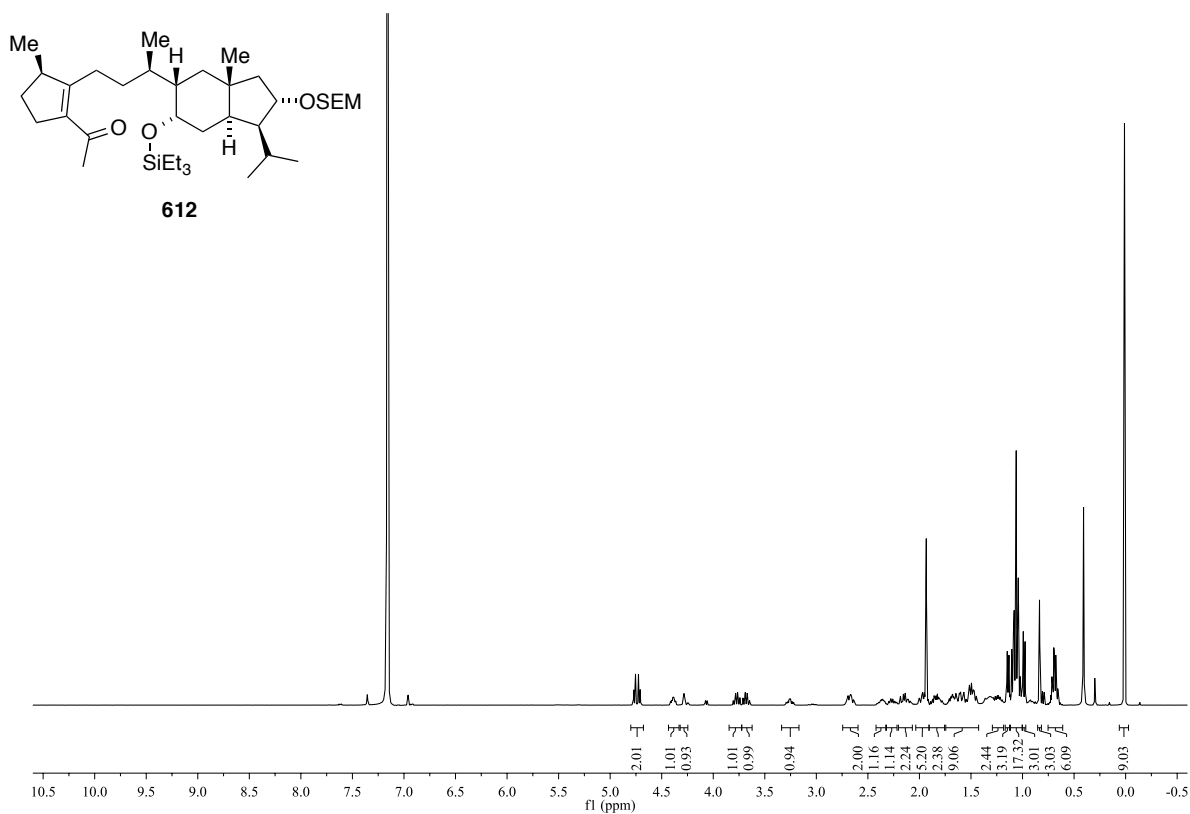
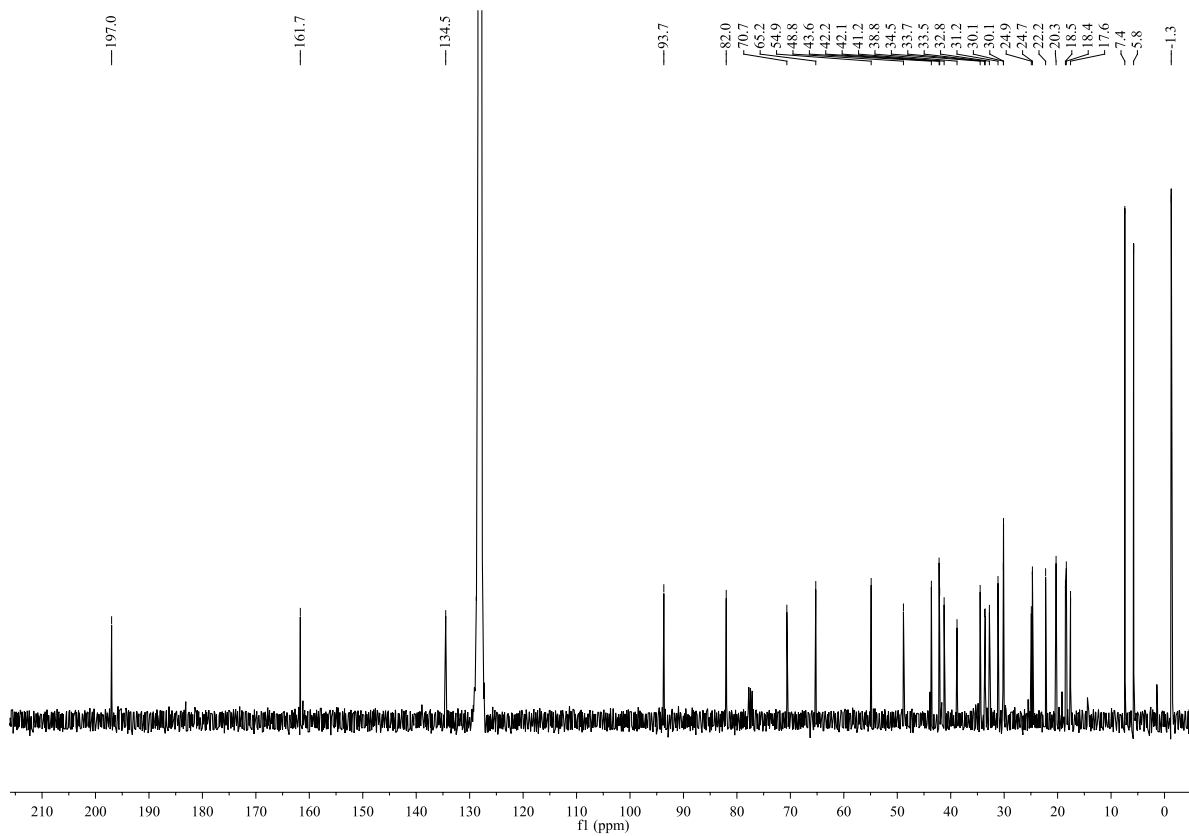


539

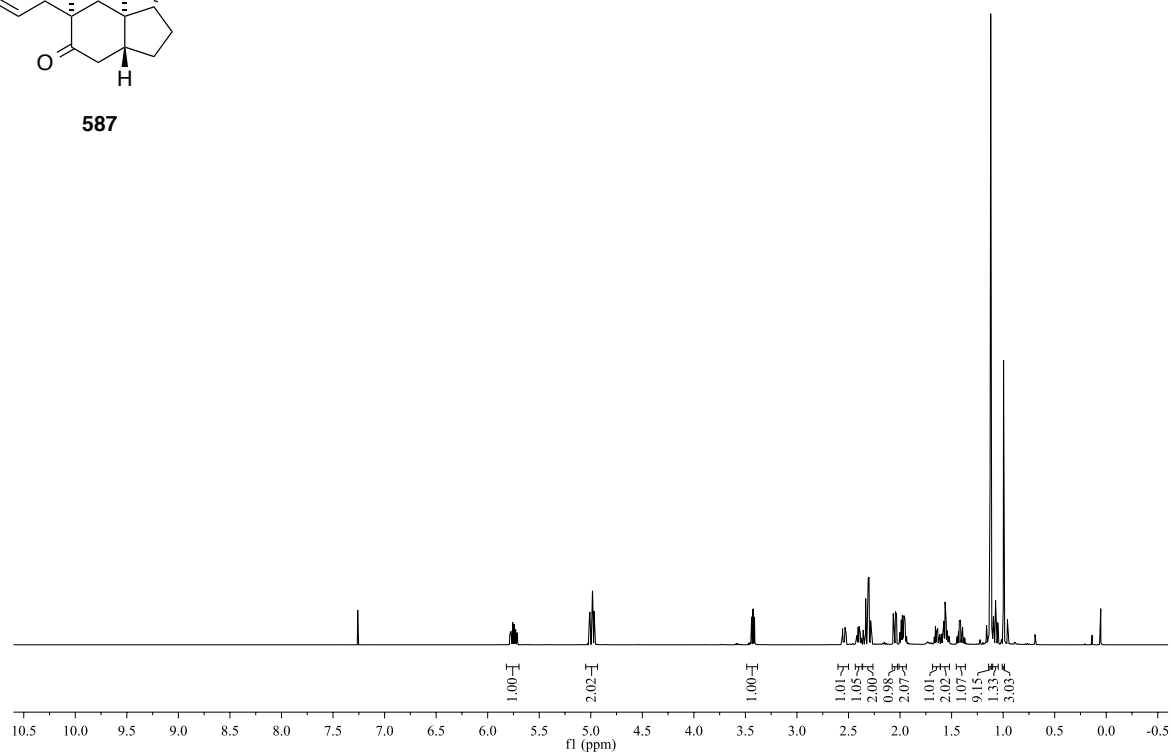
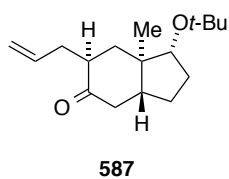


^{13}C NMR (CDCl_3 , 100 MHz):

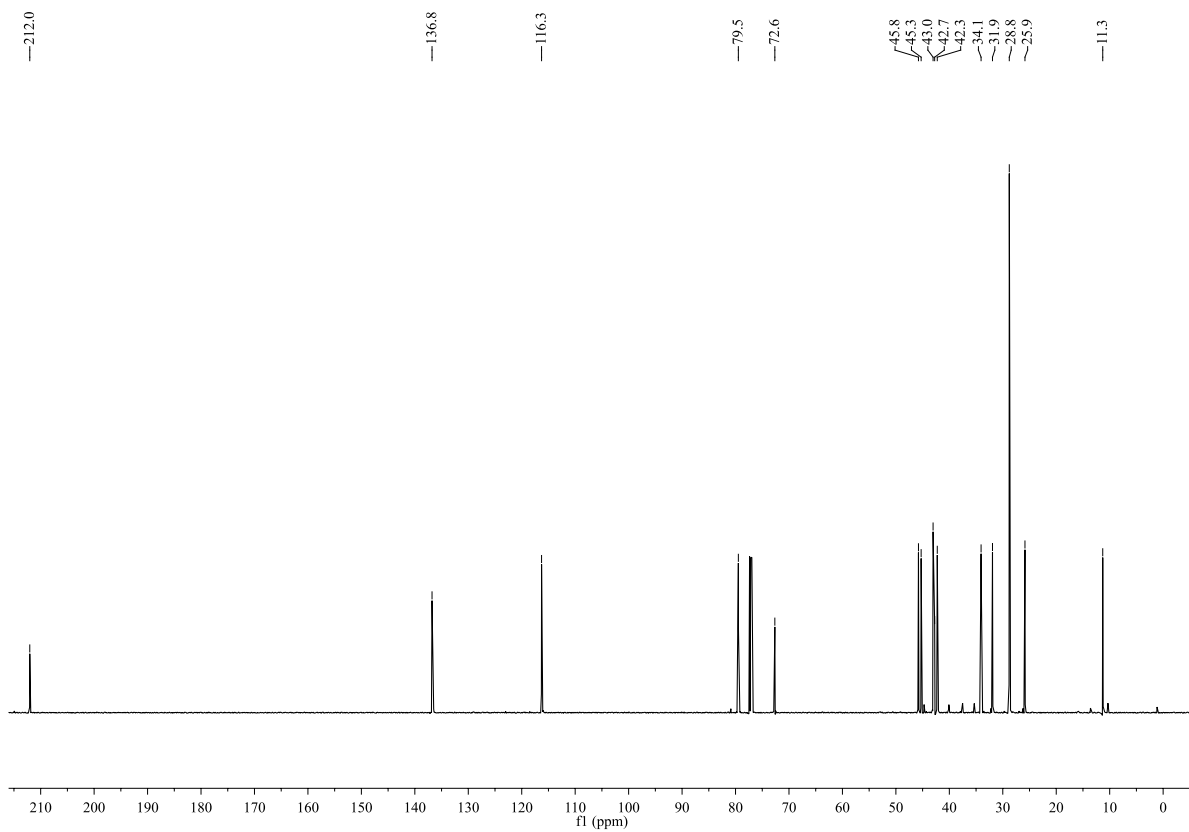


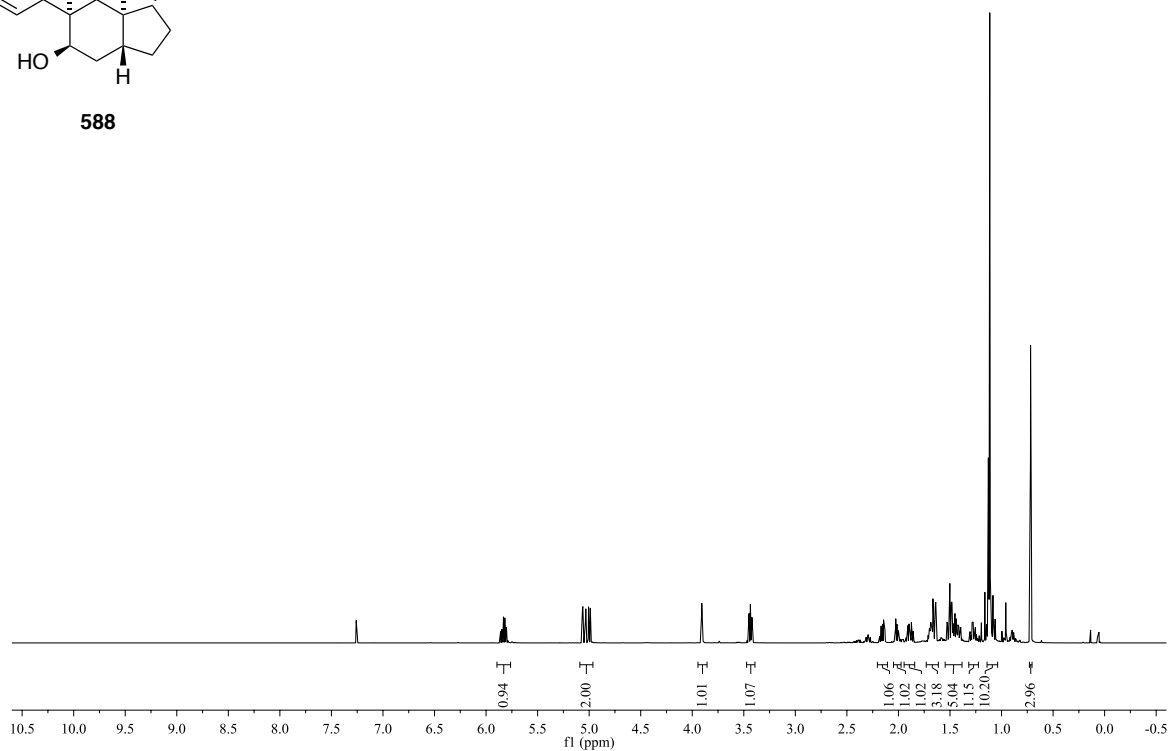
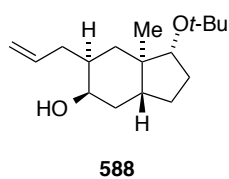
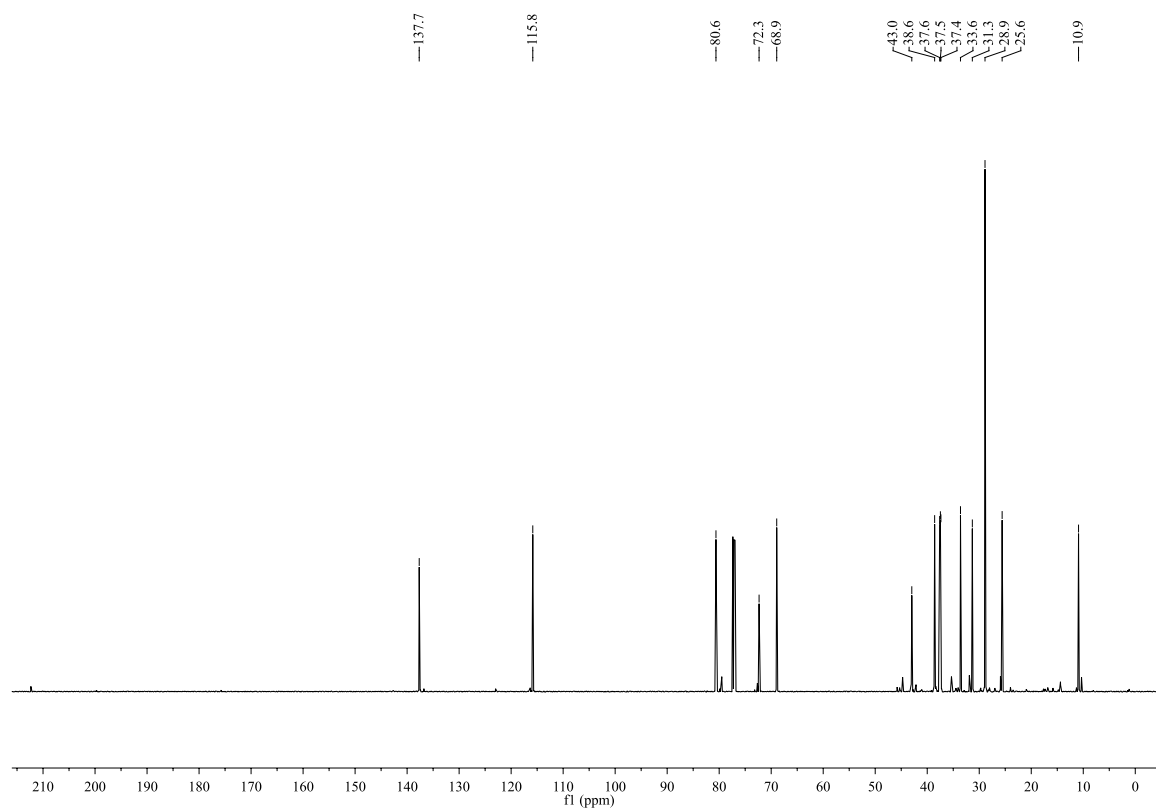
^1H NMR (C_6D_6 , 400 MHz): ^{13}C NMR (C_6D_6 , 100 MHz):

^1H NMR (CDCl_3 , 600 MHz):

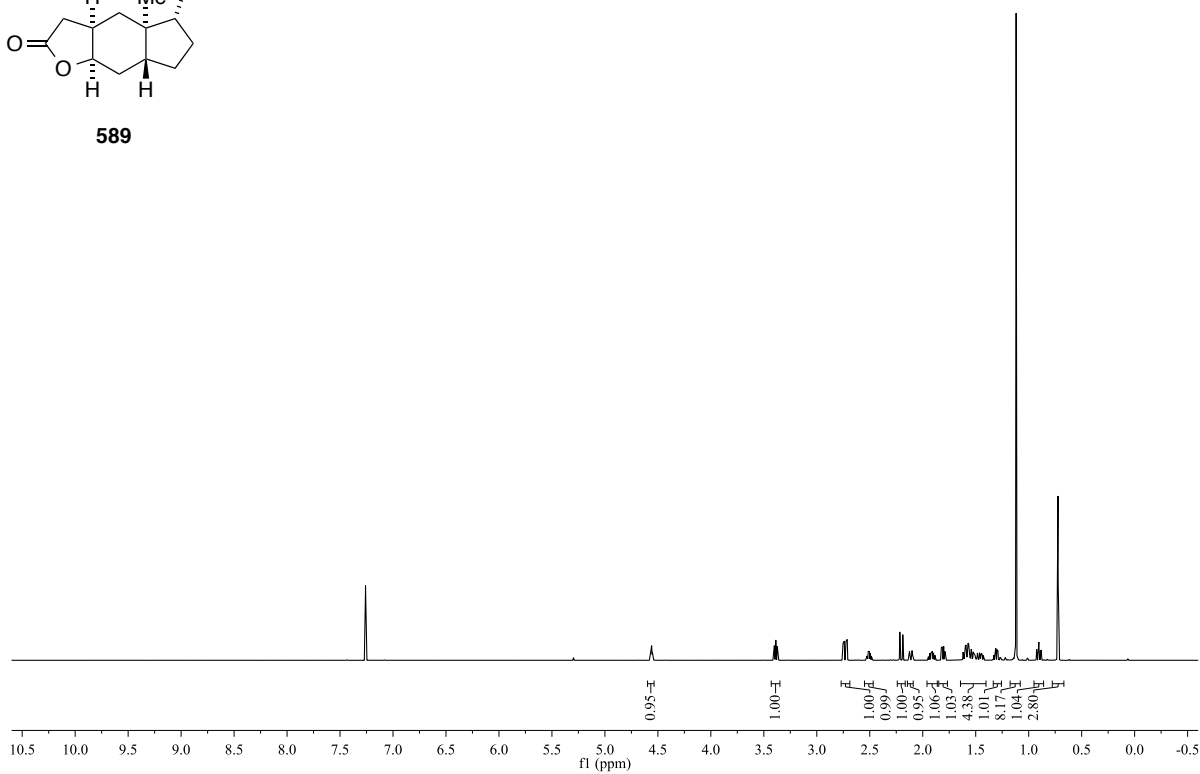
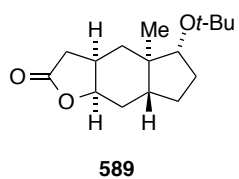


^{13}C NMR (CDCl_3 , 150 MHz):

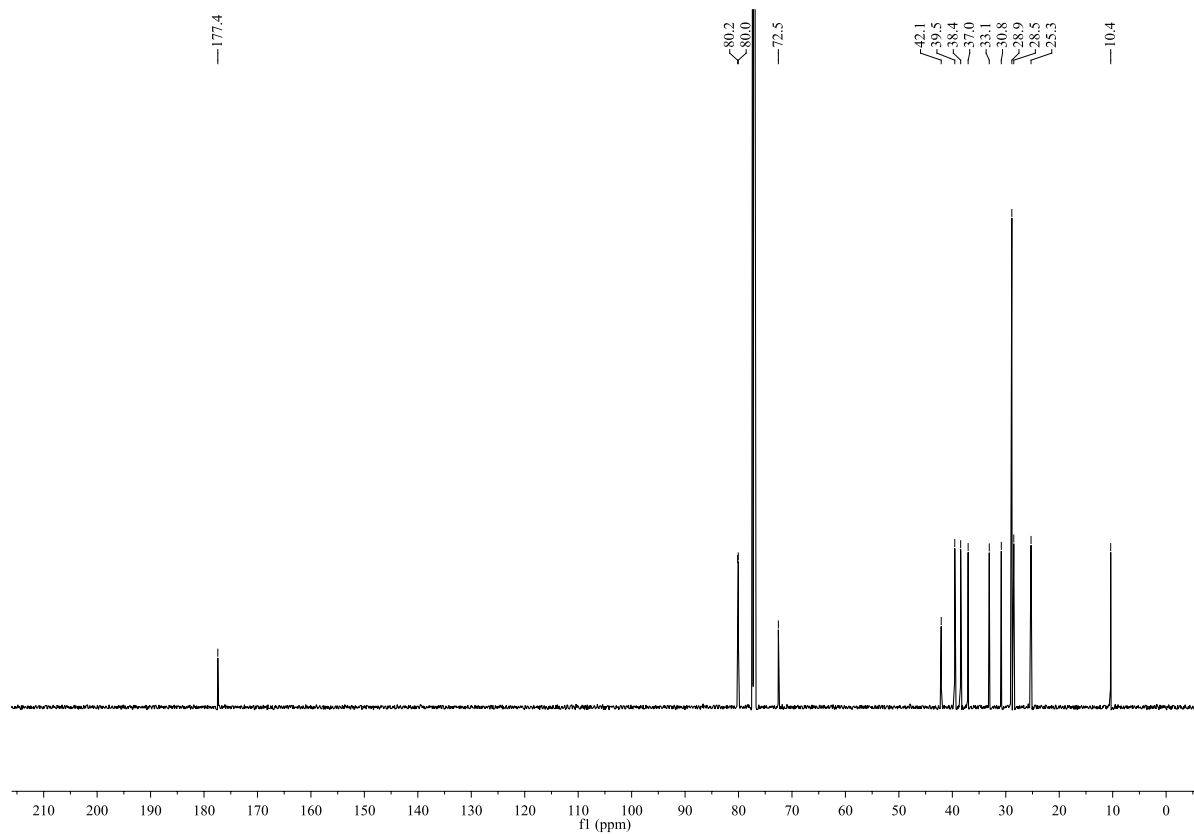


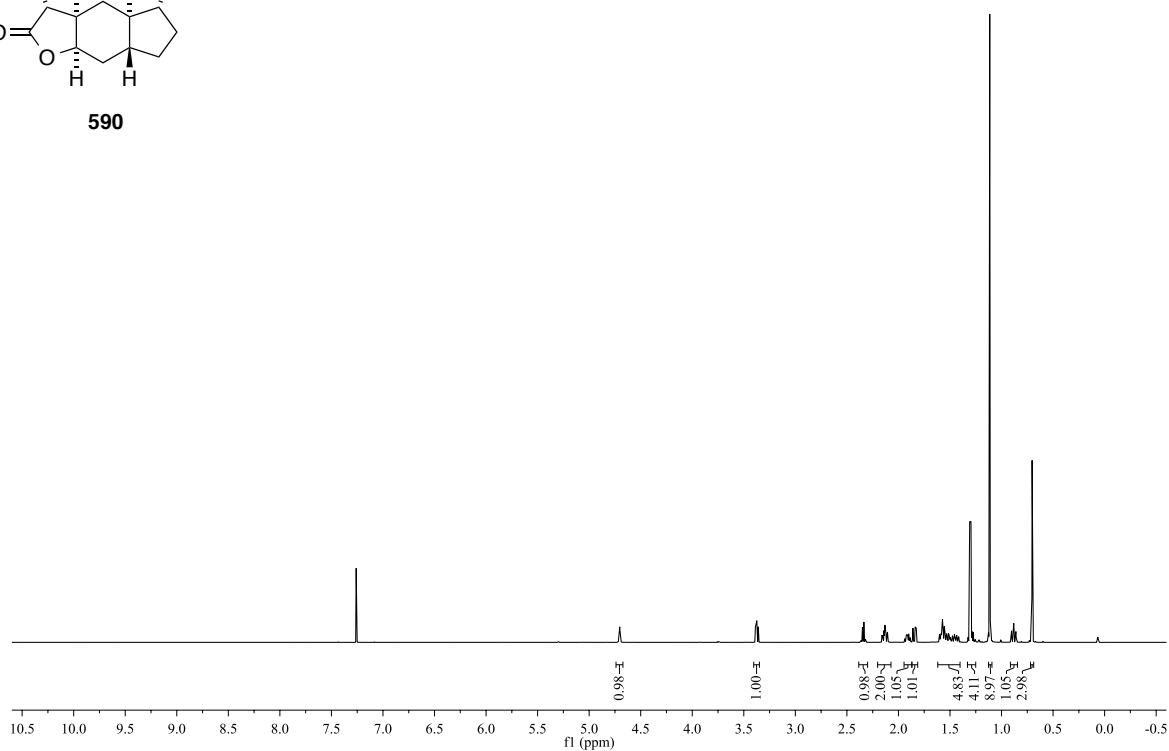
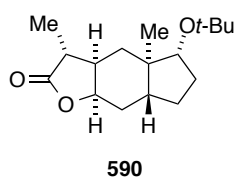
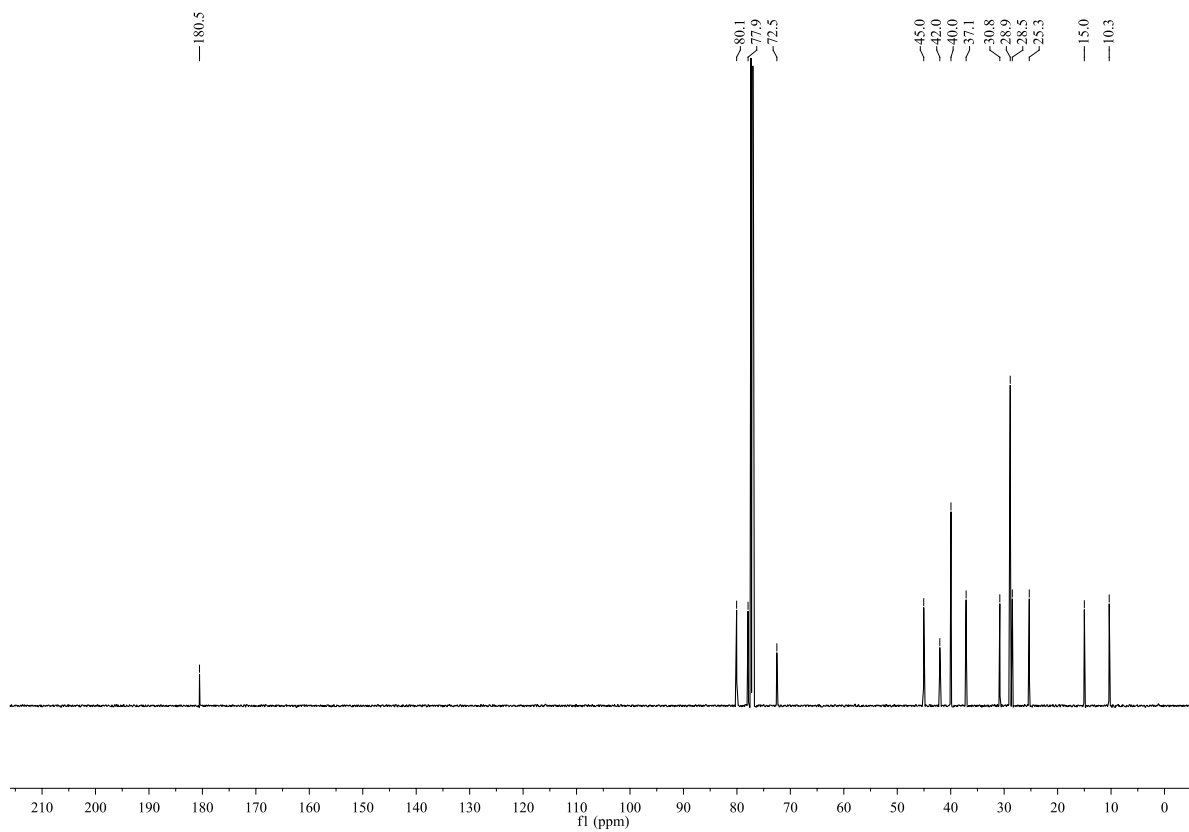
^1H NMR (CDCl_3 , 600 MHz): ^{13}C NMR (CDCl_3 , 150 MHz):

^1H NMR (CDCl_3 , 600 MHz):

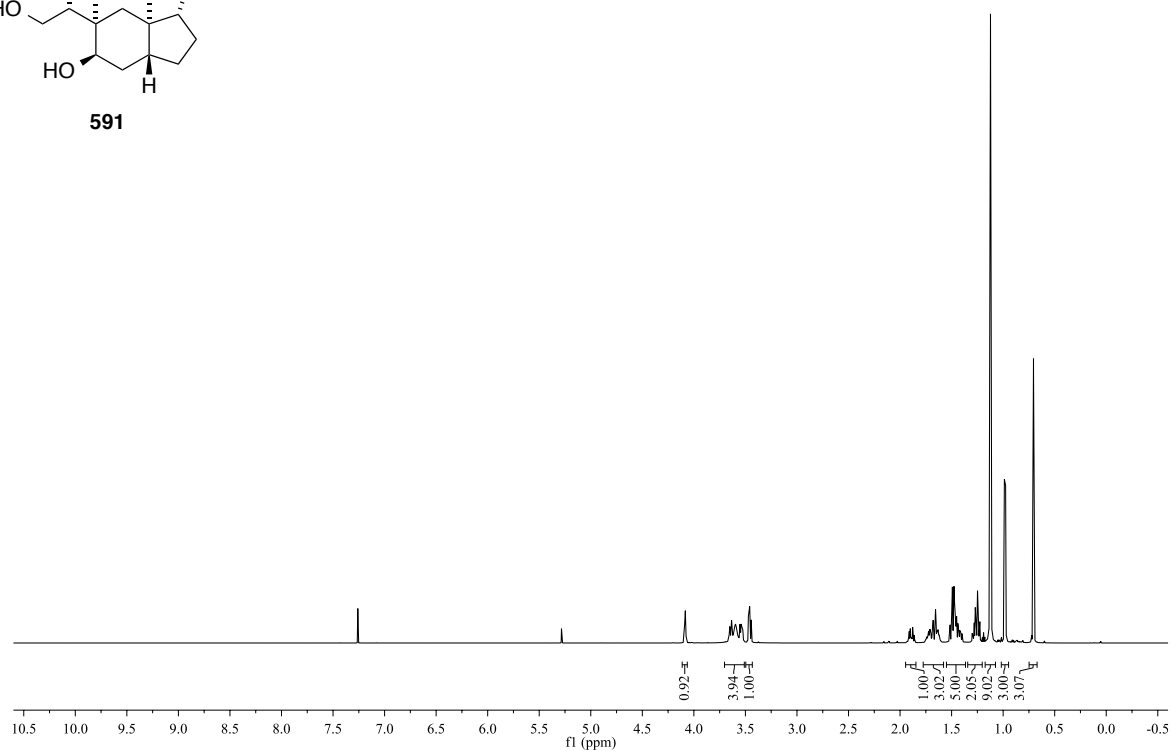
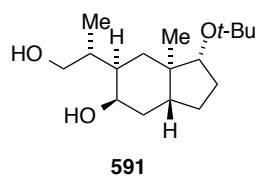


^{13}C NMR (CDCl_3 , 150 MHz):

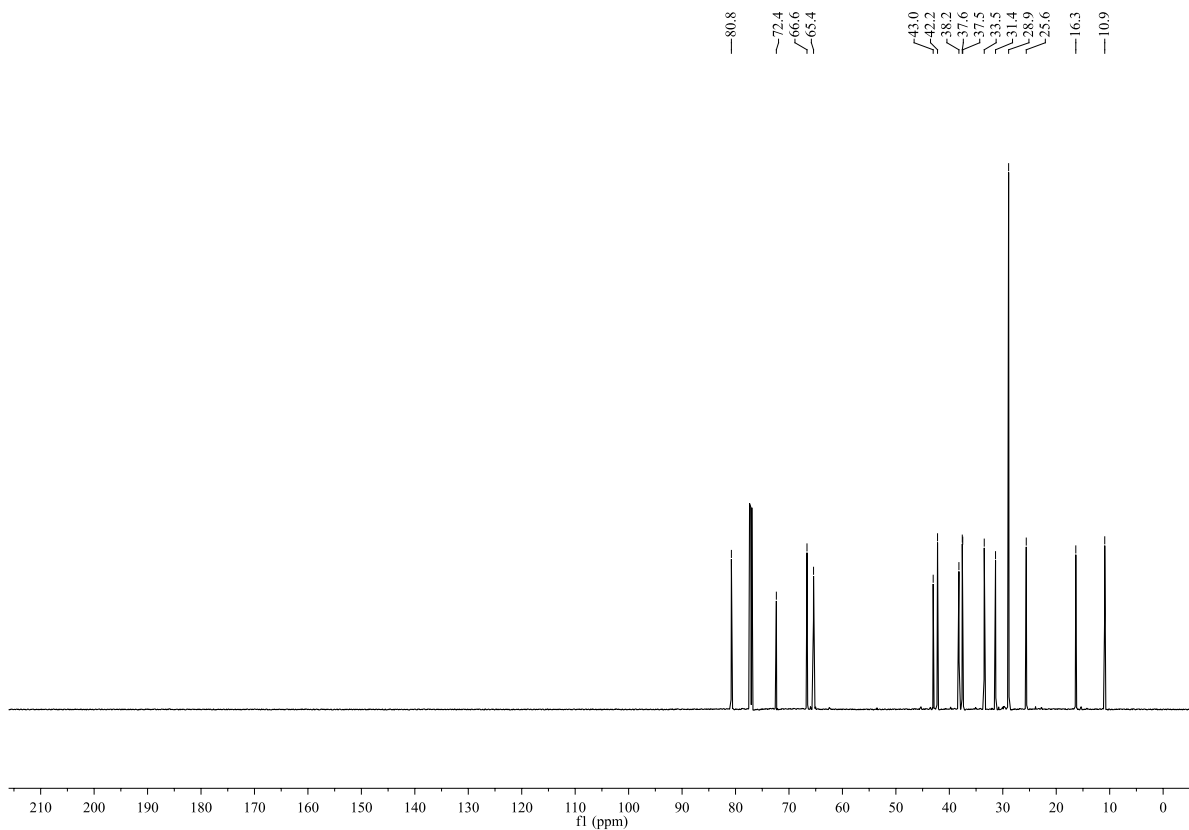


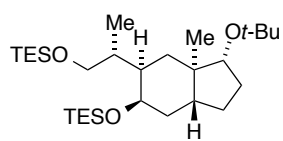
^1H NMR (CDCl_3 , 600 MHz): ^{13}C NMR (CDCl_3 , 150 MHz):

^1H NMR (CDCl_3 , 600 MHz):

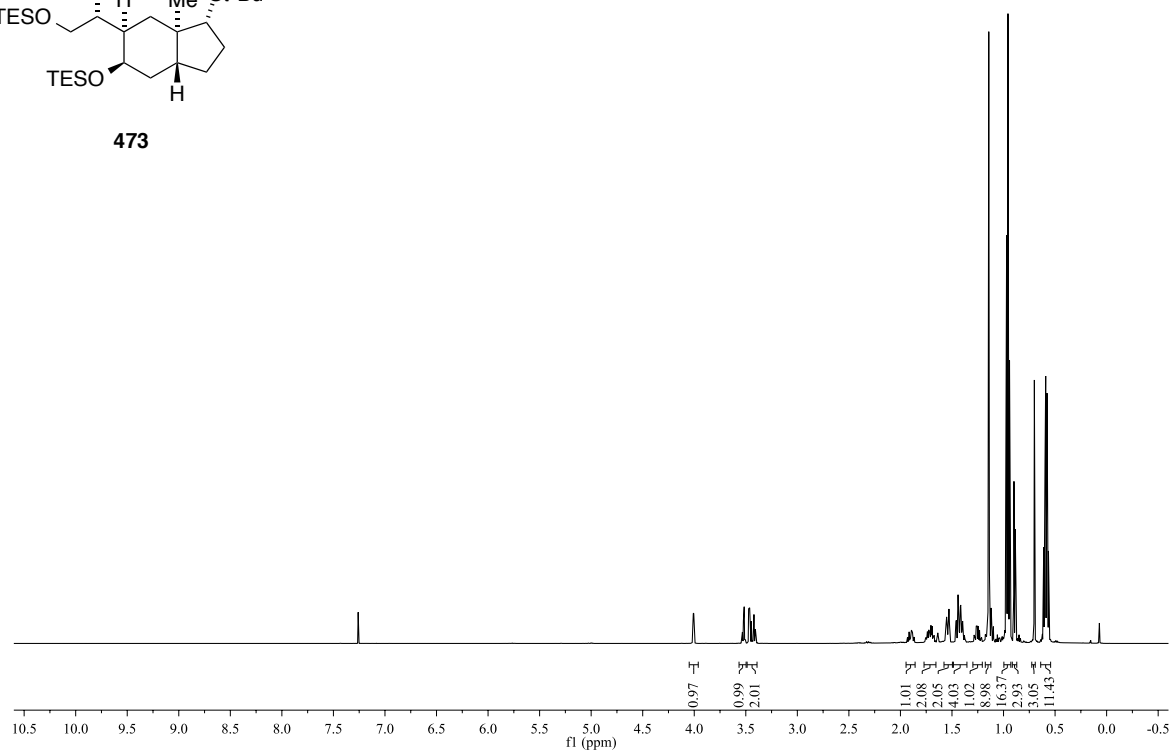
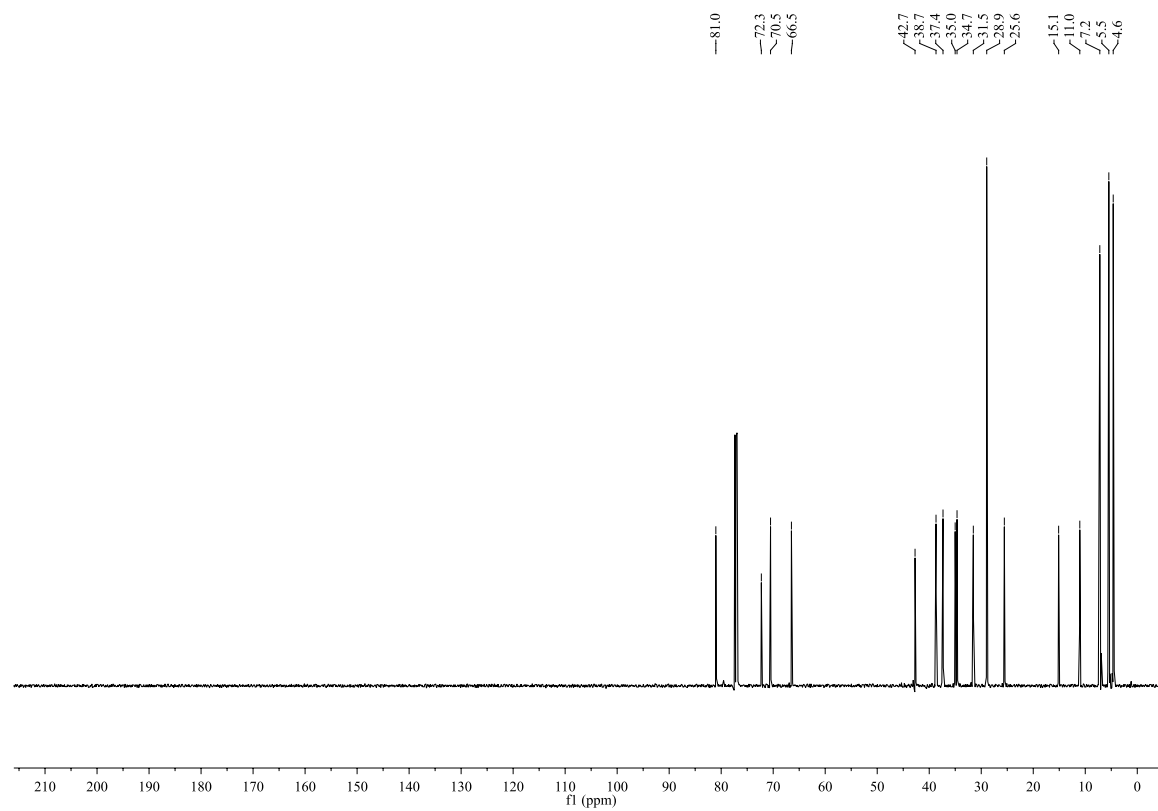


^{13}C NMR (CDCl_3 , 150 MHz):

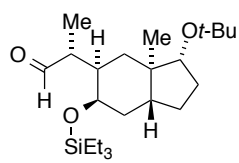


^1H NMR (CDCl_3 , 600 MHz):

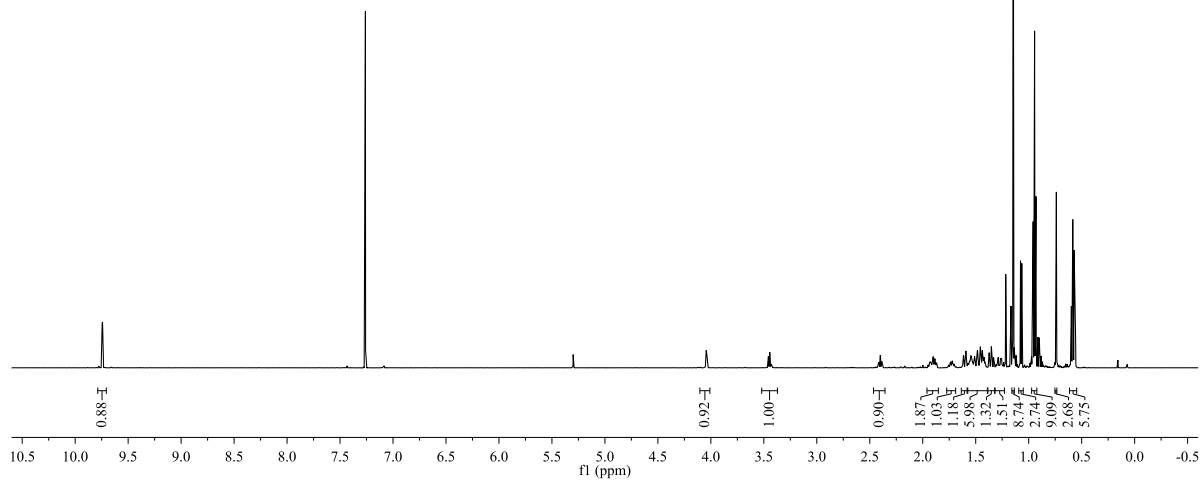
473

 ^{13}C NMR (CDCl_3 , 150 MHz):

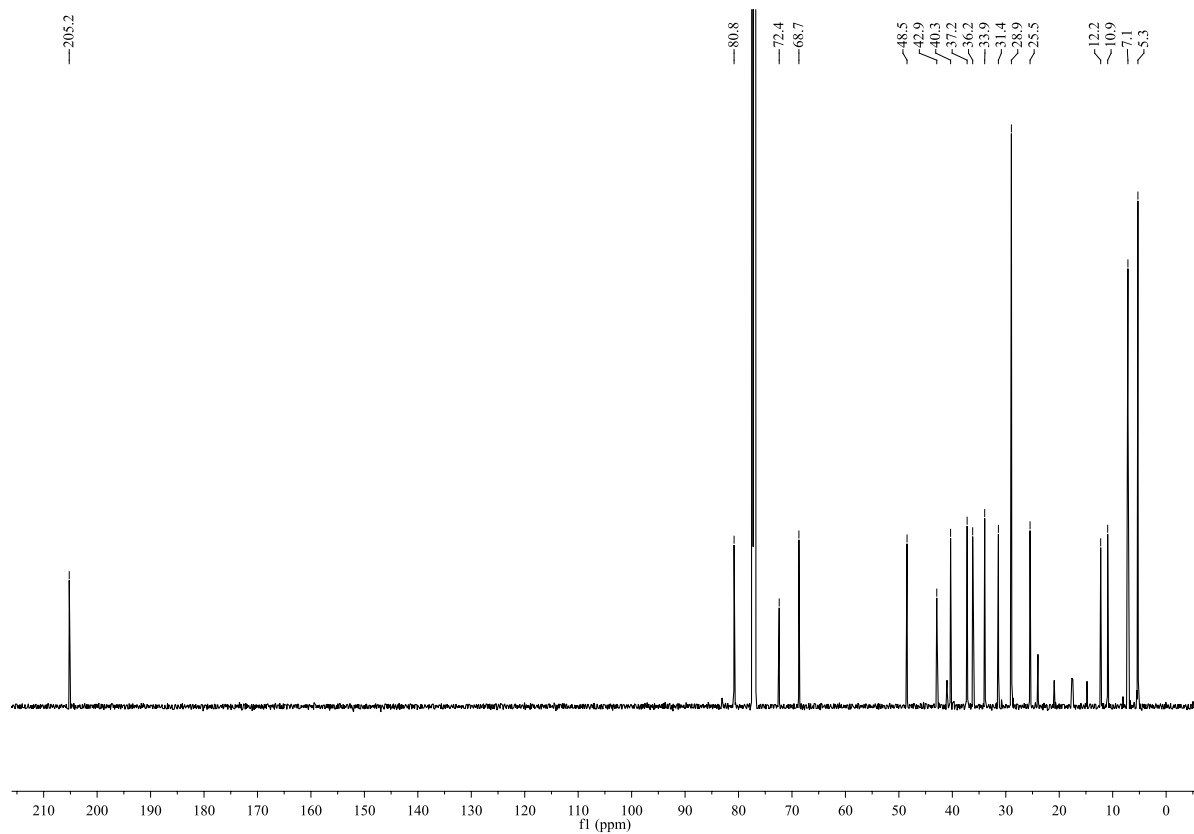
^1H NMR (CDCl_3 , 600 MHz):



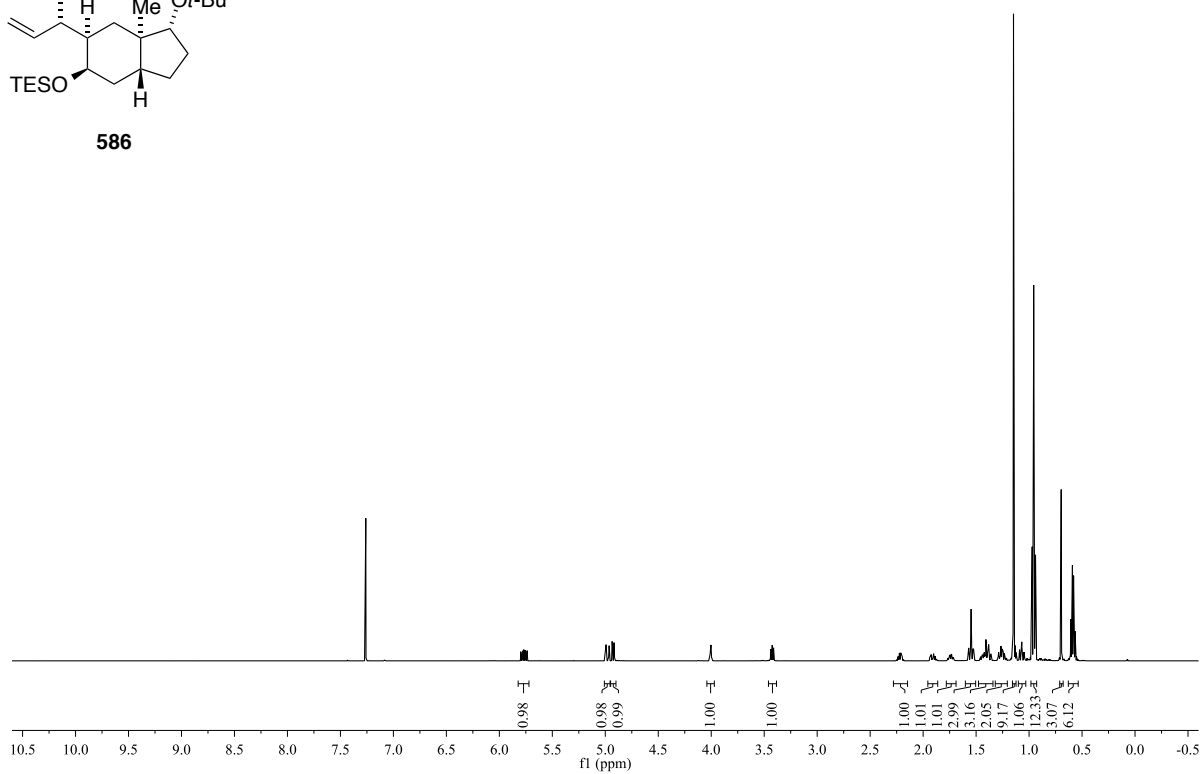
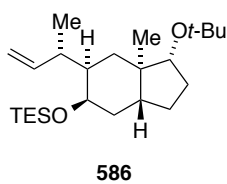
592



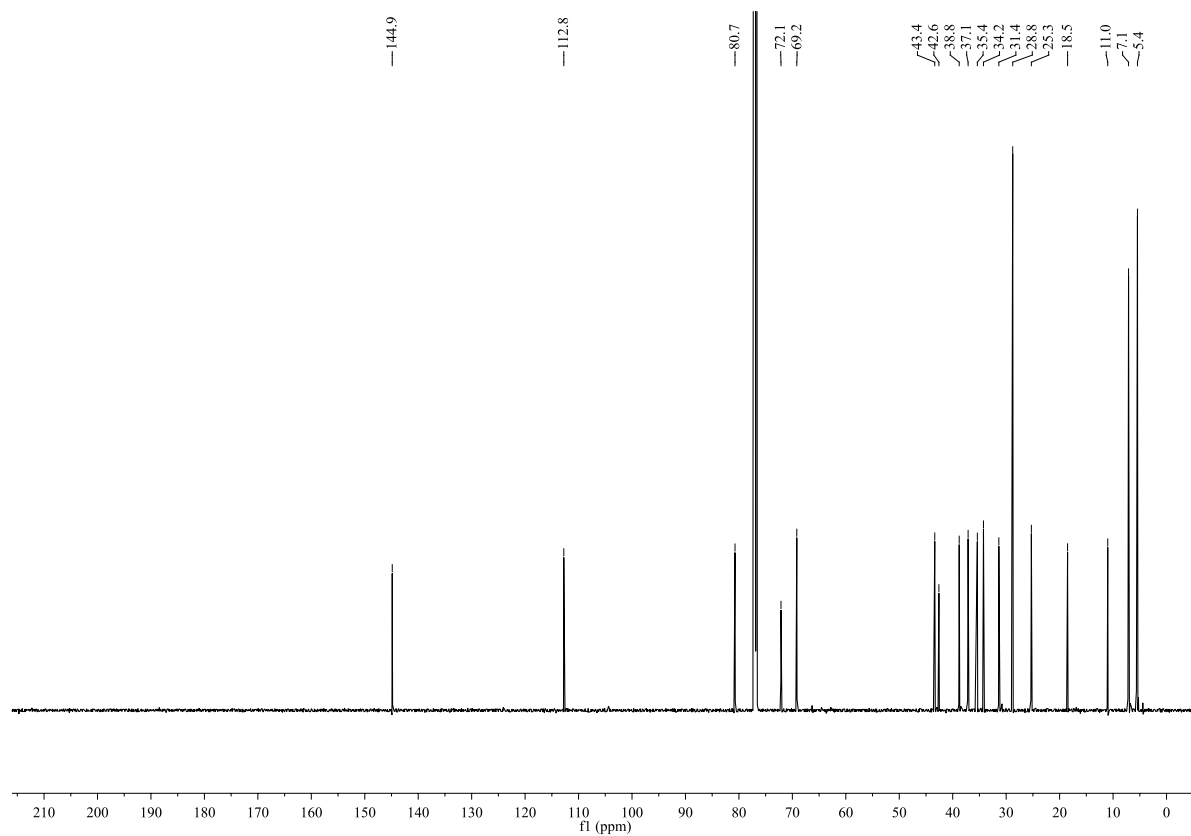
^{13}C NMR (CDCl_3 , 150 MHz):



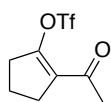
^1H NMR (CDCl_3 , 600 MHz):



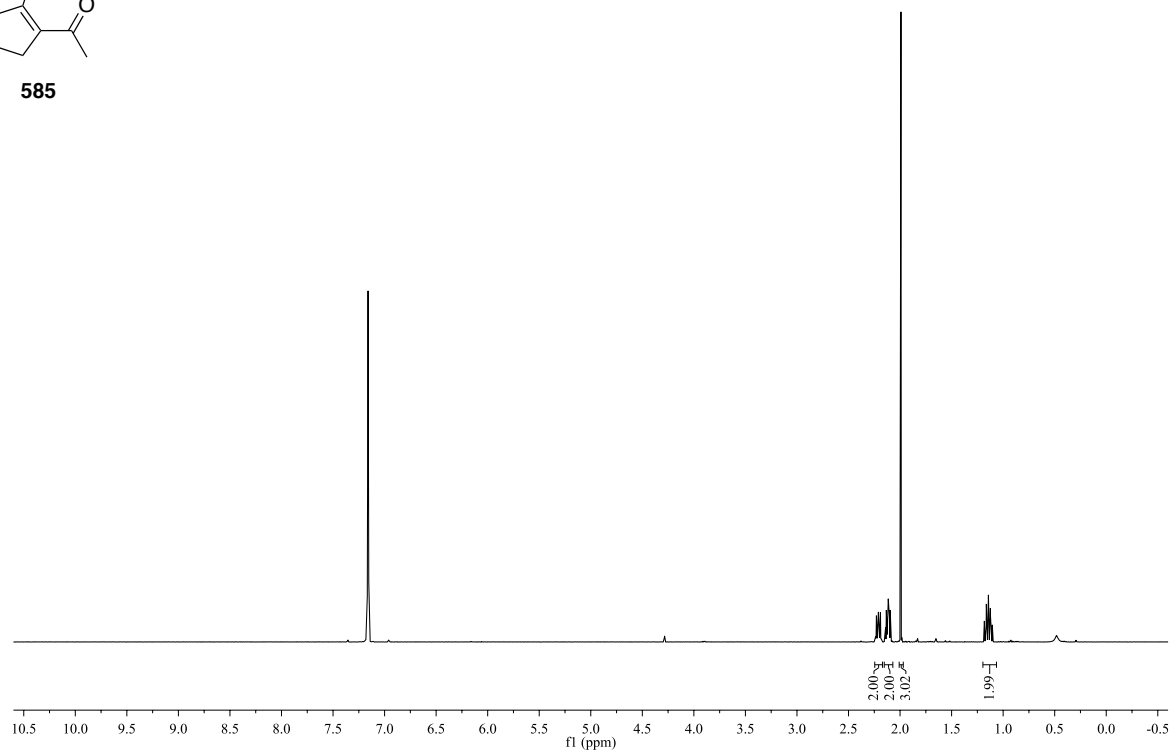
^{13}C NMR (CDCl_3 , 150 MHz):



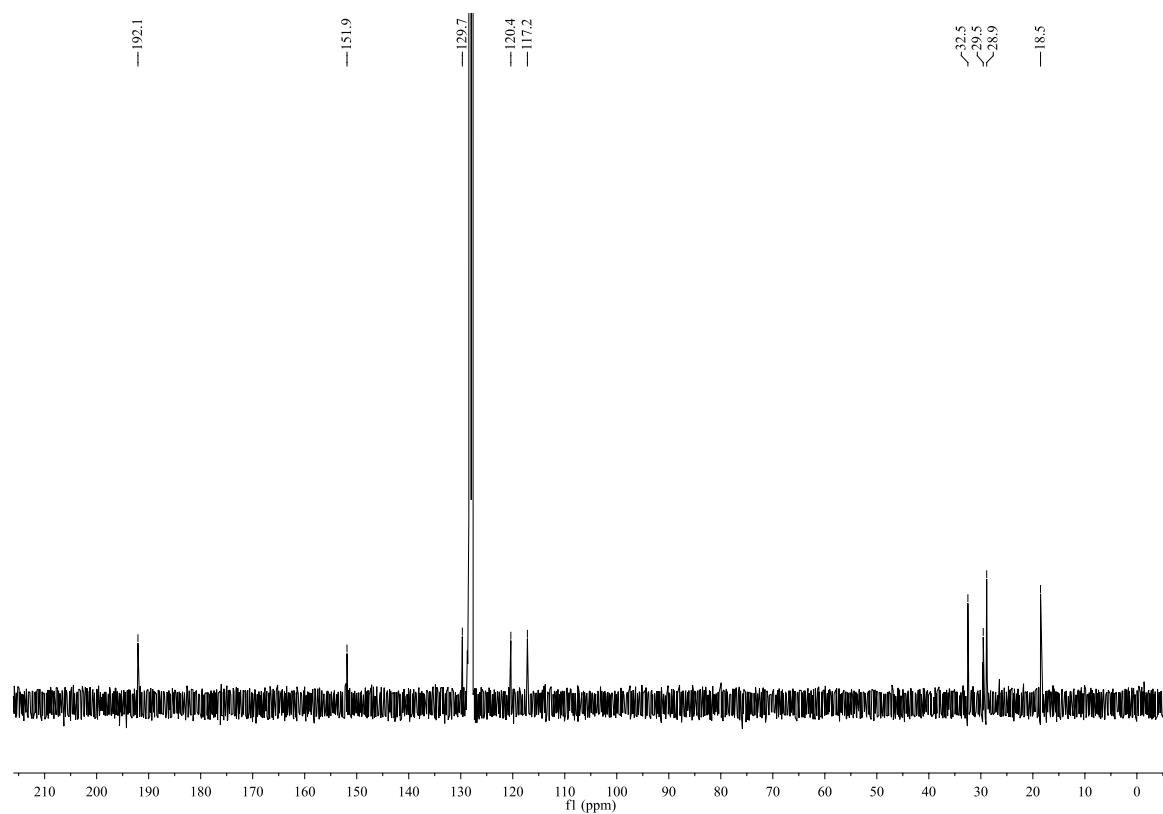
^1H NMR (C_6D_6 , 400 MHz):

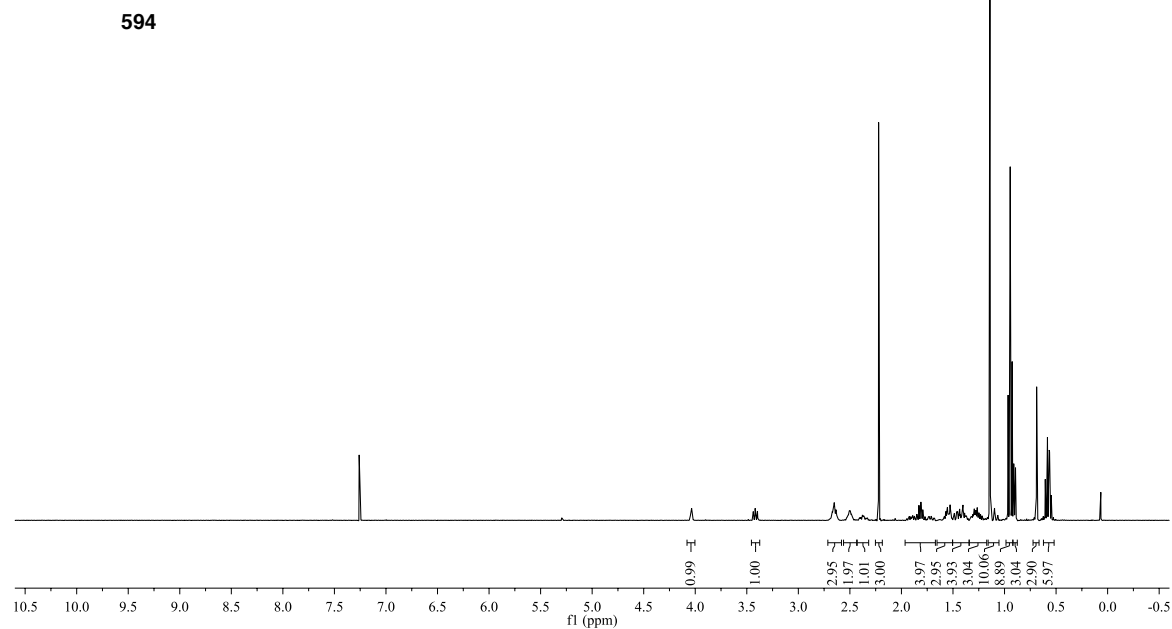
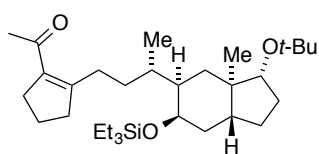
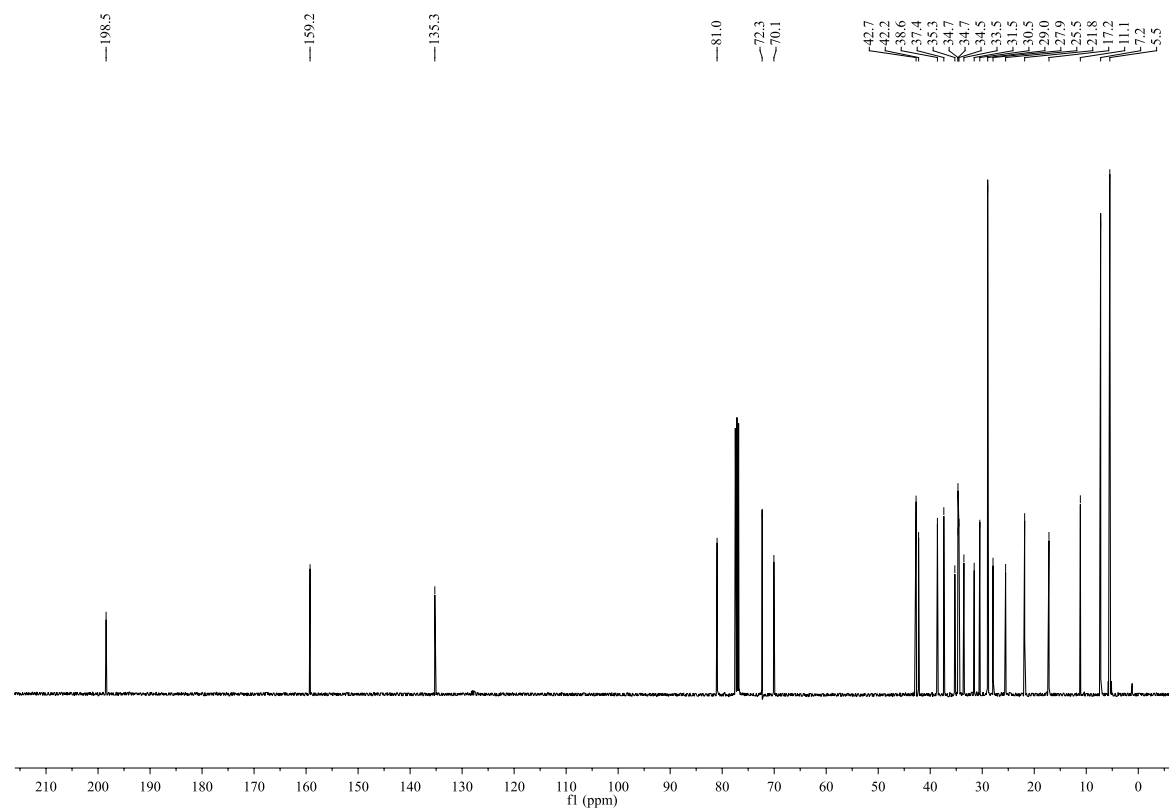


585

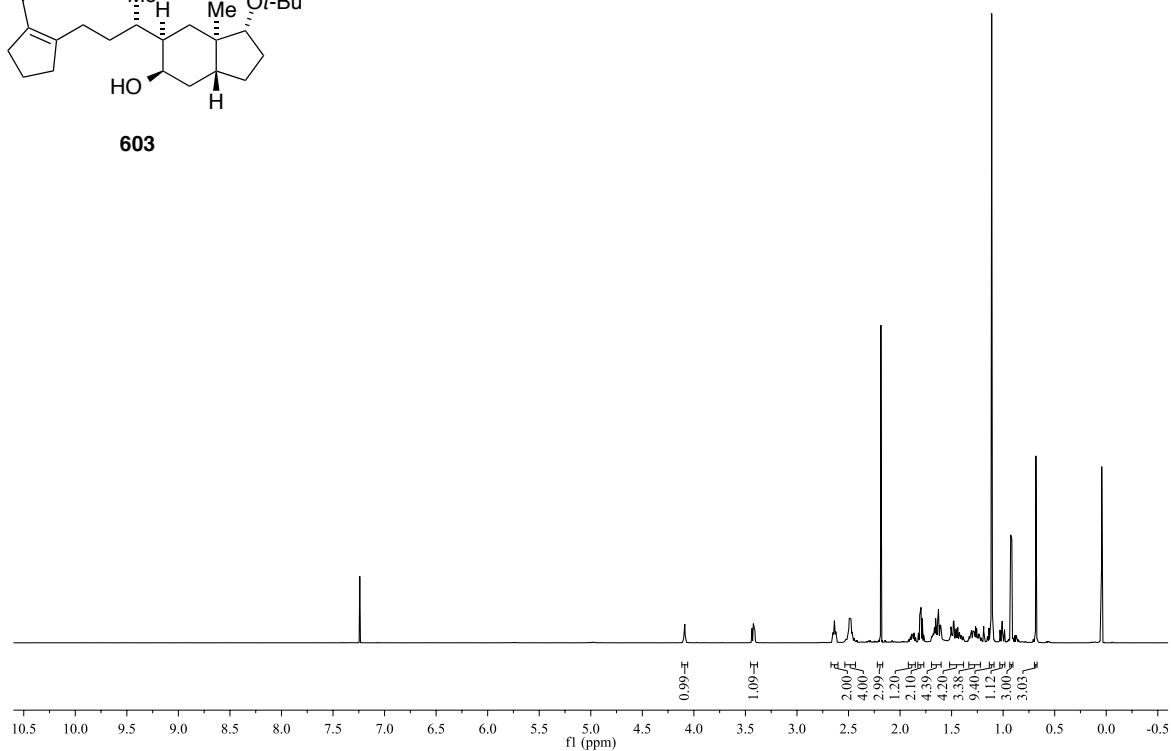
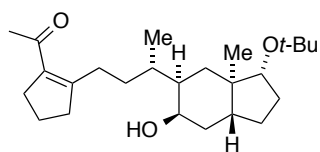


^{13}C NMR (C_6D_6 , 100 MHz):

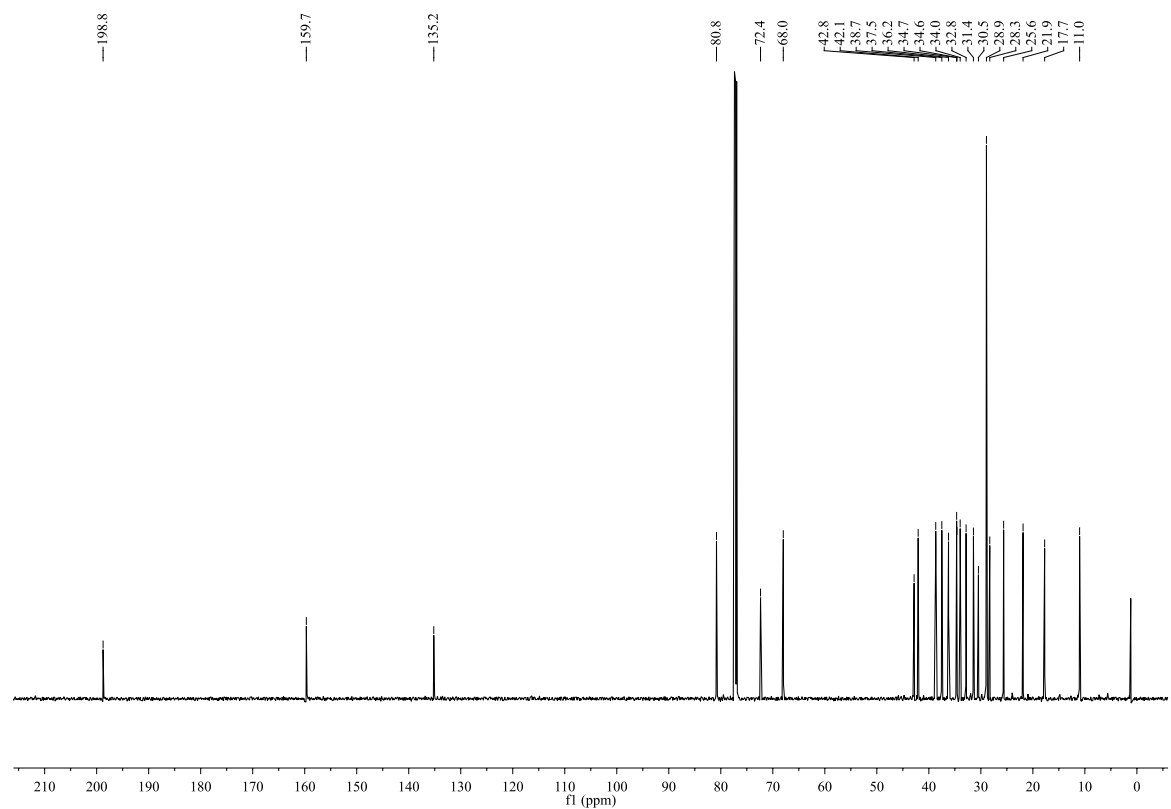


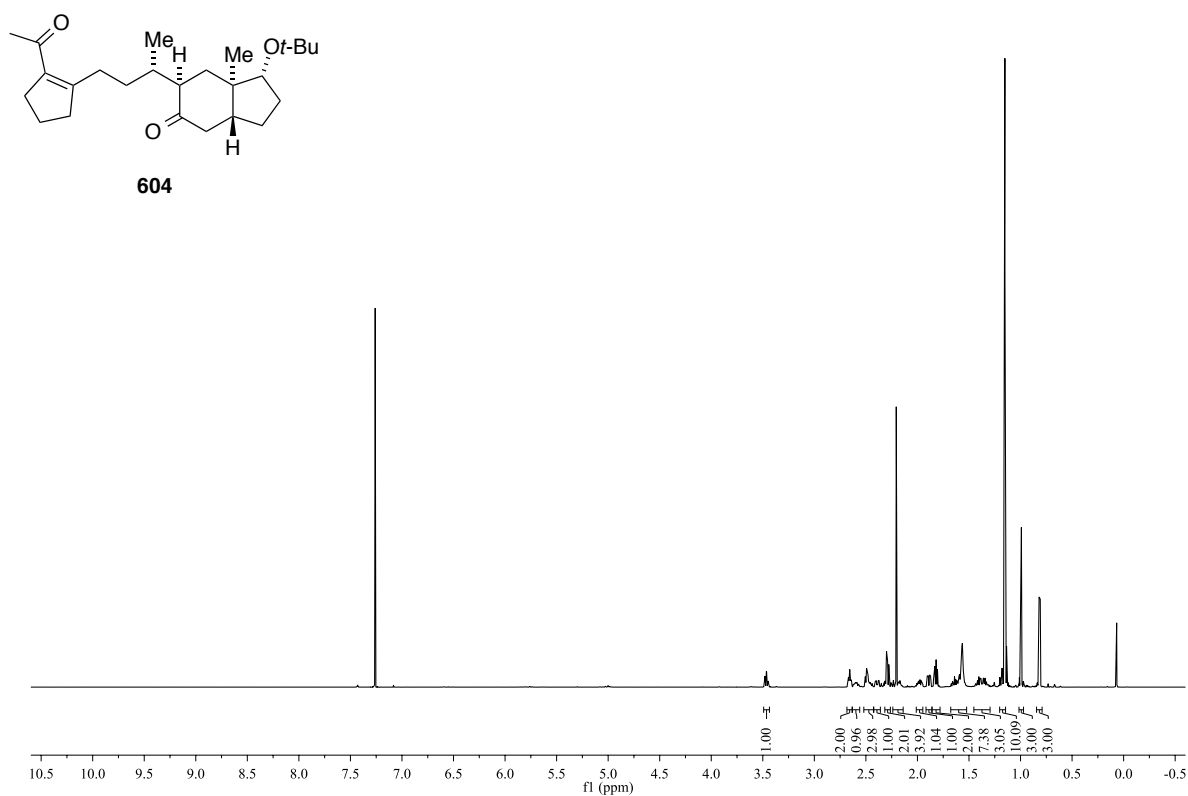
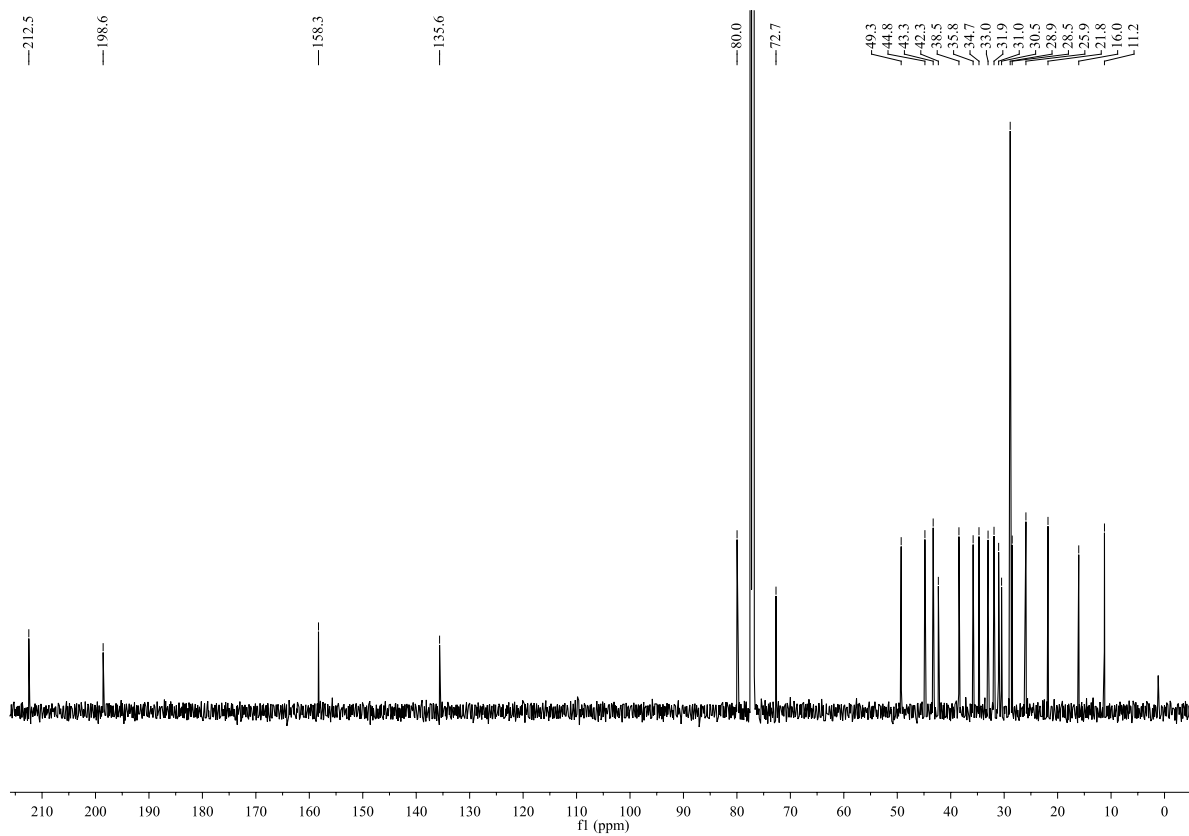
^1H NMR (CDCl_3 , 400 MHz): ^{13}C NMR (CDCl_3 , 100 MHz):

^1H NMR (CDCl_3 , 600 MHz):

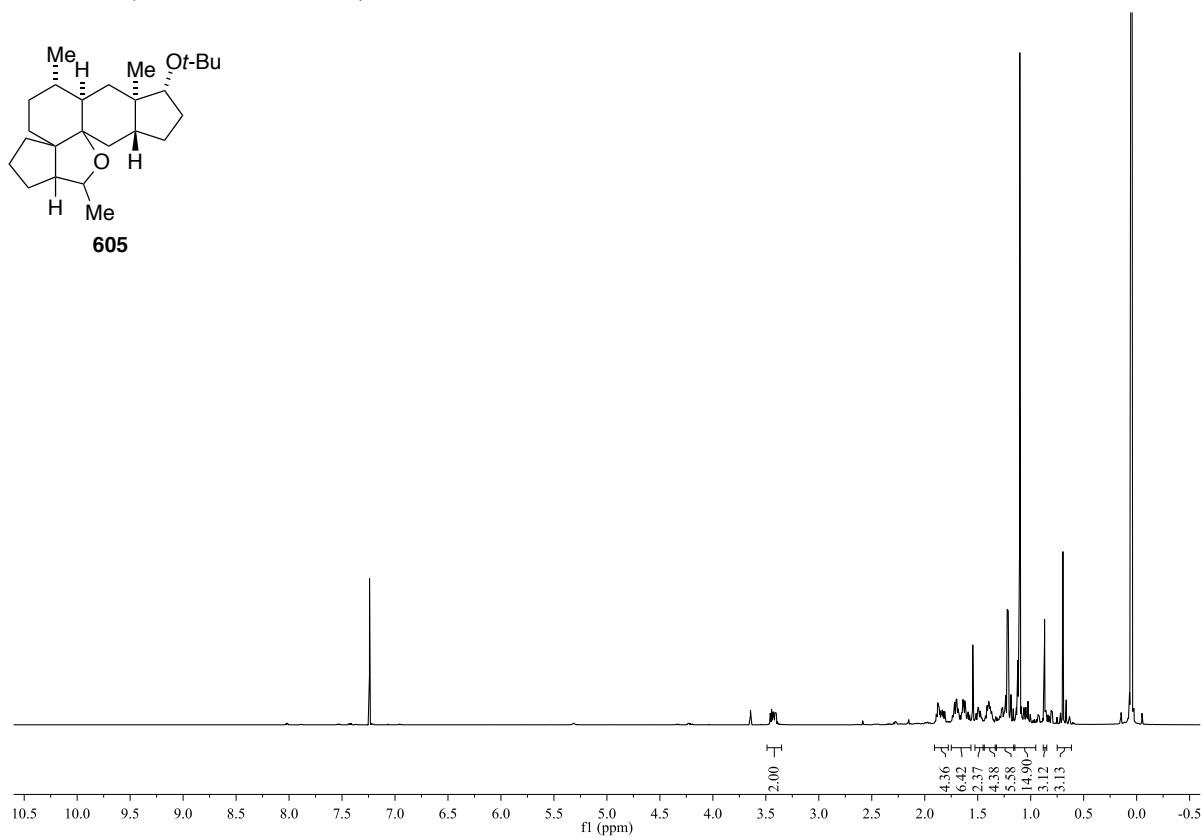
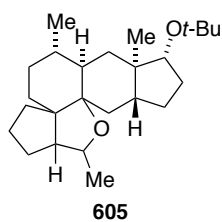


^{13}C NMR (CDCl_3 , 150 MHz):

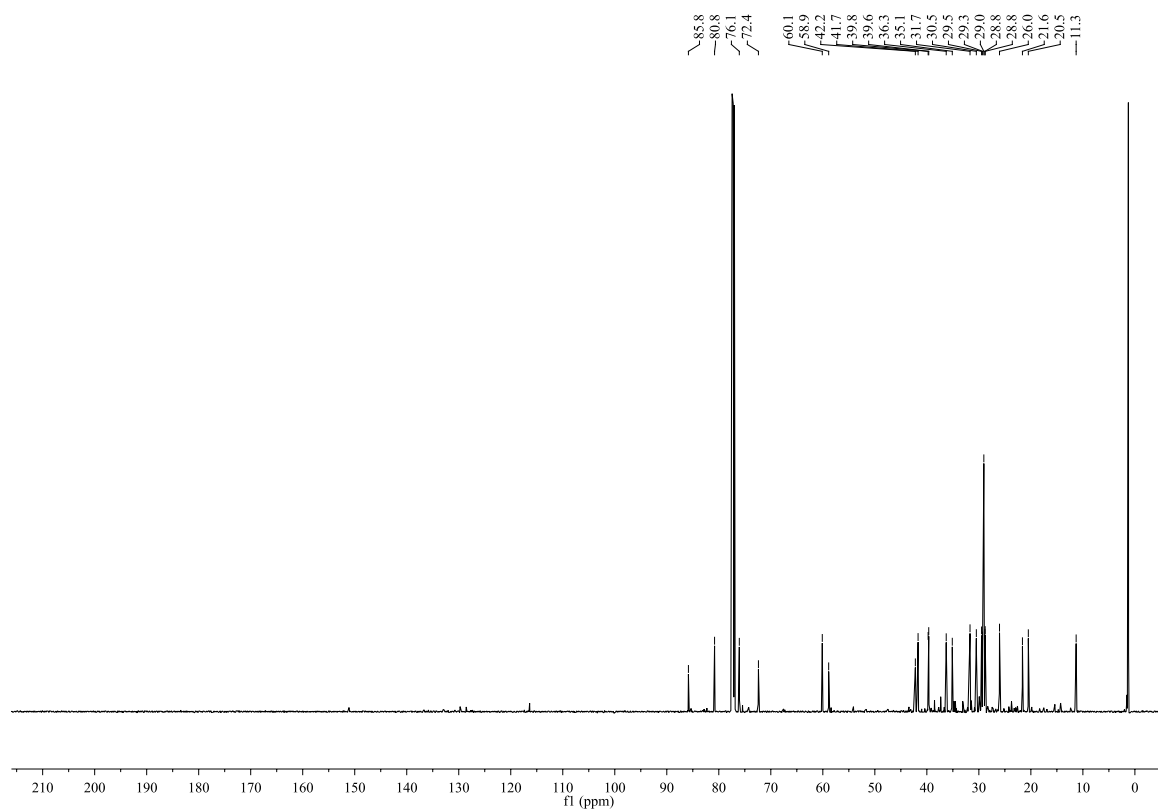


^1H NMR (CDCl_3 , 600 MHz): ^{13}C NMR (CDCl_3 , 150 MHz):

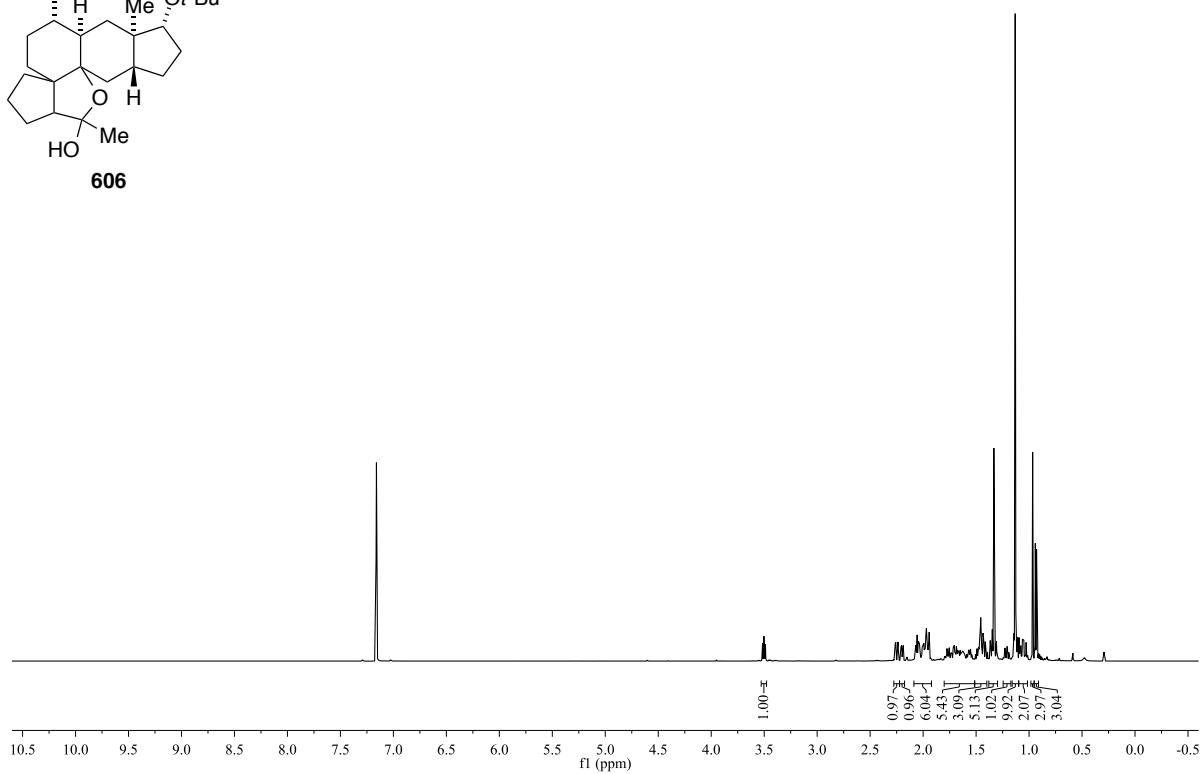
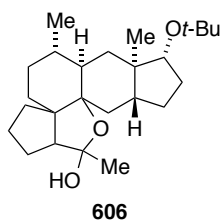
^1H NMR (CDCl_3 , 600 MHz):



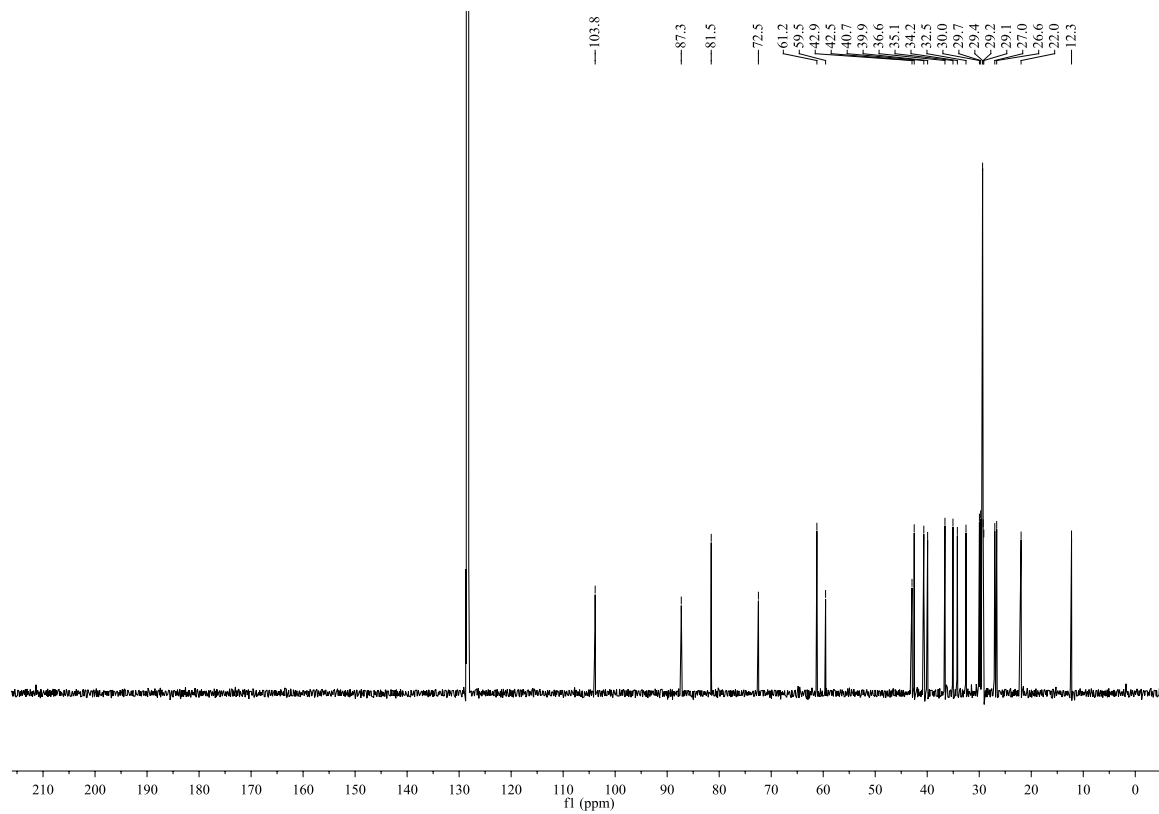
^{13}C NMR (CDCl_3 , 150 MHz):



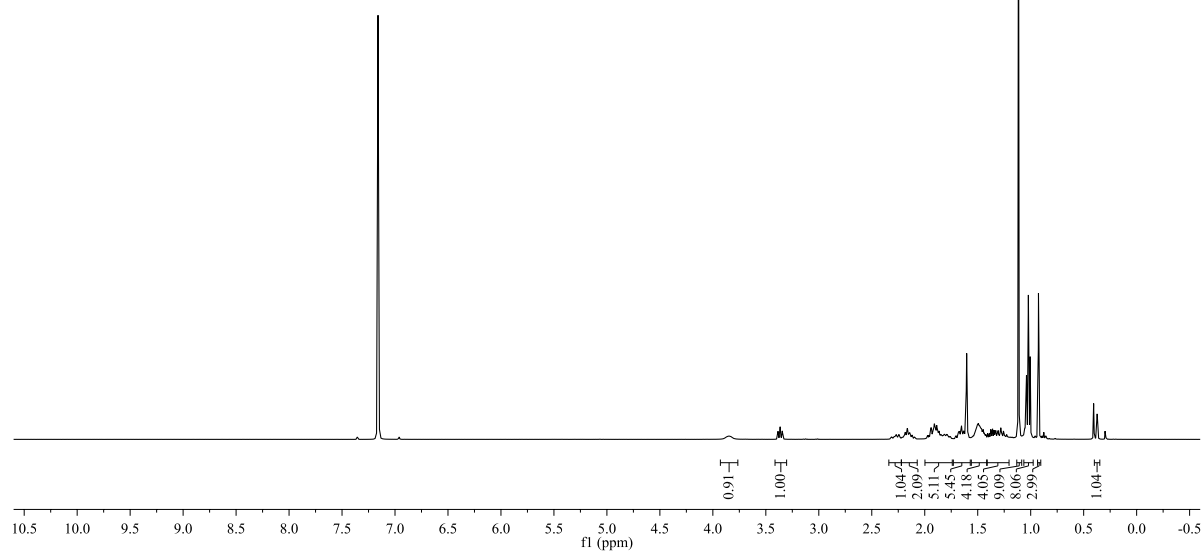
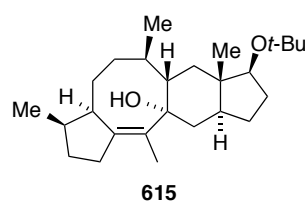
^1H NMR (C_6D_6 , 600 MHz):



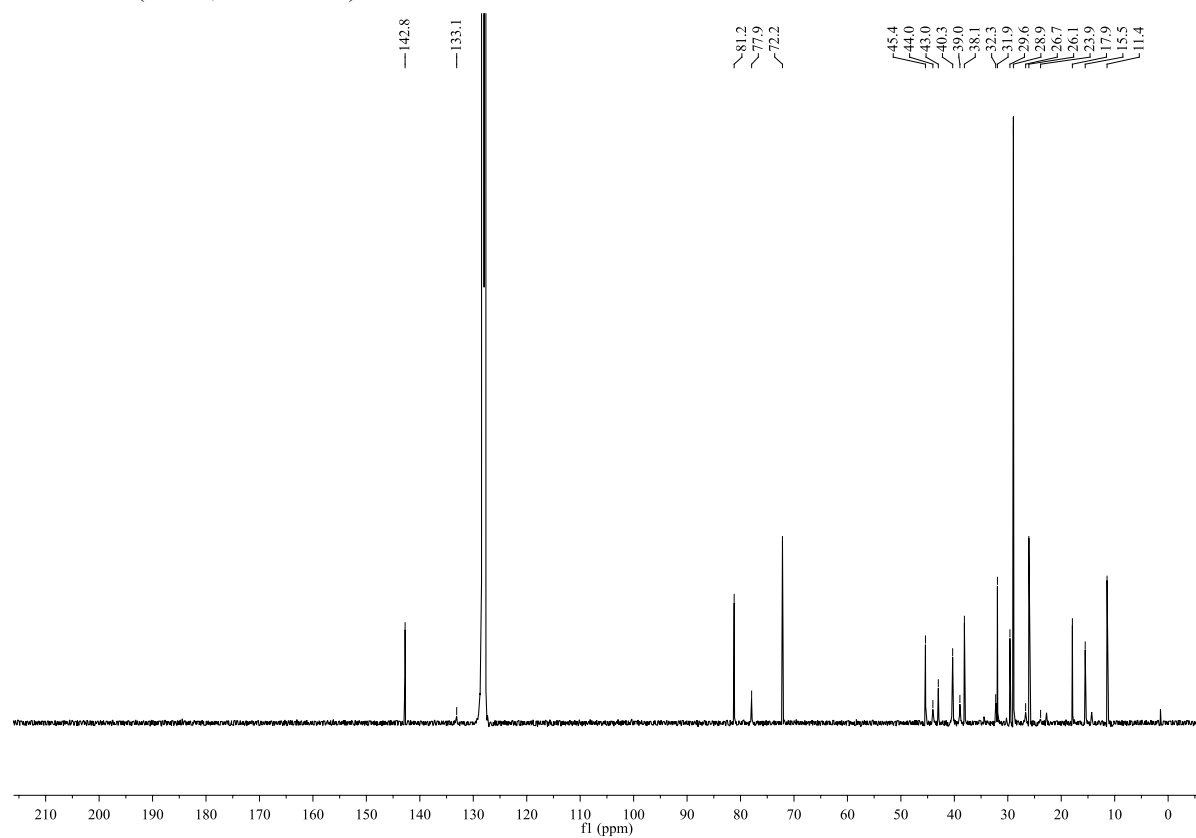
^{13}C NMR (C_6D_6 , 150 MHz):



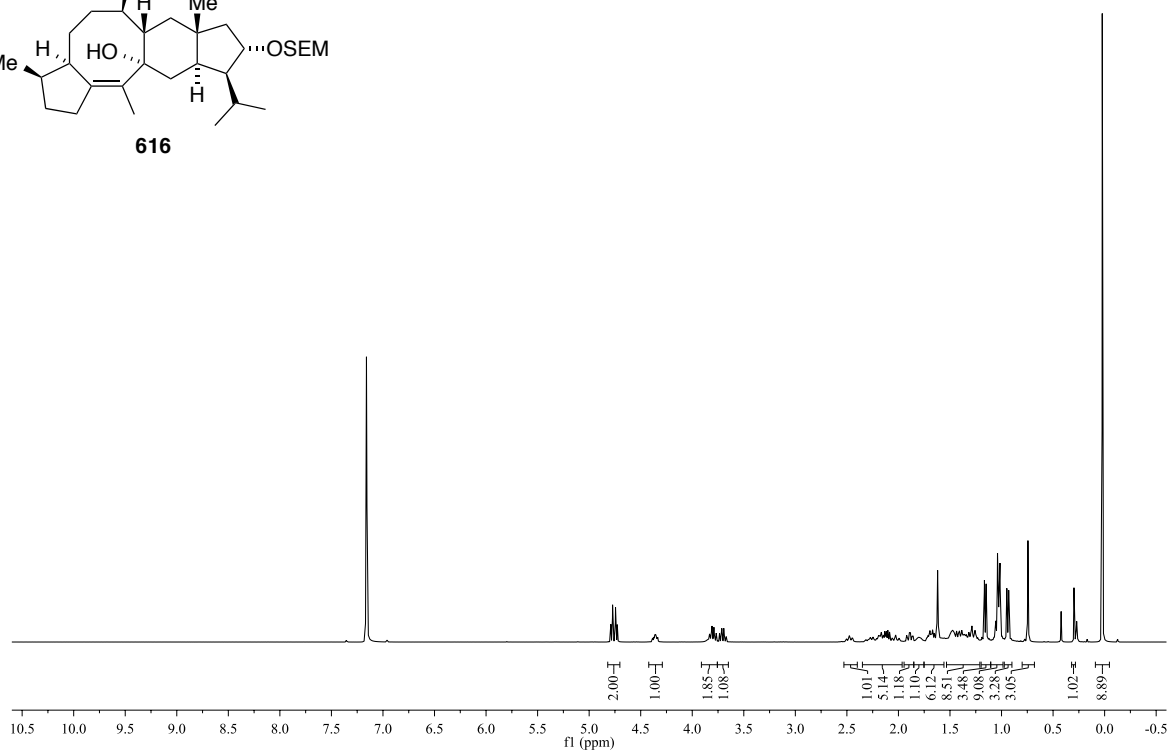
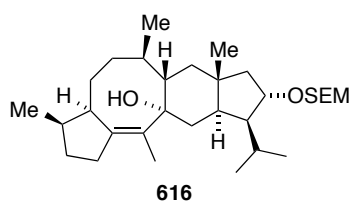
^1H NMR (C_6D_6 , 400 MHz):



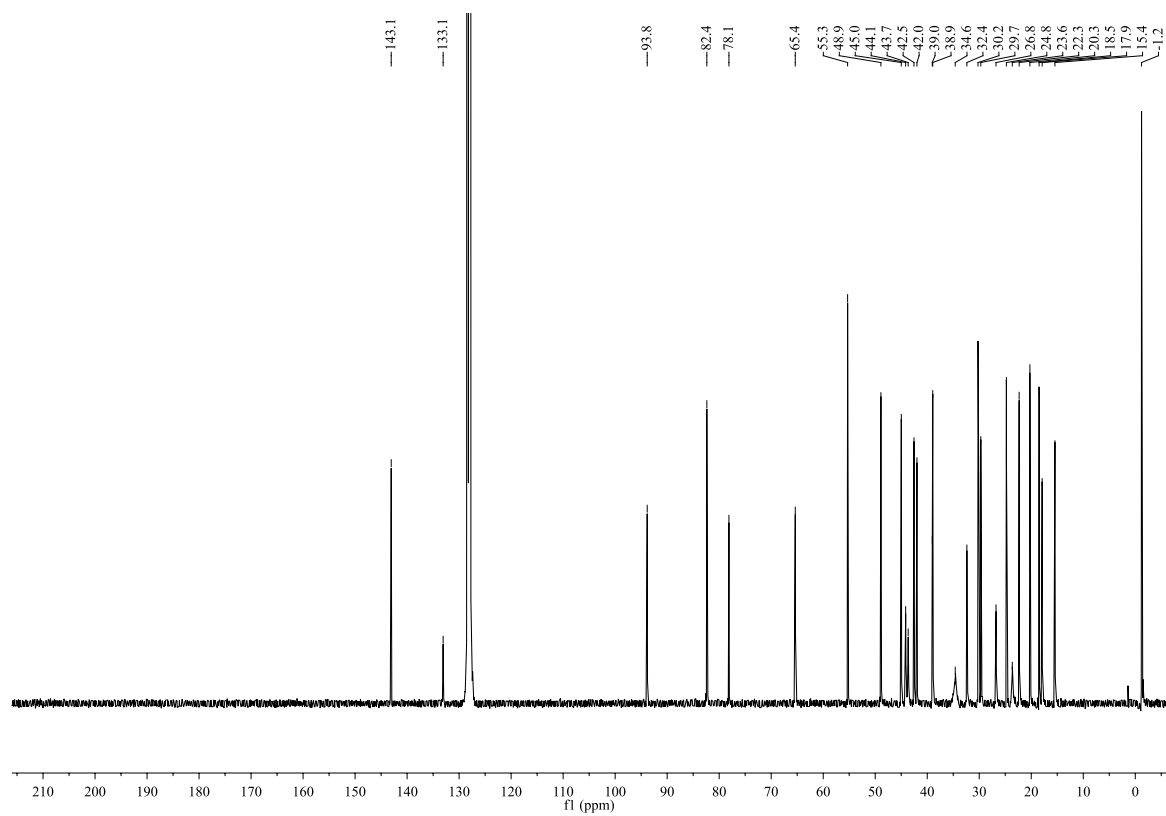
^{13}C NMR (C_6D_6 , 100 MHz):



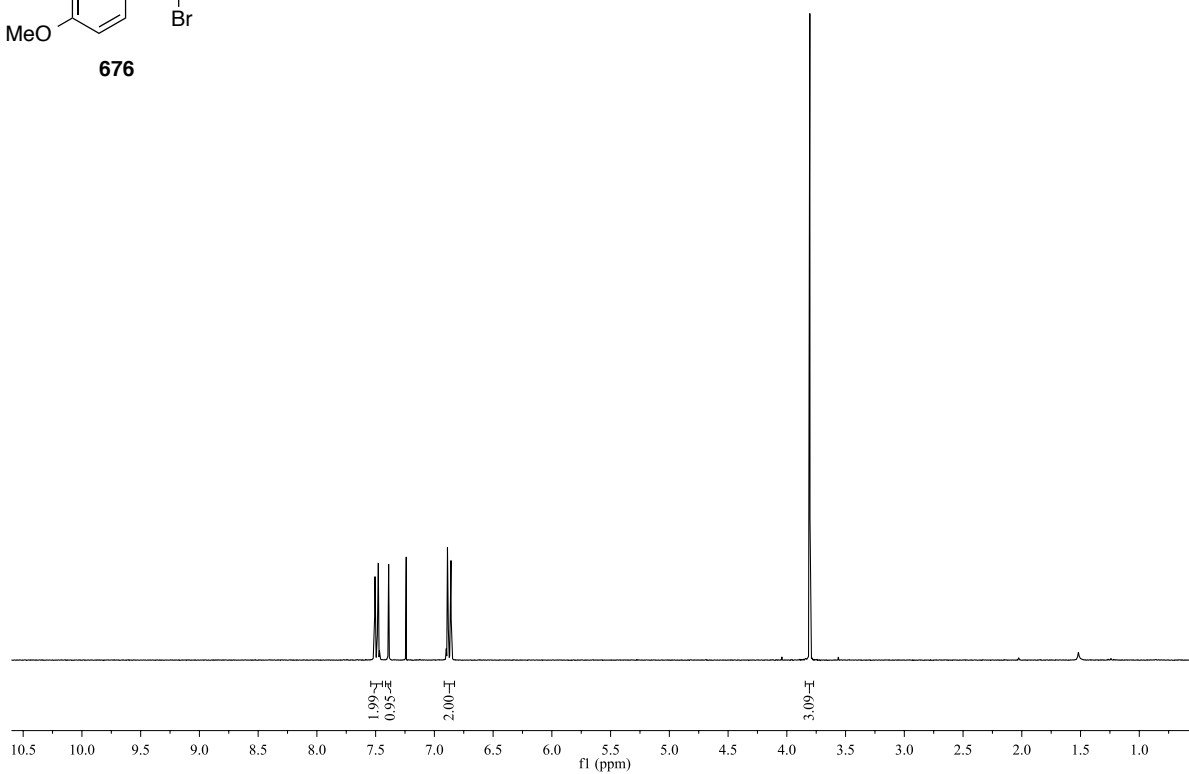
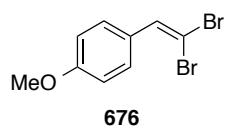
^1H NMR (C_6D_6 , 400 MHz):



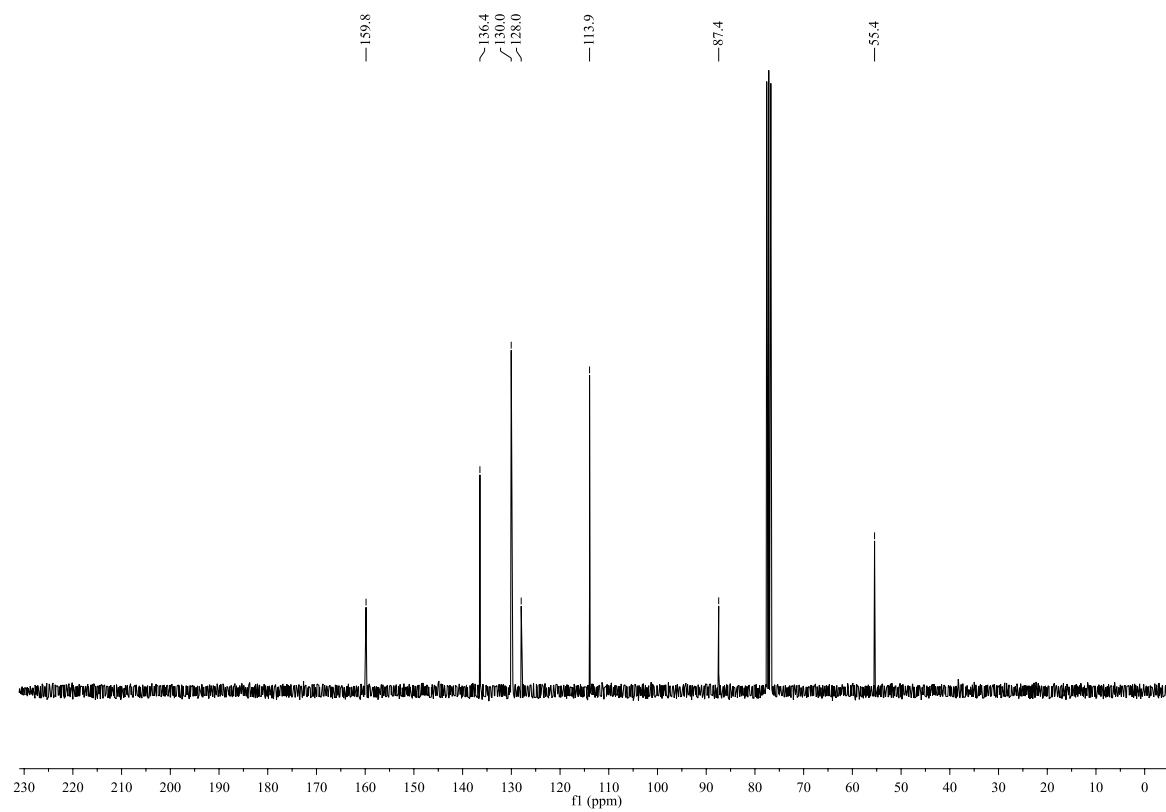
^{13}C NMR (C_6D_6 , 100 MHz, 50 °C):



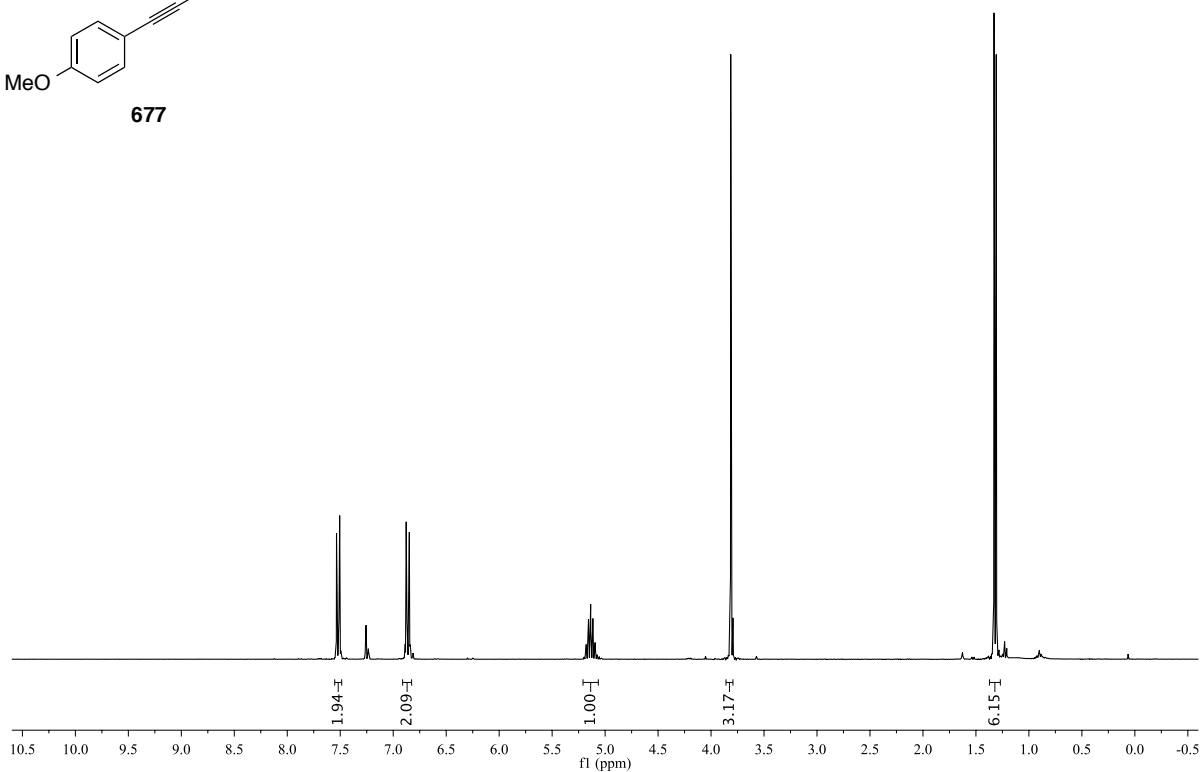
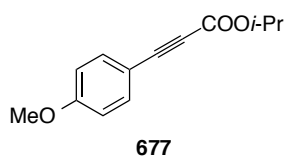
^1H NMR (CDCl_3 , 300 MHz):



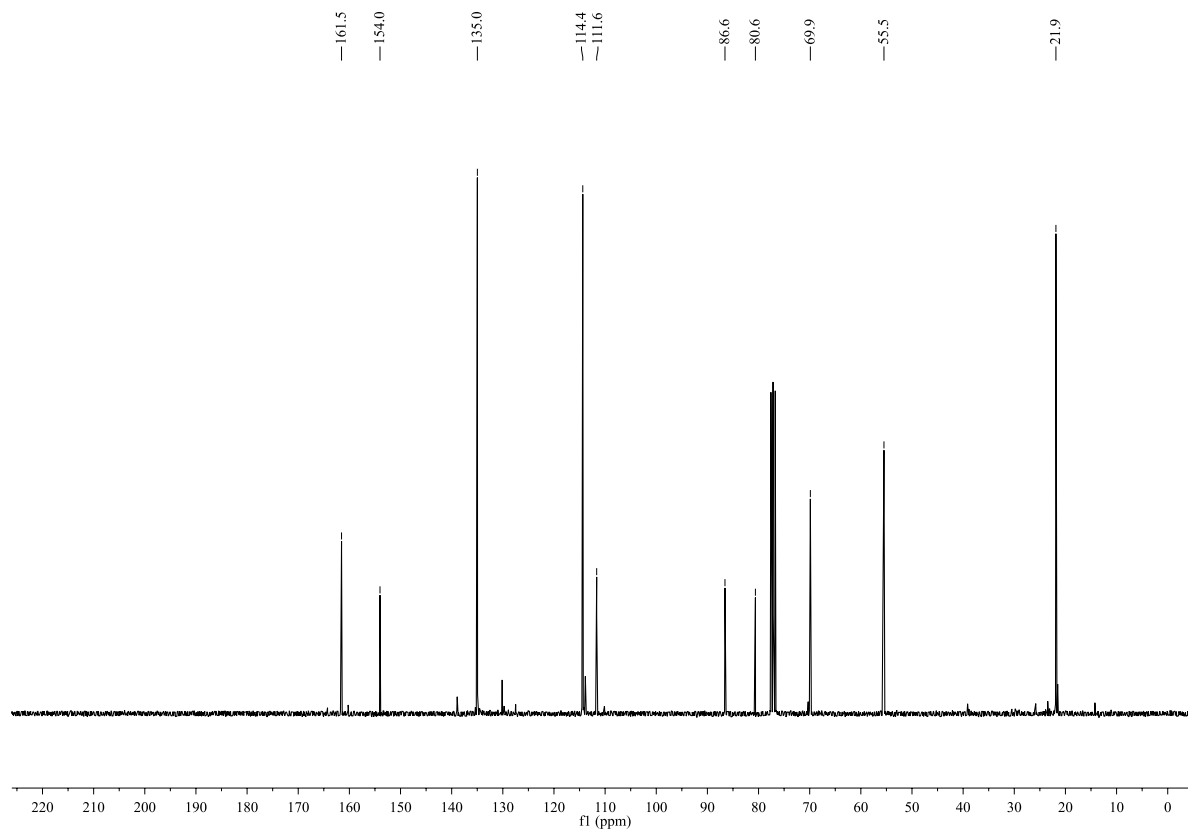
^{13}C NMR (CDCl_3 , 75 MHz):



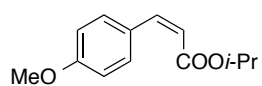
^1H NMR (CDCl_3 , 300 MHz):



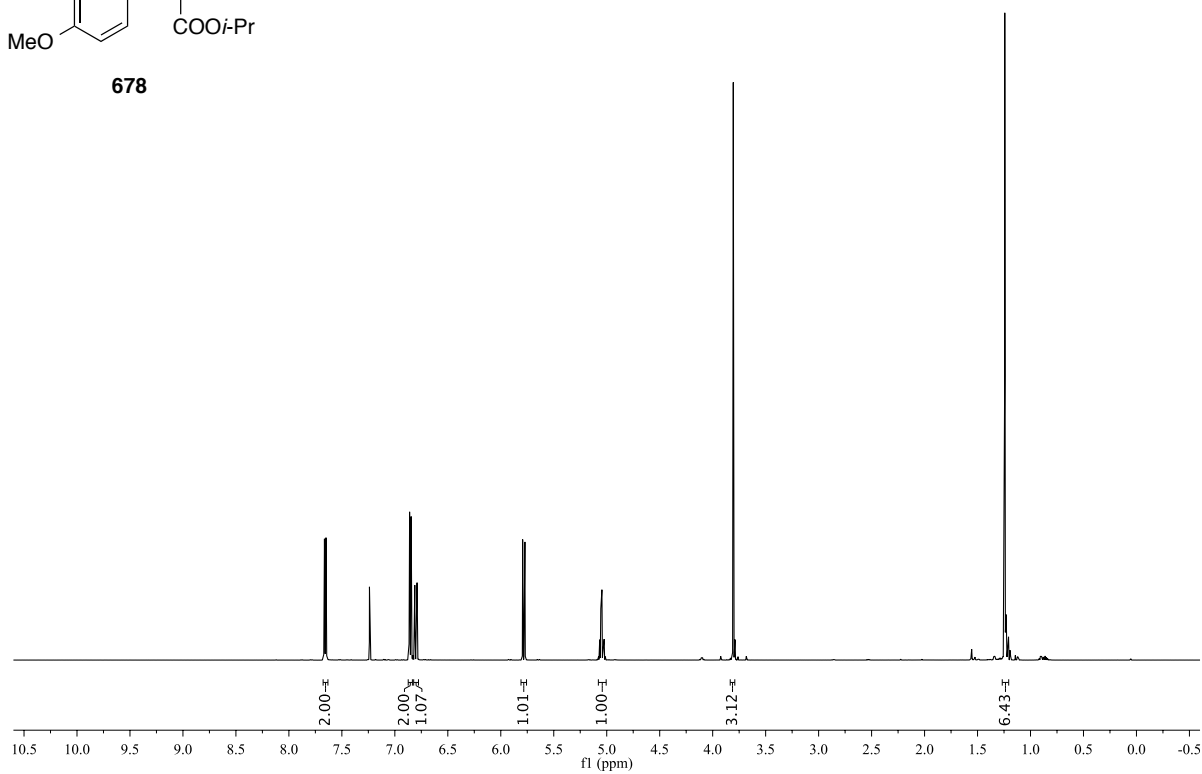
^{13}C NMR (CDCl_3 , 75 MHz):



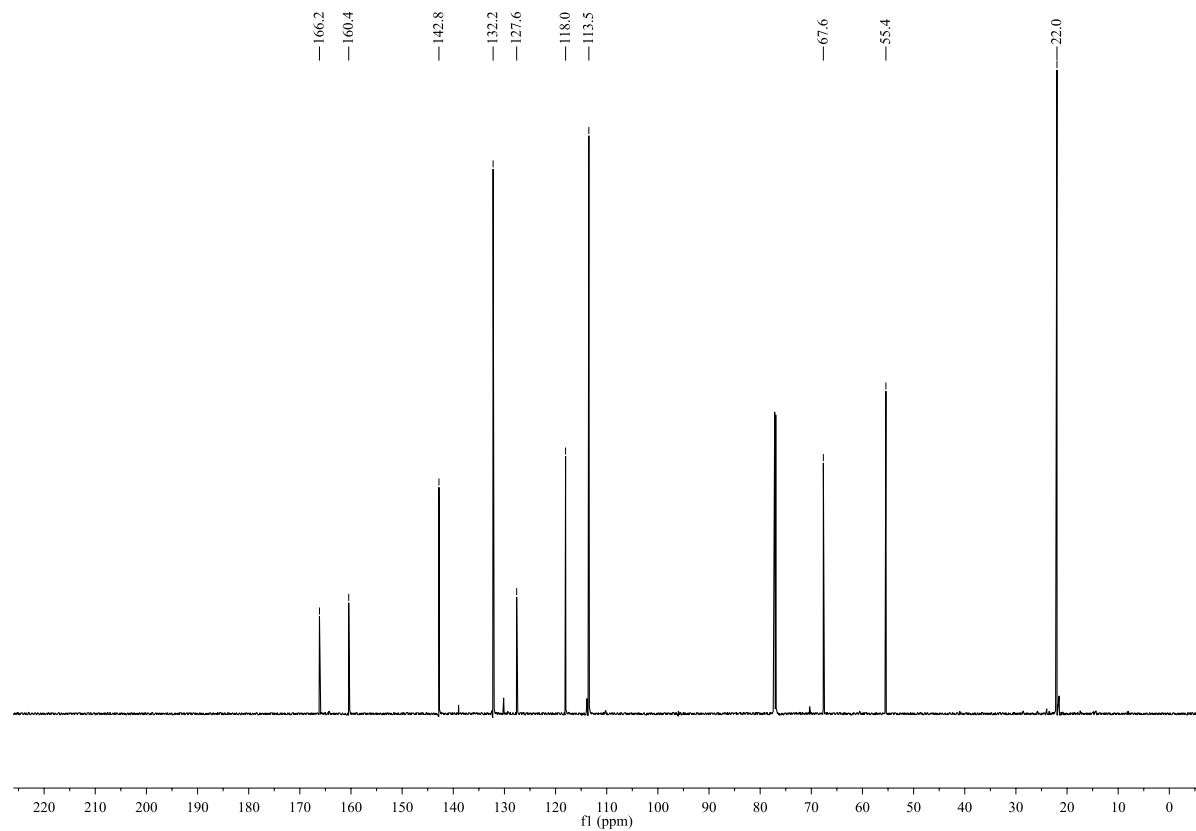
^1H NMR (CDCl_3 , 600 MHz):



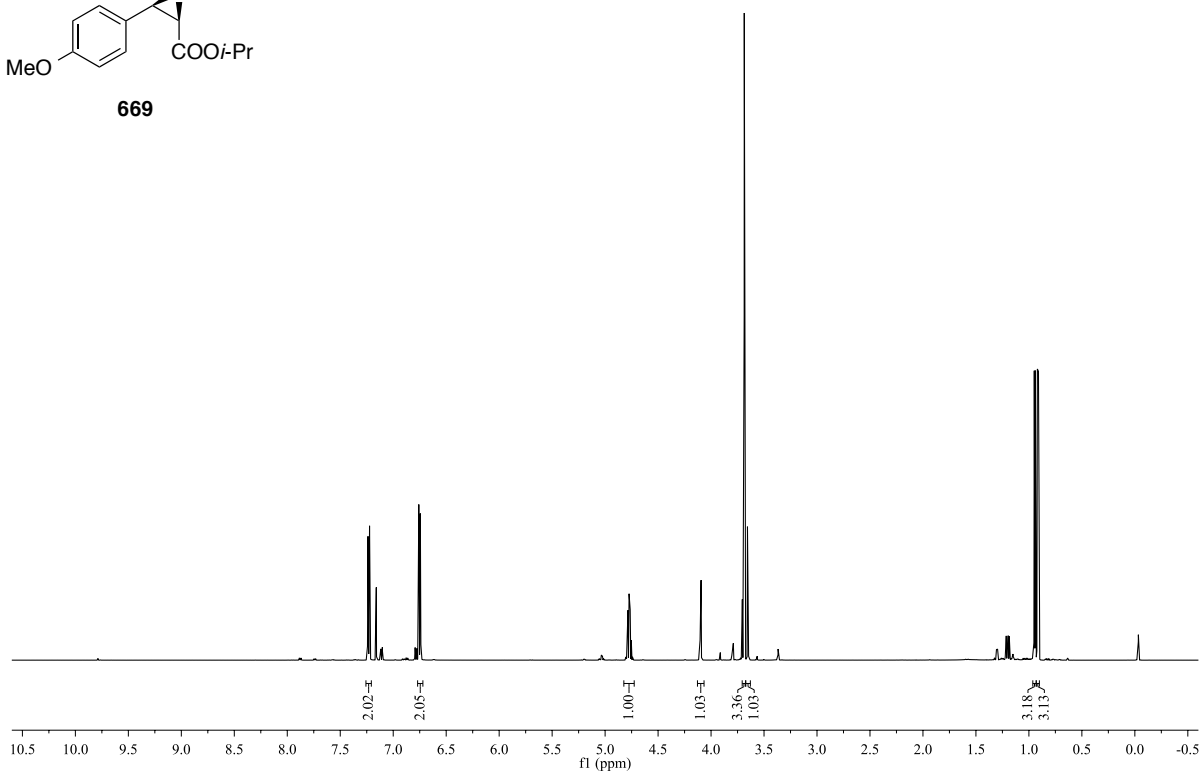
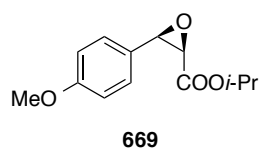
678



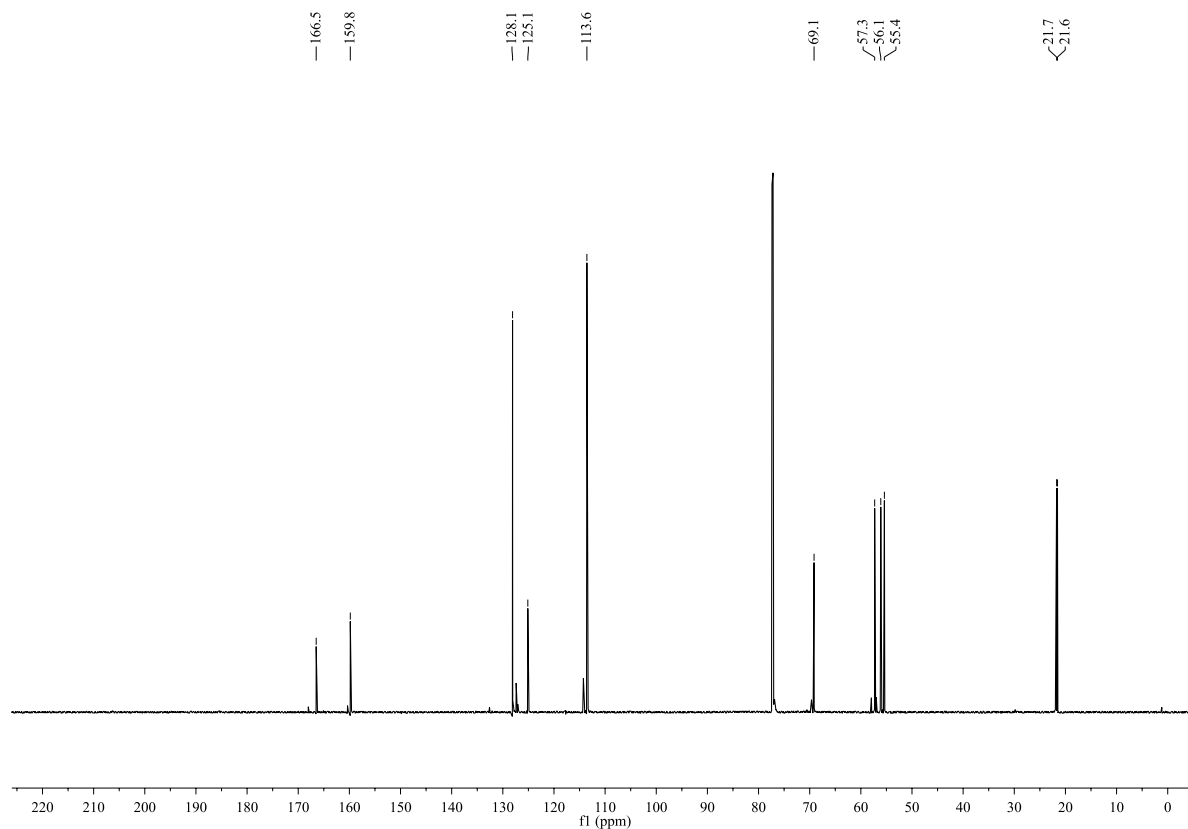
^{13}C NMR (CDCl_3 , 150 MHz):



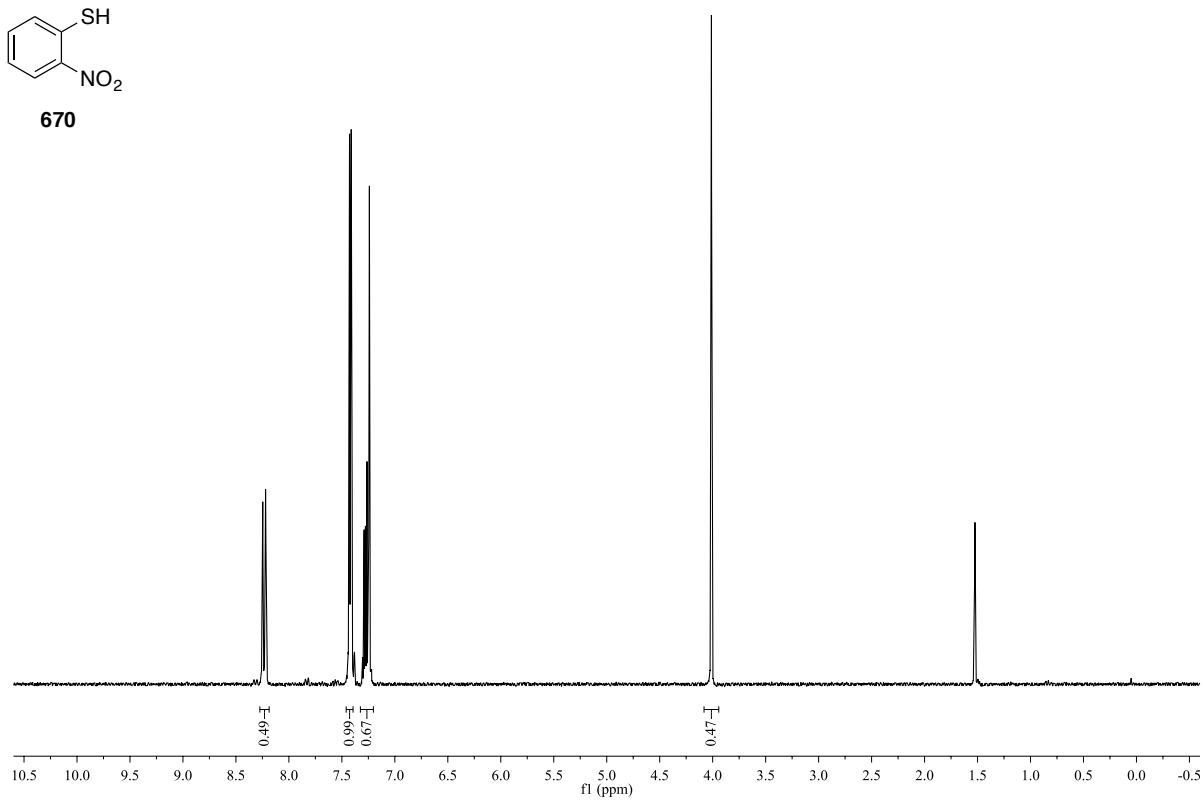
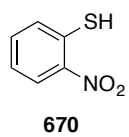
^1H NMR (CDCl_3 , 600 MHz):



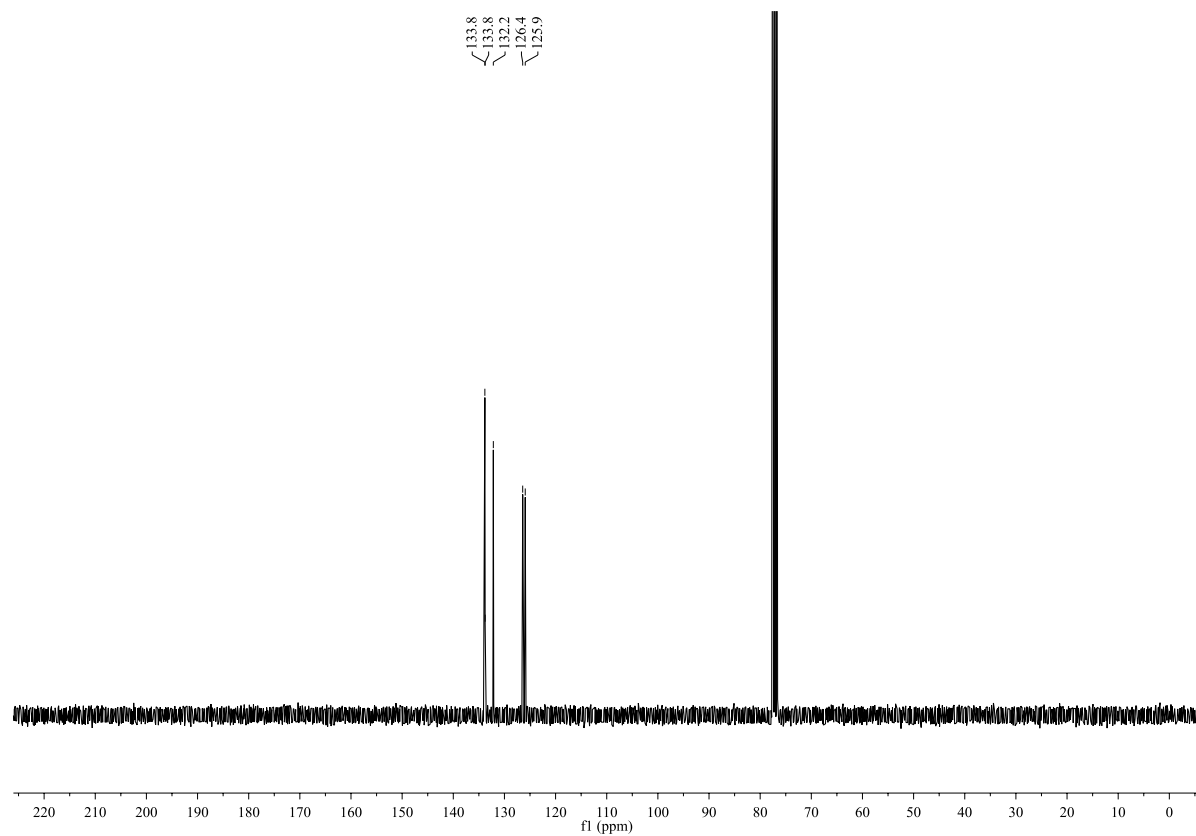
^{13}C NMR (CDCl_3 , 150 MHz):

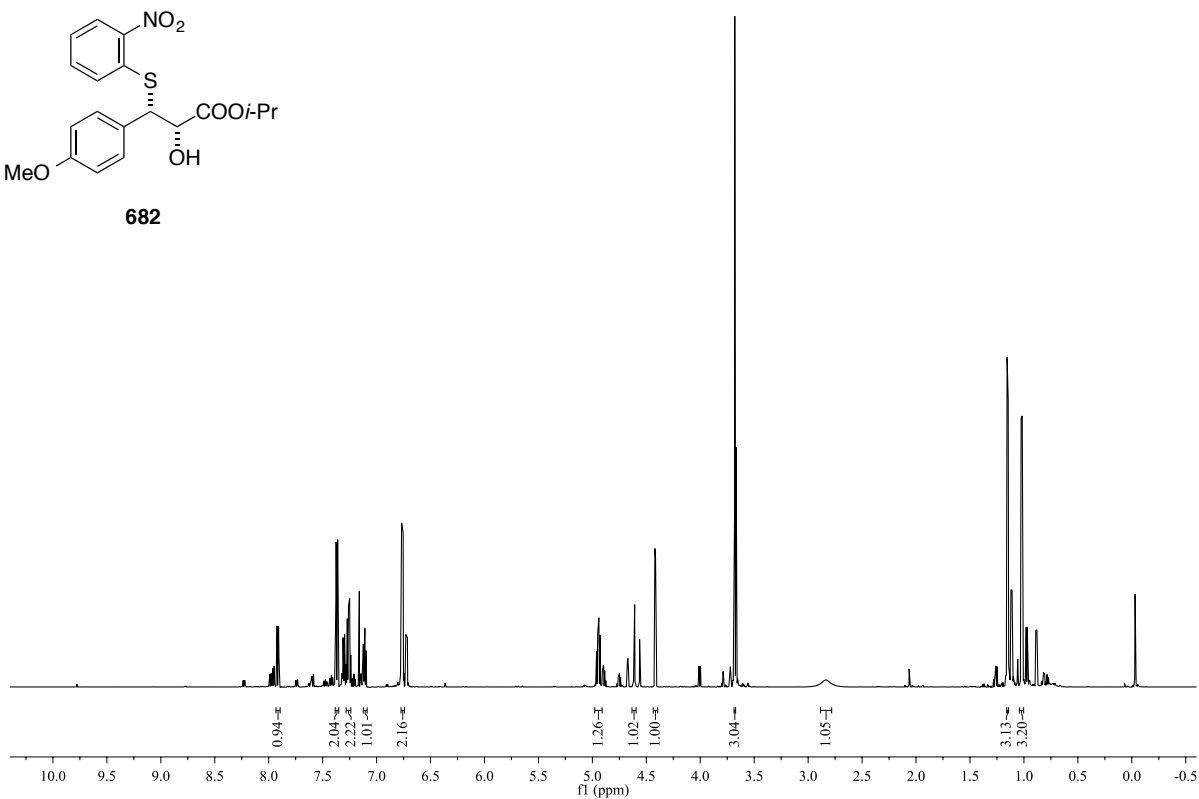
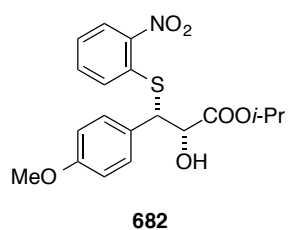
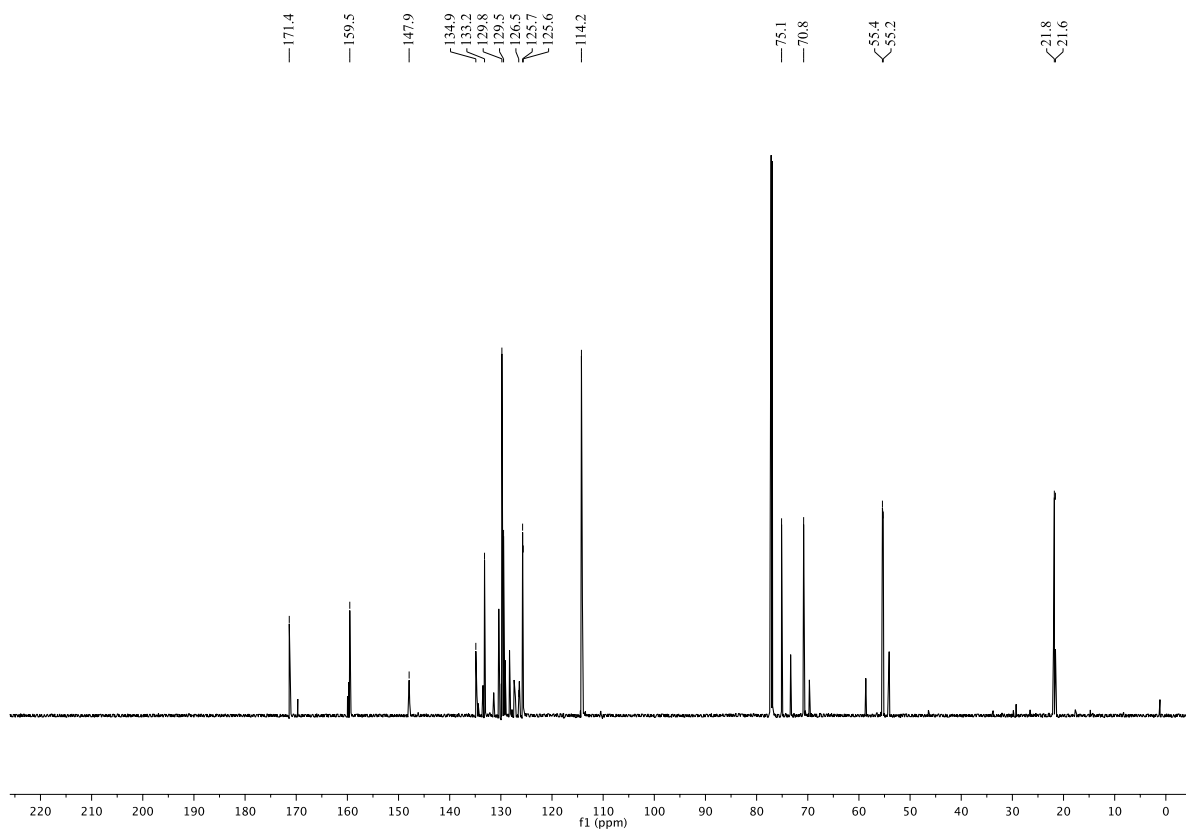


^1H NMR (CDCl_3 , 300 MHz):

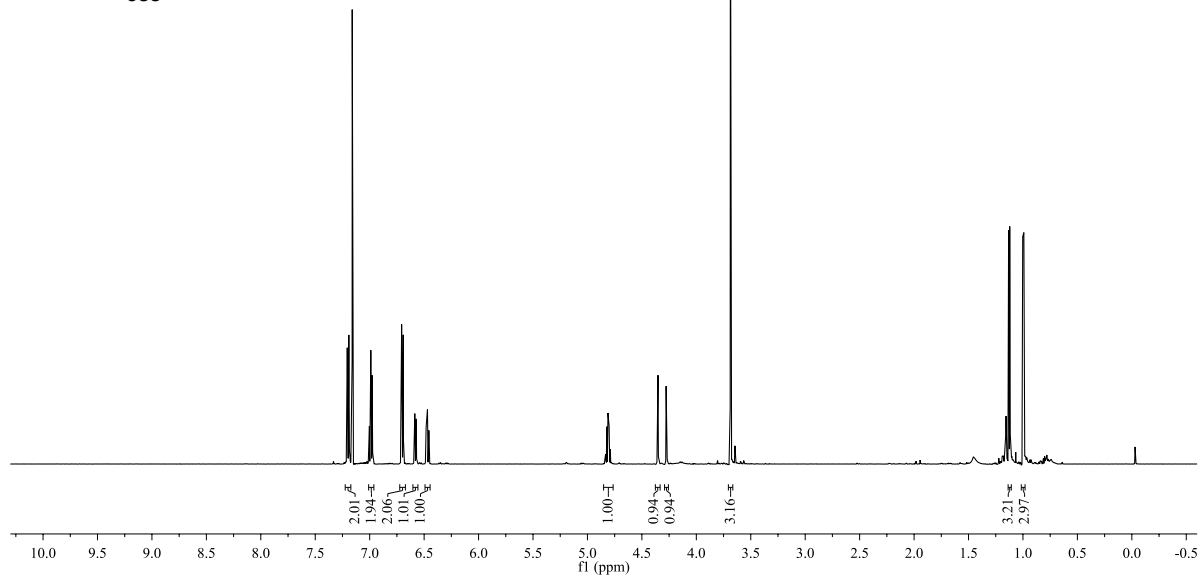
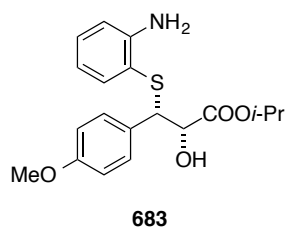


^{13}C NMR (CDCl_3 , 75 MHz):

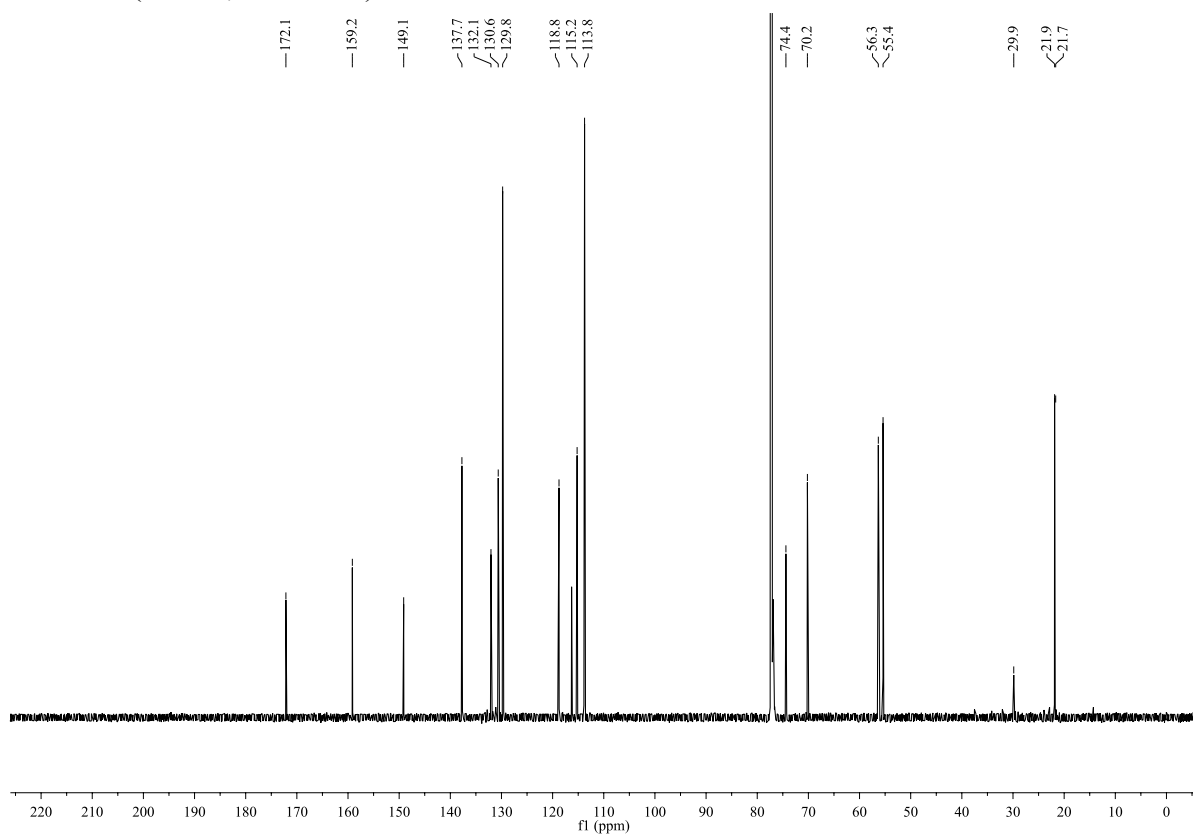


^1H NMR (CDCl_3 , 600 MHz): ^{13}C NMR (CDCl_3 , 150 MHz):

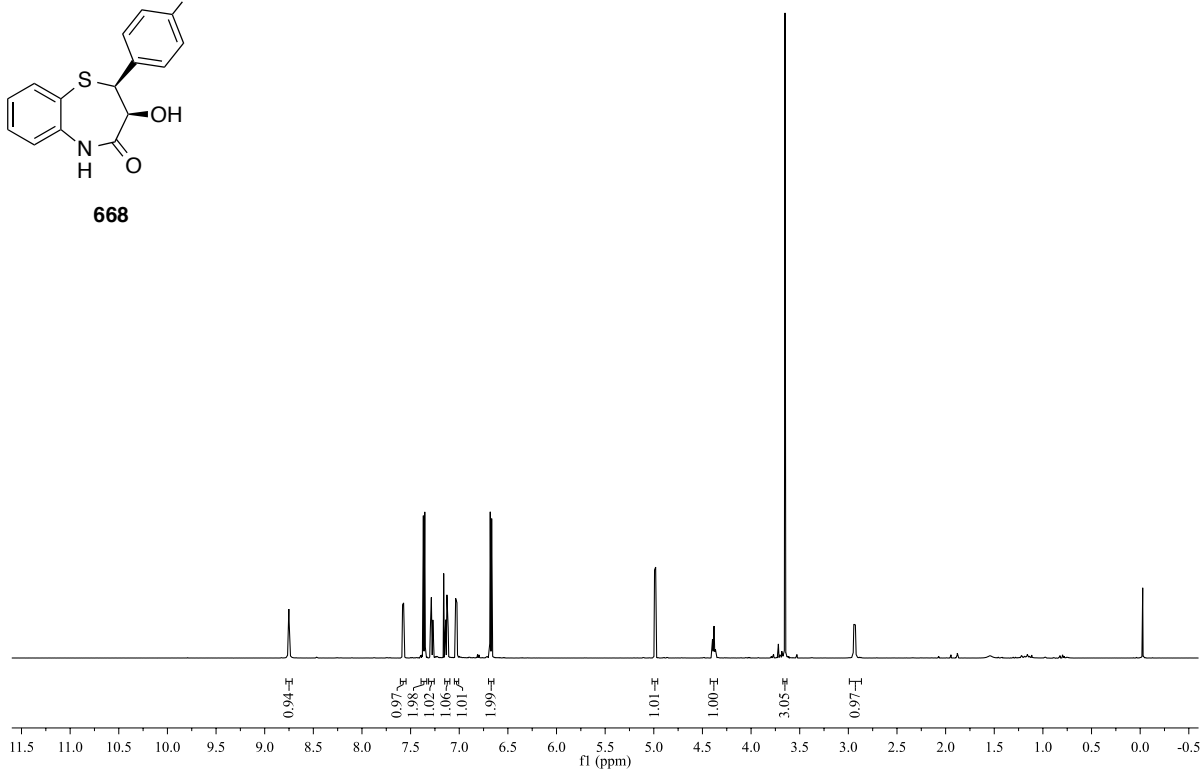
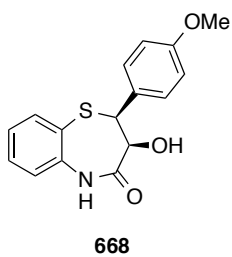
^1H NMR (CDCl_3 , 600 MHz):



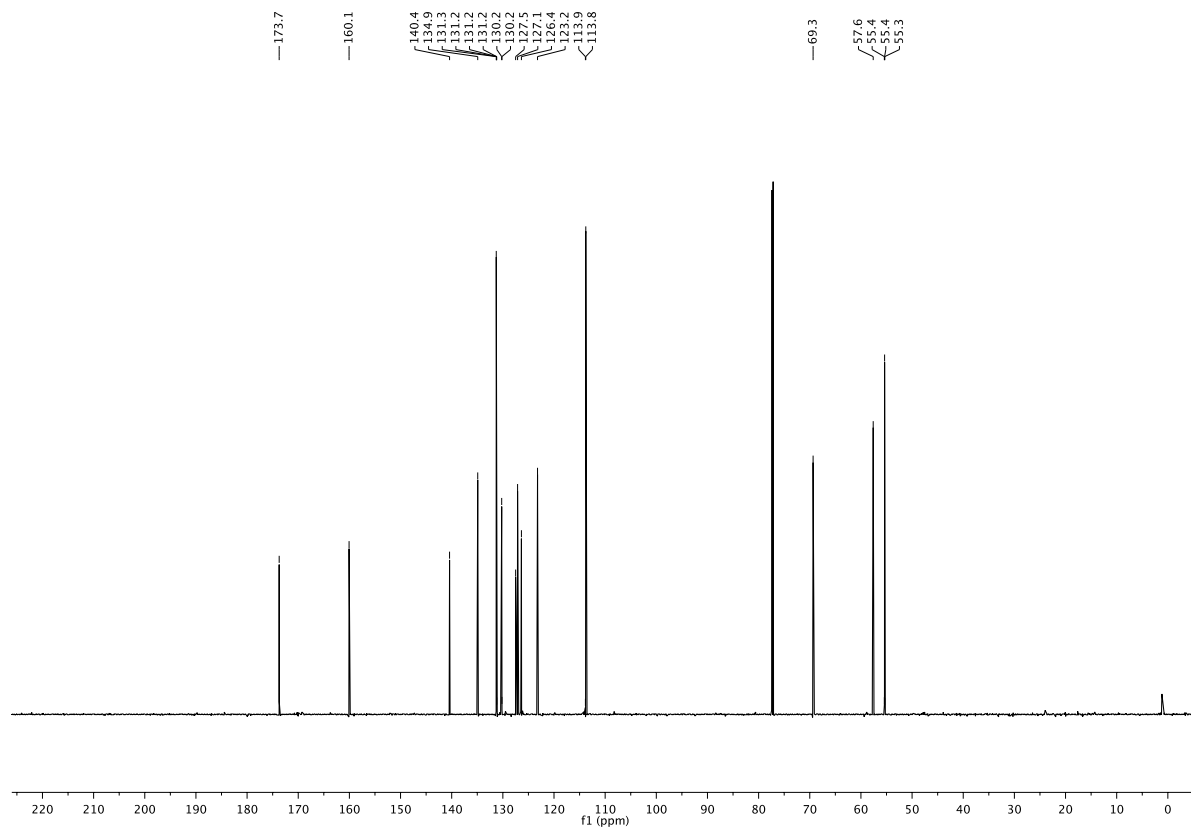
^{13}C NMR (CDCl_3 , 150 MHz):



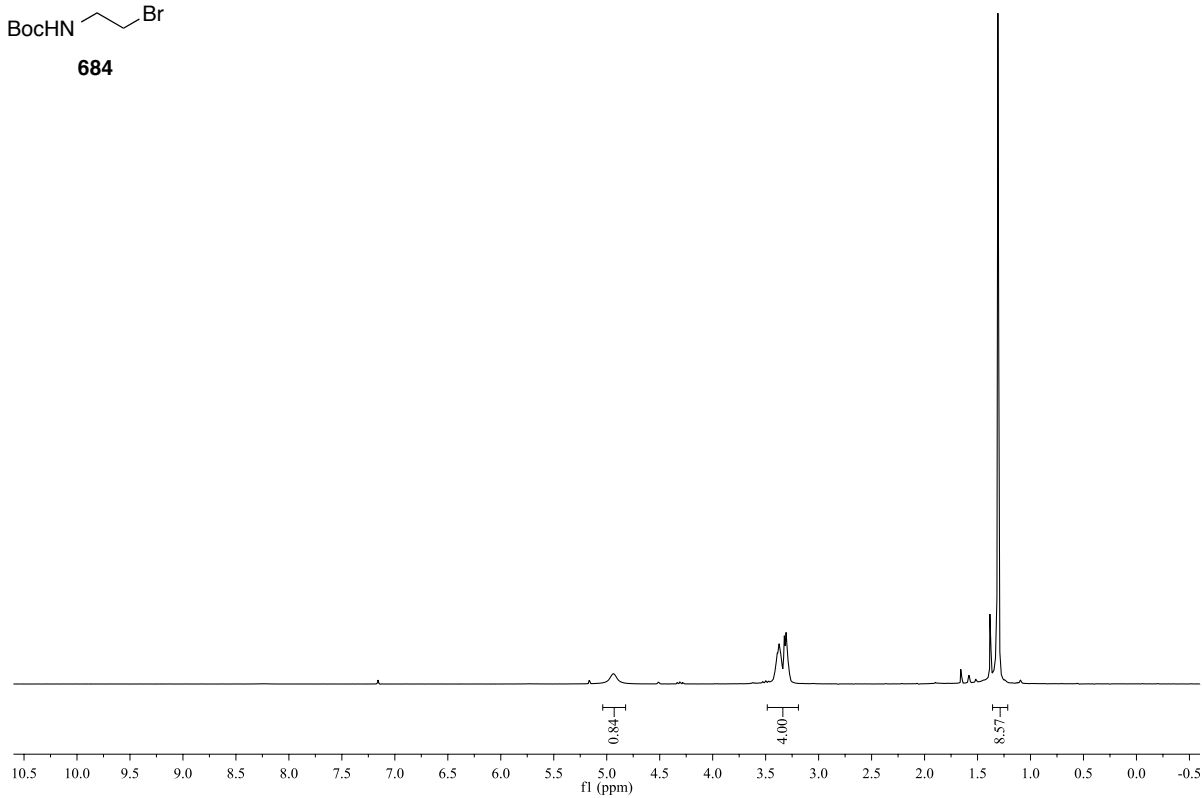
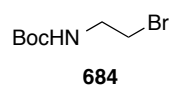
^1H NMR (CDCl_3 , 600 MHz):



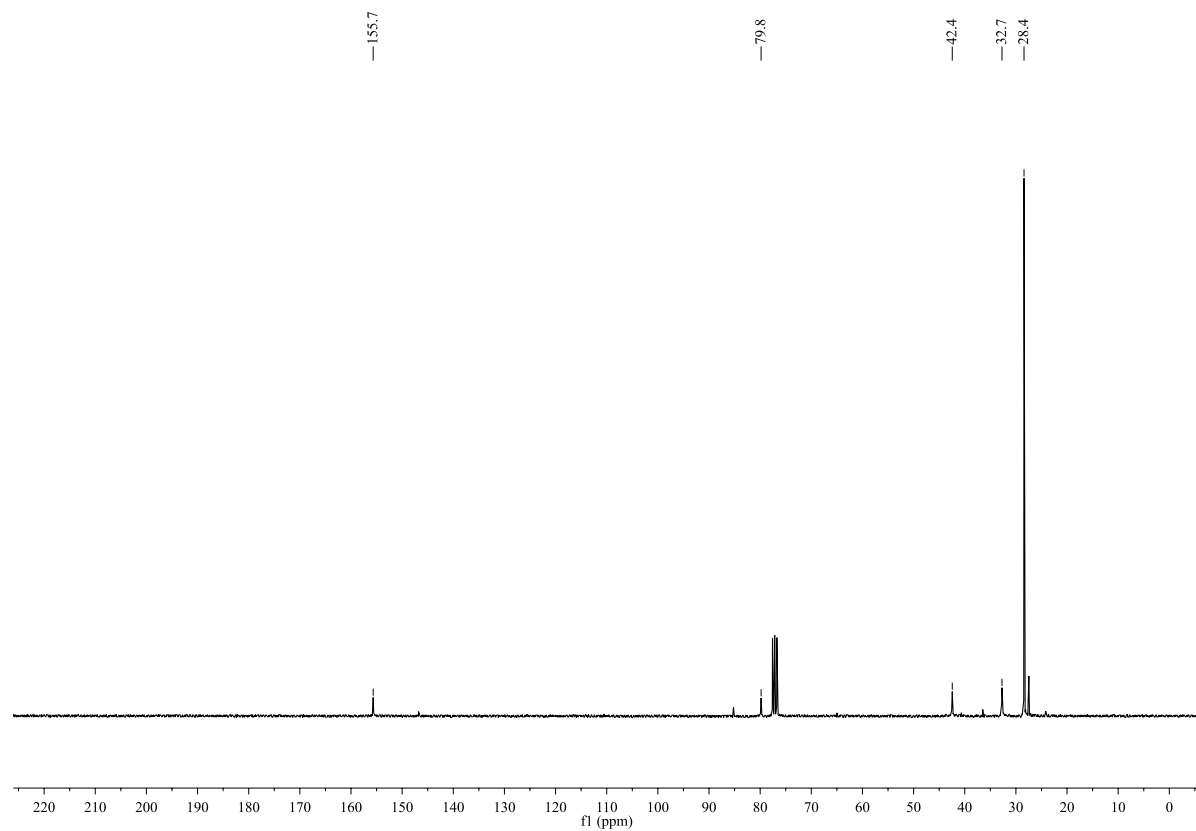
^{13}C NMR (CDCl_3 , 150 MHz):



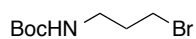
^1H NMR (CDCl_3 , 300 MHz):



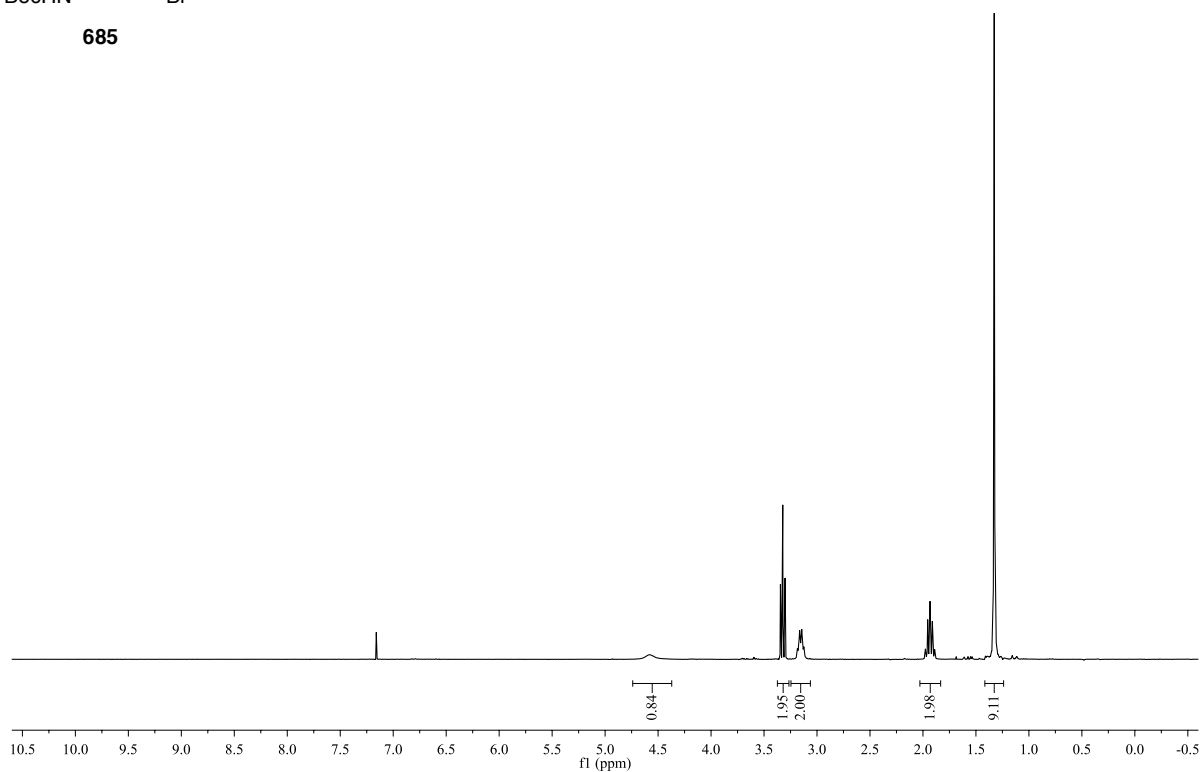
^{13}C NMR (CDCl_3 , 75 MHz):



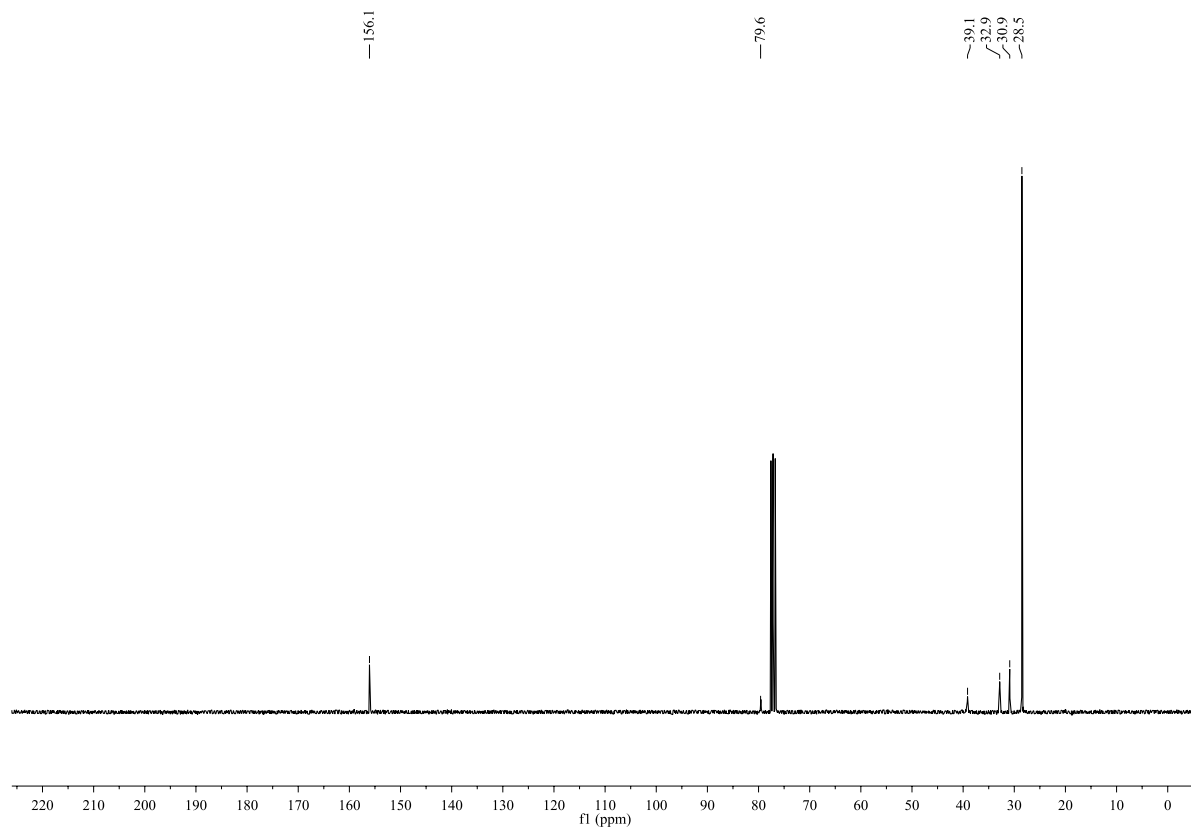
^1H NMR (CDCl_3 , 300 MHz):



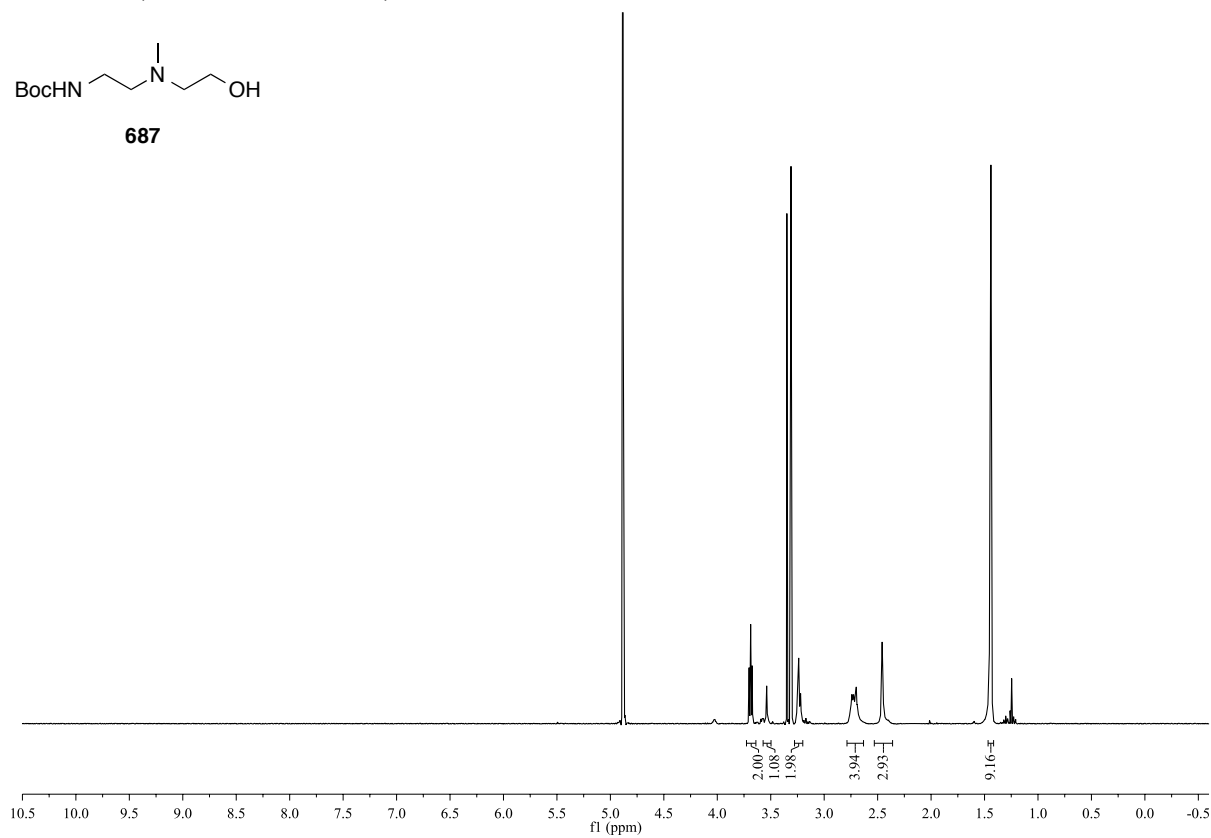
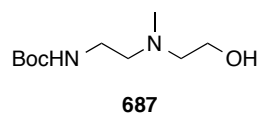
685



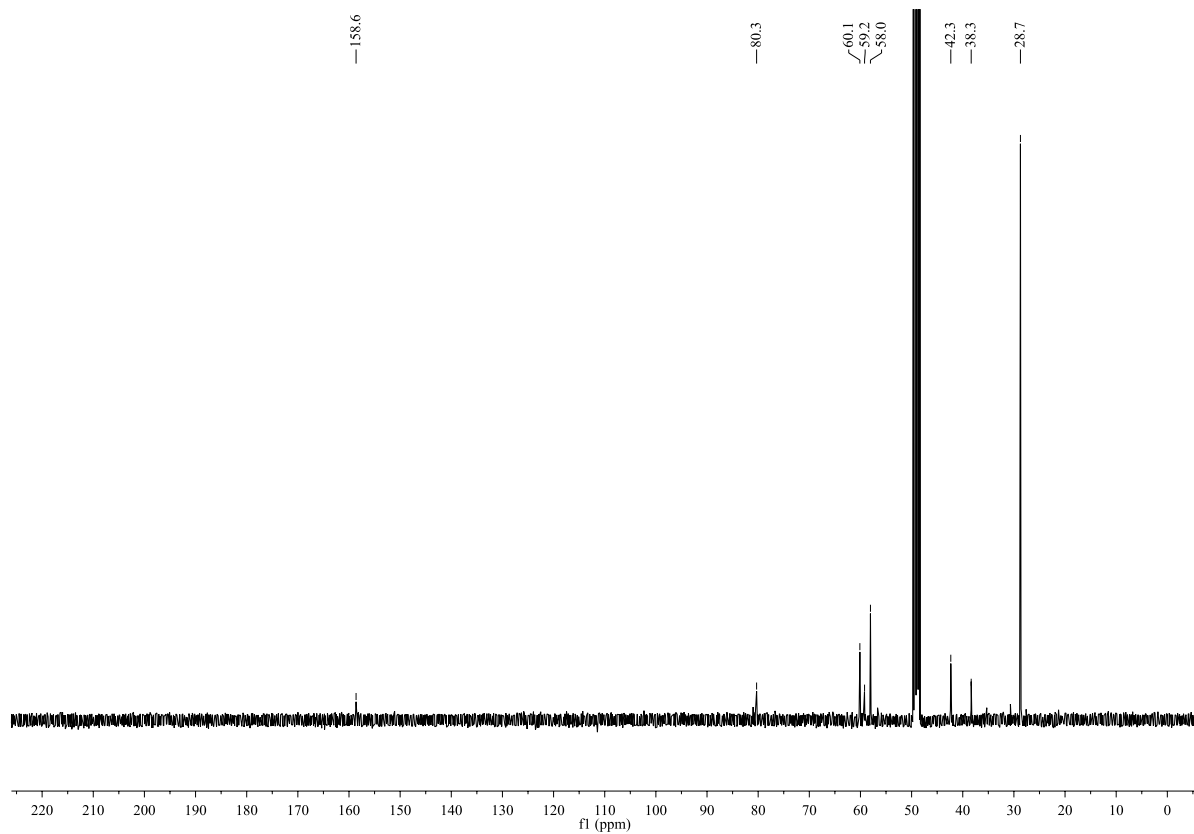
^{13}C NMR (CDCl_3 , 75 MHz):



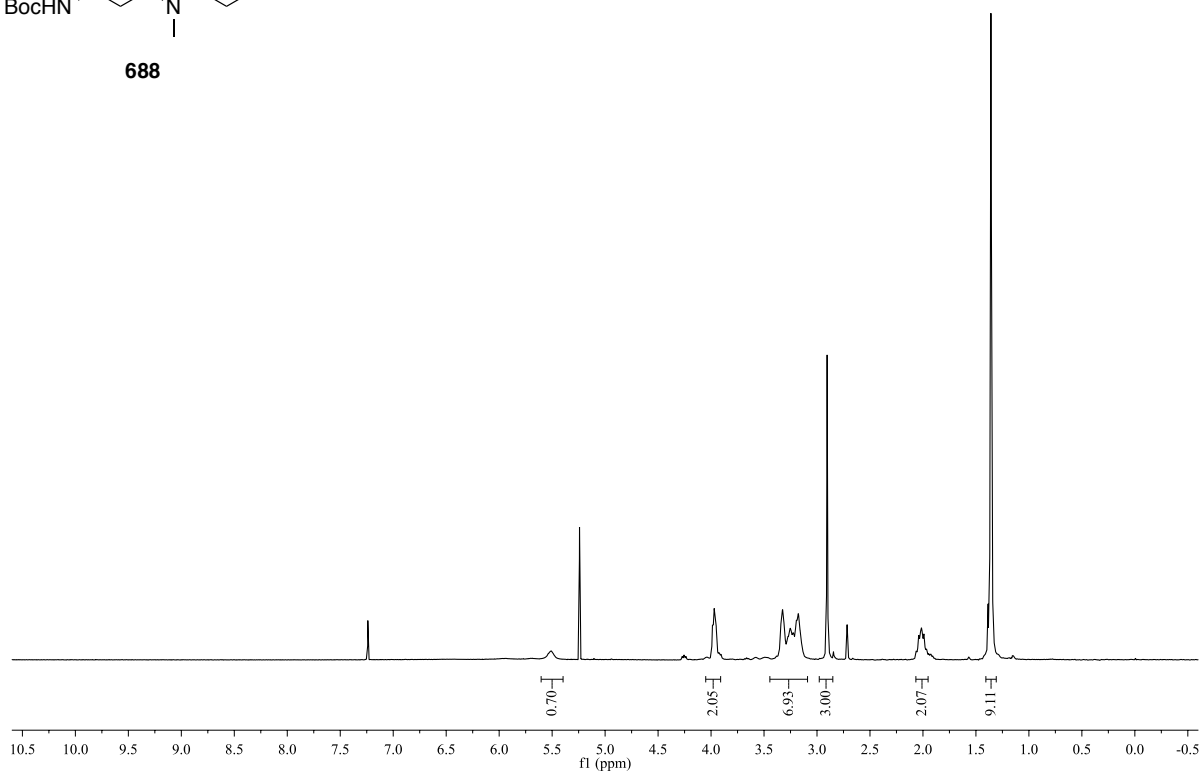
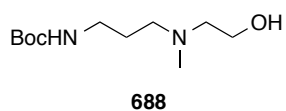
^1H NMR (CD_3OD , 400 MHz):



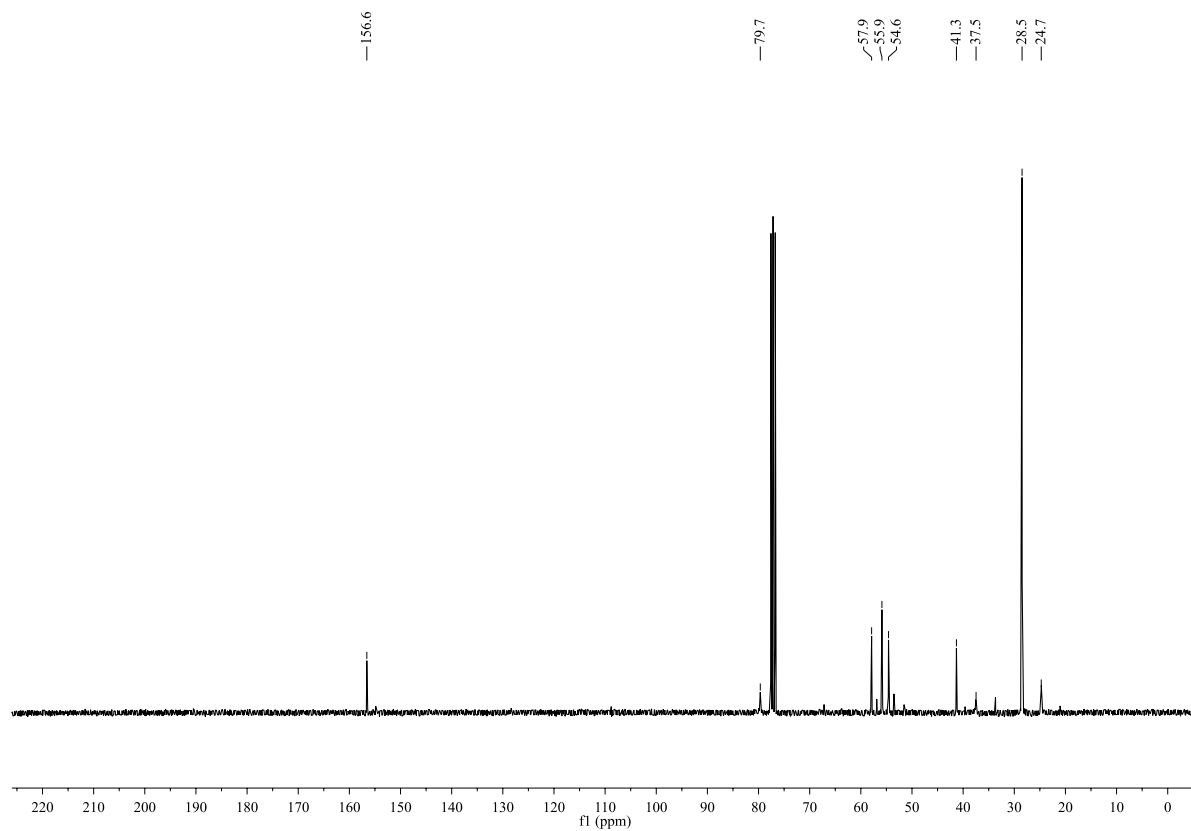
^{13}C NMR (CD_3OD , 100 MHz):



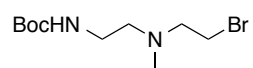
^1H NMR (CDCl_3 , 300 MHz):



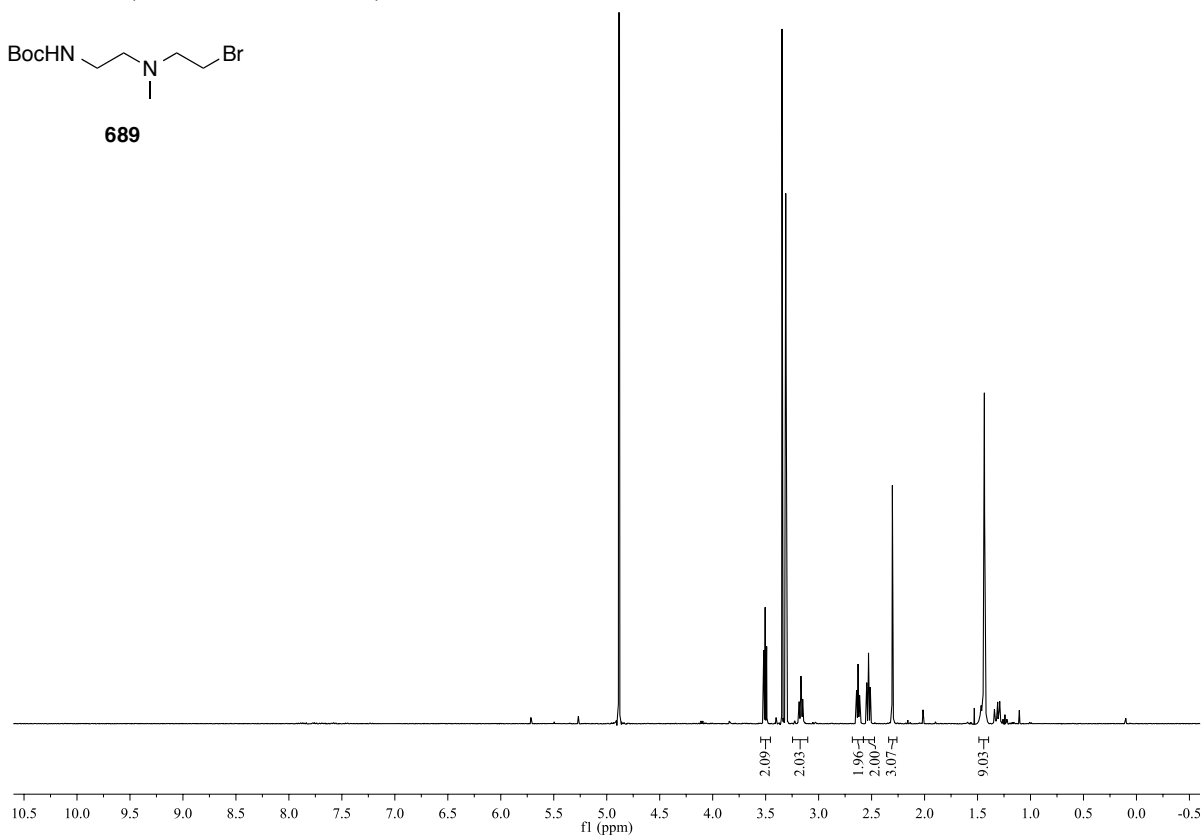
^{13}C NMR (CDCl_3 , 75 MHz):



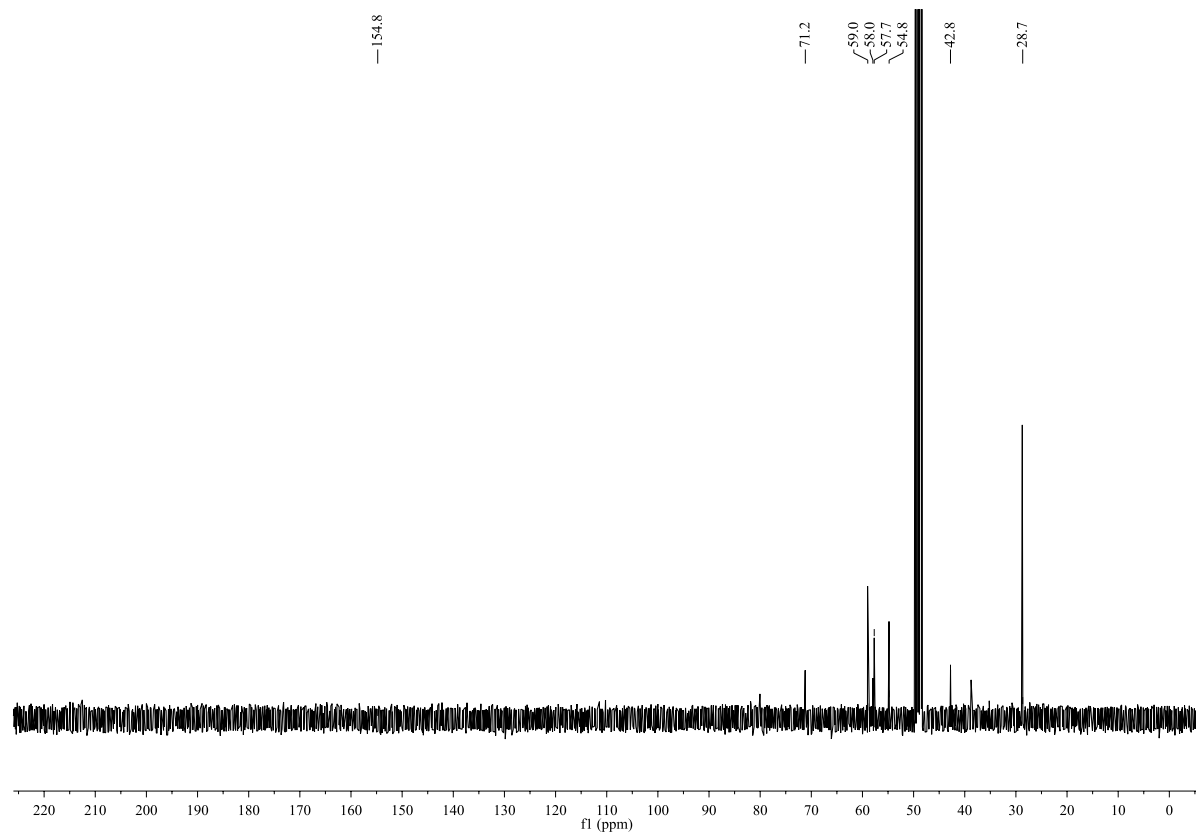
^1H NMR (CD_3OD , 400 MHz):

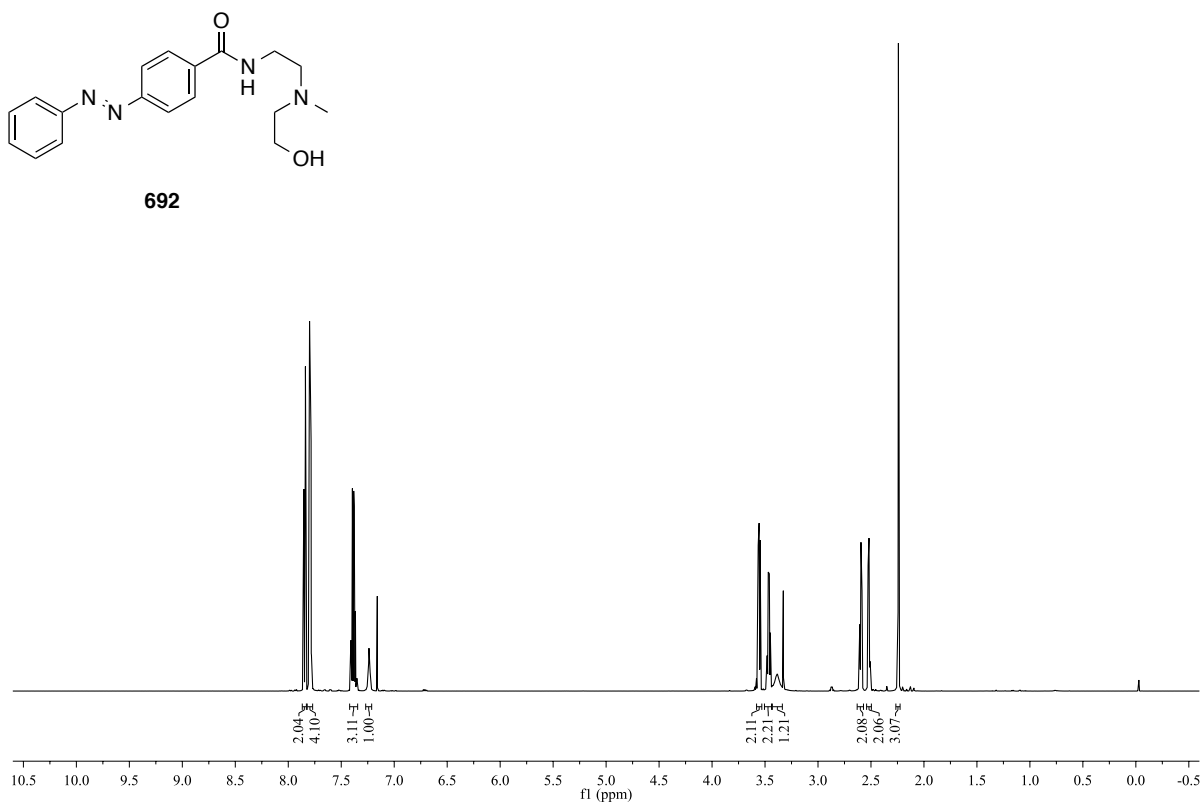
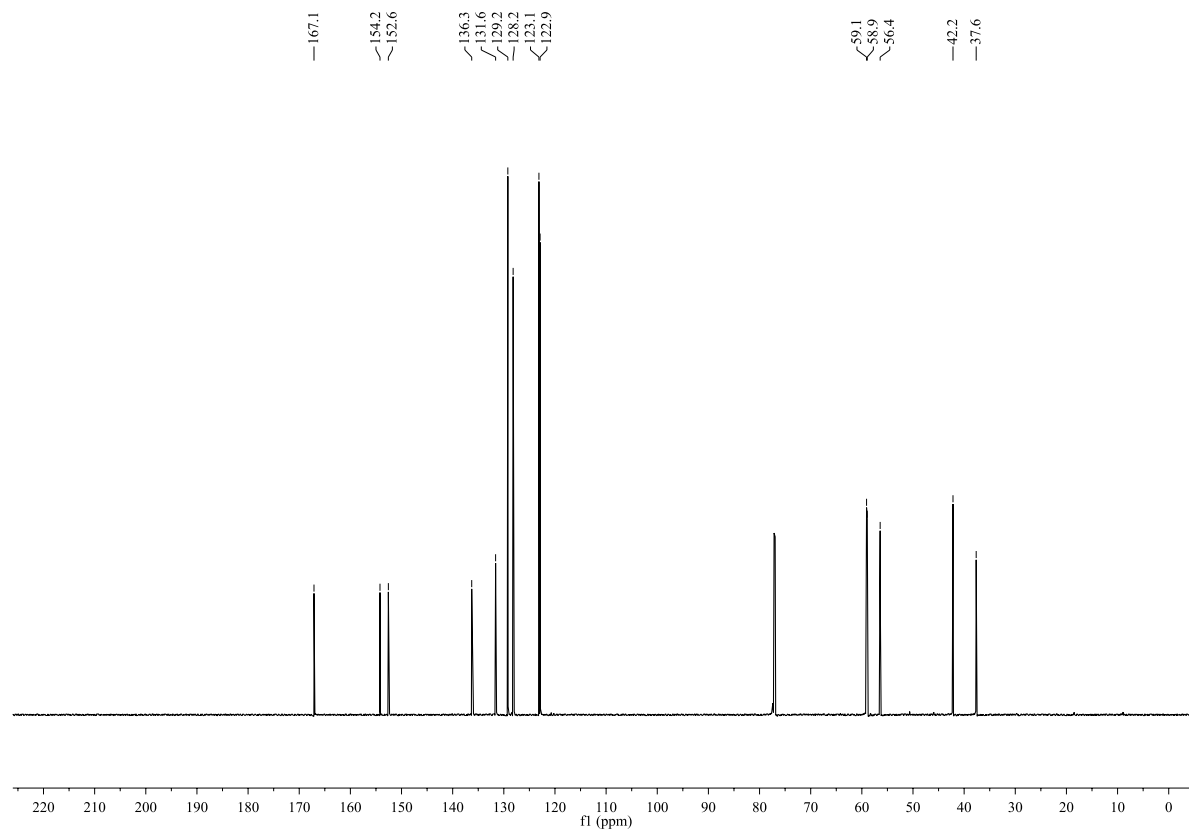


689

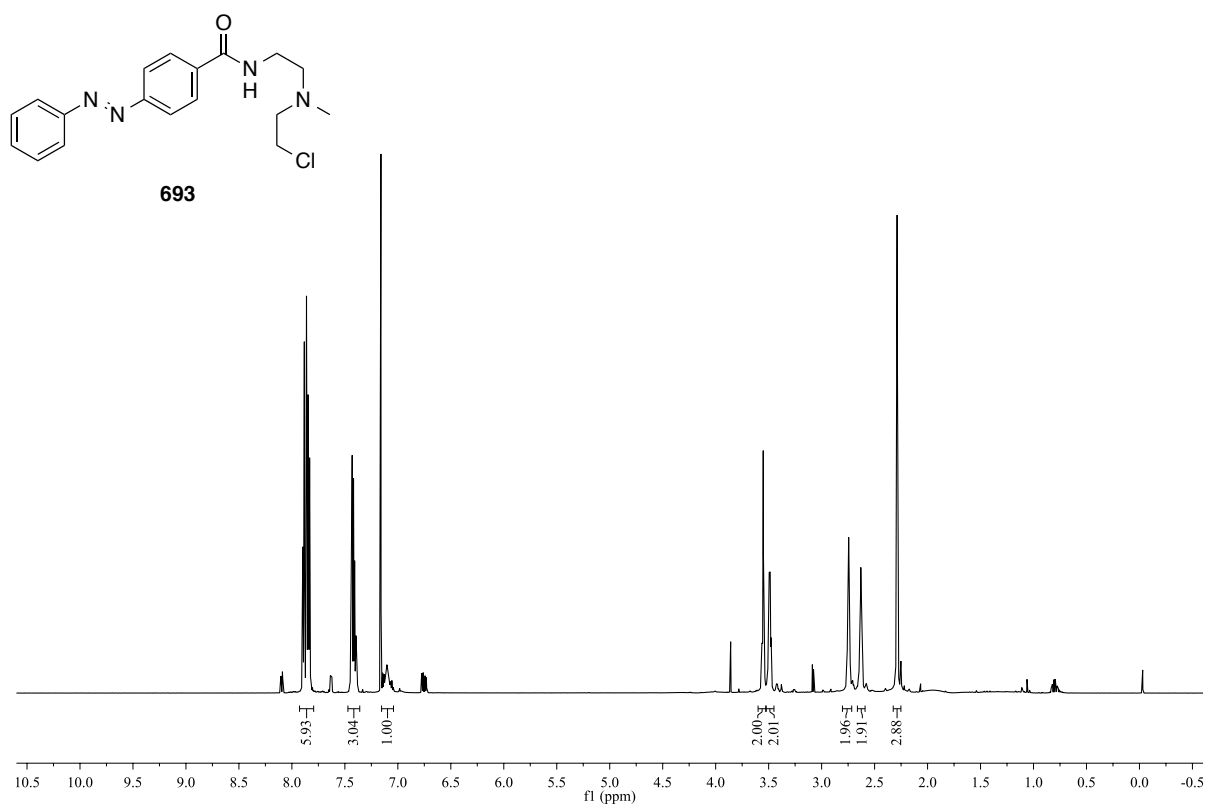


^{13}C NMR (CD_3OD , 100 MHz):

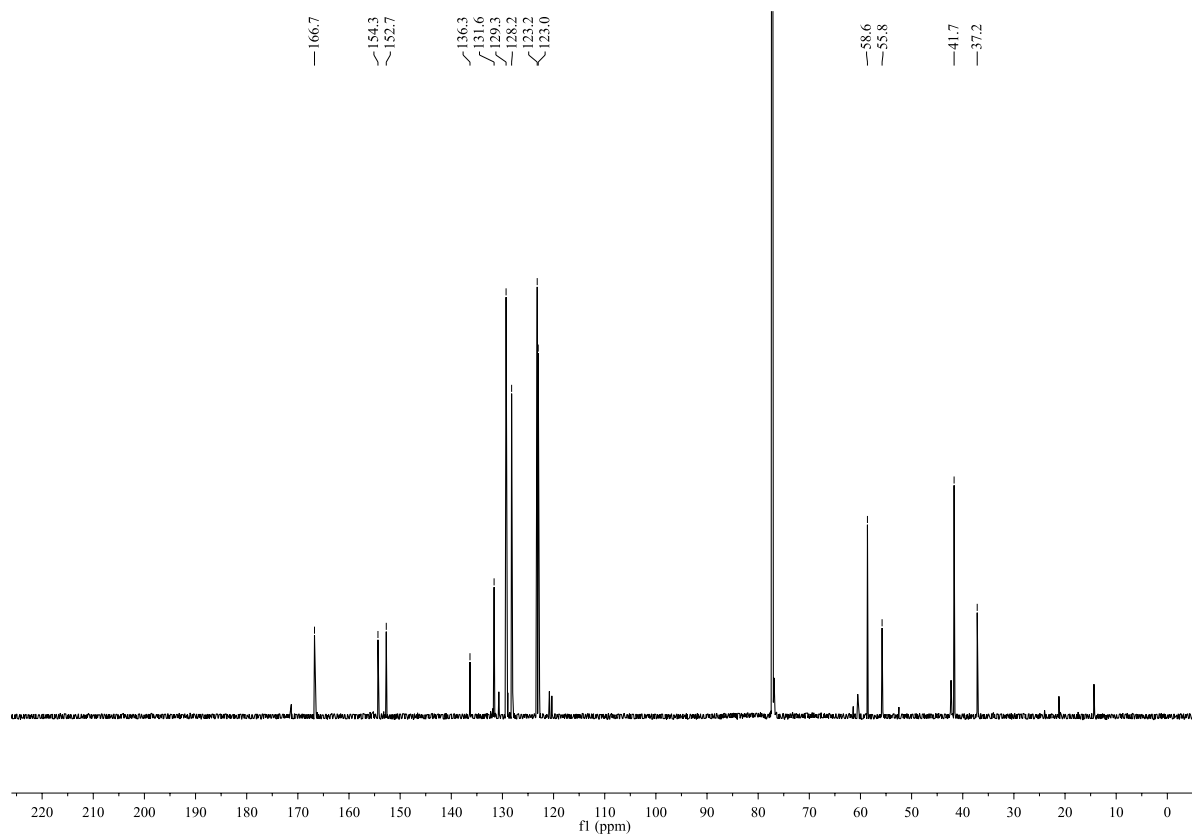


^1H NMR (CDCl_3 , 600 MHz): ^{13}C NMR (CDCl_3 , 150 MHz):

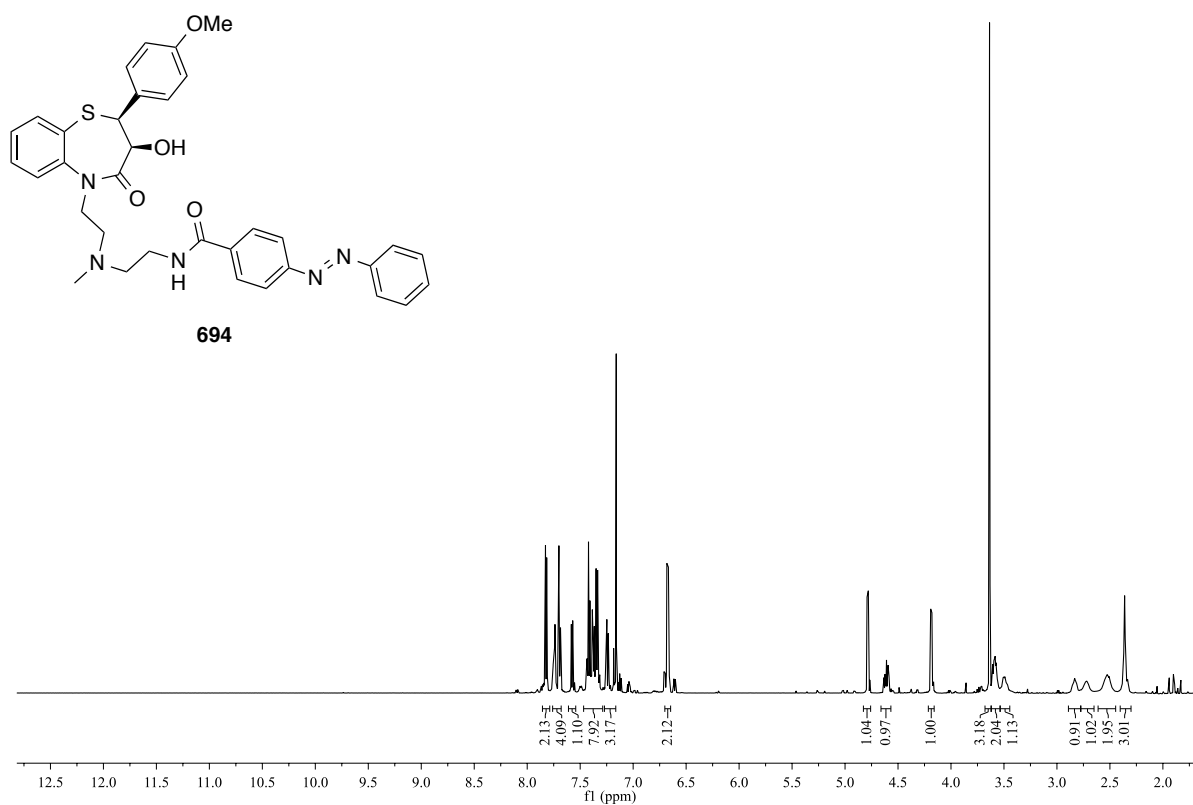
^1H NMR (CDCl_3 , 600 MHz):



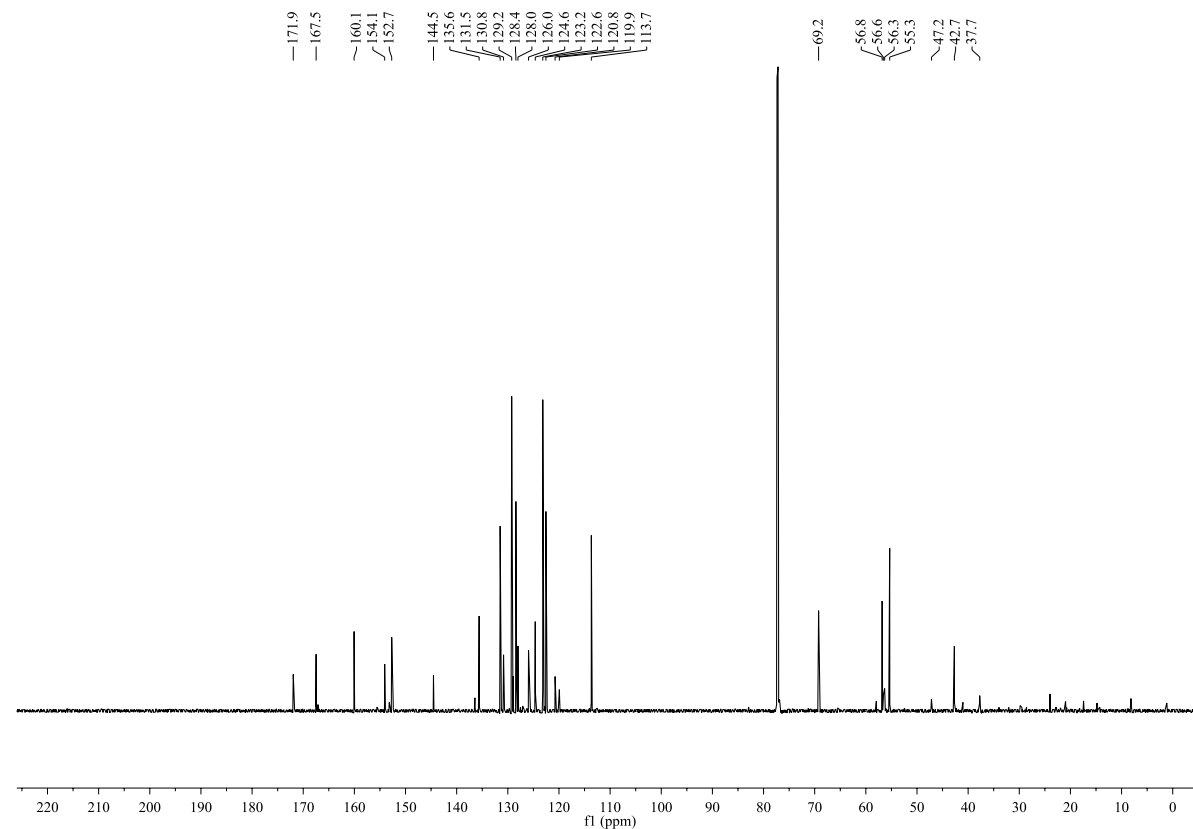
^{13}C NMR (CDCl_3 , 150 MHz):



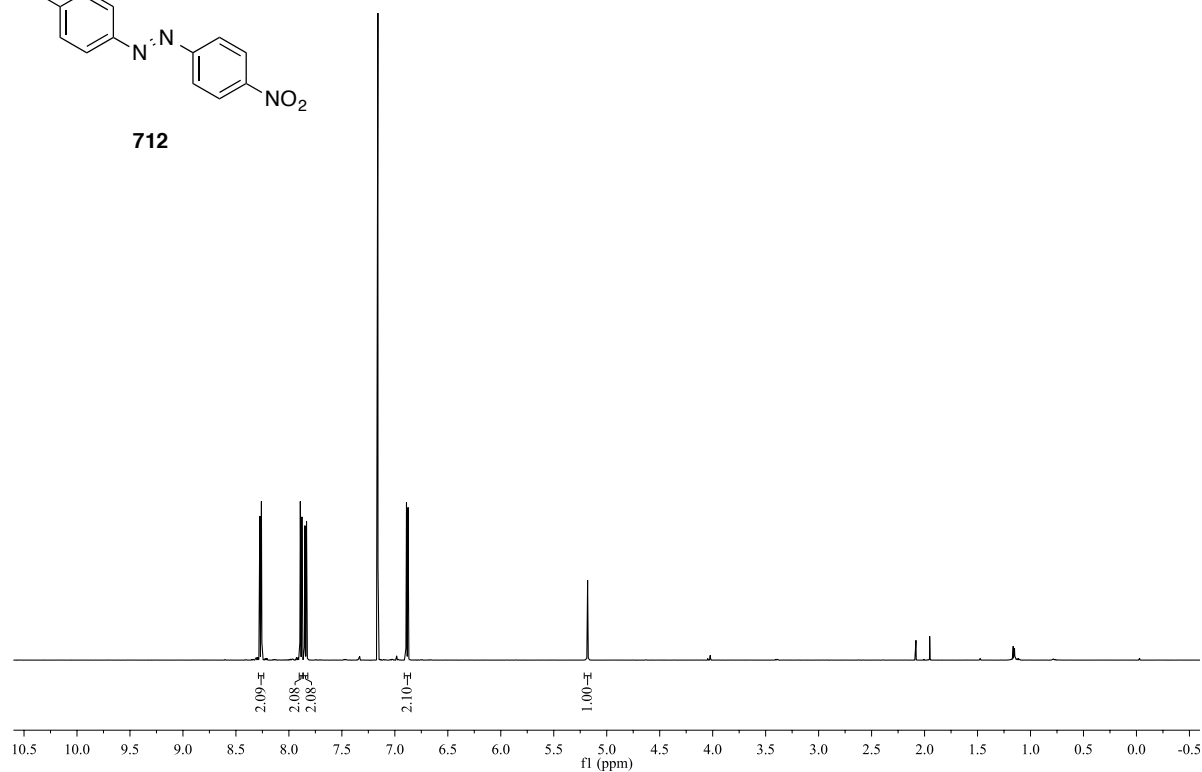
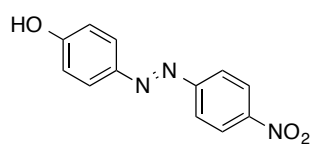
^1H NMR (CDCl_3 , 600 MHz):



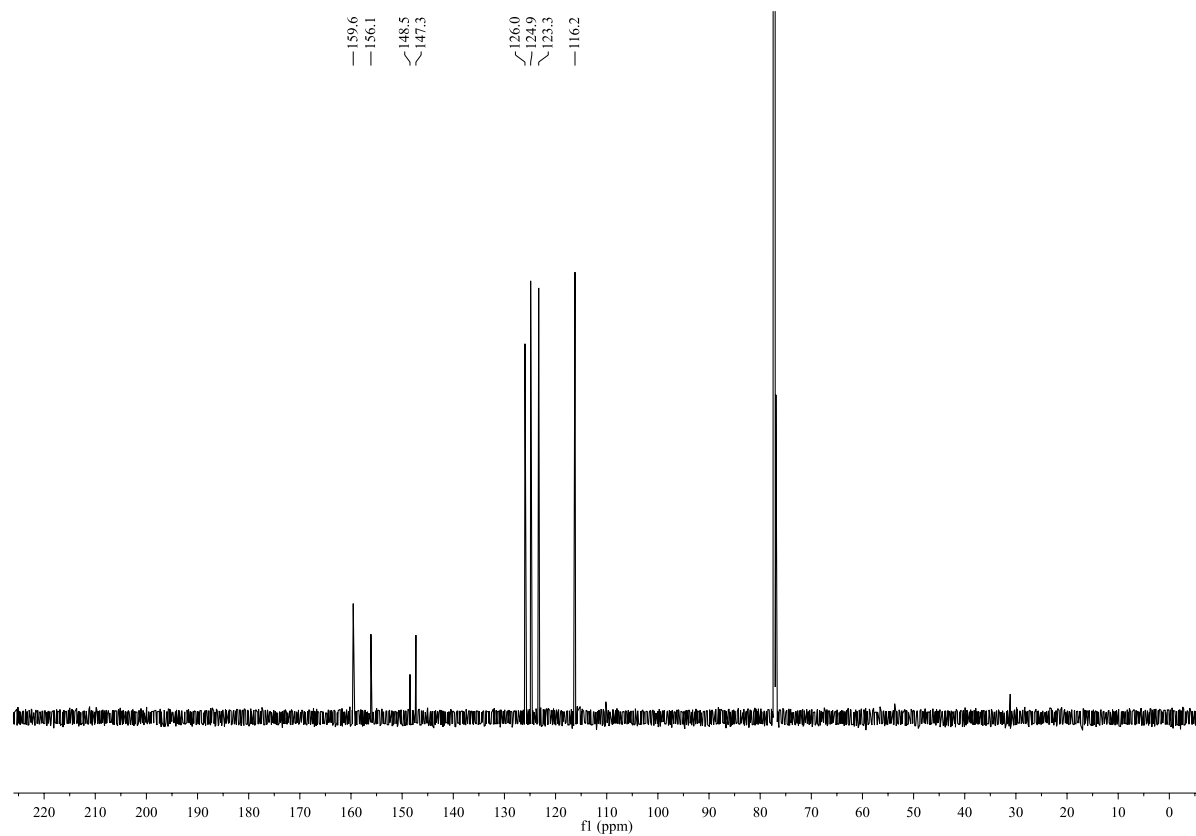
^{13}C NMR (CDCl_3 , 150 MHz):



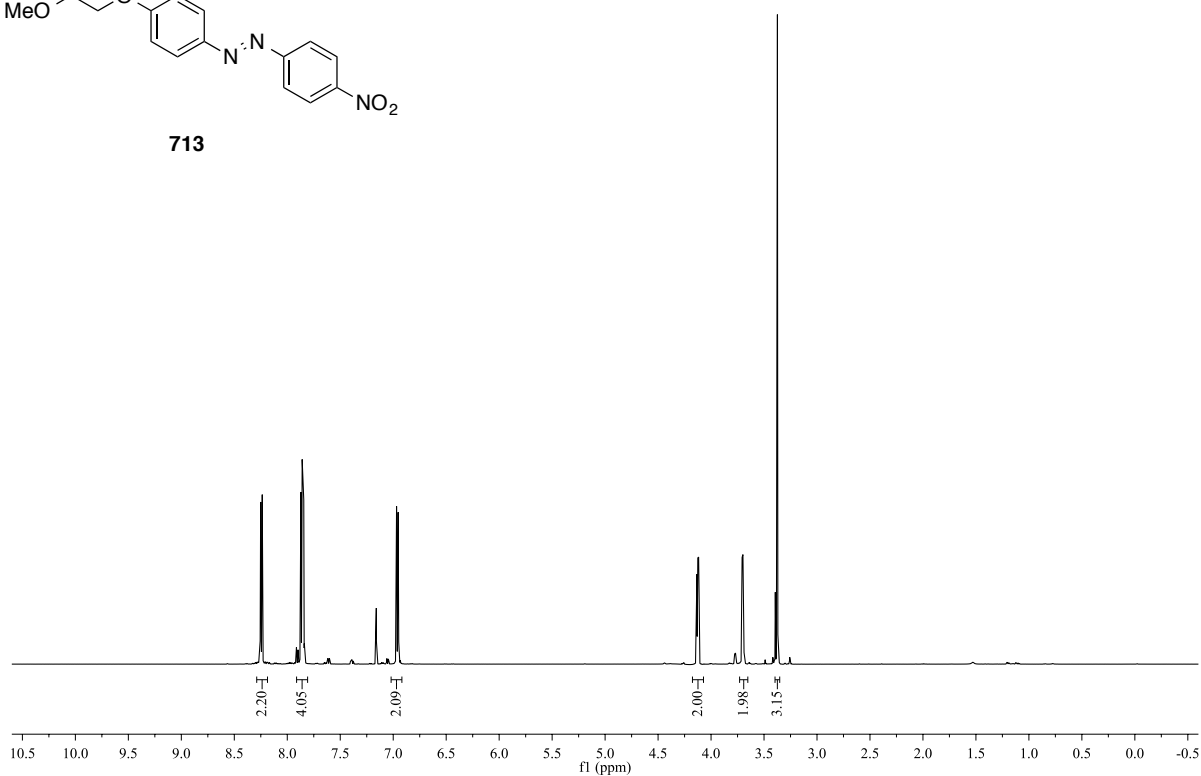
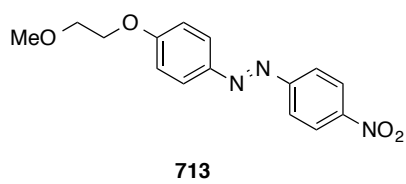
^1H NMR (CDCl_3 , 600 MHz):



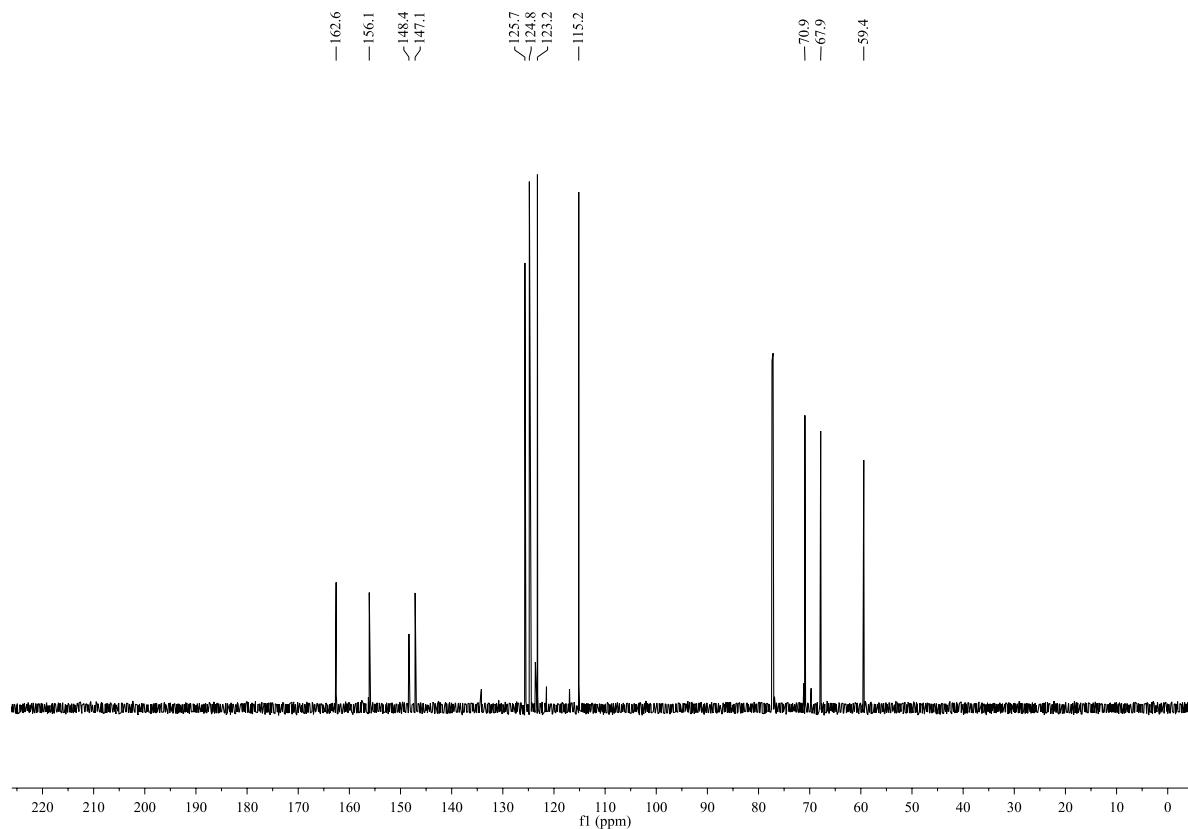
^{13}C NMR (CDCl_3 , 150 MHz):



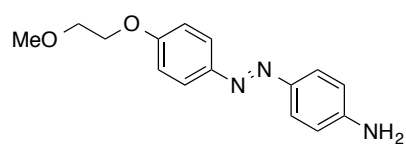
^1H NMR (CDCl_3 , 600 MHz):



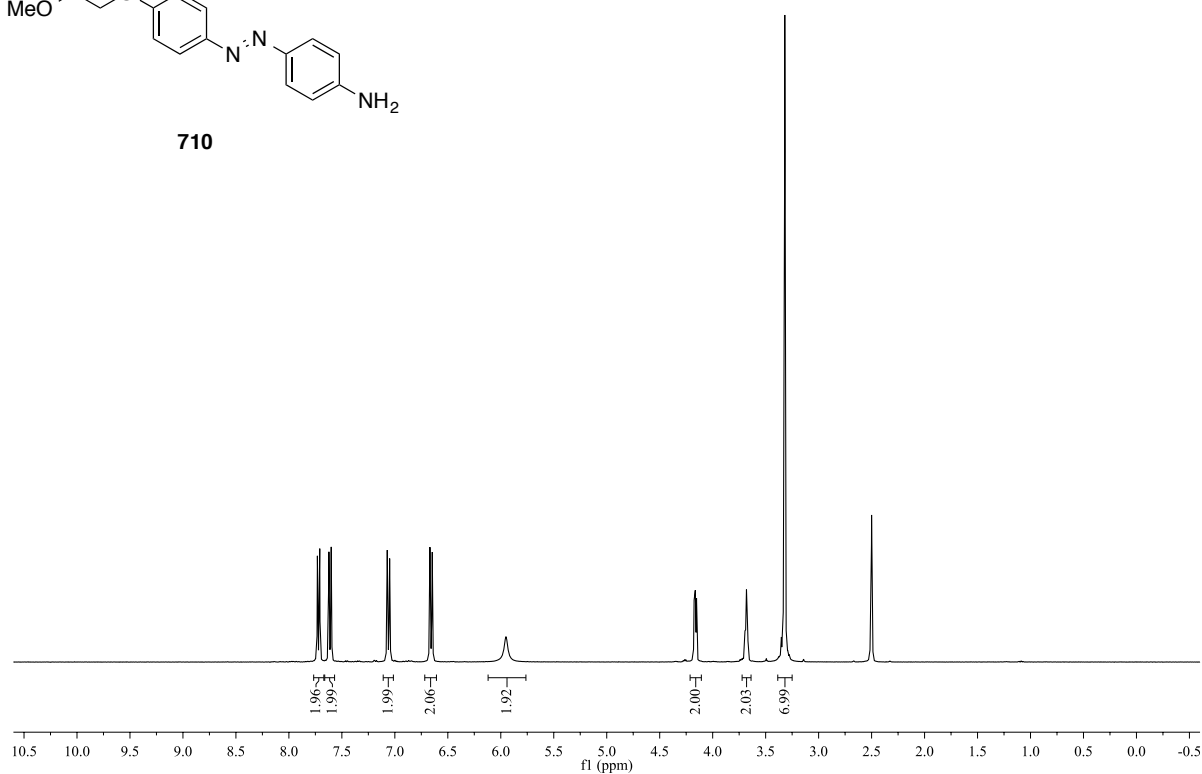
^{13}C NMR (CDCl_3 , 150 MHz):



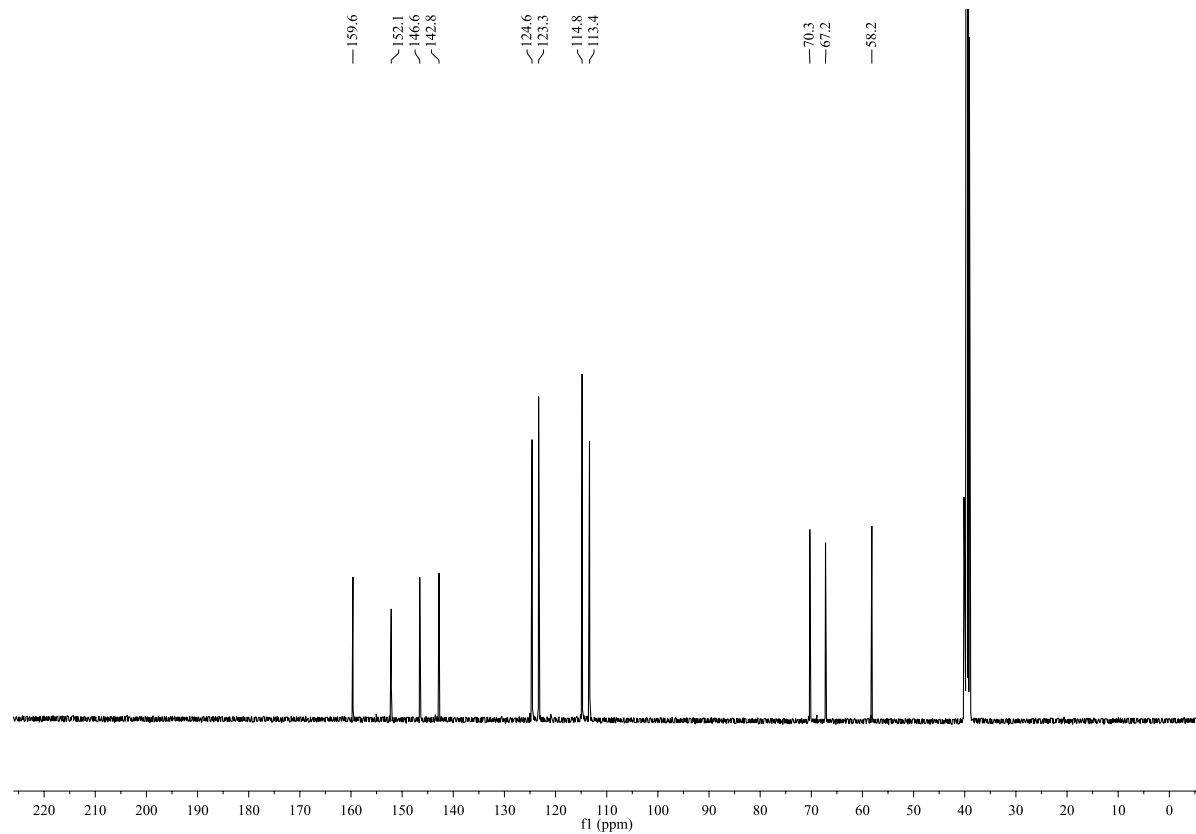
^1H NMR (DMSO- d_6 , 400 MHz):



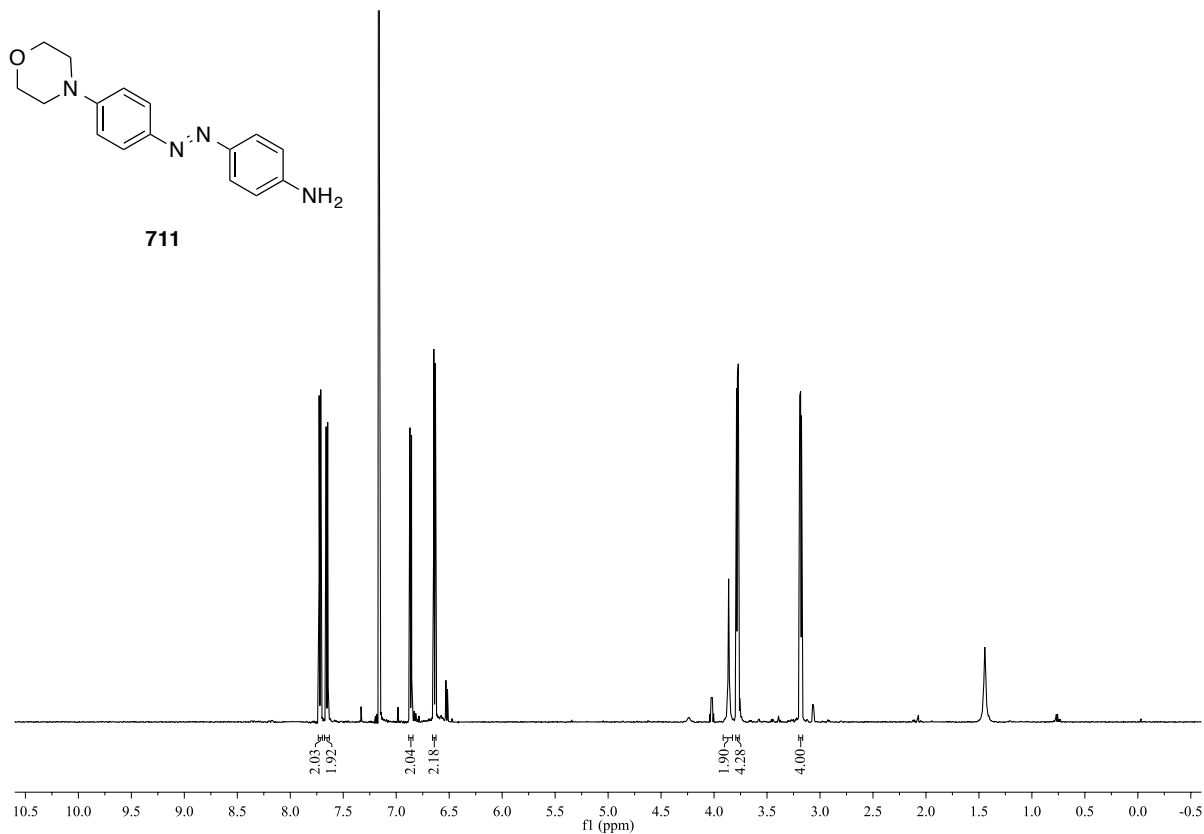
710



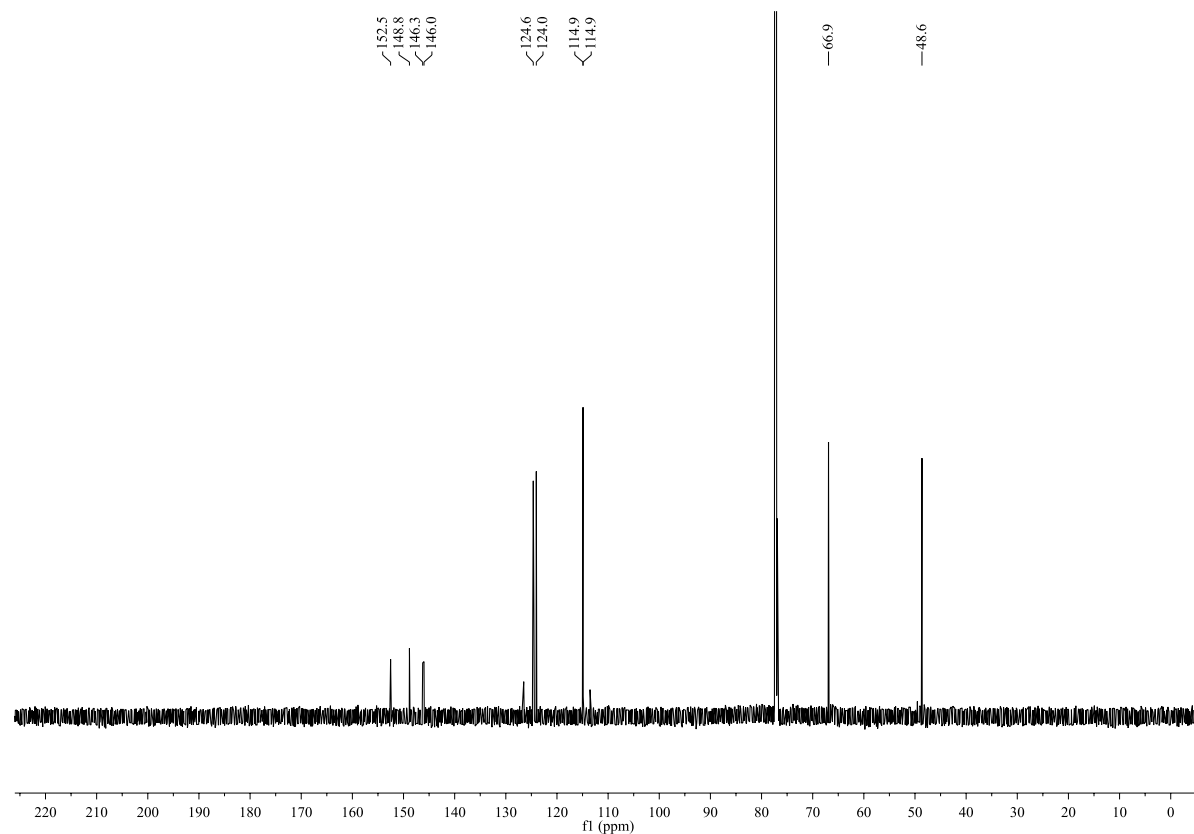
^{13}C NMR (DMSO- d_6 , 100 MHz):



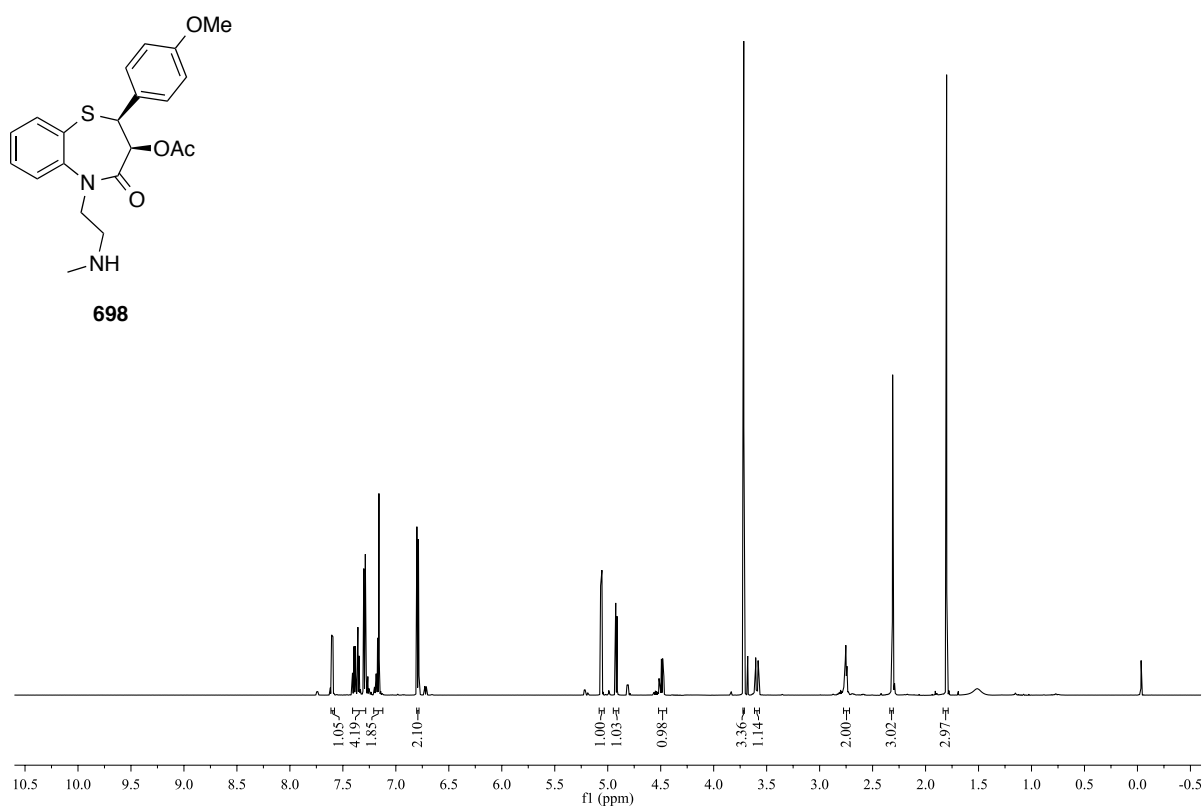
^1H NMR (CDCl_3 , 600 MHz):



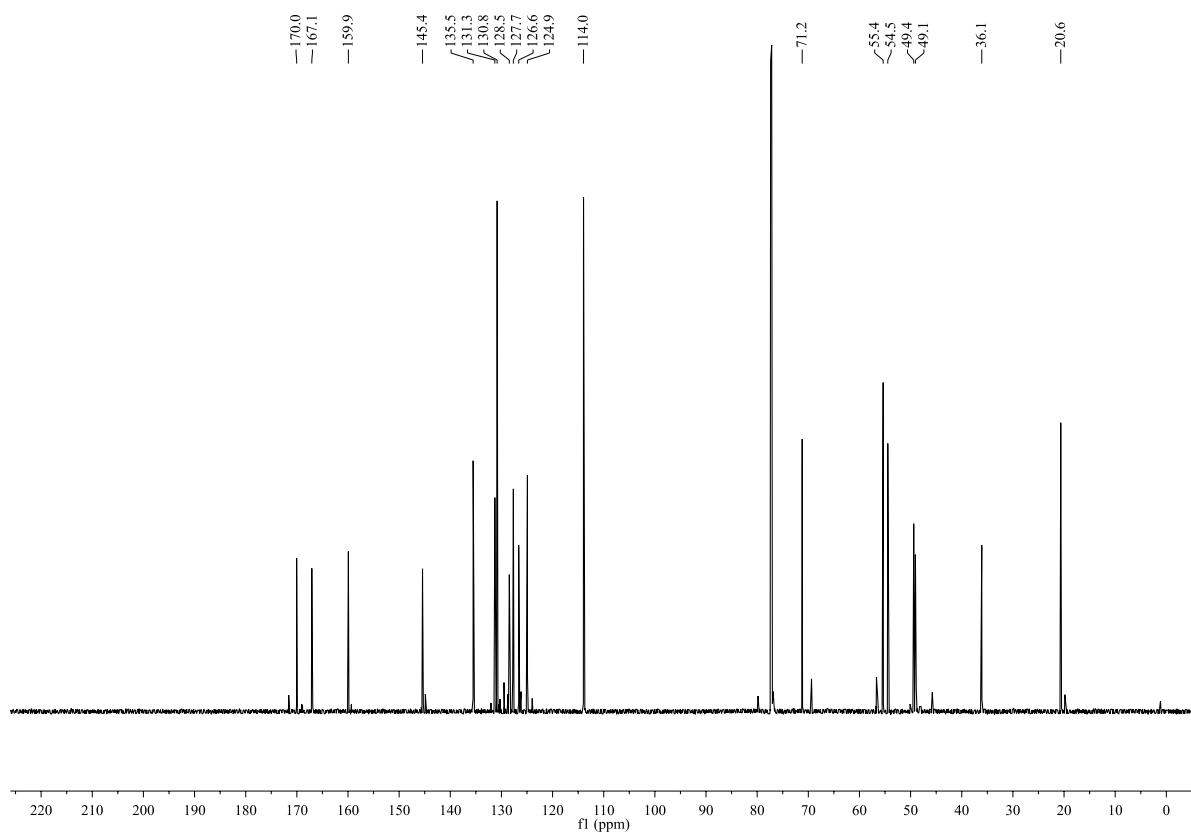
^{13}C NMR (CDCl_3 , 150 MHz):



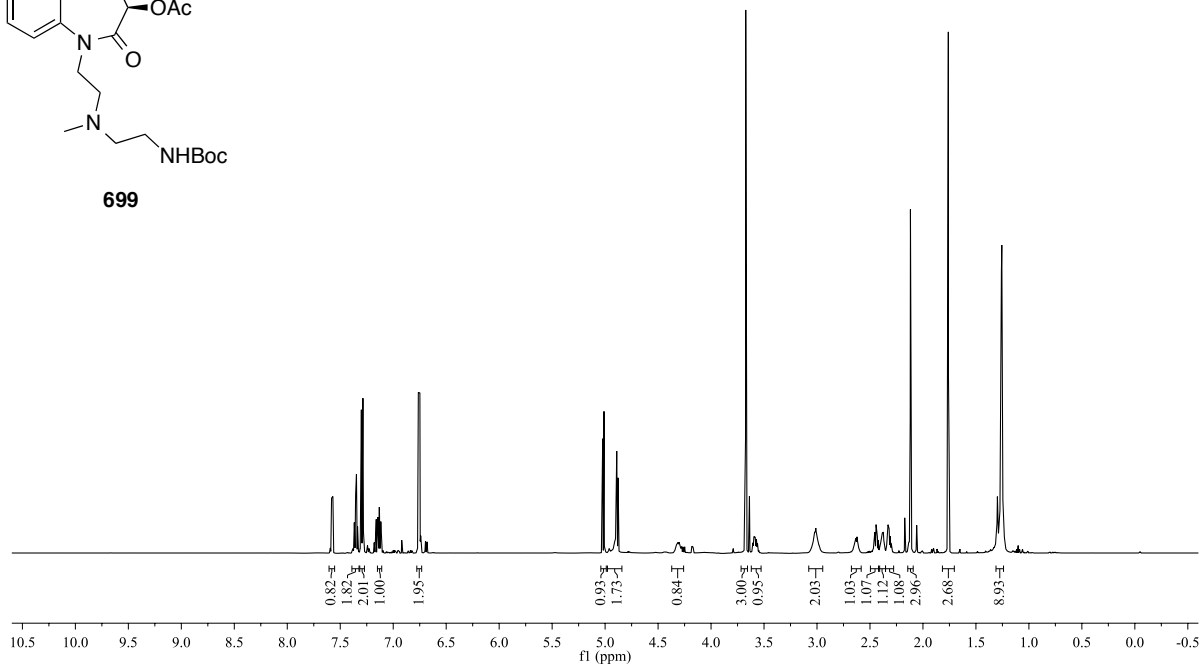
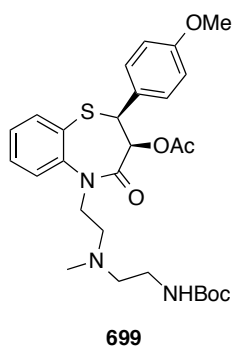
^1H NMR (CDCl_3 , 600 MHz):



^{13}C NMR (CDCl_3 , 150 MHz):

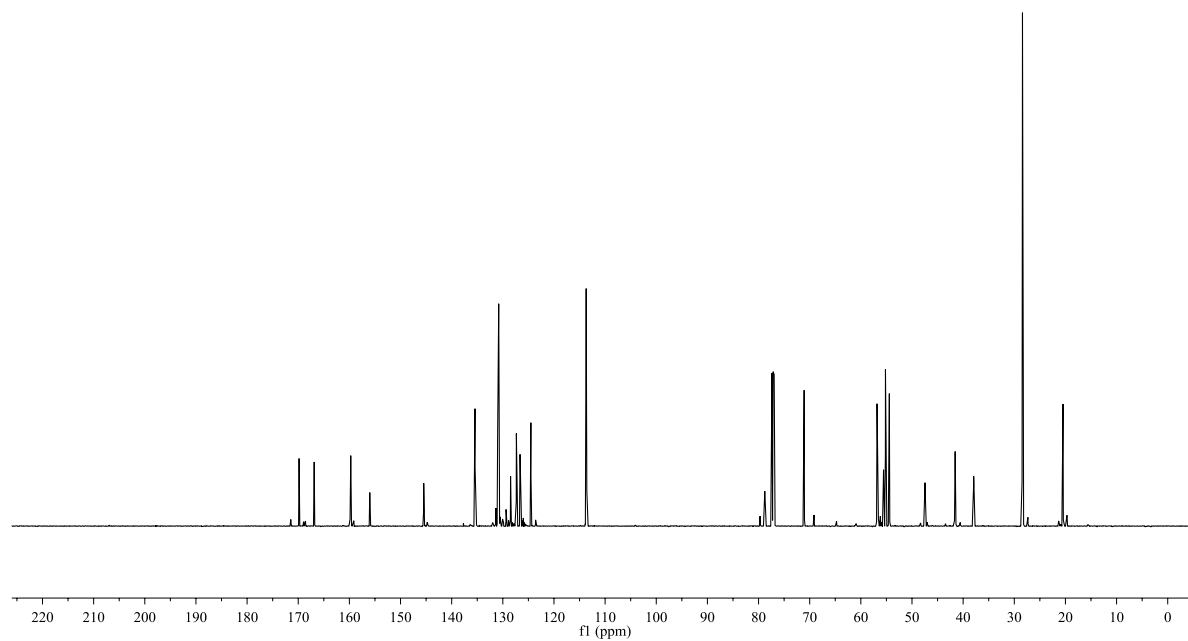


^1H NMR (CDCl_3 , 600 MHz):

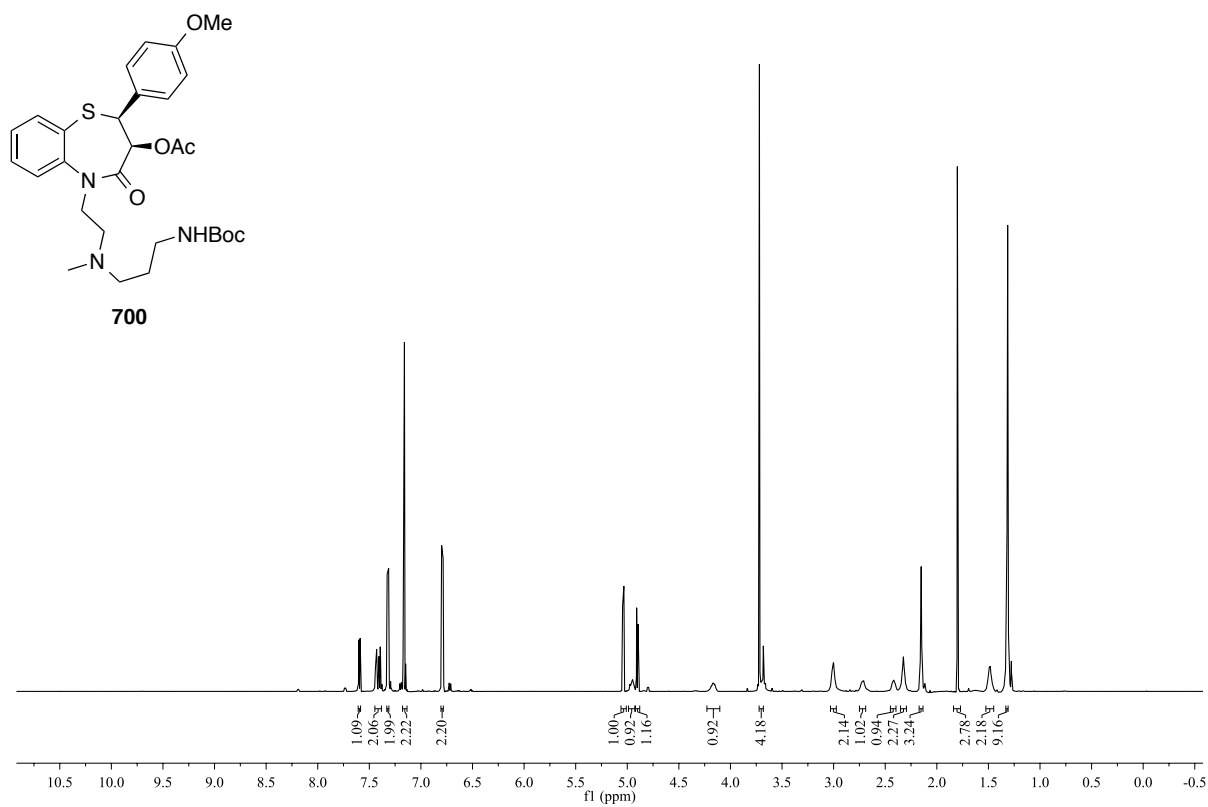


^{13}C NMR (CDCl_3 , 150 MHz):

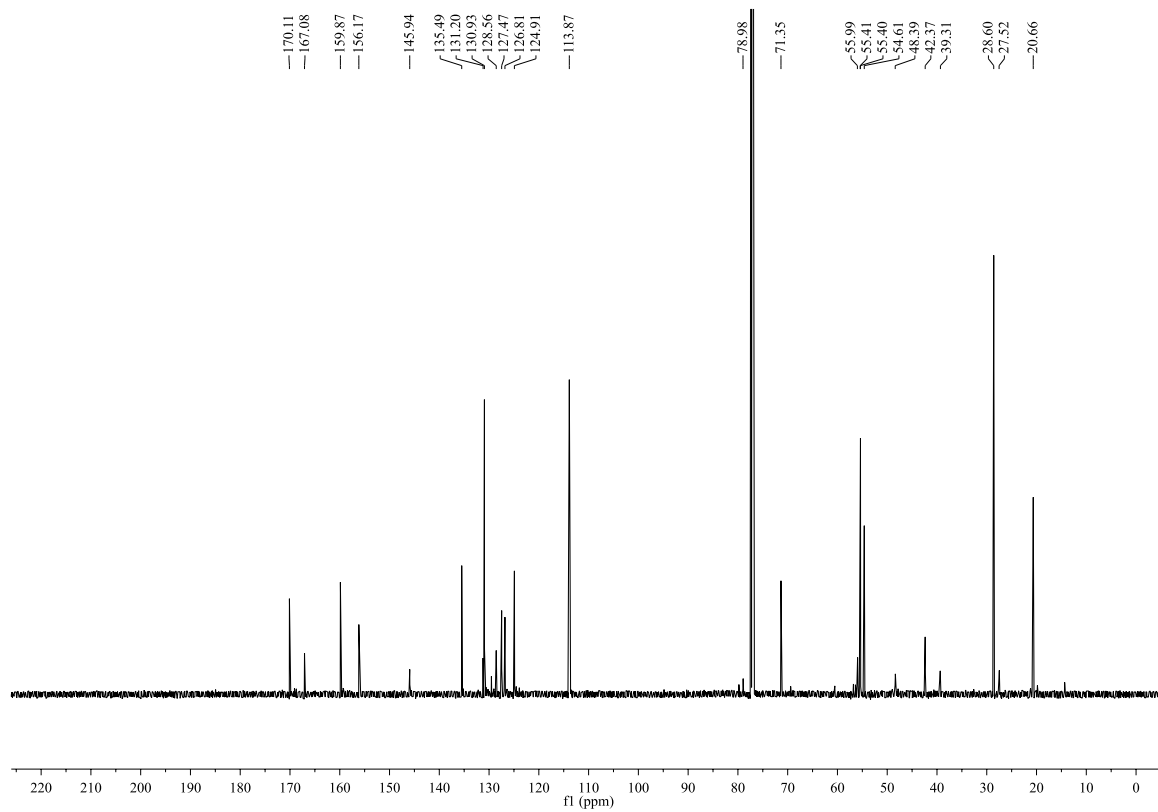
169.8, 166.9, 159.7, 156.0, 145.5, 135.4, 131.0, 130.8, 128.5, 127.3, 126.6, 124.5, 113.7, 78.8, 71.1, 56.8, 55.6, 55.2, 54.4, 47.5, 41.6, 37.9, 28.4, 20.5.



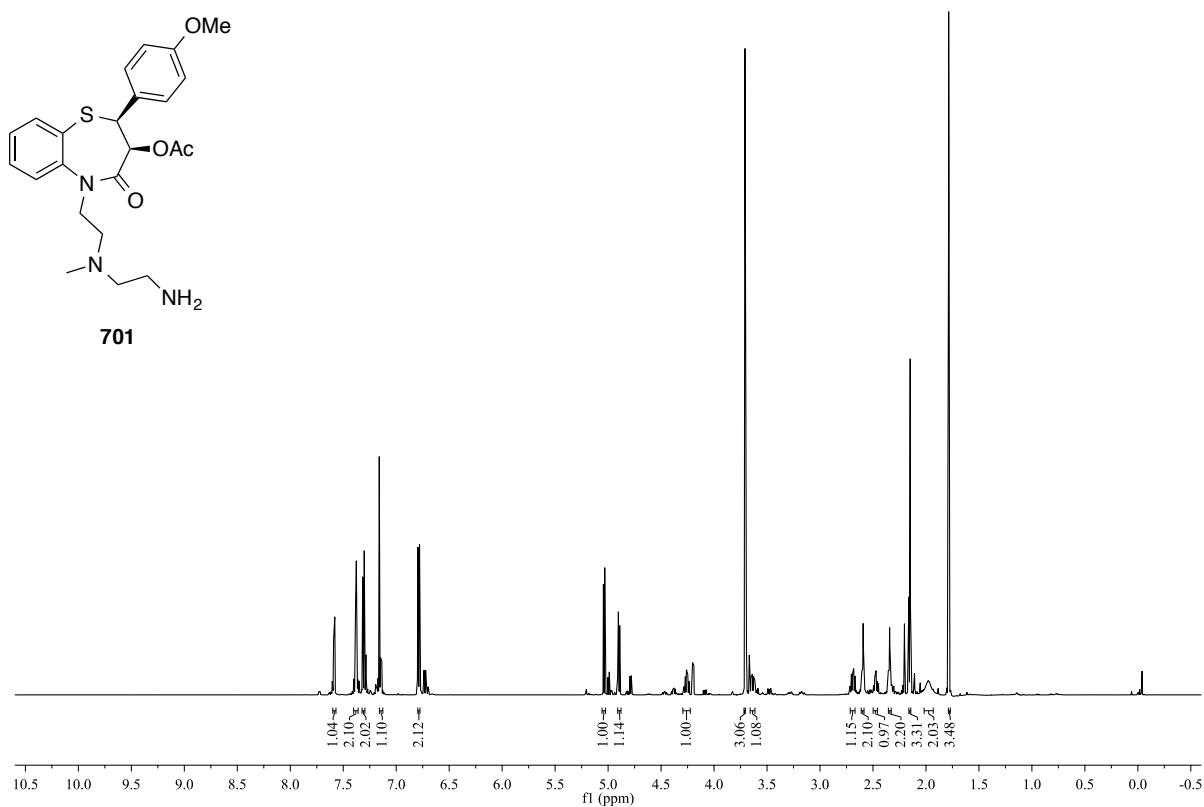
^1H NMR (CDCl_3 , 600 MHz):



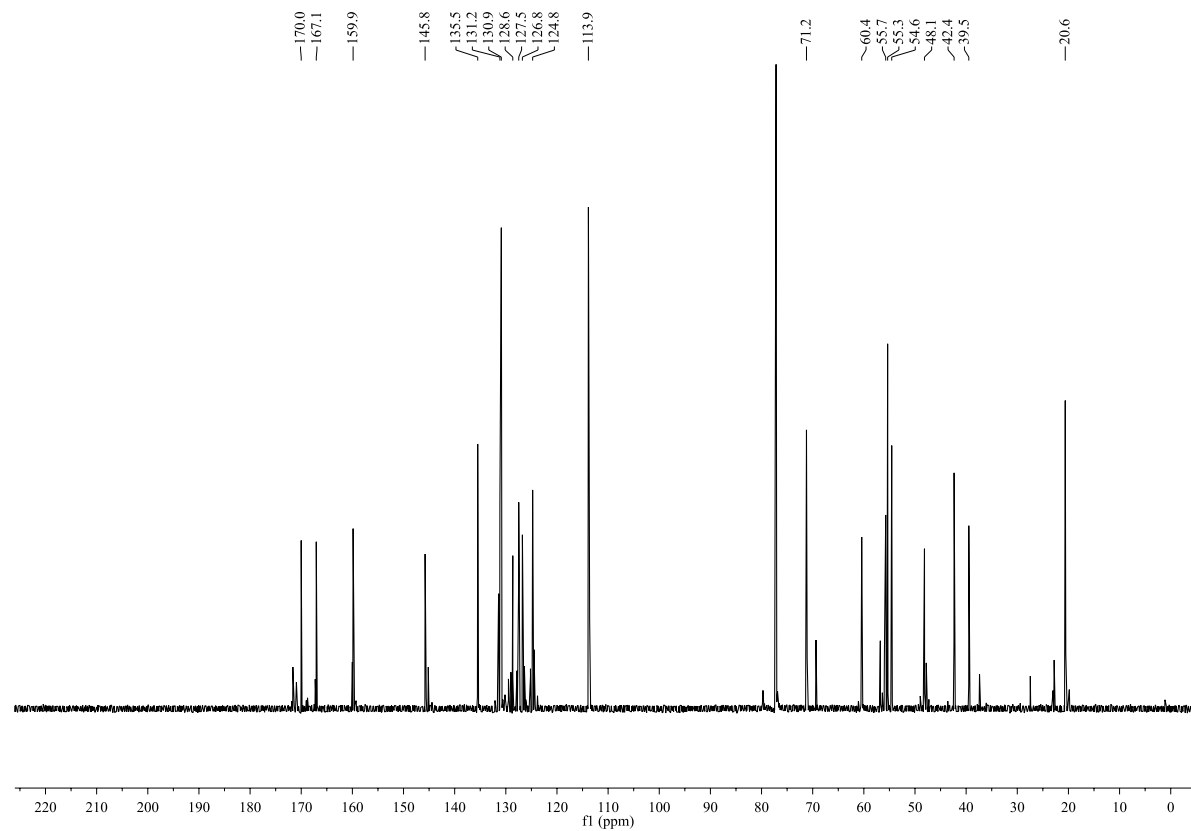
^{13}C NMR (CDCl_3 , 150 MHz):

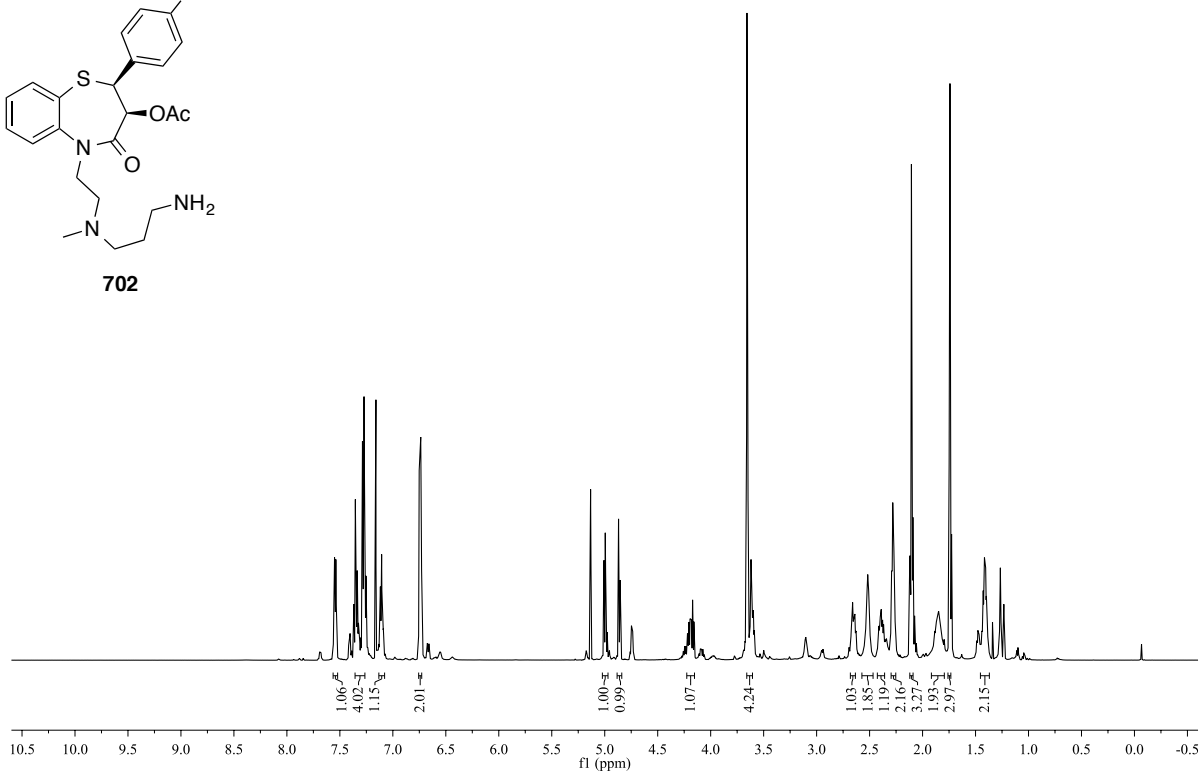
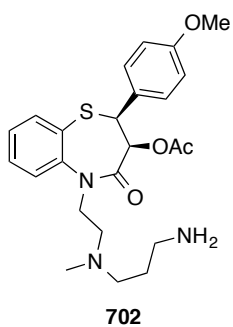


^1H NMR (CDCl_3 , 600 MHz):

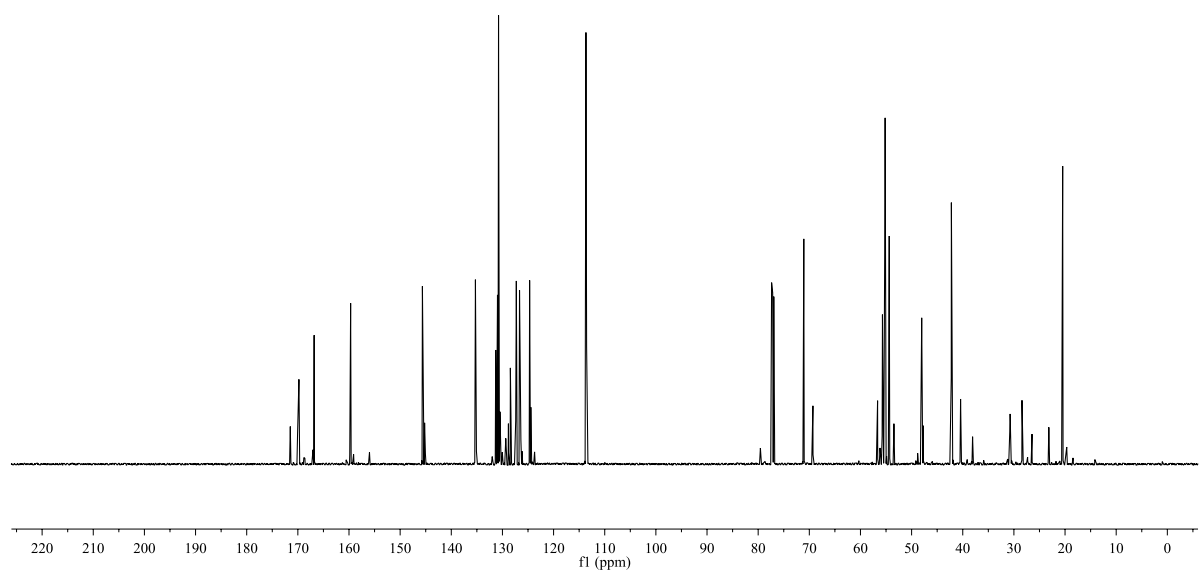


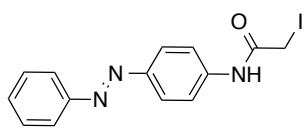
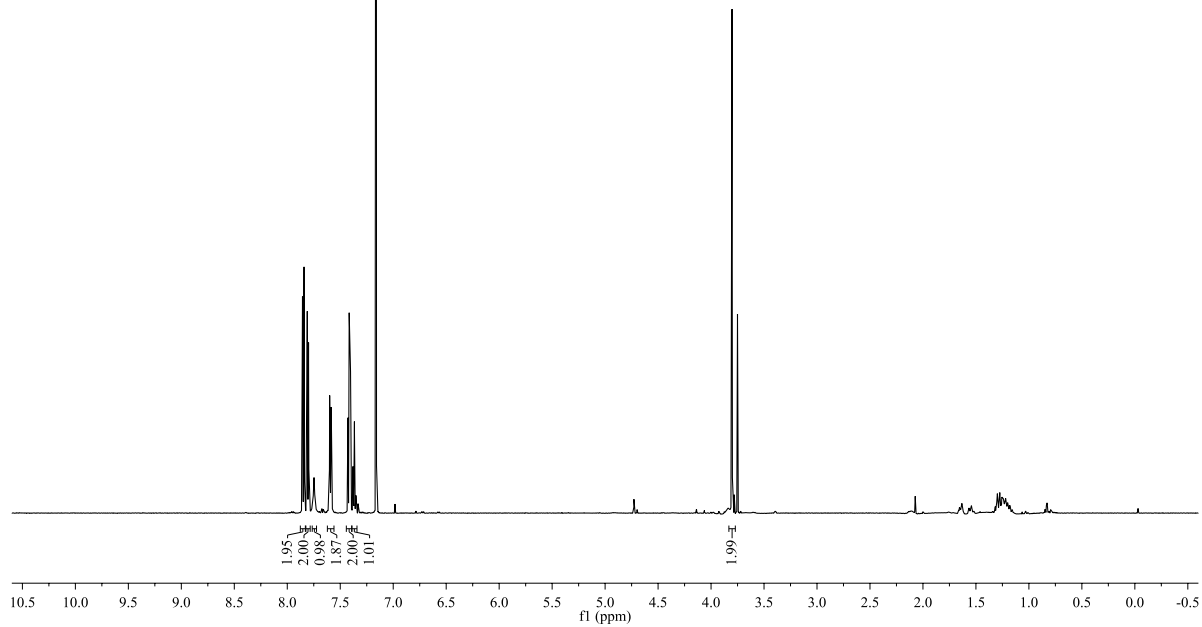
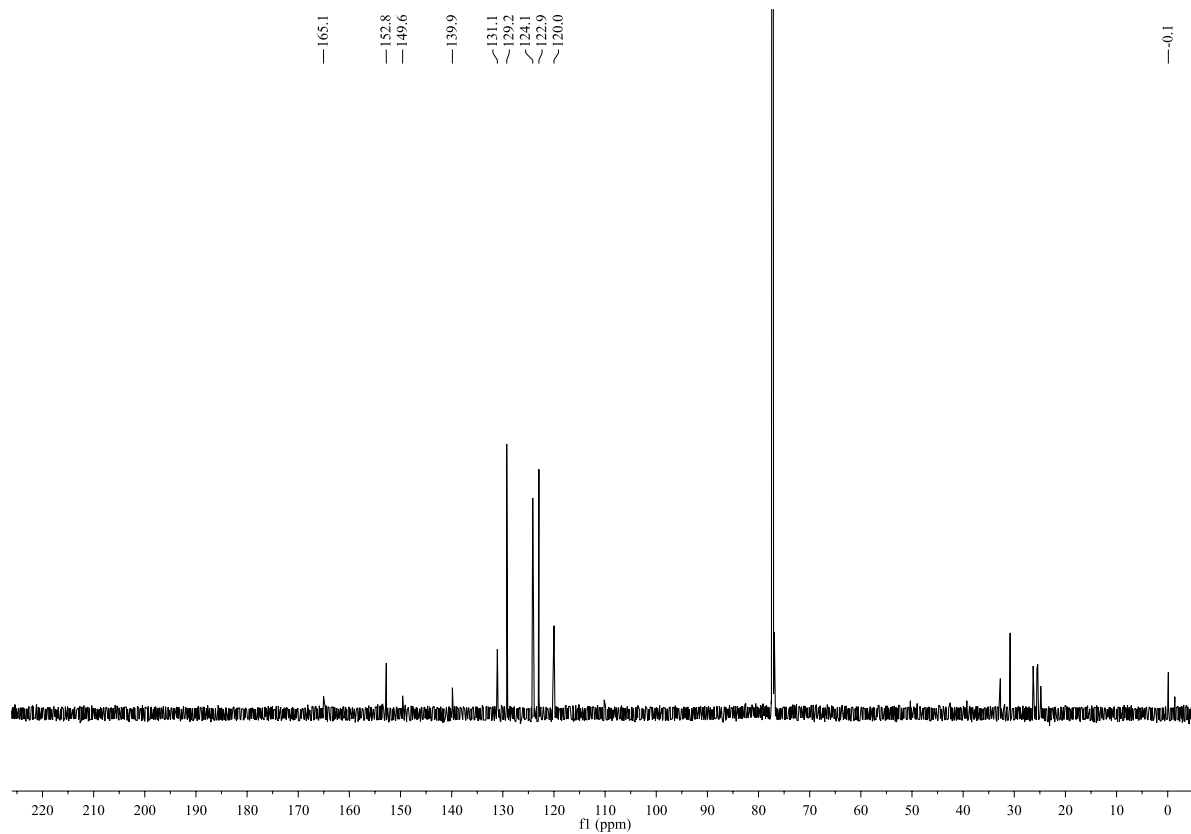
^{13}C NMR (CDCl_3 , 150 MHz):



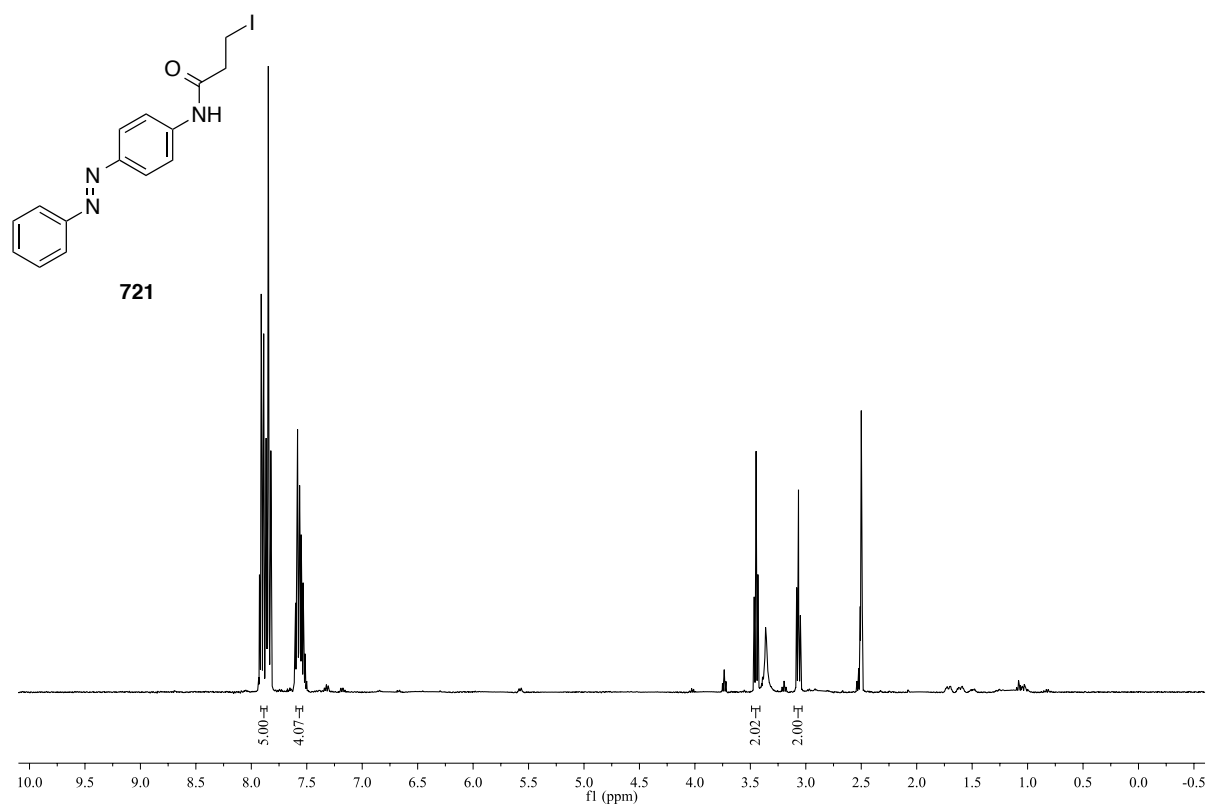
^1H NMR (CDCl_3 , 600 MHz): ^{13}C NMR (CDCl_3 , 150 MHz):

169.8 166.8 159.7 145.6 135.3 131.3 130.8 128.4 127.3 126.7 124.7 113.7 71.1 56.7 55.7 55.2 54.4 48.0 42.2 40.4 28.4 20.5

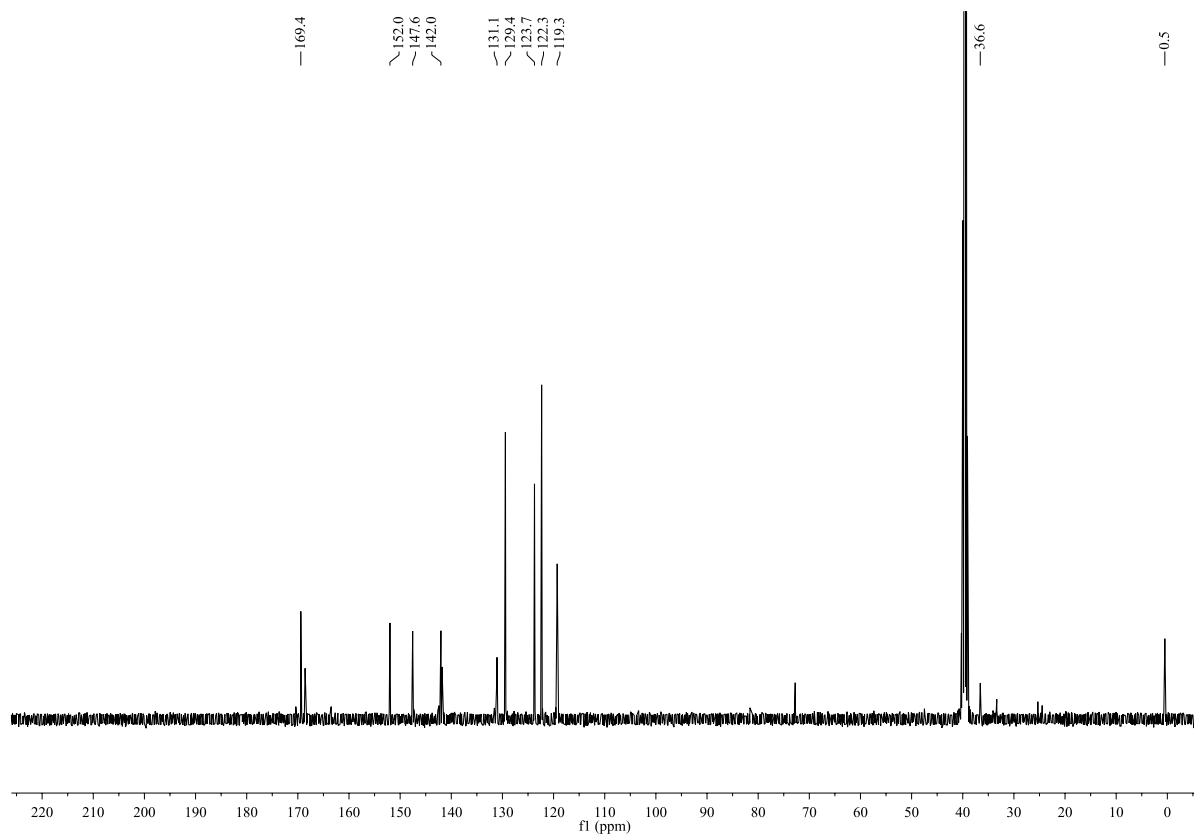


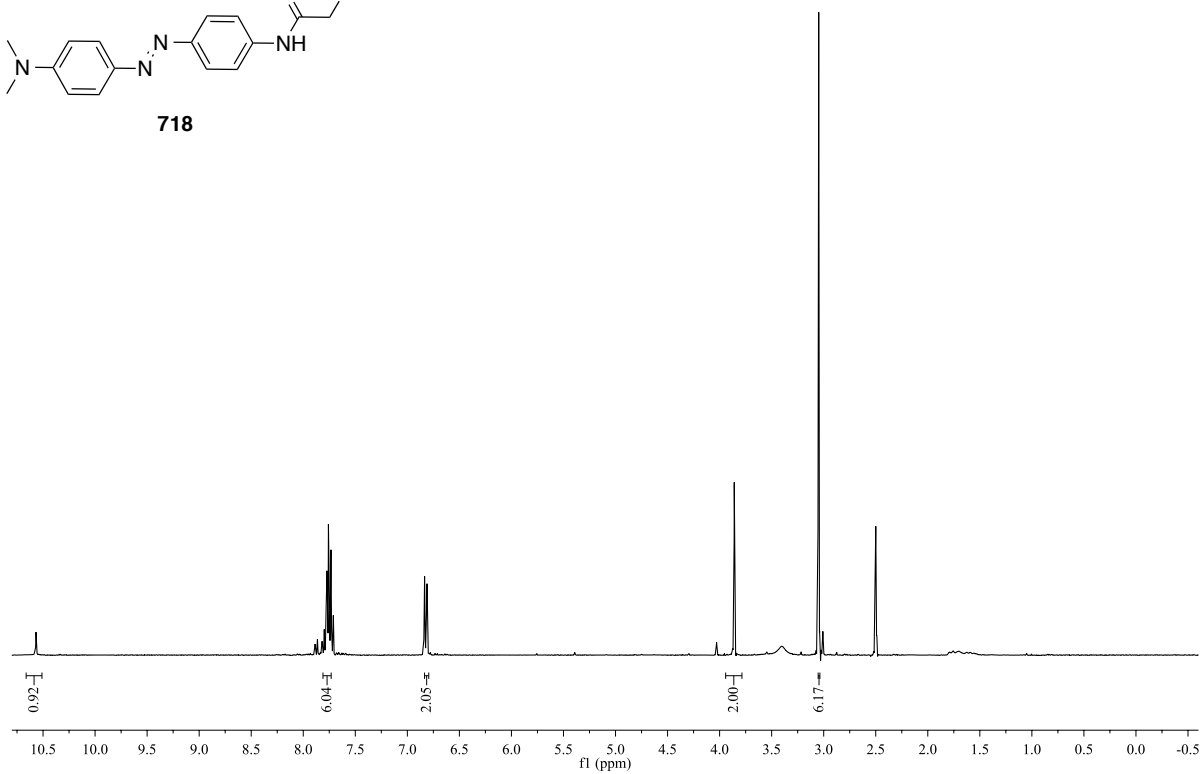
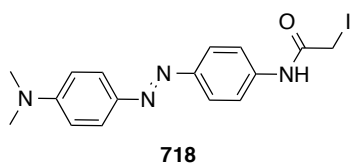
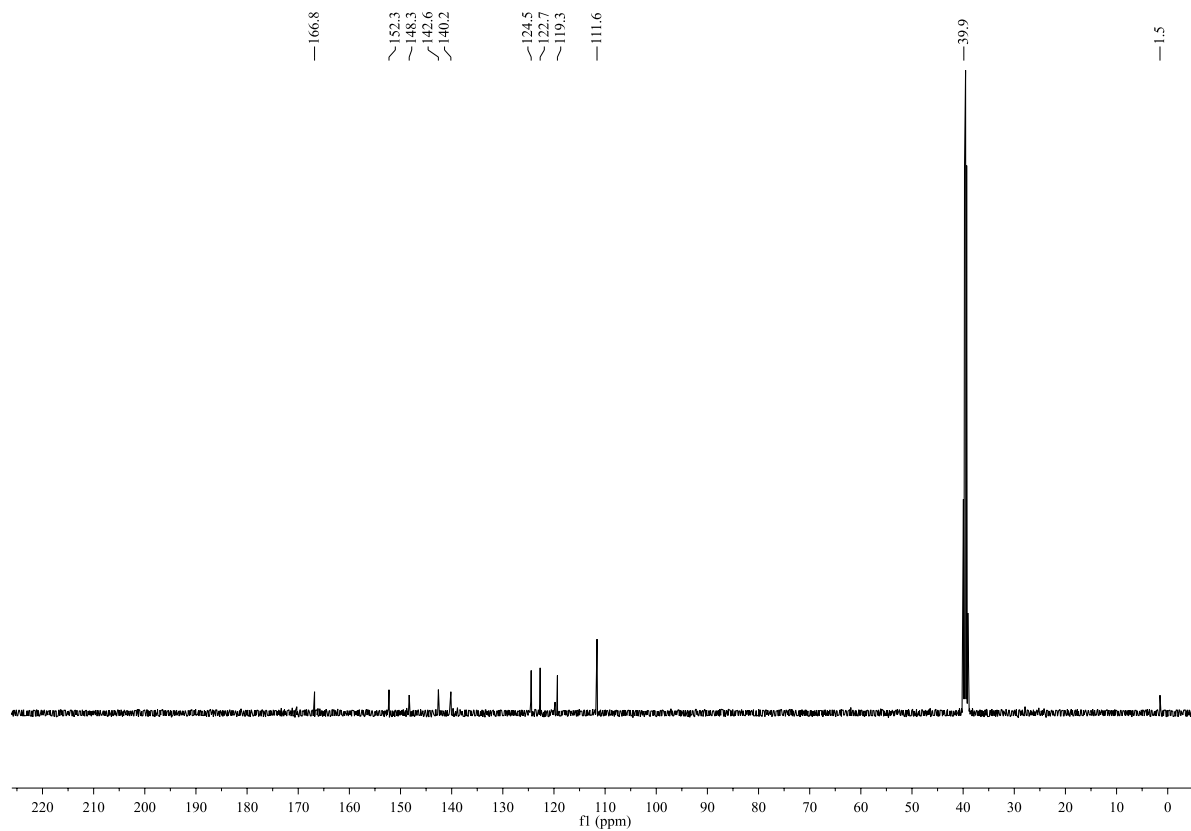
^1H NMR (CDCl_3 , 600 MHz):**703** ^{13}C NMR (CDCl_3 , 150 MHz):

^1H NMR (DMSO- d_6 , 400 MHz):

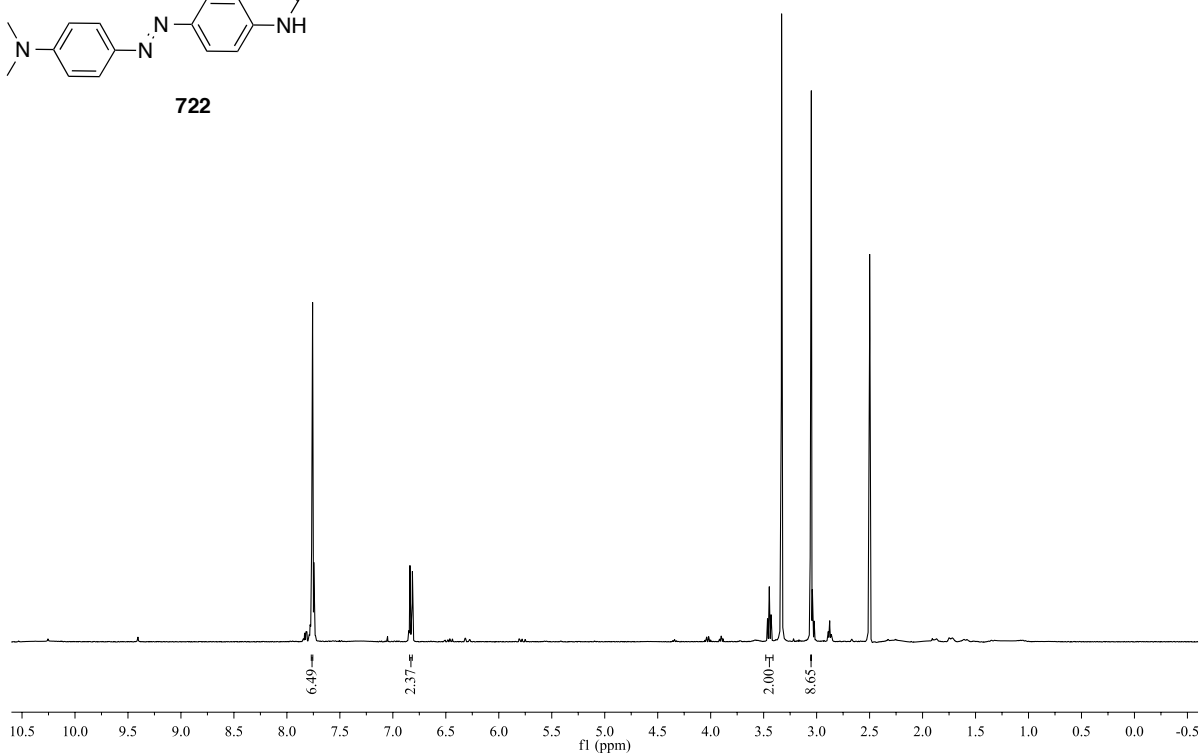
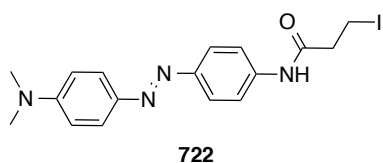


^{13}C NMR (DMSO- d_6 , 100 MHz):

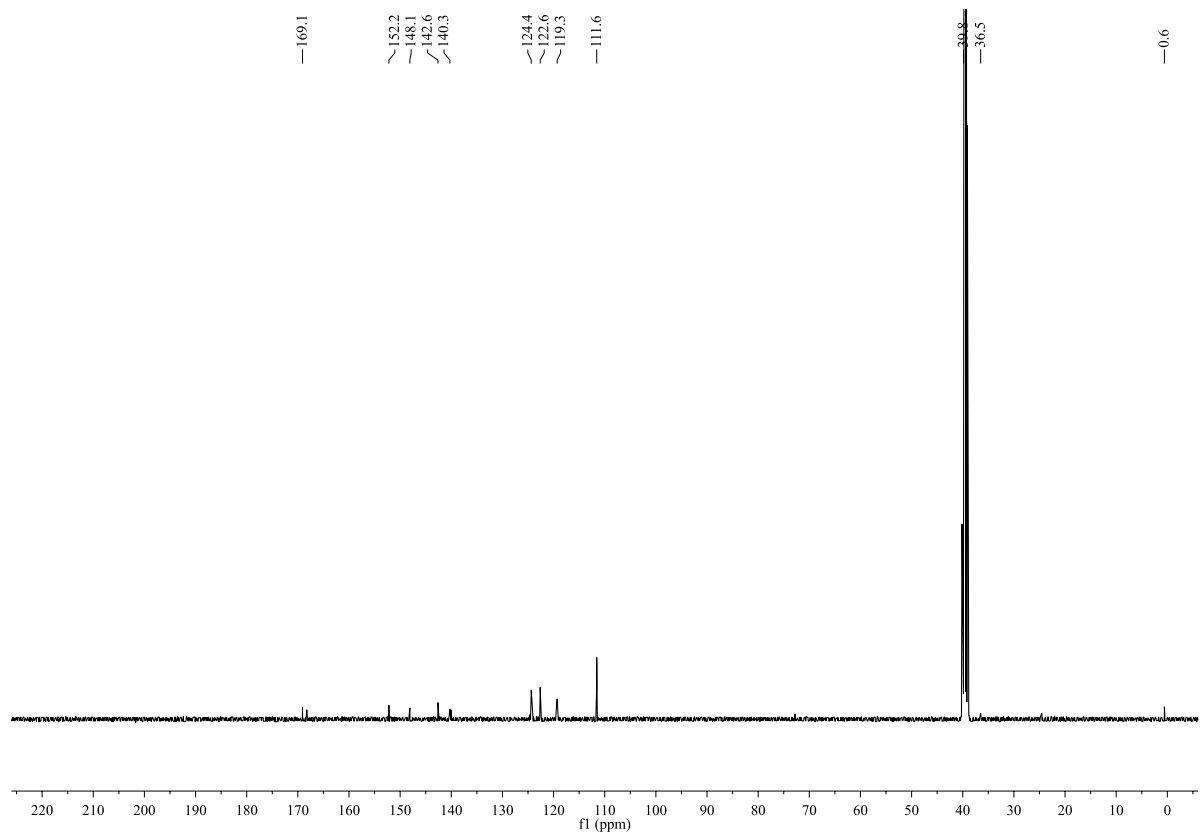


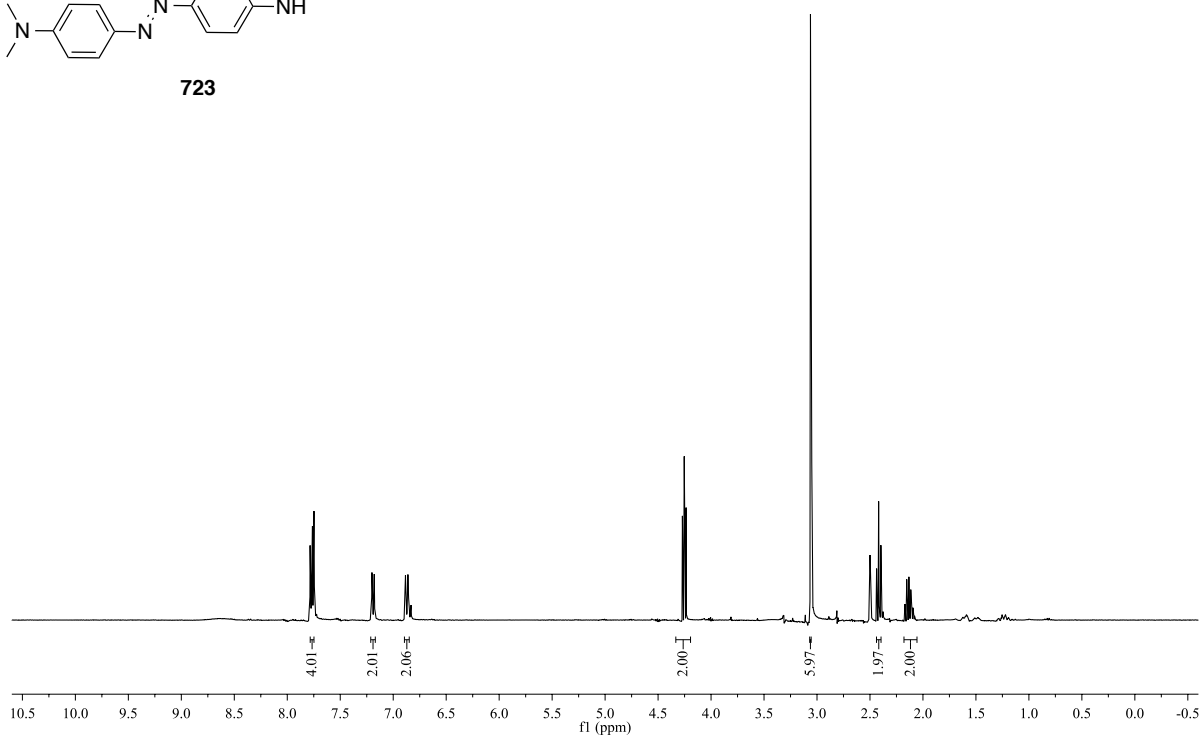
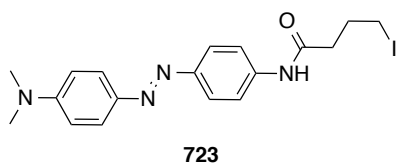
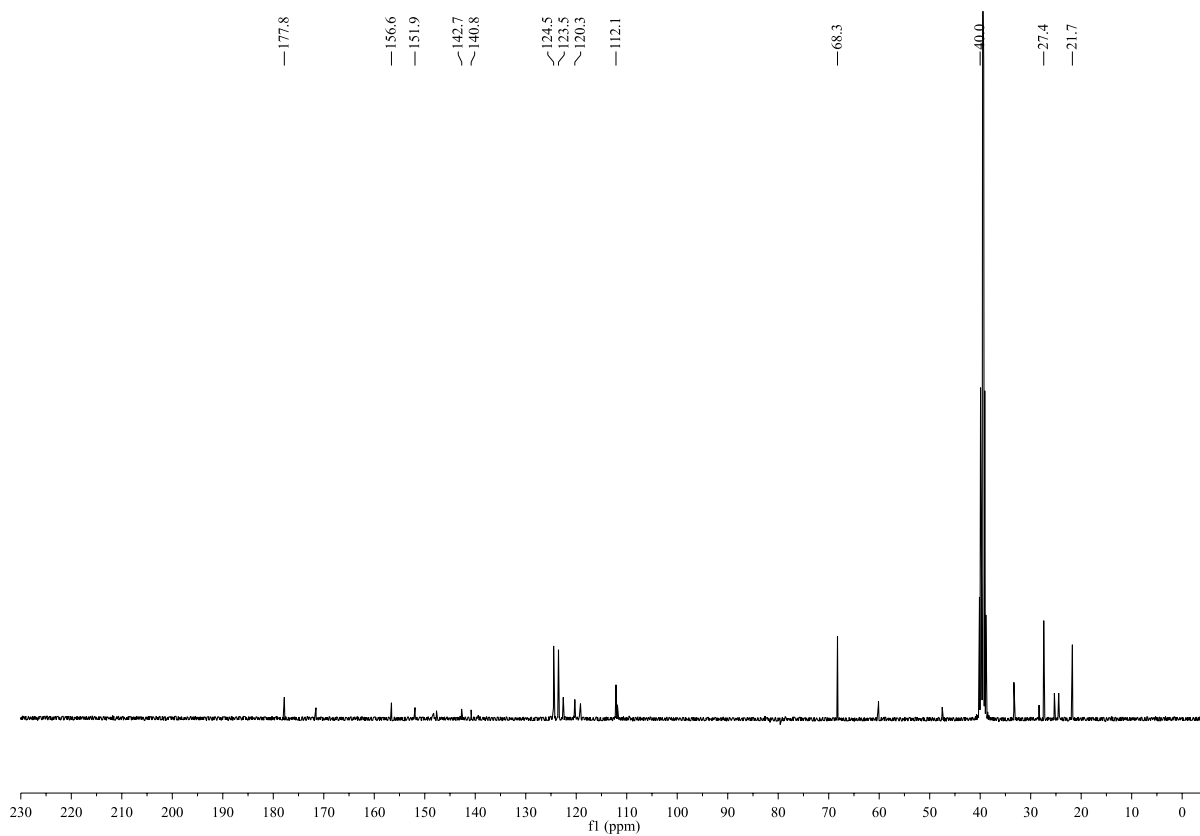
^1H NMR (DMSO- d_6 , 400 MHz): ^{13}C NMR (DMSO- d_6 , 100 MHz):

^1H NMR (DMSO- d_6 , 600 MHz):

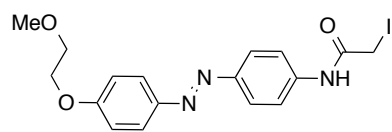


^{13}C NMR (DMSO- d_6 , 150 MHz):

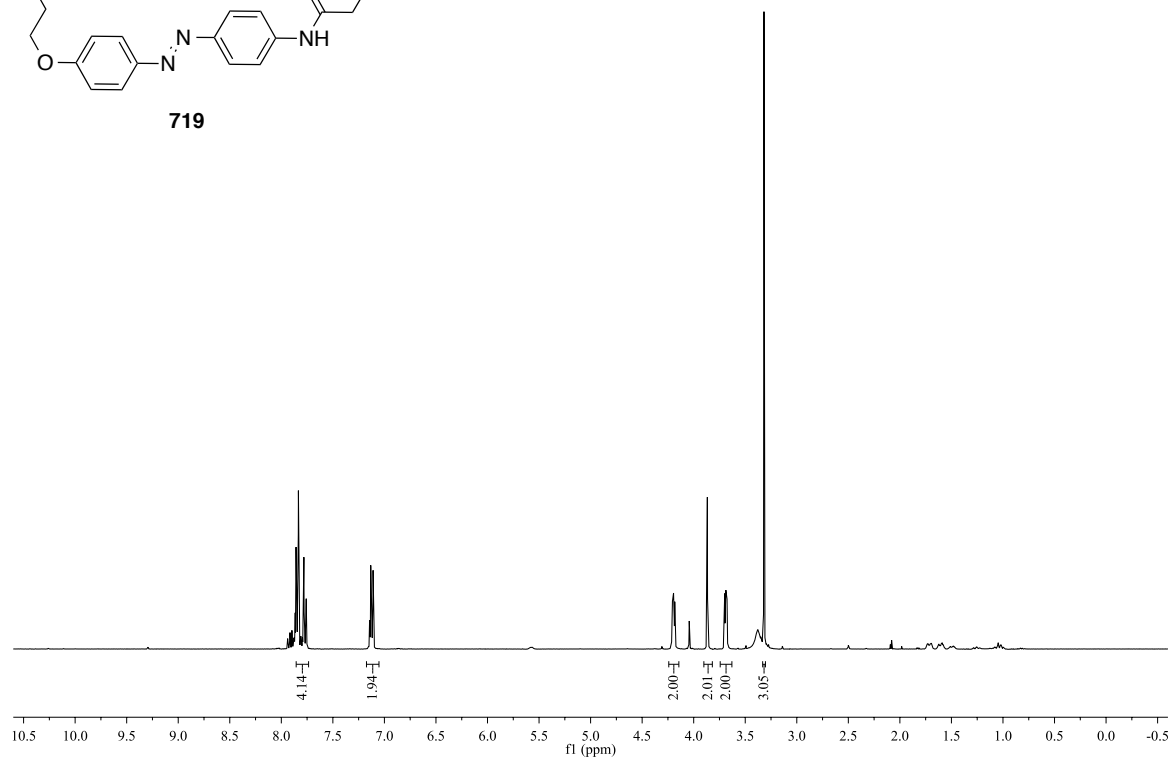


^1H NMR (DMSO- d_6 , 600 MHz): ^{13}C NMR (DMSO- d_6 , 150 MHz):

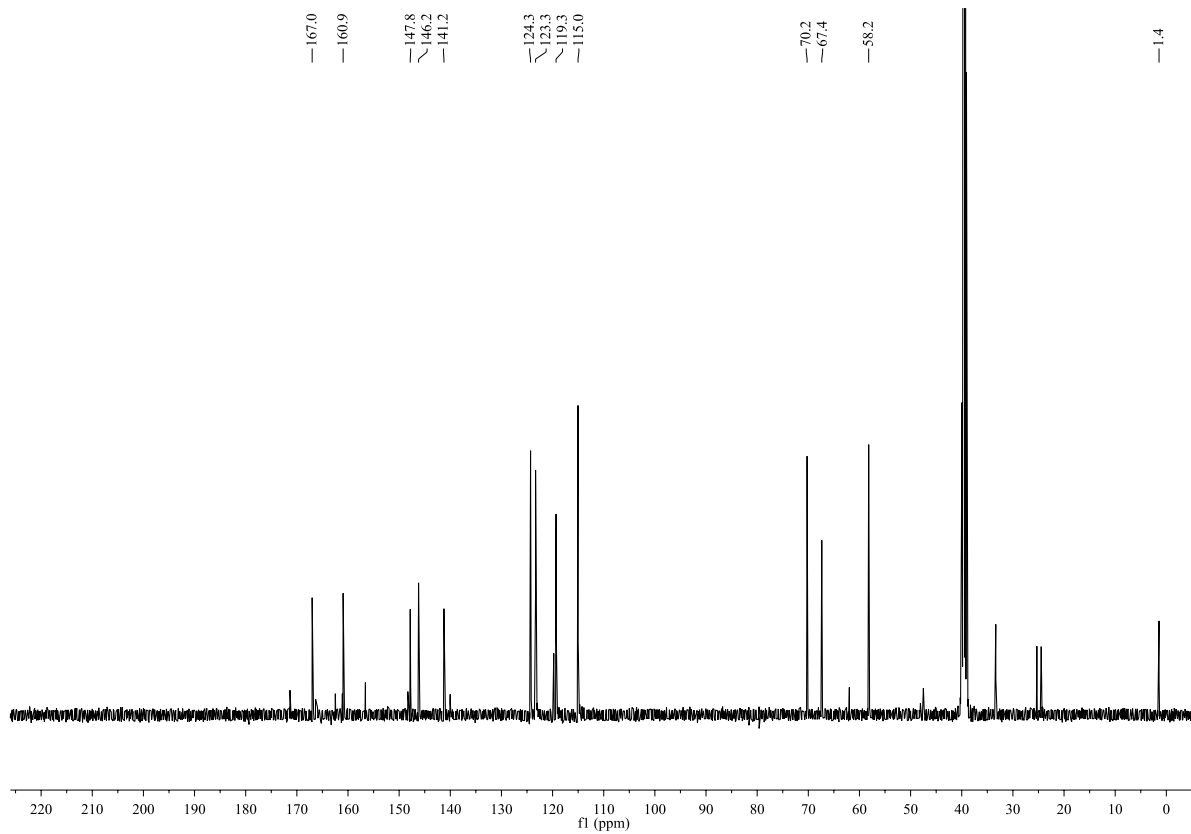
^1H NMR (DMSO- d_6 , 400 MHz):



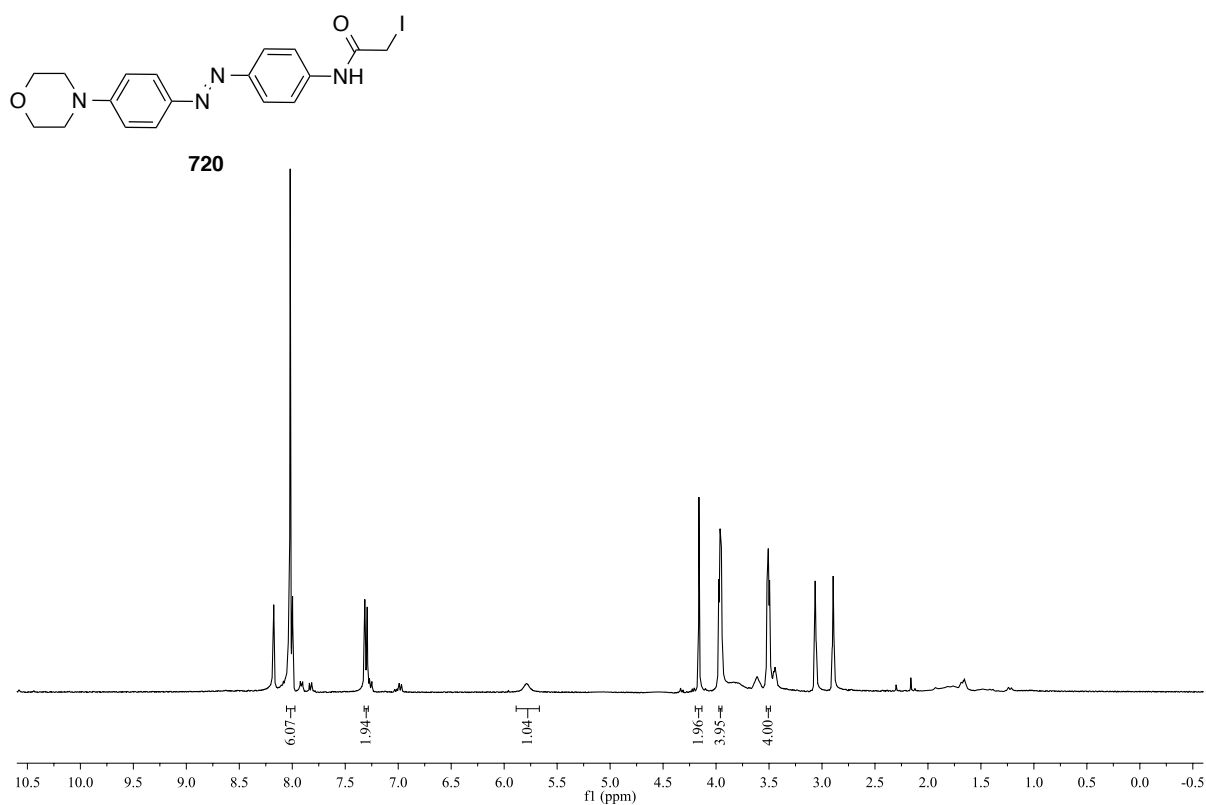
719



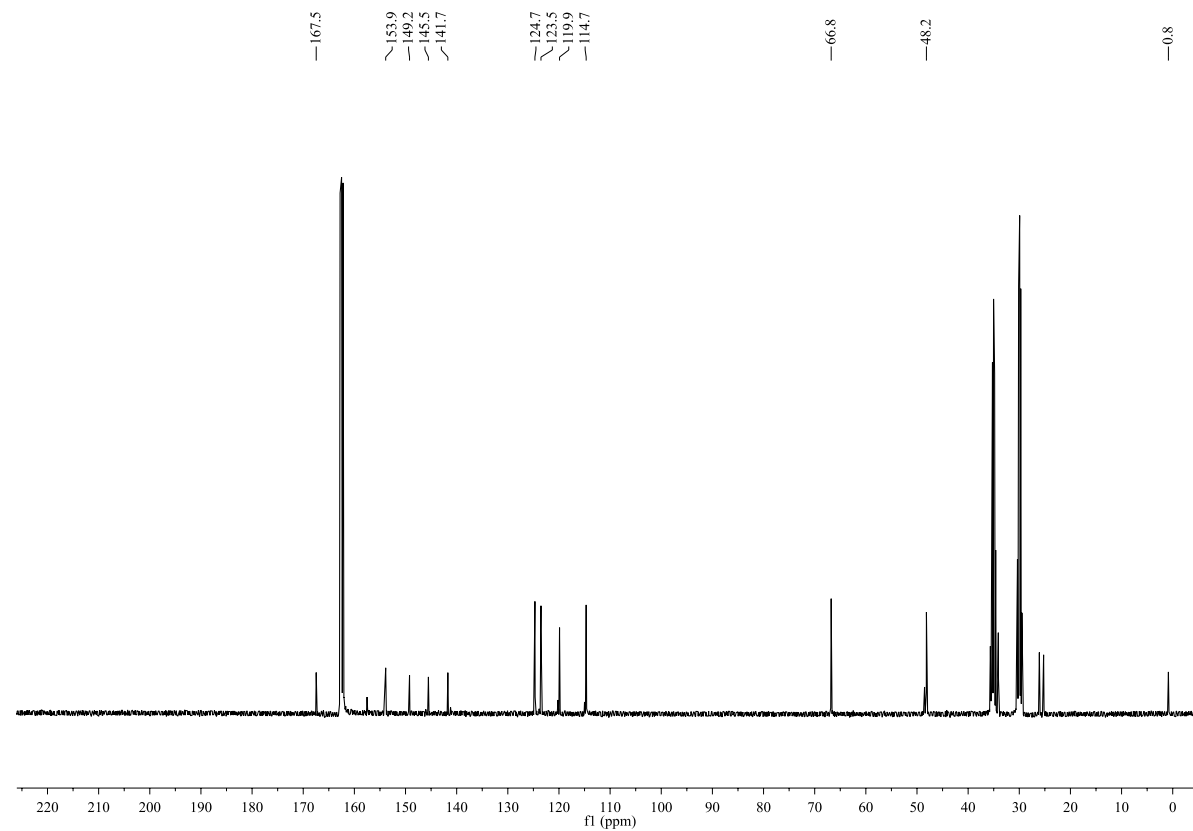
^{13}C NMR (DMSO- d_6 , 100 MHz):



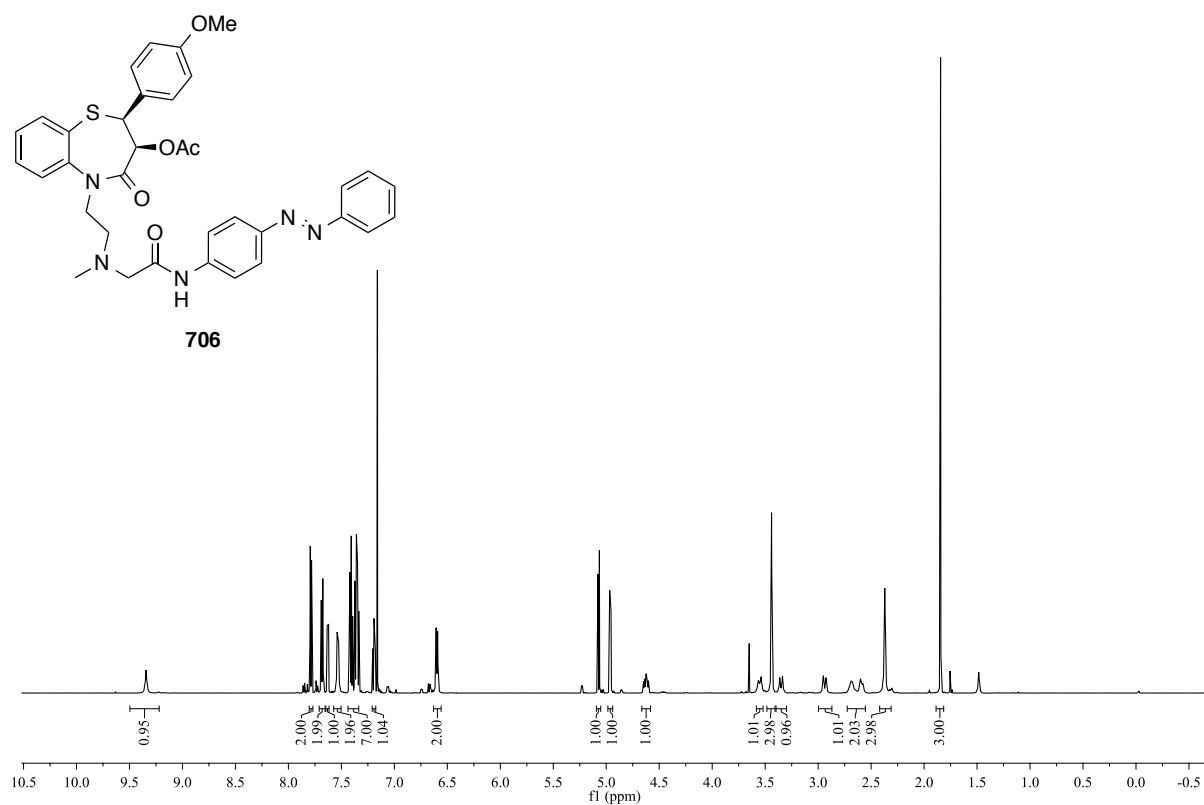
^1H NMR (DMF- d_7 , 400 MHz):



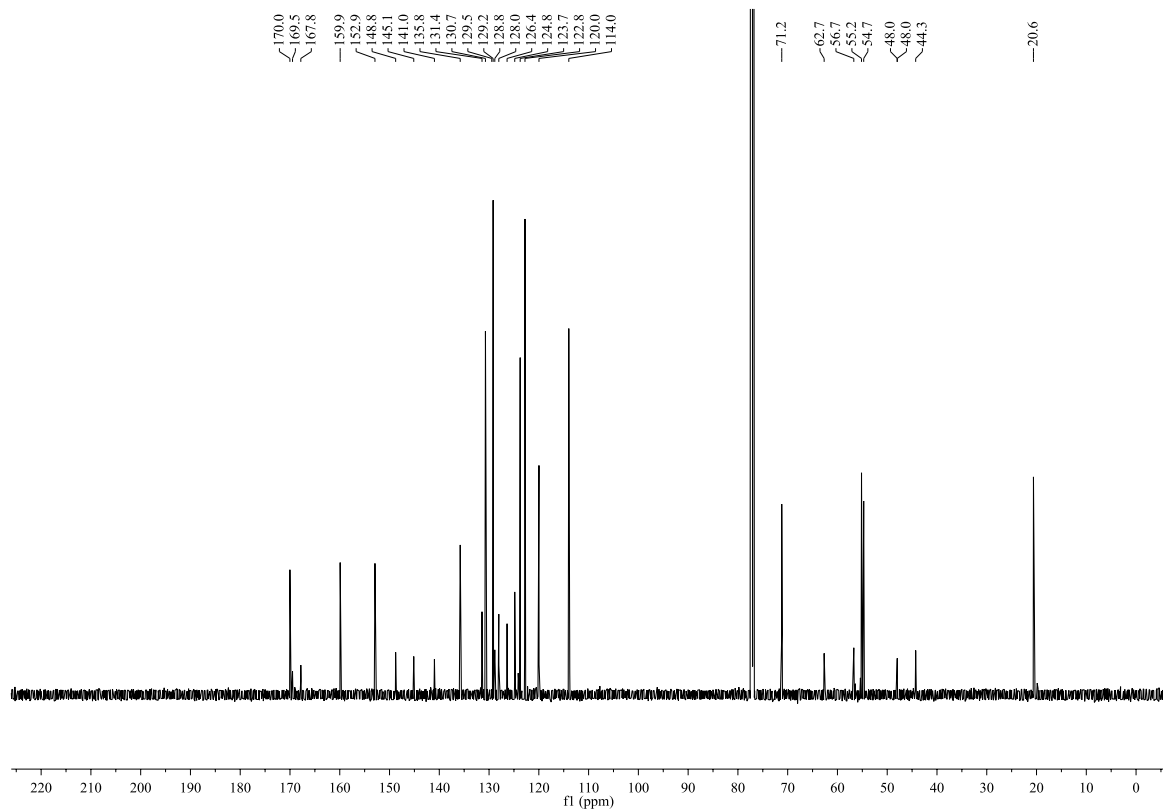
^{13}C NMR (DMF- d_7 , 100 MHz):

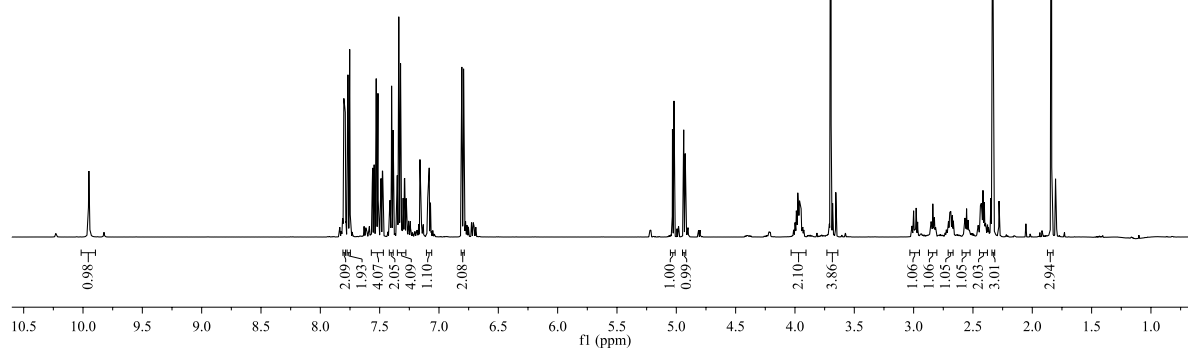
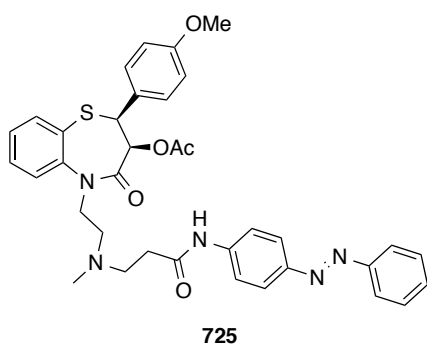
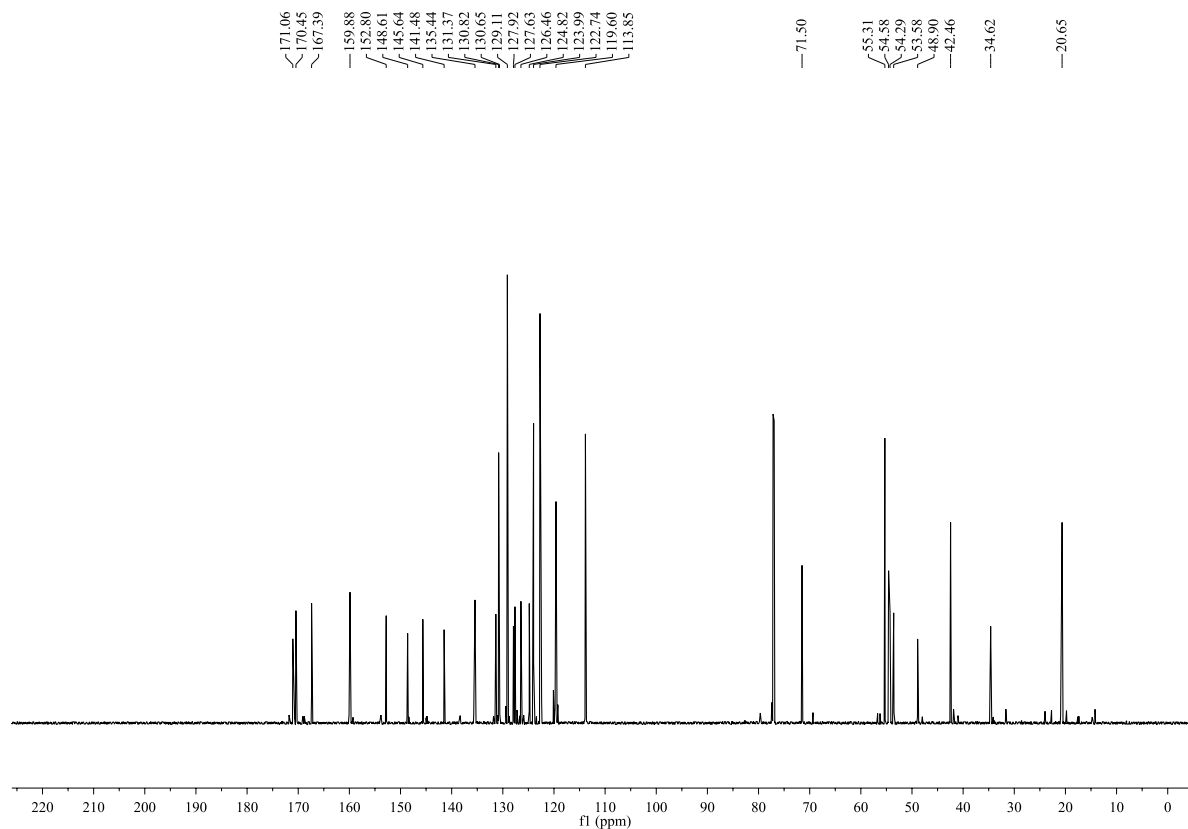


^1H NMR (CDCl_3 , 600 MHz):

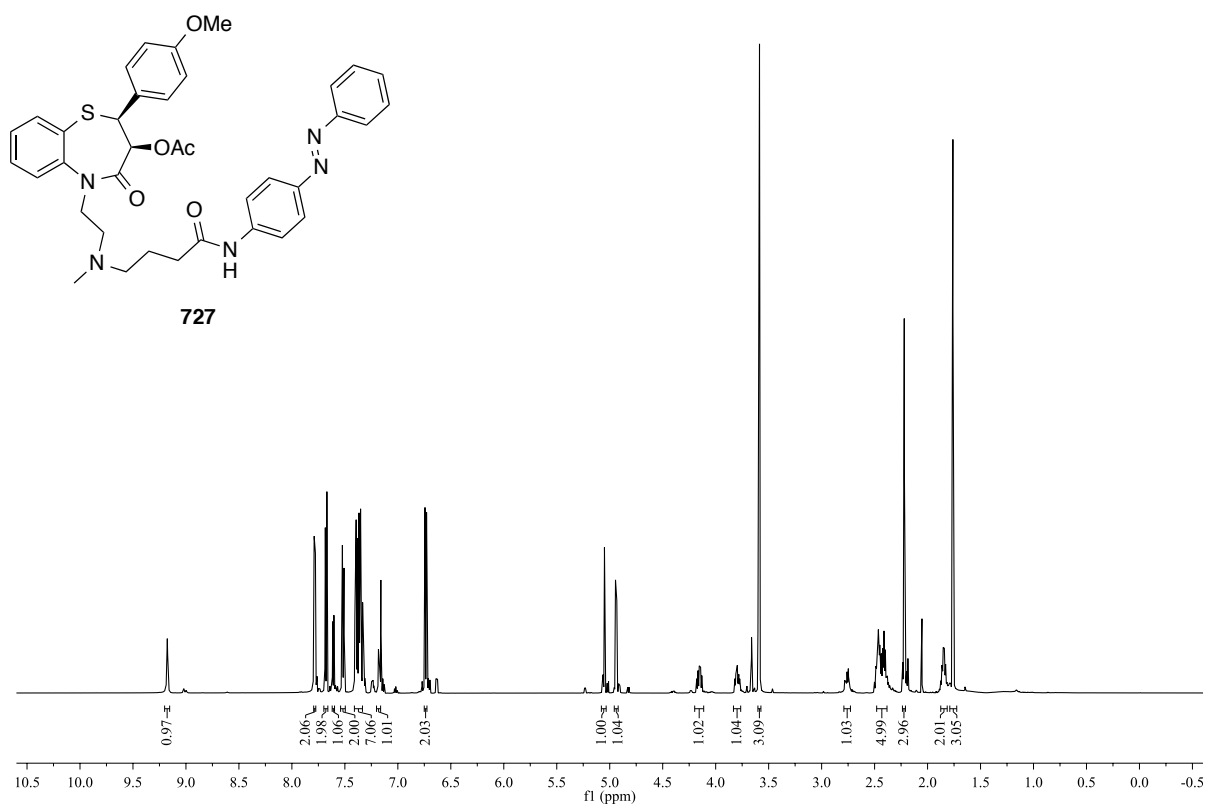


^{13}C NMR (CDCl_3 , 150 MHz):

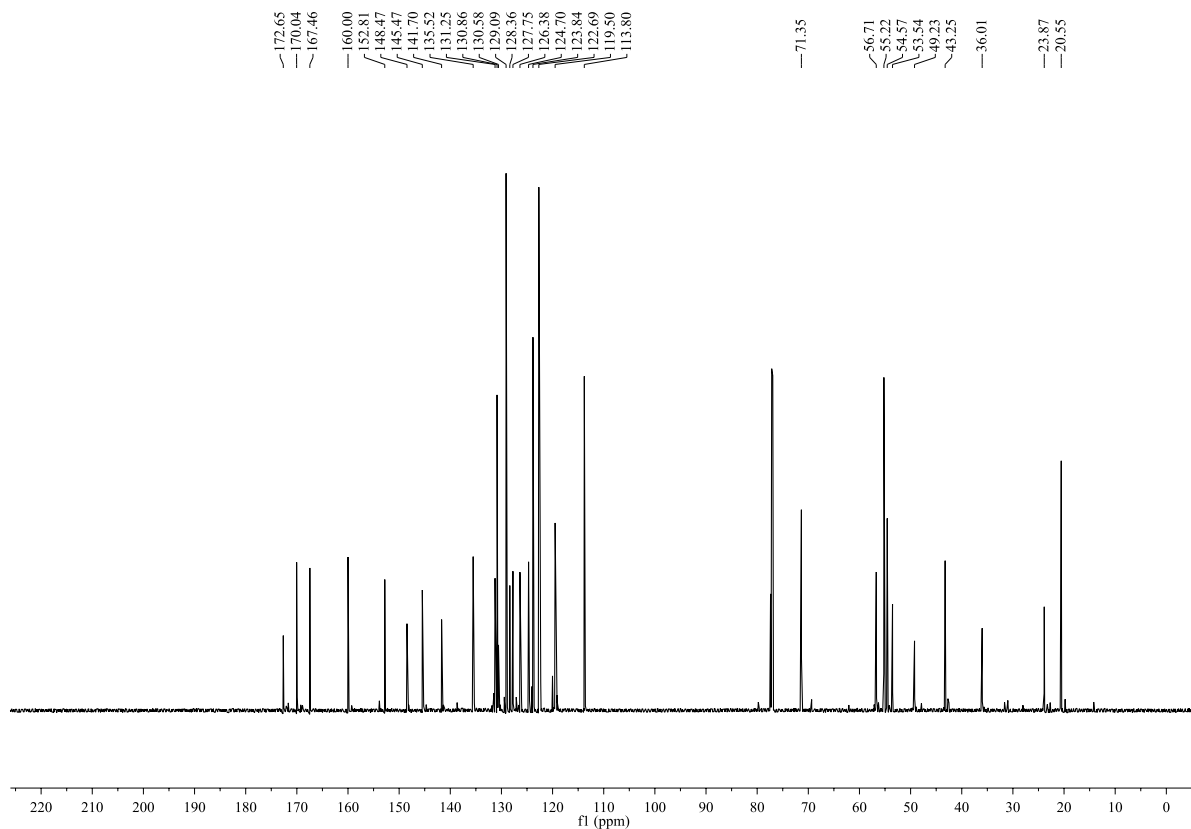


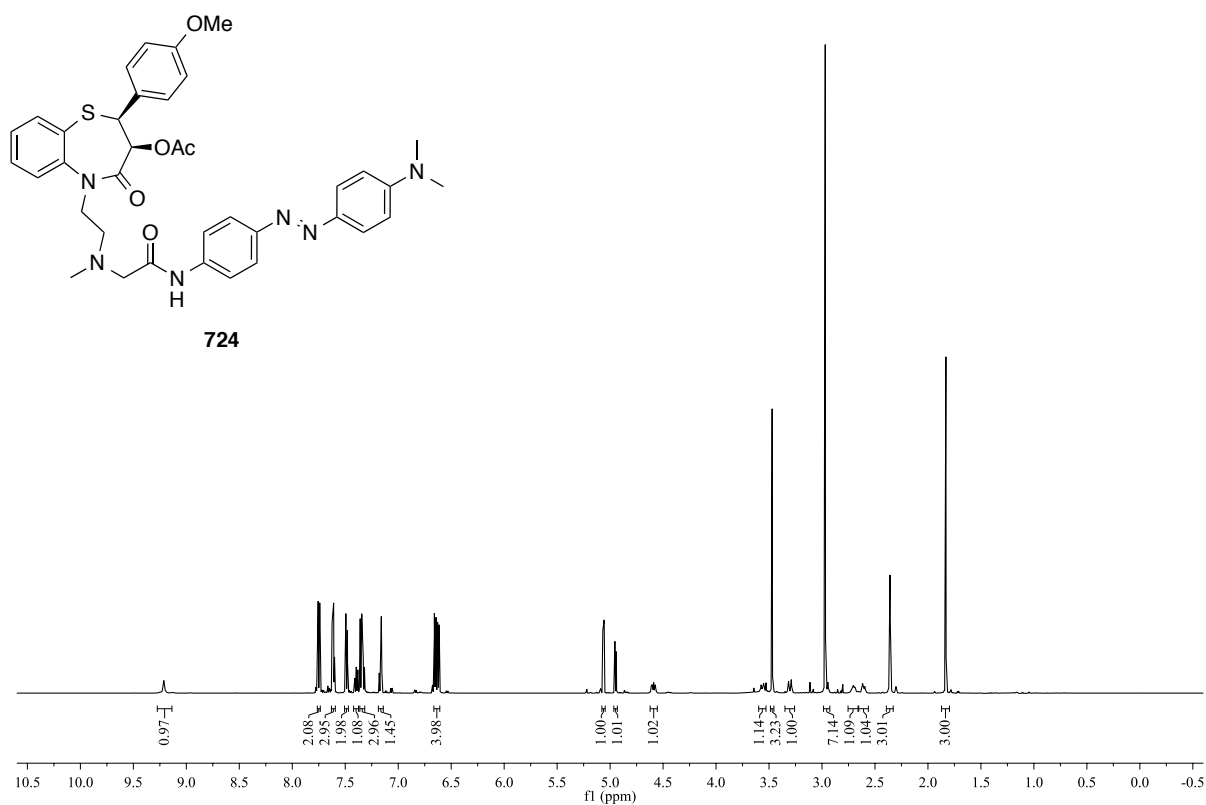
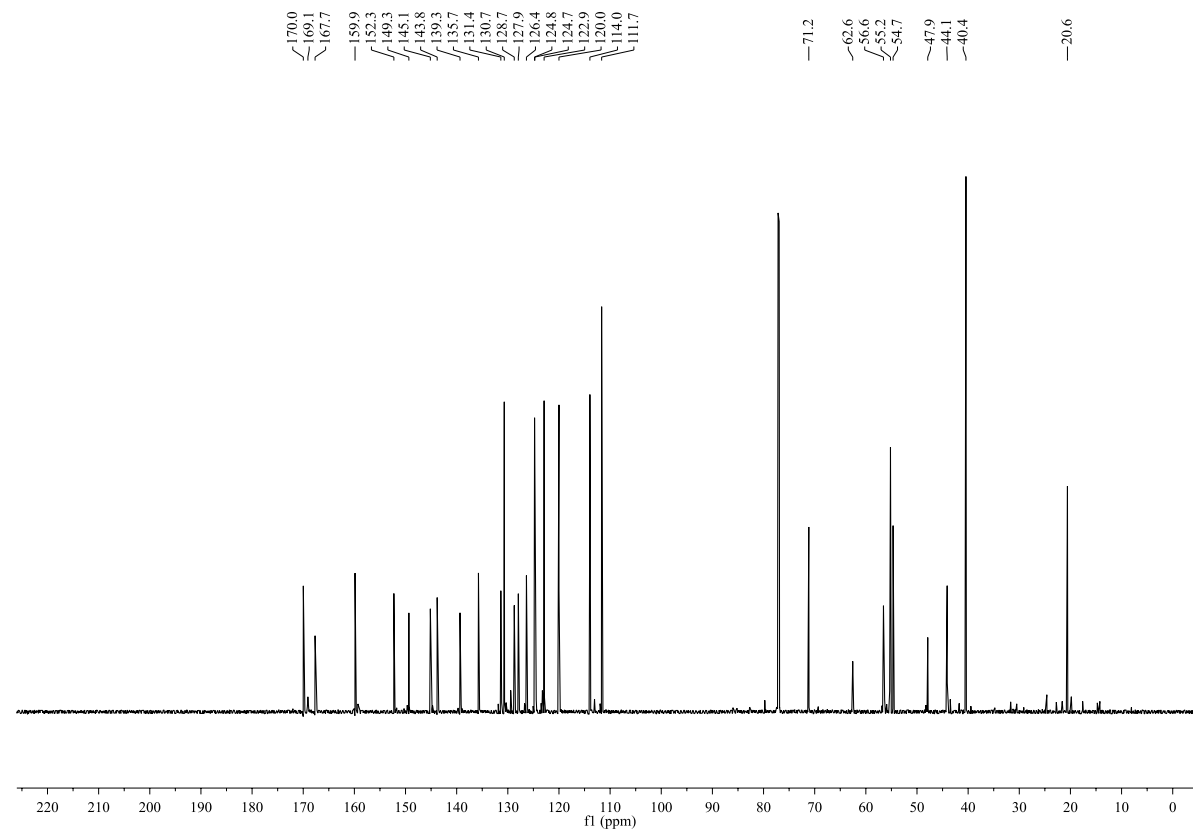
^1H NMR (CDCl_3 , 600 MHz): ^{13}C NMR (CDCl_3 , 150 MHz):

^1H NMR (CDCl_3 , 600 MHz):

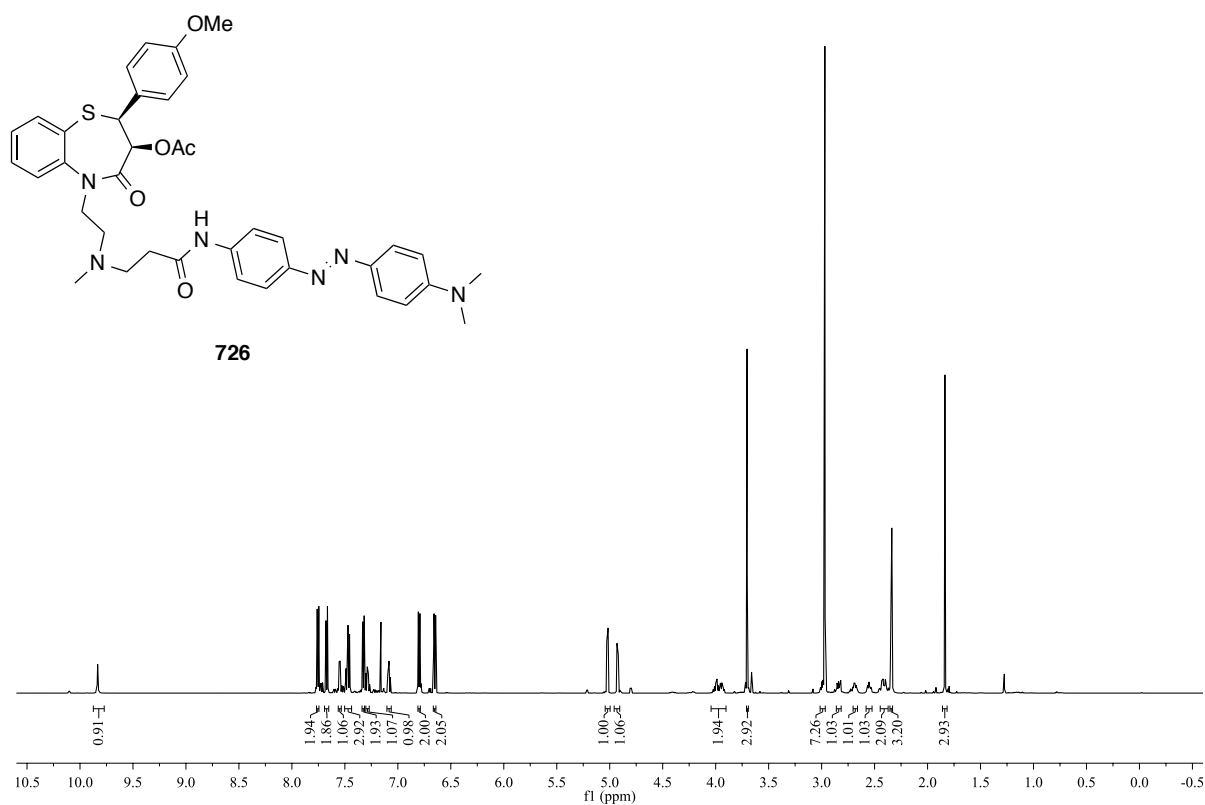


^{13}C NMR (CDCl_3 , 150 MHz):

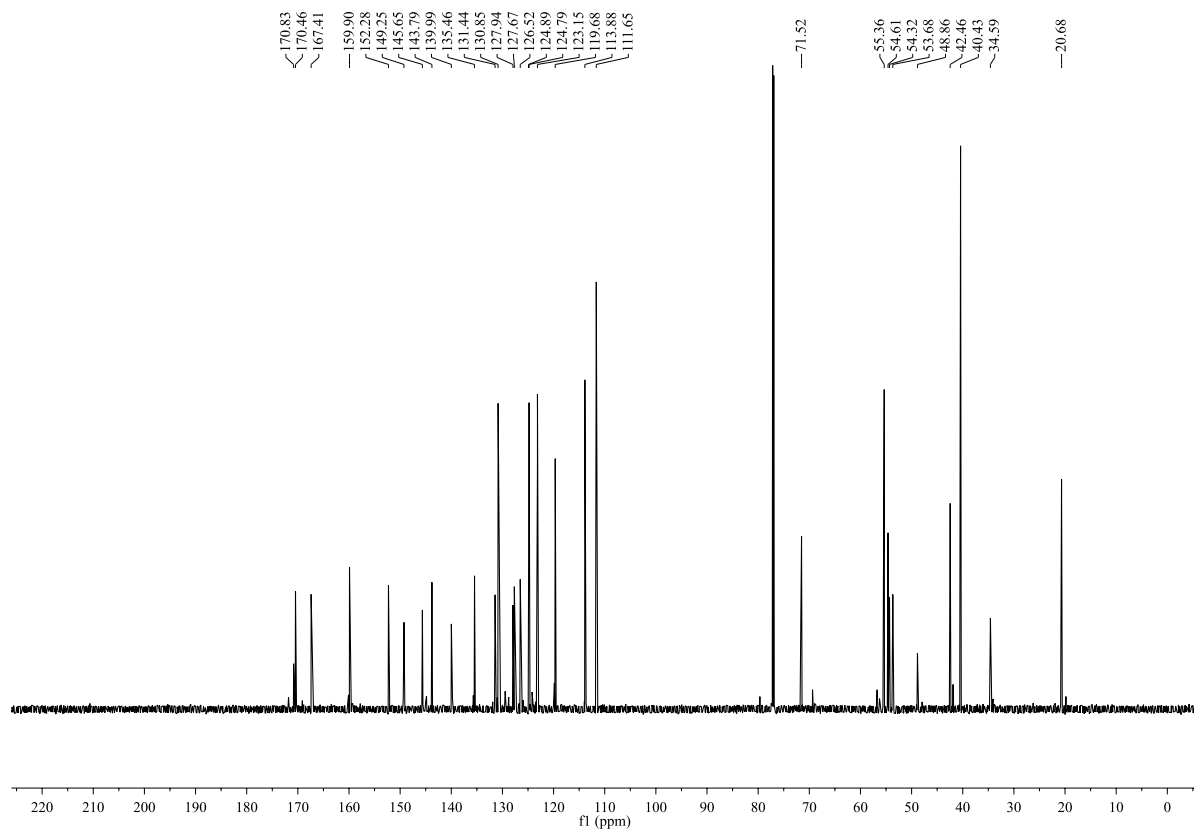


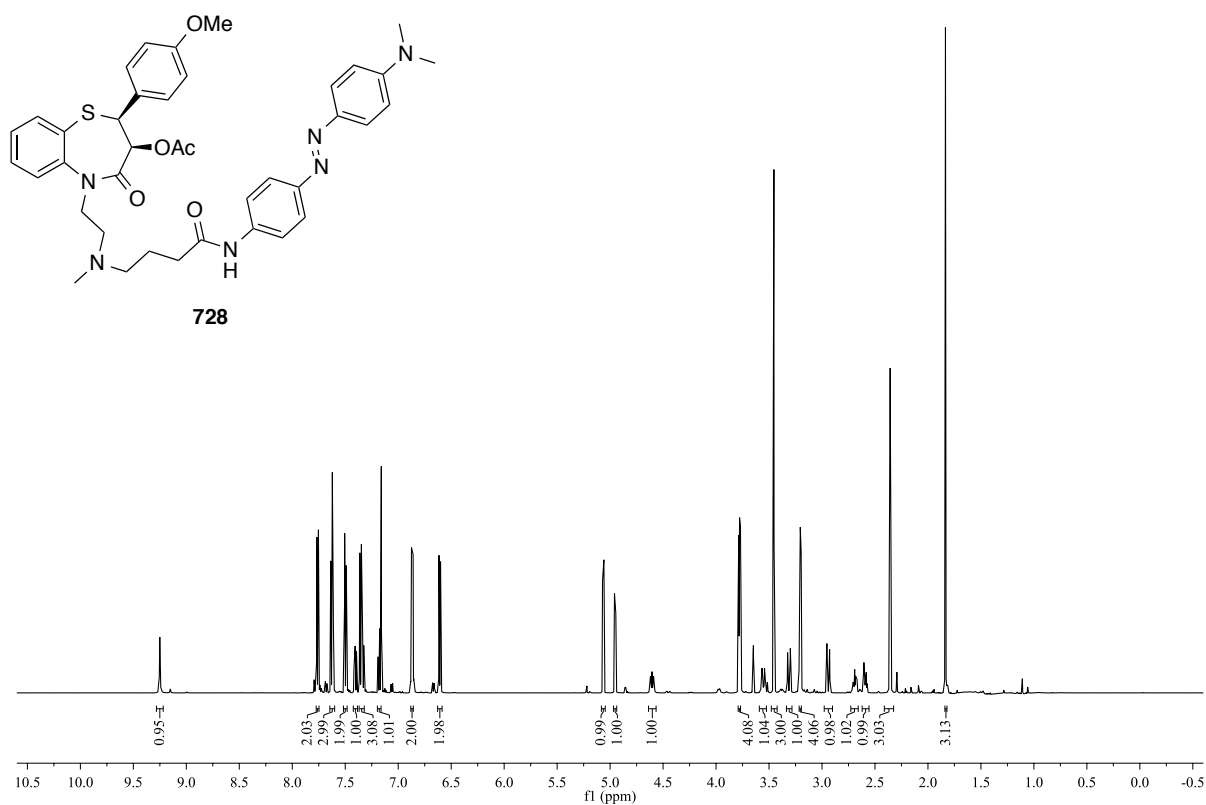
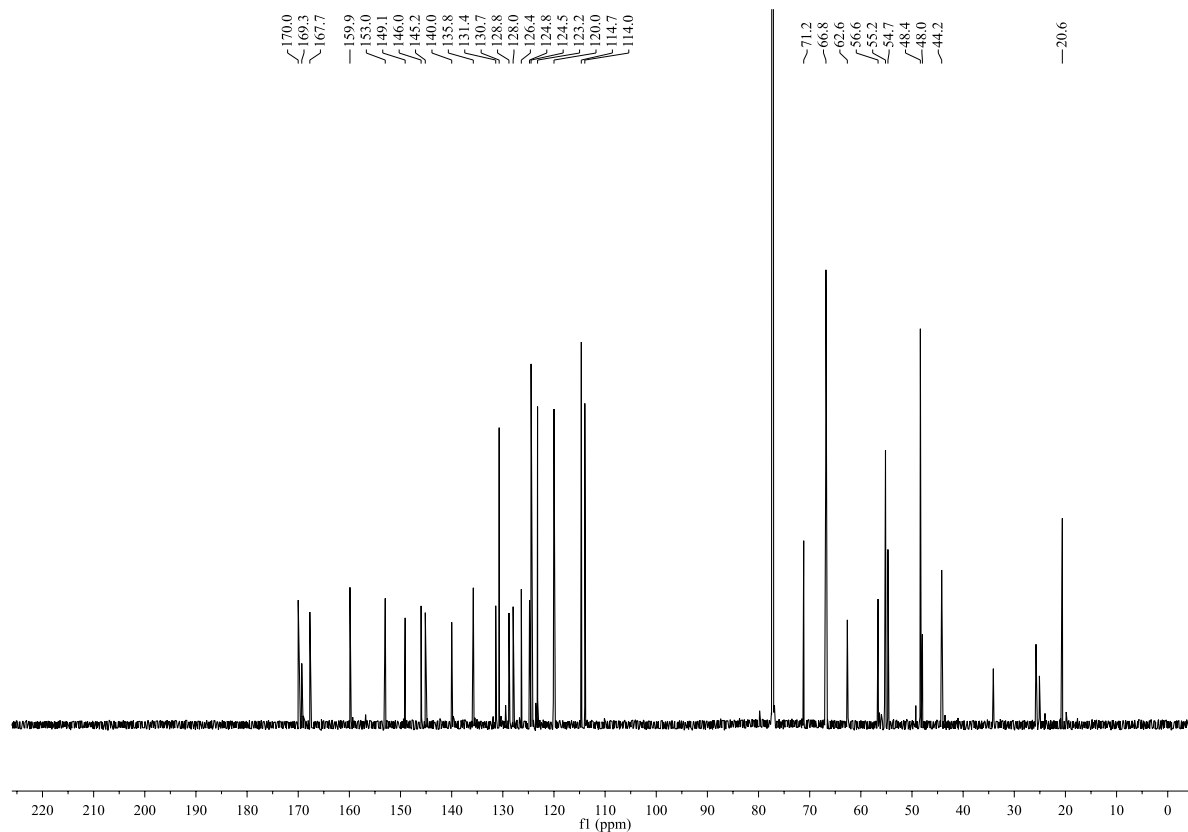
^1H NMR (CDCl_3 , 600 MHz): ^{13}C NMR (CDCl_3 , 150 MHz):

^1H NMR (CDCl_3 , 600 MHz):

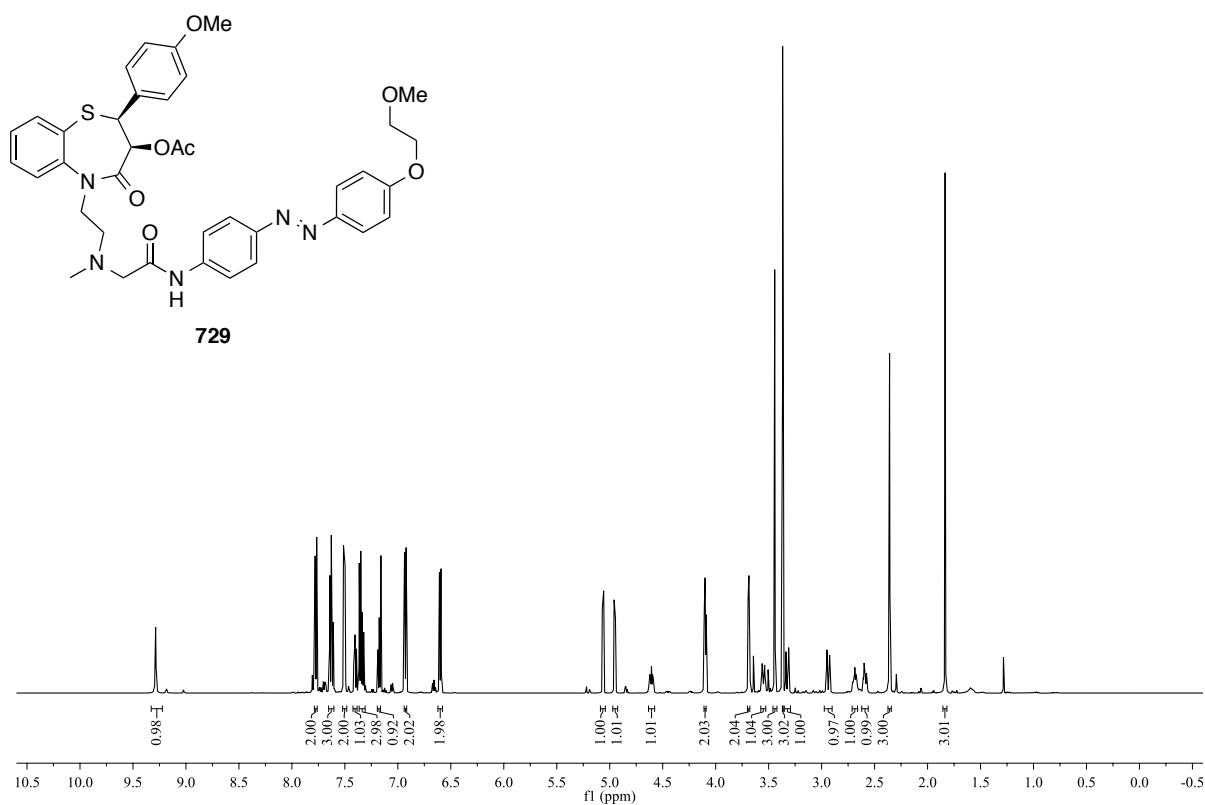


^{13}C NMR (CDCl_3 , 150 MHz):

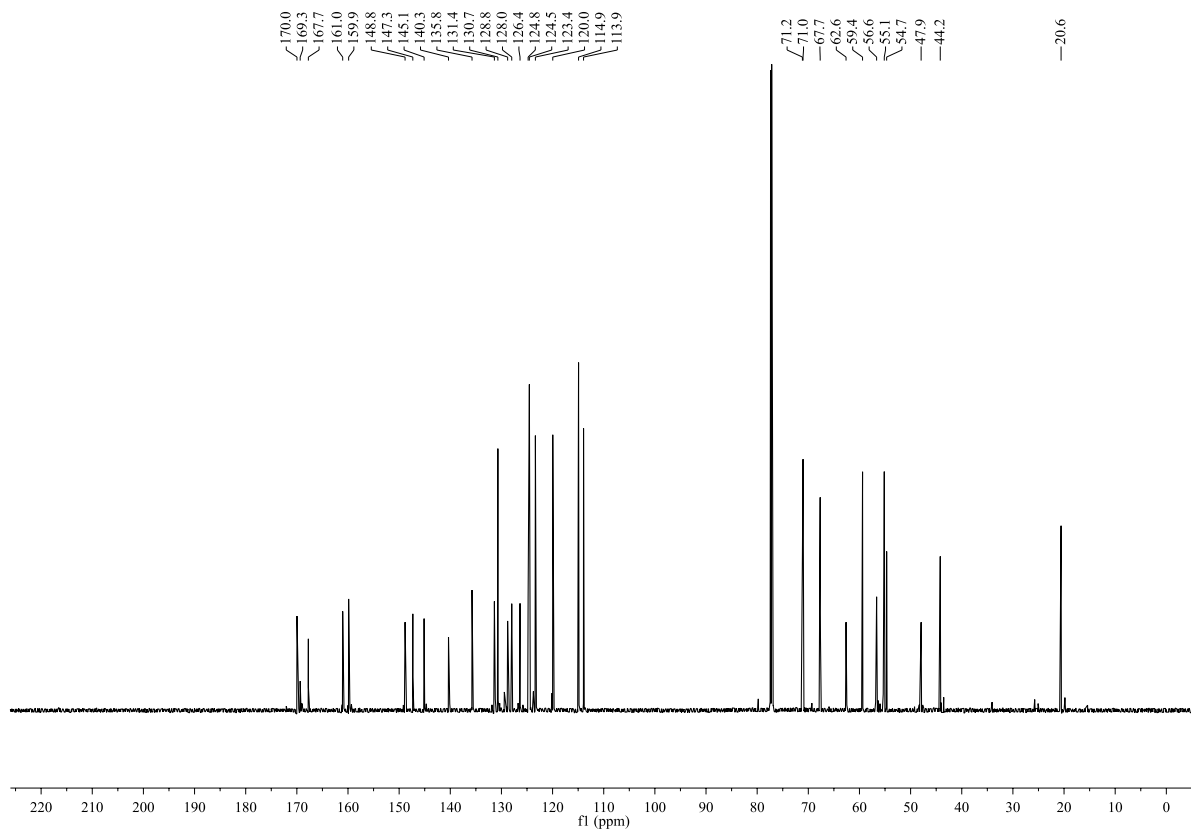


^1H NMR (CDCl_3 , 600 MHz): ^{13}C NMR (CDCl_3 , 150 MHz):

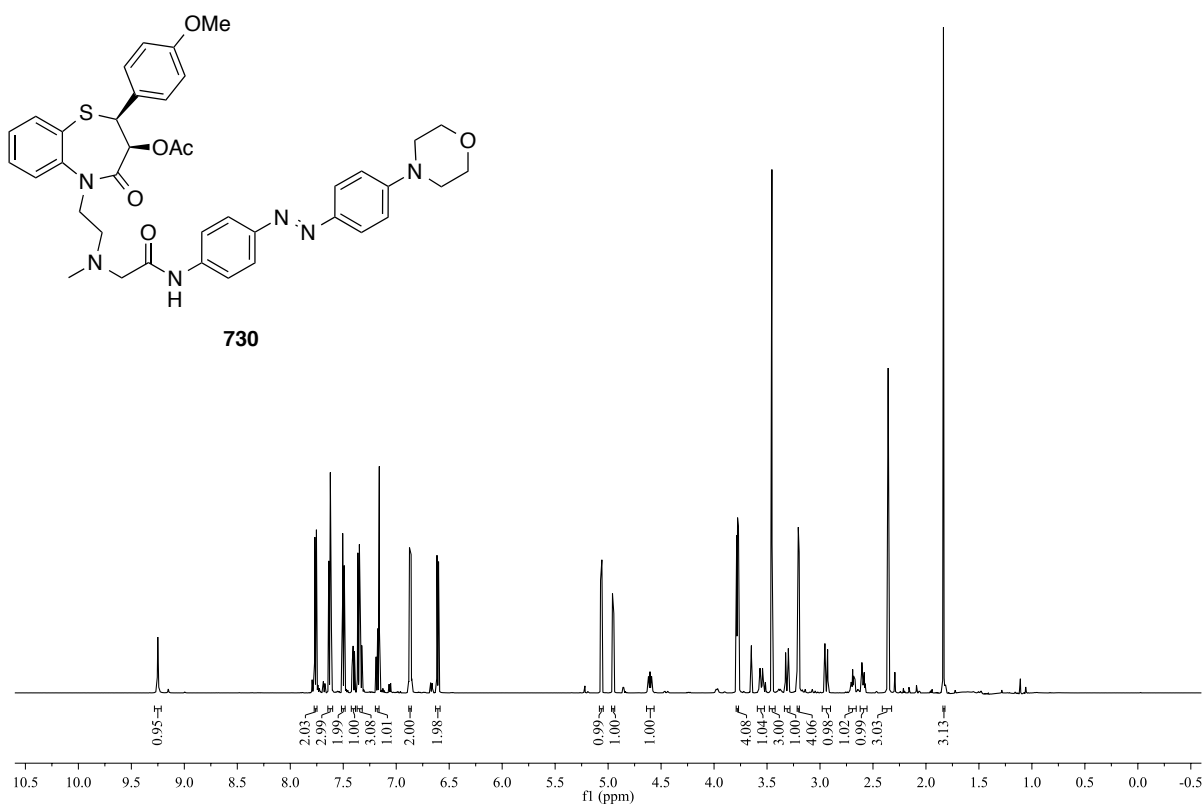
^1H NMR (CDCl_3 , 600 MHz):



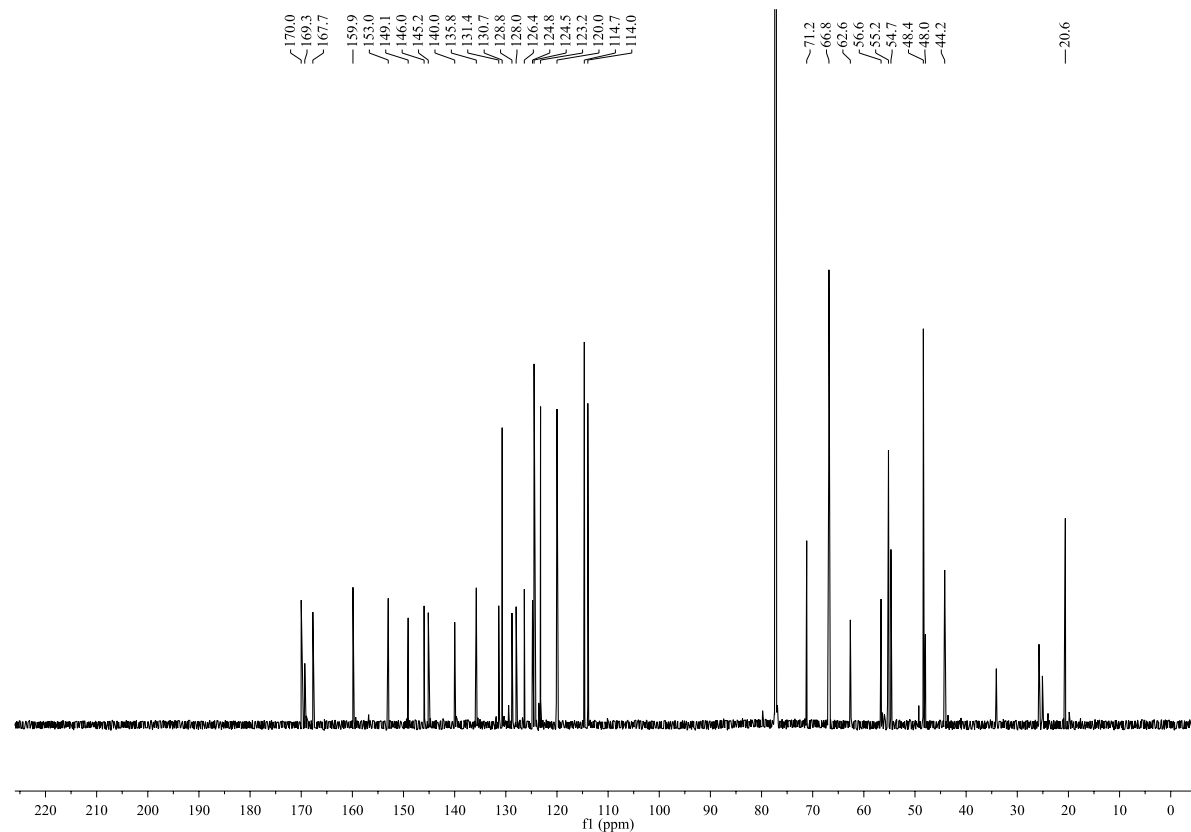
^{13}C NMR (CDCl_3 , 150 MHz):

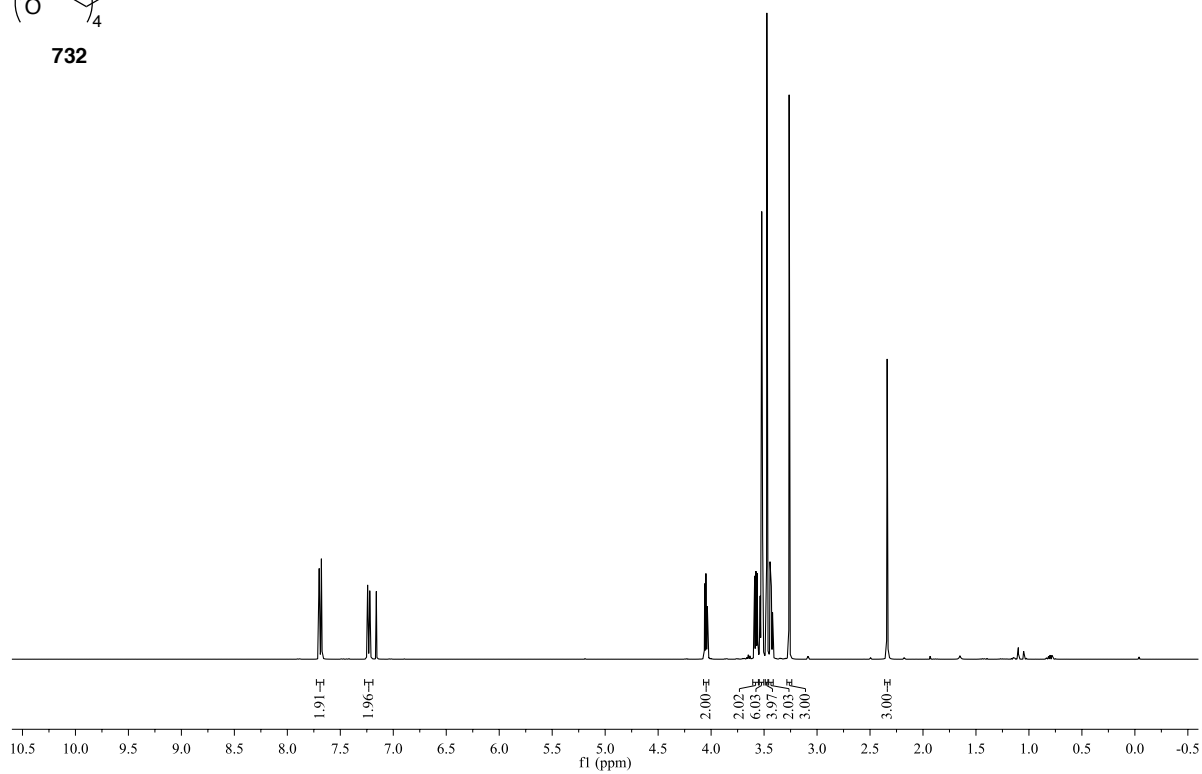
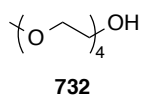
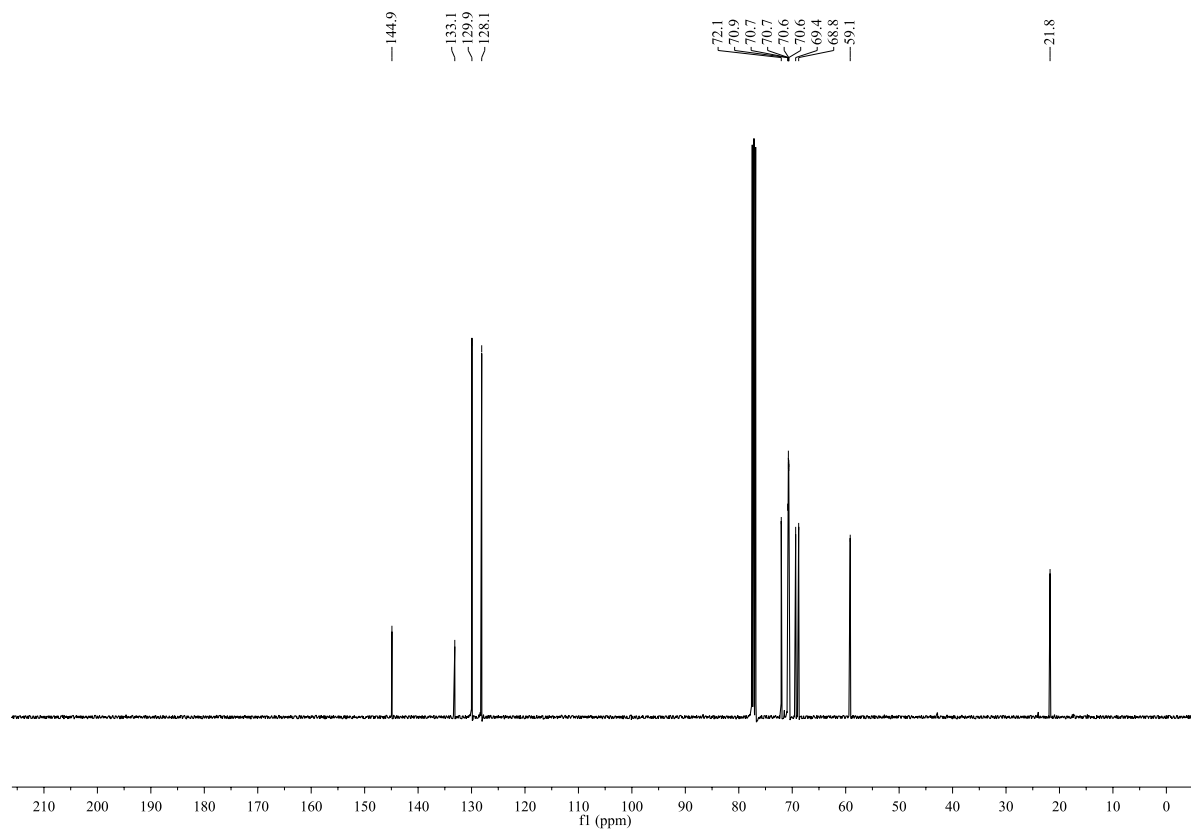


^1H NMR (CDCl_3 , 600 MHz):

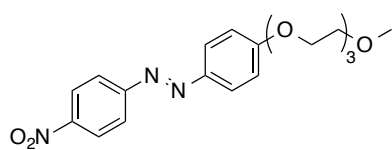


^{13}C NMR (CDCl_3 , 150 MHz):

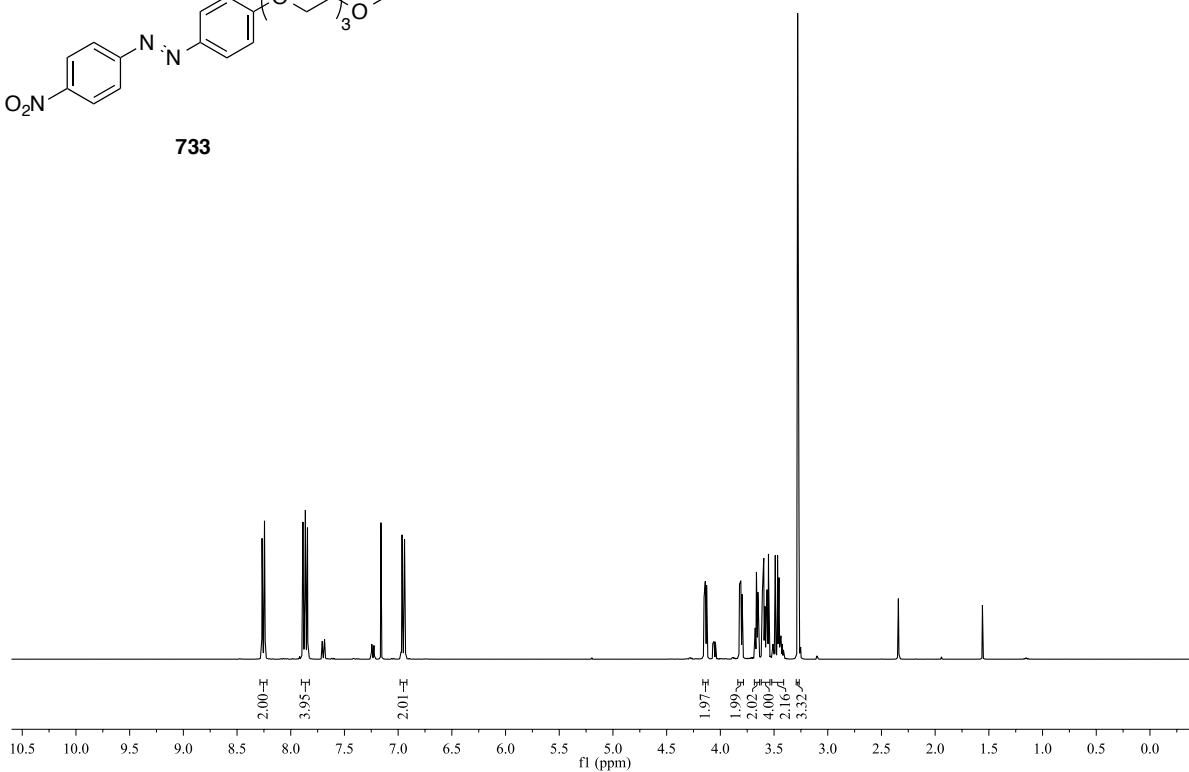


^1H NMR (CDCl_3 , 400 MHz): ^{13}C NMR (CDCl_3 , 100 MHz):

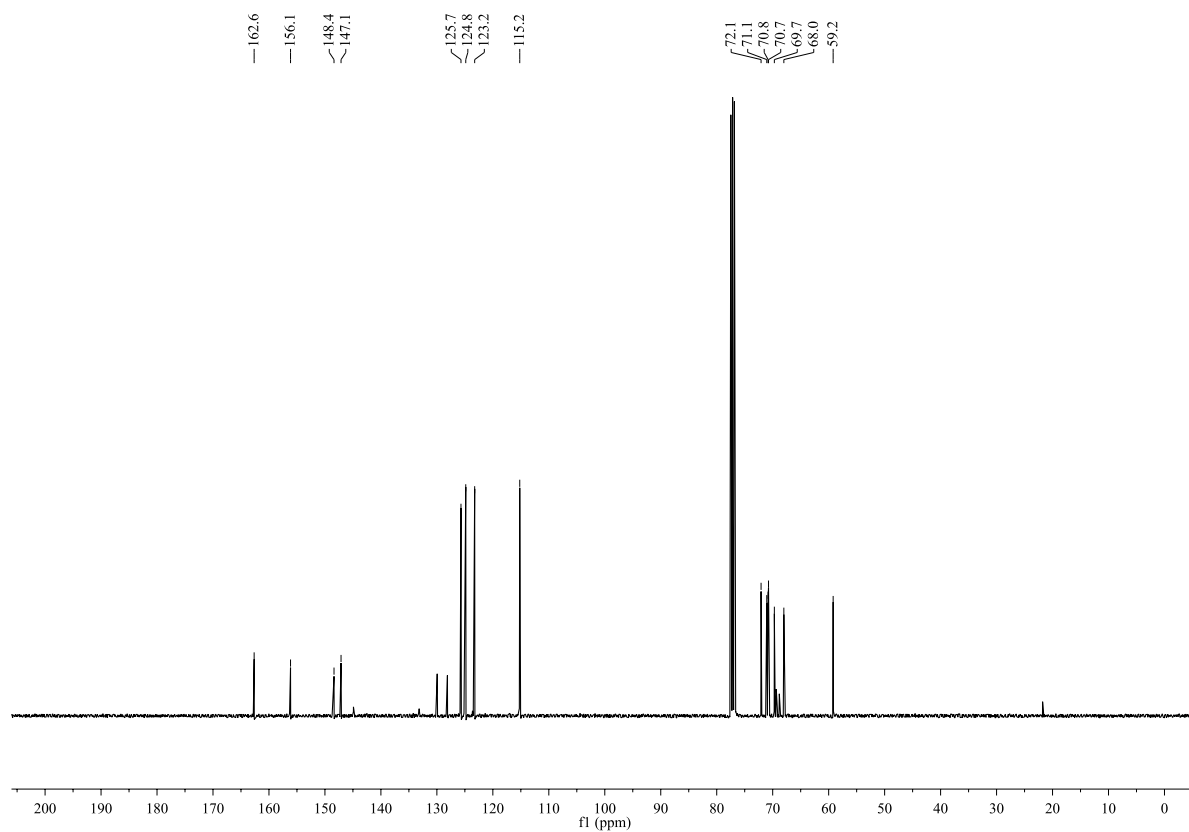
^1H NMR (CDCl_3 , 400 MHz):

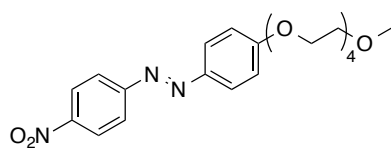
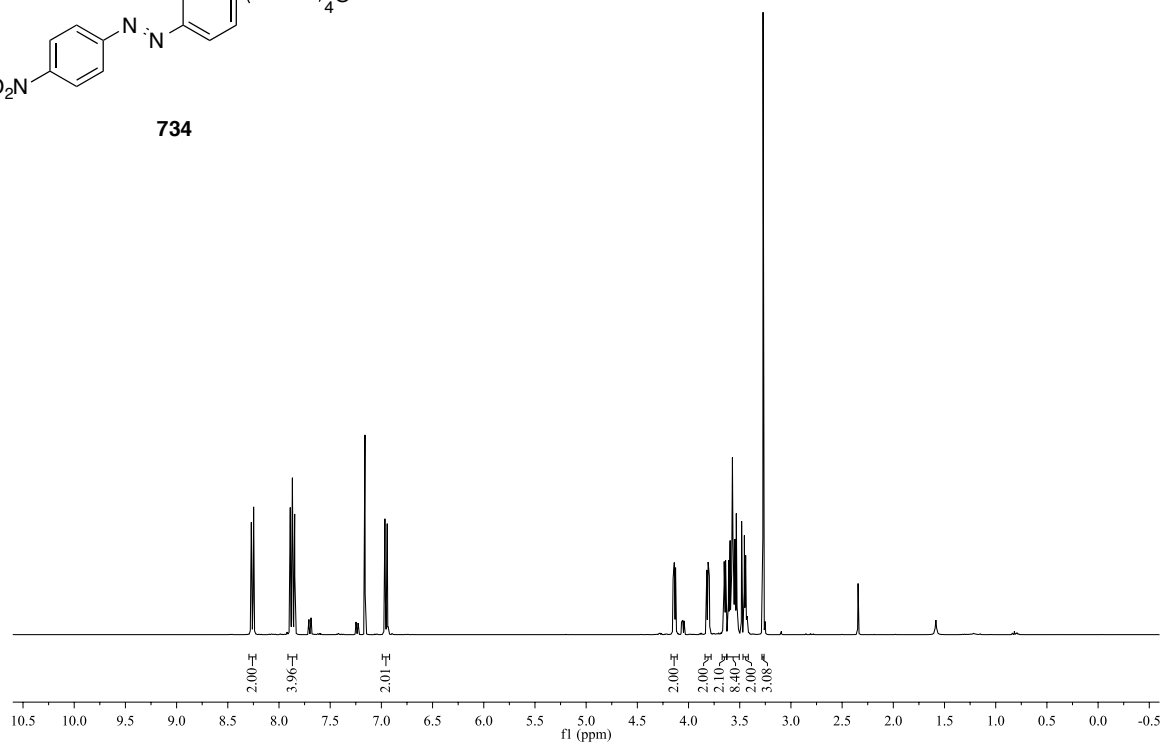
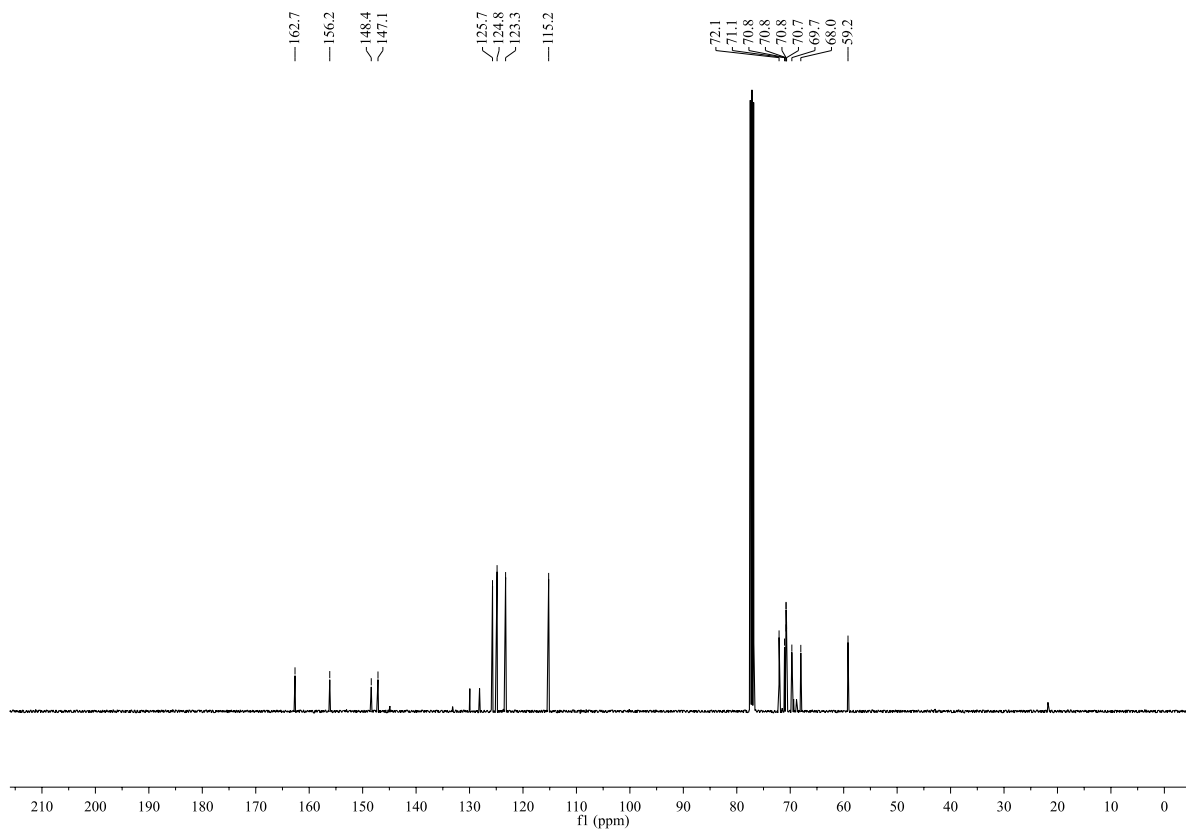


733

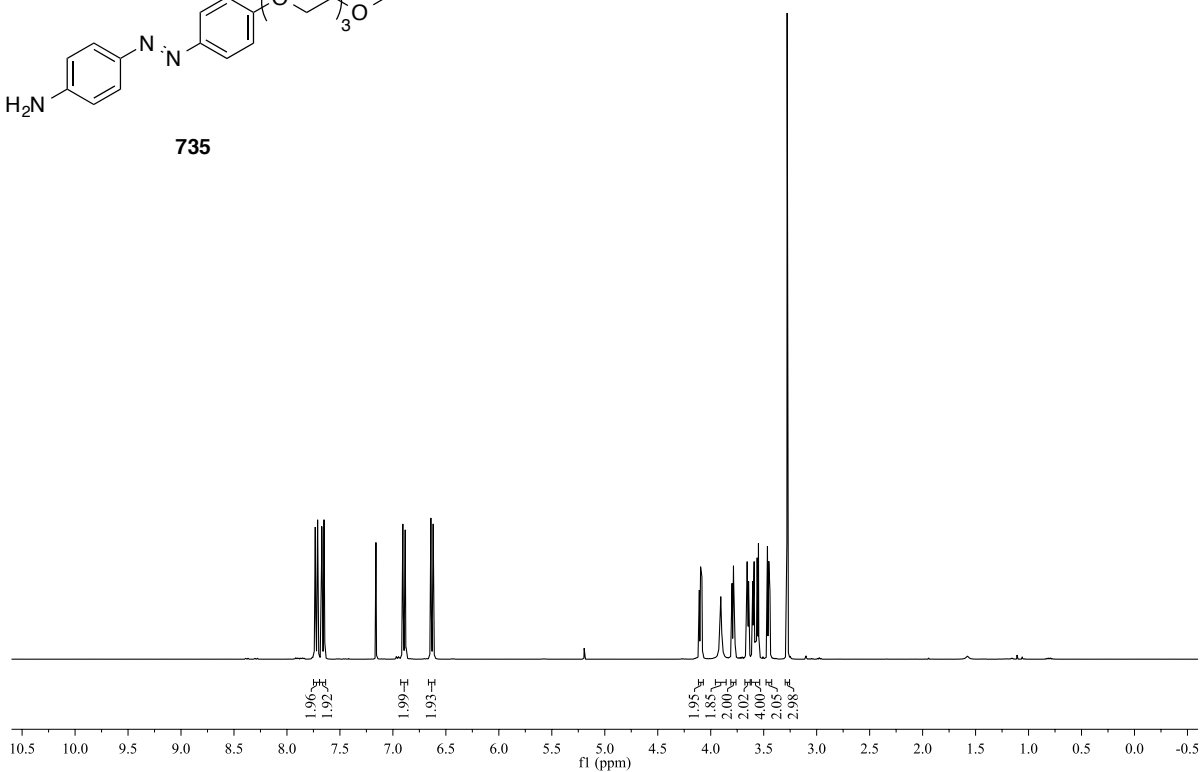
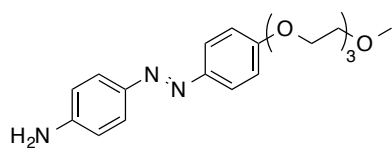


^{13}C NMR (CDCl_3 , 100 MHz):

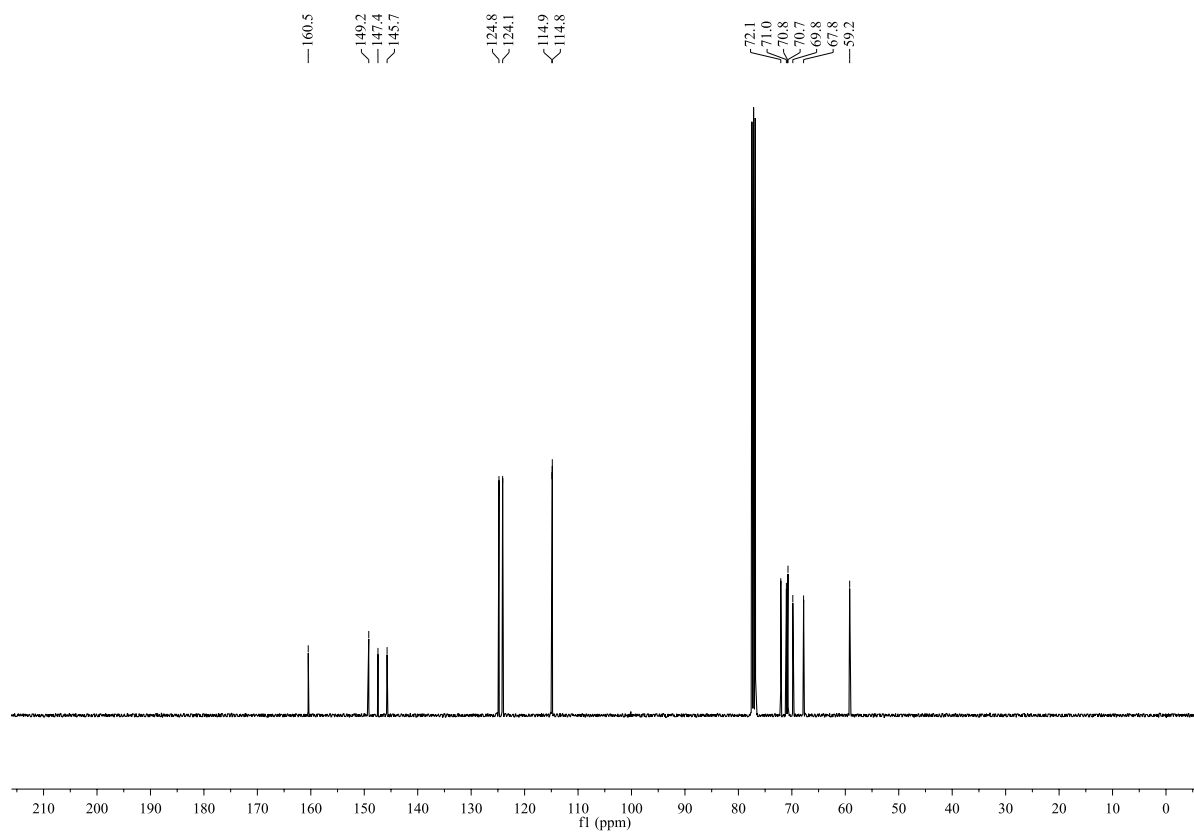


^1H NMR (CDCl_3 , 400 MHz):**734** ^{13}C NMR (CDCl_3 , 100 MHz):

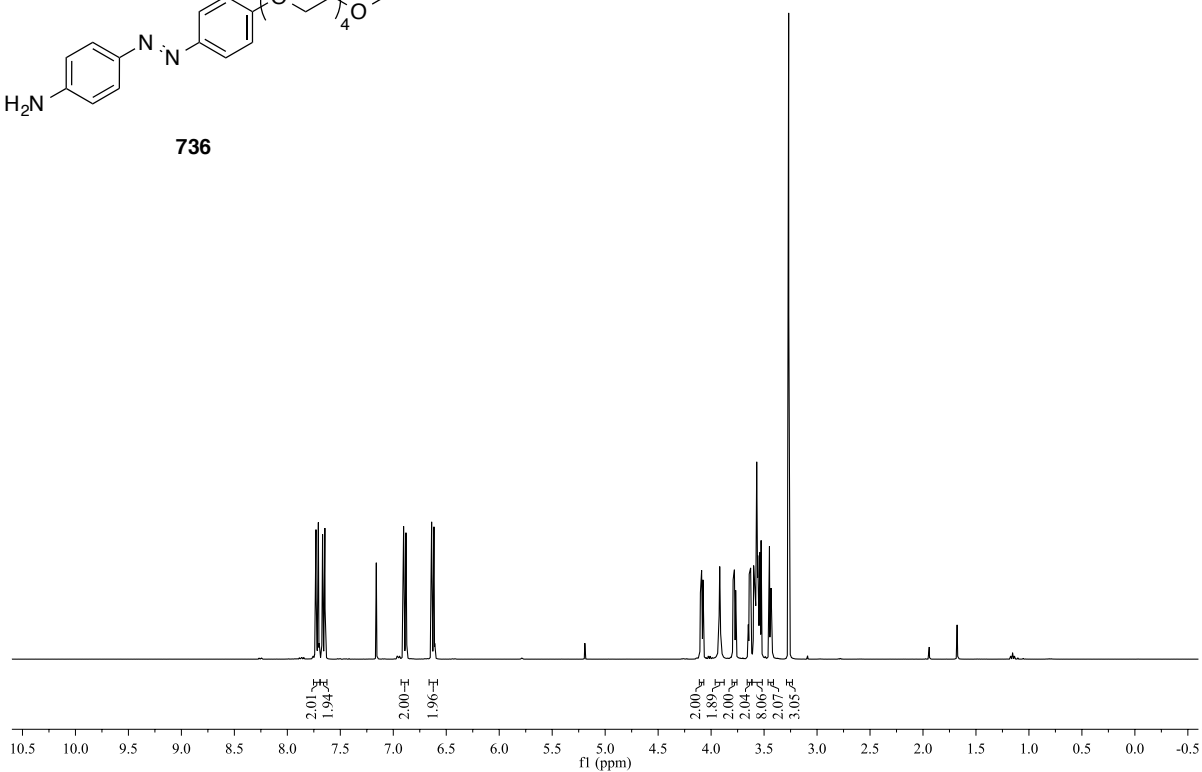
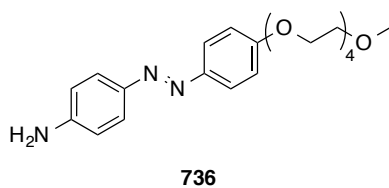
^1H NMR (CDCl_3 , 400 MHz):



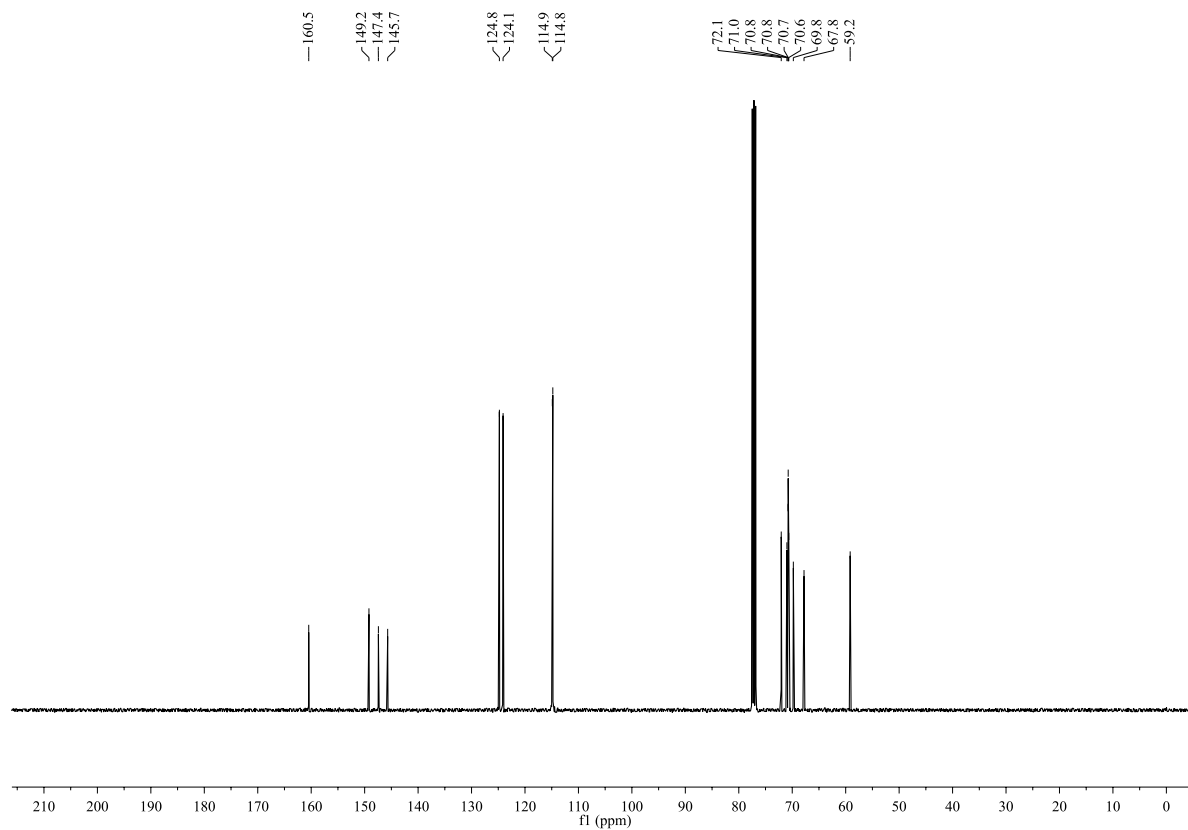
^{13}C NMR (CDCl_3 , 100 MHz):



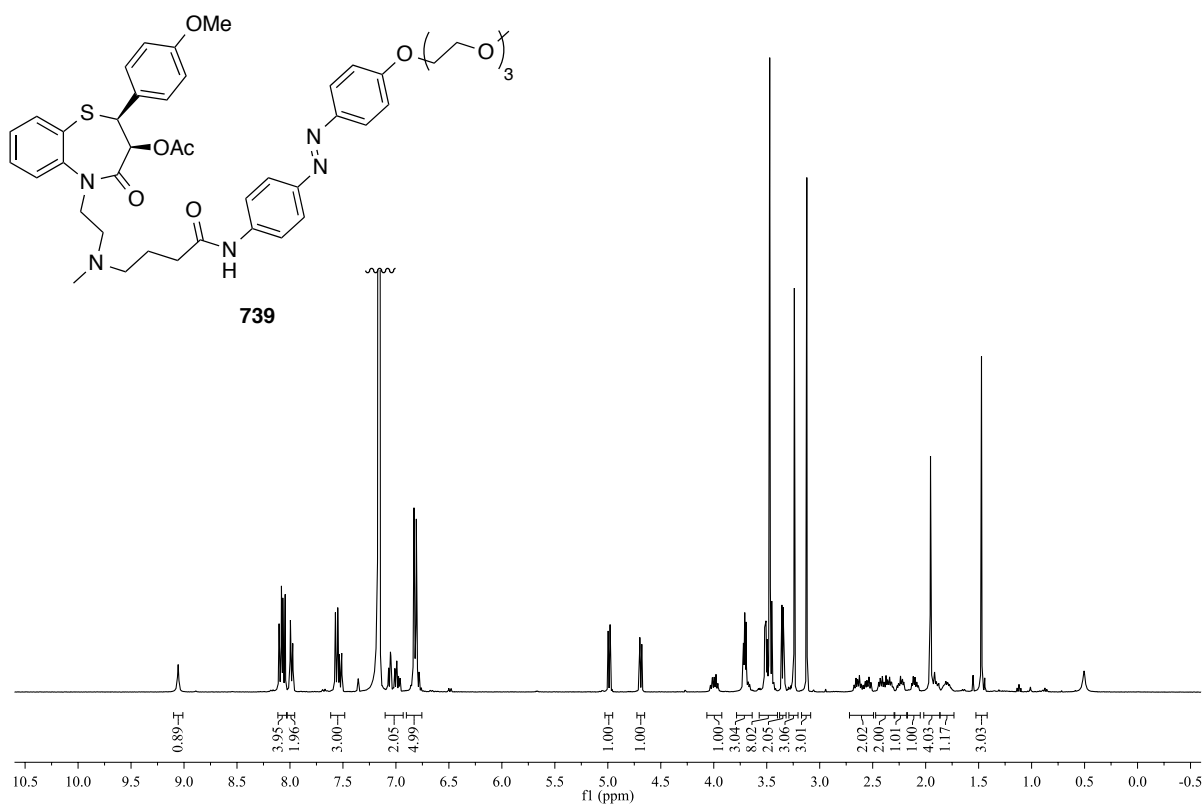
^1H NMR (CDCl_3 , 400 MHz):



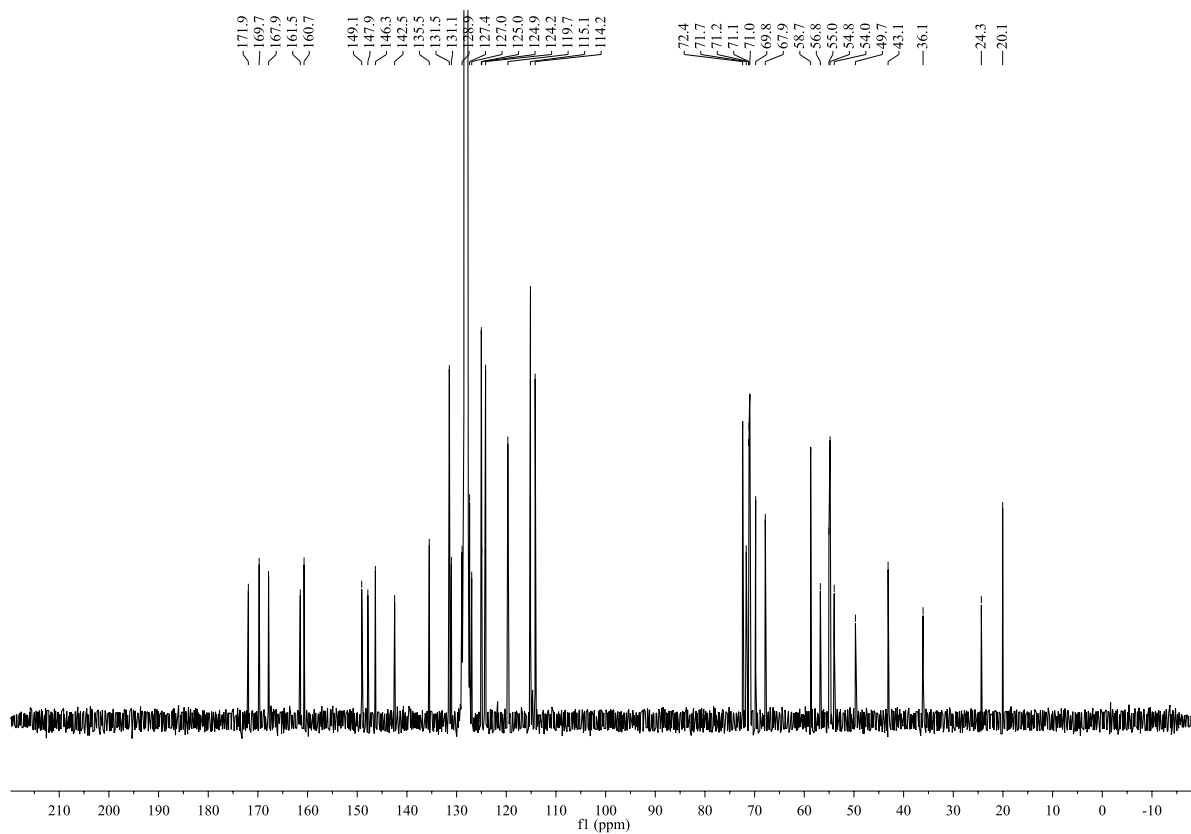
^{13}C NMR (CDCl_3 , 100 MHz):

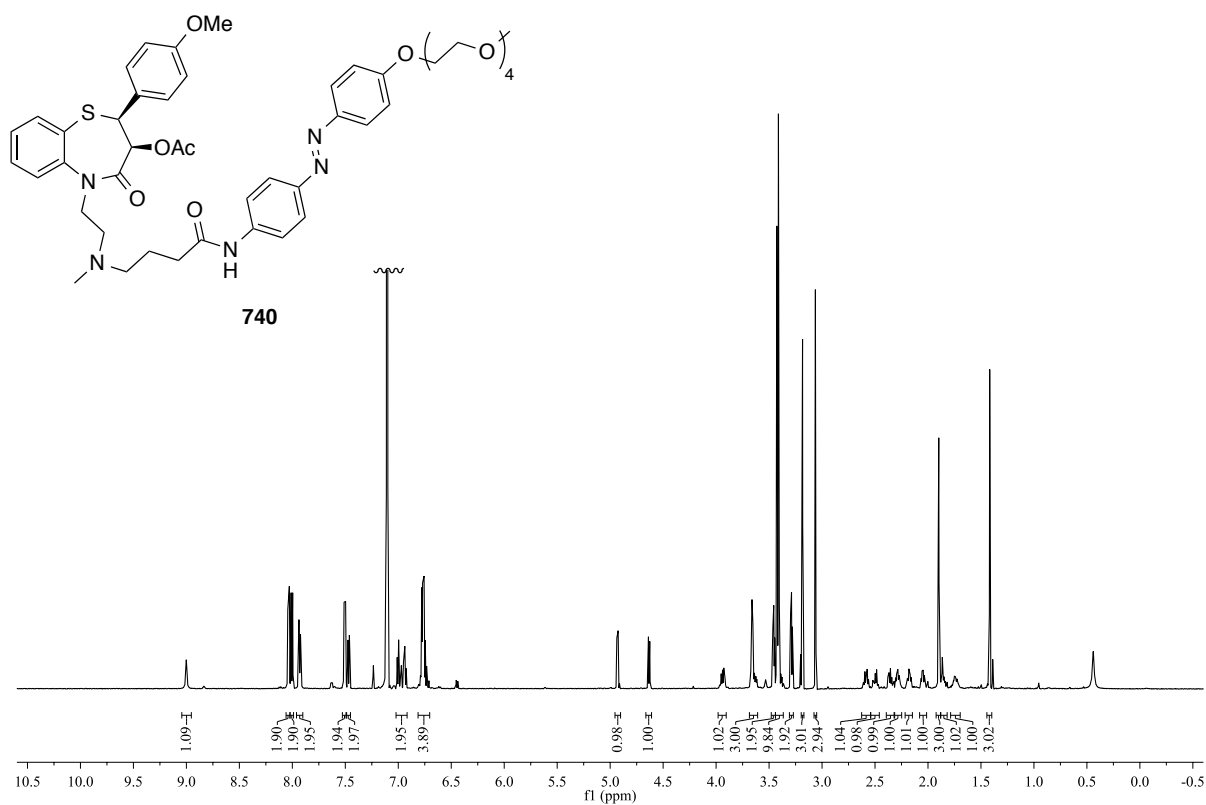
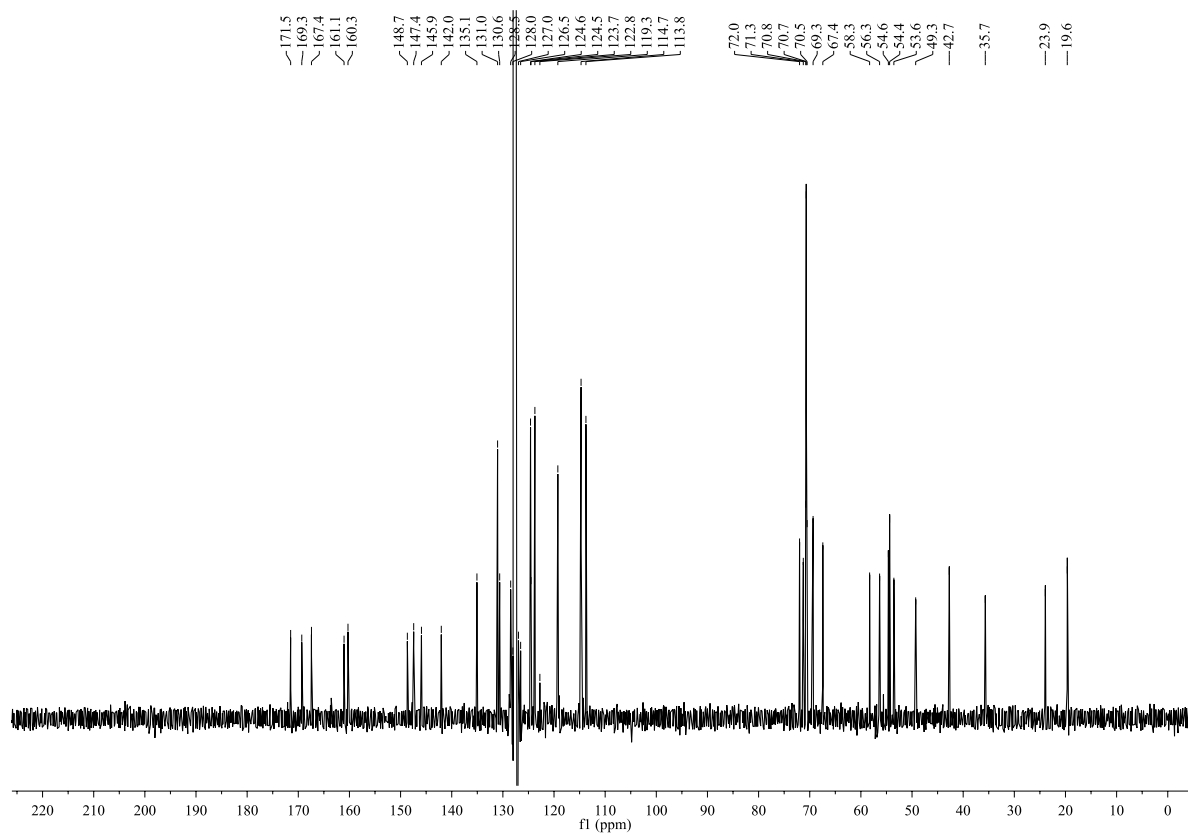


^1H NMR (CDCl_3 , 600 MHz):



^{13}C NMR (CDCl_3 , 150 MHz):

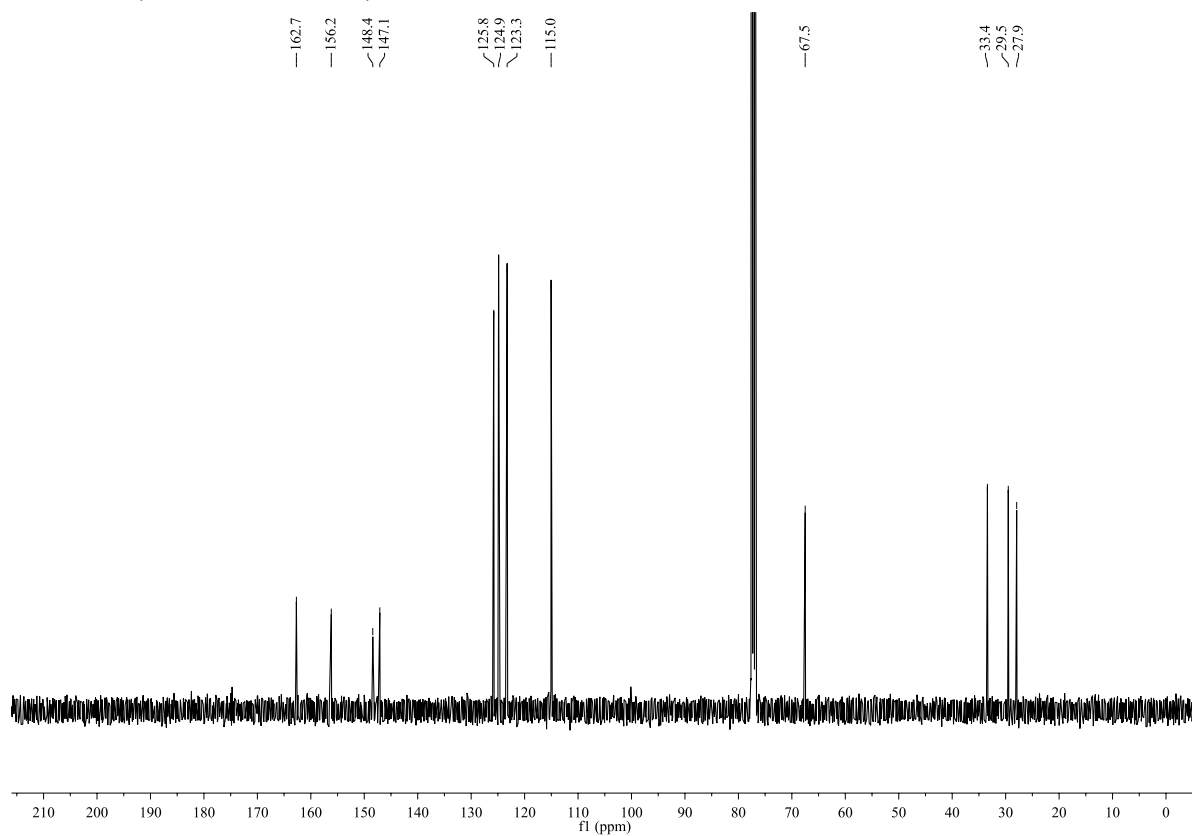


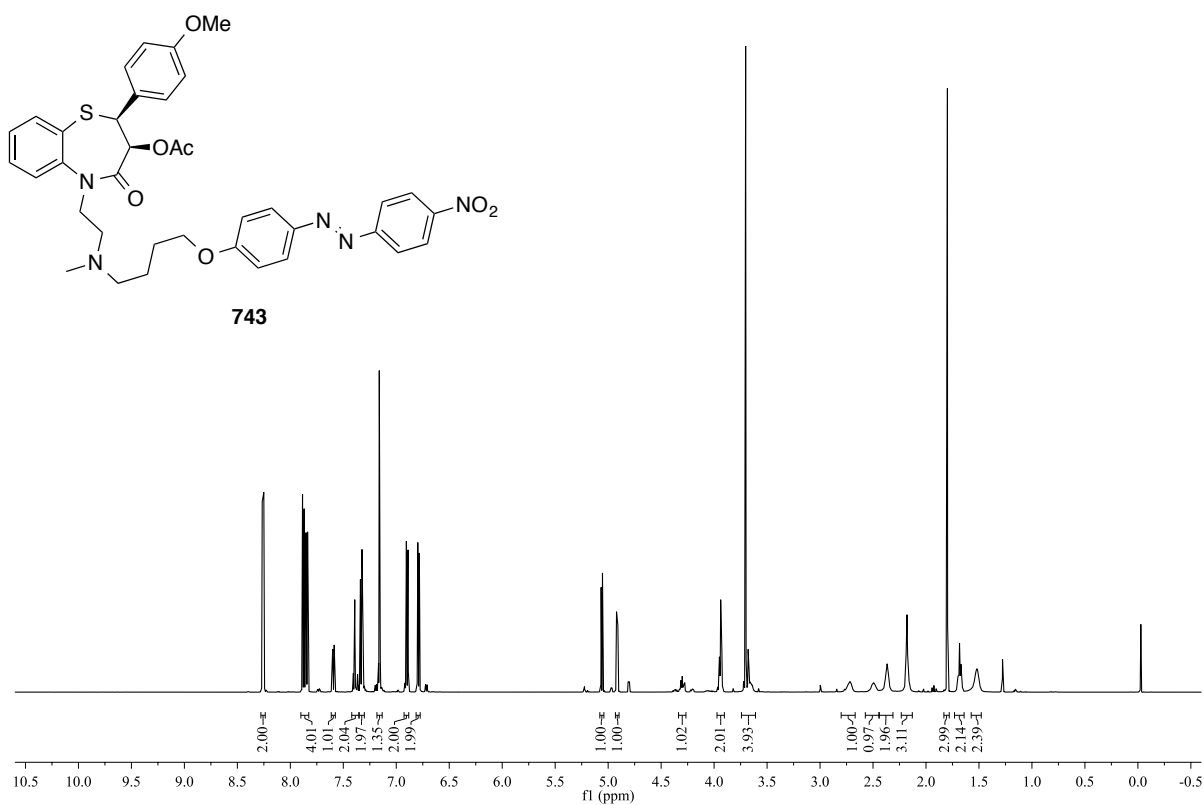
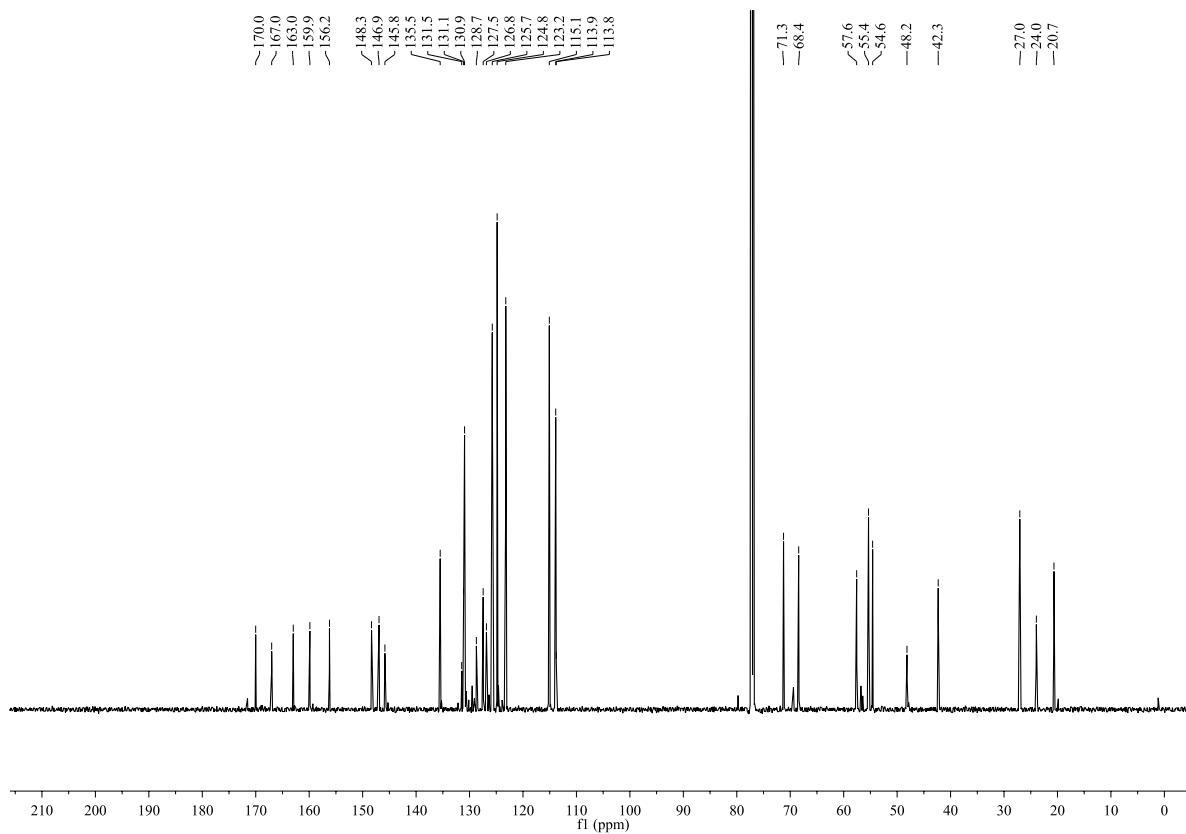
^1H NMR (CDCl_3 , 600 MHz): ^{13}C NMR (CDCl_3 , 150 MHz):

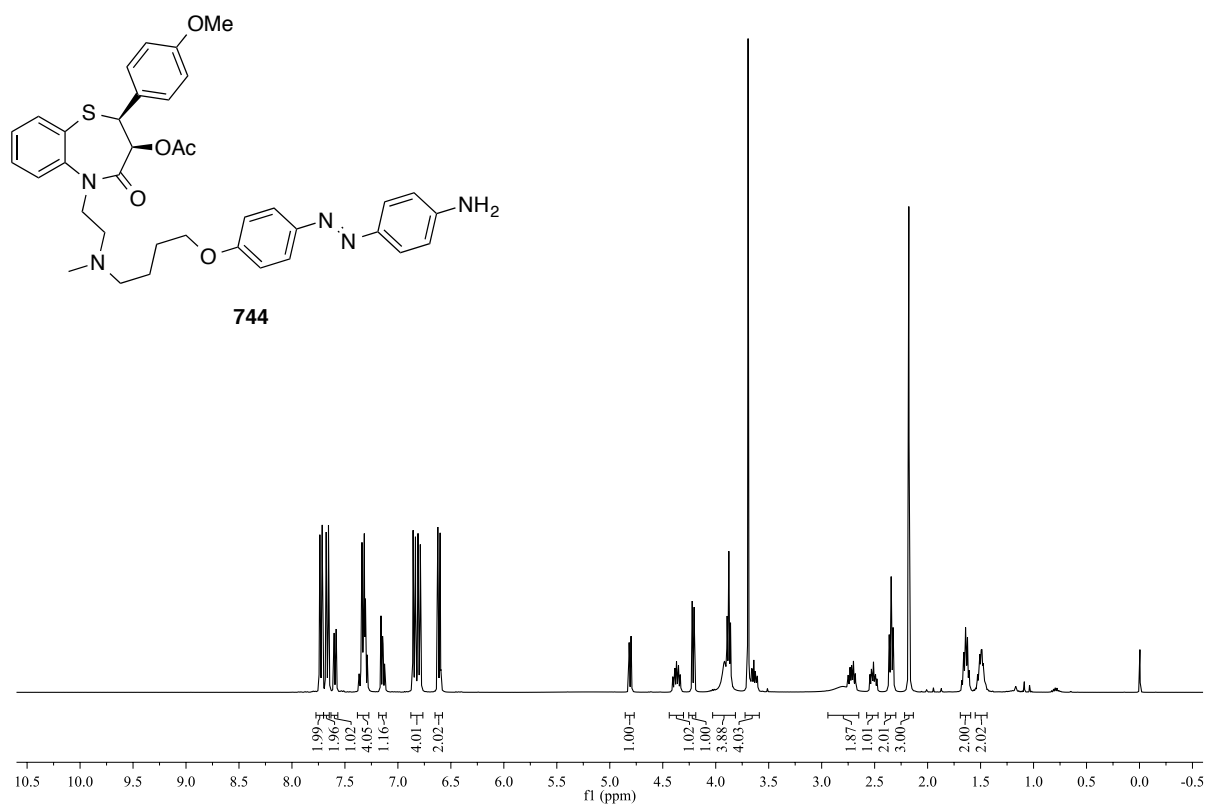
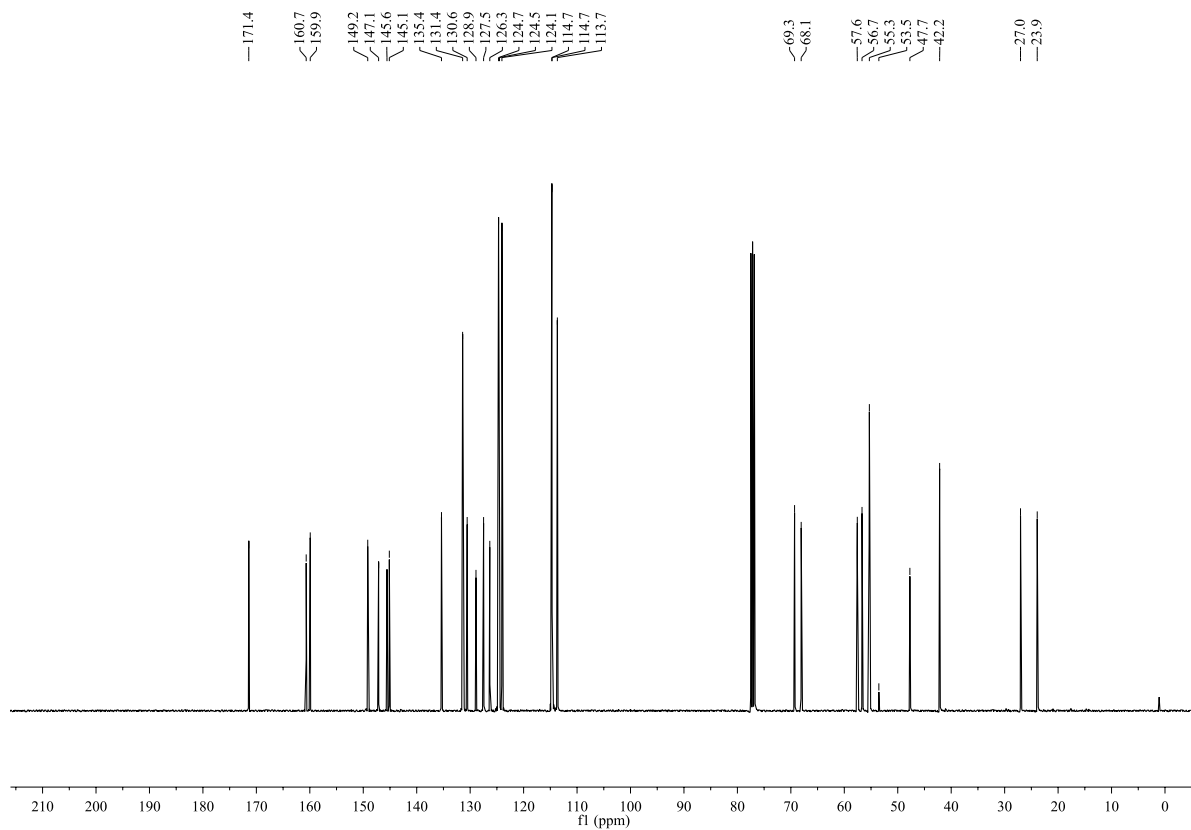
^1H NMR (CDCl_3 , 400 MHz):



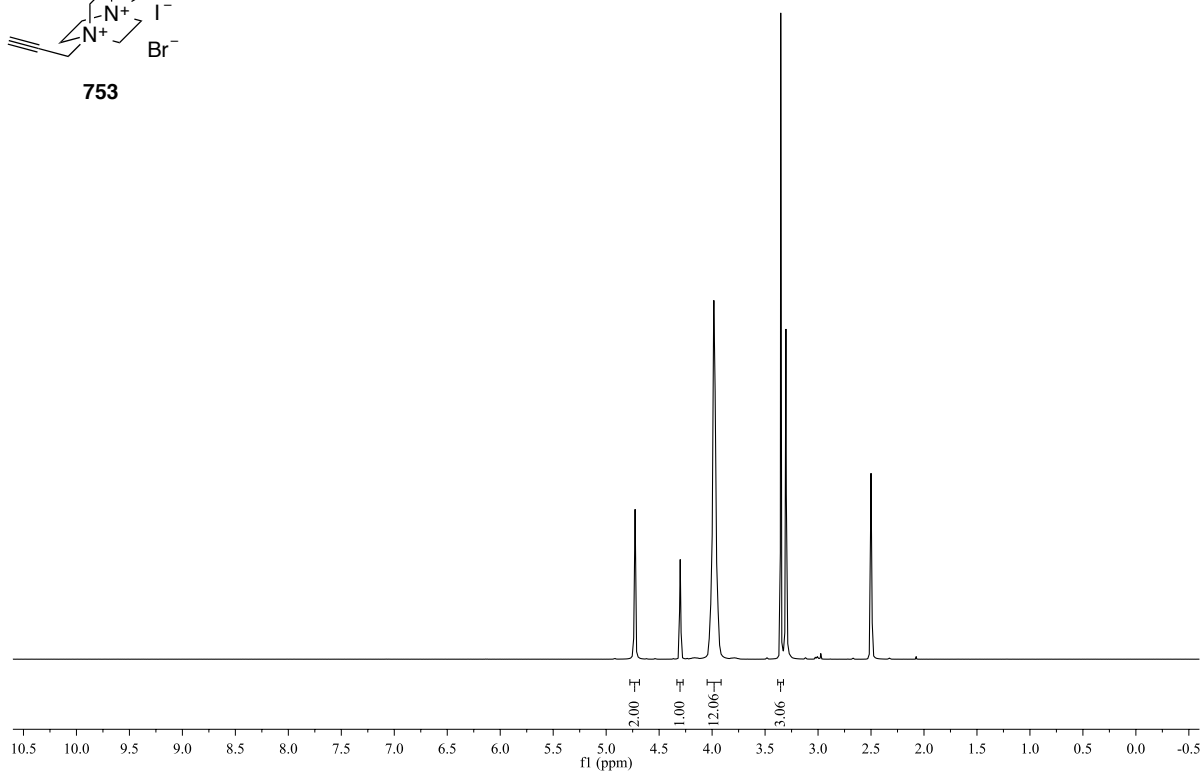
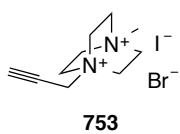
^{13}C NMR (CDCl_3 , 100 MHz):



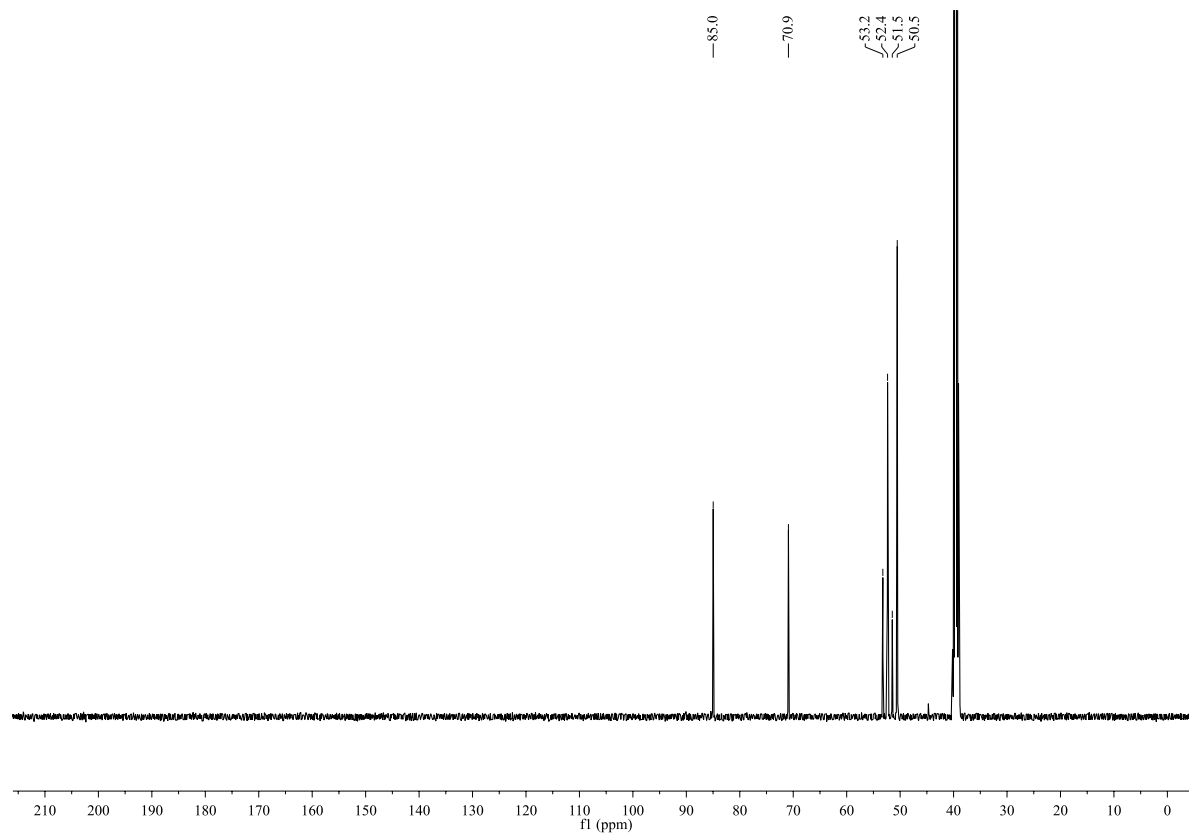
^1H NMR (CDCl_3 , 600 MHz): ^{13}C NMR (CDCl_3 , 150 MHz):

^1H NMR (CDCl_3 , 400 MHz): ^{13}C NMR (CDCl_3 , 100 MHz):

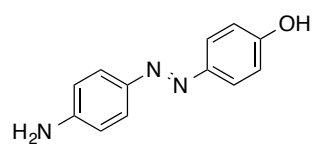
^1H NMR (DMSO- d_6 , 400 MHz):



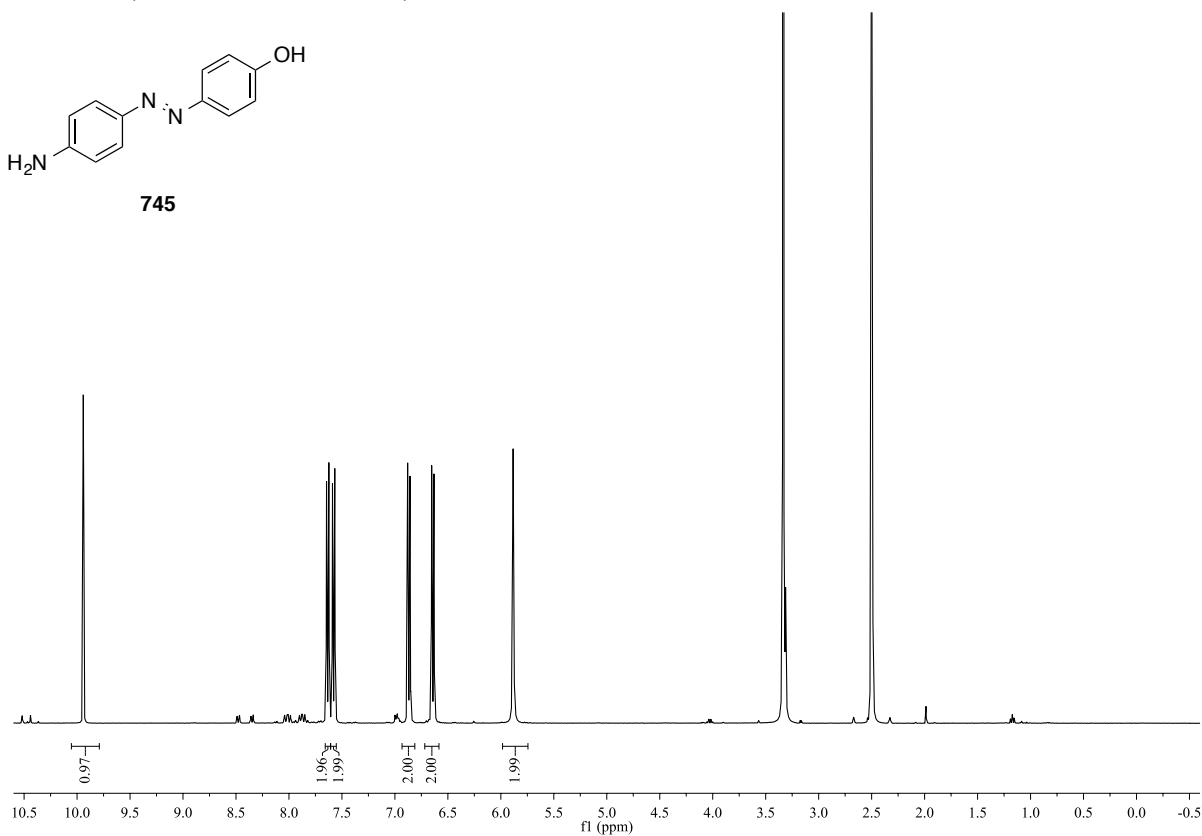
^{13}C NMR (DMSO- d_6 , 100 MHz):



^1H NMR (DMSO- d_6 , 400 MHz):

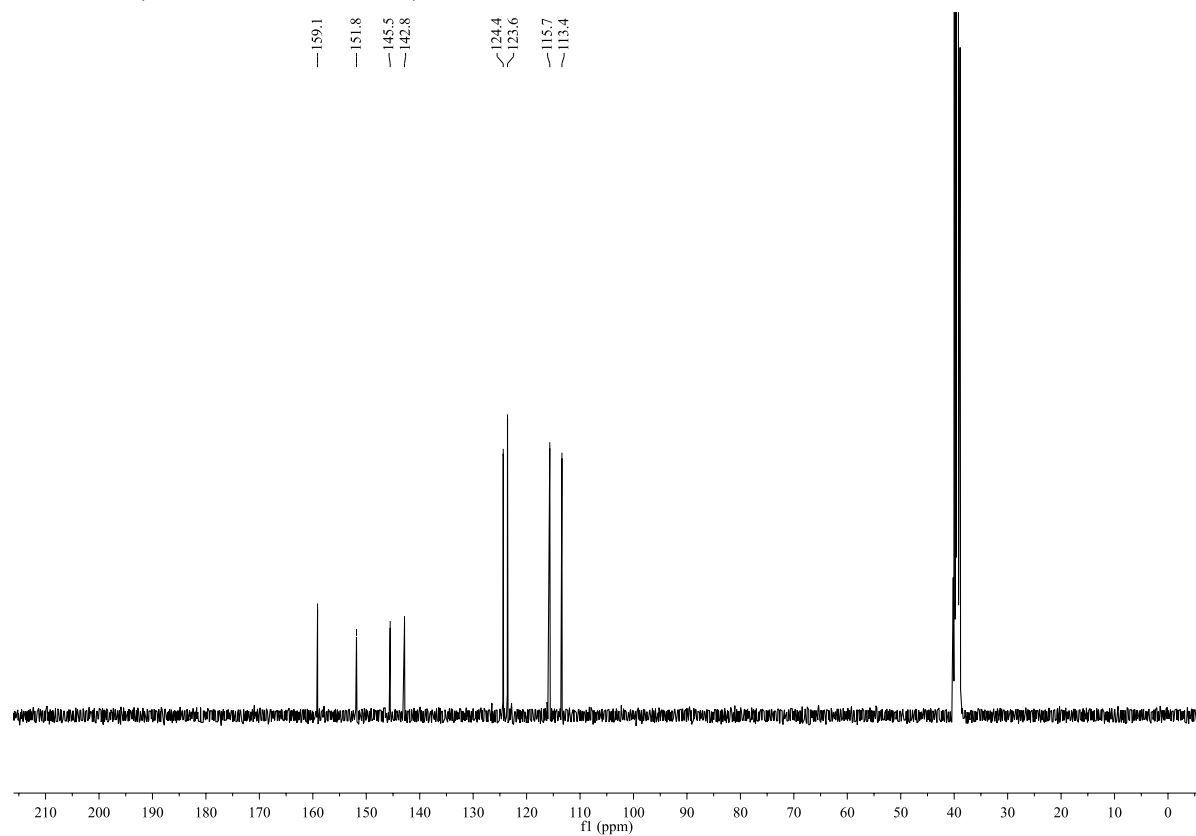


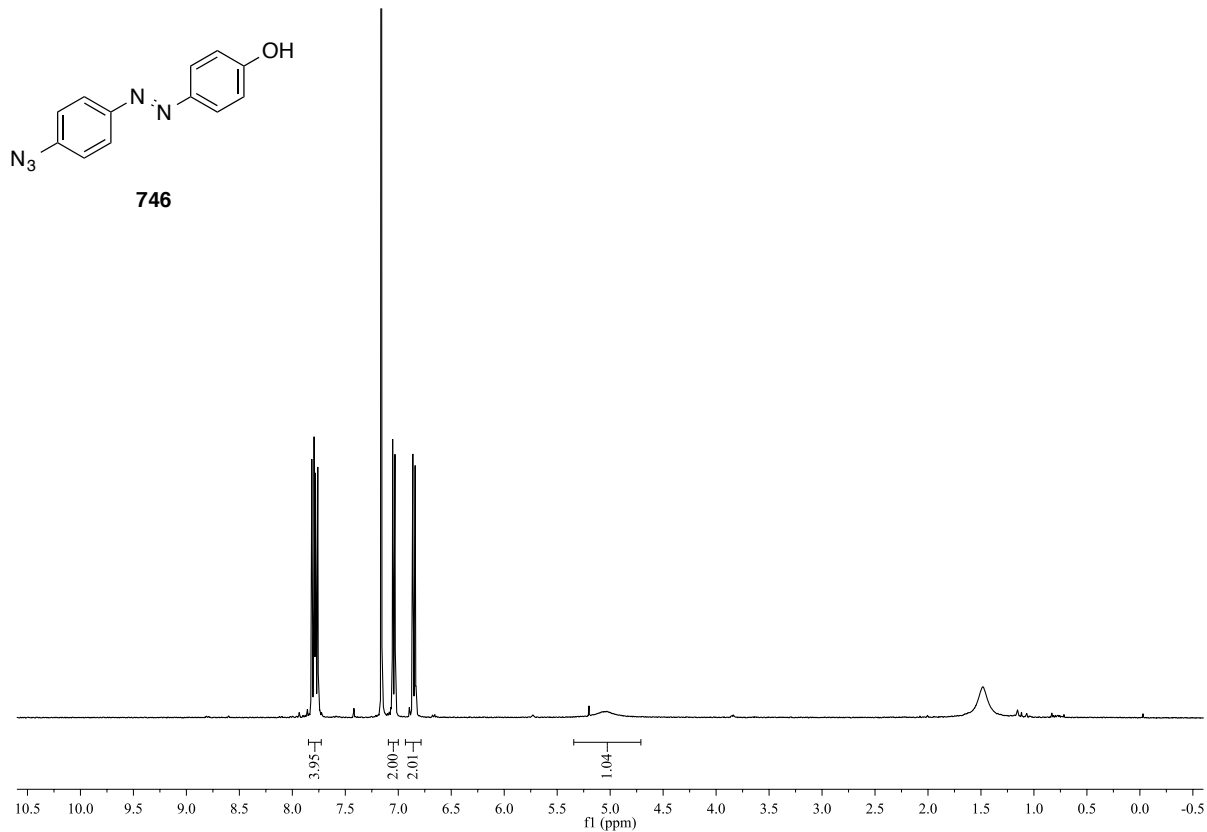
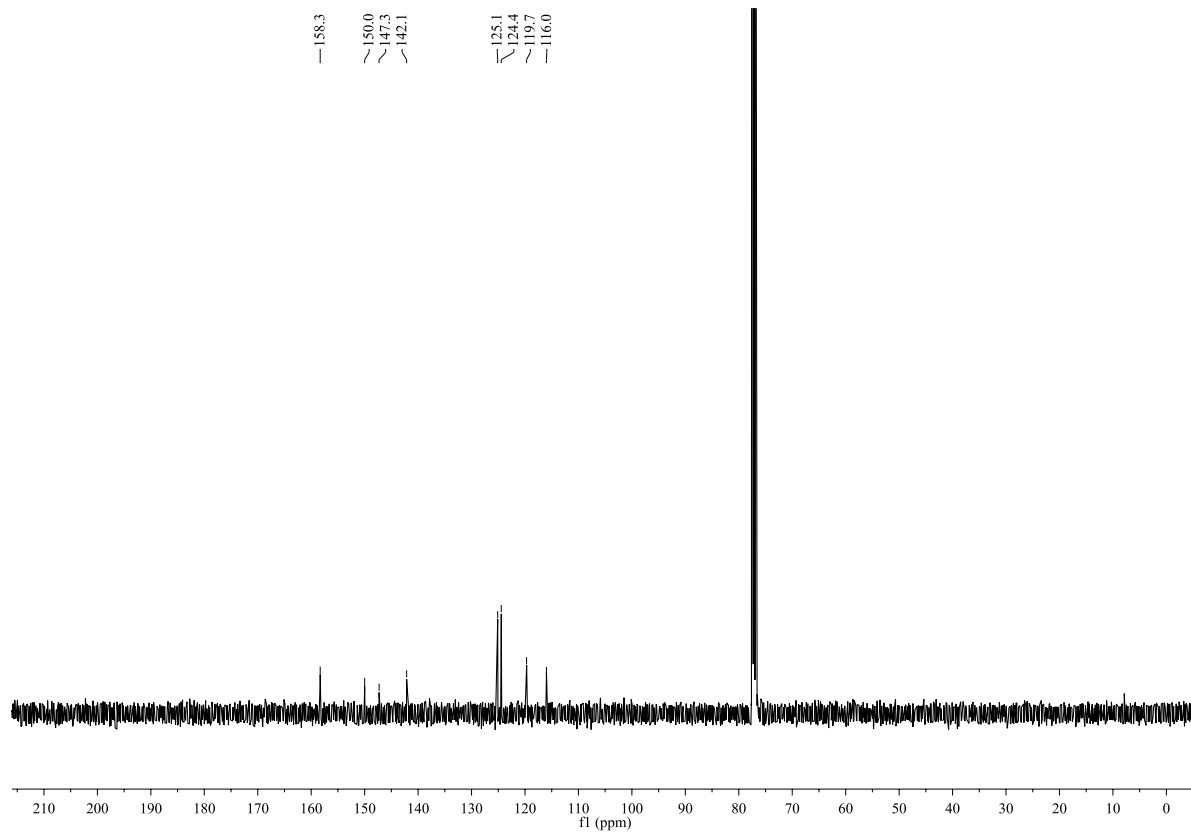
745



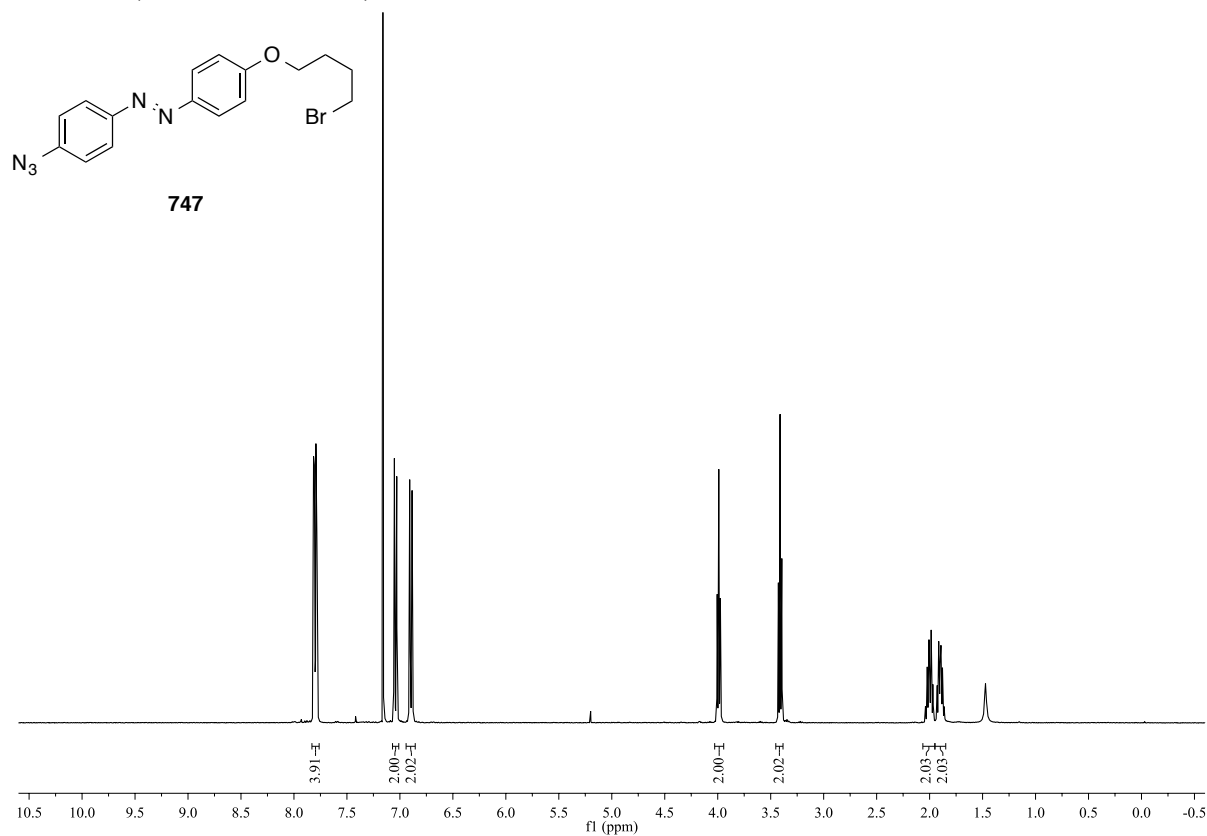
^{13}C NMR (DMSO- d_6 , 100 MHz):

— 159.1
— 151.8
— 145.5
— 142.8
— 124.4
— 123.6
— 115.7
— 113.4

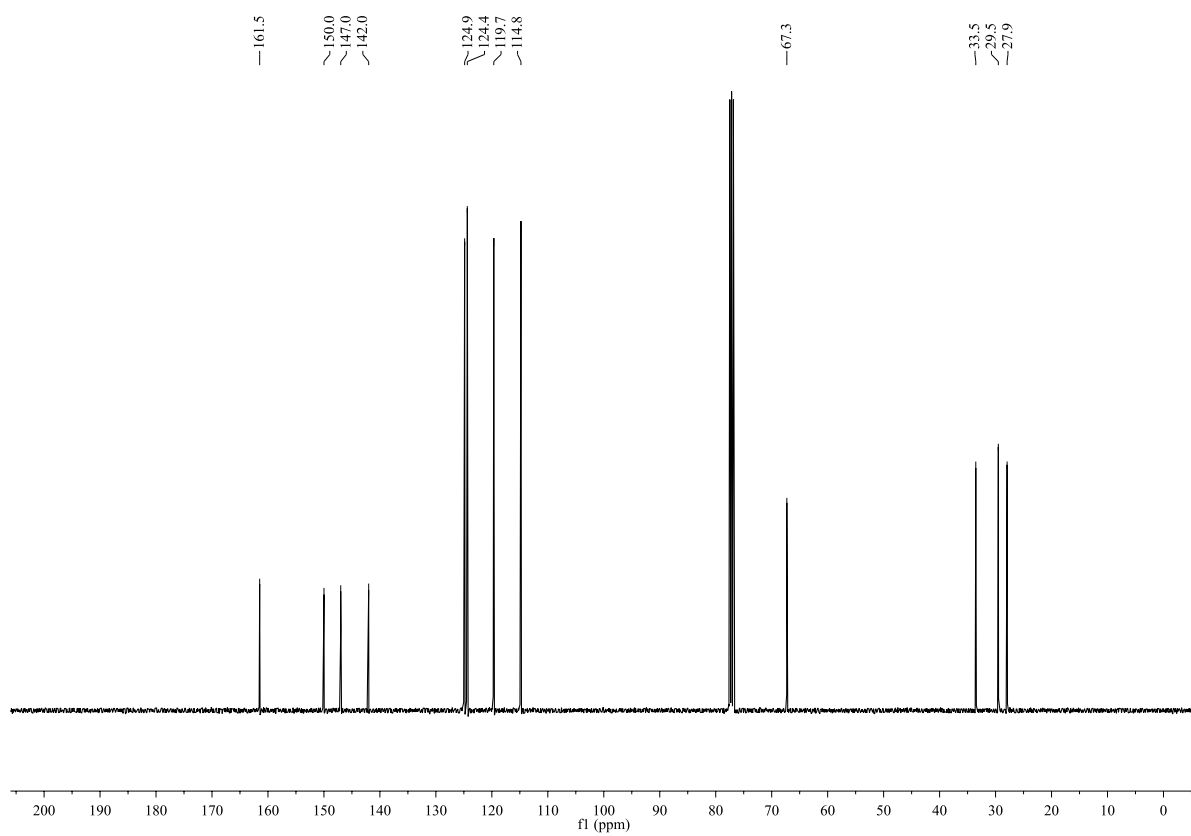


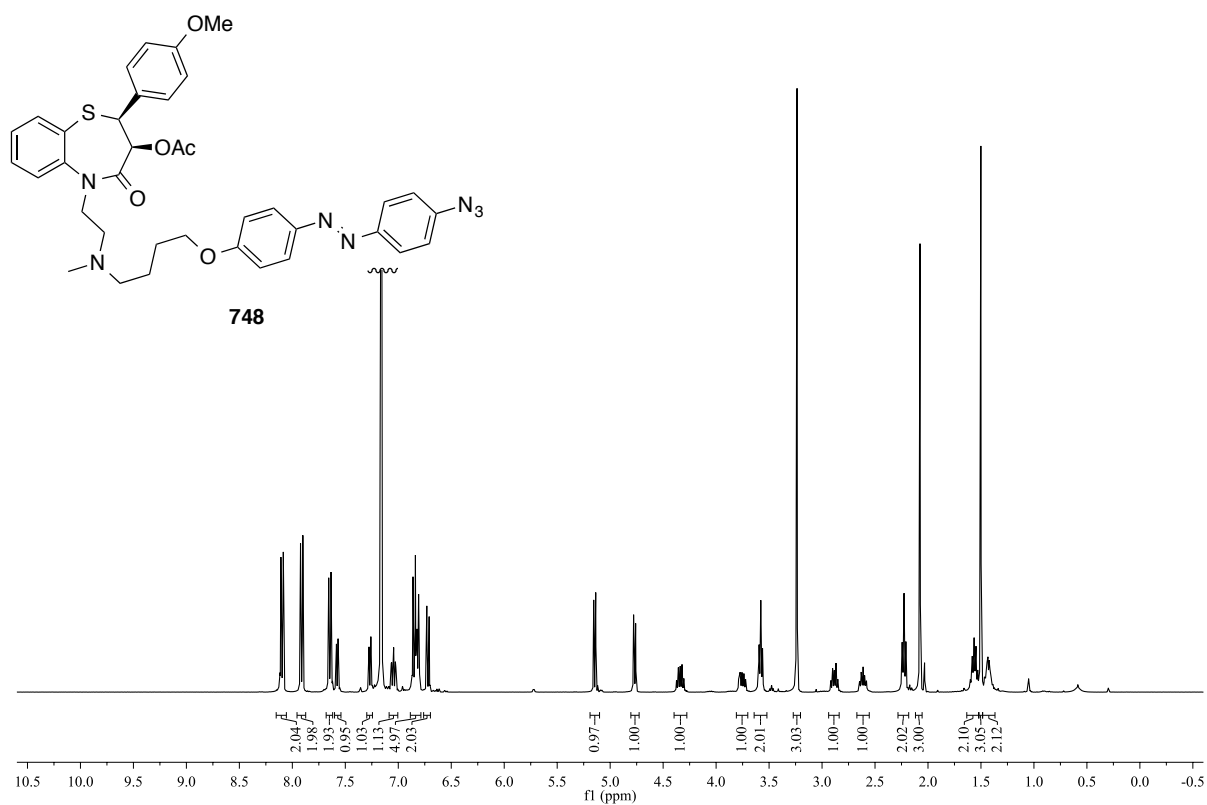
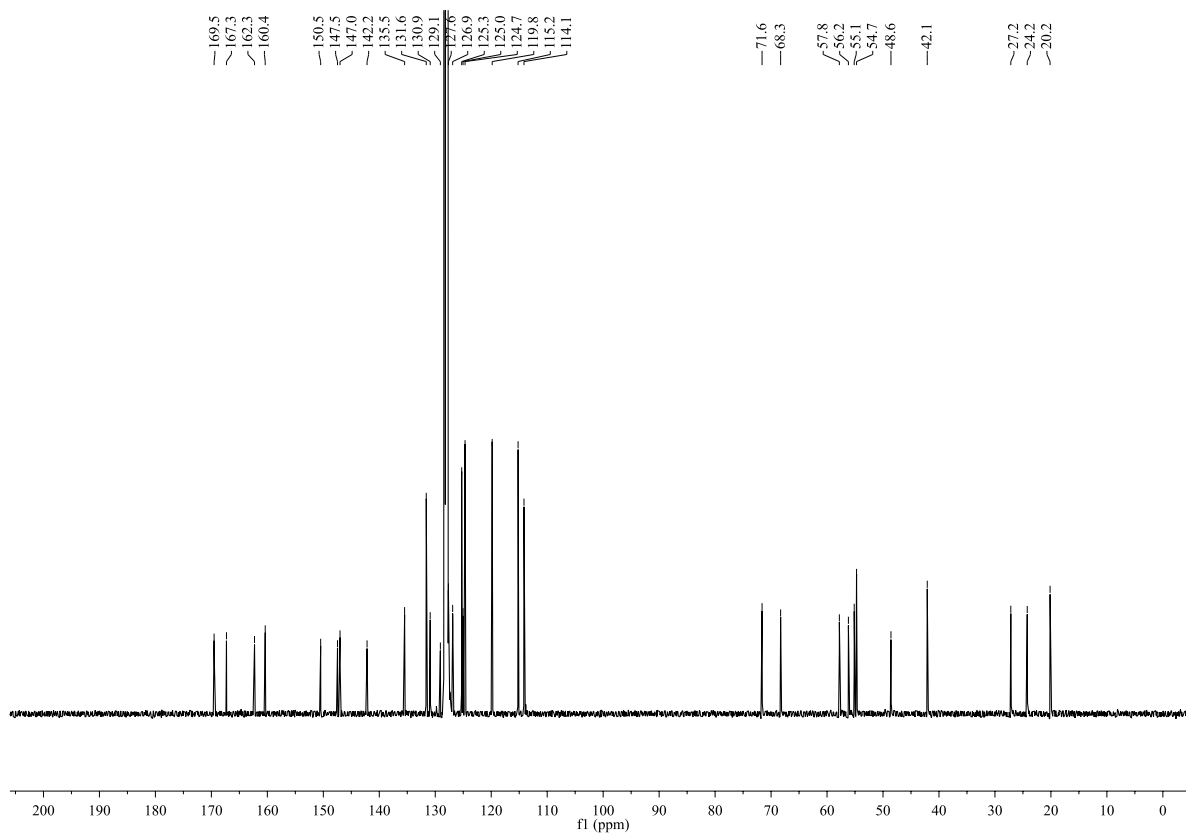
^1H NMR (CDCl_3 , 400 MHz): ^{13}C NMR (CDCl_3 , 100 MHz):

^1H NMR (CDCl_3 , 400 MHz):

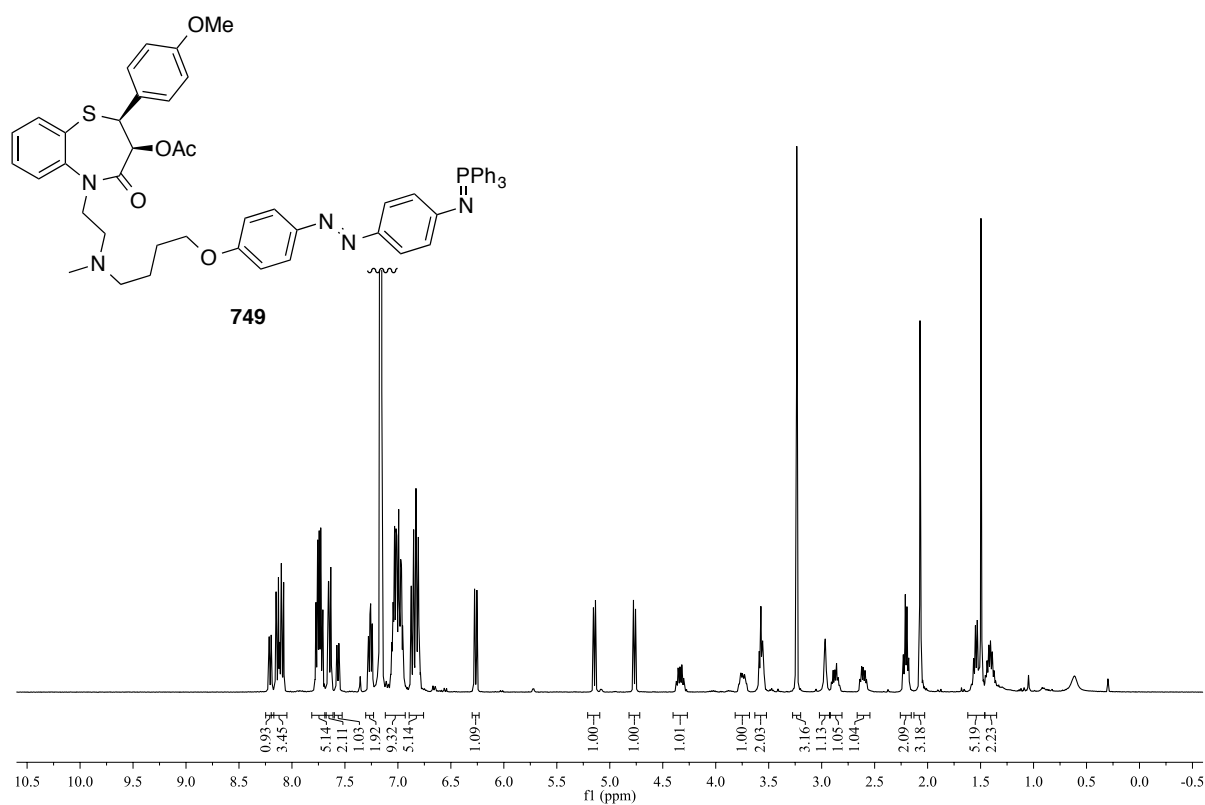


^{13}C NMR (CDCl_3 , 100 MHz):

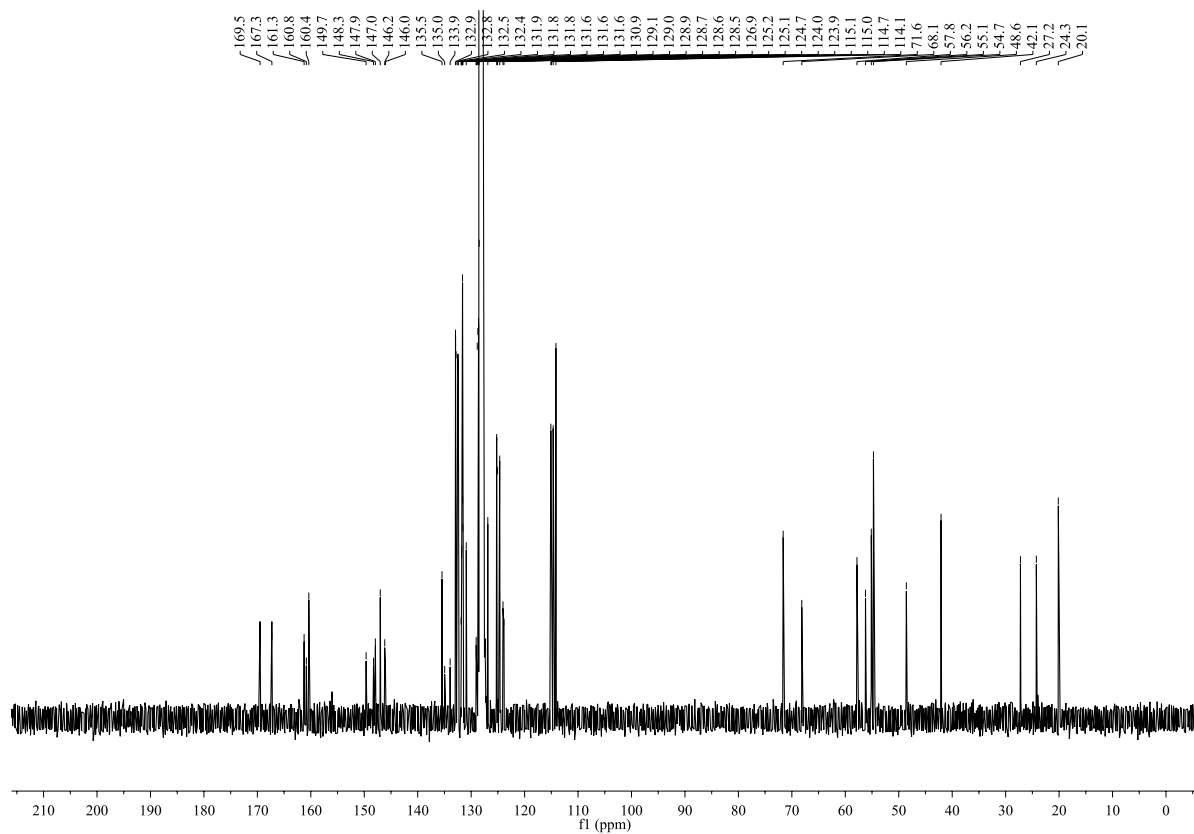


^1H NMR (CDCl_3 , 400 MHz): ^{13}C NMR (CDCl_3 , 100 MHz):

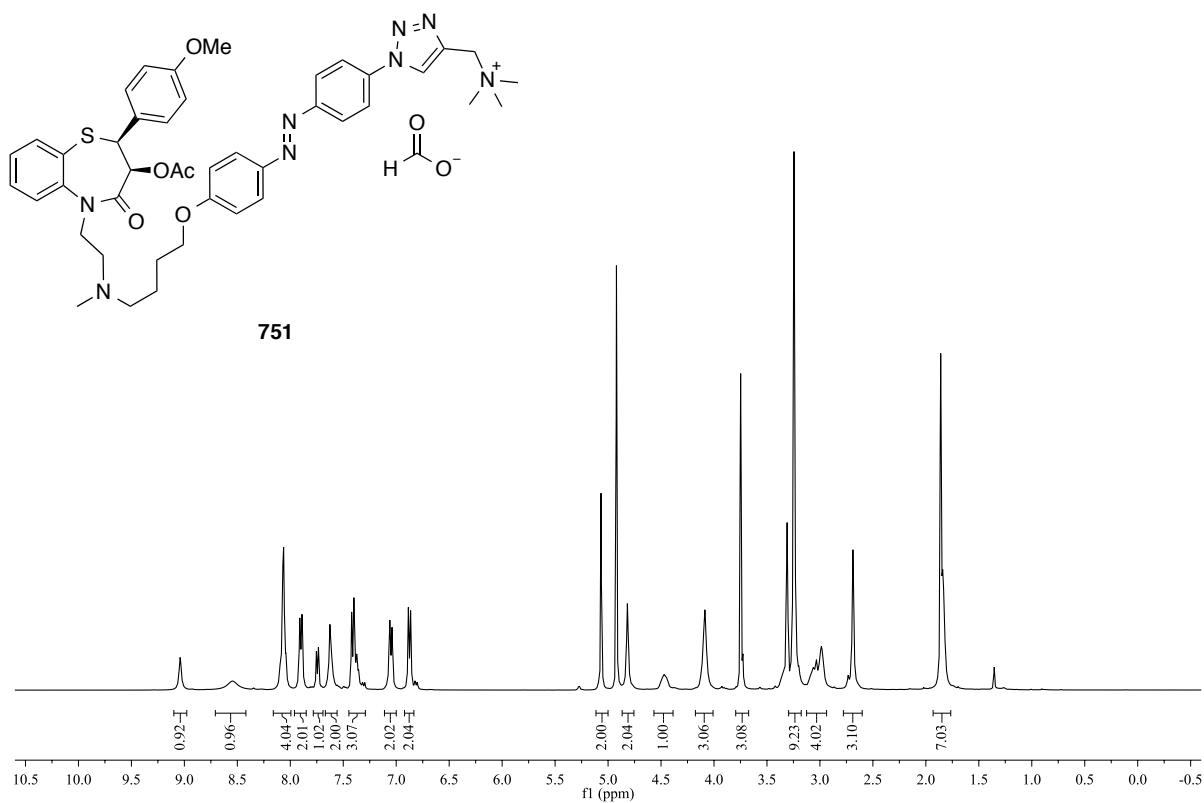
^1H NMR (CDCl_3 , 400 MHz):



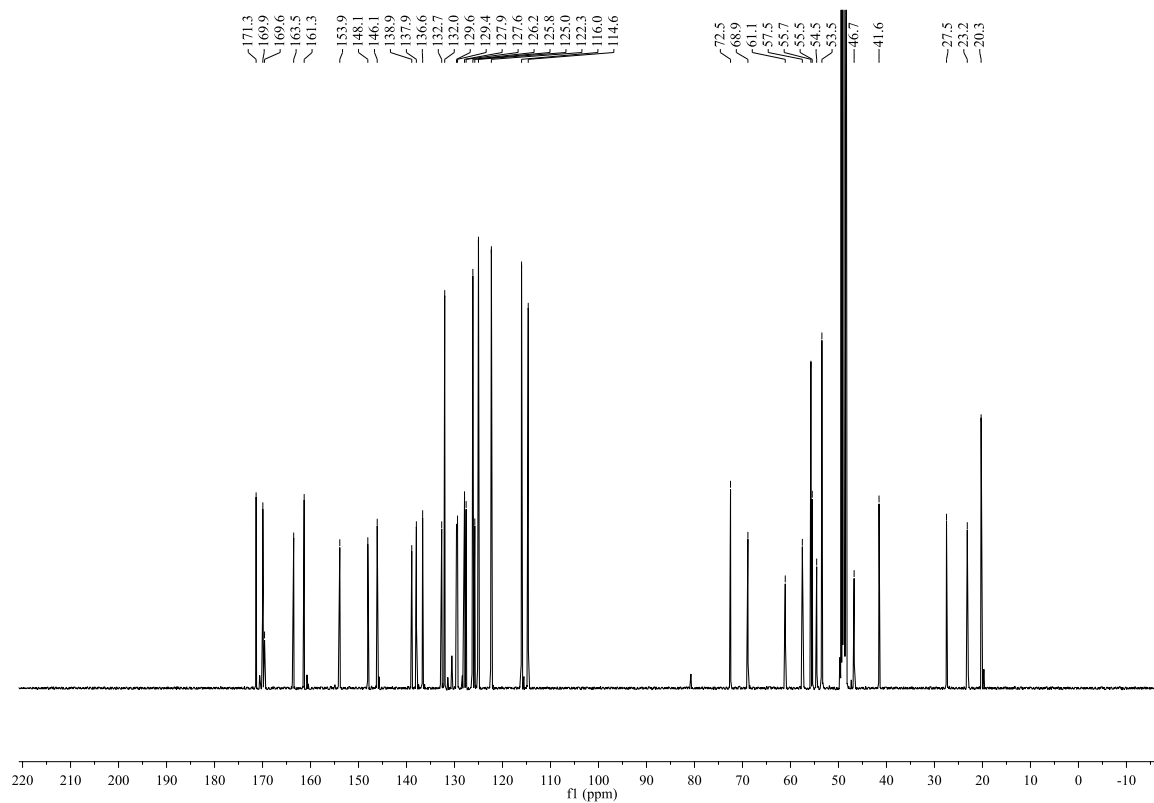
^{13}C NMR (CDCl_3 , 100 MHz):



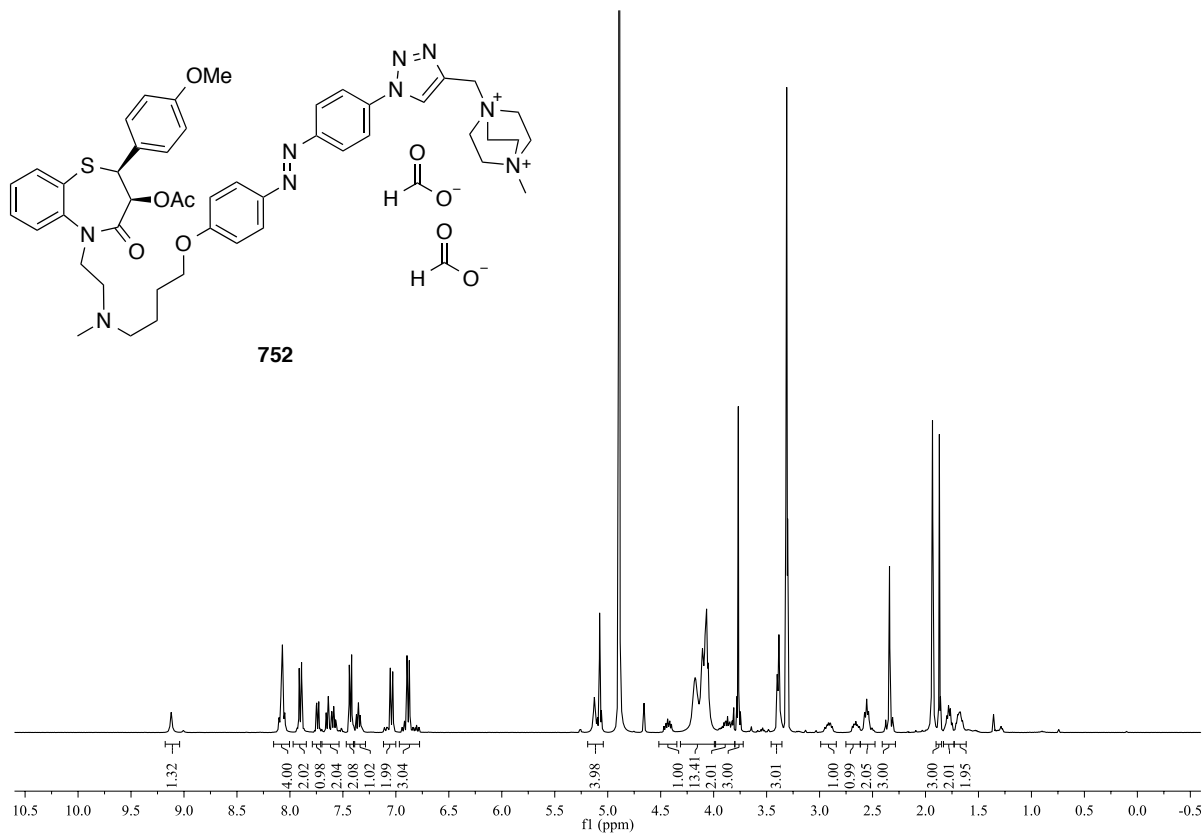
^1H NMR (CD_3OD , 400 MHz):



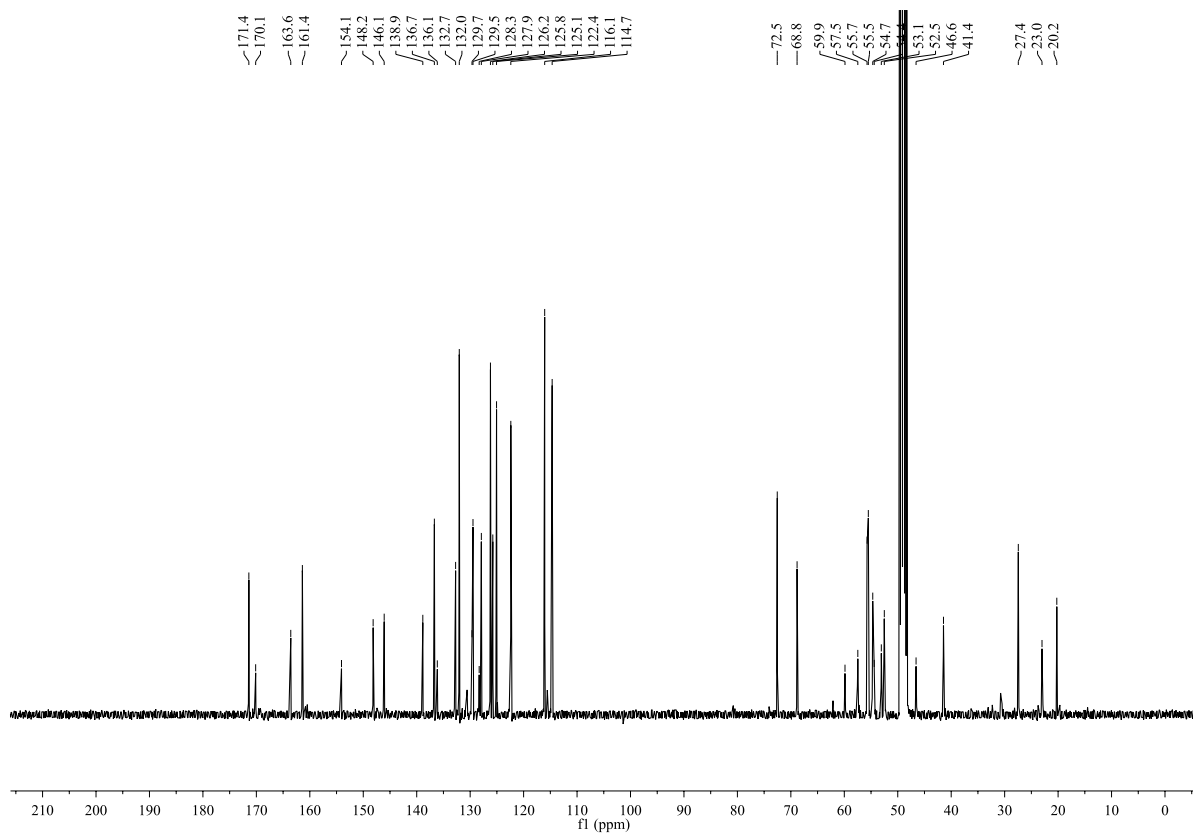
^{13}C NMR (CD_3OD , 100 MHz):



^1H NMR (CD_3OD , 400 MHz):



^{13}C NMR (CD_3OD , 100 MHz):



V. Additional Data

Comparison of NMR Data of Synthetic (–)-Nitidasin with Isolation Data

Note: Synthetic (–)-nitidasin (**238**) was highly unstable in commercially available CDCl₃. In order to circumvent decomposition due to traces of acid, molecular sieves (4 Å, activated, 20 g) was added to CDCl₃ (new 100 mL bottle), the bottle was flushed with argon and stored over night at 4 °C. Immediately prior to recording the spectra, CDCl₃ (2 mL) was filtered over basic Al₂O₃ (4 cm pad in a Pasteur pipette). The first 0.5 mL of CDCl₃ were discarded. The (–)-nitidasin (**238**) sample was dissolved in CDCl₃ (0.7 mL) and filled into a NMR tube, which was flushed with Argon and sealed. In such media, (–)-nitidasin (**238**) was stable for 48 hours. CDCl₃ was referenced to $\delta = 7.26$ and 77.00 ppm, respectively.

Table A.14: Comparison of ¹H NMR data of (–)-nitidasin (**238**).

Natural, ¹ H NMR (CDCl ₃ , 600 MHz) ^[154] δ /ppm	Synthetic, ¹ H NMR (CDCl ₃ , 600 MHz) δ /ppm
2.55 (m, 1H)	2.55 (m _C , 1H)
2.46 (m, 1H)	2.46 (m _C , 1H)
2.40 (m, 1H)	2.40 (m _C , 1H)
2.34 (s, 1H, OH)	2.34 (s, 1H)
2.17 (t, $J = 12.5$ Hz, 1H)	2.17 (t, $J = 13.0$ Hz, 1H)
2.10 (d, $J = 17.2$ Hz, 1H)	2.11 (d, $J = 17.1$ Hz, 1H)
2.06 (m, 1H)	2.09–2.03 (m, 1H)
1.98 (d, $J = 17.2$ Hz, 1H)	1.98 (d, $J = 17.2$ Hz, 1H)
1.88 (m, 2H)	1.94–1.83 (m, 3H)
1.87 (m, 1H)	
1.76 (br d, $J = 13.5$ Hz, 1H)	1.75 (dd, $J = 12.6, 2.8$ Hz, 1H)
1.65 (br d, $J = 12.5$ Hz, 1H)	1.65 (dd, $J = 13.1, 2.4$ Hz, 1H)
1.56 (m, 1H)	1.59–1.54 (m, 2H)
1.55 (m, 1H)	
1.46 (m, 1H)	1.49–1.42 (m, 2H)
1.44 (m, 1H)	
1.41 (s, 3H)	1.41 (s, 3H)
1.32 (m, 1H)	1.35–1.21 (m, 4H)
1.26 (m, 3H)	

1.12 (m, 1H)	1.12 (m _C , 1H)
1.00 (d, $J = 6.2$ Hz, 3H)	1.00 (d, $J = 6.3$ Hz, 3H)
0.98 (d, $J = 6.1$ Hz, 3H)	0.99–0.94 (m, 6H)
0.97 (d, $J = 6.1$ Hz, 3H)	
0.96 (s, 3H)	0.96 (s, 3H)
0.89 (d, $J = 5.5$ Hz, 3H)	0.89 (br d, $J = 5.8$ Hz, 3H)

Table A.15: Comparison of ^{13}C NMR data of (–)-nitidasin (**238**).

Natural, ^{13}C NMR (CDCl_3 , 150 MHz) ^[154]	Synthetic, ^{13}C NMR (CDCl_3 , 100 MHz)
δ/ppm	δ/ppm
220.50	220.51
79.17	79.18
75.06	75.07
67.29	67.30
55.83	55.83
55.77	55.78
42.35	42.35
42.18	42.19
41.84	41.85
41.70	41.71
39.11	39.11
36.00	36.01
34.83	34.83
34.20	34.22
32.22	32.23
32.13	32.13
28.35	28.36
26.56	26.57
25.32	25.36
24.67	24.67
23.08	23.09
21.16	21.16
20.11	20.12
16.34	16.35
14.89	14.89

Gas-phase Energies of Calculated Structures

Tables A.16 and A.17 list the calculated energies for all structures that are depicted in the reaction profile in scheme 4.20. Values given in the second row refer to the gas-phase. The respective reference points are allyl cation **623** and allylic alcohol **622**. Employed computational methods are outlined in section I of the appendix.

Table A.16: Relative energies for transitions states and intermediates given in scheme 4.20.

Structure	E [kJ/mol] (B3LYP/def-SVP)	E [kJ/mol] (B3LYP/def-SVP, COSMO, THF)
623	0	0
[624] [‡]	+87.6	+80.1
625	+83.0	+68.6
[629] [‡]	+84.7	+73.8
628	+25.6	+25.3
[630] [‡]	+53.9	+45.9
626	+39.9	+33.1
622	0	0
627 + H ₂ O	+31.9	+4.6

Table A.17: Absolute energies for transitions states and intermediates given in scheme 4.20.

Structure	E [Hartree] (B3LYP/def-SVP)	E [Hartree] (B3LYP/def-SVP, COSMO, THF)
623	−976.780812	−976.831410
[624] [‡]	−976.747450	−976.800896
625	−976.749199	−976.805292
[629] [‡]	−976.748561	−976.803300
628	−976.771067	−976.821776
[630] [‡]	−976.760272	−976.813926
626	−976.765602	−976.818700
622	−1052.851393	−1052.209235
627 + H ₂ O	−1052.839256	−1052.207473

Cartesian Coordinates of Calculated Structures

Table A.18: Cartesian coordinates for allylic cation **623**.

C	-6.60421657	1.66112306	2.43645479	H	-11.3997879	0.03441992	4.71281140
C	-7.83115662	1.20861517	1.60468132	C	-6.59767260	1.87114864	-2.39379619
C	-8.69409615	0.25229847	2.49683966	C	-9.05128807	2.19614339	-2.04630543
C	-7.58609419	-0.34507743	3.44597372	C	-5.22474130	4.46033771	-1.74634733
C	-6.22369624	0.29349965	3.06064492	H	-6.28439238	4.67761870	-1.98171520
C	-7.37865831	2.72874108	-0.20352423	H	-4.68122825	5.39048327	-1.99347659
C	-6.17168834	3.33160927	0.47917443	C	-4.66230645	3.34486709	-2.64124176
C	-7.61267628	2.33721124	-1.55309887	H	-3.55763470	3.36115422	-2.59155390
C	-8.45413916	2.39023535	0.79399453	H	-4.92887369	3.53052368	-3.69865069
C	-5.04546707	4.17049696	-0.23911593	C	-5.11400864	1.91696838	-2.19734174
H	-6.66865041	4.05621321	1.15597904	C	-4.57484029	0.74682055	-3.07558395
C	-5.55910005	2.25732256	1.47168976	H	-4.81551214	1.78094059	-1.14726674
H	-4.74322975	2.75923707	2.02309438	C	-6.89245207	1.15448901	-3.68963898
H	-5.09030894	1.45036987	0.87719655	C	-5.52979574	0.75036926	-4.28957441
H	-7.40944111	0.52520801	0.83748907	H	-4.76960776	-0.18051142	-2.49619519
C	-6.93942197	2.67178021	3.55819854	C	-3.08328546	0.78412139	-3.41896166
H	-7.39936359	3.60695926	3.18790683	H	-2.82540150	1.63917081	-4.06950571
H	-6.01699769	2.95401607	4.09741058	H	-2.79077476	-0.13325183	-3.96057612
H	-7.63281186	2.25075272	4.30294589	H	-2.45654956	0.84385078	-2.50986365
C	-9.93928401	0.78447033	3.26613043	H	-5.56832712	-0.22334034	-4.80682673
H	-9.07736347	-0.55012613	1.83558376	H	-5.20282609	1.49532847	-5.03907175
H	-9.38487496	2.06820824	0.31839665	H	-7.52279846	1.76941041	-4.36124614
H	-8.68081444	3.23779576	1.46282918	H	-7.52082166	0.26771168	-3.45492567
H	-5.54072735	0.38197822	3.92442897	H	-4.10096131	3.60120933	-0.13264555
H	-5.70406513	-0.32390506	2.30265547	C	-4.85335604	5.49057992	0.53919692
H	-9.61904901	1.59130534	3.95520142	H	-5.73804320	6.14782847	0.43342183
C	-10.5480361	-0.34774201	4.12195893	H	-3.97967215	6.04609212	0.15386202
C	-11.0486719	1.34779954	2.35286603	H	-4.68443741	5.31786313	1.61848917
H	-10.8041765	2.32589528	1.90700126	H	-9.12292971	2.49461117	-3.10520252
H	-11.9795585	1.49474468	2.92894787	H	-9.74609477	2.84283140	-1.49132628
H	-11.2876682	0.64349299	1.53178208	H	-9.42432480	1.15627790	-1.97291081
H	-9.82961260	-0.79095893	4.83226972	H	-7.54788235	-1.44609440	3.38259394
H	-10.9279436	-1.16456715	3.47774819	H	-7.82501130	-0.10615657	4.49672041

Table A.19: Cartesian coordinates for transition state **624**.

C	-6.79172525	1.44521780	2.60385976	H	-5.98865451	1.63188054	-2.35482174
C	-7.99038267	1.02381524	1.71135730	C	-8.44285960	1.40560191	-2.18967094
C	-9.01273942	0.28818644	2.64367842	C	-5.30752952	4.49328636	-1.27221880

C	-8.05118572	-0.33520150	3.72512783	C	-6.40468096	4.60397809	-1.25409153
C	-6.60243063	0.13266222	3.40356078	H	-4.90205113	5.51539589	-1.17224862
C	-7.17123997	2.33330709	-0.19643456	H	-4.85559387	3.97678028	-2.65291786
C	-6.02276903	2.91397641	0.63933336	C	-3.79442659	4.23479798	-2.83385714
C	-7.17201936	1.88468521	-1.48288609	H	-5.42510932	4.48733341	-3.45770424
C	-8.39516571	2.10835428	0.68373381	H	-5.01121432	2.50554132	-2.90219418
C	-4.82958588	3.61841902	-0.07248249	C	-4.13146850	1.76729484	-3.90709598
H	-6.51038589	3.73603238	1.20245126	C	-4.84939412	1.83786892	-1.72837513
C	-5.60202147	1.84839573	1.69830853	H	-5.81178897	0.24480328	-2.98817171
H	-4.77333525	2.23762619	2.31656728	C	-4.39261990	0.27265424	-3.59118433
H	-5.21066140	0.95472896	1.16946055	C	-3.07077811	2.03998799	-3.75158476
H	-7.58659801	0.19969003	1.08427591	H	-4.53341408	2.18478270	-5.34343860
C	-7.11930840	2.60201407	3.58073244	C	-5.59785094	1.97192826	-5.55543072
H	-7.55763019	3.48741861	3.08539261	H	-3.92531577	1.61820858	-6.06904181
H	-6.19996464	2.93357017	4.09821656	H	-4.34964715	3.25839194	-5.52541024
H	-7.83155775	2.29394869	4.36156309	H	-3.65988330	-0.08636729	-2.84386981
C	-10.2152908	1.04750421	3.28124845	H	-4.28778765	-0.37233223	-4.47914399
H	-9.46967541	-0.52548124	2.04524207	H	-6.58565508	0.13433390	-3.77053905
H	-9.26813233	1.76501446	0.11370877	H	-5.98394738	-0.56280872	-2.25628378
H	-8.67920765	3.05064825	1.18523781	H	-4.11092397	2.84331141	-0.42888597
H	-5.98870041	0.25889248	4.31397023	H	-4.02340215	4.48800551	0.91599410
H	-6.08423475	-0.61230065	2.76863604	C	-4.66062197	5.28112580	1.35091322
H	-9.82529746	1.82524067	3.96739744	H	-3.18331278	4.98251210	0.39503488
C	-11.0670986	0.06917713	4.12177604	H	-3.59644743	3.90365607	1.74788664
C	-11.1374149	1.74371785	2.26076526	H	-8.38504728	1.58646440	-3.27873732
H	-10.6776234	2.62655443	1.78882985	H	-9.31920365	1.96632296	-1.83102395
H	-12.0597525	2.09759817	2.75656315	H	-8.64695974	0.32747393	-2.04190891
H	-11.4474126	1.04566493	1.45830442	H	-8.12276243	-1.43639528	3.75025579
H	-10.4771312	-0.47805616	4.87719685	H	-8.34340336	0.01062799	4.73216707
H	-11.5549032	-0.68334820	3.47105532	H	-5.98865451	1.63188054	-2.35482174

Table A.20: Cartesian coordinates for homoallylic cation **625**.

C	-6.81532270	1.43222755	2.58618718	H	-11.9013752	0.82129958	4.69074140
C	-8.04892627	1.11085909	1.69289727	C	-5.78634235	1.55406950	-2.15228343
C	-9.10195106	0.41157494	2.61894868	C	-8.32337951	1.54970031	-2.27356467
C	-8.16565074	-0.31327357	3.65824625	C	-5.22414068	4.48584033	-1.23722436
C	-6.69616639	0.08485089	3.33920709	H	-6.30214779	4.70274911	-1.15609385
C	-7.14732944	2.37496028	-0.18073394	H	-4.71809193	5.46571173	-1.18662246
C	-5.97959601	2.89885983	0.66305092	C	-4.90000862	3.94498473	-2.65983938
C	-7.09542084	1.90377789	-1.44987409	H	-3.93262865	4.32665912	-3.03928355
C	-8.39674953	2.23152555	0.67732983	H	-5.65671027	4.35789654	-3.37521924
C	-4.76951993	3.60346738	-0.03425519	C	-4.98060262	2.50269747	-2.91594328

H	-6.43675343	3.72053718	1.25064928	C	-4.17017401	1.80103217	-3.95156137
C	-5.60072002	1.79309446	1.69123421	H	-4.98421706	1.47051788	-1.35177379
H	-4.75221686	2.12109443	2.31960271	C	-5.68672480	0.19985651	-2.91529977
H	-5.25721633	0.89088464	1.14307772	C	-4.31158052	0.29392693	-3.60205859
H	-7.70153458	0.27696342	1.04635136	H	-3.12506499	2.16651290	-3.94226987
C	-7.06512303	2.57377823	3.60360738	C	-4.76455102	2.16062968	-5.35841087
H	-7.46168720	3.49595881	3.14131226	H	-5.82979449	1.88169678	-5.44439949
H	-6.12261394	2.83853651	4.11813420	H	-4.19978943	1.59226334	-6.11633230
H	-7.78242069	2.28021783	4.38533112	H	-4.65383285	3.23566597	-5.58073872
C	-10.2421160	1.21815095	3.31007843	H	-3.50871953	0.00249037	-2.89891242
H	-9.62060883	-0.34799589	2.00011140	H	-4.21354144	-0.34988746	-4.49213749
H	-9.27957048	1.93703592	0.09136122	H	-6.50154308	0.12020498	-3.65616038
H	-8.63658317	3.18221047	1.18545740	H	-5.78787049	-0.65763035	-2.22958048
H	-6.06930599	0.14434608	4.24761059	H	-4.03170018	2.84871500	-0.38049919
H	-6.22494472	-0.66525459	2.67430088	C	-4.01281345	4.48701305	0.98112674
H	-9.79287583	1.93539919	4.02559326	H	-4.66115824	5.30006817	1.35885997
C	-11.1424916	0.25620689	4.11908844	H	-3.12836868	4.95432186	0.51072417
C	-11.1313313	2.02156060	2.34070203	H	-3.65812536	3.91034600	1.85169897
H	-10.6115954	2.87702623	1.88079879	H	-8.19310022	1.87109725	-3.32571662
H	-12.0056979	2.43418487	2.87681359	H	-9.22185818	2.06190709	-1.89709736
H	-11.5213289	1.37779507	1.52770546	H	-8.54313804	0.46427031	-2.29415542
H	-10.5774023	-0.35761801	4.84194402	H	-8.29945909	1.40874653	-3.63267035
H	-11.6814445	-0.43742072	3.44339509	H	-8.42567113	0.00187701	4.68411186

Table A.21: Cartesian coordinates for transition state **629**.

C	-6.81281828	1.48758859	2.67801640	H	-12.0859310	0.87397169	4.29896198
C	-7.95638372	1.09700675	1.69956101	C	-5.38378304	1.39504373	-1.92864152
C	-9.07798814	0.41984937	2.55768568	C	-7.98734619	1.42720189	-2.23776528
C	-8.23653466	-0.20289933	3.73592919	C	-4.99991531	4.44067075	-1.11318185
C	-6.74719691	0.18287715	3.51084059	H	-6.08073040	4.67432419	-1.08116506
C	-6.93061980	2.33046875	-0.13368806	H	-4.48659820	5.41797746	-1.06997311
C	-5.84021119	2.89707272	0.77148438	C	-4.65869807	3.85837086	-2.49106394
C	-6.78963382	1.79842932	-1.37973684	H	-3.54913462	3.89467654	-2.65249758
C	-8.24157044	2.17438337	0.62038556	H	-5.02368326	4.52130346	-3.30646326
C	-4.59764129	3.59196535	0.13221074	C	-4.95930528	2.46374777	-2.84996958
H	-6.34936512	3.72829986	1.29838028	C	-4.71085435	1.93722291	-4.23048648
C	-5.53492838	1.82515406	1.86610275	H	-4.69384307	1.36614554	-1.06996229
H	-4.73893767	2.19146712	2.53978567	C	-5.29629804	0.06703228	-2.73736368
H	-5.14155123	0.90699538	1.38291404	C	-4.45672448	0.42088445	-3.98828467
H	-7.53697038	0.24750629	1.11939308	H	-3.82052255	2.46551864	-4.62851853
C	-7.16489599	2.67112901	3.61177794	C	-5.85526522	2.22194275	-5.25207221
H	-7.47818924	3.58272354	3.07164751	H	-6.76167943	1.63442364	-5.03464013

H	-6.28740456	2.93824934	4.22903635	H	-5.49420131	1.92809997	-6.25223585
H	-7.98073556	2.42007945	4.30700184	H	-6.12771190	3.29138219	-5.28514524
C	-10.3083503	1.23138850	3.06366959	H	-3.38130966	0.25036382	-3.79594398
H	-9.50443832	-0.39694636	1.94171932	H	-4.72950913	-0.18679903	-4.86826662
H	-9.06278260	1.83958333	-0.02792383	H	-6.29696569	-0.29014549	-3.02882309
H	-8.54219542	3.13381798	1.07766818	H	-4.83858295	-0.73525508	-2.13513073
H	-6.19311852	0.29725410	4.46016389	H	-3.84180069	2.83856993	-0.16708793
H	-6.22482877	-0.60042926	2.92748897	C	-3.90470429	4.49763888	1.17111048
H	-9.95839310	2.01763266	3.76235258	H	-4.57840546	5.30951378	1.50487357
C	-11.2568369	0.29789809	3.84898771	H	-3.00199481	4.96780684	0.73998626
C	-11.1150389	1.92365107	1.94644183	H	-3.58575694	3.93812287	2.06658917
H	-10.5888928	2.77809928	1.49228966	H	-7.75758164	1.47972205	-3.31275488
H	-12.0652444	2.31992000	2.34888155	H	-8.83114544	2.11322139	-2.06427266
H	-11.3750854	1.21073490	1.13957336	H	-8.34747947	0.39913042	-2.03561729
H	-10.7487561	-0.24116198	4.66717585	H	-8.36609966	-1.29705755	3.80165778
H	-11.7041445	-0.46149555	3.17751199	H	-8.58720018	0.20221340	4.70143938

Table A.22: Cartesian coordinates for cyclopropylcarbinyl cation **628**.

C	-6.75570137	1.56883164	2.60209442	H	-12.1801126	1.28695054	3.84532717
C	-7.86786100	1.27415812	1.55962868	C	-5.10869159	1.04143929	-1.62530068
C	-9.09068653	0.66564169	2.32477782	C	-7.80617799	1.09651990	-1.99025133
C	-8.36651343	-0.00967427	3.55309302	C	-7.80617799	1.09651990	-1.99025133
C	-6.84064443	0.24607206	3.40676295	H	-5.61707325	4.86795420	-0.93114480
C	-6.67740159	2.42871737	-0.18533859	H	-3.91425340	5.18676631	-1.22535046
C	-5.59671076	2.93897891	0.74318322	C	-4.66481342	3.57309319	-2.39737218
C	-6.54708069	1.75458531	-1.42708774	H	-3.61994449	3.40607584	-2.73296708
C	-8.00759057	2.42647800	0.50772380	H	-5.12348638	4.20829187	-3.17732329
C	-4.29032118	3.54908915	0.17221109	C	-5.31086209	2.19736730	-2.48256903
H	-6.07471725	3.78635208	1.26791101	C	-5.45271381	1.69186951	-3.94260742
C	-5.42865497	1.82127931	1.84813007	H	-4.49233718	1.06835069	-0.72439058
H	-4.63611937	2.15624233	2.54021292	C	-5.10539297	-0.25530764	-2.42920240
H	-5.06832317	0.88402329	1.38149321	C	-5.47644351	0.13554658	-3.88647016
H	-7.47784646	0.40982340	0.98271927	H	-4.47029747	1.98822948	-4.36657731
C	-7.05811502	2.76037392	3.54087737	C	-6.51872313	2.34662345	-4.83144374
H	-7.17841914	3.72244855	3.01055417	H	-7.54782597	2.11625562	-4.50732032
H	-6.22873873	2.88734683	4.25999363	H	-6.41048884	1.98583686	-5.87011037
H	-7.97488808	2.60611359	4.13041273	H	-6.40947693	3.44571251	-4.85821394
C	-10.3014619	1.54918607	2.74486468	H	-4.75919775	-0.28948868	-4.60857362
H	-9.51530065	-0.12309026	1.67317059	H	-6.46029438	-0.26633675	-4.18482778
H	-8.84875401	2.24086214	-0.16793037	H	-5.76572041	-1.02864891	-1.99715098
H	-8.84875401	2.24086214	-0.16793037	H	-4.07877488	-0.66373280	-2.36699207
H	-6.32502980	0.29290206	4.38231348	H	-3.56027713	2.75964049	-0.09180940

H	-6.36194469	-0.56861269	2.82894445	C	-3.62777260	4.44967357	1.23072702
H	-9.95597139	2.31565090	3.46784239	H	-4.27729423	5.30872808	1.48560382
C	-11.3490925	0.66848897	3.46117336	H	-2.67487407	4.85754784	0.84842548
C	-10.9890696	2.28056903	1.57266224	H	-3.40125920	3.90969949	2.16639709
H	-10.3982289	3.11654739	1.16486591	H	-7.62771369	0.54447344	-2.91595661
H	-11.9487937	2.71631705	1.90457732	H	-8.58347700	1.84778322	-2.21060052
H	-11.2193354	1.58211167	0.74435868	H	-8.22816041	0.37437487	-1.26935004
H	-10.9286571	0.11325779	4.31734452	H	-8.59296253	-1.08733907	3.62344893
H	-11.7826964	-0.07426971	2.76291357	H	-8.73340199	0.44108626	4.49180280

Table A.23: Cartesian coordinates for transition state **630**.

C	-6.69848393	1.77294253	2.62923258	H	-5.70916520	1.18164082	-1.20397638
C	-7.60425816	1.06626984	1.59264922	C	-8.01684174	2.93143930	-2.38103442
C	-8.73813032	0.34234874	2.39836426	C	-4.19771186	4.14622671	-1.25530464
C	-8.02034659	0.07100192	3.77752244	C	-5.04146610	4.85003861	-1.41696511
C	-6.58112092	0.64487443	3.68047668	H	-3.28421499	4.75435593	-1.38568870
C	-6.55596787	2.32543668	-0.33657241	H	-4.19946747	3.06898077	-2.34171611
C	-5.59081313	3.05110615	0.67933454	C	-3.31857839	2.40493194	-2.24221546
C	-6.69289447	2.70803774	-1.74117565	H	-4.10371459	3.56160680	-3.32799977
C	-7.87898990	1.92808984	0.35512042	H	-5.45875211	2.19595375	-2.40046498
C	-4.22587722	3.62148481	0.19200956	C	-5.59706055	1.34325147	-3.69337352
H	-6.20161286	3.92672620	0.97574150	C	-4.79720096	1.01622918	-0.60859262
C	-5.38534240	2.14926265	1.92245913	H	-6.34442336	-0.08765969	-1.79900906
H	-4.70440722	2.65722001	2.62728654	C	-6.54762533	0.17846166	-3.31922676
H	-4.85339200	1.22551613	1.61114530	C	-4.58018204	0.90876114	-3.79961680
H	-6.98384707	0.22386475	1.21984512	H	-5.90993504	2.05685445	-5.01553792
C	-7.33431253	3.02674500	3.28063703	C	-6.95026154	2.42377747	-5.07566647
H	-7.69774753	3.77004883	2.54862216	H	-5.76326973	1.36177388	-5.86108340
H	-6.59213785	3.53593244	3.92261842	H	-5.23692747	2.91567523	-5.18775134
H	-8.19076892	2.77086023	3.92406021	H	-6.32986645	-0.72061525	-3.92117400
C	-10.1397398	1.00135513	2.57419000	H	-7.59692275	0.44206170	-3.54685859
H	-8.93128571	-0.62451084	1.89136034	H	-7.27900832	-0.38490933	-1.29150462
H	-8.51803410	1.37123042	-0.34887962	H	-5.63698131	-0.92033720	-1.63933933
H	-8.42866092	2.85097459	0.61498423	H	-3.46800530	2.81267579	0.26881528
H	-6.19619354	0.99702673	4.65499356	H	-3.78740557	4.76110631	1.14002226
H	-5.87501909	-0.12765434	3.31699391	C	-4.46709462	5.62944162	1.04746251
H	-10.0234607	1.94260372	3.14820065	H	-2.76981481	5.10782292	0.88743960
C	-11.0502988	0.06005252	3.39285103	H	-3.77705217	4.45423068	2.19924607
C	-10.8552733	1.33721110	1.24789561	H	-7.91204034	3.31201495	-3.40753524
H	-10.4233310	2.20293552	0.72128877	H	-8.59272450	3.64304585	-1.76033764
H	-11.9157786	1.58684921	1.43490492	H	-8.62975913	2.01162265	-2.41910745
H	-10.8420638	0.47072194	0.55731044	H	-8.01452099	-1.00122935	4.03973557

H	-10.6012408	-0.24556344	4.35358165	H	-8.56955680	0.57694910	4.59086992
H	-11.2707166	-0.86364243	2.82207875	H	-5.70916520	1.18164082	-1.20397638

Table A.24: Cartesian coordinates for cyclobutyl cation **626**.

C	-6.76248965	1.80538018	2.58705640	H	-5.53436598	1.06649210	-1.09670649
C	-7.58787658	0.98975260	1.55995700	C	-7.57225783	3.75704466	-2.19303819
C	-8.72204805	0.26658350	2.36502928	C	-4.13802206	4.05761672	-1.32417815
C	-8.03193852	0.07966947	3.77218237	C	-4.93044469	4.81810390	-1.49562759
C	-6.62966500	0.74548777	3.70677576	H	-3.18974106	4.60980482	-1.45301015
C	-6.47467087	2.13399956	-0.40401407	H	-4.20556237	2.97730633	-2.41778801
C	-5.59700569	3.04061468	0.63052971	C	-3.31625589	2.31918968	-2.38406417
C	-6.58161481	2.80568947	-1.69556345	H	-4.20787059	3.47188463	-3.40685328
C	-7.83360709	1.75422084	0.26063360	H	-5.45371238	2.05930098	-2.32588977
C	-4.21511280	3.57514581	0.14367239	C	-5.77406350	1.21737406	-3.60231731
H	-6.24063449	3.91763938	0.83351888	C	-4.59659312	0.87476492	-0.55341312
C	-5.43439271	2.20250473	1.92328618	H	-6.16633027	-0.22994705	-1.65573276
H	-4.81520519	2.78059006	2.63264495	C	-6.71573130	0.11791397	-3.05918092
H	-4.84978144	1.29160259	1.68628175	C	-4.80251591	0.74327613	-3.85591958
H	-6.91616141	0.15338186	1.27359732	H	-6.27103159	1.97194221	-4.83842054
C	-7.48248238	3.06116073	3.13812603	C	-7.29905132	2.36154843	-4.71595071
H	-7.85048158	3.74293841	2.35033440	H	-6.28585358	1.29715358	-5.71262654
H	-6.79162158	3.64222591	3.77657902	H	-5.61274407	2.81929757	-5.10347581
H	-8.35059743	2.80084917	3.76369793	H	-6.76176685	-0.76115195	-3.72584671
C	-10.1489648	0.88348407	2.48008855	H	-7.75217774	0.51372342	-2.99702708
H	-8.87054262	-0.72537693	1.89323098	H	-6.93357916	-0.66710672	-0.99267001
H	-8.41791602	1.14646361	-0.45330074	H	-5.36926159	-0.98998868	-1.74701532
H	-8.40667202	2.68267557	0.43130411	H	-3.47114090	2.76197394	0.26919454
H	-6.31611409	1.17490640	4.67587108	H	-3.78953007	4.74997338	1.05536954
H	-5.85876442	0.00266633	3.42283172	C	-4.46445504	5.61640602	0.91971192
H	-10.0873723	1.82623369	3.05925366	H	-2.76653656	5.08381403	0.80771370
C	-11.0579997	-0.08880945	3.26391824	H	-3.79786040	4.48379507	2.12517315
C	-10.8211824	1.20338683	1.12805999	H	-7.23034047	4.33041015	-3.06969671
H	-10.3853001	2.07763062	0.61814033	H	-7.95373556	4.41444984	-1.39047926
H	-11.8924980	1.43260222	1.27608907	H	-8.44770225	3.14628718	-2.52053416
H	-10.7657787	0.33828976	0.43822775	H	-7.95932177	-0.98367804	4.05969845
H	-10.6244444	-0.39389346	4.23225820	H	-8.64030900	0.56383336	4.55624879
H	-11.2392369	-1.01147930	2.67824294	H	-5.53436598	1.06649210	-1.09670649

Table A.25: Cartesian coordinates for allylic alcohol **622**.

C	-0.06567973	0.19680303	0.12116555	H	-0.90597146	1.69566124	-1.99024765
C	0.03240677	-1.21337806	0.81530966	C	0.30048348	1.31255010	-3.70624689
O	-1.46813510	0.51056379	0.03379907	C	1.01237278	2.69202718	-1.72092804

C	0.46090753	0.15151417	-1.37261304	H	-0.39590060	0.57463075	-4.13760026
C	0.67204127	1.23793606	1.02002155	H	1.32929046	1.02374894	-4.00062913
C	-0.07803612	-1.09139114	-2.14185588	H	0.07982552	2.28106701	-4.19366618
H	1.56365655	0.05204657	-1.30303560	C	1.84647650	0.72136645	1.84002909
C	0.16029188	1.46719565	-2.17529190	H	1.54012346	0.06581202	2.67780102
C	0.08488460	-2.43141894	-1.40286439	H	2.44117470	1.54036596	2.27285306
H	0.43992807	-1.15777041	-3.11571416	H	2.53633394	0.12559193	1.21153371
H	-1.15170631	-0.93409220	-2.36489655	C	-0.59767969	3.34632619	0.21103844
C	1.58562071	-2.81107505	-1.32549507	C	0.93766244	3.52987508	2.12746174
C	-0.83077413	-4.61626419	-0.84072867	C	0.20590761	3.80953413	-1.04021434
C	-0.61343408	-2.31283274	-0.02475662	H	1.52022049	3.13350131	-2.60037184
C	-0.83883641	-3.78421710	0.49590545	H	1.83117405	2.36695830	-1.05451963
H	-0.47205862	-1.10984691	1.79515280	C	0.19620087	4.87527612	1.92469107
H	1.07994095	-1.47503459	1.03286208	C	-1.06904301	4.52068675	1.11015745
H	1.98147253	-2.98624744	-2.34415674	H	0.90127981	4.62872935	-0.76958668
H	1.76424080	-3.73083031	-0.74422985	H	-0.50436127	4.24452186	-1.77155313
H	2.20627461	-2.02017443	-0.87040633	H	0.82368545	5.58618216	1.35261378
H	-1.63110667	-1.94702152	-0.26063372	H	-0.04518531	5.37492054	2.88095326
H	-1.85799363	-3.82906571	0.93140250	H	-1.81389953	4.09211094	1.81473798
C	0.09996709	-4.37743584	1.59264548	C	-1.72385116	5.70838802	0.39595399
H	1.15304238	-4.25293296	1.26377860	H	-1.00348989	6.25326668	-0.24292127
C	-0.15260963	-5.89017992	1.78595694	H	-2.12810589	6.43561751	1.12502540
C	-0.05333910	-3.69540808	2.96809664	H	-2.56208119	5.38167499	-0.24838356
H	0.02814125	-6.48154970	0.87250017	H	-1.77750773	0.70117569	0.93453026
H	-1.19716925	-6.07678883	2.10637958	C	-0.71169486	-3.60971308	-2.01035599
H	0.50909474	-6.29798162	2.57253187	H	-1.72260277	-5.26189234	-0.93385015
H	0.28861171	-2.64906315	2.97816093	H	0.03842049	-5.29793986	-0.86226986
H	0.53670562	-4.23324551	3.73332416	H	-1.71176129	-3.25254075	-2.32518300
H	-1.11021848	-3.71209654	3.30012136	H	-0.23161076	-4.05356342	-2.90341805
C	-0.06567973	0.19680303	0.12116555	C	0.32839171	2.54488913	1.11698654
C	0.03240677	-1.21337806	0.81530966	H	-1.45437154	2.75340562	-0.13721106

Table A.26: Cartesian coordinates for desoxy-astellatol (**627**).

H	-1.74356382	2.19641481	2.26926296	C	-0.18746080	-0.70547138	-0.07443316
H	-1.87386813	3.73782089	3.13744404	C	-0.48671324	0.66411847	0.57988348
H	-0.35763751	2.80878208	3.20909924	C	-0.28769653	-0.64047285	-1.64670414
C	-0.38480882	-1.85838747	-3.89836349	H	-1.35979117	-0.45459960	-1.86453930
H	-1.49153630	-1.85052903	-3.94028851	C	0.10478433	-1.94216015	-2.43557038
H	-0.04216642	-2.73800842	-4.47320000	C	0.54574063	0.55824406	-2.18600624
H	-0.01892025	-0.96350682	-4.43051874	H	-1.55610443	0.90676359	0.42986822
C	1.11742893	-1.47166881	0.37868548	C	0.40970537	1.75828451	0.00143459
C	1.75220588	-1.16440457	1.75945410	H	-0.35202988	0.56290685	1.67015272

C	0.23340098	-2.76506834	0.59905007	C	0.20596790	1.91087667	-1.52846367
C	0.64449691	-3.33142748	1.98241947	H	0.43087459	0.63913967	-3.28237412
C	-0.35613289	-4.24907846	2.69116167	H	1.61939625	0.34075217	-2.00919753
C	1.03324183	-2.07066204	2.78397463	C	-1.21481342	2.36864335	-1.94283072
H	1.57296820	-3.91750311	1.79963499	C	1.21600102	3.04467211	-1.82517564
H	1.71548355	-0.09717440	2.04164329	H	1.44270820	1.36130826	0.09393440
H	2.82483355	-1.43487814	1.72254403	C	0.53416206	3.20498753	0.59533307
H	1.66584572	-2.30352767	3.66157996	H	-1.49605709	3.33407191	-1.48915899
H	0.11542398	-1.58296930	3.16771778	H	-1.25767847	2.50091955	-3.04097994
H	0.07956116	-4.65644197	3.62305317	H	-2.00148060	1.64321857	-1.67254530
H	-0.64302267	-5.11282866	2.06251896	C	-0.66983305	3.88540683	1.31160773
H	-1.27672723	-3.70286790	2.96727784	C	1.04503033	4.03311548	-0.64426347
H	1.89487323	-1.54008108	-0.40099176	H	1.33696249	3.16803049	1.36035475
C	-0.39763331	-3.28788805	-1.85332194	H	1.05131172	3.52875493	-2.80683839
H	1.21398076	-1.99025727	-2.46479208	H	2.24262919	2.62787798	-1.83320369
C	0.26193050	-3.77901029	-0.55323557	H	1.98086119	4.57827906	-0.42473725
C	-0.99867645	-1.85511818	0.52003735	H	0.30294602	4.80535567	-0.91728973
H	-0.25581541	-4.70689140	-0.23735108	H	-1.50826568	3.98373700	0.59061667
H	1.31814538	-4.06092384	-0.74578776	C	-0.26826645	5.30826565	1.75901355
H	-0.23106023	-4.06642855	-2.62355912	C	-1.18854759	3.10719727	2.54025077
H	-1.49530139	-3.23374548	-1.71630530	H	0.05835710	5.94523695	0.91880223
C	-2.27850826	-1.95096664	0.88974806	H	0.56628180	5.26491504	2.48721863
H	-2.69322466	-2.86098643	1.34000679	H	-1.11281530	5.82261268	2.25438821
H	-2.97641261	-1.11491252	0.74442609				

Table A.27: Cartesian coordinates for diene (**631**).

C	-0.18500578	-0.18805095	-0.58867581	C	-2.22145674	-2.47941583	-1.63632480
C	1.08464816	0.65568101	-0.38975266	C	-2.49012040	-2.13235970	0.92339418
C	-0.26540524	-1.48777610	-0.20639037	H	-3.02736867	-3.23774645	-1.59801265
C	-1.29536865	0.56000389	-1.26018135	H	-1.50466687	-2.79705368	-2.41563147
C	0.94125919	-2.22156574	0.38056864	H	-2.67473757	-1.53079099	-1.96404598
C	-1.51732398	-2.37929835	-0.26676747	C	-0.98877618	1.02998304	-2.67464502
C	2.27838683	-1.49073033	0.18689122	H	-0.19762836	1.80601783	-2.68742939
H	0.76113174	-2.41071207	1.46191285	H	-1.86806475	1.45617724	-3.18465924
H	0.99236982	-3.22863823	-0.08319586	H	-0.61270909	0.19207668	-3.29285865
C	2.74624695	-1.66860584	-1.28064441	C	-2.83672979	0.46128038	0.78372428
C	4.37624881	-0.70188564	1.11787445	C	-3.62876487	1.62423188	-1.26376728
C	2.07167392	-0.00247690	0.57631129	C	-3.47333443	-0.94988670	0.87380406
C	3.50766095	0.58510633	0.88139456	H	-3.09622287	-3.05288864	1.04988368
H	1.55957598	0.85828492	-1.37061063	H	-1.88005779	-2.05174778	1.84626447
H	0.75915600	1.64174448	-0.00539194	C	-4.64107299	1.83292489	-0.10997156
H	3.05464874	-2.71690205	-1.45618218	C	-3.80925108	1.61960269	1.17453130

H	3.60574500	-1.02586298	-1.53701971	H	-4.08019568	-1.01384886	1.79669053
H	1.93832770	-1.44147222	-1.99727895	H	-4.19003062	-1.09512107	0.04107064
H	1.55831066	-0.02905331	1.55977145	H	-5.13090425	2.82385844	-0.14247513
H	3.44128298	1.13361246	1.84293394	H	-5.45288646	1.08033400	-0.15798591
C	4.14225178	1.59282511	-0.12447395	H	-3.16425987	2.51521778	1.30511078
H	4.05486913	1.17269533	-1.14849656	C	-4.63199302	1.45247962	2.45631404
C	5.64500867	1.81437782	0.15951000	H	-3.98636347	1.23456056	3.32843120
C	3.44285032	2.96691735	-0.10474840	H	-5.19446911	2.37788995	2.68338613
H	6.24779460	0.89819654	0.03958273	H	-5.37576542	0.63805636	2.37569942
H	5.80194273	2.18864745	1.19090767	C	3.40238884	-1.89900587	1.16265435
H	6.06384699	2.57075294	-0.52980090	H	4.99523390	-0.62353524	2.02986545
H	2.38900037	2.92574084	-0.42185865	H	5.08308497	-0.84732195	0.28123087
H	3.95710425	3.67751307	-0.77824988	H	3.89085063	-2.85599605	0.89699386
H	3.47268692	3.40345644	0.91326388	H	2.97762092	-2.02167844	2.17893187
H	-1.13472992	-3.40087715	-0.07443043	C	-2.46524986	0.83559001	-0.64804337
C	-0.18500578	-0.18805095	-0.58867581	H	-1.94631210	0.47294141	1.44128384

Table A.28: Cartesian coordinates for diene (**632**).

C	0.44176242	-0.19343427	-0.14963278	C	-3.07018230	-1.79782060	-0.79275502
C	0.72994697	1.25340537	-0.55564636	C	-0.87144812	-1.96927207	-2.08138206
C	-1.00333393	-0.60674985	0.14597611	H	-3.77960029	-1.11591113	-0.29152799
C	1.45801879	-1.09401551	-0.10840199	H	-2.90398417	-2.65063737	-0.10757890
C	-1.84298457	0.48382013	0.91160758	H	-3.57401350	-2.19035944	-1.69691426
C	-1.74515967	-1.09177411	-1.15074689	C	2.89878604	-0.67885835	-0.39081679
C	-1.09376594	1.81643960	1.10013527	H	3.33954073	-0.09926203	0.44635640
H	-2.17367954	0.08491001	1.89026432	H	2.97783177	-0.04091333	-1.29092405
H	-2.77032651	0.69642924	0.34659103	H	3.54623759	-1.55708520	-0.55768960
C	-0.05936647	1.67654081	2.24658832	C	0.43937658	-3.43853097	-0.31663510
C	-1.07200180	4.23102167	0.95250022	C	2.01903812	-3.12482834	1.42919028
C	-0.46431016	2.17343698	-0.28141152	C	-0.44795498	-3.34871096	-1.53828654
C	-0.34043518	3.75045075	-0.34153779	H	0.02196433	-1.40224664	-2.39653961
H	1.00782035	1.27299521	-1.62964447	H	-1.45114385	-2.14833743	-3.00932855
H	1.62681477	1.61458090	-0.01932923	C	1.81575442	-4.64525265	1.24945301
H	-0.59564463	1.59674866	3.21183380	C	0.49686419	-4.76938267	0.44114668
H	0.62875984	2.53764925	2.31579672	H	-1.35533937	-3.95841535	-1.35172524
H	0.56061827	0.76998881	2.14393803	H	0.07299587	-3.89467950	-2.35559826
H	-1.23804810	1.91488234	-1.02979219	H	1.79691226	-5.20350649	2.20360408
H	-0.95720985	4.08472277	-1.20049429	H	2.64915069	-5.05571998	0.64811522
C	1.06692374	4.35901641	-0.58518767	H	0.54508507	-5.62239000	-0.26797229
H	1.79251687	3.84975627	0.08300958	C	-0.74818596	-4.96667263	1.33455534
C	1.11425820	5.86580943	-0.25835720	H	-0.82613510	-4.16303377	2.09105258
C	1.51691308	4.15306940	-2.04689003	H	-0.71020214	-5.93369207	1.87100254

H	0.95922442	6.07461728	0.81446346	H	-1.68071688	-4.95305545	0.73988781
H	0.33834551	6.41915680	-0.82273766	C	-1.98060927	3.05513284	1.36129697
H	2.09339861	6.29622992	-0.54162219	H	-1.63063752	5.17219431	0.80062091
H	1.46888594	3.09888995	-2.36608514	H	-0.34203586	4.43463277	1.75840798
H	2.55450322	4.50465434	-2.20323192	H	-2.87405104	3.01917133	0.70594199
H	0.86824681	4.73196524	-2.73294388	H	-2.34490506	3.12804524	2.40376527
H	-2.00067826	-0.18558373	-1.74121017	C	1.26034467	-2.52046423	0.24795578
C	0.44176242	-0.19343427	-0.14963278	H	3.08738675	-2.83635161	1.44918376

Table A.29: Cartesian coordinates for diene (**633**).

C	-0.46770749	0.29918462	-0.88462699	C	1.57790662	-1.81370398	-1.73022479
C	-0.02066305	1.42900117	-0.29388256	H	-1.34924576	-2.26847479	-3.66376182
C	-0.24173126	-0.00561494	-2.37053889	H	-1.23075508	-2.72269786	-1.94600803
C	-1.32785202	-0.67744974	-0.13586950	H	-0.14739195	-3.47863583	-3.14633179
C	0.55649303	1.10032895	-3.12603922	C	-2.81955140	-0.47755206	-0.30989180
H	-1.25292036	-0.04153360	-2.82818584	H	-3.12007579	0.53479830	0.02519543
C	0.40032402	-1.40967325	-2.66695620	H	-3.42253804	-1.21323563	0.24644078
C	0.31662330	2.50769021	-2.55452236	H	-3.11069207	-0.55331248	-1.37713121
H	0.28240763	1.05302650	-4.19958626	C	0.69369154	-1.96066544	0.75861176
H	1.64050455	0.87614729	-3.06827253	C	-1.60011178	-2.73088284	1.37105002
C	-1.16779761	2.89088398	-2.77181321	C	1.31395435	-2.67262805	-0.47076530
C	1.19868217	4.70020116	-1.93824259	H	2.28648896	-2.39766362	-2.35042886
C	0.78655819	2.44046217	-1.06848663	H	2.13748751	-0.90342210	-1.43436817
C	1.06479244	3.91003380	-0.58948086	C	-0.53998069	-3.69127238	1.95310161
H	-1.43296474	2.73400152	-3.83517127	C	0.72927644	-2.81979561	2.06594961
H	-1.37772354	3.94646974	-2.53910863	H	0.70678872	-3.55800623	-0.74226370
H	-1.85505819	2.27823157	-2.16507413	H	2.29764043	-3.07914937	-0.16734510
H	1.80767811	2.00859854	-1.13977406	H	-0.35628359	-4.53582702	1.25914673
H	2.06341031	3.89473561	-0.11082642	H	-0.84399222	-4.13736005	2.91844542
C	0.14610923	4.55354914	0.48787905	H	0.55631915	-2.10607451	2.89979571
H	0.22021015	3.89595638	1.37961172	C	2.02035860	-3.58741705	2.37208306
C	-1.34684756	4.66213090	0.13111384	H	2.22383816	-4.37913115	1.62769197
C	0.69433279	5.93615743	0.90397615	H	1.95851894	-4.08275161	3.35969102
H	-1.79022517	3.68218714	-0.11225095	H	2.89740105	-2.91278033	2.39507561
H	-1.52001739	5.33508056	-0.72980015	C	1.22679245	3.64465115	-3.07732116
H	-1.91471372	5.08350470	0.98193315	H	2.09374224	5.34795320	-1.95406458
H	0.65123040	6.65737714	0.06527374	H	0.33370877	5.37492128	-2.07890646
H	1.74730864	5.87765301	1.23937052	H	2.25664726	3.26202719	-3.22335079
H	0.10376699	6.36802515	1.73343487	H	0.89605275	4.06052618	-4.04813504
H	0.86916555	-1.28085654	-3.66395933	C	-0.80094979	-1.68148579	0.59029277
C	-0.63934333	-2.52985505	-2.85657688	H	1.25366082	-1.01872652	0.91011538
C	-0.46770749	0.29918462	-0.88462699	H	-2.34463636	-3.25644870	0.74283816

Table A.30: Cartesian coordinates for diene (**634**).

C	2.00753906	-1.16074237	-1.00697967	C	-0.98822668	-1.71978779	1.14809832
C	0.69269949	-1.94115219	-0.81705895	H	-0.11697471	-1.79337748	1.83444277
C	-0.47279775	-1.08410751	-0.19169304	C	-1.07906958	1.34937086	-0.23775754
C	-0.13021623	0.40527469	-0.03081988	C	-2.48848782	1.01252720	-0.59007187
C	1.28082527	0.79315200	0.43033791	C	-0.87833736	2.84007848	-0.03389877
C	2.26197672	-0.38026753	0.31791803	H	0.12127103	3.11416977	0.33969053
H	0.91185730	-2.79790005	-0.15405332	H	-1.06571063	3.38718486	-0.97918405
H	0.36205635	-2.38278544	-1.77720303	H	-1.61803922	3.23269655	0.69150324
H	1.99799078	-1.08933952	1.12622902	C	-1.52046631	-3.15246854	0.91698569
C	1.91163413	-0.25896786	-2.26500837	H	-1.91870908	-3.58351575	1.85530456
H	2.75487325	0.44899247	-2.35394572	H	-2.34108393	-3.16586985	0.17495472
H	1.91543531	-0.89627415	-3.17040147	H	-0.74031061	-3.83854276	0.54556175
H	0.98191986	0.33434033	-2.28617766	C	-3.53583657	0.77382667	0.50236718
C	3.28430434	-2.02864008	-1.09687684	H	-3.43592021	1.53354404	1.30637142
C	3.82801270	-0.18017512	0.44278029	C	-3.03760738	0.91375707	-1.81428727
H	4.13610464	-0.66830631	1.38984272	C	-4.87475496	0.99379939	-0.28066791
C	4.40770449	-1.04364043	-0.72166520	C	-4.52295325	0.62541894	-1.75062258
C	4.37691988	1.26953104	0.53454216	H	-5.04409455	2.08989003	-0.26831727
H	3.86618490	1.89310693	-0.22873159	H	-5.11429760	1.21155282	-2.48103696
C	5.89171398	1.34243711	0.25096357	H	-4.73957746	-0.44350624	-1.97262348
H	6.14552156	1.07443651	-0.78953288	C	-6.13773380	0.32781555	0.27492446
H	6.27272501	2.36529968	0.43197155	H	-7.02251162	0.62500576	-0.31953194
H	6.45565089	0.66120464	0.91756113	H	-6.08107324	-0.77625726	0.25015683
C	4.10303889	1.87373482	1.92802913	H	-6.32777593	0.63121583	1.32214668
H	4.42780541	2.93043295	1.98162733	C	-3.39240744	-0.61480275	1.17574654
H	3.03726398	1.83499986	2.20854065	C	-2.04582507	-0.87356304	1.90288190
H	4.66689958	1.31744615	2.70228621	H	-4.21089265	-0.71766534	1.91318581
H	4.64934550	-0.40831458	-1.59419122	H	-3.57845419	-1.40388669	0.42271732
H	5.34738612	-1.55258243	-0.44057938	H	-2.25693482	-1.41126002	2.84780306
H	3.23102021	-2.84748071	-0.35110246	H	-1.59960230	0.09073113	2.21269862
H	3.43120623	-2.50052216	-2.08706838	H	-1.32416911	-1.13213134	-0.89228712
C	2.00753906	-1.16074237	-1.00697967	H	1.23240643	1.16272701	1.47414493

Table A.31: Cartesian coordinates for conformer **635**.

C	0.09374278	-0.16459038	-0.05334760	H	-3.25094725	-1.01474055	0.55520799
C	0.80548482	1.23777566	0.02394943	C	-2.11037893	-2.13991143	1.93682235
O	-0.04953665	-0.46896337	-1.44972321	C	-2.15029437	-2.36926437	-0.63241648
C	-1.34751700	-0.08482683	0.55541018	H	-2.40931390	-1.47409764	2.76859830
C	0.91868485	-1.23721157	0.69462105	H	-1.08980852	-2.50266264	2.14902558
C	-2.16160571	1.09220184	-0.05197012	H	-2.78601664	-3.01625872	1.96404102
H	-1.18137261	0.16842486	1.61968183	C	1.60270665	-0.75905540	1.96834471

C	-2.21275939	-1.39994034	0.58575924	H	2.49057745	-0.13331903	1.75223697
C	-1.44030230	2.45128942	0.06539419	H	1.94741461	-1.58835215	2.60333317
H	-3.13950099	1.14271993	0.46741790	H	0.92517400	-0.14048747	2.58751163
H	-2.37906359	0.87795223	-1.11633909	C	0.34650440	-3.26750252	-0.85702790
C	-1.37212955	2.88466411	1.55249259	C	1.82151855	-3.56614624	1.12650865
C	-0.89086344	4.61526944	-0.91120737	C	-1.15871650	-3.55514211	-0.62918406
C	-0.05276801	2.32911229	-0.62384983	H	-2.02910867	-1.78670287	-1.56130569
C	0.45583546	3.79928082	-0.87345414	H	-3.15481880	-2.83519707	-0.69866386
H	1.77616702	1.12891776	-0.49989110	C	1.55508348	-4.92940767	0.46569715
H	1.04714414	1.50549587	1.06515101	C	1.19998167	-4.57333992	-0.98980224
H	-2.39537994	2.99942613	1.95821578	H	-1.28896449	-4.14391147	0.30073323
H	-0.85746036	3.84982497	1.69065876	H	-1.48979424	-4.22653891	-1.44413104
H	-0.85082181	2.15300417	2.19284343	H	0.69452265	-5.43446936	0.94835620
H	-0.28890756	1.95057735	-1.63633231	H	2.41305249	-5.62246011	0.54795977
H	0.90907386	3.82641322	-1.88552105	H	2.14177540	-4.26545909	-1.49381768
C	1.53323994	4.41787007	0.07172452	C	0.59859153	-5.73555787	-1.78884501
H	1.19946616	4.29154014	1.12287618	H	-0.26920279	-6.18633957	-1.27268662
C	1.70615640	5.93233824	-0.18467744	H	1.34704255	-6.53880844	-1.92538113
C	2.91966550	3.75551059	-0.07106603	H	0.26202295	-5.41975403	-2.79501964
H	0.78486875	6.51202744	-0.00579446	H	0.84311088	-0.53380150	-1.82673008
H	2.02559310	6.12136075	-1.22910413	C	-2.05213731	3.60011371	-0.76903200
H	2.48634506	6.35200114	0.47717902	H	-0.98007762	5.22467466	-1.82851045
H	2.94125868	2.70764256	0.26601928	H	-0.93183876	5.33098008	-0.07087049
H	3.67259647	4.30092652	0.52775141	H	-2.35943377	3.21157548	-1.75951093
H	3.26068556	3.78172660	-1.12496917	H	-2.95096079	4.04990065	-0.30555171
C	0.09374278	-0.16459038	-0.05334760	C	1.00729390	-2.53703391	0.32613055
C	0.80548482	1.23777566	0.02394943	H	0.42688517	-2.69074948	-1.79025449

Table A.32: Cartesian coordinates for water.

O	-3.16767047	-0.72594854	0.01005517
H	-2.19860750	-0.67756464	-0.01280005
H	-3.44037202	0.11642318	-0.38788512

VI. List of Abbreviations

$\tilde{\nu}$	wavenumber
[1,2]~H	[1,2]-hydride shift
2D	two-dimensional
3D	three-dimensional
9-BBN	9-borabicyclo[3.3.1]nonane
Ac	acetyl
ADP	adenosine diphosphate
Alk	alkyl
AMPA	α -amino-3-hydroxy-5-methyl-4-isoxazolepropionic acid
Ar	aryl substituent
Arc (protein)	activity-regulated cytoskeleton-associated (protein)
atm	atmosphere(s)
ATP	adenosine triphosphate
ATR	attenuated total reflection (IR spectroscopy)
B3LYP	Becke, three-parameter, Lee-Yang-Parr
BDNF	brain-derived neurotrophic factor
BINAP	2,2'-bis(diphenylphosphino)-1,1'-binaphthalene
BINAPO	2-diphenylphosphino-2'-diphenylphosphinyl-1,1'-binaphthalene
Boc	<i>tert</i> -butyloxycarbonyl
Bn	benzyl
br	broad
brsm	based on recovered starting material
BTZ	benzo(thi)azepine
Bu	butyl
©	copyright
<i>c</i>	cyclo, concentration (optical rotation)
C _{2v}	symmetry point group
CDI	calcium-dependent inactivation
calcd.	calculated
CaM	calmodulin
cAMP	cyclic adenosine monophosphate
CaMK	calmodulin-dependent protein kinase

cat.	catalyst, catalytic
Cav (channel)	voltage-gated calcium (channel)
CCDC	Camebridge Crystallographic Data Centre
CMP	cytidine monophosphate
CoA	coenzyme A
COSMO	conductor-like screening model
COSY	homonuclear correlation spectroscopy (NMR spectroscopy)
Cp	cyclopentadienyl
CREB	cAMP response element-binding protein
CSA	camphorsulfonic acid
CTP	cytidine triphosphate
CuTC	copper(I)-thiophene-2-carboxylate
Δ	elevated temperature
δ	chemical shift (NMR spectroscopy)
D	sodium D line (optical rotation)
d	doublet (NMR spectroscopy), deuterio
dba	dibenzylideneacetone
DBU	1,8-diazabicyclo[5.4.9]undec-7-ene
DCC	<i>N,N'</i> -dicyclohexylcarbodiimide
DCE	1,2-dichloroethane
decomp.	decomposition
DFT	density functional theory
DHP	dihydropyridine
DIBAL	diisobutylaluminum hydride
DIPA	diisopropylamine
DIPEA	diisopropylethylamine
DIPT	diisopropyl tartrate
DMAP	4-(dimethylamino)pyridine
DMAPP	dimethylallyl pyrophosphate
DME	dimethoxyethane
DMF	<i>N,N</i> -dimethylformamide
DMP	Dess-Martin periodinane
DMPU	<i>N,N'</i> -dimethyl- <i>N,N'</i> -trimethyleneurea
DMSO	dimethylsulfoxide

DOXP	1-deoxy-D-xylulose 5-phosphate
DPBS	Dulbecco's phosphate-buffered saline
dppf	1,1'-bis(diphenylphosphino)ferrocene
<i>dr</i>	diastereomeric ratio
DTMB-SEGPPOS	see ref. 511
E	electrophile
e	electron
E1	unimolecular elimination
E1cB	elimination unimolecular conjugate base
E2	bimolecular elimination
EDCI	<i>N</i> -(3-dimethylaminopropyl)- <i>N</i> -ethylcarbodiimide hydrochloride
<i>ee</i>	enantiomeric excess
eGFP	enhanced green fluorescent protein
EI	electron impact ionization (mass spectroscopy)
Enz	enzyme
eq.	equivalent(s)
Et	ethyl
<i>er</i>	enantiomeric ratio
ESI	electron spray ionization (mass spectroscopy)
FAB	fast atom bombardment (mass spectroscopy)
FAD	flavin adenine dinucleotide
FDA	Food and Drug Administration
G2 (phase)	growth (phase) 2
GABA	γ -aminobutyric acid
GCMS	gas chromatography–mass spectrometry
GK	guanylate kinase
GPI	glycosylphosphatidylinositol
GPP	geranyl pyrophosphate
λ	wavelength
H	reaction enthalpy
h	Planck constant
HEK(293T cells)	human embryonic kidney (293T cells)
HEPES	2-(4-(2-hydroxyethyl)-1-piperazinyl)-ethansulfonic acid
Hex	hexane

HIV	human immunodeficiency virus
HMG-CoA	β -hydroxy- β -methylglutaryl-CoA
HPMA	hexamethylphosphoramide
HMQC	heteronuclear multiple bond coherence (NMR spectroscopy)
HPLC	high-performance liquid chromatography
HRMS	high-resolution mass spectrometry
HWE	Horner-Wadsworth-Emmons
<i>i</i>	<i>iso</i>
IBX	2-iodoxybenzoic acid
IL-2	interleukin-2
im	imidazole
INOC	intramolecular nitrile oxide cycloaddition
Ipc	isopinocampheyl
IPP	isopentenyl pyrophosphate
IR	infrared
IUPAC	International Union of Pure and Applied Chemistry
<i>J</i>	coupling constant (NMR spectroscopy)
KcsA (channel)	potassium crystallographically-sited activation (channel)
KHMDS	potassium hexamethyldisilazide
K-Selectride [®]	potassium tri- <i>sec</i> -butylborohydride
K _V (channel)	voltage-gated potassium (channel)
L	ligand
LAB	lithium amidotrihydroborate
lat.	Latin
LCMS	liquid chromatography–mass spectrometry
LDA	lithium diisopropylamide
LiHMDS	lithium hexamethyldisilazide
L-Selectride [®]	lithium tri- <i>sec</i> -butylborohydride
LTCC	L-type calcium channels
M	metal, molecule (mass spectrometry)
M (phase)	mitotic (phase)
<i>M</i>	molecular weight
M	molarity
m	multiplet (NMR spectroscopy)

MAP	mitogen-activated protein
max	maximum
m _C	centrosymmetric multiplet (NMR spectroscopy)
<i>m</i> -CPBA	<i>meta</i> -chloroperbenzoic acid
Me	methyl
ME-CDP	4-diphosphocytidyl-2- <i>C</i> -methyl-D-erythritol
MEP	methylethritol phosphate
Mes	mesityl
MMC	methoxymagnesium methyl carboxylate
MMFF	merck molecular force field
MOM	methoxymethyl
mRNA	messenger RNA
MS	mass spectroscopy, molecular sieves
Ms	mesyl
MVA	mevalonic acid
MVK	methyl vinyl ketone
ν	frequency
NADPH	nicotinamide adenine dinucleotide phosphate hydrogen
NaHMDS	sodium hexamethyldisilazide
Nap	naphtyl
Na _v (channel)	voltage-gated sodium channel
NIS	<i>N</i> -iodo succinimide
NMO	<i>N</i> -morpholino <i>N</i> -oxide
NMR	nuclear magnetic resonance
NOE	nuclear Overhauser effect
NOESY	nuclear Overhauser effect correlation spectroscopy (NMR spectroscopy)
n.r.	no reaction
O	oxidative step
<i>p</i>	<i>para</i>
PAA	phenylalkylamine
PAF	platelet-activating factor
PCC	pyridinium chlorochromate
PG	undefined protective group

Ph	phenyl
PhNTf ₂	<i>N</i> -phenyl(bistrifluoromethanesulfonate)
PIFA	(bis(trifluoroacetoxy)iodo)benzene
Pinnick	Pinnick oxidation
Piv	pivaloyl
pK _A	acid dissociation constant (negative logarithmic value)
PMB	<i>para</i> -methoxybenzyl
PMP	<i>para</i> -methoxyphenyl
ppm	parts per million (NMR spectroscopy)
PPTS	pyridinium <i>para</i> -toluenesulfonate
Pr	propyl
py	pyridine
<i>p</i> -TsOH	<i>para</i> -toluenesulfonic acid
q	quartet (NMR spectroscopy)
quant.	quantitative
quin	quintet (NMR spectroscopy)
®	registered
R	undefined or elsewhere defined substituent
<i>rac</i>	racemic
Ras	rat sarcoma (monomeric G-protein)
RCM	ring-closing metathesis
ref.	reference
R _f	retardation factor
RRCM	relay ring-closing metathesis
R _t	retention time
rt	room temperature
s	singlet (NMR spectroscopy)
SAR	structure activity relationship
<i>sec</i>	secondary
sept	septet (NMR spectroscopy)
SEM	2-(trimethylsilyl)ethoxymethyl
Ser	serine
SH3	SRC homology 3
S _N 1	nucleophilic chemical substitution of first kinetic order

S _N 2	nucleophilic chemical substitution of second kinetic order
S _N i	internal nucleophilic chemical substitution
SNARE	soluble <i>N</i> -ethylmaleimide-sensitive-factor attachment receptor
T	temperature
T (cells)	T(hymus) lymphocytes
t	time, triplet (NMR spectroscopy)
<i>t</i>	(<i>tert</i>) tertiary
TASF	tris(dimethylamino)sulfonium difluorotrimethylsilicate
TBAF	tetrabutylammonium fluoride
TBDPS	<i>tert</i> -butyldiphenylsilyl
TBS	<i>tert</i> -butyldimethylsilyl
Tebbe	Tebbe's reagent
TES	triethylsilyl
TFE	2,2,2-trifluoroethanol
TIPS	triisopropylsilyl
TFA	trifluoroacetic acid
Tf ₂ O	trifluoromethanesulfonic anhydride
Tf	triflyl
THF	tetrahydrofuran
THP	tetrahydropyranyl
TLC	thin-layer chromatography
TM	trademark
TMEDA	<i>N,N,N',N'</i> -tetramethylethylenediamine
TMS	trimethylsilyl, tetramethylsilane (NMR spectroscopy)
Tol	tolyl
TPAP	tetrapropylammonium perruthenate
TPP	tetraphenylporphyrine
trig	trigonal
Ts	tosyl
u.p.	unknown product
UV-Vis	ultraviolet-visible
VDI	voltage-dependent inactivation
wt-%	weight percent
ψ	pseudo

VII. References

- [1] a) T. J. Maimone, P. S. Baran, *Nat. Chem. Biol.* **2007**, *3*, 396–407. b) K. Chen, P. S. Baran, *Nature* **2009**, *459*, 824–828.
- [2] a) A. A. Newmann, 'Chemistry of Terpenes and Terpenoids', Academic Press, London, New York, **1972**. b) E. Breitmaier, 'Terpene – Aromen, Düfte, Pharmaka, Pheromone', Wiley-VCH, Weinheim, 2nd edition, **2005**. c) K. C. Nicolaou, T. Montagnon, 'Molecules that Changed the World', Wiley-VCH, Weinheim, **2008**.
- [3] A. Kekulé, 'Lehrbuch der organischen Chemie', Ferdinand Enke Verlag, Erlangen, **1863**.
- [4] A. D. McNaught, A. Wilkinson, 'Compendium of Chemical Terminology', Blackwell Scientific Publications, Oxford, 2nd edition, **1997**.
- [5] O. Wallach, *Liegigs Ann. Chem.* **1887**, *239*, 1–54.
- [6] a) L. Ruzicka, *Angew. Chem.* **1938**, *38*, 5–11. b) L. Ruzicka, *Experientia* **1953**, *9*, 357–367.
- [7] L. Ruzicka, *Helv. Chim. Acta* **1971**, *54*, 1753–1759.
- [8] a) S. Chaykin, J. Law, A. H. Phillips, T. T. Tchen, K. Bloch, *Proc. Natl. Acad. Sci. USA* **1958**, *44*, 998–1004. b) K. Bloch, S. Chaykin, A. H. Phillips, A. deWaard, *J. Biol. Chem.* **1959**, *234*, 2595–2604. c) K. Bloch, *Steroids* **1992**, *57*, 378–382.
- [9] a) F. Lynen, H. Eggerer, U. Henning, I. Kessel, *Angew. Chem.* **1958**, *70*, 738–742. b) F. Lynen, *Pure Appl. Chem.* **1967**, *14*, 137–168.
- [10] For a selection of reviews on the biosynthesis of terpenoid natural products, see: a) N. Qureshi, J. W. Porter, 'Biosynthesis of Isoprenoid Compounds', Wiley, New York, Vol. 1, **1981**. b) D. A. Bochar, J. A. Friesen, C. V. Stauffacher, V. W. Rodwell, 'Comprehensive Natural Product Chemistry', Vol. 2, **1999**. c) P. M. Dewick, *Nat. Prod. Rep.* **2002**, *19*, 181–222. d) P. M. Dewick, 'Medicinal Natural Products: A Biosynthetic Approach', Wiley, Chichester, 3rd edition, **2009**.
- [11] A. E. Leyes, J. A. Baker, F. M. Hahn, C. D. Poulter, *Chem. Commun.* **1999**, 717–718.
- [12] M. Rohmer, *Nat. Prod. Rep.* **1999**, *16*, 565–574.
- [13] M. Rohmer, M. Knani, P. Simonin, B. Sutter, H. Sahm, *Biochem. J.* **1993**, *295*, 517–524.
- [14] F. Rohdich, S. Hecht, K. Gärtner, P. Adam, C. Krieger, S. Amslinger, D. Arigoni, A. Bacher, W. Eisenreich, *Proc. Natl. Acad. Sci. USA* **2002**, *99*, 1158–1163.
- [15] For detailed reviews on the non-mevalonate pathway, see: a) W. Eisenreich, M. Schwarz, A. Cartayrade, D. Arigoni, M. H. Zenk, A. Bacher, *Chem. Biol.* **1998**, *5*, R221–R233. b) W. Eisenreich, A. Bacher, D. Arigoni, F. Rohdich, *Cell. Mol. Life. Sci.* **2004**, *61*, 1401–1426.
- [16] a) K. Boje, Dissertation, WWU Münster, **2002**. b) T. Wegener, Dissertation, University of Osnabrück, **2005**.
- [17] a) C. C. Hughes, A. K. Miller, D. Trauner, *Org. Lett.* **2005**, *7*, 3425–3428. b) A. K. Miller, C. C. Hughes, J. J. Kennedy-Smith, S. N. Gradl, D. Trauner, *J. Am. Chem. Soc.* **2006**, *128*, 17057–17062. c) G. Liang, I. B. Seiple, D. Trauner, *J. Am. Chem. Soc.*

- 2006**, 128, 11022–11023. d) P. A. Roethle, D. Trauner, *Org. Lett.* **2006**, 8, 345–347. e) P. A. Roethle, P. T. Hernandez, D. Trauner, *Org. Lett.* **2006**, 8, 5901–5904.
- [18] For recent reviews on the isolation of diterpenoid natural products, see: a) J. R. Hanson, *Nat. Prod. Rep.* **2002**, 19, 125–132. b) J. R. Hanson, *Nat. Prod. Rep.* **2009**, 26, 1156–1171. c) J. R. Hanson, *Nat. Prod. Rep.* **2012**, 29, 890–898. d) J. R. Hanson, *Nat. Prod. Rep.* **2013**, 30, 1346–1356.
- [19] R. Croteau, R. E. B. Ketchum, R. M. Long, R. Kaspera, M. R. Wildung, *Phytochem. Rev.* **2006**, 5, 75–97.
- [20] a) W.W. Epstein, H. C. Rilling, *J. Biol. Chem.* **1970**, 245, 4597–4605. b) C. D. Poulter, H. C. Rilling, W. W. Epstein, *J. Am. Chem. Soc.* **1971**, 93, 1783–1785.
- [21] For selected examples of studies on triterpene cyclization, see: a) K. U. Wendt, G. E. Schulz, E. J. Corey, D. R. Liu, *Angew. Chem. Int. Ed.* **2000**, 39, 2812–2833. b) K. U. Wendt, *Angew. Chem. Int. Ed.* **2005**, 44, 3966–3971. c) I. Abe, *Nat. Prod. Rep.* **2007**, 24, 1311–1331.
- [22] R.-T. Li, Q.-S. Zhao, S.-H. Li, Q.-B. Han, H.-D. Sun, Y. Lu, L.-L. Zhang, Q.-T. Zheng, *Org. Lett.* **2003**, 5, 1023–1026.
- [23] For recent reviews on meroterpenoids, see: a) R. Geris, T. J. Simpson, *Nat. Prod. Rep.* **2009**, 26, 1063–1094. b) J. W. Lockner, Dissertation, Scripps Research Institute La Jolla, **2011**.
- [24] a) K. Minagawa, S. Kouzuki, J. Yoshimoto, Y. Kawamura, H. Tani, T. Iwata, Y. Terui, H. Nakai, S. Yagi, N. Hattori, T. Fujiwara, T. Kamigauchi, *J. Antibiot.* **2002**, 55, 155–164. b) J. Yoshimoto, M. Kakui, H. Iwasaki, H. Sugimoto, T. Fujiwara, N. Hattori, *Microbiol. Immunol.* **2000**, 44, 677–685. c) J. Yoshimoto, M. Kakui, H. Iwasaki, T. Fujiwara, H. Sugimoto, N. Hattori, *Arch. Virol.* **1999**, 144, 865–878. d) J. Sakurai, T. Kikuchi, O. Takahashi, K. Watanabe, T. Katoh, *Eur. J. Org. Chem.* **2011**, 2948–2957.
- [25] N. Civjan, ‘Natural Products in Chemical Biology’, John Wiley & Sons, New Jersey, **2012**.
- [26] a) G. Sakoulas, S.-J. Nam, S. Loesgen, W. Fenical, P. R. Jensen, V. Nizet, M. Hensler, *PLoS One* **2012**, 7, e29439. b) L. Kaysser, P. Bernhardt, N.-J. Nam, S. Loesgen, J. G. Ruby, P. Skewes-Cox, P. R. Jensen, W. Fenical, B. S. Moore, *J. Am. Chem. Soc.* **2012**, 134, 11988–11991.
- [27] R. Meier, S. Strych, D. Trauner, *Org. Lett.* **2014**, 16, 2634–2637.
- [28] J. L. Bicas, A. P. Dionísio, G. M. Pastore, *Chem. Rev.* **2009**, 109, 4518–4531.
- [29] G. Wang, W. Tang, R. R. Bidigar, ‘Terpenoids as Therapeutic Drugs and Pharmaceutical Agents’, in L. Zhang, A. L. Demain, ‘Natural Products: Drug Discovery and Therapeutic Medicine’, Humana Press Inc., Totowa, **2005**, 197–227.
- [30] D. McNamee, *Lancet* **1993**, 342, 801.
- [31] a) L. R. Phillips, L. Malspeis, J. G. Supko, *Drug Metab. Dispos.* **1995**, 23, 676–680. b) G. Liu, K. Oetl, H. Bailey, L. Van Ummersen, K. Tusch, M. J. Staab, D. Horvath, D. Alberti, R. Arzooarian, H. Rezazadeh, J. McGovern, E. Robinson, D. DeMets, D. Wilding, *Invest. New Drugs* **2003**, 21, 367–372.
- [32] a) P. L. Crowell, *J. Nutr.* **1999**, 129, 775S–778S. b) C. J. Fabian, *Breast Cancer Res.* **2001**, 3, 99–103. c) P. L. Crowell, R. R. Chang, Z. Ren, C. E. Elson, M. N. Gould, *J. Biol. Chem.* **1991**, 266, 17679–17685.

- [33] a) A. Hitmi, A. Coudret, C. Barthomeuf, *Crit. Rev. Biochem. Mol. Biol.* **2000**, *35*, 317–337. b) J. George, H. P. Bais, G. A. Ravishankar, *Crit. Rev. Biotechnol.* **2000**, *20*, 49–77.
- [34] K. N. Jones, J. C. English, *Clin. Infect. Dis.* **2003**, *36*, 1355–1361.
- [35] G. D. Meng, J. C. Zhu, Z. W. Chen, L. T. Wong, G. Y. Zhang, Y. Z. Hu, J. H. Ding, X. H. Wang, S. Z. Qian, C. Wang, D. Machin, A. Pinol, G. M. H. Waites, *Contraception* **1988**, *37*, 119–28.
- [36] M. Kumar, S. Sharma, N. K. Lohiya, *Contraception* **1997**, *56*, 251–256.
- [37] G. M. H. Waites, C. Wang, P. D. Griffin, *Int. J. Androl.* **1998**, *21*, 8–12.
- [38] For a review on the discovery of the compound artemisinin (**57**), see: L. H. Miller, X. Su, *Cell* **2011**, *146*, 855–858.
- [39] R. M. Fairhurst, G. M. L. Nayyar, J. G. Breman, R. Hallett, J. L. Vennerstrom, S. Duong, P. Ringwald, T. E. Wellems, C. V. Plowe, A. M. Dondrop, *Am. J. Trop. Med. Hyg.* **2012**, *87*, 231–241.
- [40] J. N. Cumming, P. Ploypradith, G. H. Posner, *Adv. Pharmacol.* **1997**, *37*, 253–297.
- [41] a) N. Acton, R. J. Roth, *J. Nat. Prod.* **1989**, *52*, 1183–1185. b) N. Acton, R. J. Roth, *J. Org. Chem.* **1992**, *57*, 3610–3614.
- [42] L.-K. Sy, G. D. Brown, *Tetrahedron* **2002**, *58*, 897–908.
- [43] J. Turconi, F. Griolet, R. Guevel, G. Oddon, R. Villa, A. Geatti, M. Hvala, K. Rossen, R. Göller, A. Burgrad, *Org. Process Res. Dev.* **2014**, *18*, 417–422.
- [44] G. O. Schenck, *Naturwissenschaften* **1948**, *35*, 28–29.
- [45] H. Hock, O. Schrader, *Angew. Chem.* **1936**, *49*, 595–597.
- [46] D. -K. Ro, E. M. Paradise, M. Ouellet, K. J. Fisher, K. L. Newman, J. M. Ndungu, K. A. Ho, R. A. Eachus, T. S. Ham, J. Kirby, M. C. Y. Chang, S. T. Withers, Y. Shiba, R. Sarpong, J. D. Keasling, *Nature* **2006**, *440*, 940–943.
- [47] For successfully disclosed total syntheses of artemisinin (**XX**), see: a) J. M. Liu, M. Y. Ni, J. F. Fan, Y. Y. Tu, Z. H. Wu, Y. L. Wu, W. S. Chou, *Huaxue Xuebao* **1979**, *37*, 129–143. b) G. Schmid, W. Hofheinz, *J. Am. Chem. Soc.* **1983**, *105*, 624–625. c) X. X. Xu, J. Zhu, D. Z. Huang, W. S. Zhou, *Tetrahedron* **1986**, *42*, 819–828. d) A. M. Avery, C. Jennings-White, W. K. M. Chong, *Tetrahedron Lett.* **1987**, *28*, 4629–4632. e) T. Ravindranathan, M. A. Kumar, R. B. Menon, S. V. Hiremath, *Tetrahedron Lett.* **1990**, *31*, 755–758. f) M. A. Avery, W. K. M. Chong, C. Jennings-White, *J. Am. Chem. Soc.* **1992**, *114*, 974–979. g) H. J. Liu, W. L. Yeh, S. Y. Chew, *Tetrahedron Lett.* **1993**, *34*, 4435–4438. h) M. G. Constantino, M. Beltrame, J. G. V. daSilva, *Synth. Commun.* **1996**, *26*, 321–329. i) H. J. Liu, W. L. Yeh, *Heterocycles* **1996**, *42*, 493–497. j) J. S. Yadav, B. Thirupathaiah, P. Srihari, *Tetrahedron* **2010**, *66*, 2005–2009. g) C. Zhu, S. P. Cook, *J. Am. Chem. Soc.* **2012**, *134*, 13577–13579.
- [48] For a comprehensive review on the chemistry and biology of gincolides, see: K. Strømgaard, K. Nakanishi, *Angew. Chem. Int. Ed.* **2004**, *43*, 1640–1658.
- [49] K. C. Nicolaou, T. Montagnon, ‘Molecules That Changed the World’, Wiley-VCH, Weinheim, **2008**.
- [50] W. S. Fang, X. T. Liang, *Mini Rev. Med. Chem.* **2005**, *5*, 1–12.
- [51] For selected articles on the biological effects of paclitaxel (**117**), see: a) P. B. Schiff, S. B. Horwitz, *Proc. Natl. Acad. Sci. USA* **1980**, *77*, 1561–1565. b) T. H. Wang, D. M. Popp, H. S. Wang, M. Saitoh, J. G. Mural, D. C. Henley, H. Ichijo, J. Wimalasena, J.

- Biol. Chem.* **1999**, 274, 8208–8216. c) A. Ganguly, H. Yang, F. Cabral, *Mol. Cancer Ther.* **2010**, 9, 2914–2923.
- [52] N. Hall, *Chem. Commun.* **2003**, 661–664.
- [53] K. C. Nicolaou, Z. Yang, J. J. Liu, H. Ueno, P. G. Nantermet, R. K. Guy, C. F. Claiborne, J. B. Renaud, E. A. Couladouros, K. Paulvannan, E. J. Sorensen, *Nature* **1994**, 367, 630–634. b) K. C. Nicolaou, R. K. Guy, *Angew. Chem. Int. Ed.* **1995**, 34, 2079–2090.
- [54] a) R. A. Holton, C. Somoza, H. B. Kim, F. Liang, R. J. Biediger, P. D. Boatman, M. Shindo, C. C. Smith, S. Kim, *J. Am. Chem. Soc.* **1994**, 116, 1597–1598. b) R. A. Holton, C. Somoza, H. B. Kim, F. Liang, R. J. Biediger, P. D. Boatman, M. Shindo, C. C. Smith, S. Kim, *J. Am. Chem. Soc.* **1994**, 116, 1599–1600.
- [55] A. Mendoza, Y. Ishihara, P. S. Baran, *Nat. Chem.* **2012**, 4, 21–25.
- [56] J. W.-H. Li, J. C. Vederas, *Science* **2009**, 325, 161–165.
- [57] B. Ganem, R. R. Franke, *J. Org. Chem.* **2007**, 72, 3981–3987.
- [58] M. Vuagnoux-d’Augustin, A. Alexakis, *Chem. Eur. J.* **2007**, 13, 9647–9662.
- [60] S. Kobayashi, I. Hachiya, Y. Yamanoi, *Bull. Chem. Soc. Jpn.* **1994**, 67, 2342–2344.
- [61] M. Rowley, M. Tsukamoto, Y. Kishi, *J. Am. Chem. Soc.* **1989**, 111, 2735–2737.
- [62] E. Hecker, *Cancer Res.* **1968**, 28, 2338–2349.
- [63] K. Zechmeister, F. Brandl, W. Hoppe, E. Hecker, H. J. Opferkuch, W. Adolf, *Tetrahedron Lett.* **1970**, 11, 4075–4078.
- [64] For selected publications on the biological activity of ingenol derivatives, see: a) C. M. Hasler, G. Acs, P. M. Blumberg, *Cancer Res.* **1992**, 52, 202–208. b) M. Fujiwara, K. Ijichi, K. Tokuhisa, K. Katsuura, S. Shigeta, K. Konno, G. Y. Wang, D. Uemura, T. Yokota, M. Baba, *Antimicrob. Agents Chemother.* **1996**, 40, 271–273. c) S. M. Ogbourne, A. Suhrbier, B. Jones, S.-J. Cozzi, G. M. Boyle, M. Morris, D. McApline, J. Johns, T. M. Scott, K. P. Sutherland, J. M. Gardner, T. T. T. Le, A. Lenarczyk, J. A. Aylward, P. G. Parsons, *Cancer Res.* **2004**, 64, 2833–2839. d) A. Vasas, D. Rédei, D. Csupor, J. Molnár, J. Hohmann, *Eur. J. Org. Chem.* **2012**, 27, 5115–5130.
- [65] a) Lars Jrgenson, S. J. McKerrall, C. A. Kuttruff, F. Ungeheur, J. Felding, P. S. Baran, *Science* **2013**, 341, 878–882. b) L. Jrgenson, S. J. McKerrall, C. A. Kuttruff, F. Ungeheur, J. Felding, P. S. Baran, *J. Am. Chem. Soc.* **2014**, 136, 5799–5810.
- [66] a) X. Liang, G. Grue-Sørensen, A. K. Petersen, T. Högberg, *Synlett* **2012**, 23, 2647–2652. b) G. Appendino, G. C. Tron, G. Cravatto, G. Palmisano, J. Jakupovic, *Nat. Prod. Rep.* **1999**, 62, 76–79.
- [67] For reviews on approaches toward and syntheses of ingenol (XX), see: a) S. Kim, J. D. Winkler, *Chem. Soc. Rev.* **1997**, 26, 387–399. b) I. Kuwajima, K. Tanino, *Chem. Rev.* **2005**, 105, 4661–4670. c) J. K. Cha, O. L. Epstein, *Tetrahedron* **2006**, 62, 1329–1343.
- [68] K. M. Brummond, H. Chen, K. D. Fisher, A. D. Kerekes, B. Richards, P. C. Still, S. J. Geib, *Org. Lett.* **2002**, 4, 1931–1934.
- [69] G. Appendino, G. C. Tron, G. Cravotto, G. Palmisano, R. Annunziata, G. Baj, N. Surico, *Eur. J. Org. Chem.* **1999**, 12, 3413–3420.
- [70] a) G. Komppa, *Chem. Ber.* **1903**, 36, 4332–4335. b) G. Komppa, *Chem. Ber.* **1909**, 41, 4470–4474.
- [71] a) G. Wagner, W. Brickner, *Chem. Ber.* **1899**, 32, 2302–2325. b) H. Meerwein, *Liebigs. Ann. Chem.* **1914**, 405, 129–175.

- [72] R. A. Yoder, J. N. Johnston, *Chem. Rev.* **2005**, *105*, 4730–4756.
- [73] E. Poupon, B. Nay, ‘Biomimetic Organic Synthesis’, Wiley-VCH, Weinheim, Vol. 1, **2011**.
- [74] R. B. Woodward, F. Sondheimer, D. Taub, K. Heusler, W. M. McLamore, *J. Am. Chem. Soc.* **1952**, *74*, 4223–4251.
- [75] P. Wieland, M. Miescher, *Helv. Chem. Acta* **1950**, *33*, 2215–2228.
- [76] a) Z. G. Hajos, D. R. Parrish, German patent, DE 2102623, **1971**. b) U. Eder, G. Sauer, R. Wiechert, *Angew. Chem. Int. Ed.* **1971**, *10*, 496–497. c) G. Hajos, D. R. Parrish, *J. Org. Chem.* **1974**, *39*, 1615–1621.
- [77] a) E. J. Corey, M. Ohno, R. B. Mitra, P. A. Vatakencherry, *J. Am. Chem. Soc.* **1964**, *86*, 478–485. b) E. J. Corey, X.-M. Cheng, ‘The Logic of Chemical Synthesis’, Wiley-VCH, New York, **1995**. c) E. J. Corey, *Chem. Soc. Rev.* **1988**, *17*, 111–133.
- [78] D. H. R. Barton, *Experientia* **1950**, *6*, 316–320.
- [79] P. A. Wender, C. D. Jesudason, H. Nakahira, N. Tamura, A. L. Tebbe, Y. Ueno, *J. Am. Chem. Soc.* **1997**, *119*, 12976–12977.
- [80] W. P. D. Goldring, G. Pattenden, *Chem. Commun.* **2002**, 1736–1737.
- [81] J. Y. Cha, J. T. S. Yeoman, S. E. Reisman, *J. Am. Chem. Soc.* **2011**, *133*, 14964–14967.
- [82] J. Deng, S. Zhou, W. Zhang, J. Li, R. Li, A. Li, *J. Am. Chem. Soc.* **2014**, *136*, 8185–8188.
- [83] For a recent review on synthetic investigations on sesterterpenoid natural products, see: D. T. Hog, R. Webster, D. Trauner, *Nat. Prod. Rep.* **2012**, *29*, 752–779.
- [84] For reviews on marine natural products, including sesterterpenoids, see: a) D. J. Faulkner, *Nat. Prod. Rep.* **2002**, 19–41. b) R. Ebel, *Mar. Drugs* **2010**, *8*, 2340–2368. c) J. W. Blunt, B. R. Copp, W.-P. Hu, M. H. G. Munro, P. T. Northcote, M. R. Prinsep, *Nat. Prod. Rep.* **2007**, *24*, 31–86. d) R. Ebel, *Mar. Drugs* **2010**, *8*, 2340–2386. e) J. W. Blunt, B. R. Copp, R. A. Keyzers, M. H. G. Munro, M. R. Prinsep, *Nat. Prod. Rep.* **2013**, *30*, 237–323.
- [85] S. S. Ebada, W. Lin, P. Proksch, *Mar. Drugs* **2010**, *8*, 313–346.
- [86] For the majority of review articles published on, or including sesterterpenoids, see: a) G. A. Cordell, *Pytochemistry* **1974**, *13*, 2343–2364. b) J. R. Hanson, *Nat. Prod. Rep.* **1986**, *3*, 123–132. c) J. R. Hanson, *Nat. Prod. Rep.* **1992**, *9*, 481–489. d) J. R. Hanson, *Nat. Prod. Rep.* **1996**, *13*, 529–535. e) Y. Liu, S. Zhang, P. J. M. Abreu, *Nat. Prod. Rep.* **2006**, *23*, 630–651. f) Y. Liu, L. Wang, J. H. Jung, S. Zhang, *Nat. Prod. Rep.* **2007**, *24*, 1401–1429. g) N. Ungur, V. Kulcitki, *Tetrahedron* **2009**, *65*, 3815–3828. h) T. Rezanka, L. Siristova, K. Sigler, *Anti-Infect. Agents Med. Chem.* **2009**, *8*, 169–192. i) Y. Liu, Z. Wang, X. Meng, W. Fan, W. Du W. Deng, *J. Chin. Pharm. Univ.* **2010**, *41*, 289–298. j) M. A. Gonzalez, *Curr. Bioact. Compd.* **2010**, *6*, 178–206. k) L. Wang, B. Yang, X.-P. Lin, X.-F. Zhou, Y. Liu, *Nat. Prod. Rep.* **2013**, *30*, 455–473.
- [87] C. L. Hugelshofer, T. Magauer, *Angew. Chem. Int. Ed.* **2014**, DOI: 10.1002/anie.201407788.
- [88] K. Ishibashi, R. Nakamura, *J. Agr. Chem. Soc. Jpn.* **1958**, *32*, 739.

- [89] a) S. Nozoe, M. Morazaki, K. Tsuda, Y. Iitaka, N. Takahashi, S. Tamura, K. Ishibashi, M. Shirasaka, *J. Am. Chem. Soc.* **1965**, *87*, 4969–4970. b) A. Andolfi, A. Evidente, A. Santani, A. Tuzi, *Acta Cryst.* **2006**, *E62*, o2195–o2197.
- [90] For a review on the biological properties of ophiobolins, see: T. K. Au, W. S. Chick, P. C. Leung, *Life Sci.* **2000**, *67*, 733–742.
- [91] E. D. de Silva, P. J. Scheuer, *Tetrahedron Lett.* **1980**, *21*, 1611–1614.
- [92] a) S. Katsumura, S. Fujiwara, S. Isoe, *Tetrahedron Lett.* **1985**, *26*, 5827–5830. b) S. Katsamura, S. Fujiwara, S. Isoe, *Tetrahedron Lett.* **1988**, *29*, 1173–1176.
- [93] M. E. Garst, E. A. Tallman, J. N. Bonfiglio, D. Harcourt, E. B. Ljungwe, A. Tran, *Tetrahedron Lett.* **1986**, *27*, 4533–4536.
- [94] A. Soriente, M. De Rosa, A. Acipella, A. Scettri, G. Sodano, *Tetrahedron: Asymmetry* **1999**, *10*, 4481–4484.
- [95] J. Coombs, E. Lattman, H. M. R. Hoffmann, *Synthesis* **1998**, 1367–1371.
- [96] a) P. Bury, G. Hareau, P. J. Kocienski, D. Dhanak, *Tetrahedron* **1994**, *50*, 8793–8808. b) A. Pommier, P. J. Kocienski, *Chem. Commun.* **1997**, 1139–1140. c) A. Pommier, V. Stepanenko, K. Jarowicki, P. J. Kocienski, *J. Org. Chem.* **2003**, *68*, 4008–4013.
- [97] A. Soriente, M. De Rosa, A. Scettri, G. Sodano, M. Terencio, M. Payá, M. J. Alcaraz, *Curr. Med. Chem.* **1999**, *6*, 415–431.
- [98] V. Martin, S. Woodard, T. Katsuki, Y. Yamada, M. Ikeda, K. B. Sharpless, *J. Am. Chem. Soc.* **1981**, *103*, 6237–6240.
- [99] G. Hareau-Vittini, P. J. Kocienski, G. Reid, *Synthesis* **1995**, 1007–1013.
- [100] For the isolation and biological properties of terpestacin (**161**), see: a) M. Oka, S. Iimura, O. Tenmyo, S. Yosuke, M. Sugawara, N. Okhusa, H. Yamamoto, K. Kawano, S.-L. Hu, Y. Fukagawa, T. Oki, *J. Antibiot.* **1993**, *46*, 367–373. b) S. Iimura, M. Osa, Y. Narita, M. Konishi, H. Kakisawa, Q. Gao, T. Oki, *Tetrahedron Lett.* **1993**, *34*, 493–496. c) M. Oka, S. Iimura, Y. Narita, T. Furumai, M. Konishi, T. Oki, Q. Gao, H. Kakisawa, *J. Org. Chem.* **1993**, *58*, 1875–1881.
- [101] a) K. Tatsuta, N. Masuda, H. Nishida, *Tetrahedron Lett.* **1998**, *39*, 83–86. b) K. Tatsuta, N. Masuda, *J. Antibiot.* **1998**, *51*, 602–606.
- [102] a) G. O. Berger, M. A. Tius, *J. Org. Chem.* **2007**, *72*, 6473–6480. b) G. O. Berger, M. A. Tius, *Org. Lett.* **2005**, *7*, 5011–5013.
- [103] Y. Jin, F. G. Qiu, *Org. Biomol. Chem.* **2012**, *10*, 5452–5455.
- [104] I. N. Nazarov, I. I. Zaretskaya, *Izv. Akad. Nauk. SSSR, Ser. Khim* **1941**, 211–224.
- [105] M. A. Blanchette, W. Choy, J. T. Davis, A. P. Essensfeld, S. Masamune, W. R. Roush, T. Sakai, *Tetrahedron Lett.* **1984**, *25*, 2183–2186.
- [106] A. G. Myers, M. Siu, F. Ren, *J. Am. Chem. Soc.* **2002**, *124*, 4230–4232.
- [107] A. G. Myers, B. H. Yang, H. Chen, L. McKinstry, D. J. Kopecky, J. L. Gleason, *J. Am. Chem. Soc.* **1997**, *119*, 6496–6511.
- [108] a) J. Chan, T. F. Jamison, *J. Am. Chem. Soc.* **2003**, *125*, 11514–11515. b) J. Chan, T. F. Jamison, *J. Am. Chem. Soc.* **2004**, *126*, 10682–10691.
- [109] a) B. M. Trost, G. Dong, J. A. Vance, *J. Am. Chem. Soc.* **2007**, *129*, 4540–4541. b) B. M. Trost, G. Dong, J. A. Vance, *Chem.–Eur. J.* **2010**, *16*, 6265–6277.
- [110] M. I. Choudhary, R. Ranjit, Atta-ur-Rahman, S. Hussain, K. P. Devkota, T. M. Shrestha, M. Parvez, *Org. Lett.* **2004**, *6*, 4139–4142.

- [111] a) S.-H. Luo, J. Hua, X.-M. Niu, Y. Liu, C.-H. Li, Y.-Y. Zhou, S.-X. Jing, X. Zhao, S.-H. Li, *Phytochemistry* **2013**, *86*, 29–35. d) S.-H. Luo, J. Hua, C.-H. Li, Y. Liu, X. N. Li, X. Zhao, S.-H. Li, *Tetrahedron Lett.* **2013**, *54*, 235–237.
- [112] J. Xie, Y. Ma, D. A. Horne, *J. Org. Chem.* **2011**, *76*, 6169–6176.
- [113] X. Huang, L. Song, J. Xu, G. Zhu, B. Liu, *Angew. Chem. Int. Ed.* **2013**, *52*, 952–955; *Angew. Chem.* **2013**, *125*, 986–989.
- [114] a) C. O. Kappe, S. S. Murphree, A. Padwa, *Tetrahedron* **1997**, *53*, 14179–14233. b) D. Mal, P. Pahari, *Chem. Rev.* **2007**, *107*, 1892–1918. c) C. L. Hugelshofer, T. Magauer, *Synthesis* **2014**, 1279–1296.
- [115] W. Hofheinz, P. Schönholzer, *Helv. Chim. Acta* **1977**, *60*, 1367–1370.
- [116] R. P. Gregson, D. Ouvrier, *J. Nat. Prod.* **1982**, *45*, 412–414.
- [117] K. Takeda, M.-a. Sato, E. Yoshii, *Tetrahedron Lett.* **1986**, *27*, 3903–3906.
- [118] J. Uenishi, R. Kawahama, O. Yonemitsu, *J. Org. Chem.* **1997**, *62*, 1691–1701.
- [119] a) Y. Okude, S. Hirano, T. Hiyama, H. Nozaki, *J. Am. Chem. Soc.* **1977**, *99*, 3179–3181. b) H. Jin, J. Uenishi, W. J. Christ, Y. Kishi, *J. Am. Chem. Soc.* **1986**, *108*, 5644–5646.
- [120] A. Fontana, I. Fakhr, E. Mollo, G. Cimino, *Tetrahedron: Asymmetry* **1999**, *10*, 3869–3872.
- [121] For reviews on the construction of cyclootanol systems, see: a) G. Mehta, V. Singh, *Chem. Rev.* **1999**, *99*, 881–930. b) N. A. Petasis, M. A. Patane, *Tetrahedron* **1992**, *48*, 5757–5821.
- [122] K. Tsuna, N. Noguchi, M. Nakada, *Angew. Chem. Int. Ed.* **2011**, *50*, 9452–9455.
- [123] K. Tsuna, N. Noguchi, M. Nakada, *Chem. Eur. J.* **2013**, *19*, 5476–5486.
- [124] M. Rowley, Y. Kishi, *Tetrahedron Lett.* **1988**, *29*, 4909–4912.
- [125] For recent reviews on metal catalyzed olefin metathesis, see: a) R. H. Grubbs, ‘Handbook of Metathesis’, Wiley-VCH, Weinheim, **2003**. b) K. C. Nicolaou, P. G. Bulger, D. Sarlah, *Angew. Chem. Int. Ed.* **2005**, *44*, 4490–4527. c) A. H. Hoveyda, A. R. Zhugralin, *Nature* **2007**, *450*, 243–251. d) C. Samojłowicz, M. Bieniek, K. Grela, *Chem. Rev.* **2009**, *109*, 3708–3742. e) A. Fürstner, *Science* **2013**, *341*, 1357–1364.
- [126] a) S. Reformatsky, *Ber. Dtsch. Chem. Ges.* **1887**, *20*, 1210–1211. b) K. Nozaki, K. Oshima, K. Utimoto, *Tetrahedron Lett.* **1988**, *29*, 1041–1044. b) K. Nozaki, K. Oshima, K. Utimoto, *Bull. Chem. Soc. Jpn.* **1991**, *64*, 403–409.
- [127] a) T. Ríos, F. Colunga, *Chem. Ind. (London)* **1965**, 1184–1185. b) Y. Itake, I. Watanabe, I. T. Harrison, S. Harrison, *J. Am. Chem. Soc.* **1968**, *90*, 1092–1093.
- [128] a) N. Kato, H. Kataoka, S. Ohbuchi, S. Tanaka, H. Takeshita, *J. Chem. Soc., Chem. Commun.* **1988**, 354–356. b) N. Kato, H. Takeshita, H. Kataoka, S. Ohbuchi, S. Tanaka, *J. Chem. Soc., Perkin Trans. I* **1989**, 165–174.
- [129] a) T. Ríos, L. Quijano, *Tetrahedron Lett.* **1969**, *10*, 1317–1318. b) T. Ríos F. Gómez, *Tetrahedron Lett.* **1969**, *10*, 2929–2930.
- [130] For Kato’s preliminary synthetic studies on the construction of ceroplastol II (**211**), see: a) H. Takeshita, T. Hatsui, N. Kato, T. Madsuda, T. Tagoshi, *Chem. Lett.* **1982**, 1153–1156. b) N. Kato, S. Tanka, H. Takeshita, *Chem. Lett.* **1986**, 1989–1992. c) N. Kato, K. Nakanishi, H. Takeshita, *Bull. Chem. Soc. Jpn.* **1986**, *59*, 1109–1123.
- [131] R. K. Boeckman, Jr., A. Arvantis, M. E. Voss, *J. Am. Chem. Soc.* **1989**, *111*, 2737–2739.

- [132] L. A. Paquette, T. Z. Wang, N. H. Vo, *J. Am. Chem. Soc.* **1993**, *115*, 1676–1683.
- [133] C. A. Grob, W. Baumann, *Helv. Chim. Acta* **1955**, *38*, 594–610.
- [134] F. N. Tebbe, G. W. Parshall, G. S. Reddy, *J. Am. Chem. Soc.* **1978**, *100*, 3611–3613.
- [135] L. Claisen, *Ber. Dtsch. Chem. Ges.* **1912**, *45*, 3157–3166.
- [136] For semisyntheses of scalarane-type sesterterpenoids, see: a) X.-J. Meng, Y. Liu, W.-Y. Fan, B. Hu, W. Du, W.-D. Deng, *Tetrahedron Lett.* **2009**, *50*, 4983–4985. b) W.-Y. Fan, Z.-L. Wang, Z.-G. Zhang, H.-C. Li, W.-P. Deng, *Tetrahedron* **2011**, *67*, 5596–5603. c) W.-Y. Fan, Z.-L. Wang, H.-C. Li, J. S. Fossey, W.-P. Deng, *Chem. Commun.* **2011**, *47*, 2961–2963. d) X.-B. Chen, Q.-J. Yuan, J. Wang, S.-K. Hua, J. Ren, B.-B. Zeng, *J. Org. Chem.* **2011**, *76*, 7216–7221. e) Z.-L. Wang, Z.-G. Zhang, H. C. Li, W.-P. Deng, *Tetrahedron* **2011**, *67*, 6939–6964. f) H. N. Kamel, Y. B. Kim, J. M. Rimoldi, F. R. Fronczek, D. Ferreira, M. Slattery, *J. Nat. Prod.* **2009**, *72*, 1492–1496.
- [137] L. A. Paquette, B. Y. Dyck, *J. Am. Chem. Soc.* **1998**, *120*, 5953–5960.
- [138] a) C. Yuan, B. Du, L. Yang, B. Liu, *J. Am. Chem. Soc.* **2013**, *135*, 9291–9294. b) B. Du, C. Yuan, L. Yang, B. Liu, S. Qin, *Chem. Eur. J.* **2014**, *20*, 2613–2622.
- [139] L. Acebey, M. Sauvain, S. Beck, C. Moulis, A. Gimenez, V. Jullian, *Org. Lett.* **2007**, *9*, 4693–4696.
- [140] D. T. Hog, P. Mayer, D. Trauner, *J. Org. Chem.* **2012**, *77*, 5838–5843.
- [141] S. C. Agarwal, K. A. Aghoramurty, K. G. Sarma, T. R. Seshadri, *J. Sci. Industr. Res.* **1961**, *20B*, 613.
- [142] P. S. Rao, K. G. Sarma, T. R. Seshadri, *Curr. Sci.* **1965**, *34*, 9–11.
- [143] P. S. Rao, K. G. Sarma, T. R. Seshadri, *Curr. Sci.* **1966**, *35*, 147–148.
- [144] M. Kaneda, R. Takahashi, J. Iitaka, S. Shibata, *Tetrahedron Lett.* **1972**, *45*, 4609–4611.
- [145] M. Kaneda, J. Iitaka, S. Shibata, *Acta Cryst.* **1974**, *B30*, 358–364.
- [146] H. Sugawara, A. Kasuya, Y. Iitaka, S. Shibata, *Chem. Pharm. Bull.* **1991**, *39*, 3051–3054.
- [147] E. J. Corey, M. C. Desai, T. A. Engler, *J. Am. Chem. Soc.* **1985**, *107*, 4339–4341.
- [148] E. J. Corey, T. A. Engler, *Tetrahedron Lett.* **1984**, *26*, 149–152.
- [149] a) L. A. Paquette, J. Wright, G. J. Drtina, R. A. Roberts, *J. Org. Chem.* **1987**, *52*, 2960–2962. b) J. Wright, G. J. Drtina, R. A. Roberts, L. A. Paquette, *J. Am. Chem. Soc.* **1988**, *110*, 5806–5817.
- [150] L. A. Paquette, R. A. Roberts, G. J. Drtina, *J. Am. Chem. Soc.* **1984**, *106*, 6690–6693.
- [151] T. Hudlicky, L. Radesca-Kwart, L.-q. Li, T. Bryant, *Tetrahedron Lett.* **1988**, *29*, 3283–3286.
- [152] a) T. Hudlicky, R. P. Short, *J. Org. Chem.* **1982**, *47*, 1522–1527. b) T. Hudlicky, A. Flemming, L. Radesca, *J. Am. Chem. Soc.* **1989**, *111*, 6691–6707.
- [153] P. A. Wender, S. K. Singh, *Tetrahedron Lett.* **1990**, *31*, 2517–2520.
- [154] N. Kawahara, M. Nozawa, D. Flores, P. Bonilla, S. Sekita, M. Satake, K.-i. Kawai, *Chem. Pharm. Bull.* **1997**, *45*, 1717–1719.
- [155] I. H. Sadler, T. J. Simpson, *J. Chem. Soc., Chem Commun.* **1989**, 1602–1604.
- [156] D. T. Hog, F. M. E. Huber, P. Mayer, D. Trauner, *Angew. Chem. Int. Ed.* **2014**, *53*, 8513–8517; D. T. Hog, F. M. E. Huber, P. Mayer, D. Trauner, *Angew. Chem.* **2014**, *32*, 8653–8657.

- [156] D. T. Hog, Dissertation, LMU Munich, **2013**.
- [157] U. Lauer, T. Anke, W. S. Sheldrick, A. Scherer, W. Steglich, *J. Antibiot.* **1989**, *152*, 875–882.
- [158] Y. Wang, M. Dreyfuss, M. Ponelle, L. Oberer, H. Riezman, *Tetrahedron* **1998**, *54*, 6415–6426.
- [159] Y. Wang, L. Oberer, M. Dreyfuss, C. Sütterlin, H. Riezman, *Helv. Chim. Acta* **1998**, *81*, 2031–2942.
- [160] a) C. Sütterlin, A. Horvath, P. Gerold, R. T. Schwarz, Y. Wang, M. Dreyfuss, H. Riezman, *EMBO J.* **1997**, *16*, 6374–6383. b) C. Sütterlin, M. V. Escibano, P. Gerold, Y. Maeda, M. J. Mazon, T. Kinoshita, R. T. Schwarz, H. Riezman, *Biochem. J.* **1998**, *332*, 153–159.
- [161] O. D. Hensens, D. Zink, J. M. Williamson, V. J. Lotti, R. S. L. Chang, M. A. Goetz, *J. Org. Chem.* **1991**, *56*, 3399–3403.
- [162] For the structural elucidation of ceriferene-type natural products, see: a) J. K. Pawlak, M. S. Tempesta, T. Iwashita, K. Nakanishi, Y. Naya, *Chem. Lett.* **1983**, 1069–1072. b) S. Fujiwara, M. Aoki, T. Uyehara, and T. Kato, *Tetrahedron Lett.* **1984**, *25*, 3003–3006.
- [163] H. Takahashi, T. Hosoe, K. Nozawa, K. Kawei, *J. Nat. Prod.* **1999**, *62*, 1712–1713.
- [164] H. Fujimoto, E. Nakamura, E. Okuyama, M. Ishibashi, *Chem. Pharm. Bull.* **2000**, *48*, 1436–1441.
- [165] K. Yoganathan, C. Rossant, R. P. Glover, S. Cao, J. J. Vittal, S. Ng, Y. Huang, A. D. Buss, M. S. Butler, *J. Nat. Prod.* **2004**, *67*, 1681–1684.
- [166] X. Huang, H. Huang, H. Li, X. Sun, H. Huang, Y. Lu, Y. Lin, Y. Long, Z. She, *Org. Lett.* **2013**, *15*, 721–723.
- [167] D. Butler, *Nature* **2000**, *406*, 670–672.
- [168] a) A. Nören-Müller, W. Wilk, K. Saxena, H. Schwalbe, M. Kaiser, H. Waldmann, *Angew. Chem. Int. Ed.* **2008**, *47*, 5973–5977. b) V. V. Vintonyak, K. Warburg, H. Kruse, S. Grimme, K. Hübel, D. Rauh, H. Waldmann, *Angew. Chem. Int. Ed.* **2010**, *49*, 5902–5905. c) N. J. Beresford, D. Mulhearn, B. Szczepankiewicz, G. Liu, M. E. Johnson, A. Fordham-Skelton, C. Adab-Zapatero, J. S. Cavet, L. Tabernero, *J. Antimicrob. Chemother.* **2009**, *63*, 928–936.
- [169] N. Kawahara, M. Nozawa, Diana Flores, Pablo Bonilla, S. Sekita, M. Satake, *Phytochemistry* **2000**, *53*, 881–884.
- [170] S. B. Singh, R. A. Reamer, D. Zink, D. Schmatz, A. Dombrowski, M. A. Goetz, *J. Org. Chem.* **1991**, *56*, 5618–5622.
- [171] N. Kawahara, M. Nozawa, A. Kurata, T. Hakamatsuka, S. Sekita, M. Satake, *Chem. Pharm. Bull.* **1999**, *47*, 1717–1719.
- [172] a) M. S. Wilson, G. R. Dake, *Org. Lett.* **2001**, *3*, 2041–2044. b) M. S. Wilson, J. C. S. Woo, G. R. Dake, *J. Org. Chem.* **2006**, *71*, 4237–4245.
- [173] a) R. G. W. Norrish, F. W. Kirkbride, *J. Chem. Soc.* **1932**, 1518–1530. b) For a review that includes Norrish-type reactions, see: W. M. Harspool, F. Lenci, ‘CRC Handbook of Photochemistry and Photobiology’, CRC Press, New York, 2nd edition, **2004**.
- [174] a) D. Milstein, J. K. Stille, *J. Am. Chem. Soc.* **1978**, *100*, 3636–3638. b) J. K. Stille, *Angew. Chem. Int. Ed.* **1986**, *25*, 508–524.

- [175] R. Mizutani, K. Nakashima, Y. Saito, M. Sono, M. Tori, *Tetrahedron Lett.* **2009**, *50*, 2225–2227.
- [176] a) R. H. Shapiro, M. J. Heath, *J. Am. Chem. Soc.* **1967**, *89*, 5734–5735. b) R. H. Shapiro, M. F. Lipton, K. J. Kolonko, R. L. Buswell, L. A. Capuano, *Tetrahedron Lett.* **1975**, 1811–1814.
- [177] For reviews on the synthesis of cyclooctenes *via* RCM, see: a) M. Tori, R. Mizutani, *Molecules* **2010**, *15*, 4242–4260. b) A. Michaut, J. Rodriguez, *Angew. Chem Int. Ed.* **2006**, *45*, 5740–5750.
- [178] L. A. Paquette, T. M. Heidelbaugh, *Synthesis* **1998**, 495–508.
- [179] B. B. Snider, T. C. Kirk, *J. Am. Chem. Soc.* **1983**, *105*, 2364–2368.
- [180] B. B. Snider, D. J. Rodini, J. van Straten, *J. Am. Chem. Soc.* **1980**, *102*, 5872–5880.
- [181] C. R. Johnson, M. Haake, C. W. Schroeck, *J. Am. Chem. Soc.* **1970**, *92*, 6594–6598.
- [182] G. M. Atkins, E. M. Burgess, *J. Am. Chem. Soc.* **1968**, *90*, 4744–4745.
- [183] D. A. Evans, A. M. Golob, *J. Am. Chem. Soc.* **1975**, 9716, 4765–4766.
- [184] E. Piers, S. L. Boulet, *Tetrahedron Lett.* **1997**, *38*, 8815–8818.
- [185] G. A. Molander, M. S. Quirnbach, L. F. Silva, Jr., K. C. Spencer, J. Balsells, *Org. Lett.* **2001**, *3*, 2257–2260.
- [186] S. D. Walker, Dissertation, University of British Columbia, **2002**.
- [187] a) E. Piers, P. C. Marais, *Tetrahedron Lett.* **1988**, *29*, 4053–4056. b) E. Piers, K. L. Cook, C. Rogers, *Tetrahedron Lett.* **1994**, *35*, 8573–8576. c) E. Piers, S. D. Walker, R. Armbrust, *J. Chem. Soc., Perkin Trans. I* **2000**, 635–637.
- [188] W. G. Dauben, D. M. Michno, *J. Org. Chem.* **1977**, *42*, 682–685.
- [189] J. C. Collins, W. W. Hess, F. J. Frank, *Tetrahedron Lett.* **1968**, *9*, 3363–3366.
- [190] W. S. Rapson, R. Robinson, *J. Chem. Soc.* **1935**, 1285–1288.
- [191] E. Arundale, L. A. Mikeska, *Chem. Rev.* **1952**, *51*, 505–555.
- [192] K. Bowden, I. M. Heilbron, E. R. H. Jones, B. C. L. Weedon, *J. Chem. Soc.* **1946**, 39–45.
- [193] B. S. Bal, W. E. Childers, H. W. Pinnick, *Tetrahedron* **1981**, *11*, 2091–2096.
- [194] A. E. Favorskii, *J. Russ. Phys. Chem. Soc.* **1894**, *26*, 590.
- [195] L. Tschugaeff, *Ber. Dtsch. Chem. Ges.* **1899**, *32*, 3332–3335.
- [196] For a review on the Wittig-Still rearrangement, see: N. Mikami, *Chem. Rev.* **1986**, *86*, 885–902.
- [197] A. P. Krapcho, G. A. Glynn, B. J. Grenon, *Tetrahedron Lett.* **1967**, *3*, 215–217.
- [198] P. A. Wender, T. W. Von Geldern, B. H. Levine, *J. Am. Chem. Soc.* **1988**, *110*, 4858–4860.
- [199] V. Voorhees, R. Adams, *J. Am. Chem. Soc.* **1922**, *44*, 1397–1405.
- [200] T. J. Simpson, *J. Chem. Soc., Perkin Trans. I* **1994**, *21*, 3055–3056.
- [201] For selected studies on the homoallyl-cyclopropylcarbinyl-cyclobutyl rearrangement, see: a) M. Geisel, C. A. Grob, W. Santi, W. Tschudi, *Tetrahedron Lett.* **1972**, *42*, 4311–4314. b) M. Geisel, C. A. Grob, R. P. Traber, W. Tschudi, *Helv. Chim. Acta* **1976**, *59*, 2808–2820. c) K. B. Wiberg, D. Shobe, G. L. Nelson, *J. Am. Chem. Soc.* **1993**, *115*, 10645–10652. And ref. 319.
- [202] For selected recent syntheses that are based on cascade reactions and were disclosed by the Trauner research group, see: a) C. A. Kuttruff, H. Zipse, D. Trauner, *Angew. Chem. Int. Ed.* **2011**, *50*, 1402–1405. b) R. Webster, B. Gaspar, P. Mayer, D. Trauner,

- Org. Lett.* **2013**, *15*, 1866–1869. c) F. Löbermann, L. Weisheist, D. Trauner, *Org. Lett.* **2013**, *15*, 4324–4326. d) S. Strych, D. Trauner, *Angew. Chem. Int. Ed.* **2013**, *52*, 9509–9512.
- [203] Q. Xiong, W. K. Wilson, J. Pang, *Lipids* **2007**, *42*, 87–96.
- [204] S. Nozoe, J. Furukawa, U. Sankawa, S. Shibata, *Tetrahedron Lett.* **1976**, *17*, 195–198.
- [205] L. H. Zalkow, R. N. Harris III, D. Van Derveer, J. A. Bertrand, *J. Chem. Soc., Chem. Commun.* **1977**, 456–457.
- [206] L. H. Zalkow, R. N. Harris III, D. Van Derveer, *J. Chem. Soc., Chem. Commun.* **1978**, 420–421.
- [207] H. Stephen, international patent, WO 89/12626, **1989**.
- [208] E. J. Enholm, A. Trivellas, *Tetrahedron Lett.* **1989**, *30*, 1063–1066.
- [209] a) G. A. Molander, J. B. Etter, *J. Org. Chem.* **1986**, *51*, 1778–1786. b) P. A. Zoretic, B. C. Yu, M. L. Caspar, *Synth. Commun.* **1989**, *19*, 1859–1863. c) A. R. Daniewski, M. R. Uskokovic, *Tetrahedron Lett.* **1990**, *31*, 5599–5602. d) For a review on SmI₂-mediated cyclizations, see: G. A. Molander, C. R. Harris, *Chem. Rev.* **1996**, *96*, 307–338.
- [210] R. Mahrwald, ‘Modern Aldol Reactions’, Wiley-VCH, Weinheim, Vol. 1: ‘Enolates, Organocatalysis, Biocatalysis and Natural Product Synthesis’, **2004**.
- [211] Z. G. Hajos, D. R. Parrish, *Org. Synth.* **1985**, *63*, 26–31.
- [212] J. N. Marx, L. R. Norman, *J. Org. Chem.* **1975**, *40*, 1602–1606.
- [213] a) S. Bahmanyar, K. N. Houk, *J. Am. Chem. Soc.* **2001**, *123*, 11273–11283. b) S. Bahmanyar, K. N. Houk, *J. Am. Chem. Soc.* **2001**, *123*, 12911–12912.
- [214] B. List, *Angew. Chem. Int. Ed.* **2010**, *49*, 1730–1734.
- [215] a) A. R. Daniewski, J. Kiegel, *Synth. Commun.* **1988**, *18*, 115–18. b) A. R. Daniewski, K. Kiegel, E. Pietrwska, T. Warchol, W. Wojchiechowska, *Liebigs Ann. Chem.* **1988**, 593–594.
- [216] A. R. Daniewski, J. Kiegel, *J. Org. Chem.* **1988**, *53*, 5534–5535.
- [217] a) Y. Moritani, D. H. Apella, V. Jurkauskas, S. L. Buchwald, *J. Am. Chem. Soc.* **2000**, *122*, 6797–6798. b) J. Yun, S. L. Buchwald, *Org. Lett.* **2011**, *3*, 1129–1131. c) J. Chae, J. Yun, S. L. Buchwald, *Org. Lett.* **2004**, *6*, 4809–4812.
- [218] R. A. Micheli, Z. G. Hajos, N. Cohen, D. R. Parrish, L. A. Portland, W. Sciamanna, M. A. Scott, P. A. Wehrli, *J. Org. Chem.* **1975**, *40*, 675–681.
- [219] For recent synthetic studies, using this protocol on large scale, see: a) R. C. A. Pearson, M. J. Digrandi, S. J. Danishefsky, *J. Org. Lett.* **1993**, *58*, 3938–3941. b) K. C. Nicolaou, Y. P. Sun, X. S. Peng, D. Polet, D. Y.-K. Chen, *Angew. Chem. Int. Ed.* **2008**, *47*, 7310–7313. c) J. L. Frie, C. S. Jeffery, E. J. Sörensen, *Org. Lett.* **2009**, *11*, 5349–5397. d) A. N. Flyer, C. Si, A. G. Myers, *Nat. Chem.* **2010**, *2*, 886–892.
- [220] E. J. Corey, A. X. Huang, *J. Am. Chem. Soc.* **1999**, *121*, 710–714.
- [221] M. Stiles, *J. Am. Chem. Soc.* **1959**, *81*, 2598–2599.
- [222] R. Webster, A. Boyer, M. J. Fleming, M. Lautens, *Org. Lett.* **2010**, *12*, 5418–5421.
- [223] a) O. Wallach, *Ann. Chem.* **1918**, *414*, 233–243. b) O. Wallach, *Ann. Chem.* **1895**, 289, 349.
- [224] J. Wolinsky, H. Wolf, T. Gibson, *J. Org. Chem.* **1963**, *28*, 274–275.
- [225] J. Cossy, S. Boubouz, A. Hakiki, *Tetrahedron* **1999**, *55*, 11289–11294.
- [226] R. B. Loftfield, *J. Am. Chem. Soc.* **1951**, *73*, 4707–4714.

- [227] J. Wolinsky, D. Chan, *J. Org. Chem.* **1965**, *30*, 41–43.
- [228] N. Ouvrard, J. Rodriguez, M. Santelli, *Angew. Chem. Int. Ed.* **1992**, *31*, 1651–1653.
- [229] T. Tsunoda, M. Suzuki, R. Noyori, *Tetrahedron Lett.* **1980**, *21*, 1357–1358.
- [230] O. Piccolo, F. Spreafico, G. Visentin, *J. Am. Chem. Soc.* **1985**, *50*, 3946–3948.
- [231] a) K. Kagechika, M. Shibasaki, *J. Org. Chem.* **1991**, *56*, 4093–4094. b) K. Kagechika, T. Ohshima, M. Shibasaki, *Tetrahedron* **1993**, *49*, 1773–1782. c) T. Ohshima, K. Kagechika, M. Adachi, M. Sodeoka, M. Shibasaki, *J. Am. Chem. Soc.* **1996**, *118*, 7108–7116.
- [232] A. Nangia, G. Prasuna, *Tetrahedron* **1996**, *52*, 3435–3450.
- [233] a) T. Magauer, J. Mulzer, K. Tiefenbacher, *Org. Lett.* **2009**, *11*, 5306–5309. b) M. Ohba, T. Haneishi, T. Fuji, *Chem. Pharm. Bull.* **1995**, *43*, 26–31.
- [234] R. J. Arhart, J. C. Martin, *J. Am. Chem. Soc.* **1972**, *94*, 5003–5010.
- [235] For a recent example, see: D. B. Ushakov, V. Navickas, M. Ströbele, C. Maichle-Mössmer, F. Sasse, M. E. Maier, *J. Org. Chem.* **2011**, *13*, 2090–2093.
- [236] S. Aoki, S. Kotani, M. Sugiura, M. Nakajima, *Chem. Commun.* **2012**, *28*, 5524–5526.
- [237] T. Mukaiyama, K. Narasaka, K. Banno, *Chem. Lett.* **1973**, *2*, 1011–1014.
- [238] A. R. Bassindale, T. Stout, *J. Organomet. Chem.* **1984**, *271*, C1–C3.
- [239] K. Ishihara, Y. Hiraiwa, H. Yamamoto, *Synlett* **2001**, *12*, 1851–1854.
- [240] S. R. Crabtree, W. L. A. Chu, L. N. Mander, *Synlett* **1990**, *3*, 169–170.
- [241] S. Nahm, S. M. Weinreb, *Tetrahedron Lett.* **1981**, *22*, 3815–3818.
- [242] D. Liotta, G. Zima, M. Saindane, *J. Org. Chem.* **1982**, *47*, 1258–1267.
- [243] R. Rej, P. Pal, S. Nanda, *Tetrahedron* **2014**, *70*, 4457–4470.
- [244] I. C. Stewart, C. J. Douglas, R. H. Grubbs, *Org. Lett.* **2008**, *10*, 441–444.
- [245] For an *O*-alkylation reaction on a similar system, see: A. Kuramochi, H. Usuda, K. Yamatsugu, M. Kanai, M. Shibasaki, *J. Am. Chem. Soc.* **2005**, *127*, 14200–14201.
- [246] F. Senatore, V. D. Feo, Z. L. Zhou, *Ann. Chim. (Rome)* **1991**, *81*, 269–274.
- [247] R. Rojasa, V. Doroteoa, B. Bustamantec, J. Bauerd, O. Locka, *Fitoterapia* **2004**, *75*, 754–757.
- [248] T. R. Malek, *Annu. Rev. Immunol.* **2008**, *26*, 453–479.
- [249] a) Y. Q. Tu, A. Hübener, H. Zhang, C. J. Moore, M. T. Fletcher, P. Hayes, K. Dettner, W. Francke, C. S. P. McErlean, W. Kitching, *Synthesis* **2000**, 1956–1978; b) T. Magauer, H. J. Martin, J. Mulzer, *Angew. Chem. Int. Ed.* **2009**, *48*, 6032–6036.
- [250] K. C. Nicolaou, G. Vassilikogiannakis, W. Mägerlein, R. Kranich, *Angew. Chem. Int. Ed.* **2001**, *40*, 2482–2486.
- [251] A. Stolle, B. Ondruschka, W. Bornath, *Eur. J. Org. Chem.* **2007**, 2310–2317.
- [252] For mechanistic studies on the pyrolytic formation of (–)-citronellene (**413**), see: A. Stolle, B. Ondruschka, W. Bornath, T. Netscher, M. Findeisen, M. M. Hoffmann *Chem. Eur. J.* **2008**, *14*, 6805–6814; and references cited therein.
- [253] T. P. Sieber, Dissertation, University Freiburg (Switzerland), **2000**.
- [254] a) T. Hanazawa, T. Wada, T. Masuda, S. Okomato, F. Sato, *Org. Lett.* **2001**, *3*, 3975–3977. b) W. A. Nugent, J. Feldman, J. C. Calabrese, *J. Am. Chem. Soc.* **1995**, *117*, 8992–8998.
- [255] N. B. Desai, K. McKelvie, F. Ramirez, *J. Am. Chem. Soc.* **1962**, *84*, 1745–1747.
- [256] E. J. Corey, P. L. Fuchs, *Tetrahedron Lett.* **1972**, *13*, 3769–3772.

- [257] a) P. Fritsch, *Libiegs Ann.* **1894**, 279, 319–323. b) W.P. Buttenberg, *Libiegs Ann.* **1894**, 279, 324–337. c) H. Wichell, *Libiegs Ann.* **1894**, 279, 337–344.
- [258] For reviews on metal mediated enyne cyclizations, see: a) B. M. Trost, *Acc. Chem. Res.* **1990**, 23, 34–42. b) I. Ojima, M. Tzamarioudaki, Z. Li, R. J. Donovan, *Chem. Rev.* **1996**, 96, 635–662. c) B. M. Trost, M. J. Krische, *Synlett* **1998**, 1–16. d) C. Aubert, O. Buisine, M. Malacria, *Chem. Rev.* **2002**, 102, 813–834.
- [259] a) S. Ma, G. Zhu, X. Lu, *J. Org. Chem.* **1993**, 58, 3692–3696. b) M.-S. J. Wang, W.-Y. Jang, H.-Y. Jang, *Organometallics* **2009**, 28, 4841–4844.
- [260] G. Zhu, X. Tong, J. Cheng, Y. Sun, D. Li, Z. Zhang, *J. Org. Chem.* **2005**, 70, 1712–1717.
- [261] a) G. Agnel, Z. Owczarczyk, E.-i. Negishi, *Tetrahedron Lett.* **1992**, 33, 1543–1546. b) D. R. Swanson, C. J. Rousset, E.-i. Negishi, *J. Org. Chem.* **1989**, 54, 3521–3523. c) E.-i. Negishi, S. J. Holmes, J. M. Tour, J. A. Miller, F. E. Cederbaum, D. R. Swanson, T. Takahashi, *J. Am. Chem. Soc.* **1989**, 111, 3336–3346.
- [262] A. M. García, J. L. Mascareñas, L. Castedo, A. Mouriño, *J. Org. Chem.* **1997**, 62, 6353–6358.
- [263] J.-L. Montchamp, E.-i. Negishi, *J. Am. Chem. Soc.* **1998**, 120, 5345–5346.
- [264] a) W. P. Griffith, S. V. Ley, G. P. Withcombe, A. D. White, *J. Chem. Soc., Chem. Commun.* **1987**, 1625–1627. b) S. V. Ley, J. Norman, W. P. Griffith, S. P. Marsden, *Synthesis* **1994**, 639–666.
- [265] F. G. Bordwell, G. E. Drucker, H. E. Fried, *J. Org. Chem.* **1981**, 46, 632–635.
- [266] P. G. M. Wuts, T. W. Greene, ‘Greene’s Protective Groups in Organic Synthesis’, John Wiley & Sons, Hoboken, **2007**.
- [267] Y. Ito, T. Hirao, T. Saegusa, *J. Org. Chem.* **1985**, 63, 26–31.
- [268] a) M. Toyota, M. Ihara, *Synlett* **2002**, 1211–1222. b) S. Porth, J. W. Bats, D. Trauner, G. Giester, J. Mulzer, *Angew. Chem. Int. Ed.* **1999**, 38, 2015–2016.
- [269] For the laboratory preparation of Pd(OAc)₂ from powdered Pd⁰, see: V. I. Bakhmutov, J. F. Berry, F. A. Cotton, S. Ibragimov, C. A. Murillo, *Dalton Trans.* **2005**, 1989–1992.
- [270] Y. Ito, T. Hirao, T. Saegusa, *J. Org. Chem.* **1978**, 43, 1011–1013.
- [271] a) R. C., Larock, T. R. Hightower, G. A. Kraus, P. Hahn, D. Zheng, *Tetrahedron Lett.* **1995**, 36, 2423–2426. b) J. Zhu, J. Liu, R. Ma, H. Xie, J. Li, H. Jiang, W. Wang, *Adv. Synth. Catal.* **2009**, 351, 1229–1232.
- [272] J. Q. Yu, H. C. Wu, E. J. Corey, *Org. Lett.* **2005**, 7, 1415–1417.
- [273] a) I. Shimizu, I. Minami, J. Tsuji, *Tetrahedron Lett.* **1983**, 24, 1797–1800. b) I. Shimizu, I. Minami, J. Tsuji, *Tetrahedron Lett.* **1983**, 24, 5635–5638. c) I. Shimizu, I. Minami, J. Tsuji, *Tetrahedron Lett.* **1983**, 24, 5639–5640.
- [274] Y. Lu, P. L. Nguyen, N. Lévaray, H. Lebel, *J. Org. Chem.* **2013**, 78, 776–779.
- [275] a) G. A. Molander, M. S. Quirmbach, L. F. Silva, Jr., K. C. Spencer, J. Balsells, *Org. Lett.* **2001**, 3, 2257–2260. b) J. R. Bull, M. C. Loedolff, *J. Chem. Soc., Perkin Trans. 1* **1996**, 1269–1276.
- [276] a) S. H. Bertz, J. Human, C. A. Ogle, O. Seagle, *Org. Biomol. Chem.* **2005**, 3, 392–394. b) S. H. Bertz, G. Dabbagh, *J. Chem. Soc., Chem. Commun.* **1982**, 1030–1032.
- [277] C. Smit, M. W. Fraaje, A. J. Minnaard, *J. Org. Chem.* **2008**, 73, 9482–9485.

- [278] T. J. Reddy, G. Bordeaux, L. Trimble, *Org. Lett.* **2006**, 8, 5585–5588.
- [279] a) S. Cacchi, E. Morera, G. Ortar, *Tetrahedron Lett.* **1984**, 25, 4821–4824. b) K. C. Nicolaou, Q.-Y. Toh, D. Y. –K. Chen, *J. Am. Chem. Soc.* **2008**, 130, 11292–11293. c) P. Hauwert, R. Boerleider, S. Warsink, J. J. Weigand, C. J. Elsevier, *J. Am. Chem. Soc.* **2010**, 132, 16900–16910.
- [280] H. C. Brown, J. R. Schwier, B. Singaram, *J. Org. Chem.* **1978**, 43, 4395–4397. b) A. K. Mandal, P. K. Jadhav, H. C. Brown, *J. Org. Chem.* **1980**, 45, 3543–3544. c) H. C. Brown, K. Mandal, N. M. Yoon, B. Singaram, J. R. Schwier, P. K. Jadhav, *J. Org. Chem.* **1982**, 47, 5069–5074. d) H. C. Brown, P. K. Jadhav, A. K. Mandal, *J. Org. Chem.* **1978**, 47, 5074–5083.
- [281] a) K. Toshima, T. Jyojima, H. Yamaguchi, Y. Noguchi, T. Yoshida, H. Murase, M. Nakata, S. Matsamura, *J. Org. Chem.* **1997**, 62, 3271–3284. b) P. J. Kocięński, ‘Protecting Groups’, Thieme, Stuttgart – New York, 3rd edition, **2005**.
- [282] a) For recent advances, using symmetrical allyl carbonates, see: M. Braun, T. Meier, *Angew. Chem. Int. Ed.* **2006**, 45, 6952–6955; and references cited therein. b) M. Kimura, Y. Horino, R. Mukai, S. Tanaka, Y. Tamaru, *J. Am. Chem. Soc.* **2001**, 123, 10401–10402. c) T. Graening, J. F. Hartwig, *J. Am. Chem. Soc.* **2005**, 127, 17192–17193. d) For a comprehensive review on transition metal catalyzed decarboxylative allylations, see: J. D. Weaver, A. Recio, III, A. J. Grenning, J. A. Tunge, *Chem. Rev.* **2011**, 111, 1846–1913.
- [283] I. Jastrzbska, J. B. Scaglione, G. T. DeKoster, N. P. Rath, D. F. Covey, *J. Org. Chem.* **2007**, 72, 4837–4843.
- [284] a) E.-i. Negishi, M. J. Idacavage, *Tetrahedron Lett.* **1979**, 10, 845–848. b) E.-i. Negishi, H. Matsushita, S. Chatterjee, R. John, *J. Org. Chem.* **1982**, 47, 3188–3190. c) E.-i. Negishi, F. Luo, *J. Org. Chem.* **1983**, 48, 2427–2430.
- [285] a) J. A. Keith, D. C. Behenna, J. T. Mohr, S. Ma, S. C. Marinescu, J. Oxgaard, B. M. Stoltz, W. A. Goddard, III, *J. Am. Chem. Soc.* **2007**, 129, 11876–11877. b) J. A. Keith, D. C. Behenna, N. Sherden, J. T. Mohr, S. Ma, S. C. Marinescu, R. J. Nielsen, J. Oxgaard, B. M. Stoltz, W. A. Goodard, III, *J. Am. Chem. Soc.* **2012**, 134, 19050–19060.
- [286] P. Zhang, H. Le, R. E. Kyne, J. P. Morken, *J. Am. Chem. Soc.* **2011**, 133, 9716–9719.
- [287] H. Steinhausen, M. Reggelin, G. Helmchen, *Angew. Chem. Int. Ed.* **1997**, 36, 2108–2110.
- [288] a) L. O. Jeronicic, M.-P. Cabal, S. J. Danishefsky, *J. Org. Chem.* **1991**, 56, 387–395. b) T. Hoye, J. R. Vyvyan, *J. Org. Chem.* **1995**, 60, 4184–4195.
- [289] a) S. Krishnamurthy, *Aldrichim. Acta* **1974**, 7, 55–60. b) S. Wittmann, B. Schönecker, *J. prakt. Chem.* **1996**, 338, 759–762.
- [290] a) R. Pappo, D. S. Allen, Jr., R. U. Lemieux, W. S. Johnson, *J. Org. Chem.* **1956**, 21, 478–479. b) J. Xu, L. Trzoss, W. K. Chang, E. A. Theodorakis, *Angew. Chem. Int. Ed.* **2011**, 50, 3672–3676.
- [291] a) P. Wipf, S. R. Rector, H. Takahashi, *J. Am. Chem. Soc.* **2002**, 124, 14848–14849. b) P. Wipf, S. R. Spencer, *J. Am. Chem. Soc.* **2005**, 127, 225–235.
- [292] For selected examples, see: a) M. Carda, J. A. Marco, *Tetrahedron* **1992**, 48, 9789–9800. b) P. Wipf, Y. Kim, D. M. Goldstein, *J. Am. Chem. Soc.* **1995**, 117, 11106–11112. c) Y. Morimoto, M. Iwahashi, T. Kinoshita, K. Nishida, *Chem. Eur. J.*

- 2001**, 7, 4107–4116. d) Y. Morimoto, M. Iwahashi, K. Nishida, Y. Hayashi, H. Shirahama, *Angew. Chem.* **1996**, 108, 968–970. e) J. Chen, J. Chen, Y. Xie, H. Zhang, *Angew. Chem. Int. Ed.* **2012**, 51, 1024–1027. f) H. Fujioka, K. Nakahara, N. Kotoku, Y. Ohba, Y. Nagatomi, T.-L. Wang, Y. Sawama, K. Murai, K. Hirano, T. Oki, S. Wakamatsu, Y. Kita, *Chem. Eur. J.* **2012**, 18, 13861–13870.
- [293] CCDC 934939 contains the supplementary crystallographic data for lactone **470** and can be obtained free of charge from Cambridge Crystallographic Data Centre via www.ccdc.cam.ac.uk/data_request/cif.
- [294] a) A. Rodríguez, M. Nomen, B. W. Spur, J. J. Godfroid, *Tetrahedron Lett.* **1999**, 40, 5161–5164. For selected recent examples, see: b) A. J. Ndakala, M. Hashemzadeh, R. C. So, A. R. Howell, *Org. Lett.* **2002**, 4, 1719–1722. c) J. Ramharter, J. Mulzer, *Org. Lett.* **2009**, 11, 1151–1153. d) A. R. Henderson, J. Stec, D. R. Owen, R. J. Whitby, *Chem. Commun.* **2012**, 48, 3409–3411.
- [295] N. Aloune, K. Bentayeb, E. Vrancken, H. Gérard, R. Mangeney, *Chem. Eur. J.* **2009**, 15, 45–48.
- [296] a) W. F. Bailey, J. J. Patricia, *J. Organomet. Chem.* **1988**, 352, 1–46. b) F. Leroux, M. Schlosser, ‘The Preparation of Organolithium Reagents and Intermediates’, Wiley-VCH, New York, **2004**.
- [297] For selected examples on the addition of tetrasubstituted alkenyl lithium species to aldehydes, see: a) L. E. Overman, M. J. Sharp, *J. Am. Chem. Soc.* **1988**, 110, 612–614. b) M. J. Di Grandi, D. K. Jung, W. J. Krol, S. J. Danishefsky, *J. Org. Chem.* **1993**, 58, 4989–4992. c) A. Melekhov, P. Forgione, S. Legoupy, A. G. Fallis, *Org. Lett.* **2000**, 2, 2793–2796. d) J. Chen, Q. Song, P. Li, H. Guan, X. Jin, Z. Xi, *Org. Lett.* **2002**, 4, 2269–2271. e) R. Nakajima, C. Delas, Y. Takayama, F. Sato, *Angew. Chem. Int. Ed.* **2002**, 41, 3023–3025. f) M.-Y. Lin, A. Das, R.-S. Liu, *J. Am. Chem. Soc.* **2006**, 128, 9340–9341. g) M. E. Jung, M. Murakami, *Org. Lett.* **2006**, 8, 5857–5859.
- [298] For similar oxidative intramolecular lactol formations, see: a) A.-M. Periers, P. Laurin, Y. Benedetti, S. Lachaud, D. Ferroud, A. Iltis, J.-L. Haesslein, M. Klich, G. L’Hermite, B. Musicki, *Tetrahedron Lett.* **2000**, 41, 867–871. b) J. Aigner, E. Gössinger, H. Kählig, G. Menz, K. Pflugseder, *Angew. Chem. Int. Ed.* **1998**, 37, 2226–2228.
- [299] For selected examples of lactol-based Wittig olefinations, see: a) C. Taillier, B. Gille, V. Bellosta, J. Cossy, *J. Org. Chem.* **2005**, 70, 2097–2108. b) M. Lautens, C. Meyer, A. van Oeveren, *Tetrahedron Lett.* **1997**, 38, 3833–3836.
- [300] P. J.-L. Hérisson, Y. Chauvin, *Makromol. Chem. (French)* **1971**, 141, 161–176.
- [301] R. H. Grubbs, *Tetrahedron* **2004**, 60, 7117–7140.
- [302] E. L. Dias, T. S.-B. Nguyen, R. H. Grubbs, *J. Am. Chem. Soc.* **1997**, 119, 3887–3897.
- [303] For selected examples, involving especially the formation of 8-membered rings, see: a) L. A. Paquette, I. Efremov, *J. Am. Chem. Soc.* **2001**, 123, 4492–4501. b) J. R. Rodriguez, L. Castedo, J. L. Mascarenas, *Chem. Eur. J.* **2002**, 8, 2923–2930.
- [304] T. R. Hoye, H. Zhao, *Org. Lett.* **1999**, 1, 1123–1125.
- [305] a) M. Ullman, R. H. Grubbs, *Organometallics* **1998**, 17, 2484–2489. b) H. E. Blackwell, D. J. O’Leary, A. K. Chatterjee, R. A. Washenfelder, D. A. Bussmann, R. H. Grubbs, *J. Am. Chem. Soc.* **2000**, 122, 58–71.

- [306] T. R. Hoye, C. S. Jeffery, M. A. Tennakoon, J. Wang, H. Zhao, *J. Am. Chem. Soc.* **2004**, *126*, 10210–10211; and references cited therein.
- [307] H. Helmboldt, M. Hiersemann, *J. Org. Chem.* **2009**, *74*, 1698–1708.
- [308] R. Appel, *Angew. Chem. Int. Ed.* **1975**, *14*, 801–811.
- [309] a) R. R. Schrock, J. S. Murdzek, G. C. Bazan, J. Robbins, M. DiMare, M. O'Regan, *J. Am. Chem. Soc.* **1990**, *112*, 3875–3885. b) G. C. Bazan, J. H. Oskam, H. N. Cho, L. Y. Park, R. R. Schrock, *J. Am. Chem. Soc.* **1991**, *113*, 6899–6907.
- [310] A. Vakalopoulos, H. M. R. Hoffmann, *Org. Lett.* **2000**, *2*, 1447–1450.
- [311] a) R. H. Crabtree, *Acc. Chem. Res.* **1979**, *12*, 331–337. For an example of the application of Crabtree's catalyst to the hydrogenation of hindered alkenes see: b) T. J. Maimone, J. Shi, S. Ashida, P. S. Baran, *J. Am. Chem. Soc.* **2009**, *131*, 17066–17067.
- [312] G. C. Bond, J. J. Philipson, P. B. Wells, J. M. Winterbottom, *Trans. Faraday Soc.* **1966**, *62*, 443–454.
- [313] For this purpose commercial CDCl₃ was stirred over molecular sieves under exclusion of light for 24 hours. Prior to use, it was additionally filtered through basic alumina, discarding the first fractions gathered.
- [314] H. Fujioka, S. Matsuda, M. Horai, E. Fujii, M. Morishita, N. Nishiguchi, K. Hata, Y. Kita, *Chem. Eur. J.* **2007**, *13*, 5238–5248.
- [315] D. J. Morgans, Jr., K. B. Sharpless, *J. Am. Chem. Soc.* **1981**, *103*, 462–464.
- [316] M. A. Umbreit, K. B. Sharpless, *Org. Synth.* **1981**, *60*, 29–32.
- [317] I. H. Sadler, T. J. Simpson, *J. Magn. Res. Chem.* **1992**, *30*, S18–S30.
- [318] J. R. Hansen, *Nat. Prod. Rep.* **1986**, *3*, 123–132.
- [319] M. Geisel, C. A. Grob, W. Santi, W. Tschudi, *Helv. Chim. Acta* **1973**, *56*, 1055–1062.
- [320] For early investigations on ketene-based [2+2]-cycloadditions, see: a) F. Chick, N. T. M. Wilshire, *J. Chem. Soc.* **1908**, 946–950. b) H. W. Moore, D. S. Wilbur, *J. Org. Chem.* **1980**, *45*, 4483–4491. c) M. Rey, S. Roberts, A. Dieffenbacher, A. S. Dreiding, *Helv. Chim. Acta* **1970**, *53*, 417–432.
- [321] For reviews on intramolecular ketene-based [2+2]-cycloadditions, see: a) B. B. Snider, *Chem. Rev.* **1988**, *88*, 793–811. b) E. Lee-Ruff, G. Madenova, *Chem. Rev.* **2003**, *103*, 1449–1483.
- [322] J. E. McMurry, M. P. Fleming, *J. Am. Chem. Soc.* **1974**, *96*, 4708–4709.
- [323] For reviews on carbonyl-carbonyl couplings using low valent titanium, see: a) A. Fürstner, B. Bagdanović, *Angew. Chem. Int. Ed.* **1996**, *35*, 2442–2469; b) J. E. McMurry, *Chem. Rev.* **1989**, *89*, 1513–1524.
- [324] For an application of McMurry conditions for the construction of an 8-membered ring system, see: A. S. Kende, S. Johnson, P. Sanfilippo, J. C. Hodges, L. N. Jungheim, *J. Am. Chem. Soc.* **1988**, *110*, 3513–3515.
- [325] a) R. Huisgen, *Angew. Chem. Int. Ed.* **1963**, *2*, 565–598. b) R. Huisgen, *Angew. Chem. Int. Ed.* **1963**, *2*, 633–645.
- [326] For an review on the use of chiral auxiliaries in chemical synthesis, see: Y. Gnar, F. Glorius, *Synthesis* **2006**, *12*, 1899–1930.
- [327] D. A. Evans, M. D. Ennis, D. J. Mathre, *J. Am. Chem. Soc.* **1982**, *104*, 1737–1739.
- [328] D. A. Dickman, A. I. Meyers, G. A. Smith, R. E. Gawley, *Org. Synth.* **1985**, *63*, 136; **1990**, *7*, 530.
- [329] C. J. MacNevin, R. L. Moore, D. C. Liotta, *J. Org. Chem.* **2008**, *73*, 1264–1269.

- [330] A. E. May, P. H. Willoughby, T. R. Hoye, *J. Org. Chem.* **2008**, *73*, 3292–3294.
- [331] a) D. R. Williams, J. M. McGill, *J. Org. Chem.* **1990**, *55*, 3457–3459. b) C. P. Decicco, P. Grover, *J. Org. Chem.* **1996**, *61*, 3534–3541.
- [332] a) H. Lindlar, *Helv. Chim. Acta* **1952**, *35*, 446–450. b) H. Lindlar, R. Dubuis, *Org. Synth.* **1973**, *5*, 880.
- [333] a) D. A. Kummer, W. J. Chain, M. R. Morales, O. Quiroga, A. G. Myers, *J. Am. Chem. Soc.* **2008**, *130*, 13231–13233. b) M. R. Morales, K. T. Mellem, A. G. Myers, *Angew. Chem. Int. Ed.* **2012**, *51*, 4568–4571.
- [334] J. J. W. Juan, A. B. Smith III, *J. Org. Chem.* **1993**, *58*, 3073–3711.
- [335] A. G. Myers, B. H. Yang, K. J. David, *Tetrahedron Lett.* **1996**, *37*, 3623–3626.
- [336] For selected examples on the *in situ* generation of nitrile oxides, see: a) A. P. Kozikowski, P. D. Stein, *J. Am. Chem. Soc.* **1982**, *104*, 4023–4024. b) M. E. Jung, B. T. Vu, *J. Org. Chem.* **1996**, *61*, 4427–4433. c) O. Irie, Y. Fujiwara, H. Nemoto, K. Shishido, *Tetrahedron Lett.* **1996**, *37*, 9929–9232. d) I. N. N. Namboothiri, N. Rastogi, ‘Synthesis of Heterocycles via Cycloadditions’, Springer, Berlin, Heidelberg, **2008**, 12, 1–44; e) D. Bonne, L. Salat, J.-P. Duclère, J. Rodriguez, *Org. Lett.* **2008**, *10*, 5409–5412.
- [337] F. K. Brown, L. Raimondi, Y. -D. Wu, K. N. Houk, *Tetrahedron Lett.* **1982**, *33*, 4405–4408.
- [338] A. P. Kozikowski, Y. Y. Chen, *Tetrahedron Lett.* **1982**, *23*, 2081–2084.
- [339] P. W. Atkins, J. de Paula, ‘Physikalische Chemie’, Wiley-VCH, Weinheim, 5th edition, **2013**.
- [340] D. P. Curran, *J. Am. Chem. Soc.* **1982**, *104*, 4024–4026.
- [341] a) S. Y. Lee, B. S. Lee, C. W. Lee, D. Y. Oh, *Synth. Commun.* **1999**, *29*, 3621–3626. b) S. Y. Lee, B. S. Lee, C. W. Lee, D. Y. Oh, *J. Org. Chem.* **2000**, *65*, 256–257.
- [342] K. S. L. Huang, E. H. Lee, M. M. Olmstead, M. J. Kurth, *J. Org. Chem.* **2000**, *65*, 499–503.
- [343] R. Lin, J. Castells, H. Rapoport, *J. Org. Chem.* **1998**, *63*, 4069–4078.
- [344] P. N. Confalone, G. Pizzolato, D. L. Confalone, M. R. Uskoković, *J. Am. Chem. Soc.* **1980**, *102*, 1954–1960.
- [345] For a recent synthetic application of a selective hydrogenative N–O bond cleavage, see: V. S. Enev, W. Felzmann, A. Gromov, S. Marchart, J. Mulzer, *Chem. Eur. J.* **2012**, *18*, 9651–9668.
- [346] For selected reviews on B-alkyl Suzuki cross-couplings, see: a) G. Seidel, A. Fürstner, *Chem. Commun.* **2012**, *48*, 2055–2070. b) S. R. Chemler, D. Trauner, S. J. Danishefsky, *Angew. Chem. Int. Ed.* **2001**, *40*, 4544–4568.
- [347] T. Ohe, N. Miyaura, A. Suzuki, *J. Org. Chem.* **1993**, *58*, 2201–2208.
- [348] C. R. Johnson, M. P. Braun, *J. Am. Chem. Soc.* **1993**, *115*, 11014–11015.
- [349] M. E. Weiss, E. M. Carreira, *Angew. Chem. Int. Ed.* **2011**, *50*, 11501–11505.
- [350] a) C. A. Tolman, *Chem. Rev.* **1977**, *77*, 313–348. b) T. Hayashi, M. Konishi, Y. Kobori, M. Kumada, T. Higuchi, K. Hirotsu, *J. Am. Chem. Soc.* **1984**, *106*, 158–163.
- [351] a) J. E. McMurry, M. P. Fleming, K. L. Kees, L. R. Kepski, *J. Org. Chem.* **1989**, *54*, 3748–3749. b) J. E. McMurry, T. Lectka, J. G. Rico, *J. Org. Chem.* **1989**, *54*, 3748–3749.

- [352] For reviews on carbonyl-couplings *via* the reagent SmI₂, see: a) G. A. Molander, *Chem. Rev.* **1992**, *92*, 29–68. b) D. P. Curran, T. L. Fevig, C. P. Jasperse, M. J. Tottleben, *Synlett* **1992**, 943–961. c) G. A. Molander, C. R. Harris, *Chem. Rev.* **1996**, *96*, 307–338. d) A. Krief, A.-M. Laval, *Chem. Rev.* **1999**, *99*, 745–777. e) D. J. Edmonds, D. Johnston, D. J. Procter, *Chem. Rev.* **2004**, *104*, 3371–3403.
- [353] For the utilization of SmI₂ in taxane synthesis, see: a) S. Arseniyadis, D. Yashunsky, R. Pereira de Freitas, M. Muñoz Dorado, E. Toromanoff, P. Portier, *Tetrahedron Lett.* **1993**, *34*, 1137–1140. b) C. S. Swindell, W. Fan, *J. Org. Chem.* **1996**, *61*, 1109–1118.
- [354] M. Kito, T. Sakai, N. Haruta, H. Shirahama, F. Matsuda, *Synlett* **1996**, *11*, 1057–1060.
- [355] M. Schwaebe, R. D. Little, *J. Org. Chem.* **1996**, *61*, 3240–3244.
- [356] For recent applications of tungsten(IV)-based deoxygenations in total synthesis, see: a) K. Molawi, N. Delpont, A. M. Echavarren, *Angew. Chem. Int. Ed.* **2010**, *49*, 3517–3519. b) T. Sengoku, S. Xu, K. Ogura, Y. Emori, K. Kitada, D. Uemura, H. Arimoto, *Angew. Chem. Int. Ed.* **2014**, *53*, 4213–4216.
- [357] For selected examples of perrhenate-based protocols transposing allylic alcohols, see: a) K. Nakasaka, H. Kusama, Y. Hayashi, *Chem. Lett.* **1991**, 1413–1416. b) S. Bellemin-Laponnaz, *ChemCatChem* **2009**, *1*, 357–362. c) Y. Xie, P. E. Floreancig, *Angew. Chem. Int. Ed.* **2013**, *52*, 625–628.
- [358] a) A. Pedretti, L. Villa, G. Vistoli, *J. Mol. Graphics Modell.* **2002**, *21*, 47–49. b) A. Pedretti, L. Villa, G. Vistoli, *Theor. Chem. Acc.* **2003**, *109*, 229–232. c) A. Pedretti, L. Villa, G. Vistoli, *J. Comput. Aided Mol. Des.* **2004**, *18*, 167–173.
- [359] a) A. D. Becke, *Phys. Rev. A* **1988**, 3098–3100. b) C. Lee, W. Yang, R. G. Parr, *Phys. Rev. B* **1988**, *37*, 785–789. c) A. D. Becke, *J. Chem. Phys.* **1993**, *98*, 5648–5652.
- [360] a) S. Grimme, *J. Comput. Chem.* **2004**, *25*, 1463–1473. b) S. Grimme, *J. Comput. Chem.* **2006**, *27*, 1787–1799. c) S. Grimme, S. Ehrlich, L. Goerigk, *J. Comput. Chem.* **2011**, *32*, 1456–1465. d) S. Grimme, J. Antony, S. Ehrlich, H. Krieg, *J. Chem. Phys.* **2010**, *132*, 154104. e) H. Kruse, S. Grimme, *J. Chem. Phys.* **2012**, *136*, 154101.
- [361] S. Sinnecker, A. Rajendran, A. Klamt, M. Diedenhofen, F. Neese, *J. Phys. Chem. A* **2006**, *110*, 2235–2245.
- [362] a) F. Neese, *J. Comput. Chem.* **2003**, *24*, 1740–1747. b) S. Kossmann, F. Neese, *Chem. Phys. Lett.* **2009**, *481*, 240–243. c) F. Neese, F. Wennmohs, A. Hansen, U. Becker, *Chem. Phys.* **2009**, *356*, 98–109. d) R. Izsak, F. Neese, *J. Chem. Phys.* **2011**, *135*, 144105. e) S. Kossmann, F. Neese, *J. Chem. Theory Comput.* **2010**, *6*, 2325–2338.
- [363] H. Kruse, L. Goerigk, S. Grimme, *J. Org. Chem.* **2012**, *77*, 10824–10834.
- [364] D. L. Comins, A. Deghani, *Tetrahedron Lett.* **1992**, *33*, 6299–6302.
- [365] B. H. Lipshutz, J. M. Servesko, T. B. Petersen, P. P. Papa, A. A. Lover, *Org. Lett.* **2004**, *6*, 1273–1275.
- [366] For reviews on conjugate reductions that are mediated by metal hydrides, see: a) V. Jurkauskas, Dissertation, Massachusetts Institute of Technology, **2004**. b) E. Keinan, N. Greenspoon, ‘Partial Reduction of Enones, Styrenes and Related Systems’, in B. M. Trost, I. Fleming, ‘Comprehensive Organic Synthesis’, Elsevier, Oxford, Vol. 8: ‘Reductions’, **2005**.

- [367] a) G. M. Rubottom, M. A. Vazquez, D. R. Pelegrina, *Tetrahedron Lett.* **1974**, 49–50, 4319–4322. b) G. M. Rubottom, J. M. Gruber, *Tetrahedron Lett.* **1974**, 19, 4319–4322.
- [368] For common asymmetric modifications of the Rubottom oxidation, see: a) F. A. Davis, A. C. Sheppard, *J. Org. Chem.* **1987**, 52, 954–955. b) T. Hashiyama, K. Morikawa, K. B. Sharpless, *J. Org. Chem.* **1992**, 57, 5067–5068. c) Y. Zhu, Y. Tu, H. Yu, Y. Shi, *Tetrahedron Lett.* **1998**, 39, 7819–7822. d) W. Adam, R. T. Fell, C. R. Saha-Möller, C.-Gui Zhao, *Tetrahedron: Asymmetry* **1998**, 9, 397–401. e) W. Adam, R. T. Fell, V. R. Stegmann, C. R. Saha-Möller, *J. Am. Chem. Soc.* **1998**, 120, 708–714.
- [369] DMP was provided by Dr. D. Stichnoth and prepared according to: R. E. Ireland, L. Liu, *J. Org. Chem.* **1993**, 58, 2899.
- [370] a) M. Brini, T. Calì, D. Ottolini, E. Carafoli, ‘Intracellular Calcium Homeostasis and Signaling’, in L. Banci, ‘Metalloomics and the Cell’, ‘Metal ions in Life Sciences’, Springer Netherlands, **2013**, 12, 119–168. b) M. Brini, D. Ottolini, T. Calì, E. Carafoli, ‘Calcium in Health and Disease’, in A. Sigel, H. Sigel, R. K. O. Sigel, ‘Interrelations between Essential Metal Ions and Human Diseases’, ‘Metal ions in Life Sciences’, Springer Netherlands, **2013**, 13, 81–137.
- [371] a) K. E. S. Poole, J. Reeve, *Curr. Opin. Pharmacol.* **2005**, 5, 612–617. b) A. K. Prahalad, R. J. Hickey, J. Huang, D. J. Hoelz, L. Dobrolecki, S. Murthy, T. Winata, J. M. Hock, *Proteomics* **2006**, 6, 3482–3493.
- [372] D. Voet, J. G. Voet, ‘Biochemistry’, John Wiley & Sons, Hoboken, 4th edition, **2011**.
- [373] D. H. Copp, B. Cheney, *Nature* **1962**, 193, 381–382.
- [374] W. F. Boron, ‘Medical Physiology: A Cellular And Molecular Approach’, Saunders/Elsevier, Philadelphia, 2nd edition, **2009**.
- [375] X. Pan, J. Liu, T. Nguyen, C. Liu, J. Sun, Y. Teng, M. M. Fergusson, I. I. Rovira, M. Allen, D. A. Springer, A. M. Aponte, M. Gucek, R. S. Balaban, E. Murphy, T. Finkel, *Nat. Cell. Biol.* **2013**, 15, 1464–1472.
- [376] For reviews on Ca²⁺-mediated signaling, see: a) E. Carafoli, *Biochem. Biophys. Res. Commun.* **2004**, 322, 1097. b) M. J. Berridge, *Annu. Rev. Physiol.* **2005**, 67, 1–21. c) O. H. Petersen, *Cell Calcium* **2005**, 38, 171–200. d) D. E. Clapham, *Cell* **2007**, 131, 1047–1058. e) P. E. Greer, M. E. Greenberg, *Neuron* **2008**, 59, 846–860.
- [377] For reviews on the role of Ca²⁺ in neurotransmitter release, see: a) R. D. Burgoyne, *Nat. Rev. Neurosci.* **2007**, 8, 182–193. b) E. Neher, T. Sakaba, *Neuron* **2008**, 59, 861–872.
- [378] M. W. Berchtold, H. Brinkmeier, M. Münter, *Physiol. Rev.* **2000**, 80, 1215–1265.
- [379] G. E. Hardingham, S. Chawla, C. M. Johnson, H. Bading, *Nature* **1997**, 385, 260–265.
- [380] For a selection of Ca²⁺-dependent enzymes, see: a) W. N. Fishbein, S. P. Bessman, *J. Biol. Chem.* **1966**, 241, 4842–4847. b) M. Sugiura, T. Kawasaki, I. Yamashina, *J. Biol. Chem.* **1982**, 257, 9501–9507. c) N. Takahashi, Y. Takahashi, F. W. Putnam, *Proc. Natl. Acad. Sci. USA* **1986**, 83, 8019–8023. d) S. G. Rhee, Y. S. Bae, *J. Biol. Chem.* **1997**, 272, 15045–15048.
- [381] a) J. Tang, A. Maximov, O. H. Shin, H. Dai, J. Rizo, T. C. Südhof, *Cell* **2006**, 126, 1175–1187. b) A. Maximov, J. Tang, X. Yang, Z. P. Pang, T. C. Südhof, *Science* **2009**, 323, 516–521.
- [382] M. M. Dale, H. P. Rang, M. M. Dale, ‘Pharmacology’, Churchill Livingstone, Edinburgh, 6th edition, **2007**.

- [383] S. Hochman, J. Schreckengost, H. Kimura, J. Quevodo, *Ann. N. Y. Acad. Sci.* **2010**, *1198*, 140–152.
- [384] I. Parnas, G. Rashkovan, R. Ravin, Y. Fischer, *J. Neurophysiol.* **2000**, *84*, 1240–1246.
- [385] M. E. Greenberg, E. B. Ziff, L. A. Greene, *Science* **1986**, *234*, 80–83.
- [386] For selected studies on gene regulation by neuronal activity, see: a) C. A. Altar, P. Laeng, L. W. Jurata, J. A. Brockman, A. Lemire, J. Bullard, Y. V. Bukhman, T. A. Young, V. Charles, M. G. Palfreyman, *J. Neurosci.* **2004**, *24*, 2667–2677. b) S. J. Hong, H. Li, K. G. Becker, V. L. Dawson, T. M. Dawson, *Proc. Natl. Acad. Sci. USA* **2004**, *101*, 2145–2150. c) H. Li, X. Gu, V. L. Dawson, T. M. Dawson, *Proc. Natl. Acad. Sci. USA* **2004**, *101*, 647–652. d) E. Nedivi, D. Hevroni, D. Naot, D. Israeli, Y. Citri, *Nature* **1993**, *363*, 718–722. e) C. S. Park, R. Gong, J. Stuart, S. J. Tang, *J. Biol. Chem.* **2006**, *281*, 30195–30211.
- [387] D. D. Ginty, J. M. Kornhauser, M. A. Thompson, H. Bading, K. E. Mayo, J. S. Takahashi, M. E. Greenberg, *Science* **1993**, *260*, 238–241.
- [388] K. Deisseroth, E. K. Heist, R. W. Tsien, *Nature* **1998**, *392*, 198–202.
- [389] M. Naraghi, E. Neher, *J. Neurosci.* **1997**, *17*, 6961–6973.
- [390] H. Bito, K. Deisseroth, R. W. Tsien, *Cell* **1996**, *87*, 1203–1214.
- [391] H. Tokumitsu, T. R. Soderling, *J. Biol. Chem.* **1996**, *271*, 5617–5622.
- [392] D. G. Wheeler, C. F. Barrett, R. D. Groth, P. Safa, R. W. Tsien, *J. Cell Biol.* **2008**, *183*, 849–863.
- [393] A. Hudmon, H. Schulman, J. Kim, J. M. Maltez, R. W. Tsien, G. S. Pitt, *J. Cell Biol.* **2005**, *171*, 537–547.
- [394] R. E. Dolmetsch, U. Pajvani, K. Fife, J. M. Spotts, M. E. Greenberg, *Science* **2001**, *294*, 333–339.
- [395] R. D. Zuhlke, G. S. Pitt, K. Deisseroth, R. W. Tsien, H. Reuter, *Nature* **1999**, *399*, 159–162.
- [396] B. Katz, R. Miledi, *J. Physiol.* **1967**, *189*, 535–544.
- [397] S. Hagiwara, S. Nakajima, *J. Gen. Physiol.* **1966**, *49*, 807–818.
- [398] H. Reuter, *J. Physiol.* **1967**, *192*, 479–492.
- [399] B. A. Simms, G. W. Zamponi, *Neuron* **2014**, *82*, 24–45.
- [400] W. A. Catterall, *Cold Spring Harb. Perspect. Biol.* **2011**, 1–23.
- [401] B. M. Olivera, J. M. McIntosh, L. J. Cruz, F. A. Luque, W. R. Gray *Biochemistry* **1984**, *23*, 5087–5090.
- [402] For a review on the different types of agatoxin peptides, see: M. E. Adams, *Toxicon* **2004**, *43*, 509–525.
- [403] R. Newcomb, B. Szoke, A. Palma, G. Wang, X.-h. Chen, W. Hopkins, R. Cong, J. Miller, L. Urge, K. Tarczy-Hornoch, J. A. Loo, D. J. Dooley, L. Nadasdi, R. W. Tsien, J. Lemos, G. Miljanich, *Biochemistry* **1998**, *37*, 15353–15362.
- [404] B. M. Curtis, W. A. Catterall, *Biochemistry* **1984**, *23*, 2113–2118.
- [405] W. A. Catterall, *Neuron* **2010**, *67*, 915–928.
- [406] A. Randall, R. W. Tsien, *J. Neurosci.* **1995**, *15*, 2995–3012.
- [407] For additional reviews on voltage-gated calcium channels, see: a) F. Hofmann, M. Biel, V. Flockerzi *Annu. Rev. Neurosci.* **1994**, *17*, 399–418. b) W. A. Catterall, *Annu. Rev. Cell Dev. Biol.* **2000**, *16*, 521–555. c) F. H. Yu, V. Yarov-Yarovoy, G. A. Gutman, W. A. Catterall, *Pharmacol. Rev.* **2005**, *57*, 387–395.

- [408] R. W. Tsien, D. Lipscombe, D. V. Madison, K. R. Bley, A. P. Fox, *Trends Neurosci.* **1988**, *11*, 431–438.
- [409] B. E. Flucher, C. Franzini-Armstrong, *Proc. Natl. Acad. Sci. USA* **1996**, *93*, 8101–8106.
- [410] a) W. Almers, P. T. Palade, *J. Physiol.* **1981**, *312*, 159–176. b) E. Rios, G. Brum, *Nature* **1987**, *325*, 717–720. c) T. Tanabe, K. G. Beam, J. A. Powell, S. Numa, *Nature* **1988**, *336*, 134–139.
- [411] a) J. W. Hell, R. E. Westenbroek, C. Warner, M. K. Ahljianian, W. Prystay, M. M. Gilbert, T. P. Snutch, W. A. Catterall, *J. Cell Biol.* **1993**, *123*, 949–962. b) R. W. Westenbroek, L. Hoskins, W. A. Catterall, *J. Neurosci.* **1998**, *18*, 6319–6330.
- [412] D. Lipscombe, T. D. Helton, W. Xu, *J. Neurophysiol.* **2004**, *92*, 2633–2641.
- [413] a) H. Reuter, H. Porzig, S. Kokubun, B. Prod'hom, *Ann. NY Acad. Sci.* **1988**, *522*, 16–24. b) T. Tanabe, A. Mikami, S. Numa, K. G. Beam, *Nature* **1990**, *344*, 451–453.
- [414] J. P. Weick, R. D. Groth, A. L. Isaksen, P. G. Mermelstein *J. Neurosci.* **2003**, *23*, 3446–3456.
- [415] H. Zhang, Y. Fu, C. Altier, J. Platzer, D. J. Surmeier, I. Bezprozvanny, *Eur. J. Neurosci.* **2006**, *23*, 2297–2310.
- [416] For a review on Cav1.2- and Cav1.3-mediated catecholamine release, see: D. H. Vandael, S. Mahapatra, C. Calorio, A. Marcantoni, E. Carbone, *Biochim. Biophys. Acta* **2013**, *1828*, 1608–1618.
- [417] a) N. T. Bech-Hansen, M. J. Naylor, T. A. Maybaum, W. G. Pearce, B. Koop, G. A. Fishman, M. Mets, M. A. Musarella, K. M. Boycott, *Nat. Genet.* **1998**, *19*, 264–267. b) J. Striessnig, H. J. Bolz, A. Koschak, *Pflug. Arch. Eur. J. Phy.* **2010**, *460*, 361–374.
- [418] M. Murakami, O. Nakagawasai, S. Fujii, K. Kameyama, S. Murakami, S. Hozumi A. Esashi, R. Taniguchi, T. Yanagisawa, K. Tan-no, T. Tadano, K. Kitamura, K. Kisara, *Eur. J. Pharmacol.* **2001**, *419*, 175–181.
- [419] S. Barnes, M. E. Kelly, *Adv. Exp. Med. Biol.* **2002**, *514*, 465–476.
- [420] C. Wahl-Schott, L. Baumann, H. Cuny, C. Eckert, K. Griessmeier, M. Biel, *Proc. Natl. Acad. Sci. USA* **2006**, *103*, 15657–15662.
- [421] T. Tanabe, H. Takeshima, A. Mikami, V. Flockerzi, H. Takahashi, K. Kangawa, M. Kojima, H. Matsuo, T. Hirose, S. Numa, *Nature* **1987**, *328*, 313–318.
- [422] a) I. I. Serysheva, S. J. Ludtke, M. R. Baker, W. Chiu, S. L. Hamilton, *Proc. Natl. Acad. Sci.* **2002**, *99*, 10370–10375. b) M. Wolf, A. Eberhart, H. Glossmann, J. Striessnig, N. Grigorieff, *J. Mol. Biol.* **2003**, *332*, 171–182. c) C. P. Walsh, A. Davies, A. J. Butcher, A. C. Dolphin, A. Kitmitto, *J. Biol. Chem.* **2009**, *284*, 22310–22321. d) C. P. Walsh, A. Davies, M. Nieto-Rostro, A. C. Dolphin, A. Kitmitto, *Channels (Austin)* **2009**, *3*, 387–392.
- [423] L. Tang, T. M. Gamal El-Din, J. Payandeh, G. Q. Martinez, T. M. Heard, T. Scheuer, N. Zheng, W. A. Catterall, *Nature* **2014**, *505*, 56–61.
- [424] a) G. W. Zamponi, E. Bourinet, D. Nelson, J. Nargeot, T. P. Snutch, *Nature* **1997**, *385*, 442–446. b) S. Dai, D. D. Hall, J. W. Hell, *Physiol. Rev.* **2009**, *89*, 411–452. c) D. D. Hall, S. Dai, P. Y. Tseng, Z. Malik, M. Nguyen, L. Matt, K. Schnizler, A. Shephard, D. P. Mohapatra, F. Tsuruta, R. E. Dolmetsch, C. J. Christel, A. Lee, A. Burette, R. J. Weinberg, J. W. Hell, *Neuron* **2013**, *78*, 483–497.

- [425] For a review on $\text{Ca}_v\beta$ subunits, see: Z. Buraei, J. Yang, *Physiol. Rev.* **2010**, *90*, 1461–1506.
- [426] N. L. Brice, A. C. Dolphin, *J. Physiol.* **1999**, *515*, 685–694.
- [427] For a recent review on $\text{Ca}_v\alpha 2\delta$ subunits, see: A. C. Dolphin, *Biochim. Biophys. Acta* **2013**, *1828*, 1541–1549.
- [428] a) A. Davies, I. Kadurin, A. Alvarez-Laviada, L. Douglas, M. Nieto-Rostro, C. S. Bauer, W. S. Pratt, A. C. Dolphin, *Proc. Natl. Acad. Sci. USA* **2010**, *107*, 1654–1659. b) I. Kadurin, A. Alvarez-Laviada, S. F. Ng, R. Walker-Gray, M. D’Arco, M. G. Fadel, W. S. Pratt, A. C. Dolphin, *J. Biol. Chem.* **2012**, *287*, 33554–33566.
- [429] T. Yasuda, L. Chen, W. Barr, J. E. McRory, R. J. Lewis, D. J. Adams, G. W. Zamponi, *Eur. J. Neurosci.* **2004**, *20*, 1–13.
- [430] M. B. Hoppa, B. Lana, W. Margas, A. C. Dolphin, T. A. Ryan, *Nature* **2012**, *486*, 122–125.
- [431] J. Arikath, K. P. Campbell, *Curr. Opin. Neurobiol.* **2003**, *13*, 298–307.
- [432] a) P. J. Chu, H. M. Robertson, P. M. Best, *Gene* **2001**, *280*, 37–48. b) R. S. Chen, T. C. Deng, T. Garcia, Z. M. Sellers, P. M. Best, *Biophys.* **2007**, *47*, 178–186.
- [433] M. Rousset, T. Cens, S. Restituto, C. Barrere, J. L. Black, 3rd, M. W. McEnery, P. Charnet, *J. Physiol.* **2001**, *532*, 583–593.
- [434] S. Matsuda, K. Kakegawa, T. Budisantoso, T. Nomura, K. Kohda, M. Yuzaki, *Nat. Commun.* **2013**, *4*, 2759.
- [435] D. L. Minor, Jr., F. Findeisen, *Channels (Austin)* **2010**, *4*, 459–474.
- [436] a) G. H. Hockerman, B. Z. Peterson, B. D. Johnson, W. A. Catterall, *Annu. Rev. Pharmacol. Toxicol.* **1997**, *37*, 361–396. b) G. H. Hockerman, B. Z. Peterson, E. Sharp, T. N. Tanada, T. Scheuer, W. A. Catterall, *Proc. Natl. Acad. Sci.* **1997**, *94*, 14906–14911.
- [437] D. B. Tikhonov, B. S. Zhorov, *J. Biol. Chem.* **2008**, *283*, 17594–17604.
- [438] S. Berjukow, R. Marksteiner, F. Gapp, M. J. Sinnegger, S. Hering, *J. Biol. Chem.* **2000**, *275*, 22114–22120.
- [439] S. C. Stotz, S. E. Jarvis, G. W. Zamponi, *J. Physiol.* **2004**, *554*, 263–273.
- [440] a) R. L. Spaetgens, G. W. Zamponi, *J. Biol. Chem.* **1999**, *274*, 22428–22436. b) S. C. Stotz, J. Hamid, R. L. Spaetgens, S. E. Jarvis, G. W. Zamponi, *J. Biol. Chem.* **2000**, *275*, 24575–24582. c) S. C. Stotz, G. W. Zamponi, *Trends Neurosci.* **2001**, *24*, 176–181.
- [441] M. R. Tadross, M. Ben Johny, D. T. Yue, *J. Gen. Physiol.* **2010**, *135*, 197–215.
- [442] J. P. Imredy, D. T. Yue, *Neuron* **1994**, *12*, 1301–1318.
- [443] M. Ben Johny, P. S. Yang, H. Bazzazi, D. T. Yue, *Nat. Commun.* **2013**, *4*, 1717.
- [444] G. W. Zamponi, *Neuron* **2003**, *39*, 879–881.
- [445] a) T. N. Marks, S. W. Jones, *J. Gen. Physiol.* **1992**, *99*, 367–390. b) S. I. McDonough, Y. Mori, B. P. Bean, *Biophys. J.* **2005**, *88*, 211–223.
- [446] a) A. Welling, Y. W. Kwan, E. Bosse, V. Flockerzi, F. Hofman, R. S. Kass, *Circ. Res.* **1993**, *73*, 974–980. b) A. Welling, A. Ludwig, S. Zimmer, N. Klugbauer, V. Flockerzi, H. Hofmann, *Circ. Res.* **1997**, *81*, 526–532. c) J. Striessnig, *Cell Physiol. Biochem.* **1999**, *9*, 242–269.
- [447] S. A. Ringer, *J. Physiol. (London)* **1882**, *4*, 29–42.
- [448] A. Fleckenstein, *Verh. Dtsch. Ges. Inn. Med.* **1964**, *70*, 81–99.

- [449] A. Fleckenstein, *Circ Res.* **1983**, 52(2 pt. 2), 13–16.
- [450] H. Nakajima, M. Hoshiyama, K. Yamashita, A. Kiyomoto, *Jpn. J. Pharmacol.* **1975**, 25, 383–392.
- [451] M. Kohlhardt, *Recent Adv. Stud. Cardiac. Struct. Metab.* **1975**, 5, 19–26.
- [452] S. J. Goldmann S., *Angew. Chem. Int. Ed.* **1991**, 30, 1559–1578.
- [453] J. Striessnig, A. Pinggera, G. Kaur, G. Bock, P. Tuluc, *WIREs Membr. Transp. Signal.* **2014**, 3, 15–38.
- [454] a) H. Glossmann, D. R. Ferry, J. Striessnig, A. Goll, K. Moosburger, *Trends Pharmacol. Sci.* 1987, 8, 95–100. b) W. A. Catterall, J. Striessnig, *Trends Pharmacol. Sci.* **1992**, 13, 256–262.
- [455] J. Striessnig, M. Grabner, J. Mitterdorfer, S. Hering, M. J. Sinnegger, H. Glossmann, *Trends Pharmacol. Sci.* **1998**, 19, 108–115.
- [456] I. Bezprozvanny, R. W. Tsien, *Mol. Pharmacol.* **1995**, 48, 540–549.
- [457] B. A. Kenny, S. Fraser, A. T. Kilpatrick, M. Spedding, *Br. J. Pharmacol.* **1990**, 100, 211–216.
- [458] O. Fagbemi, K. A. Kane, F. M. McDonald, J. R. Parratt, A. L. Rothaul, *Br. J. Pharmacol.* **1984**, 83, 299–304.
- [459] J. Hendrich, A. T. Van Minh, F. Hebllich, M. Nieto-Rostro, K. Watschinger, J. Striessnig, J. Wratten, A. Davies, A. C. Dolphin, *Proc. Natl. Acad. Sci. USA* **2008**, 105, 3628–3633.
- [460] M. Schramm, G. Thomas, R. Towart, G. Franckowiak, *Nature* **1983**, 303, 535–537.
- [461] W. Zheng, D. Rampe, D. J. Triggle, *Mol. Pharmacol.* **1991**, 40, 734–741.
- [462] S. Herzig, *Eur. J. Pharmacol.* **1996**, 295, 113–117.
- [463] W. Xu, D. Lipscombe, *J. Neurosci.* **2001**, 21, 5944–5951.
- [464] D. Vo, W. C. Matowe, M. Ramesh, N. Iqbal, M. W. Wolowyk, S. E. Howlett, E. E. Knaus, *J. Med. Chem.* **1995**, 38, 2851–2859.
- [465] a) N. Baidur, A. Rutledge, D. J. Triggle, *J. Med. Chem.* **1993**, 36, 3743–3745. b) R. Bangalore, N. Baidur, A. Rutledge, D. J. Triggle, R. S. Kass, *Mol. Pharm.* **1994**, 46, 660–666.
- [466] a) R. S. Kass, J. P. Arena, *J. Gen. Physiol.* **1989**, 93, 1109–1127. b) R. S. Kass, J. P. Arena, S. Chin, *J. Gen. Physiol.* **1991**, 98, 63–75. c) Y. W. Kwan, R. Bangalore, M. Lakitsh, H. Glossmann, R. S. Kass, *J. Mol. Cell. Cardiol.* **1995**, 27, 253–262.
- [467] For selected articles on the elucidation of DHP binding in Cav channels, see: a) J. Mitterdorfer, M. Grabner, R. L. Kraus, S. Hering, H. Prinz, H. Glossmann, J. Striessnig, *J. Bioenerget. Biomembr.* **1998**, 30, 19–333. b) references 436a and 455. c) B. S. Zhorov, E. V. Folkman, V. S. Ananthanarayanan, *Arch. Biochem. Biophys.* **2001**, 393, 22–41. d) D. J. Triggle, *Cell. Mol. Neurobiol.* **2003**, 23, 293–303. e) D. B. Tikhonov, B. S. Zhorov, *J. Biol. Chem.* **2009**, 284, 19006–19017. f) M. A. Shaldam, M. H. Elhamamasy, E. A. Esmat, T. F. El-Moselhy, *ISRN Med. Chem.* **2014**, 203518.
- [468] a) S. Cosconati, L. Marinelli, A. Lavecchia, E. Novellino, *J. Med. Chem.* **2007**, 50, 1504–1513. b) G. M. Lipkind, H. A. Fozzard, *Mol. Pharmacol.* **2003**, 63, 499–511. c) references 467c and 467e.
- [469] T. Fehrentz, Dissertation, LMU Munich, **2012**.

- [470] a) K. S. Lee, R. W. Tsien, *Nature* **1983**, 302, 790–794. b) A. Uehara, J. R. Hume, *J. Gen. Physiol.* **1985**, 85, 621–647. c) S. Herzig, H. Lullmann, H. Sieg, *Pharmacol. Toxicol.* **1992**, 71, 229–235.
- [471] N. Dilmac, N. Hillard, J. H. Hockerman, *Mol. Pharmacol.* **2003**, 64, 491–501.
- [472] a) K. Seydl, D. Kimball, H. Schindler, C. Romanin, *Pflugers Arch.* **1993**, 424, 552–554. b) J. Kurokawa, S. Adachi-Akahane, T. Nagao, *Mol. Pharmacol.* **1997**, 51, 262–268. c) S. Hering, A. Savchenko, C. Strubing, M. Lakitsch, J. Striessnig, *Mol. Pharmacol.* **1993**, 43, 820–826.
- [473] W. Shabbir, S. Beyl, E. N. Timin, D. Schellmann, T. Erker, A. Hohaus, G. H. Hockerman, S. Hering, *Br. J. Pharmacol.* **2011**, 162, 1074–1082.
- [474] R. Kraus, B. Reichl, S. D. Kimball, M. Grabner, B. J. Murphy, W. A. Catterall, J. Striessnig, *J. Biol. Chem.* **1996**, 271, 20113–20118.
- [475] a) G. H. Hockerman, N. Dilmac, T. Scheuer, W. A. Catterall, *Mol. Pharmacol.* **2000**, 58, 1264–1270. b) S. Hering, S. Aczel, M. Grabner, F. Doring, S. Berjukow, J. Mitterdorfer, M. J. Sinnegger, J. Striessnig, V. E. Degtiar, Z. Wang, H. Glossmann, *J. Biol. Chem.* **1996**, 271, 24471–24475.
- [476] D. M. Floyd, S. D. Kimball, J. Krapcho, J. Das, C. F. Turk, *J. Med. Chem.* **1992**, 35, 756–772.
- [477] Y.-H. Ji, M. Natarajan, J. H. Griffin, international patent, WO 99/63992, **1999**.
- [478] a) J. Das, D. M. Floyd, S. D. Kimball, K. J. Duff, M. W. Lago, J. Krapcho, R. E. White, R. E. Ridgewell, M. T. Obermeier, S. Moreland, D. McMullen, D. Normandin, S. A. Hedberg, T. R. Schaeffer, *J. Med. Chem.* **1992**, 35, 2610–2617. b) J. Das, D. M. Floyd, S. D. Kimball, K. J. Duff, T. C. Vu, M. W. Lago, R. V. Moquin, V. G. Lee, J. Z. Gougoutas, M. F. Malley, S. Moreland, R. J. Brittain, S. A. Hedberg, G. G. Cucinotta, *J. Med. Chem.* **1992**, 35, 773–780. c) S. D. Kimball, D. M. Floyd, J. Das, J. T. Hunt, J. Krapcho, G. Rovnyak, K. J. Duff, V. G. Lee, R. V. Moquin, C. F. Turk, S. A. Hedberg, S. Moreland, R. J. Brittain, D. M. McMullen, D. E. Normandin, G. G. Cucinotta, *J. Med. Chem.* **1992**, 35, 780–793.
- [479] S. Ikeda, J. Oka, T. Nagao, *Eur. J. Pharmacol.* **1991**, 208, 199–205.
- [480] For selected recent publications on the photocontrol of receptor or channel enzymes, see: a) A. Mourot, M. A. Kienzler, M. R. Banghart, T. Fehrentz, F. M. E. Huber, M. Stein, R. H. Kramer, D. Trauner, *ACS Chem. Neurosci.* **2011**, 2, 536–543. b) J. Levitz, B. Gaub, H. Janovjak, P. Stawski, D. Trauner, E. Y. Isacoff, *Biophys. J.* **2011**, 100, 177–177. c) T. Fehrentz, C. A. Kutttruff, F. M. E. Huber, M. A. Kienzler, P. Mayer, D. Trauner, *ChemBioChem* **2012**, 13, 1746–1749. d) A. Mourot, T. Fehrentz, D. Bautista, D. Trauner, R. Kramer, *Nat. Methods* **2012**, 9, 396–402. e) I. Tochitsky, A. Polosukhina, V. E. Degtyar, N. Gallerani, C. M. Smith, A. Friedman, R. N. Van Gelder, D. Trauner, D. Kaufer, R. H. Kramer, *Neuron* **2014**, 81, 800–813.
- [481] For selected synthetic approaches toward diltiazem (**645**), see: a) H. Inoue, H. Kugita, M. Ikezaki, M. Konda, S. Takeo, *Chem. Pharm. Bull.* **1971**, 19, 595–602. b) S. Tanabe, *Chem. Abstr.* **1983**, 100, 85733. c) E. Decorte, F. Moimas, B. Kojic-Prodic, Z. Ruzic-Toros, V. Sunjic, *Helv. Chim. Acta* **1984**, 67, 916–926. d) K. G. Watson, Y. M. Fung, M. Gredley, G. J. Bird, R. W. Jackson, H. Gountzos, B. R. Matthews, *J. Chem. Soc., Chem. Commun.* **1990**, 15, 1018–1019. e) A. Schwartz, P. B. Madan, E. Mohacsi, J. P. O'Brien, L. J. Todaro, D. L. Coffen, *J. Org. Chem.* **1992**, 57, 851–856.

- f) H. Inoue, K. Matsuki, M. Sobukawa, A. Kawai, M. Takeda, *Chem. Pharm. Bull.* **1993**, *41*, 643–648. g) E. N. Jacobsen, L. Deng, Y. Furukawa, L. E. Martínez, *Tetrahedron* **1994**, *50*, 4323–4334. h) S. Yamada, I. Tsujioka, T. Shibatani, R. Yoshioka, *Chem. Pharm. Bull.* **1999**, *47*, 146–150. i) R. Imashiro, T. Kuroda, *Tetrahedron Lett.* **2001**, *42*, 1313–1315. j) B. M. Choudary, N. S. Chowdari, S. Madhi, L. K. Mannepalli, international patent, WO 2004058734 A1, **2004**.
- [482] For a review on syntheses of optically active 1,5-benzothiazepines, see: A. Lévai, A. Kiss-Szikszai, *ARKIVOC* **2008**, *1*, 65–86.
- [483] A. Béchamp, *Ann. de Chimie et de Physique* **1854**, *4*, 186–196.
- [484] a) W. Zhang, J. L. Loebach, S. R. Wilson, E. N. Jacobsen, *J. Am. Chem. Soc.* **1990**, *112*, 2801–2803. b) E. N. Jacobsen, W. Zhang, A. R. Muci, J. R. Eck2qaer, L. Deng, *J. Am. Chem. Soc.* **1991**, *113*, 7063–7064. c) R. Irie, K. Noda, Y. Ito, N. Matsumoto, T. Katsuki, *Tetrahedron: Asymmetry* **1991**, *2*, 481–494.
- [485] T. Hashiyama, H. Inoue, M. Konda, M. Takeda, *J. Chem. Soc., Perkin Trans. I* **1984**, 1725–1732.
- [486] B. M. Adger, J. V. Barkley, S. Bergeron, M. W. Cappi, B. E. Flowerdew, M. P. Jackson, R. McCague, T. C. Nugent, S. M. Roberts, *J. Chem. Soc., Perkin Trans. I* **1997**, 3501–3507.
- [487] N. Hosoya, A. Hatayama, K. Yanai, H. Fujii, R. Irie, T. Katsuki, *Synlett* **1993**, 641–645.
- [488] C. C., Lee, J. W. Clayton, D. G. Lee, A. J. Finlayson, *Tetrahedron* **1962**, *18*, 1395–1402.
- [489] J. Alexander, *Org. Prep. Proced. Int.* **1993**, *25*, 133–137.
- [490] R. A. Olofson, *Pure Appl. Chem.* **1988**, *60*, 1715–1724.
- [491] S. C. Wallwork, *Acta Cryst.* **1962**, *15*, 758–759.
- [492] A. V. Shcherbatiuk, O. S. Shyshlyk, V. D. V. Yarmoliuk, O. V. Shishkin, S. V. Shishkina, V. S. Starova, O. A. Zaporozhets, S. Zozulya, R. Moriev, O. Kravchuk, O. Manoilenko, A. A. Tolmacheva, P. K. Mykhailiuka, *Tetrahedron* **2013**, *69*, 3796–3804.
- [493] T. D. Choudhury, Y. Shen, N. V. S. Rao, N. A. Clark, *J. Organomet. Chem.* **2012**, *712*, 20–28.
- [494] K. Barral, A. D. Moorhouse, J. E. Moses, *Org. Lett.* **2007**, *9*, 1809–1811.
- [495] R. N. Butler, A. Fox, S. Collier, L. A. Burke, *J. Chem. Soc., Perkin Trans. 2* **1998**, 2243–2247.
- [496] H. Staudinger, J. Meyer, *Helv. Chim. Acta* **1919**, *2*, 635–646.
- [497] For an example for the hydrolysis of a similar phosphazene compound, see: C. W. Lindsley, Z. Zhao, R. C. Newton, W. H. Leister, K. A. Strauss, *Tetrahedron Lett.* **2002**, *43*, 4467–4470.
- [498] a) H. C. Kolb, M. G. Finn, B. K. Sharpless, *Angew. Chem. Int. Ed.* **2001**, *40*, 2004–2021. b) H. C. Kolb, B. K. Sharpless, *Durg Discov. Today* **2003**, *8*, 1128–1137.
- [499] R. Huisgen, *Proc. Chem. Soc. (London)* **1961**, 357–396.
- [500] A. M. Gurney, H. A. Lester, *Physiol. Rev.* **1987**, *67*, 583–617.
- [501] F. A. Gobas, J. M. Lahittete, G. Garofalo, W. Y. Shiu, D. Mackay, *J. Pharm. Sci.* **1988**, *77*, 265–272.
- [502] E.-H. Ryu, Y. Zhao, *Org. Lett.* **2005**, *7*, 1035–1037.

- [503] J.-Y. Kazock, M. Taggougui, B. Carré, P. Willmann, D. Lemordant, *Synthesis* **2007**, 24, 3776–3778.
- [504] A. J. Brouwer, S. J. E. Mulders, R. M. J. Liskamp, *Eur. J. Org. Chem.* **2001**, 10, 1903–1915.
- [505] S. Kohmoto, E. Mori, K. Kishikawa, *J. Am. Chem. Soc.* **2007**, 129, 13364–13365.
- [506] F. Neese, *Wiley Interdiscip. Rev. Comput. Mol. Sci.* **2012**, 2, 73–78.
- [507] N. Kawahara, M. Nozawa, D. Flores, P. Bonilla, S. Sekita, M. Satake, K.-i. Kawai, *Chem. Pharm. Bull.* **1997**, 45, 1717–1719.
- [508] CrysAlisPro, *Oxford Diffraction Ltd.*, Version 1.171.33.41 (release 06-05-2009 CrysAlis171.NET).
- [509] A. Altomare, M. C. Burla, M. Camalli, G. L. Cascarano, C. Giacovazzo, A. Guagliardi, A. G. G. Moliterni, G. Polidori, R. Spagna, *J. Appl. Crystallogr.* **1999**, 32, 115–119.
- [510] G. M. Sheldrick, *Acta Cryst.* **2008**, A64, 112–122.
- [511] T. Saito, T. Yokozawa, T. Ishizaki, T. Moroi, N. Sayo, T. Miura, H. Kumobayashi, *Adv. Synth. Catal.* **2001**, 343, 264–267.

VIII. Curriculum Vitae

FLORIAN MAURITIUS ERASMUS HUBER

Personal Information

Date of birth	Born in Großhadern/Munich on April, 22 nd 1984.
Nationality	German.
Marital status	Unmarried.

*Education*

Since 2010	Ph.D. studies (doctoral studies) in organic chemistry in the research group of Prof. Dr. Dirk Trauner at Ludwig-Maximilians-Universität in Munich.
2004 – 2010	Study of chemistry at Ludwigs-Maximillians-Universität in Munich and graduation with diploma in chemistry (average grade: 1.28). ^{xiv}
2003 – 2004	Basic military service at German Bundeswehr (facilities at Bayreuth and Penzing).
1994 – 2003	Student at Ignaz-Kögler-Gymnasium in Landsberg am Lech. Graduation with Abitur (average grade: 1.7).
1990 – 1994	Elementary school in Finning.

Spoken languages

German	Mother language.
English	Fluently.
French	Advanced: student exchange (Nice, 1999), student courses at Ludwig-Maximilians-Universität in Munich (2013 – 2014).

^{xiv} Title: 'I. Synthesis of Red-shifted and Z-stable Diazene Compounds as Photochromic, Internal Blockers of Voltage-gated Potassium Channels. II. Progress Toward the Co-crystallization of the Potassium Channel KcsA and Photochromic, Internal Blockers of Voltage-gated Potassium Channels'.

Practical experience

2009	Internship in the working group of Prof. Dr. J. Schmedt auf der Gönne (LMU Munich, <i>Synthesis and solid state NMR analysis of alkaliphosphate glasses</i>).
2008 – 2009	Internship in the working group of Prof. Dr. T. Bein (LMU Munich, <i>Drug delivery and biodegradation studies on mesoporous silica nanoparticles</i>).
2008	Internship in the working group of Prof. Dr. T. Carell (LMU Munich, <i>Synthesis of hypermodified tRNA nucleosides</i>).
2008	Internship in the working group of Prof. Dr. T. M. Klapötke (LMU Munich, <i>Synthesis of organosulfonium and organotellurium azides and dinitramides</i>).
2005	Temporary substitute at MicroCoat Biotechnologie GmbH (Bernried, Germany, <i>Preparation of diversely loaded microtitre plates</i>).
2004	Temporary substitute at Roche Diagnostics GmbH (Penzberg, Germany, <i>Order processing and packing</i>).
2000 – 2003	Undisclosed partner with the company 'Impuls Produkt & Service KG' (student project, <i>Maintenance and distribution of computer soft- and hardware</i>).

Publication list

First author:	D. T. Hog, [#] F. M. E. Huber, [#] D. Trauner, 'The Total Synthesis of (–)-Nitidasin', <i>Angew. Chem. Int. Ed.</i> 2014 , 53, 8513–8517; <i>Angew. Chem.</i> 2014 , 126, 8653–8657; <i>Synfacts</i> 2014 , 10, 902.
Others:	T. Fehrentz, [#] C. A. Kuttruff, [#] F. M. E. Huber, M. A. Kienzler, P. Mayer, D. Trauner, 'Exploring the Pharmacology and Action Spectra of Photochromic Open-Channel Blockers', <i>ChemBioChem</i> 2012 , 13, 1746–1749. A. Mourot, [#] M. A. Kienzler, [#] M. R. Banghart, T. Fehrentz, F. M. E. Huber, M. Stein, R. H. Kramer, D. Trauner, 'Tuning Photochromic Ion Channel Blockers', <i>ACS Chemical Neuroscience</i> 2011 , 2, 536–543.

[#]These authors contributed equally.

Presentations

Oral presentations

- 2014 'The Total Synthesis of (–)-Nitidasin and Synthetic Studies Toward Astellatol', *Seminar at the University of Toronto*, invited by Prof. Dr. M. Lautens.

Poster presentations

- 2014 'The Total Synthesis of (–)-Nitidasin and Synthetic Studies Toward Astellatol', *GRC The Central Role of Natural Products in Biology and Chemistry* (Andover, NH).
- 2014 'The Total Synthesis of (–)-Nitidasin', *SFB-749 annual meeting* (Venice).
- 2013 'Photocontrolling Ca_v Channels: Design and Synthesis of Potential Photochromic Blockers', *Frontiers in Medicinal Chemistry* (Munich).
- 2012 'Dynamic Nanosystems for the Temporal and Spatial Control of Cell Functions with Light', *SFB-1032 annual meeting* (Hohenkammer).
- 2011 'Dynamics of Photoswitchable Channel Blockers and Biomimetic Cascade Reactions', *SFB-749 annual meeting* (Munich).

– Munich, October 12th 2014